

ESEN-CPS-BK-0000001058-ESE

00471219

مجلة جمعية المهندسين المصرية

المجلد الرابع عشر

العدد الأول (يناير - فبراير - مارس ١٩٧٥)

هيئة التحرير

رئيس التحرير

دكتور سيد مرتضى

سكرتير التحرير

وأمين الصندوق

دكتور جمال الدين نصار

مهندس توفيق أحمد عبد الجواد

دكتور حامد حسنين عامر

مهندس عبد الملك العصفورى

دكتور فؤاد بهجت

دكتور محمد فهم صقر

دكتور محمود أبو زيد

دكتور محيى الدين سليم

- تصدر المجلة ربع سنوية
- ترسل النصوص المطلوب موافقة هيئة التحرير على نشرها باسم السيد / رئيس التحرير . وهو غير مسئول عن فقد أو تلف أى نص .
- تنشر المجلة المقالات التى تسهم فى رفع مستوى العلوم الهندسية وطرق ممارستها .
- تقبل للنشر المقالات باحدى اللغتين العربية أو الانجليزية ، على أن تقدم من ثلاث نسخ مكتوبة على الآلة الكاتبة ومعها ملخص بكل من اللغتين .
- تذكر أسماء أصحاب المقالة كاملة باللغتين ومعها ألقابهم العلمية ووظائفهم .
- يراعى ألا تتجاوز المقالة ٨ صفحات بالمجلة ، وفى سبيل ذلك يختصر الاشتقاق الرياضى ويستعاض عن الجداول بمنحنيات مرسومة بالحبر الشينى الأسود ، على أن يشغل المنحنى نصف صفحة على الأكثر ولا يشغل صفحة كاملة الا فى حالات استثنائية وسيصفى أى منحن الى تلك المقاسات .

- ويراعى ألا يقل ارتفاع الحروف أو الأرقام على المنحنيات المنشورة عن ٣ مم بعد التصغير .
- يعنى بذكر المراجع المستقى منها المقال وتصنف تبعاً لاسم المؤلف ثم العنوان ثم المجلة أو الكتاب وتاريخه .

- تقدم لصاحب المقال تجربتان للطباعة وتفرق بالأولى نسخة من مصطلحات التصحيح التى يؤدى اتباعها الى رفع كفاية التصحيح وتقليل الوقت الضائع فيه .

اشتراكات الجمعية :

قرشا

٢٠٠

١٥٠

١٠٠

العضو

العضو المنتسب

المنتسب

اشتراكات المجلة :

يتلقى أعضاء الجمعية نسخهم مجاناً .

ولغير الأعضاء :

قرشا

١٠٠

٣٠٠

٥٠٠

الاشتراك السنوى للمهندسين

الاشتراك السنوى لغير المهندسين

الاشتراك السنوى للهيئات

تعطى أولوية النشر بالمجلة للسادة

الزملاء أعضاء جمعية المهندسين المصرية

الاعلانات :

مؤسسة مصر للطباعة والنشر

القاهرة ١٩ شارع سوق التوفيقية ت ٧٢١٩٢

محتويات العدد

التشييد والبناء	التصنيع والانتاج	الخامات الأولية والصناعات الكيميائية
القسم العربى :	القسم العربى :	القسم العربى :
— مؤثر المباني رخيصة التكاليف . للدكتور جمال نصار ٨٤		
— التكنولوجيا والعمارة . « التقدم التكنولوجى وأثره على العمارة والمدينة والمجتمع » . العماري توفيق عبد الجواد ١٧		
القسم الأفرنجى :	القسم الأفرنجى :	القسم الأفرنجى :
— طريقة بيانية لحساب المعاملات الهيدروليكية للخزانات الجوفية الدكتور محمود أبو زيد والمهندس صالح رشوان ٣٤	— الاتزان العابر لنظم القوى الكهربائية دكتور مدحت أديب نصر ١٠٧	— الاجهادات فى الصخور المحيطة بفتحات منجم المغارة للفحم . للدكتور محب الدين حسين والدكتور حسن فهمى امام جيولوجى ناجى نصيف ١٥١
— تحليل سلوك مجموعات الخزائيق المحملة عرضيا . ١ - الطريقة الترويجية المعدلة للدكتور محمد عادل بركات ٤٠	— تحليل اهتزازات التلى فى منظومات دفع ناقلات البترول الكبيرة - حساب اجهادات التلى . للدكتور فؤاد بهجت والدكتور نعمان محارم والمهندس على العراقي ١١٧	— التطور الحديث فى الفناطيسات السيراميكية الدائمة . للدكتور احمد مراد جاد الله والدكتور ه . و . هينك ١٦٦
— معالجة مخلفات الصناعة المفتقرة الى النسبة اللازمة من النيتروجين والفوسفور للمعالجة البيولوجية باستخدام طريقة الحماة المعاد تشغيلها . الدكتور احمد عبد الوارث والدكتورة فاطمة الجوهري والمهندس مدحت صالح ٥٢		
— خواص الخزان الجوفى فى الوجه القبلى . للدكتور محمد حمدي الكاتب والمهندسة فاطمة عبد الرحمن ٦٣		

التشييد والبناء

جمعية المهندسين المدنيين
جمعية المهندسين المعماريين
جمعية مهندسي الري

جمعية المهندسين المصرية

يسرني أن أوضح فيما يلي التشكيل الجديد لمجلس ادارة الجمعية عن عام ١٩٧٥ :

رئيس	١ - الأستاذ الدكتور أحمد محرم أحمد
وكيل	٢ - المهندس أمين حلمى كامل
وكيل	٣ - المهندس حسن ناجى
أمين عام	٤ - الأستاذ الدكتور محمد محمد الهاشمى
أمين صندوق	٥ - الدكتور محيى الدين سليم
أمين عام مساعد	٦ - الأستاذ الدكتور محمد فهم صقر
أمين صندوق مساعد	٧ - المهندس مدحت العلالى
أعضاء	٨ - المهندس أحمد على كمال
	٩ - المهندس ابراهيم نجيب
	١٠ - الأستاذ الدكتور مصطفى الحفناوى
	١١ - المهندس عبد الحميد الزنفل
	١٢ - الدكتورة أمينة الحفنى
	١٣ - الدكتور جمال الدين نصار
	١٤ - المهندس ابراهيم كامل أحمد
	١٥ - الأستاذ الدكتور أحمد أمين مختار

راجيا أن يستمر التعاون بيننا بما يعود على أمتنا العربية بالخير والبركات .

وتفضلوا بقبول فائق الاحترام ،

الأمين العام

أ.د. محمد محمد الهاشمى

ble feedback on the success off meeting the project's objectives.

- 3) An efficient and capable project management system is essential. The quality of existing management skills effectively limit all subsequent activity.
- 4) More positive directives and fewer preventive restrictions, are called for.

HOUSING SYSTEMS AND METHODS :

- 1) Prefabricated systems in some countries have shown a significant on-site saving in time (in Japan total site time of units : 2 to 6 weeks).
- 2) High-rise should be used when needed. When needed, it should be accompanied with more planning than single storey developments. The consequent costs are believed to be more than offset by the saving in urban infrastructure.
- 3) Encourage cooperative housing projects. Provide flexibility.

SERVICES :

- 1) "Services" should be extended to include not only the facilities in the house but also public utilities and also social services.
- 2- There should be a future conference on public utilities. Extension of facilities in built-up areas. Provision of utilities in new areas (new towns).
- 3) Reduce costs of service equipment in the home as compared to total costs.
- 4) It is essential that all energy usage be optimized.

CONCRETE SYSTEMS :

- 1) Use of concrete Systems not suitable to rural areas or developing countries.
- 2) Prefabrication carries with it the responsibility for success of repeating details.
- 3) Prefab concrete used up to 25 stories, exception, up to 30 stories.
- 4) Possibility of fibrous reinforcement/bamboo.
- 5) The need to conserve concrete.

G. NASSAR

ECONOMICS :

- 1) The overall housing policy must not only embrace the city. It must also be at least regional, and is even better if it is national. In some parts of the world, coordination considering adjacent nations may be essential.
- 2) Design must consider concentration of industry as well as population growth.

SOCIAL EFFECTS :

- 1) Not only self-help in construction should be developed but also self-help in design.
- 2) Find out what people want. Consideration of social effects should be an integral part of the initial planning process.
- 3) Find the link between the researcher and the planner.
- 4) The incorporation of health, educational and cultural services and other amenities is essential.

MAINTENANCE AND MANAGEMENT:

- 1) Professional managers should be engaged to handle occupancy problems on public housing projects.
- 2) Since the most serious vandalism is to lifts, this argues for limiting heights to 4 and 5 storeys, where possible.
- 3) Provide opportunity for tenants to purchase their flats, thus affording the incentives of private ownership.

IMPLEMENTATION :

- 1) Top level government support is crucial if housing goals are to be accomplished.
- 2) Government agencies must be strengthened.
- 3) Close coordination is needed between government, private sector, developers.
- 4) A monitoring effort would be useful to assess the effects of building construction as they arise. This will be useful to the decision makers in their future projects.
- 5) Feedback and follow-up is essential.
- 6) The environmental impact should be evaluated and considered.
- 7) Provide for natural mobility of people by provision of medium and-high-income housing.
- 8) Availability of building materials must be planned.
- 9) More research in the building industry should be supported.

PROJECT MANAGEMENT :

- 1) The ordinary loose alliance of designer, client and contractor will not do on major projects. "Project Management" techniques are needed that put these in closer relationship with the investor and government.
- 2) The developer consultant should stay with the project through the occupancy, operation phase. This will ena-

- 9) Design the ("Self-help") construction to enable residents to apply as much of their own efforts as possible.
- 19) International coordination would be desirable in the categorization of the problems.
- 11) Each country should analyse where the cost of the housing lies.
- 12) Priorities should be determined (who gets the housing first).

HISTORICAL, CULTURAL, ARCHITECTURE:

- 1) Units must be designed to meet the needs of extended family. (Adjacent units can frequently serve).
- 2) Provision should be made for transition of life style... from rural to city, from city slums to improved housing. Educational aspects are included here (i.e. educating people to cope with urban life).
- 3) The historical and cultural value of older housing schemes should be considered prior to any planned demolition in the belief that renovation is preferable, if possible.
- 4) Private open space - in the form of a courtyard or terrace large enough to be used as a flexible living space (for sleeping, eating, living, etc. in privacy) — should be provided.
- 5) Designs should use native materials and available skills as much as possible.
- 6) Consider clustering of dwelling units to enable small neighbourhoods to develop with in large projects by studying the optimal functional size of men in groups (9 to 11).

URBAN PLANNING :

- 1) Diversity is essential. Must provide for schools, employment, cultural, entertainment.
- 2) Avoid waste of land by dependence on the automobile. Cluster the (housing) demands, or lay them out in linear fashion to facilitate transportation scheme.
- 3) Lay out the transportation network as one of the first steps.
- 4) Develop an urban design plan (Ex: San Francisco), describing the desired visual, physical, sensual aspects of the city.
- 5) Exploit all available resources, squeeze in shops.
- 6) Provide opportunity for people to make alterations in their homes.
- 7) Self-help projects are important. These can even include work on the infrastructure.
- 8) Open space must be treated critically. Usually it is better to provide opportunity for productive use of such with middle class mentality.
- 9) Don't approach Low-Income Housing spaces.
- 10) Urban planning legislation or enabling acts should be issued and zoning ordinances must be adopted for each urban center.
- 11) A long range housing policy should be drawn in such a way that it is not liable to subjective changes.
- 12) The provision of industrial housing should be executed at the same time of constructing industrial plants, with due care to pollution probability. Emphasis should be placed on the provision of opportunities for employment to housing occupants.

RECOMMENDATIONS COMING FROM

CONFERENCE SESSIONS

APPROACHES. SUGGESTIONS AND

PREAMBLE :

- 1) Housing is one of the most crucial problems facing Egypt. It must be considered so by all concerned.
- 2) The housing situation is actually deteriorating in most developing countries.
- 3) The approach to solution of low-income housing problems will vary, depending on whether it is for rural people, for the new urban dweller, or for people accustomed to city life.
- 4) Poverty is a process of exclusion or denegration.
- 5) Eighty percent of past housing projects have overrun their cost.
- 6) By Low Cost Housing is meant those housing projects built for low-income groups, where families cannot afford to pay the rent or the cost of their dwellings if calculated on an economic basis. (Perhaps "Low-Income Housing" is more descriptive of housing for people of limited income).

NEEDS FOR EGYPT :

- 1) 1.500.000 units 15 years.
- 2) Decrease construction costs.
- 3) Healthful social and human town.
- 5) Control land speculation.
- 5) Increased public transport/lower costs.
- 6) Subsidy to provide homes for lower income.
- 7) Control of noise, nuisance and pollution.

- 8) Provision of parks, green belts, playgrounds.
- 9) Codes of practice.
- 10) Develop trained workers (60,000 needed).
- 11) Control population density and generated traffic.
- 12) Develop financing system.
- 13) Introduce efficient management system.

SUGGESTIONS

GENERAL :

- 1) Every country must develop its own national housing policy.
- 2) Each country must develop its own way to solve the same basic housing problems.
- 3) A strong government land use policy is essential to stop land speculation (example : Iran's policy).
- 4) Government subsidies should be realistic.
- 5) Government can provide the amenities and infrastructure that people cannot provide.
- 6) Standards are required, but should allow for flexibility.
- 7) Adjust housing to the people, not people to the housing.
- 8) Consider the needs of the present people, recognizing that planning should incorporate the dynamic aspects of future needs.

Implementation of Housing Goals was discussed during Session 8. Chairmen : Mr. J. Fitzgerald (USA) and Mr. M. El Hifnawy (ARE). Speakers : Prof. Re. Rooseno (Indonesia), Eng. A. Idris (ARE) Prof. L. Rudrelman (USA) Mr. J. Murply (USA). The paper presented by Prof. Rooseno was a case study of the Indonesia situation and efforts towards the implementation of housing goals.

Project Management was subject of the following session. Chairmen were Dr. E. Gaylord (USA) and Dr. Gamal Nassr (ARE). Speakers Mr. C. Jha (USA) Mr. I. Osman (ARE), Mr. A. Haddon (Hong Kong) Mr. Andrews (UK).

Session 10 dealt with Housing Systems and Methods. Chairmen, Mr. Codella (ARE). Speakers were Dr. P. Barnard (Canada), Mr. F. Sironi (Italy), Mr. M. Holley (France), Mr. Krell (USA) and Mr. Watabe (Japan).

Services were discussed during Session 11. Chairmen : Mr. R. Baum (USA) and Eng. E. Farag (ARE). Speakers : Eng. E. Farag (ARE). Mr. T. Sun (USA).

Safe Housing and Safe Homes were subject of session 12. Chairmen : Mr. J. Chiristiansen (U.S.A) and Gen. Badr (ARE). Speakers : Mr. R. Mainstone (UK), Dr. M. Kamel (ARE) and Mrs. M. Law (UK). In her paper, presented to the Conference, Mrs. Law emphathized that : for most countries it could be said, that the majority of deaths and casualties by fire would takeplace in the home. If safe housing could be designed, therefore a significant reduction in life loss and injury could be achieved.

Session 13 discussed : Application : Steel and Mixed Coustruction. Chairmen : Dr. T. Naka (Japan) and Eng. A. Morsy (ARE) Speakers Eng. F. Zaghla (ARE), Dr. M. Watabe (Japan) Mr. Viest (USA) and Mr. Kato (Japan).

The following session delt with Applications : Masonry systems - Chairmen M.H. Cheng (Hong Kong) and Eng. A. Talaat (ARE). Speakers : Prof. B. Lewicki (Poland), Mr. M. Rophael (ARE) Mr. B. Sundara Rao (India) Mr. Paxton (USA) and Mr. Macchi (Italy). Applications : Concrete Systems formed the subject of session 15. Chairmen :

Prof. A. Coul (U.K.) and Dr. W. S. Hanna (ARE), Speakrs Mr. B. Vavaroutas (Greece) and Dr. B. Goschy (Hungary).

neers, Dr. R. El Mahgoub, First Secretary of the Arab Socialist Union, Mr. Michael Gaus, Director, National Science Foundation, and Dr. Lynn S. Beedle, Chairman of the Joint Committee on Tall Buildings. Dr. Gamal Nassar, Conference Organizer introduced the speakers, in this session.

On the First Session spoke Dr. D. Sfintesco (France) Eng. H. Kaddah A.R.E. and Mr. P. Kimm (USA) on Global Needs.

The second session discussed the: Recent Solutions and Needs. Chairmen of the session were Dr. T Kavanagh (USA) and Eng. S. Habib (ARE). Speakers were : Mr. P. Selvanayatnam (W. Indies), Dr. P. Varghese (India) Eng. I. Kenawy (ARE), Mr. N. Khalili (Iran) and Mr. Wanjchi (Kenya).

In his speech Mr. Khalili outlined the Iranian Experience in housing underlining the fact that Iran's housing need is fourtimes that of Egypt, to be met in two thirds the time. He also stated the fact that in its rapid industrialization, Iran has admittedly made mistakes in the housing development field, which were recognized by now and which are being corrected.

Subject of the third session were : Historical Aspects and Cultural Values Chairmen of this session were : Dr. F. Khan (U.S.A.) and Dr. Y. Eid (A.R.E.) Speakers were : Mrs. M. Khalili (Iran) Eng. H. Fathi (A.R.E) Prof. H. Cowan (Australia), C. Correa (U.S.A.) and Mr. Wanjchi (W. Indies). In this speech Mr. Wanjchi pointed out the following : Real breakthrough in low cost housing can only occur when the peoples' right to shelter just as used to be in the «bushages» is accepted. The minimum standard and density of housing should be left to ei-

ther the occupier who pays for what he can afford, or to the government whenever it may fall that people need certain standards. During sessions : Urban Planning, Housing, Transport, Land Use were discussed. Chairmen of the session were : Mr. J. Linville (U.S.A.) and Dr. A. Moéram (ARE) Speakers : Mr. R. Okamoi (USA) Eng. S. Nasr Habib (ARE), Mr. R. Seiz (USA) and Mrs. L. de Gouffray, Colombia, Speaking of : Condensed Approach to Urban Development. Mrs. Lee de Gouffray said that, this planning technique is based on the establishment of a group of self - contained, high - density cities especially designed for pedestrians.

Economic Aspects were discussed during fifth session : Chairmen : Dr. F. Reinitzhuber (BRD) and Eng. Michel Rophail (ARE). Speakers were Mr. S. Mathur (India), Mr. J. Linville (USA), Mr. S. Sardjouna (Indonesia), and Mr. Correa (USA).

In Session 6 special attention was given the Social Effects. Chairmen : Dr. M. Gauss (USA) and Mr. Hassan (ARE) Speakers : Dr. Noha Fahmy (ARE) Mrs. J. O'Neill (Australia), Mrs. J. Conway (UK) Prof. R. Herrenkohl (USA.) and Mr. J. Friedman (France). Dr. Noha Fahmy, Head of the urbanization Unit at the National Center for Social and Criminological Research, spoke of the relation between Social Researches and Planning in form of Housing.

Subject of Session 7 was Maintenance and Management. Chairmen : Mr. J. Rankine (Australia) and Mr. Farag (ARE). Speakers : Mr. E. Kennard (Hong Kong), Eng. A. Abou Youssef (ARE) and Eng. H. Barboura (Tunis). Eng. Barboura especially dealt with the Tunisian Problem.

FROM THE CAIRO CONFERENCE ON LOW COST HOUSING IN DEVELOPING COUNTRIES

CAIRO : APRIL, 20 — 25, 1975

by

G. NASSAR

CONFERENCE REVIEW

More than 300 from 54 countries (a new record for a Joint Committee-related conference) met in Cairo for the April 20 — 25 week to make specific recommendations on Low Income Housing. The opening speech of President Sadat was delivered by Osman A. Osman, Minister of Housing and Reconstruction.

One hundred specialist-participants (coming from 24 countries) attended through the efforts of the Joint Committee. Each responded very well to «last minute» arrangements. The «OK» from NSF came only 26 days from conference opening.

His Excellency Eng. Osman Ahmed Osman said that it was a major international Conference on Low Cost Housing in Developing Countries. The aim of this conference was to bring specialists from all over the world and from a wide variety of disciplines. in order to adapt the best of their experiences to our needs.

The Conference was sponsored by the Egyptians Society of Civil Engineers, Egyptian Academy of Science & Technology, the U.S. Agency for International Development (Office of Housing) and the Joint Committee on Tall Buildings, headquartered at Lehigh University, Bethlehem, Pennsylvania.

Dr. Micheal Gaus, Head of Section, Engineering Devision, NSF announced be-

fore the conference not only would it enable a worldwide audience to exchange the latest from recent housing research, but it would also help identify important topics for future research, and indeed it did.

Participating Countries were : USA, France. W. Indies, India, Iran, Australia, Bahrain, Columbia, Federal Republic of Germany, Indonesia, Britain, Hong-Kong, Tunis, Canada, Italy, Japan, Poland, Sudan, Greece, Hungary, Singapore, Norway, Syria, Irak, Austria, Omman, Kuwait, Morocco, Algeria. Lebanon, Jordan, Libya, Ghana. Sierra Leonē, Jugoslavia, Bengladesh, Kenya, Peru, Rhodesia, Mali, Ivory Coast, Chechoslovakia. Zaire, Mexico, Senegal, Nepal, Brazil and Nigeria.

The sessions went beyond specific Housing systems. The 5 days conference included 15 sessions in addition to the opening and closing address session.

Eng. Osman A. Osman also emphasized the national problem of skilled labor. At the opening address spoke also: Dr. A. Mohram, President of the Egyptian Society of Engineers, H.E. Eng. Abdul Azim Abul Ata of the Syndicate of Engi-

**FROM THE CAIRO
CONFERENCE ON LOW
COST HOUSING IN DEVELOPING COUNTRIES**

CAIRO : APRIL, 20 — 25, 1975

by

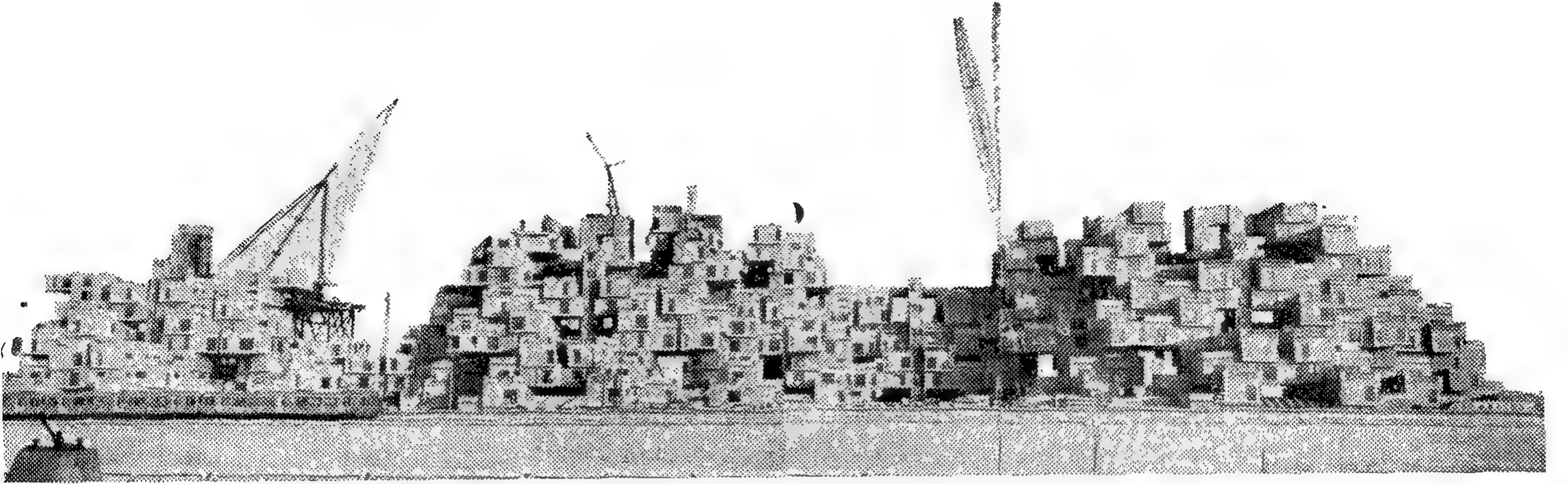
G. NASSAR

التقدم التكنولوجي واثره على العمارة والمدنية والمجتمع

(١)

المعماري : توفيق أحمد عبد الجواد

The Influence of Technology on Architectural Creativity,
Town Planning & Society.
Dr. Tawfik Abdel-Gawad. Cairo.



١ - مونتريال كندا ٦٧ - الوحدات الجاهزة الصنع
بالتجميع للاسكان العصري وطريقة الميكاتنو ويسمونها
بالتكنولوجيا الحديثة في العمارة .. ؟

التكنولوجيا فوضعت بصماتها على حضارة العصر
في مختلف مجالاتها ومقوماتها لصالح العصر أو لغير
صالحه . ولما كانت العمارة هي المرآة التي تعكس
جميع تلك المتوازيات ، حيث تتأثر بشكل حياة
الشعب والمرحلة التي يمر بها والتركيب الاجتماعي
له ، فقد سجلت ذلك الانقلاب ، أو مرحلته الانتقائية
التي وصفت عمارة القرن العشرين بأنها ثورة
معمارية عكست مختلف الثورات الفكرية- الادبية
والاجتماعية والفنية .

ظهر من أعمال رواد العمارة الأربعة الكبار
الأوائل وهم : فرانك لويد رايت F.L. Wright
١٨٦٩ - ١٩٥٩ وتصويراته للعمارة التي كانت نوعية
ديموقراطية ، لو كوربوزيه Le Corbusier
١٨٨٨ - ١٩٦٥ الذي اتجه بكل قوته نحو التحول
الشامل الذي طرأ على الأشكال الخارجية للقوى
الميكانيكية أو القوى الآلية ، حيث تجسدت أمامه
النظرية التكعيبية Cubism ولتر جروبياس
W. Gropius ١٨٨٣ - ١٩٦٩ وهو أول من نادى
بتطبيق العلم والتكنولوجيا في العمارة ، والذي عمق
المفاهيم باستخدام الحديد والزجاج في العمارة ،
وتطبيق الطرق المستحدثة في صناعة مواد البناء
السابقة الصنع Prefabricated Units

— من الخيمة في الصحراء الى الوصول للقمر ..
— ومن المنقذ في الكهف الى التدفئة المركزية ..
— ومن الثقب في الحائط الى المسطحات الزجاجية .
— ومن نور الشموع الى الأسطح المضاءة .

كان الهدف دائما هو العمل على راحة الانسان
ولكن هل سيصبح الانسان شامة في هذا العصر ؟
وهل ارتاح الانسان .. ؟

● لقد سارت الحضارات السابقة على ناموس
التطور على مدى آلاف السنين ، وأسرفت وتباطأت
هذه الحضارات في تطورها على مختلف العهود ،
وسجلت العمارة هذا التطور . ظاهرة جديدة تميز
بها هذا العصر في القرن العشرين ، وهي خروج
العمارة من التطور الهاديء الى ما يمكن أن يطلق
عليه ما يسمى بالانقلاب - أي عصر السرعة
والتكنولوجيا .

انقلاب في التفكير .. ، انقلاب في الطاقة والقوى
المحركة .. ، انقلاب في الصناعة وفي التكنولوجيا
.. ، انقلاب في كل شيء حتى في علاقة الانسان
مع نفسه ومع معتقداته ، مع مفاهيمه وتقاليده .
وكما أحدث البخار انقلابا في الحضارة ، وقامت
الكهرباء بانقلاب آخر ، جاءت الطاقة العملاقة في

الحال فيما يتعلق بالمهندس المدني والانشائي والاقتصادي والاجتماعي والجغرافي وغيرهم - انشغل المعمارون بالتصميم وتركوا المدينة يتولى أمرها غيرهم - فكان هذا الارتباك والخلط وسوء التخطيط ، حتى مدارس العمارة التي كانت لها منذ عهد قريب رسالة وفلسفة وأنصار ، وكانت لكل مدرسة منها قوة ورأى في وضع الأسس والمعايير والمفاهيم في العمارة وتخطيط المدن مثل الباو هاوس في ألمانيا ، وليفربول في إنجلترا ، والبوز آرت في باريس ، وزبورخ في سويسرا ، ومدارس نيويورك وهارفارد تخلفت عن رسالتها واهتمت بالتصميم العملي . تركوا عمارة وتخطيط المدينة يتولى أمورهما المتفعون والمستغلون ، والمحترفون ، والدخلاء ، والوسطاء ، والعملاء ، وتجار المهنة فكانت هذه الفوضى المعمارية وكان هذا الارتباك المدني المروع . حتى أطلق المجتمع على طابع العمارة الحديثة - عمارة الربع قرن الماضي - استعارات مختلفة ، سماها بطابع « **علب السجائر** » Cigar Boxes وسماها أيضا **بصناديق الأحذية** Shoe Boxes كما أطلق على المجاورات والمجمعات السكنية اسم **معامل أو مصانع التفریح** .

● تكونت في مدينة لندن ، التي تتفجر مبانيها الحديثة في كل اتجاه وفي غير اتجاه جمعية تسمى « **جماعة أعداء المناظر الكثيفة** » تضع لافتاتها على المباني العالية وتصفها بأنها « **عمليات أجهاض** » أو مباني غير شرعية ، وسميت فورة البناء في لندن « **جنون البلدية** » Municipal madness

● ولأول مرة في تاريخ العمارة يتظاهر آلاف الفرنسيين في شوارع باريس يعلنون سخطهم احتجاجا على مشروعات البلدية وانقاذ باريس من المباني العالية ذات - المسطحات الزجاجية الرهيبة حيث رفضوا أن يضعوا على وجه باريس قناع شيكاغو ومائتات .

وصف « لو . كوريوزيه » المباني العالية في نيويورك وشيكاغو بأنها عمليات اعلان وشهرة لأسماء أصحابها وأنها أعمال بهلوانية والعب نارية في دنيا المال . وقال عنها « فرانك لويد رايت » - أن كانت هذه المباني العالية انتصار للهندسة فانها بالقطع هزيمة للعمارة ..

● وظهر في اليابان مذهب جديد يسمى **ميتابوليزم** Metabolism تكوينات معمارية جديدة وانشائها في الفضاء وسميت بالمدن الفضائية ، عبارة عن قوائم رأسية اسطوانية الشكل كنقط ارتكاز يحشر فيها جميع عناصر الاتصال الرأسى والخدمات ، ويتفرع من هذه الاسطوانات كوابيل

والتوحيد القياسي Standardisation . . . ميزفان درروه Mies Van der Roche عن المبني وعن مواد البناء . . كيف عاصر انتساجهم الضخم وأعمالهم المعمارية الخالدة تلك الثورة المعمارية وساروا في طليعتها ، فسجوا بذلك ما يمكن أن يسمى بطابع أو طراز القرن العشرين .

● ان التطورات السياسية في مختلف أنحاء العالم في هذا القرن فرضت مطالب واحتياجات ثورية لحل مشاكل المجتمع أو عمارة المجتمع لمختلف مطالبه من سكنية واجتماعية وصحية وثقافية ومختلف نواحي أنشطته الأخرى . وبذلك فرضت على المماريين وضع نظريات واساليب معمارية جديدة لكي تواجه ذلك الانقلاب ولكي تحقق مطالبهم .

ان المجتمع الاشتراكي التعاوني ، والذي هو طابع المجتمع العالمي اليوم ، لم يكن له وجود أو كيان فعلى حقيقى قبل الحرب العالمية الأولى . فالمصنع الحديث ، والمدن الصناعية ، والمجمعات السكنية التي اتجهت الى التفكير في انشاء الحي السكني بجميع خدماته في عمارة واحدة ، بل ونادى البعض الى أبعد من ذلك بانشاء المدينة بأكملها على شكل عمارة تعاونية اشتراكية واحدة ، لم تكن الاشتراكية التعاونية للثقافة أو الترفيه أو التعليم أو التموين أو التأمين الصحى . . لها وجود قبل ذلك وهو الاتجاه الصحيح الجديد الذي يحدد وضوح الرؤية لعمارة الغد ومدينة الغد .

ولكن ما الذى حدث . . ؟ حدث أن التقدم الصناعى الآلى والتطور التكنولوجى سبق التقدم المعمارى ، وظهر ذلك الشبح المخيف الذى هدد كيان المدن وهو ما يسمى بالانفجار السكانى ، ومشاكل المرور وخطاره ، سرعة النقل والانتقال ، وتآوثر في الهواء والماء والوقت وضجيج وضوضاء . . حتى فقد المرء كرامته في هذا الخضم الانسانى دون أن يشعر المجتمع به . بالدرجة التي رأينا أن شباب هذا الجيل أصبح مسلوب الايمان بحاضره ، مرعوب من الشك في مستقبله .

ويسبب التقدم الصناعى ، والتطور التكنولوجى ، وبعض العوامل الأخرى ظهر الارتباك المعمارى والكابوس المدنى على المدينة والمجتمع ، حيث لم يحدد المعمارى طريقه ، ولم يرسم للمخطط خط سيره ، ولم يضع لمهندس الطرق حدود ، وكذلك



برج نوبل/باريس ١٩٧١

● تبلغ مساحة منطقة الدفاع La Defence خارج مدينة باريس نحو ٧٠٠ هكتار ، خصص منها نحو ١٢٠ هكتار للمركز التجاري الذي يقع على المحور الرئيسى للمدينة الذى يمتد من متحف اللوفر الى الكلونكور ، ومن أفنيو الشنليريه الى الاتوال .

ويقع برج نوبل باريس Noble Tower - الموضح اعلاه - على هذا المحور مارفاعة ١٠٥ م مكون من ٣٠ طابق بخلاف ٣ طوابق قاعدة لهذا البرج .

وتعتبر باريس إحدى المدن الكبرى التى تواجه تلك المشكلة المخيفة وهى التضخم السكانى حيث أصبحت مدينة مخيفة مزدحمة ومركزا لتجمع بشرى رهيب . لذلك تتم دراسات جادة مختلفة على أساس تخفيض نسبة عدد سكانها وتخطيط ضواحي باريس وخلق مناطق تجمعات جديدة فيها . ومنها « مشروع الأحزمة المشقة » ، « مشروع المدينة المتوازية » . ومشروع « باريس تحت الأرض » وغيرها وكما يصفها ابتاؤها من المعماريين الكبار بأنها « مدينة يعوزها الدفء وتنقصها الروح والحياة .. » لابد اذن من اعادة الحياة اليها ، لان المدينة ماهى الا كائن حى مهدد بالتآكل والانقراض اذا مادب الفساد الى اى جزء من اجزائه . لابد اذن من القاء مغناطيس على الاحياء والمناطق التى فقدت حياتها لتجمع أنسجتها وربط أوردتها وشريبتها لاعادة الحياة اليها .. بالعلم والتخطيط والعمارة .

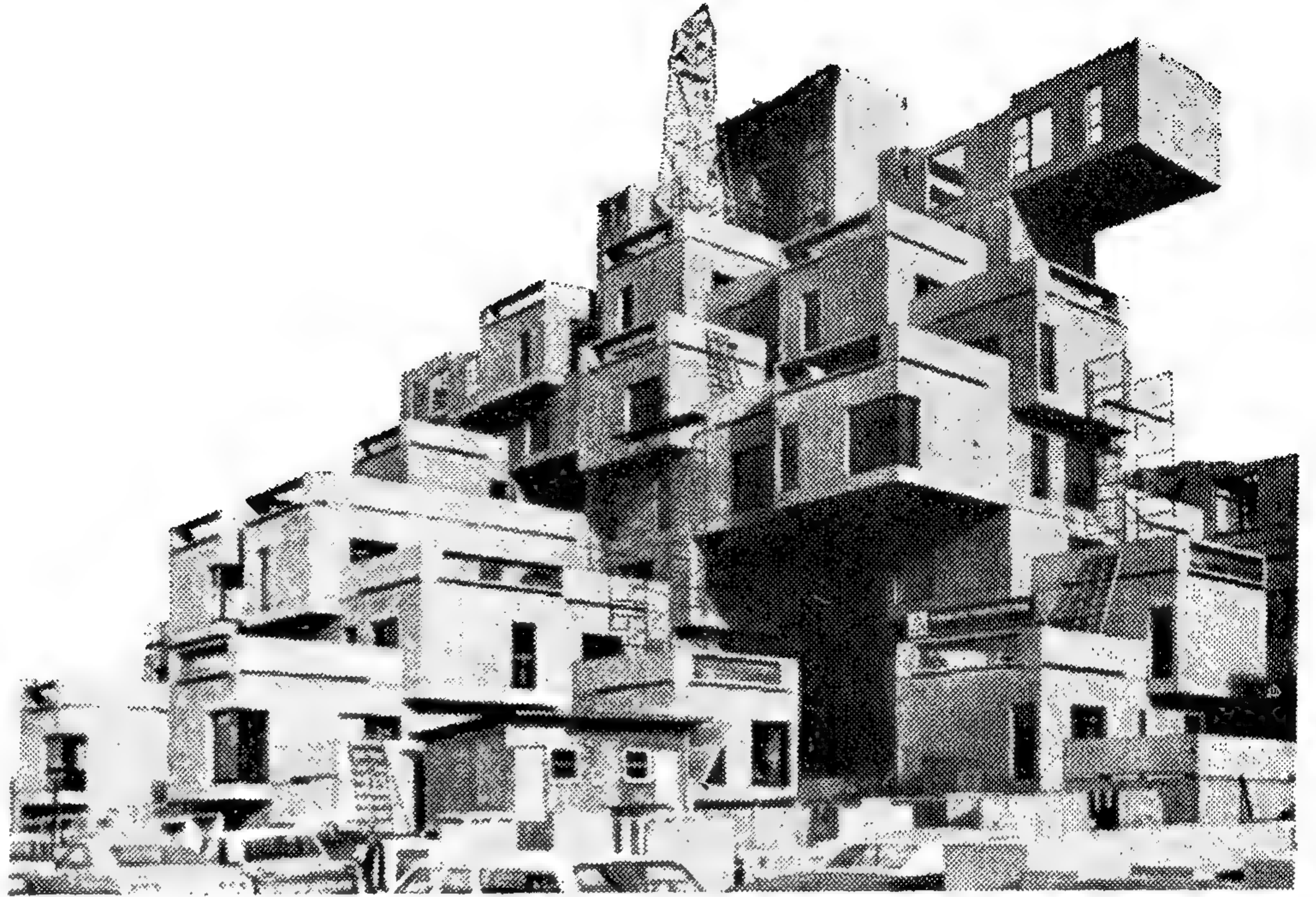
تحمل المكاتب الادارية أو الوحدات السكنية على شكل شجرة وذلك لاختلاء سطح أرض المدينة للسيارة

وبسبب التقدم التكنولوجى فى مجال البناء والانشاء والتعمير وجدنا ان بعض عواصم المدن الكبرى هربت من حل مشاكلها وحددت مناطق الامتداد الجديدة المطلوبة للملاحقة هذا التطور وشيدت المباني فوق مياه البحر أو مياه الخليج مثل سيدنى وروتردام وأمستردام وطوكيو ، أو بالبناء تحت الأرض - وكأن هذا العمل ليس معناه دفن الأحياء مثل ما حدث فى باريس وتورنتو ومونتريال .

● ومن خلال دراستنا لتاريخ العمارة على مر العصور حتى منتصف هذا القرن ومن خلال تدريسنا لهذا التاريخ فاننا لم نصادف حتى الآن طبعا من الخيال يشبه فى طرافته أو ايلامه أو ارتبائه أو فتنته ما يظهر الى الوجود فى عواصم مدن العالم اجمع . اننا نرى فى مدينة القرن العشرين خلط معمارى ومدنى ، وفوضى تخطيطية وفنية غير مألوفة - ويقال انها التطور التكنولوجى ، أعمال لا تمت بصلة الى البيئة من حيث الموقع والمناخ ، غير متناسقة مع مقتضيات البيئة الأساسية وظروف الاجتماعية والقيم الحضارية ، هزيلة من الناحية الفلسفية والعملية والوظيفية والفنية . من المسئول عن هذا .. ؟ الجواب هو بالقطع المعمارى ، الذى سمح للالة أن تنتصر عليه وتستعبده بعد ان كانت هى عبدا له . المعمارى الذى نسى الحقيقة وهى ان العمارة تولد ولا تصنع .

لقد حاول الجيل السابق قطع علاقته وارتباطه بالماضى وطرزه ، ونحن حططنا تلك القيود التى فرضت على التصميم المعمارى وتخطيط المدن . واليوم ونحن فى حيرة من المستقبل وبعد ان حررنا العمارة من قيود الماضى وخلقنا عمارة حديثة نجد أنفسنا نعيش فى كابوس مدنى كثيف مخيف ينتشر حولنا فى كل اتجاه . يحاول هذا الكابوس أن يجرنا ويسجننا فى مركزه . ومن داخل هذا الكابوس ننظر حولنا لنبحث عن ثمرة الحرية التى حصلنا عليها بصعوبة كبيرة .

والسؤال هنا هو ، هل ستصبح المدن فى عالمنا الجديد مأجاً للانسان الساعى للحرية .. أو انها ستصبح أداة طغيان جديد ومصدر قلق وارهاق لهذا الانسان ؟



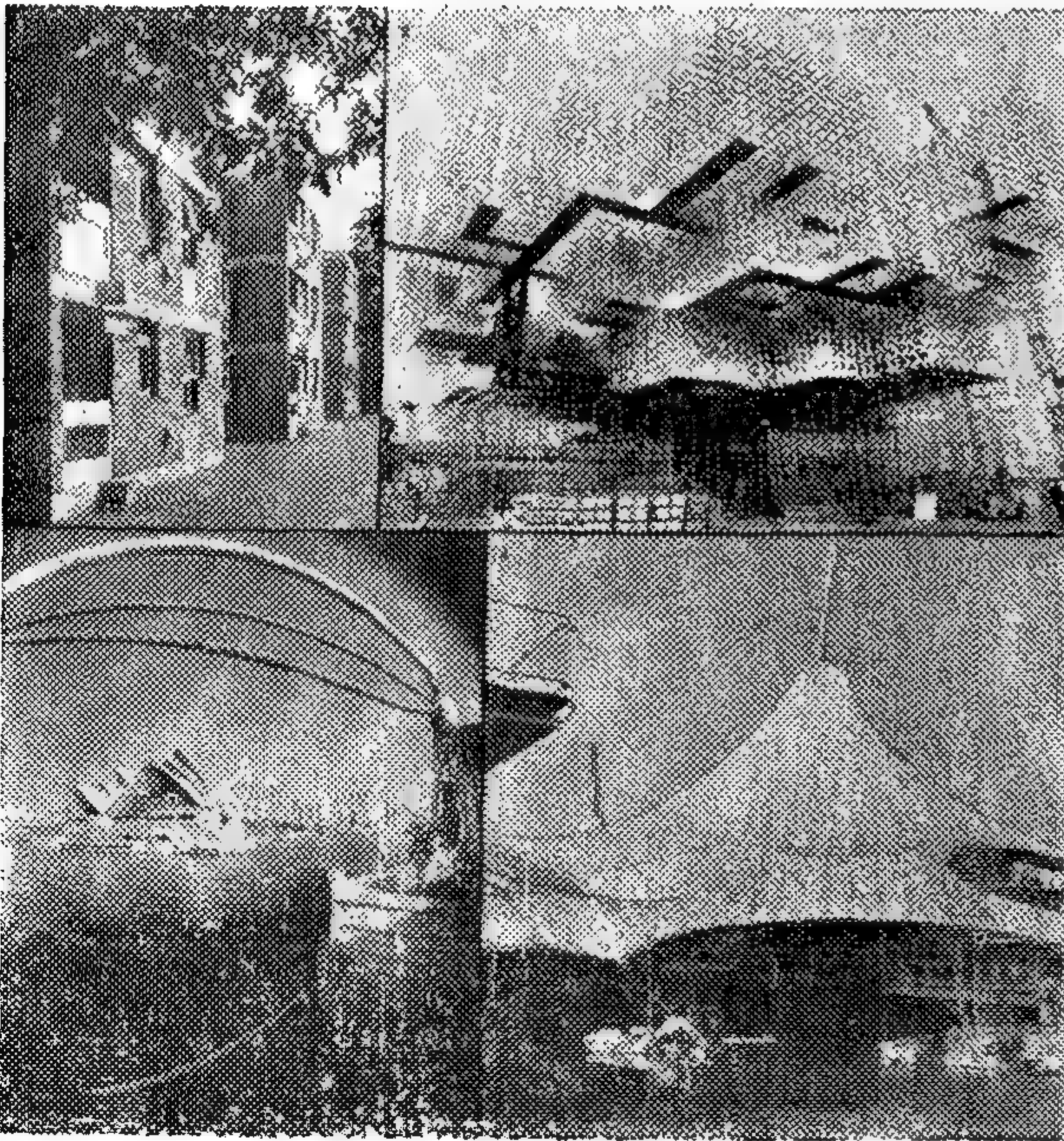
٣ - يمين : اسكان ٦٧ مونتريال
كندا

٤ - أسفل : مساكن « هام كومن »
انجلترا ، أوبرا سيدني استراليا ،
جناح معرض سويسرا ١٩٧٠ ، جناح
معرض المانيا ١٩٦٧

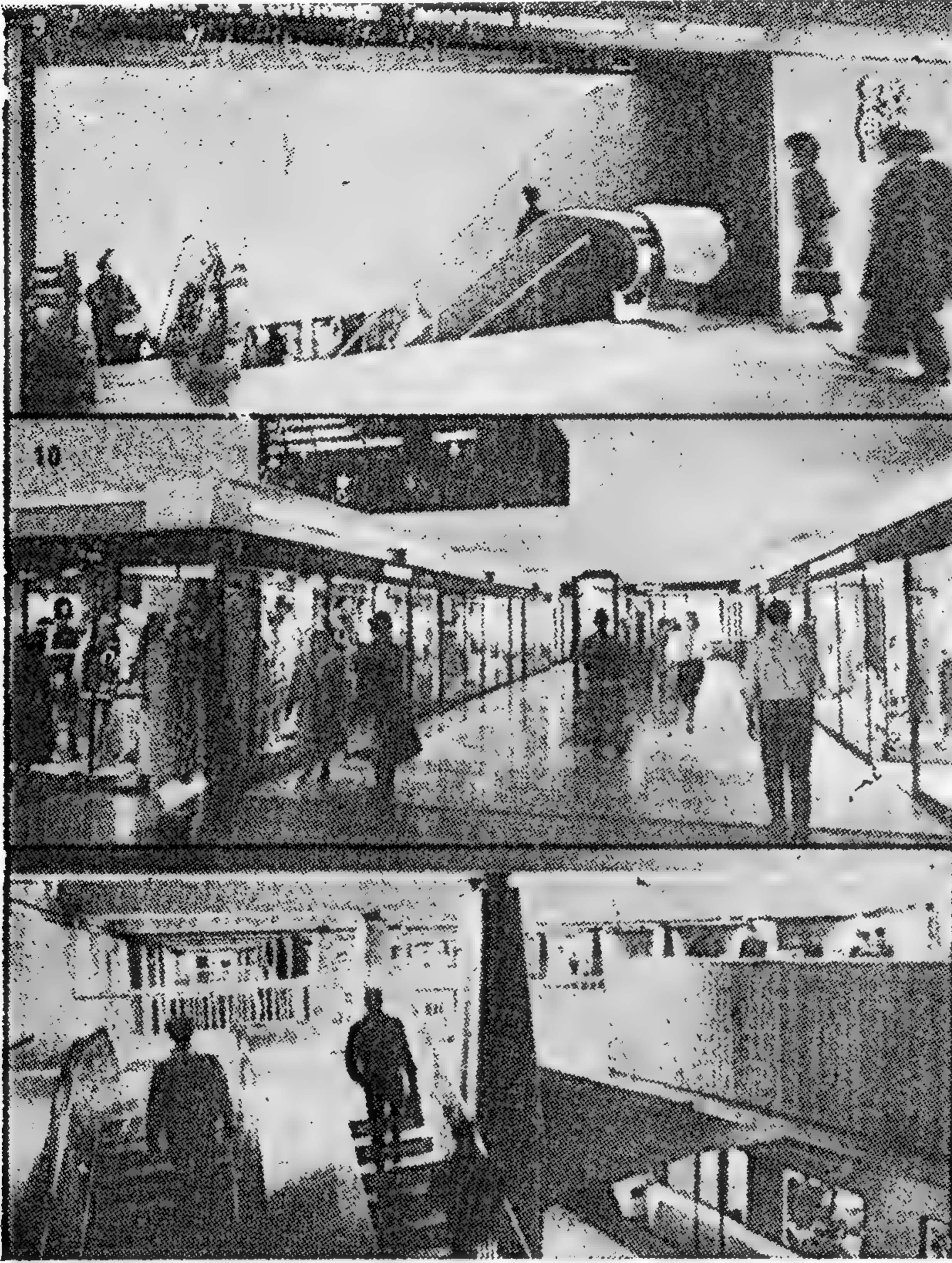
● العمارة الحديثة تطور ثوري :

نطرح سؤالاً على جانب كبير من الأهمية وهو :
ما هي العمارة الحديثة ، Modern Architecture
وما هو رأى الشعوب فيها ..؟ ولماذا تعنى كلمة
« العمارة » عند الكثير من الناس حتى اليوم انها
مفهوم لمسجد هام أو كاتدرائية أو مبنى تذكاري
Monumental .. ولا تدل هذه الكلمة «العمارة»
أو هذا التعبير على السكن أو الوحدة السكنية التي
يعيش الانسان فيها .

اعتقد أن السبب في ذلك يرجع بأنه لا يزال حتى
الآن معظم سكان العالم يعيشون حياة بدائية ، رغم
انتشار التطور العلمي والتكنولوجي الحديث ،
ولا تختلف حياتهم كثيراً عن حياة أسلافنا سكان
المغارات والكهوف . حيث لدينا القليل جداً من
وسائل التحكم على مساكننا الحالية مثلهم ..
بالدرجة التي تحاول أن نختار المسكن ضمن اطار
مجموعات أخرى من الشقق التي يبنها تجار هذه
المهنة أملاً في توفير عامل الامن على هذه الصورة .
تماماً مثل الطيور التي تبنى أعشاشها متجاورة على
أعلى الشجر لحماية نفسها وفقسها ، محاولين أن
نجعل من هذه العلب السكنية أماكن صالحة للمعيشة
بوضع محتويات الأمتعة حولنا ، باحثين عن متطلبات
وفاء الحياة التي نهتم بها ، وخاصة من الناحية
الاقتصادية في حين أنه لا تهتمنا القيم المعمارية .



● أطلق المجتمع على عمارة العصر الحديث استعارات
مختلفة : سماها أحيانا بطابع «علب السيجار» Gigar Boxes
وأحيانا آخر « بصناديق الأحذية » shoe Boxes ، كما
أطلق على المجموعات السكنية الحديثة «معامل التفريخ البشرى»
أو أبراج حمام المجتمع الانساني أو « معتلات العصر الحديث »
أو « خرائب الاسكان العصري »



● تخطيط وتحسين مراكز المدينة تحت الأرض

علم جديد ودراسة حديثة لتخطيط وتحسين مراكز المدينة تحت الأرض محطات السكك الحديدية، محطات المترو، محطات السيارات، المراكز التجارية، المطاعم والمقاهي وأماكن الترفيه - الخدمات الثابتة مثل مواقف الانتظارات بمختلف أنواعها، المخازن - إلى غير ذلك من الخدمات اللازمة للمدينة ..

هذا الفرع الجديد من العمارة الحديثة ليس المقصود به دفن الإسكان المدني تحت الأرض، ولكنه في الواقع هو نقل هذه المنشآت من سطح المدينة إلى منسوب سفلى كالساحر وصلات العرض والأسواق التجارية والمخازن وغيرها لخلق أماكن متسعة على سطح المدينة لاستغلالها بصورة أفضل في إطار مشروعات تخطيط المدن الكبرى وخاصة في المدن التي تعزى بتراتها وثرواتها التاريخية الأصلية مثل باريس وروما ولندن والقاهرة . وبذلك يمكن أن نمنع تلك الصور الهزلية والمناظر المؤذية المشوشة والفوضى والهرجلة التي تظهر الآن على سطح الأرض في المدن القائمة والمدن الحديثة .

ورجال المال والاقتصاد والمشتغلين في صناعة مواد البناء وطرق الإنشاء، وتنشر هذه الأسئلة في الصحف والمجلات، وتناقش هي والإجابات عنها في ندوات تعقدها الجمعيات التخصصية وفي مؤتمرات هندسية على المستوى المحلي والدولي بين المؤيدين والمعارضين بين المتفائلين والمتشائمين، بينما تسير عجلة البناء وتدور في سرعة مذهلة .

هل يجب أن يكون الوضع كذلك ..؟ يجب المعماري ويقول لا .. لأن العمارة الحديثة التي ترتفع حولنا اليوم في مدننا القديمة والحديثة ما هي إلا تطور ثوري بالمعنى التكنووجي في مجال استخدام طرق إنشاء جديدة للمباني ومواد بناء مستحدثة - الحديد والخرسانة والزجاج والبلاستيك وغيرها - ويقول المعماري أيضا أن العمارة الحديثة تطور ثوري في مجال آخر . فعند القرن التاسع عشر اثبتت لنا العلوم الاجتماعية والاقتصادية والسيكولوجية أن

وهل فكر الإنسان الذي يسكن ويعيش في هذه المباني الجديدة في صلاحيتها ونوعيتها وملاءمتها للحياة العصرية .. والتي تقام هذه المنشآت الضخمة حولنا كل يوم في جميع مدن العالم .. في لندن وباريس وبرلين وطوكيو والقاهرة .. هل فكرنا في أنها ربما تكون هذه المباني انذار بالحكم بالاعدام على هذه المدن نتيجة لازدحام السكان المروع ..؟ هل لاحظنا أن بعض هذه المباني العالية جيد وبعضها رديء؟ هل لم نلاحظ أن هناك مبنى يدخل على نفوسنا السرور والآخر تضيق به النفس عند رؤيته وما أكثره؟ لقد ظلت العمارة دائما في الماضي وستظل في الحاضر والمستقبل هي المرآة التي تعكس الحضارة والمدنية والتقدم، وتعبر عن احتياجات الإنسان ومطالبه وتفوقه وطموحه . فما هو الرأي إذن فيما يقام حولنا من هذه المنشآت في هذا العصر؟

ويضع هذه الأسئلة كثير من المعماريين والمخططين

التكنولوجى وبسرعة الانشاء . ولكن من المحتمل جدا ، ما لم يحدث من التطورات الغير منظورة ، أن تستمر الطرق التقليدية فى البناء كدالة لها أهميتها ومغزاها ، ولكن ليست كجزء فى المسرح البنائى .

والسؤال هنا هو : هل من الممكن وجود تطورات مشهدية منظرية على المسرح البنائى ؟ يعتقد البعض أنه من الممكن ، وخاصة شباب المعمارين الذين يرحبون بالانتاج الصناعى بالجملة فى المباني ويأملون فى توسيع نطاق هذا الانتاج الآلى الذى بدأ منذ بداية هنرى فورد ، وتطبيقه فى المباني بطرق هندسية سفسطائية كالتى ظهرت فى المجالات الهندسية الأخرى ، وكانت نتيجة تفكيرهم على هذه الأسس أن أخذت المباني شكل الانشاءات الحديدية الضخمة المشابهة لتلك التكوينات والتركيبات البتروكيميائية .

وربما نجد أن أقرب الأمثلة التى تشير الى هذه الخطوة المترددة نحو المستقبل هى تلك المشروعات الضخمة لملاصكان اتى بنيت مؤخرا فى مونتريال وفرانكفورت واليابان وميلانو وغيرها . ومن المؤكد أن الكثير يفضلون السكنى فى المباني الحالية القائمة على السكن فى هذه المجاورات السكنية الحديثة برغم ما بها من معدات مستحدثة . ان حلم التكنولوجيا هو أن يرى بأن جميع الاحتياجات الانسانية يمكن الحصول عليها بالضغط على زر . ولكننى أشك فى أن التكنولوجيا سوف لا تحقق المتطلبات الأساسية للحياة اليومية الطبيعية . وان حققتها اليوم فى بعض الظروف فنجد أنها تتطلب من النفقات الشئ الكثير التى لا يمكن توفرها الا لرؤساء مجالس إدارة المؤسسات والشركات الرأسمالية فى العالم . ومن حسن الحظ فانه يوجد الان الكثير من التطورات الحديثة الأقل مظهرية ، وهى التى ظهرت نتيجة لقدرتنا على التحكم فى البيئة الداخلية لمبانينا على أحسن وجه لم يسبق له مثيل . وهذه التطورات هى التحكم فى تكييف الهواء ، والاضاءة الصناعية ، والاتصال الداخلى بالمصاعد الكهربائية الرأسية والأفقية ، ولو أن الأخيرة لم يتم انتشارها بعد ، توضح هذه الطريقة فى قدرتنا على التحكم ان تاريخ العمارة يمكن رؤيته كانه امتداد ثابت لمقدرتنا على المحافظة لتوفير الراحة لأنفسنا بمثل هذه العوامل والخطوات الغير مظهرية .

فالحالات الطويلة من نار الموقد فى الكهف الى التدفئة المركزية وتكييف الهواء . . ومن الثقب فى الحائط الى المسطحات الزجاجية ووسائل التحكم فى الاضاءة ، ومن نور الشموع الى الأسقف المضاء . تمت كلها بخطوات متتلة ناجحة نحو حياة أفضل ونحو راحة الإنسان .

الإنسان هو حصيلة ونتاج المجال الذى يعيش فيه كما انه نتاج والديه . فاذا كان الإنسان هو حصيلة جزئية للمجتمع الذى يعيش فيه ، فان تحسين البيئة بالطبع تحسين للإنسان ، وتحسين الإنسان معناه تحسين المجتمع . وتقف هذه المعدلة الصعبة وراء العمارة وتخطيط المدن فى القرن العشرين .

وسواء اكانت هذه الحقيقة التى تتسم بالبساطة واضحة ام غير واضحة ، فاننا متفقون تماما ان المساكن والمدن فى عصرنا الحالى فى حالة سيئة . فقد امتدت كثير من المدن فى اواخر القرن الماضى تبعا للامتداد الصناعى على غير أسس تخطيطية سليمة . ولان الامتداد الصناعى يسبق الامتداد العمرانى والتخطيطى ، وهذا خطأ وقعت فيه كثير من المدن ، ويعاد اليوم بناء هذه المدن . حتى ولو تم ذلك فنرى ظهور مشاكل جديدة منها مشاكل النقل والمواصلات ، وتتجسد هذه الأسئلة الصعبة التى تواجه المعمارى والمخطط فى هذا العصر ، ويحاول كل منهما الاجابة عنها وهى : كيف واين نعيش او يجب ان نعيش فى هذه المدن . . وما هى نوع او أنواع الخدمات التى يمكن توافرها لنا . .؟ كيف يمكن الوصول الى مقر العمل . . الى المدرسة واجامعة . . الى المركز التجارى والمالى . . الى النادي الرياضى او أى مكان للترفيه فى المدينة . .؟

ولكن فى الواقع نرى ان القضية هى قضيتنا على مستوى المجتمع كله . ولذلك يجب توسيع قاعدة المعرفة فى هذا المجال الحيوى . يجب نشر وتوضيح وعرض مقدمات ومقتطفات لأراء بعض رواد العمارة - لوكوربوزيه ، فرانك لويد رايت ، ولتر جروبياس ، ميزفان درروه ، سارائين ، ياما ساكى . . وغيرهم فى حل مشاكل التعمير وتخطيط المدن .

● الانتاج بالجملة Mass Production

نحن متفقون تماما أن أهم ظاهرة مميزة لهذا العصر التى نتجت عن استخدام التكنولوجيا فى مجتمعنا الحديث هى الانتاج بالجملة Mass Production فى مجال صناعة مواد البناء وطرق الانشاء . حتى وطرق الانشاء . حتى رأينا مثلاً انه امكن طلب انشاء مئات المدارس وآلاف المساكن بالجملة طبقا لرسومات ونماذج معدة لذلك ، بالرغم من ان طرق انشائها أكثر كلفة من الطرق التقليدية التى اثبتتها التجارب حتى الآن .

انقسم المعمارين فى هذا المجال الى فريقين . الأول غير راض عن هذه الطريقة وهى « طريقة الميكانو » فى العمارة ، والفريق الثانى يرحب بالتأكيد

استعملوها بينما كانوا يبحثون عن نظرية أو قاعدة جديدة . وبظهور الاتجاهات الحديثة في العمارة التأثرية

Cubists والتكعيبية Impressionists

وعماراة المستقبل Futurists ظهرت تصورات وأفكار تفهم جديد الحقيقة بصرية للمنظور للمبنى أو المدينة أو الحي فكانت العمارة التأثرية تختص بتأثير الضوء في المبنى بالإضافة الى التكوين الغير متمائل Informal ، والتكعيبية بالشفافية والتكوين والتغير الاجتماعي .

تابعت العمارة حينئذ حركات التطور واندمجت في اطارها وظهر أسلوب جديد في المباني باستخدام التكنولوجيا في الحديد والخرسانة والزجاج، ونظرية جديدة في التكوين والتركيب المعماري وبدأت عمارة القرن العشرين عمارة رمزية ، وتجربة تعليمية مهيبة . ولكن منذ الحرب العالمية الثانية بدأت العمارة تفقد هذه الظاهرة ظاهرة الاحترام والأدب والوقار في الانتاج المعماري في معظم أنحاء العالم ولم تسجل هذه الأعداد الضخمة من المباني التي أنشئت أسماء آلاف شباب المعماريين واختفت في سجل النسيان لأن -الوقار والأدب والاحترام يحدد الفرق بين المبنى الجيد والمبنى الرديء .

فالزيادة المستمرة الواسعة النطاق في انشاء المساكن للطبقات المحدودة الدخل وغيرها والمساحات الشاسعة التي تشغلها هذه المساكن تهدد خطر على البيئة والمجتمع . وتزداد المدن في توسعاتها نحو الريف بطرق مرتجلة رغم أنف مخططي المدن والمعماريين ، ويتم البناء بواسطة المستقلين والمتفعين والمحترفين ومهندسي البلديات وتجار المهنة .

فأول خطوة للقضاء على هذه المشكلة وحلها هي عزل هذا المحترف أو ذلك المتفع والمستغل من التحكم في البناء أو التخطيط ، يجب أن تصمم المباني بواسطة معماريين مؤهلين ، وأن هذه المباني يجب أن ترقى الى مستوى عال من الأدب والوقار والاحترام . وعلى هذا الأساس يمكن أن تعالج وتحل جميع المشاكل الكبرى الأخرى المتعلقة بالبيئة والمجتمع ، وبدونها سوف لا يمكن الوصول الى حل مشاكل المدن سوى القليل جدا منها .

تطورات العصر الحديث فرضت إعادة النظر في نظريات العمارة وأسس التصميم وشروط التنفيذ والتخطيط العمراني على أسس إنسانية . . ولكن هل اتبعت هذه الأسس ؟ كان التطور الصناعي والتطور التكنولوجي أسرع من التطور المعماري والتخطيط العمراني .

● النظام المرئي وعدم النظام في العمارة وتخطيط المدينة

Visual order & disorder in Architecture & Town Planning.

ان الشيء الوحيد الذي يميز الانسان عن سائر الحيوانات هو قدرته على الابتكار والابداع وخلق النظم . ومن هذه القدرة في تعريف الأشياء وتسميتها يمكنه تصنيفها وترتيبها الى عديد من الأنواع والفصائل . وبمجرد معرفة الشيء ، طائر أو وردة مثلاً ، ففي مقدورنا أن نخصص الصفحات لتسجيل عادات هذا الشيء ونحدد نقط ضعفه وقوته ونشرح للناس كيف تؤيد الحكم وكيف نتحكم في التعريف على هذه الأسماء .

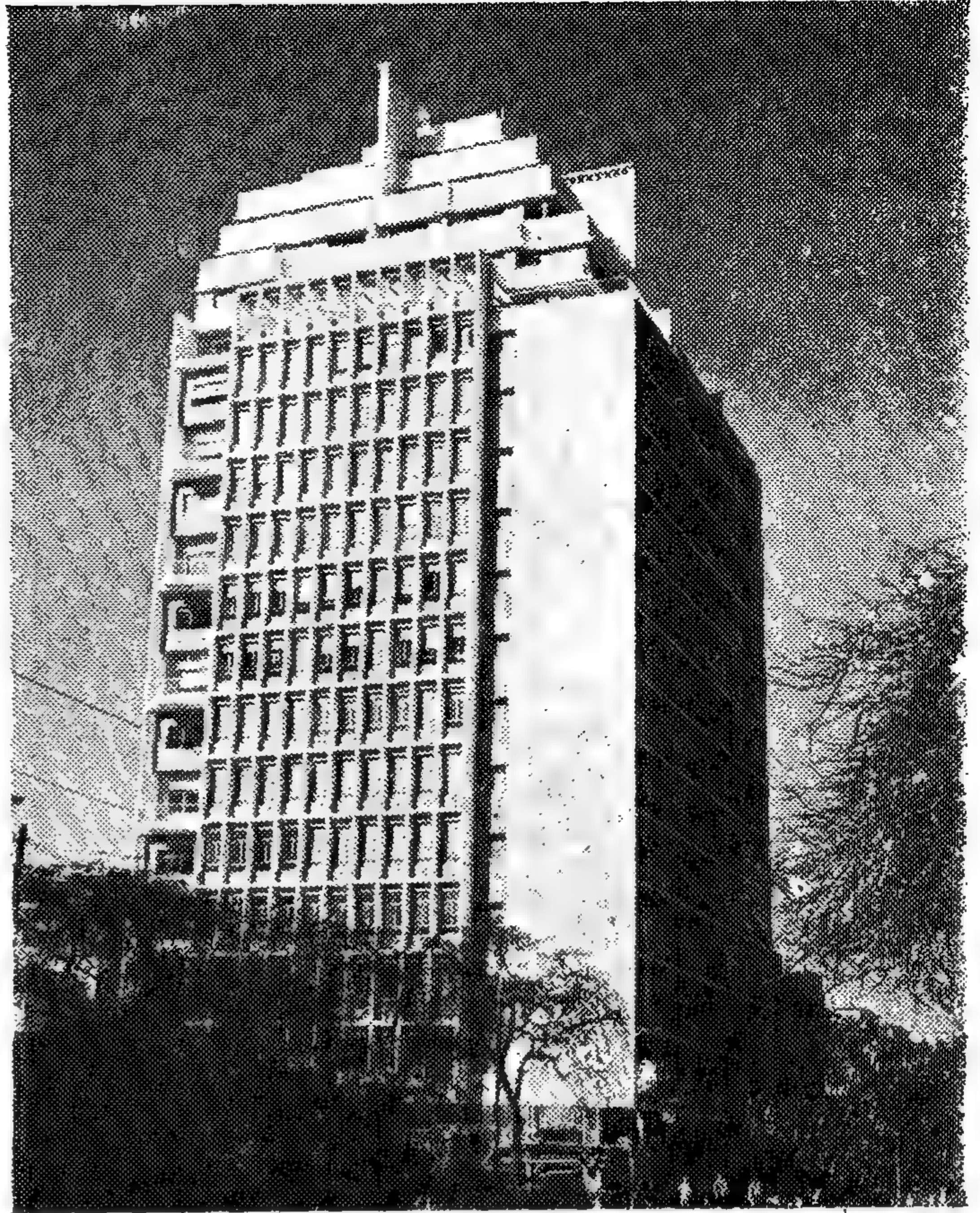
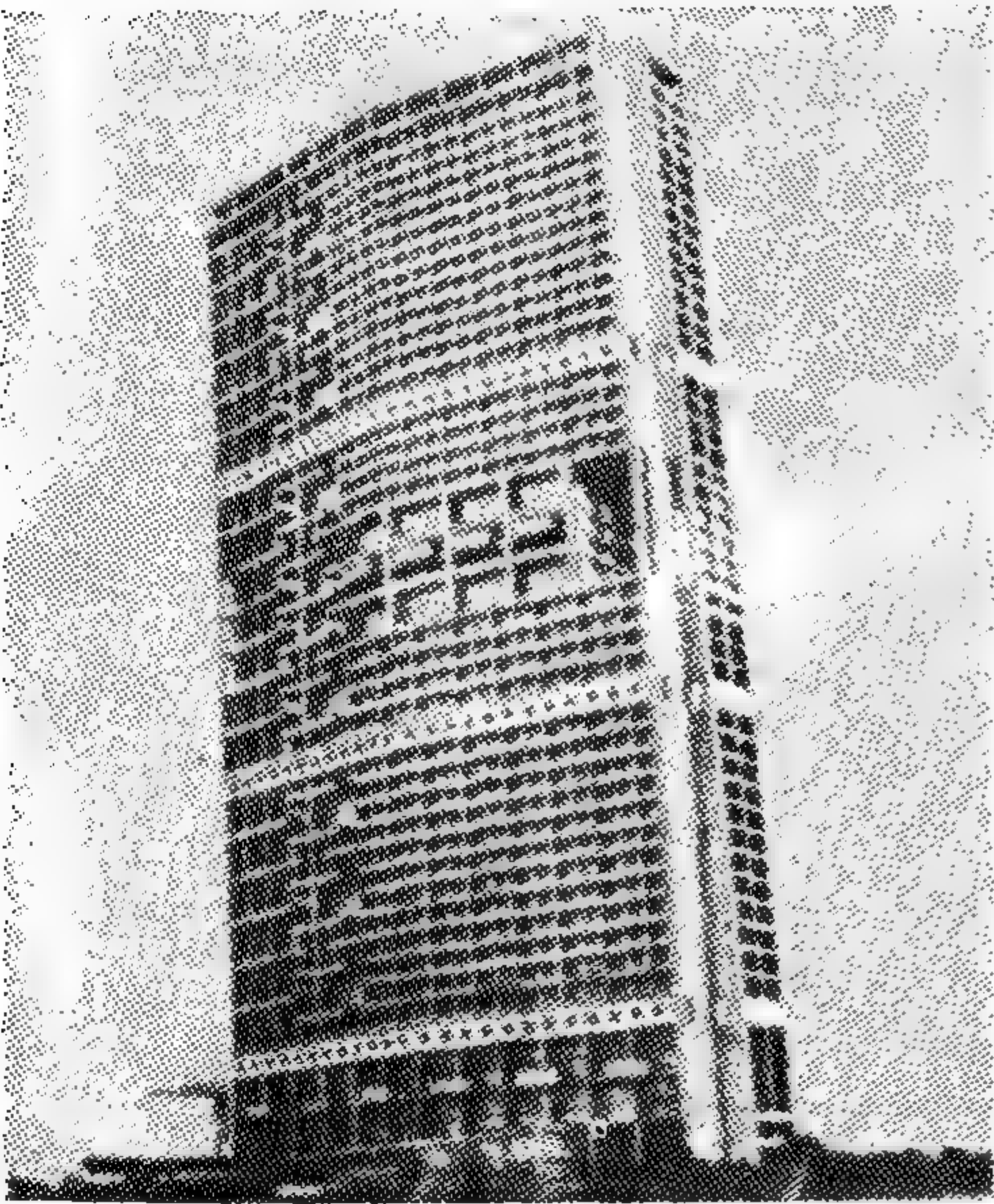
هناك نوعان من المعرفة : معرفة عامة أو عادية متفق عليها ، وهي التي تعكس العلم العادي المؤلف لدى الجماهير ، ومعرفة تخصصية ، وهي التي تتعلق وتختص بالدين والعلوم والفنون والآداب والحرف والصناعة . فهناك اذن معرفة أو علم مؤلف أساسه الأشياء المنظورة ، ومعرفة أو علم خفي أو مستقر أساسه الأشياء المعروفة ، والمعرفة المستترة تنتشر تدريجياً في الثقافة العامة . مثلاً : يعرف الجمهور بصفة عامة ما هو المنظور Perspective ، لأن تأثيره يمكن ادراكه والشعور به بمجرد أن تكون العين مستعدة له وبمعرفة متقنة ، ومع ذلك فقد أصبح معرفة المنظور الآن جزء من الثقافة ، ولذلك نرى الأشياء الآن في المنظور ونهتم بها أكبر الاهتمام . ولكن من الواضح ان معرفة طريقة رسم المنظور للمبنى أو لمنظر عام لموقع ما يحتاج الى معرفة متخصصة على أساس الايزومتري الهندسي والنظام الحسابي . وهناك طرق أخرى أكثر دقة استخدمها القدماء في نظرياتهم لعمل المنظور على أساس حسابات هندسية وعلاقات بين اعداد بسيطة لها علاقة وارتباط بنظريات فلسفية وأخرى دينية . وعلى هذه الاسس أنشئت أروع الآثار المصرية القديمة الفرعونية والافريقية والرومانية . هذه الاسس التي نعرف القليل عنها تتعلق بنظرية النسبية في العمارة والعلاقة بين الأرض والمعد والالهة .

ولكن نلاحظ في القرن الثامن عشر ان هذه النظرية قد ازدادت تعقيداً وأصبحت غير واقعية واختفت بظهور الثورة على الطرز الكلاسيكية وانتشار الحركة الرومانسية .

وام يجهل الفنانون والمعماريون هذه النظريات في القرن التاسع عشر والقرن العشرين ، ولكنهم لم يتمكنوا من مشاركة قواعد القرن السادس عشر الدينية والفلسفية وعدم احترامها ومع ذلك فقد

٦ - يمين : برج الزمالك بالقاهرة للمعماري
الدكتور سيد كريم

٧ - أسفل : برج الجزائر للمعماري ل .
كوروبونيه .



● الجدية والوقار واحترام ..

أمثلة معمارية جادة تعبر بصدق عن كيفية استخدام العلم والتكنولوجيا في خدمة العمارة لتحقيق الوظيفة والغرض والجمال. .. أمثلة تتسم بالوقار والأدب والتعبير والشخصية ، وتنسجم مع الواقع والحاضر ، وتعيش مع البيئة والمجتمع في توافق تام .

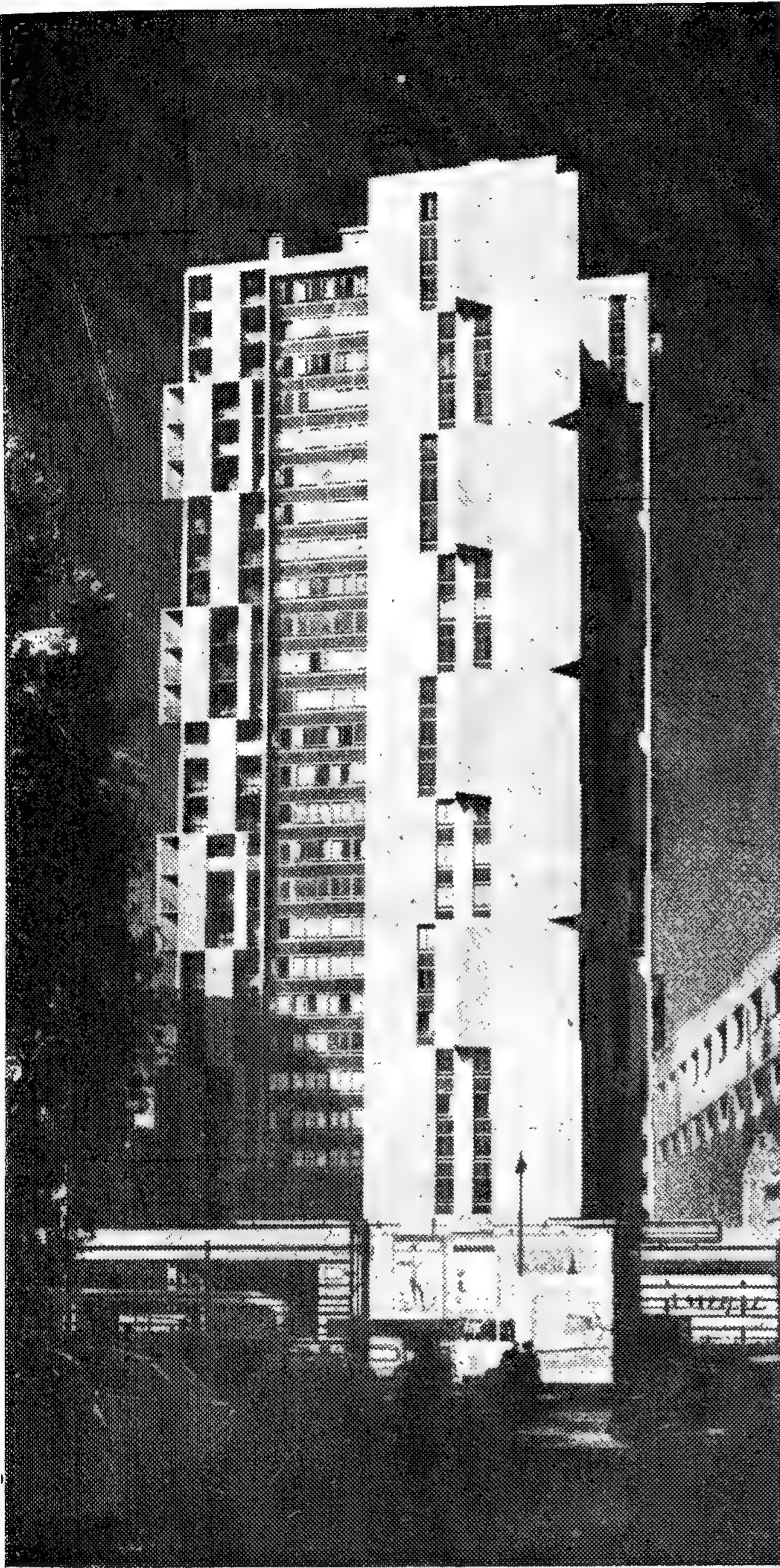
الدراسة العلمية والهندسية حينذاك الا انه اتضح فيما بعد ان ظهرت الكثير من العيوب والاختفاء في هذه التخطيطات والتي كانت تنقصها الخبرة العلمية والاجتماعية والنفسية والثقافية .

وبعد انتهاء الحرب العالمية الثانية - ١٩٤٥ برزت مشكلة تخطيط المدن بصورة أقوى لاعادة تخطيط المدن التي دمرتها الحرب وزادت أهمية التخطيط على أساس البحث والدراسة الدقيقة لوائح المجتمع للحصول على أحسن وأفضل النتائج للوصول الى مستوى حياة أفضل . وقبل ان ينتهي المخططون من دراساتهم ومشروعاتهم وبدء بالفعل في تنفيذ البعض منها فوجئوا بضرورة إعادة النظر في هذه المشروعات على أسس حديثة مختلفة تتماشى ومتطلبات العصر وسرعة تقدمه .

تطور سريع في الصناعة .. زيادة مخيفة مذهلة في السكان ما يسمى بالتفجير السكاني ، نمو كيفي

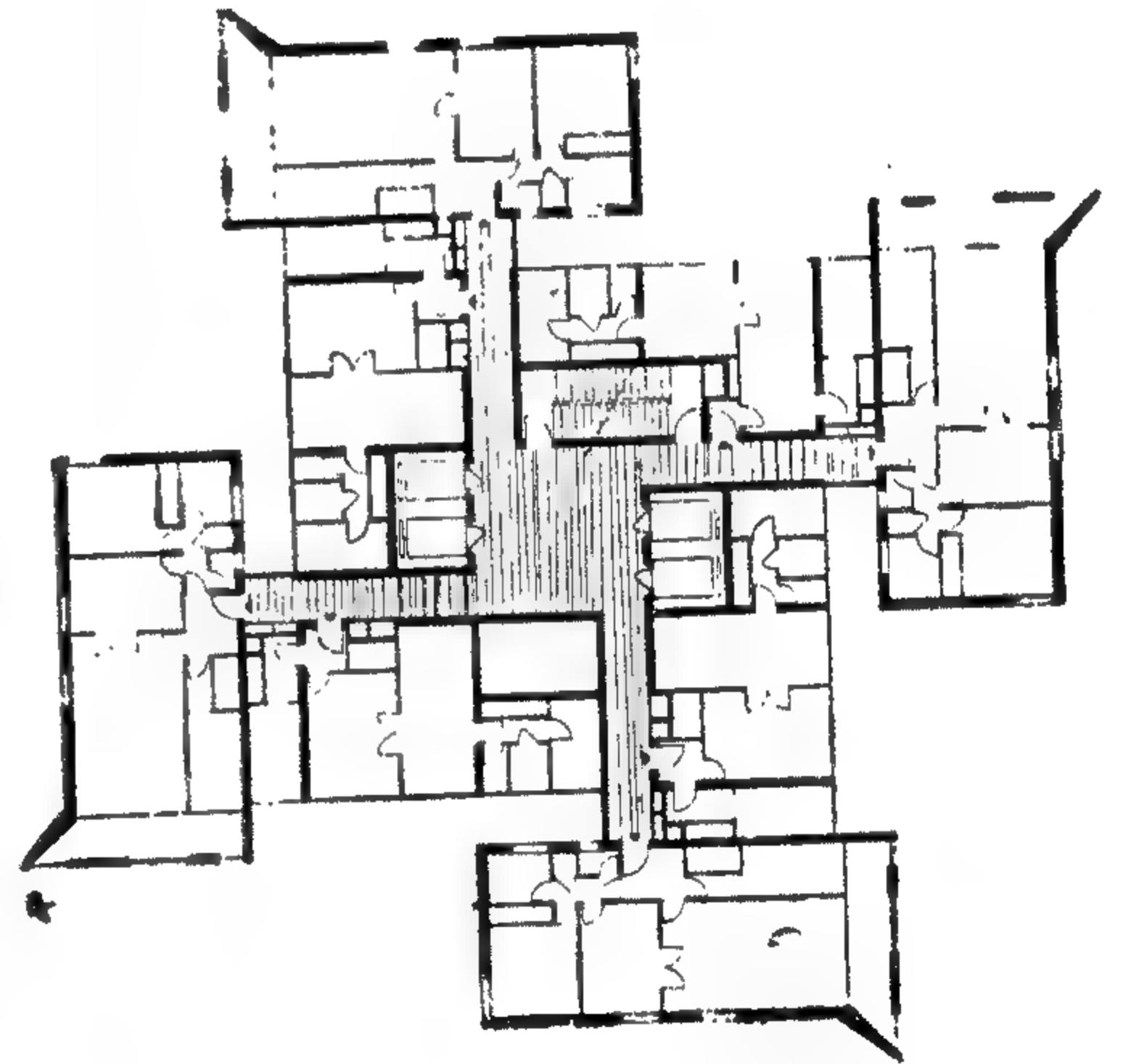
● **المدينة المثالية** هي وسيلة لقيام المودة ، فخير نظام للمدن هو ما يقوم على العناية بسكانها وتحضرهم فالمهمة الرئيسية للمدينة انى جانب توفير الوسائل لأوجه الأنشطة اليومية هي تحويل القوة الى نظام ، والطاقة الى حضارة ، والمادة الجامدة الى رموز حية للفن ، والتكاثر البيولوجي الى قدرة اجتماعية خلاقة « أو بعبارة أخرى تنمية تراث الحضارة ونقله من جيل الى جيل ، وكذلك نقل موارد الحضارة الى أصغر الوحدات الحضارية مما يؤدي الى وحدة العالم وقيام التعاون بين أرجائه .

لقد ظهرت أهمية التخطيط بصورة ملحة بعد الحرب العالمية الاولى مباشرة ١٩٢٠ وأعيد تخطيط الكثير من الأحياء القديمة في مدن متعددة في أوروبا ، هذا فضلا عن تخطيط وبناء ضواحي حديثة لمدن متصلة أو منفصلة . وعلى الرغم من أن مشروعات التخطيط والتصميم كانت على جانب كبير من



● مجموعة فلاندرز السكنية/باريس ، تصميم المعمارى أنجير ١٩٦٧ تقع هذه المجموعة السكنية فى شارع فلاندرز : باريس وتتكون من برج سكنى بارتفاع ٣٠ طابق يحتوى كل منها على ٨ شقق سكنية .

خطوط مستقيمة جادة فى المساقط الأفقية والوجهات ، فى الفراغ وفى الحجم . علاقة أكيدة صريحة تجمع بين الموقع والمبنى . اتجاه محدد بأسلوب لطابع معمارى يعبر أصدق تعبير فى كيفية تطبيق العلم والتكنولوجيا فى العمارة الحديثة ، عمارة القرن العشرين .



٨ - أعلا : المسقط الأفقى للدور المتكرر للعمارة .

٩ - يسار : منظور عام لبرج فلاندرز السكنى

بأساليب ديناميكية معاصرة لبناء مجتمعات حية نخلقها من التخطيط المستوحى من واقع المجتمع الحالى المتفاعل مع التطورات السريعة المستمرة حاضرا ومستقبلا .

ان معظم الحلول التى وضعت والنظريات التخطيطية التى اتبعت كانت كلها لحل مشاكل مدن معينة مرتبطة بزمان معين وعوامل تأثيرية محددة معينة . اننا فى الواقع نواجه فى هذا العصر الحديث - عصر الالة - مشكلة من أعقد المشاكل وهى إعادة

للمدن القائمة .. مشاكل المرور وخطاره .. ظهور الأحياء الغير صحية .. سرعة النقل والانتقال .. انتشار المصانع بصورة مبعثرة هنا وهناك .. نزوح سكان الريف الى المدن بصورة مستمرة سعيا وراء الرزق أو حياة أفضل .. تلوث فى الهواء وضجيج وضوضاء .. الخ مما أدى الى توتر أعصاب سكان تلك المدن وسلبهم راحتهم وصحتهم وشخصيتهم حتى فقد الفرد كرامته فى هذا الخضم الانسانى دون أن يشعر بالمجتمع أو يشعر المجتمع به . كل هذا أدى الى إعادة النظر فى نظريات التخطيط وقواعد التخطيط والمفاهيم التخطيطية التى كانت متبعة لى تكون صالحة لخلق مجتمعات أفضل

ان مؤتمر المباني العالية الذي عقد في جامعة بنسلفانيا ١٩٧٣ ثم في القاهرة ١٧٩٤ والذي ضم مئات المماريين والمخططين والانشائيين رأى أنه ليس متأكد تماماً أن مثل هذه المباني العالية يجب أن تنشأ - قرر أنه ما من أحد يمكنه أن يجزم حتى الآن ما سوف يترتب عنها من مشاكل اجتماعية أو مسلكية أو معرفة تأثير هذه المباني العالية على الاقتصاد أو البيئة المحيطة بالمبنى .

أثير في هذا المؤتمر ان هذه المباني العالية ، سواء الأبراج السكنية أو المكتبية لم تنشأ في كثير من الحالات بسبب الحاجة الملحة اليها ، ولكنها أنشئت اما للتعبير عن اعلان وشهرة لأسماء أصحابها أو رمز لعمل ناجح . أوضح بعض علماء هذا المؤتمر أن هذه المباني لم تنشأ طبقاً لمواصفات محددة أو توحيد قياسي محدد ، كما أضاف البعض الآخر من هؤلاء العلماء أنه يخشى على سلامة أرواح السكان في حالة حدوث حريق أو هزة أرضية أو أى خطر آخر . ومن المقترحات التى تستلفت النظر اقتراح بإنشاء « مناطق أمان » Safety Zones داخل المبنى في أحد الطوابق العلوية محصنة ضد الحريق ومكيفة الهواء لالتجاء سكان الطوابق العليا لفترة الحالة النفسية التى تنتاب سكان هذه الطوابق العليا وشعورهم في حالة انقطاع التيار الكهربائي انعزالهم وخاصة المتقدمين في السن ، كما تقرر أن تستمر مناقشة هذا الموضوع الهام على ٢٤ دورة تعقد مرة كل ٦ أشهر في عاصمة من عواصم العالم . ويصف فرانك لويد رايت ١٨٦٩ - ١٩٥٩ المباني العالية بقوله :

« ان الراسية تسبب الدورار لحياة الانسان ، اما الخط الأفقى فهو خط الحياة لبنى الانسان وربما تصبح أمة بأسرها في يوم ما ، مدينة حرة الامتداد يعيش موظفوها على مسافات متباعدة فوق أرض يحتلونها وعلى هيئة حرة ، حيث يختلط كل من العاملين في الحقل والمصنع ، في الفنون والصناعات وفي العلوم والتربية والتجارة والنقل ، ويصبح سعى كل منهم منتهاى الى كل فرد آخر ، وعلى أساس خطوط طبيعية بالنسبة لهم جميعاً تتخذ الحياة الانسانية صورة جديدة وطرقاً أفضل للعمل دون حركة ضائعة أو اضطراب أو تداخل أو الزام .

ان كانت ناطحات السحاب انتصار للهندسة فانها بالقطع هزيمة للعمارة انها هياكل من الصلب ترتفع مختلفة تحت كساء من رقائق من الحجر مشبه فيها . انها صورة أخاذة تحاكى أبراج عهود الاقطاع ، ولكنها عمارة زائفة .. »

● الارتباك المعماري والكابوس المبنى

Architectural Confusion & Urban Nightmare

علمت المدينة الانسان كيف يطير في السماء كالطير ويفرّو الفضاء ويصل الى القمر وكيف يفوص

التوازن في حياة المجتمع واخضاع الالة لمطالب الانسان . ومن هنا تظهر أهمية وضع أسس جديدة وأساليب جديدة ومفاهيم جديدة للتخطيط العمرانى بشرط أن يسيطر عليها العامل الانسانى أو الناحية الانسانية لمجتمع يجب أن يعيش وينمو ويتحرك .

● المدينة والشبح :

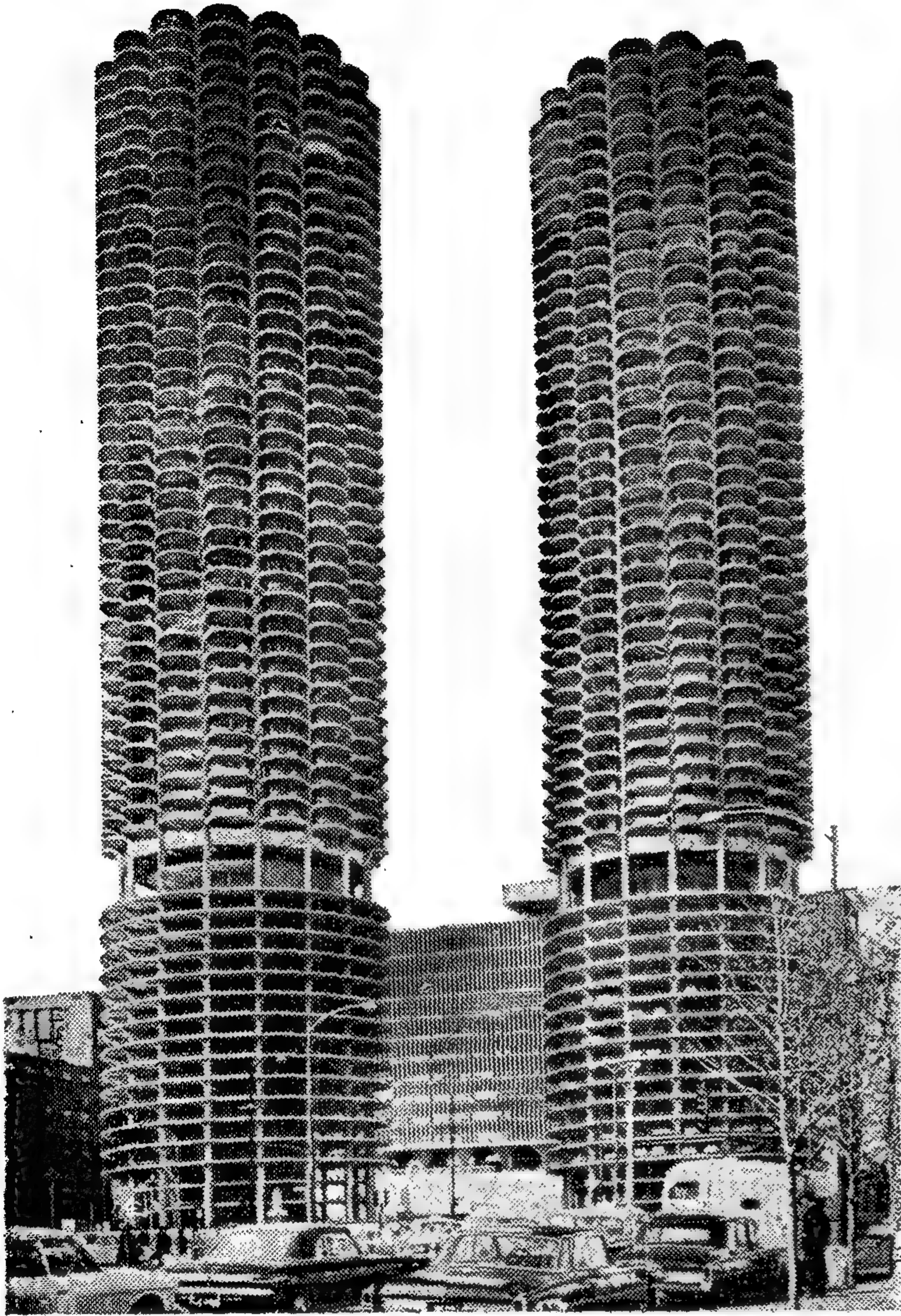
الانفجار السكاني . . شبح مخيف يهدد سكان المدن . سيدفع الانفجار السكاني البشرية الى الانتحار الجماعى ، وهذا ما تنبأ به بعض علماء العصر لأن الازدحام الرهيب على سطح الكرة الأرضية سوف يدفع الانسان الى القيام بعمليات انتحار جماعية كما تفعل بعض الحيوانات . وهناك شبح مخيف يهدد المدن العضوية التكوين بالدمار حتى المدن التى أعيد تخطيطها وتمت على أسس تضمن لها النمو العضوى والتطور والبقاء . ويتمثل هذا الشبح في عدة عوامل تسيطر عليها نزعات الدفاع عن البقاء ، وتتلخص هذه العوامل فيما يلى :

- ١ - الزيادة المستمرة في عدد سكان العالم مع انخفاض موارد تموينه ، وقد أكد بعض الاقتصاديين ان العالم ان لم يتدارك تلك المشكلة الحيوية فسوف تجتاحه المجاعة قبل مضي نصف قرن .
- ٢ - عدم الاستقرار السياسى لكثير من الشعوب وعدم تحقيق مبدأ الاشتراكية التعاونية الاقتصادية الفعلية .
- ٣ - أثر الصناعة الآلية في اختلال التوازن الاقتصادى في العالم ، وأثر انتاج الجملة Mass Production في اختلال توازن النقد والعلاقة بين الانتاج والتوزيع .
- ٤ - ازدياد الفارق في مستوى المعيشة بين مختلف طبقات الشعب الواحد من جهة ومختلف طبقات الشعوب من جهة أخرى .
- ٥ - الزيادة المضطردة في استنفاد موارد الدول في شؤون اوقاية والدفاع وازدياد فقدان الثقة والتي يمكن التعبير عنها بمختلف أنواع التضخم الغير متوازن في جسم الكرة الأرضية أن كل مشكلة من هذه المشاكل العالمية لن تحل الا بالمشروعات العالمية المشتركة . فمشكلة زيادة السكان ، وهى الشبح الأكبر المخيف الذى يهدد كيان العالم ومدنياته لن تحلها الحروب هذه المرة ولا مختلف وسائل الاستعمار التى حلتها في الماضى ، بل ستحل بايجاد مكان جديد للعيش أو توسيع الرقعة الزراعية والسكنية على سطح الكرة الأرضية ، واستغلال المدفونة وقواه الحركة الكامنة وذلك لصالح المجتمع العالمى وزيادة المسطحات اللازمة لاستيعاب تلك الزيادة في السكان لبضعة قرون .

في البحار كالأسماك ولكنها لم تعلمه حتى الآن كيف يعيش على الأرض كإنسان .

لم أجد تسمية صحيحة لمدينة اليوم أنسب من تسميتها « باكابوس المذنب Urban Nightmare »

حيث ان الناس في المدينة اليوم يسومون بسوء العذاب من الحياة فيها . ويكفى القاء نظرة سريعة من أعلى على أى مدينة في العالم لنرى ذلك الخلط والتخبط والتخطيط الغير منطقي واللاعقل . نرى تلك الكتل البشرية المتحركة ببطء على الأرصفة ، ان كان هناك أرصفة ، صراع وكفاح ، حركة وضجيج سيارات « سرعة » واندفاع امواج بشرية ، وآلاف السيارات ، أصوات مزعجة ، حوادث ، جو خانق ملوث .. الخ فنشعر باننا نعيش في حلم مخيف ونحيا في كابوس مدني مروع . حتى المدن والاحياء القديمة التي كانت تعيش في أحلام ماضيها الحلوة الهائلة . نراها تعاني اليوم من هذا الكابوس المزعج الذي فرض نفسه وخيم عليها وذلك بعد ان تحولت هذه المدن وتلك الاحياء القديمة لتخدم أغراض الحاضر ومتطلباته واحتياجاته الآلية وسرعة سياراته ذات الاعداد الرهيبة .

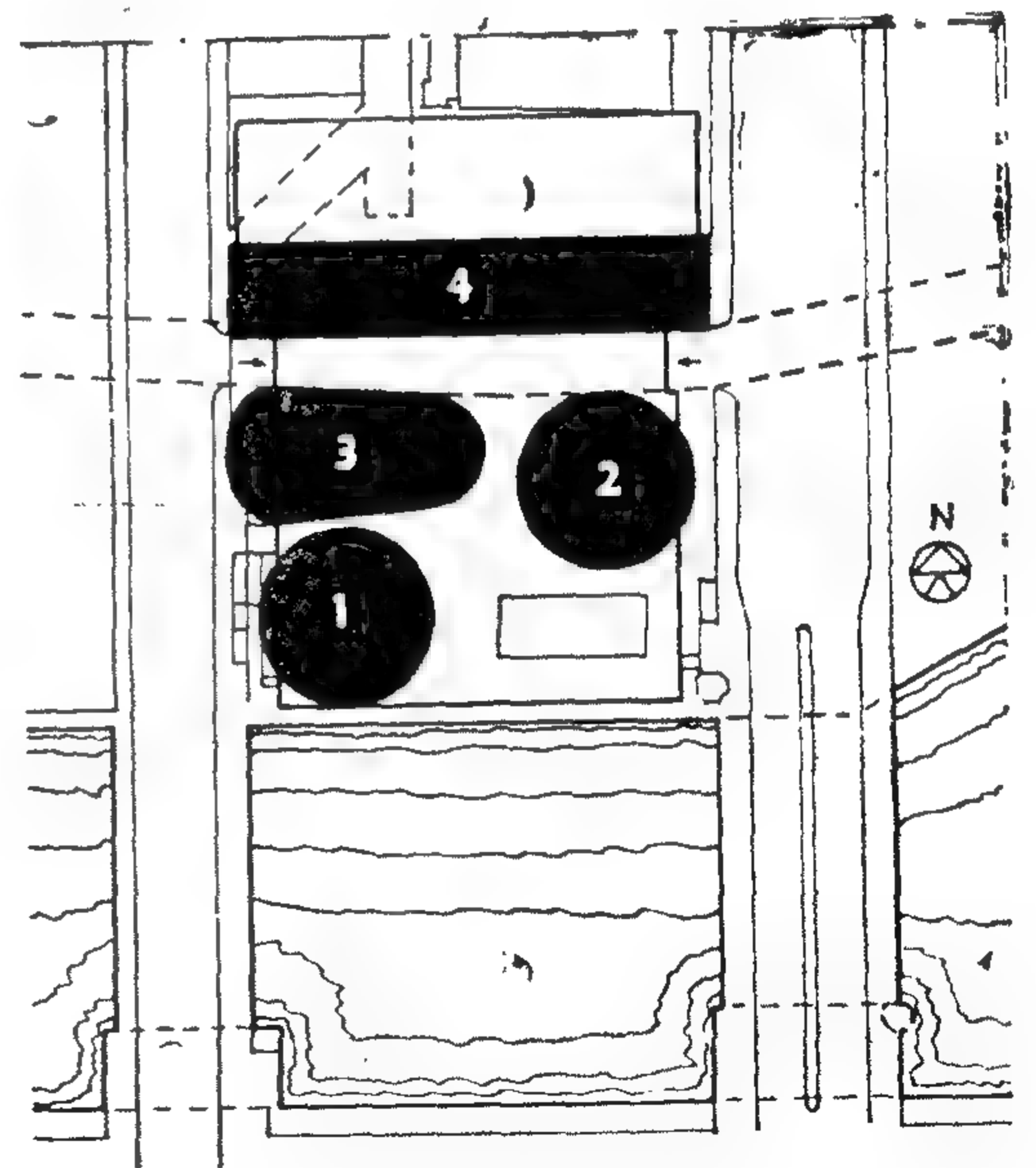


والسؤال هنا هو : هل ستصبح المدن في عالمنا الجديد ملجأ للإنسان الساعي للحرية ، ام ستصبح أداة طفيان جديد ومصدر قلق وارهاق لهذا الإنسان .

● العمارة والمجتمع

كانت العمارة دائماً وستظل اصدق واشرف تعبير على تقدم الأمم وحضارتها فهي التي تعكس وجه التقدم ، وهي احد الدعائم الأساسية واحد وجه التقدم الانساني . وعلى ذلك تحتل العمارة مكاناً هاماً في الحياة الاجتماعية للمجتمع .

ان المعمارى يبني للإنسان ، ويبني للشعب ، يبني للإنسان ويعمل على توفير الراحة والمتعة في مسكنه . يبني له البيت لسكنه ، ودور العلم لثقافته والمستشفيات أصحته والنوادي والمسارح لتسليته والترفيه عنه . يبني للإنسان ولأولاده المسكن الصحي الملائم الذي يتفق مع احتياجاته ومطالبه



١٠ ، ١١ - منظور : وتخطيط عام لمجموعة ماريناسيتي السكنية شيكاغو ١٩٦٨ . برجان دائريان كل منهما مكون من ٦٠ طابق : الطوابق ١٥ السفلية مخصصة للسيارات ، والمتوسطة مخصصة مكاتب والعلوية مخصصة للسكن . تجميع غير متلاحم وتكوينات معقدة غير متزنة . فضلاً عن أن جميع الوحدات المكتبية والسكنية على اشكال دائرية يصعب الانتفاع بها من حيث الوظيفة والغرض والانتفاع .

تصنيع مواد البناء) بدراستها وعلاقتها بالمبنى الذي يقوم بتصميمه وإنشائه ومعنى ذلك هو العمارة والمعماريين ، والبناء والبنائين . نريد هذا الاتجاه وهذا التطور أو ذلك التحول ولكن نضيف على ذلك بان التصنيع لا يجب أن يكون له تأثير على العمارة الا اذا اراد المعماري ذلك .

وعلى ذلك نرى أن كل شيء يدل على أن عمل المعماري Architect ينقسم إلى مرحلتين . المرحلة الأولى هي الخلق Creation والمرحلة الثانية هي التكوين Composition تجميع عناصر التكوين المطلوبة للمبنى . فالمعماري دائما يخلق ويبدع طبقا لمواد البناء المتاحة له ووفقا لظروف وطبيعة المنطقة ، واذا لم تتوفر له هذه المواد وتلك الظروف فليس هناك عمارة بل هي انشاء وبناء والتاريخ القديم يثبت لنا ذلك بوضوح وأمانة .

فلا تقبل أبدا بل ونرفض الاعتراف بانتصار الآلة المزيف على الانسان ، حيث الحقيقة أن الآلة اخترعها الانسان لخدمته . اننا نستعمل الآلة الكاتبة والآلة الحاسبة والعقل الالكتروني ونتحكم فيها ونخضعها لعلمنا وعلما واحتياجاتنا ولا نجد في ذلك ما يشير الى أن هذه الآلات سيدة نفسها وتنتصر علينا ، فيجب إذن أن لا نقف بل نبحث عن الحقيقة ، حقيقة مواد البناء ، حقيقة التصنيع لخدمة العمارة ، فالعمارة تولد ولا تصنع .

ومن الحقائق الثابتة أن العمارة كانت دائما في العهود السالفة هي الصورة الصادقة والتعبير الدقيق لحضارة الانسان وتطوره . وسارت حضارة الانسان وسارت معها العمارة في تطور هادئ رزين لا يفارقها طابعا المميز . وكانت العمارة دائما تتميز بصفتين ملازميتين لا يمكن فصلهما . فالى جانب الوجود المادى المسمد من مواد البناء وطرق الانشاء هناك المحتوى الحسى للمبنى ، وهو ما يتمتع به المبنى من صفات فنية وهى **الشخصية والغرض والوظيفة** بأسلوب خاص وتعبير معين تماما « كالكلام » فالى جانب البناء اللفظى هناك المعنى الذى يعبر عن هذا الكلام وأسلوب التعبير به .

فالحياة والمدنية الحديثة مهما اتجهت ناحية الآلة ونحو المادية ونحو التكنولوجيا ، فهى لن تستغنى أبدا عن الفن ولن تنفصل عن عجلته فى سيرها التقدمى ، بل هى توجه كل قواها الآلية والمادية لتعميم الفن ونشره ليلعب دوره فى حياة المجتمع ويحتل مكانه فى كل ركن من أركان مقومات حياته . فى كفاحه ونضاله . . فى سلمه وحربه . . فى عمله ولهوه . . فى كل ما يرتبط بإحساسه فى الوجود كعنصر انشائي فعال فى المجتمع الانسانى .

توفيق أحمد عبد الجواد

يتبع [٢]

يراعى فى المسكن أن تدخله أشعة الشمس الدافئة والتهوية المستمرة . يحيط المبنى - بالحدائق والخضرة ليشعر بالحياة ومباهجها ، يحاول أن يجعل المبنى كأنه جزء من الطبيعة أو أن الطبيعة جزء منه ، يحول شوارع المدن الى ميادين مظلة بالأشجار ، ويحول الميادين الى حدائق مزدهرة . ومعنى ذلك أن العمارة عامل أساسى فى حياة الانسان فى المجتمع الذى يعيش فيه . وهذا هو المعنى الحقيقى لتلك العبارة التى عبر عنها فيكتور هوجو عن العمارة بقوله « أن العمارة هى تلك السمفونية العظيمة الخالدة من الحجر ، وهى ذلك العمل الضخم لانسان وامة » .

ولذلك لا يمكن للمجتمع أن يتجاهل هذه الحقيقة وبالتالي لا يمكن أن يتجاهل المجتمع المعماري وذلك لسبب الدور الذى يقوم به المعماري أولا فى مهمته ثم كيفية التعبير عنها وهى الحقيقة ، التناسب والتوازن ومعنى ذلك العمارة نفسها . فالعمارة إذن موضوع اجتماعى عمرانى وتفرض نفسها على المجتمع لمدة طول أو تقصر . فمن الخطورة بمكان أن نعبّر عن العمارة بالقول هذه العوامل . فبالرغم من أن هذه العوامل هى بأنها نتيجة تحقيق العوامل التكنولوجية والاقتصادية والاجتماعية وأن القيم المعمارية تتحقق اذا اكتملت فعلا لازمة وضرورية فى العصر الحالى ولكنها يجب أن لا تتحكم فى العمارة .

فالانسان وحده وليست الآلة هو الذى يحدد شكل العمارة وشكل المبنى ، والانسان وحده هو الذى يحدد نوعية المبنى وليست التكنولوجيا ولا العوامل الاقتصادية أو الاجتماعية .

حقيقة بان هذه العوامل مجتمعة وغيرها تلعب دورا كبيرا فى تطور مواد البناء وطرق الانشاء ، وأن هذه المواد التقليدية القديمة وهى الطوب والحجر والخشب وايضا طرق البناء تطورت نتيجة للتطور العلمى والصناعى والتكنولوجى ولكن هناك مشتقات وعوامل أكثر أهمية وأكثر انسانية لا يمكن تحقيقها الا بالمعماري وحده وأهمها الشخصية القوة ، التعبير ، الوظيفة ، الغرض ، الصراحة .

فرسالة المعماري واضحة تمام الوضوح وثابتة راسخة عما كانت عليه من قبل ، بل وتزداد ثباتا الى أن يتم عملية انقائهم بسلام هذا بالإضافة الى وضوحها بأنه مطالب أيضا بأن يبحث ويكشف الكثير من العلوم المتعلقة بمواد البناء وسيصبح المعماري بل ويجب عليه أن يكون الممول الأول للتصنيع وتحديد الأغراض الأساسية المراد تحقيقها وتحويل المواد الصماء الى مواد جميلة أو « مواد الجمال » ، عليه أن يقود هذه الحركة الآن (حركة

The true drawdown or drawdown due to formation loss = observed drawdown -
 $cQ^2 = (D.D)f$

If $(D.D)f$ is multiplied by the correction factor due to full penetration which can be determined by KOZENY equation

$$S = CPP \times SPP$$

where $S = D.D$ for pumped well fully penetrating aquifer

CPP = Partial penetration constant for pumped well (fraction).

SPP = Observed drawdown for partial penetration conditions.

Generally for the New Valley CPP =

$$\frac{\text{Net opened sand thickness}}{\text{Total net sand thickness}}$$

The corrected SP.C can be obtained by deviding the discharge by the corrected $(D.D)f$ for full penetration, or it can be determined by multiplying local SP.C by the reciprocal of CPP (Fig. 4) shows the curve for the same well Nasser I after correction for partial penetration. From this curve $T/S = 1470 \text{ m}^2/\text{day}$.

$$T/S = 4 \times 10^5, S = 3.7 \times 10^{-3}$$

Comparison between value of T & S calculated by SP.C method and values obtained by INZ (Industro Project ZEGRAB Consultant Company) are shown in the following table :

Well Name	Corrected T by INZ	Corrected T by SP.C	Corrected S by INZ	Corrected S by SP.C
Nasser I	1210	1470	2.8×10^{-3}	3.7×10^{-3}

SUMMARY AND CONCLUSION

The proposed graphical method is a rapid and easy one to determine T & S simultaneously for wells of 4 "to 9", diameters without serious errors. For diameters more than 10" other set of calculations and T/S sheets must be prepared.

Electronic computer can give a rapid and accurate results for all variables in eq. 9 & 10.

The graphs of T groups can be used efficiently if the necessary adjustment and

limitations taken in consideration as illustrated before.

REFERENCES

- 1,2 & 3 : Theory of Aquifer Tests. Geological Survey water supply paper No. 1536 Page 331-340.
- 4 : The Jornal American Water Work Association Vol. 58 No. 5, May 1966 Printed in USA.
- 5 : Selected Analytical Methods for well and aquifer evaluation. By WILLIAM C. WALTON.

termine the values of specific capacities at time equals 0.01 day (14.4 minutes) and at time equals 2.1 day (144 minutes) respectively. From the difference between these two values, the values of T & S can be obtained as shown in the next solved example.

Solved Example :

The following table shows the observed data for one of the wells in Kharga - New Valley Project. This well is Nasser I (85/8" surface casing 9 5/8" of drilling in producing zone) and well loss $c = 0.2 \times 10^{-6}$ determined from step drawdown test.

Well name Date of test	Time of measurement min.	Constant discharge test Qm ³ /day	Observed Drawdown mt.	Obs. D.D C Q ² = (D.D)f	SP.C $\frac{Q}{(D.D)}$ - local
Nasser I	1				
	2				
	3				
	4				

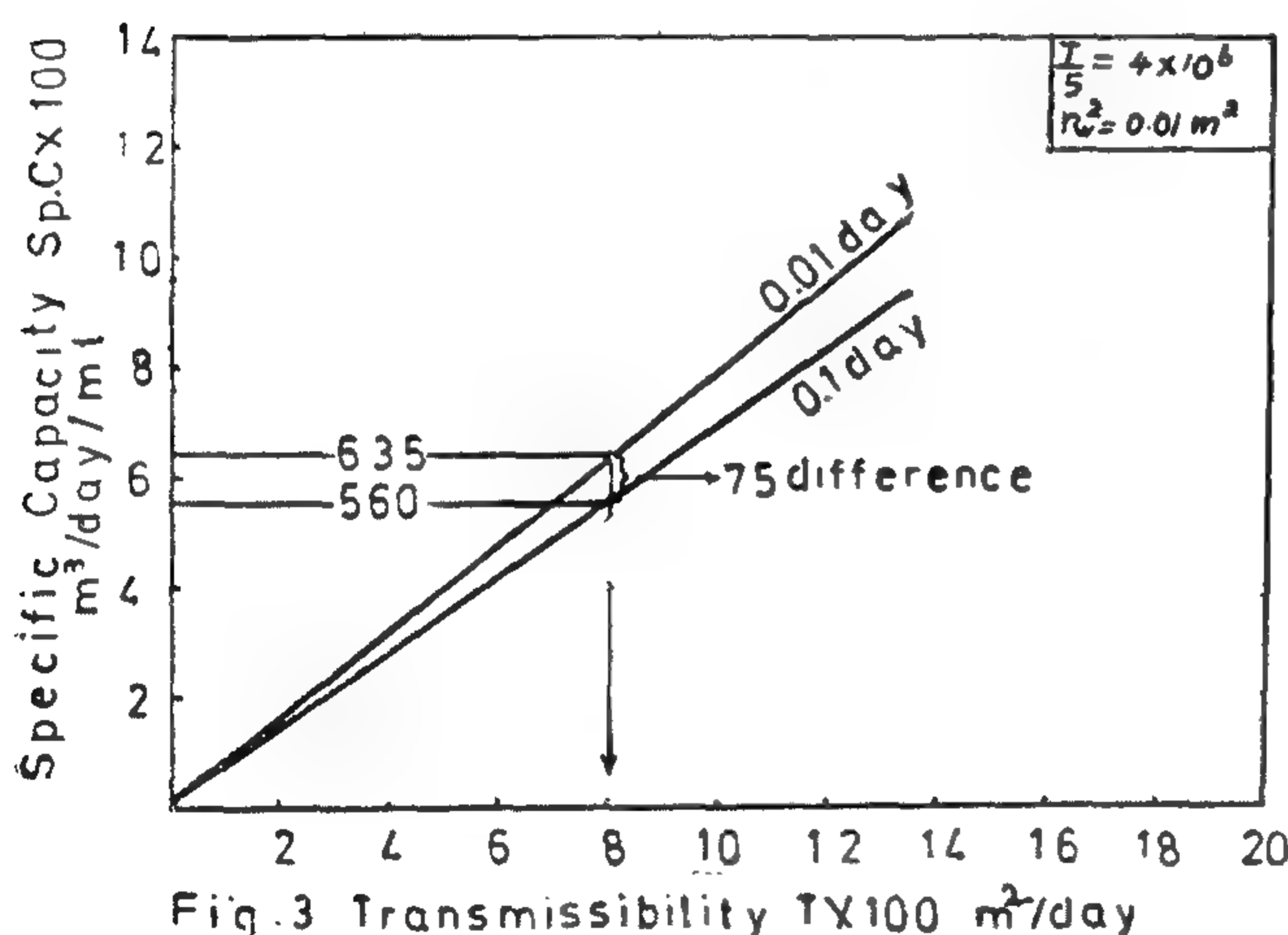


Fig. 2 shows the time - SP.C curve.

From Fig. 2 the following values are obtained:

The SP.C at time 14.4 min. (0.01 day)
= 635 m²/day.

The SP.C at time 144 min. (0.1 day)
= 560 m²/day.

Therefore the difference equals 75. This difference, according to Fig. 3 between PS.C 635 & 560 = 75 is only found in the sheet of $T/S = 4 \times 10^6$. Drop a vertical line on the x-axis one gets a value of $T/S = 800$ m²/day. From this value and for $T/S = 4 \times 10^6$, $S = 800/4 \times 10^6 = 2 \times 10^{-4}$.

Comparison between value of T & S calculated by SP.C method and JACOB method (Straight line method).

Well Name	Local T by St. line method	Local T by SP.C method	Local S by St. line method	Local S by SP.C method
Nasser I	790	800	7.4×10^{-4}	2×10^{-4}

Corrections of T & S for Partial Penetrations :

It is possible to correct values of trans-

missibility and storativity by using the proposed procedure after calculating the total SP.C as follows :

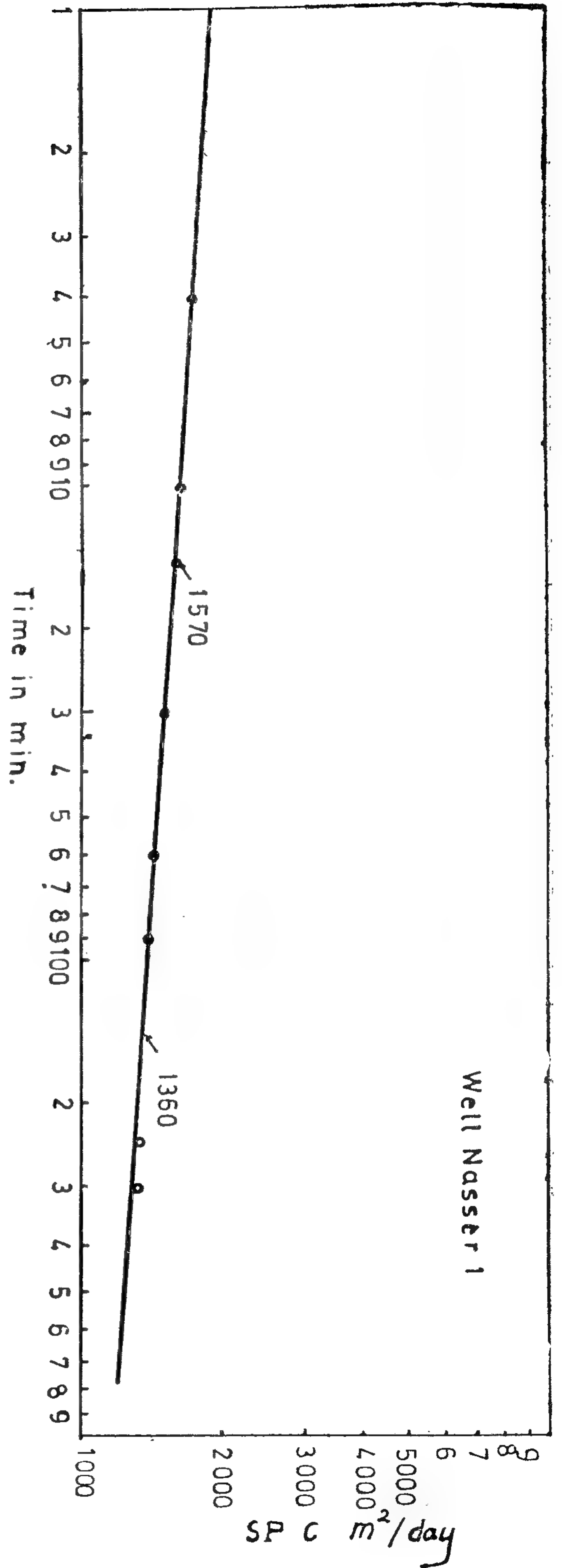
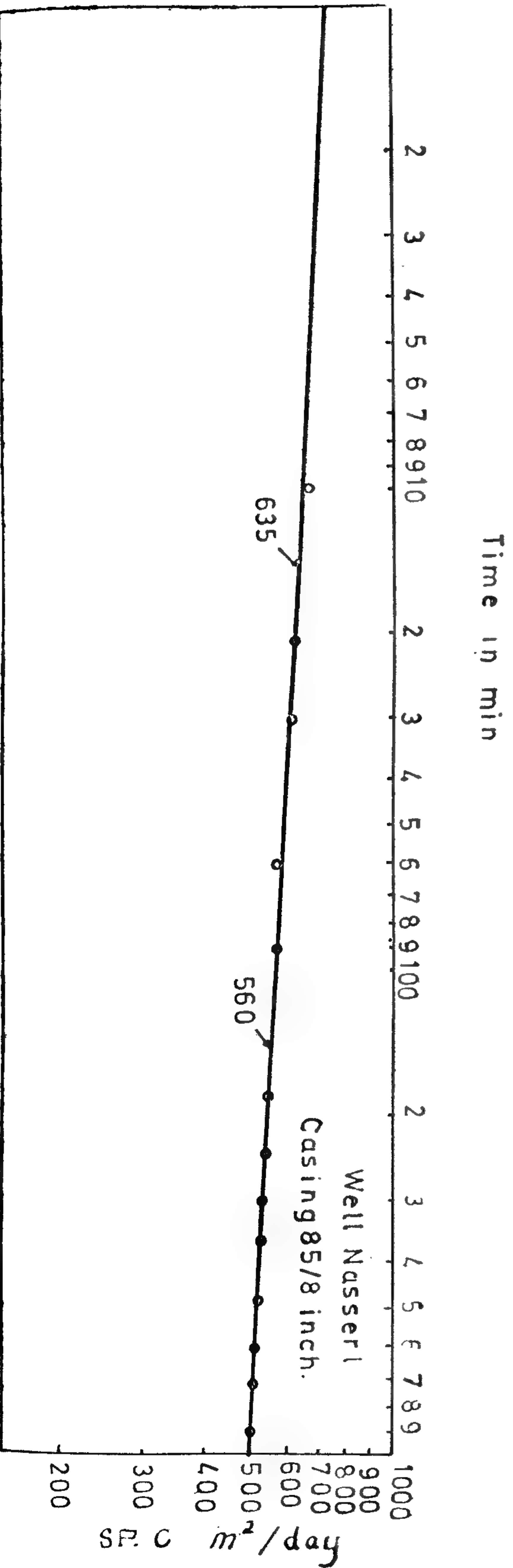


Fig 4 (Time, S.P.C. Curve Corrected for full penetration)



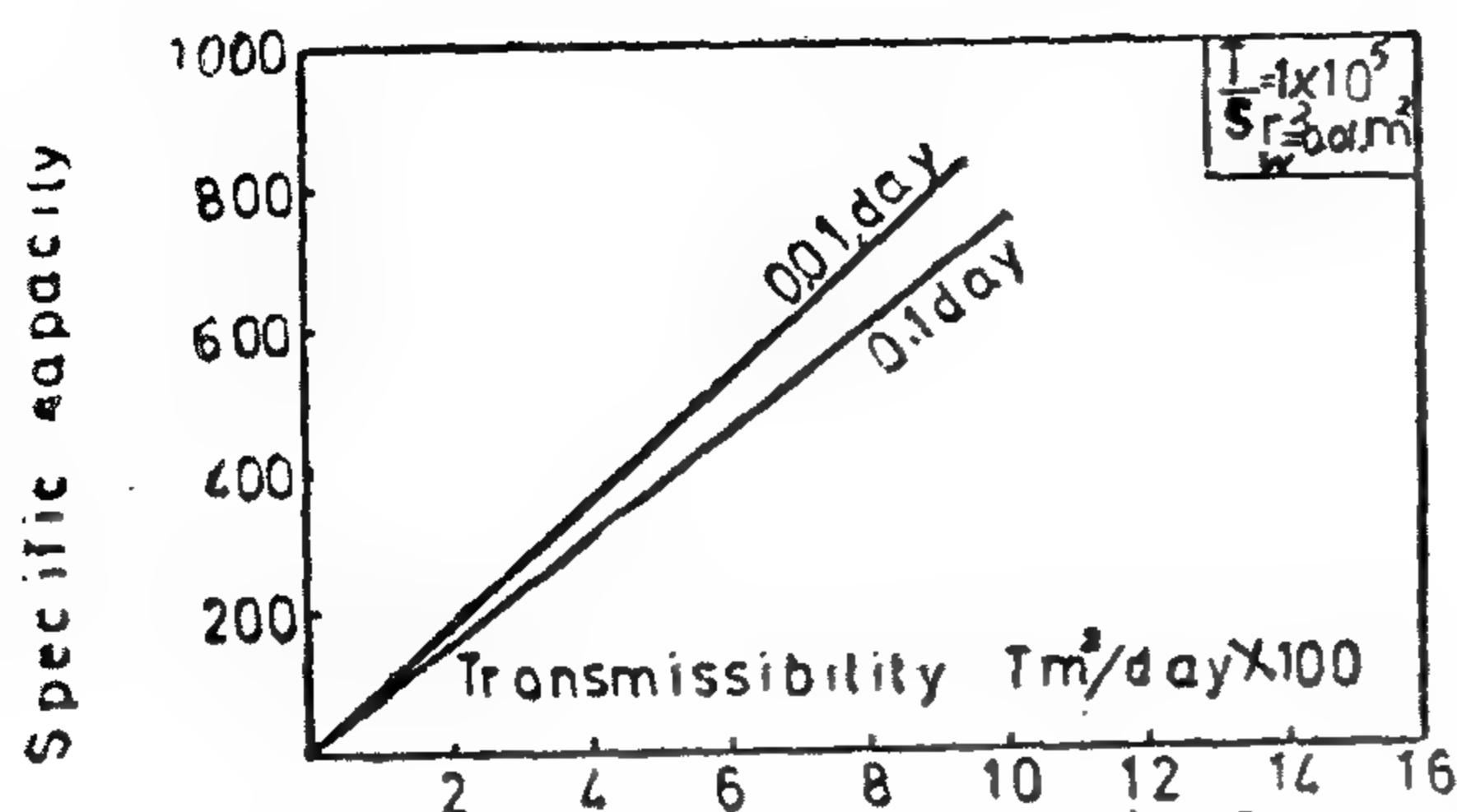


Fig 1-values of T & sp. cap. $T/S = 1 \times 10^5$ & $r_w = 0.01 \text{ m}$

dial lines decreases as time increase and as T/S value increase. The slope of these lines decreases as T/S values increases.

Conditions and Limitations of Applying the Method :

This method is based on the THIES non-equilibrium formula, and its modification made by JACOB.

The following boundry conditions are assumed :

- 1 — The aquifer is homogenous, isotropic, constant thickness and have infinte areal extent.
- 2 — The well loss should be taken in consideration if it is valuable.
- 3 — The effective radius of the well has not been affected by the drilling and development of the well, and is equal to the nominal radius of the well.

- 4 — The discharge, coefficient of transmissibility and storativity is constant during the period of the test.

Method of Application

Application of this method can be carried out according to the following steps :

- 1 — Determine the value of the well loss coefficient "c" from step discharge test.
- 2 — Run a pumping test with constant discharge test and tabulate the measured drawdown and time.
- 3 — Subtract from each drawdown the value of cQ^2 which equals the well loss constant during the test. Then obtain the net D.D. of the aquifer.
- 4 — Devide the value of the constant discharge Q by each net drawdown obtained from step "3" to obtain the values of specific capacity. It decreases with time.
- 5 — Plot the obtained values of specific capacity and corresponding time on log-log paper where time "t" in minutes as x-axis and specific capacity values as Y-axis.
- 6 — A straight line will be obtained from step "5". From this straight line de-

Table(1): Computed Values for B and Specific C apacities which are the Reciprocal of B at $T/S = 1 \times 10^6$

$\frac{T}{S}$	t day	$\frac{(x)t}{T}$	Transmissibility										
			200	400	600	800	1000	1200	1400	1600	1800	2000	
1×10^6	0.01	$\frac{1.17}{T}$	5.85	2.93	1.96	1.46	1.17	0.975	0.836	0.732	0.650	0.585	$B \times 10^{-3}$
			171	341	510	685	855	1030	1200	1365	1540	1710	SP.C
	0.1	$\frac{1.35}{T}$	6.75	3.38	2.25	1.69	1.35	1.12	0.965	0.845	0.75	0.675	$B \times 10^{-3}$
			148	296	445	592	740	890	1038	1180	1330	1480	SP.C
	1.0	$\frac{1.53}{T}$	7.68	3.83	2.55	1.92	1.53	1.275	1.09	0.96	0.85	0.768	$B \times 10^{-3}$
			130	260	392	520	654	785	918	1045	1175	1300	SP.C
	10.	$\frac{1.75}{T}$	8.75	3.37	2.9	1.75	1.46	1.25	1.09	0.97	0.875	0.875	$B \times 10^{-3}$
			114	228	345	455	570	685	800	920	1030	1140	SP.C
	100	$\frac{1.89}{T}$	9.5	4.75	3.15	2.36	1.89	1.57	1.35	1.18	1.05	0.95	$B \times 10^{-3}$
			105	210	318	425	530	635	740	850	1050	1050	SP.C

The ratio of discharge to the drawdown, called the "specific capacity" according to equation (1) is equal to :

$$Q/S_w = 1/B + cQ \quad (2)$$

If the discharge Q is constant during pumping period, then, the specific capacity must decrease with time. This is due to the fact that the formation resistance B increases with time as the everwinding area of influence of well expands.

For small values of well loss c which usually ranges between 0.2×10^{-5} and 6×10^{-6} , the quantity cQ in equation (2) will be very small if it is compared to " B " and it can be neglected from the denominator without any serious error and equation (2) will be :

$$Q/S_w = 1/B \quad (3)$$

Non Steady Radial Flow in an Extensive Aquifer

The equation developed by Theis for the non steady radial flow is :

$$S_w = Q/4\pi T W(u) \quad (4)$$

where: $W(u)$ is the well function and equals :

$$W(u) = (-0.5772 - \ln u + u - u^2/2 \times 21 \\ - u^3/3 \times 31, \dots \dots \dots)$$

and

$$S_w = \text{drawdown in mt.}$$

$$u = r_w^2 S / 4 T t$$

where : S = coefficient of storage

T = coefficient of transmissibility (m^2/day),

t = time in days since pumping began,

r_w = effective radius of the pumped well in mt.

For sufficiently large values of t , the well function may be approximated by a simple logarithmic expression. Thus the

drawdown after sufficient time has elapsed is given approximately by:

$$S_w = Q/4\pi T (\ln 4Tt/r_w^2 S - 0.5772) \quad (5)$$

When the well-loss is appreciable the drawdown in the well is :

$$S_w = Q/4\pi T (\ln 4Tt/r_w^2 S - 0.5772) + cQ^2 \quad (6)$$

$$S_w = Q/4\pi T (2.303 \log 4Tt/r_w^2 S - 0.5772) + cQ^2 \quad (7)$$

Comparing eq. (7) with eq. (1), therefore :

$$B = 1/4\pi T (2.303 \log 4Tt/r_w^2 S - 0.5772) \quad (8)$$

or:

$$B = 1/T (0.183 \log 4Tt/r_w^2 S - 0.046) \quad (9)$$

In equation (9) the value of T/S is usually defined as the diffusivity, calculations of this parameter in this paper run in the range of $T/S = 1 \times 10^{-4}$ to 1×10^9 . r is considered to be 0.10 mt which is a practical value for well diameter in the New Valley Project.

Values of t vary between 0.01 day to 100 days. If one takes $x(t)$ equals the term $(0.183 \log 4Tt/r_w^2 S - 0.046)$ in equation (9), then :

$$B = x(t) / T \quad (10)$$

Table (1) shows some computed values of B for T/S equals 1×10^6 .

From Table (1), it is clear that the values of Specific capacity are the reciprocal for values of B (formation resistance).

Values of transmissibility and corresponding values of specific capacities, on graph paper give a family of straight lines for the time interval 0.01 day, 0.1 day, 1, 10 and 100 days. (Figure 1).

These straight lines pass through the origin.

A set of graphs similar to Figure 1 can be plotted for values of $T/S = 1 \times 10^4$, 2×10^4 1×10^9 . These graphs give a clear variation in its divergent and slope. The divergence between two ra-

AGRAPHICAL METHOD FOR

ESTIMATING THE TRANSMISSIBILITY & STORATIVITY OF AQUIFERS FROM THE SPECIFIC CAPACITY OF WELLS

By

Eng. SALAH RASHWAN* & Dr. MAHMOUD ABU-ZIED**

INTRODUCTION

The specific capacity of the well, which is the discharge per unit drawdown, decreases with time. If the discharge during the pumping test is constant, then the specific capacity should vary with time. Transmissibility and storativity of the aquifer are two main factors for shaping the slope of time - specific capacity curve.

The specific capacity of a well can be used for estimating the hydrologic parameters of the aquifer by the use of formulas developed by THEIS (1935) (1), or by BROWN (2), and chart developed by MAYER (3). The principle of these methods is to determine the specific capacity after certain constant period of pumping usually one day, also assuming the value of the coefficient of storage to get a value for the coefficient of transmissibility. But the value of specific capacity varies with time. SANDOR C. CSALLANY (4), developed another method in which time factor is taken in consideration to determine the coefficient of transmissibility. In this method the value of storage coefficient has to be assumed. Four values only for the storage coefficient have been considered in CSALLANY method. These values are : $S = 2 \times 10^{-1}$, 2×10^{-2} , 2×10^{-3} , 4×10^{-4} . In the proposed method no as-

sumptions for the hydrologic parameters are required, and the coefficient of transmissibility and storativity can be determined simultaneously.

Drawdown Distribution in an Artesian Well :

The drawdown in an artesian well that is pumped, is the difference between the static water level and the pumping level.

This drawdown has two components :

The first, arising from the resistance of the formation, and is proportional to the discharge.

And the second, termed "well loss" and represents the loss of head that accompanied the flow through the screen and upward inside the casing to the surface; this part is approximately proportional to the square of the discharge.

$$S_w = B Q + c Q^2 \quad (1)$$

where: S_w = drawdown inside the well
in mt.

B = Formation resistance

c = well loss

Q = discharge (m^3/day).

** Senior Research Engineer, Ministry of Irrigation, UAR.

* E.G.D.O.A., U.A.R., Korga, New Valley.

- P_p, P_r — maximum stress in the
— soil, in the vicinity of the
single pile and the pier,
respectively.
- R_r — Poulos group reduction
factor.
- S — spacing between piles.
- ϱ_o — single pile deflection at
mud line under a load
 H
- $\varrho_p, \varrho_r, \varrho_g$ — total deflections of the
single pile, pier and pile
group, respectively.
- ϱ_{pr} — total deflection of a pier,
having an assumed stiff-
ness equal to the sum of
stiffnesses of the single
piles.
- ϱ^e — deflection due to elastic
strains in the soil.
- ϱ^p — deflection due to plastic
strains in the soil.

REFERENCES

1. Barakat, M.A. (1974).
Modifications to two methods of anal-
ysis of laterally loaded pile groups.
Norwegian Geotechnical Institute,
Internal report, No. 51503-2. Not pu-
blished.
2. Focht, J.A. and K.J. Kenneth (1973).
Rational analysis of the lateral per-
formance of offshore pile groups.
Offshore Technology Conference, 5,
Houston. Vol. 2, p. 701-708.
3. Hetenyi, M. (1946).
Beams on elastic foundations.
University of Michigan press, Ann
Arbor, Michigan.
4. Matlock, H. and L.C. Reese (1960).
Generalized solution for laterally loa-
ded piles.
American Society of Civil Engineers.
Proceedings, Vol. 86, No. SM5, p.
63-91.
5. Poulos, H.G. (1971).
Behaviour of laterally loaded piles;
II-Pile groups.
American Society of Civil Engineers.
Proceedings, Vol. 97, No. SM 5, p.
733-751.
6. Schjetne, K. (1973).
Design of piled foundation at the
Frigg field, Norwegian Sector. Norwe-
gian Geotechnical Institute, Internal
report, No. 72007-6.
Not published.

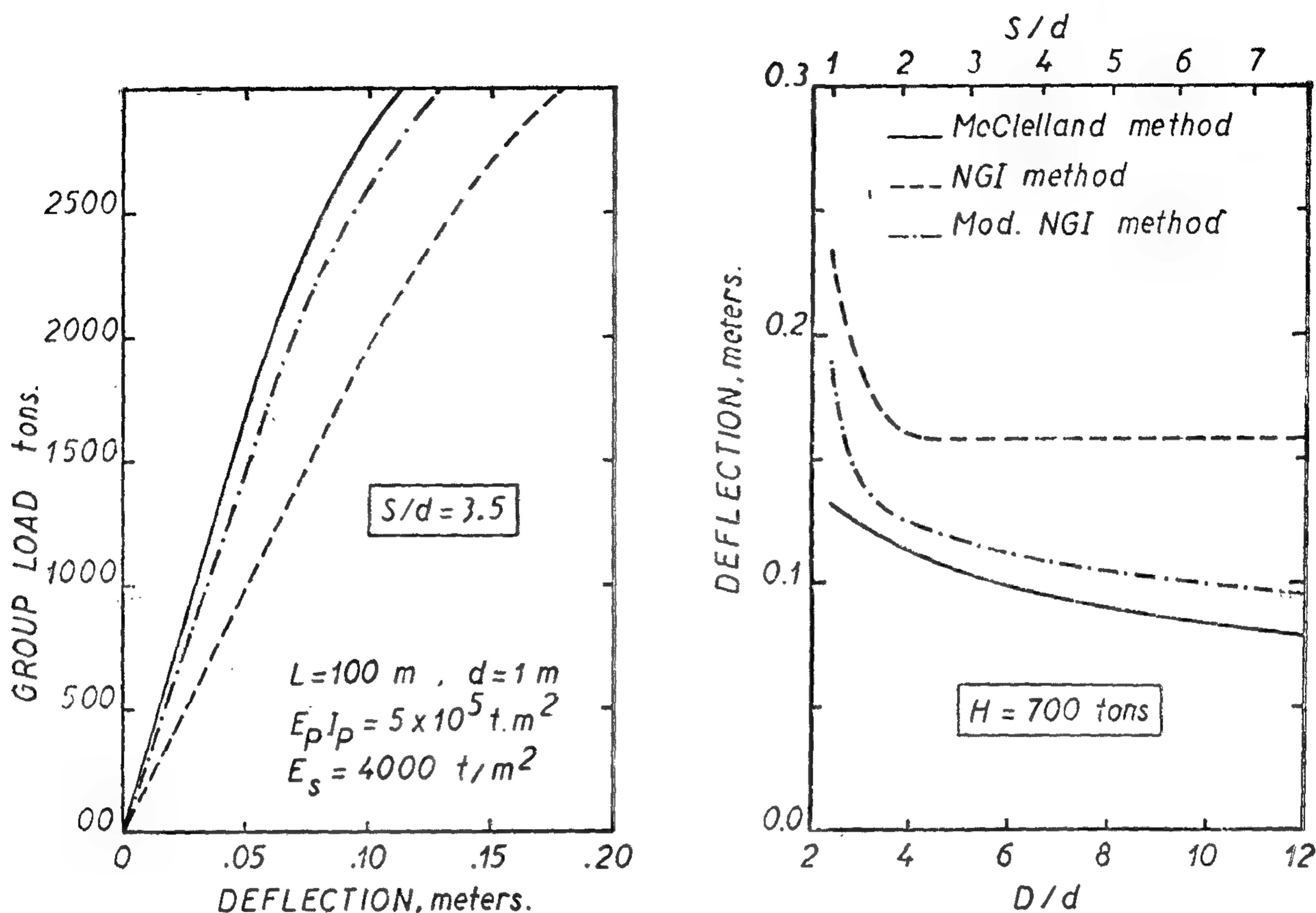


FIG. 3-DEFLECTION OF A 4-PILE GROUP IN STIFF CLAY.

For the investigated pile groups, the NGI method yielded deflections 8 to 70% bigger than those computed by McClelland method. The suggested modified NGI method yielded results mostly on the conservative side. Compared to the deflections computed by McClelland, the deviations ranged between - 7 % and + 21 %. Typical results of the computed load/deflection and deflection/pile spacing relationships, for the pile group at the first site, are represented on figure 3.

CONCLUSIONS

As a simple method for predicting the deflection of a laterally loaded pile group the modified NGI method is suggested. The method accounts for the actual stiffness of the soil-pile pier and corrects for the part of deflection, twice considered in the NGI method. Computed deflections are expected to be mostly on the conservative side.

NOTATIONS

- | | |
|-----------------|--|
| d, D | — diameters of pile and pier, respectively. |
| E_p, E_r, E_s | — moduli of elasticity of pile, pier and soil, respectively. |
| F_{pr} | — pier reduction factor. |
| H | — average pile load in a group. |
| H_p | — single pile load. |
| H_o | — a single pile load, producing a stress level in the soil equal to that due to a pier with a load $n.H$. |
| I_p, I_r, I_s | — moments of inertia of pile, pier and area bounded by pile perimeter, respectively. |
| K | — coefficient of subgrade reaction. |
| n | — number of piles in a group. |

pier enclosing the pile group, then to the soil which surrounds the pier. In the immediate adjacency of the piles, a high level of stress is reached and elastic as well as plastic strains take place in the soil. In the pier vicinity, a relatively low level of stress is reached and elastic strains mainly take place in the soil.

The lateral deflection of any pile in the group, or the group deflection ρ_g , may be regarded as the sum of:

- 1 — The deflection ρ_p of the single pile, at the average pile load H .
- 2 — The increase in the single pile deflection due to the effect of the other piles in the group. This deflection increase, which also can be referred to as the net pier effect, is equal to the difference between the deflection ρ_r of the pier under the total load nH , and the deflection ρ_o of the single pile at a load H_o , corresponding to the same low stress level of pier performance.

$$\begin{aligned} \rho_g &= \rho_p + \rho_R - \rho_o \quad \text{Hence,} \\ &= \rho_p + \rho_R \left(1 - \frac{d}{D}\right) \quad (11) \end{aligned}$$

The lateral deflection ρ_r of the pier, with the actual stiffness $E_r I_r$, can be correlated to the deflection ρ_{pr} of the pier, with an assumed stiffness equal to the sum of the single pile stiffnesses $n \cdot E_p I_p$, by the expression

$$\rho_R / \rho_{pr} = \sqrt[4]{n} \cdot R_R \quad (12)$$

From 11 and 12, it follows that

$$\rho_g = \rho_p + F_{pr} \cdot \rho_{pr} \quad (13)$$

were

$$F_{pr} = \sqrt[4]{n} \cdot R_R \left(1 - \frac{d}{D}\right) \quad (14)$$

F_{pr} is the pier reduction factor which accounts for the actual interaction between piles and soil, considers the difference between the correct and the assumed stiffness of the pier, and corrects for the

uplicated part of deflection. F_{pr} can be obtained from the chart in figure 2.

The lateral deflections, ζ_p of the single pile at the average pile load and ρ_{pr} of the enclosing pier at the total horizontal load, can be computed as in the NGI method by a subgrade reaction procedure, using p-y data modified for each particular diameter.

CASE STUDIES

The lateral deflection of a 4-pile group has been computed by three different procedures: NGI, suggested modified NGI and McClelland methods. Comparatively, McClelland method can be considered as the best, available at present, analytical procedure. Comparison between the computed deflections is carried out, at different loads and pile spacings, in three different soil conditions. Homogeneous stiff clay, very loose sand, and nonhomogeneous layers of dense sand followed by layers of stiff clay represent the prevailing soil conditions at the investigated sites.

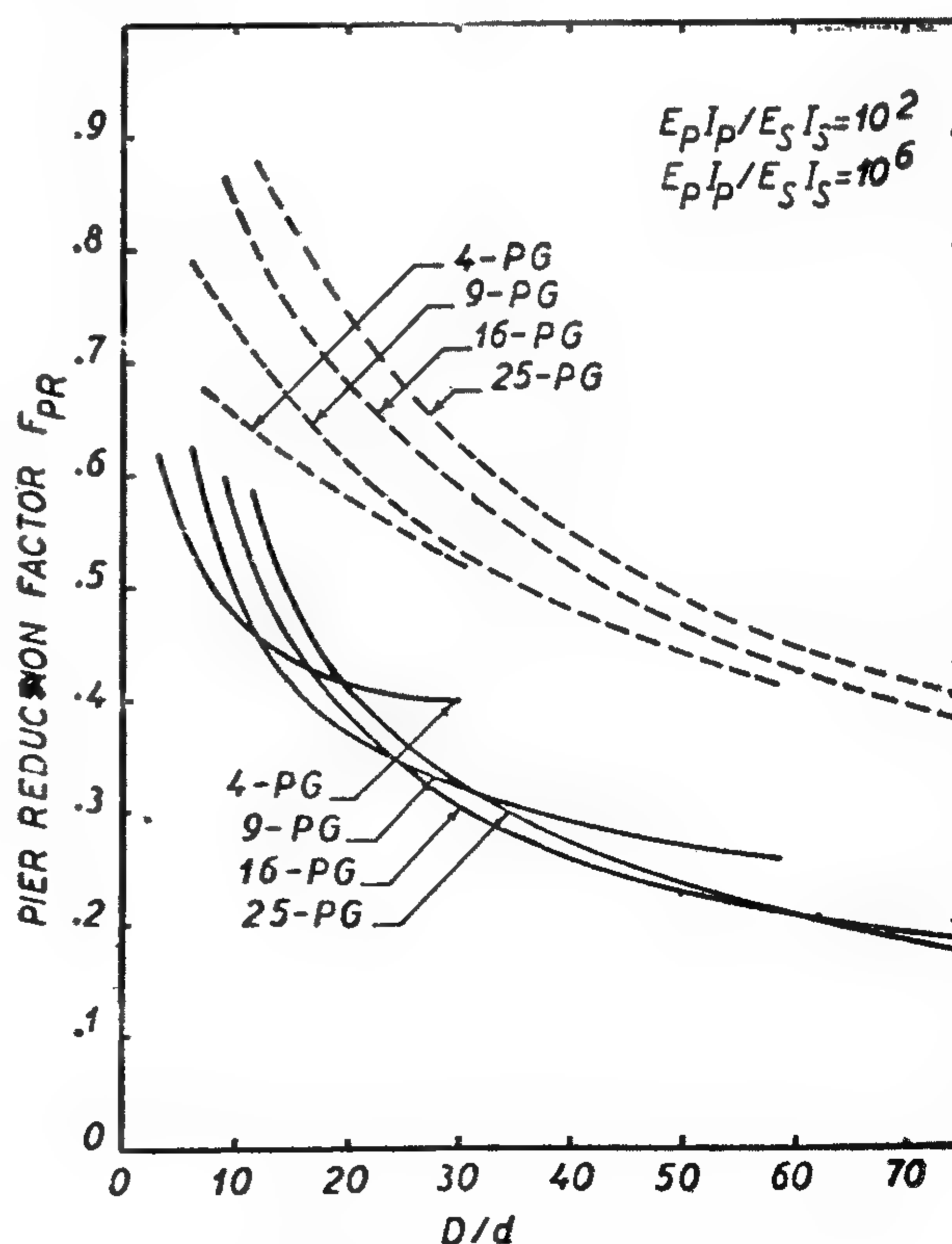


FIG. 2-PIER REDUCTION FACTOR F_{pr} .

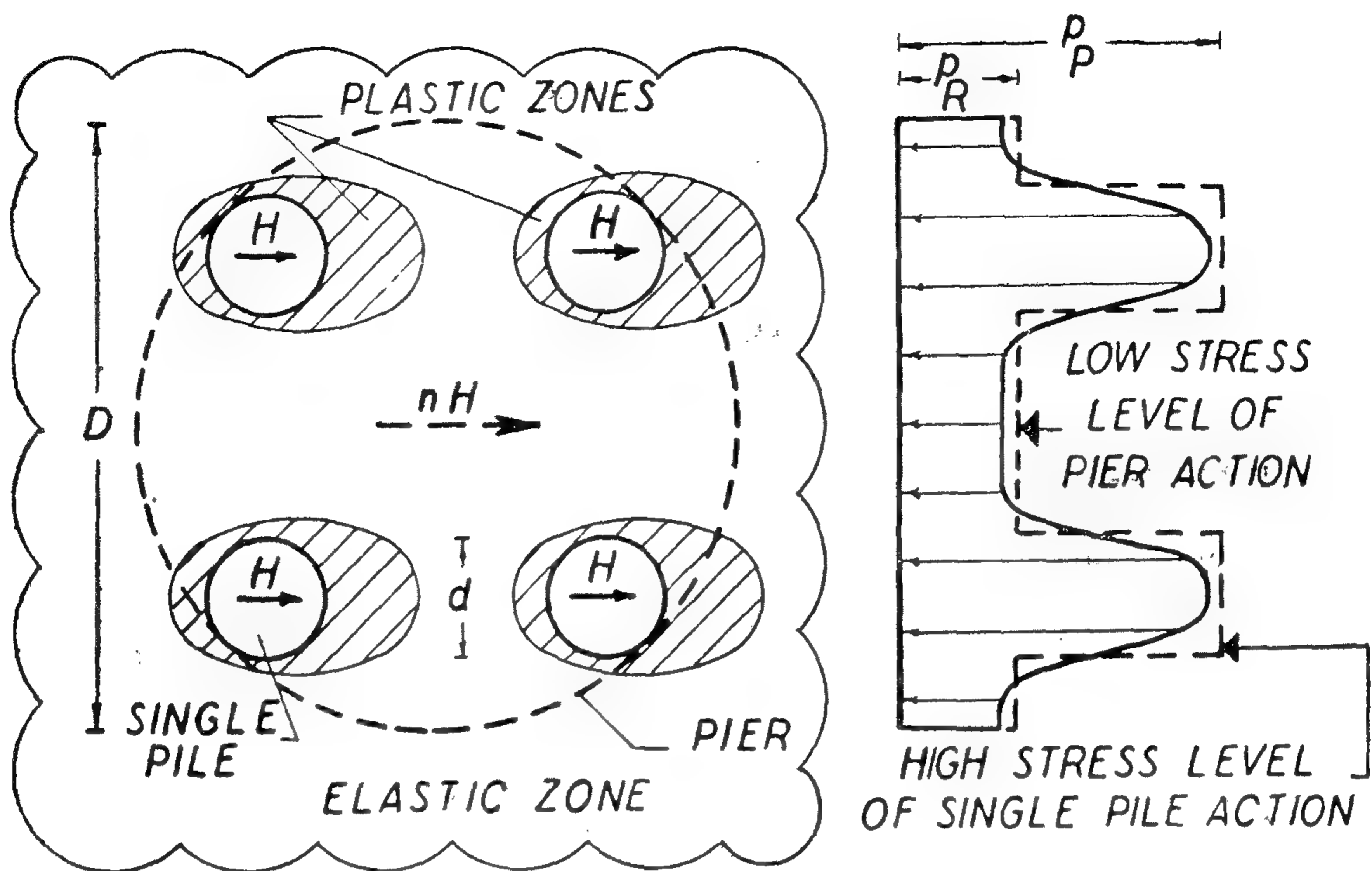


FIG.1.a- STRESS LEVELS IN THE SOIL, IN VICINITY OF A PILE GROUP.

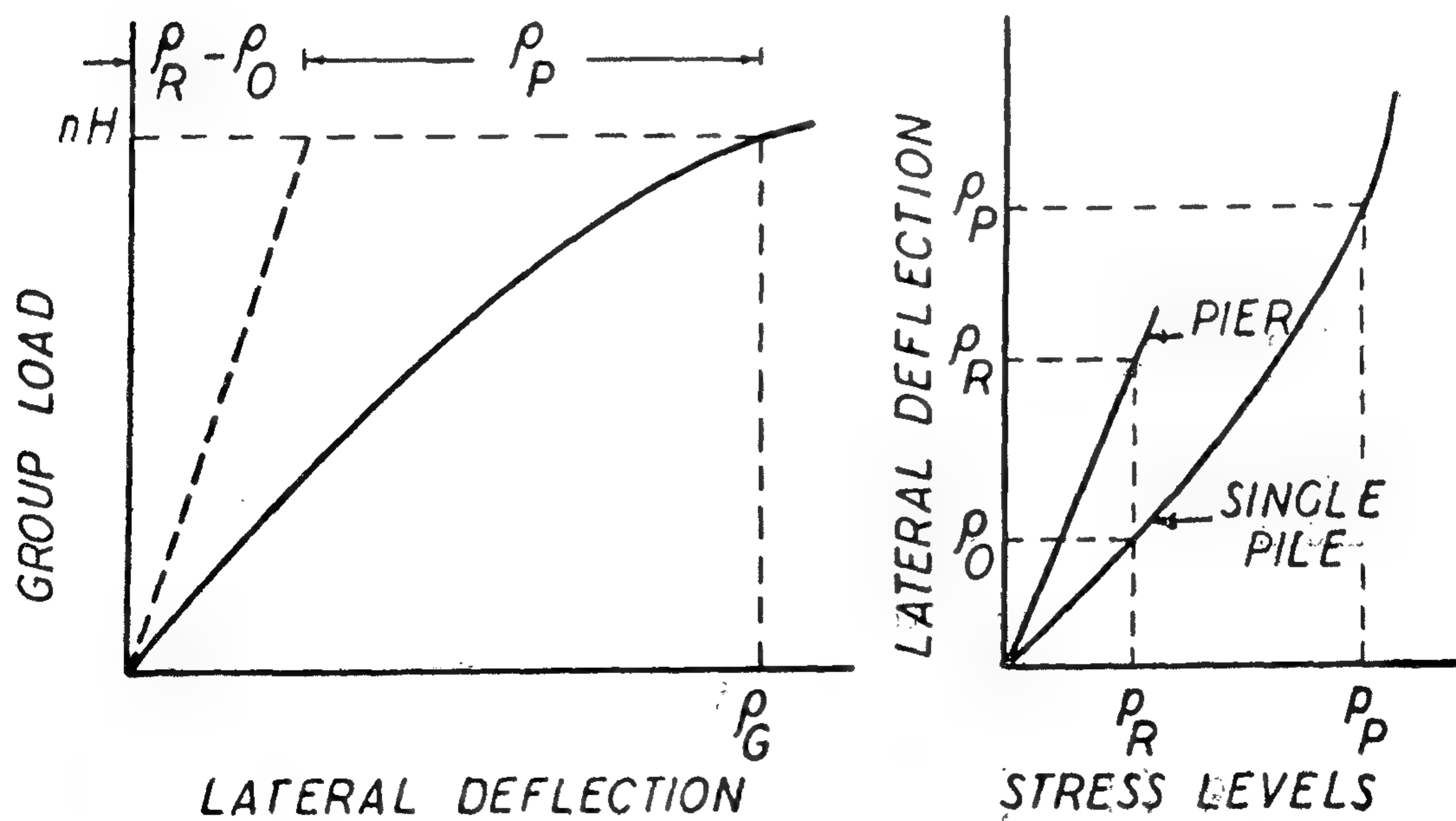


FIG.1.b- LATERAL DEFLECTIONS, OF SINGLE PILE, PIER AND PILE GROUP.

where : H_p — horizontal pile load at mud line,

$E_p I_p$ — flexural rigidity of the pile,
 d — pile diameter,

K — coefficient of subgrade reaction,

E_s — modulus of soil elasticity;
 $E_s = k.d.$

Consider that a group of n such piles, acted upon by a total horizontal load $n.H$, is substituted by a pier of diameter D , large enough to enclose all the piles of the group. The elastic deflection δ_o^e of the pier can be expressed as

$$\rho_R^e = nH / \sqrt[4]{4E_R I_R E_s^3} \quad (3)$$

where : $E_R I_R$ is the flexural rigidity of the pier.

From numerical solutions, based on the elastic half-space procedures, a correlation between the lateral deflections of the single pile and the pile group has been suggested by Poulos. This correlation can be rewritten in the following form:

$$R_R = \frac{\rho_R^e}{\rho_p^e} \cdot \frac{H_p}{nH} \quad (4)$$

Where : R_R is a group reduction factor.

Combining equations 2,3 and 4, the following expression for the flexural rigidity of the pier can be deduced.

$$E_R I_R = E_p I_p / R_R^4 \quad (5)$$

The use of equation 5 to express the flexural rigidity of the pier provides that the lateral deflection, computed by the subgrade reaction procedure, will account for the actual interaction between piles and soil.

STRESS LEVELS IN THE SOIL

From equation 2, the maximum stress p_p in the vicinity of the single pile may

be expressed as :

$$P_p = \frac{H_p}{\sqrt[4]{4E_p I_p E_s^3}} \cdot \frac{E_s}{d} \quad (6)$$

A similar expression for the maximum stress P_r in the soil surrounding the pier is

$$P_R = \frac{n H R_R}{\sqrt[4]{4E_p I_p E_s^3}} \cdot \frac{E_s}{D} \quad (7)$$

using expressions 6 and 7 for P_p and P_r to compare the stress levels in the soil in vicinity of the single pile and the pier, figure 1-a, we get:

$$\frac{P_p}{P_R} = \frac{H_p}{H} \cdot \frac{D}{n d R_R} \quad (8)$$

At a single pile load H_p equal to the average pile load H in the group, equation 8 shows that the stress level in the soil due to the action of the single pile is much higher than that due to the action of the pier.

At the same stress level in the soil, the following correlations between the single pile and pier loads and deflections can be deduced.

$$H_o = n H R_R \cdot \frac{d}{D} \quad (9)$$

$$\rho_o^e = \rho_R^e \cdot \frac{d}{D} \quad (10)$$

Where H_o and ρ_o^e are the single pile load and elastic deflection, corresponding to the stress level of pier action. These expressions show that, at any given level of stress in the soil, the load and the deflection of the single pile are comparatively smaller than those of the pier, figure 1-b.

GROUP DEFLECTION

The group load is assumed to be uniformly distributed between the piles. The pile loads are transferred, first to the

ANALYSIS OF THE PERFORMANCE OF Laterally LOADED PILE GROUPS

I — MODIFIED NGI METHOD

By

Dr. ADEL BARAKAT,

ABSTRACT

In this paper the NGI method for computing the deflection of laterally loaded pile groups is developed. The soil-piles interaction is accounted for in the modified method by correlating available solutions based on the subgrade reaction and the elastic half-space analyses. The NGI duplicate consideration of a part of the elastic deflection is corrected. Computed deflections of some case studies confirmed the privileges of the suggested modifications.

INTRODUCTION

Among the several methods, commonly used to predict the performance of laterally loaded pile groups, the NGI and McClelland methods represent the available analytical procedures which consider the elastic plastic behaviour of soil in the vicinity of piles. McClelland method is a rational procedure which can be used to predict the group deflection, the load distribution between piles and the stresses along the piles. The NGI method is a simple approach which only gives the lateral deflection of the pile group at mud line.

In the NGI method a group of n piles is substituted by a pier, large enough to enclose all the piles and with a stiffness equal to the sum of stiffnesses of the single piles. The deflection ρ_g of the group is found by summing up : the deflection ρ_{pr} of the pier, acted upon by the total horizontal load, and the deflection ρ_p of a single pile, acted upon by the average pile load; that is $\rho_g = \rho_p + \rho_{pr}$ (1)

Deflections are computed by the subgrade reaction procedure using p/y data developed for each particular diameter.

The NGI assumption of a pier stiffness only dependent upon the number of piles in the group disregards the interaction between the piles and the soil. Moreover, a part of the elastic deflection is twice considered, and consequently, the computed deflection will be always bigger than the expected deflection.

The development of the NGI method, by considering the soil-pile interaction and eliminating the duplicated part of elastic deflection, represents the aim of the present work.

ANALYSIS

Account for Soil-Piles Interaction

The subgrade reaction analysis, applied in the NGI method to compute the group deflections does not account for the actual interaction between piles and soil; whereas the elastic half-space analysis can consider for it. To extend this important feature of the halfspace analysis to the subgrade reaction analysis, available solutions based on both methods of analysis are correlated.

Consider a fixed-head long pile, embedded in an elastic Winkler's subgrade of constant with depth coefficient of subgrade reaction. The elastic deflection ρ_p^e of the pile at mud line can be expressed as

$$\begin{aligned}\rho_p^e &= H_p / \sqrt[4]{4 E_p I_p d^3 \nu^3} \\ &= H_p / \sqrt[4]{4 E_p I_p E_s^3} \quad (2)\end{aligned}$$

* Assistant Professor, Faculty of Engineering, Alerandria University.

- activated sludge process.
J.W.P.C.F., 39, 251.
8. Klegerman, M.H. (1962),
High-rate activated sludge treatment process.
Ind. Water and Wastes, 97.
9. Levin, G.V.; and Shapiro, J. (1965),
Metabolic uptake of phosphorus by waste water organisms.
J.W.P.C.F., 37, 800.
18. McKinney, R.E. (1960),
Complete mixing activated sludge.
Water and Sewage Works, 107, 2, 69.
11. Randall, C.W.; and King, P.H. (1970),
Phosphate release in the activated sludge process.
A.S.C.E., 96, 395.
12. Randall, C.W. (1971).
Microbial release of soluble phosphate in an activated sludge environment. Presented at the summer Institute on environmental quality, Now or Never- Michigan State University- June 29- July 1, 1970.
13. Rich, L.G. (1963),
Unit processing of sanitary engineering, John Wiley and Sons, New York.
14. Sawyer, C.N. (1940),
Activated sludge oxidation.
Sewage Works J., 12, 244.
15. Sawyer, C.N.; Helmers, E.N.; Frame, J.D. (1951),
Nutritional requirements in the biological stabilization of industrial wastes.
Sew. and Ind. Wastes, 23, 884.
16. Schulze, K.L. (1964),
The activated sludge process as a continuous flow process. Water and Sewage Works, 111, 12, 526.
17. Sekikawa, J.; Nishikawa, S.; Okazaki, M. and Kato, K. (1966), A release of soluble ortho-phosphate in activated sludge process. Advances in water pollution research, 2, WPCF, Washington, D.C., 261.

18. Stewart, M.J. (1964),
Activated sludge process variations, the complete spectrum, Water and Sewage Works, R. 241, 246.
- 19 — Symons, J.M.; and McKinney, R.E., (1958),
The biochemistry of nitrogen in the synthesis of activated sludge. Sew. and Ind. Wastes, 30, 874.

ZUSAMMENFASSUNG

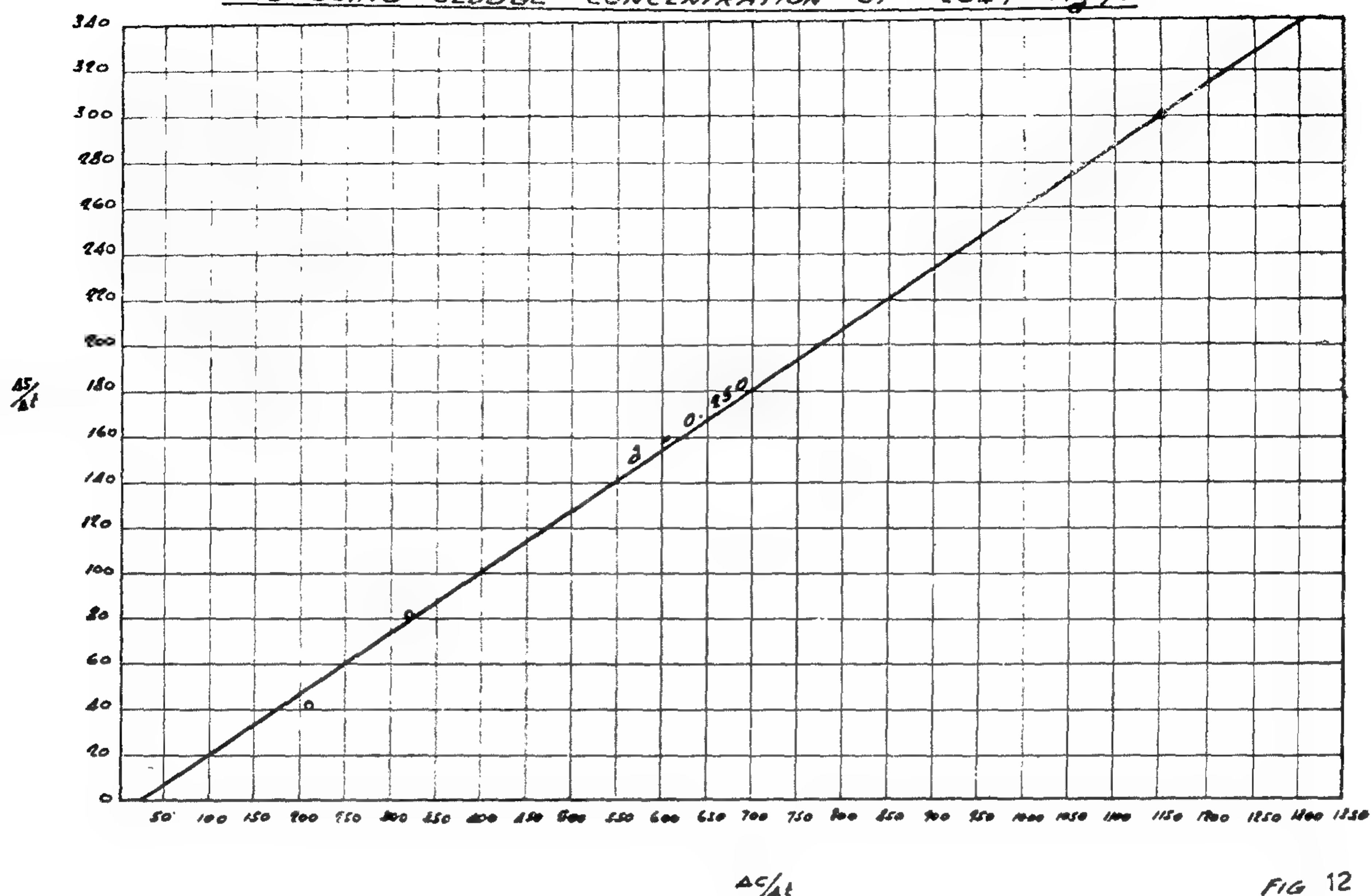
Kontaktstabilisierungsprozess als einer der konventionellen Belebtschlammverfahren, hat die biologische Behandlung der Industrie-Abwasser die unter Nährstoff Mangel leiden ermöglicht. Die Versuche haben ausserdem gezeigt, dass für eine bestimmte BSB -Belastung, die Notwendige Nährstoff Zusatz darf nicht nur auf Basis der Ablauf Qualität, beziehungsweise BSB -Abnahme berechnet werden. Belüftungsbecken Aufenthaltszeit und Schlamm Gehalt müssen berücksichtigt werden.

Wenn diese Grundsätze sorgfältig beachtet werden, ist im Vergleich mit dem konventionellen Belebtschlamm-verfahren, biologische Behandlung mit grössere BSB: P : N Verhältnisse zulässig.

SUMMARY

Contact stabilization as one of the modifications of activated sludge appears to offer a satisfactory and economical solution to the problem of treatment of wastes deficient in nitrogen and phosphorus. The evaluation of nutrient requirements in terms of BOD removal during the operational conditions showed that, for a given BODload, the optimum nutrient supplementation cannot be selected solely on the basis of the desired effluent quality with respect to BOD removal, but also on the reactor detention time and aeration solids concentration.

THE RATE OF CHANGE IN ORGANIC SOLIDS CONCENTRATION AND
COD USING SLUDGE CONCENTRATION OF 2649 mg/l



REFERENCES

1. Gool, K.C. and Gaudy, A.F. (1969), Regulation of nitrogen levels for heterogeneous populations of sewage origin grown in completely mixed reactors. *Biotechnology and Bioengineering*, vol. XI, 79.
2. Hall, M.W.; and Engelbrecht, R. (1967), Uptake of soluble phosphorus by activated sludge. *Proc., 7th. Ind. Water and Waste Conference, Univ. of Texas, Austin, Tex., Section II.*
3. Helmers, E.N.; Frame, J.D.; Greenberg, A.E.; and Sawyer, C.N. (1951), Nutritional requirements in the biological stabilization of wastes. II — Treatment with domestic sewage. *Sew. and Ind. Wastes*, 23, 884.
4. Helmers, E.N.; Frame, J.D.; Greenberg, A.E.; and Sawyer, C.N. (1952), Nutritional requirements of industrial wastes. III — Treatment with supplementary nutrients. *Sew. and Ind. Wastes*, 24, 496.
5. Henkelekian, H.; Orford, H.E.; and Manganelli, R. (1951), Factors affecting the quantity of sludge production in the activated sludge process. *Sew. and Ind. Wastes*, 23, 945.
6. Jenkins, D.; and Menar, A. (1967, A study of the fate of phosphorus during primary sedimentation and activated sludge treatment. *Serl. Report 67-6, Sanitary Eng. Research Lab., Univ. of Calif., Berkley Calif.,*
7. Komolrit, K.; Geol, K.C.; and Gaudy, A.F., Jr. (1967), Regulation o exogenous nitrogen supply and its possible applications to

THE RATE OF CHANGE IN ORGANIC SOLIDS CONCENTRATION AND
COD USING SLUDGE CONCENTRATION OF 1382 MG/L

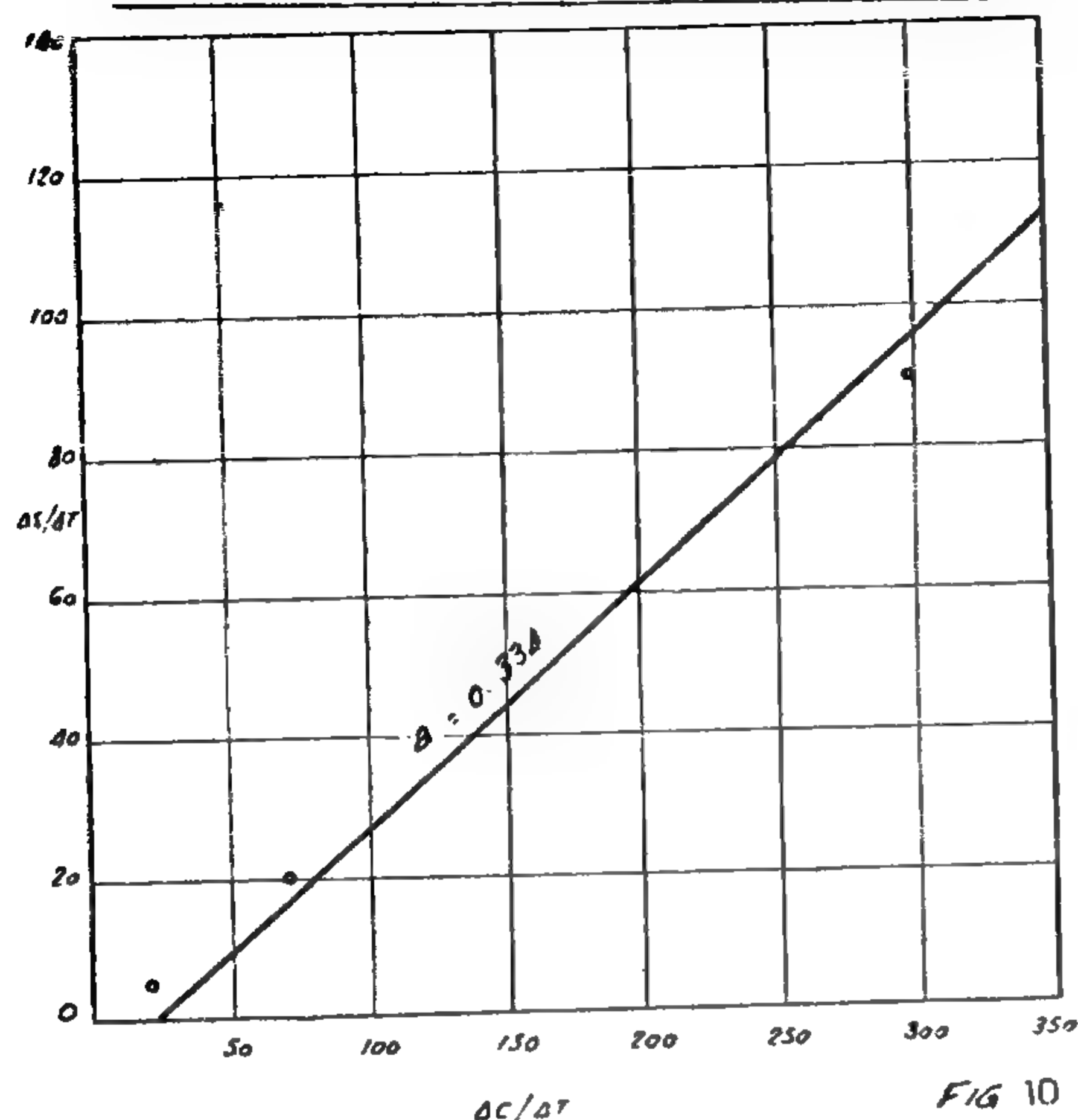


FIG 10

cess should allow a saving in the costs of supplemental nitrogen and phosphorus and should prevent leakage of these elements into the receiving stream.

2 — For a given BOD load, the amount of nitrogen and phosphorus required decreases by increasing aeration solids which may be attributed to reduction in sludge growth rate. Since the required nutrients for microorganisms in such a culture is low, the overall growth pattern is expectedly low in terms of rate of growth.

3 — The optimum BOD : N ratio and BOD : P ratio to be employed for the

treatment of organic wastes cannot be selected solely on the basis of the desired effluent quality with respect to carbon removal, since the optimum nitrogen and phosphorus supplementation will be somewhat dependent upon the reactor detention time employed.

THE RATE OF CHANGE IN ORGANIC SOLIDS CONCENTRATION AND COD USING SLUDGE
CONCENTRATION OF 1580 MG/L.

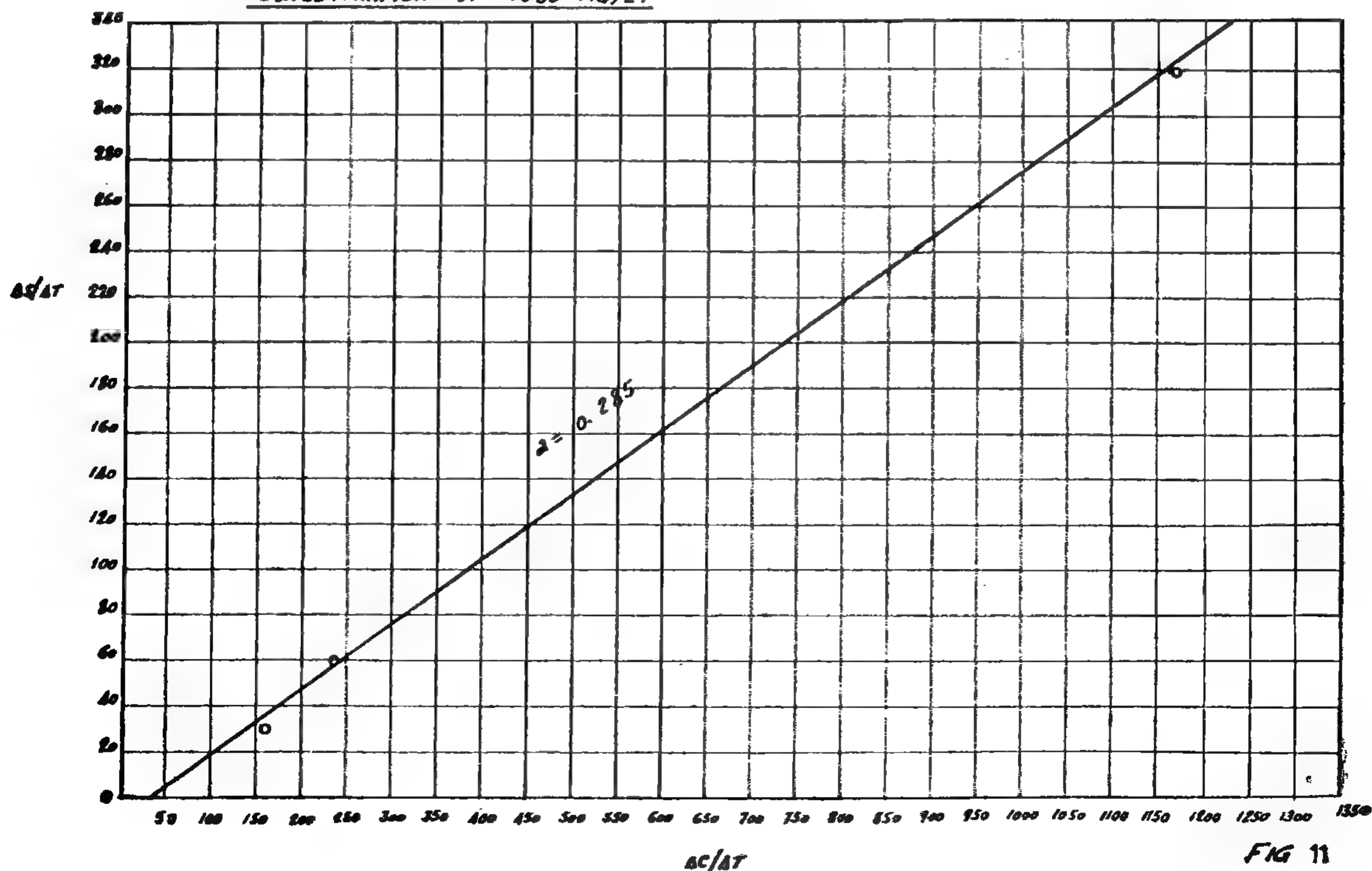


FIG 11

(vi) Batch process kinetics

Batch laboratory studies were carried out to derive criteria concerning the rates of organic removal, sludge production, sludge oxidation and initial adsorption. Activated sludge from the stabilization was used for this purpose. The following formula recommended by Rich, (1963); for short intervals of time was used.

$$\Delta S / \Delta t = \alpha \Delta C / \Delta t - \alpha b \bar{S}$$

where α and b = constants

\bar{S} = mean sludge concentration

The effects of varying the initial aeration solids concentrations over the range of 573 to 2649 mg/l was investigated. The rate of change in volatile solids concentration and COD during the aeration period examined were computed. Corresponding values are plotted on arithmetic coordinates. The value of " α " was determined by the slope of the straight line of best fit constructed through the plotted points, (Figs. 9, 10, 11 and 21). These values were found to be 0.670, 0.334, 0.285 and 0.250 respectively. From Fig. (9), it is seen that when $\Delta S / \Delta t = 0$; $\Delta C / \Delta t = 55$.

These values represent the rate of change in organic concentration that is attributable to the basal metabolic requirements of the activated sludge organisms.

The data obtained showed definite reductions in sludge growth as the aeration sludge organisms.

The data obtained showed definite reductions in sludge growth as the aeration solids increased. The same trend was noted by Heukelekian, et al., 1951; and Sawyer, 1940; in some studies on domestic sludge. This may be explained as a result of the decrease in the feed to microorganisms ratio (F/M). Since the ratio of nutrients to microorganisms in such a culture is low, the overall growth pattern reflects the competition for nutrient and is predominantly one of the declining growth.

THE RATE OF CHANGE IN ORGANIC SOLIDS
CONCENTRATION AND COD USING SLUDGE
CONCENTRATION OF 573 MG/L.

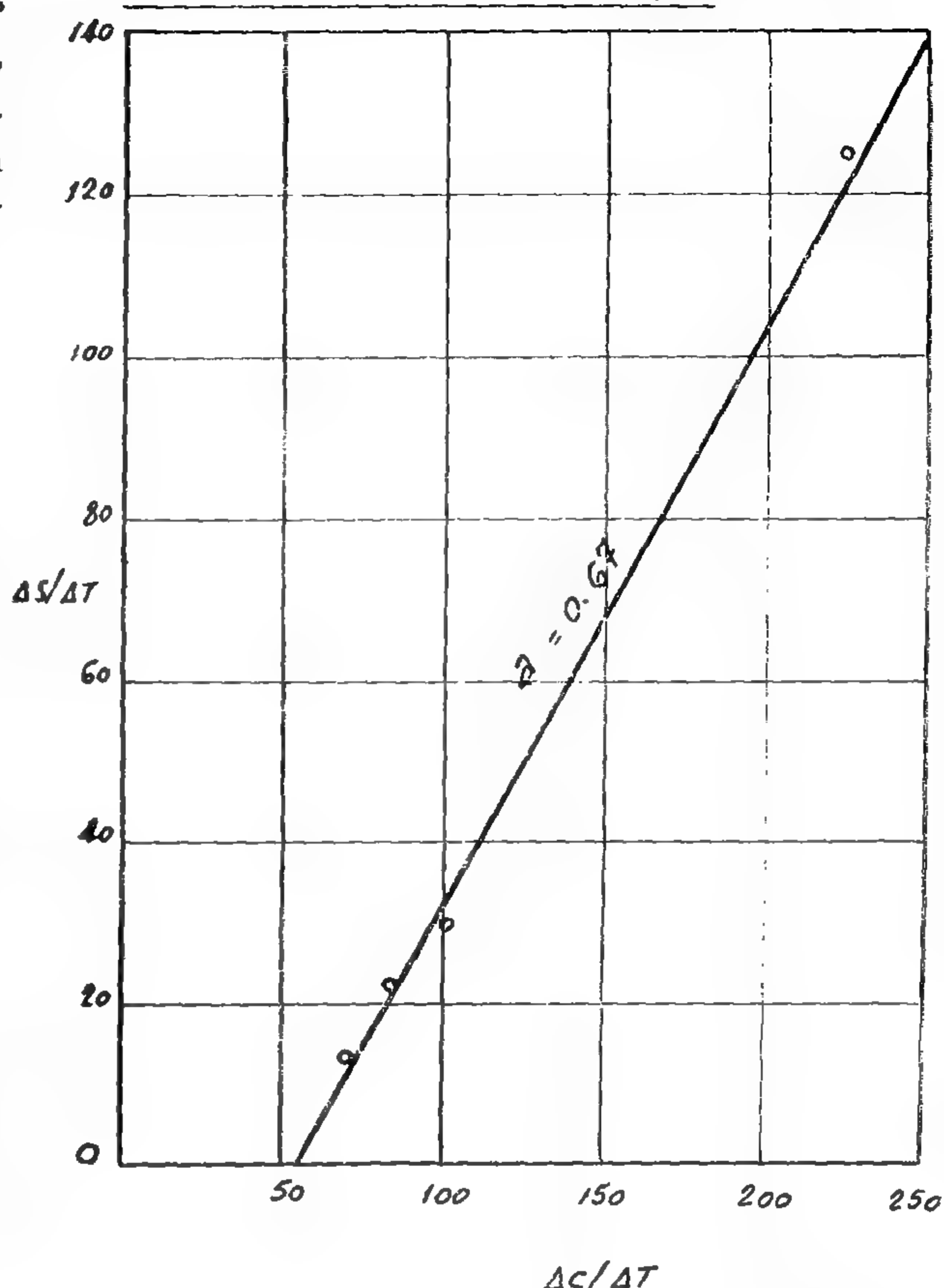


FIG 9

Mckinney, 1960; reported that at a loading ratio below 0.45 lb of ultimate BOD/lb of biological solids/day, 93% of the removed BOO would be expected to be oxidized to carbon dioxide and water and 7% converted to new cells. At a loading ratio of about 2, 45% would be oxidized, and 55% converted to cells. The relationship between process loading and system performance have been studied by many investigators, (Klegerman, 1962; Stewart, 1964; Schulze, 1964).

IV. Conclusion

Based on the available data and their discussions, the major findings may be summed up as follows :

1 — The adoption of the contact stabilization method appears to offer a satisfactory and economical solution to the problems of treatment of wastes, deficient in nitrogen and phosphorus. Such a pro-

Table (4)

The effect of aeration solids concentration
on nitrogen and phosphorus requirements

Period of retention(hr)		BOD ppm		Nitrogen utilized kg N/100kg BOD removed	Phosphorus utilized kg P/100 kg BOD removed	Aeration volatile solids (mg/l)
Contact zone	Stab. zone	Waste water	Effl.			
1	6	204	16	3.34	1.0	1467
1	6	200	12	3.03	1.28	1570
1	6	200	11	2.57	0.75	1795
1	6	230	6	2.14	0.70	1860
1	6	300	20	2.00	0.65	2340

Stab. = Stabilization zone

Effl. = Effluent

(v-2) Effect of aeration solids concentration

The effect of varying the aeration solids concentration over the range of 1467 and 2340 mg/l is shown in Table (4) and illustrated in Fig. (8). The results ob-

tained showed that for a given BOD load, nitrogen and phosphorus requirements decreased with increasing aeration solids concentration. The results also showed that as little as 2.0 kg nitrogen and 0.65 kg of phosphorus would suffice for the removal of 100 kg of BOD.

RELATIONSHIP BETWEEN VOLATILE SOLIDS CONCENTRATION AND UTILIZATION
OF NITROGEN AND PHOSPHORUS.

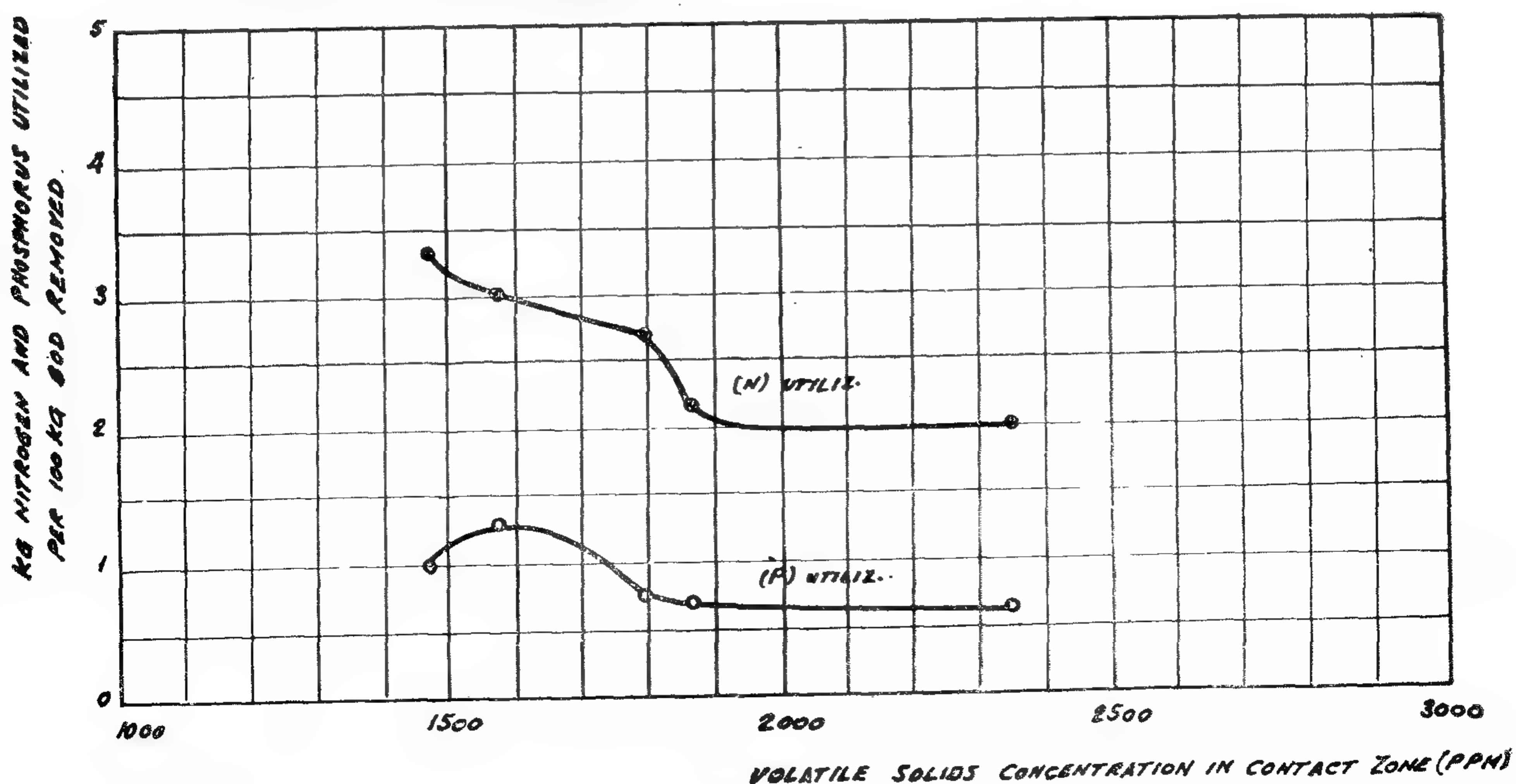


FIG 8

RELATIONSHIP BETWEEN BOD LOAD AND
SVI (CONTACT ZONE, CASE 4)

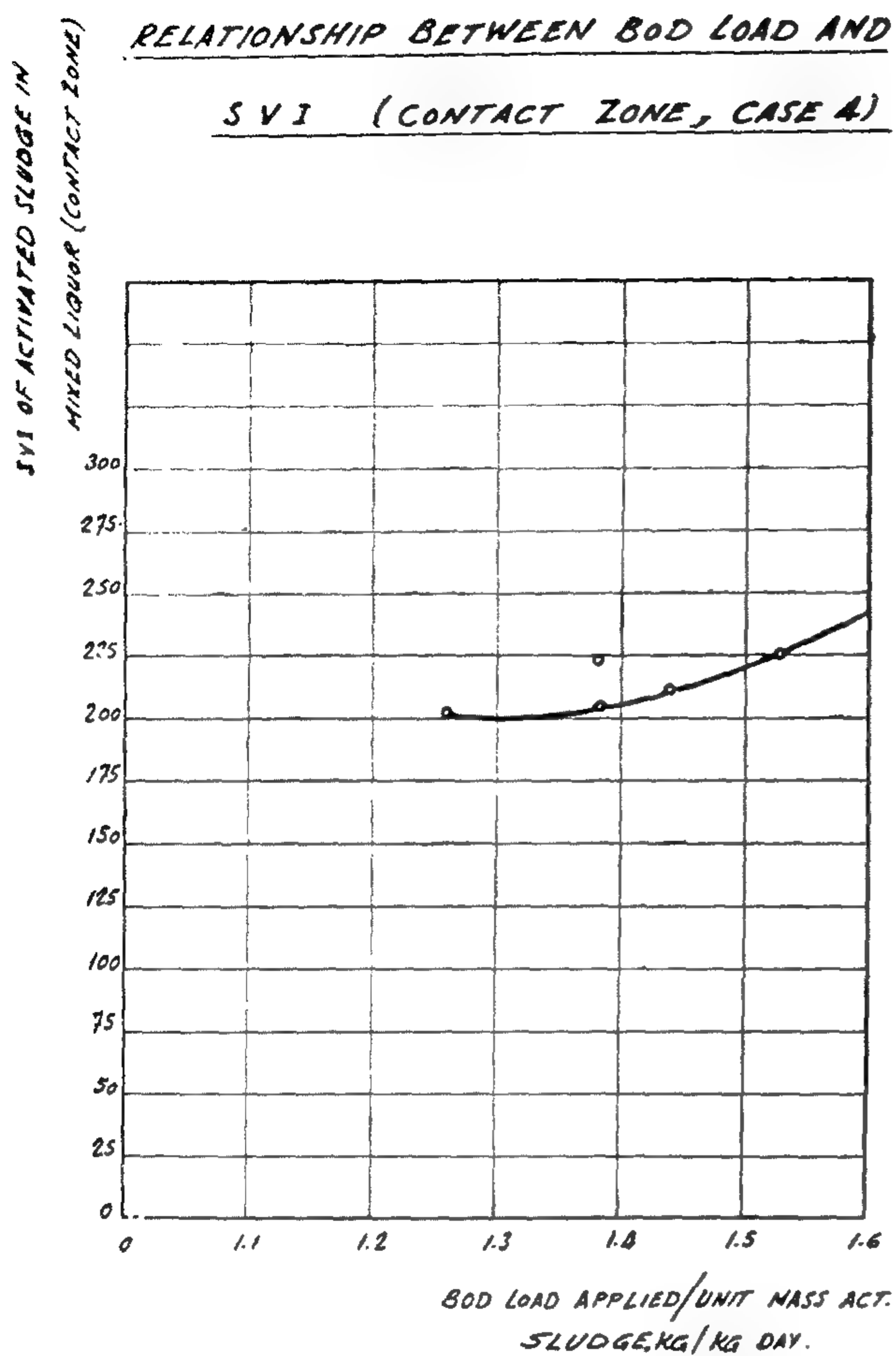


FIG 5

RELATIONSHIP BETWEEN SVI AND BOD
REDUCTION (CASES N° 3 & 4)

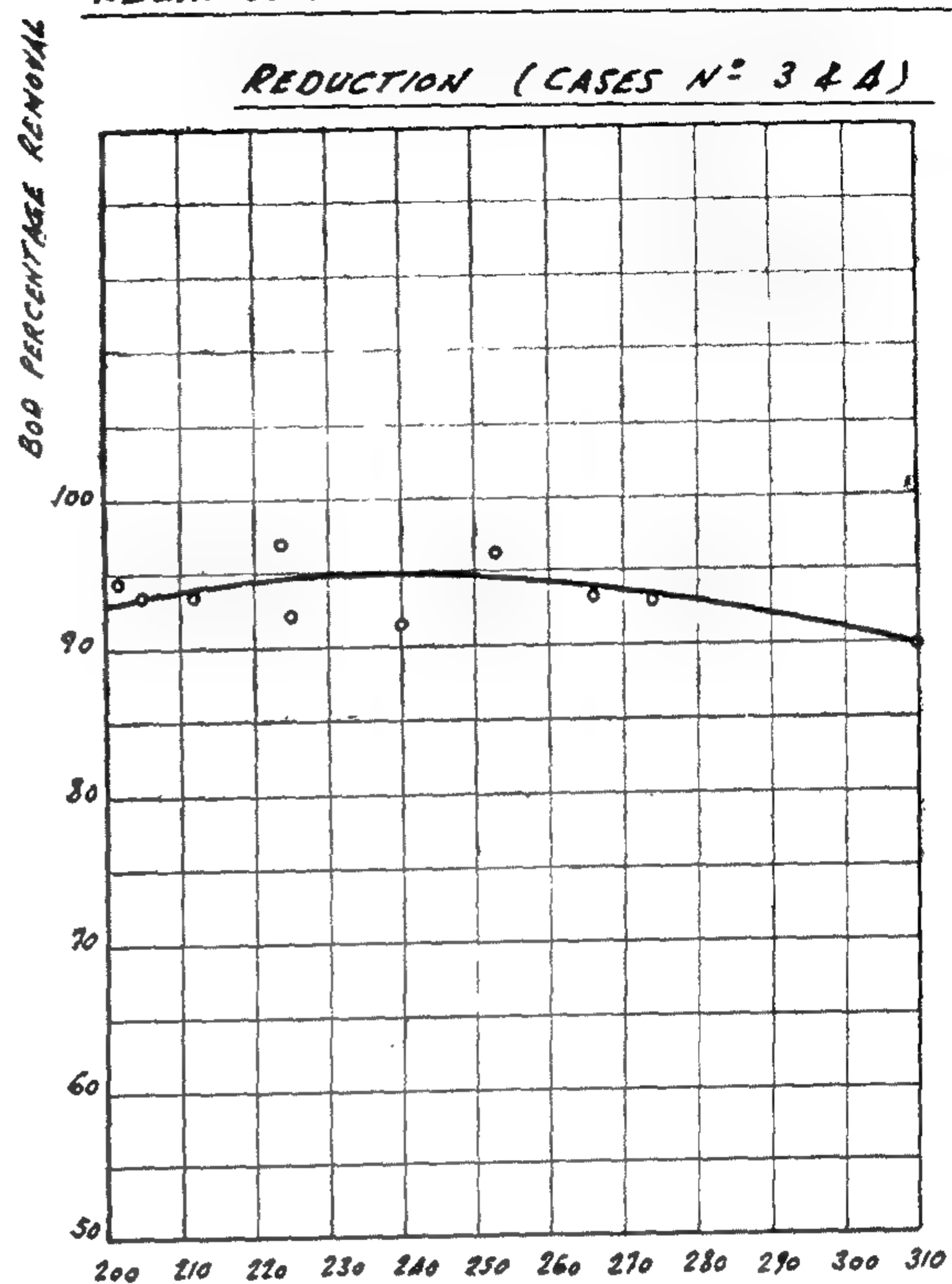
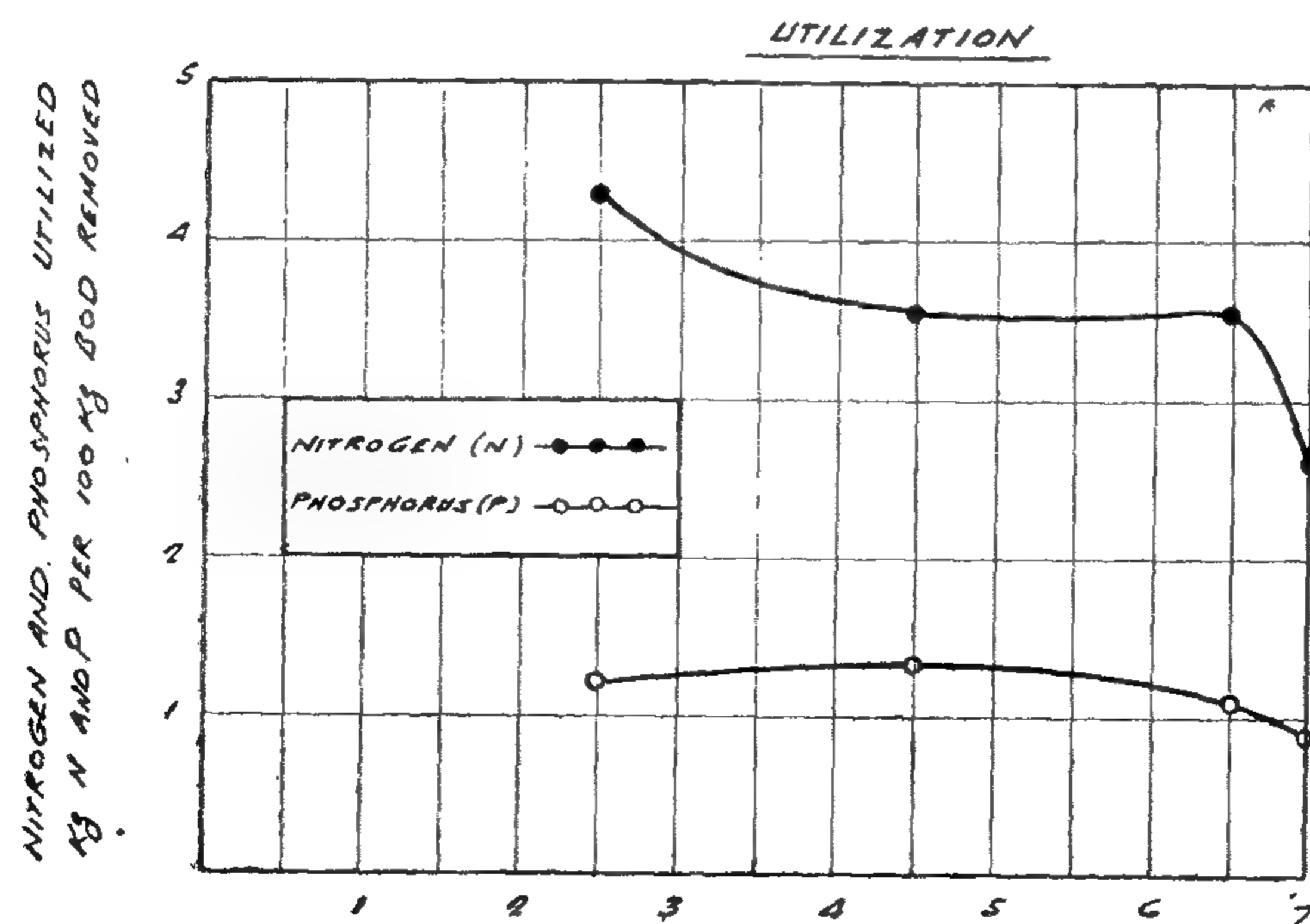


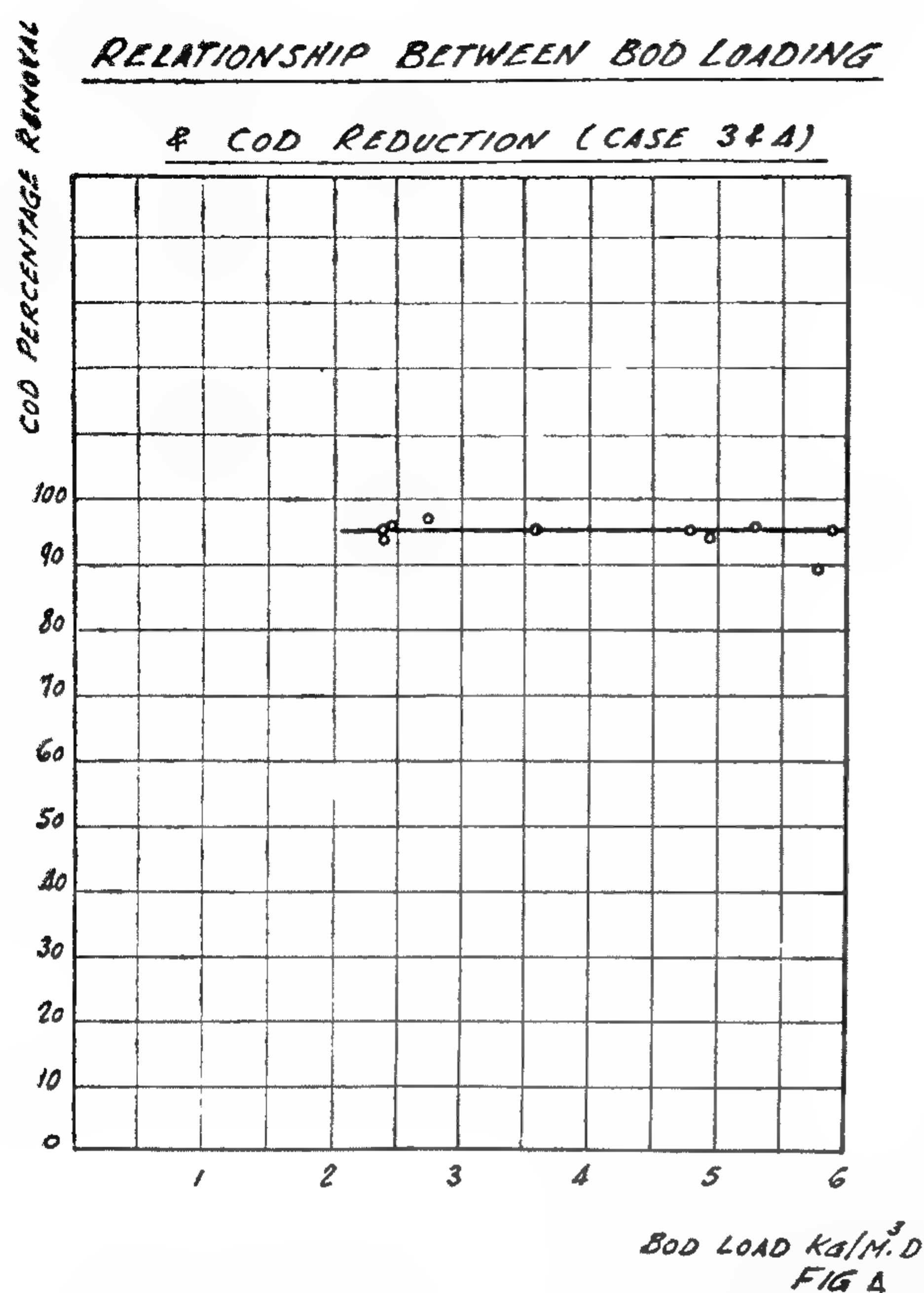
FIG 6 SVI

EFFECT OF THE DETENTION PERIOD ON THE NITROGEN AND PHOSPHORUS



HOURS OF AERATION

FIG 7



graph shown in Flg. (5) is obtained. From this graph, it appears that the sludge volume index of the activated sludge in the contact zone appears to correspond to variations in sludge loadings. Values around 200 ml/g were observed when the sludge load was about 1.26 kg/kg.d. compared to 240 ml/g when the sludge load was around 1.6 kg/kg.d. However, it should be noted that no marked variation was observed over the range from 1.26 to 1.38 kg/kg.d, after which a comparatively marked increase was attained when the sludge load was increased. This indicates that the organism are less tolerant to this load range and react more sharply to any change in the load.

The relationship between sludge volume index and BOD removal is illustrated in Fig. (6). From this graph, it may be seen that the optimum sludge volume index ranges from 230 to 250 ml/g.

(v) Nitrogen and phosphorus requirements

Among the most important variables which occur in the operation of biological treatment units and affect nitrogen and phosphorus requirements are the period of aeration and solids concentration.

(vi) Effect of aeration period

An evaluation of nutrient requirements in terms of BOD removed during the operational conditions showed that the amount of nitrogen and phosphorus required decreases by increasing the hours of aeration (Fig. 7). When a detention period 2.5 hours was used, average nitrogen and phosphorus utilized were 4.3 kg N and 1.16 kg P per 100 kg BOD removed compared to 1.61 kg N and 0.85 kg P at 7 hours aeration. These results are in agreement with those given by Randall (1971) who claimed that if aeration is continued after substrate removal is complete, desorption of phosphorus from sludge will occur.

During extended aeration, the soluble phosphate concentration always increased as a straight line function of aeration time indicating a steady release that would continue until the supply was exhausted. One relationship which is reasonably typical of all plants is that the soluble phosphorus concentration tends to decrease during organic substrate removal and then tends to increase again during subsequent treatment, particularly final settling (Levin and Shapiro, 1965; Randal and King, 1970; Randal. 1971). It is generally agreed when a carbon source is being metabolized that phosphate uptake occurs only utilized by the microorganisms.

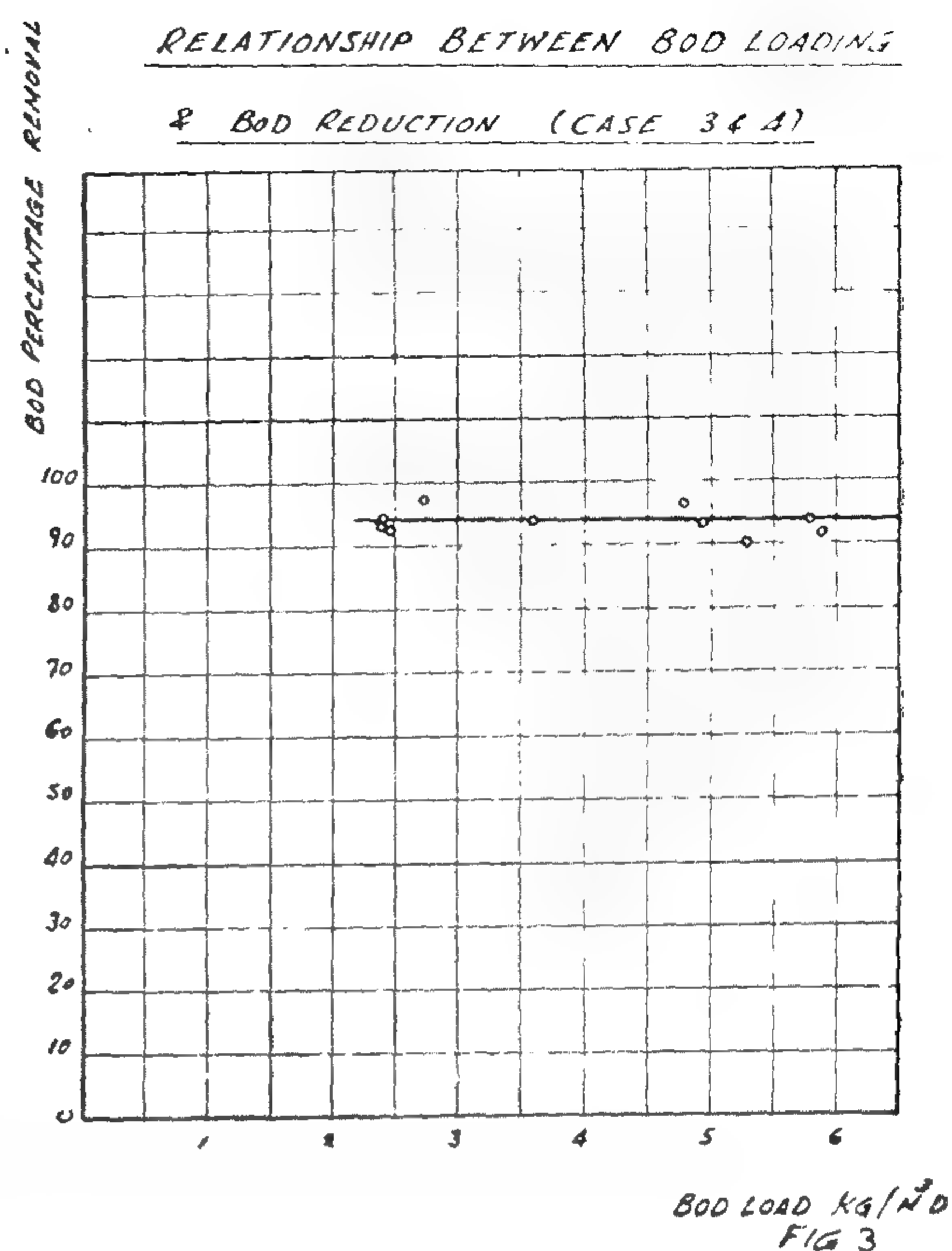
When the relationship between increased hours of aeration in both contact and stabilization zones was plotted against percentage BOD and COD removals, the curves given in Fig. (2) were obtained.

(iii) **Effect of BOD-load on purification efficiency**

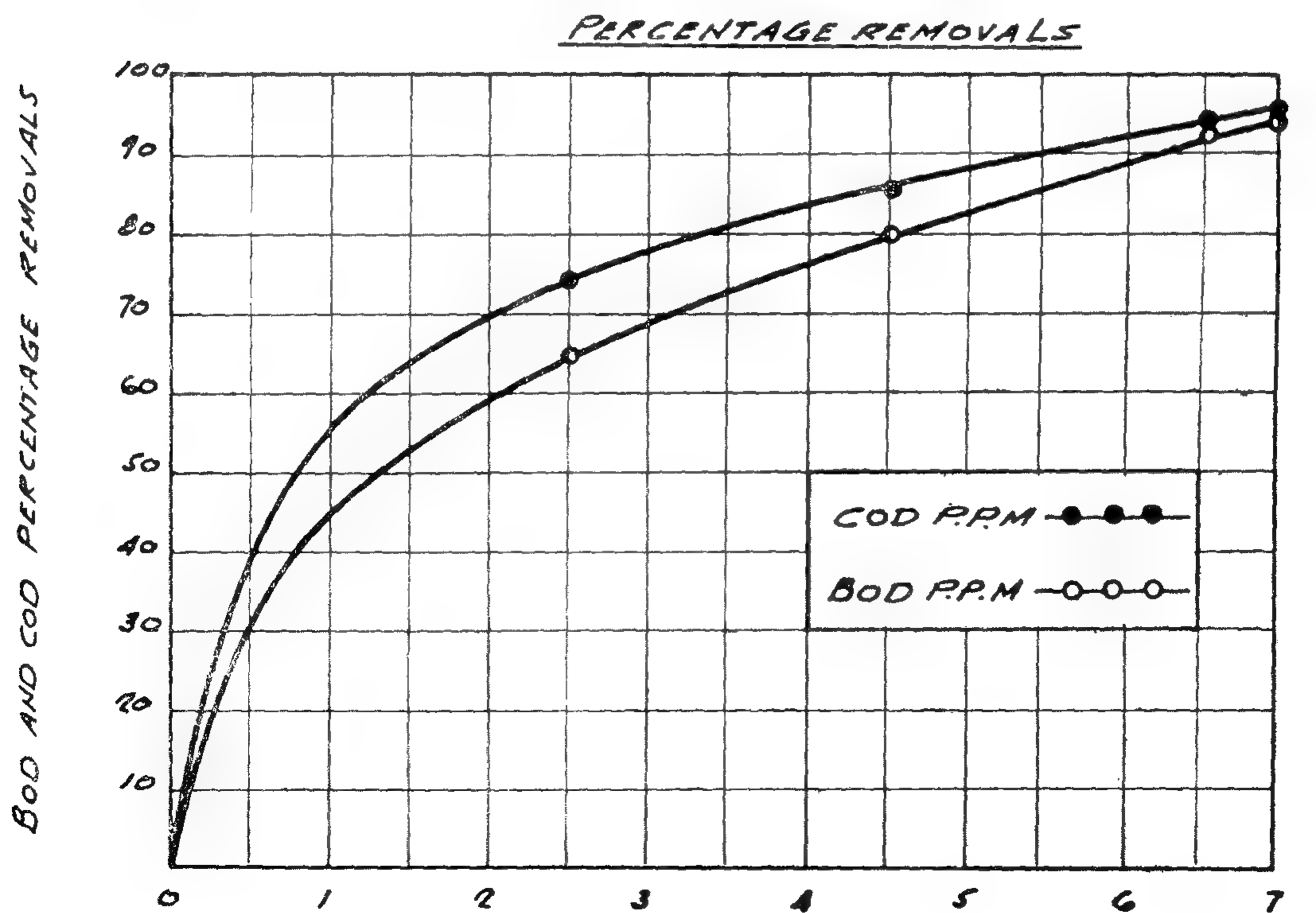
The purification efficiencies in percentage of BOD and COD removed for the last two experimental series were plotted against the loadings fed of the aerator. From Figures (3) and (4), it follows that the purification efficiency does not seem to be affected by changes in the BOD load in the range examined.

(iv) **Effect of sludge loading on sludge volume index**

When the BOD load applied per unit mass of activated sludge is plotted against the sludge volume index, the



RELATIONSHIP BETWEEN HOURS OF AERATION AND AVERAGE BOD AND COD



(ii) Effect of detention period in reaeration zone

Three experimental runs in which different reaeration periods, namely, 2, 4, and 6 hours were carried out. The rate of waste water and of returned activated sludge to the plant were kept constant at about 48 m³/m³.d. The resulting average retention period of mixed liquor in the contact zone was 30 minutes.

From the results recorded in table (3), it could be seen, that when the retention period in the reaeration zone was 2 hours, average BOD removal up to 65% may be recorded. Corresponding removal in permanganate value was 74.3%. However it should be noted that during this period of operation the percentage BOD and COD removal fluctuated somewhat. BOD removal range varied between 56% and 87% while that for permanganate ranged from 70 to 86%.

When the retention period in the reaeration zone was raised from 2 to 4 hours, the BOD and COD removal ratios increased from 65 to 80% and from 74.4 to 85.4% respectively.

With a reaeration time of 6 hours and a contact period of 30 minutes, COD and BOD removals were raised to the order of 94% and 93% respectively.

When the BOD load was changed from 5.35 kg-m³.d to 2.72 kg/m³.d by increasing the detention period in the contact chamber from 30 to 60 minutes and the subsequent decrease of the hydraulic load from 48 m³/m³.d to 24 m³/m³.d, BOD removal up to 94.2% was obtained. Corresponding permanganate value removal was 95.4%. It is important to note that during this period of operation the system operated in a relatively stable manner with respect to effluent COD and BOD.

Table (3)
Average conditions of operation and performance of contact-stabilization plant treating onion dehydrating wastewater

Characters	Time of aeration (hr)	Contact zone	0.5	0.5	1.0
		Stabil. zone	2	4	6
Waste hydraulic load (m ³ /m ³ .d)		24	28	24	12
BOD load (kg/m ³ .d)		5.7	6.23	5.35	2.72
Sludge load (kg/kg.d)		2.54	4.07	2.87	1.4
(Raw)		812	711	625	570
COD(mg KMnO ₄ /l)(Effl.)		208	106	30	26
(% R)		74	85	94	95
(Raw)		237	222	211	223
BOD (mg O ₂ /l) (Effl.)		85	45	15	13
(%R)		65	80	93	94
(Raw)		17	16	17	9
Suspended solids(Effl)		10	1.4	0.8	0.8
(mg/l) (% R)		40	91.5	95.5	91.0
pH-value (Raw)		7.2	7.14	6.9	7.0
(Effl.)		7.1	7.43	7.8	7.7

% R = Percentage Removal

Table (1)

Flow rates and retention periods in contact
stabilization activated sludge plant

BOD- load kg/m ³ .d	Sludge load kg/kg.d	Hydraulic load m ³ /m ³ .d		Periods of retention of liquid (hr)		
		Waste water	Returned sludge	Contact zone	Stabil. zone	Sediment. tank
5.7	2.54	24	24	0.5	2	2.16
6.23	4.07	28	20	0.5	4	2.16
5.35	2.87	24	24	0.5	6	2.16
2.72	1.4	12	12	1.0	6	2.16

III. RESULTS AND DISCUSSION

(i) Waste characteristics

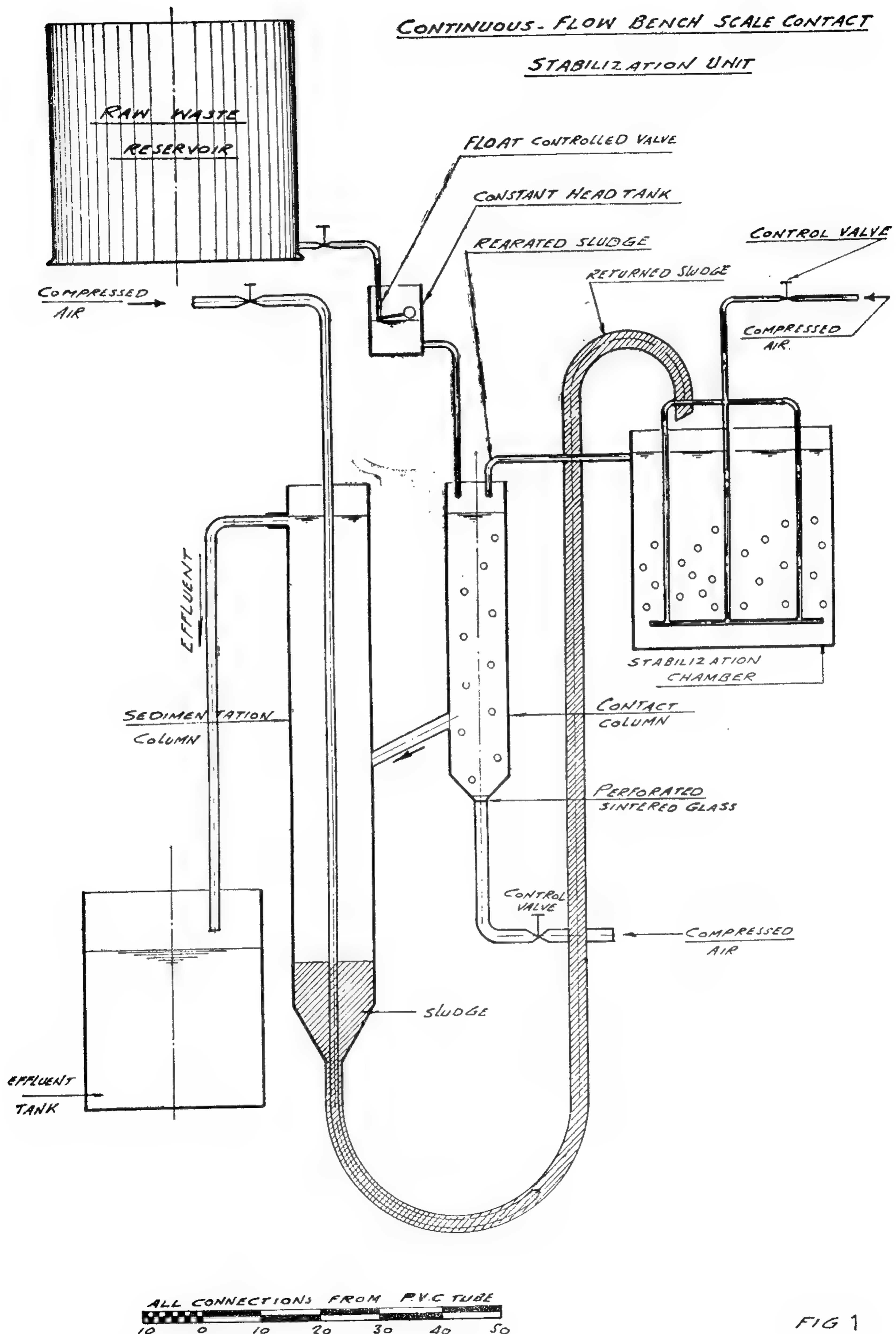
Detailed pollutional characters of the waste are recorded in Table (2). nature of the waste in question indicates the presence of phosphorus in rather low amo-

unts. The ratio of P/BOD may be set as 1 : 280 which is not sufficient to support biological oxidation. The total nitrogen content being around 4 mg/l representing the lowest range for any acceptable biological treatment of a waste having BOD level within the denoted average.

Table (2)

Average character determinations for onion wastewater

Character		Average
pH-value		7.05
COD	(mg KMnO ₄ /l)	712
BOD ₅	(mg O ₂ /l)	238
Ammonia	(mg N/l)	traces
Organic nitrogen	(mg N/l)	3.32
Nitrite	(mg N/l)	traces
Nitrate	(mg N/l)	1.12
Phosphate	(mg P/l)	0.85
Suspended solids, 105°C	(mg/l)	39.30
Suspended solids	(% OVM)	92.7
Total residue, 105°C	(mg/l)	510
Total residue	(% OVM)	65.5



Division of Water Pollution Control
National Research Centre
Dokki, Cairo, U.A.R.

ACTIVATED SLUDGE PROCESS MODIFICATION FOR PHOSPHORUS DEFICIENT WASTES

Dr.-ENG. FATMA A. EL-GOHARY; PROF. Dr.-ENG. A.M. ABDEL-WARITH;
AND ENG. M. SALEH

I. INTRODUCTION :

A well-balanced substrate is necessary to allow unrestricted growth of bacteria cells. However, it has been recognized for several years that many industrial wastes are poorly balanced from a nutritional point of view. Since the supplementation of chemicals containing such salts obviously affects the economics of the treatment process, much work bearing upon the appropriate amount of nutrient supplement for a given strength of waste has been accomplished, (Helmerts, et al., 1951; Helmerts, et al., 1952; Sawyer, 1951; Symons, and McKinney, 1958; Geol and Gaudy, 1969).

It has been reported that the amount of nutrients required is always proportional to the new sludge growth, (Helmerts, et al., 1951 Hall and Engelbrecht, 1967; Jenkins, and Menar, 1967; Sekikafa, et al. 1966). Therefore, if sludge synthesis can be controlled, the nitrogen and phosphorus requirements can be controlled. However, as the total removal is the sum of oxidation and synthesis, the reduction of synthesis necessitates an increase in oxidation, if total removal is to remain the same.

It was therefore decided to investigate the removal of organic material from solution by a low-synthesis high-oxidation, consequently low phosphorus and nitrogen demand system. Contact stabilization as one of the modifications of activated sludge treatment was selected for experimentation. It is a good example of the advantageous use of changes in the physiological properties of microorganisms, (Rich, 1963; and Komolrit, et al. 1967).

II. METHODS OF STUDY

Studies were conducted using nitrogen and phosphorus deficient waste obtained from onion drying industry. A phosphorus deficient waste obtained from onion drying industry. A schematic drawing of the continuous flow bench-scale pilot plant used in this study is shown in Fig. (1). Detention times for sludge stabilization and mixed liquor contact were varied to establish failure levels and peak efficiencies. Sludge from the activation tank was mixed with the raw waste within a volumetric ratio of one part of sludge to one part of onion waste. The detention time in the contact basin was based upon total flow to the separator. Table (1) shows the average ratio of flow and the equivalent periods retention of liquid in the various compartments of the plant.

4. The width of the Nile Valley in Upper Egypt ranges between 7 and 21 kilometers.
5. In places where the porosity of the aquifer is available, Terzaghi empirical formula is found to give good values of permeability.
6. The empirical relation developed by Hazen is noticed to give higher values of permeability than those values obtained from pumping tests. Hazen relation is found to be reduced by a correction value of 0.27 to estimate the average permeability of the aquifer depending only on results of seiving analysis.
7. The permeability coefficient of the semi-permeable silty-clay cap has been determined and found to vary between 0.04 and 5 meters per day.
8. The permeability coefficient of the sand and gravel aquifer has been determined by pumping tests and empirical relations of Terzaghi and Hazen. It ranges between 18 and 85 meters per day.
2. Hashem, A.S., "Effect of the High Dam on the Nile Hydrology and its Relation to Expansion Projects in Arab Republic of Egypt," Vol. II, Government Press, Ministry of Irrigation, Oct. 1972.
3. Hazen, A., "Some Physical Properties of Sands and Gravels with Special Reference to their Use in Filtration". 24th Ann. Rep., Mass. State Bd. Health, Boston, pp. 541-556, 1893.
4. Jacob, C.E., "Flow of Ground Water in Engineering Hydraulics", (H. Rouse Ed.), John Wiley, and Sons, New York, 1950.
5. Kozeny, J., "Das Wasser in Boden, "Grundwasser-bewegung, in Hydraulik, Springer, Verlag., Vienna, 1953.
6. Said, R. "The Geology of Egypt, "Elsevier Publishing Company, Amsterdam — New York, 1962.
7. Terzaghi, C., "Principle of Soil Mechanics, "Eng. New record, Vol. 95, 1925.
8. Willcocks, W., and J.I. Craig, "Egyptian Irrigation", Vol. 1, E. & F. Spon. Ltd., London, 1913.

APPENDIX REFERENCES

1. Attia, M.I., "Deposits in the Nile Valley and the Delta," Government Press, Cairo, 1954.

**TAMLE 2. — COEFFICIENTS PERMEABILITY OF THE
SAND AGUIFER AND SILTY-CLAY FORMATIONS**

Sec. No.	Distance from Aswan, in kms.	k, of sand aquifer, in meters/day	k, of silty-clay, in meters/day
1	115.2	36	0.40
2	242.0	72	—
3	285.8	50	—
4	325.6	31.5	0.15
5	574.0	45	—
6	661.2	35	—
7	143.6	31.5	1.00
8	809.3	24	—
9	838.5	24	—
10	868.0	21	—
11	904.4	20	—

PERMEABILITY OF SILTY-CLAY

TOP LAYER

The auger-hole method is adopted in the field for the measurement of the permeability coefficient of the top silty-clay layer. Two bore holes had been tested at each cross-section to obtain an average permeability value. The simplest method is to dig an auger hole into the soil below the water table. First, the elevation of the water table is determined by allowing the water surface in the hole to reach equilibrium with the soil water. Afterwards, the hole is pumped out to a new lower water level, the rate of rise of water in the hole is then measured. From the measurements, the permeability is calculated by the following relation;

$$k = C \Delta h / \Delta t \quad (9)$$

in which Δ_s is the rise of water during the change in time Δt . The coefficient C has to be determined from known diagrams. Results are listed in Table 2.

CONCLUSIONS

From the study represented in this paper the principal conclusions are summarized as follows :

1. From the geological study, the aquifer is formed of sand and gravel located between an impermeable bed at the bottom and sides, while at the top it is covered with a semi-permeable silty-clay layer.
2. The bed of the Nile is found to cut into the sand and gravel aquifer causing a response between the Nile water and ground water.
3. The average thickness of the top silty-clay layer varies between 6 and 14 meters while the average thickness of the aquifer varies between 18 and 245 meters.

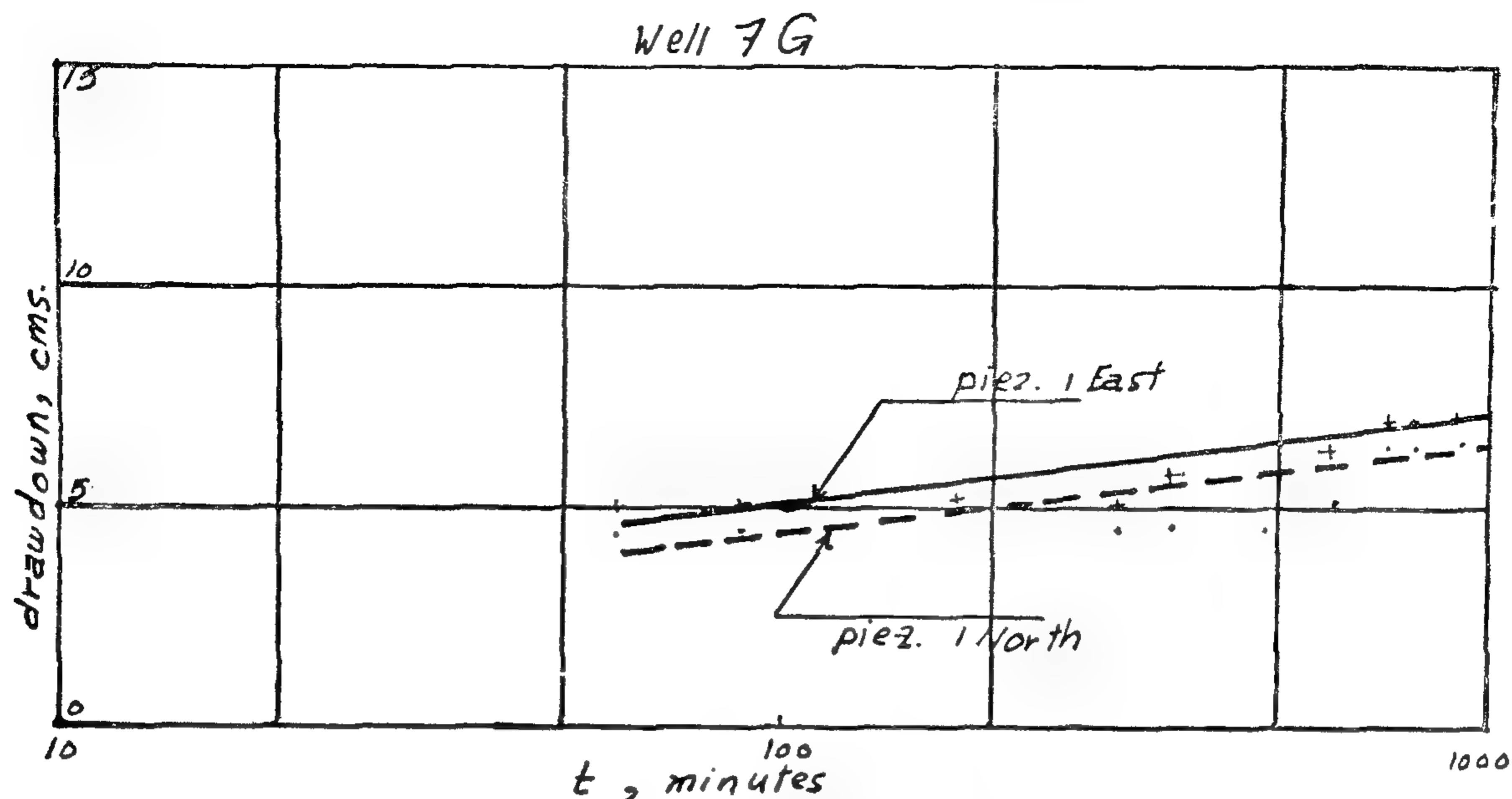


Fig. 5. — Field curve at the pumping well 9G for Jacob method of solution

b) Empirical Relations

The permeability coefficient of the aquifer can be determined approximately by Hazen formula (3) given in the form,

$$k = 1300 d_{10}^2 \quad (6)$$

where, k = sand permeability, in meters/day, and

d_{10} = sieve diameter, in mms, for which 10% by weight of the sand sample is finer.

In places where the porosity of the aquifer is available, the permeability can also be determined by Terzaghi formula (7) reduced in the form,

$$k = 6350 d_{10}^2 \left[\frac{N - 0.13}{3\sqrt{1 - N}} \right]^2 \quad (7)$$

in which k is the permeability in meters per day; d is the effective grain diameter in mms; and N is the porosity. Applying Terzaghi formula given by Eq. 7

for the permeability determination by samples taken from the bore holes 6G, and 9G results are obtained as follows :

$$k = 60 \text{ m/day; at well No. 6G}$$

$$k = 74.5 \text{ m/day; at well No. 9G}$$

which are in good agreement with those values obtained from pumping tests. For the same samples the permeability was also determined by Hazen formula which gave higher values. This means that Hazen equation must be reduced by a correction factor. As a result, the permeability has been determined using both Terzaghi and Hazen formulae at many other deep borings. From these values a graphical correlation was plotted between the permeability values obtained by Eq. 6 and that by Eq. 7. The corrected form of Eq. 6 is reduced in the following relation

$$k = 350 d_{10}^2 \quad (8)$$

Results of permeability values are listed in Table 2.

in which s = drawdown in the observation well; Q = discharge; T = transmissivity $k.B$; k = permeability; B = thickness of aquifer; S = storativity; r = distance between pumping well and observation well; and t = time since beginning of pumping. For an observation well as a particular distance, one can demonstrate from Eq. 2 that :

$$s_2 - s_1 = \frac{Q}{4\pi T} \ln \frac{t_2}{t_1}$$

$$\text{or } s_2 - s_1 = \frac{2.3 Q}{4\pi T} \log \frac{t_2}{t_1} \quad \dots (3)$$

in which s_1 and s_2 are the values of drawdown at times t_1 and t_2 , respectively. When s is plotted against time on semi-logarithmic paper, the relation will be a straight line. If s_1 and s_2 are chosen for one logarithmic cycle, $\log t_2/t_1 = 1$.

In this this case, Eq. 3 will be simplified as

$$\Delta s = (s_2 - s_1) = \frac{2.3 Q}{4\pi T} \quad (4)$$

From which

$$k = \frac{2.3 Q}{4\pi \cdot b \cdot \Delta s} \quad (5)$$

After the measured data had been adjusted by the correction factor given by Eq. 1, they were plotted on semi-logarithmic paper, as shown in Figs. 4 & 5. Results of the permeability are obtained as follows :

$k = 64$ meters/day, at pumping well No. 6 G.

and

$k = 82$ meters/day, at pumping well No. 9 G.

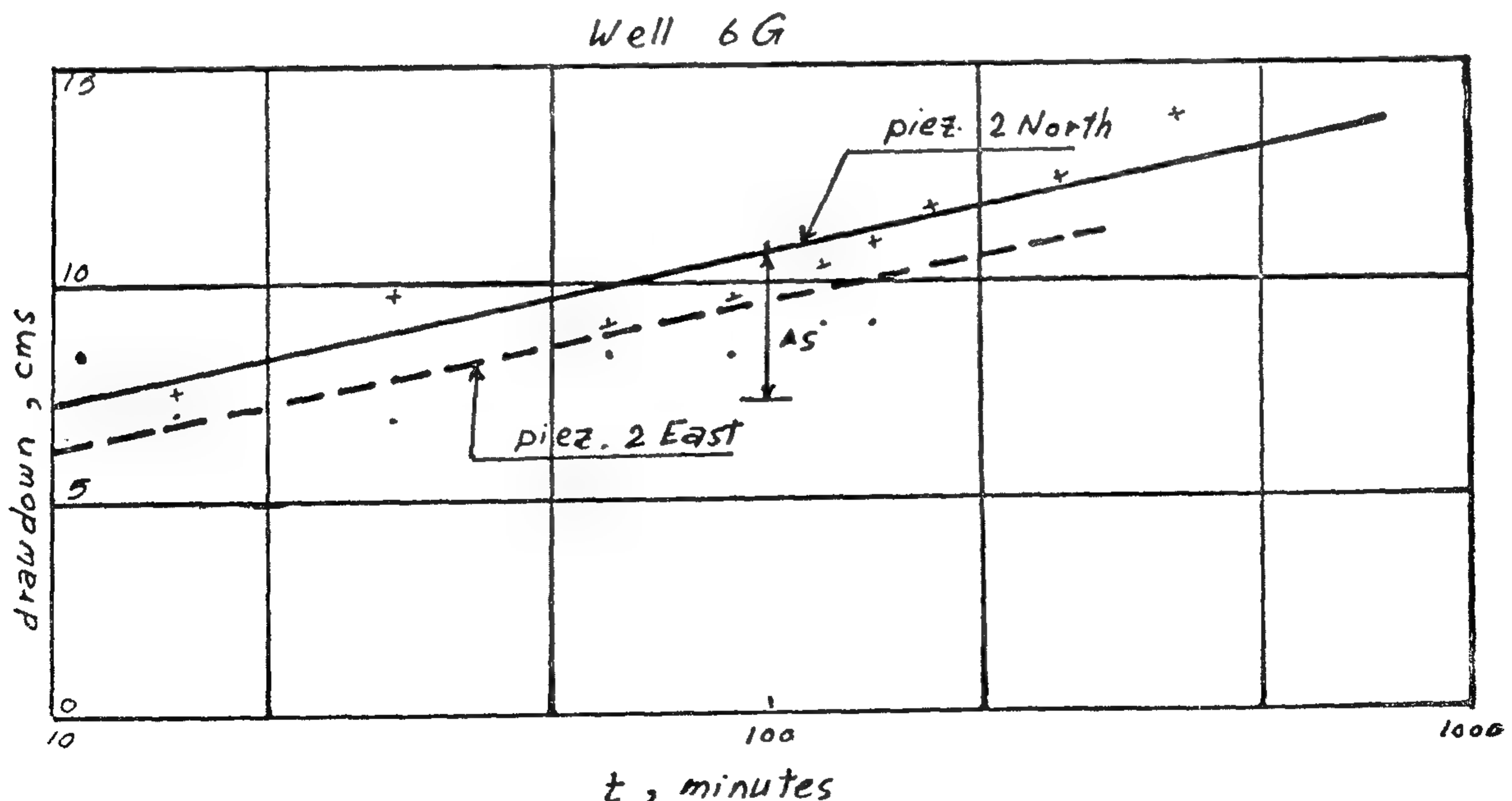


Fig. 4. Field curve at the pumping well 6G for Jacob method of solution

TABLE 1. — AVERAGE DIMENSIONS OF THE AQUIFER AS DETERMINED FROM THE TRANSVERSAL SECTIONS

Sec. No.	Dist. from Aswan, in kilometers	Thick. of top silty — clay layer, in meters	Thick. of aquifer, in meters	Total width of valley, in kilometers
1	115.2	8	20	6.5
2	242.0	12	70	11.5
3	285.8	8	75	8.5
4	325.6	14	62	13.0
5	574.0	10	110	10.0
6	661.2	12	170	18.5
7	743.6	12	140	18.5
8	809.3	8	100	13.5
9	838.5	8	85	10.0
10	868.0	10	26	8.5
11	904.4	14	50	7.0

PERMEABILITY OF THE AQUIFER

The permeability of the sand and gravel aquifer has been evaluated in the field using results of pumping tests available at two locations only. It is well known that many empirical formulae are developed for determination of the permeability based on the pore-size distribution of the soil. Application of these empirical relations was also made at the same pumping tests using relations proposed by Terzaghi and Hazen. Hazen equation has been adjusted for use at other places for determination of permeability by means of sieving analysis.

Measurements were available from pumping tests at two locations, namely: deep boring No. 6 G at Istal in El-Minia Province and deep boring No. 9 G at Sanabo in Assuit Province. A network of 6 piezometers were installed around each pumping well, 3 piezometers to the north and 3 piezometers to the east at distances 5, 15 and 40 meters from the well. Readings were taken during the non-steady flow conditions of drawdown and recovery tests. A full record of the

elapsed time and drawdowns were recorded.

Since the wells were partially penetrating the aquifer, the recorded values of drawdowns were first corrected according to Kozeny (5) approach. His correction factor is given in the form,

$$\eta = \frac{S_f}{S_p} = \frac{1}{\left[1 + 7 \sqrt{\frac{r_w}{2b}} \cos \frac{\pi b}{2B} \right]} \quad (1)$$

in which S_f = drawdown in a fully penetrating well; S_p = drawdown in a partially penetrating well; b = depth of partial penetration of pumping well in the aquifer; B = the aquifer thickness, and r_w = well radius.

For pumping well No. 6 G, it is found that $Q = 2450$ m³/day; $r_w = 0.10$ m; $b = 25$ m; $B = 200$ m; and $\eta = 0.69$. Also for pumping well No. 9 G, it is found that $Q = 2568$ m³/day; $r_w = 0.10$ m; $b = 31.40$ m; $B = 240$ m; and $\eta = 0.64$. All measured drawdowns were first reduced by the correction factors before being used in Jacob approach (4) represented by solving the following modified relation

$$s = \frac{Q}{4\pi T} \ln \frac{2.25 T t}{r^2 S} \quad (2)$$

surface with nearly uniform thickness, while it vanishes at the far ends of the valley giving place to the sand formation to appear. The thickness of the aquifer is always bigger in the west.

7. From Naga Hammadi to the south of Sohag, between kilometer 358 and kilometer 415 from Aswan, the plain is narrow in the east where the limestone hills approaches the river. Formations of sand and gravel underlie the top silty layer with maximum thickness near the river channel, vanishing at both sides of the valley where the limestone formations appear at the surface.

8. At Akhmim, the width of the valley becomes bigger in the western side. Going northward to Assuit, the bounding cliffs sometimes approach the river channel from the east. The aquifer has a maximum thickness of 150 meters. Clay layers are bounding the aquifer from the bottom, while limestone cliffs are bounding it from the sides.

9. At Abnub, 18 kilometers north of Assuit, the eastern valley valley is wide due to change in the regime of the Nile channel. Northward at Qusiya, 35 kilometers north of Assuit, the eastern cliffs are approaching the river and the plain extends to the west.

10. From Dairut to Samallut, between kilometer 605 and kilometer 709 from Aswan, the eastern side nearly vanishes and the river washes the limestone cliffs. The valley extends to the west with an average width of 12 kilometers. The aquifer takes more or less an oval shape with a maximum thickness of 230 meters at the middle of the plain. Clay formations are bounding the aquifer at the bottom, while limestone hills are bounding it from both sides.

11. From Beni Mazar to south of Maghaga, kilometer 728 to kilometer 744 from Aswan, the eastern cliffs are far from the river. The western plain is very wide compared to that of the east. It is underlain with the sand and gravel aquifer having an average thickness of 260 meters. Limestone formations appear at the surface bounding the plain from the sides.

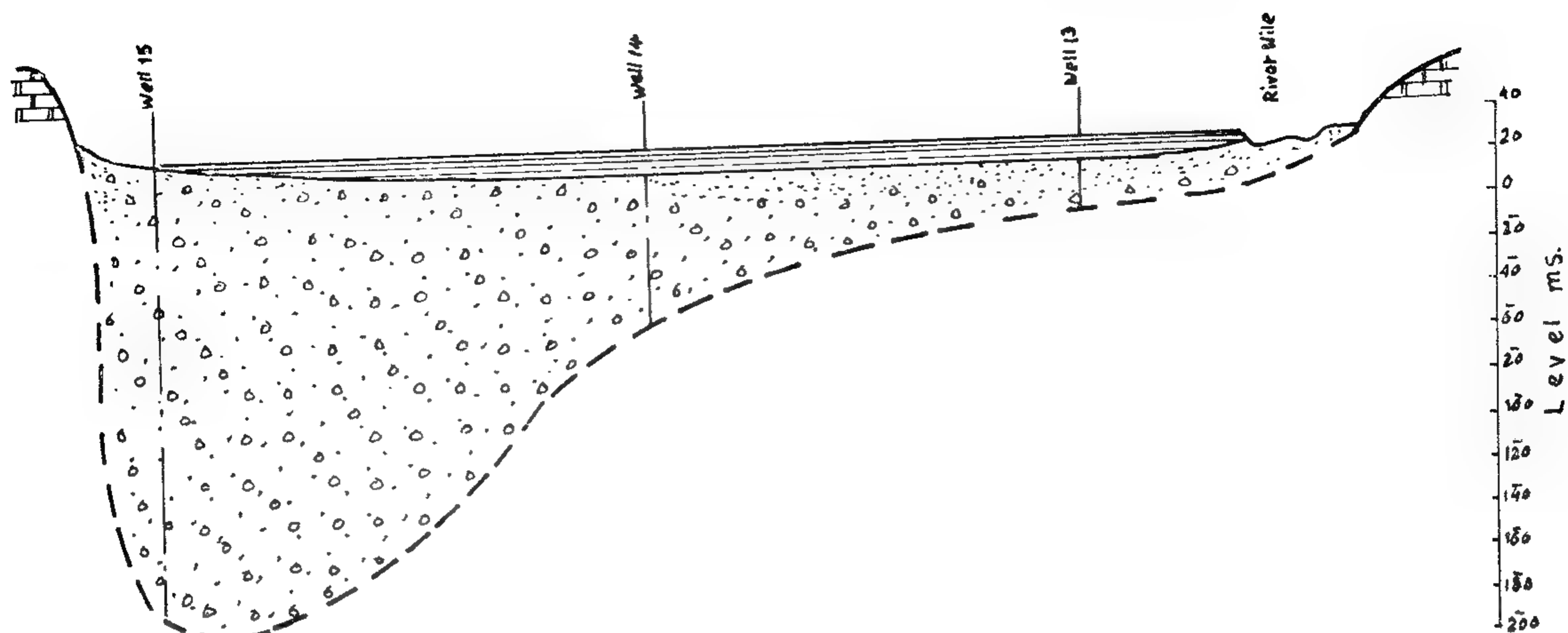
12. From Maghaga to Beni-Suef, kilometer 755 to kilometer 799 from Aswan, the eastern valley vanishes again giving place to limestone formations. Silty-clay layer exists at the surface of the western plain for a big length, then vanishes towards the far end giving place to sand transported from the desert to appear. The aquifer takes again an oval shape with a maximum thickness of 250 meters. Limestone formations are bounding the valley from both sides.

13. Between Beni-Suef and El-Wasta, kilometer 799 to kilometer 820 from Aswan, the Aquifer still has an oval shape with a thickness of 170 meters in the middle of the western plain. Limestone formations are bounding the valley from the west, while the river is washing the limestone cliffs in the east.

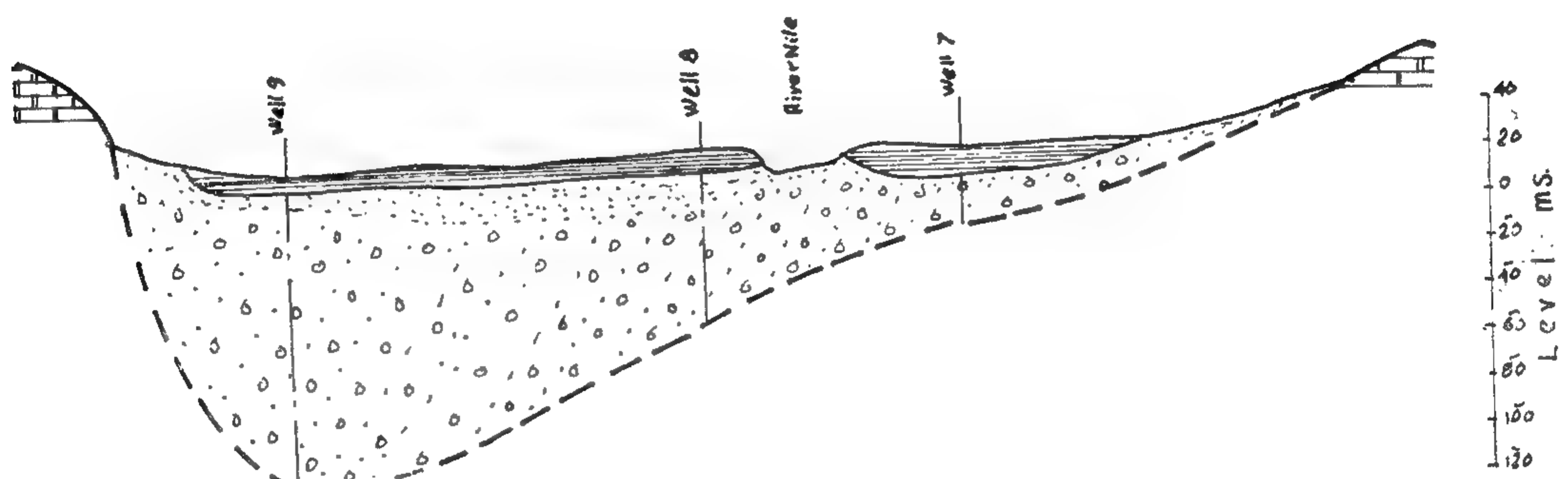
14. From El-Wasta to Giza, kilometer 820 to kilometer 910 from Aswan, the plain extends on both sides of the river having a big width in the west. The silty-clay cap appears at the surface with an average thickness of 20 meters. The aquifer underlies both sides of the valley being confined at the bottom by clay formations and limestone cliffs from both sides.

Based on these cross-sections, the average dimensions of the aquifer are determined and listed in Table 1.

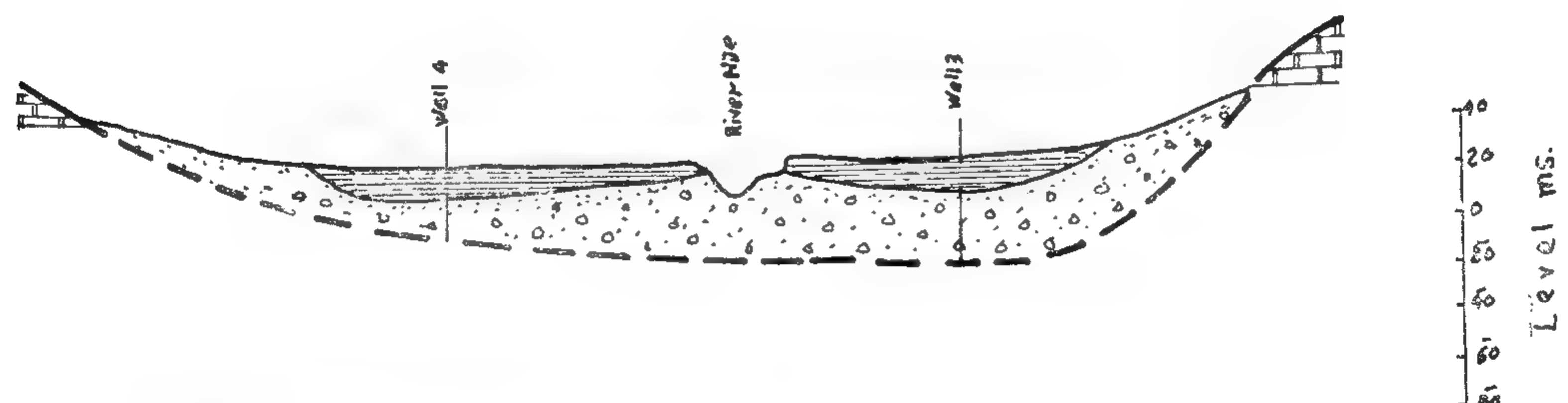
CROSS SECTION № 8, km 809.3



CROSS SECTION № 9, km 838.5



CROSS SECTION № 10, km 868.0



CROSS SECTION № 11, km 904.4

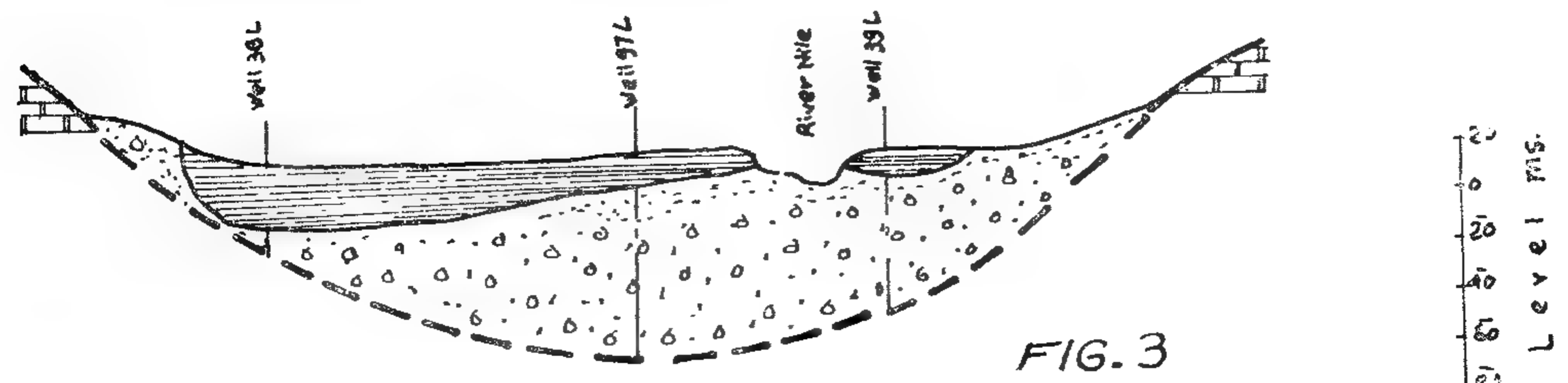
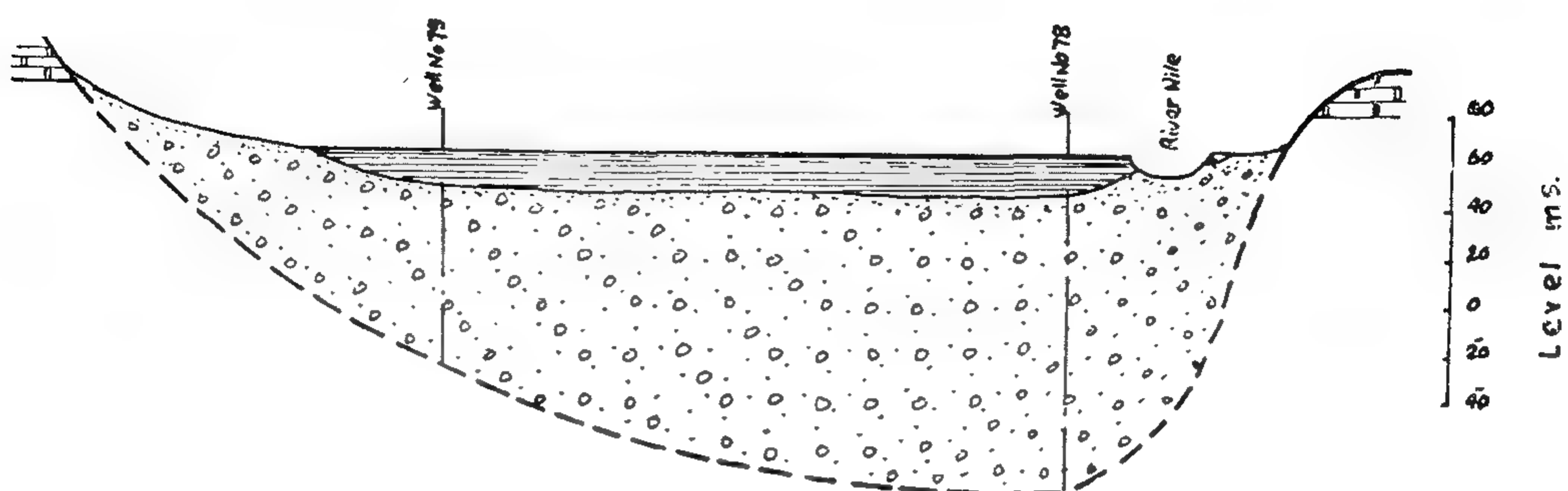
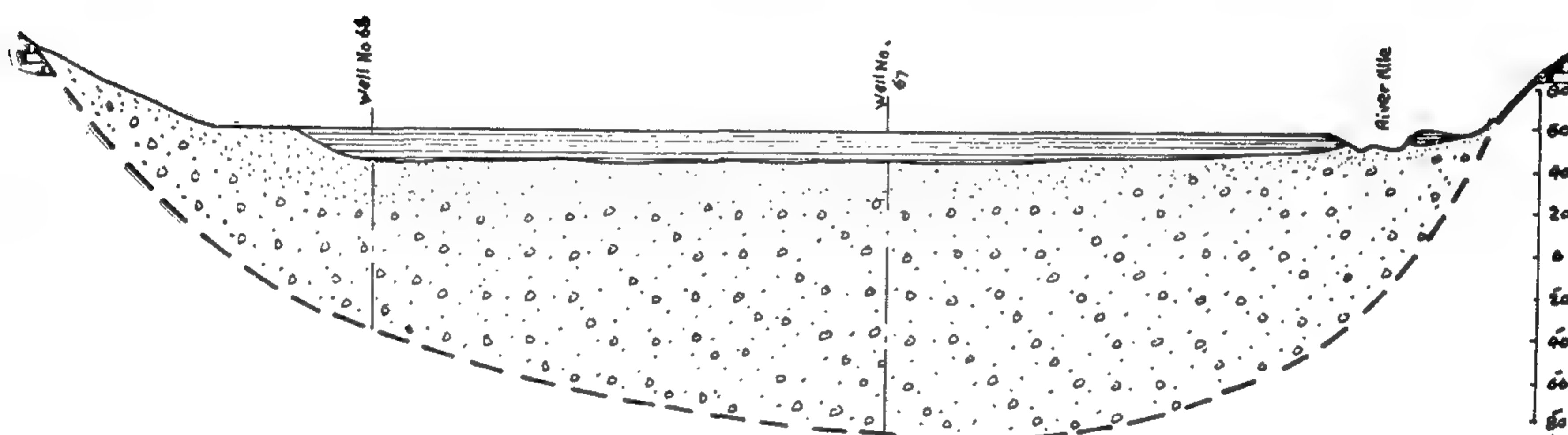


FIG. 3

CROSS SECTION N° 5, km 574.0



CROSS SECTION N° 6, km 661.2



CROSS SECTION N° 7, km 743.6

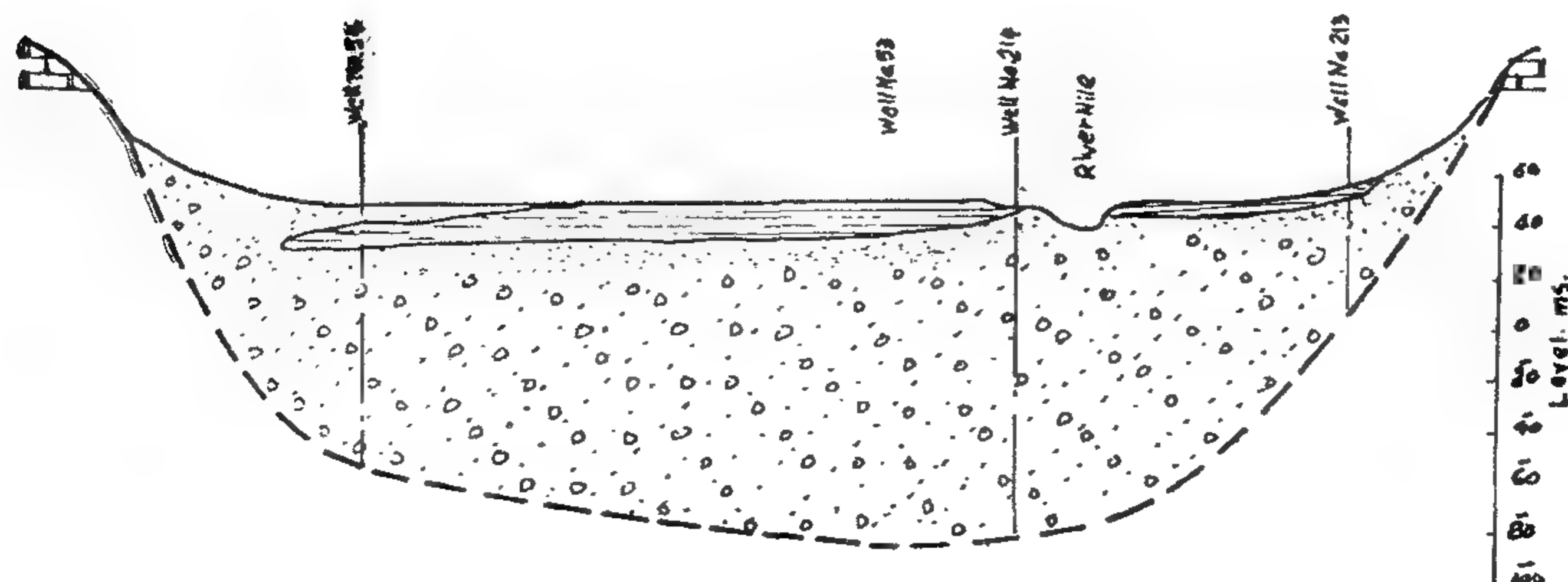
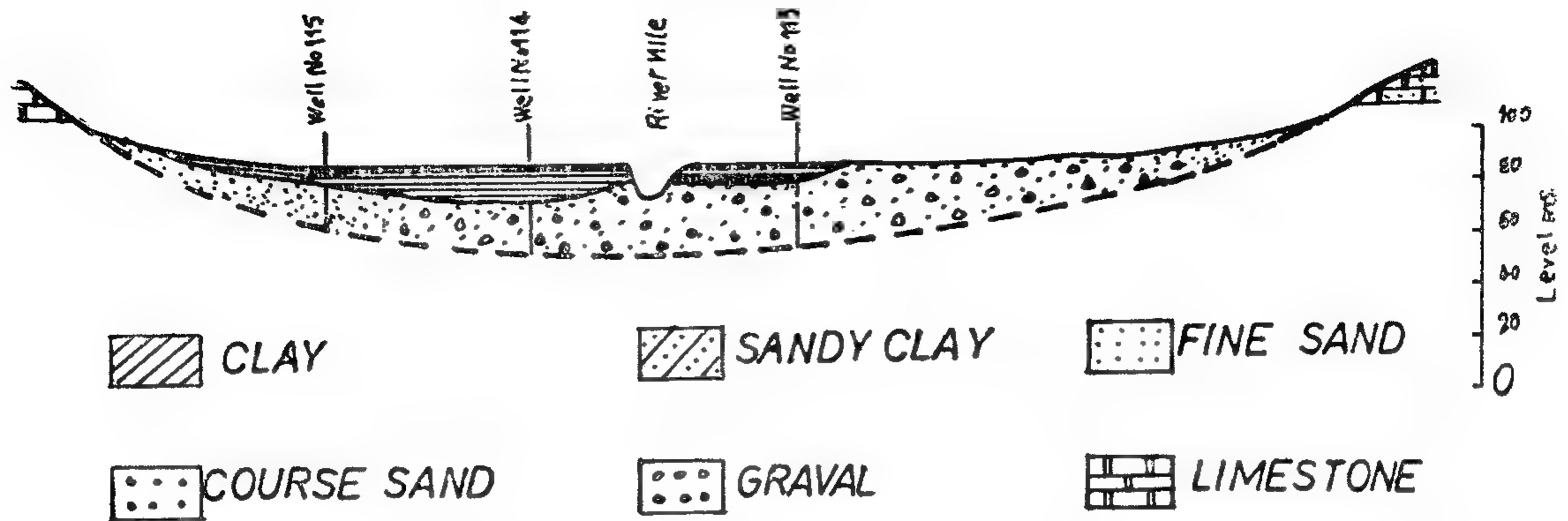
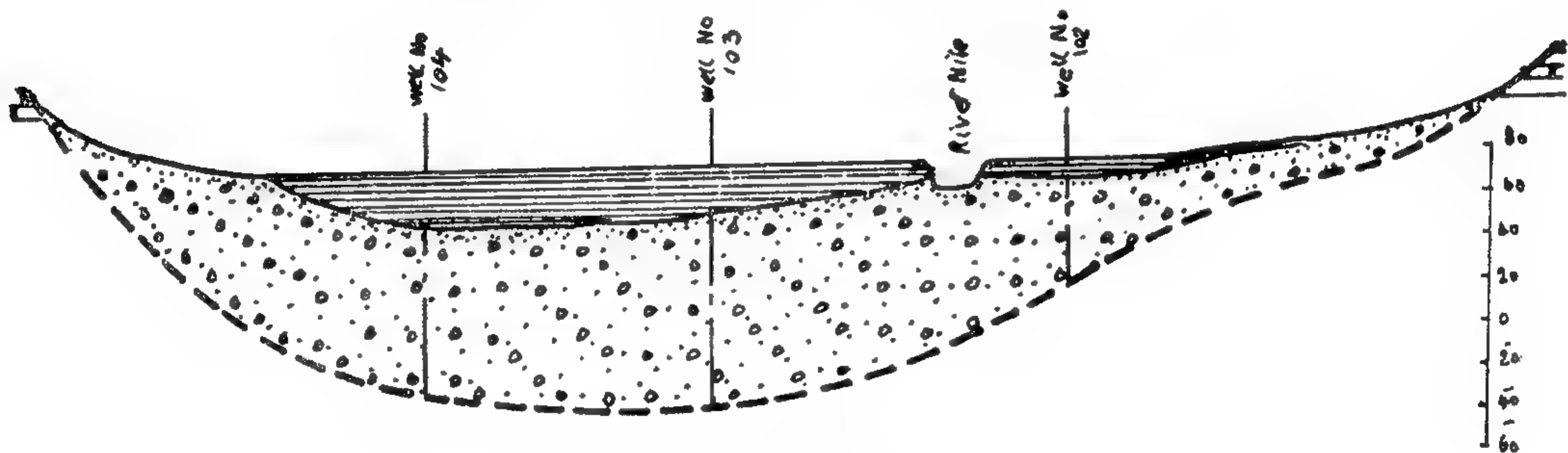


FIG. 2

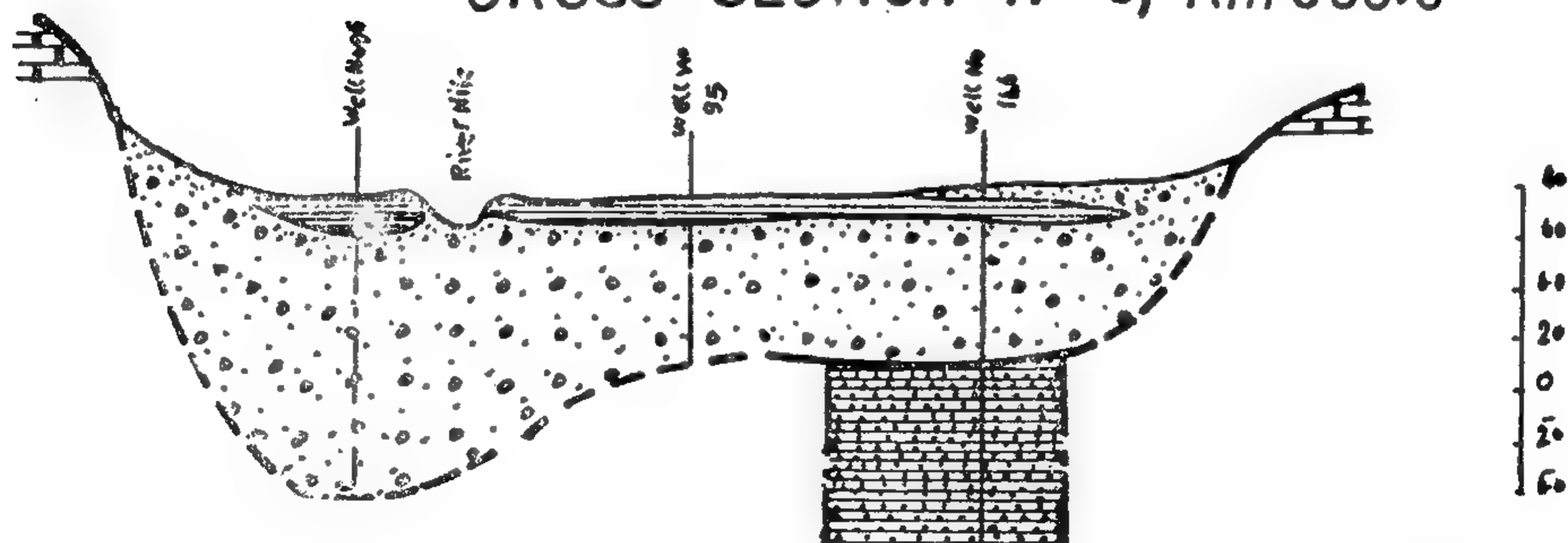
CROSS SECTION N° 1, Km 115.2 from Aswan



CROSS SECTION N° 2, Km 242.0



CROSS SECTION N° 3, Km 385.3



CROSS SECTION N° 4, Km 325.6

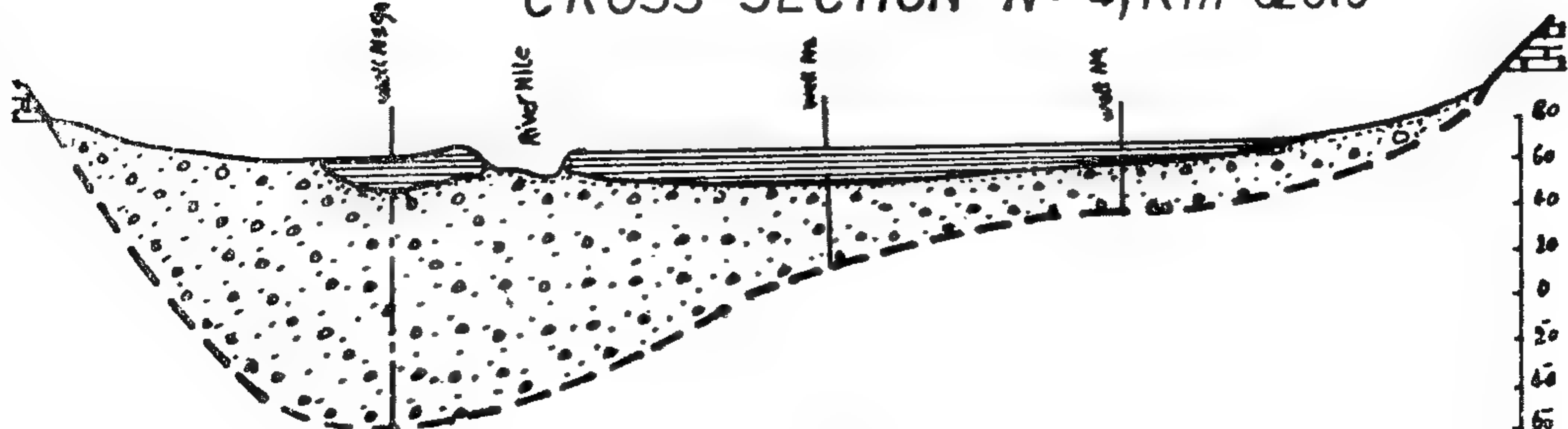


FIG. 1

ducted by examining the specimens of old borings available at the Geological Survey Museum. He made some more borings to obtain an approximate picture of the different formations and their continuity.

In 1962, Said (6) made a geological study of the Nile Valley of Upper Egypt. He confirmed that the Nile River would probably be eroded on a line of faulting and rifting. In 1966, Hashem (2) gave a brief survey of the geological characteristics of Upper Egypt through longitudinal and transversal sections showing the lithology of the groundwater reservoir. His study had been based on deep borings explored in the Nile Valley by the Ground-Water Research Office initiated in 1953 by the Ministry of Irrigation.

GEOLOGICAL ANALYSIS OF NILE VALLEY

In order to determine the type and extent of the ground water bearing formations in Upper Egypt between Aswan and Cairo, it has been necessary to start with collecting data concerning the various bore holes. The principal sources of data were available at the Ground-Water Research Office of the Ministry of Irrigation and the Geological Survey Department of the Ministry of Industry.

From the details of the bore loggings of the available data, it has been possible to draw four longitudinal sections in the eastern and western sides of the river. In addition, fifty-one transversal sections perpendicular to the Nile channel have been drawn to give a fairly clear idea about the lithology of the Nile Valley. With regard to the longitudinal sections, the bottom end of the aquifer has been estimated on the basis of data of deep borings. The same results have been introduced for use in tracing the transversal sections. Examples of traced sections are shown in Figs. 1, 2, & 3.

Geological results from the sections of the Nile Valley between Aswan and Cairo are summarized as follows :

1 Along the eastern bank between Aswan and Assuit, the silty-clay top layer has smaller thickness than that in the west.

2. At Kom Ombo, 60 kilometers north of Aswan, the plain extends 15 kilometers to the east of the river, while the sandstone formations bound the river from the west. The sand and gravel formations exist only below the silty-clay top layer of the eastern valley with a maximum thickness of 27 meters in the middle of the plain.

3. At Edfu, 115 kilometers north of Aswan, the Valley extends on both sides of the river. The silty-clay top layer covers the western plain to a distance of about 4.5 kilometers from the river channel and with a maximum thickness of 14 meters. In the east, the silty-clay top layer covers only a length of about 1.5 kilometers. The aquifer extends under both sides with a maximum thickness of 22 meters.

4. Going northward, the width of both the Nile Valley and the silty-clay become smaller giving place to the fine sand transported from the desert. The thickness of the aquifer becomes bigger with a maximum value of 95 meters under the western plain.

5. To the north, 16 kilometers from Isna barrage, the eastern plain sometimes vanishes giving place to the limestone hills to appear. Northward, the silty-clay on both sides of the Nile with bigger width in the west.

6. From Qus to the south of Naga Hammadi, between kilometer 256 and kilometer 325 from Aswan, the western plain becomes narrower than that of the eastern plain and vanishes sometimes. The silty-clay layer appears always at the

CHARACTERISTICS OF THE GROUND WATER RESERVOIR IN UPPER EGYPT

By

Dr. MOHAMED HAMDY EL-KATEB, Ph. D¹, and

FATMA ABDEL — RAHMAN, M.Sc.²

INTRODUCTION

Full use of water resources can be increased by operating the ground-water basins in coordination with storage of surface water to meet the growing water demands. The greater the detailed knowledge of the ground-water reservoirs, the more effectively and efficiently ground water can be developed and utilized. The water resources are not successfully managed if only the Nile water is considered and the ground water resources are neglected. In fact, the study of ground water in Upper Egypt has had too little attention.

The study represented in this paper is concerned with the ground water reservoir in Upper Egypt between Aswan and Cairo. Its better understanding can assist in solving the additional problem of drainage. The cultivated land in large areas has been water logged because of excessive irrigation after the conversion from basin to perennial irrigation. It is obvious that pumping the ground water can be useful in certain cases for developing irrigation water and at the same time draining the land. The use of the tile drainage system may not provide a feasible means of drainage, specially where the silty-clay layer overlies an artesian aquifer.

The objective of this study is to obtain complete information of the ground-water basin in Upper Egypt by knowledge of its geology, geometry and its physical properties such as the permeability coefficient of the aquifer.

PREVIOUS INVESTIGATIONS

It is of great importance to review all the literature that pertains to the geological characteristics of the different formations of the Nile Valley between Aswan and Cairo. Although some investigations have been conducted in the past, there is little information in the literature on the ground-water reservoir in Upper Egypt.

In 1913, Willcocks and Craig (8)³ discussed briefly the geologic formations of the Nile Valley as a basis for the study of the ground water basin. They stated that away from the river, the top clay attains a considerable thickness and the sand cannot be reached till a depth of 10 meters.

In 1954, Attia (1) made an investigation for the sediment deposits in the Nile Valley. His study had not been purely geological and academic, but it aimed to an economic subject. His work was con-

1. Assist. Prof. of Irrig. Eng., Cairo Univ., Giza, Arab Republic of Egypt.

2. Civil Engineer, Ground-Water Research Office, Ministry of Irrig., Cairo, Arab Republic of Egypt.

3. Numerals in parentheses refer to corresponding items in the Appendix-References.

BUILDING & CONSTRUCTION

**INSTITUTION OF CIVIL ENGINEERS
INSTITUTION OF ARCHITECTS
INSTITUTION OF IRRIGATION ENGINEERS**

التصنيع والانتاج

جمعية المهندسين الكهربائيين
والإلكترونيين

جمعية الهندسة الإدارية
جمعية المهندسين الميكانيكيين

- AIEE, Vol. 75, pt. III, pp. 1321-1329, 1956.
6. Aylett, P.D.: "The Energy-Integral Criterion of Transient Stability Limits of Power Systems", *Proc. IEE*, Vol. 105, pt. C, pp. 527-536, 1958.
 7. Dyrkacz, M.S., and Lewis, D.G. : "A New Digital Transient Stability Program", *Trans. AIEE*, Vol. 78, pt. III, pp. 913-919, 1959.
 8. Lane, C.M., Long, R.W., and Powers, J.N. : "Transient-Stability Studies, II", *Trans. AIEE*, Vol. 78, pt. III, pp. 1291, 1959.
 9. Rindt, L.J., Long, R.W., and Byerly, R.T. : "Transient Stability Studies, Part III, Improved Computational Techniques", *Trans. AIEE*, Vol. 78, pt. III, pp. 1673-1677, 1959.
 10. Dyrkacz, M.S., Young, C.C., and Maginniss, F.J.: "A Digital Transient Stability Program Including the Effects of Regulator, Exciter, and Governor Response", *Trans. AIEE*, Vol. 79, pt. III, pp. 1245-1257, 1960.
 11. Fitzgerald, A.E., and Kingsley, C. : "Electric Machinery", 2nd ed., McGraw-Hill, New York, 1961.
 12. Miles, J.G.: "Analysis of Overall Stability of Multimachine Power Systems", *Proc. IEE*, Vol. 108, pt. A, pp. 203, 1961.
 13. Gupta, P.P., and Humphery Davies, M.W.: "Digital Computers in Power System Analysis", *Proc. IEE*, Vol. 108, pt. A, pp. 383, 1961.
 14. Dharma Rao, N. : "A New Approach to the Transient Stability Problem", *Trans. AIEE*, Vol. 81, pp. 186-190, 1962.
 15. Taylor, D.G. : "Analysis of Synchronous Machines Connected to Power System Networks", *Proc. IEE*, Vol. 110, pt. C, pp. 606, 1963.
 16. Dharma Rao, N., and Ramachandra Rao, H.N. : "Phase-Plane Techniques for the Solution of Transient Stability Problems", *Proc. IEE*, Vol. 110, pt. C, pp. 1451-1461, 1963.
 17. Dienneley, J.L., and Kennedy, M.W. : "Influence of Governors on Power System Transient Stability", *Proc. IEE*, Vol. 111(1), pp. 98-106, 1964.
 18. Dharma Rao, N., and Ramachandra Rao, H.N. : "Solution of Transient Stability Problems Through the Number-Series Approach", *Proc. IEE*, Vol. 111(4), 1964.
 19. Humpage, W.D., and Stott, B. : "Effect of Autoreclosing Circuit Breakers on Transient Stability in E.H.V. Transmission Systems", *Proc. IEE*, Vol. 111(7), pp. 1287, 1964.
 20. Venikov, V.A. : "Transient Phenomena in Electrical Power Systems", (translated from the Russian), Pergamon, London, 1964.
 21. Humpage, W.D., and Stott, B.: "Predictor-Corrector Methods of Numerical Integration in Digital Computer Analysis of Power System Transient Stability", *Proc. IEE*, Vol. 112, pp. 1557-1565, 1965.
 22. Gless, G.E. : "Direct Method of Lyapunov Applied to Transient Power System Stability", *Trans. IEEE*, Vol. 85, pp. 159-168, 1966.
 23. El-Abiad, A.H., and Nagappan, K.: "Transient Stability Region of Multimachine Power Systems", *Trans. IEEE*, Vol. 85, pp. 169-179, 1966.
 24. Stagg, G.W., and El-Abiad, A.H. : "Computer Methods in Power System Analysis", McGraw-Hill, New York, 1968.
 25. Dharma Rao, N.: "Routh-Hurwitz Conditions and Lyapunov Methods for the Transient Stability Problem", *Proc. IEE*, Vol. 116(4), pp. 539-547, 1969.
 26. Elgerd, O.I.: "Electric Energy Systems Theory", McGraw-Hill, New York, 1971.

ces the risk of instability. Compensation for line reactance by series capacitors is economical for increasing the stability of lines more than 200 miles long. Increasing the number of parallel lines between two points is a common means of reducing reactance.

It has been pointed out that there is a critical clearing time before which circuit breakers must operate to clear the fault if stability is to be maintained, and the quicker a fault is isolated from a system, the less disturbance it causes. The use of high-speed circuit breakers on power systems has greatly improved their stability and at the same time has reduced the need for making other changes in design to effect stable operation.

CONCLUSIONS

Maintaining synchronism between the various parts of a power system becomes increasingly difficult, however, as the systems and interconnections between systems continue to grow.

The choice of the most suitable method for solving the differential swing equations of the synchronous machines connected to a power system subjected to a transient disturbance, in order to check the system stability or to define a critical condition, depends upon many factors. Among these factors are the nature of the system under consideration being large, small, or involving two machines only; and the type of the control apparatus used. Another factor is that of obtaining the required accuracy with a minimum of computer time. If it is required to define a critical stability condition, the swing equation may be solved numerically, and to observe through the resulting swing curves whether the machines tend to lose or maintain synchronism. In general, one solution is not enough to define the critical condition; but it is necessary to solve several times, for different assumed conditions, till the critical condition is reached. Instead of solving the differential swing equations several times, the appli-

cation of the transient stability criteria may reduce the amount of work to one numerical solution only.

One advantage of the digital calculation of stability in comparison with the A.C. network analyser is that human intervention is unnecessary as the digital solution progresses. Speed is another great advantage of a digital computation. A calculation of transient stability on a system having 16 generators, 71 busses, and 89 lines required 16 minutes on a large digital computer. The same study would require about 4 hours on an A.C. network analyser. Other advantages of the digital computer are its availability for a single study, the possibility of sending input data to the computer location for processing by nonengineering personnel, and the avoidance of human error in recording results.

In order to improve the stability of a power system modern high-speed quick-acting automatic voltage regulators and autoreclose circuit breakers are used. Auto-reclosing coupled with the use of high-speed protective gear, forms one of the more economical methods of improving stability, thereby reducing the need for other changes in design in order to effect stable operation of the power system.

REFERENCES

1. Dahl, O.G.C. : "Electric Power Circuits", Vol. II, McGraw-Hill, New York, 1938.
2. Crary, S.B. : "Power System Stability", Vol. II, John Wiley and Sons, New York, 1947.
3. Kimbark, E.W.: "Power System Stability", Vol. III, John Wiley and Sons, New York, 1950.
4. Rudenberg, R. : "Transient Performance of Electric Power Systems", McGraw-Hill, New York, 1950.
5. Johnson, D.L., and Ward, J.B.: "The Solution of Stability Problems by Means of Digital Computers", Trans.

val of time. Comparing P_s and P_e for each machine (whether P_e is determined by a digital computer or read on an A.C. network analyser) gives the accelerating power of the machine for the torque angles at the beginning of an interval. One program for calculating P_e on the digital computer employs an iterative method very similar to that of calculating load flow.

The calculation of the change in angle of each machine over an interval of time can be performed by programming to computer to solve the equation

$$\Delta\delta_n = \Delta\delta_{n-1} + \frac{P_{a(n-1)}}{M} (\Delta t)^2$$

for each machine. Such a simple approximation of the solution of a second-order differential equation is necessary for a hand calculation, but the digital computer solves the swing equation more accurately by other methods of numerical evaluation of angular change. The problem still requires a step-by-step solution, and the challenge of programming is one of obtaining the required accuracy with a minimum of computer time. The iterative method of computing the power output of each machine is time-consuming unless the time intervals are small. The more accurate numerical approximations of the change of torque angle during an interval are justified only if longer time intervals are chosen.

METHODS OF IMPROVING TRANSIENT STABILITY

There are certain factors which affect transient stability and which may be altered in order to raise the transient stability limit of the system. Inspection of the equation

$$\Delta\delta_n = \Delta\delta_{n-1} + \frac{P_{a(n-1)}}{M} (\Delta t)^2$$

indicates that an increase in the inertia constant M of a machine reduces the angle through which it swings during any time interval and thus allows a longer time for circuit breaker operation to isolate the fault before the machine passes through its critical clearing angle. An increase in M offers a means of increasing stability, but it has not been used extensively for economic reasons.

The methods frequently used to increase stability are :

1. Increase in the system voltage.
2. Reduction of series reactance by parallel lines.
3. Use of high-speed circuit breakers, including reclosing breakers.

The maximum value P_{max} of a power/angle curve is proportional to the per unit excitation. Field forcing can therefore cause the machine to work on a higher power/angle curve, thereby allowing it to swing through a larger angle from its original position before it reaches the critical clearing angle. P_{max} is increased by an increase in the internal voltage of a machine or in the voltage of the infinite bus to which the machine is connected through a reactance. Thus, raising P_{max} increases the critical clearing time and the probability of maintaining stability.

Reducing the reactance of a transmission line has the same effect as raising P_{max} . Compensation for line inductive reactance can be obtained by the use of parallel transmission lines instead of a single line. In general, more power is transferred during a fault on one of the lines if there are two lines in parallel, than would be transferred over a single faulted line. Increased power transfer means less available accelerating power, because the accelerating power is the difference between power input and power transfer. Lower accelerating power redu-

USE OF A.C. ANALYSERS AND DIGITAL COMPUTERS FOR OBTAINING SWING CURVES

In a multi-machine system, hand computation is impractical even for a small system because of the great amount of time required, and it is necessary to use A.C. analysers or digital computers for determining the swing curves for all the machines of the system. Often a small digital computer is used as an adjunct to the A.C. analyser. However, the step-by-step methods still form the basis of solution.

When the effects of automatic voltage regulators and governors are represented in the equation of motion as follows:

$$M \frac{d^2\delta}{dt^2} + K_d \frac{d\delta}{dt} = (P_s - \Delta P_s) - P_e$$

where K_d is the damping coefficient,

P_s is the power input,

ΔP_s is the change in input power due to governor action,

P_e is the electrical power output modified by the voltage regulator.

This equation is best solved by means of an analogue or digital computer. In most studies the governor and voltage regulator effects are ignored but their influence on stability limits have been analysed in recent investigations.

The function of the A.C. analyser is to determine the accelerating power for each machine as part of the step-by-step calculation. The positive-sequence network is set up on the A.C. analyser. Each machine is represented by its transient reactance in series with its voltage behind transient reactance adjusted to the phase angle and magnitude to give the power flow and bus voltage existing under normal conditions. The output of each generator before any transient condition occurs is P_s . Changes on the analyser are then made to represent the fault or the new network after a switching operation. The accelerating po-

wer is the difference between the new reading of power P_e for each machine and the constant value of P_s . The change in angular position with respect to the synchronous position is then calculated for each machine over the chosen time interval according to the equation

$$\Delta\delta_n = \Delta\delta_{n-1} + \frac{P_a(n-1)}{M} (\Delta t)^2$$

The calculation may be made by hand or on a small digital computer. The generators representing each machine on the analyser are then adjusted to agree with the new rotor positions. The power P_e is read again for each machine, and new angular positions are computed. The step-by-step analysis is continued in this manner until enough points on the swing curves have been found to indicate which machines, if any, are unstable.

When a computer is used to calculate the change in angular position of each machine at each step, the values of M and P_s for each machine are stored in the computer. Output power is read from the A.C. analyser for each generator and fed into the computer, which then calculates and prints out the new generator angles. When each generator angle has been adjusted to the new angle, a new set of accelerating powers is read and supplied to the computer. Except that the angles are calculated by the computer, the step-by-step process is the same, although the computer offers the possibility of more elaborate methods of calculating the change in δ for each step.

Digital computers replace A.C. network analysers entirely to determine the swing curves of the machines of a power system in a manner most easily understood by a comparison with the A.C. network analyser method. The problem divides into two parts. One part is the calculation of the accelerating power of each machine. The second part is obtaining the change in angle of each machine over a small inter-

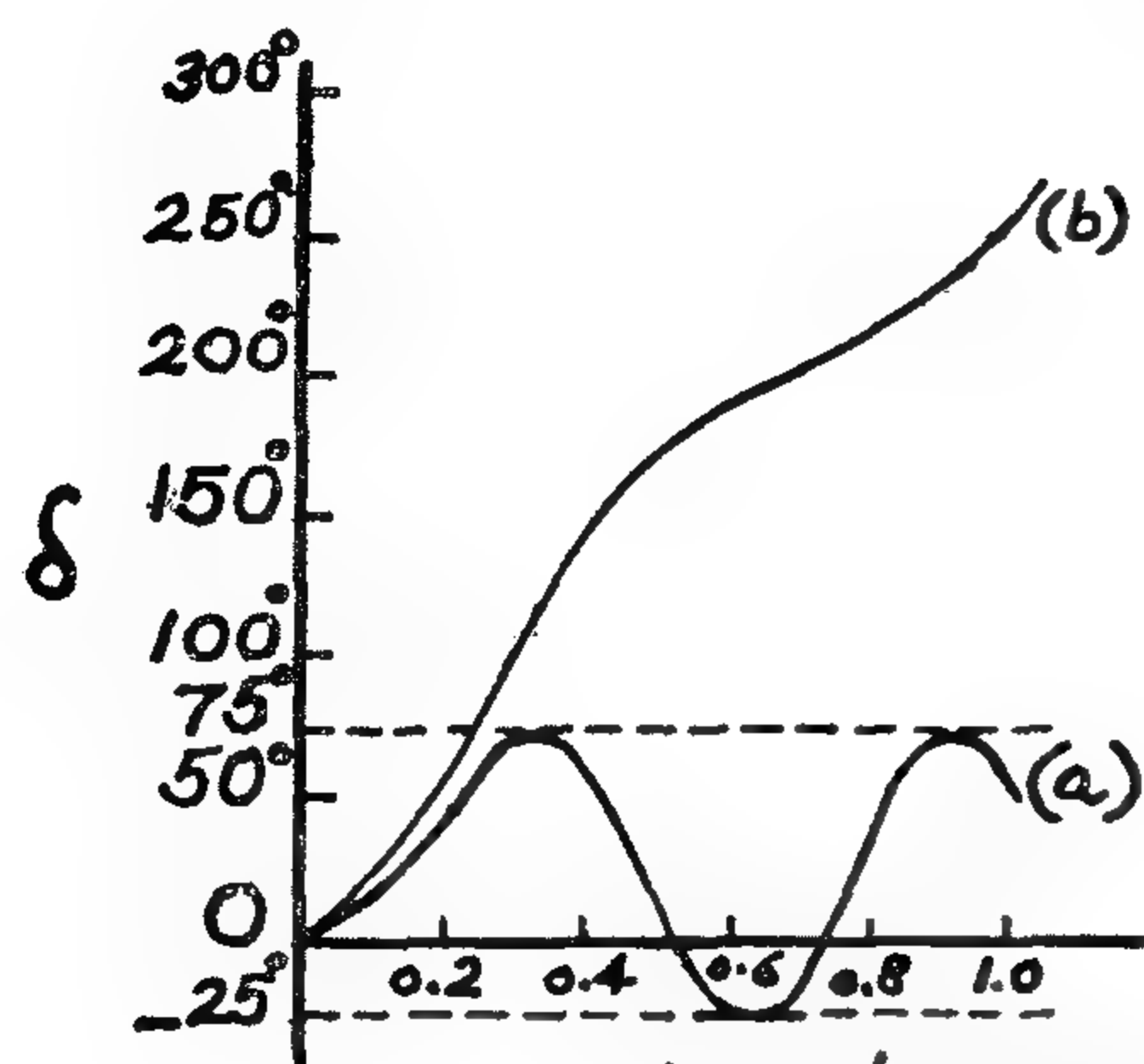


Figure 4. Typical Swing Curves
(a) Stable condition
(b) Unstable condition
Damping ignored.

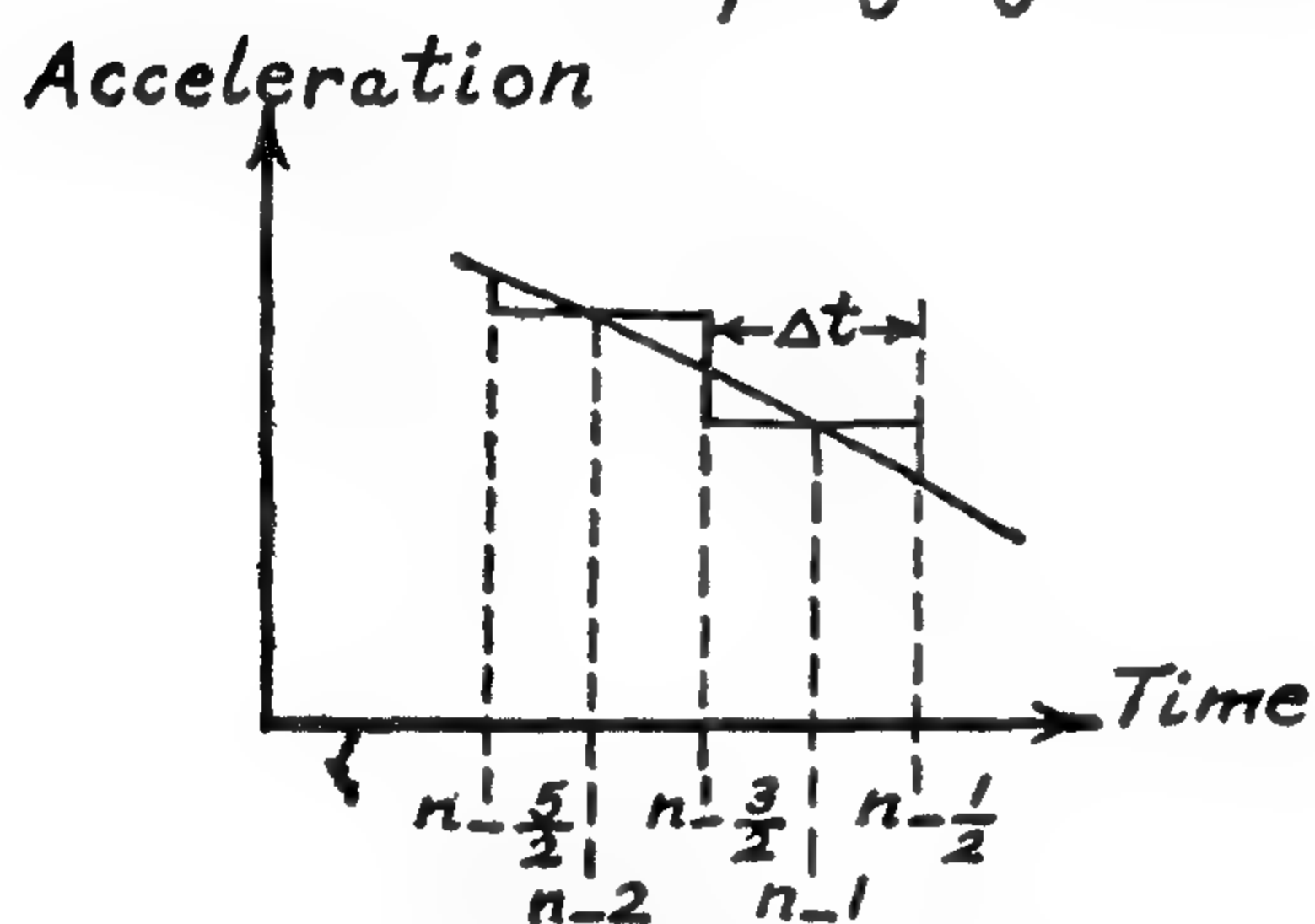


Figure 6. Acceleration/time curve.

rence now being used for the accelerating power.

Dharma Rao and Ramachandra Rao, in reference (18), apply the number-series approach to solve transient stability problems, by essentially converting a non-linear differential equation into a non-linear integral equation of the convolution type. The convolution integral is then approximated by the trapezoidal rule.

The Runge-Kutta Fourth-Order method depends mainly on the formulae derived by Runge and Kutta for the numerical solution of linear and non-linear differential equations. This method has the advantage of being self-started i.e. the point $(n+1)$ can be found from the point n only. On the other hand, it is considered to be a time-consuming method be-

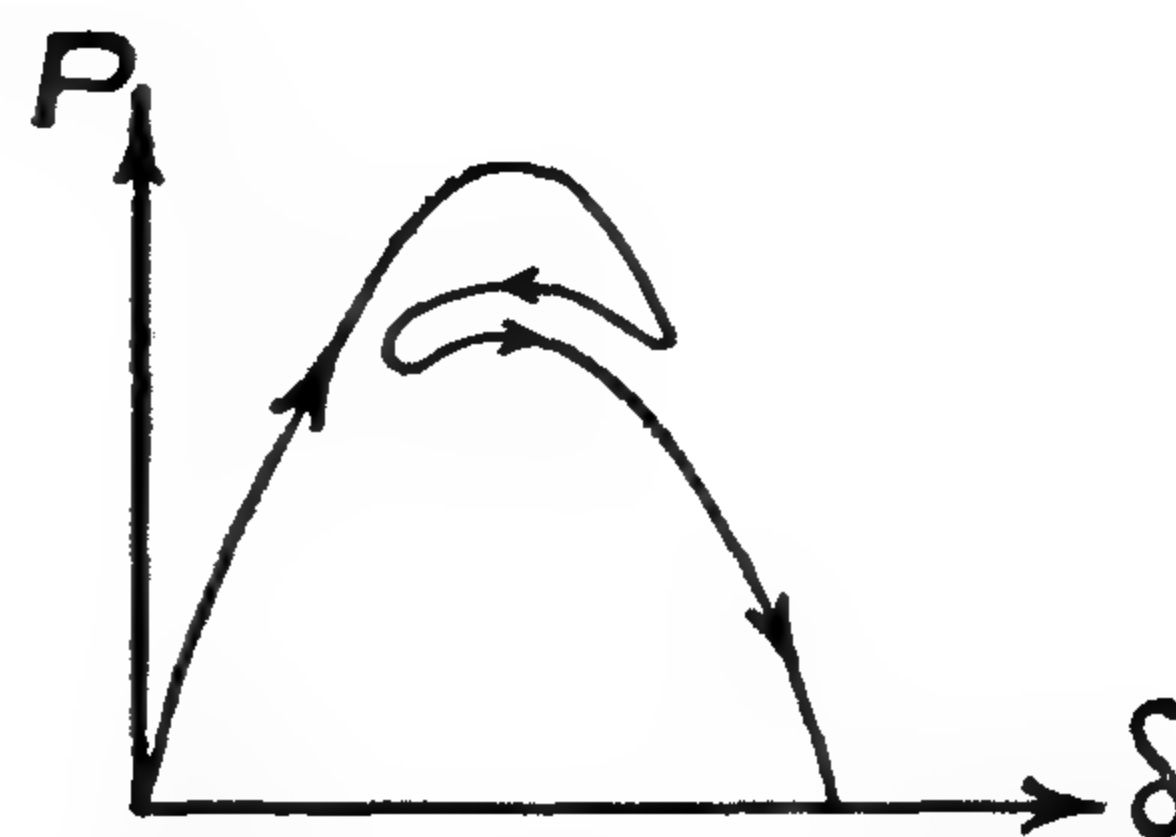


Figure 5. Loss of synchronism due to decline of field flux.

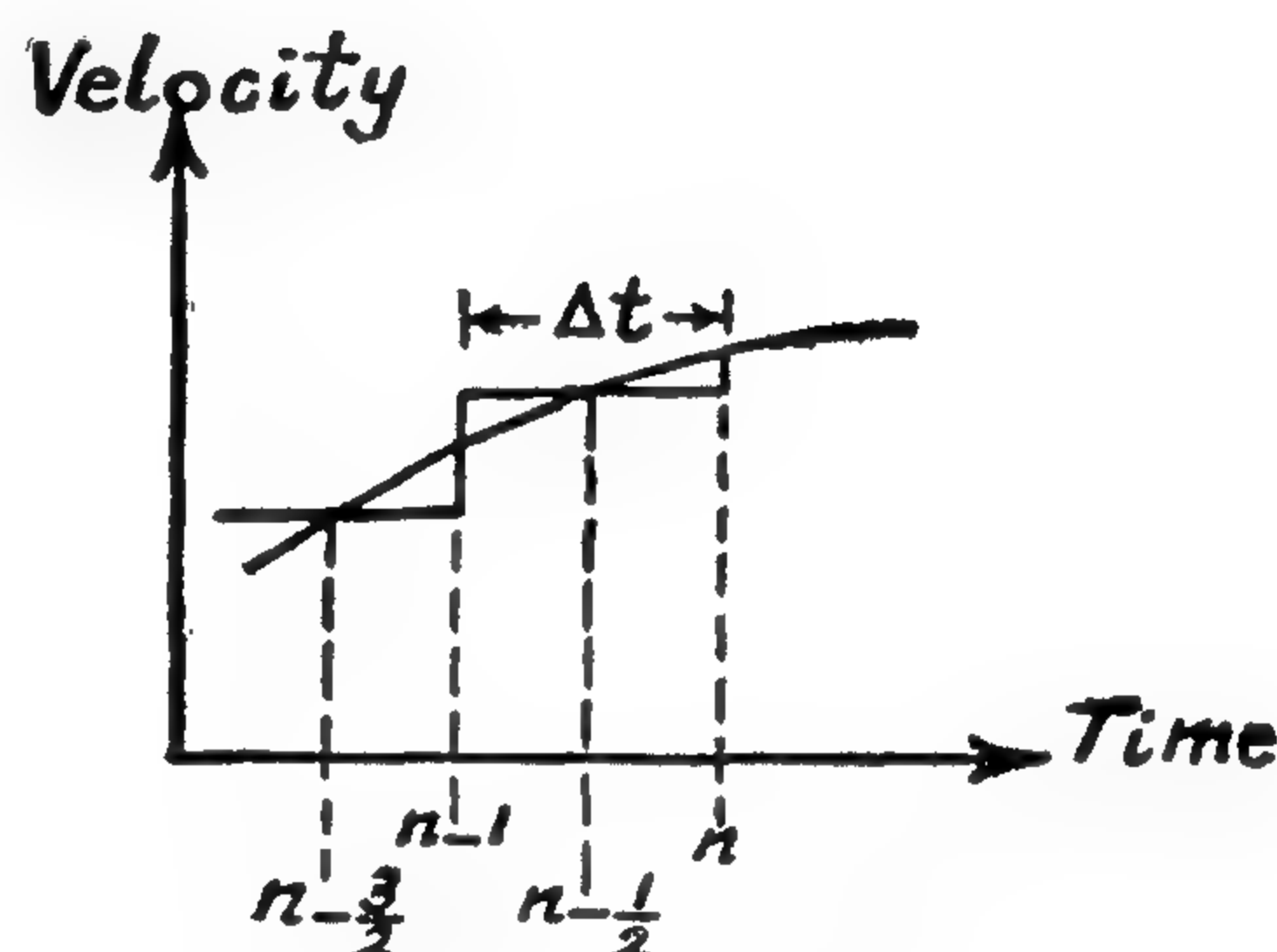


Figure 7. Velocity/time curve.

cause the swing equation has to be solved many times within a step.

The predictor-corrector method is based on applying two formulae. The first, called the predictor formula, is to find an approximate value for the point (x_{n+1}, y_{n+1}) if the points $n, n-1, \dots$ are known. The predictor formula should not contain the unknown derivatives at the points $n+1$. This formula may be obtained by extrapolation as in Adam's predictor formulae or by integration ahead as in Euler's predictor formulae. The second, called the corrector formula, is a more accurate formula used to correct the predicted value of y_{n+1} by iteration. The predictor-corrector method is an elaborate but more accurate method for solving differential equations.

Now, the angle θ is continually changing with time, and we are concerned with an angular displacement δ from the reference axis, which is rotating at synchronous speed w_s , so that

$$\theta = w_s t + \delta$$

$$\frac{d\theta}{dt} = w_s + \frac{d\delta}{dt} \quad \text{and} \quad \frac{d^2\theta}{dt^2} = \frac{d^2\delta}{dt^2}$$

$$\text{Therefore } T_a = J \frac{d^2\delta}{dt^2}$$

and since power is equal to torque times angular velocity, the accelerating power is

$$P_a = T_a w = w J \frac{d^2\delta}{dt^2} = M \frac{d^2\delta}{dt^2}$$

where M is the product $w J$ and is normally expressed in megawatts per radian and second². The above equation is called the "swing equation", P_a being given by $P_s - P_e$, where P_s is the shaft power and P_e the electrodynamic power. We have, therefore, a differential equation which, if solved, will give the angular displacement at various time intervals after the disturbance, and will enable the maximum angle of swing to be ascertained. If the swing curve (Figure 4) so plotted shows that the angle tends to increase without limit, the system is unstable. If, however, the angle reaches a maximum and then returns, it is probable that the system is stable. Unless quick-acting voltage regulators are used, it is possible for a machine to retain synchronism during the first swing, but to lose it during the next swing as a result of decline of field flux, as shown by Figure 5.

When solving the swing equation, the shaft power P_s is assumed constant and the effect of damping is ignored. It will be appreciated that the accelerating power (which depends on the difference between output and input quantities) is a variable, and it is necessary to use a step-by-step method of solution.

SOLUTION OF SWING EQUATION BY STEP — BY — STEP METHOD

Consider the acceleration/time curve, and assume that the acceleration changes in steps at Δt intervals. From Figure 6 it can be seen that the acceleration for the $(n-1)$ th interval is constant. Now,

$$w_{n-\frac{1}{2}} = w_{n-\frac{3}{2}} + \Delta t \alpha_{n-1}$$

where w and α represent angular velocity and acceleration respectively. Or,

$$w_{n-\frac{1}{2}} - w_{n-\frac{3}{2}} = \Delta t \alpha_{n-1} = \frac{P_{a(n-1)}}{M} \Delta t$$

Now consider the velocity/time curve, Figure 7.

Let the velocity be constant for intervals Δt from $(n-2) \Delta t$ to $(n-1) \Delta t$, and so on.

The increase in δ_n is

$$\Delta \delta_n = w_{n-\frac{1}{2}} \Delta t$$

and the increase in δ_{n-1} is

$$\Delta \delta_{n-1} = w_{n-\frac{3}{2}} \Delta t$$

$$\therefore \Delta \delta_n - \Delta \delta_{n-1} = (w_{n-\frac{1}{2}} - w_{n-\frac{3}{2}}) \Delta t$$

$$= \frac{P_{a(n-1)}}{M} (\Delta t)^2$$

$$\text{or } \Delta \delta_n = \Delta \delta_{n-1} + \frac{P_{a(n-1)}}{M} (\Delta t)^2$$

Suppose some disturbance occurs to cause acceleration : immediately before the disturbance $P_a = 0$, and immediately afterwards $P_a = P_s - P_e$, so that the average accelerating power is $(P_a + 0)/2$. Thus, the first step in the solution will be written as

$$\Delta \delta_1 = \Delta \delta_0 + \frac{(\Delta t)^2}{M} P_{a_0} = \Delta \delta_0 + \frac{(\Delta t)^2}{M} \frac{P_a}{2}$$

and $\Delta \delta_0$ will be zero. Subsequent steps are

$$\Delta \delta_2 = \Delta \delta_1 + \frac{(\Delta t)^2}{M} P_{a_1}$$

and so on.

In the subsequent steps the new P_e is evaluated from a knowledge of the new load angle, the actual $(P_s - P_e)$ diffe-

In the phase-plane technique, it is necessary to plot velocity versus displacement by solving the system equation to obtain a direct relation between these ordinates. If the equation cannot be solved, the phase-plane diagram is graphically constructed by the aid of isoclinicals, or numerically by the point-by-point calculations. The term phase-plane is used because each point on a given trajectory describes a particular state or phase of the system.

The basis of the direct-Lyapunov method is the Lyapunov's theorem which states that the equilibrium is stable if there exists a positive definite function $V(X, t)$ such that its total derivative dV/dt for the differential equation $dX/dt = f(X, t)$ is not positive. The function $V(X, t)$ is called a Lyapunov function, and has the following properties :

1. The function is positive definite.
2. It is a function of the time "t" and the "n" variables X_1, X_2, \dots, X_n of the system represented by the equation $dX/dt = f(X, t)$.
3. dV/dt along the trajectories of the system is not positive.

It is to be noted that the Lyapunov function for any system is not unique. If a Lyapunov function of the state variables fails to show that the system is stable or unstable, another function may succeed. It is also worth mentioning that the stability limit determined by a certain Lyapunov function may not be the actual critical limit i.e. exceeding this limit, may not cause instability. In other words, the checking of stability by the direct-Lyapunov method gives sufficient conditions but may not be necessary.

TRANSIENT STABILITY — CONSIDERATION OF TIME. THE SWING CURVE

In the previous section attention has been mainly directed towards the determination of rotor angular position; in prac-

tice the corresponding times are more important. The protection engineer requires allowable times rather than angles when specifying relay settings. The solution of the equation $\frac{d^2\delta}{dt^2} = \frac{P_a}{M}$ with respect to time is performed by means of numerical methods and the resulting time-angle curve is known as the swing curve, which determines the change in the angular position of the rotor over a short time interval.

Thus, a general approach is required to assess the system performance, including circuit breakers effects and the significant generator characteristics such as saliency, damping, and field decrement, which may be difficult to be treated by the direct methods previously mentioned. This approach has been to obtain a general time solution, and to observe through the swing curves whether the machines tend to lose or maintain synchronism; using the point-by-point calculations. Among the recent and most important methods are the step-by-step method, the number-series approach, the Runge-Kutta Fourth-Order method, and the predictor-corrector method.

THE SWING EQUATION

Assuming that corrections have been made for losses, under normal steady conditions the synchronous machine shaft torque T_s is equal to the electrodynamic torque T_e . In the event of a disturbance, acceleration (or retardation) occurs, and the resultant torque T_a is given by $T_s - T_e$:

$$T_a = T_s - T_e = J \frac{d^2\theta}{dt^2}$$

T_a is in newton-metres and the moment of inertia J is in Kilogram-metres²

the initial operating power and angle could be increased to such values that the shaded area between δ_0 and δ_1 is equal to the shaded area between δ_1 and δ_3 where $\delta_3 = 180 - \delta_1$; this would be the condition for maximum input power. Beyond δ_3 energy would again be absorbed by the rotor from the turbine.

The power angle curves pertaining to a fault on one of two parallel lines is shown in Figure 2. The fault is cleared in a time corresponding to δ_1 and the shaded area δ_0 to δ_1 indicates the energy stored. The rotor swings until it reaches δ_2 when the two areas are equal. In this particular case P_0 is the maximum operating power for a fault clearance time corresponding to δ_1 , and conversely δ_1 is the "critical clearing angle" for P_0 . If the angle δ_1 is decreased it is possible to increase the value of P_0 without loss of synchronism. The general case where the clearing angle δ_1 is not critical is shown in Figure 3. Here the rotor swings to δ_2 where the shaded area from δ_0 to δ_1 is equal to the area δ_1 to δ_2 . Critical conditions are reached when $\delta_2 = 180 - \delta_1$. The time corresponding to the critical clearing angle is called the "critical clearing time" for the particular (normally full load) value of power input. This time is of great importance to protection and switchgear engineers as it is the maximum time allowable for their equipment to operate without instability occurring. The critical clearing angle for a fault on one of two parallel lines may be determined as follows.

Applying the equal-area criterion to Figure 2

$$\int_{\delta_0}^{\delta_1} (P_0 - P_1 \sin \delta) d\delta + \int_{\delta_1}^{\delta_2} (P_0 - P_2 \sin \delta) d\delta = 0$$

$$\therefore [P_0 \delta + P_1 \cos \delta]_{\delta_0}^{\delta_1} + [P_0 \delta + P_2 \cos \delta]_{\delta_1}^{\delta_2} = 0$$

from which as $\delta_2 = 180 - \delta_1$,

$$\cos \delta_1 = \frac{P_0(\delta_0 - \delta_2) + P_1 \cos \delta_0 - P_2 \cos \delta_2}{P_1 - P_2}$$

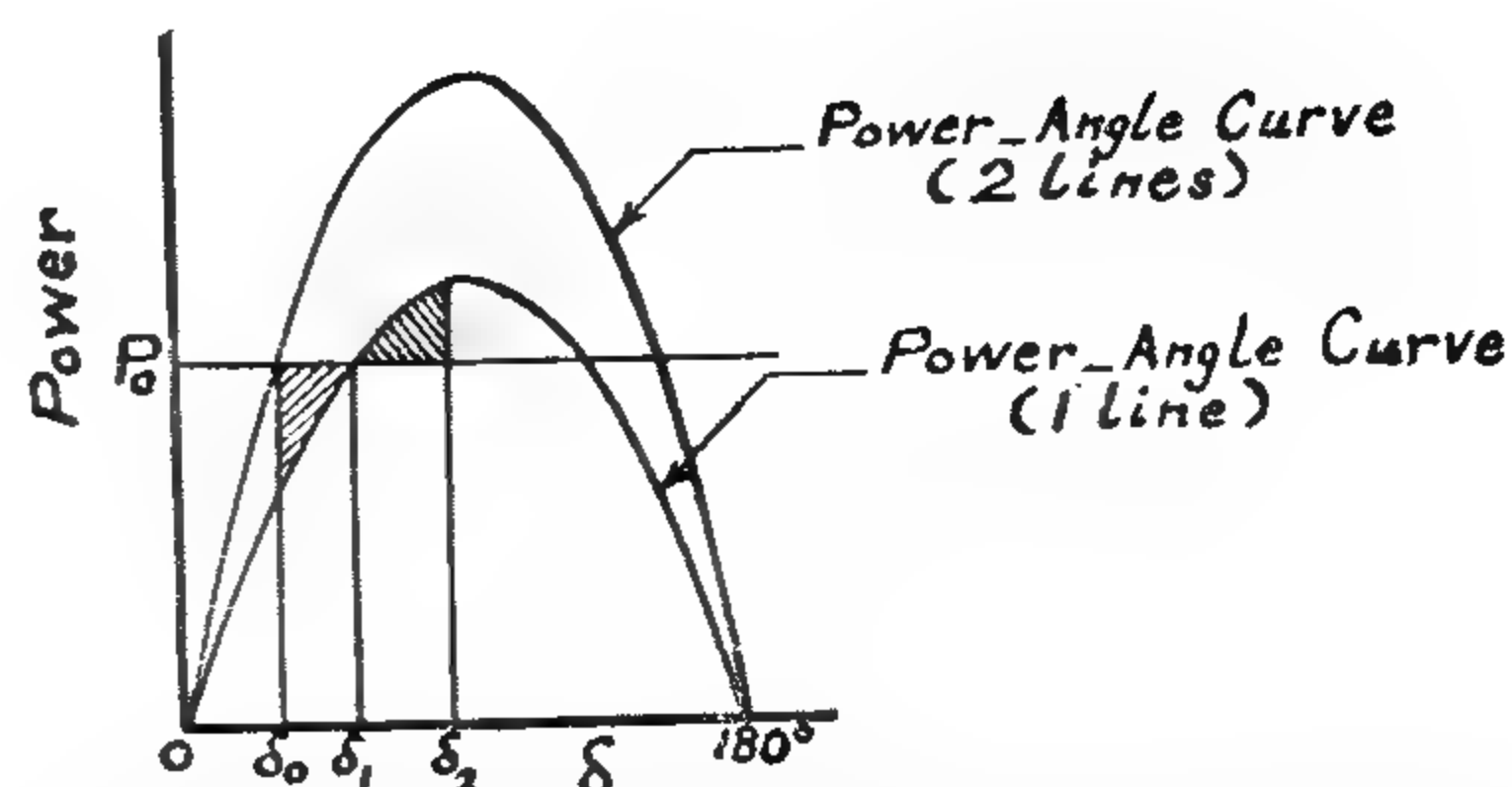


Figure 1. Power-angle curves for one line and two lines in parallel. Equal area criterion. Resistance neglected.

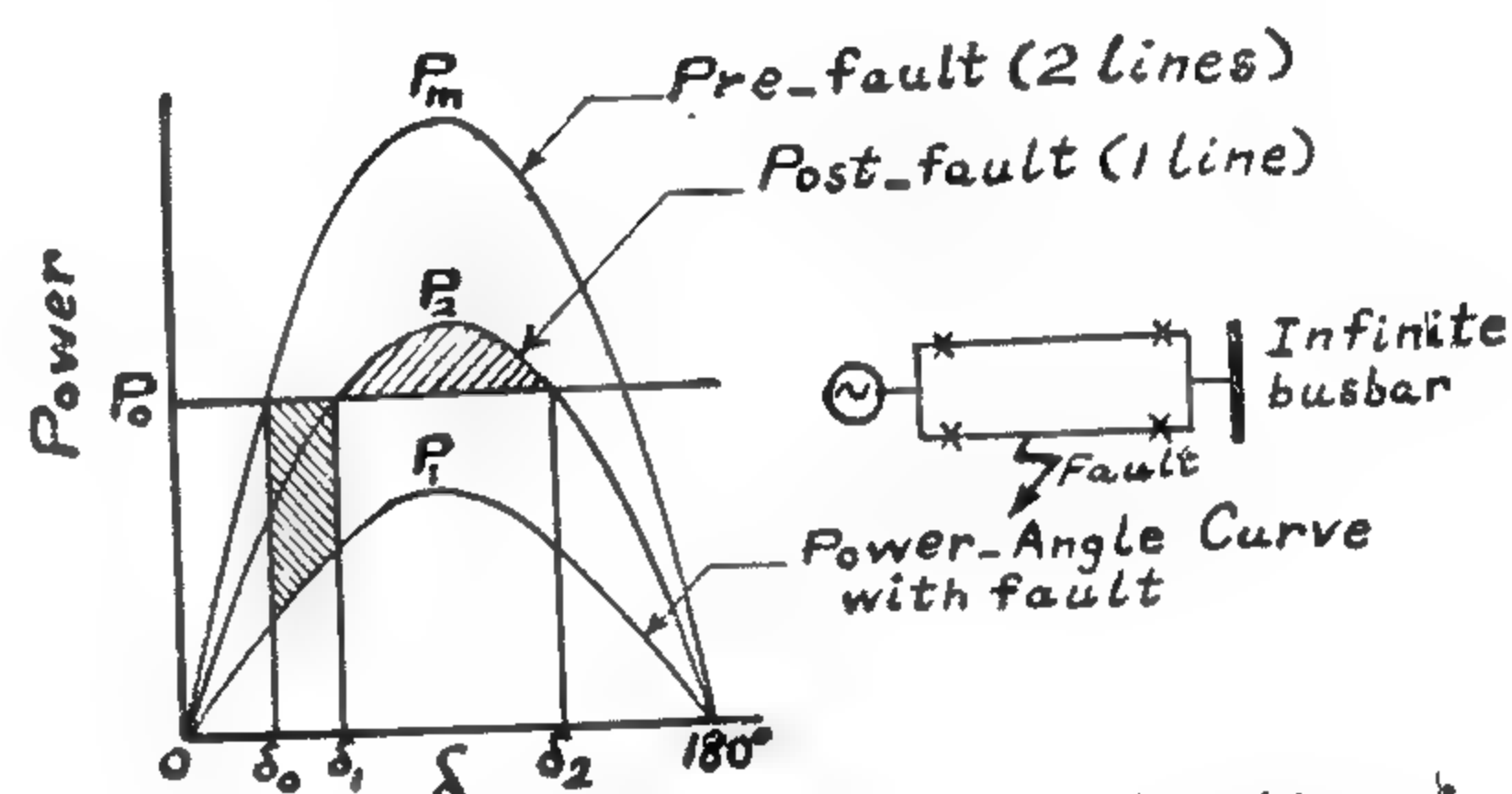


Figure 2. Fault on one line of two lines in parallel. Equal area criterion. Resistance neglected. δ_1 is critical clearing angle for input power P_0 .

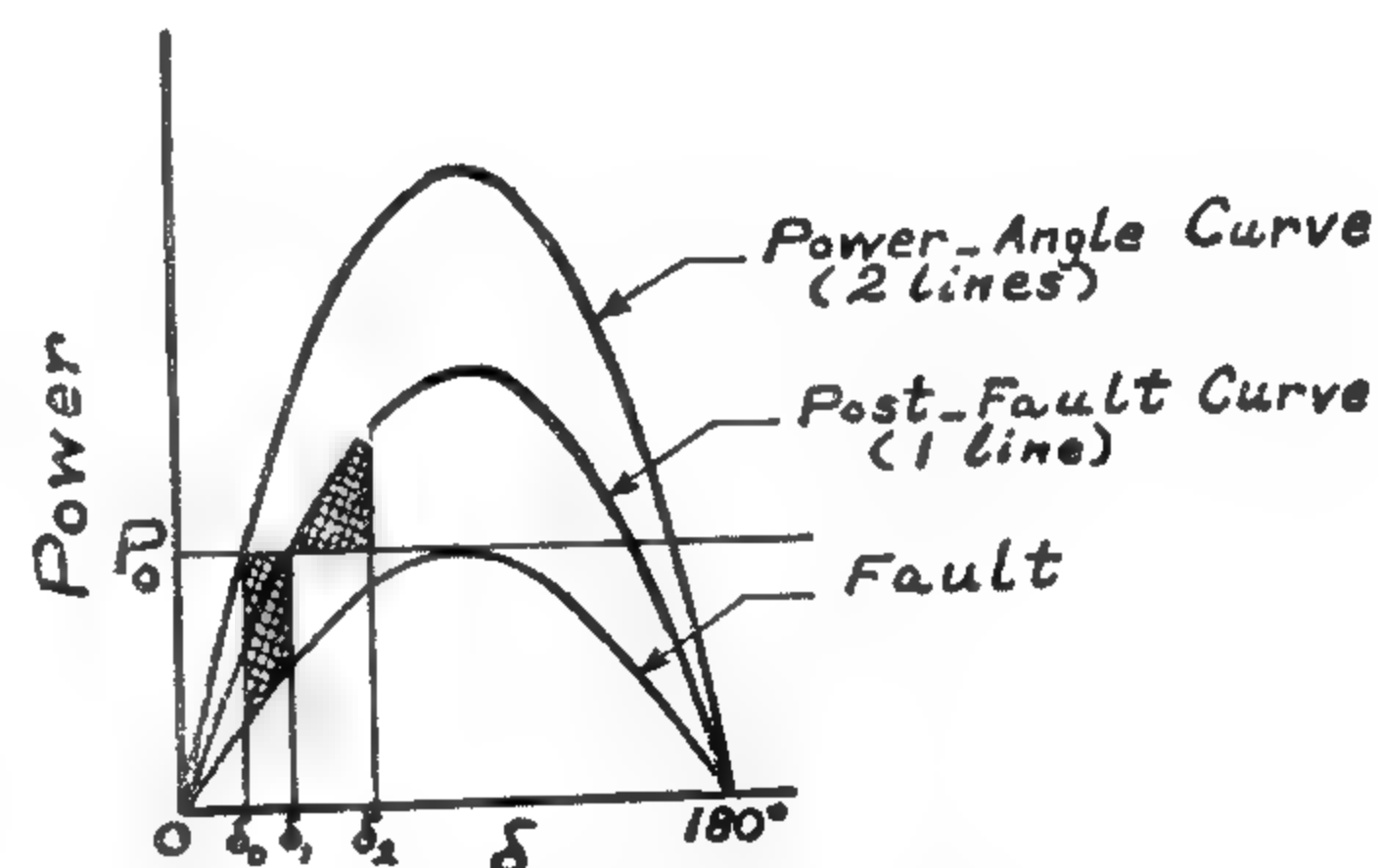


Figure 3. Situation as in Figure 2, but δ_1 not critical.

Hence the critical clearing angle δ_1 is determined.

The energy-integral criterion is based on the law of conservation of energy; that is, for a stable system, the energy stored in it remains constant at any instant, if damping is neglected; or decreases continually during oscillations, if damping is considered.

fault disturbances it may be assumed that the voltage behind transient reactance is constant, a method commonly used in practice because of its simplicity. There are, however, more rigorous methods available, and these take saliency into account.

Transient disturbances may occur owing to differences in the input/output balance as a result of sudden load changes. Switching operations and faults with subsequent clearance are other causes of transient disturbance. In the latter case there may be auto-reclosure to consider.

TRANSIENT STABILITY — CONSIDERATION OF ROTOR ANGLE

When a fault occurs at the terminals of a synchronous generator the power output of the machine is greatly reduced as it is supplying a mainly inductive circuit. However, the input power to the generator from the turbine has not time to change during the short period of the fault and the rotor endeavours to gain speed to store the excess energy. If the fault persists long enough the rotor angle will increase continuously and synchronism lost. Hence the time of operation of the protection and circuit breakers is all-important.

An aspect of increasing importance is the use of autoreclosing circuit breakers. These open when the fault is detected and automatically reclose after a prescribed period (usually less than one second). If the fault persists the circuit breaker reopens and then recloses as before. This is repeated once more, when, if the fault still persists, the breaker remains open. Owing to the transitory nature of most faults often the circuit breaker successfully recloses and the rather lengthy process of investigating the fault and switching in the line is avoided. The length of the auto-reclose operation must be considered when assessing transient stability limits; in particular analysis must include the mo-

vement of the rotor over this period and not just the first swing as is often the case.

The equation of motion of a rotating machine (which will be derived later) is

$$\text{given by } \frac{d^2\delta}{dt^2} = \frac{P_a}{M}$$

If in the above equation both sides are multiplied by $2 (d\delta/dt)$,

$$2 \left(\frac{d\delta}{dt} \right) \left(\frac{d^2\delta}{dt^2} \right) = \frac{d}{dt} \left(\frac{d\delta}{dt} \right)^2 = \frac{2P_a}{M} \left(\frac{d\delta}{dt} \right)$$

$$\therefore \left(\frac{d\delta}{dt} \right)^2 = \frac{2}{M} \int_{\delta_0}^{\delta} P_a d\delta$$

The rotor will swing until its angular velocity is zero in which case the machine remains stable; if $d\delta/dt$ does not become zero the rotor will continue to move and synchronism lost. Hence the criterion for stability is that the area between the $P - \delta$ curve and the line representing the power input must be zero. This is known as the "equal - area criterion". It should be noted that this is based on the assumption that synchronism is retained or lost on the first swing or oscillation of the rotor, which in certain cases is subject to doubt. Physically the criterion means that the rotor must be able to return to the system all the energy gained from the turbine during the acceleration period.

The equal-area criterion, the energy-integral criterion, the phase-plane technique, and the direct-Lyapunov method are some methods that may be applied directly, with certain assumptions, for determining the relative transient stability of a power system without developing the time response.

A simple example of the equal-area criterion may be seen by an examination of the switching out of one of two parallel lines which connect a generator to an infinite busbar (Figure 1). For stability to be retained the two shaded areas are equal and the rotor comes initially to rest at angle δ_2 , after which it oscillates until completely damped. In this particular case

THE TRANSIENT STABILITY OF ELECTRIC POWER SYSTEMS

By

Dr. Eng. MEDHAT ADIB NASR*

INTRODUCTION

The tendency of a power system or its component parts to develop forces to maintain synchronism and equilibrium is known as "stability". Much study has been devoted to stability since about 1920.

The stability of a system of interconnected dynamic components is its ability to return to normal or stable operation after having been subjected to some form of disturbance.

When the rotor of a synchronous generator advances beyond a certain critical angle, the magnetic coupling between the rotor (and hence the turbine) and the stator fails. The rotor, no longer held in synchronism with the rotating field of the stator currents, rotates relative to the field and pole slipping occurs. Each time the poles traverse the angular region where stability obtains, synchronizing forces attempt to pull the rotor into synchronism.

There are two forms of instability in power systems; the loss of synchronism between synchronous machines, and the stalling of asynchronous loads. Synchronous stability may be divided into two types, steady-state and transient. Steady-state stability is basically the ability of the power system when operating under given load conditions to retain synchronism when subject to small disturbances such as the continual changes in load or generation and the switching out of lines. It is most likely to result from the changes in source-to-load impedance resulting

from changes in the network configuration.

Transient stability is concerned with sudden and large changes in the network condition such as brought about by faults. The maximum power transmittable, the stability limit, is less than that for the corresponding steady-state condition.

The stability of an asynchronous load is controlled by the voltage across it; if this becomes lower than a critical value, induction motors may become unstable and stall. In a power system it is possible for either synchronous or load instability to occur. The former is more probable and hence has been given much more attention.

TRANSIENT STABILITY

When a sudden short-circuit occurs at the terminals of a turbo-alternator, the effective reactance varies with time, from the sub-transient value, through the transient value to the steady-state synchronous value.

During a disturbance the period of mechanical oscillation may be of the order of one second. The sub-transient time-constant will be about 0.3 second, so it is usually ignored in transient stability studies. A typical armature time-constant would be about 0.2 second, so in many studies the direct component of armature current is ignored. The transient component of armature current may have a time-constant of a few seconds, which is longer than the period of mechanical oscillation, so it is necessary to consider the transient reactance. When considering

* Assistant Professor, Department of Electrical Power and Machines,
Faculty of Engineering, Cairo University.

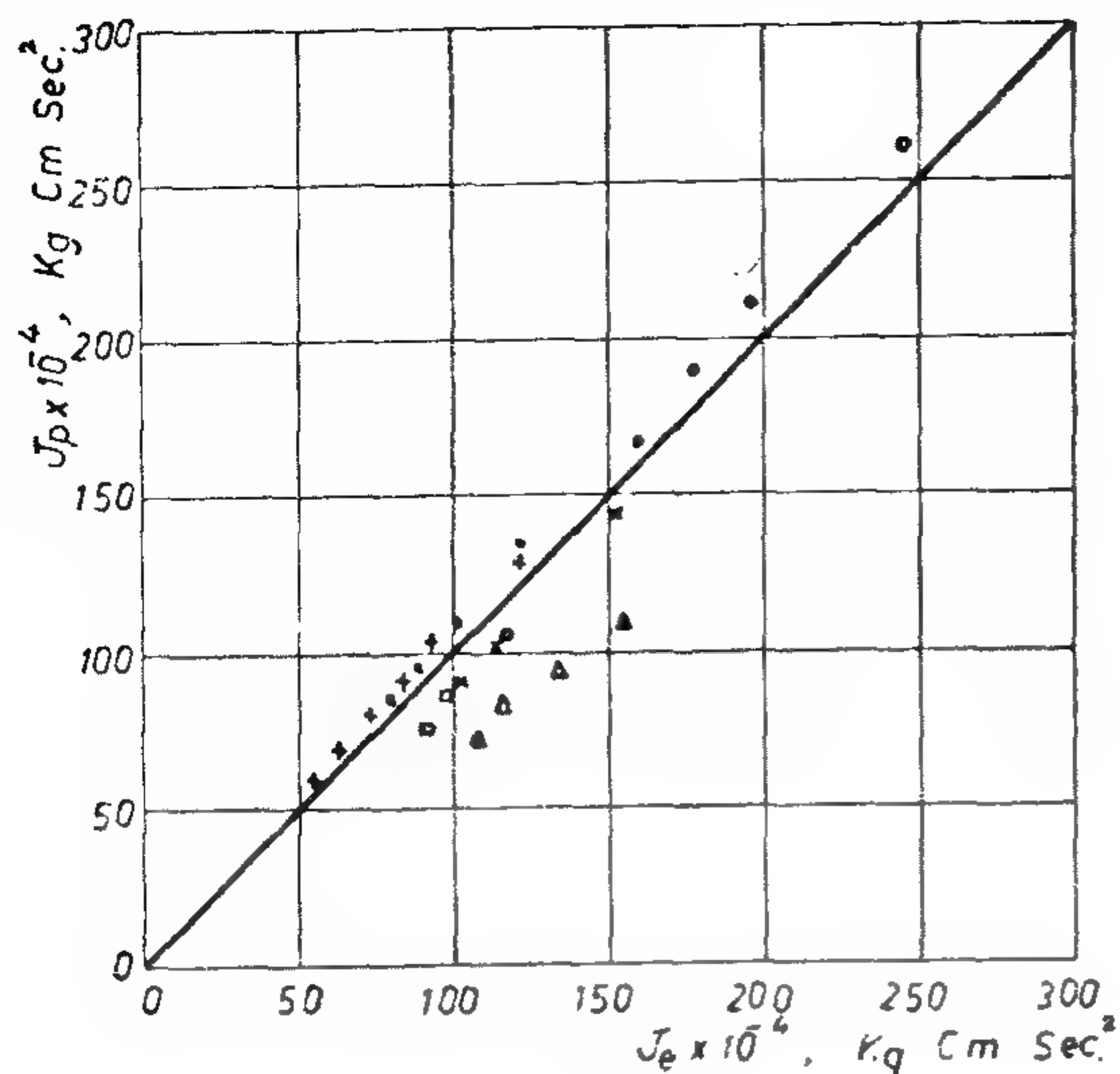


FIG (5)

REFERENCES

- 1 — E. Panagopules. "Design-Stage Calculations of Torsional, Axial, and Lateral Vibrations of Marine Shafting", S.N.A.M.E, Vol. 58. 1950.
- 2 — A. Emerson, L. Sinclair and P.A. Milne, "The Propulsion of a Million Ton Tanker", Stone Manganese Marine Technical Papers, No. 9. Aug. 1971.
- 3 — W. Ker Wilson, Practical Solution of Torsional Vibration Problems, Vol. 2, Chapman and Hall, 1963.
- 4 — R. Steidel, An Interoduction to Mechanical Vibrations, John Wiley, 1971.
- 5 — T.P. O'Brien, The Design of Marine Screw Propellers, Hutchinson Scientific and Technical, London, 1962.
- 6 — "Rules and Regulations for the Construction and Classification of Steel Ships", Lloyds Register of Shipping, 1973.
- 7 — N. Petrovsky, Marine Internal Combustion Engines", Mir Publishers, Moscow.
- 8 — F. Lewis, Dynamic Effects, Marine Engineering, Vol. II, (Edited by H.E. Seward), S.N.A.M.E., 1960.
- 9 — J.P. Van Mannen, "Fundamentals of Ship Resistance and Propulsion", N.S.M.B., Pub. No. 1320.
- 10 — "Rules for the Construction and Classification of Steel Ships", Det. Norske Vertas, 1973.

involving the fifth power) thus giving rise to the proposed modified equation:

$$w^2 = \frac{2000}{L_i + 0.4L_p} \left(\frac{L}{L + 0.5N} \right) \left(\frac{H}{R} \right)^{1/3} \quad (16)$$

RESULTS AND DISCUSSION

Six groups of engines belonging to different Diesel engine makers with powers ranging from 2300 to 4000 hp/cyl., and with number of cylinders from 8 to 12 with a total of 24 engines were considered. Engine data (inertias and stiffness) were available from engine builders. Propeller inertia was either given, or was calculated with the help of Fig. (4). Lengths of intermediate and propeller shafts were arbitrarily chosen as 12 and 6 meters respectively for the sole purpose of comparing the results, that is why they were assigned the same values for all cases.

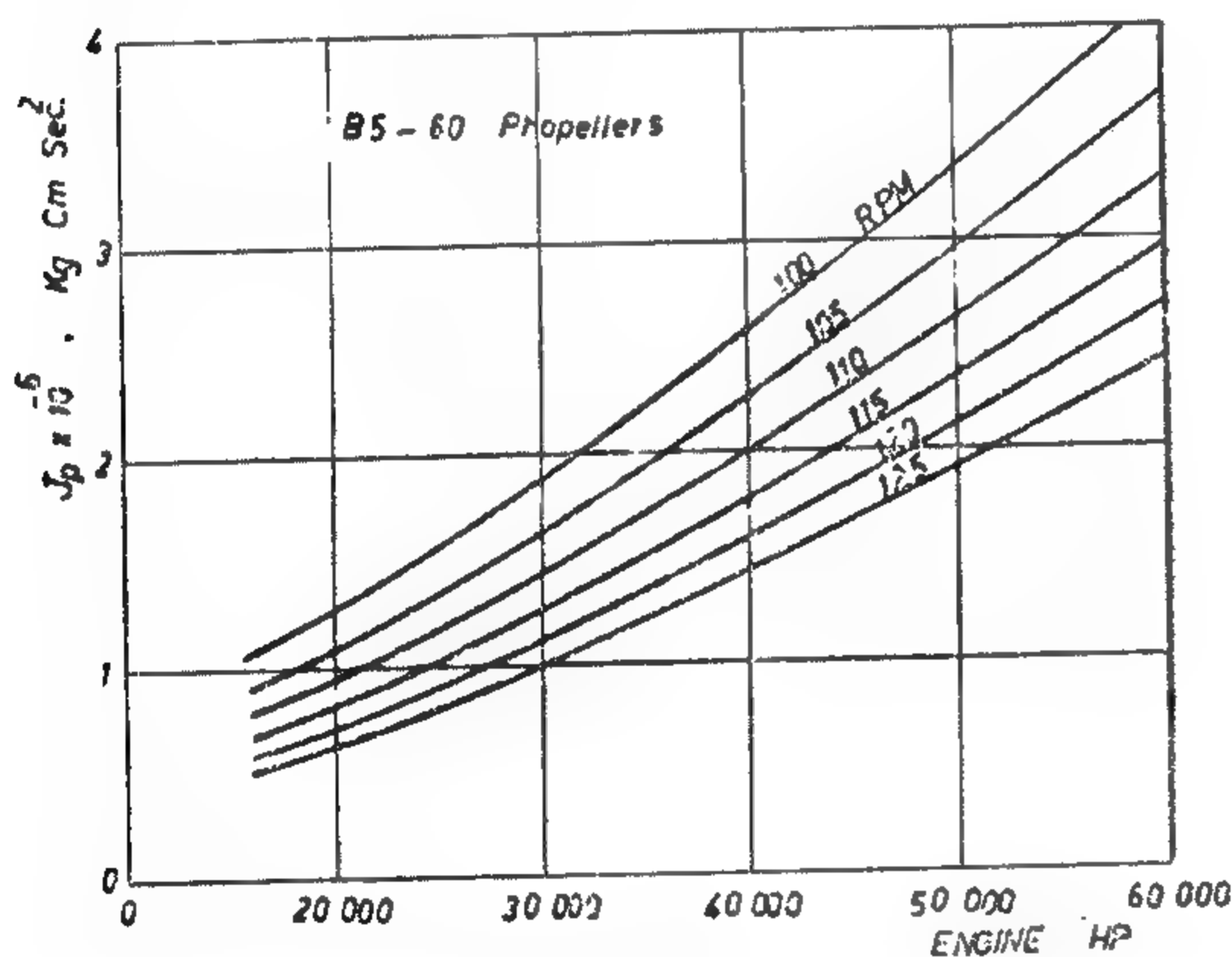


FIG.(4)

Such data was then fed to the computer and by means of a standard program for the Holzer method; the first mode frequency, labeled w_c , was obtained.

The values w_1 and w_m were then calculated by means of both the proposed equations, namely; Eq. (15) and (16).

The following table shows a comparison of the different values of w and the percentage error of the six engine groups.

From the mentioned table, the following conclusions and remarks can be drawn:

- 1 — The original equation gives better accuracy than the modified equation, which is expected.
- 2 — For groups 2, 4 and 5, the error in the original equation is large compared to group 1, 3 and 6. This is due to the fact that J_e for the former groups lies far from the straight line approximation, given by Eq. (2), for the engine inertia, hence the deviation in w . On the other hand, the latter groups are exactly represented by Eq. (2), hence the smaller errors.
- 3 — In the modified Eq. (16):
 - The error is not influenced appreciably if J_e equals J_p as in group 1 and 3
 - The error decreases if J_e is larger than J_p which compensates for the effect of J_e approximation as in group 2.
 - The error increases if J_e is less than J_p which has an additive effect to the approximation of J_e as in groups 4 and 6.

- 4 — The number of cylinders has no effect upon the accuracy of the results.

The above analysis of the results is in effect a theoretical rationalization of the trends shown in the results. However, from the point of view of the user of the equations (the designer) he should be satisfied by either one since even with the most preliminary data available (as in the modified equation) the error is in general less than 10 % and in fact for most cases it is much less.

$$d_p = 1.14 d_i + D/C. \quad (16)$$

where

- d_p = propeller shaft diameter, ins.
 d_i = intermediate shaft diameter, ins.
 C = constant which equals 144 for the type of ships under consideration.

In order to simplify the expression for d_p we try to write it down as a function of d_i only, i.e.

$$d_p = \lambda d_i. \quad (17)$$

For several existing installations, the propeller shaft diameter d_p was calculated using Eq. (16) and checked against Eq. (17) in a way to determine the constant of proportionality λ . It turns out that the value $\lambda = 1.23$ gives a very close approximation.

Finally, the stiffness of the intermediate as well as the propeller shaft can thus be written as:

$$K_i = \frac{\pi G}{32 L_i} (8.9)^3 \left(\frac{H}{R} \right)^4$$

$$K_p = \frac{\pi G}{32 L_p} (1.23 \times 8.9)^3 \left(\frac{H}{R} \right)^4$$

and the equivalent stiffness of both shafts :

$$K_e = K_i K_p / (K_i + K_p).$$

hence

$$K_e = \frac{\pi G (8.9)^4 (H/R)^{4/3}}{32 (L_i + 0.436 L_p)} \quad (14)$$

The Proposed Equation :

Having derived expressions for the items J_e , J_p and k , one can substitute these values into the expression for the frequency given by Eq. (1). Before doing that, however, the following observations has to be made.

The system as described above concentrates the engine inertia at the last cylinder,

this implies that the crankshaft is infinitely rigid. In order to approach the actual system the stiffness as given by Eq. (14) should be modified (reduced) to account for the elasticity of the crankshaft. Suppose we consider the engine inertia to be concentrated at the middle cylinder. This does not mean that we have to add half the engine length to the length of the equivalent shaft due to the difference in diameters. In fact, if this is taken into consideration, the engine inertia will be concentrated at a point such that a little more than one fourth the engine length should be added to the length of the equivalent shaft. Knowing that the centre line distance between two consecutive cylinders is of the order of 1.8 mt, then the shaft extension will be equal to 0.5 N, or the stiffness Eq. (14) will be multiplied by the factor

$$L / (L + 0.5 N)$$

where

N = number of cylinders

$L = L_i + L_p$ mt

Hence the frequency equation takes the form :

$$\omega^2 = \frac{5.1 \times 10^6}{L_i + 0.436 L_p} \cdot \frac{L}{L + 0.5 N} \left(\frac{H}{R} \right)^{4/3} \left[\frac{1}{5.16 \times 10^3 H} + \frac{1}{\left(\frac{1057}{R} + 0.043 \sqrt{H} \right)^5} \right] \quad (15)$$

In order to simplify Eq. (15) we turn our attention to the term in brackets which represents $(1/J_e + 1/J_p)$.

Figure (5) shows a plot of J_e against J_p , from which one directly observes that J_e and J_p are, in the case of large tankers, more or less equal. This allows us to eliminate the second term (the one

$$D = \frac{474}{R} + 0.0194 \sqrt{H} \text{ mt.} \quad (11)$$

Substituting this value for D into Eq. (8), the latter takes the form :

$$J_p = \left(\frac{1057}{R} + 0.043 \sqrt{H} \right)^5 \text{ kg.cm.soo}^2 \quad (12)$$

Furthermore, and in order to facilitate the calculation of J_p Eq. (12) is represented graphically on Fig. (4) for a range of engine power H from 20,000 to 60,000 hp and from 100 to 125 rpm covering the range of large tankers in operation.

3 — Propulsion Shafting Stiffness:

The elasticity in the "Two-degree-of-freedom model", described previously, is provided by means of the intermediate and propeller shafts.

The torsional stiffness of a shaft is given by:

$$K = \frac{G J}{L} = \frac{\pi G d^4}{32 L} \quad (13)$$

where

L = length of the shaft.

d = diameter of the shaft.

G = shear modulus of the shaft material.

The determination of the stiffness of either the intermediate or propeller shaft (hence the equivalent stiffness of the system) boils down to the determination of their respective diameters.

Consider first the intermediate shaft. According to the Lloyds Register of Shipping [6] the shaft diameter is given by :

$$d = 89 \sqrt[3]{\frac{H}{R} \left(\frac{X+A}{1+A} \right) \left(\frac{60}{T+16} \right)} \text{ mm} \quad (14)$$

where

H = engine brake horsepower.

R = r.p.m.

T = specified minimum tensile stress for shaft material (taken as 44 kg/mm² according to the same rules).

X = ratio of maximum to mean indicated torque at the after cylinder (taken 1 for two stroke engines having 6 cylinders or more) [10].

A = J_e / J_p .

= ratio of engine to propeller inertia.

Performing the necessary substitutions, Eq. (14) can take the final form; namely:

$$d = 8.9 \sqrt[3]{\frac{H}{R}} \quad (15)$$

In order to arrive at an average value of d the rules of several Classification Societies were considered. After performing the necessary substitutions and unifying the symbols and the units the diameter of the intermediate shaft was shown to be given by the general formula :

$$d = C \sqrt[3]{\frac{H}{R}}$$

where C takes the following values :

according to	Lloyds Register of Shipping	8.9
according to	Det norske Veritas	8.9
according to	The Bureau Veritas	8.9
according to	The American Bureau	9.14
according to	The Germanischer Lloyd	10.0

Hence the value for C of 8.9 was adopted since it suits the majority of the different Classification Societies.

The next step was to determine the diameter of the propeller shaft. According to Lloyds Register, the propeller shaft diameter d_p is given by the following formula

COMPARISON OF FREQUENCY RESULTS

Engine Group	Engine's Characteristics	No. of Engine Cyl ²	Exact Frequency (ω_c) rad/sec	Proposed Formulae			
				Original		Simplified	
				freq. (ω) rad/sec	error %	freq. (ω_s) rad/sec	error %
I	Builder Mitsubishi	8	26.45	25.50	- 3.59	25.10	- 5.10
	Type KSZ 86/160 E	9	26.77	26.00	- 2.34	25.50	- 4.52
	HP/Cyl 2300	10	26.93	26.20	- 2.39	25.63	- 4.47
	RPM 118	12	26.91	26.30	- 1.83	25.87	- 3.56
II	Builder Gotaverken	8	25.12	26.10	+ 3.93	25.38	+ 1.20
	Type DM 830/1700 VGS U	9	25.66	26.30	+ 2.60	25.60	- 0.04
	HP/Cyl 2400	10	25.53	26.40	+ 3.59	25.80	+ 1.09
	RPM 119	12	25.86	26.55	+ 2.76	26.00	+ 0.74
III	Builder Mitsubishi	8	26.98	26.40	- 1.79	26.20	- 2.72
	Type KSZ 93/170 E	9	27.22	26.60	- 1.94	26.40	- 2.74
	HP/Cyl 2780	10	27.30	26.80	- 1.83	26.50	- 2.93
	RPM 115	12	27.13	26.80	- 0.94	26.80	- 0.94
IV	Builder Sulzer	8	28.99	27.10	- 5.93	26.10	- 9.41
	Type RND 90	9	29.10	27.25	- 5.78	26.33	- 9.01
	HP/Cyl 2900	10	29.43	27.35	- 6.51	26.50	- 9.40
	RPM 122	12	28.48	27.37	- 3.53	26.73	- 5.72
V	Builder MAN	8	28.80	27.00	- 6.25	26.20	- 9.02
	Type KSZ 90/160	9	29.25	27.40	- 5.82	26.47	- 8.95
	HP/Cyl 3000	10	29.30	27.45	- 5.75	26.60	- 8.54
	RPM 122	12	28.89	27.45	- 4.47	26.90	- 6.48
VI	Builder Sulzer	8	27.20	27.40	+ 0.85	27.05	+ 3.36
	Type RND 105	9	27.20	27.50	+ 1.31	28.35	+ 4.18
	HP/Cyl 4000	10	27.06	27.60	+ 2.08	28.50	+ 5.36
	RPM 108	12	26.39	27.60	+ 4.60	28.80	+ 8.88

Adding 25 % of the above value to account for the entrained water [6] and transforming to the (kg-cm-sec) metric units, J_p takes the final form:

$$J_p = 50.25 D^5 \text{ kg.cm.sec}^2 \quad (7)$$

where D is the propeller diameter in meters.

Two other formulae for the determination of the mass moment of inertia of the propeller and entrained water were used to check the value obtained by means of Eq. (7). Due to space limitations, we give only the final form of both formulae :

i) Kutuzov's formula [7]

$$J_p = 59.87 D^5$$

ii) Formula quoted by Seward [8].

$$J_p = 57.8 D^5$$

From the above three formulae evolves the expression used in this paper which represents their average, hence J_p was taken as :

$$J_p = 56 D^5 \text{ kg.cm.sec}^2 \quad (8)$$

It thus remains to derive an expression for the propeller diameter D .

This can easily be done as shown below with the help of the B 5-60 systematic-screw series design [9]. We have

$$B_p = \frac{R \sqrt{P}}{V^{2.5}}$$

and
$$\delta = \frac{R D}{V_a} \quad (9)$$

$$V_a = V_s (1 - w)$$

where

R = propeller rpm

P = horsepower delivered to the propeller.

V_a = speed of advance in knots.

V_s = ship's speed in knots.

w = wake factor.

a = pitch ratio = p/D .

P = propeller pitch in ft.

Taking the maximum propeller efficiency as the design criterion for an optimum propeller, a direct relation between B_p and δ for such a condition is derived and shown in Fig. (3). It is obvious that

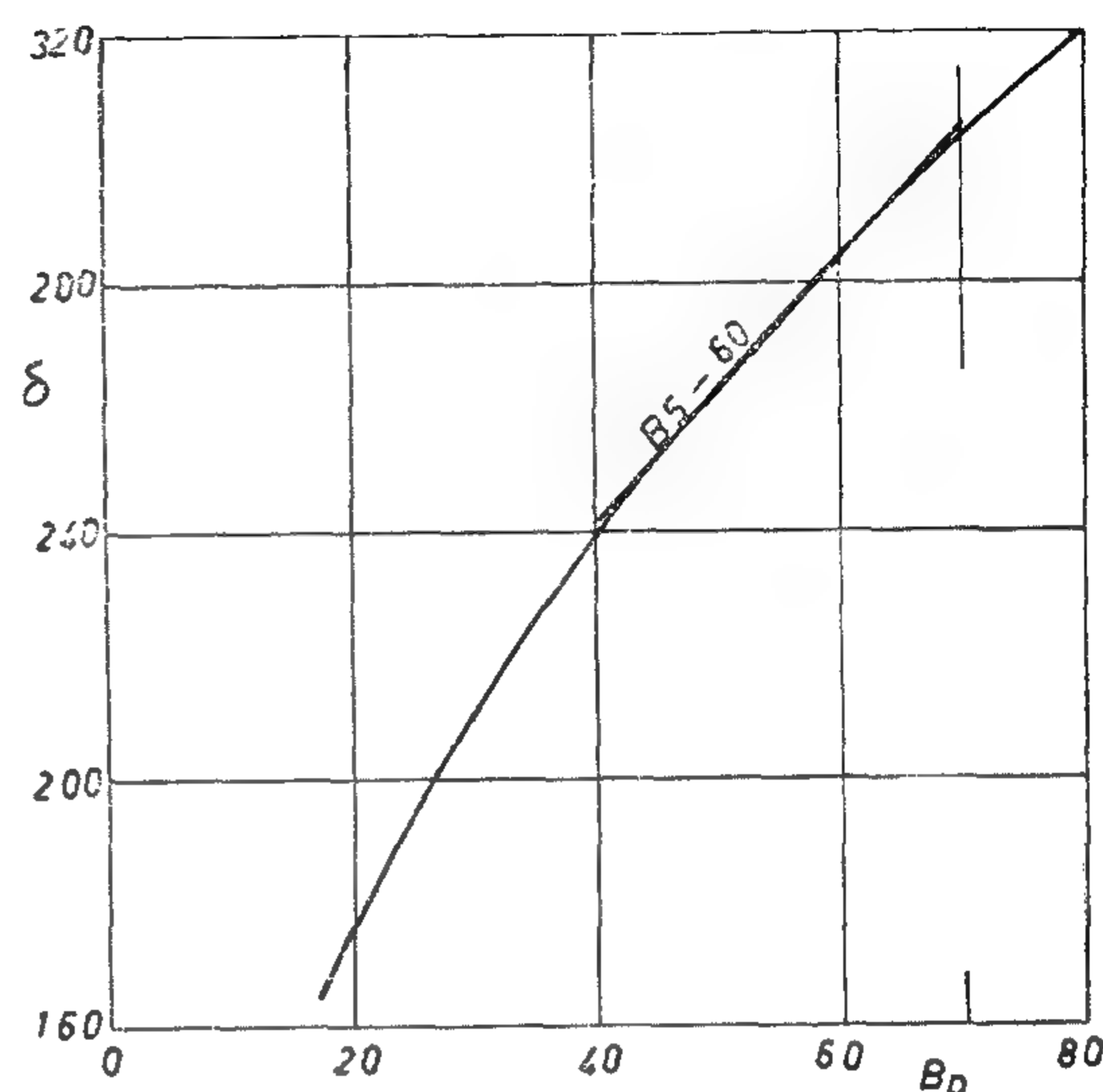


FIG. (3)

this relation for the range of B_p corresponding to the large tankers under consideration here; namely, $(40 < B_p < 70)$ is very nearly a straight line. Such line is given by the following expression:

$$\delta = 2.136 B_p + 156.54$$

Substituting from Eq. (9) into this expression, and assuming the wake factor to be equal to 0.36 [2], and the mechanical transmission efficiency of 0.98, the propeller diameter in meters can be estimated from :

$$D \approx \frac{489}{R} + 0.0197 \sqrt{H} \text{ mt.} \quad (10)$$

The accuracy of Eq. (10) has been checked against propellers of known data. It turned out that the equation yielded values approximately 3 % higher than the existing values. Hence, Eq. (10) is modified to take the final form:

A plot of J_c against (H/R) representing existing engines is shown in Fig. (2). A considerable scatter is noticed, but this is to be expected since different builders have, essentially, different designs and construction experience.

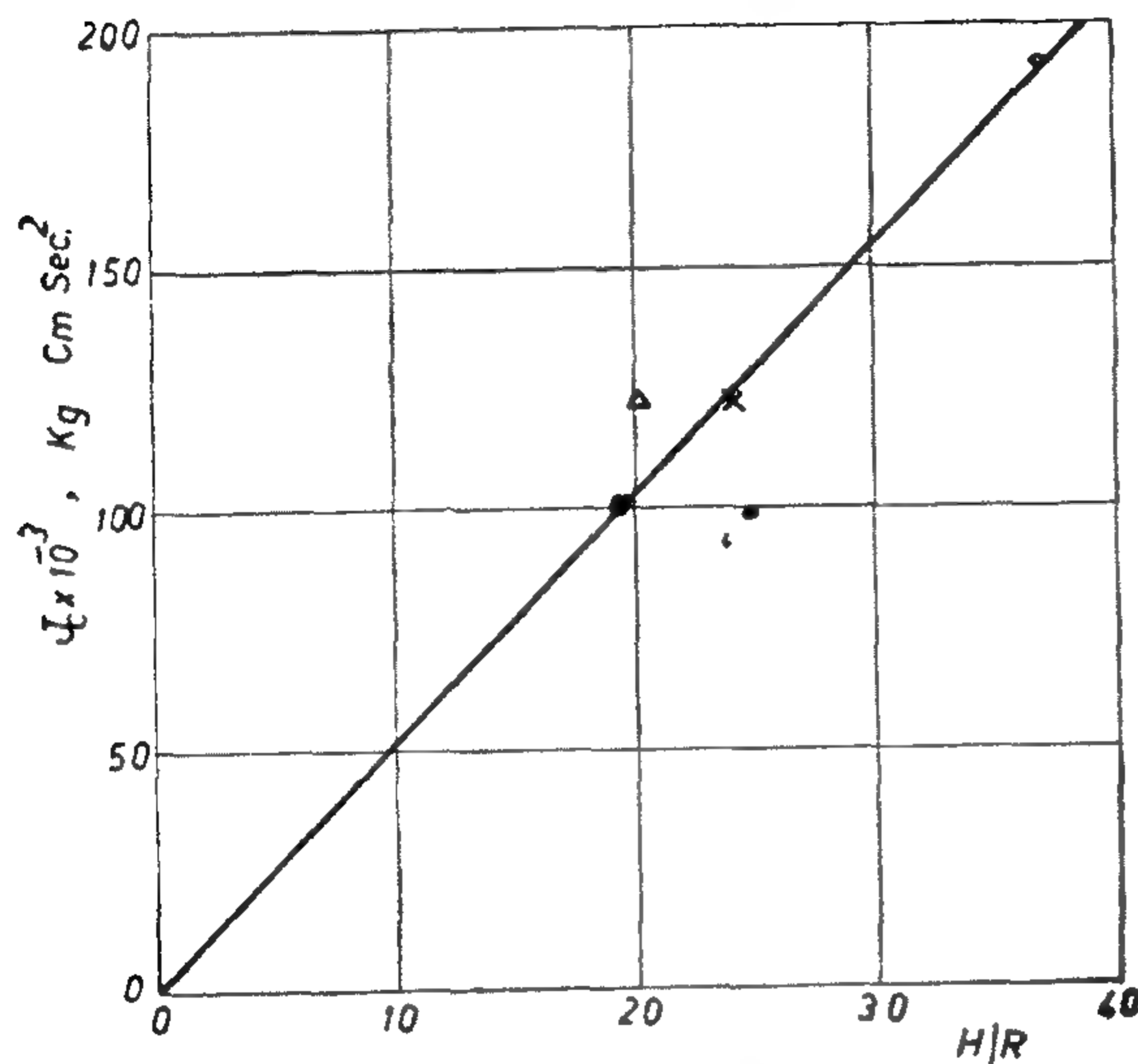


FIG. (2)

However, a very simple relationship that furnishes a fair representation of the available data in the given range can be derived and is given by

$$J_c = 5160 (H_c/R) \quad (2)$$

and

$$J_c = N J_c$$

where

$$\begin{aligned} H_c &= \text{Horsepower per cylinder} \\ N &= \text{Number of cylinders} \end{aligned}$$

2 — The Propeller Inertia :

The propeller mass moment of inertia is a function of many geometrical factors. Hence, an exact determination of the propeller inertia is not only a tedious job but also requires complete propeller drawings. Therefore, we have resorted to the empirical formulae in a way to reduce them to the most simple form.

Consider first the formula given by O'Brian [5], by which the moment of inertia of the propeller in lb.ft² is given by:

$$J_p = \frac{BD^2W_B}{15.7} + \frac{1}{8}W_H(d_b^2 + d_s^2) \quad (3)$$

The first term represents the moment of inertia of the blades while the second represents the moment of inertia of the blades while the second represents the moment of inertia of the boss, and

$$W_B = \frac{wD^3 a \tau}{3.69 B} \quad (4)$$

$$W_H = \frac{\pi}{4} w L_b (d_b + d_s)(d_b - d_s) \quad (5)$$

where

W_b = approximate weight of one blade in lbs.

W_h = approximate weight of boss in lbs.

w = density of screw material in lb/cu.ft.

D = propeller diameter in ft.

τ = blade thickness fraction.

a = developed blade area ratio.

B = number of blades.

L_b = propeller boss length in ft.

d_b = propeller boss outer diameter in ft.

d_s = propeller shaft diameter in ft.

The following parameters are usually expressed in terms of the propeller diameter and within practical applications could be expressed as follows :

$$\begin{aligned} L_b &= D \\ d_b &= 0.2D \\ d_s &= 0.1D \end{aligned} \quad (6)$$

Substituting by the appropriate values for some parameters and making use of Eq. (3) the moment of inertia of the propeller J_p can be simplified in the form:

$$J_p = 0.2485 D^5 \quad \text{lb.ft}^2$$

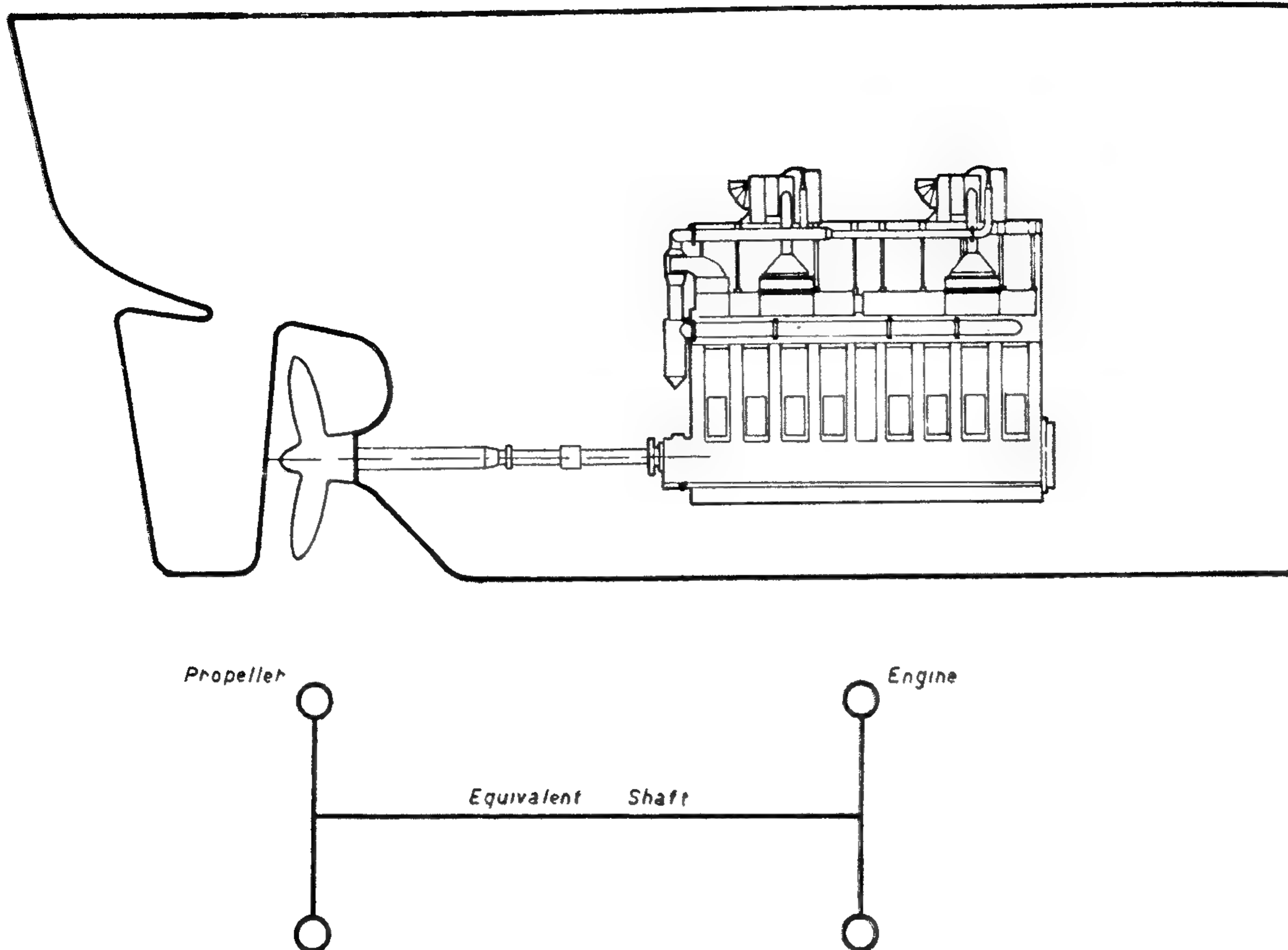


FIG.(1) REDUCTION OF THE PROPULSION SHAFTING SYSTEM
TO A TWO MASS SYSTEM

$$J_c \approx J_r + \frac{1}{2} m L_c^2$$

where

- J_c = mass moment of inertia per cylinder.
- J_r = mass moment of inertia of rotating parts per cylinder
- m = mass of reciprocating parts per cylinder.
- L_c = crank radius.

The above expression does not furnish an easy way for the calculation of the cylinder inertia, since it requires the knowledge of J_r , m , L_c which are not usually available especially in the early design

stages. Hence, the need arises for a different approach. It is clear that J_c is a function of L_c as well as the mass of the moving parts (rotating and reciprocating).

This in turn, though dependent on the particular engine construction, can be considered as a function of the piston area A and the piston length or in general J_c is proportional to (AL_c) .

Now since the mean effective pressure for the type of engines considered here is more or less constant. One can readily conclude that J_c is proportional to (H/R) . Where H is the engine horsepower and R is the engine rpm.

ratios around 0.6. The wake pattern, which plays a role in the propeller design, is influenced by the tanker block coefficient, hence the need for the choice of a definite value of that coefficient is essential. Fortunately, the great increase in tanker capacities has led to ships that are quite full, i.e. having an almost constant block coefficient of about 0.85 [2].

From the survey it was also clear that the engines of such tankers are almost invariably located far aft, due to constructional and strength considerations, which led, in turn, to relatively short intermediate shafts. The length of shafting may vary appreciably, that is why no attempt to standardize such length was made.

Moreover, large motor-tankers are usually propelled by directly - coupled large-bore, 2-stroke, slow speed Diesel engines. The engine speed is mostly around 110 rpm, ranging between 108 and 122 rpm. The horsepower ranges between 2300 and 4000 hp per cylinder, while the mean effective pressure is more or less constant as it ranges from 10.6 to 12 kg/cm².

THEORETICAL FREQUENCY CONSIDERATION :

In general, the propulsion system of a large motor tanker consists essentially of three main components, namely, the engine, the driving shaft and the propeller.

In the study of torsional vibrations, such a system is usually depicted by a model consisting of a disc to represent the propeller's inertia, a shaft to represent the elasticity of the driving shaft and many discs each representing the inertia of the moving parts of each cylinder. These are connected to each other by means of a shaft having the same stiffness as that portion of the crankshaft between each two consecutive cylinders.

Thus we generally have a many-degree-of-freedom system. The natural frequency of such a system is usually determined by means of the well known Holzer tabulation method [3].

In order to employ that technique one needs an approximate value for the natural frequency. This is always obtained by reducing the system to a two-degree-of-freedom system. Fortunately in our case, since the total crankshaft stiffness is much larger than that of the driving shaft (15 to 20 times), one is not far away from the actual system if all the engine inertia is lumped at the after most cylinder.

Having thus arrived at the two-degree-of-freedom system shown in Fig. (1), one can apply the well known formula for the natural frequency of the system, namely:

$$\omega^2 = K_{eq} \left(\frac{1}{J_e} + \frac{1}{J_p} \right) \quad (1)$$

where

- ω = natural frequency of the system.
- K_{eq} = equivalent stiffness of driving shaft.
- J_e = total mass moment of inertia of engine's moving parts.
- J_p = mass moment of inertia of propeller including entrained water.

As mentioned before, Eq. (1) gives a first trial value for the frequency. However, in reducing the multi-mass system to a two-degree-of-freedom system, one has to be very careful to have the various approximations in such a way that the frequency based on Eq. (1) approaches, and in fact be a good deal close to, that of the actual system.

The Propulsion System Parameters :

1 — Engine Inertia :

The equivalent mass moment of inertia per cylinder is usually given by [4].

TORSIONAL VIBRATION ANALYSIS FOR THE PROPULSION SYSTEMS OF LARGE MOTOR TANKERS

Part I : NATURAL FREQUENCY EVALUATION

PROF. F. BAHGAT, M. SC., PH.D.

Professor of Marine Engineering
and Ship Machinery
Marine Engineering and Naval
Architecture Department

N. MAHAREM, M. SC., PH.D.

Asst. Prof. of Mechanical
Vibrations
Mechanical Engineering
Department

A. EL-IRAKI, B.SC.

Teaching Assistant
Marine Engineering

and Naval Architecture Department
Faculty of Engineering, Alexandria University

INTRODUCTION

Ship vibrations can be classified into two main broad groups; namely, the hull and the propulsion system vibrations. Both groups, have received a great deal of attention from research workers over a long period of time.

The propulsion system vibrations, on the one hand, generally involve three different types of vibrations, namely; lateral, longitudinal as well as torsional vibrations. Meanwhile, all types may be excited either by the engine or the propeller or both [1].

In recent years, there has been a continuous trend towards the increase in the size of oil tankers and consequently their engine power. This led to the evolution of new category of ships better known as the super, the monster as well as the mammoth types or otherwise commonly known as VLCCs. Such state of affairs, in turn, has posed certain considerations, from the vibration point of view, which was partly responsible for initiating the present work.

Since the effect of the torsional vibration presents the most significant of all

three types to the extent of being sometimes disastrous, we have confined our attention in this paper to its study and in particular to the determination of its first mode natural frequency. Our objective was to arrive at a simple formula for that frequency which requires the knowledge of the basic data of such propulsion shafting systems; normally available at the early design stages.

Characteristics of the Selected Tankers :

Although ships possess individual characteristics, yet large size tankers have many common features that allow some degree of standardization to the extent that they can be treated sometimes as groups. A general survey of existing large oil tankers throws some light and justifies the choice of certain particular values for some of the main parameters involved in this study.

It was observed that, despite the ever increasing carrying capacity of large oil tankers, their speed has remained almost unchanged ranging around 16 knots. Moreover, the great majority of such tankers were single screw ship driven by five bladed propellers with blade area

INDUSTRY & PRODUCTION

**INST. OF MECHANICAL ENGINEERS
INST. OF ELECTRICAL ENGINEERS**

الخامات الأولية والصناعات الكيماوية

جمعية مهندسي المناجم والبترو
والفلزات
جمعية المهندسين الكيماويين

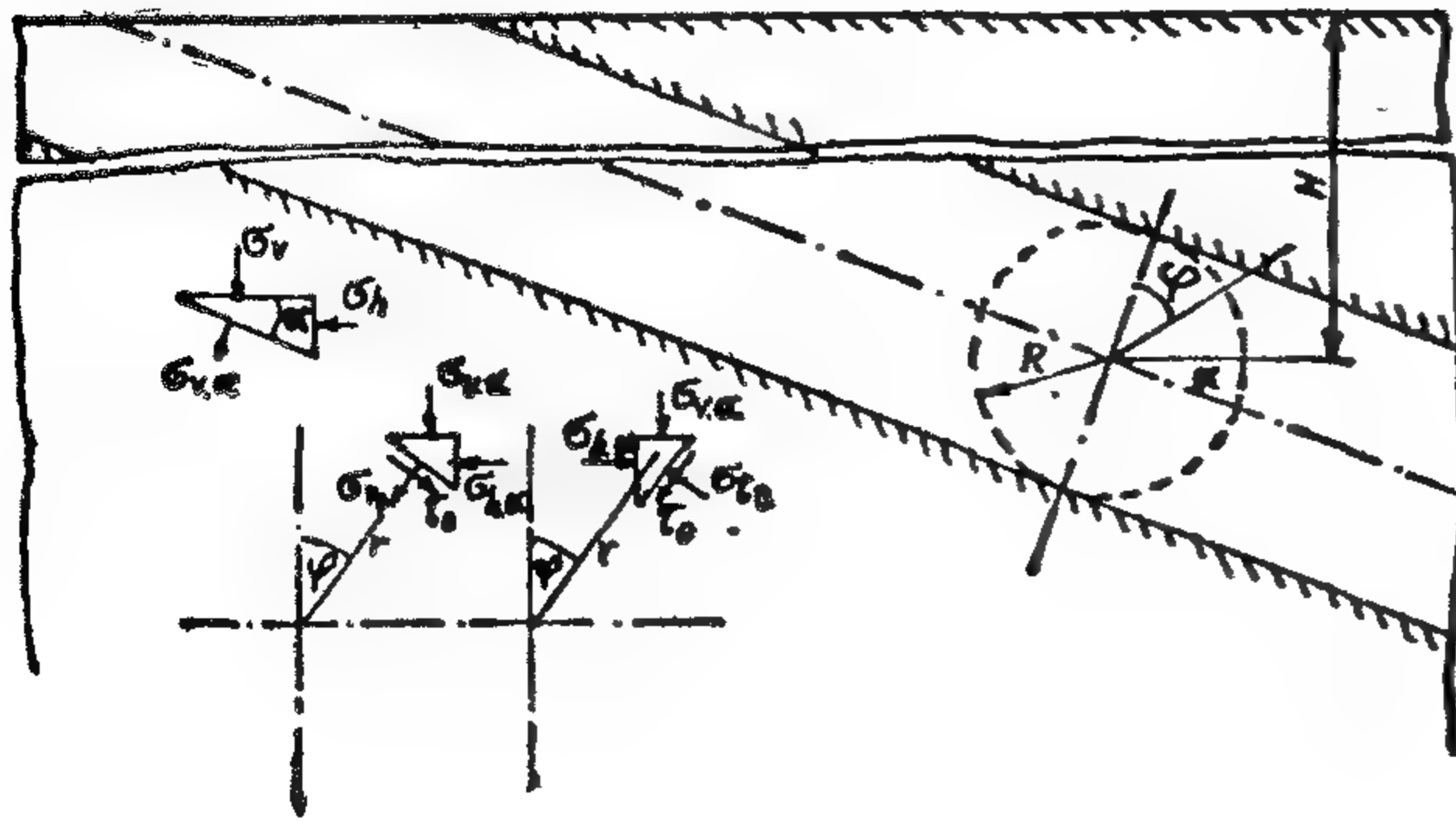


Fig. (6)

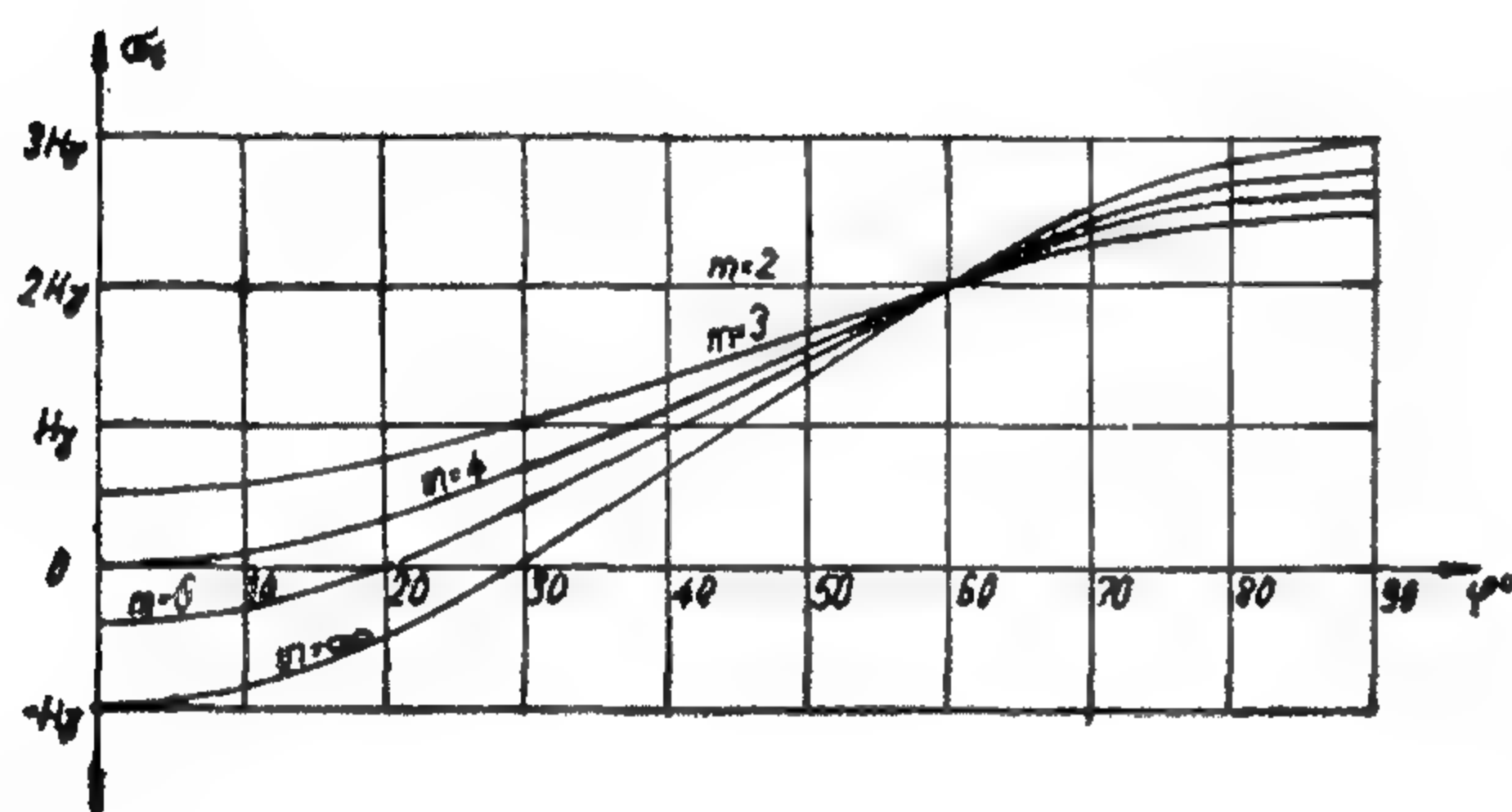


Fig. (7)

It is sufficient to plot the variation of σ_t only from $\phi = 0^\circ$ to $\phi = 90^\circ$.

The diagram proves the existing relation between Poisson's ratio and the tangential stress. The greater the Poisson's ratio, the more the tangential stress will concentrate around the gallery and vice versa.

(5) Conclusions :

1. It is essential before carrying out Maghara mine excavations to know the state of stress about these excavations.
2. The rupture of rocks starts usually at the roof or the floor of the mine excavations when the shear stress reaches the shear strength of the rocks. The correct determination of Poisson's ratio and a knowledge of to what height the effect of shearing stress extends will prevent rock fractures and bursts which may cause disasters.
3. The study of Maghara coal mine field reveals that clay beds and underground water appears to be very important factors in determining the stress distribution about mining excavations.

(6) References

- (1) Timoshenko & Goodier: Theory of Elasticity. (1951).
- (2) Terzaghi-Richart : Stresses in Rocks about Cavities. (1952).
- (3) Tsimbarievich: Stresses in Main Haulage Road Pillars. (Russian) Ugol (1951).
- (4) Isaacson, E. DE ST. Q. : Rock Pressure in Mines. Mining Publications Ltd., Salisbury House, London (1958).

the shaft wall will deform beyond the elastic range but will not fail. It also signifies that beyond elastic deformation permanent set has also taken place.

The stress state caused by the excavation of the shaft has only been considered. However, around the shaft, in the shaft pillar itself, landings, machine rooms and beyond the shaft pillar coal seams shall be extracted. Underground excavations will cause of course additional loading and thrust, transmitted to the shaft pillar. Its magnitude varies as a function of time.

In order to make a good design for a shaft, the most disadvantageous state should be taken into consideration.

The Hungarian Research Centre of Mining gives an approximate solution by adding a correction factor (k) to the equation of the stresses on the shaft walls given in equation (3).

$$\begin{aligned}\sigma_v &= kH \\ \sigma_r &= 2(k-1) \frac{H}{m-1} \\ \sigma_t &= 0 \\ \tau &= 0\end{aligned}\quad (8)$$

In the case of plastic rocks, failure starts at the shaft wall and progresses inward as a function of time.

Rock in non-plastic state may become plastic on absorbing water, or water accelerates the velocity of spread of plasticity. The assumption of the hydrostatical state is on the safe side, because it presents itself only in relatively soft, water-logged strata in periods after the excavations.

In great depths, if the hydrostatical state is to be considered, the shaft is lined with ductile materials, generally with steel, for even high-strength rigid materials would require large dimensions. Steel lining is generally ribbed, because this saves considerable material without substantially reducing load carrying capacity.

b) Inclined Shafts :

According to Fig. (6), the centre line of the shaft dips at angle α to the horizontal.

The original stress-state before sinking the shaft which were given in equations (4) can be expressed in polar coordinates as follows :

$$\begin{aligned}\sigma_r &= H\gamma \left\{ \frac{1}{m-1} + \frac{m-2}{2(m-1)} \cos^2 \alpha + \frac{m-2}{2(m-1)} \cos^2 \alpha \cos 2\phi \right\} \\ \sigma_t &= H\gamma \left\{ \frac{1}{m-1} + \frac{m-2}{2(m-1)} \cos^2 \alpha - \frac{m-2}{2(m-1)} \cos^2 \alpha \cos 2\phi \right\} \\ \tau &= -H\gamma \frac{m-2}{2(m-1)} \cos^2 \alpha \sin 2\phi\end{aligned}\quad (9)$$

The variation of loading which results from the opening of the inclined shaft can be solved by

Timoshenko's stress function :

$$\Phi = \left\{ A r^2 + B r^4 + \frac{C}{r^2} + D \right\} \cos 2\phi \quad (10)$$

Terzaghi-Richart give the final result of the stress field around the inclined shaft as follows :

$$\begin{aligned}\sigma_r &= \frac{H\gamma}{m-1} \frac{r^2 - R^2}{r^2} + H\gamma \frac{m-2}{2(m-1)} \frac{r^2 - R^2}{r^2} \cos^2 \alpha \\ &\quad + H\gamma \frac{m-2}{2(m-1)} \left\{ 1 - 4 \frac{R^2}{r^2} + 3 \frac{R^4}{r^4} \right\} \cos^2 \alpha \cos 2\phi \\ \sigma_t &= \frac{H\gamma}{m-1} \frac{r^2 + R^2}{r^2} + H\gamma \frac{m-2}{2(m-1)} \frac{r^2 + R^2}{r^2} \cos^2 \alpha \\ &\quad - H\gamma \frac{m-2}{2(m-1)} \left\{ 1 + 3 \frac{R^4}{r^4} \right\} \cos^2 \alpha \cos 2\phi \\ \tau &= -H\gamma \frac{m-2}{2(m-1)} \left\{ 1 + 2 \frac{R^2}{r^2} - 3 \frac{R^4}{r^4} \right\} \cos^2 \alpha \sin 2\phi.\end{aligned}\quad (11)$$

c) Galleries :

If $\alpha = 0$ is substituted into the groups of equations (11), the stress components of the country rock of circular horizontal galleries are obtained :

$$\begin{aligned}\sigma_r &= \frac{H\gamma}{2} \frac{m}{m-1} \frac{r^2 - R^2}{r^2} + \frac{H\gamma}{2} \frac{m-2}{m-1} \left\{ 1 - 4 \frac{R^2}{r^2} + 3 \frac{R^4}{r^4} \right\} \cos 2\phi \\ \sigma_t &= \frac{H\gamma}{2} \frac{m}{m-1} \frac{r^2 + R^2}{r^2} - \frac{H\gamma}{2} \frac{m-2}{m-1} \left\{ 1 - 3 \frac{R^4}{r^4} \right\} \cos 2\phi \\ \tau &= -\frac{H\gamma}{2} \frac{m-2}{m-1} \left\{ 1 - 2 \frac{R^2}{r^2} - 3 \frac{R^4}{r^4} \right\} \sin 2\phi\end{aligned}\quad (12)$$

The variation of the tangential stress presenting itself on the rock surface of the gallery is represented by Fig. (7).

Fig. (4) shows the variation of stresses. It is evident that as compared to the original stress state there is a substantial change of stress only in the immediate neighbourhood of the shaft. At a distance of twice the shaft diameter from the shaft axis the original stress state is present. The most disadvantageous intensity of stress in rocks about the shaft presents itself at the shaft wall, and ground failure starts at this place. According to Fig. (4) the stresses arising on the shaft wall are independent of the shaft diameter. In the same time it is clear that the shaft diameter will affect the penetration of stresses into the country rocks.

The stress state of the immediate neighbourhood is three dimensional. Biaxial deformation would arise if the vertical stress H is constant. According to the natural order of things H changes and this change generates shearing stress in the shaft lining on horizontal planes and on the tangential planes. The variation of H being linear, this shearing stress is constant, independent of depth. With increasing depth this shearing stress loses importance, and it is not essential from a mining point of view.

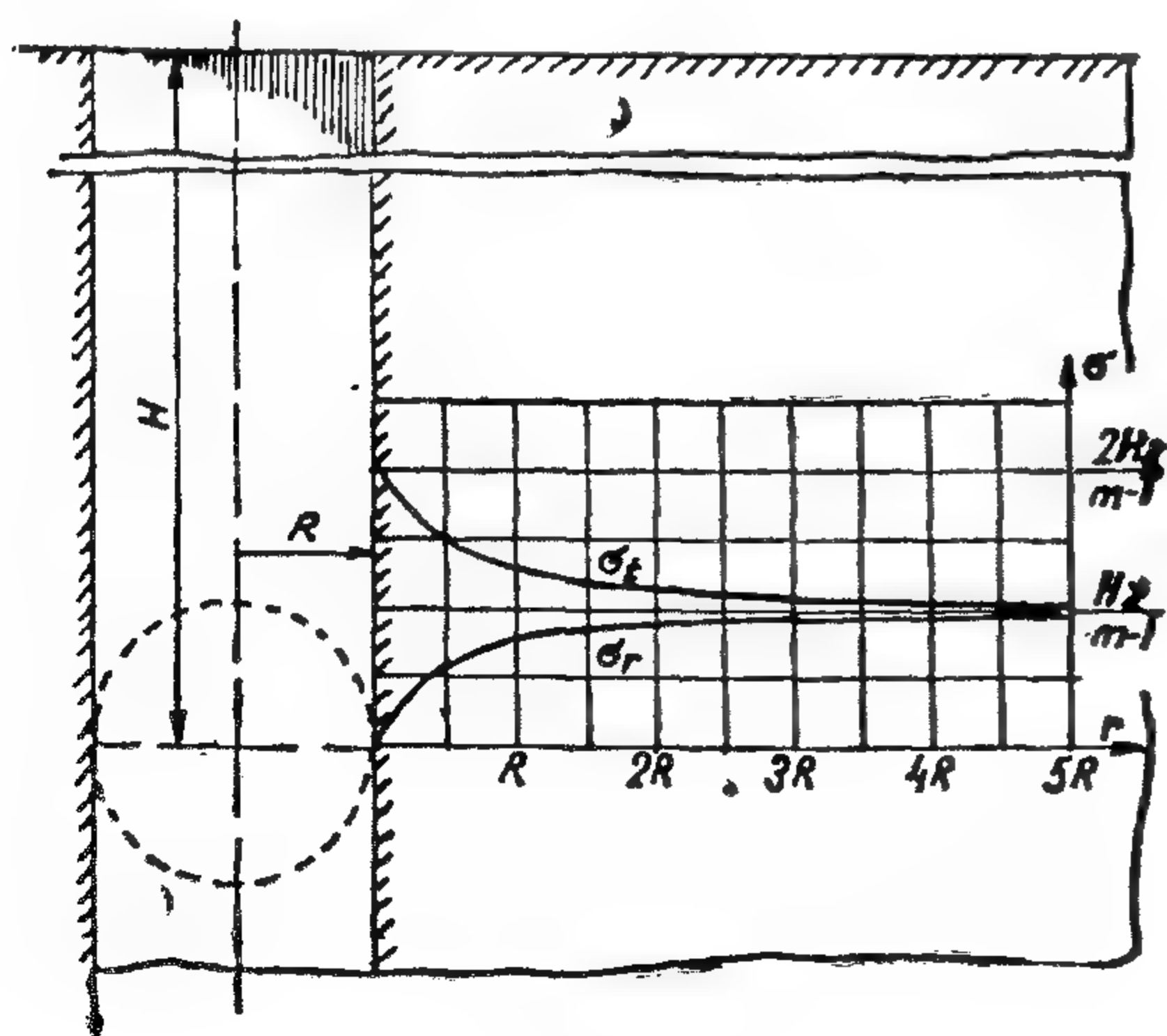


Fig. (4)

It is well established by laboratory experiments carried out by the authors on the different types of the Maghara coal mine rocks, that the stress-strain relationship can be represented by Fig. (5).

The perfectly elastic region ($O \rightarrow a$), the elasto-plastic ($a \rightarrow p$) and the perfectly plastic region beyond the point p .

Relationships derived on the basis of the theory of elasticity will hold only up to point a . Let point b be chosen along

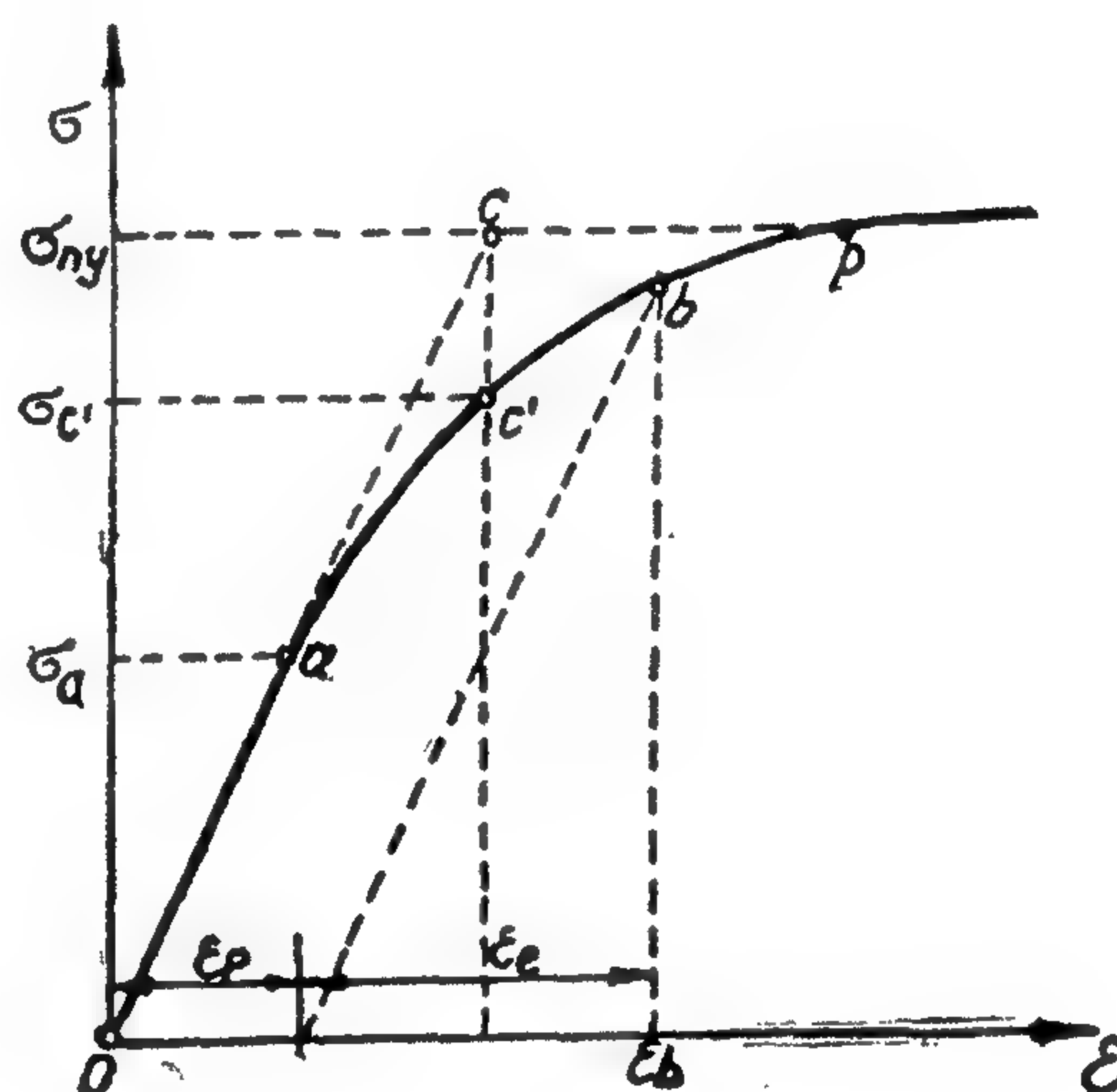


Fig. (5)

the elasto-plastic section $a-p$. It is clear that the deformation, measured on the abscissa axis can be divided into two parts ϵ_e which is the elastic and ϵ_p the plastic deformation.

If the relationships, obtained on the basis of the theory of elasticity, are extended to section $a-p$ too, a neglect has been committed. A practically admissible error is if the relationships are assumed valid for section oc' . This means that as long as:

$$\sigma_c' > \frac{2H\gamma}{m-1} \text{ or } \sigma_c' > H\gamma$$

(7)

If the infinite strip loading extends on both sides to infinity, i.e., the width (2a) becomes infinite, then the stress state of the infinite half space is very simple :

$$\begin{aligned}\sigma_r &= q \\ \sigma_h &= \frac{q}{m-1} \\ \tau &= 0\end{aligned}\quad (3)$$

where m is Poisson's ratio.

(4) Prediction of the state of stress around excavations :

In order to extract coal efficiently and safely, the stress state around different excavations should be well studied in order to avoid troubles which may arise in the case of wrong planning of the mine excavations. The following is a critical discussion of stress distributoin around some mining openings.

a) Vertical Shafts :

Let the state around vertical shafts be established. The cross section is circular, the shaft penetrates different strata. Two physical characteristics of the different layers have to be known: compressive strength and Poisson's ratio of the rocks.

The stress state before shaft sinking can be expressed by the following equations :

$$\begin{aligned}\sigma_v &= H\gamma \\ \sigma_h &= \frac{H\gamma}{m-1} \\ \tau &= 0\end{aligned}\quad (4)$$

where H stands for distance from the surface.

γ for the volumetric weight of rocks.

σ_v vertical (component) of the stress.

σ_h horizontal (component) of the stress.

τ shear stress.

Stress distribution is shown in Fig. (3).

σ_t is the tangential stress.

σ_r is the radial stress.

r is the radial distance.

R is the radius of the shaft.

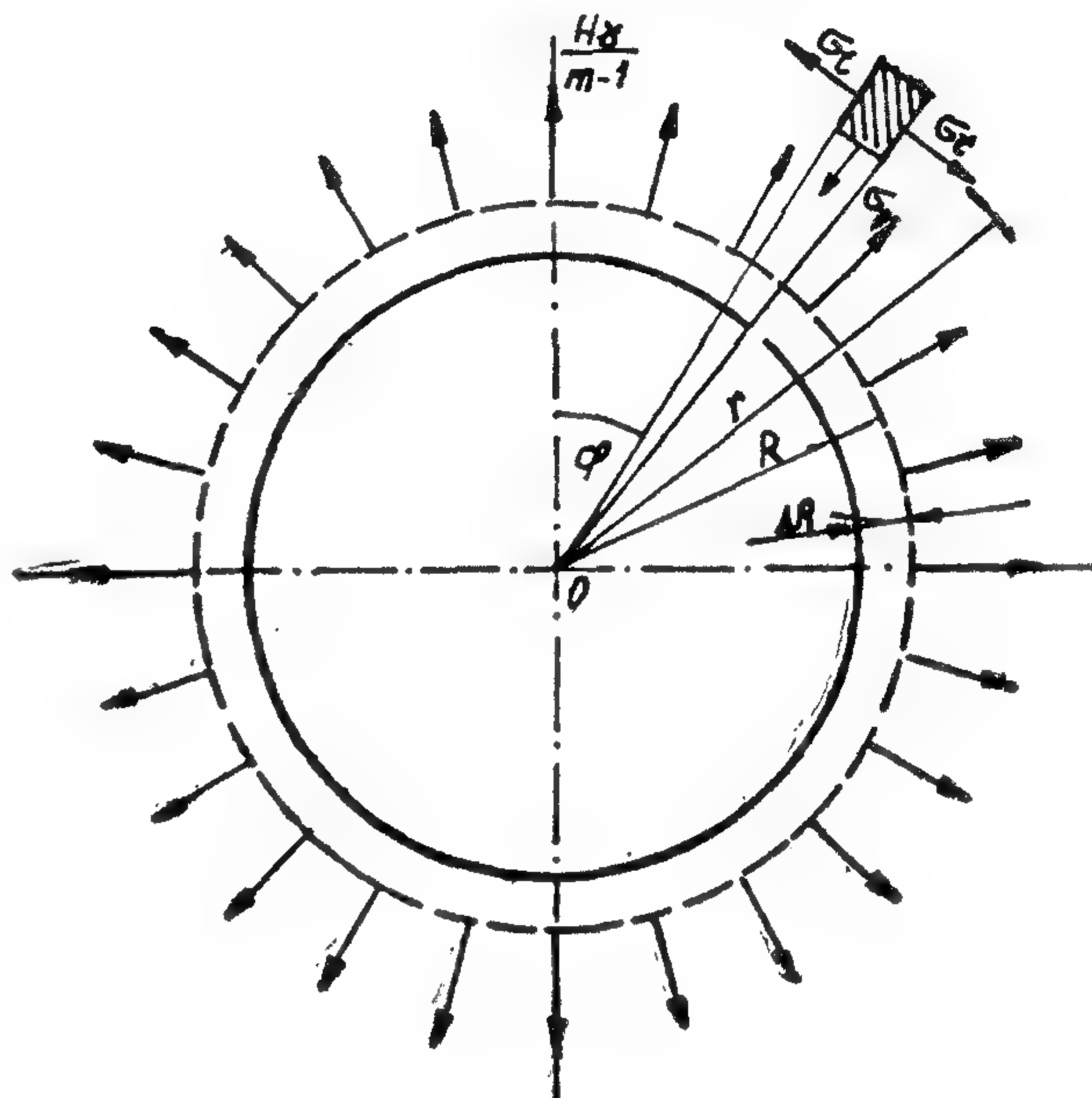


Fig. (3)

The problem is turned to be similar to that of a thick walled tube and the internal pressure equals $H\gamma / m-1$ the tangential and radial stresses are accordingly :

$$\begin{aligned}\sigma_t &= \frac{H\gamma}{m-1} \frac{r^2 + R^2}{r^2} \\ \sigma_r &= \frac{H\gamma}{m-1} \frac{r^2 - R^2}{r^2} \\ \tau &= 0\end{aligned}\quad (5)$$

If $R = r$, that is the border of the shaft wall or on the shaft wall stresses will be:

$$\begin{aligned}\sigma_t &= \frac{2 H \gamma}{m-1} \\ \sigma_r &= 0 \\ \tau &= 0\end{aligned}\quad (6)$$

Moreover, in upper seam horizon, there is an evidence from the many boreholes driven in the area that the sandstone beneath the upper coal seam is saturated with water. This water is a source of static pressure at that depth. Some of the boreholes indicate that the coal seam itself contains a certain degree of humidity which may be of importance in predicting the behaviour of rocks around mine excavations. The sandstone beneath the main coal seam is also saturated with water in the present dip drainage system. The main seam dip workings are wet, and part of the first main seam production face "No. 1 east" is below the natural water level.

Informations obtained from boreholes logs show that there is often heavy roof- and sometimes weaker floor.

Immediately beneath the upper coal seam, there is 20 to 30 cms. of clays, with thin carbonaceous shale at the top. This carbonaceous shale is weak and may be of some importance to the workable thickness, as it appears probable that the coal seam can be undercut in it.

(3) Theoretical Fundamentals :

In Maghara area two main sources of stresses should be considered. First, stresses produced by the load due to weight of the superincumbent rock, which is a function of depth, and second, the unrelieved tectonic stresses which should be evaluated according to the structures in the area.

Theory of elasticity postulates that stress components of the stress field produced in the isotropically elastic infinite half space along an infinite straight line by uniform vertical loading are formulated when the material of infinite half space is assumed as weightless:

$$\begin{aligned}\sigma_v &= \frac{2}{\pi} \frac{q}{r} \cos^3 \phi \\ \sigma_h &= \frac{2}{\pi} \frac{q}{r} \cos \phi \sin^2 \phi \\ \tau &= \frac{2}{\pi} \frac{q}{r} \cos^2 \phi \sin \phi\end{aligned}\quad (1)$$

where :

σ_v denotes vertical stress, σ_h horizontal normal stress, and τ the shear stress. q expresses the intensity of vertical loading, r & ϕ are defined by Fig. (1).

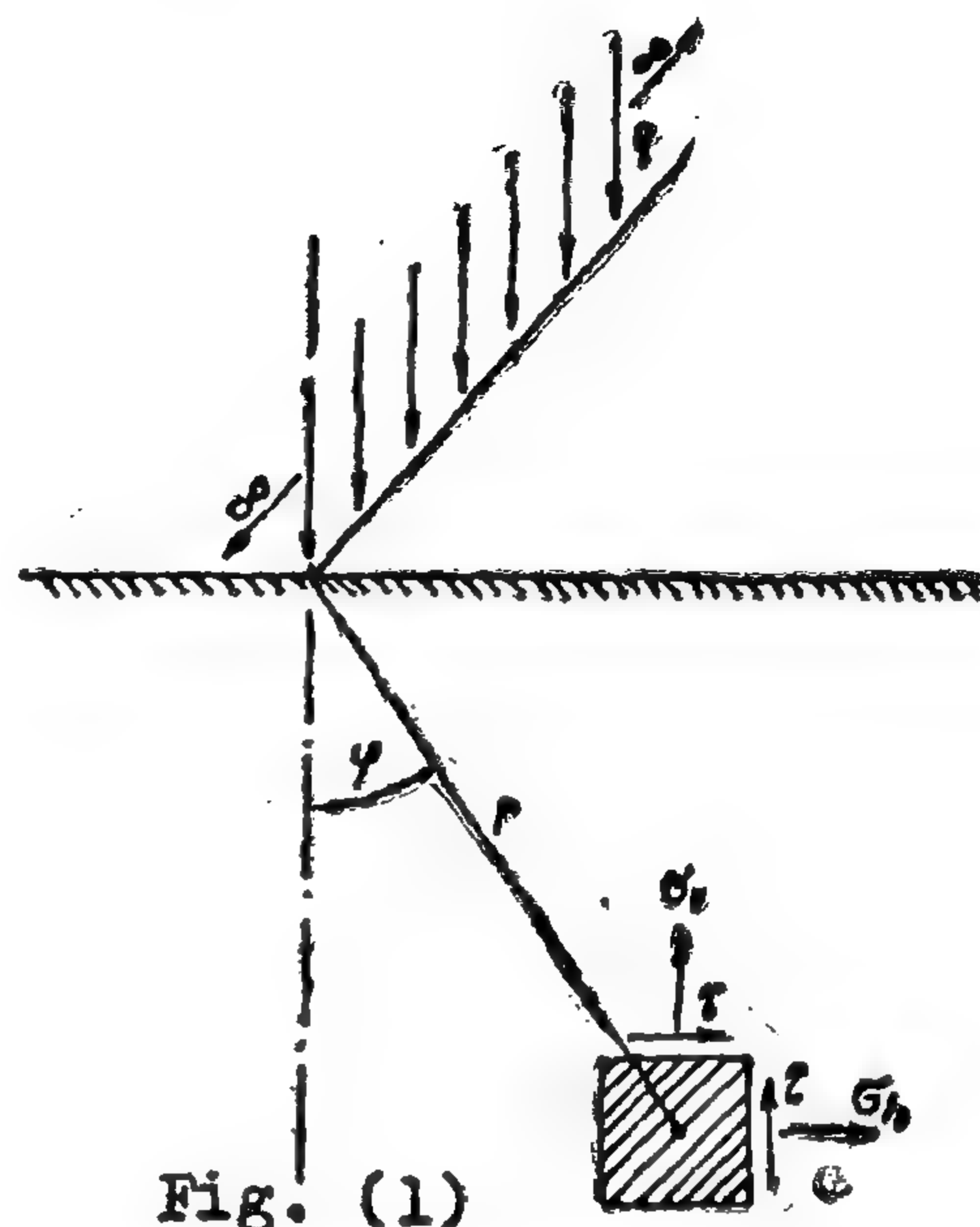


Fig. (1)

The known relationships of the loading of the infinite strip will be written with reference to the notations given in Fig. (2).

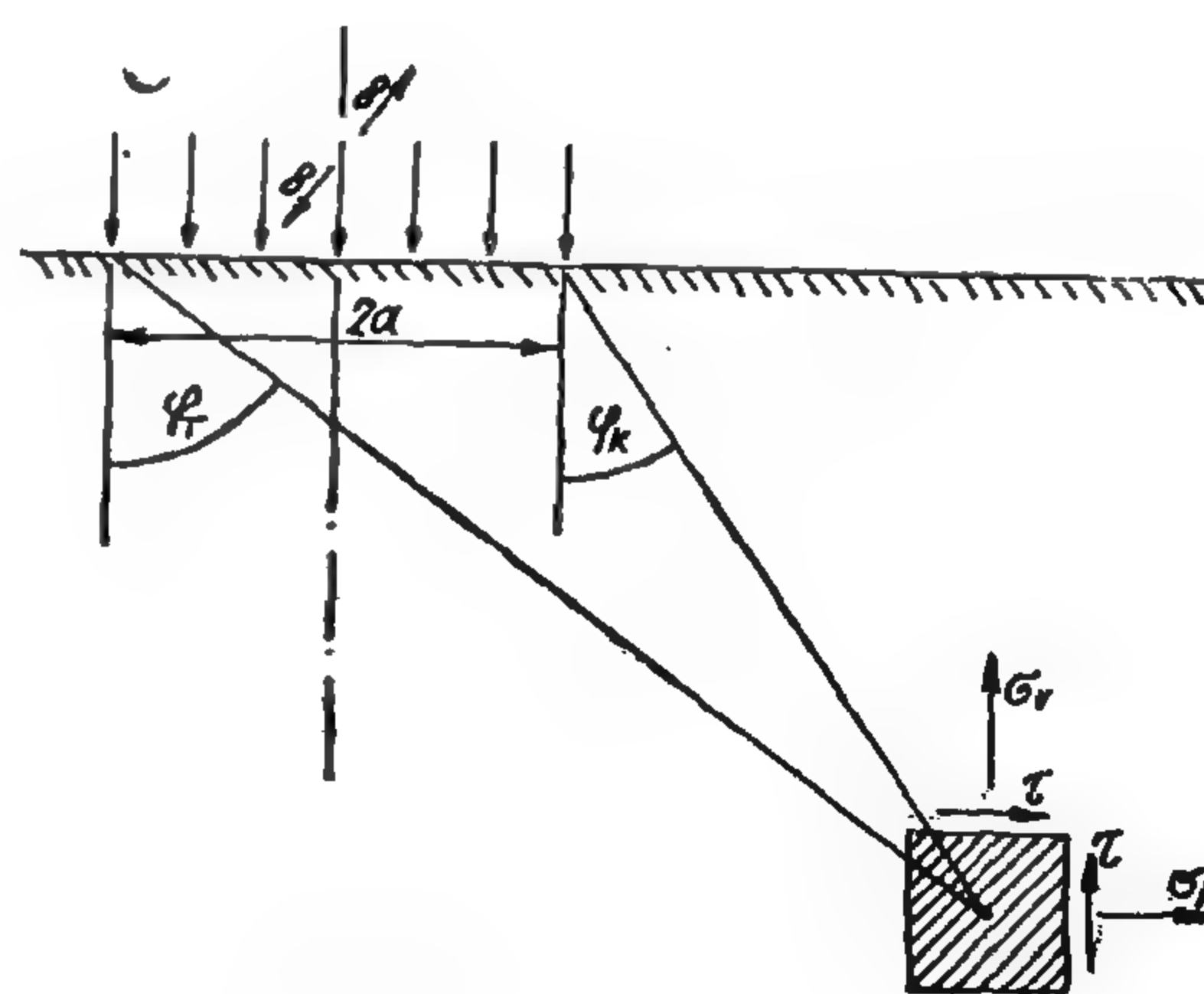


Fig. (2)

$$\begin{aligned}\sigma_v &= \frac{q}{\pi} (\sin \phi_T \cos \phi_T - \sin \phi_K \cos \phi_K + \hat{\phi}_T - \hat{\phi}_K) \\ \sigma_h &= \frac{q}{\pi} (-\sin \phi_T \cos \phi_T + \sin \phi_K \cos \phi_K + \hat{\phi}_T - \hat{\phi}_K) \\ \tau &= \frac{q}{\pi} (\cos^2 \phi_K - \cos^2 \phi_T)\end{aligned}\quad (2)$$

THE STATE OF STRESS IN ROCKS AROUND MAGHARA COAL MINE OPENNINGS

By

MOHEB EL-DIN HUSSEIN, Ph.*

HASSAN F. IMAM, Ph. D**

NAGY N. YANNI M.Sc.***

(1) INTRODUCTION :

The aim of this article is to obtain an approximate formula to predict the stress-state of the country rocks around vertical shafts, inclines and galleries which is necessary for the exploitation of underground mines. The analysis is based essentially on the fundamentals of the theory of elasticity, laboratory experiments and field observations.

A knowledge of stress distributions and how they are related to the excavations, an appreciation of where the maximum stress concentrations may be and of what regions may be considered as substantially distressed are questions of vital importance to the practising mining engineer.

However, one may summarise the main factors controlling the behaviour of rocks around mine openings as follows :

1. The geological considerations of rocks (presence or absence of fissures, discontinuities, mineralogical structures, ... etc.).
2. The depth of the openings from the surface.
3. Underground water conditions.
4. Physical and mechanical properties of rocks (porosity, ultimate shear strength, ultimate compression strength, creep effects, angle of repose... etc.).
5. Mining operations (blasting effects, the advance of the longwall face ... etc.).

(2) GEOLOGICAL CONSIDERATIONS

The thickness of the overburden in Maghara coal field ranges from less than 45 m. to about 150 m. The dip of the coal seam is about 9° to 11°.

Examination of the exposed rocks in the mine and of hand specimens taken from cores show that the coal seams and associated rocks have been strongly affected by folds, shear planes, fractures, joints and faults. Shear planes are developed in the coal seams forming a system of planes of weakness, most probably due to several intercalations of clays and shales. Also, failure of clay may take place along bed separation planes.

Presence or absence of fractures and joints is an important structural factor which may effects the mechanical behaviour of coal and associated rocks. For instance, fractures and joints occur in sandstones, clays and coal in Maghara coal field. In coal seams joints are mainly of rectilinear type and fractures are often at 45° to the bedding and to a less extent parallel to the bedding. Argillaceous strata have a tendency to develop fractures at about 30° to the bedding. Oolitic limestone formation, overlying the coal seams, is hard and free from fractures and joints.

Other structural defects are the faults and shear zones. There are some faults affecting the face heading of the upper seam. These faults are of small throw (about 20 to 30 cm.) and fault zones are of limited effect.

* Associate Prof., El-Azhar University.

** Associate Prof., Cairo University.

*** Research Assistant, N.R.C., Cairo.

- Compounds", J. Canad. Ceram. Soc., 33, 127-137, 1964.
17. J. Beretka & M.J. Ridge, "The Reaction Between Iron III Oxide and Barium Carbonate in Vacuo", J. Chem. Soc. (A), 2463, 1968.
 18. H. Stäblein & W. May, "Phasen Untersuchungen im System BaO. Fe_2O_3 - Fe_2O_3 ", Berichte der Deutschen Keram. Ges., 64, 126, 1969.
 19. H. Stäblein & J. Willbrand, "Texture and Reaction Mechanism in the Formation of Barium Hexaferrite", Reactivity of Solids, Proc. of the 7th Intern. Symposium on Reactivity of Solids, Bristol 1972. Ed. : J.S. Anderson, N.W. Roberts & F.S. Stone, Chapman & Hall, London 1972.
 20. J. Suchet, "Synthese De La Magnetobaryte Par Frittage", Bull de La Societe Franc. de Ceramique, 33, 33, 1965.
 21. G.C. Bye & C.R. Howard, "The Synthesis of Barium Hexaferrite from Iron Oxide and Barium Carbonate", J. Appl. Chem. Biotechnol., 21, 319-23, 1971.
 22. F. Haberey, M. Velicescu & A. Kocktel, "Ablauf der Herstellung von $\text{BaFe}_{12}\text{O}_{16}$ aus BaCO_3 & $\alpha\text{-Fe}_2\text{O}_3$ ", To be published.
 23. A.J. Mountvola, "Electrical and Magnetic Behaviour of Ultrafine Grain Ceramics", Ultrafine Grain Ceramics, Ed. : J. Burke, N.L. Reed & V. Weiss, Syracuse Univ. Press, 1970.

REFERENCES

1. D.J. Iden, C.E. Ehrenfried & H.J. Garnett, "Present & Future Applications of High Coercive Force Magnets", AIP Conference Proceedings, Magnetism & Magnetic Materials. Ed: C.D. Graham & J.J. Rhyne, New York 1972.
2. G. Heimke & J.D. Nye, "Ferrite Permanent Magnets From Prefabricated Powders", Powder Metallurgy International, 5 (1), 28-33, 1973.
3. H.B. Ries, "The Technology of the Ferrite Manufacture" and Applications", Interceram, 1, 84-92, 1966.
4. H. Wüllkopf, "Einfluss von Rohstoffeigenschaften und Stöchiometrie auf die Sinterkinetik von Bariumferriten", Int., J. Magnetism, 5, 147-155, 1973.
5. A.L. Stuijts, "Sintering of Ceramic Permanent Magnetic Materials" Trans. Brit. Ceram. Soc., 55, 57-74, 1956.
6. H. Wüllkopf, Unpublished Work.
7. A.M. Gadalla & H.W. Hennicke, "On the Reactivity of Ferric Oxide", Powder Metallurgy International, 5 (4), 196-200, 1973.
8. Y. Goto & T. Takada, "Phase Diagram of the System BaO-Fe₂O₃", J. Amer. Ceram. Soc., 43, 150-153, 1960.
9. P. Batti, "Diagramma d'equilibrio del sistema BaO-Fe₂O₃", Annali Di Chimica Rome, 50, 1461-78, 1960.
10. S. Mori, Y. Tawara, E. Hirota, T. Miyawa, H. Mitsuda & C. Okazaki, "Magnetic properties of various phases of barium orthoferrate BaFeO_x", Ferrites Proc. Intern. Conference July 1970, Japan. Ed.: Y. Hoshino, S. Iida & M. Sugimoto, Univ. Park Press, Baltimore, London, Tokio.
11. S. Mori, "Phase Transformation in Barium Orthoferrate", J. Amer. Ceram. Soc., 49, 600, 1966.
12. C.M. Wilson, G.C. Bye, C.R. Howard, J.H. Sharp, D.M. Tinsley & S.A. Wentworth-Rossi, "Solid state Reactions of carbonates with oxides", Reactivity of Solids, Ed.: J.S. Anderson & F.S. Stone, Chapman and Hall, London 1972.
13. G. Sloceri, "Phase Equilibrium in the Subsystem BaO. Fe₂O₃ - BaO. 6 Fe₂O₃", J. Amer. Ceram. Soc., 56, 489-490, 1973.
14. H.J. Van Hook, "Thermal Stability of Barium Ferrite", J. Amer. Ceram. Soc., 47, 579-81, 1964.
15. G. Winkler, "Die Bildung und Umwandlung Hexagonaler und Trigonaler und Trigonaler Magnetischer Phasen in Dreistoffsystem BaO-MeO-Fe₂O₃", Reactivity of Solids, Ed.: G.M. Schwab, Elsevier Publishing Co., 1965.
16. A.G. Sadler, W.D. Westwood & D.C. Lewis, "Differential Thermal Analysis of Ferrite Raw Materials and

Initial permeability increases by grain size and values of saturation magnetization decreases with decreasing grain size.

In view of the above facts, a program of research was planned in Clausthal Technical University aiming to increase sintering rate and to achieve better magnetic properties by controlling microstructure of the product. This include studying the effect of limited additions, in and outside the solubility limits, on densification during various sintering stages, on grain size produced and on magnetic properties.

The latter will be followed using the Permagraph shown in Figure 14. It measures the induction B of the test specimen with the aid of measuring coils arranged immediately on the specimen, in connection with a fluxmeter, while the field intensity H is measured by means of a probe close to the test specimen. It could be used for powder materials and for various cross sections without determining them. It measures also the polarization directly and records the demagnetization curves automatically.

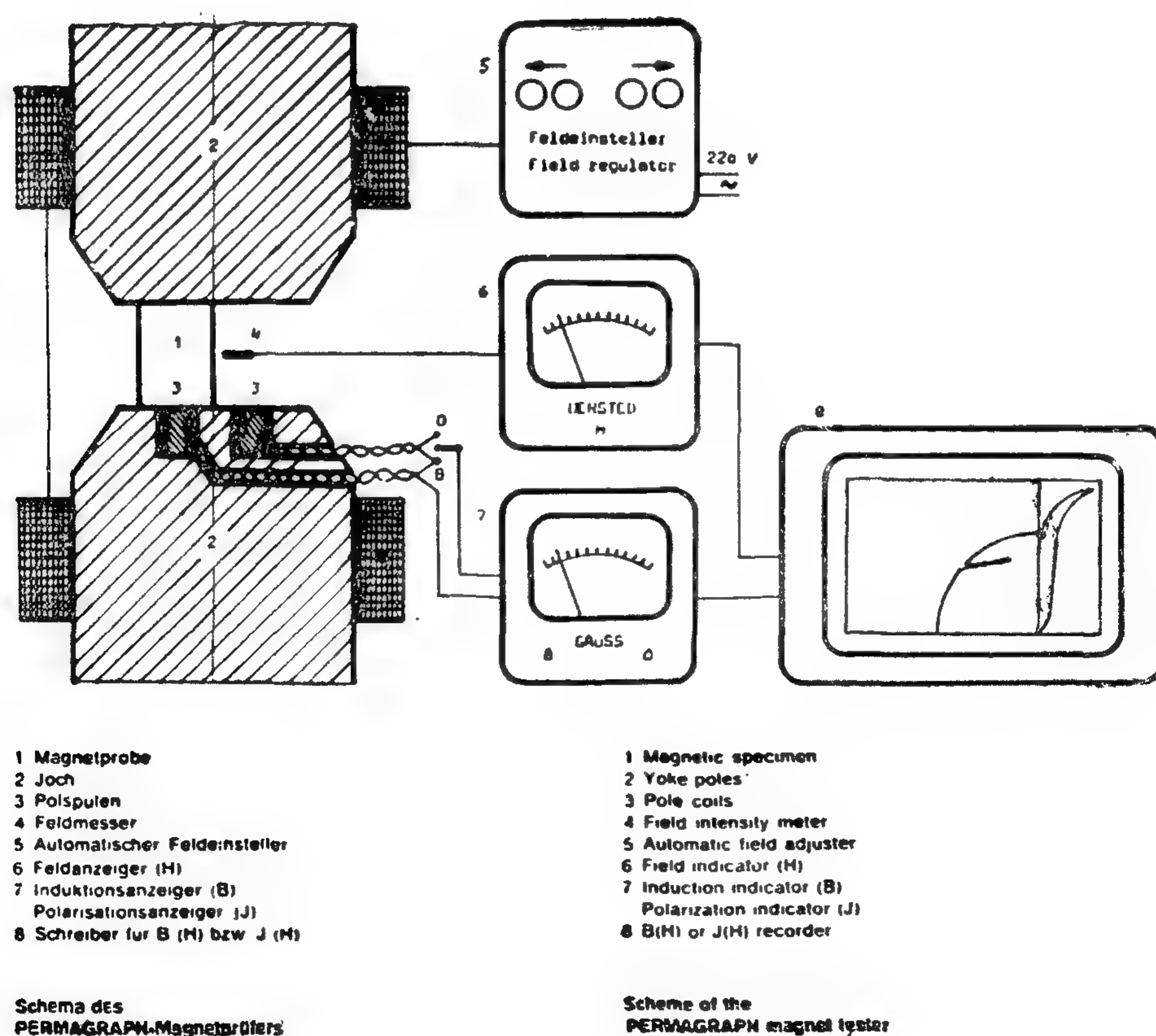


Fig. 14 : Permagraph magnet tester.

Also Figure 12 shows that using $\text{BaO}/\text{Fe}_2\text{O}_3$ of 1 : 5.6 gave at 1300°C pure hexaferrite with smaller crystals after one hour, instead of three hours, thus giving smaller grains after sintering. It should be noted that BaO in excess than required for hexaferrite formation increased the rate of formation of monoferrite at low temperatures and the rate of formation of hexaferrite at high temperatures, as indicated by Figure 9.

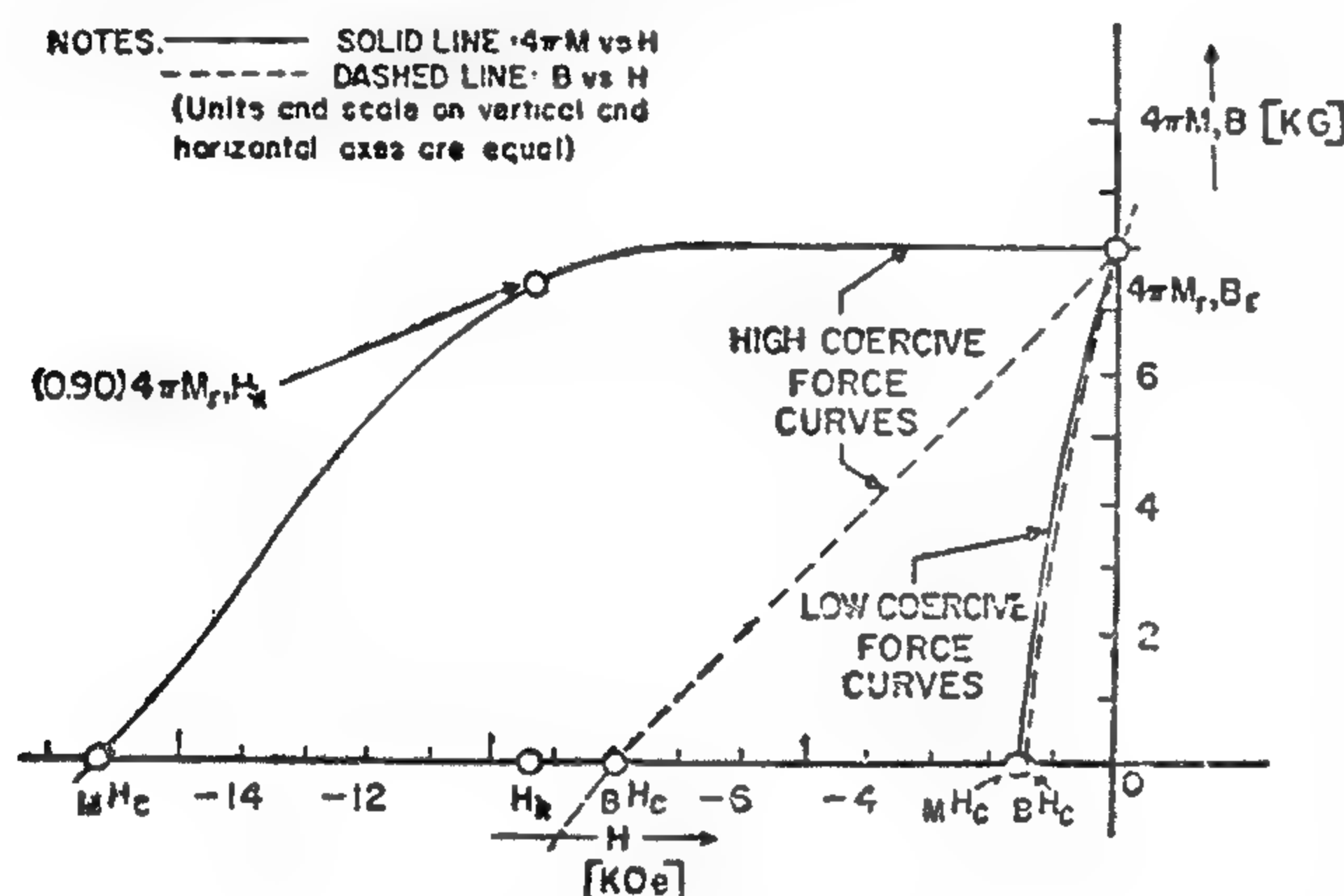


Fig. 13 : Demagnetization curves.

4. CRUSHING AND MILLING :

Usually wet milling is used and further research should be carried out in this field to study the effect of water on the constituents present especially in presence of excess BaO where a change in colour and expansion were observed and could not be explained.

For dry pressing in magnetic field, the water must be removed but for wet pressing in magnetic field the slurry can be used immediately. For isotropic magnets, water must be removed and the powder must be granulated to obtain good flow properties using spray drying or mechanical granulation.

5. FABRICATION PROCESS :

For producing anisotropic magnets the powder is oriented by applying a magnetic field to the die cavity. The green density should be as high as possible to ob-

tain minimum shrinkage with maximum strength. Sintering should be carried out to reach the best mechanical and magnetic properties.

Figure 13 shows demagnetization curves for high and conventional low coercive force permanent magnet materials. The two types of curves ($B-H$ and $4\pi M-H$) used to characterize permanent magnets are shown. The induction or normal coercive force bH_c is the value of the demagnet to zero. The intrinsic coercive force mH_c is the value of the demagnetization field that will reduce the magnetization of a magnet to zero. For conventional magnets values of bH_c and mH_c are nearly equal but for high coercive force magnets $mH_c \geq bH_c$. H_k represents the knee or the limiting field for useful performance and is the value at which the magnetization is reduced to 90% of the residual level.

A useful set of criteria for classification of high coercive force materials are:

- $H_k / 4\pi M$ between 0.5 & 1.0 for moderate demagnetization fields and greater than 1 for magnets with very high stability.
- bH_c approximates to $4\pi M_r$.
- Recoil permeability u_r (the slope $\Delta B / \Delta H$ of a minor loop of $B-H$ demagnetization curve) approximates to unity.
- $mH_c \geq bH_c$.

The highest coercive force is obtained when the energy necessary to change the domain structure is the greatest, i.e. in small grains where domain rotation is predominant this energy is very high compared to wall displacement occurring in large grains. Accordingly decreasing particle size increases coercivity up to critical particle size ($1\mu\text{m}$ in case of barium hexaferrite) below which coercivity falls rapidly until a non-magnetic stage is reached.

and appeared at higher temperatures. In contrast to curves shown in Figure 4, a constant weight corresponding to complete dissociation of carbonate was not reached implying that the presence of excess Fe_2O_3 accelerated the reaction rate. It is also evident that nitrate dissociated at 400°C gave more reactive iron oxide than that prepared at 500°C . This

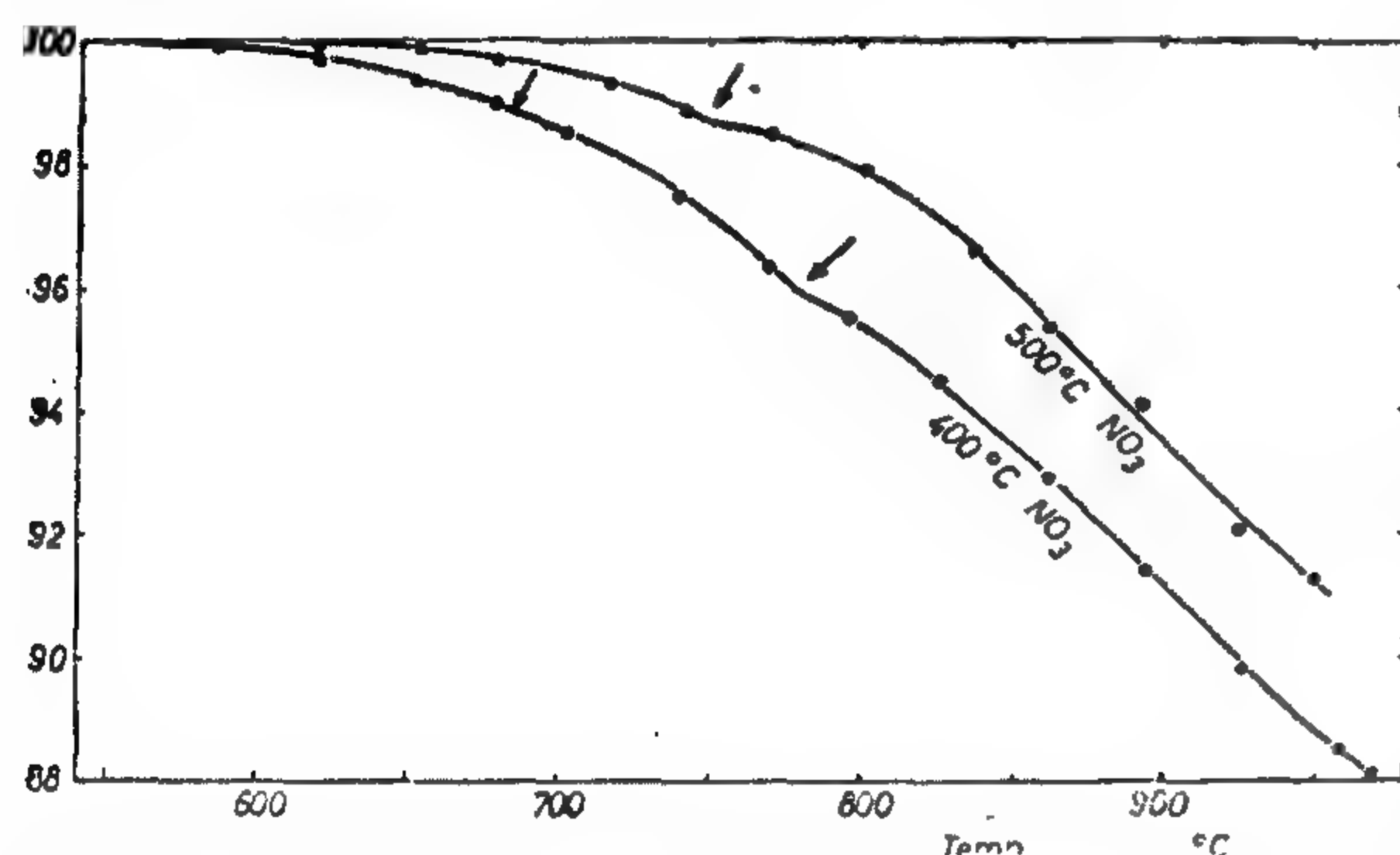


Fig. 10 : Change in weight in mixtures of BaCO_3 & Fe_2O_3 to form monoferrite indicating its formation in at least three steps

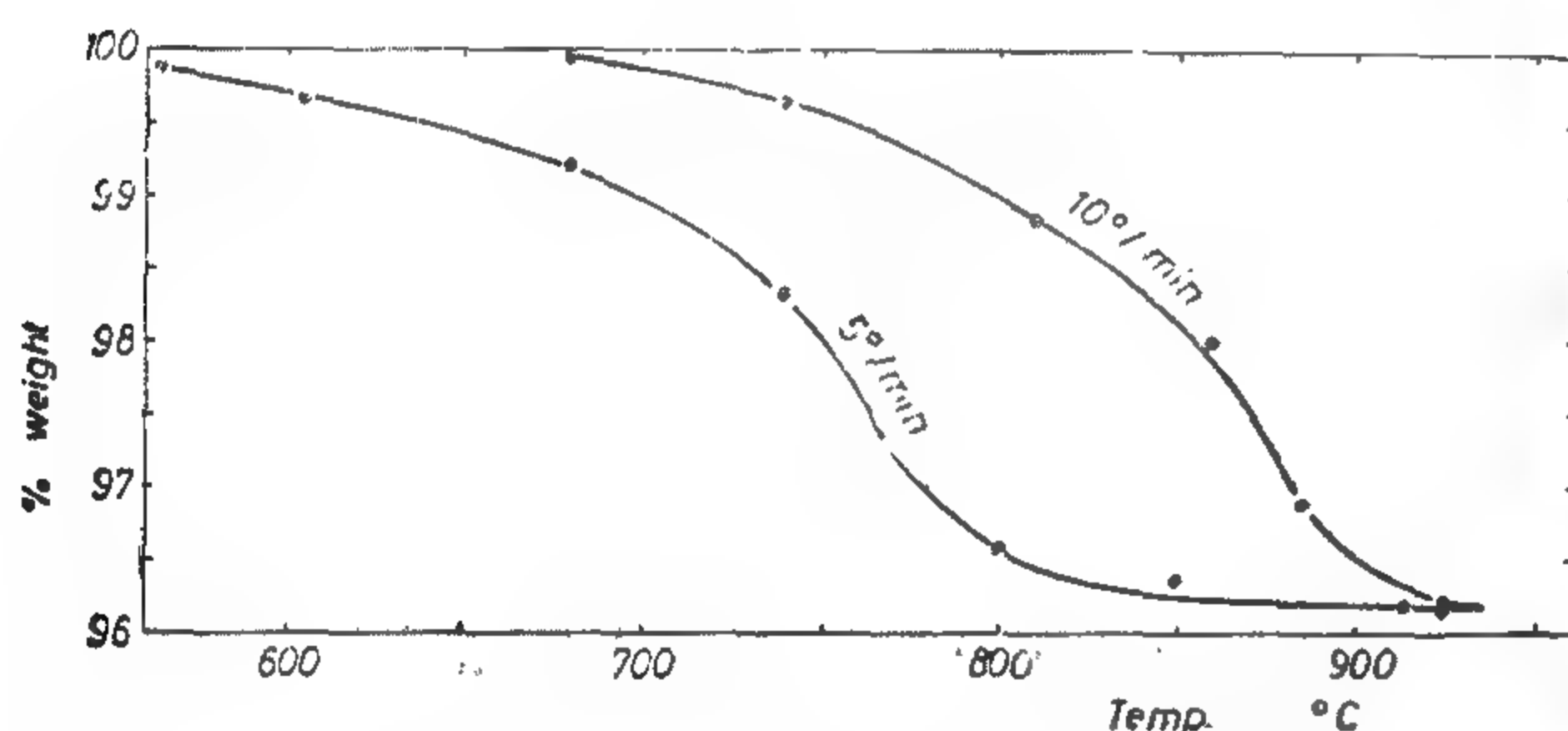


Fig. 11 : Effect of rate of heating on change in weight in mixtures forming hexaferrite

result is in accordance with those discussed earlier. Figure 11 shows the effect of heating rate on weight changes, indicating that higher efficiencies of reactions are obtained with slow heating rates, a result contradicting Winkler's statement that heating and cooling rates of 200°C/hr did not affect the reactions. Also present results are not in agreement with Wullkopf(4) who stated that the formation of monoferrite is not affected by stoichiometric ratio of $\text{BaO}/\text{Fe}_2\text{O}_3$ and is little affected by grain size of raw materials.

To compare the hexaferrite prepared at various temperatures, it was found by X-ray that the reaction was nearly complete at 1100°C after $8\frac{1}{2}$ hrs., at 1200°C after 5 hrs. and at 1300°C after 3 hrs. Electron micrographs for these three conditions are shown in Figure 12 indicating that firing at low temperatures for a long time gave hexaferrite crystals very small and of nearly uniform size but strongly adhering to each other. Such material is expected to be reactive and will form small grains on sintering suitable for isotropic magnets. Firing at high temperatures for short periods gave well formed large crystals which can be easily broken by grinding into particles consisting of individual single crystals suitable for anisotropic or plastically bonded magnets

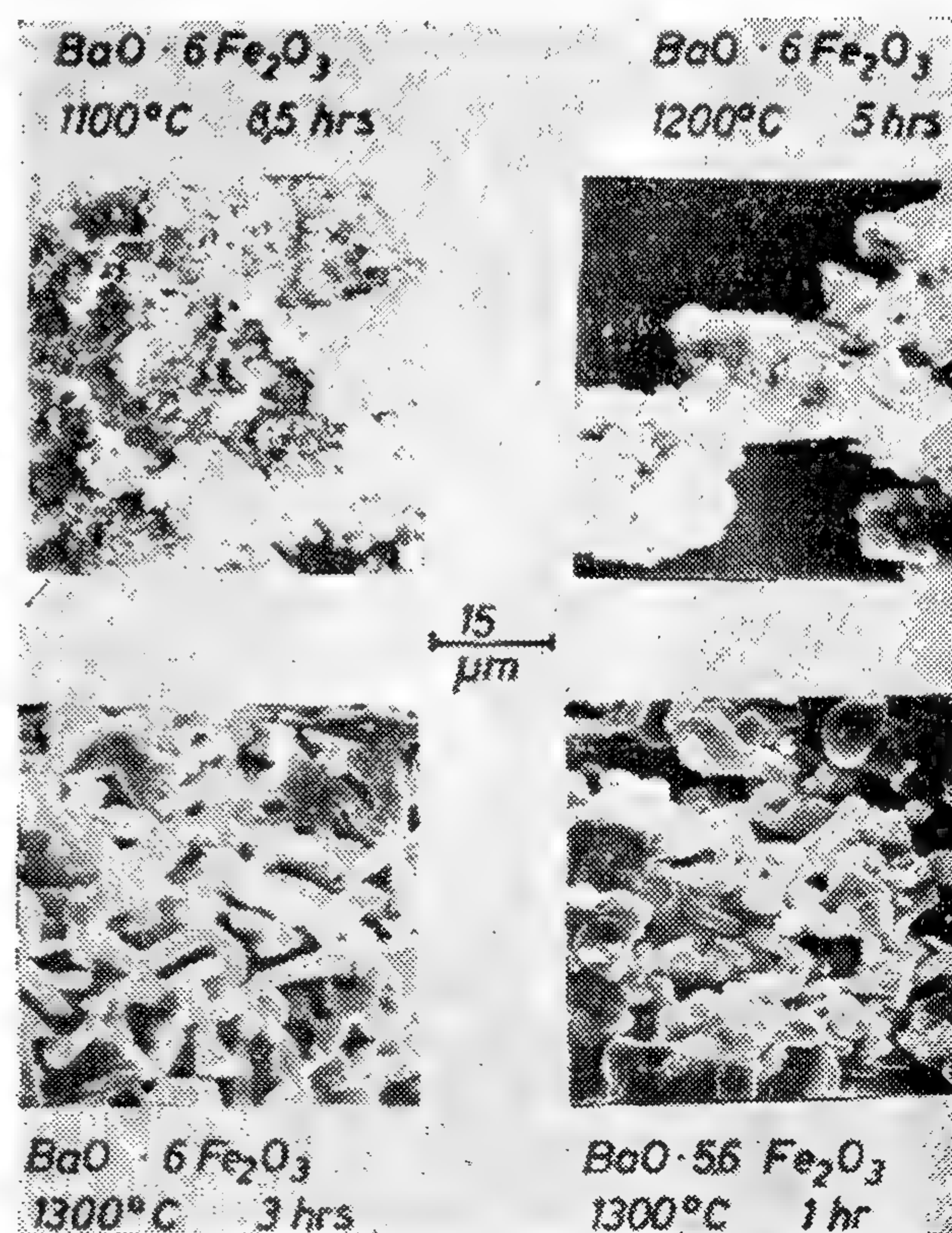


Fig. 12 : Electron micrographs for barium hexaferrite prepared by firing BaCO_3 and Fe_2O_3 at various temperatures for the shortest time required for formation of hexaferrite. They show the effect of preparation conditions; Temperature, time, $\text{BaO}/\text{Fe}_2\text{O}_3$ ratio

ferrite. Suchet⁽²⁰⁾ showed also that the monoferrite was formed between 700-900°C but below 800°C he stated the formation of a compound considered to be BFe_4O_7 .

Recently Bye & Howard⁽²¹⁾ showed that although x-ray showed monoferrite as the intermediate phase, a number of infra red absorption peaks appeared and could not be referred to the known compounds implying a complex sequence of events. Also Habery et. al.⁽²²⁾ noticed at low temperatures the presence of X-ray pattern other than monoferrite and considered it to be Fe_3O_4 . They showed Fe_3O_4 & Fe_2O_3 to exist over a wide range of temperature (700-775°C) in air, and such result is against the phase rule. Bye & Howard⁽²¹⁾ noticed also that the rate of disintegration of $BaCO_3$ was far more rapid than the weight loss and accordingly they suggested that the formation of monoferrite involved a number of fast steps in which high barium ferrites were formed but were not in sufficient quantity or crystallinity to appear using X-ray or to upset weight loss. Later they showed in polished sections⁽¹²⁾ that $5BaO \cdot Fe_2O_3$, $3BaO \cdot Fe_2O_3$, $2BaO \cdot Fe_2O_3$ & $BaO \cdot Fe_2O_3$ were present and that $3BaO \cdot Fe_2O_3$ was the major product. They attributed the disappearance of these compounds when using x-rays to their dispersion at points of contacts between reacting particles.

Using x-ray after firing $BaCO_3$ & Fe_2O_3 prepared from various origins, the main phase present as intermediate phase was found to be monoferrite with some extra lines decreasing in intensity with higher temperatures and disappearing at a temperature higher than 1200°C. These lines could be considered $2BaO \cdot 3Fe_2O_3$, the d-spacings of which were published very recently⁽¹³⁾. Compounds higher in BaO than monoferrite, were not detected. Using the internal standard method the percentage of monoferrite and hexaferrite at various temperatures are

shown in Figure 9. It is evident that the formation of both depend on raw materials and their ratio. High $BaCO_3$ content increased the rate of formation of monoferrite at low temperatures and the hexaferrite at high temperatures.

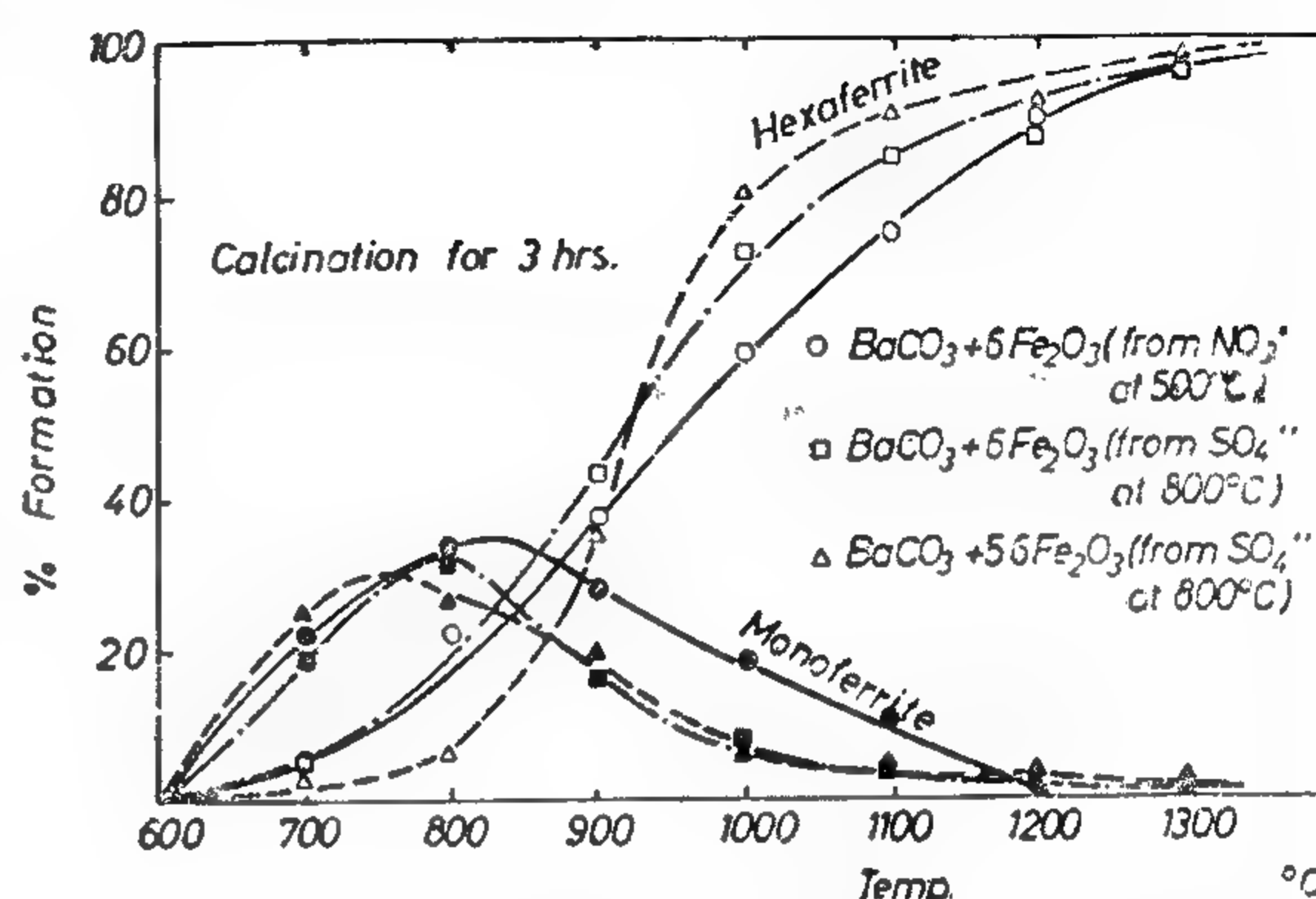


Fig. 9 : Variation of the relative amounts of the main phases detected by X-ray on firing $BaCO_3$ & Fe_2O_3 after soaking for three hours. It shows the effect of nonstoichiometric ratio and the origin of Fe_2O_3

Following the reaction using the thermobalance was discussed earlier (Fig. 4) showing all the curves to be smooth and the corresponding DTG curves gave only one peak suggesting one reaction to occur; presumably that of the formation of monoferrite. After a weight loss corresponding to the disappearance of the carbonate, the mixtures should consist of monoferrite and Fe_2O_3 as well as a small amount of hexaferrite, but the unexplained extra lines mentioned earlier were also present. This confirms that the reaction is more complicated. To increase the sensitivity of the thermobalance, mixtures containing high $BaCO_3$ content, just to form the monoferrite, were examined. The curves are shown in Figure 10 showing breaks and the DTG curves gave also three peaks corresponding to three different reactions; formation of $5BaO \cdot Fe_2O_3$ which was difficult to detect by x-ray owing to its low crystallinity, formation of $3BaO \cdot Fe_2O_3$ and formation of $2BaO \cdot Fe_2O_3$. Monoferrite increased

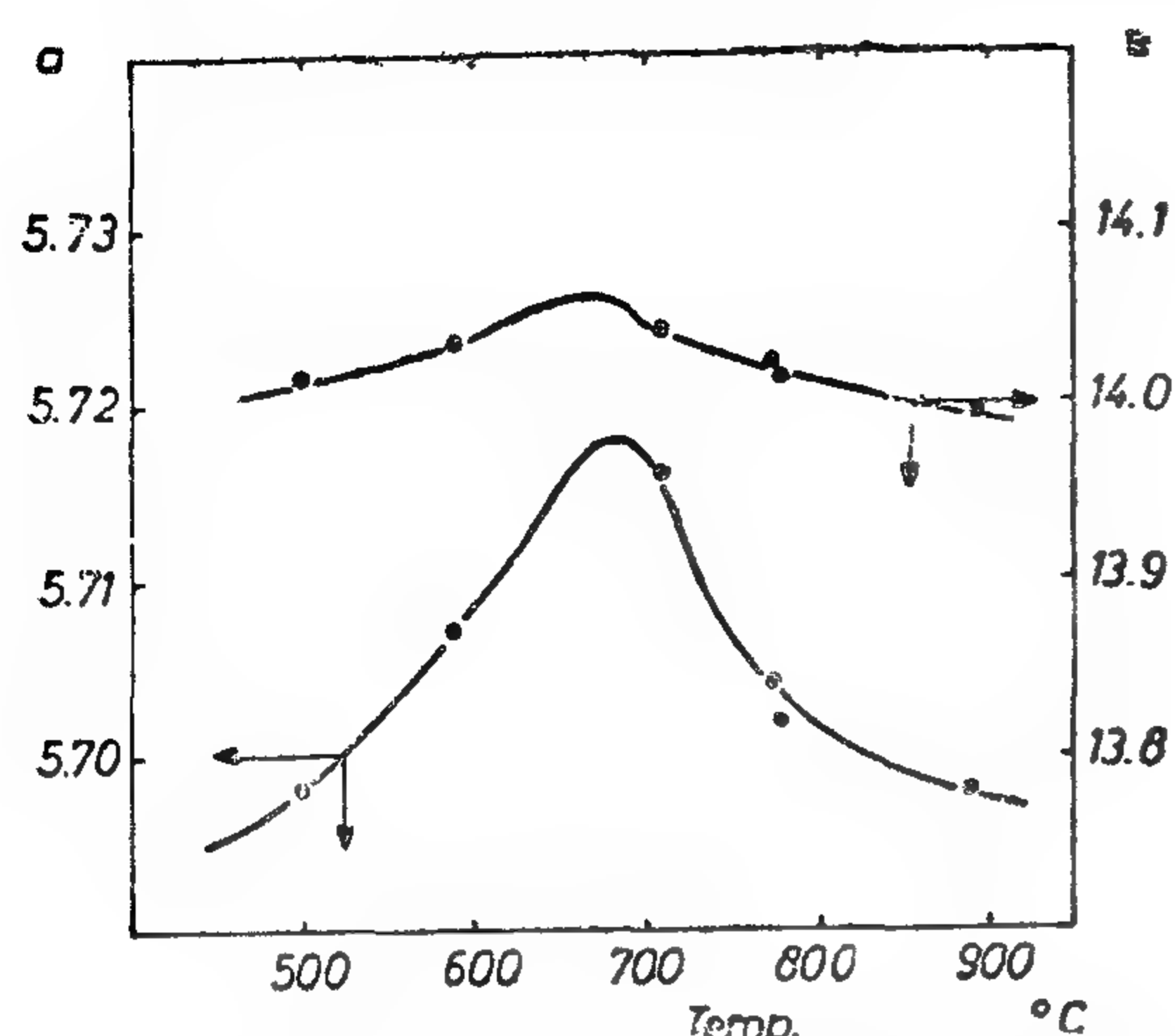


Fig. 8 : Variation of lattice parameters of hexagonal $BaFeO_{3x}$ with temperature

This compound was found by Wilson et. al.⁽¹²⁾ when they fired pellets of Fe_2O_3 surrounded by $BaCO_3$. According to present results, this compound could be prepared by firing $BaCO_3$ & Fe_2O_3 above $740^\circ C$ in air for a long time, then quenching to prevent oxidation back to ferrate and $BaCO_3$. $BaCO_3$ is formed by the action of CO_2 in atmosphere on BaO .

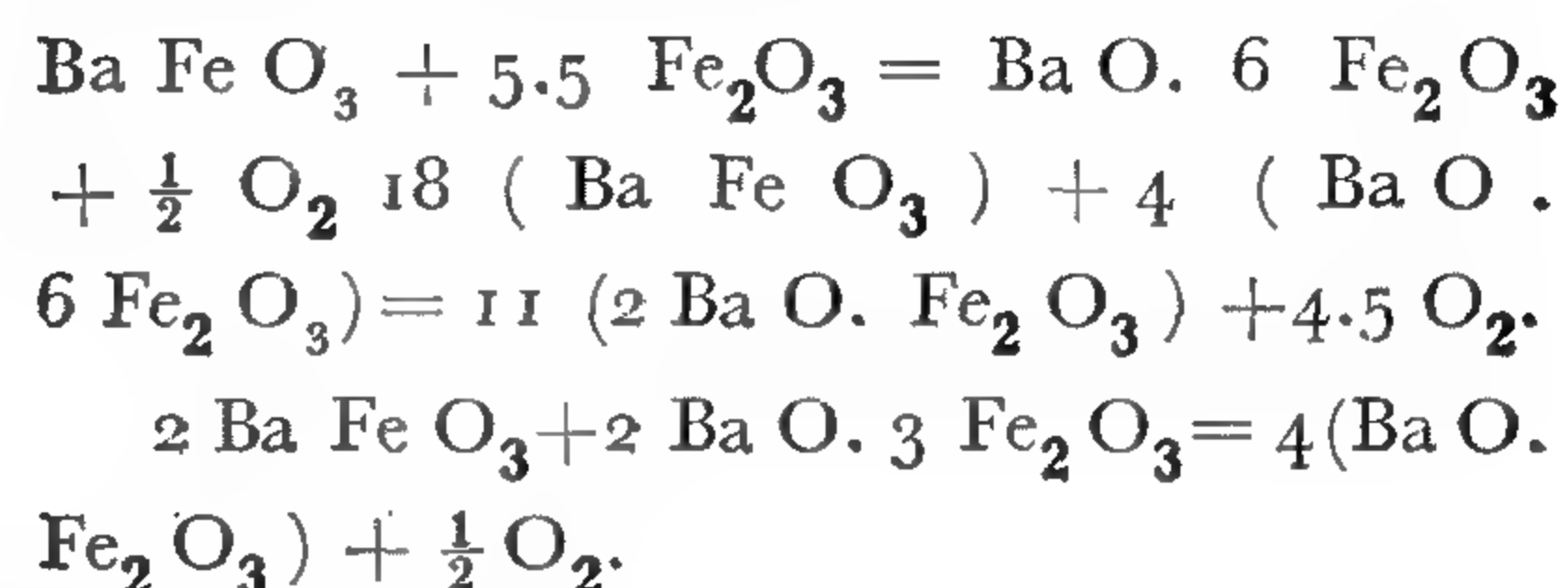
$5BaO \cdot Fe_2O_3$ was found to melt peritectically at about $1150^\circ C$ with slight isothermal oxygen loss.

Above $740^\circ C$, mixtures of $5BaO \cdot Fe_2O_3$ & Ferrate will lose oxygen progressively up to about $920^\circ C$ at which the composition $BaFeO_{2.63}$ loses oxygen isothermally giving a solid solution of $2BaO \cdot Fe_2O_3$ rich in oxygen. This phase is triclinic but its limits of solid solubility was not fixed and is shown tentatively on the diagram. Above $920^\circ C$ mixtures of $5BaO \cdot Fe_2O_3$ & $2BaO \cdot Fe_2O_3$ form $3BaO \cdot Fe_2O_3$ with isothermal oxygen loss at about $930^\circ C$.

$5BaO \cdot Fe_2O_3 + 2(2BaO \cdot Fe_2O_3) = 3(3BaO \cdot Fe_2O_{3-x}) + \frac{3x}{2}O_2$
The latter phase was found by Batti⁽⁹⁾ to form solid solution ranging from $3BaO \cdot Fe_2O_3$ to $7BaO \cdot Fe_2O_3$ and was found by the authors to be tetragonal with

$a=4.212$ & $c = 9.718$ and at $1300^\circ C$ it was found completely molten.

Transition temperatures for the following reactions, which should occur according to the present phases, were relatively low and could not be fixed correctly due to the sluggishness of the reactions and their irreversibility. The tie lines are thus shown dashed.



It should be mentioned that $2BaO \cdot 3Fe_2O_3$ dissociates at high temperatures to mono and hexaferrites⁽¹³⁾.

At higher temperatures monoferrite and hexaferrite form eutectic liquid at $1388^\circ C$ and hexaferrite dissociates peritectically to liquid and compound X ($BaFe^{2+}Fe^{3+}O_{23}$). The latter dissociates at higher temperature to compound W ($BaFe_2^{2+}Fe_{16}^{3+}O_{27}$) which dissociates to magnetite⁽¹⁴⁾.

According to the above results, it could be seen that the compound $4BaO \cdot Fe_2O_3$ reported by Winkler⁽¹⁵⁾ does not exist and the published d-spacings were found to be $BaFeO_3$, $5BaO \cdot Fe_2O_3$ & $BaCO_3$. Also this diagram explains the complicated patterns mentioned by Stäblein & Willbrand for this mixture⁽²¹⁾.

3.2. Mechanism Of Hexaferrite Formation:

Several research workers studied the formation of hexaferrite from $BaCO_3$ & Fe_2O_3 in oxygen, air and in vacuum using various techniques. They noticed the formation of intermediate phase which was considered by Sadler et. al.⁽¹⁶⁾ as BaO and by various authors^(15,17,18,19) as $BaO \cdot Fe_2O_3$. Accordingly they suggested that the monoferrite is formed first and at higher temperatures it reacts with remaining Fe_2O_3 forming the hexa-

reached depend on the raw materials and the applications required for the product. For isotropic magnets the reaction can be interrupted at an early stage when the particles are still very small and strongly adhering together, for anisotropic magnets, larger, well formed crystals are preferred which during milling can be easily broken into particles consisting of individual single crystals⁽²⁾.

3.1. Equilibrium Relationships Between Iron Oxides & Barium Oxide in Air :

To understand the effect of temperature and oxygen partial pressure on hexaferrite formation, changes in weight accompanying annealing and storage of some mixtures as well as the conflicting data about the existing compounds, equilibrium relationships in the system $\text{FeO}_2\text{-Fe}_3\text{O}_4\text{-BaO}$ was studied in air. Such study is also essential to understand expansion and change in colour observed in mixtures containing high BaO content, to follow changes in magnetic properties and to fix conditions for preparing mixtures of reproducible properties. It is thought that the magnetic properties of Fe^{4+} containing compounds are not yet understood due to difficulties in preparing specimens containing reproducible concentrations. It should be noted that phase relationships in such system are complicated due to the fact that changes in phases are not only function of initial composition and temperature but also depend on the oxygen partial pressure and most of the previous investigations in this system were explained and represented as binary condensed systems^(8,9).

Figure 7 was based on previous and present results obtained by following changes in weight and x-ray examination. On heating mixtures having BaO content (more) than $2\text{BaO} \cdot \text{Fe}_2\text{O}_3$ reversible oxidation-reduction reactions occurred and the latter composition gave on complete oxidation BaFeO_3 & BaCO_3

indicating that the composition of the ferrate is deficit in BaO as shown in the diagram. Mixtures of BaFeO_3 & Fe_2O_3 lose oxygen irreversibly on heating implying that mixtures of BaCO_3 and Fe_2O_3 having BaO content lower than $2\text{BaO} \cdot \text{Fe}_2\text{O}_3$. Fe_2O_3 will not oxidize on heating since iron oxide decreases the stability of the ferrate. This conclusion is very important in manufacturing hexaferrite since after forming or sintering, quenching or cooling slowly will always preserve the high temperature phases to room temperature.

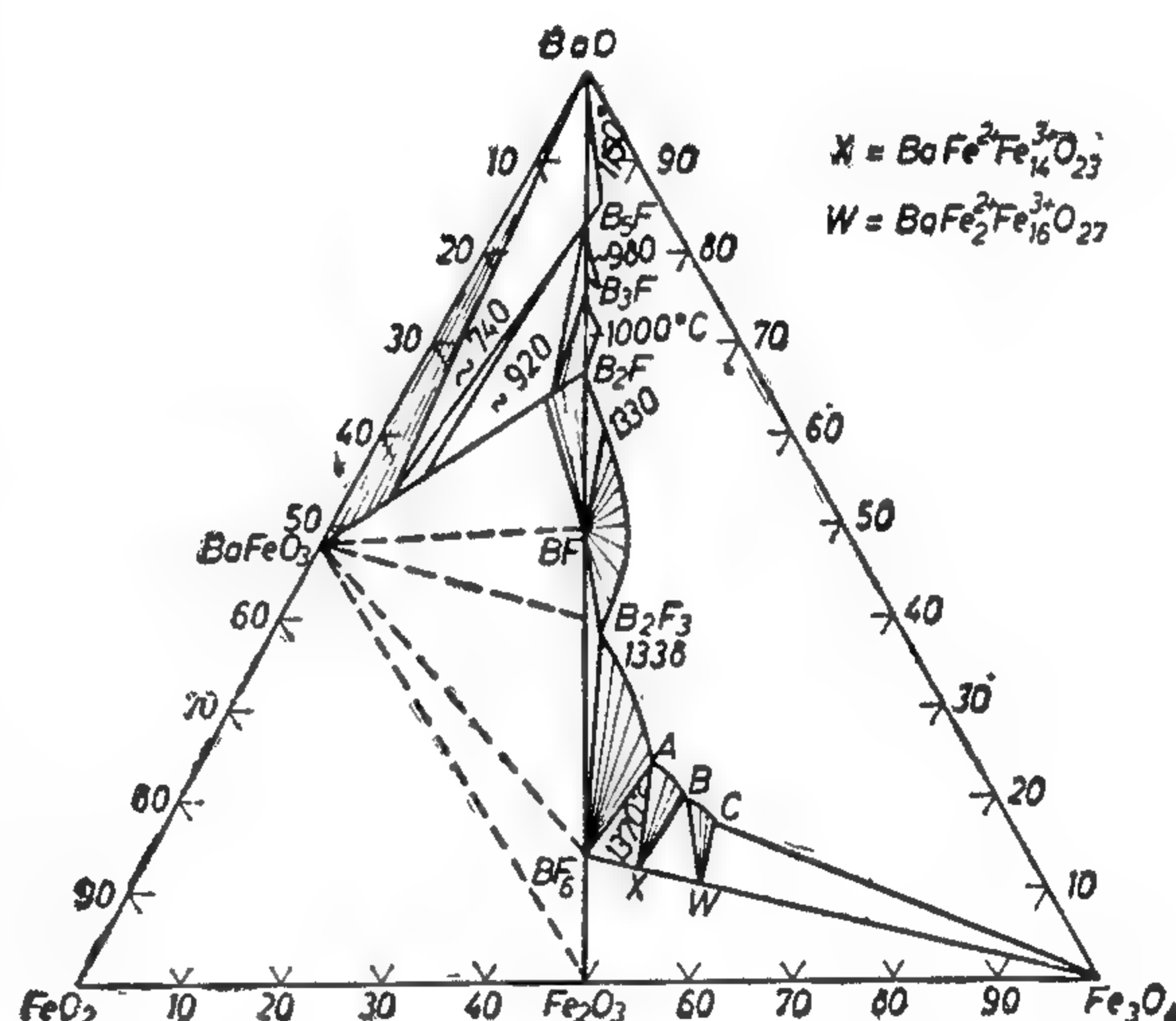
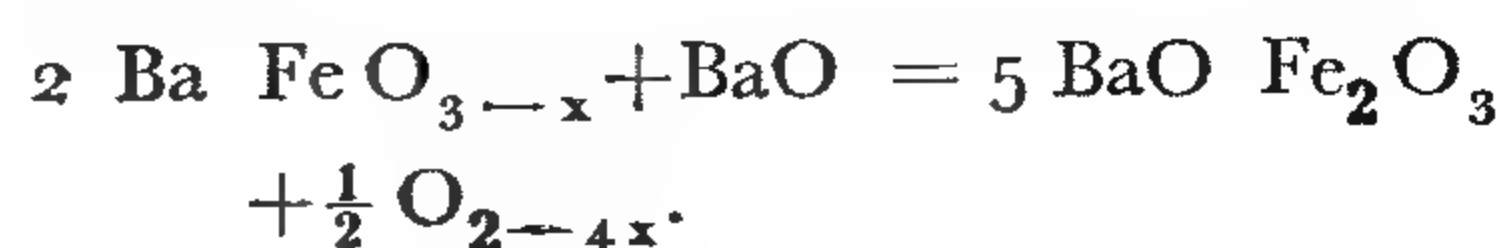
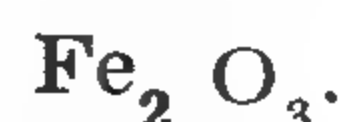


Fig. 7 : The system $\text{BaO-Fe}_2\text{O}_3$ in air.

Mixtures of BaCO_3 & BaFeO_3 lose oxygen over a range of temperature due to the formation of hexagonal ferrate solid solution, the variation of its lattice parameter with temperature is shown in Figure 8. This solid solution can extend to the composition $\text{BaFeO}_{2.63}$ (10,11). At about 740°C isothermal oxygen loss occurred due to the formation of 5BaO .



At high temperatures, sintering was observed and was excessive in case of oxide from oxalate and sulphate. Sintering produced particles with a wide particle size distribution, which tend to be rounded, i.e. with lower surface energy. It is also evident that not only at low temperatures but also at high temperatures, small particles tend to stick to large particles.

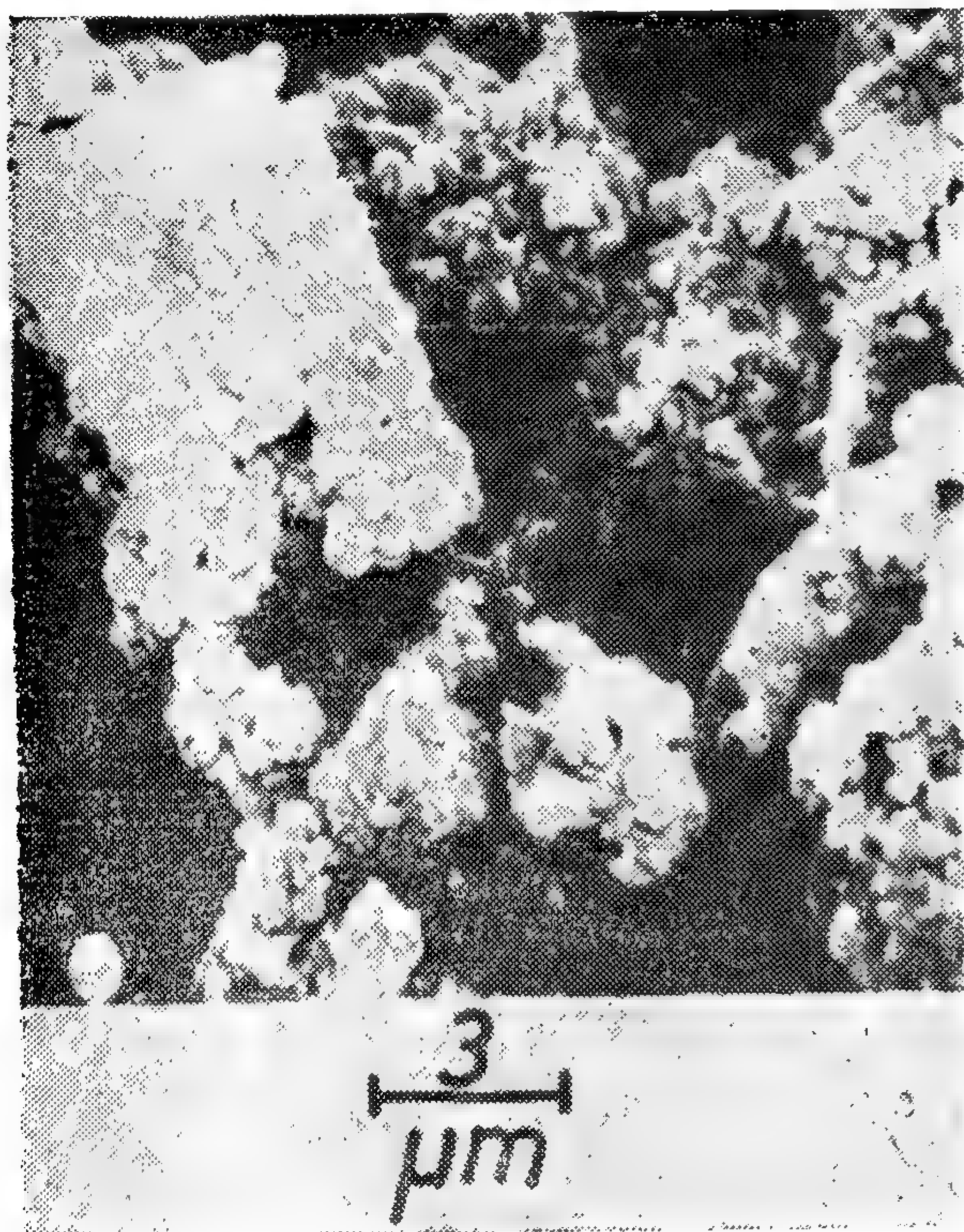


Fig. 6 : Electron micrograph for iron oxide prepared from sulphate at 650°C for one hour showing the formation of agglomerates inside the mother crystal.

The high surface area associated with Fe_2O_3 from nitrate at low temperature may explain the reason for its capability for retaining adsorbed gases up to high temperatures. The lower values of reactivity of iron oxide prepared from nitrate and hydroxide, in spite of their high specific surfaces, may be due to their high agglomeration tendency. Particles of extremely fine ferric oxide, with very high specific surface tend to floc and adhere to each other rather than to mix with barium carbonate, thus decreasing the num-

ber of contacts and the rate of reaction. During firing, such agglomerates are expected to shrink giving also loose contacts. Increasing the temperature of preparation decreases the surface area to an optimum limit, thus decreasing the agglomeration tendency but with a surface area large enough for solid state reactions. Accordingly the oxide prepared from nitrate at 300°C was less reactive than that prepared at 400 or 500°C. This may also explain the unexpected results that activity increased with particle size, as was concluded by Blum and Li(7).

It should be also noted that the large difference in particle size is not recommended as a raw material for ultrafine grain ceramics since this will enhance exaggerated grain growth. Accordingly the iron oxide prepared from the sulphate at moderate temperatures (650-850°C) is recommended.

In view of the above results it could be concluded that while the reactivity of the oxide prepared from sulphate or oxalate is proportional to the specific area irrespective to its origin, or method of preparation, the reactivity of the oxide from nitrate or hydroxide exhibit high cohesion tendency decreasing their reactivity. Original oxalate needle crystals were preserved giving ideal material for magnetic tapes, but at higher temperatures $\gamma\text{-Fe}_2\text{O}_3$ gives $\alpha\text{-Fe}_2\text{O}_3$ with low reactivity.

Returning back to the flow sheet shown in Fig. 1, the suitable raw materials are weighed then mixed to give homogeneous mixture. Mixing may be carried in the dry or in the wet state. In the latter case the powder is dried and the mixture is then pelletized or pressed into tablets.

3. FORMATION OF HEXAFERRITE :

Rotary kiln or tunnel kiln can be used for forming the hexaferrite in order to give homogeneous calcination. The rate of heating and the maximum temperature

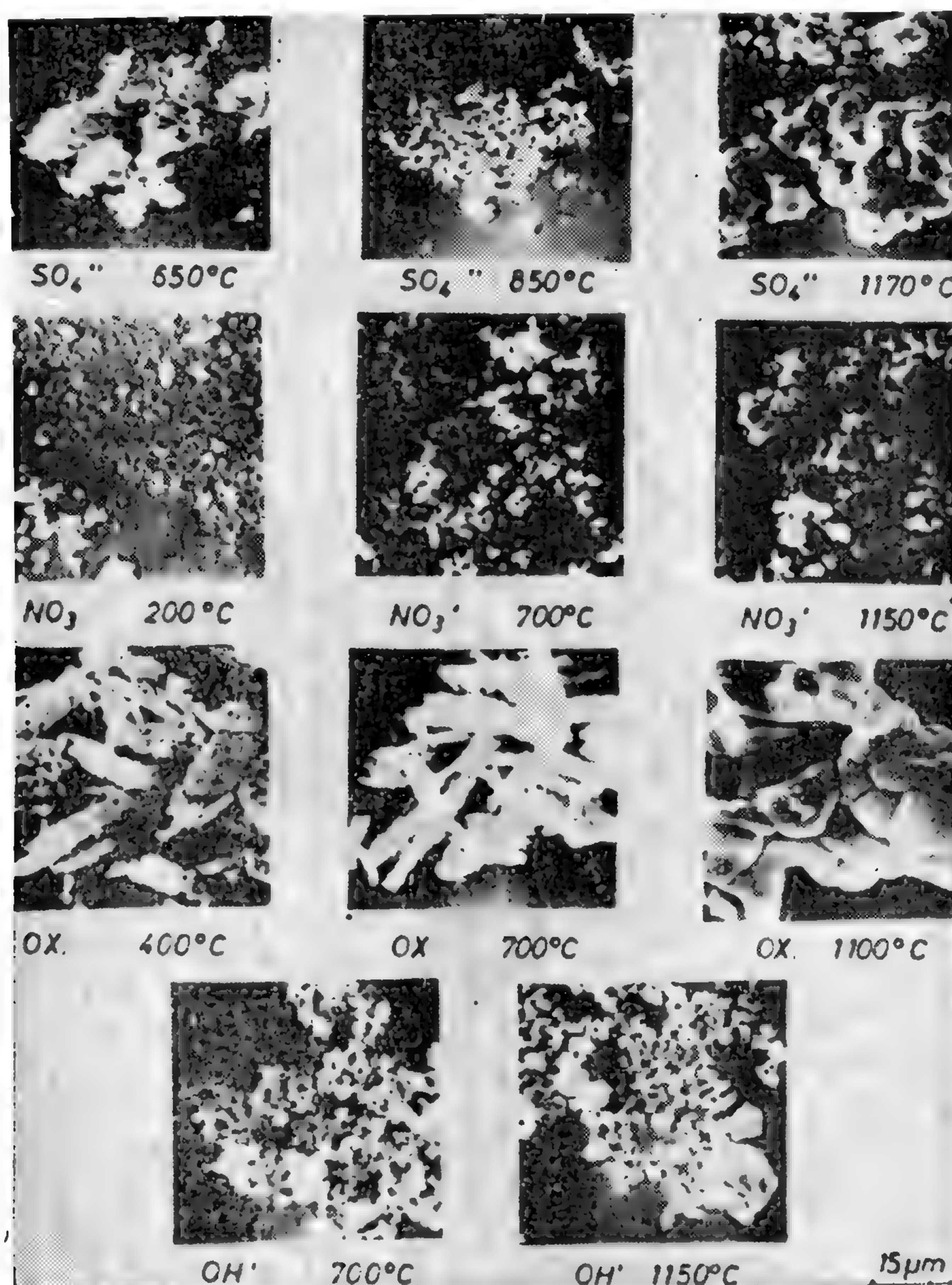


Fig. 5 : Electron micrographs for α Fe_2O_3 prepared at various temperatures from various salts

them to fine rounded particles with uniform size distribution. On the other hand, the oxide produced from oxalate was retained in the original crystal with high surface roughness. This roughness may be due to the growth of the various crystallites formed inside the mother crystal and the tendency to acquire spherical shape by surface diffusion. In view of the large crystal size obtained by X-ray for Fe_2O_3 from oxalate it could be concluded that the oxide crystallites formed in-

side the mother crystal of salt are formed and grow in certain preferred directions, that all produced crystallites have the same orientation giving high values by X-ray and enhancing grain growth.

In case of using nitrate or hydroxide, higher temperatures caused the agglomerates to shrink to much smaller particles eliminating the micropores. This explains the observed increase in density as well as the rapid increase in crystal size especially in case of iron oxide produced from nitrate.

ranges, on the formation of hexaferrite and stages of sintering as well as on controlling microstructure and magnetic properties* is needed and is carried now in TU. Clausthal. It is also aimed to achieve rigid specifications for the raw materials and recently Wullkopf studied the effect of chloride, nitrate, and sulphate and found that the first enhances monoferrite formation and volatilities at high temperatures causing corrosion problems.

For iron oxide, generally a mixture of natural ore and synthetic oxide is used. It is recommended that the mixture contains 98-99.6% Fe_2O_3 with specific gravity of 4.9-5.2, grain size 0.1-0.5 μm and specific surface area of 3-20 m^2/gm .⁽²⁾ (some factories prefer to use 0.8-7 m^2/gm)⁽⁶⁾.

Recent work by the authors showed that reactivity of iron oxide is not only a function of crystal size or specific surface but the reaction with BaCO_3 should also be followed using a thermobalance. The latter apparatus was proved to be the best tool to assess the iron oxide⁽⁷⁾.

Hydrated iron sulphate, nitrate, oxalate and hydroxide were fired at various temperatures above that required for producing $\propto\text{-Fe}_2\text{O}_3$. Figures 2 & 3 show that at low temperatures when iron oxides can be prepared from nitrate or oxalate, higher specific area were obtained but the rate of crystal growth was very high. Surface area drops at high temperatures due to increase in particle size. Thermogravimetric changes are shown in Figure 4. In all mixtures, a progressive weight loss occurred far below the dissociation temperature of pure BaCO_3 , indication that the iron oxide decreased its stability with various values depending on the reactivity of ferric oxide. With active oxide the loss was rapid and a constant weight was reached at low temperature. The curves were classified in two groups; (a) those showing reactivity in proportion to values of specific surface as in Figure 2 and (b) those giving values unexpected from the

point of view of surface energy. It was found that while ferric oxide produced from sulphate or oxalate has reactivity in proportion to specific surface independent of the method of preparation, that produced from nitrate or hydroxide gave lower reactivity than expected. This could be seen when one overlaps the two diagrams. This effect was referred to agglomeration tendency, discussed later in view of electron micrographs. Moreover, ferric oxide prepared from nitrate at 300°C gave reactivity between that prepared at 400 and 500°C, inspite of its very high surface area. This shift to the right could not be attributed to weight change due to evolution of gases adsorped on due to evolution of gases adsorped on ultrafine grains (produced at low temperatures) but was also attributed to high agglomeration tendency.

To compare particle size, particle size distribution, shape and tendency for agglomeration for the oxides prepared from the various salts, at various temperatures, some specimens were selected and examined in a Jeol JSM-U3 electron microscope using 25 KV. In preparing the specimens, ether was used to decrease the agglomeration tendency. The micrographs obtained are shown in Figure 5 with the same magnification for the sake of comparison. It is evident that the oxide produced at low temperature agglomerates within the framework of the original crystals. This is very clear in case of iron oxide from the oxalate at 400 & 700°C and from the sulphate at 650°C (See also Fig. 6). In the mother crystal extremely small pores exist between the crystallites and with the oxalate the pores were so fine to be detected by surface area measurement. On the other hand crystals of nitrate and hydroxide were precipitated from liquid and were very fine with high cohesive power, producing agglomerates with wide agglomerate size distribution.

At higher temperatures, gases evolving from the sulphate crystals, shattered

* Tech. University Clausthal, Zellerfeld West Germany.

ratures (Fig. 9). Fig. 12 shows also that finer hexaferrite is produced by firing at lower temperatures and for shorter time than that produced with stoichiometric composition. It is also known that BaO increases the density with minimum grain growth during sintering process (2).

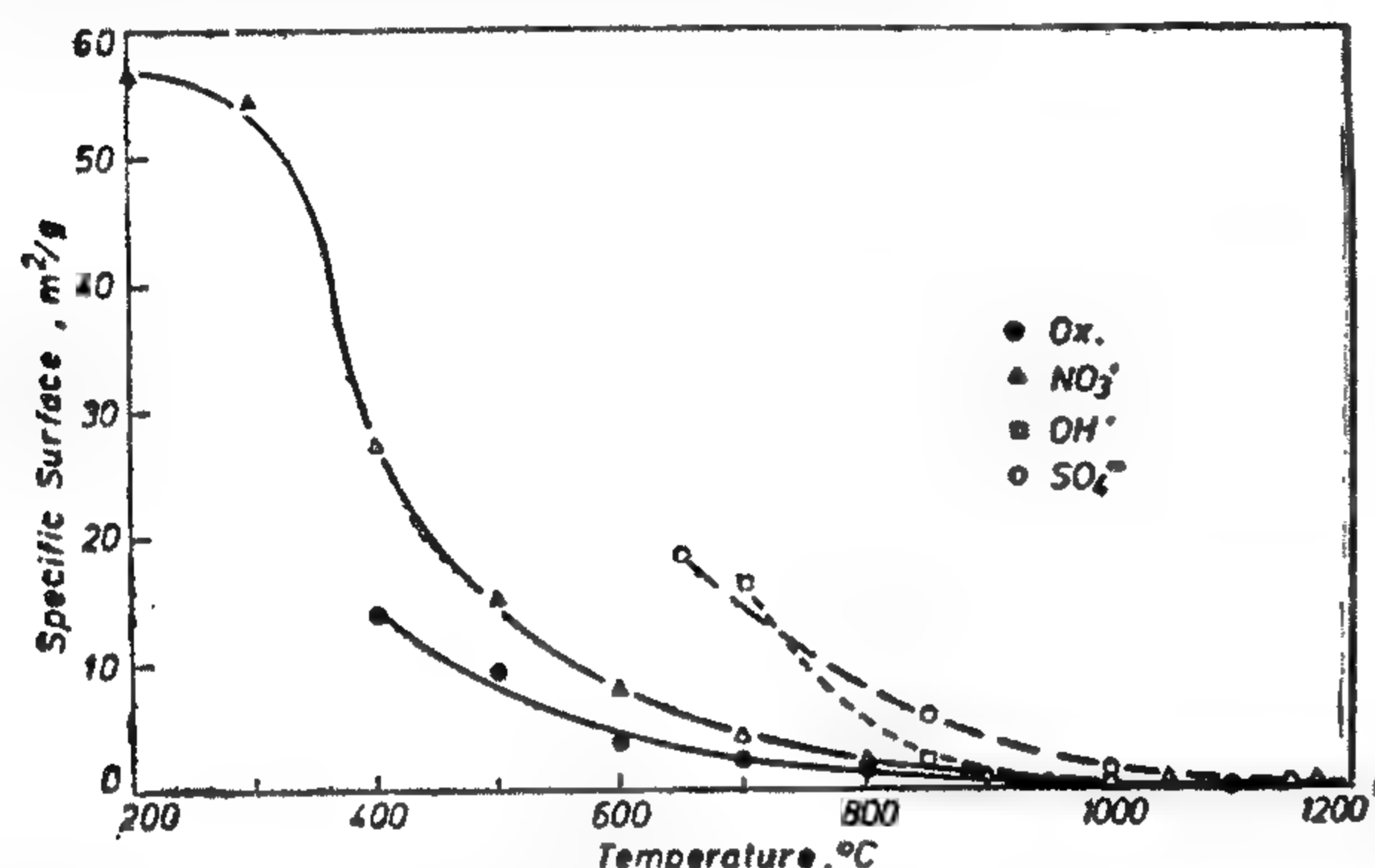


Fig. 2: Specific surface of α -Fe₂O₃ produced by firing hydrated iron sulphate, nitrate, oxalate and hydroxide at the indicated temperatures for one hour

Some additions as Al₂O₃ & SiO₂ less than 1% are added and it is thought that while SiO₂ increases sintering rate, Al₂O₃ inhibits grain growth. As mentioned earlier, systematic study for the role of additives, in and outside the solubility

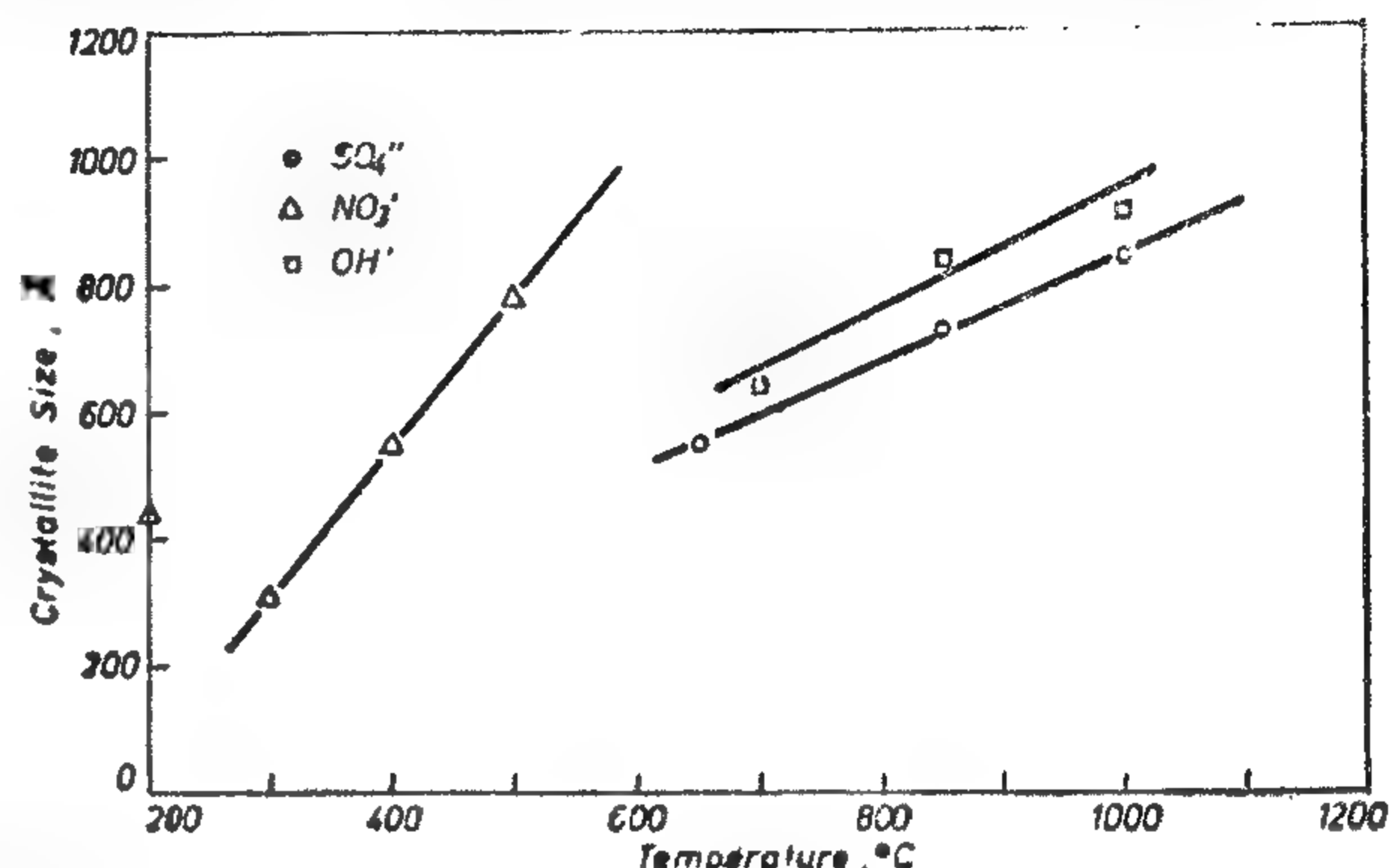


Fig. 3: Crystallite size of α -Fe₂O₃ produced by firing hydrated iron sulphate, nitrate and hydroxide. Crystal size for oxide from oxalate was large and could not be measured by X-ray.

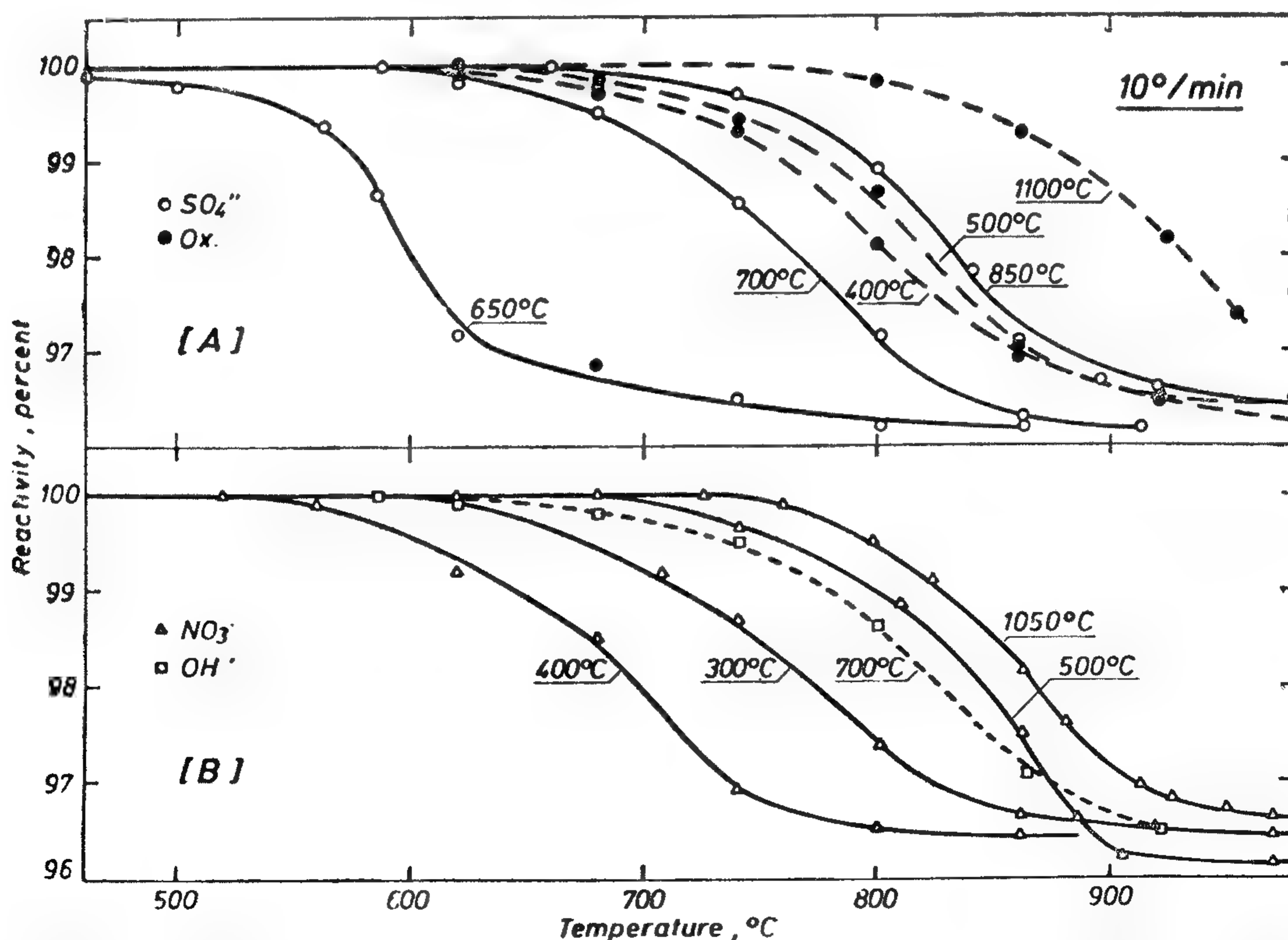


Fig. 4: Reactivity of various types of Fe₂O₃ with BaCO₃ using the thermobalance with a rate of heating of 10°C/min

tion range on the formation, sintering stages, microstructure and hence on magnetic properties will increase our present knowledge and may put us in a position to achieve better quality and to increase productivity and to lower the price by decreasing sintering temperature and time.

The sequence of unit operations and processes in the production of hexaferrite was summarized by Heimke & Nye(2) and is shown in Figure 1. Here the steps will be reviewed with special emphasis on process variables and production pro-

blems as well as the results obtained by the authors. For details of the equipment used reference should be made to Ries(3).

2. RAW MATERIALS :

Practically excess BaO than required to form the stoichiometric composition is used since it was found that using 5.6 moles of Fe_2O_3 instead of 6 moles gives optimum magnetic properties(4). As will be discussed later, present authors found that excess BaO increases the percentage monoferrite formed at low temperatures and the hexaferrite formed at high tempe-

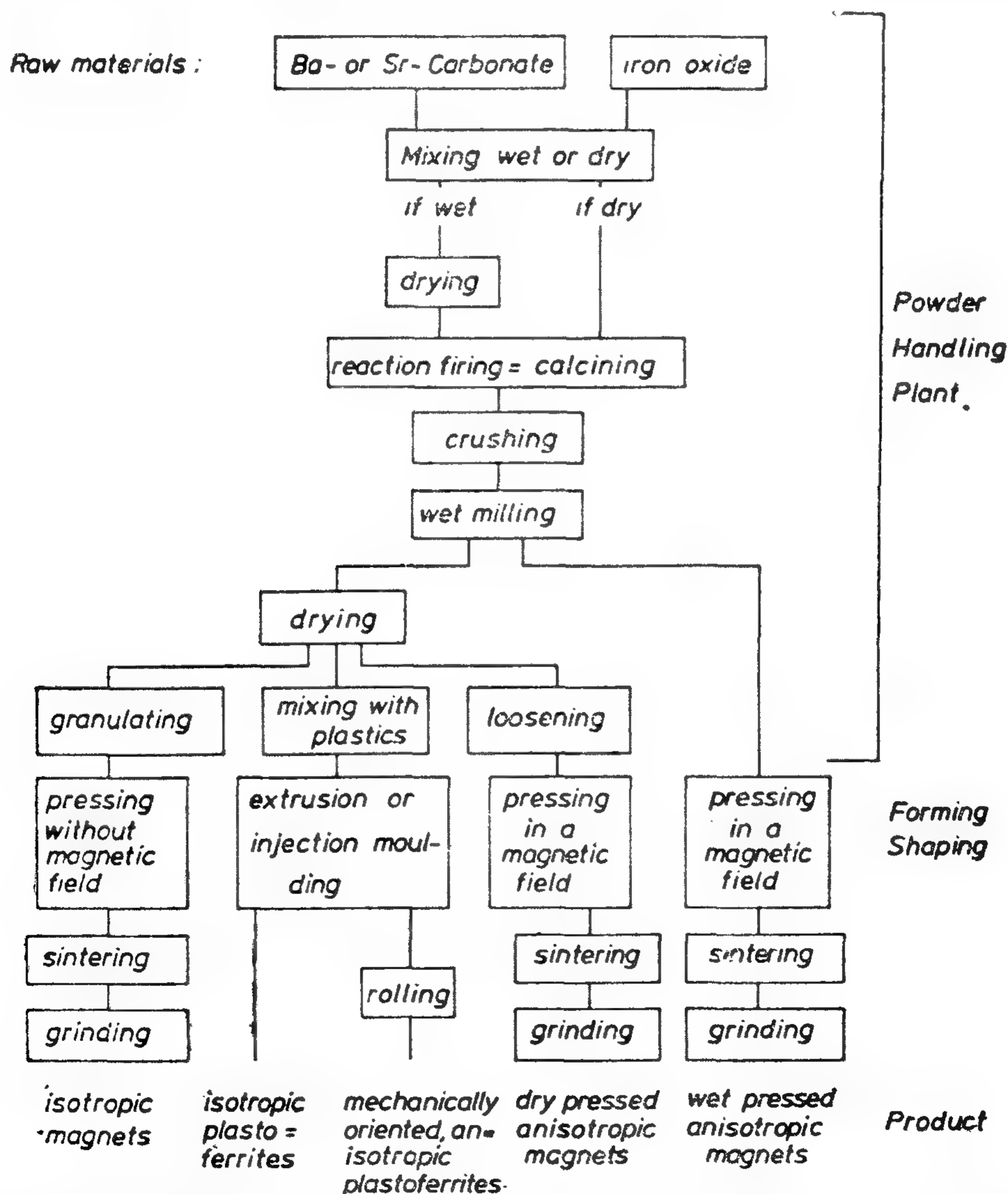


Fig. 1 : Flow Sheet for the possible steps for manufacturing barium hexaferrite

RECENT DEVELOPMENTS IN CERAMIC PERMANENT MAGNETS

By

Dr. A.M. GADALLA* & Prof. Dr. H.W. HENNICKE**

ABSTRACT

The parameters affecting various steps in barium hexaferrite manufacture as well as the existing conflicting data are reviewed. Present results dealing with the effect of raw materials and methods for assessing different grades of iron oxide and the oxidation-reduction reactions occurring in various mixtures of oxides of iron and barium were established. Kinetics of hexaferrite formation was followed and proved to be not as simple as previously reported but occurring in various steps.

Importance of current research in sintering and effect of additives on sintering stages, microstructure and magnetic properties is also mentioned.

1. INTRODUCTION :

Permanent magnets of the magnetoplumbite structure (Ba, Sr) $0.6 \text{ Fe}_2 \text{O}_3$ were discovered recently (from 23 years) and due to continuous research they are now manufactured in large industrial scale. They have high coercivities, high electrical resistivity, low density and low price. High coercivity means that this kind of magnet can be built into the operating zones of electrical machines and equipment which handle power without risk of demagnetization. High resistivity enables massive blocks of this insulating material to have low flux leakage and to be magnetized by very short pulses of

heavy current that consumes negligible power. Ceramic magnets can be made with an almost linear demagnetization curve which means that it has excellent recoil properties, i.e. it remains magnetically stable. The main disadvantage is the relatively high decrease in saturation magnetization with temperature.

Important applications are their use in rotor or stator in electrical machinery and lifting and holding magnets. Future applications of significant potential include passive frictionless suspension for tracked ground vehicles which may solve transportation problems and low power long lived friction free bearings for spacecraft systems(1).

Although the technology of formation is now known, several points need further research to explain the conflicting data regarding the intermediate compounds formed during fabrication, or to understand peculiar behaviours noticed such as changes in weight accompanying annealing and storage of same mixtures or expansion and changes in magnetic properties in mixtures having excess BaO content.

Detailed studies on raw materials are needed to establish rigid specifications for chemical composition, particle size and particle size distribution. The role of limited additions inside and outside solid solu-

* Dr. A.M. Gadalla is associate Professor in Faculty of Engineering Cairo University, Egypt.

** "Prof. Dr. H.W. Henricke is Lehrstuhl für Glas Keramik, Clausthal Technical University, West Germany.

RAWMATERIALS & GHEMICAL INDUSTRIES

**INST. OF TINING, PETROLEUM &
METALLURGICAL ENGINEERS —
INST. OF CHEMICAL ENGINEERING**

CONTENTS

GENERAL SECTION :

BUILDING & CONSTRUCTION	INDUSRTY & PRODUCTION	RAW MATERIALS & CHEMICAL ENGINEERING
(ARABIC)	(ARABIC)	(ARABIC)
— Cairo Conference on Low Cost Housing Dr. G. NASSAR 4		
— The Influence of tec- hnology on architec- tural-creativity town Planning & Society Dr. T. ABDEL-GA- WAD 17		
—O—	—O—	—O—
(ENGLISH)	(ENGLISH)	(ENGLISH)
— A Graphical method for estimating the transmissibility & storativity of equifers from the specific capa- city of wells. Dr. M. ABU-ZIED, & S. RASHWAN 34	— The Transient stabl- ility of electric power systems Dr. M.A. NASR 107	— The state of stress in Rocks around mag- hara coal mine open- nings Dr. M. EL-DIN-HUS- SEIN, Dr. H.F. IMAM & NAGY. N. YANNI ... 151
— Analysis of the Per- formance of laterally loaded Pile groups Dr. M. ADEL BARA- KAT 40	— Torsional vibration analysis for the Pro- pulsion systems of Large motor tankers Part I. Dr. F. BAHAT, N. MAHAREM & A. EL- IRAKI 117	— Recent developments in Ceramic Permanent magntes Dr. A.M. GADALLA, Dr. H.W. HENNICKE 156
— Activated sludge Pro- cess Modification for Phosphorus- Deficient wastes. Dr. A.M. ABD EL- WARITH, Dr. F.A. EL-GOHARY & M. SALEH 52		
— Characteristics of the ground water reser- voir in upper Egypt Dr. M.H. EL-KATEB & F. ABD EL-RAH- MAN 63		

JOURNAL OF THE EGYPTIAN SOCIETY OF ENGINEERS

VOL. XIV.

ISSUE No. 1 —

(JAN-FEB-MARCH 1975)

EDITING BOARD

Editor

Dr. S. MORTADA

Assist. Editor &

Treasurer

Dr. G. NASSAR

Dr. H. AMER

Eng. T. ABD EL - GAWAD

Dr. F. BAHGAT

Dr. M.F. SAKR

Dr. M. ABU-ZIED

Dr. M. E. SELIM

Eng. A. EL-ASFORY

- Issued Quarterly Contributors are invited to submit material for editorial consideration addressed to the Editor. The Journal cannot accept responsibility for loss or damage to any material.

INSTRUCTIONS FOR AUTHORS OF ARTICLES

- The Journal publishes articles contributing to the advancement of engineering science and applications.
- Articles may be written in Arabic or English and presented in triplicate with an abstract in both languages.
- Authors' names to be given in full, together with their academic titles and professional occupation.
- Articles may not exceed 8 pages. In this respect, mathematical derivations may be abbreviated and tables replaced by curves.
- Curves to be drawn in black china ink, and to occupy half a page at most. Exceptionally, full page curves or plates are admitted. Curves presented will be scaled down to these sizes. Figures & lettering on curves should not be less than 3 mm even after scaling down.
- References to be given at the end of each article and classified alphabetically according to author's name followed by the name of the journal or book and the date of issue.
- Authors will be presented with two proofs, the first one accompanied by a correction convention chart to ease the work of type correction.

Society Subscriptions

Member	200 P.T.
Associate member	150 P.T.
Associate	100 P.T.

Magazine Subscriptions

Society members Free	
Engineers subscriptions	100 P.T.
Non-engineers subscription	300 P.T.
Organisations subscriptions	500 P.T.

ADVERTISING AGENT

Moassasset Misr for Printing and Publication
10, Souk El Tawfikieh Str. Cairo. Tel. 72192

مجلة جمعية المهندسين المصرية

المجلد الرابع عشر

العدد الثانى (ابريل - مايو - يونيو ١٩٧٥)

- تصدر المجلة ربع سنوية
- ترسل النصوص المطلوب موافقة هيئة التحرير على نشرها باسم السيد / رئيس التحرير . وهو غير مسئول عن فقد أو تلف أى نص .
- تنشر المجلة المقالات التى تسهم فى رفع مستوى العلوم الهندسية وطرق ممارستها .
- تقبل للنشر المقالات باحدى اللغتين العربية أو الانجليزية ، على أن تقدم من ثلاث نسخ مكتوبة على الآلة الكاتبة ومعها ملخص بكل من اللغتين .
- تذكر أسماء أصحاب المقالة كاملة باللغتين ومعها ألقابهم العلمية ووظائفهم .
- يراعى ألا تتجاوز المقالة ٨ صفحات بالمجلة ، وفى سبيل ذلك يختصر الاشتقاق الرياضى ويستعاض عن الجداول بمنحنيات مرسومة بالحبر الشينى الأسود ، على أن يشغل المنحنى نصف صفحة على الأكثر ولا يشغل صفحة كاملة الا فى حالات استثنائية وسيصفى أى منح إلى تلك المقاسات .
- ويراعى ألا يقل ارتفاع الحروف أو الأرقام على المنحنيات المنشورة عن ٣ مم بعد التصغير .
- يعنى بذكر المراجع المستقى منها المقال وتصنف تبعاً لاسم المؤلف ثم العنوان ثم المجلة أو الكتاب وتاريخه .
- تقدم لصاحب المقال تجربتان للطباعة وترفق بالاولى نسخة من مصطلحات التصحيح التى يؤدى اتباعها الى رفع كفاية التصحيح وتقليل الوقت الضائع فيه .

اشتراكات الجمعية :

قرشاً

٢٠٠

١٥٠

١٠٠

العضو

العضو المنتسب

المنتسب

اشتراكات المجلة :

يتلقى أعضاء الجمعية نسخهم مجاناً .

قرشاً

١٠٠

٣٠٠

٥٠٠

الاشتراك السنوى للمهندسين

الاشتراك السنوى لغير المهندسين

الاشتراك السنوى للهيئات

تعطى أمانة النشر بالمجلة للسادة

الزملاء أعضاء جمعية المهندسين المصرية

الاعلانات :

مؤسسة مصر للطباعة والنشر

القاهرة ١٩ شارع سوق التوفيقية ت ٧٢١٩٢

هيئة التحرير

رئيس التحرير

دكتور سيد مرتضى

سكرتير التحرير

وأمين الصندوق

دكتور جمال الدين نصار

مهندس توفيق أحمد عبد الجواد

دكتور حامد حسنين عامر

مهندس عبد الملك العصفورى

دكتور فؤاد بهجت

دكتور صلاح السبكى

دكتور محمود أبو زيد

دكتور محيى الدين سليم

محتويات العدد

التشييد والبناء	التصنيع والانتاج	الخدمات الأولية والصناعات الكيماوية
القسم العربى :	القسم العربى :	القسم العربى :
— مؤثر المباني رخيصة التكاليف . للدكتور جمال نصار ٨	— التنظيم ومراجعة الهياكل التنظيمية للمهندس حسن ناجي ٧٤	
— التكنولوجيا والعمارة . « التقدم التكنولوجى وأثره على العمارة والمدينة والمجتمع - ٢ » . المعماري توفيق عبد الجواد ١١		
القسم الافرنجى :	القسم الافرنجى :	القسم الافرنجى :
— تحليل القوى فى الفراغ بالاسقاط المتعامد . للمهندس سمير حنا عبد الشهيد ٢٦	— تأثير الانهيار الكهربى للتربة على قيمة المقاومة الأرضية . للدكتور مهندس أسعد زيتون والمهندسة اهداب محمد كامل المرشدى ٩٣	— موديل رياض لميكانيكية التركيز بالترسيب . للدكتور محمد فكرى شلبى والدكتور محمد زكى حتوت ١٤٧
— تأثير الاجهادات على قوى القص للرمل . للدكتور عبد المنعم موسى ٢٣	— تحليل اهتزازات اللى من منظومات دفع ناقلات البترول الكبيرة . حساب اجهادات اللى - ٢ - . للدكتور فؤاد بهجت والدكتور نعمان محارم والمهندس على العراقى ١٠٢	
— تحليل الكمرات الخرسانية سابقة الاجهاد ذات الفتحات بطريقة العناصر المحددة . للدكتور محمد محمد الهاشمى والدكتور عبد الوهاب أبو العينين والمهندس أحمد أحمد عبد الحميد ٤١	— زمن انهيار الاكسوجين . حساباته ودراسته النظرية . للدكتور محمد رضوان والدكتور محمد سعيد أبو سعده والمهندس عبد الرحمن زغلول ١٠٩	

THE NEW BOARD OF THE EGYPTIAN OF SOCIETY OF ENGINEERS.

- | | |
|--------------------------------------|--|
| 1 — PROF. DR. AHMED MOHARRAM. | Chairman. |
| 2 — ENG. AMIN HELMI KAMEL. | Deputy-Chairman,
Representative of Institution of Mechanical
Engineers. |
| 3 — ENG. HASSAN NAGUI. | Deputy-Chairman,
Representative of Institution of Manage-
Engineers. |
| 4 — PROF. DR. MOHAMED M. EL-HASHIMY. | Secretary — General |
| 5 — DR. MOHYI EL-DIN SELIM. | Treasurer. |
| 6 — PROF. DR. MOHAMED FAHIM SAKRE. | Assistant General Secretary,
— Representative of Institution of Electric &
Electronic. |
| 7 — ENG. MEDHAT EL-ALAYLI. | Assistant Treasurer,
Representative of Institution of Chemical
Engineers. |
| 8 — ENG. ABDEL HAMID EL-ZANFALY | Member,
Representative of Institution of Planning. |
| 9 — ENG. AHMED ALI KAMAL. | Member,
Representative of Institution of Irrigation
Engineers. |
| 10 — Dr. MOUSTAFA EL-HEFNAWY. | Member,
Representative of Institution of Civil Engi-
neers. |
| 11 — ENG. IBRAHIM KAMEL AHMED. | Member,
Representative of Institution of Mines &
Petroleum. |
| 12 — ENG. IBRAHIM NAGUIB. | Member. |
| 13 — Dr. AMINA EL-HEFNI. | Member. |
| 14 — Dr. GAMAL NASSAR. | Member. |
| 15 — PROF. AHMED AMIN MOUKHTAR. | Member. |

تشكيل مجلس إدارة جمعية المهندسين المصرية لعام ١٩٧٥

- | | |
|------------------|---------------------------------------|
| رئيس | ١ — الأستاذ الدكتور أحمد محرم أحمد |
| وكيل | ٢ — المهندس أمين حلمي كامل |
| وكيل | ٣ — المهندس حسن ناجي |
| أمين عام | ٤ — الأستاذ الدكتور محمد محمد الهاشمي |
| أمين صندوق | ٥ — الدكتور محيي الدين سليم |
| أمين عام مساعد | ٦ — الأستاذ الدكتور محمد فهمي صقر |
| أمين صندوق مساعد | ٧ — المهندس مدحت العلاليلي |
| | ٨ — المهندس أحمد علي كمال |
| | ٩ — المهندس ابراهيم نجيب |
| | ١٠ — الأستاذ الدكتور مصطفى الحفناوي |
| | ١١ — المهندس عبد الحميد الزنفلي |
| أعضاء | ١٢ — الدكتورة أمينة الحفني |
| | ١٣ — الدكتور جمال الدين نصار |
| | ١٤ — المهندس ابراهيم كامل أحمد |
| | ١٥ — الأستاذ الدكتور أحمد أمين مختار |

التشييد والبناء

جمعية المهندسين المدنيين
جمعية المهندسين المعماريين
جمعية مهندسي الري

as sand filters, retaining sand but allowing passage of the water. The causeway may thus be constructed of crushed rock of large size and the need for protective stone linings eliminated.

Figure 12 shows the construction of such a dual causeway construction with sand infilling which in fact forms part of one of the cofferdams for the High Island Dam and Reservoir in Hong Kong.

8. USE IN ASPHALT REINFORCEMENT

The cracking and fatigue of asphaltic overlays on concrete pavements is a very serious problem in road and airfield construction. This problem derives from the low tensile strength of asphalt. The inclusion of a flexible fabric membrane at the concrete/asphalt interface has been found to increase the tensile capacity of the overlay thus reducing and redistributing the amount and degree of reflection and shrinkage cracks. This is one of the newer areas of fabric use and installation techniques are developing and long term trials are underway.

9. CONCLUSION

It may now be stated that the use of fabric membranes in civil engineering construction has three specific advantages. Firstly, they have cost benefits accrued from saving on materials, reduction in construction time, reduction in maintenance. Secondly, technical benefits

derived from more efficient performance of structures such as roads, railways, drains and asphaltic overlays. Thirdly, the use of fabrics have opened up new construction possibilities in terms of land use not previously possible, use of construction techniques not previously technically or financially viable.

10. REFERENCES

- CEDERGREN, H.R. 1967. Seepage, Drainage and Flow Nets. Wiley, New York.
- MARKS, B.S. 1975. The Behaviour of Aggregate and Fabric Filters in Sub-drainage Applications. Univ. of Tennessee. Report (unpublished).
- McGOWN, A. and OZELTON, M.W. 1973. Fabric Membranes in Flexible Pavement Construction over Soils of Low Bearing Strength. Civ. Eng. Pub. Works Review, January.
- McGOWN, A., SWEETLAND, D.B., PERTTMAN, A. and GOLDSMITH, P.L., 1973. Fabric Screen Research and Development. University of Strathclyde Report (unpublished).
- TERZAGHI, K. 1925. *Erdbaumechnik auf Bodenphysikalischer Grundlage*. Deuticke, Vienna.
- U.S.W.E.S. 1941. Investigation of Filter Requirements for Undrains. Technical Memorandum No. 183-1.

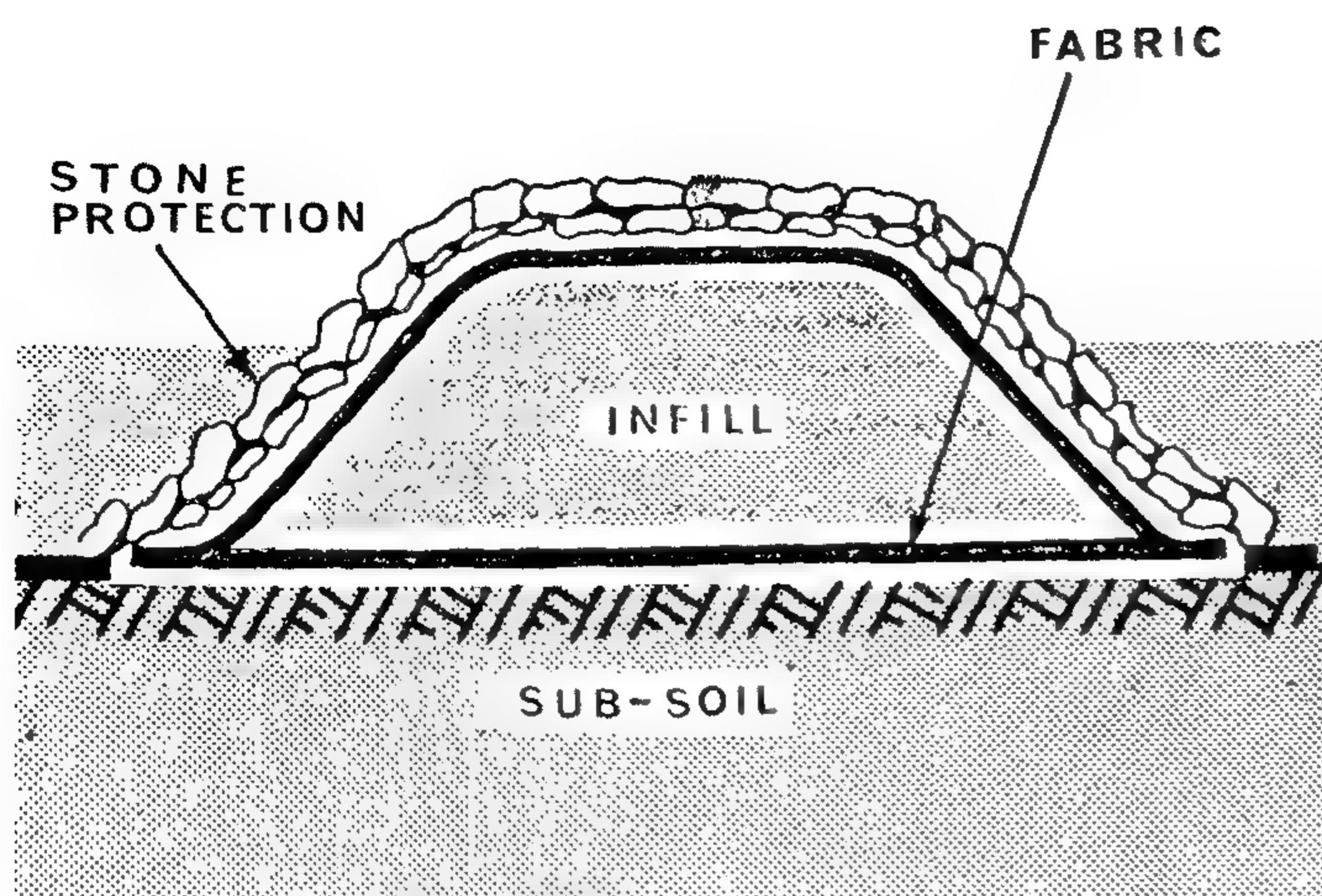


Fig. 9. Single Causeway Construction

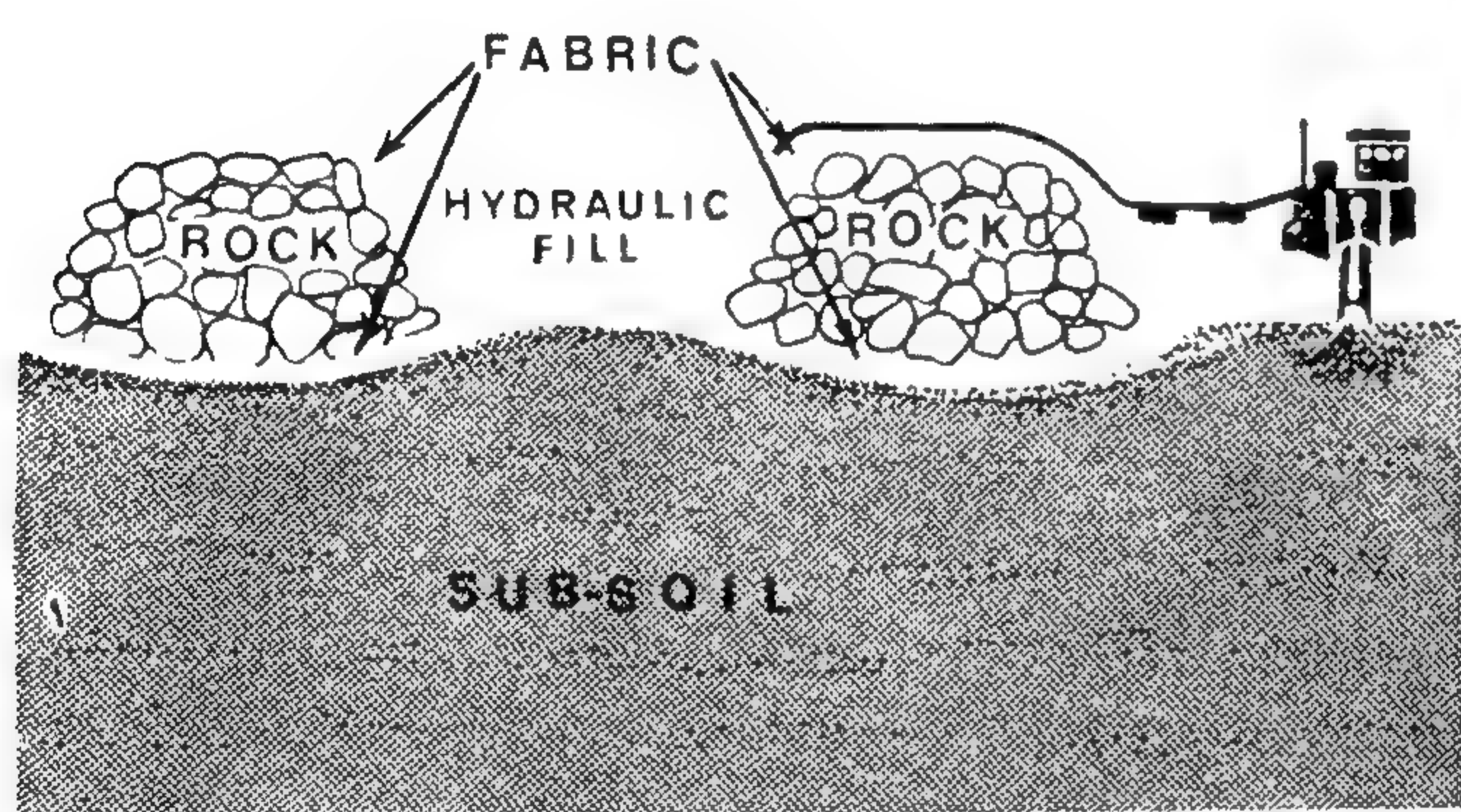


Fig. 10. Dual Causeway Construction

7. USE IN LAND RECLAMATION AND CAUSEWAYS

The need for new land for agricultural and industrial purposes is increasing rapidly and consideration must now be given to the reclamation of land from the sea or inland waters. The use of fabric in construction of single and dual causeways has therefore been developed and been developed and been proven to be a very economical and technically efficient mode of construction. The fabric is used as shown in Figs. 9 and 10. The reclaimed land may be obtained by pumping out the water and draining the soil behind a single enclosure causeway, by end tipping suitable fill from the land out to the single causeway or by pumping sand into the area between dual causeways.

With single causeways, the use of fabric in a filtration function as shown in Fig. 9 on the sides reduces the number of layers of protective filter stones. The use of fabric beneath the general fill also allow the easy construction of a working platform. Figure 11 shows this procedure being adopted in the construction of a causeway for land reclamation in United Kingdom. The use of fabric in dual causeway construction, as shown in Fig. 10, is very similar to that in single causeways except that the fabric on the inner faces act



Fig. 11. Land Relamation, United Kingdom

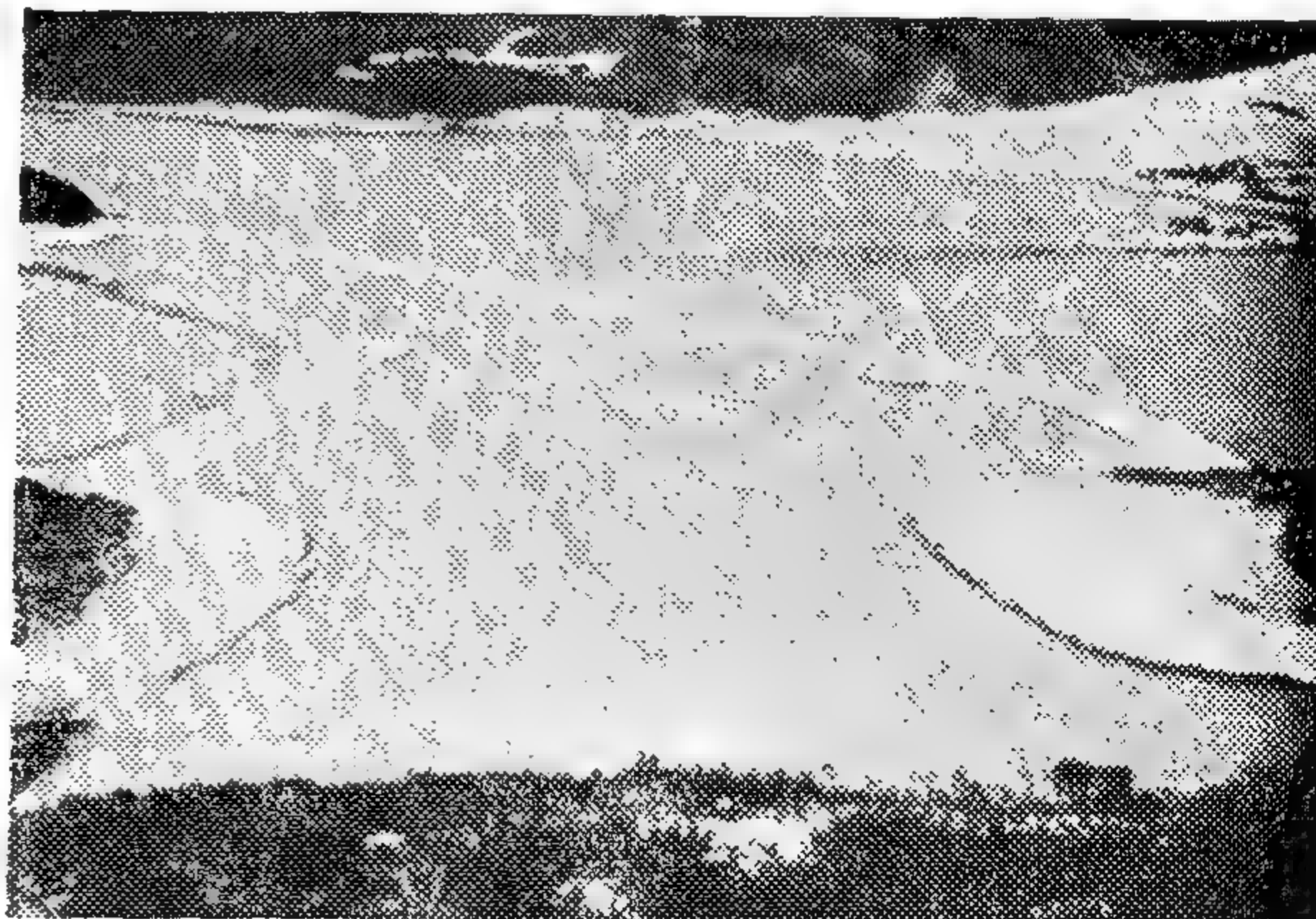


Fig. 12. Dual Causeway Construction for Cofferdams, High Island Dam, Hong Kong

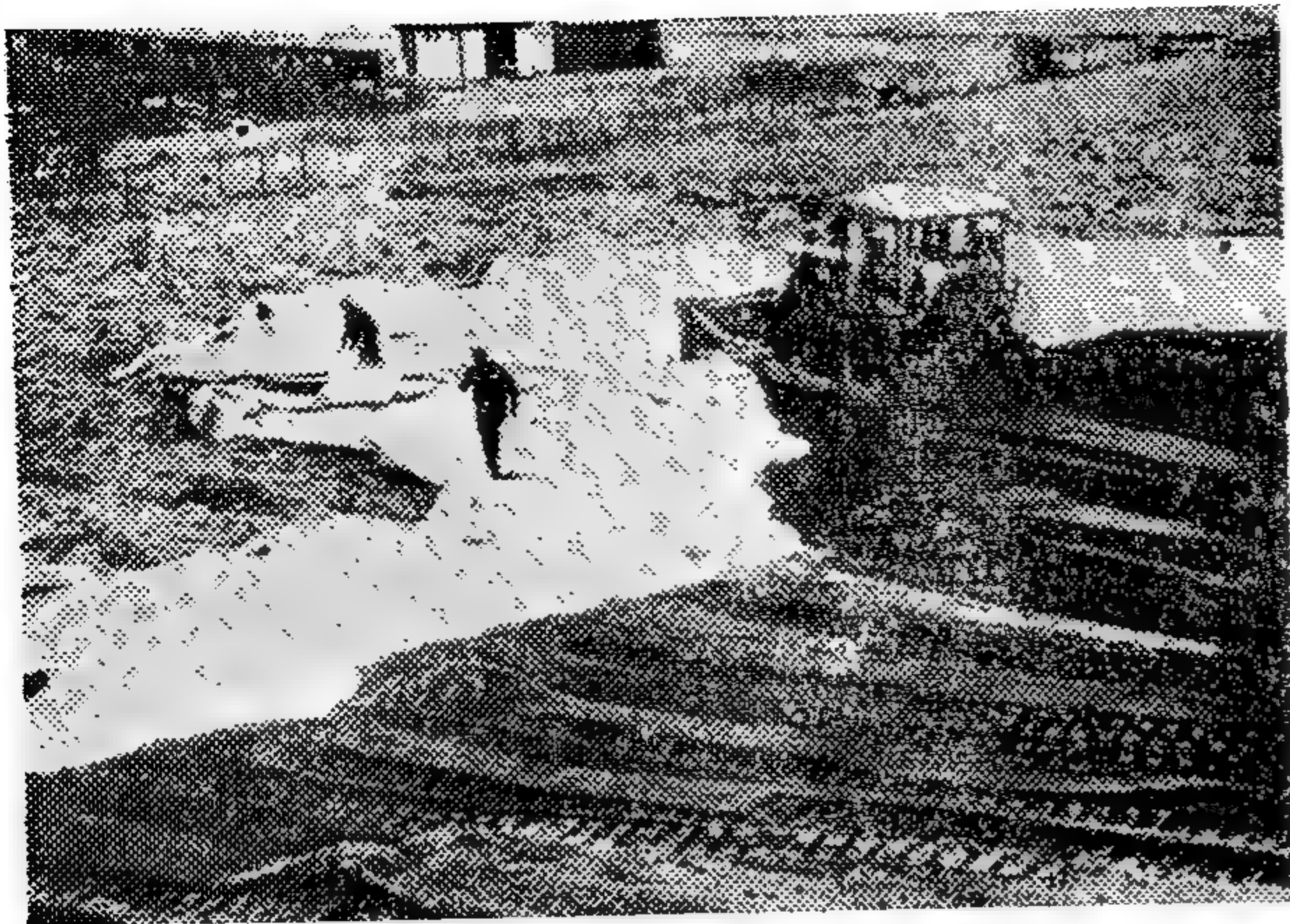


Fig. 5. A Motorway Embankment in Scotland

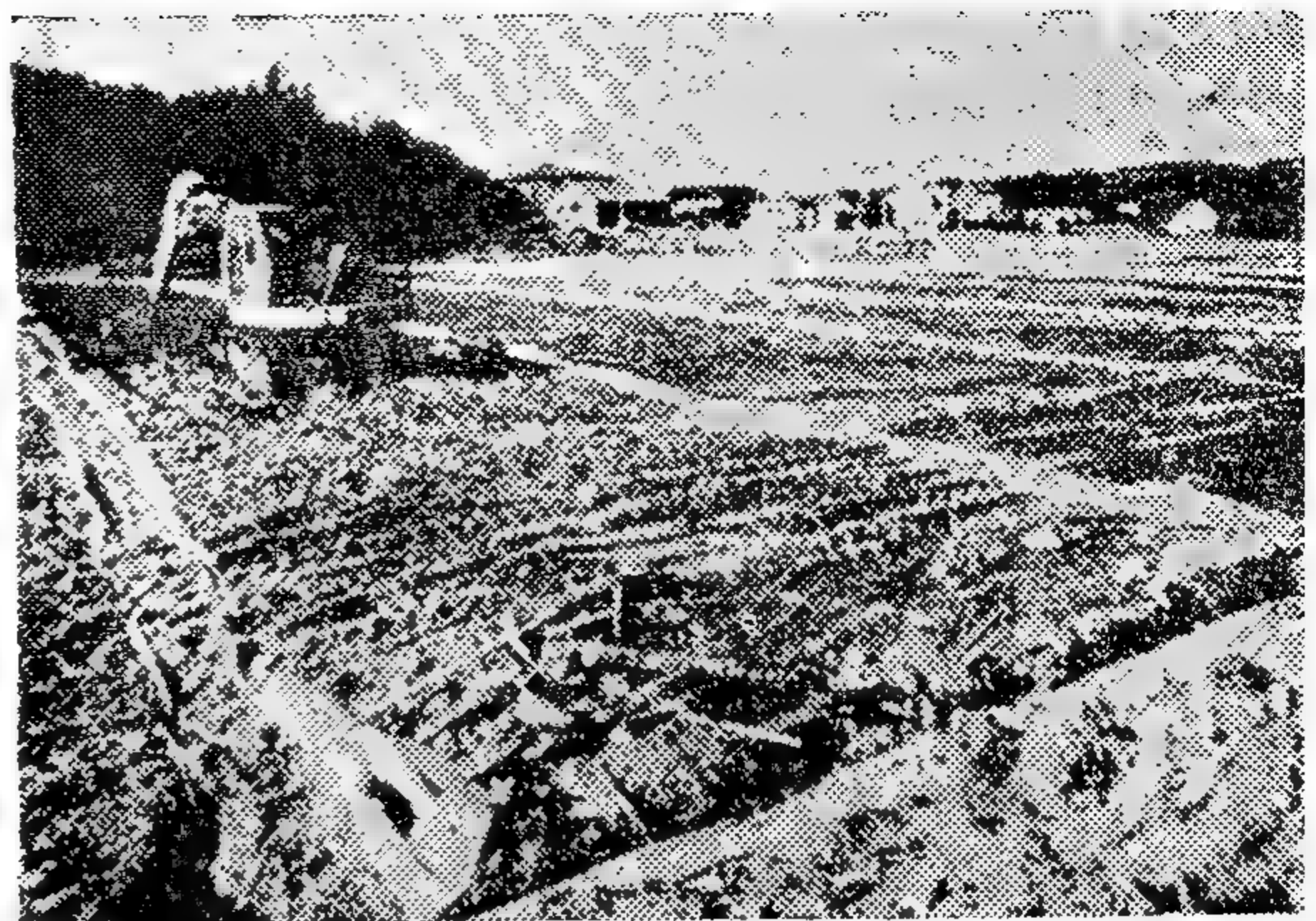


Fig. 7. A Fabric Lined Drainage Grid, Sweden

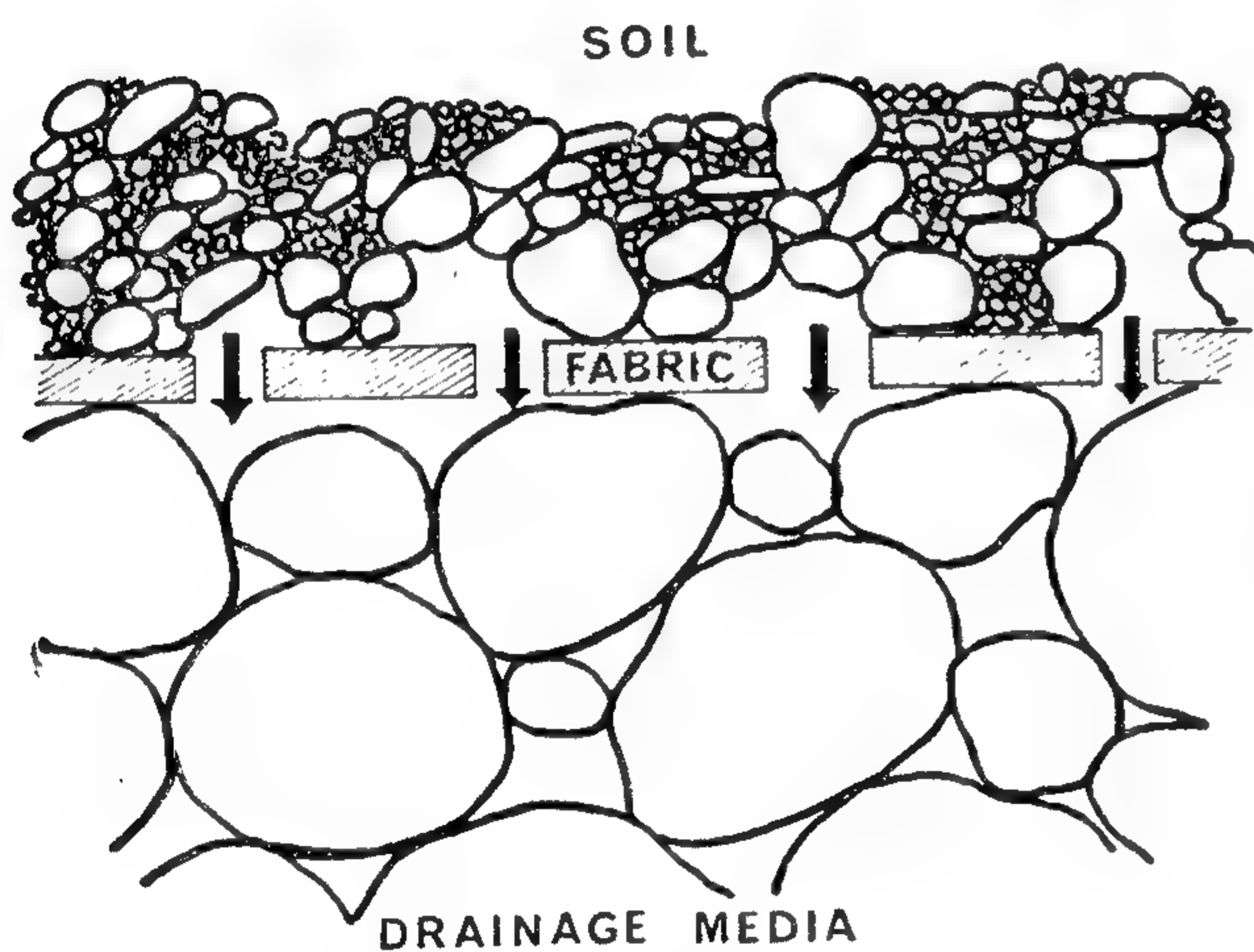


Fig. 6. The Development of a Self Induced Filtration Layer

to be built up in the soil, a phenomenon which is known as Self Induced Filtration. Thus three layers are in fact active in the fabric drain, the natural soil filter, the fabric and the drainage media. The cost of such a fabric multi layer drain is, however, much less than the Cedergren type drain.

Considerable research and development studies have been undertaken in Europe McGown (1973) and United States of America Marks (1975) and the



Fig. 8. Fabric Lined Revetments, Great Lakes, Canada

efficiency of the self induced filtration principle is now well proven over a wide range of soils and hydraulic conditions. Also fabric drains have been successfully used in practice. For example, Fig. 7 shows the grid of fabric lined drains laid in soft clayey silt as undrainage for a playing field in Sweden and Fig. 8 shows the use of fabric in the lining of revetments on the shores of the Great Lakes in Canada. Fabrics have also been used in road under drainage, canal linings and to protect drainage blankets beneath stabilised areas and embankments.

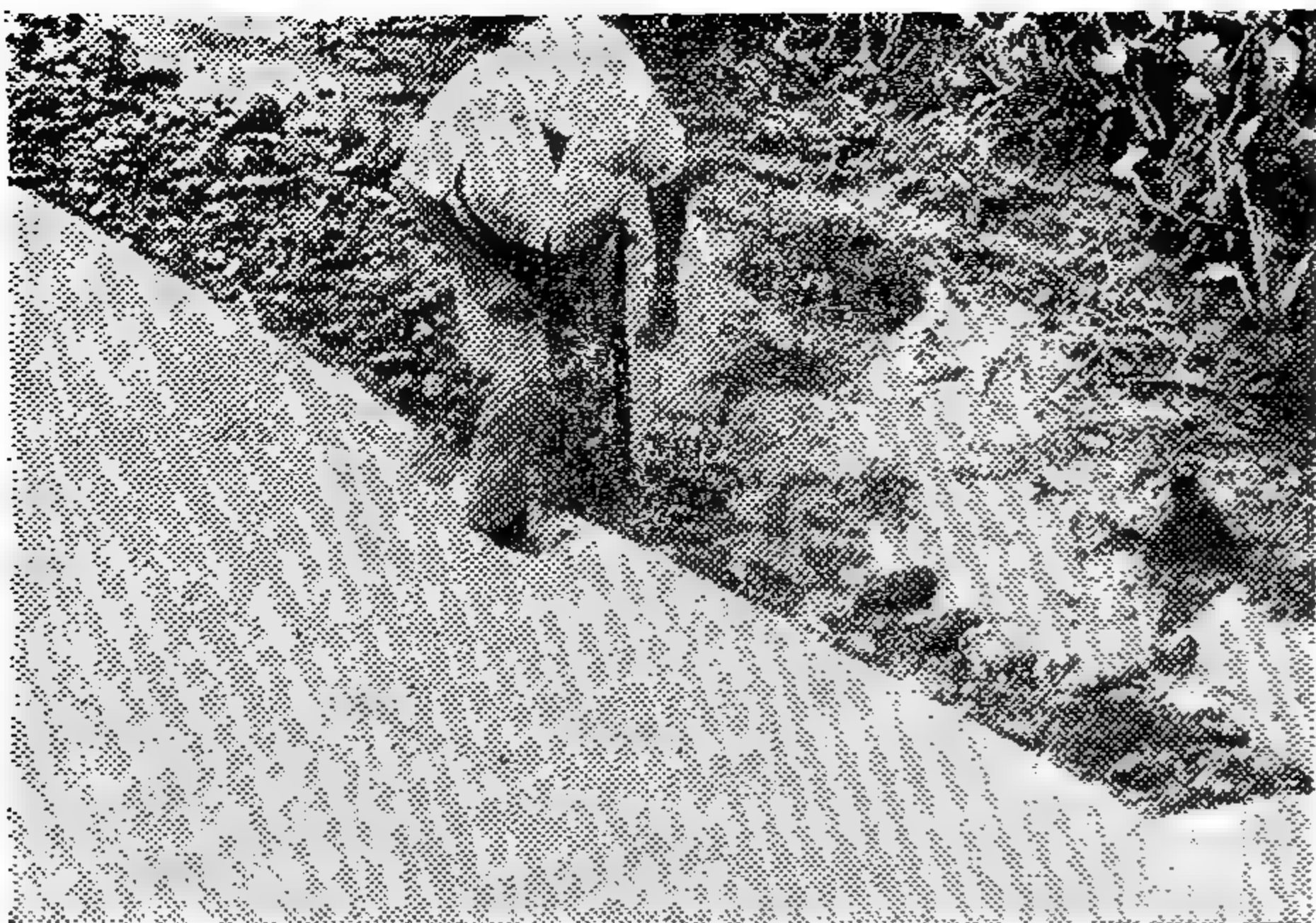


Fig. 3. Laying Fabric in Tropical Rainforest in Columbia

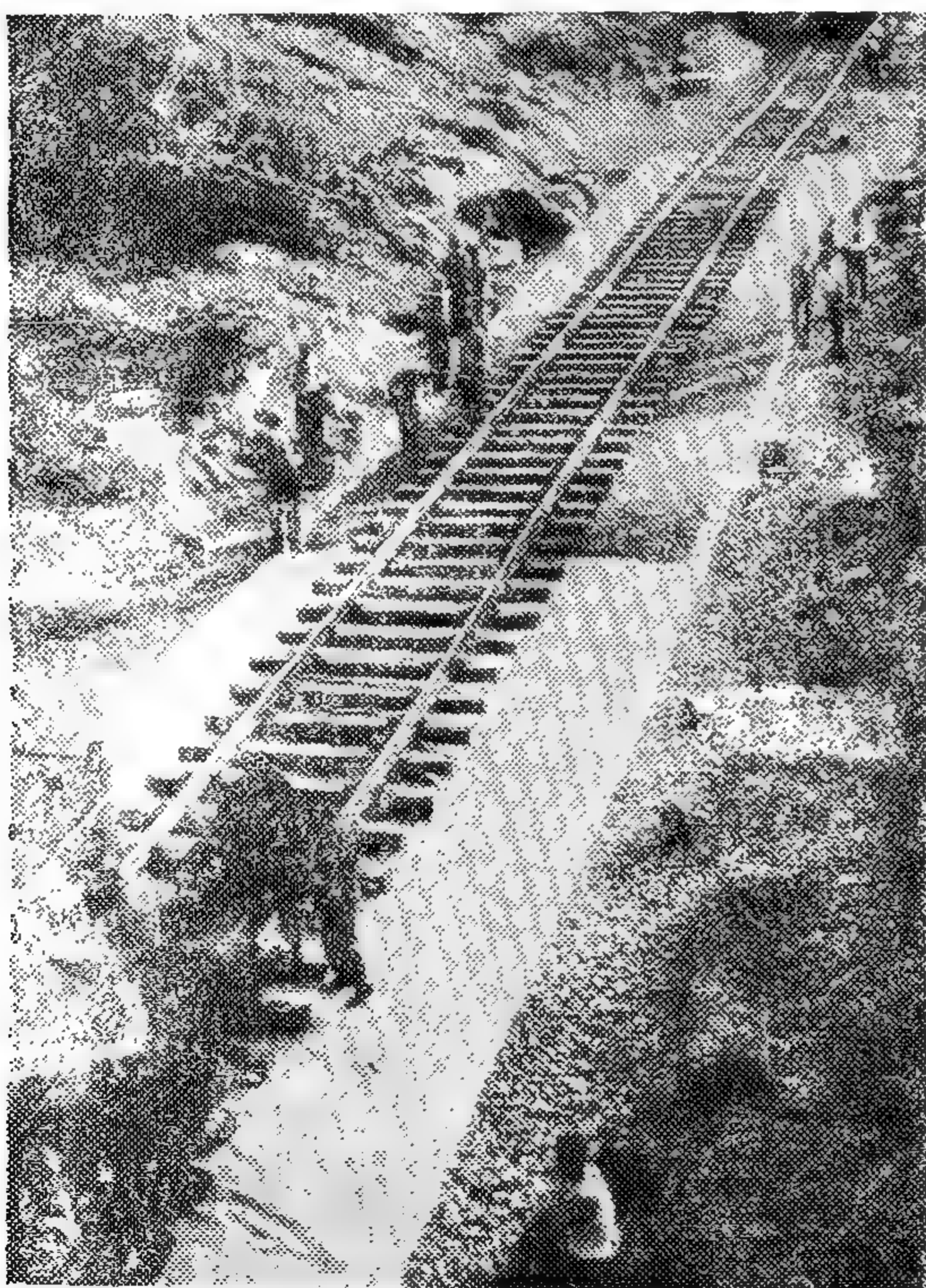


Fig. 4. Construction of Railway Track, Austria

stabilised in a very similar manner in the United States, and the land later used for the construction of large industrial complexes.

6. USE IN DRAINAGE APPLICATIONS

In many civil engineering problems a principle feature of the design solution is the provision of adequate drainage. Difficulty is, however, experienced particularly in soils with high silt contents in obtaining suitably graded filter sands and in controlling the installation of these in the correct manner and position. In addition the multi-layer drain consisting of two or three different but uniform gradings, has been shown by Cedergren (1967) to be a technical improvement over the conventional Terzaghi (1925) or U.S.W.E.S. (1941) single layer drain composed of well graded materials. The problem with the multi-layer drain is of course the costs and difficulties of installation. The use of fabric drains can in various situations overcome many of these problems.

Firstly, fabric is manufactured off site under closely controlled conditions and is widely available. As discussed later, it will carry out the filtration function of drainage layer, therefore when replacing a single layer drain the drainage media behind the fabric does not require to be closely controlled. The problem of the availability of suitable drainage media is therefore largely overcome.

Secondly, the fabric will maintain its filtration properties during the relatively simple laying operation thus the installation difficulties of conventional drains are largely overcome.

Thirdly, the placement of a fabric membrane at the boundary of a trench or on the surface of a drainage blanket, will when backed by drainage media, control the passage of some of the soil particles close to the membrane, as shown in Fig. 6. This causes a natural filter layer

so that the surface layer of vegetation can be left. In soft or loose sub-soils, this vegetable layer has the greatest intrinsic strength of any of the surface layers, therefore the final structure can gain from its remaining.

Where either the width or length of a project is greater than the dimensions of one roll of fabric overlapping is the recommended jointing procedure. In average conditions, 0.3 m overlap is sufficient but in extreme conditions, an overlap of 1 m may be necessary.

As shown in Fig. 1, and previously detailed by McGown and Ozelton (1973), the principle function in roads, railways and area stabilisation is separation. The fabric is generally placed between soft or loose soils and the road sub-base, railway ballast or good quality infill materials used for area stabilisation. In road and area stabilisation, the fabric gives the cost benefits of saving in the amount of material that would normally penetrate into the soil and of increased speed of construction. By eliminating the penetration of the good quality aggregate into the soil, the fabric retaining the aggregates intrinsic strength and permeability. This permits the technical benefit of the formation of a working surface in roads and area stabilisation at depths of infill considerably less than by conventional displacement techniques. In railways the fabric plus a thin sand layer has the technical benefit of reducing pumping of soft clays up into the ballast and therefore it reduces maintenance and increases the life of the track.

In all applications, the sub-soil is not disrupted or remoulded when fabric is used and the soil therefore retains any strength it may have. The maintained high permeability of the fabric and the overlying materials also allows for the easy drainage of the sub-soil and by so doing the strength of the soils will be

increased with time. Additionally, the presence of the fabric causes the overlying materials to be maintained in compression simply by containing them and preventing a great deal of the spreading normally occurring. This has the effect of increasing the strength of the overlying material over that where no fabric is used. Accumulatively these effects of reduction in sub-soil disruption, improved drainage and fill containment give to these roads, railways and stabilised areas with fabric included an increase in strength over those systems without fabric included an increase in strength over those systems without fabric.

The use of fabric membranes in these applications is now widespread both in geographical terms and in terms of the sub-soil types covered. To exemplify their use, Fig. 3 shows fabric being laid in very wet sub-soils for a road through tropical rain forests in Columbia. The extremely poor ground conditions are apparent but with the use of fabric, the road was constructed using 1 m of good quality, well graded sandy gravel. Fig. 4 shows the construction of a section of railway track in Austria including fabric. On this site pumping of clay into the ballast had previously been a problem but the use of a 75 mm layer of sand laid into a layer of fabric prior to placing of the ballast has proven to be a solution. Fig. 5 further shows the construction of a very wide motorway embankment in United Kingdom which traverses very soft, deep clay and where the water table is at or above ground level. Great difficulty was experienced with movement of earth moving plant and piling equipment of fabric onto the soil by and tipping, careful spreading and compaction of crushed rock, provided with only 0.5 m of fill, an excellent working surface. This layer also served as a drainage blanket onto which the motorway embankment, composed of oil spent shale, was placed. Very large areas have also been

technically superior design in many cases. The relative weightings of the three principle functions in various applications are shown in Fig. 1.

APPLICATION	FUNCTION		
	Separation	Filtration	Reinforcement
Roads, Railways and area subgrade stabilisation	Shaded	White	White
Drainage	White	Shaded	White
Coastal and River Bank Protection	Shaded	Shaded	White
Land Reclamation	White	Shaded	White
Asphalt Reinforcement	White	White	Shaded

Fig. 1. Principle Functions of Membranes in Various Applications

3. THE NATURE OF CIVIL ENGINEERING FABRICS

The optimum physical properties of a fabric must vary with the requirements of the various functions. For example, an ideal separation membrane would be a complete film of material whereas a filtration fabric obviously requires that a large number of apertures are available to allow free passage of water. A particular membrane must therefore have properties which are a compromise between the various, often conflicting, property requirements of the different functions.

The real break-through in manufacturing that has occurred is the development of non-woven membranes which are manufactured from man-made plastic fibres. The plastics used are generally rot-proof although like most plastics they do degrade in ultra-violet light. However, when buried in Civil Engineering Structures these materials have a very long life expectancy.

For example, Figure 2 shows the complex structure of the ICI Terram fabric. It is a melded fabric constructed of 25

per cent polyamide (nylon) and 75 per cent polypropylene. In this case no glueing is used which could degrade with time, in fact, the polyamide forms a sheath around some of the polypropylene filaments and where polyamide crosses over polyamide the manufacturing process causes them to fuse together. The remainder of the filament cross overs are mechanically interlocking but allow mobility of the filaments. These materials in this structural arrangement produces a lightweight, highly frictional, relatively high strength fabric with high extensibility. It also has high resistance to tear propagation but has sufficient rigidity of structure to retain its filtration properties in a wide variety of stress and strain conditions. Such a combination of properties is important for satisfactory use of fabrics in civil engineering and care must therefore be exercised in the selection of fabric type for any application.

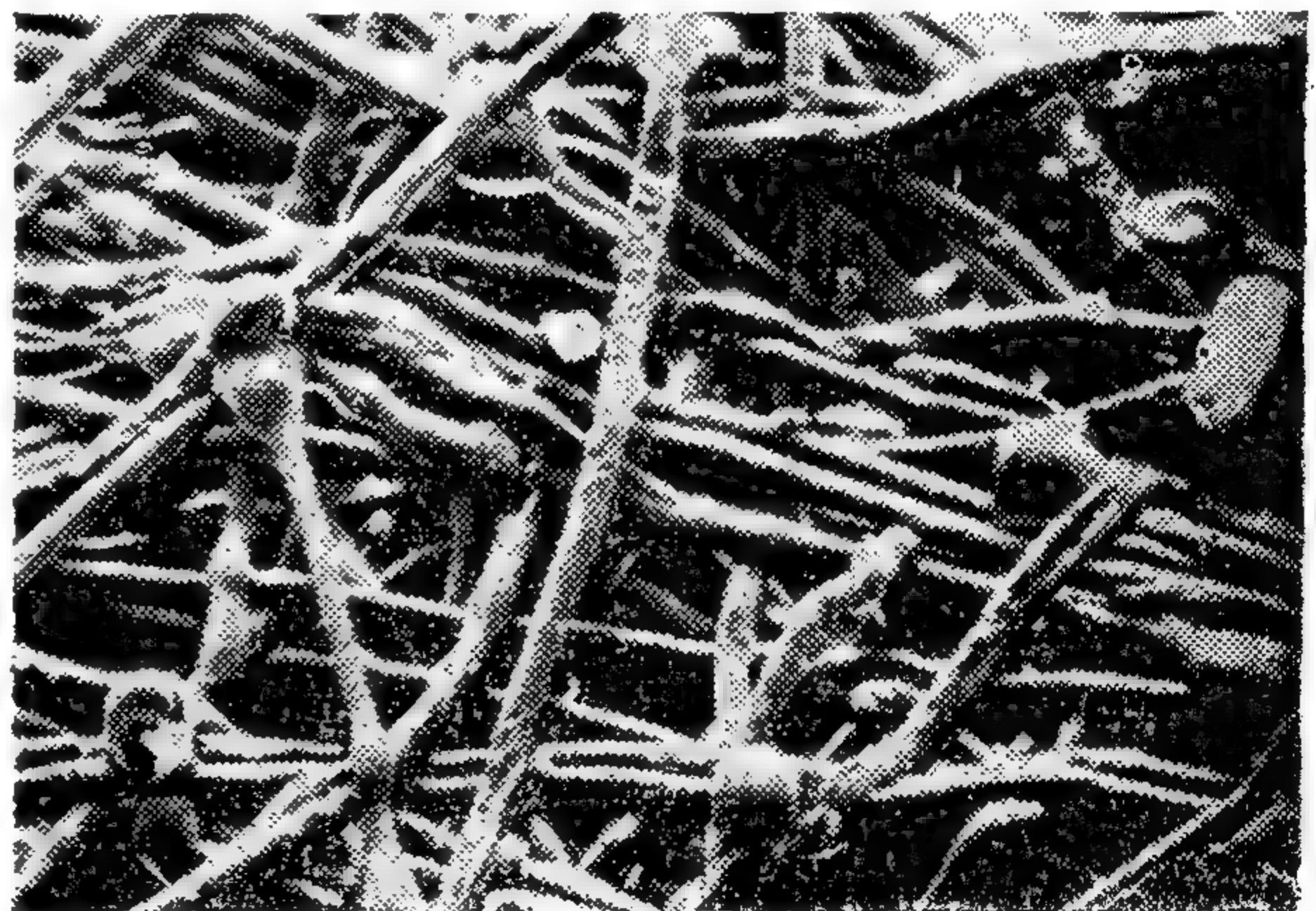


Fig. 2. The Structure of ICI Terram Fabric

4. METHOD OF INSTALLATION

Fabric membranes generally come in rolls 100 m long and 4 to 5 m wide. With a lightweight fabric the weight of a roll is about 60 Kg, which can easily be carried by two men. Laying out is simply a matter of rolling the fabric directly onto the surface of the soil. Only large stones or tree stumps need be removed,

THE USE OF NON-WOVEN PERMEABLE FABRIC MEMBRANES IN THE SOLUTION OF SOME CONSTRUCTION PROBLEMS

By : G. NASSAR*

AFTER A LECTURE GIVEN

BY ALAN McGOWN**

SUMMARY

The principal fabric membrane functions of separation, filtration and reinforcement are described and the relative importance of these various uses are outlined. The nature of fabric suitable for civil engineering is discussed and the method of installation briefly described. The use of fabrics in various applications such as roads, railways and area stabilisation, drainage, land reclamation and causeway construction together with asphalt reinforcement are described and practical examples are cited. The various cost and technical benefits are indicated and new construction possibilities noted.

1. INTRODUCTION

The use of permeable fabric membranes has been accepted for a number of years in a few countries, in a few specialised branches of our technology. Over the last three years, however, new fabrics with radically different forms of non-woven construction have become available and these new materials permit the much more widespread application of fabrics.

Research and application development work is now getting underway in Europe and the United States of America and so called Membrane Technology is fast developing. This paper therefore attempts to describe the functions of fabric membranes and illustrates the applications range which have so far been identified.

2. THE FUNCTIONS OF FABRIC MEMBRANES

The principle functions of fabric membranes are to keep apart different layers of construction materials, to freely allow passage of water while controlling the passage of solids and to alter the stress-strain behaviour of systems in which they are included. These three functions are known as Separation, filtration and Reinforcement, but a fourth function of drainage in the plane of the fabric may also be operable, particularly in thick membranes.

By a combination of these various functions in different relative weightings, the the fabrics can in fact be used to assist in the solution of a wide range of civil engineering problems, providing not only a cost effective solution but also a

* Assist. Prof., Structural Department, Faculty of Engineering, Ain Shams University.

** B.Sc. Ph.D., M.I.C.E., M.I.H.E., M. ASCE., F.G.S.

Department of Civil Engineering, University of Strathclyde, Glasgow U.K.

TALL BUILDING NEWS

The ten		Tallest Buildings in the World		
Building	City	Yr.	St.	M.
Sears Tower	Chicago	73	110	442
World Trade	New York	73	110	412
Empire State	New York	31	102	381
Standard Oil	Chicago	73	80	346
John Hancock	Chicago	68	99	344
Chrysler	New York	29	77	264
United Calif. Bank	Los Angeles	74	65	262
40 Wall St.	New York	30	71	259
First Nat. Bank	Chicago	68	60	259
Water Tower Plaza	Chicago	74	70	259

TOKYO & HONG KONG CONFERENCE

Sept. 5-11, 1976 :

10th congress of IABSE, Tokyo

Sept. 12, 1976:

Tall Building Symposium, Tokyo

Sept. 20-22, 1976:

Tall Building Conference. Hong Kong. The tall building activities have been planned to coincide with the special travel rates made possible by virtue of the already assured group flights for the IABSE Congress and the attractive post-conference tours.

INFORMATION NEEDED

Committee 21A (Selection of Structural Systems) wants information on structural systems used in tall concrete buildings from all geographic regions. Descriptions and selection criteria for systems not commonly used in the United States are particularly desired. Please send information to Headquarters, or directly to :

Mr. Victor F. Leabu
Chairman, Committee 21A
Giffels Associates, Inc.
1000 Marquette Bldg.
Detroit, Michigan 48226, USA

CAIRO DEVELOPMENTS

(From Times : Vol. 6, No. 3)

Work on the Proceedings of our Low-Income Housing Conference is moving apace: photos selected, typing underway. We've been promised a "Christmas present".

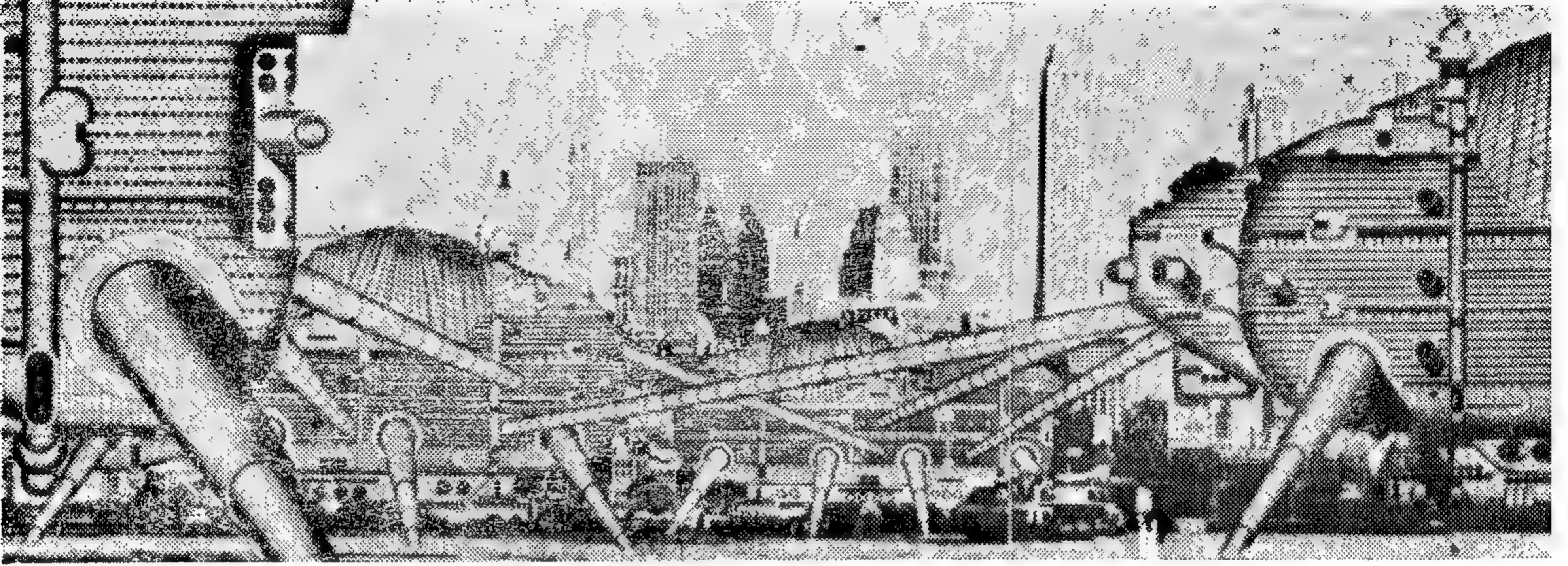
The development of the master plan for the Suez Zone reconstruction is coming along well. The plans are expected to be submitted this fall.

10,000 housing units in Ismailia and Suez have been completed in 8 months.

The new bridge across the Nile continues to "grow".

Ismailia and Port Said are now bustling communities. The contrast with a year ago is remarkable.

G. NASSAR



١٢ : استخدم الإنسان في العصر الماضي الآلة كي تكون عبداً
له يستخدمها ويطوعها لصالح الإنسانية .. ولكن في العصر
الحديث ، عصر الصناعة والتكنولوجيا بدأت الآلة تستخدم
الإنسان وأصبح عبداً لها . ظهر المسكن الجاهز المصنع المتحرك
أو المتقل ، وسيظهر قريباً مدينة كاملة متحركة متنقلة
Walking City — كما هو موضح أعلاه . والسبب
في ذلك سيطرة الآلة والتكنولوجيا على العمارة .

مقدمة

في الجزء الأول من هذا البحث
الذي نشر في العدد الماضي أوضحت
كيف سجلت العمارة الحديثة تطور
العصر الحديث أو ما يسمى بالانقلاب
لصالح العصر أو لغير صالحه ..
وشرحت أن العمارة الحديثة ما هي
الا تطور ثوري ، وأطلق المجتمع عليها
استعارات مختلفة سماها بعلب
السيجار ، أو صناديق الأحذية ، أو
معامل التفريخ البشرية ، أو معتقلات
العصر الحديث ، أو خرائب الإسكان
العصري ..

وفيما يلي أهم عناصر الجزء
الثاني من البحث والذي نشر ضمن
بحوث المؤتمر الهندسي العربي الثالث
عشر في تونس ٢١/١٧ مارس ١٩٧٥
وكما نشر أيضاً باللغة الإنجليزية في
المؤتمر الدولي لاتحاد الممارين الذي
عقد في مدريد ١٢/٥ مايو ١٩٧٥ .

- الولايات المتحدة الأمريكية وحضارة المادية
والنفعية .
 - اليابان : طوكيو تبنى فوق مياه الخليج ...
 - الاتحاد السوفيتي : العمارة الحديثة ليست
عمارة ماركسية .
 - المملكة المتحدة/بريطانيا والتعمير الديموقراطي .
 - فرنسا : باريس تبنى تحت الأرض ..
 - عواصم البلاد العربية تعيش في فوضى معمارية .
- سأحاول لقاء الضوء على ما وصلت اليه العمارة
في هذا العصر الحديث في أهم عواصم بلاد العالم
وتأثير التقدم الصناعي والتكنولوجي عليها .. في
نيويورك وشيكاغو ، في الاتحاد السوفيتي ، في لندن
وباريس في طوكيو والقاهرة ..

● الولايات المتحدة الأمريكية :

وحضارة المادية والنفعية

تتسم الملامح الأمريكية في الحياة العامة بشتى صورها بصفة واحدة مميزة قد لا تتوفر في غيرها من البلاد الأخرى . هذه الصفة أو هذا الطابع المميز يتلخص في انطلاقة الحركة الغير مقيدة ببداية ونهاية ، ولكي تكون الحركة حرة الخطوات ، أن تكون مؤلفة من وحدات متكررة الى غير نهاية معلومة . وتتمثل هذه الصفة الواحدة في تخطيط المدن الأمريكية ، وناطحات السحاب ، وفي الثقافة والأدب وموسيقى الجاز ، والتصنيع الآلى ذات الوحدات المتكررة ، والتجميع المتكرر .. الخ

فتخطيط المدينة الأمريكية يتبع طريقة الشبكة Grid System خطوط مستقيمة متوازية ومتعامدة كأنها شبكة من القضبان تتوازي وتتعامد في مربعات صغيرة . وكذلك ناطحات السحاب التي هي في هيكلها المعماري والانشائي كالقفص ترتفع أعمدته الرأسية الى أعلا تعترضها كمرات أفقية للطوابق المتكررة .. وهكذا فيما يتعلق بموسيقى الجاز ذات الوحدة المتكررة ، والشعر والأدب والانتاج بالجملة . فان أهم ما تتميز به الثقافة الأمريكية أساسا ، هو الاهتمام بطريق السير والحركة أكثر من الاهتمام بما ينتج عن ذلك السير ويتجسد على صورة محدودة .

فالمدينة المخططة على أساس تكرار وحدة المربعات باستقامة الشوارع وتعامدها بمنتهى الدقة قد تنمو بنفس الطريقة بغير حدود دون أن تنكسر وحدتها الفنية ، وناطحة السحاب التي تتكرر طوابقها الى أعلا تبعا لمقياس وحدة ارتفاع يمكن أن يستمر ارتفاعها الى غير حد دون أن ينكسر شكلها المعماري . وكذلك الحال فيما يتعلق بالانتاج الاقتصادي من حيث قابلية البناء لتكرار الوحدات أو الطوابق وهكذا .

● حضارة الولايات المتحدة الأمريكية اذن حضارة ناجحة على المستوى الانتاجي والمادى ، حققت السيطرة الكاملة على الانسان الأمريكى في الداخل والخارج ، ووصلت الى الاتزان الذى يضمن لها الاستمرار والاتساع . وربما يقدر لهذه الحضارة السيطرة على التجمعات الرأسمالية الأخرى ذات التاريخ العريق والتراث القومى والدينى . حتى المجتمعات الاشتراكية نجدها اليوم مهددة بهذا الغزو الحضارى الأمريكى أكثر من غيرها ، لأنها مجتمعات قد قطعت صلتها بتراتها القومى والدينى والروحى ، وخلقت فراغا حضاريا لا يمكن أن تزدهر فيه الا القيم المادية . خاصة وان هذه المجتمعات الاشتراكية لا تزال تقيم نجاحها وانجازاتها بمعايير مادية ميكانيكية غير انسانية .

● أن الحضارة الرأسمالية هي حضارة المادة والانتفاع ، أى حضارة الماديين النفعين ، حضارة ترى الانسان على أنه كمية من الاحتياجات من السهل ارضاؤها ، والحضارة الاشتراكية باستمرارها في التركيز على الآلة وعلى الانتاج وعلى الكم دون ذكر للهدف الانسانى ، وبإهمالها خلق وعى تاريخى انسانى عند المواطنين قد تقع في برائن هذه الرؤية النفعية المعادية للفكر والانسان ، وقد تظل تابعة لعبودية عالم الضرورة والكم . وناطحات السحاب مثلا ما هي الا عنوان لهذه الحضارة الأمريكية على المستوى الانتاجي والمادى .

كان سكان نيويورك يعانون من ارتفاع أجور المساكن ويطالبون الحكومة بوضع حد لشر الملاك وجشعهم ، والحكومة لا تقوى على اجابة مطلبهم لعدم شرعيته . فظهرت فكرة انشاء أعلى مبنى في نيويورك ، وكان الهدف بناء أعلى مبنى في العالم عرفه التاريخ - دعاية واستثمار رؤوس أموال . وأقيم مبنى امير ستيت Empire State Building في الشارع الخامس بمدينة نيويورك عام ١٩٣٠ وتربع على عرش أعلى مبنى في العالم أكثر من ٤٠ عاما .

وتكونت مظلة من المماريين على المستوى العالمى لانشاء مبنى سكرتارية هيئة الامم المتحدة في نيويورك عام ١٩٥٠ برياسة « ولاس هاريسون » التي أعلنت فيها ظهور هذا الحجاب المسمى الحائط الزجاجى الساتر Curtain Wall . ولو أن فكرتها كانت مقترحة من قبل في أعمال ميزفان درروه ، والترجروبياس ، ودادوك . غير أنه كان على هذه المشروعات المقترحة أن تنتظر بعض الوقت لانتظار الميتالرجى والبلاستيكي الصناعى ، حيث كانت هناك بعض الأمور والمشاكل الفنية تنتظر الحل مثل العزل ضد الحرارة والرطوبة والمياه والتمدد والانكماش للمواد المستعملة .

وكان أن أعطت الولايات المتحدة الأمريكية جميع فرص الامكانيات الى « ميزفان درروه » ١٨٨٦ بعد أن هاجر من ألمانيا واستوطن أمريكا سنة ١٩٢٨ لتنفيذ رسالته وفلسفته في العمارة ووجد نفسه محاط بالعملاء . هذه الفلسفة التي عبر عنها « ميز » بأن « القليل يكفى ، ويكاد أن لا يكون » .

Less is more والتي عبر عنها البعض « عدم وجود عمارة » م يكن مبنى سيجرام ٣٧٥ بارك آفينيو بنيويورك عام ١٩٥٨ تصميم « ميز » وعمره ٧٣ عاما أول ناطحة سحاب من زجاج وحديد ، بل كان حلمه الاول الذى تحقق في بناء ناطحة سحاب في شيكاغو عام ١٩٥٧ على نمط ما قام به من مشروعات مماثلة في برلين ، وتشير هذه الأمثلة وغيرها الى درجة التحكم في صياغة المدن والزجاج والحديد في العمارة .

أفادت وأضرت في نفس الوقت . تكاد البحار تصبح مسمومة من كثرة ما يفرغ فيها من فضلات المصانع من الكيماويات والمواد السامة . المدن مزدحمة والحياة فيها رهيبة ، والمرافق مثقلة بما فيها وما عليها من أعباء . وبهذا الشكل سنقتل الطبيعة .

استطاع اليابان أن يخلق معجزة خلال الربع قرن الماضي على مجموعة تنقصها المواد الخام والأراضي الخصبة والمواد الأولية وذلك بفضل التكنولوجيا الحديثة واستخدامها ، واستطاعت الإدارة البشرية وقدرة الخلق أن تحلق بالشعب الياباني إلى آفاق بعيدة ومجالات متشعبة تطورا وابتكارا وتجديدا . حيث أن الدولة بكامل مؤسساتها الرسمية والأهلية والاقتصادية قد اتخذت من العلم والأبحاث منهجا وسبيلا للتقدم .

وتقوم معاهد البحوث الحكومية أو الخاصة بالأبحاث في مجال تنمية التكنولوجيا اليابانية والأبحاث التي تساعد على رفع مستوى رفاهية الشعب وتحسين أحوال معيشته الصحية والنفسية . واهتمت بأبحاث الفضاء والأقمار الصناعية ونقل البرامج التليفزيونية ودراسة الأحوال الجوية وبحوث الزلازل والأعاصير والتنبؤ بها ، واستحداث النظريات الهندسية لإنشاء مباني ضد الزلازل .

أما فيما يتعلق بتلوث البيئة والمحيطات فقد صممت محطات التنقية لعوادم المصانع التي لايسمح الآن بالتخلص منها في الأنهار والمحيطات ، مع الاستفادة من مخلفات الصناعة كمصادر للمواد الأولية . حتى أنه أمكن إنتاج البترول من مخلفات البلاستيك، وكذلك إنتاج مواد بناء لرصف الشوارع من المخلفات المنزلية ، وتحويل مياه المجارى بالمعالجات الكيماوية والبكتريولوجية للحصول على مياه الشرب . وهذه هي القدرة الحقة على كيفية استخدام العلم والتكنولوجيا لتحسين أحوال معيشة الانسان في هذا العصر الحديث .

وتعتبر اليابان فعلا احدى الدول التي يقلقها معدلات نموها . وذلك أن اندفاعاتها التكنولوجية تعرض البيئة اليابانية للتلوث بسبب ما يستتبعها من تركيز المصانع وتركيز السكان . ومعنى ذلك تلوث في الجو والمياه والأرض والانسان . ومن هنا ظهر مشروع جديد يطلق عليه اسم « مشروع خدمة المدينة » City Service Project ويتلخص بأن كل محافظ مسئول عن وضع الخطط اللازمة لإدارتها وسلامتها وأمنها وتقديمها ونموها . ومن أهم بنوده:

— حماية السكان وتأمين حياتهم وممتلكاتهم من أخطار الزلازل وتشقق الأرض والحرائق والفيضانات وزيادة توسيع رقعة المسطحات الخضراء والحدائق العامة ، وإنشاء مسارات جديدة للمواصلات داخل

— وتطالعنا شيكاغو أيضا بنوع آخر أو بمجموعة أخرى من الابراج التي تحتوى على ٢٠ طابق للسيارات يعملوها ١٠ طوابق أخرى للمكاتب الادارية ثم ٤٠ طابق للوحدات السكنية . ويبلغ قطر الدائرة التي تحدد كل طابق ٣٢ م ، ومحيط الدائرة مقسم الى ١٥ قطاع : وتتمركز هذه القطاعات حول نواة مركزية قطرها ٩٧٥ م تتجمع في داخلها الخدمات الرأسية . أطلق على هذه المجموعة اسم « ماريناستى » Marina City تصميم المعماري برتراند جولدبرج ١٩٦٦ . نجد أن هذا المشروع بتصميمه وتوزيعه بطريقة أو بأخرى مصمم ، قد يكون انعكاسا لقريئة اجتماعية موجودة وهى السيارة التي وجدت مكشوفة في هذه الطوابق المخصصة ، وتقارب الكتل الغير ناجح كأنها محصلة خدمات مختلفة مؤدية الى تجميع غير متلاحم وكأنها تكوينات غير مترنة . وواضح أن العوامل الانشائية تغلبت على النواحي المعمارية والفنية ، فكانت هذه التكوينات الدائرية للوحدات الادارية والسكنية التي تتنافى مع الوظيفة والغرض والانتفاع .

— وأخيرا مركز التجارة الدولي/نيويورك ١٩٧١ تصميم المعماري « منرو ياماسكى » الذى حطم الرقم القياسى لأعلى مبنى فى العالم ، ويتكون من برجين يصل ارتفاع كل منهما الى ٤١٠ م ويحتوى على ١١٠ طابق بخلاف الطوابق السفلية . خصص لاسكان وخدمة عدد ٥٠ ألف شخص يعملون فى مؤسسة روكفلر بمدينة نيويورك الواجهات مكسوة بألواح الألومينيوم المؤكسد لتأكيد الاستقامة الرأسية والتعبير عن القدرة والتحكم فى كيفية تطبيق العلم والتكنولوجيا فى العمارة الحديثة .

ويقول ل . كوربوزيه ١٨٨٨ - ١٩٦٥ : فى هذا الموضوع بلهجة ساخرة « لم تنشأ ناطحات سحاب نيويورك بحكمة جدية ونوايا جديدة . يحتفون بها ويهتفون لها على أنها أعمال بهلوانية خارقة ، نجحت ناطحات السحاب على أنها اعلان وشهرة لأسماء اصحابها . ليست ناطحات السحاب والأبراج العالية هنا عنصر هام فى تخطيط المدن ، وإنما هى علم مرفوع الى السماء ، والعب نارية لشهرة أسماء اصحابها فى دنيا المال ، نيويورك كارثة ولكنها كارثة ساحرة .

● طوكيو تبني فوق مياه الخليج :

يواجه اليابان مشكلة تلوث خطيرة فى المدن ، وأصبحت مشاكل نمو المدن اليابانية من أهم المشاكل الرئيسية لعلاقة الانسان بالبيئة وضرورة حماية الأرض والماء والهواء والانسان ، علاوة عن موضوع زيادة السكان ، وازدحام المدن ، والانتقال من الريف الى المدينة .

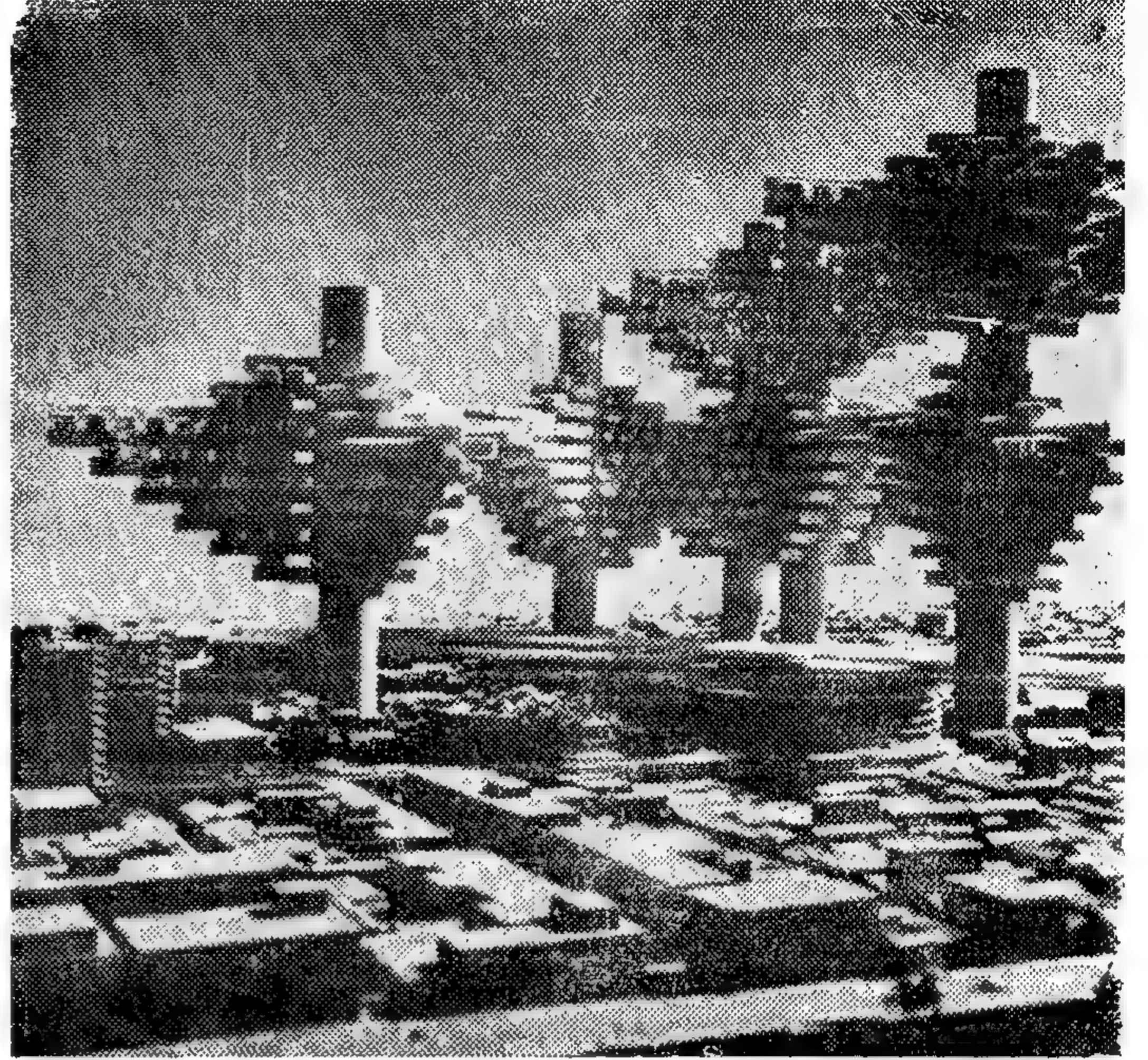
ويقول رئيس وزراء اليابان الحالى ، حينما تحدث عن التقدم الصناعى والتكنولوجى « ان اليابان تعيش على جزر يحيط بها البحر من كل جهة . . حفروا الجبال بحثا عن الطعام ، وحصدوا البحار لنفس السبب . . أكلوا جذور الشجر وأكلوا أعشاب المياه . . ان عمليات الصناعة والتصنيع

والادارية والصناعية . ولكن بأساليب جديدة .
اختلفت عن مثيلاتها في العالم ، سمحت بالحصول
على تكوينات معمارية وتخطيطية في الفضاء . حيث
تتلخص في انشاء قوائم رأسية من الحديد أو
الخراسانة المسلحة قطر حوالى ١٢م كنقط ارتكاز
ودعائم للعناصر الأفقية الممتدة منها أو بينها ، وهى
في نفس الوقت عناصر الاتصال الرأسى وتجميع
الخدمات . ومن أغرب الأمثلة في هذا الشأن مبنى
مكاتب جريدة حى جنزا طوكيو تصميم المعماري
كنزو تانج سنة ١٩٦٧ ، أسطوانة ضخمة يتجمع
داخلها جميع الخدمات ، الحركة والماكينات والناس
داخل الماسورة ، ويتفرع منها كوابيل تحمل المكاتب
الادارية للجريدة يرجى أن ينظر شكل ١٣ ، ١٧ ، ١٨

— وضعوا العديد من المشروعات لتخطيط المدن
الطولية أو المدن الشريطية وكان من أهمها امتداد
مدينة طوكيو نحو الخليج والبناء فوق الماء واخضاع
التربة المائية للبناء فوقها . . مثل مشروع « مدينة
المحيط » Ocean City ١٩٦٤ للمعماري كيكوتيك
Kikutake الأسطوانات العالية للمجموعات السكنية
على أقراص وحلقات مستديرة وكأنها أجسام لفرقة
راقصة على سطح الماء ، ومشروع مدينة المصاطب
Neo-Mastaba City طوكيو شكل ١٤ ، ١٥ ، ١٦
للمعماريان آكى ، نوزاوا حيث يعتقدان أنه اذا أمكن
لقدماء المصريين منذ آلاف السنين بناء الهرم الأكبر
بالجيزة بهذا المقياس الضخم ، فان مثل هذا
المقياس يمكن تحقيقه بوسائل العصر الحديث العلمية
والتكنولوجية ، حيث تحتوى كل وحدة من وحدات
هذه المصاطب على ٣٠ ألف ساكن . . ومشروع
الانشاء الفضائى Spatial Construction
للمعماري « آن أوسوزاكي » ، والمدينة الفضائية
Cluster in the Air شكل ١٣ عبارة عن انشاء
نقط ارتكاز ضخمة تحتوى على مجموعة الخدمات
ومنها تتفرع المساكن على شكل عناقيد .

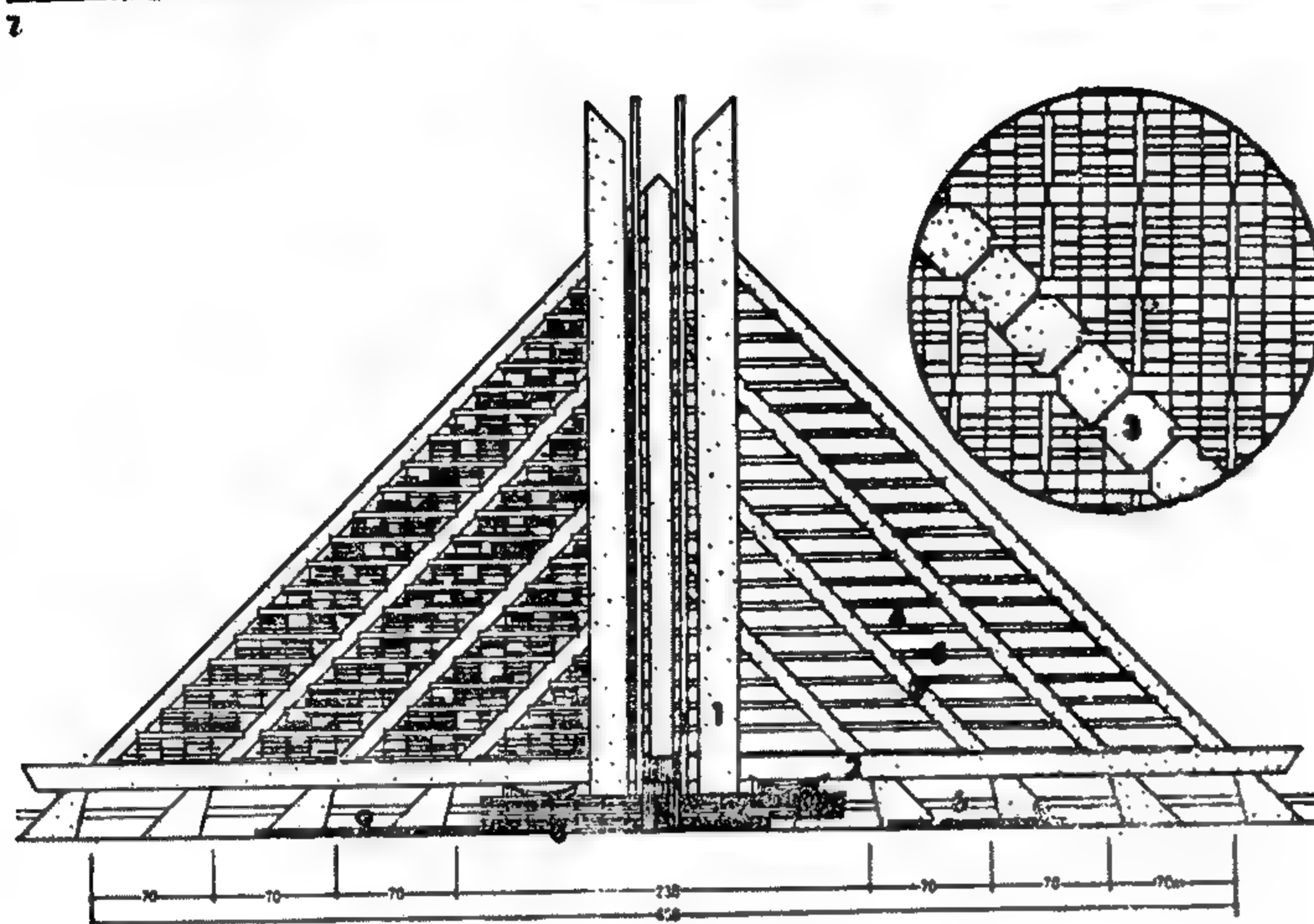
● الاتحاد السوفيتى والتطور العمارى :

كان أسلوب الحكم السوفيتى فى الأربعينيات
وما بعدها بكل تأكيدات الاجتماعية ملائما لكى يشع
وينشر عمارة تؤكد الطابع الاجتماعى والقومى
والتكنيكى البنائى . وكان هناك أكثر من سبب يوحى
بأن روسيا لابد وأن تكون فى مقدمة حركة التطور
المعماري الحديث . ولكنها بدلا من ذلك اتجهت الى
الوراء نحو هذا الأسلوب المسكن أو المهديء
النيوكلاسيك الذى يمكن الحصول عليه من أى بلد
فى أوروبا . مع أنه كان فى روسيا فى ذلك الوقت
حركتان أخذتا شكلا محددا فى البناء وهما :
« الانشائية » Constructionism
و « الرسمية الرمزية » Symbolic Formalism
حيث تهدف الحركة الأولى الى الديناميكية الثورية

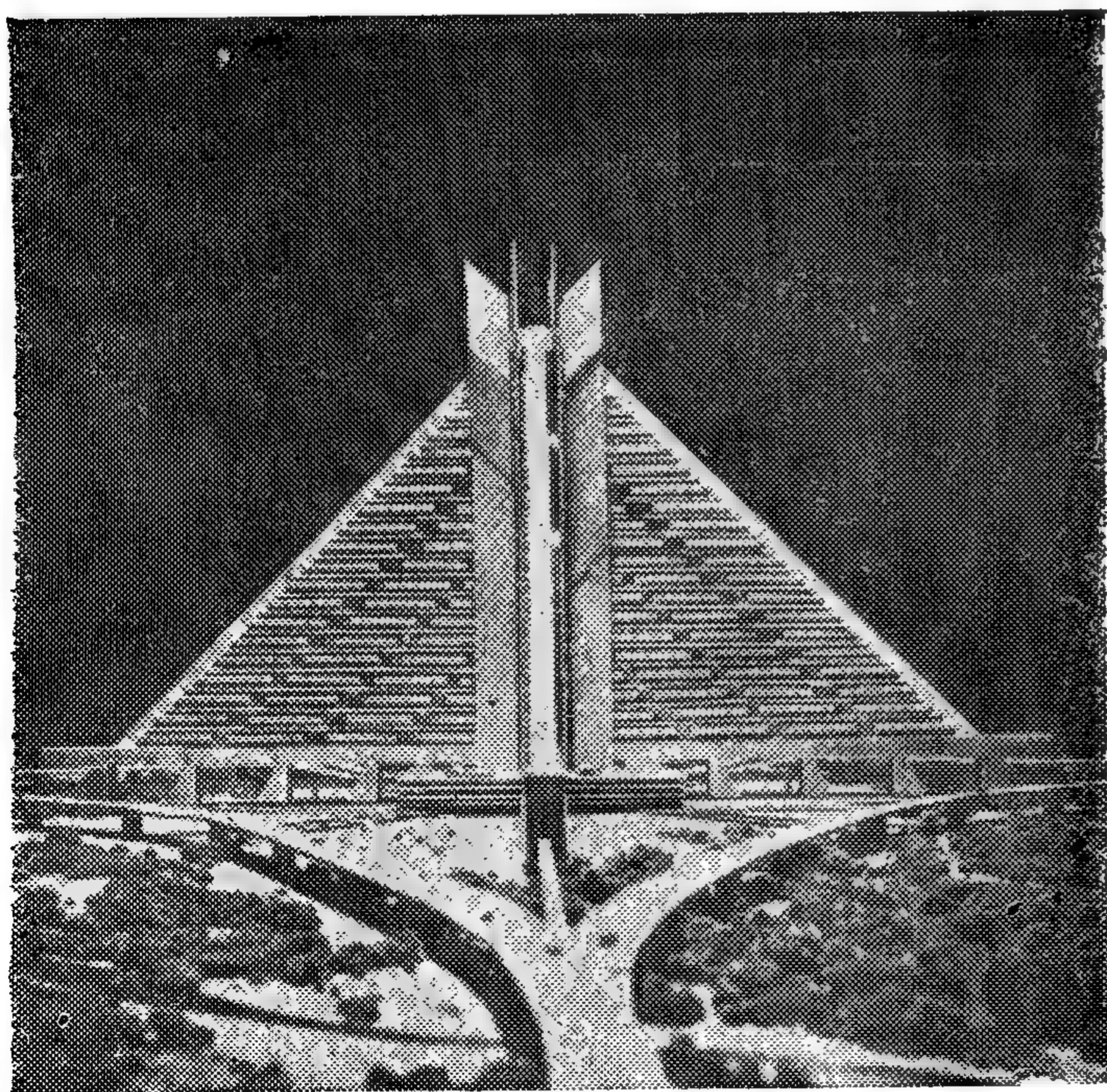


١٣ : مذهب جديد لعمارة العصر الحديث ينادى به المهندس
المعماري فى اليابان ويسمى ميتابوليزم Metabolism
تكوينات معمارية وتخطيطية وكتل فى الفراغ وانشائها فى الفضاء ،
عمارات سكنية ومباني ادارية وصناعية ومدن فضائية . . .
عبارة عن قوائم رأسية قطر ١٢م كنقط ارتكاز ودعائم
للعناصر الأفقية الممتدة منها أو بينها . وتحشر داخل هذه
الماسورة الرأسية جميع الخدمات وهى - الحركة والناس
والماكينات - واخلاء سطح المينة للمارة والمشاة والسيارات .
فلسفة جديدة لمذهب جديد أدخلته أو فرضته تكنولوجيا
العصر الحديث ، وربما تكون عودة الى حياة الانسان الأول على
أعلى الشجر طلبا للأمان .

وخارج المدينة ، ومشروعات الاسكان والتعمير ،
والتحكم فى تلوث الأرض والماء والهواء .
● نرى أنه فى اليابان ظهرت حركة جديدة متطورة
يتزعمها المعماري « كينزو تانج » Kinzo Tange
ومذهب جديد فى العمارة ويسمى « ميتابوليزم »
Metabolism للمباني وانشاء المدن الفضائية
وتتلخص هذه الحركة فى مجموعة العمليات
المتصلة بالخلايا والأنسجة التى تؤمن الطاقة
الضرورية للعمل والأنشطة المختلفة التى تتميز بها
المواد الجديدة للبناء والتعويض بها عن المواد
التقليدية القديمة . . واستحداث الأفكار الحديثة
المتطورة التى تناسب مشاكل المدن من حيث التربة
والمواقع والعوامل الطبيعية والجغرافية التى تنفرد
بها اليابان دون غيرها من بلاد العالم .
— اتجهوا الى الاتجاه الرأسى فى المباني السكنية



١٤ ، ١٥ ، ١٦ : مدينة المصاطب السكنية طوكيو يعتقد مصمم هذا المشروع وهما المعمارين آكي ونوزاوا اليابانيان أنه إذا امكن لقدماء المصريين منذ آلاف السنين بناء الاهرام بهذا المقياس الضخم ، فان مثل هذا المقياس يمكن تحقيقه بوسائل العصر الحديث العلمية والتكنولوجية . ويرى الى اليمن شكل ١٤ . التخطيط العام للمصاطب السكنية وتوضيح ربط المصاطب ومسار المشاة والسيارات . ويوضح الشكل رقم ١٥ اعلا : مقارنة حجم المصطبة بأهم المباني العالية ثم التفاصيل الداخلية للمصطبة من سلالم متحركة وشوارع ومونورتل واماكن العيشة ومحلات تجارية ترفية وانتظار سيارات وخلافه . شكل رقم ١٦ أسفل ماكيت المصطبة أو المدينة السكنية الكاملة .



لم تبتدع الثورة الاشتراكية السوفيتية أساليب جديدة أو طرق معقدة في عمارة العصر الحديث ، ولكنها أوجدت الوسائل والطرق التي أمكن بواسطتها العمل على قومية الأرض ، ونهاية الملكية الفردية ،



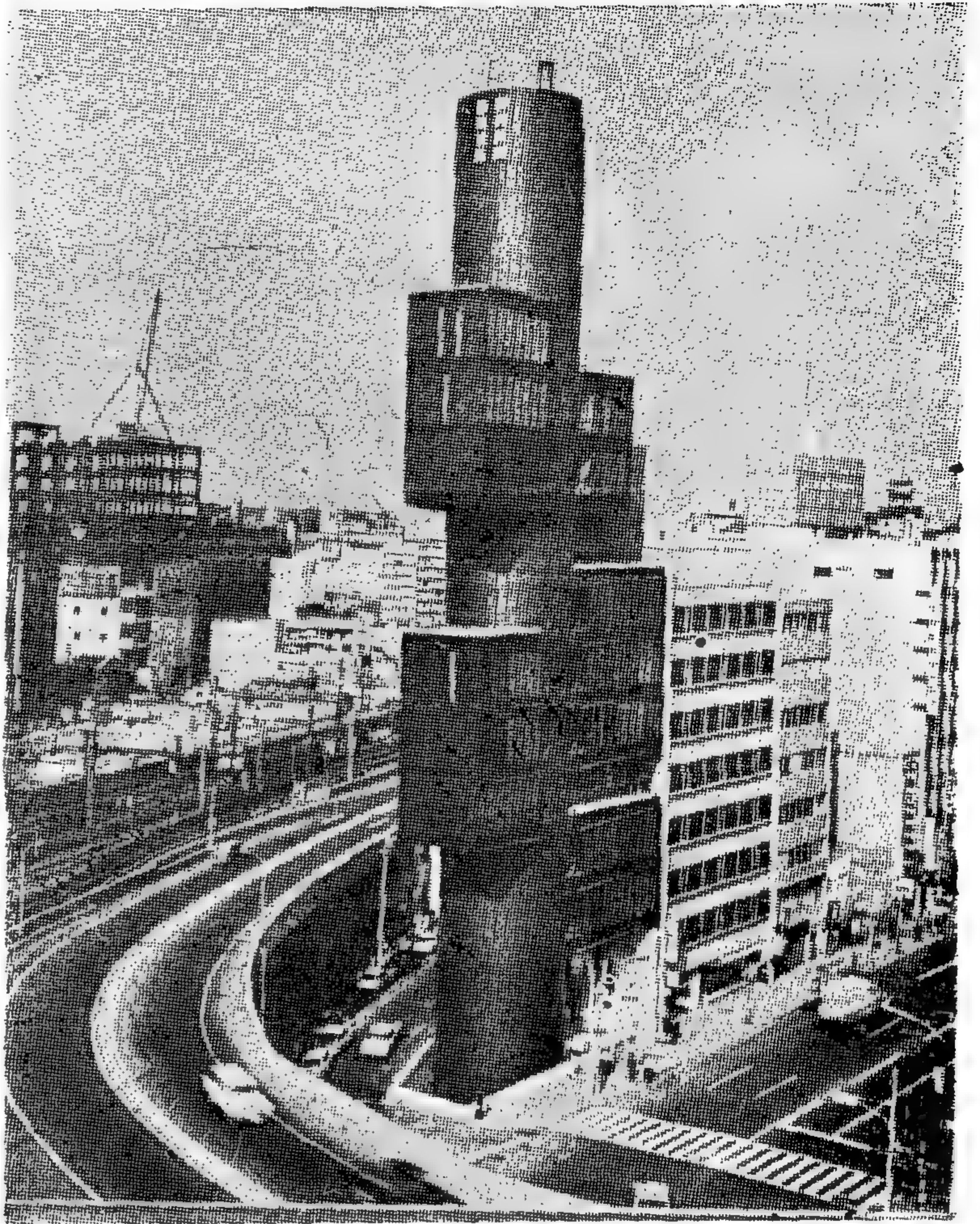
وتعميم الملكية الجماهيرية لوسائل الإنتاج ، وأسلوب العمل الجماعى ... الى غير ذلك من المفاهيم الاشتراكية . ومن العلامات الواضحة والخطوط العريضة في مجال البناء والانشاء في الاتحاد السوفيتى ما يسمى « استمرار زيادة معدل النمو في مجال صناعة مواد البناء وطرق الانشاء » . فمثلا نرى انه اذا كان حجم انشاء المساكن قد بلغ مليون مترا مربعا في سنة ١٩٥٣ نلاحظ انه في السنوات الخمس ١٩٥٩/٥٤ بلغ ٣٨٧٠ مليون م^٢ ، ثم وصل في ١٩٦٥/٥٩ الى ٥٥٠ مليون م^٢ .

ومما يذكر بخصوص مزاوله مهنة الهندسة المعمارية في الاتحاد السوفيتى انه لا توجد مكاتب معمارية حرة ، حيث ان كل معمارى موظف في الدولة . ويعمل المعمارى الروسى مع مجموعة من الفنيين والانشائيين والاقتصاديين كوحدة تسمى « لواء » تحت رئاسة معمارى أو مدنى . واللواء هو أصغر وحدة ، وكل مجموعة ألوية أى وحدات تشكل « قطاع » Sector ويسند « معهد التخطيط الاقتصادى الوطنى » المسمى Gosplan كل عام الى كل قطاع جزء من مشروع الخطة ، ويقوم كل قطاع بتوزيع المشروع على كل وحدة للقيام بدراسته ، واحسن تصميم هو الذى يجرى العمل به . وبعد اعتماد المشروع من رئيس القطاع يرفع الى المجلس الأعلى للسوفيت - القسم الفنى ، ثم الى المسؤولين المحليين بالمنطقة .

● المملكة المتحدة والتعمير الديموقراطى :

لقد تخلت الثقافة الانجليزية - بريطانيا - عن تقاليد البالية برغبة أكيدة وعزم قوى حتما ، ومضت في البناء والانشاء والتعمير بعد الحرب العالمية الثانية ٣٩ - ١٩٤٥ بما يتمشى مع عصر القدرة الآلية ، واعادة تخطيط مدينة لندن وغيرها من المدن الكبرى على مبادئ أساسية أهمها : أن تكون المساكن قريبة من أماكن العمل ومتصلة بشبكة ملائم بجميع الخدمات والمرافق مثل السواق والمدارس والمستشفيات والكنائس والمسارح والحدائق ، ثم الاتصال بالريف الانجليزى المفتوح . وواضح انهم اهتموا اهتماما بالغا بمبدأ « اللاتجميع » Decentralisation والخروج من المدن والعيش في مدن حائقية تبعية . وتخفيض عدد سكان مقاطعة لندن بمقدار ٥ ملايين للتخفيف عن المدينة ، واحاطة الكتلة البنائية للندن بحزام أخضر Green Belt يتراوح عرضه بين ٧ ، ١٠ أميال حتى لا يمكن هناك أى احتمال لامتداد المدينة .

هذه هي الأسس التخطيطية التى روعيت في تخطيط لندن وغيرها من المدن البريطانية ، ولكن الذى يعنينا في هذا الموضوع الأسس الانسانية التى روعيت في التطبيق وهى الأسس الحقيقية لما نسميه بالديموقراطية وأهمها ما يأتى :

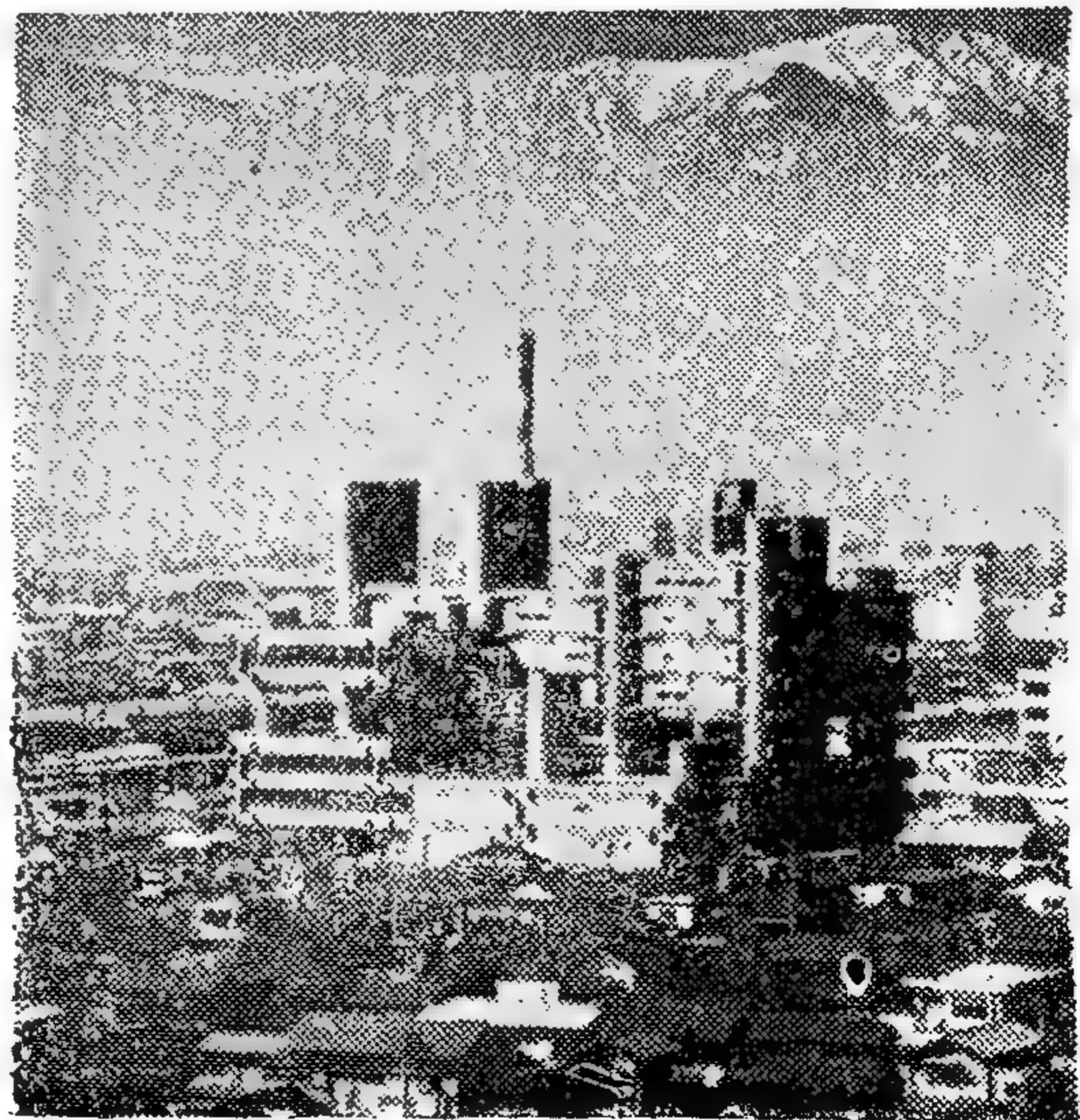


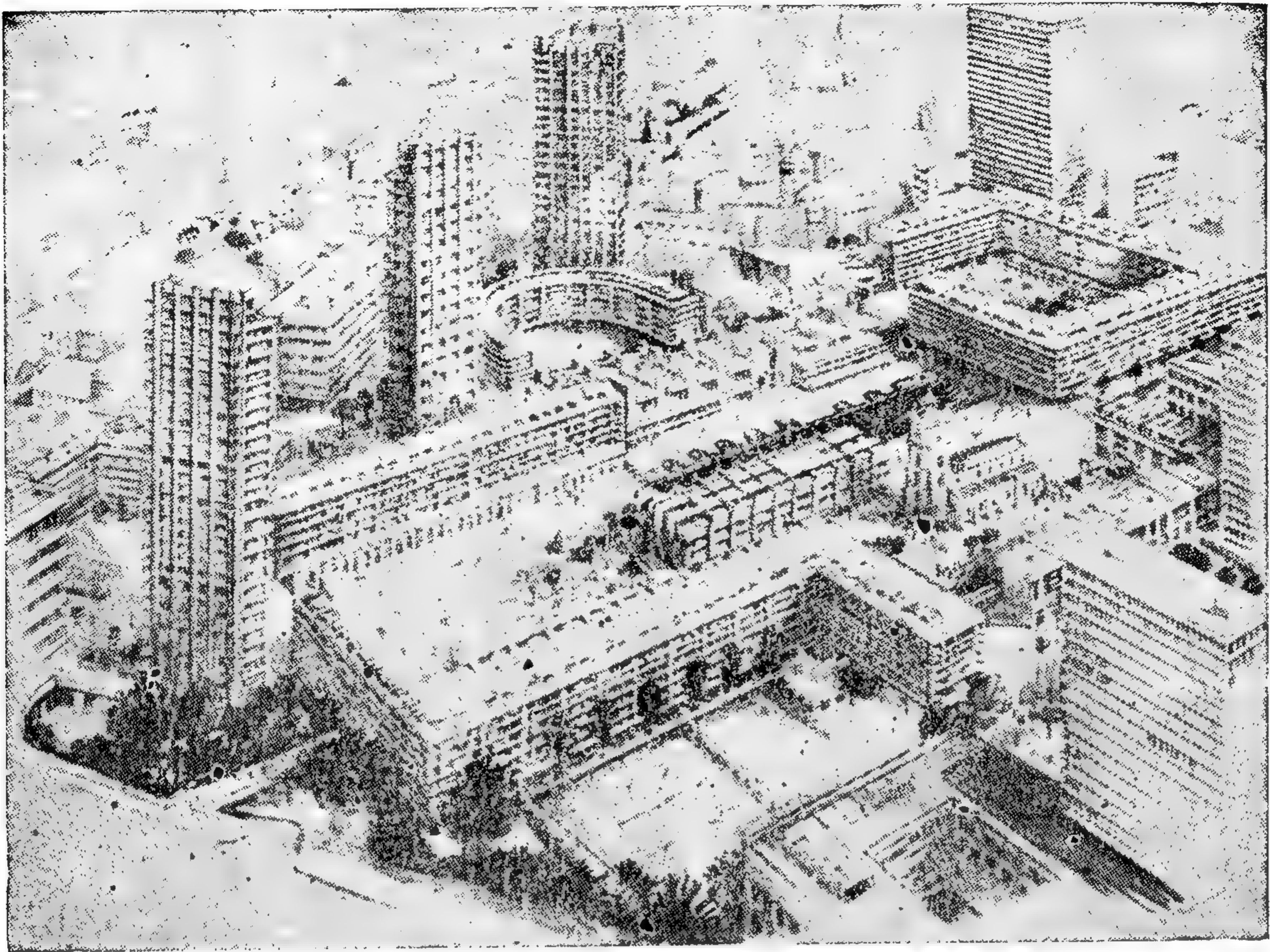
١٧ : مبنى مكاتب وإدارة جريدة حى جنزا طوكيو -

تصميم المعمارى كنزو تانج ١٩٦٧

١٨ : مبنى مكاتب إدارية لمحطة إذاعة ياماناشى

كوتو - اليابان ١٩٦٨





١٩ : إعادة تخطيط وتعمير منطقة « باربيكان »
لندن - يتسم هذا المشروع بالجدية والرزانة والتعقل

● لندن ، تتفجر في كل اتجاه ..

وأبراجها السكنية عملية اجهاض :

لندن تتفجر في كل اتجاه - ولكنها تحترم ماضيها وتعيش في حاضرها وتعمل لمستقبلها . منذ عام ١٩٤١ والسلطات المدنية في لندن وغيرها من المدن البريطانية تضع الخطط والمشروعات والتخطيط العام Master Plans لإعادة البناء وفقا لمشروعات وتجمعات سكنية مدروسة . وهكذا أعدوا المسرح البنائي لظهور لندن وغيرها من المدن الكبرى مثل ليفربول وبرمنجهام ومانشستر كمدينة ناطحات السحاب تعبيرا عن العصر الحديث .

ومن هذه المشروعات الحديثة : مشروع التخطيط العام لمنطقة باربيكان Barbican شكل ١٩ شمال لندن لاسكان ٦٥٠٠ شخص ويتكون من ٢١١٧ وحدة سكنية يحتوى على ٣ أبراج بارتفاع ٤٣ طابق ومجموعات أخرى أفقية مستطيلة مكونة من ١١ طابق . ثم مشروع مجاورة سكنية بحى توستن Tustin Estate جنوب لندن ويتكون من ٣ أبراج سكنية بارتفاع ١٩ طابق ومجموعات أخرى بارتفاع

أولا - أن الجسم المادى للمدينة الحديثة الديمقراطية اليوم ينبغي أن لا يكون له مركز واحد ، بل مراكز متعددة ، متضافرة كلها بعضها مع بعض . بحيث يزداد ارتفاع المباني كلما اقتربنا من محيط النشاط وهذا هو التخطيط العضوى السليم Organic Planning

ثانيا - حيث أن الازدحام البشرى إنما هو من سبيل القتل ، وإذا لم يكن قتلا للجسد فهو قتل للشعور ، لذا يجب تخفيض عدد سكان المدن المزدحمة ووقف معدلات النمو .

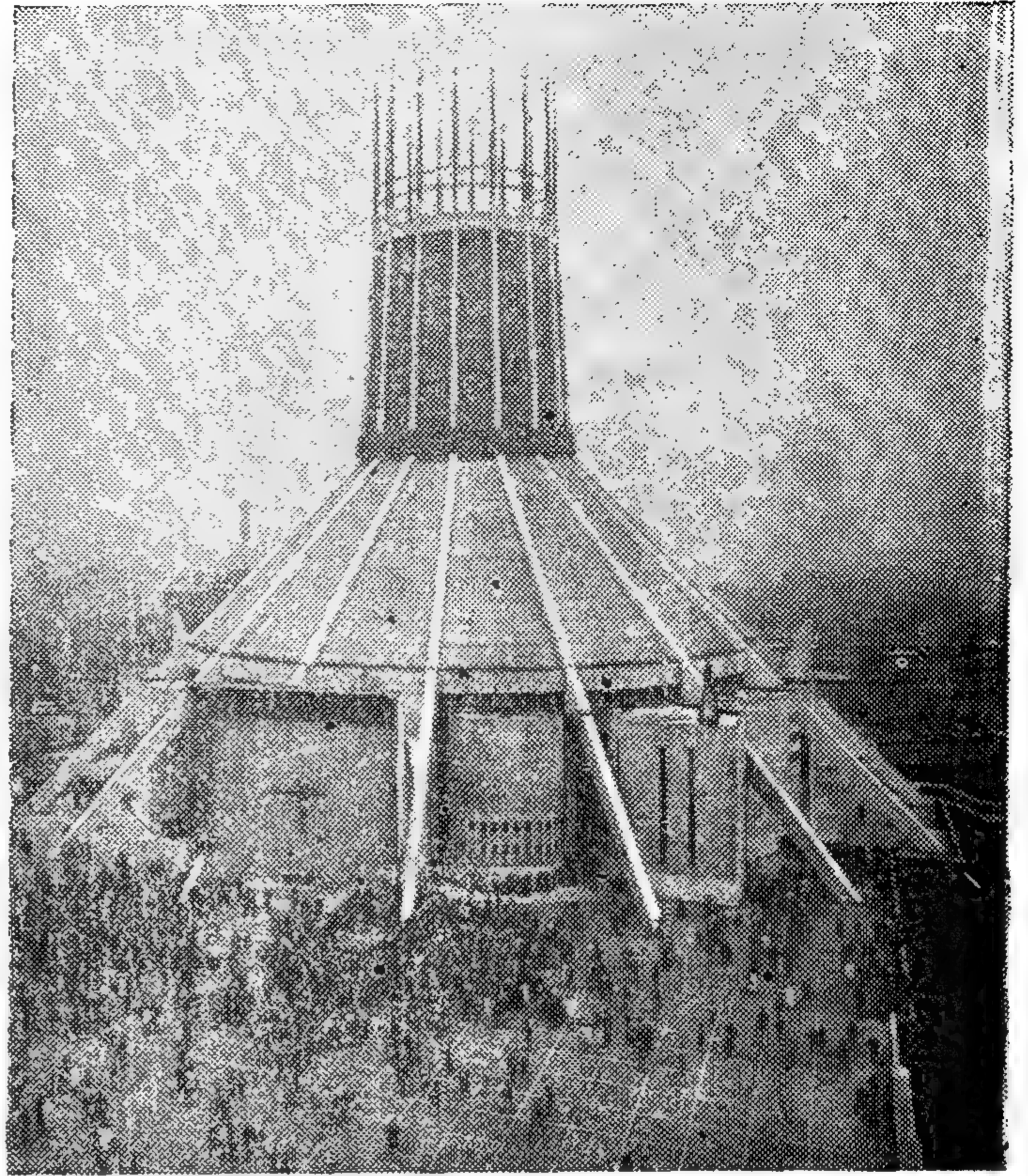
ثالثا - يجب أن لا يراعى في البناء أن هناك أغنياء موسرين أو فقراء معدمين . إذ لا محل هنا لمقياس الذهب .

رابعا - عدم تعطيل الأراضى الفضاء الا لفرض المناظر الطبيعية التى يشترك فيها الجميع بالتمتع بها ، وان لا يكون هناك مستغلون للممتلكات .

خامسا - لا حرمان للمجتمع من الأفكار التى يعيش عليها ، فلا احتكار .

واتجه التفكير في التوسع الرأسى للمدينة حيث الحاجة الملحة تضطر تلك العاصمة الى الارتفاع الى أعلا وتجميع الخدمات الصحية والترفيهية والاجتماعية اللازمة للسان ، بحيث يرتفع البرج السكنى الى اعلا مرتكزا على قاعدة مستطيلة أو مربعة أو مستديرة على شكل باكو تجمع فيها هذه الخدمات كما كان يفعل الاغريق والرومان من قبل.

غير أن هناك خطورة من حدوث تكرار هذا النوع من الأبراج أو الطابع المعمارى التكوينى لهذه المباني العالية وهو البرج والقاعدة Tower & Podium وهى الملل والسامة من رؤية هذه المباني المرتفعة التى تجاوزت خط السماء للمدينة Skyline of Town اذا لم تصمم بمهارة وعناية ، وهو ما يعلمه المعماري الانجليزى الذى يحاول التغلب عليها بشتى المعالجات المعمارية سواء من حيث التصميم أو من حيث اضافة بعض العناصر الزخرفية كالحوائط الساترة Curtain Wall أو بالاقتراب بالعمارة نحو الفن وعمل الفنان بالتأثير الذى يعتمد أساسا على التنظيم المجرد المطلق على الألوان .



٢٠ - حتى المباني الدينية لم تسلم من سيطرة التكنولوجيا . ويرى اعلاندرائية الروم الاورثوذكس فى مدينة ليقربول - ١٩٦٨

ان عشاق « لندن القديمة » يعارضون « لندن الحديثة » . وتكونت جماعات منها « جماعة أعداء المناظر الكئيبة » تضع لافتات السخط على المباني التى لا تحبها مثل - مبنى شركة شل مثل عملية اجهاض - ناطحات السحاب تكشف أسرار الحياة الملكية . غير أن هناك مؤيدون لهذا الأسلوب حيث عبر عن رأيهم أحد الكتاب فى الصحف بقوله « اننى أرحب بالأبراج العالية التى ترتفع فى سماء لندن الفسيحة الممتدة .. فمن الكآبة أن يتمسك المرء بأن القديم والجديد لا يستطيعان العيش معا فى راحة . واننى أعطف على هؤلاء الزائرين القادمين من الخارج الذين يصيبهم الهلع للتغيير الذى حدث فى أفق لندن ، ولكنى لا أرى سببا يوجب علينا أن نعيش فى متحف لمجرد ادخال السرور على قلوبهم .. وأعتقد أن هذا الرأى يترجم رأى الشباب الذى يطرب للطفرة المتجهة الى أعلا .

● باريس تبني تحت الأرض :

يظهر أن موضوع انشاء ناطحات سحاب والعمارة الحديثة - عمارة علب السيجار أو صناديق الأحذية - ما يشغل بال الفرنسيين أنفسهم ، حيث أدلى الرئيس الفرنسى الراحل « جورج بوميدو » بحديث غير سياسى الى صحيفة «لوموند» الفرنسية فى ١٥/١١/١٩٧٢ تناول فيه هذا الموضوع الذى يشغل بال الرأى العام بالدرجة الأولى الآن وهو : هل تقام ناطحات سحاب فى مدينة باريس ؟

ومشروعات اعادة تخطيط أحياء Westbory Lambath ٦ طوابق ومشروع منطقة وستبرى لامبث كنزنجتون وكرويدون وفوكسهول ، بريكستون Brixton وتيمسيد وغيرها .

ومما لا شك فيه أن لندن التى عاش فيها أوليفر تويست ، وبيتر بان ، وشارلوك هولمز ، وشكسبير تختلف كثيرا عنها الآن . حقا أن المباني الرمادية التاريخية الجديدة ذات الأصالة المعمارية ستبقى دائما فى لندن الجديدة وفى ليفربول الحديثة وفى أوكسفورد القرن العشرين . ستبقى هذه المباني خالدة قوية معبرة عن ماضيها وحاضرها وحتى عن مستقبلها بالرغم من ذلك التطور التكنولوجى الذى طغى على عمارة العصر . ستبقى هذه المباني التاريخية التذكارية دائما كمبنى البرلمان وكاتدرائية سان بول ، وبرج لندن وآلاف الحدائق وأركان الجمال فيها ، وغيرها ولكن هل ستبدو هذه الروائع هزيلة ضائعة الى جوار هذه المباني الحديثة الشامخة الارتفاع ، والتى تتفجر حولها ؟ .. هذا ما سوف نتحدثنا به الأجيال القادمة .

عام ١٩٧٧ ويعتبر برج نوبل Noble Tower أعلى الأبراج المكتبية في المدينة شكل ٢ العدد الأول .

وبتطبيق أسس ونظريات التخطيط الحديث لمدن تحت الأرض ، واستخدام التكنولوجيا جعل من السهولة بمكان تخصيص مساحات تحت الأرض تقاس بقدر يصل من ثلاثة الى ستة المساحة فوق سطح الأرض المراد تخطيطها وتصميمها . وبذلك يمكن ايجاد العلاج النافذ الفعال لأمراض وعيوب الحياة الحديثة للكتل البشرية في المدينة مثل باريس، التي تعجز بتراتها وثروتها التاريخية . (بتطبيق هذا العمل الفني الحديث - تخطيط وتحسين المدن تحت الأرض - يجعل من الضرورة بمكان السير في مختلف « العمليات الجراحية للمدينة » على مناسيب شوارعها والتي غالبا ما تكون مكلفة فيما يتعلق بنزع ملكيات ضخمة تزيد تكاليفها عن تكاليف الإنشاء تحت الأرض .

وأهم مثل على ذلك هو المشروع الجارى تنفيذه حاليا تحت حدائق قصر التولارى في باريس ، والتي تبلغ مساحتها نحو ٨٠ فدانا لاستغلالها لعمل جراجات وأماكن انتظار سيارات وخطوط المترو والمعارض والمتاحف ومباني الخدمات الأخرى اللازمة لتلك المنطقة . وبذلك يترك السطح العلوى للمشاة والنزهة والاستمتاع بقصر التولارى واللوفر والكونكورد وغيرها من الأماكن التاريخية . وهو مما لا شك فيه اتجاه سليم من جميع الوجوه معماريا وتخطيطيا وحضاريا وتكنولوجيا .

● غواصم البلاد العربية تعيش في فوضى معمارية :

ان مصر كانت دائما ولا تزال نموذجا فريدا لدول العالم بالنسبة لحفظ التوازن مع البيئة والمناخ والمجتمع . وكانت كل حضاراتها القديمة أساسها حفظ التوازن مع النيل واحترام الطبيعة الى درجة العبادة - عبادة النيل ، وعبادة الشمس، الحضارات المصرية القديمة ، الحضارة العربية والحضارة الإسلامية . ولأن الحضارة المصرية اعتمدت على هذا التوازن لذلك بقيت هذه الحضارة بينما اندثرت حضارات أخرى غيرها كثيرة .

ان أبسط تعريف للعمارة بأنها « تفاعل وجدان الانسان مع البيئة » . تفاعل وجدان الانسان العربى مع البيئة العربية هي عمارة عربية ، وتفاعل وجدان الانسان الأوروبى مع البيئة الأوروبية هي عمارة أوروبية . ولكن تفاعل وجدان الانسان الأوروبى مع بيئة عربية شرقية ليست عمارة بل هي خلط ومسوخ معمارى . لا يمكن للمعماري الأجنبى أو المخطط الأوروبى مهما أوتى أى منهما من علم ومعرفة أن يشعر بذلك ويخضع أحاسيسه لى تفاعل مع البيئة العربية .

ولم يشأ الرئيس الفرنسى أن يتخذ موقف التأيد أو المعارضة في هذا الموضوع وإنما قال : ان ناطحات السحاب - في حد ذاتها - ليست شيئا جميلا أو قبيحا ، وإنما الأمر يتوقف على ما يحيط هذه المباني المرتفعة والنسب بينها وبين المباني المجاورة . الى ان قال - ان مدينة النور - باريس - ليست متحفًا ولا هي مدينة ميتة ، وإنما هي مدينة قابلة للتطور . ثم قال « بومبيدو » في هذا الحديث الطويل - ليس هناك فن معمارى فرنسى ، لأن فن العمارة لغة دولية ، وأبدى أسفه لأن مبدأ مراعاة التوفيق بين اشكال المباني والهدف التي شيدت من أجله لا يراعى في المباني الفرنسية .

ولقد تظاهر في العام الماضى ١٩٧٢ مائة ألف فرنسى لانقاذ منطقة « حى الصالات » Les Halles سوق الخضار التاريخى القديم ، ويقع في وسط العاصمة ، والتي وصفها « اميل زولا » بمعدة باريس ، وطالبوا الحكومة بعدم هدمها لإنشاء مشروع مركز تجارى ذا أبنية مرتفعة يسمى - Plateau Beaubourg بلاتو بوبرج ، حيث تم نقل السوق فعلا الى ضاحية من ضواحي باريس بالقرب من مطار أورلى Only Airport وفى شهر يونيو من نفس العام كانت هناك مظاهرات في شوارع باريس احتجاجا على التصميمات التي أعدت لإنشاء طريق سريع على الضفة الشرقية لنهر السين ويتبع ذلك انشاء المباني العالية على ذلك الجانب للنهر . واليوم ولأول مرة يسير الناس في الشوارع يحتجون على اقامة منشآت جديدة ويتساءلون... هل ستتحول مدينة النور والحرية الى مدينة المباداة والنفعية...؟ وهل سيتغير وجه باريس وتلبس قناع شيكاغو ومانهاتن القرن العشرين...؟ وهل ستصبح مدينة الفنون والجمال مدينة صناعية واستغلال المال...؟

● ومن نقطة الانطلاق هذه والرغبة الجامحة نحو المحافظة على باريس شرعت البلدية فوراً في تعمير منطقة الدفاع La Défense والتي تبلغ مساحتها ٧٠٠ هكتارا وضعت تحت تصرف هيئة عامة للتخطيط والتعمير . ويربط هذه المنطقة محور رئيسى هام يمتد من قصر اللوفر الى قصر الكونكورد وآفنيو الشانزلزيه الى الاتوال . ولذلك أعطيت مشروعات تحت الأرض Underground Projects شكل ه العدد الأول أهمية خاصة نظرا لفرق المناسيب وقدره ٢٢ مترا بين نهايتى قطاع هذا المحور . ويشمل مشروع تعمير منطقة الدفاع على عدد كثير من المباني العالية استخدمت فيها كل وسائل التكنولوجيا ، منها المباني المكتبية تتسع لعدد ١٠٠ ألف موظف وعامل ، وعمارات سكنية لعدد ١٢ ألف عائلة وكثير من مباني الخدمات العامة ستتم جميعها

● نرى في البلاد العربية مع الأسف الشديد أن النجاح في الكثير من المنشآت المعمارية الضخمة الكبرى ، وفي ظل هذا التطور العالمى السريع ، هو الشيء الشاذ الذى ما كان ينتظر حدوثه ، وقد كان العكس فى الماضى .

كان الاخفاق فى المشروعات المعمارية فى الماضى هو الشيء البعيد الاحتمال . ان عمالقة الأساطير الشرقية ومشيدوا قصور صلاح الدين وقلاعه ومصمموا جامع السلطان حسن وابن طولون وسمراء وبابل والقيروان والفسطاط .. وغيرها من الروائع الخالدة ليسوا بسحرة ولكنهم عمالقة فعلا . وكما ينقصنا فى أيامنا هذه من هؤلاء العمالقة الكثير وهذا هو سر تخلفنا . والسبب فى ذلك أن هذه المشروعات التى تعهد بها الدول العربية الى المعمارين تحتاج فعلا الى عمالقة لصعوبتها وضخامة مسئوليتها التاريخية . فانشاء مدينة أو تخطيط قرية ، واقامة دار للبلدية أو مبنى للاذاعة أو دار للوبرا أو مكتبة عامة أو جامعة ليس الاعمال من أعمال العمالقة فهل من العسير مؤاخذه المعمارى من أن يكون عملاقا ؟

— لماذا ننكر هذا الاخفاق الذى بدأ يتكاثر حولنا فى كل مكان من البلاد العربية حتى لكأننا نعانى من حمى الاخفاق ، اذا استثنينا بعض الأمثلة القليلة النادرة التى أنشأها قليل من المعمارين الذين يعرفون ما لهم من حقوق وما عليهم من واجبات ، هؤلاء الذين يخلصون لمهنتهم ويؤمنون برسالتهم وهم ليسوا تجار مهنة وهم قلة .

— اننا نشعر بالمرارة حينما نرى تلك الأمثلة المتعددة من المباني الهامة والعامة فى المدن العربية على تلك الصور الهزيلة التافهة التى ان دلت على شيء فانما تدل على ضعف المهندس أو استهتاره بقدرسية المهنة وكرامتها ويساعده على ذلك قصور القوانين وضعف اللوائح والتشريعات الخاصة بالمباني والتخطيط وأعمال التنظيم والتى لا تحمى المدينة من هذا العبث ومن هذا الارتجال .

— اننا نشعر بالضيق والضرر حينما نرى تلك الأبنية والتى تحمل اسم هيئات حكومية جادة أصيلة أو تحمل اسم مؤسسات عامة لها شأنها ومكانتها ، نرى هذه الأبنية مصممة على شكل طائرة أو بارجة أو قاطرة وما أكثرها فى المدن العربية المنشأة فى بيروت والكويت والقاهرة والاسكندرية والرياض وجدة . نرى تلك المناظر الغير لائقة فهما ومعنى ونساءل — هل قصد المعمارى أن يصمم مبناه على تلك الصورة .. ؟ أم هذه هى التكنولوجيا الحديثة فى العمارة .. ؟

نريد عمارة نابغة من أصالتنا وواقعنا ومجتمعنا ، لا عمارة مستوردة من الخارج تفرض علينا ونحن الذين علمنا العالم أجمع كيف تكون الحضارة وكيف تكون العمارة .

اننا لا نريد مأساة مشروع شانديجار بالهند أن يتكرر عندنا فى الشرق حيث ثبت فشله ، ولا نريد مهزلة برازيليا التى صفق لها العالم يوم انشائها ثم حكم عليها حكما آخر مخالف بعد ذلك لأنها عمارة دخيلة على البيئة والمناخ والمجتمع ..

● ان القاهرة كغيرها من المدن تفقد السيطرة على أمور نفسها بالتدريج ، مثلها فى ذلك كمثل السفينة الضخمة التى تفرق ببطء تحت موج يزيد ارتفاعا . فالاعداد الهائلة من السكان التى تتزايد عليها بنسب لا مثيل لها ، وعدم القدرة على مجازاة هذه الزيادة بالتخطيط السليم وحسن التوزيع وزيادة المرافق . كل هذا يجعلها كالسفينة الضخمة التى تفقد السيطرة على أمور نفسها .

ولعل بيت الداء لاصيل يكمن من مشكلة ادارية .. فالمرافق تتبع عدة جهات والاختصاصات مبشرة ، واللوائح والقوانين وكثرتها وتعددتها فحدث عنها ولا حرج : ومحافظ المدينة عاجز فى حقيقة الأمر عن حكمها . فالأمر اذن يحتاج الى اعادة النظر جذريا فى جميع هذه الأمور مع ايجاد الحلول السليمة التى تلازم تطور العصر والبيئة والمجتمع والتى تستند الى الاساليب العلمية وتتفق مع سرعة التطور .

وهناك اجماع على ضرورة انشاء المدن التابعة ، وفعلا تم اختيار المساحات اللازمة لانشاء ثلاثة مدن تبعية وهى مدينة السادات ومدينة العبور ومدينة ١٠ رمضان .

ولكن ظهرت نغمة شاذة وخطيرة ، ولعلها هى موضة العصر الحديث فى الدول الرأسمالية وهى انشاء المباني العاليه السكنية والمكتبية . واشيع فعلا أن هناك اتجاه بتعديل قانون المباني واستثناء بعض المناطق المطلة على النيل فى الزمالك وغيرها وبدات بعض الأجهزة الحكومية تحدد بعض المواقع واختيارها لمثل هذه المباني . ونشط العملاء والسمايرة استعدادا لتلك الفرصة الذهبية وفجأة ارتفع سعر المتر المربع فى بعض المواقع من ٦٠ ، ٨٠ جنيه الى ٥٥٠ جنيه .

ان المرحلة التى نمر بها اليوم هى مرحلة تحول ويجب أن يكون طابع مشروعات هذه المرحلة يتسم بالتواضع لا بالضخامة والمقياس الكبير ، فالمستقبل هو للعمل المتواضع وليس للأعمال الضخمة . ومن حسن الحظ استقر رأى أخيرا على عدم السماح بانشاء المباني العالية Tall Buildings داخل كوردون مدينة القاهرة .



١٢ : الانتاج بالجملة
Mass Production
في العمارة الحديثة
وطريقة الميكانو والمتبعة
الآن من الاسكان
العصرى ، والتي اطلق
عليها المجتمع في كثير
من الأحيان اسم
« معامل التفريخ
البشرى » او « أبراج
حمام المجتمع الانساني »
أو مقتعلات العصر
الحديث

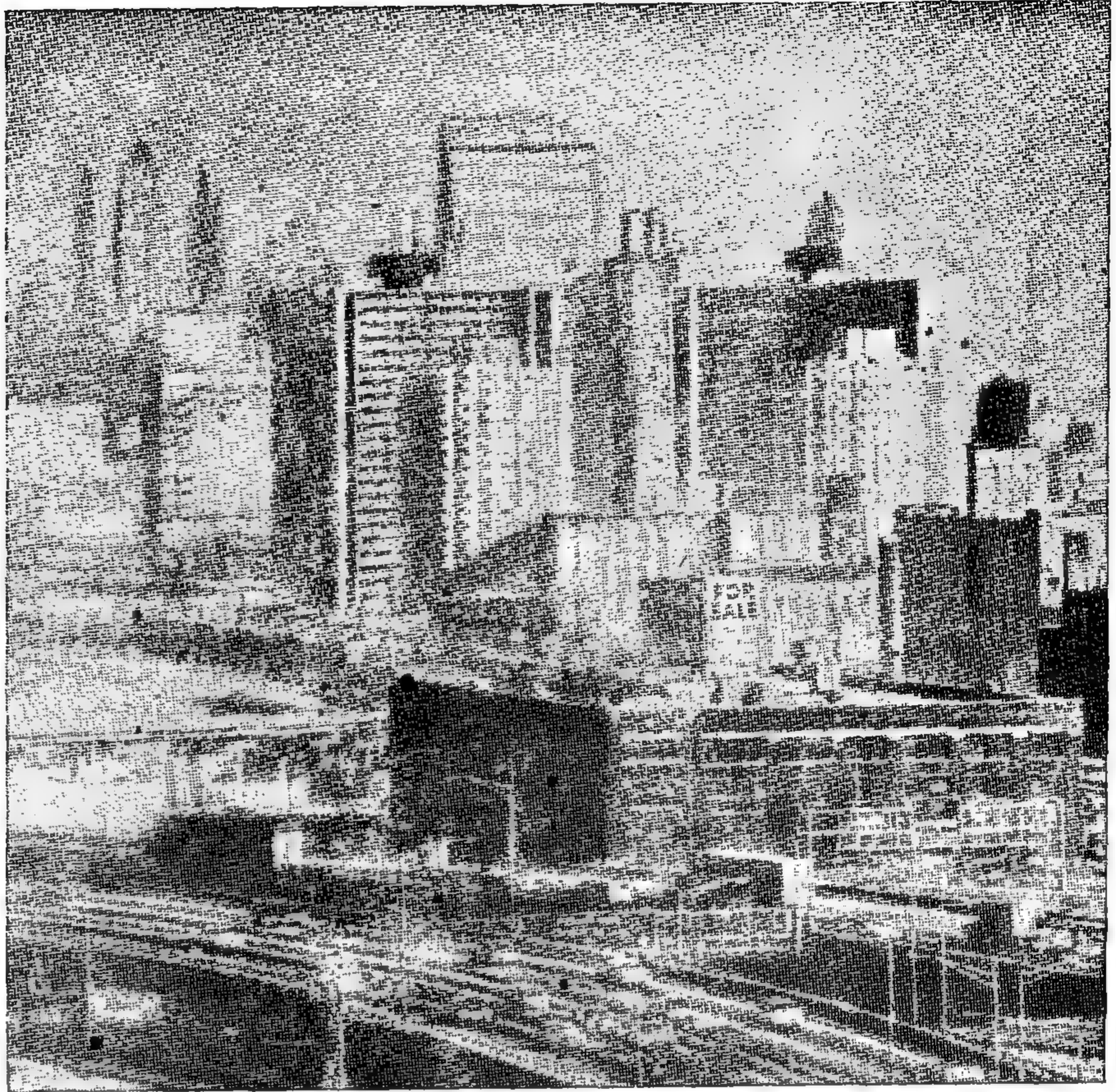
والفش والتضليل ، لأن شركات التأمين تدفع قيمة الإيجار في حالة الخلو .

— رأيت المباني العالية التي تجاوزت خط السماء وكأنها عمليات أجهزة للمدن ، وشاهدت ناطحات السحاب التي يعيش معظم سكانها في رعب وخوف وقلق خشية حدوث أى طارئ من انقطاع تيار الكهرباء أو هزة أرضية أو نشوب حريق مفاجئ .

— رأيت في الركن المقابل لتلك الأعمال البهلوانية العالية وهذه الألعاب النارية مجموعات أخرى من المباني الجاهزة الصنع داخل المصنع وكأنها معرض لمواد البناء وطرق الإنشاء معروضة للإعلان عنها وليست للسكن . ورأيت أيضا تلك الأحياء المنتشرة والمتداخلة في قلب المدن والذي أطلق عليها خطأ اسم مناطق الإسكان الشعبي أو الإسكان الاقتصادي ، وصحتها مناطق « مساكن التفريخ » يخيم عليها الكآبة بحوائطها الصماء المظلمة .

يقول « جوته » أن أى نظام للمجتمع لا يكون عضويا Organic من حيث تكوينه بما يضمن له التطور والنمو المتجانس والمتماثل في جميع أعضائه ، نظام يحول المجتمع بأكمله إلى شكل شجرة ترتبط جميع فروعها وخلاياها ببعضها وترتكز جذورها على أرض صلبة بما يضمن لها البقاء نظام مصيرة الانهيار فكذلك الحال في العمارة .

● تجولت في كثير من مدن العالم قديمها وحديثها رأيت الخلط المعماري والفوضى المدنية والارتباك الانشائي ، وشاهدت الحيرة والقلق المرسومة على وجوه أهل هذه المدن . رأيت عن قرب تلك الأبراج العالية للأعمال الإدارية والسكنية والتي تفجرت في كل اتجاه من المدينة تعلن عن أسماء وشهرة أصحابها بالأنوار الصناعية المؤذية ، مع أن معظم طوابقها غير مستغل ومهجور ولكنه مضاعف من الداخل للخداع



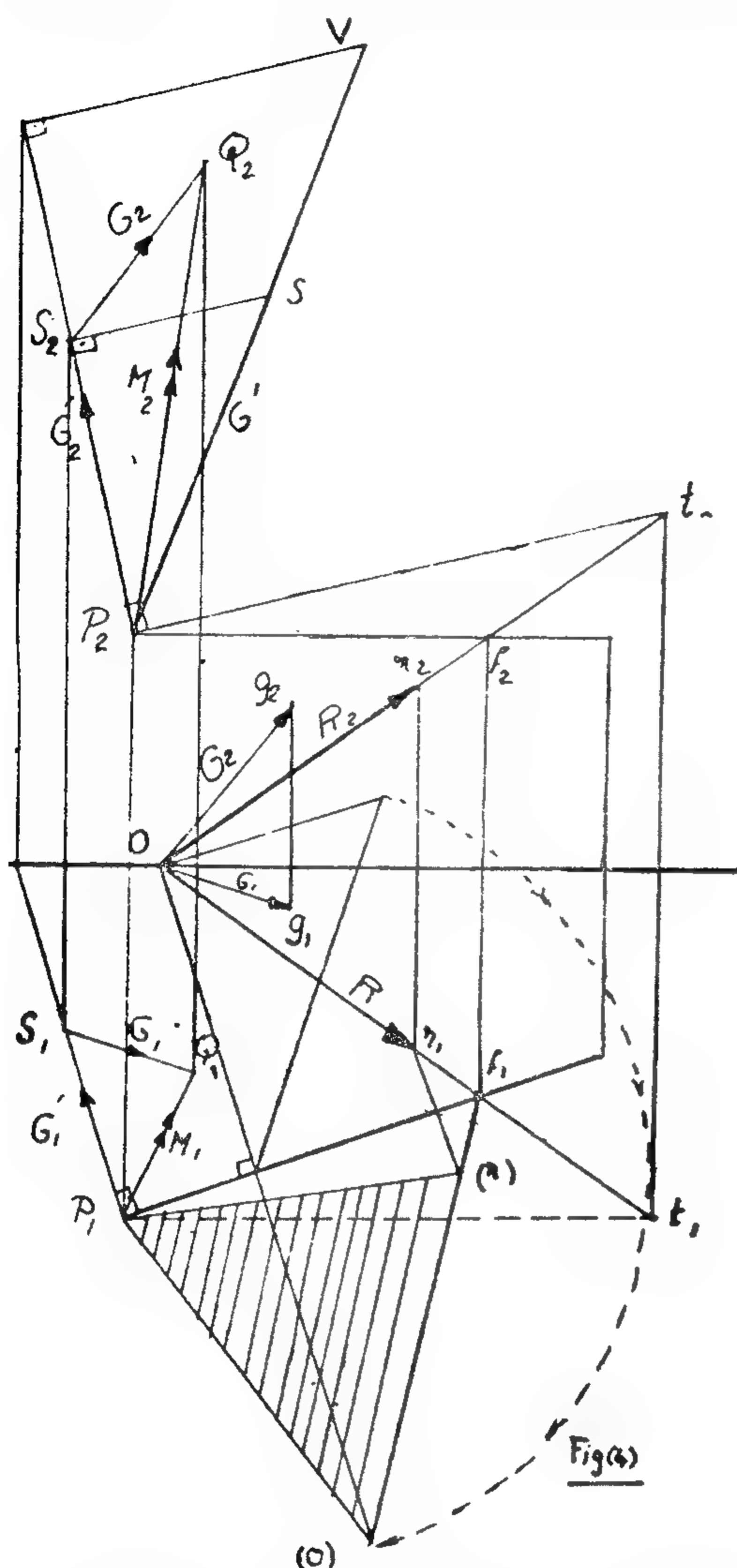
٢٢ : نيويورك ومثلها شيكاغو وغيرها
من المدن الأمريكية وكأنها غابة
استوائية للمباني العالية للسكان
البشرى . أن الازدحام البشرى هو
من سبيل القتل ، وإذا لم يكن قتلا
للجسد فهو قتل للشعور الانساني .

— ومن خلال افكارى المضطربة فى هذا المجال ،
وما رأيته من المناقشات فى المدينة العصرية كنت
أرى عمارة تذكارية ضخمة خالدة Monumental
عمارة لآثار الماضى وعمارة لآثار الحاضر —
الأكروبول ، الشانزليزيه ، الانفاليد ، جامع السلطان
حسن ، تاج محل ، ميدان الطرف الأغر ، فلورنسا
... تزحف حولها وفى كل اتجاه مدينة السيارات
مدينة القرن العشرين — مساكن ومصانع من كل
نوع وطرق سريعة تعبر هذه المدن ، وبالإضافة الى
كل هذا سيارات وسيارات تسير فى الظلام مارة
بعمارة الماضى وعمارة الحاضر . وهنا أقف خائفا
مضطربا كالطفل الضائع فى الظلام حائرا أى الطريق
أسلك وفى أى اتجاه أسير . . . وعندئذ أحاول أن أجد
طريقى ، وأتفادى هذا الكابوس المدنى لأواجه المأزق
الذى أنا فيه كمعمارى باستخدام الخبرة التى
اكتسبتها كبناء متفوق . والله ولى التوفيق .

توفيق أحمد عبد الجواد

— رأيت فى مدينة القرن العشرين خلط معمارى
ومدنى ، وفوضى تخطيطية وفنية غير مألوفة ، أعمال
لا تمت بصلة الى البيئة من حيث الموقع والمناخ ،
غير متناسقة مع مقتضيات البيئة الأساسية والظروف
الاجتماعية والقيم الحضارية ، هزيلة من الناحية
الفلسفية والعملية والوظيفية والفنية ، من المسئول
عن كل هذا . . ؟ هو بالقطع المهندس المعمارى ويشترك
معه المجتمع فى المسئولية .

— أن المباني التى شيدتها الأجيال السابقة تتفوق
كثيرا على معظم مباني الجيل الحالى خاصة اذا
ما أخذ فى الاعتبار عدم توفر معدات البناء الحديثة
فى تلك العصور . وتكمن بعض أسباب تفوق البناء
القديم على الحديث فى أن العمل كان يتصف فى
الماضى بالتروى والصدق والاخلاص والأمانة
العلمية والفنية والمهنية وباعتزاز المرء بما تصنعه
يداه ، وأن البناء كان يشيد فى الماضى لكى يبقى
طويلا ، وبسبب نظام التدريب وجدت اعظم براعة
مهنية .



moment \bar{M} of the system about P can be expressed as

$$\bar{M} = \bar{G} + \bar{G}'$$

In fig. (4) \bar{PS} represents \bar{G}' , \bar{SQ} represents \bar{G} and \bar{PQ} represents the required moment \bar{M}_p .

6. RESOLUTION OF A SYSTEM OF FORCES TO A FORCE \bar{H} ALONG A GIVEN LINE PQ AND ANOTHER FORCE \bar{F} WHOSE LINE OF ACTION IS TO BE DETERMINED

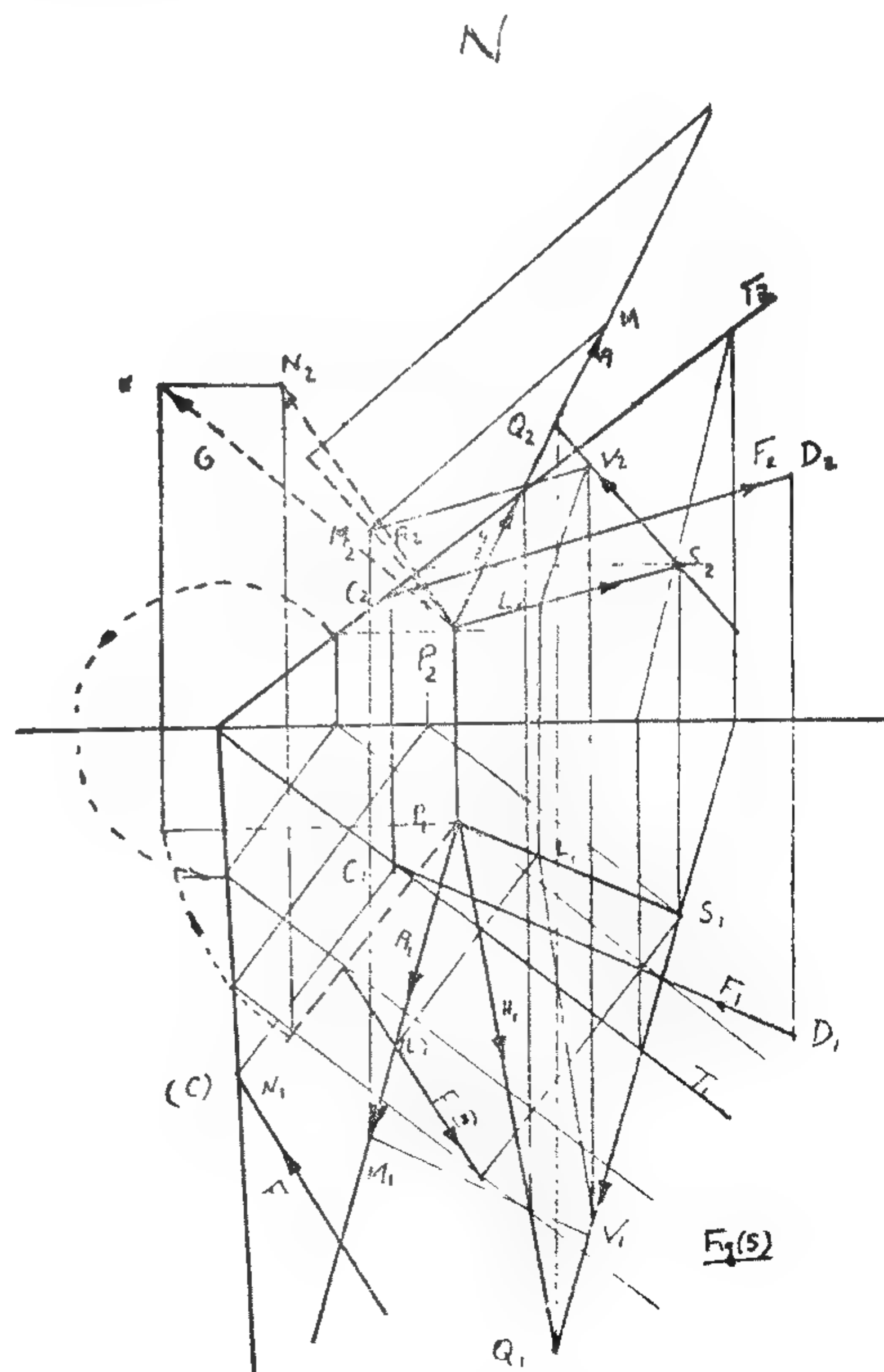
Consider the point P as origin and reduce the system to a force \bar{R} and a couple

\bar{G} at the origin. From point Q on PQ a parallel is drawn to the line of action of \bar{R} to intersect the plane of the couple \bar{G} at point S. Taking V on QS such that SV represents \bar{R} , then LV represents the force \bar{H} that acts along the line PQ. If the force acting along LS is denoted by \bar{F} ; then

$$\bar{H} = \bar{R} + \bar{F}$$

The plane of the couple \bar{G} is rotated about its horizontal trace T_1 until it coincides with the horizontal plane of projection. The couple \bar{G} is replaced by two forces in this plane: \bar{F} along LS and another equal, parallel & opposite force \bar{F} acting along CD such that the perpendicular distance between them is G/F .

The two required forces are \bar{H} acting PQ and \bar{F} acting along CD. This is shown in Fig. (5).



- | | | |
|------------|--------------|---|
| REFERENCES | F. ALEXANDER | : Mechanics of Structures |
| | A. CHAHLY | : Descriptive Geometry |
| | L. LEVINSON | : Fundamentals of Engineering Mechanics |
| | M. MOVNIN | : Theoretical Mechanics |
| | S. TARG | : Theoretical Mechanics |

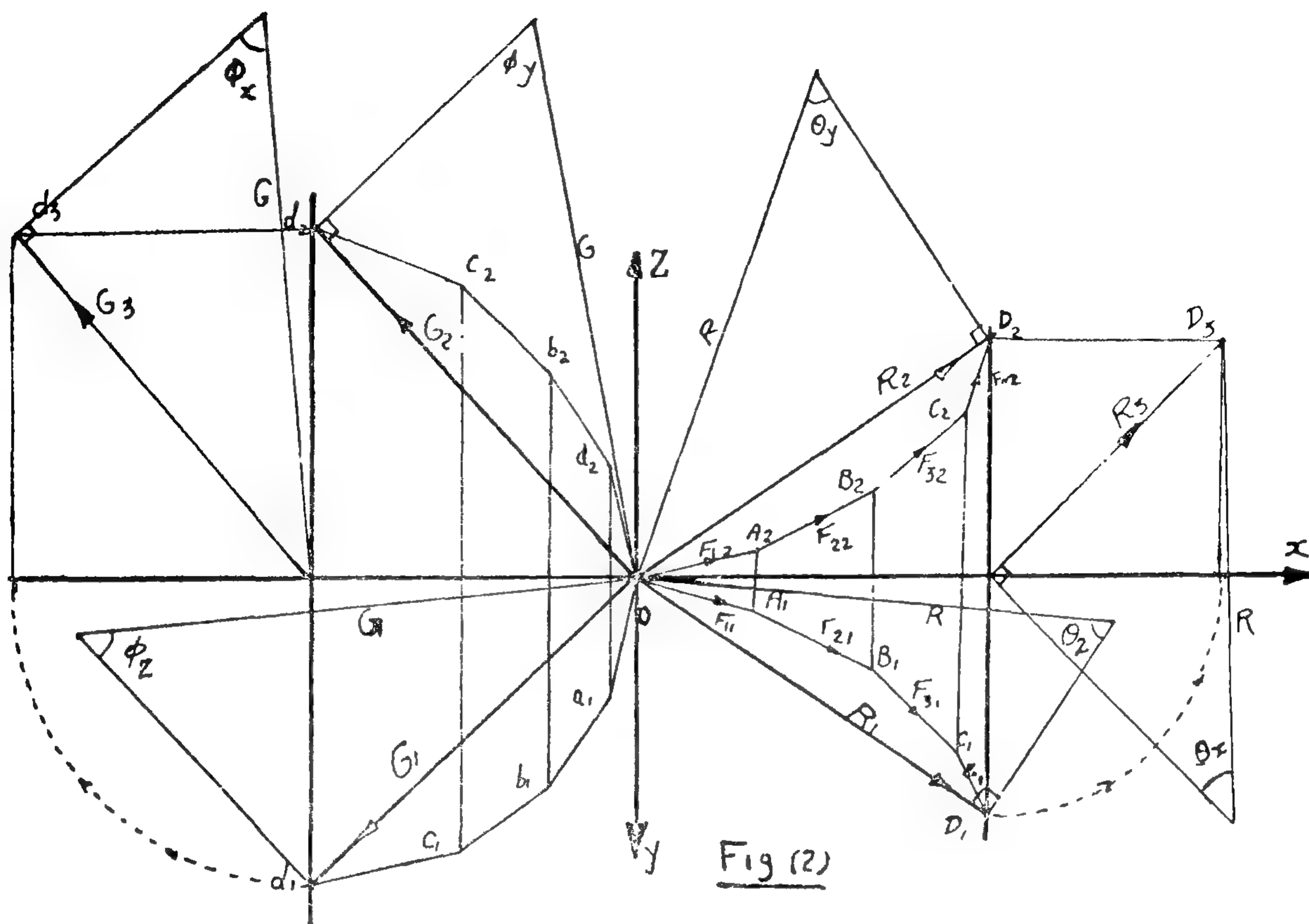


Fig (2)

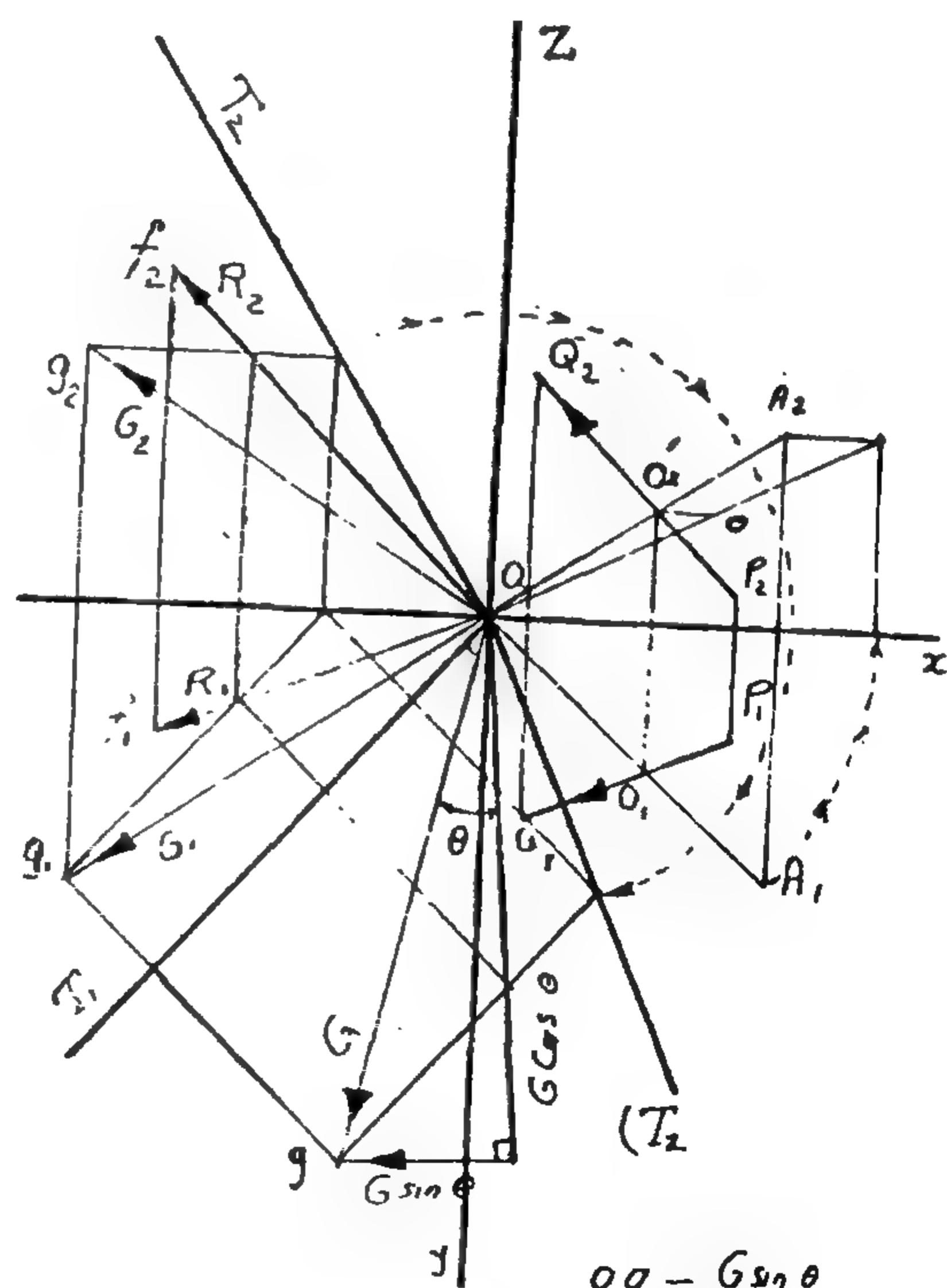
couple of magnitude $G \cos \theta$ whose axis coincides with the line of action of the force \mathbf{R} through O' .

Force \mathbf{R} represents the intensity of the wrench, $G \cos \theta$ represents the couple of the wrench and $p = \frac{G \cos \theta}{R}$ represents the pitch of the wrench. The line of action of \mathbf{R} at O' which in the same time coincides with the axis of the couple ($G \cos \theta$) is the central axis. This is shown in fig. (3).

5. MOMENT OF A SYSTEM OF FORCES ABOUT ANY POINT P

Let the given system be reduced to a force \mathbf{R} and a couple \mathbf{G} at the origin O .

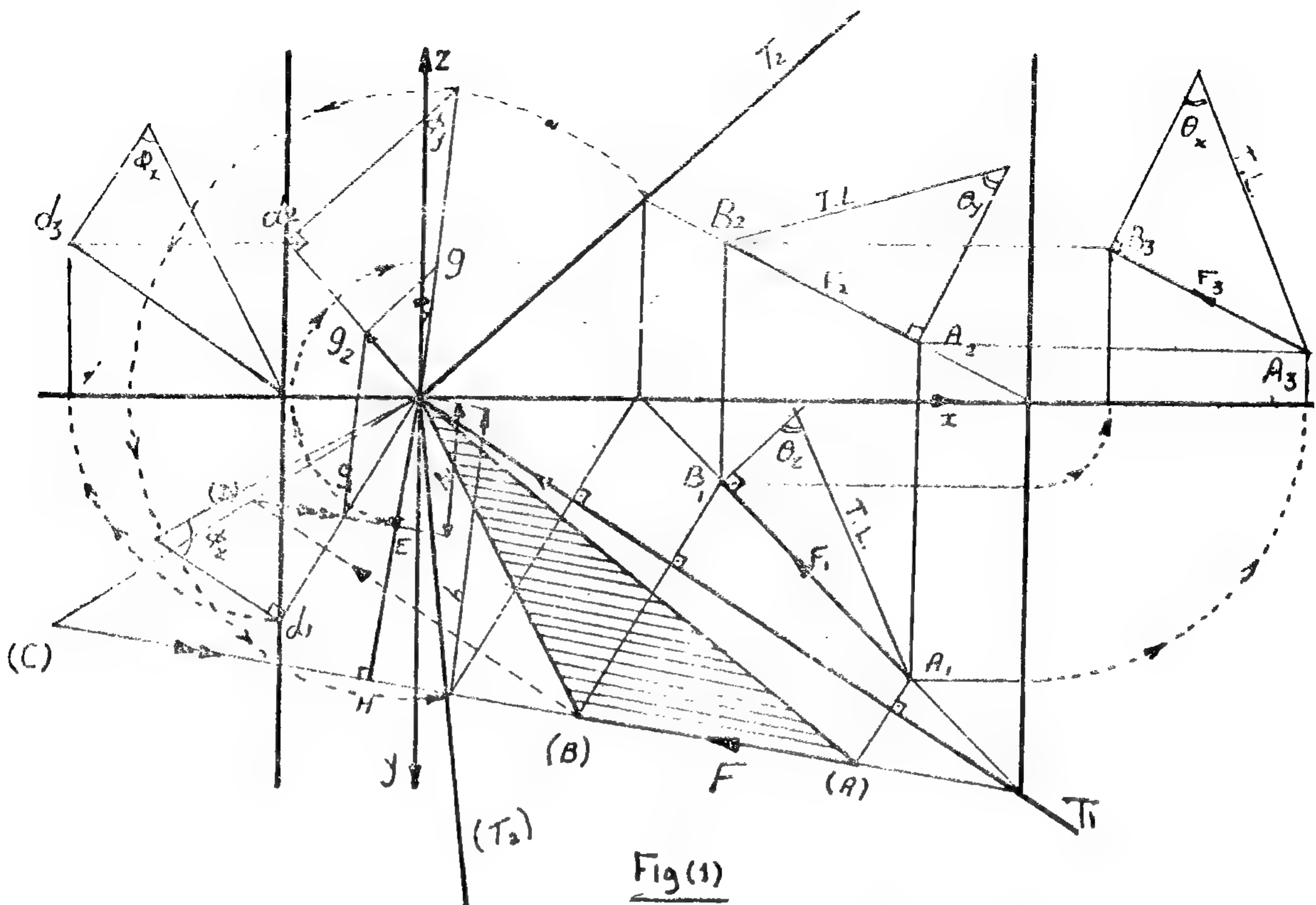
The moment G' of the force \mathbf{R} at O about the point P is represented in magnitude by twice the area of the triangle formed from the line of action of the force \mathbf{R} (representing its magnitude) and the point P . The vector \overrightarrow{PS} represents this moment G' . The moment \mathbf{G} at the origin



$$OQ = \frac{G \sin \theta}{R}$$

$$PQ \approx \text{central axis}$$

O is shifted to P without any change neither in magnitude nor direction. Thus the



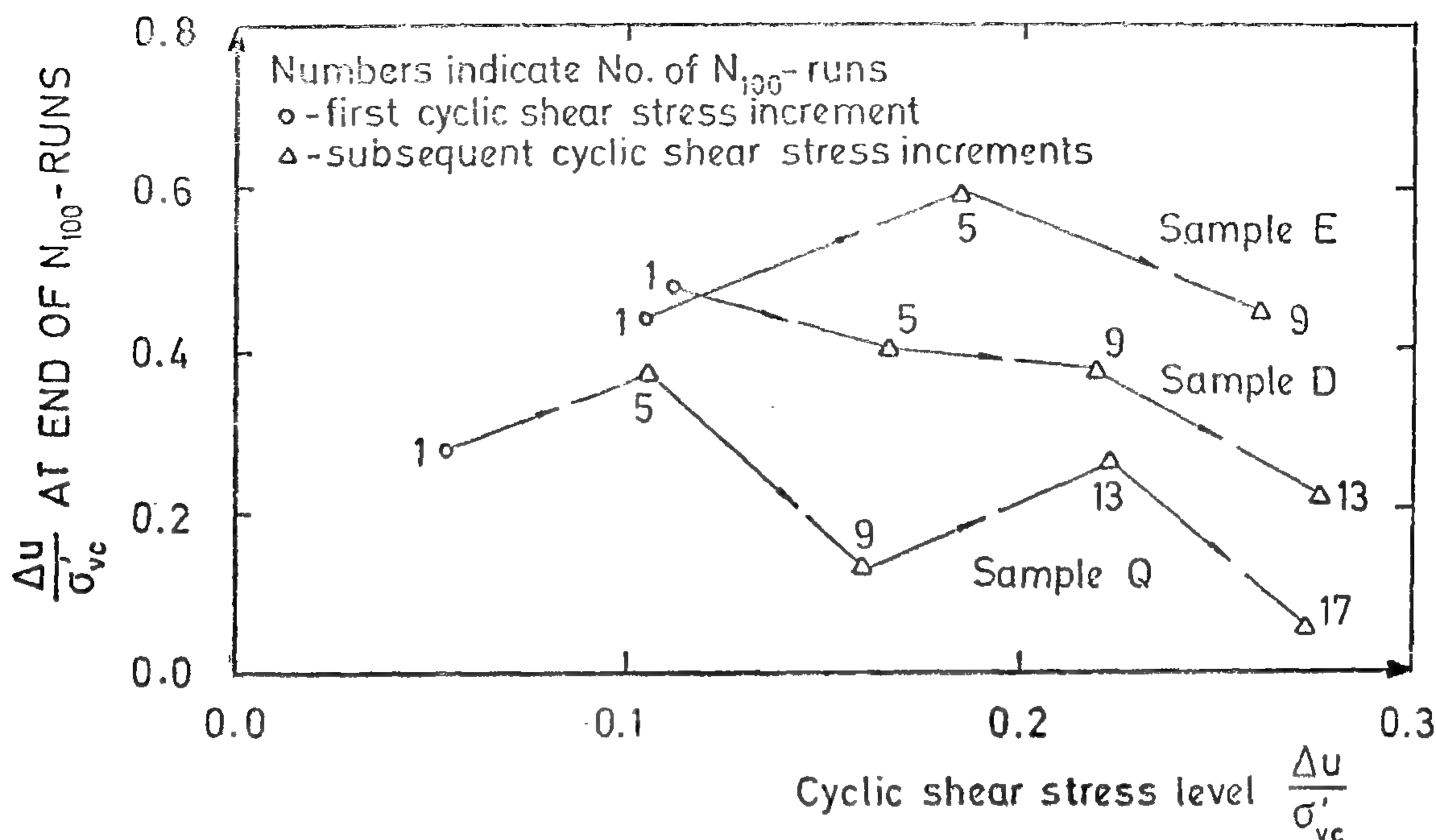


Fig. 5 Effect of increased cyclic shear stress increments on the cyclic "pore pressure".

According to the above findings, it can be concluded that the stability of offshore structures against cyclic shear stresses resulting from sea waves increases if the structure is subjected to periods of minor waves each followed by a relatively quiet period before the occurrence of the maximum design wave load.

SUMMARY AND CONCLUSIONS

Constant-volume cyclic simple shear tests were carried out on ten samples of dense sand whose initial relative densities varied from 80.6% to 89.7%. The samples were 50 cm² and 103.7 cm² in cross-sectional area. Each sample was subjected to different cyclic shear stress levels and tested for a run of 100 stress cycles repeated at least four times. At the end of each N_{100} -run the induced cyclic "pore pressure" was dissipated by restoring the effective vertical stress to the original consolidation pressure. The cyclic shear stress levels used in the tests varied from $\tau_h / \sigma'_{vc} = 0.038$ to $\tau_h / \sigma'_{vc} = 0.277$. The test results showed that.

1. The cross-sectional area of the sand sample has practically no effect on the cyclic "pore pressure".
2. If the sand has been subjected to previous cyclic loading, this will result in a significant decrease in "pore pressure" induced by subsequent cyclic shear stresses.

ACKNOWLEDGEMENTS

The work described in the preceding pages was carried out at the Norwegian Geotechnical Institute which kindly provided the laboratory facilities. Sincere thanks are due to Mr. Knut Andersen for his valuable discussions and to Mr. Einar Stensby for his assistance in the experimental part of the work.

The research grant offered by the Norwegian Agency for International Development is gratefully acknowledged.

The effect of preshearing at low cyclic shear stress level on the undrained shearing resistance of sand was investigated by the tests carried out on samples A-A, B-B, C-C, and D-D. These samples were first presheared for $N_{100} = 4$ at a cyclic shear stress level $\tau_h / \delta'_{vc} = 0.038$ and then tested for levels equal to 0.095, 0.142, 0.189, and 0.236, the fifth N_{100} -run at cyclic shear stress respectively. The normalized "pore pressure" at the end of the fifth N_{100} -run was recorded and given by the triangles in Fig. 3. Comparing the results indicated by the solid and dashed lines in Fig. 3 for virgin and cyclically presheared samples of sand respectively, it can be seen that preshearing of sand results in a decrease in cyclic "pore pressure", and hence the resistance to liquefaction is considerably increased. As another example, sample R (not shown in Fig. 3) reached liquefaction after applying 36 stress cycles with cyclic shear stress level $\tau_h / \delta'_{vc} = 0.159$, while it was possible to run the test in the presheared sample C-C for 100 stress cycles at $\tau_h / \delta'_{vc} = 0.189$ without it showing any sign of liquefaction. The corresponding induced horizontal shear strains were $\epsilon_h = \pm 1.733\%$ in sample R and $\epsilon_h = \pm 0.244$ in the presheared sample C-C.

In another series of tests, samples D,E and Q were subjected to increased cyclic shear stress increments, and were tested with four N_{100} -runs at each increment. The test results are illustrated by Fig. 5, in which the normalized "pore pressure" at the end of the first N_{100} -runs are plotted against the corresponding cyclic shear stress levels. In general, the test results showed that cyclic "pore pressure" is appreciably affected by both the cyclic shear stress

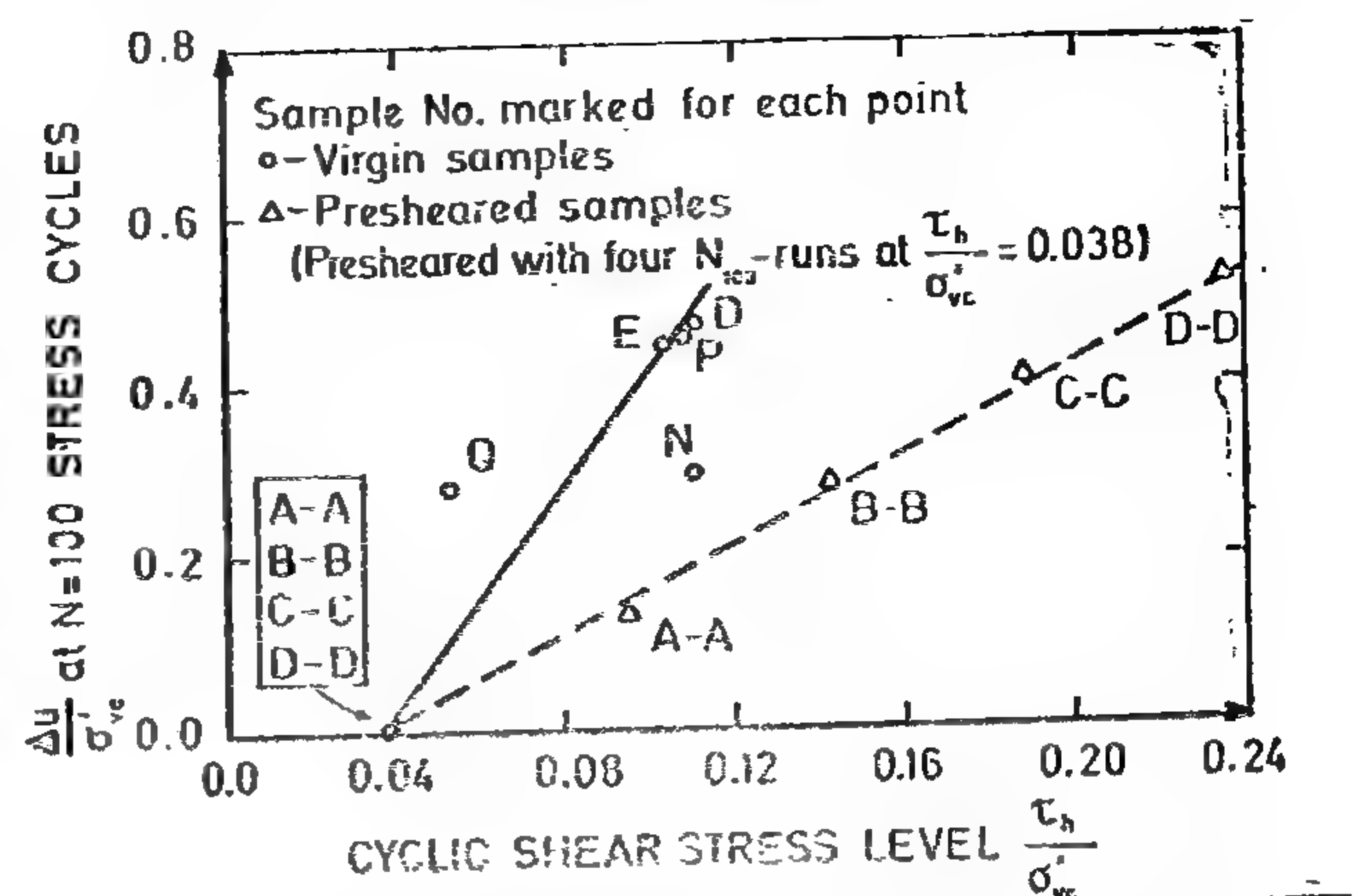


Fig. 3 Relationship between the normalized "pore pressure" $\Delta u / \delta'_{vc}$ and cyclic shear stress level τ_h / δ'_{vc} .

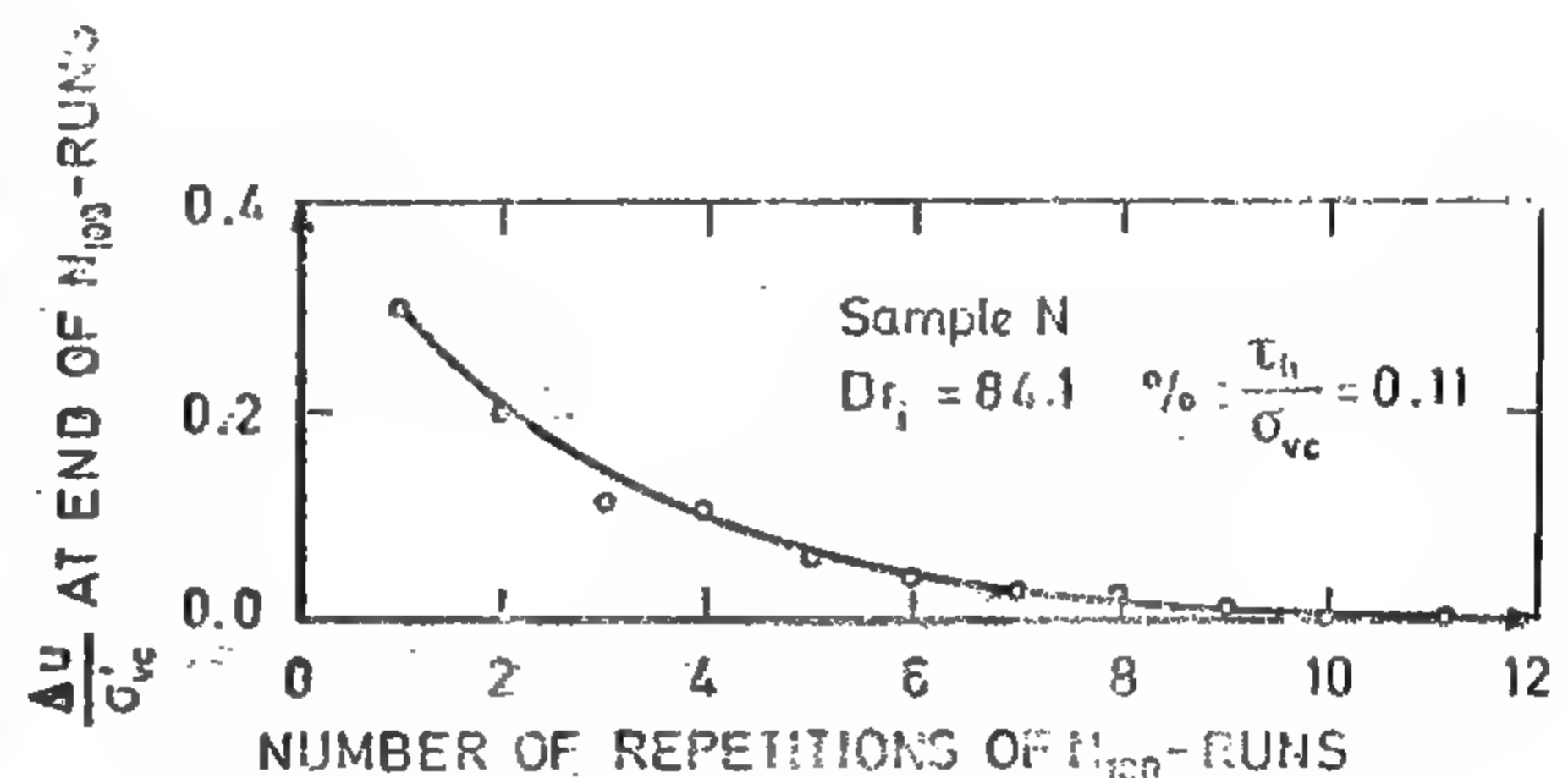


Fig. 4. Effect of repetition of N_{100} -runs on the cyclic "pore pressure"; Test No. N.

level applied to the virgin samples and the ratio between each two consecutive cyclic shear stresses $(\tau_h / \delta'_{vc}) R$.

Samples Q and D were tested for approximately equal ratios $(\tau_h / \delta'_{vc}) R$, but with different initial cyclic shear stress levels, $\tau_h / \delta'_{vc} = 0.053$ and 0.111 , respectively. Sample Q showed lower cyclic "pore pressures" in all the stages of the test than those in sample D. In another case, samples D and E were tested at equal initial cyclic shear stress levels, $\tau_h / \delta'_{vc} = 0.11$. Sample E was subsequently subjected to higher ratios of $(\tau_h / \delta'_{vc}) R$ than on sample D. As a result, the "pore pressures" induced in sample E were higher than those in sample D.

DESCRIPTION OF SAND

The sand used in the tests was obtained by grab sampling from the Frigg Field area in the North Sea. The microscopical examination incated that approximately 90% of the grains were composed of quartz, and the remainder was mostly plagioclase and alkali feldspars. The sand was uniform, medium to fine, with grain diameters between 0.06 mm and 0.59 mm; $D_{10}=0.15$ mm, and $D_{50}=0.2$ mm. The particles were subrounded in shape. The maximum and minimum void ratios were 0.835 and 0.450 respectively. The coefficient of permeability k of the sand at a relative density of 75% was 3×10^{-4} cm/sec.

TEST PROCEDURE AND EXPERIMENTAL PROGRAM

As pointed out by Peacock and Seed (1968), the cyclic loading conditions in the field are best simulated by carrying out the cyclic shear tests in a simple shear apparatus. Therefore, all the tests were carried out in the Norwegian cyclic simple shear apparatus. The apparatus was originally designed to apply static simple shear loading (Bjerrum and Landva, 1966). In November 1972, the apparatus was modified to apply horizontal cyclic shear stresses. The present description of the apparatus will be limited to the main features. These are: the vertical loading system which applies the vertical stress to the sample and can be controlled to retain constant specimen height in constant volume tests; the horizontal cyclic shear loading device with an adjustable frequency; the cylindrical reinforced rubber membrane which allows the sample to strain in simple shear and plane strain;

the gauges for measuring the magnitudes of stresses and strains. The cyclic loading wave form shown in Fig. 1 was used in all tests described herein.

The test results were evaluated by means of a computer program. Corrections were made for the resistance of the reinforced rubber membrane.

Terzaghi and Peck (1967) pointed out that the shearing strength of cohesionless soils is not appreciably different whether the soil is "wet or dry". This is because most of the shearing resistance of these soils is caused by interlocking of the grains. Previous constant volume static and cyclic simple shear tests (Moussa, 1973 and 1974), carried out on the same sand used herein, showed that the results obtained from dry samples were in good agreement with those obtained from saturated samples. Preparing dry samples of sand is easier and less time consuming than with completely saturated ones. Therefore, all the tests were carried out on dry samples of sand.

The change in vertical effective stress in constant-volume simple shear test corresponds to the change in pore water pressure Δu which develops in a conventional undrained test on saturated soil with pore water pressure measurements (Bjerrum and Landva, 1966). Accordingly, the term "pore pressure" used in this paper when interpreting the test results refers to the change in the effective vertical stress.

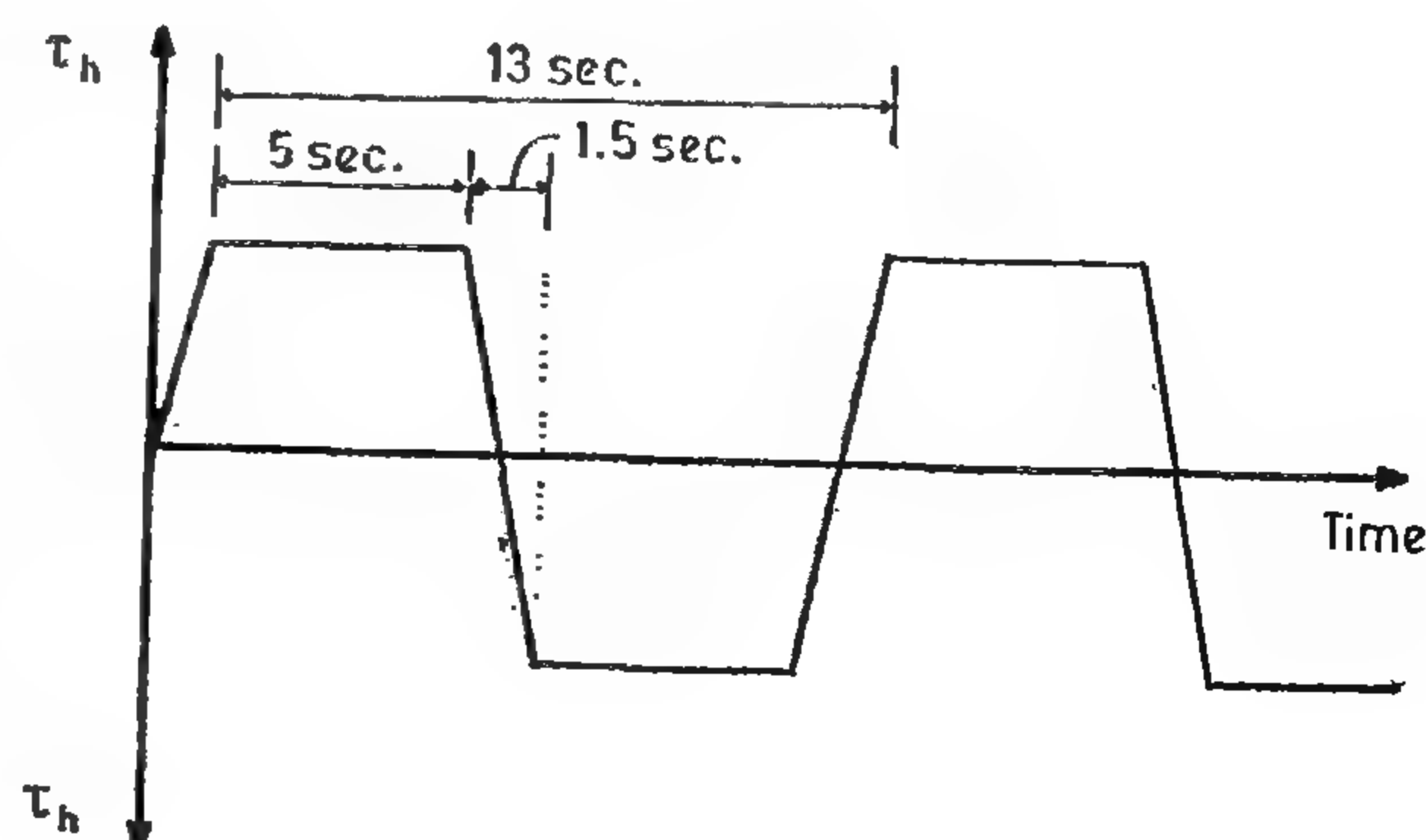


Fig. 1 Cyclic wave form of shear loading.

EFFECT OF STRESS HISTORY ON CPCLIC SHEAR STRENGTH OF SAND

By

ABDELMONEM AHMED MOUSSA, DR. - ING.*

SYNOPSIS

The pore pressure induced by cyclic shearing under equivalent undrained conditions in dense sand which has been subjected to previous cyclic shear stresses is less than that in virgin sand. The amount of decrease in cyclic pore pressure at a given cyclic shear stress level and number of load cycles depends on the magnitude and duration of the previous cyclic shearing.

INTRODUCTION

The strength of sand under cyclic loading has drawn the attention of many investigators during the last twenty years. It has been found that a cohesionless soil can deform and fail by virtue of fact that the pore water pressure induced by cyclic loading is not dissipated during the short duration of load application. Florin and Ivanov (1961) observed that even coarse sand deposits remain essentially undrained for several minutes after being loaded. The strains induced by cyclic loading are very small up to a certain number of load cycles, while the pore water pressure shows a cumulative increase. Shear strains subsequent to liquefaction are extremely large (Finn et al., 1971, and others).

Liquefaction phenomena of sand have been thoroughly investigated and it can be concluded that the number of cycles required to cause liquefaction of sand depends on: (i) grain structure; (ii) density; (iii) initial stresses; (iv) magnitude of cyclic loading; (v) failure mode; (vi) previous stress history, and (vii) type of testing equipment. The effect of strain history was investigated by Finn et al. (1970). It has been found that partial liquefaction in which strains are quite small leads to a considerable increase in the resistance of the sand to subsequent liquefaction.

It is the purpose of this paper to study the effect of previous stress history on the equivalent undrained shearing resistance of sand under equally reversed cyclic simple shear stresses. The results obtained will lead to a lower factor of safety against the applied loads than that which can be expected in the field where some drainage will probably take place.

The paper reports on current research work at the Norwegian Geotechnical Institute on cyclic loading on sand, as related to the offshore structures in the North Sea.

Associate Professor of Soil Mechanics and Foundations

Faculty of Engineering, Ain Shams University Cairo, Egypt.

NOTATIONS

A_s	=	Area of prestressing tendons.
b	=	Breadth of beam.
E_s	=	Modulus of elasticity of prestressing steel.
f_{bo}	=	Maximum compressive bottom fibre stress at mid-span section of a beam with opening at transfer.
f_{eo}	=	Maximum tensile stress at mid-height of the vertical edge of the opening at transfer.
f_{to}	=	Maximum compressive top fibre stress at mid-span section of a solid beam at transfer.
f_{ts}	=	Maximum compressive top fibre stress at mid-span section of a solid beam at working.
h_o	=	Height of opening.
l_o	=	Length of beam.
L	=	Length of beam.
δ_h	=	Horizontal displacement of the nodal point at which the prestressing force is applied.
δ_{to}	=	Upward central deflection of top fibres of a beam with opening at transfer.

δ_{bo} = Downward central deflection of bottom fibres of a beam with opening at working.

δ_{bs} = Downward central deflection of bottom fibres of a solid beam at working.

δ_{ts} = Upward central deflection of top fibers of a solid beam at transfer.

REFERENCES

1. Ali I. Mohammed, «The Effect of Openings on Structural Elements with particular reference to Reinforced Concrete Beams». M.Sc. thesis, Cairo University, 1962.
2. Nga, D. and Scordelis, A.C., «Finite Element Analysis of Reinforced Concrete Beams», ACI Journal, Proceedings, Vol. 64, No. 3, March 1967, pp. 152 — 163.
3. Dmetrov, C.A., and Kalatuav, «Design of Prestressed Concrete Structures, Moscow, 1967.
4. Zeinkiewicz, O.C., The Finite Element Method in Structural and Continuum Mechanics, McGraw Hill Book Co., New York, 1967.
5. A.A. Hamid, Effect of Openings in prestressed Concrete Beams, M. Sc. Thesis, Faculty of Engineering, Ain Shams University, Cairo, 1974.

* * *

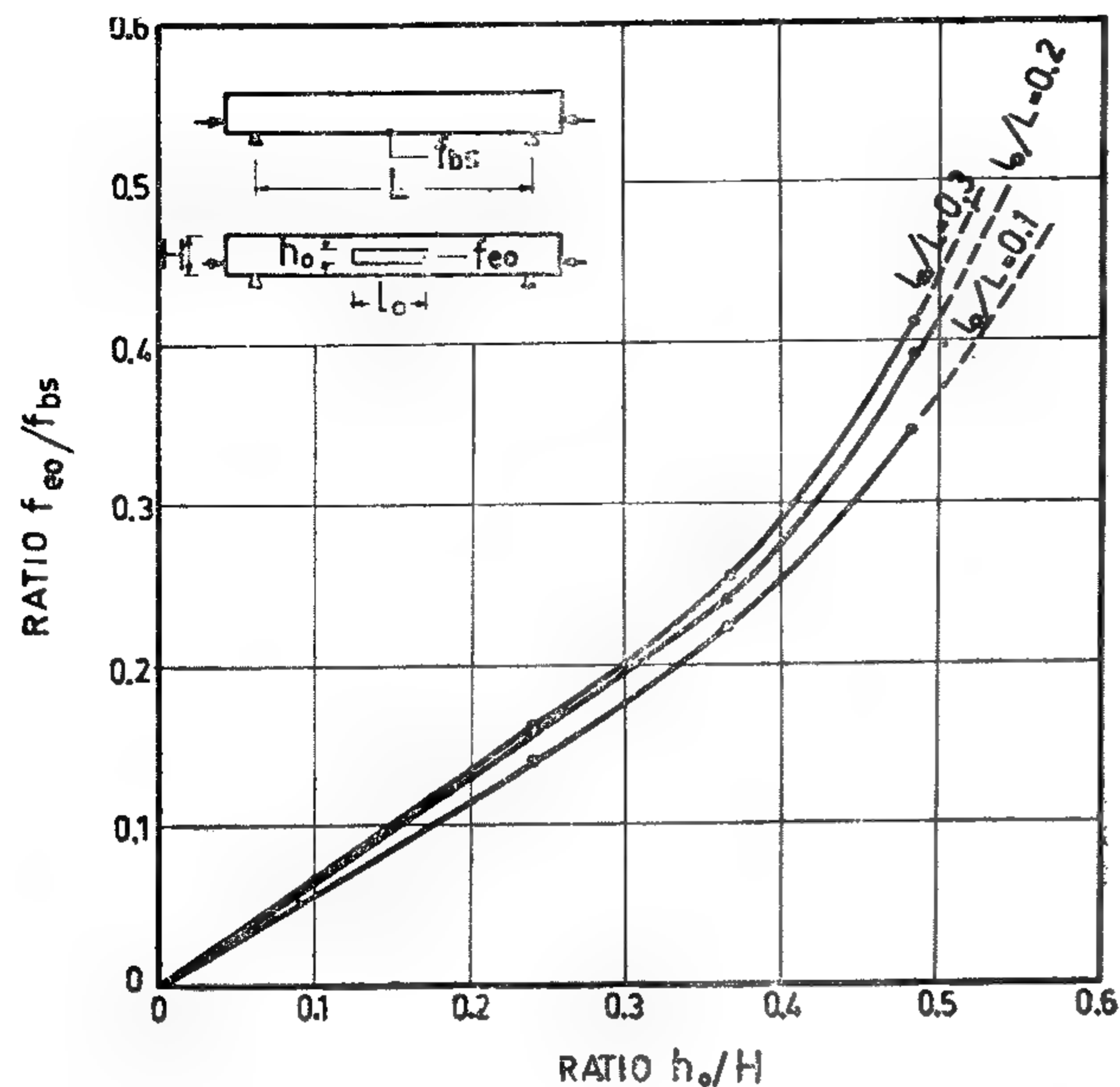


FIG. 12 - TENSILE STRESSES AT THE EDGE OF THE OPENING AT TRANSFER

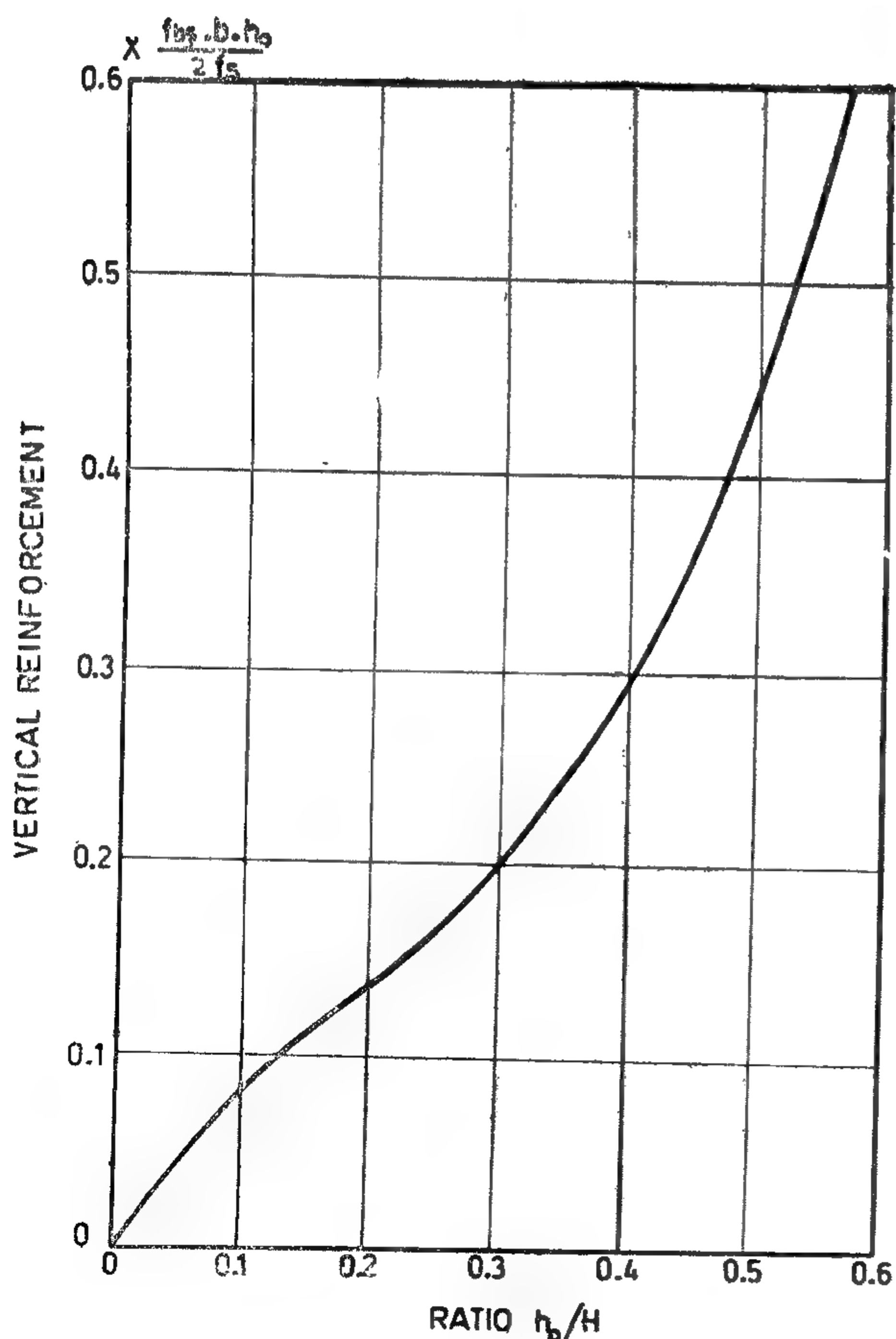


FIG. 13 - PROPOSED CHART FOR THE CALCULATION OF REQUIRED VERTICAL REINFORCEMENT AT THE SIDE END OF A RECTANGULAR OPENING

2. Providing one central rectangular opening in the pure bending zone of a prestressed concrete beam increases central deflection and extreme fibre stresses to an extent depending on both relative height and relative length of such opening. This increase reaches more than 100% for extreme ratios of $h_o/H > 0.5$, and $l_o/L > 0.3$. The designer, using the proposed design aid chart, can check and control central deflection and extreme stresses.

3. Providing a central rectangular opening in the pure bending zone of a prestressed concrete beam creates tensile stresses around the opening nearly in the vertical direction and extend up to a distance equal one half the opening length from each side. Required vertical edge reinforcement can be provided using the proposed aid chart. The horizontal edge reinforcement proved to be of less efficiency than the vertical one.

4. Existence of an opening in the bending zone of a prestressed concrete beam makes separation between the deformation of the top and bottom chords of such opening. These chords cannot act together as one unit and assumption of plane section (composed of top and bottom chords) remains plane after deformations is not valid, especially for cases of high slenderness ratios of opening's chords. Accordingly, providing of intermediate posts between such chords is recommended to have less difference of deflection and less tendency of buckling of chords.

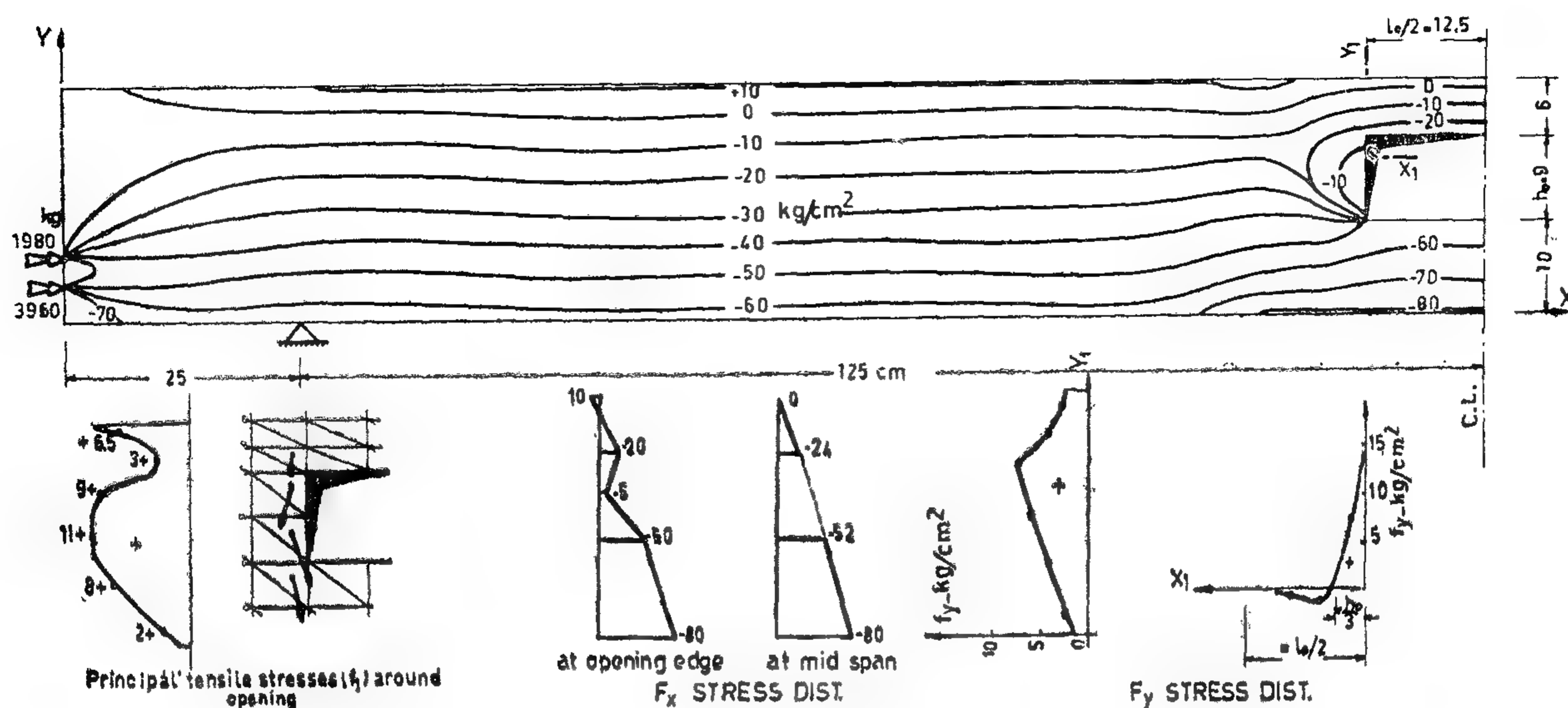


FIG. 10 - CONTOUR LINES OF LONGITUDINAL STRESSES AT TRANSFER FOR BEAM B-32

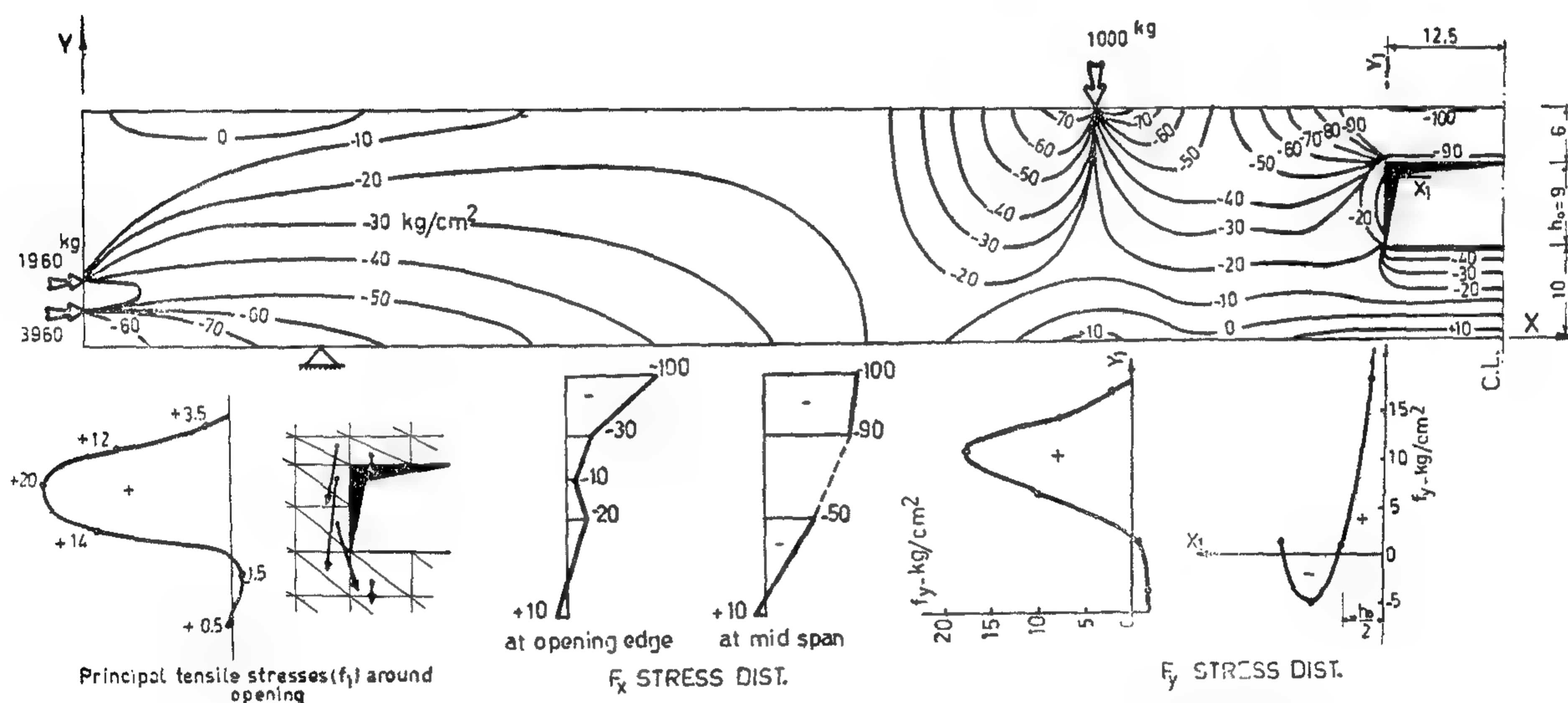


FIG. 11 - CONTOUR LINES OF LONGITUDINAL STRESSES AT WORKING FOR BEAM B-32

The tensile stresses, see Fig. (10), created around the opening are found to extend up to a distance equal to one half the height of the opening from each of both its sides. The required vertical reinforcement provided at the vertical sides of the rectangular opening can be calculated using the design aid chart shown in Fig. (13).

CONCLUSIONS

1. The finite element method offers a powerful tool to be used as the basis for development of an analytical model of a prestressed concrete element with openings, which permits a detailed study of the complicated nature of the deformations and stress concentration around openings.

fibre compressive stresses at mid-span section for a beam with one central opening, (f_o), can be expressed in terms of the corresponding stresses in a similar beam without opening, (f_s), such as :
at transfer

$$f_{bo} = R_{ct} \cdot f_{bs} \quad \dots\dots (6)$$

at working

$$f_{to} = R_{cw} \cdot f_{ts} \quad \dots\dots (7)$$

where

$$R_{ct} = 1 + 1.45 (h_o/H) - 4.75 (h_o/H)^2 + 7.5 (h_o/H)^3 \quad \dots\dots (8)$$

$$R_{cw} = 1 + 3.25 (h_o/H) - 10.75 (h_o/H)^2 + 18.5 (h_o/H)^3 \quad (9)$$

The above-mentioned proposed formulae for (R_{ct} & R_{cw}) are represented by a design aid chart shown in Fig. (9).

The stress distribution over the X-sections passing near the edge of the opening is non linear, while it is nearly linear at mid-span sections. See Figs. (10) and (11).

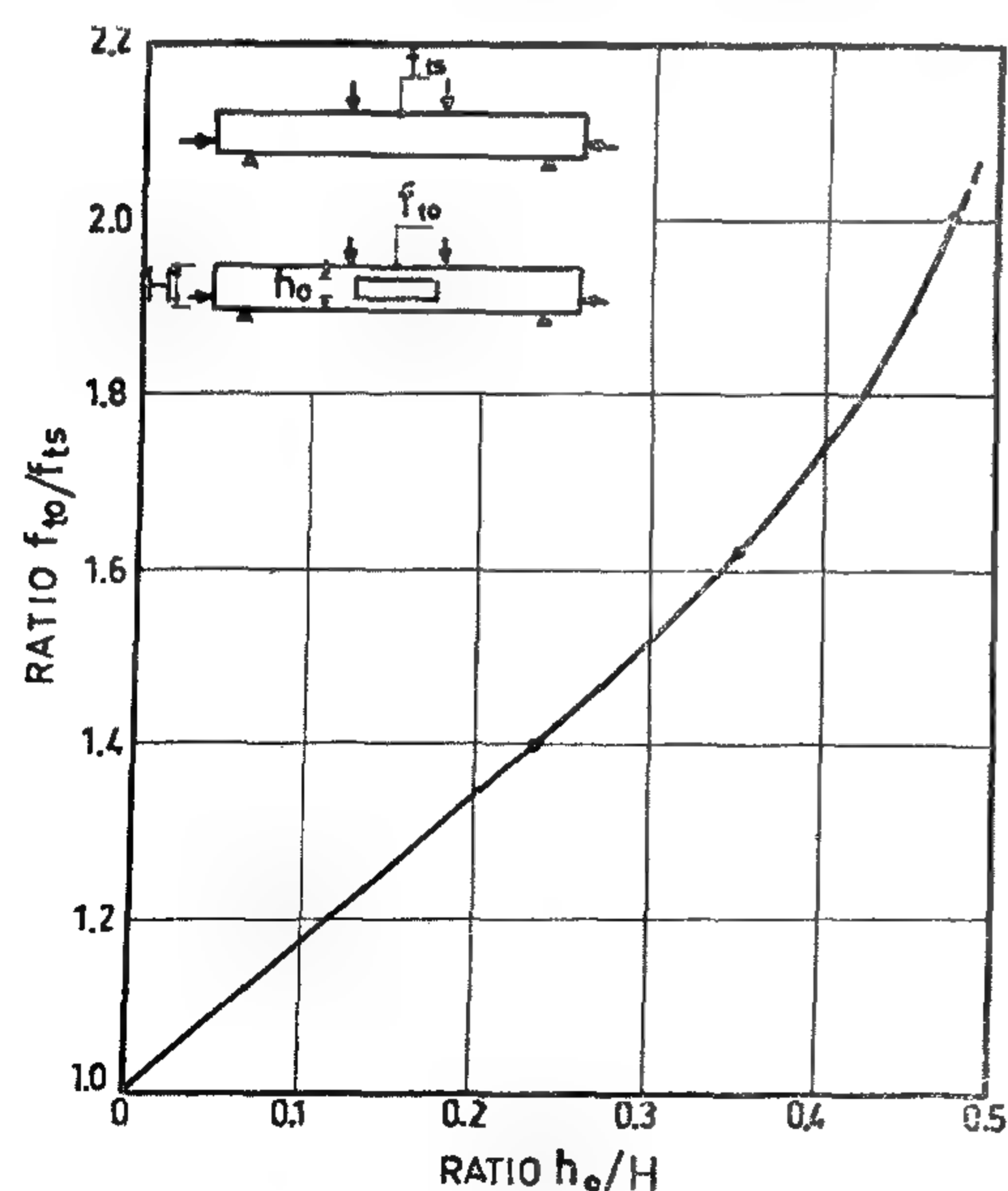


FIG. 8 -EXCESS OF TOP FIBER STRESSES AT WORKING STAGE

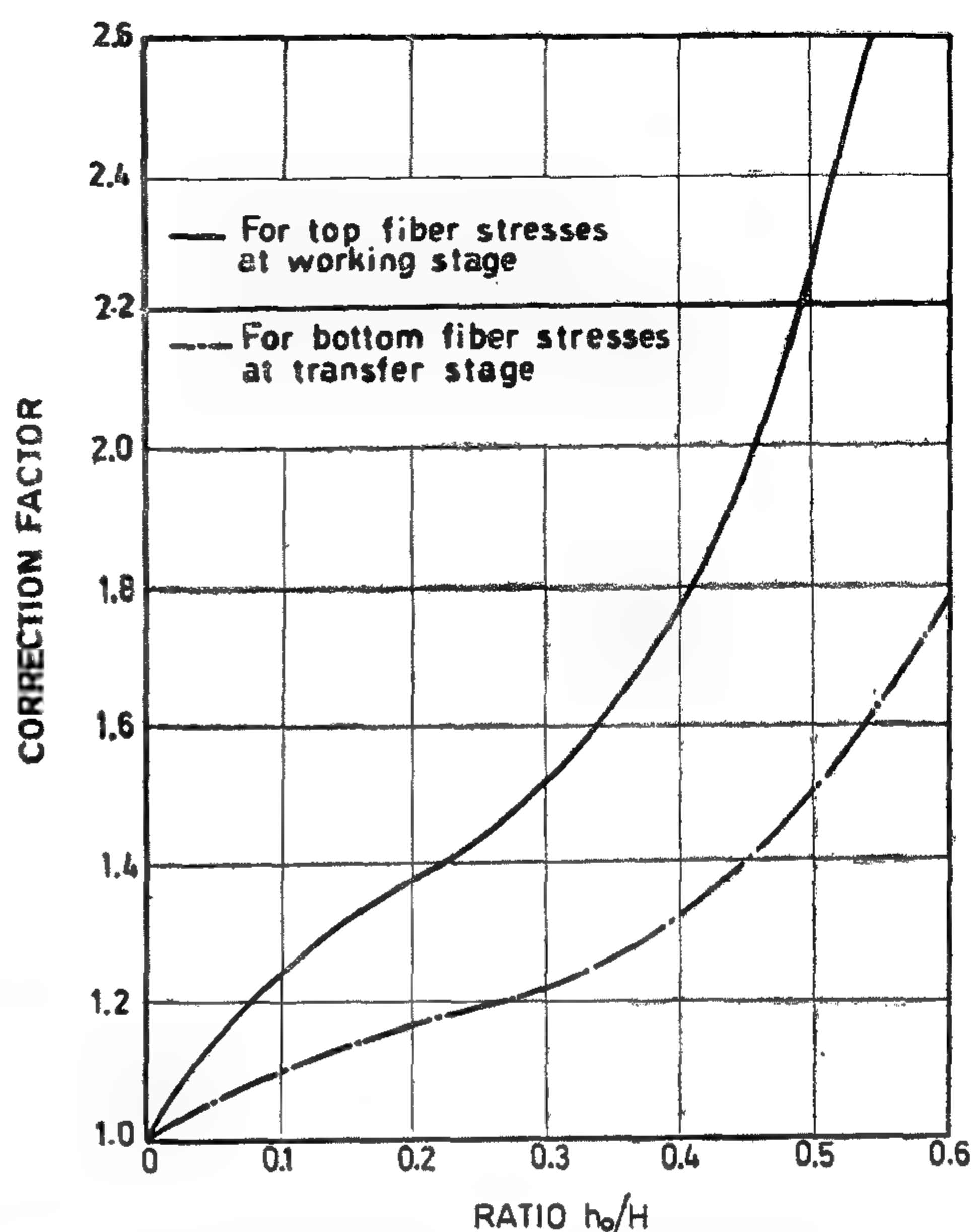


FIG. 9 -PROPOSED CHART FOR THE CORRECTION FACTOR OF COMPRESSIVE STRESSES AT MID-SPAN SECTION

c) Stress Concentration around the Opening :

The existence of the opening in the bending zone of a prestressed concrete beam makes a disturbance in the flow of stresses and creates excessive principal tensile stresses nearly in the vertical direction. See (Figs. (10) and (11)).

The maximum tensile stresses created at mid-height of the vertical edges of the opening at transfer, (f_{eo}), is represented by the curves shown in Fig. (12). Such tensile stresses can be expressed in terms of mid-span extreme fibre stresses in a similar solid beam at transfer, (f_{bs}), as

$$f_{eo} = f_{bs} [(h_o/H) - 2.5 (h_o/H)^2 + 4.5 (h_o/H)^3] \dots (1)$$

UPward deflection at transfer stage :

$$\delta_{to} = R_{dt} - \delta_{ts} \quad (2)$$

Downward deflection at working stage :

$$\delta_{bo} = R_{dw} \cdot \delta_{bs} \quad \dots\dots (3)$$

where

$$R_{dt} = 1 + 0.72 l_o/L (h_o/H)^{\frac{1}{2}} \quad \dots\dots (4)$$

$$R_{dw} = 1 + 11.5 l_o/L (h_o/H)^2 \quad \dots\dots (5)$$

The above-mentioned proposed formulae for (R_{dt} & R_{dw}) are represented by a design aid chart shown in Fig. (5).

The vertical displacement of the extreme fibres show a difference between the deflection of the top and bottom chords of the opening in different stages of loadings by an amount up to 5 % at transfer, and by 10% at working load of $p = 1.0$ t. This difference

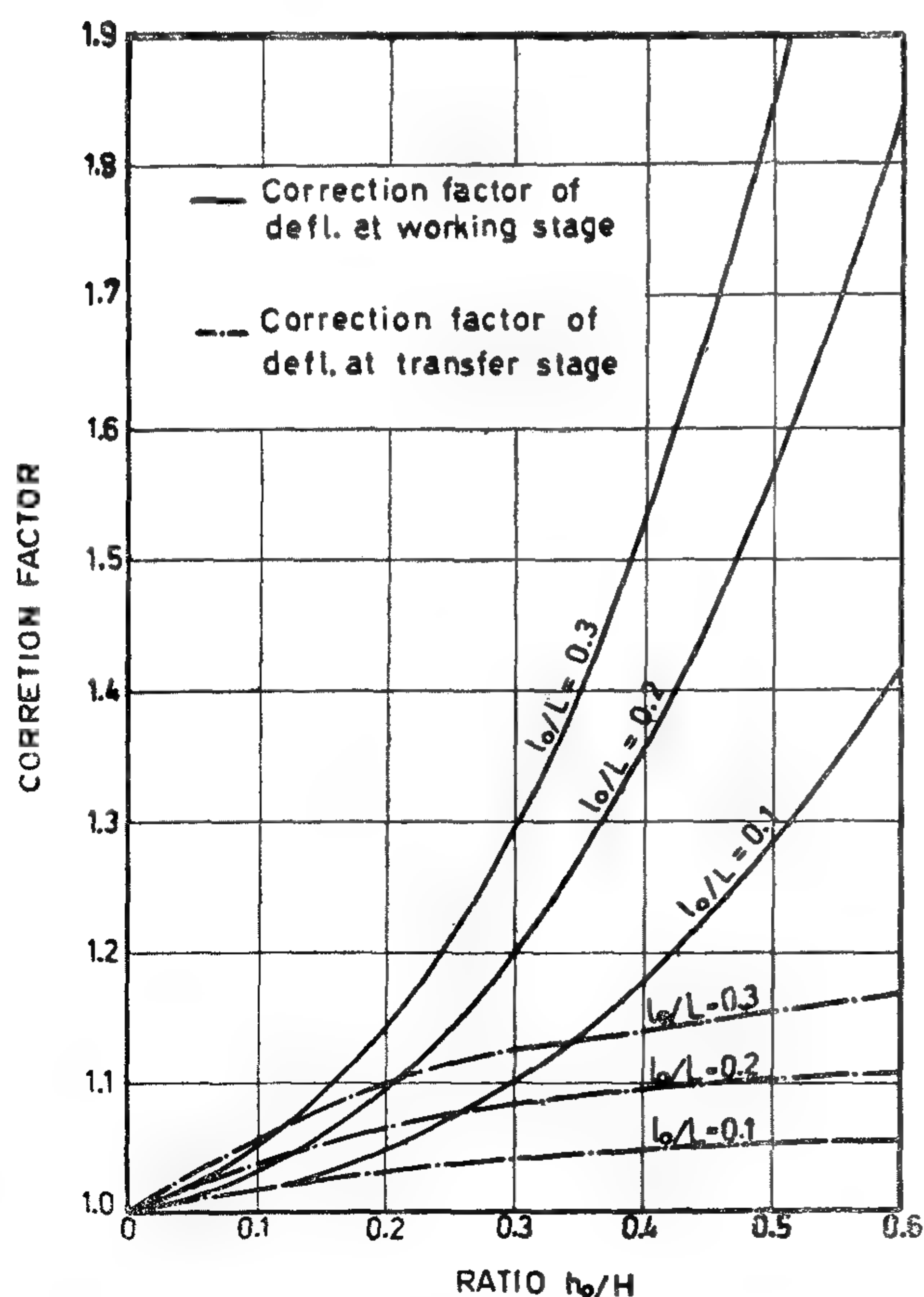


FIG. 5 — PROPOSED CHART FOR THE CORRECTION FACTOR OF CENTRAL DEFLECTION

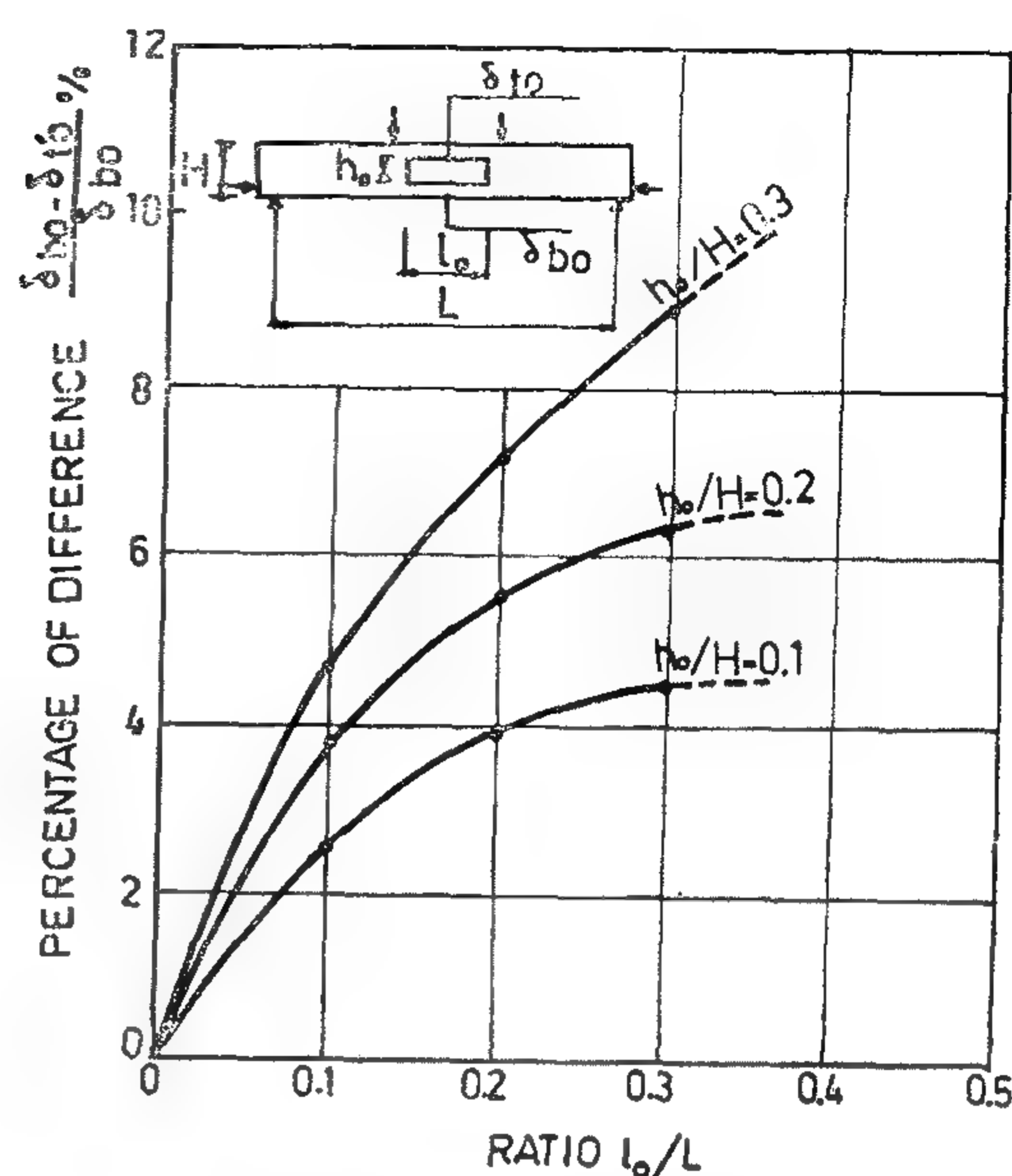


Fig. 6 — Difference of Deflection of Bottom Fibers for Upper and Lower Chords
of deflection is increased with the increase of h_o / H and l_o/L ratios, see Fig. (6).

b) Stresses of Extreme Fibres :

The excess of compressive fibres stresses at mid-span sections is represented by the curves shown in Fig. (7) and Fig. 8 Using statistical techniques, the extreme

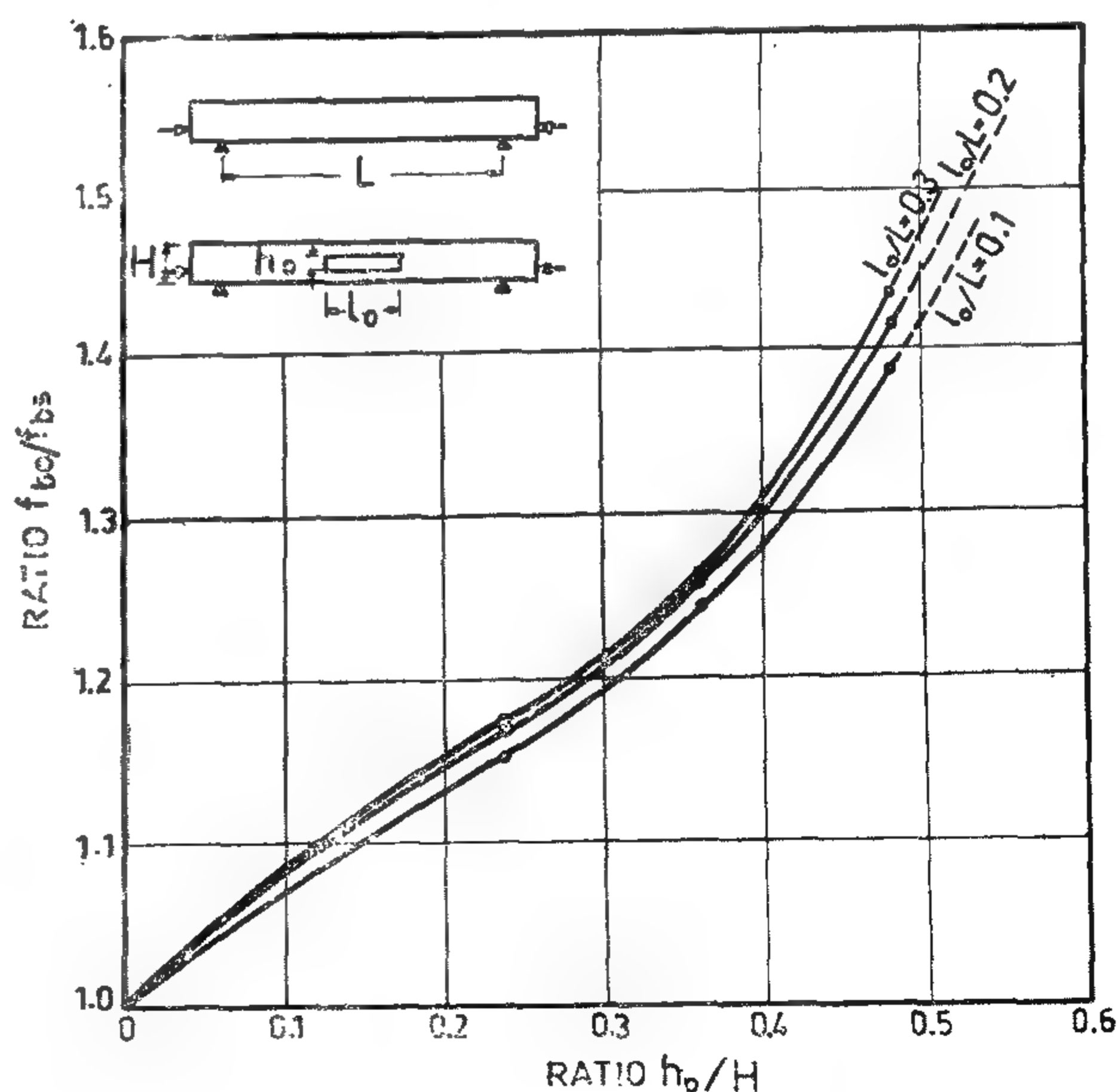


FIG. 7 — EXCESS OF BOTTOM FIBER STRESSES AT TRANSFER

Beam	Dimensions of opening		Effective Parameters	
	Length (l) cm	Height (h _o) cm	l/L	h _o /H
B —	—	—		
B — 1.1	75	6	0.30	0.24
B — 1.2	75	9	0.30	0.36
B — 1.3	75	12	0.30	0.48
B — 2.1	50	6	0.20	0.24
B — 2.2	50	9	0.20	0.36
B — 2.3	50	12	0.20	0.48
B — 3.1	25	6	0.10	0.24
B — 3.	25	9	0.10	0.36
B — 3.	25	12	0.10	0.48

L = 250 cm, H = 25 m for all model beams.

Table (1) — Dimensions and parameters of the Idealized beams.

ANALYSIS OF COMPUTER RESULTS

The existence of a central opening in the pure bending zone of rectangular prestressed concrete beam creates excess of central deflection and extreme fibre stresses at mid-span sections relative to that of a similar beam without openings. Also, principal tensile stresses exist around the opening which need special reinforcement.

a) Central Deflection :

The excess of central deflection is presented in Fig. (3) and Fig. (4) at transfer and working stages, respectively. Using statistical techniques, the central deflection of beams with openings, (δ_o), can be expressed in terms of the corresponding deflection of a solid beam (δ_s)

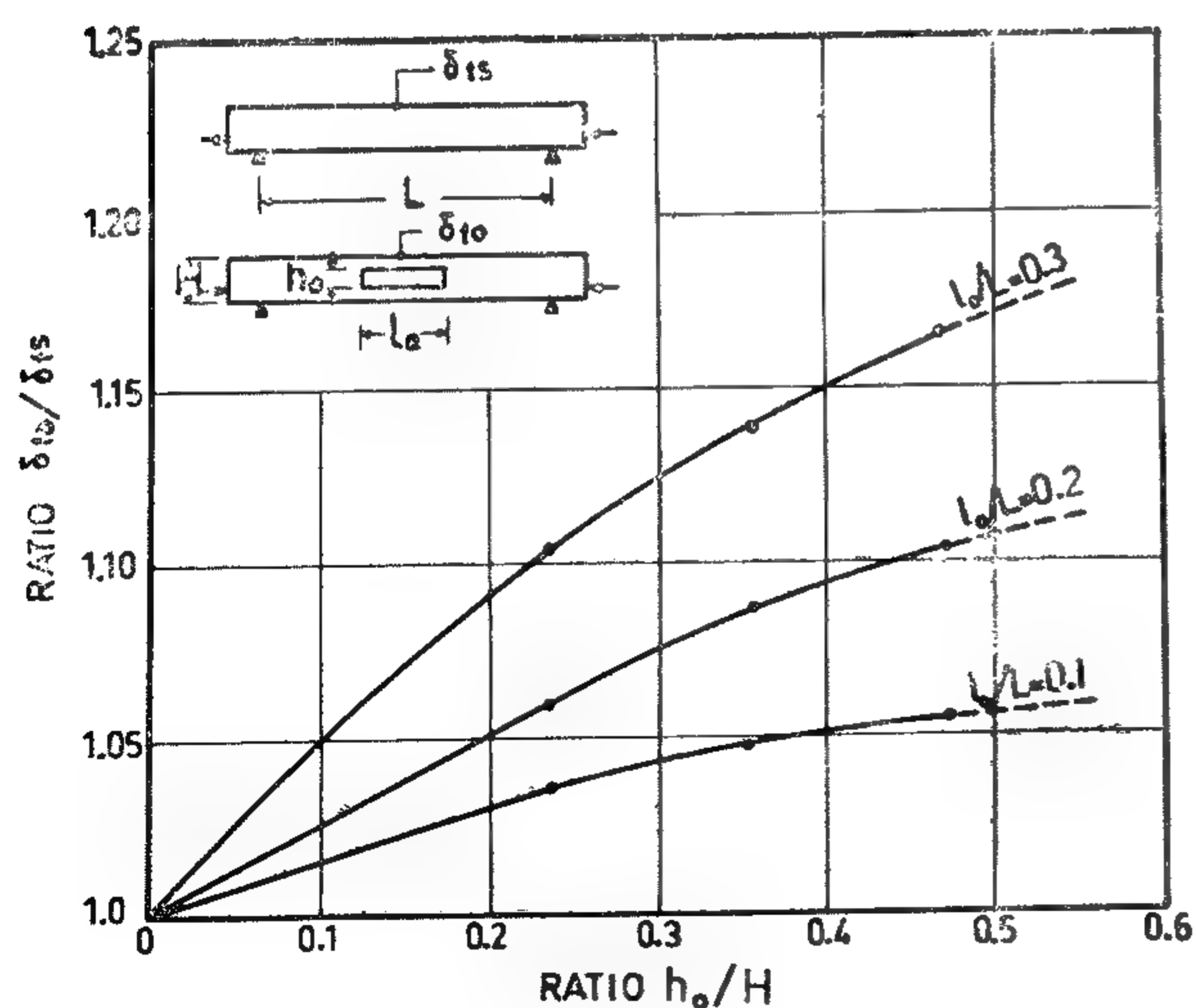


FIG. 3 — EXCESS OF DEFLECTION AT TRANSFER

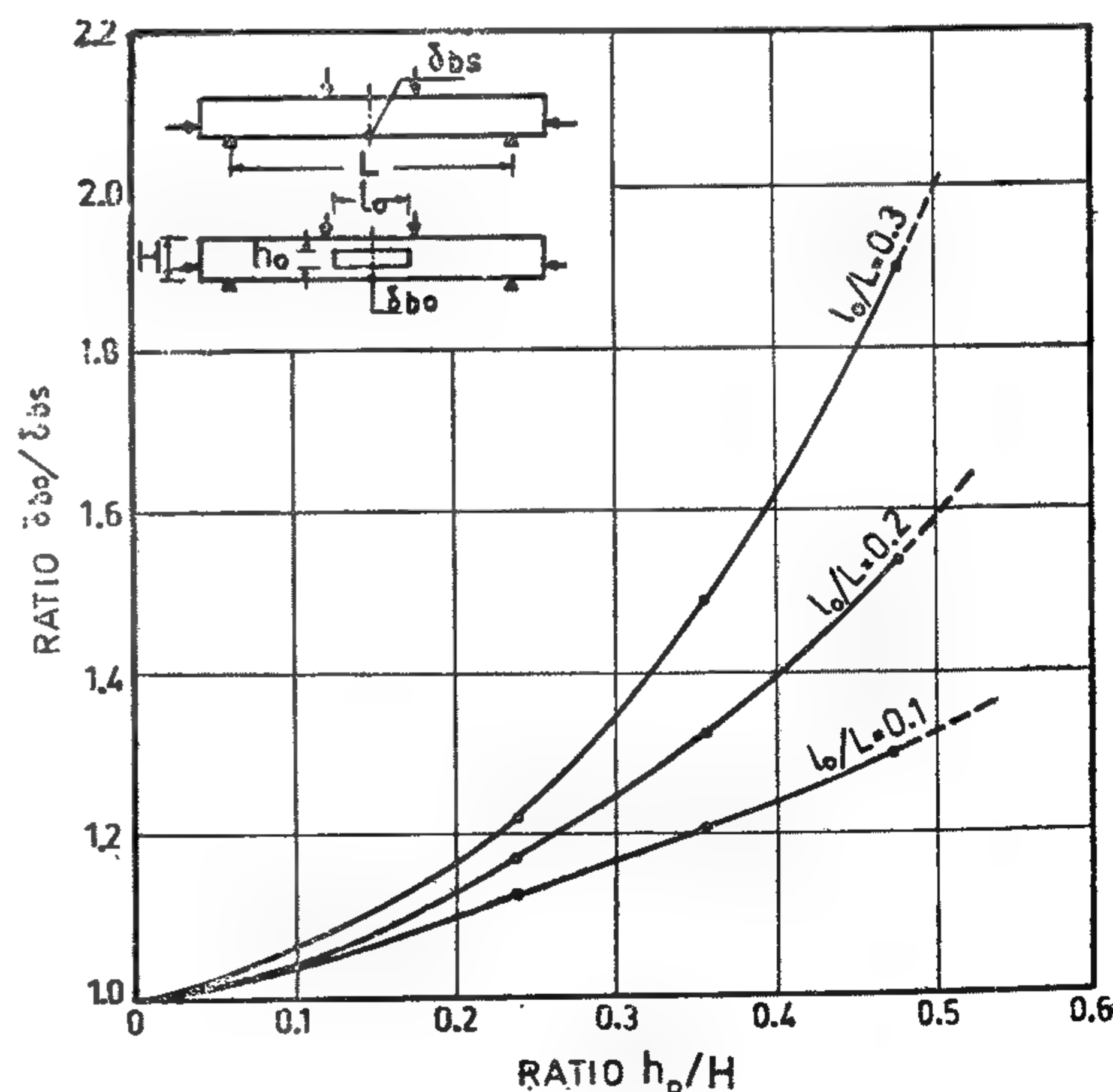


FIG. 4 — EXCESS OF DEFLECTION AT WORKING STAGE

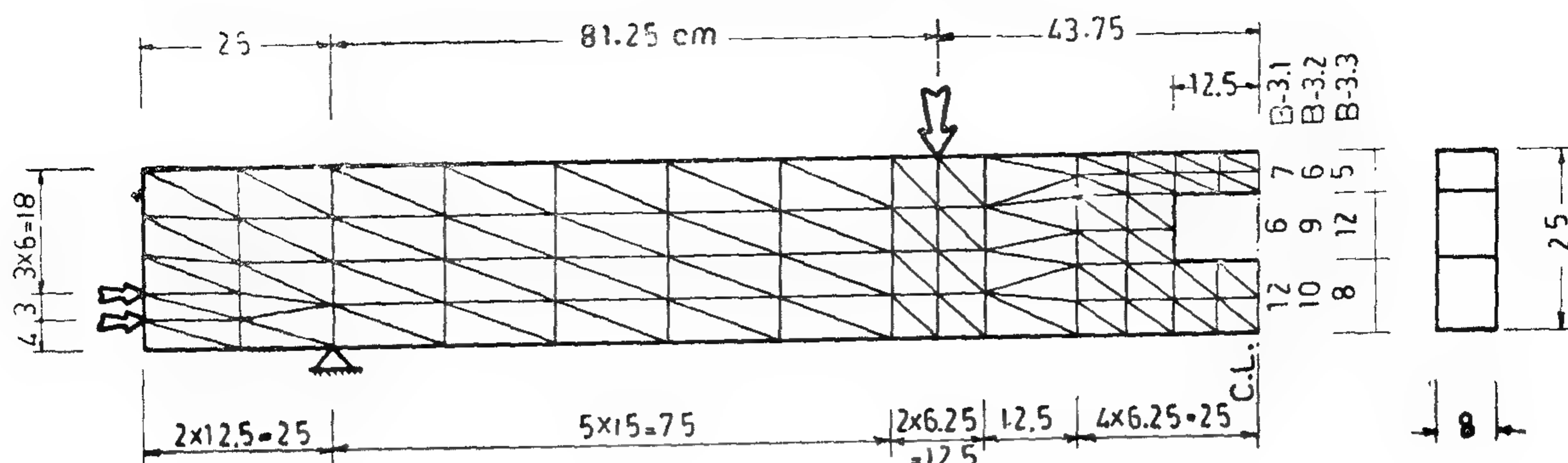


FIG. 1 - IDEALIZATION OF BEAM B-3

$$\Delta F = A_s \left(\frac{\delta h \cdot E_s}{L/2} \right) \quad \dots (1)$$

Linear displacement functions are considered for the typical triangular element. After formulation and solution of equilibrium equation, (4) the horizontal and vertical displacements at each nodal point can be obtained. Normal Stresses, principal and shear stresses are also obtained for individual element (5).

A computer program for the equilibrium equations and stress calculations has been written in Fortran II Language. This program has been run on IMB 1130 available at the Computing Centre of Ain Shams University, Cairo. For the flow diagram of this program, see Fig. (2).

PRESENT STUDY SCHEME

In this study, ten rectangular prestressed concrete beams, table (1), are analysed at transfer stage under prestressing forces besides the own weight, and at working stage under two symmetrical middle third point loadings.

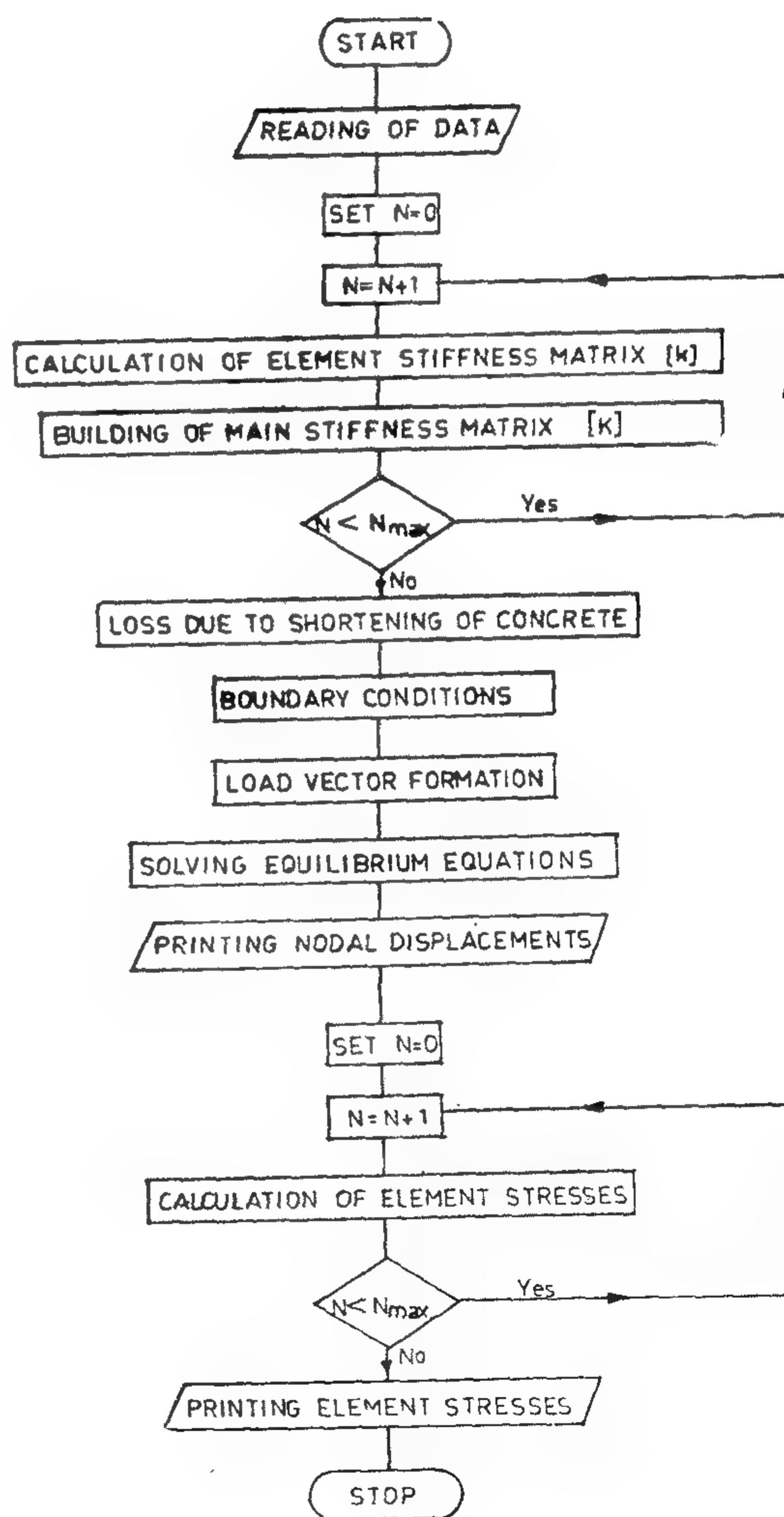


FIG. 2 - FLOW DIAGRAM FOR THE FINITE ELEMENT METHOD

FINITE ELEMENT ANALYSIS OF PRESTRESSED CONCRETE BEAMS WITH OPENINGS

by

M.M. EL-HASHIMY¹, A. ABU EL-ENEIN²
and A.A. HAMID³

INTRODUCTION

In construction practice, architects and engineers generally specify that holes and openings have to be provided in the webs of beams to accommodate the passage of utility components. Openings may be of different sizes and shapes and may cross the beams in different positions. The presence of such openings affect the behaviour of the beams to an extent depending on their positions and relative sizes.

Providing openings in structural members changes their simple mode of failure to complex and highly indeterminate one (1). In view of such complexity, the application of the classical methods of strength of materials may not give a true picture about the behaviour of such members.

Herein, the finite element method is presented to analyse rectangular prestressed concrete beams having one central rectangular opening in the pure bending zone.

THEORETICAL APPROACH AND BASIC ASSUMPTIONS

The aim of the present application of the finite element method to the problem of openings in prestressed concrete beams is to calculate the deformations and stresses of

such beams compared to that of a solid beam, which can be easily treated by the designer using the classical methods of analysis.

The following basic assumptions are taken all through the analysis. These assumptions are considered to be valid within the range of interest of prestressed concrete beams at both transfer and working stages :

a) The problem is considered a two dimensional plane stress problem.

b) Concrete ,in compression, is still in the elastic range; thus linear response of material to load is considered.

c) No cracks are allowed at both transfer and working stages; the modulus of elasticity in tension is assumed equal to that in compression.

The beam is divided into a finite number of triangular elements which are found to be very convenient to have a gradual gradation in the size throughout the beam as desired around opening.(2) As an example of the idealization, see Fig. (1).

Prestressing force is represented, in this study, as an external applied force,(3) taking into consideration the loss due to shortening of concrete :

-
1. Prof. of Reinf Conc. Str., Dept. of Struct. Eng., Ain Shams Univ., Cairo, Egypt.
 2. Lecturer, Dept. of Struct. Eng., Ain Shams Univ., Cairo Egypt.
 3. Assist. Lecturer, Dept. of Struct. Eng., Ain Shams Univ., Cairo, Egypt.

BUILDING & CONSTRUCTION

**INSTITUTION OF IRRIGATION ENGINEERS
INSTITUTION OF ARCHITECTS
INSTITUTION OF CIVIL ENGINEERS**

التصنيع والانتاج

جمعية المهندسين الكهربائيين
والإلكترونيين

جمعية الهندسة الإدارية
جمعية المهندسين الميكانيكيين

يسعد جمعية الهندسة الادارية أن تقدم للسادة الزملاء
المهندسين تباعاً موضوعات تطبيقية في فنون الادارة لتكون في
متناول أيديهم اسهاماً منها في اثراء المكتبة الهندسية بهذا
الجانب الذي يجدر بهم الاهتمام به استكمالاً لقدراتهم في ادارة
المشروعات الكبيرة التي يتولون ادارتها .
مهندس عبد الملك محمد العصفوري

التنظيم ومراجعة الهياكل التنظيمية

للمهندس حسن ناجي

أدى توسع أعمال المنشآت المختلفة وتطورها الى اهتمام الادارة بإجراء
الدراسات التنظيمية بأنواعها المختلفة ووضع النظم التي تكفل تحقيق هدف من
أهم أهدافها وهو الحصول على أفضل استخدام للمواد والطاقات المختلفة ،
بشرية وآلية وحرارية مما يسهل معه مراقبة تنفيذ العمليات المختلفة ويؤدي
عامة الى رفع الانتاجية عن طريق تكوين الجهاز الذي يباشر هذه الدراسات ويكون
رائدة الأسس السليمة للادارة والتنظيم ، وبهذا يتسع وقت الادارة لتركيز جهوداتها
في رسم السياسات ووضع التخطيطات القريبة والبعيدة المدى للمنشأة ومتابعتها .
وقبل التعرض الى هذه الدراسات والأسس الحديثة نود أن نستعرض
التطورات التي مرت بها الصناعة منذ بدئها حتى وقتنا الحاضر من حيث أسس التنظيم
والأساليب الادارية وأثر مجهودات بعض الأشخاص ممن يعتبروا رواداً في هذا
المجال .

نبذة تاريخية

عندما توسع نشاط أصحاب الأعمال ، تبين
لصاحب العمل صعوبة مباشرته لجميع المهام
بالكفاءة المطلوبة ، ويتطلب الأمر استعانتة
بمساعدين له متخصصين في مباشرة أوجه النشاط
المختلفة وبدأ التفكير في الأساليب السليمة للتشغيل
وبدا في هذا الوقت ظهور رواد الادارة والتنظيم
وكان أولهم هو شارلس بابيج Charles Babbage
بانجلترا (١٧٩٢ - ١٨٧٣) وهو عالم في الطبيعة
والرياضيات . وكان يعتقد أن هناك بعض الأسس
للادارة السليمة ولكنه لم يتمكن من تبينها أو
تحديدها .

وتلى ذلك ظهور هنري فايول (Henri Fayol)
بفرنسا (١٨٤١ - ١٩٢٥) وهو مهندس وكان
يعمل بمنجم للفحم وكان أول من أرسى بعض
قواعد الادارة السليمة التي ما زال مأخوذاً بها
حتى وقتنا الحاضر ألا وهي :

- * تحديد اختصاصات لكل وظيفة بالمنشأة .
- * تفويض السلطة لشاغل الوظيفة حتى
يمكنه القيام بواجباتها على الوجه المطوب .
- * تقسيم محدود لأوجه النشاط المختلفة
بالمنشأة واسناد الاشراف على كل منها الى فرد
واحد مسئول .
- * حصر مسئولية الفرد أمام رئيس مباشر
واحد فقط .
- وظهر في نفس الوقت تقريباً والتر راتينو
(Walter Ratnenau) بألمانيا (١٨٦٧ - ١٩٢٢)
وقد شغل مناصب ادارية متعددة في الصناعة
وكان يهتم بالسياسة وتناول في كتاباته علاقة
الادارة بالمجتمع ، وأهمية العلاقات الانسانية
وأثرها على الانتاج .
- ثم ظهر فردريك تايلور (Frederick Taylor)
بالولايات المتحدة (١٨٥٦ - ١٩١٥) وكان مهندساً
انصب اهتمامه في دراسة وتحسين طرق العمل

أسس التنظيم السليم

تعتمد هذه الأسس على الافادة بالطاقات البشرية وامكانياتها لتحقيق أعلى درجات الكفاية الانتاجية عن طريق :

- ١ - تحديد واضح للأهداف الرئيسية لنشاط المنشأة .
- ٢ - تخطيط سليم للهيكل التنظيمي للعمل الذي تمارسه المنشأة .
- ٣ - تخفيض عدد مستويات الوظائف الاشرافية الى أقل عدد ممكن مع الاطمئنان الى فاعلية الاشراف .
- ٤ - تحديد اختصاصات الادارات والأقسام المختلفة .
- ٥ - تركيز واجبات الوظائف الرئيسية كل منها في نشاط خاص .
- ٦ - تحديد واضح لواجبات وسلطات ومسئوليات شاغلي الوظائف .
- ٧ - تفويض السلطة من أعلى المستويات الى أقلها بالتسلسل الطبيعي .
- ٨ - تحميل الرئيس كامل المسؤولية عن نتائج العمل الموكل اليه .
- ٩ - حصر مسؤولية الموظف عن نتيجة عمله أمام رئيس واحد فقط .
- ١٠ - اقران المسؤولية بالمحاسبة وتسهيل الرقابة الذاتية .

وسائل التنظيم الصناعي

وتشغل الوسائل التي تكفل تحقيق أهداف التنظيم الأوضاع الآتية :

- ١ - تهيئة النظم التي تؤدي الى تبسيط العمليات الصناعية ومحو العوائق التي تعترض الانتاج (Time & Motion & Method Study)
- وتحديد الأعباء والمسؤوليات المتصلة بمختلف الأعمال (Job Descriptions)
- وتنظيم الصلة بين الجهات المختلفة المشتركة في نشاط المنشأة (Communications)
- ٢ - الاختيار والتكوين على جميع المستويات للقوى المدربة ذات الكفاية المهنية العالمية مع تحقيق العدالة في الأجر عن طريق تقييم الوظائف (Job Rating) وتسعيرها (Job Pricing)
- وتهيئة وسائل التشجيع (Incentives)
- وايجاد الجو الصالح لرفع الروح المعنوية

وكيفية الحصول على أفضل استخدام للآلات المختلفة للاقلال من الجهد وزيادة الانتاجية وكان أول من وضع جداول حدد بها أنسب السرعات لتشغيل ماكينات الصناعات المعدنية (Speed and Feeds) كما كان يركز دراساته المختلفة المستويات القريبة لمجرى العمل بخلاف هنري فايول الذي انصبت دراساته للمستويات العليا للإدارة .

ثم ظهر في نفس الوقت هنري جانت (Henri Gantt) بالولايات المتحدة (١٨٦١ - ١٩١٩) وانصبت دراساته للحوافز وأثرها على الانتاجية وخاصة المكافآت التشجيعية كما أجرى عدة دراسات للعلاقة بين الإدارة والمجتمع .

ثم ظهرت ماري فوليت (Mary Follet) بالولايات المتحدة (١٨٦٨ - ١٩٣٢) وكانت متخصصة في العلوم السياسية وأرست بعض المبادئ الخاصة بسياسة شئون الأفراد والعلاقات الجماعية .

وظهر في نفس الفترة فرانك جيلبرت (Frank Gilbreth) بالولايات المتحدة (١٨٦٨ - ١٩٢٤) وركز أبحاثه في دراسة ظروف العمل والمجهود البشري وعلاقة ذلك بدراسة الوقت والحركة وجعل منها إحدى الوسائل الأساسية للإدارة في رفع الكفاية الانتاجية كما كان أول هؤلاء الرواد في وضع قواعد سليمة لسلم الترقى . وكيفية التأهيل لضمان استتباب العمل .

وقد تلى ذلك اتساع حجم المنشآت وتعدد مصالحها في جهات مختلفة وتنوع منتجاتها وأغراضها وازدياد المنافسة مما حتم على الإدارة وضع السياسات والتخطيط البعيد المدى بجانب مراقبة سير العمليات المختلفة وتطويرها وذلك بالاستعانة بالأجهزة المختلفة كالتخطيط ومراقبة الجودة والتنظيم الصناعي والبحوث الفنية والتدريب والأمن الصناعي والطب الصناعي .

أهداف التنظيم الصناعي

يهدف التنظيم الصناعي الى رفع الانتاجية أي الحصول على استخدام أفضل للطاقات البشرية والآلية والحرارية والخامات والمواد ، كما يعتمد على سلسلة من القيادات والمشرفين والمتصلين بمجرى الأعمال لاصدار القرارات العاجلة حتى يتسع وقت الإدارة للتخطيط والرقابة والمتابعة ، وبذا يتيسر لها تطبيق مبدأ اللامركزية في التنفيذ مع مركزية التخطيط والرقابة والمتابعة عن طريق وضع النظم السليمة التي تكفل سهولة متابعة سير العمل والاطمئنان الى نتائجه .

— أن تكون طرق الاتصالات وكذلك المسئوليات والسلطات المتصلة بكل وظيفة واضحة وسليمة (في هذا المجال يحسن تفادى انشاء وظيفة الوكيل الذى له نفس اختصاص الرئيس) . . (Line Assistant) وربما ليس له سلطاته وكذلك وظيفة المساعد (Staff Assistant)

— أن يكون هناك تجانس في الهدف للوظائف التى تتكون منها وحدة عمل واحد ، (بمعنى ألا يكون هناك مثلا شخص واحد مسئول عن التشغيل وفي نفس الوقت مسئولا عن مراقبة الجودة) .

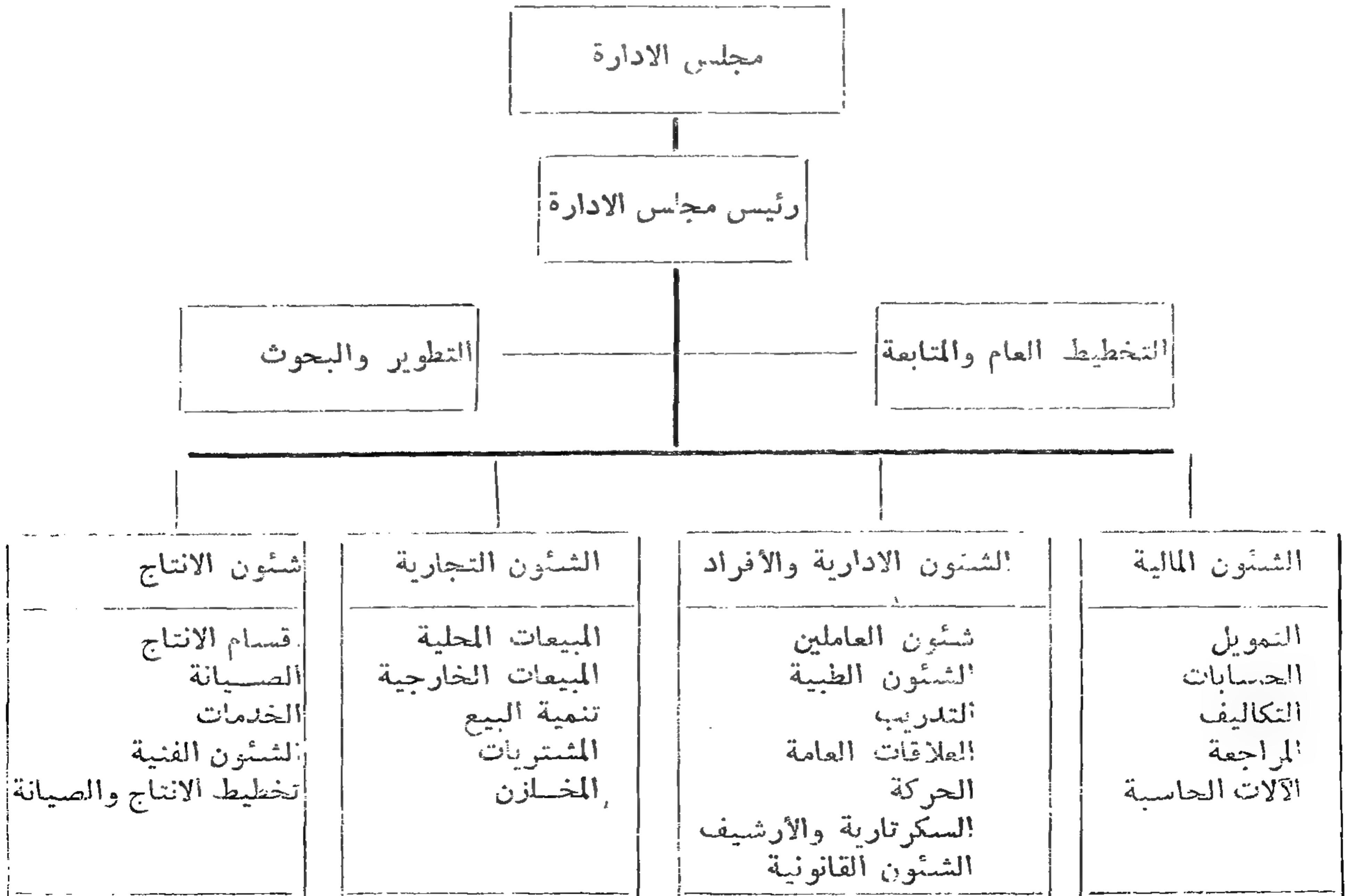
— أن يكون عدد الوظائف الخاضعة لاشراف أى رئيس طبقا لقواعد العرف الحديث عددا مناسبيا لضمان فاعلية الاشراف والتخطيط والرقابة من جهة ولضمان توزيع المسئوليات وتفويض السلطة للمرؤوسين من جهة أخرى (بمعنى أنه اذا كان عدد المرؤوسين أكثر من اللازم فان الرئيس لن يتمكن من توجيههم التوجيه السليم ولن يكون لديه الوقت الكافي للقيام بمهام التخطيط ورقابة العمل ، أما اذا كان عدد المرؤوسين أقل من اللازم فان الرئيس لى يشغل

بين العاملين وذلك للحصول على أكبر فائدة وأحسن انتاج من العنصر البشرى الذى يشغل الآن مركزا ممتازا بين العناصر الأخرى المشتركة في الانتاج .

٣ — الاستعانة قدر المستطاع بنظام آلية العمليات (Automation) للوصول الى التبسيط في الأعمال المطلوب انجازها ولزيادة الطاقة الانتاجية للعاملين ، ولتحسين النوع وثبات الجودة وتخفيض الفاقد والعدم والمعيوب ولتلافي الأخطاء .

٤ — وضع المعدلات النمطية لمختلف عناصر الانتاج ليسهل الرقابة على سلامة العمل ومراجعة نتائج التشغيل وذلك باتباع نظم ومراقبة الميزانية (Budgetary Control) ومراقبة جودة الانتاج (Quality Control) وكذلك الكفاية الانتاجية (Human Productivity) والنسب المالية للميزانات وعناصر الإيرادات والمصروفات (Financial Ratios) .

٥ — وضع الهيكل التنظيمى السليم للمنشأة ، لتوزيع أوجه النشاط المختلفة على أقسام مستقلة (أنظر خريطة رقم ١ التالية) على أن يراعى فيها القواعد الآتية :



(خريطة رقم ١)

(ب) دراسة أساليب العمل (Method Study) وهو تحليل كل عملية من حيث كيفية أدائها لالغاء الحركات الغير ضرورية بهدف تبسيط العمل ورفع الكفاءة الانتاجية .

(ج) تحديد الواجبات التي يقوم بها شاغلو الوظائف (Job Analysis and Description) وهو البيان الكتابي الواضح للواجبات التي يقوم بها شاغل الوظيفة بهدف تحديد المسؤولية .

(د) تقييم الوظائف وتسعيرها (Job Rating and Pricing) وهو تحديد قيمة نسبية لأعباء كل وظيفة بالمقارنة بالوظائف الأخرى بالمنشأة من حيث الجهد والمسئولية والمهارة ثم تصنيفها في فئات مختلفة للمرتبات بهدف تحقيق العدالة في تناسب المرتب مع أعباء الوظيفة .

(هـ) الاتصالات (Communications) وهو ايضاح

وقته سيلجأ الى المركزية ولن يقوم بتوزيع المسئوليات وتفويض السلطة للمرؤوسين .

— أن يكون الموظف مسؤولاً أمام رئيس مباشر واحد فقط . (أى يجب ألا يكون الموظف مسؤولاً عن بعض اختصاصاته أمام رئيس آخر) .

شئون العمل

ومن المجالات الرئيسية في التنظيم الصناعي دراسة شئون العمل وهي تشمل :

(أ) دراسة الحركة والوقت (Time and Motion Study) وهو تحليل كل عملية لتحديد الحركات التي يتطلب العمل اجرائها والوقت الذي تستغرقه لانجازها على الوجه المطلوب ، بهدف تساوى مستوى الجهد بين العاملين في الوظائف المختلفة .

القيادة الجماعية في إدارة الشركات

م	نوع العمل	التخطيط والتوجيه	التطوير والتحكم	الشؤون المالية	الشؤون الادارية	الشؤون التجارية	شؤون الإنتاج	ملاحظات	
								الوقت	الجهد
١	تحديد أهداف الشركة	Δ	Δ	Δ	Δ	Δ	Δ	×	×
٢	تحديد البنية التنظيمية للشركة	Δ	Δ	Δ	Δ	Δ	Δ	×	×
٣	تحديد برامج التشغيل	Δ	Δ	Δ	Δ	Δ	Δ	×	×
٤	تحديد هيكل التنظيم	Δ	Δ	Δ	Δ	Δ	Δ	×	×
٥	تحديد طرق العمل	Δ	Δ	Δ	Δ	Δ	Δ	×	×
٦	تحديد طرق العمل	Δ	Δ	Δ	Δ	Δ	Δ	×	×
٧	تحديد طرق العمل	Δ	Δ	Δ	Δ	Δ	Δ	×	×
٨	تحديد طرق العمل	Δ	Δ	Δ	Δ	Δ	Δ	×	×
٩	تحديد طرق العمل	Δ	Δ	Δ	Δ	Δ	Δ	×	×
١٠	تحديد طرق العمل	Δ	Δ	Δ	Δ	Δ	Δ	×	×
١١	تحديد طرق العمل	Δ	Δ	Δ	Δ	Δ	Δ	×	×
١٢	تحديد طرق العمل	Δ	Δ	Δ	Δ	Δ	Δ	×	×
١٣	تحديد طرق العمل	Δ	Δ	Δ	Δ	Δ	Δ	×	×
١٤	تحديد طرق العمل	Δ	Δ	Δ	Δ	Δ	Δ	×	×
١٥	تحديد طرق العمل	Δ	Δ	Δ	Δ	Δ	Δ	×	×
١٦	تحديد طرق العمل	Δ	Δ	Δ	Δ	Δ	Δ	×	×
١٧	تحديد طرق العمل	Δ	Δ	Δ	Δ	Δ	Δ	×	×
١٨	تحديد طرق العمل	Δ	Δ	Δ	Δ	Δ	Δ	×	×
١٩	تحديد طرق العمل	Δ	Δ	Δ	Δ	Δ	Δ	×	×
٢٠	تحديد طرق العمل	Δ	Δ	Δ	Δ	Δ	Δ	×	×
٢١	تحديد طرق العمل	Δ	Δ	Δ	Δ	Δ	Δ	×	×
٢٢	تحديد طرق العمل	Δ	Δ	Δ	Δ	Δ	Δ	×	×
٢٣	تحديد طرق العمل	Δ	Δ	Δ	Δ	Δ	Δ	×	×
٢٤	تحديد طرق العمل	Δ	Δ	Δ	Δ	Δ	Δ	×	×
٢٥	تحديد طرق العمل	Δ	Δ	Δ	Δ	Δ	Δ	×	×
٢٦	تحديد طرق العمل	Δ	Δ	Δ	Δ	Δ	Δ	×	×
٢٧	تحديد طرق العمل	Δ	Δ	Δ	Δ	Δ	Δ	×	×
٢٨	تحديد طرق العمل	Δ	Δ	Δ	Δ	Δ	Δ	×	×
٢٩	تحديد طرق العمل	Δ	Δ	Δ	Δ	Δ	Δ	×	×
٣٠	تحديد طرق العمل	Δ	Δ	Δ	Δ	Δ	Δ	×	×
٣١	تحديد طرق العمل	Δ	Δ	Δ	Δ	Δ	Δ	×	×
٣٢	تحديد طرق العمل	Δ	Δ	Δ	Δ	Δ	Δ	×	×
٣٣	تحديد طرق العمل	Δ	Δ	Δ	Δ	Δ	Δ	×	×
٣٤	تحديد طرق العمل	Δ	Δ	Δ	Δ	Δ	Δ	×	×
٣٥	تحديد طرق العمل	Δ	Δ	Δ	Δ	Δ	Δ	×	×
٣٦	تحديد طرق العمل	Δ	Δ	Δ	Δ	Δ	Δ	×	×
٣٧	تحديد طرق العمل	Δ	Δ	Δ	Δ	Δ	Δ	×	×
٣٨	تحديد طرق العمل	Δ	Δ	Δ	Δ	Δ	Δ	×	×
٣٩	تحديد طرق العمل	Δ	Δ	Δ	Δ	Δ	Δ	×	×
٤٠	تحديد طرق العمل	Δ	Δ	Δ	Δ	Δ	Δ	×	×
٤١	تحديد طرق العمل	Δ	Δ	Δ	Δ	Δ	Δ	×	×
٤٢	تحديد طرق العمل	Δ	Δ	Δ	Δ	Δ	Δ	×	×
٤٣	تحديد طرق العمل	Δ	Δ	Δ	Δ	Δ	Δ	×	×
٤٤	تحديد طرق العمل	Δ	Δ	Δ	Δ	Δ	Δ	×	×
٤٥	تحديد طرق العمل	Δ	Δ	Δ	Δ	Δ	Δ	×	×
٤٦	تحديد طرق العمل	Δ	Δ	Δ	Δ	Δ	Δ	×	×
٤٧	تحديد طرق العمل	Δ	Δ	Δ	Δ	Δ	Δ	×	×
٤٨	تحديد طرق العمل	Δ	Δ	Δ	Δ	Δ	Δ	×	×
٤٩	تحديد طرق العمل	Δ	Δ	Δ	Δ	Δ	Δ	×	×
٥٠	تحديد طرق العمل	Δ	Δ	Δ	Δ	Δ	Δ	×	×

بمستوى الأداء الذي سبق الاتفاق عليه (Standards of Performance) أو بنتائج تقارير النشاط (Merit Rating).

وبمقتضى هذه الدراسات الأساسية يمكن تحديد وصف واجبات الوظائف والمواصفات المطلوب توافرها في شاغليها وعددهم وتقييم الوظائف وتسعيرها ومراقبة نتائج التشغيل لمكافحة المجتهد ومحاسبة الذي لم يحقق النتائج المطلوبة رغم تهيئة الظروف المناسبة.

الدراسات التنظيمية

تبين الخريطة رقم ٣ التالية المجالات المختلفة التي تشملها الدراسات التنظيمية والوسائل المتبعة لأجرائها وتسلسلها والتي سبق شرح الدراسات الأساسية منها بالتفصيل.

وسنتولى باختصار شرح هذه الوسائل بصفة عامة، دون شرحها بأسهاب.

وتبين الخريطة أن هناك ترابطا وتسلسلا لهذه الدراسات، بحيث تعتمد كل منها على نتائج الدراسة السابقة لها - مما يتعذر معه إجراء أية دراسة منها إلا بعد إجراء الدراسات السابقة لها متدرجين من البداية وفقا لخطوط التدرج الموضحة بالخريطة.

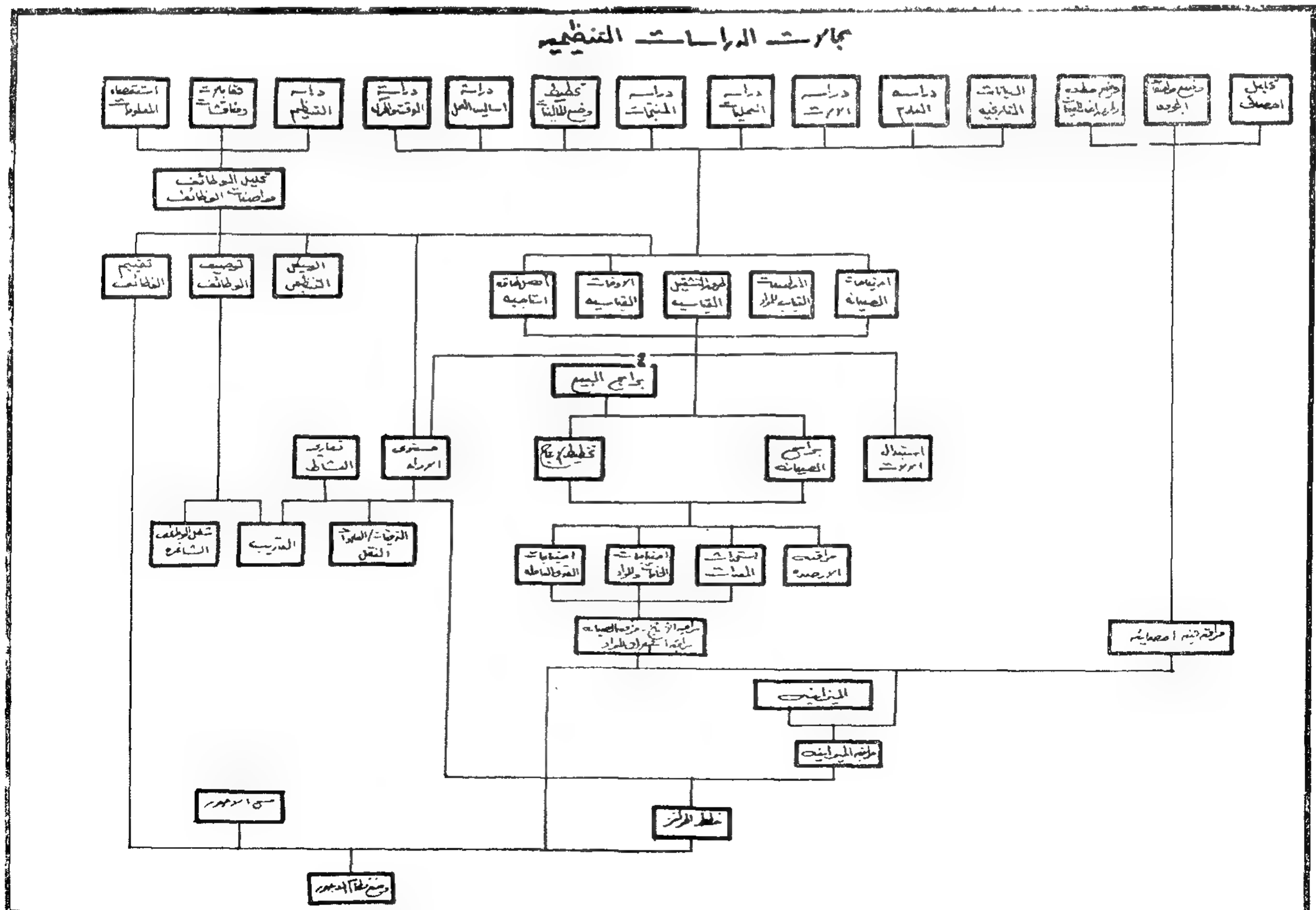
الهيكل التنظيمي للمنشأة وعلافة الأقسام المختلفة ببعضها البعض وإنشاء دليل تنظيمي (Organization Manual) يشمل تفاصيل الهيكل التنظيمي للمنشأة وتوزيع العمل على جميع مستويات الإدارة العليا وبين مختلف الأقسام (انظر جدول رقم ٢ خريطة القيادة الجماعية والتي يمكن عن طريقها كذلك تحديد اللجان المختلفة بالشركة وأعضائها ومسئولية كل منهم).

شئون العاملين

كذلك فلا بد أن تشمل شئون العاملين :

(١) المواصفات الواجب توافرها في شاغل الوظيفة (Job Occupant Specifications) وهو البيان الكتابي للقدرات والصفات المطلوب توافرها في شاغل الوظيفة بهدف وضع الشخص المناسب في المكان المناسب.

(ب) المحفزات (Incentives) ومنها المادية كالمكافآت التشجيعية (Financial Incentives) والغير مادية كرفع المهارة عن طريق التدريب والبعثات (Training and Missions) ليتأهيل والترقية ويحسن أن ترتبط المحفزات بنتائج الميزانيات التقديرية (Budgetary Control) أو بالنتائج التي حققها شاغل الوظيفة ومقارنتها



(الخريطة رقم ٣)

– دراسة توزيع ووضع الهيكل التنظيمي
(Organization Structure)

الناحية الرئيسية الثانية :

وتتضمن الدراسات لأوجه النشاط المختلفة ،
الفنية والإدارية ، وهي دراسات تم شرح بعضها
بالدراسات التنظيمية الأساسية ، ويمكن
تقسيمها إلى المراحل المبينة فيما بعد :

المرحلة الأولى :

وتشمل الدراسات التي تجرى والنتائج
التي يمكن التوصل إليها وهي :

- دراسة الوقت والحركة (Time & Motion Study)
- دراسة أساليب العمل (Method Study)
- تخطيط وضع الماكينات (Plant Lay-out)
- دراسة المنتجات (Product Analysis)
- تحليل العمليات ودراساتها (Process Analysis)
- دراسة الآلات (Machine Analysis)
- دراسة العادم (Waste Analysis)

ويستعان عند إجراء هذه الدراسات
بالبينات التاريخية السابقة والتطورات المختلفة
التي تمت (Historical Data) .

ومن المعلومات المستقاة من هذه الدراسات
ومن تحليل ووصف واجبات الوظائف السابق
الإشارة إليه في الدراسة الرئيسية الأولى يمكن
تحديد :

- * أفضل قدرة إنتاجية (Optimum Capacity)
- * الأوقات القياسية (Time Standards)
- * المواصفات المحددة لطرق التشغيل
(Standard Procedures)
- * المواصفات القياسية للمواد
(Material Standards)
- * احتياجات الصيانة
(Maintenance Requirements)

المرحلة الثانية :

وهي مرحلة التخطيط لاستخدام نتائج
الدراسات السابقة في تطبيق الأنظمة المقترحة فمن
معرفة سياسة وبرامج البيع (Sales Program)
ومع أخذ النتائج السابقة في الاعتبار يمكن
تخطيط ووضع برامج الإنتاج والصيانة :
(Production Planning & Maintenance)

والخريطة تبين ثلاث نواحي رئيسية
للدراسات – سنتولى شرحها كل على حدة وبيان
النتائج التي يمكن الحصول عليها ، ثم نبين في
النهاية الدراسات العامة التي يمكن إجراؤها
والنتائج النهائية التي يمكن التوصل إليها من
واقع هذه الدراسات .

والنواحي الرئيسية الثلاث هي :

- دراسات خاصة بالوظائف والهيكل
التنظيمي لتوزيع العمل .
- دراسات تخصصية للنواحي الفنية
والإدارية للعمل .
- دراسات مواصفات الجودة ومراقبتها .

الناحية الرئيسية الأولى :

تتضمن الدراسات الخاصة بالوظائف بحث
الهيكل التنظيمي لتوزيع العمل لتعديله وفقا
للاسس التنظيمية السليمة واعداد وصف
واجبات الوظائف ومواصفاتها وتقييمها ، ويتم
ذلك عن طريق أحد أو كل الوسائل التالية :

– اعداد صحائف استقصاء المعلومات عن
شاغلي الوظائف (Questionnaires) تملأ بواسطة
العاملين بالمنشأة .

– ملاحظة ومناقشة (Interviews and
Observations) شاغلي الوظائف أثناء تأديتهم
لعملهم مع مناقشة رؤسائهم المباشرين لمعرفة
واجباتهم .

– تحليل ودراسة التنظيمات
(Organization Analysis) بالمنشأة من توزيع
أوجه النشاط الرئيسية والفرعية وعلاقتها
ببعضها .

ومن واقع عملية جمع المعلومات السابقة يمكن
تحليل الوظائف (Job Analysis) واعداد وصف
لواجبات كل وظيفة بالمنشأة (Job Description)
الذي يستعان بالمعلومات المستفادة منه في :

– تقييم الوظائف (Job Evaluation)
أحد الدعائم التي يبنى عليها نظم المرتبات والأجور
السليمة المرتبطة بالانتاجية والتي سنتعرض
لذكرها فيما بعد .

– اعداد المواصفات المطلوب توافرها في شاغلي
الوظائف (Job Specification) التي يستعان بها
في شغل الوظائف الشاغرة (Hiring) وللتدريب
ببرامج تتمشى مع احتياجات العمل والافراد تحدد
من مقارنة مدى ادائهم الفعلي (Merit-Rating)
بالمواصفات التي يجب توافرها فيهم .

* وضع خطة وطرق أخذ العينات
(Sampling-Plan and Procedures)

* وضع مواصفات الجودة
(Quality Specifications)

* التحليل الإحصائي
(Statistical Analysis)

ومن واقع النتائج التي حصلنا عليها من
إجراء الدراسات السابقة يمكن إجراء الدراسات
التالية والمبينة بالخريطة وهي :

— المراقبة عن طريق الميزانيات التقديرية
(Budgetary Control) ومقارنة ما تحققه مراكز
النشاط المختلفة للمنشأة مع التقديرات الموضوعة
لنواحي التشغيل لأفتردة المحددة المستقبلية .

— مكافآت التشغيل (Incentive Plans)
ومنها المرتبطة بالانتاجية كوظائف الأعمال
المصنعية اليدوية أو المرتبطة بمستوى الأداء .
(Standards of Performance) كالوظائف

الرئيسية أو المرتبطة بنتائج الميزانيات التقديرية
كالوظائف الإشرافية والرئيسية أو المرتبطة بالنتائج
العامة للتشغيل كالوظائف الإدارية والكتابية
والأعمال المتنوعة .

— ربط نظام المرتبات

(Salary Administrations)

بتقييم الوظائف مع أخذ المرتبات السائدة في
الاعتبار (Salary Survey) أو القوانين المنظمة
لها وكذلك مع أخذ مكافآت التشغيل ان وجدت
في الاعتبار .

ومن نتائج الدراسات السابقة ووفقا
لاحتياجات وامكانيات المنشأة تحدد الآلات
والمعدات التي يجب استبدالها لتتمشى مع
المطالب والتطور (Machine Replacement)
وتشمل هذه المرحلة أيضا تحديد احتياجات
تنفيذ الخطة الموضوعة من قوى عاملة
(Man-power Requirement) وخامات ومواد
(Material Requirements) ومراقبة أرصدها :
(Inventory Control)

وكذلك أفضل طريقة لاستخدام المعدات الموجودة
(Machine Utilization)

المرحلة الثالثة :

وبعد تحديد هذه الاحتياجات يبدأ في التنفيذ
طبقا للتخطيط الموضوع مما يتطلب المتابعة للتأكد
من تحليل النتائج ، أو تعديل الخطة لتحقيقها
وتتم المتابعة بمقارنة النتائج الفعلية بالأهداف
الموضوعة طبقا للخطة وذلك بالنسبة للإنتاج
والصيانة واستهلاك المواد :

مراقبة الإنتاج (Production Control)
مراقبة الصيانة (Maintenance Control)
مراقبة استهلاك المواد (Materials Control)

الناحية الرئيسية الثالثة :

وتتناول هذه المرحلة مراقبة وتطوير جودة
الإنتاج عن طريق المراقبة الفنية الإحصائية
(Statistical Quality Control) وتقوم هذه
الدراسة أساسا على :

* * *

REFERENCES

2. The impulse breakdown voltage-time characteristics of soil samples, for dry and moist samples, show that the time to breakdown increase as the impulse ratio (impulse voltage/static breakdown voltage) decreases.
3. For a certain soil sample, the volt-time characteristics for different field configurations, are different.
4. The type of soil and the shape of graine effect the impulse characteristics.
5. For the different soil samples, the time to breakdown voltage increases with its moisture content and the impulse breakdown voltage is considerably higher than the static breakdown voltage.
6. The impedance of a dry soil sample decreases with the increase in frequency. But when the soil sample is wet the impedance is approximately constant.
7. There is a remarkable difference between the 50 Hz and impulse impedances for the different soil samples. The ratio between the impulse impedance to the impedance under power frequency lies between 0.154 and 0.531.
8. The resistance of concentrated earth electrode at high impulse currents, which lead to the development of the ionization zone, does not depend on the geometric dimension but is determined by the amplitude of the current, the resistivity of the soil, and the impulse characteristics of the electrode itself.
9. The impulse impedances as a function of time of a distributed earth electrode consists of two terms, a steady state resistance R and an additional transient inductive resistance, which depends on the instant at which the current passes, $\frac{Ll'}{3t}$ The impulse impedance Z (i) tends to approach its steady state value R , especially for rods of smaller length l .

1. H.M. Towne, «Impulse characteristics of driven grounds», General Electric Review, Vol. 31, November 1928, pp. 605 — 609.
2. G.G. Brown and others, «Unit operation», Book, John Wiley and Sons, London 1960.
3. H.O. Buckman, «The nature and properties of soils», Book, MacMillan Company, London, 1960.
4. D.V. Razing, «High Voltage Technology», Book, Moscow, 1963.
5. P.L. Bellaschi, R.E. Armington, and A.E. Snowden, «Impulse and 60 — cycle characteristics of driven grounds II», AIEE Trans, Vol. 61, June 1942, pp. 349 — 363.
6. E.D. Sunde, «Earth conduction Effect in Transmission Systems» D. Van Norst and blook Company, 1949.
7. S.S. Devgan and E.R. White head, «Analytical models for distributed grounding systems», IEEE trans., September/October 1973, Vol. 92, No. 5.
8. A.G. Zeitoun, «Breakdown Characteristics of long air gaps using long duration impulse waves», University of Libya Bulletin of the Faculty of Engineering, Vol. 1, 1971.
9. J.R. Eaton, «Impulse characteristics of electrical coonections to earth», General Electric Review, Vol. 47, October 1944, pp. 41 — 50.
10. P.L. Bellaschi, «Impulse and 60 — cycle characteristics of driven grounds» AIEE trans. Vol. 60, 1941, p. 123.

$$\begin{aligned}
 Z(0, t) &= \frac{1}{g_1'} \left[1 + \frac{2T_1}{t} \sum_{k=1}^{\infty} \frac{1}{k^2} \right] \\
 &= \frac{1}{g_1'} \left[1 + \frac{2T_1}{t} \frac{\pi^2}{6} \right] \\
 &= R + \frac{L_1'}{3t} \dots \dots (7)
 \end{aligned}$$

From equation (7) it is clear that the impulse impedance of a distributed earth electrode consists of two terms, 1) steady state resistance R . 2) Additional transient inductive resistance, which depends on the instant at which the current passes,

$$\frac{L_1'}{3t}$$

(2) With the Effect of the Ionization Zone :

If the current density i , based on the flowing current from the earth electrode to the surrounding earth, leads to the appearance of a gradient $E > E_{cr}$, breakdown in the earth near the electrode would take place. The ionization zone occurred has a radius depending on the current density.

The decrease of the potential, and hence the current density in parts far from the beginning of the distributed earth electrode, causes the discharge at the end of the electrode to be more limited than that at the beginning of the electrode. As a result of this the conductivity of the distributed earth electrode at its end will be reduced, i.e. it depends not only on the amplitude of current I and resistivity ρ but also on its position.

If the conductance per unit length of the distributed earth electrode in the steady state operation is (4) :

$$g = \frac{1}{R_1'} = \frac{\pi}{\rho \ln \frac{r}{r_0}}$$

The the impulse conductance g_i , with the existence of an ionization zone radius

$$Ph = \frac{l's}{\pi \epsilon r} \quad \text{will be :}$$

$$\begin{aligned}
 g_i &= \frac{\pi}{\rho \ln \frac{r}{r_{Ph}}} = \frac{\pi}{\rho \ln \frac{r \pi E_{cr}}{i \rho}} \\
 &= \frac{\pi}{\rho \ln \frac{i \pi E_{cr}}{V g_i \rho}} \dots \dots (8)
 \end{aligned}$$

Where i is the current flowing from a unit length of earth electrode and $V = f(x)$ is the potential of the earth electrode.

Calculation of the impulse resistance of a distributed earth electrode using an equivalent circuit consisting of an inductance and a non linear conductance $g_i = f(V)$, will lead to non linear differential equations which can be only solved by approximate methods.

At relatively small lengths of earth electrodes, when the current density is maximum, ionization process in the soil not only compensate the effect of the inductive resistance of the electrode, but leads to a decrease in its resistance. In this case the impulse coefficient of the earth electrode α_i is less than unity.

As the length of the earth electrode increases, the effect of the inductance will increase and the impulse coefficient will first be equal to unity, and then increases. For this condition the use of earth electrode is not advisable, since the impulse resistance will not decrease with the increase of length l .

CONCLUSIONS

1. Sand, Loamy Sand, and clay loam, when subjected to impulse voltages will puncture in a fashion very similar to insulating material when the voltage gradient exceeds a certain critical value, dependent upon the type of soil and the moisture content.

Equation (4) has been also solved by computer.

The dependence of an impulse coefficient α_i on I is illustrated in Fig. (10), for $E_{cr} = 6, 9, 12$ and 15 KV/cm, and K equals 0.01 and 0.05 . The value of r used in the computation is that of the equivalent hemisphere radius for a driven rod of length 6 m. and radius 5.08 cm (standard rod used in practice).

The value of the impulse resistance of a cylindrical electrode can be calculated in a similar way, but with the addition of new assumptions because the shape of electric field near the electrode is somewhat complicated.

Impulse Resistance of Distributed earth electrode :

(1) Without the Ionization Zone :

In this case the amplitude of the impulse current is relatively small, and the resistivity of the earth is constant i.e. $\rho_i = \rho$

The equivalent circuit of the earth electrode in this case is illustrated in Fig. (11). where, L = inductance/unit length

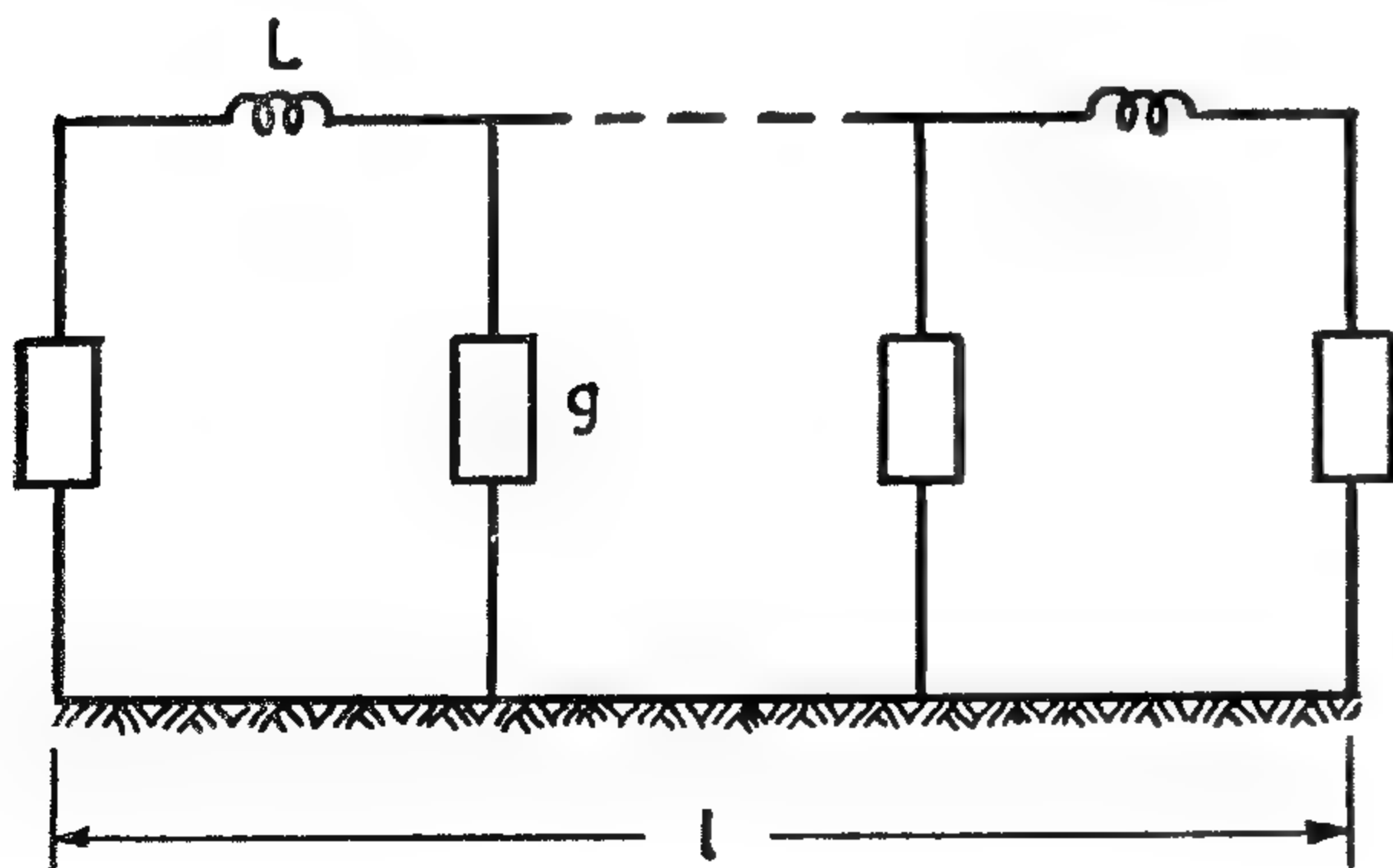


FIG. (11) EQUIVALENT CIRCUIT OF DISTRIBUTED EARTH ELECTRODE.

g = conductance/unit length

$L = 0.2 \rho_r - 0.31) \mu \text{ H/m}$

where, l' = length of the earth electrode

r = the radius of the earth electrode.

The differential equations of this equivalent circuit are as follows :

$$-\frac{\partial v}{\partial x} = L \frac{\partial i}{\partial t}$$

$$-\frac{\partial i}{\partial x} = v g$$

By solving these equations, assuming a linear current time relation at the beginning of earth electrode ($I(0,t) = at$), the voltage on the earth electrode is found to be.

$$v(x,t) = \frac{\alpha}{g l} \left[t + 2 \tau_1 \sum_{k=1}^{\infty} \frac{1}{k^2} (1 - e^{-t/\tau_k}) \cos \frac{k\pi x}{l} \right] \dots (5)$$

where

$$\tau_k = \frac{L g l^2}{k^2 \pi^2}, \tau_1 = \tau_k = 1 - \frac{L g l^2}{\pi^2}, \tau_k = \frac{\tau_1}{k^2}$$

From this results, the impulse impedance of the distributed earth electrode can be obtained :

$$Z(0,t) = \frac{V(0,t)}{I(0,t)} = \frac{1}{g l} \left[1 + \frac{2 \tau_1}{t} \sum_{k=1}^{\infty} \frac{1}{k^2} (1 - e^{-t/\tau_k}) \right]$$

If $\frac{t}{\tau_1} > 3, \tau_0 e^{-t/\tau} < 0.05$

$$1 - e^{-\frac{t}{\tau_1}} = 1 \dots (6)$$

Then equation (6) can be simplified to

$\alpha_i = \frac{R_i}{R_o}$ (proportional to $\frac{1}{\sqrt{I\rho}}$)
or, generally,

$$\alpha_i = F(I\rho) \quad \dots (3)$$

In fact this important function can be used for any shape of electrodes.

For a hemisphere electrode of radius r
the impulse coefficient α_i is :

$$\alpha_i = \frac{R_i}{R} = \frac{2\pi r}{\rho} \sqrt{\frac{\rho}{2\pi L K}} \left(\frac{\pi}{2} - \tan^{-1} \sqrt{\frac{1}{K E_{cr}}} \right) \\ = \sqrt{\frac{2\pi r^2}{I \rho K}} \left(\frac{\pi}{2} - \tan^{-1} \sqrt{\frac{1}{K E_{cr}}} \right) \dots (4)$$

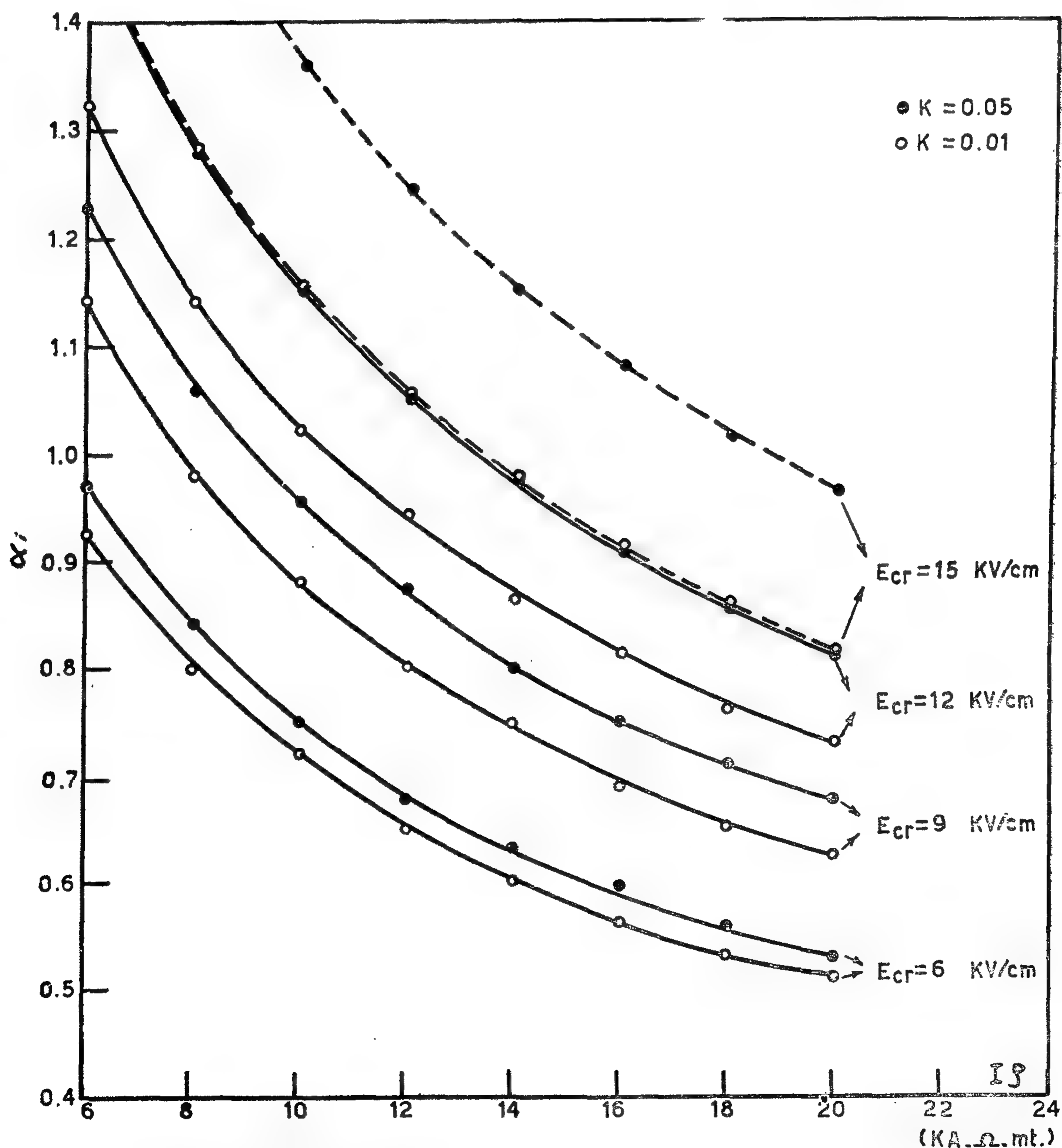


FIG. (10) RELATION BETWEEN THE IMPULSE COEFFICIENT α_i WITH $I\rho$ FOR A DRIVEN ROD OF 6 mt. LENGTH AND 5.08 cm RADIUS.

Equation (2) has been solved by translating the procedure of calculation into a FORTRAN IV program which is used with an I.C.L. 1905 digital computer.

Curves relating the impulse resistance R_i and the impulse current I are illustrated in Fig. (9), for critical field intensity $E_{cr} =$

6KV/cm. The resistivity ranges from $100 \Omega m$ to $500 \Omega m$, and K equals 0.01 and 0.05.

It is known that the steady state resistance R_o is proportional to the earth resistivity and hence the impulse coefficient for a hemisphere electrode equals :

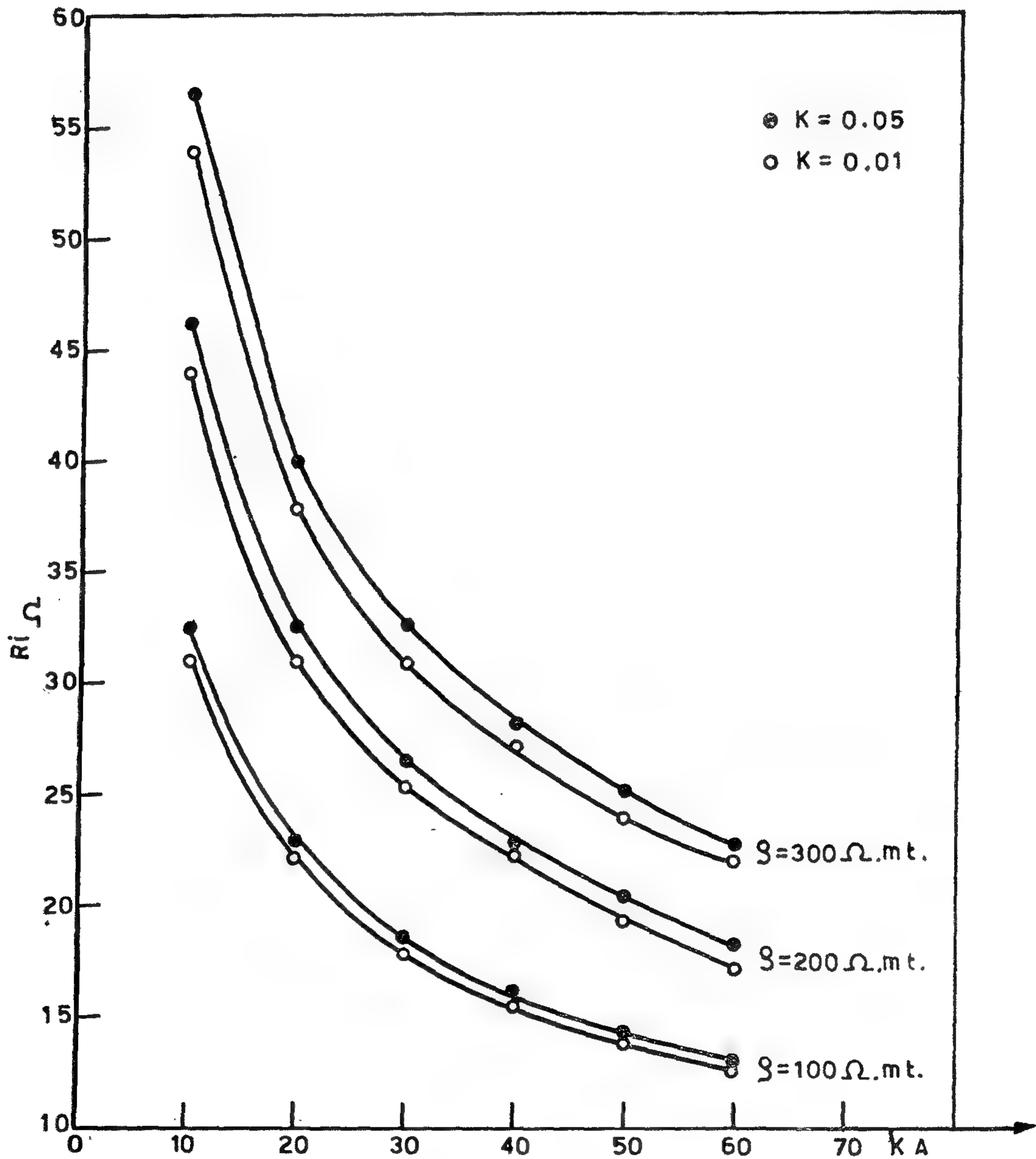


FIG. (9) RELATION BETWEEN THE IMPULSE RESISTANCE OF A HEMISPHERE ELECTRODE AND THE IMPULSE CURRENT, $E_{cr} = 6 \text{ KV} / \text{cm}.$

resistance R_0 , then R_i goes to its minimum value which occurs, after the maximum value of current. Following that R_i starts to increase again. As a result of this, the maximum value of the voltage wave comes before that of the current wave.

For the purpose of calculating R_i we have to assume that the development of the ionization zone is uniform, i.e. assuming that the limits of the ionization zone are those defined by the area and a field intensity equal to E_{cr} .

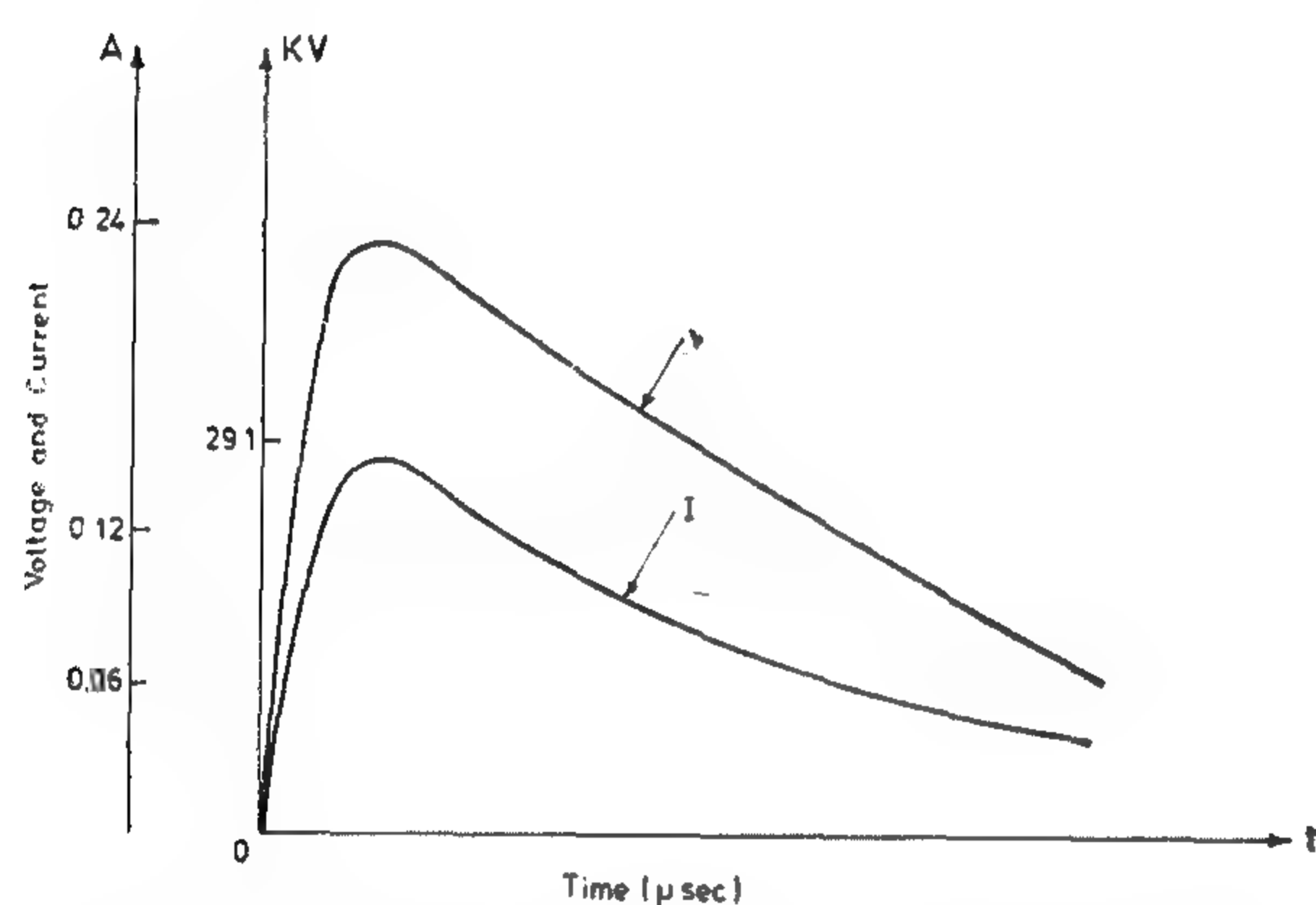


Fig. (7). Typical oscillograms of impulse current voltage during impulse discharge of a sand sample (Mesh number 20, plate to plate electrode with 10 cm separation, Moisture content 0.23%).

To simplify the analysis, the impulse characteristics of the earth $p_i/p = f(E)$, is assumed to be a straight line between $E = 0$ and $E = E_{cr}$. Therefore,

$$\frac{p_i}{p} = 1 - K E_{cr}.$$

The value of K for sandy clay, and organic soils, with waves of front times $t_f = 2$ to 4μ Sec. is from (0.01 to 0.05) (4).

The impulse resistance R_i of a hemispherical electrode, of radius r_0 replaced at the surface of an earth having a resistivity will be calculated.

For a current of amplitude I , whose front time is t_f the limit of the ionization zone which agrees with the above assumptions

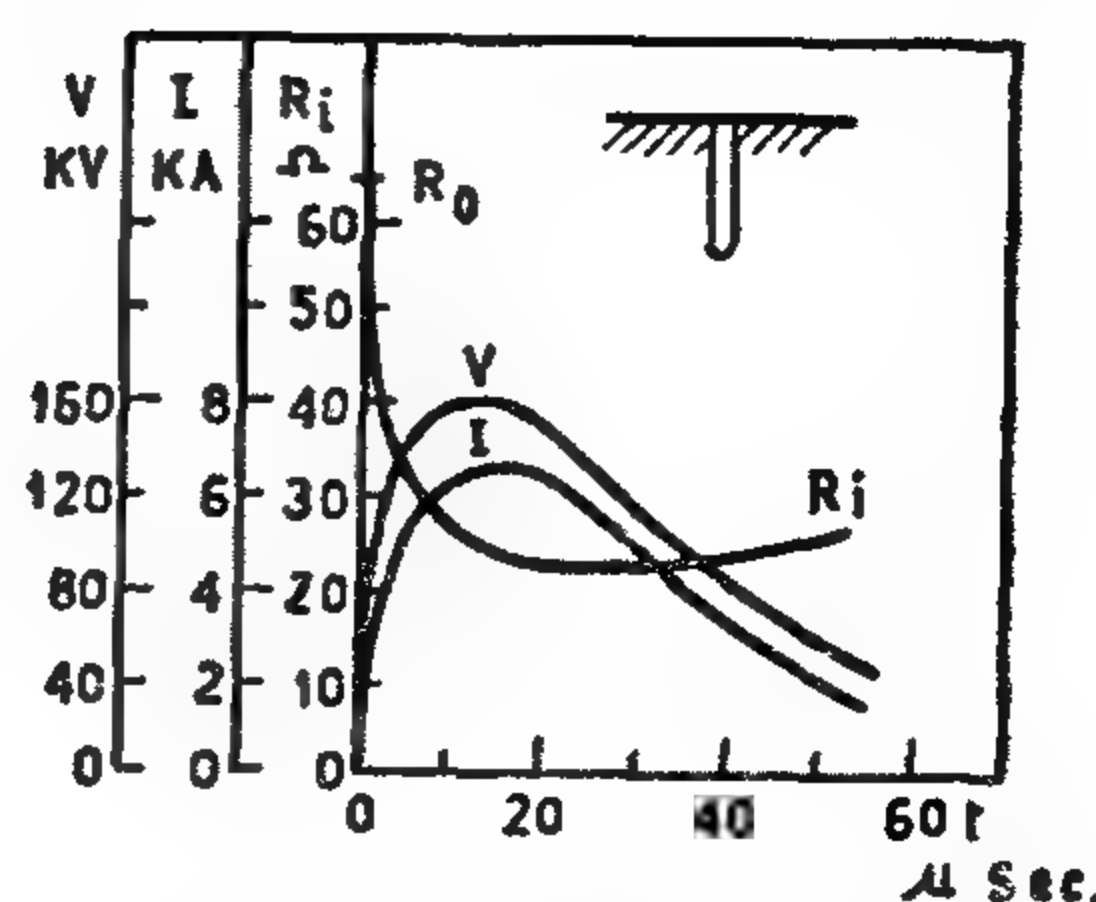


FIG. (8) CHANGE OF IMPULSE VOLTAGE, CURRENT AND RESISTANCE WITH TIME:

will be a hemisphere of radius r_{ph} at which electric field intensity E equals the breakdown field intensity of the earth E_{cr} . at time equal t_f one can write :

$$E = i \rho_i = \frac{I}{2\pi r_{ph}} \rho (1 - KE)$$

where, i = current density.

From this equation, when $E = E_{cr}$, the virtual radius of electrode equals.

$$r_{ph} = \sqrt{\frac{I \rho (1 - K E_{cr})}{2\pi E_{cr}}} \dots \dots (1)$$

Then the impulse resistance of a hemisphere electrode for a current I , which causes the development of the ionization zone, is,

From this equation it is shown that the

$$R_i = \frac{V}{I} = \sqrt{\frac{\rho}{2\pi I K}} \left[\frac{\pi}{2} - \tan^{-1} \sqrt{\frac{1}{K E_{cr}} - 1} \right] (2)$$

resistance of a concentrated electrode, for high impulse currents, does not depend on the geometric dimension but it is rather determined by the amplitude of the current I , the resistivity of soil p and the impulse characteristic of the electrodes itself.

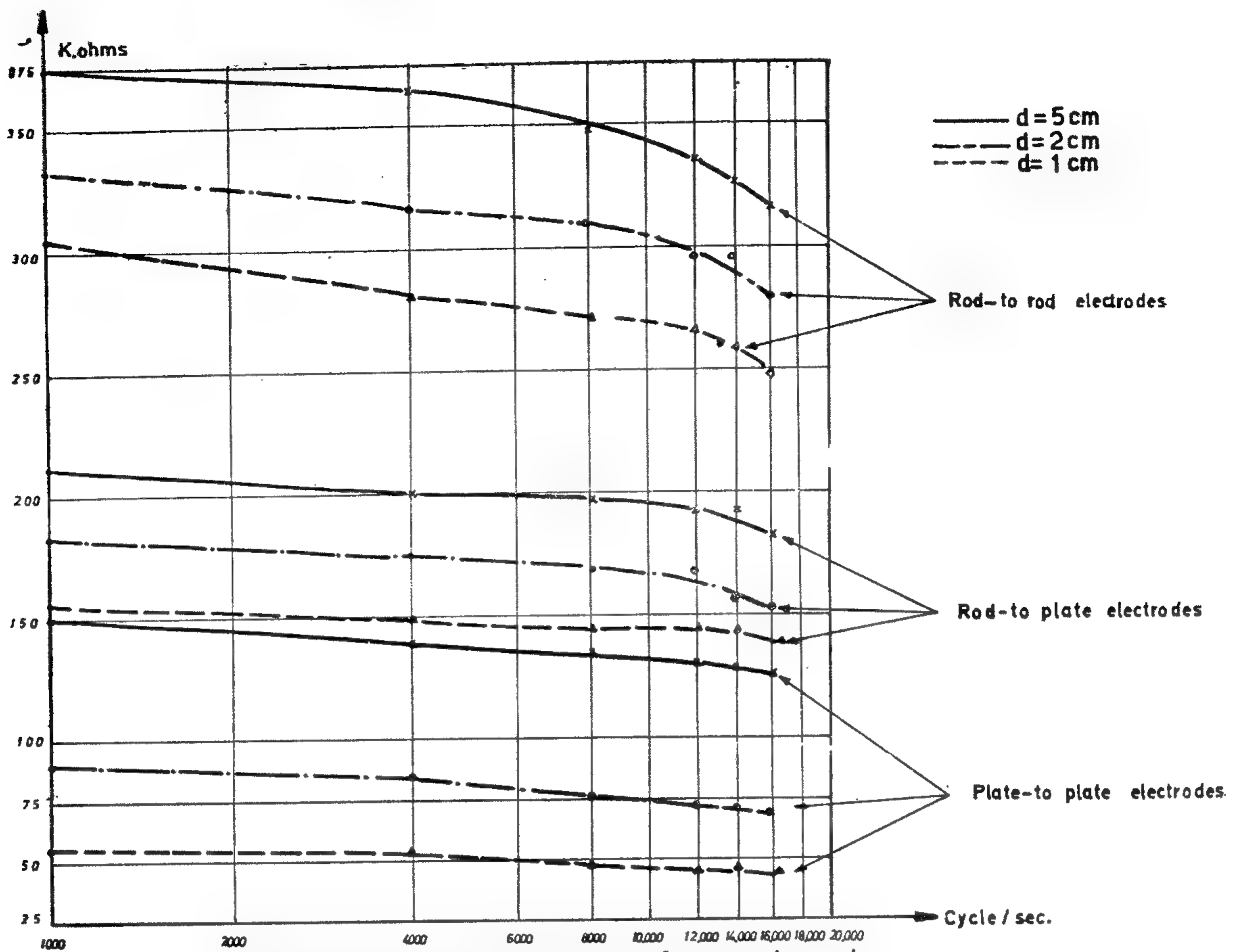


FIG. (5) Variation of impedance with frequency for a sand sample (Mesh No.20, Moisture content 0.23%)

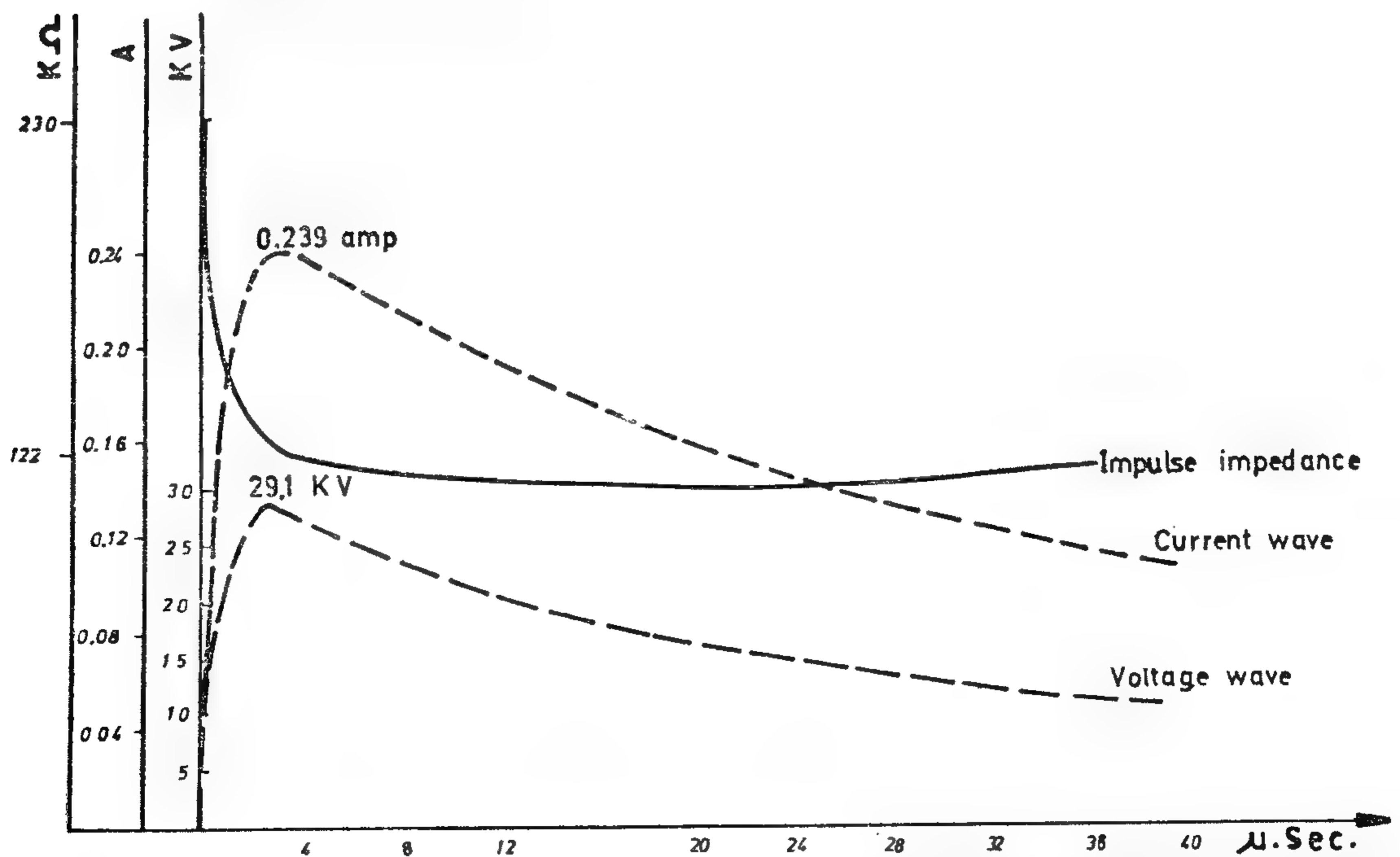


FIG. (6) Variation of impedance during impulse discharge of a sand sample of mesh number 20 between plate-to-plate electrodes with 10 cm separation moisture content 0.23%

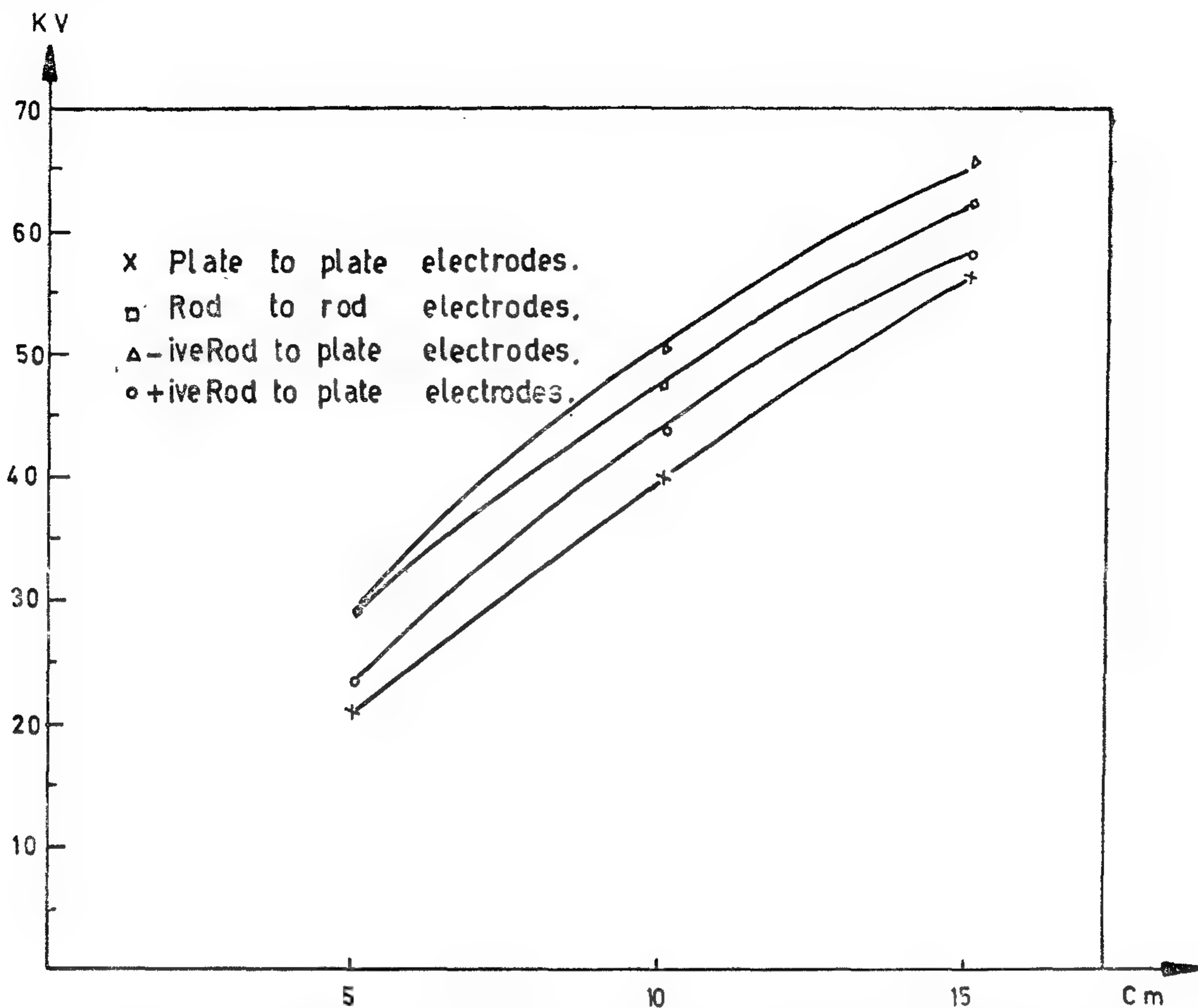


FIG. (4) Variation of critical breakdown impulse voltage with the separation between electrodes for clay loam. (Moisture content 0.23%)

CALCULATION OF THE IMPULSE-EARTH RESISTANCE OF ELECTRODES :

Grounding Arrangements :

Grounding arrangements may be classified as concentrated, distributed, or a combination of both. Concentrated grounds take a variety of forms, among them are driven rods, tower footings, metal plates, or relatively short radial conductors from the tower buried a few centimeters below the surface of the earth. The last configuration is sometimes called a «crow foot» counterpoise and the conductors commonly terminate in short driven rods. More sophisticated arrangements involve large diameter pipes in drilled holes, sometimes with special conducting slurries. Distributed grounding sys-

tems usually consist of buried conductors running parallel to the transmission conductors. Frequently, such conductors extend from one tower to another and are called «continuous counterpoises» in this case.

Impulse Resistance of Concentrated Earth Electrode :

During the impulse current, the impulse resistance of the earth electrode will vary due to the change of the volume of the ionization zone around the electrode. Fig. (8) shows the variation of the impulse voltage V , the impulse current I , and the impulse resistance R_i with time for a concentrated earth electrode. As the impulse wave is applied R_i initially will be the steady state

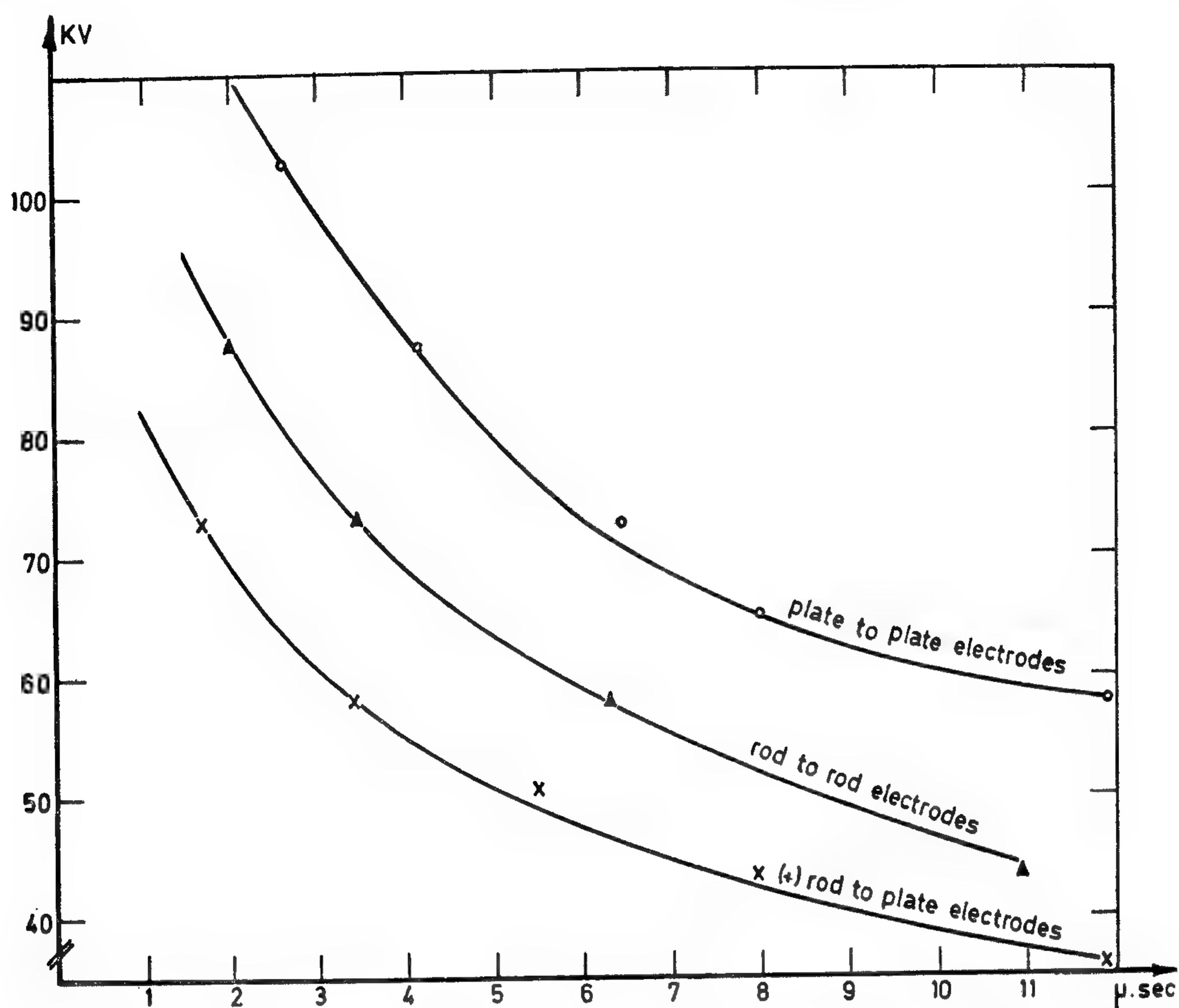


FIG. (3) IMPULSE BREAKDOWN OF SAND (Mesh No.: 20, Moisture content: 4.8%, separation between electrodes = 10 cm)

4—Variation of Impedance with Frequency:

To examine the change of the impedance z with the frequency f , an oscillator was used, it gives out-put voltage frequencies from zero up to 16 KHz. The oscillator voltage was applied to a sand sample of a mesh number 20. Accurate measurements of voltage across the specimen and current flowing through it were achieved by using a cathod-ray-ascillograph of high input impedance. Different electrodes with different spacings were used in these experiments. For each value of frequency the values of both voltages and current were recorded and the impedance was calculated. It has been noticed that for the same frequency, the impedance is independent of the voltage level. (Fig. 5) shows the variation of impedance

with frequency for a sand sample (Mesh Number 20, Moisture content 0.23%).

5—Impulse Impedance of Different Types of Soil Samples :

The volt-ampere relations for the different types of soil samples were recorded for voltages below the disruptive discharge level. The impulse impedance is calculated by dividing the maximum value of the voltage by the maximum value of the current. For the different soil samples with different shapes of electrodes, the impulse impedances were calculated for a separation of 10cm between the electrodes. Figs (6) and (7) represent the V-I characteristics of a sand sample (Mesh Number 20, moisture content 0.23%), with plate-to-plate electrodes.

This test was done for the different types of electrodes and for different spacings Fig. (1). Shows the voltage, current characteristics of loamy sand, moisture content 0.23%.

2 — Impulse Characteristics : volt-time characteristics of impulse breakdown)

The impulse breakdown voltage and the time to breakdown (V-t) characteristics of soil samples have been determined by applying impulse voltages between two electrodes buried in the soil under consideration. A curve of time to breakdown against the ac-

tual value of the applied voltage was then plotted.

The V-t characteristics of the different soil samples are shown in Figs. (2,3).

3 — Relation between the Critical Breakdown Impulse Voltage ; and the Separation between the Different Electrodes :

These results have been obtained from the volt-time characteristics of the impulse breakdown of soil samples having moisture content of 0.23%. Fig. (4) shows the critical breakdown voltages as a function of the separation between the electrodes for clay loam with moisture content 0.23%.

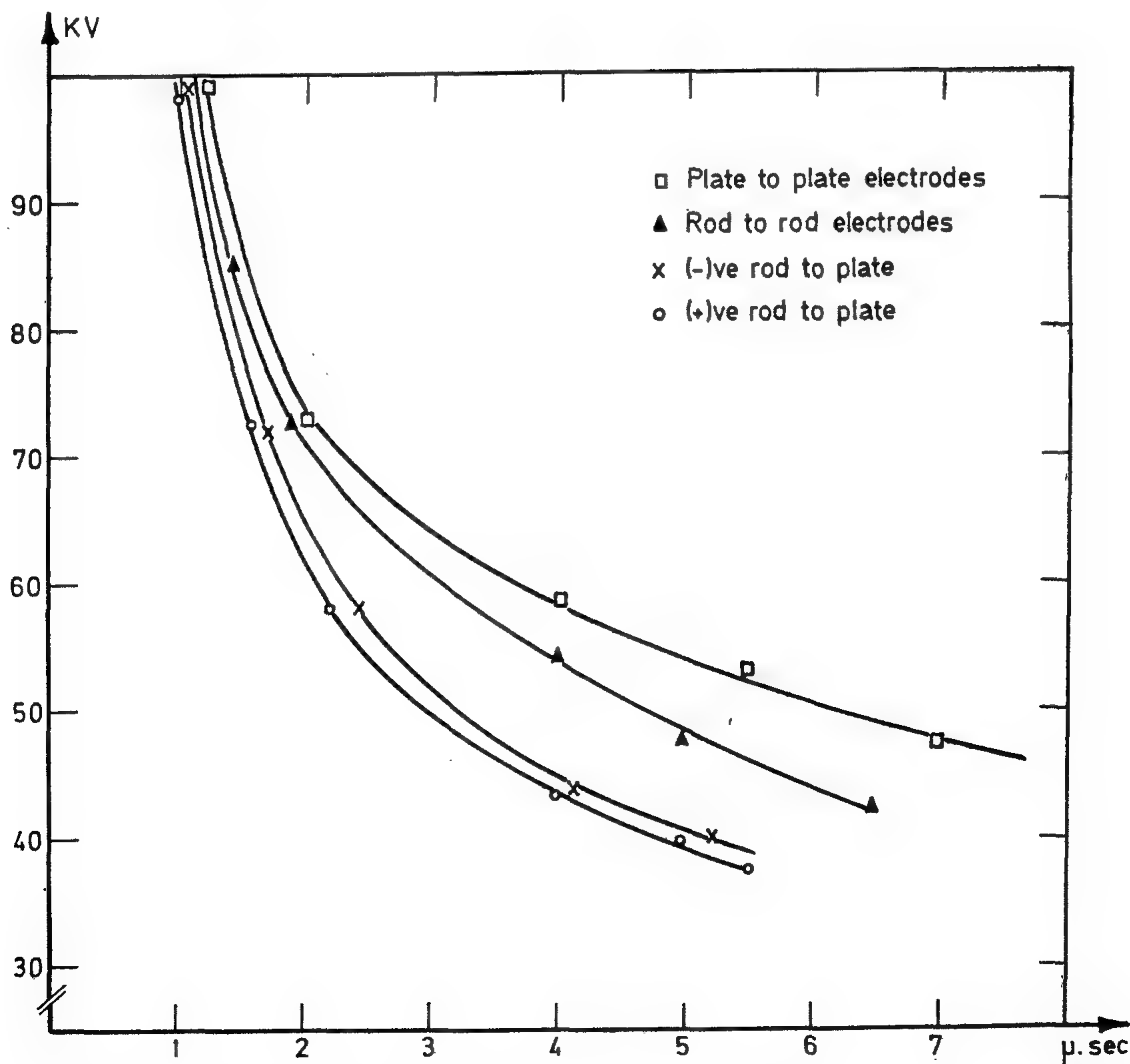


FIG. (2) IMPULSE BREAKDOWN OF SAND (Mesh No.: 20 , Moisture content : 0.23%
separation between electrodes = 10 cm)

country. The soil has been chosen to be different in characteristics as greatly as possible. The classification of soil samples investigated are :

- (a) Sand. (b) Clay loam. (c) Loamy sand.

(7) Tests have been done to determine the effect of the moisture content on the impulse characteristics of the soil.

(8) Tests have been done to determine the effect of the voltage frequency on the impedance of a soil sample using low voltages.

Types of Electrode Arranged :

- (a) Plate-to-plate, the plate was made of

copper, 10 cm in diameter, and thickness 1mm.

- (b) Rod-to-plate, a hemispherically ended rod of diameter 1cm, the plate is the same as above.

- (c) Rod-to-rod, the rods are the same as above.

Experimental Results :

1 — 50 Hz Characteristics :

Each soil sample was subjected to the 50 Hz a.c. voltage. The voltages across the soil sample and the current flowing through it were recorded and the 50 Hz impedance was calculated.

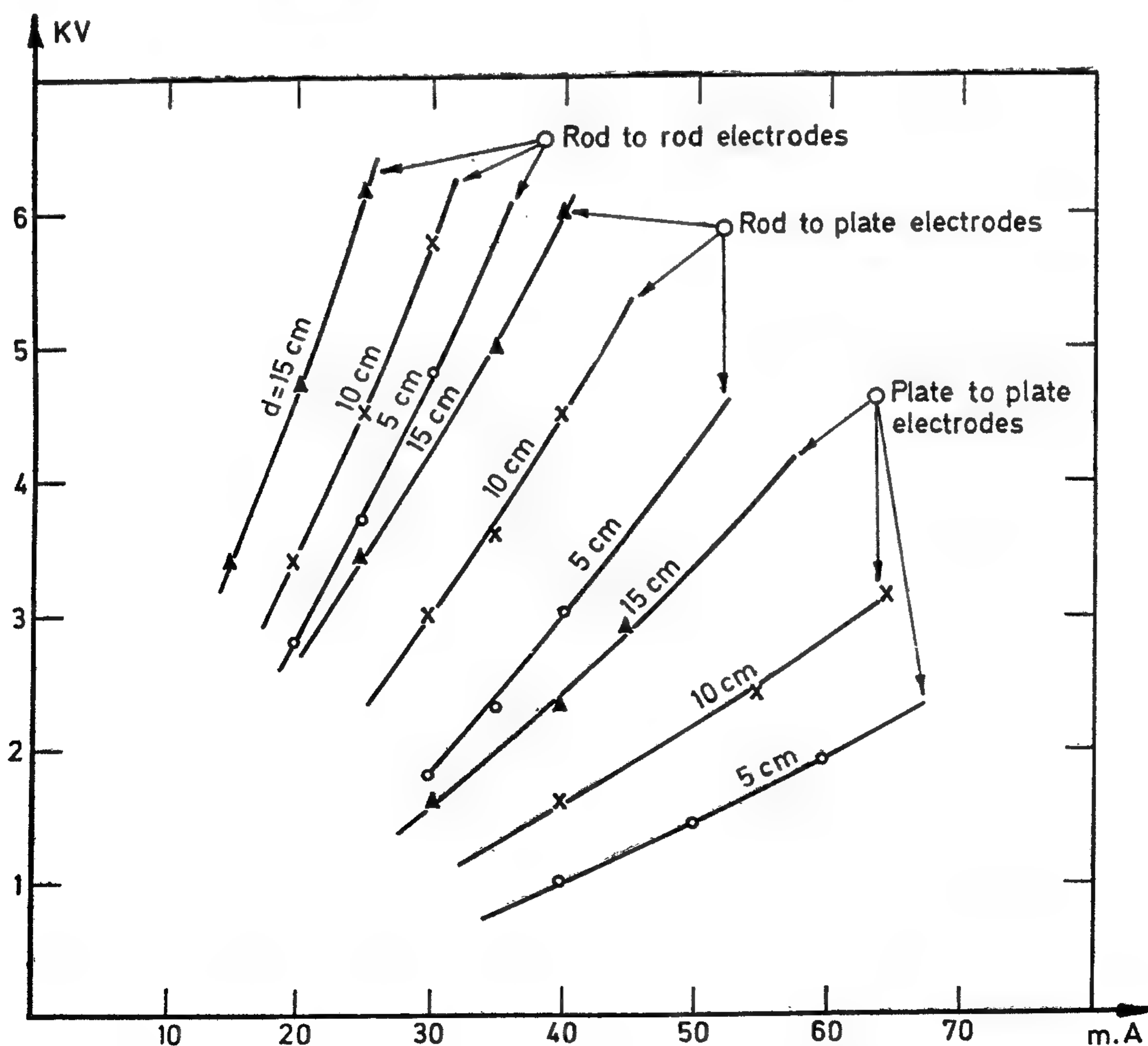


FIG. (1) VOLTAGE-CURRENT CHARACTERISTICS OF LOAMY SAND
(Moisture content: 0.23%)

The impulse generator used in this work was a marx type impulse generator consisting of eight stages, each of a single condenser whose capacitance is 0.1385 micro Farad. The value of the front resistances was 126 ohms. The load resistance was 14,750 ohms.

To study the impulse characteristics, a cathode ray oscillograph was used to measure the time to breakdown and the breakdown voltage accurately.

Soil Samples Under Test :

Three soil samples were used. They represented different types of soil in three areas in Egypt. The first one was taken from El-Barageal, 2 meters under the ground. The second one was taken from El-Basateen, 2 meters under the ground. The third one was taken from El-Basateen Hills, from which three samples of different grain sizes were obtained using screen analysis. The first has a mesh number 10 (i.e. the diameter of its grains ranges from 1.651 to 1.168 mm), the second was of mesh number 14 (the diameter ranges from 1.168 to 0.833 mm), while the third one was of mesh number 20 (the diameter is less than 0.833 mm).

The mechanical analysis of the three main samples was done in the soil and water research Institute, Soil Survey Research division. Sedimentation methods(2) were used in determining the mechanical analyses of the different samples. By the aid of the mechanical analysis, it was possible to determine the soil class of each sample using the laboratory method(3). It was found that :

The sample taken from El-Barageal has the textural name of clay loam, the sample taken from El-Basateen has the textural name of loamy sand, while the sample taken from El-Basateen Hills has the textural name of sand.

The chemical analysis of the different soil samples was also done in the Soil and Water Research Institute, Soil Survey Research Division.

Experimental Procedure :

It is apparent that soil possesses many of the characteristics of resistance materials, and at the same time many of the characteristics of insulating materials. To obtain a better understanding of the performance of soil when subjected to impulse voltages and of the impulse characteristics of complicated earthing systems, the following steps have been followed :

(1) Tests have been made to determine the 50 Hz impedance of different soils.

(2) Tests have been made to determine the time lag of impulse voltage breakdown of soil samples between electrodes for which the voltage gradient distribution is readily known, in addition to the critical breakdown voltage. The critical breakdown voltage of soil samples between rod-to-plate, rod-to-rod, and plate-to-plate electrodes have been measured.

(3) The volt-ampere relations for different soil samples have been obtained for a range of voltage below the disruptive discharge level,

(4) Tests have been made on electrode arrangements simulating installed ground rods to determine whether the model installations, which are possible in the high-voltage laboratory, agree in performance with the actual ground electrode systems.

(5) A sufficient number of tests have been made with both negative and positive—waves to determine the effect of polarity on the breakdown characteristics.

(6) Representative tests have been carried out on different types of soil. In fact it was not possible to study every soil type which could be found throughout the

SOIL BREAKDOWN AND ITS EFFECT ON THE EARTH RESISTANCE

By

A.G. ZEITOUN and A.M.K. EL- MORSHEDY

INTRODUCTION :

Although driven grounds are essential elements in lightning protection, the quantitative assessment of their effect under actual operating conditions of lightning discharge is difficult. The reason lies partly in the lack of fundamental knowledge of their impulse characteristics. The difficulty is also due to the numerous factors that affect driven grounds and ground systems.

Tests by Towne (1) have pointed out the significance of the impulse characteristics of driven grounds and the errors encountered in the use of the megger values as a basis for design. These, and tests by other investigators, have shown that under impulse conditions, ground connections have an apparent resistance somewhat below the value observed when the resistance is measured under conditions of power frequency and small currents. The ratio between the resistance as observed in tests made on installed grounds has ranged from 0.05 to 0.10 depending on the type of electrodes employed, the nature of the soil, and the magnitude and shape of the impulse current. No attempt has been made to examine the separate effect of each of these factors on the ratio. A limited number of measurements taken under natural lightning conditions have confirmed the conclusions drawn from these tests.

All previous investigations have been confined to electrodes of known dimensions

installed into natural ground. The material of the ground, the moisture content, the temperature, and the stratification have not been observed. As in other resistance measurements, the test technique has been to measure the voltage applied to the impedance under consideration and to observe the current through it. In studies of ground resistance, particularly with impulse currents, this type of measurement presents certain inherent difficulties due to the necessity of measuring current and voltage in a test circuit having a rather large physical dimensions. Also generators of impulse voltages and currents are not usually accessible outside the laboratory. For these reasons it was decided to carry out the present experimental work inside the laboratory and to use relatively small soil samples. The details of the experimental work are given below.

EXPERIMENTAL WORK :

Experimental set-up :

The a.c. voltage source used for measuring the 50 Hz impedance of the different soil samples is a single phase, 400 V/40 KV, 50 Hz, 40 KVA test transformer. The rated input voltage was 220 V and the output voltage adjustment was achieved by an induction regulator which could raise the secondary voltage up to 400 volts. A water resistance of 125 K ohms was used in series with the soil sample, on the high voltage side of the transformer to limit the current.

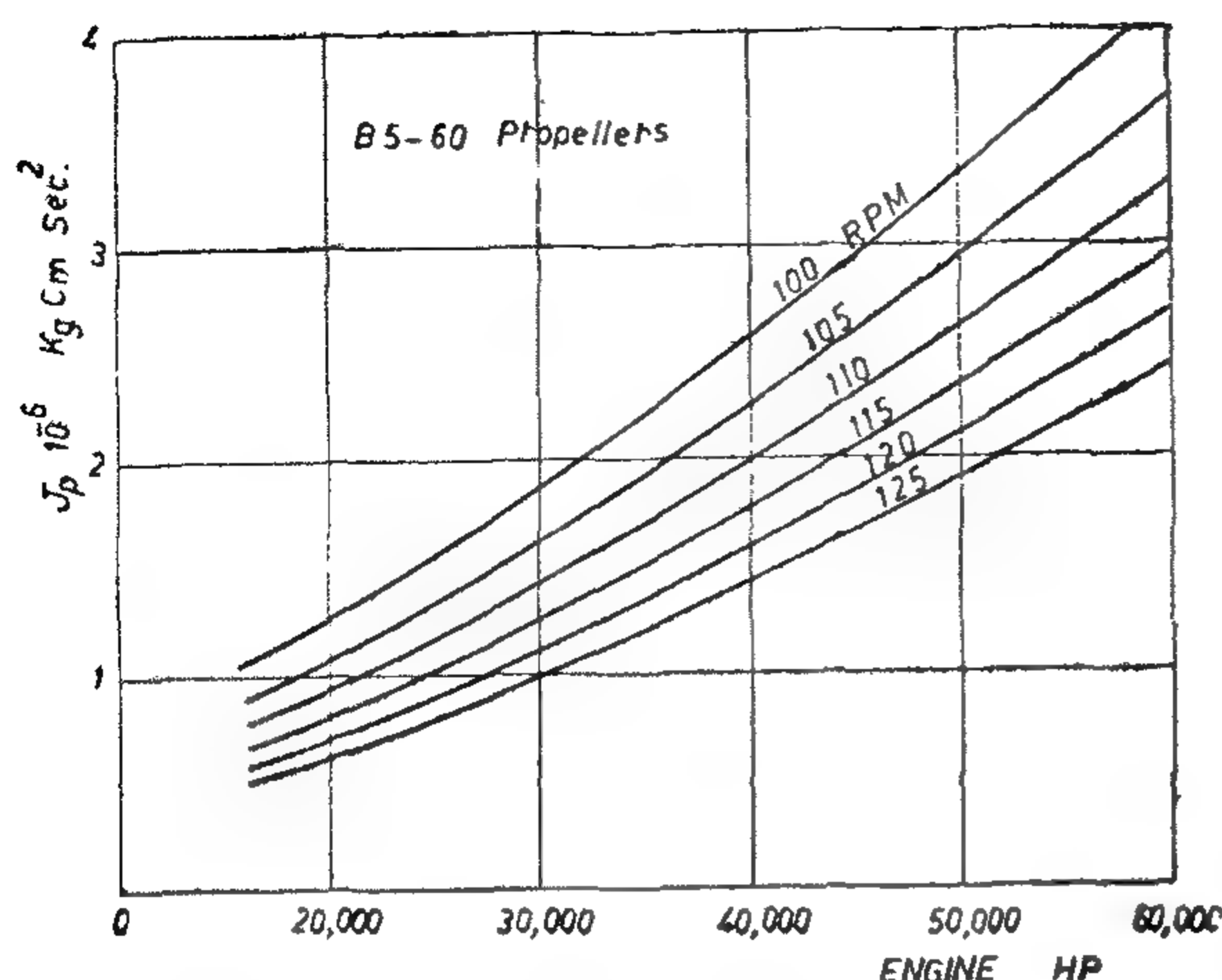


FIG. (3)

(17). The results are presented in Table (2).

From Table (2) the following remarks and conclusions can be drawn.

- 1 — The values of the shear stresses in the table may seem high but it should be pointed out that these are the maximum possible stresses. Fortunately these occur at speeds approximately from 20 — 30 rpm (for orders 12 — 8) which are far from the average rated speed of 110 rpm. These stresses do not build up unless the engine is left to run at that particular speed (between 20 — 30) for a considerable time.
- 2 — The actual stress ζ_{act} compares favourable with the exact stress ζ_e which shows that the various approximations and simplifications leading to Eq. (17) have no significant effect on its accuracy.
- 3 — In view of the above statement and in comparing ζ_{eq} , ζ_1 with ζ_e . One expects the deviation to be mainly due to the approximation in J_e . This we take up in more details in the following :
 - i — for groups 1,3,6 (where J_e is exactly represented by the straight line equation) ζ_{eq} is very close to ζ_{act} .
 - ii — for group 2,4,5 the difference between ζ_{eq} and ζ_{act} increases for group 4,5 $\zeta_{eq} < \zeta_{act}$ since

$$J_e (\text{actual}) < J_e (\text{Eq.})$$

for group 2 $\zeta_{eq} > \zeta_{act}$

since $J_e (\text{actual}) > J_e (\text{Eq.})$

iii — for groups 1,3 where $J_p/J_e = 1$, the difference between ζ_1 and ζ_{act} is not great.

iv — for groups 4,5,6 (where $J_e/J_e > 1$) $\zeta_1 < \zeta_{act}$.

v — for group 2 ($J_p/J_e < 1$).
 $\zeta_1 > \zeta_{act}$.

All the above results are in agreement with our expectations. In conclusion, for the determination of the shear stress we recommend the use of J_e obtained from the equation thus confining the error (and its direction above or below the actual value) to how close does the straight line equation approximate the actual engine inertia. In a later stage when J_e is known the required correction can be made.

REFERENCES

- 1 — F. Bahgat, et al, "Torsional Vibration Analysis for the Propulsion Systems of Large Motor Tankers", Jor. of Egyptian Society of Engineers, to appear.
- 2 — W. Ker Wilson, Practical Solution of Torsional Vibration Problems, Vol. 2, Chapman and Hall, 1963.
- 3 — B.I.C.R.A, A Handbook on Torsional Vibration, Cambridge Univ. Press, (Compiled by E.J. Nestorides), 1958.
- 4 — Macduff and Curreri, Vibration Control, McGraw-Hill, 1958.
- 5 — N. Petrovsky, Marine Internal Combustion Engines, Mir Publishers, Moscow.
- 6 — F. Lewis, Dynamic Effects, Marine Engineering, Vol. 2, (edited by H.E. Seward), S.N.A.M.E, 1960.

TABLE (2)
COMPARISON OF STRESS RESULTS

Engine Group	Engine's Characteristics		No. of Engine Cyl. ²	Rigorous Procedure τ_c kg/cm ²	Proposed Formulae			
					$\frac{J_p}{J_c}$ Actual		$\frac{J_p}{J_c} = 1$ τ_c (kg/cm ²)	$\frac{J_p}{J_c}$ Eqn. τ_{eq} (kg/cm ²)
					kg/cm ² τ_{act}	error %		
I	Builder	Mitsubishi	8	815	769	-4.52	873	762
	Type	KSZ 06/160 E	9	770	735	-4.55	882	728
	HP/Cyl.	2300	10	697	666	-4.45	740	660
	RPM	118	12	810	486	-4.70	521	481
II	Builder	Götaverken	8	791	750	-5.18	1150	851
	Type	DM 850/1700 V6S U	9	683	637	-6.73	906	723
	HP/Cyl.	2400	10	540	504	-6.66	743	572
	RPM	119	12	415	373	-10.00	525	423
III	Builder	Mitsubishi	8	1092	1040	-4.76	1152	1030
	Type	KSZ 93/170 E	9	890	840	-5.62	917	832
	HP/Cyl.	2780	10	750	685	-8.64	748	679
	RPM	115	12	526	501	-4.75	531	496
IV	Builder	Sulzer	8	1170	1247	+6.58	1163	942
	Type	RND 90	9	947	1010	+6.65	930	763
	HP/Cyl.	2900	10	785	844	+7.52	762	638
	RPM	122	12	545	587	+7.70	547	444
V	Builder	MAN	8	1125	1250	+11.10	1200	974
	Type	KSZ 90/160	9	918	986	+7.40	933	768
	HP/Cyl.	3000	10	764	825	+8.00	766	643
	RPM	122	12	568	615	+8.27	551	480
VI	Builder	Sulzer	8	1160	1218	+5.00	1170	1223
	Type	RND 105	9	950	995	+4.74	938	1000
	HP/Cyl.	4000	10	796	836	+5.02	773	841
	RPM	108	12	534	597	+7.76	555	600

No. of cylinders	Firing order
8	1, 8, 3, 4, 7, 2, 5, 6.
9	1, 6, 7, 3, 4, 9, 2, 5, 8.
10	1, 9, 5, 6, 2, 10, 4, 3, 8, 7.
12	1, 9, 11, 4, 3, 8, 10, 6, 2, 7, 12, 5.

The correction factor λ was calculated and presented in Table (1).

Table (1)			
No. of Cyl.	Orders		
	4	5	6
8	0.049	0.126	0.017
9	0.097	0.062	0.133
10	0.200	0.218	0.079
12	0.210	0.050	0.118

For orders less than 4, only the third order appears to be of significance because while the first order lies usually by far outside the operating speed range for the considered engines, the second order excitation is very weak as may be shown clearly in Fig. (1).

For the third order, the harmonic component T_3 is given by

$$T_3 = \sqrt{(a_n + T_{ni})^2 + b_n} \quad (19)$$

where

a_n = sine term of the harmonic component due to gas pressure

$$= 0.2 \sqrt{(P_m + 300)(P_m + 110)}$$

b_n = cosine term of the harmonic component due to gas pressure

$$= -0.1 P_m$$

T_{ni} = inertia harmonic component given by [2]

$$T_{ni} = I H$$

I = inertia factor

= 180 for the considered category of engines

H_{ni} = inertia harmonic component coefficient

$$= -0.2212 \text{ for order 3}$$

Finally the correction factor λ_3 takes the form

$$\lambda_3 = T_3 \left[\left(\frac{N^3}{2200} \right) \left(\frac{\sum \bar{d}_{min}}{\sum \bar{d}_{maj}} \right) \left(\frac{n}{N} \right) \right] \quad (20)$$

The factor λ_3 can be calculated and has the following values

C_{yI}	8	9	10	12
λ_3	0.157	0.240	0.274	0.730

RESULTS AND DISCUSSION

Equation (17) aside from the horsepower, rpm and numbers of cylinders involves also the engine and propeller inertias J_e , J_p yet to be determined. The propeller inertia can be determined as a function of H , R [1] as shown in Fig. (3). As for the engine inertia J_e one can substitute either one of the following values:

- i — the actual value or J_e (if known)
- ii — the approximate value obtained from the equation [1]

$$J_e = 5160 N (H_e/R).$$

- iii — the rough approximation

$$J_e/J_p = 1 [1].$$

For each one of the above alternatives one obtains a different value for the stress, σ_{act} , σ_{eq} and σ_1 respectively.

Six engine groups belonging to different makers with powers ranging from 2300 to 4000 H.P/cylinder and with number of cylinders from 8 to 12, with the appropriate propellers and shafts are considered.

The specific stress for each case is obtained on the digital computer by means of a standard program. Then, the actual amplitude, hence the actual stress (labeled σ_c) is calculated. Also the three possible (according to which value of J_e one uses) values of stress σ_{act} , σ_{eq} and σ_1 are calculated by means of Eq.

Hence $d^3 = C^3 (H/R)$ (14)

Next consider $\sum J_i a_i$ this can be written as

$$a_m \sum J_i = a_m J_e$$

where J_e is the total engine inertia

$$J_e = N J_c$$

a_m the mean values of the amplitudes of the engine inertias.

$$a_m = \sum a/N$$

Therefore the specific stress takes the form

$$\tau_{sp} = \frac{1.5 W_e J_e \sum a \cdot R}{N \pi (8.9)^3 H} \quad (15)$$

4 — The Propeller Amplitude :

The propeller amplitude a_p is obtained from the Holzer's table which cannot be done unless all the details of the system are available. This, of course, is not possible in early design stages. However knowing that the node for the first mode of vibrations lies on the intermediate shaft one can make use of the two mass approximation (were the engine inertia is concentrated at the mid cylinder) and reach the following relation:

$$J_e/J_p = a_p/a_m$$

$$\text{or } a_p = J_e/J_p a_m$$

$$a_p = J_e/J_p \sum a/N \quad (16)$$

The Proposed Stress Equation :

The shear stress, due to torsional vibrations, in the intermediate shaft of the propulsion system under consideration is given by Eq. (6) above.

Now substituting equations 8, 9, 13, 15 and 16 into equation (6) and confining attention to major orders (for two - stroke engines the major order no. n is the same as the number of cylinders N), the stress takes on the final form

$$\tau = \left[1.167 \times 10^{-3} \left(\frac{R}{N} \right)^3 \frac{J_p}{H_c} \right] \left(\frac{J_p}{J_e} \right) \quad (17)$$

where

R : engine rated rpm

N : No. of cylinders

J_p : propeller inertia, kg cm sec²

J_e : total engine inertia, kg cm sec²

H_c : brake horsepower per cylinder

τ : torsional stress, kg/cm²

In the derivation of Eq. (17) due to cancellation of some parameters the only approximations involved in the equation are the value of T_n (Eq. 8) and that of a_m and both are very close to reality. As for the propeller damping S_p the fact that it is being given by an empirical formula does not detract from the accuracy of Eq. (17) since it is exactly the same value for S_p (Eq. 13) that would have been used in connection with any exact analysis.

It has been stated at several points in the previous analysis that we are concerned only with major orders. However Eq. (17) can be modified to evaluate the stresses for minor orders. The correction for the minor order n takes place for the following parameters :

- i — the vector sum $\sum a_{min}$ corresponding to the star diagram of the order n is used instead of $\sum a_{maj}$ that corresponds to the major order N ,
- ii — the propeller damping coeff. S_p also involves n
- iii — the torque excitation is proportional to $(1/n^3)$ for orders higher than 3,
- iv — the torque excitation should be corrected for the inertia effect for orders lower than 4.

Hence for a minor order n ($n > 3$) equation (17) is multiplied by the correction factor λ to give the stress at that order where

$$\lambda_n = \frac{\sum \bar{a}_{min}}{\sum a} \cdot \left(\frac{N}{n} \right)^2 \quad n > 3 \quad (18)$$

It should be pointed out that the calculation of $\sum a_{min}$ depends on the particular firing order.

Here it is calculated for the most common firing orders, namely;

the same number of cylinders the elastic curves (for the engine portion) are substantially identical. This fact enables us to express $\sum a$ as a function of the number of cylinders as is shown in Fig. (2) from which one can deduce the relation

$$\sum a = 0.75 N + 1.3 \quad (10)$$

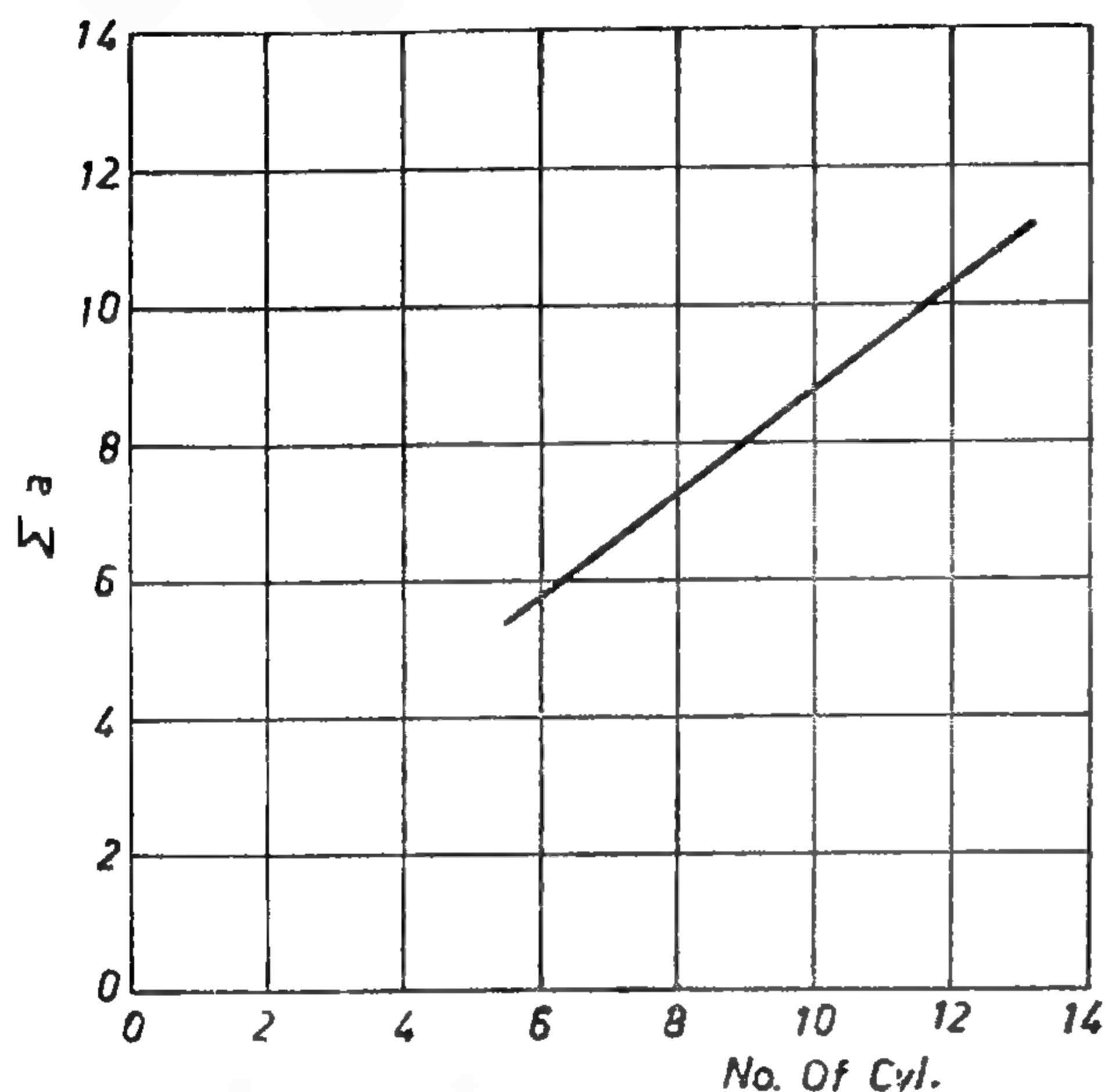


FIG.(2)

3 — Propeller Damping Coefficient

For the calculation of propeller damping coefficient several procedures were considered in order to arrive at a formula combining as far as possible the various experiences.

Archer's Method [2,3]

The propeller damping coefficient is given by

$$S_p = a T_{pc} / R_c \quad (11)$$

$$T_{pc} = 63030 (H_{pr} / R_c) (R_c / R)^3$$

where

- T_{pc} : mean propeller torque at critical speed
- H_{pr} : horse power delivered to the propeller at the rated speed
- H_{pc} : $H_{pr} (R_c / R)^3$
- R_c : critical rpm
- R : rated rpm
- a : factor to be determined from tables or graphs.

For the determination of the factor 'a' one needs to know

- i — the number of propeller blades
- ii — the developed area ratio D.A.R.
- iii — the pitch ratio P/D
- iv — propeller torque coefficient A q

$$Aq = \frac{9.5 H_{pr}}{D^2 (R D / 1000)^3}$$

Recall that the propeller diameter D was expressed as a function of the horse power and rpm [1], hence Aq is calculated for the set of engine installations considered in this work. These values for Aq ranged from 19.7 to 21.4 with most of the values close to 21.0 which is adopted here.

For the B 5-60 propeller series and from the mentioned tables and using the appropriate values for D.A.R, P/D, Aq the value of 'a' was found to be 35.

Hence Eq. (11) takes the final form

$$S_p = 22 \times 10^5 H_{pr} / R^2 (R_c / R)^3 \quad \text{ib. in. sec/red.} \quad (12)$$

Other methods for the determination of S_p are used. For space limitations we do not present them here. However when S_p as obtained by these methods was reduced to a form similar to Eq. (12) the constant term took the following values

Method	Ref.	Constant
Petrovsky	[5]	18×10^5
Ker Wilson	[2]	21.1×10^5
BICERA	[3]	19×10^5
Lewis	[6]	25×10^5

From the above analysis an average value for S_p to be used below is chosen. This in our nomenclature will read

$$S_p = 20 \times 10^5 H / R^3 (60 W_c / 2\pi n) \quad (13)$$

3 — Specific Stress :

The specific stress defined above by Eq. (5) should be expressed in different terms. Consider first the modulus of section at the intermediate shaft,

$$Z = \frac{\pi d^3}{16}$$

It was found [1] that $d = C$ where $C = 8.9$

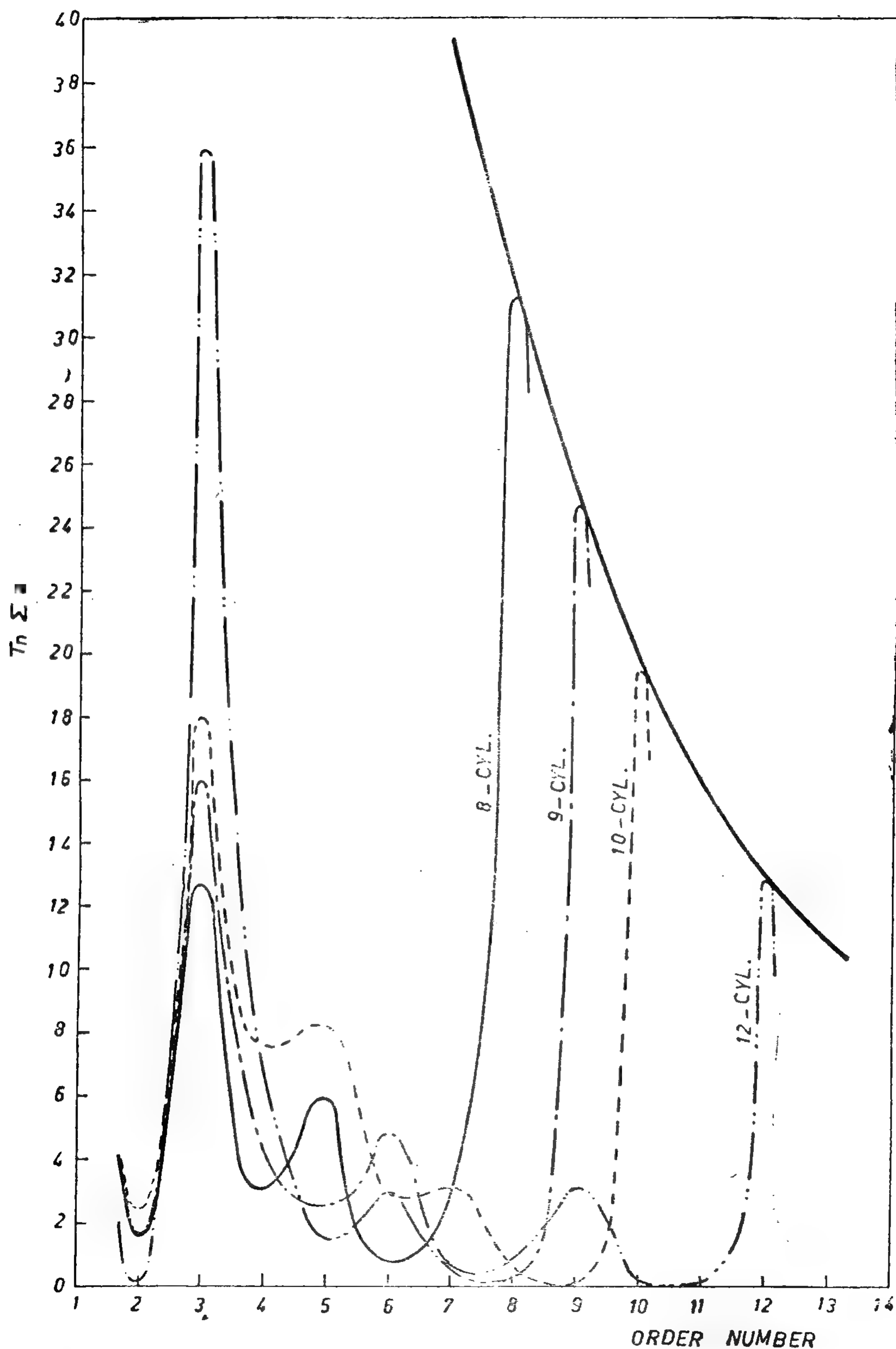


FIG.(1)

For the time being we confine our attention to major orders then later on we introduce a modifying factor to account for the minor orders.

For the major order, $\sum a$ will be the arithmetic sum $\sum a$ of the cylinder amplitudes. A study of the elastic curves for the first mode of vibration show that for

$$\tau = \tau_{sp} \theta_1$$

$$\tau = \frac{Q_n \sum \bar{a}_i}{W_c S_p \bar{a}_p^2} \frac{16 W_c^2 \sum J_i d_i}{\pi d_s^3} \quad (6)$$

where d_s : diam. of the intermediate shaft

\sum is the summation from $i = 1$ to $i = N$

N number of cylinders.

Determination of the Parameters :

It is our purpose here to express the different parameters in Eq. (6) in a more simplified — though approximate — form involving only the most preliminary data.

1 — The Exciting Torque :

The torque of an internal combustion engine is usually given by

$$Q = T A L_c$$

where A : piston area

L_c : crank length

T : tangential effort (resultant force perpendicular to the crank per unit piston area).

The tangential effort is drawn against the crank angle. The resulting periodic curve can be analyzed by Fourier's series [3] resulting into a constant term (representing the mean value) and a series of harmonically varying terms having 1, 2, 3, ... etc. repetitions per cycle (this no. of repetitions is known as the order number).

For a two-stroke, single-acting Diesel engine these harmonic components are given by the following expression [2] :

$$T_n = \frac{2000}{50/\sqrt{n} + n^3} + \frac{10 P_m}{20 + n^3} \quad (7)$$

where :

n : order no.

P_m : mean indicated pressure (lb/in²) at the particular speed exciting the order n

Substituting the appropriate value for p_m

and noting that for higher order numbers T_n becomes approximately inversely proportional to the cube of the order numbers, a simpler form for Eq. (7) that gives reasonably accurate values in comparison with the original Eq. will be adopted. This equation has the form

$$T_n = 2200 / n^3 \quad (1b/in^2) \quad (8)$$

The value of T_n given by Eq. (7) or (8) is based only on gas pressure that is the effect of the inertia of the moving parts is neglected. This is justifiable since by inspecting the expression for the inertia torque [2,3] one observes that for orders higher than the fourth they drop sharply and are safely ignored in comparison with the gas torque. (As will be discussed below we are concerned with orders higher than the fourth).

Next we proceed to eliminate the term ALc . From the well known relation,

$$H = \frac{P L_c A R N}{\text{const.}}$$

where R : RPM

N : number of cylinders.

and substituting the appropriate value for the mean pressure $P = 160$ lb/in² and assuming a mechanical efficiency of 0.88 we get :

$$ALc = 1375 H / R N \text{ in}^3 \quad (9)$$

2 — The Resultant Amplitudes :

The resultant amplitude is the vector sum of the relative amplitudes a_i taken in the directions of the star diagram for a certain order.

It is a well known fact that maximum stress occurs for maximum value of the product $Q_n \sum a$ and not necessarily for the majors ($\max. \sum a$).

However a study of six engine groups (by different makers) presented in Fig. (1), reveals that $Q_n \sum a$ is actually maximum for the major order except for the twelve cylinder engine. Moreover Fig. (1) also points out the importance of some minor orders which should be checked.

dings. This throws some light on the complexity of the problem and shows the difficulty in expressing this torque fluctuation in a formula based on strictly theoretical consideration. Fortunately the torque variation of a 5-bladed propeller does not normally exceed 3% of the mean torque [2] and is usually considerably smaller in modern designs. Moreover with five-bladed propellers — adopted in this study — the frequency of torque fluctuation is much higher than (hence does not excite) the principal mode of vibration.

Engine damping is also a complex phenomenon and is calculated with the aid of empirical formulae [3]. However in the case of a marine installation, engine damping is very small in comparison with the damping effect produced by the propeller [2].

In this study both propeller excitation and engine damping are neglected not only because each is small in comparison with the main source of excitation or damping (respectively) but also because their effects tend to cancel each other.

The Actual Amplitudes :

In view of the above discussion the system is considered to be excited only by the engine and the propeller offers the only source of damping. At resonance the energy input by the engine to the system is given by [3],

$$W_{\text{input}} = \pi Q_n \sum_{i=1}^N \theta_i \quad (1)$$

and the energy dissipated by propeller damping is given by [4]

$$W_{\text{diss}} = \pi W_c S_p \theta_p^2 \quad (2)$$

where

- Q_n : the torque component of order n
- W_c : the natural circular frequency of the mode under consideration.
- S_p : damping coefficient of the propeller
- θ_i : the actual amplitudes at the cylinders,

$i = 1, 2, \dots, N$ (No. of cylinders)

θ_p : the actual propeller amplitude.

$\sum \bar{\theta}_i$: the vector sum of the θ_i in the directions of the star diagram corresponding to the particular order n [3].

At a particular mode the actual amplitudes θ_i are proportional to the relative amplitudes a_i [2]. The latter being obtained from the Holzer table with the usual assumption that the datum amplitude at cylinder (1) $a_1 = 1$ that is

$$\theta_i/a_i = \theta_2/a_2 = \dots = \theta_p/a_p \quad (3)$$

Equating the energy input to the energy dissipated by damping to obtain the steady state amplitudes θ_i and making use of Eq. (3) one gets

$$\pi Q_n \theta_i \sum \bar{a}_i = \pi W_c S_p \theta_i^2 a_p^2$$

or

$$\theta_i = \frac{Q_n \sum \bar{a}_i}{W_c S_p a_p^2} \quad (4)$$

The Specific and Actual Stress :

The specific stress is defined as the stress at any particular section in the system resulting from a unit displacement (1 rad) at the reference mass (cylinder no. 1). This is readily obtained from the Holzer table

$$\tau_{sp} = \frac{W_c^2 \sum J_i a_i}{Z} \quad (5)$$

- where : J_i is the mass moment of inertia of the disc (i) in the system
- a_i is the relative amplitude of the disc (i) in the system
- \sum the summation from $i = 1$ up to the disc prior to the section in consideration.
- Z the modulus of the section in consideration

$$(Z = \pi d^3/16)$$

The actual stress at any section is equal to the specific stress multiplied by the actual amplitude. Hence the torsional stress at the intermediate shaft

TORSIONAL VIBRATION ANALYSIS FOR THE PROPULSION SYSTEMS OF LARGE MOTOR TANKERS

Part II : STRESS EVALUATION

F. BAHGAT, M. Sc, Ph.D.
Prof. of Marine Engineering
and Ship Machinery,
Marine Engineering and Naval
Architecture Department,

N. MAHAREM, M.Sc., Ph.D.
Asst. Prof. of Mechanical
Vibrations,
Mechanical Engineering
Department,

A. EL-IRAKI, B.Sc.
Teaching Assistant
Marine Engineering
and Naval Architecture Department,
Faculty of Engineering, Alexandria University

INTRODUCTION

Torsional vibrations, being the most significant type of vibrations present in marine propulsion installations, deserves — and in fact have received — considerable attention in the literature. Meanwhile, the continuous trend towards the increase in the size of ships has led to the evolution of a new family of ships namely; the large tankers. An interesting feature of large tankers is that they have so much in common that they can be treated as a group. For instance they are mostly propelled by slow-speed 2-stroke Diesel engines of high powers (2000 — 4000 HP/cylinder) with average speed around 110 rpm and mean effective pressure of about 11 Kg/cm² [1].

The engines are located far aft, directly coupled through a relatively short shaft to a five-blade screw.

This degree of standardization enhances the study of torsional vibration problems with the aim of arriving at particular formulae applicable to large tankers.

In a previous work [1] an expression for the first mode natural frequency of torsional vibration of the propulsion system was developed. The purpose of the present work is to develop a simple for-

mula for predicting the stresses due to torsional vibrations in the propulsion system. Our objective is that this formula will involve the preliminary data available at the early design stages. The accuracy of the formula is checked against existing installations as solved by the computer.

THEORETICAL CONSIDERATION

In a marine propulsion system torsional oscillations — hence stresses — are usually excited by either the engine, the propeller or both. Also damping (energy dissipation) is present at both the engine and the propeller.

At resonance the steady state amplitude is reached as a result of the balance between the energy input by excitation and the energy dissipated by damping; hence the need to consider each of the sources of energy input or damping in details.

Consider first the propeller excitation, the propeller blades experience flow velocities which vary both radially and circumferentially leading to fluctuating torques. The magnitudes of these fluctuating torques depend on the wake field, number and design of the blades, position of the propeller and its relation to its surrcun-

. As the percentage overvoltage increases the electric field strength E increases leading to the increase of the positive ion energy. Hence, γ_i will increase. Therefore, its effect in Eq. (5) will decrease. Accordingly, the two results get closer.

Also, we can see that at constant pressure and percentage overvoltage the deviation between the two results obtained from the two equations increases as the electrode separation increases. This is due to the fact that as the electrode separation increases, and as the percentage overvoltage is constant, the electric field strength decreases. Therefore, the effect of γ_i in Eq. (5) increases because its value decreases.

V. CONCLUSIONS

1. Using the published data [5] for the first ionization coefficient α the coefficients A and B of the familiar equation of α , $\alpha = A \exp(-BE/p)$, are obtained. (See Table 1). These values are used in the calculations of the characteristic time T .

2. The transition between the Townsend's and the streamer mechanisms cannot be found from a plot of the logarithm of the formative time lag against the logarithm of the percentage overvoltage in Oxygen as was proposed by Kohrmann [6].

3. The characteristic time T , hence the formative time lag t_f , is almost independent

of the electrode separation d at constant ratio of the electric field strength to the gas pressure E/p (in the pressure range from 250 to 1000 torr). This holds for different electrode separation ranges.

4. The characteristic time T , hence the formative time lag t_f , takes the form

$T = K_1/pK_2$ at constant percentage overvoltage ΔV and constant product of the gas pressure and electrode separation pd . K_1 and K_2 depend on ΔV , pd , and the gas itself.

REFERENCES

1. Schade, R., *Über Die Aufbauzeit Einer Glimmentladung*, Z Phys. 104, 1937, 487.
2. Loeb, L.B., *Basic Processes of Gaseous* University of California Press, Berkeley, 1955.
3. Raether, M., *Electron Avalanches and Breakdown in Gases*, Butterworths, London, 1964.
4. Abou-Seada, M. S., Unpublished report, Iowa State University, Ames, Iowa, 1968.
5. Brown, S. C., *Basic Data of Plasma Physics*, MIT Press, 1966.
6. Kohrmann, W., *Über Den Elektrischen Durchschlag In Luft*, Z. Angew. Phys. 7, 1955, 183.

* * *

where K_1 and K_2 are constants that depend on the gas itself, the percentage overvoltage ΔV , and the product of the gas pressure and electrode separation pd .

Eq. (7) shows that the characteristic time T is inversely proportional to the gas pressure p raised to a constant power at constant percentage overvoltage ΔV and constant product of gas pressure and electrode separation pd . This fairly simple expression gives a powerful tool to predict the value of the characteristic time. By calculating the value of the characteristic time T at a value of the product of gas pressure and electrode separation pd , and using the simple expression of Eq. (7), we can know the characteristic time T at any pressure p and electrode separation d , for a constant percentage overvoltage ΔV . Alternatively, we can use the generated sets of curves of T versus pd , similar to Figs. (8) and (9). Table 2 gives the values of K_1 and K_2 at different values of ΔV .

Table 2:

The constants K_1 and K_2 of the equation $T = K_1/pK_2$ for different values of the percentage overvoltage ΔV .

Percentage Overvoltage ΔV	K_2	K_1
1	0.0234	6.615×10^6
10 —	0.0118	2.245×10^5
20	0.0092	3.79×10^3
30 —	0.0062	343
40 — —	0.0054	114

D. Effect of Electrode Separation on the Characteristic Time at Constant Electric Field Strength and Gas Pressure

Calculations were carried out to estimate the characteristic time T at constant electric field strength E and pressure p to reveal the effect of the cathode-anode separation d . It was found that the characteristic time T is almost constant over a certain range of gap

length; this range depends on the ratio E/p . The gas pressure may range from 250 to 1000 torr. (See Table 3).

Also, it was found that as the electric field strength E increases, the range of the electrode separation d for which the characteristic time T is almost unchanged is increased. As the gas pressure p increases with unchanged electrode separation d , we found that the electric field strength E , for which the characteristic time T is almost constant, increases. Also, for the same electrode separation d and gas pressure p the characteristic time T decreases as the ratio E/p increases.

Our calculations show that for the same E/p and for the same range of electrode separation, the percentage change of the characteristic time decreases as the pressure increases. This may be interpreted as follows: as the pressure increases, the number of electrons that may succeed to cause avalanche is increased and the characteristic time is decreased.

E. Comparison Between Calculating the Characteristic Time Using Schade Equation and the More Exact Equation

From our calculations, it can be seen that at constant pressure p and electrode separation d the difference between the two results decreases as the percentage overvoltage ΔV increases. This may be attributed to the effect of the second Townsend ionization coefficient due to positive ion bombardment

Table 3 :

The ranges of the electrode separation d , over which the characteristic time T is constant*, for different values of the ratio E/p .

E/p (volt/cm. torr)	d (mm)
45	7 — 12
50	5 — 12
55	4 — 12

* The percentage change in T over each of the specified ranges of d is much less than 1%.

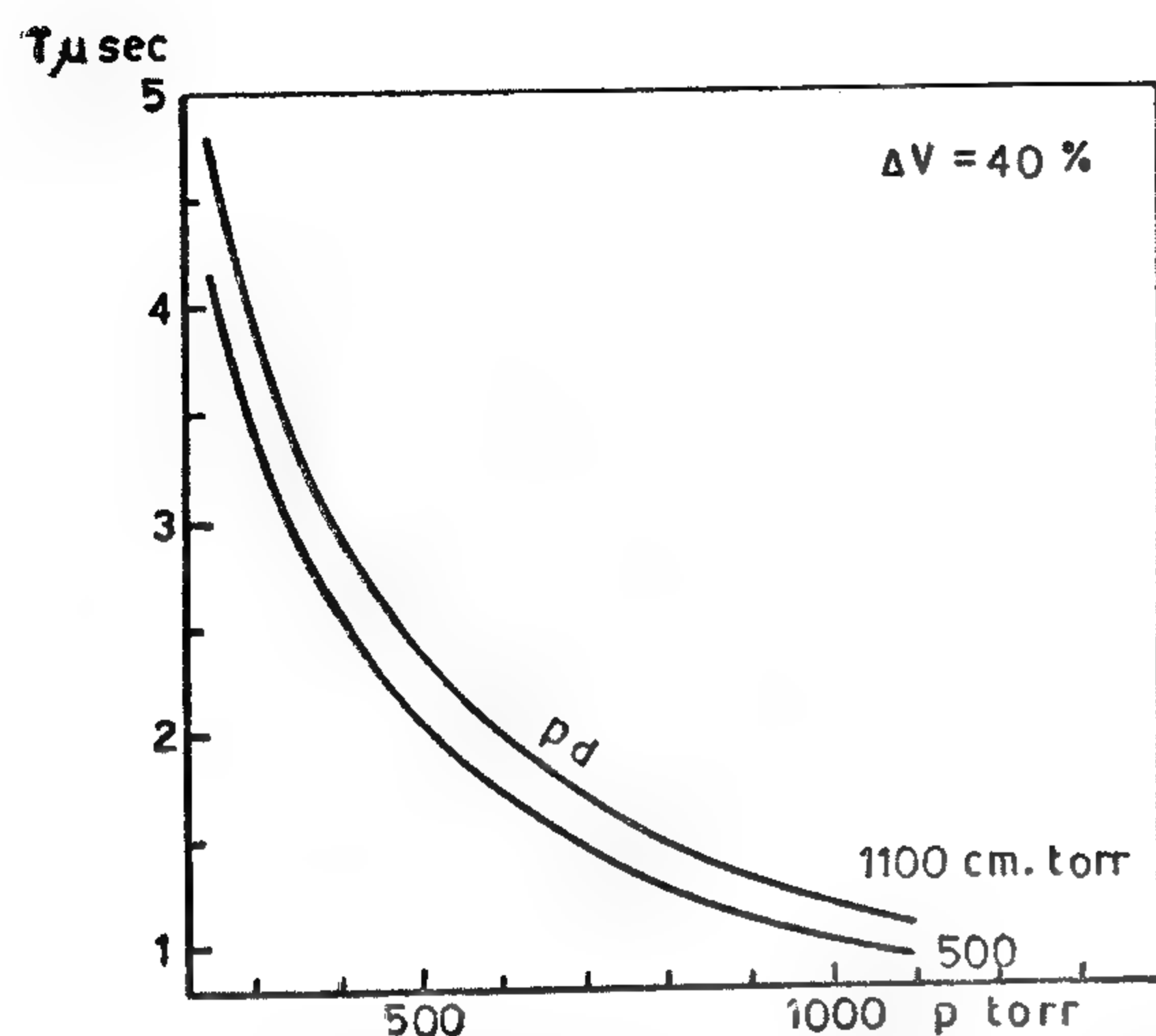


FIG. (7) THE CHARACTERISTIC TIME τ VERSUS THE GAS PRESSURE p AT CONSTANT PERCENTAGE OVERVOLTAGE $\Delta V (=40\%)$ AND CONSTANT PRODUCT OF GAS PRESSURE AND ELECTRODE SEPARATION pd .

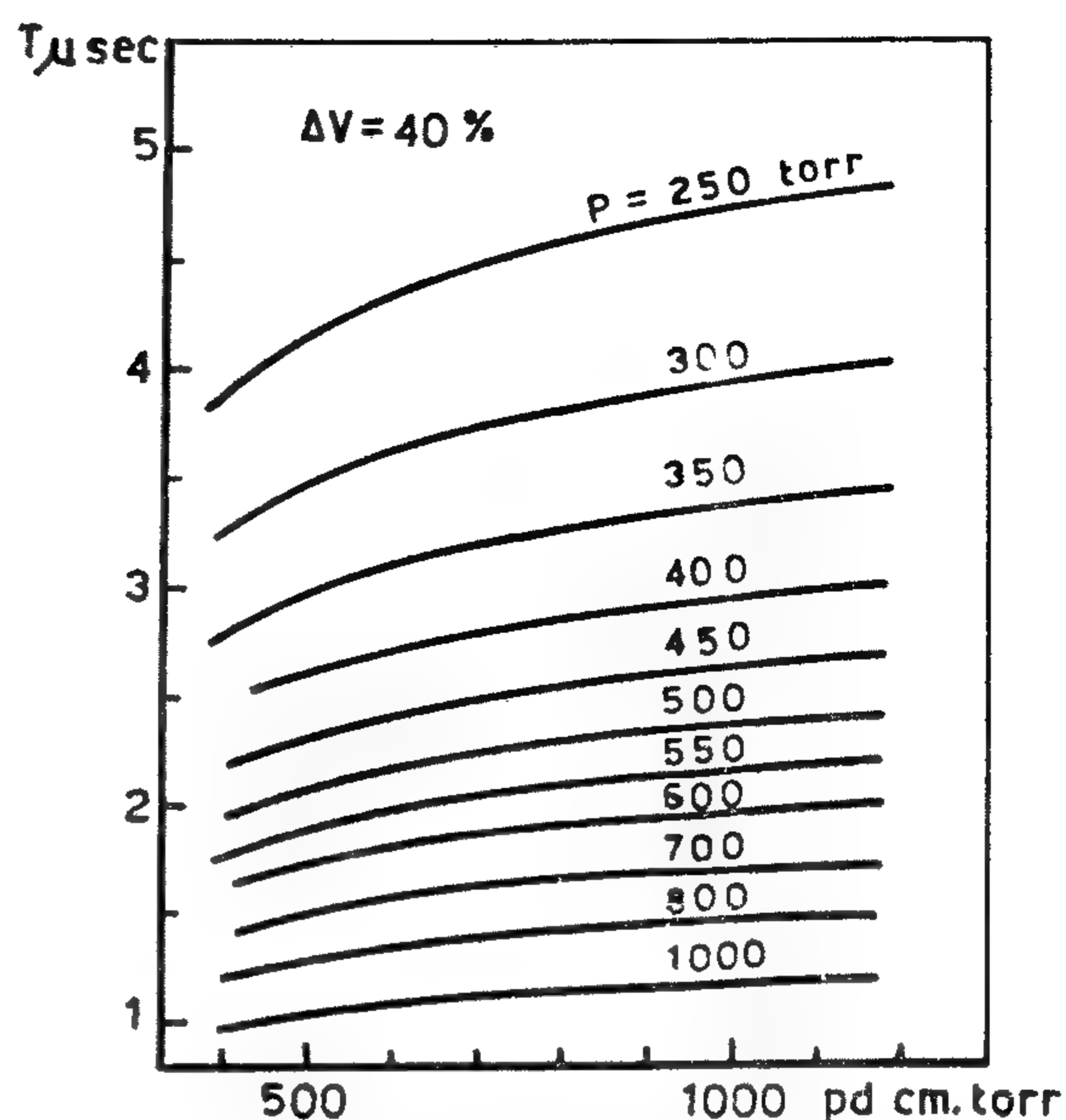


FIG. (9) THE CHARACTERISTIC TIME τ VERSUS THE PRODUCT pd AT CONSTANT $\Delta V (=40\%)$ AND CONSTANT GAS PRESSURE p .

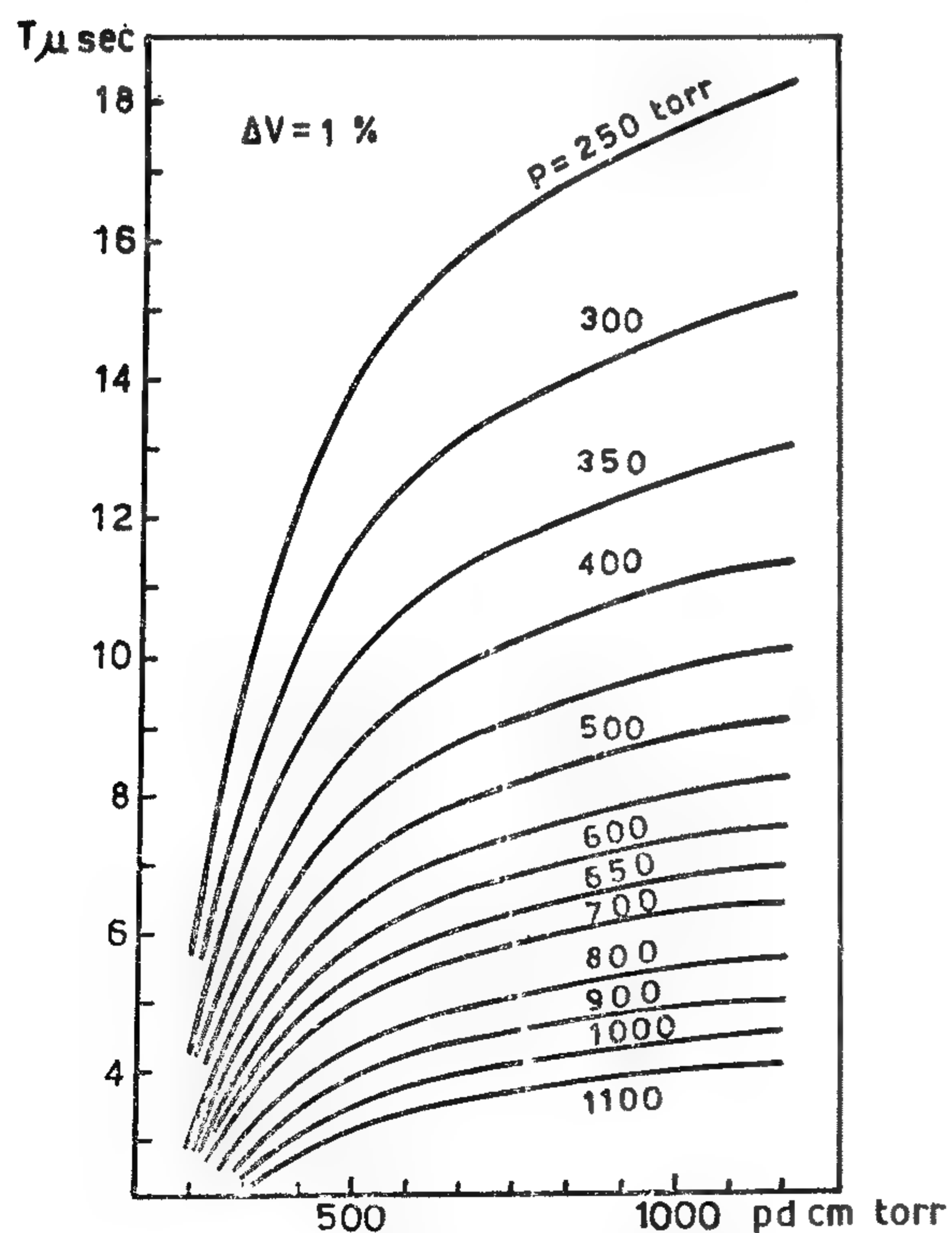


FIG. (8) THE CHARACTERISTIC TIME τ VERSUS THE PRODUCT pd AT CONSTANT $\Delta V (=1\%)$ AND CONSTANT GAS PRESSURE p .

obtained curve will be a straight line as shown in Figure (10) which yields an equation of the form

$$\tau = \frac{K_1}{p^{K_2}} \quad (7)$$

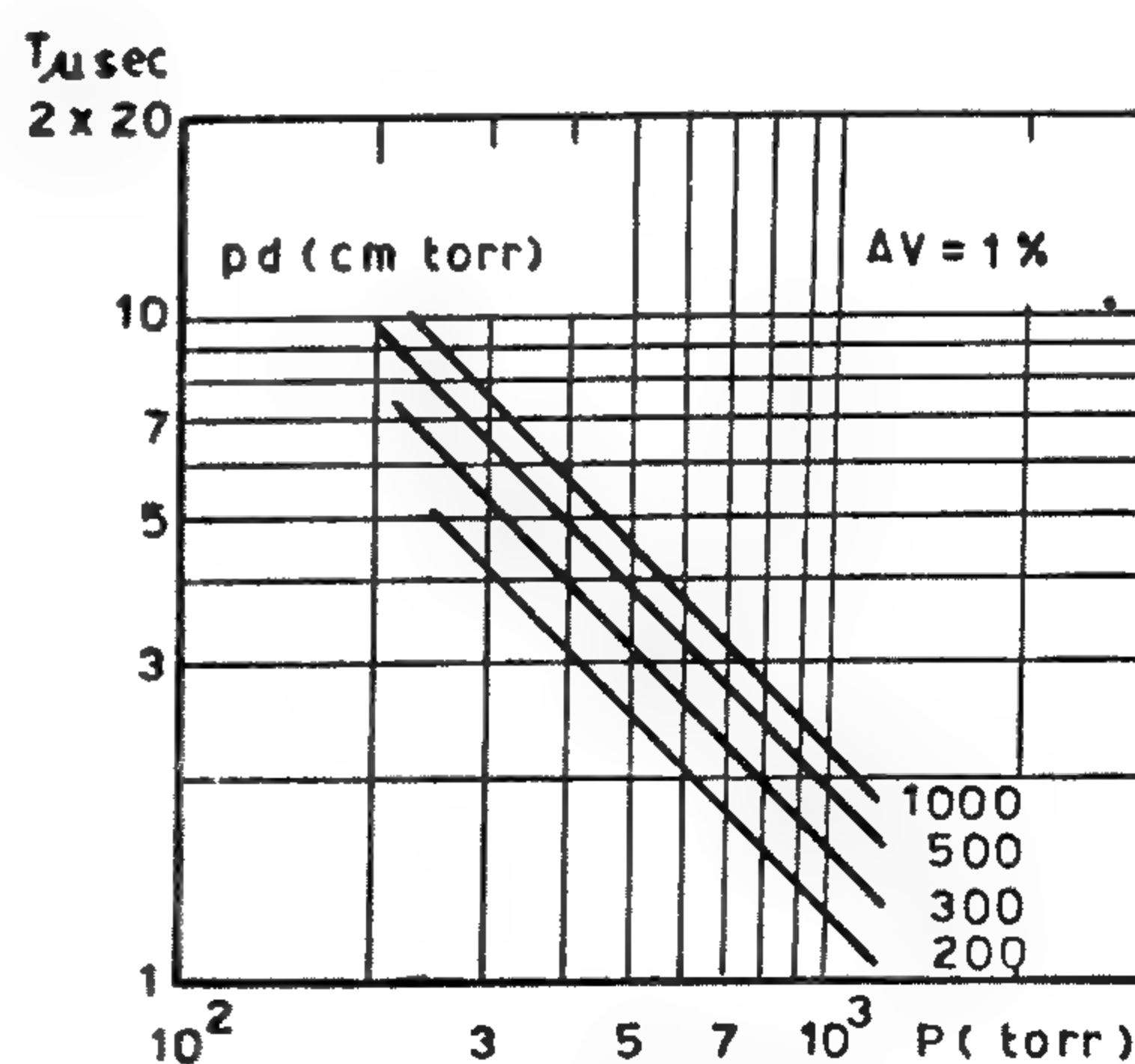


FIG. (10) THE CHARACTERISTIC TIME τ VERSUS THE GAS PRESSURE p AT CONSTANT PERCENTAGE OVERVOLTAGE $\Delta V (=1\%)$ AND CONSTANT PRODUCT OF GAS PRESSURE AND ELECTRODE SEPARATION pd ON A LOG-LOG SCALE

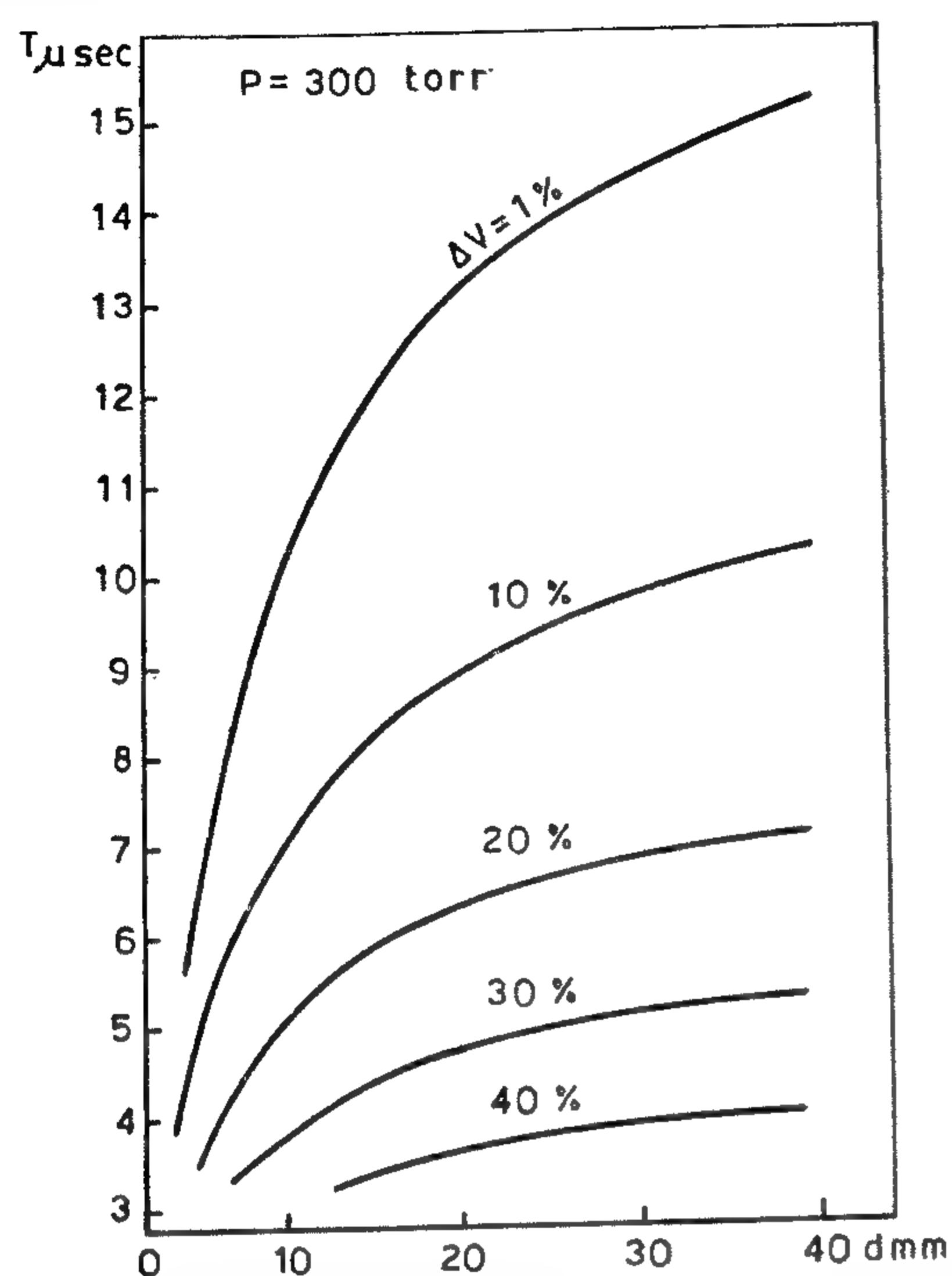


FIG.(4) THE CHARACTERISTIC TIME τ AS A FUNCTION OF THE ELECTRODE SEPARATION d AT CONSTANT GAS PRESSURE AND DIFFERENT PERCENTAGE OVERVOLTAGE ΔV AT $P = 300$ TORR

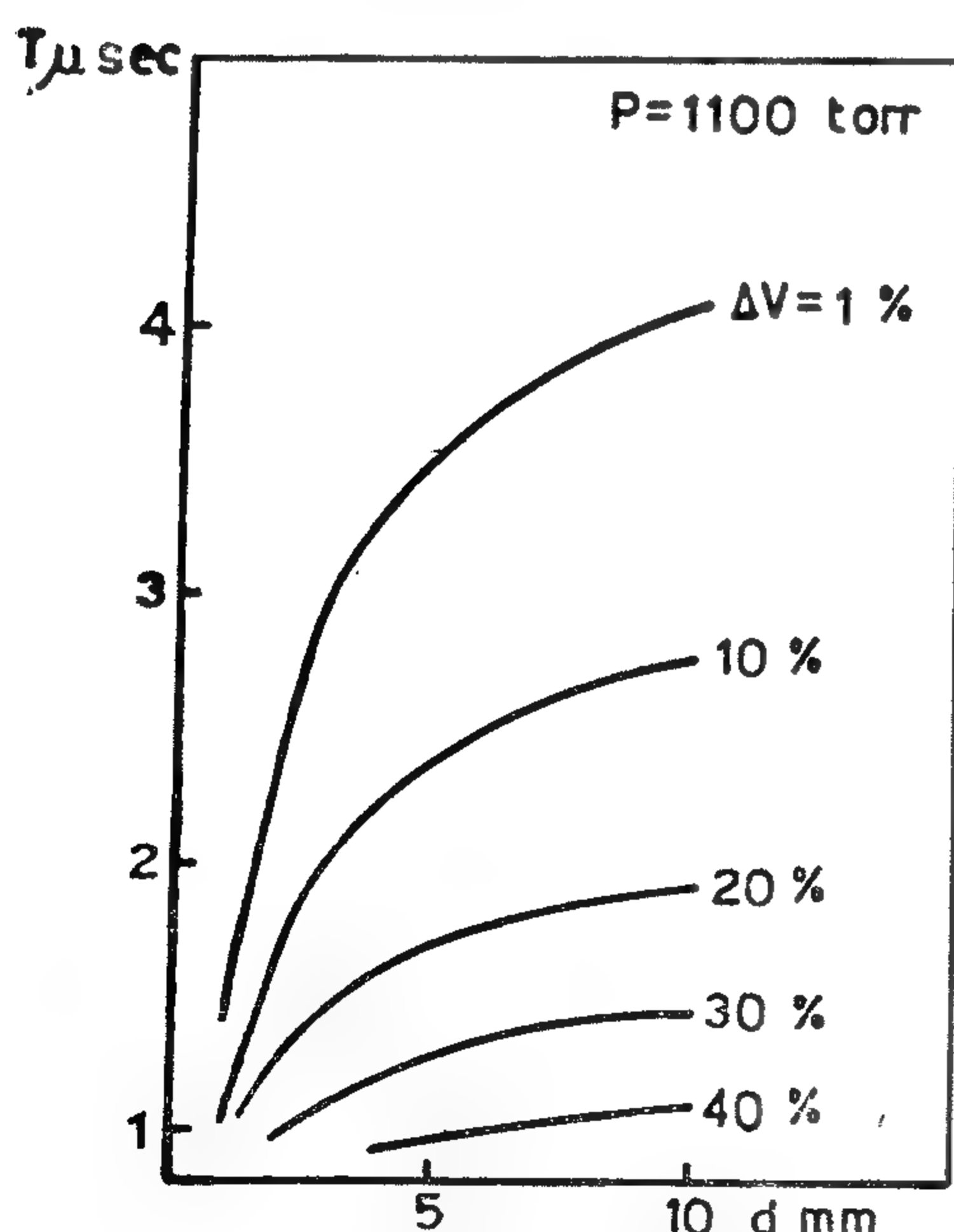


FIG.(5) THE CHARACTERISTIC TIME τ AS A FUNCTION OF THE ELECTRODE SEPARATION d AT CONSTANT GAS PRESSURE AND DIFFERENT PERCENTAGE OVERVOLTAGE ΔV AT $P = 1100$ TORR

The streamer mechanism may be responsible for the saturation of the curves. At large electrode separations any electron in the gap will help to form a streamer which will cross the gap at almost constant time independent of the position at which the electron started or the length of the gap.

C. Dependency of the Characteristic Time on Gas Pressure

At constant percentage overvoltage ΔV , and constant product of gas pressure and electrode separation pd , the variation of the characteristic time T with the gas pressure p is shown in Figures (6) and (7). These figures are deduced from Figures (8) and (9), respectively.

If the relation between the characteristic time T and the gas pressure p is plotted on a log-log scale at constant ΔV and pd , the

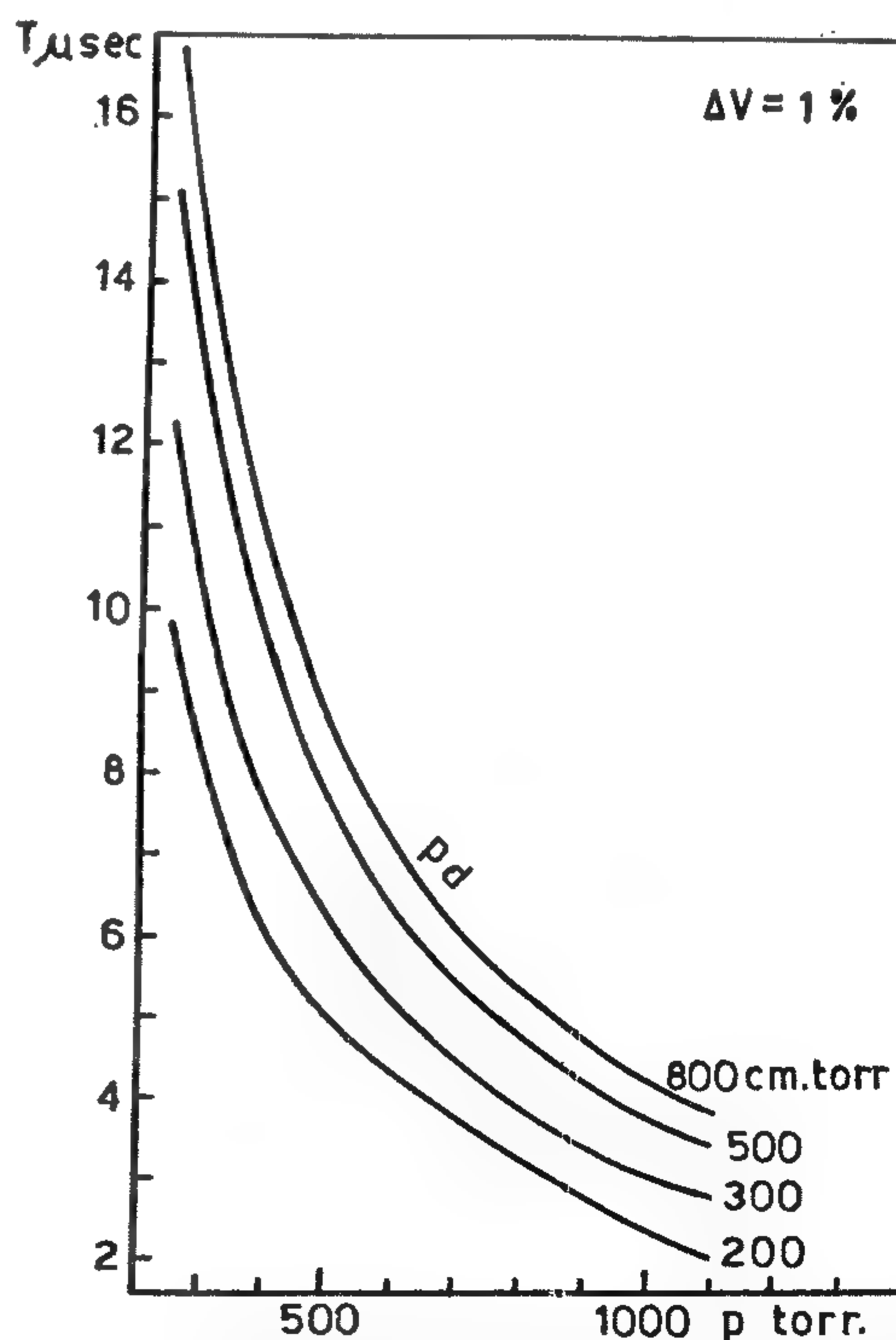


FIG.(6) THE CHARACTERISTIC TIME τ VERSUS THE GAS PRESSURE P AT CONSTANT PERCENTAGE OVERVOLTAGE $\Delta V (=1\%)$ AND CONSTANT PRODUCT OF GAS PRESSURE AND ELECTRODE SEPARATION pd

Other breakdown parameters used to calculate the characteristic time, as the second Townsend ionization coefficient due to positive ion bombardment, are also obtained from the published data [5] for Oxygen. For the calculation of the harmonic average of the positive ions and electrons drift velocities, $1/v = (1/v^+) + (1/v^-)$, we used the approximation $1/v = 1/v^+$, since $v^- \gg v^+$.

IV. RESULTS AND DISCUSSIONS

From the above, we calculate the characteristic time T using Eq. (5). In this section, the obtained results for Oxygen are presented with a brief discussion.

A. Dependency of the Characteristic Time on the Percentage Overvoltage

The family of curves of Figure (2) shows the dependency of the characteristic time T on the percentage overvoltage ΔV at constant pressure p and electrode separation d . From Figure (2), notice that the characteristic time decreases as the percentage overvoltage increases. The tendency of the curves to saturate at higher overvoltages is clear. This may be explained as follows: as the overvoltage increases, the field will reach a certain value at which any electron in the gap will have a high probability of causing breakdown.

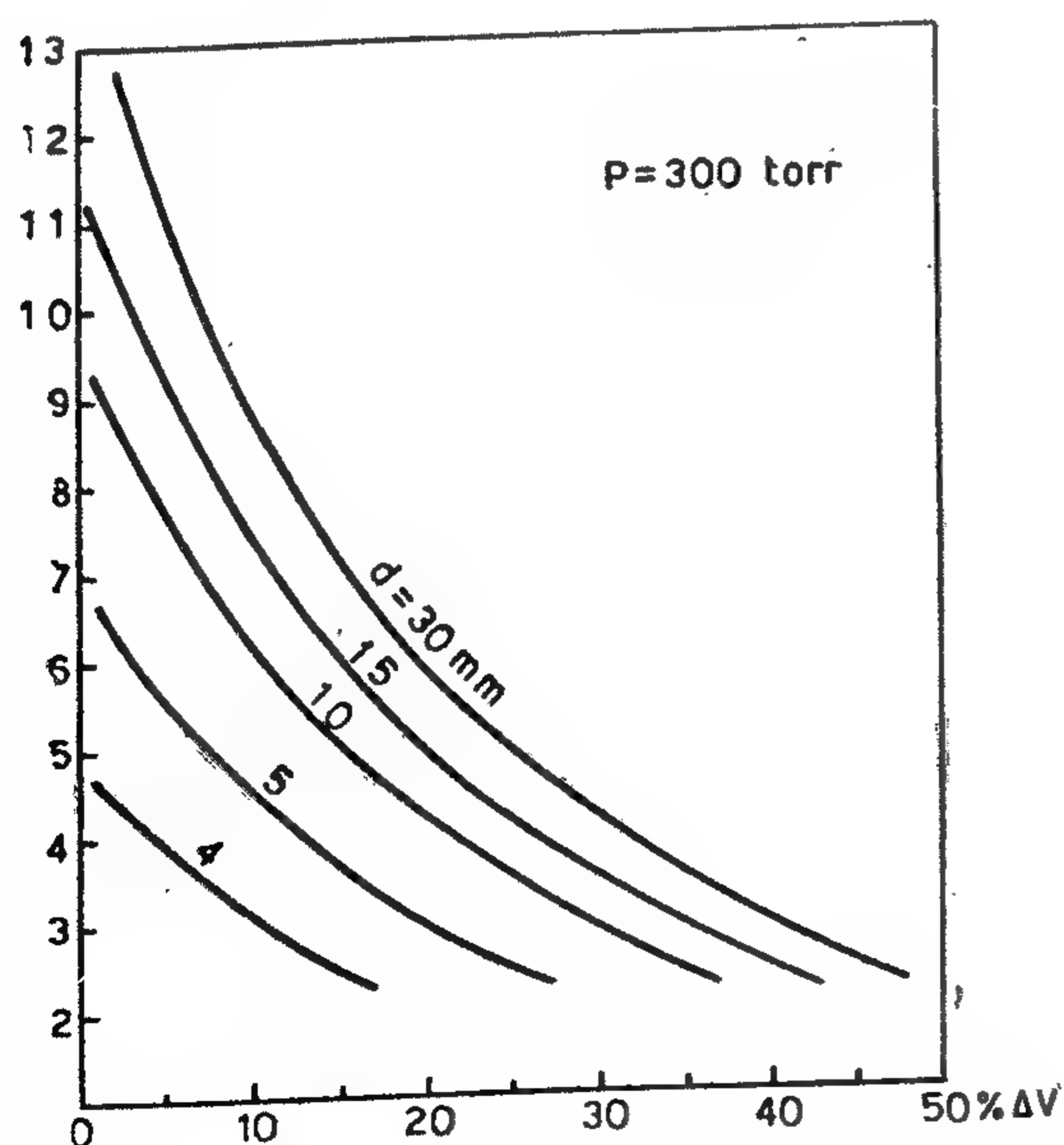


FIG. (2) THE CHARACTERISTIC TIME T AS A FUNCTION OF THE PERCENTAGE OVERVOLTAGE ΔV AT CONSTANT GAS PRESSURE $P (=300 \text{ TORR})$ AND DIFFERENT ELECTRODE SEPARATIONS D ,

The relation between the characteristic time T , and the percentage overvoltage ΔV , is plotted on log-log scales as shown in Figure (3) as a smooth continuous curve. Kohrmann [6] stated that the transition from a Townsend mechanism to a streamer one can be detected by drawing the relation between the logarithm of the formative time lag and the logarithm of the overvoltage at constant pressure and electrode separation. The curve thus obtained will show an abrupt change in the formative time lag indicating the transition. Our analysis shows that when a set of these curves are drawn, they are similar to Figure (2), showing no abrupt change.

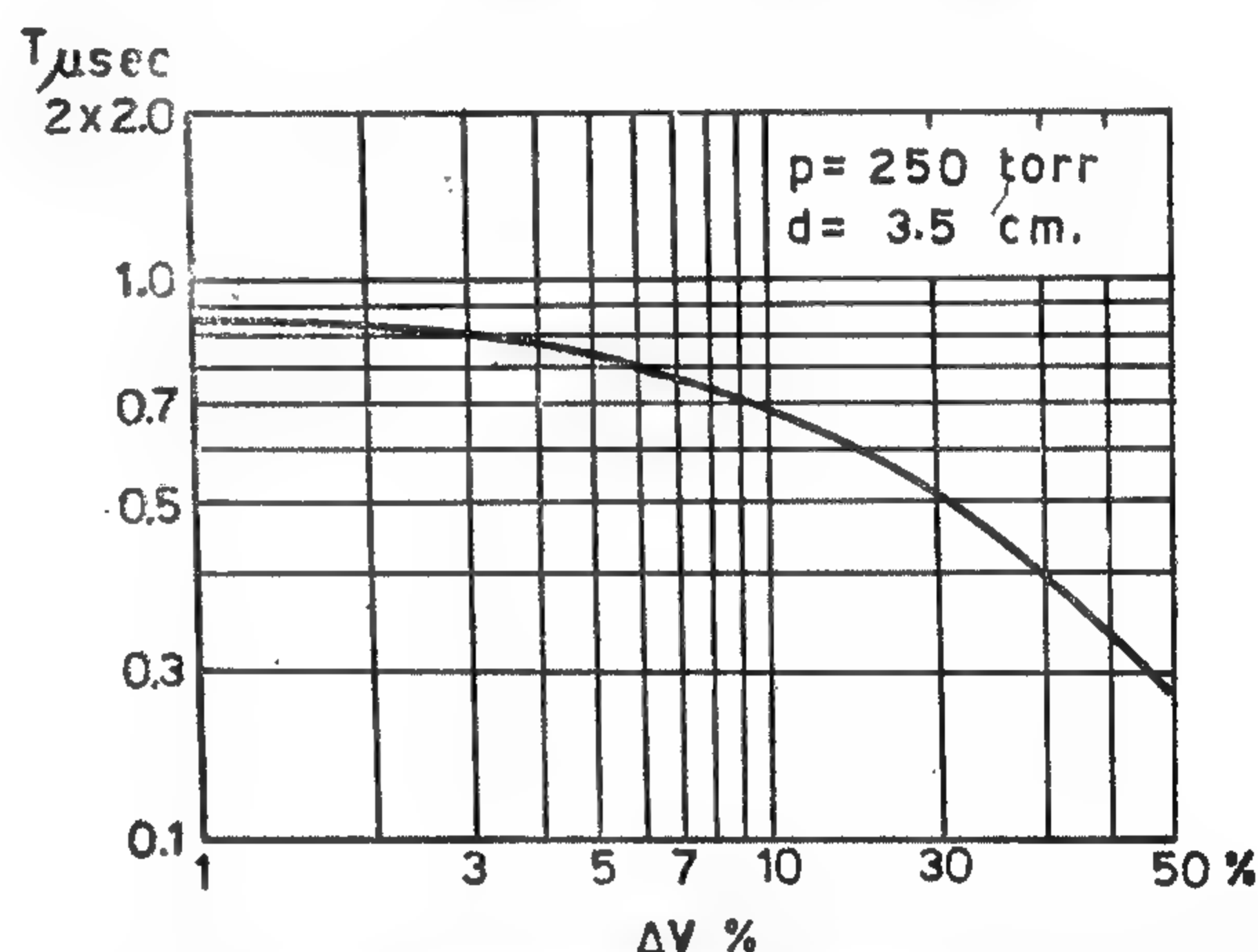


FIG. (3) THE CHARACTERISTIC TIME T VERSUS THE PERCENTAGE OVERVOLTAGE ΔV AT $P = 250 \text{ TORR}$ AND $d = 3.5 \text{ cm}$ ON A LOG-LOG SCALE

B. Dependency of the Characteristic Time on Electrode Separation

Figure (4) shows a set of curves of the characteristic time T versus the electrode separation d at constant pressure p ($p = 300 \text{ torr}$) and different values of the percentage overvoltage ΔV . Figure (5) shows a similar set of curves at a different value of pressure p ($p = 1100 \text{ torr}$). From Figures (4) and (5), it is seen that as the electrode separation increases, the characteristic time increases tending to saturate at higher values of electrode separation. The electrode separation at which the characteristic time T saturates decreases as the percentage overvoltage ΔV increases.

Schade [1] derived an equation for the formative time lag t_f that takes the form

$$t_f = [a'/(v - v_0)] \exp(b/v), \quad (2)$$

which he found that it fits his experimental measurements for Neon. From Eqs. (1) and (2) it is obvious that the formative time lag t_f is a linear function of the characteristic time T . Accordingly, by calculating the characteristic time T , the formative time lag t_f can easily be obtained. And a study of the characteristic time T can reveal the behaviour of the formative time lag t_f for the same substance under the same conditions of pressure p , electrode separation d , and electric field strength E .

The previous theoretical work [2 — 3] for calculating the formative time lag was either inaccurate or complicated in accounting for the effect of the secondary electron emission. It is our aim in this work to present an equation and a study of the formative time lag taking into consideration the effect of the secondary electron emission due to positive ion bombardment. Therefore, in this paper we will devote ourselves to the study of the characteristic time T for Oxygen, which is a linear function of the formative time lag t_f , under the effect of uniform electric field strength E and different conditions of applied voltage V , pressure p , and electrode separation d .

II. EVALUATION OF THE CHARACTERISTIC TIME

Starting with the exact solution [4] of the continuity equation we obtain the equation.

$$\gamma_i \alpha \exp(\xi d) - 1 = 1,$$

where

$$\xi = \alpha - \frac{1}{v\tau}, \quad (3)$$

and v is the harmonic average of the drift velocities of the electrons (-) and positive ions (+). v is given by

$$\frac{1}{v} = \frac{1}{v^+} + \frac{1}{v^-}. \quad (4)$$

Near threshold, we have

$$\frac{1}{v\tau} \ll \alpha,$$

therefore, Eq. (3) takes the form

$$\gamma_i \left\{ \exp \left[d \left(\alpha - \frac{1}{v\tau} \right) \right] - 1 \right\} = 1$$

rearranging, we obtain

$$\tau = 1/v \left\{ \alpha - (1/d) \ln[(1 + \gamma_i)/\gamma_i] \right\} \quad (5)$$

Further simplification of Eq. (5) leads to Eq. (1). Eq. (5) is a more accurate equation to calculate the characteristic time T which holds in the vicinity of breakdown. It is clear that it accounts for the effect of the secondary electron emission due to positive ion bombardment represented by the second Townsend ionization coefficient γ_i .

III. BREAKDOWN PARAMETERS

Using the published data [5] of the first Townsend ionization coefficient α for Oxygen and the well known equation

$$\alpha = A \exp(-BE/p), \quad (6)$$

the constants A and B and their range of application are obtained, see Table 1. The calculated values of α using the obtained values of A and B in the indicated regions, Table 1, are of very high accuracy.

Table 1:

The constants A and B of the equation $\alpha = A \exp(-BE/p)$ and their range of application

E/p (volt/cm. torr)	A	B
35 — 45	1.75	18.44
45 — 60	3.84	9.667

CHARACTERISTIC TIME OF OXYGEN CALULATIONS AND THEORETICAL STUDY

By

A. R. M. ZAGHLOUL, R. M. RADWAN,
AND M. S. ABOU-SEADA

ABSTRACT

We present an equation for the characteristic time t , through which we can calculate the formative time lag of breakdown t_f more accurately than previously obtained. This equation takes into consideration both the effect of the first Townsend ionization coefficient α and the second Townsend ionization coefficient due to positive-ion bombardment

. Calculations of the characteristic time T were carried out for Oxygen, using the presented equation, at uniform field and over wide ranges of the breakdown parameters.

The results obtained are presented together with a brief study. It was found that the characteristic time is independent of the electrode separation d , with an error much less than 1%, at constant gas pressure p and electrif field strength E , over certain ranges of d . Also, it was found that the characteristic time is inversely proportional to the gas pressure raised to a constant power over a wide range of pressure, at constant percentage overvoltage and constant product of gas pressure and electrode separation. In addition, the coefficients A and B of the well known equation of the first Townsend ionization coefficient a , $a = A \exp (-BE/p)$, are obtained.

Electrical Engineering Department, Faculty
of Engineering, Cairo University, Cairo,
Egypt

I. INTRODUCTION

We consider the case of uniform electric field using the well known configuration of parallel-plate electrodes, Figure (1), for the study of the characteristic time T in Oxygen. The obtained expression of the characteristic time T from the exact solution of the continuity equations by approximating the effects of the second Townsend ionization coefficient due to positive-ion bombardment γ_i and the first Townsend ionization coefficient a takes the form

$$r = [a/(V - V_0)] \exp(b/V). \quad (1)$$

where a and b are constants, and V and V_0 are the applied voltage and breakdown voltage of the substance under study, Oxygen in our case, respectively. The values of a , b , V , and V_0 are, of course, dependent on the substance in use and its conditions.

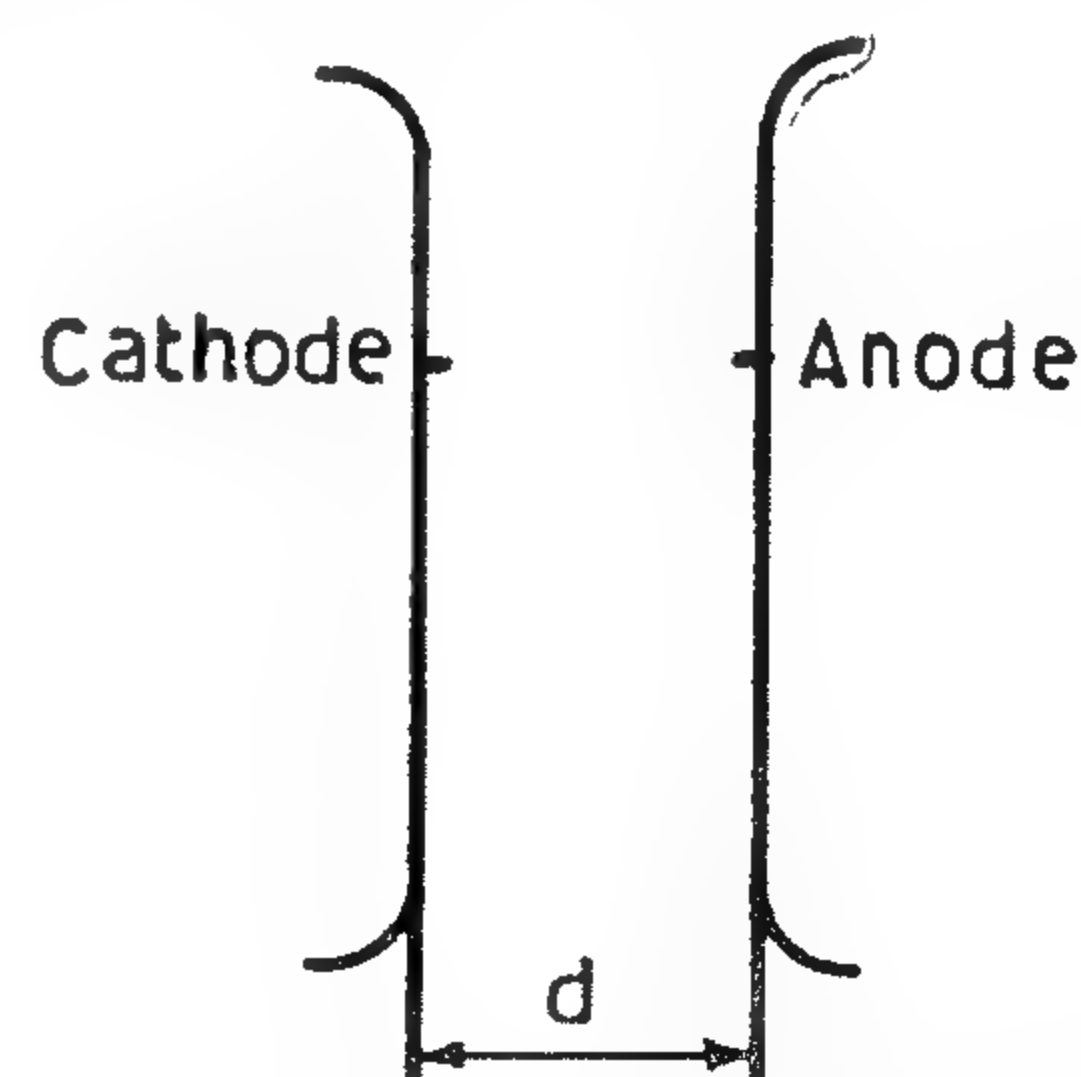


FIG.(1) PARALLEL PLATE ELECTRODES
CONFIGURATION

INDUSTRY & PRODUCTION

**INST. OF MECHANICAL ENGINEERS
INST. OF ELECTRICAL ENGINEERS**

الخدمات الأولية والصناعات الكيماوية

جمعية مهندسي المناجم والبترو
والفلزات
جمعية المهندسين الكيمائيين

REFERENCES

- (1) Gaudin, A.M., Fuerstenan, M.C., International Mineral Processing Congress, Institution of Mining and Metallurgy, London, 1960, pp. 115-27.
- (2) Gandin, A.M., Fuerstenau, M.C., Ibid., 223, 122 (1962).
- (3) Keith J. Scott, Ind. Eng. Chem. Fundamentals, Vol. 5 No. 1. February 1966 — pp. 109-113.
- (4) Carman, P.C.; Trans. Inst. Chem. Engrs. 15,150 (1937).
- (5) Michaels, O.S., Bolger, J.C., Ind. Eng. Chem. Fundamentals 1,24 (1962).
- (6) Colin Harris, Nature, Vol. 183, pp. 530-531, Feb. 21, 1959.
- (7) Whitmore, R.L., Brit. J. App. Physics., 6, 239 (1955).
- (8) Hathout M.Z., Chalabi, M.F., El. Gindi M.M., Assuit University Tech. Bulletin, 1966.
- (9) Whitmore, R.L., J. Inst. Fuel (May 1957).

* * *

The same figure illustrates the sedimentation results obtained by Whitmore (9) for different graded sizes of rough methyl methacrylate powders and represented according to equations (8,9). It is observed from the figure that there is agreement between experimental sedimentation rates and the predicted rates from equation (13) which is based on flow through porous beds.

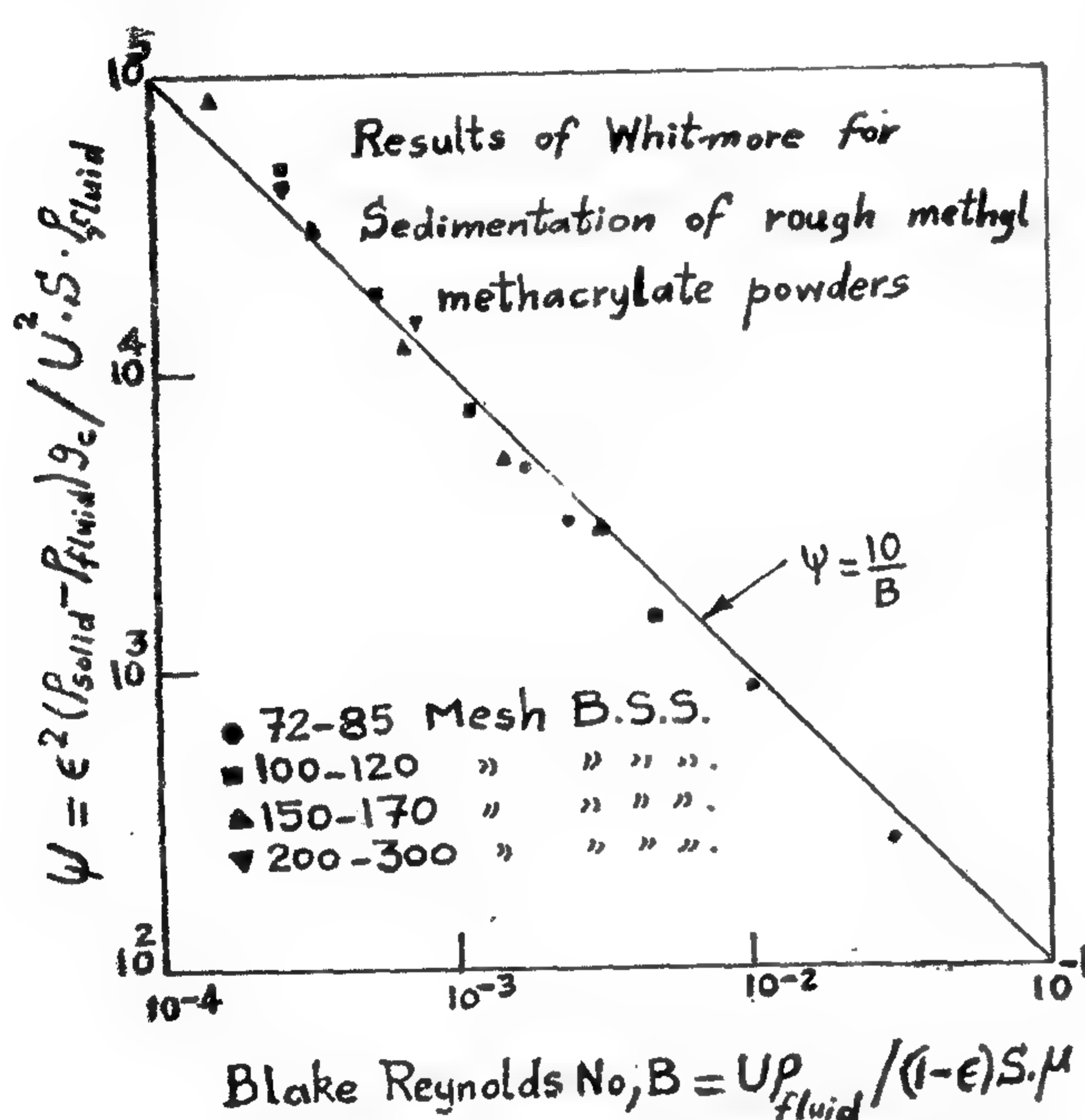


FIG.5. Comparison between Correlation obtained with streamline flow through porous beds and sedimentation rates of rough particles.

Conclusions :—

The model predicted in this work as represented by equation (17) provides a preferable means for predicting experimental settling rates at different volume concentrations. The value of the constants k , K , and the ratios c , C vary from one system to the other and should be determined for each system

under the prevailing operating conditions. The model adds to the importance of applying the correlated data of flow through porous beds in the field of sedimentation and thickening.

The theoretical model given by Colin (6) as represented by equations (7, 8, 9) is proved by this work to provide a satisfactory method for correlating experimental data in the fields - of porous beds flow and sedimentation rates, Colin's model verifies the validity of the correlation used as basis for the prediction of this work's model in the following general form for stream flow conditions :

$$U \cdot \mu \cdot L / \Delta p \cdot g_c = \epsilon^2 / K \cdot S^2 \cdot (1 - \epsilon)^2 \quad (22)$$

Symbols :

- B = Modified or Blake Reynolds number.
- c, C = Ratio of volume of water plus solid to volume of solid.
- d = Mean spherical diameter of a particle, (cm).
- g_c = Local gravitational acceleration, (980 cm/sec²).
- k, K = Constants.
- L = Thickness of bed, (cm).
- U = Descent rate of particles relative to sides, apparent velocity, (cm/sec).
- S = specific surface of solid per unit volume, (cm²/cm³).
- Z = Volume fraction of dry solid.
- ϵ = Volume fraction of voids (porosity).
- ρ = Density, (gm/cm³).
- μ = Viscosity of fluid, (poise).
- ψ = Friction factor.
- Δp = Pressure Difference, (gm/cm²).

Below $z = 0.09$, both inter and intrafloc flow occur simultaneously and the interfloc flow may be estimated by subtracting from the total measured values of "U" at each concentration, a value of "U" calculated from the determined equation (19). These differences, expressing the net flow between the flocs, can be treated in the same way as before and a straight line is obtained when $(U_{\text{diff}} z)^{\frac{1}{2}}$ is plotted against z . Figure (3) shows a comparison of the functions $(U_{\text{diff}} z)^{\frac{1}{2}}$ and $(U_{\text{diff}} z)^{\frac{1}{2}}$ plotted against the volume concentration of kaolin. The corresponding values of C and K are determined and equation (17) can be completely determined with C, K, c, and k replaced by their numerical values, thus :

$$U = \frac{1.01 \times 10^{-3} (1 - 13 z)^2}{z} + \frac{2.42 \times 10^{-5} (1 - 5.4 z)^2}{z} \dots (20)$$

Figure (4) illustrates the predicted settling rates applying three models of thickening, two of which are based on flow through porous beds, against the volume concentration of kaolin; and compares it with the experimental data reported by Gaudin and Fuerstenau (1) for the settling rates of kaolin at an alkalinity level of 0.1 gm. CaO / liter. It is observed that the model developed in this work, and is represented by equation (20), fits the experimental data better than the other models.

Another mode of using the correlation obtained for flow through porous beds (8) in sedimentation can be achieved by comparing equation (13) derived from this correlation with the work reported by Colin (6). From equation (13) we get the following equation

$$\frac{\epsilon^2}{U^2 S} \cdot \frac{\rho_{\text{solid}} - \rho_{\text{fluid}}}{\rho_{\text{fluid}}} \cdot g_c = 10 \frac{(1 - \epsilon) \cdot S \cdot \mu}{U \cdot \rho_{\text{fluid}}} \quad (21)$$

(e.) $\psi = 10 / B$ -----

This last equation (21) is analogous to equation (7) reported by Colin. The left hand

side of equation (21) was plotted versus B on log log scales as shown in figure "5" to get a straight line representing the equation.

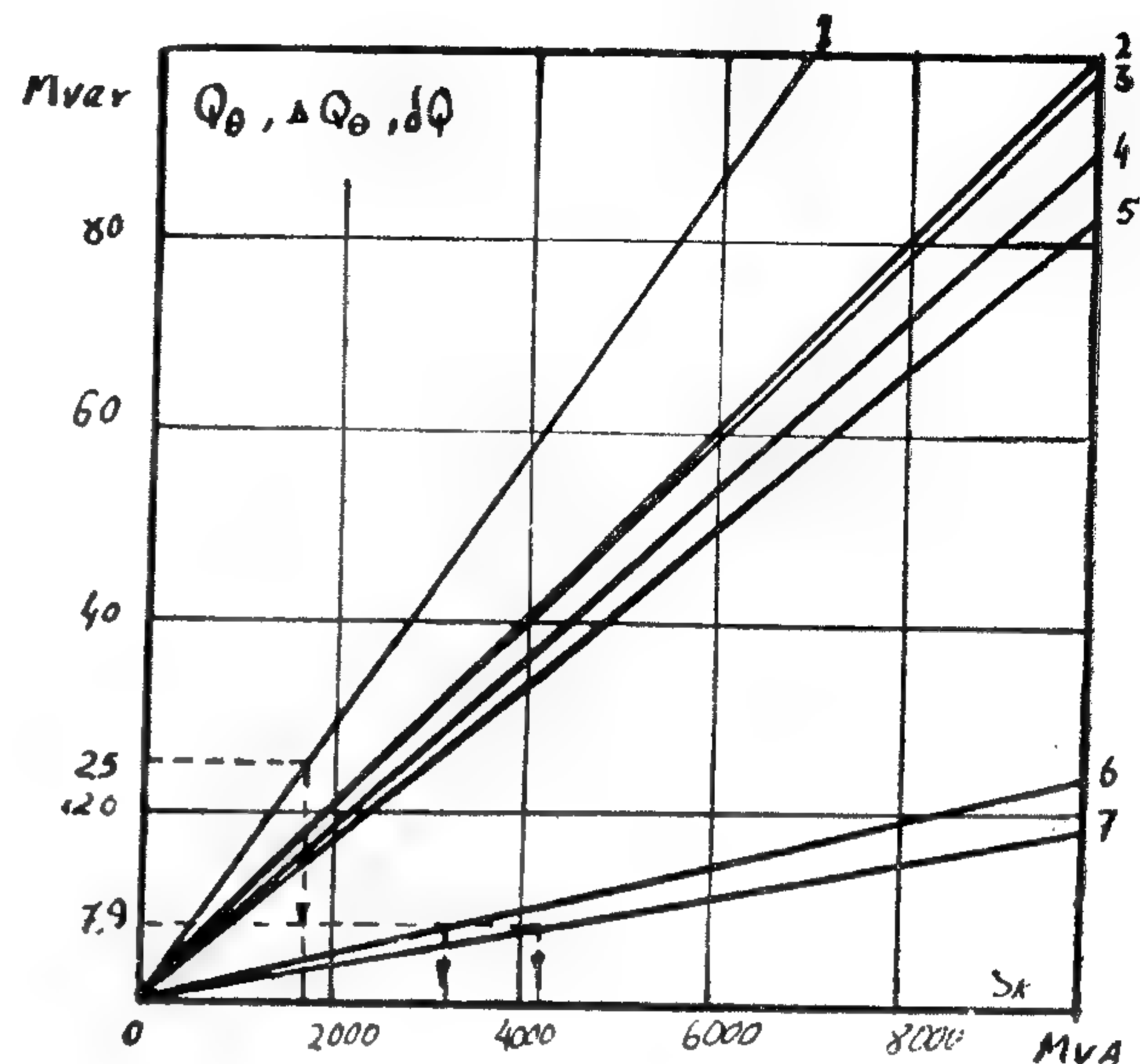


Fig (3)

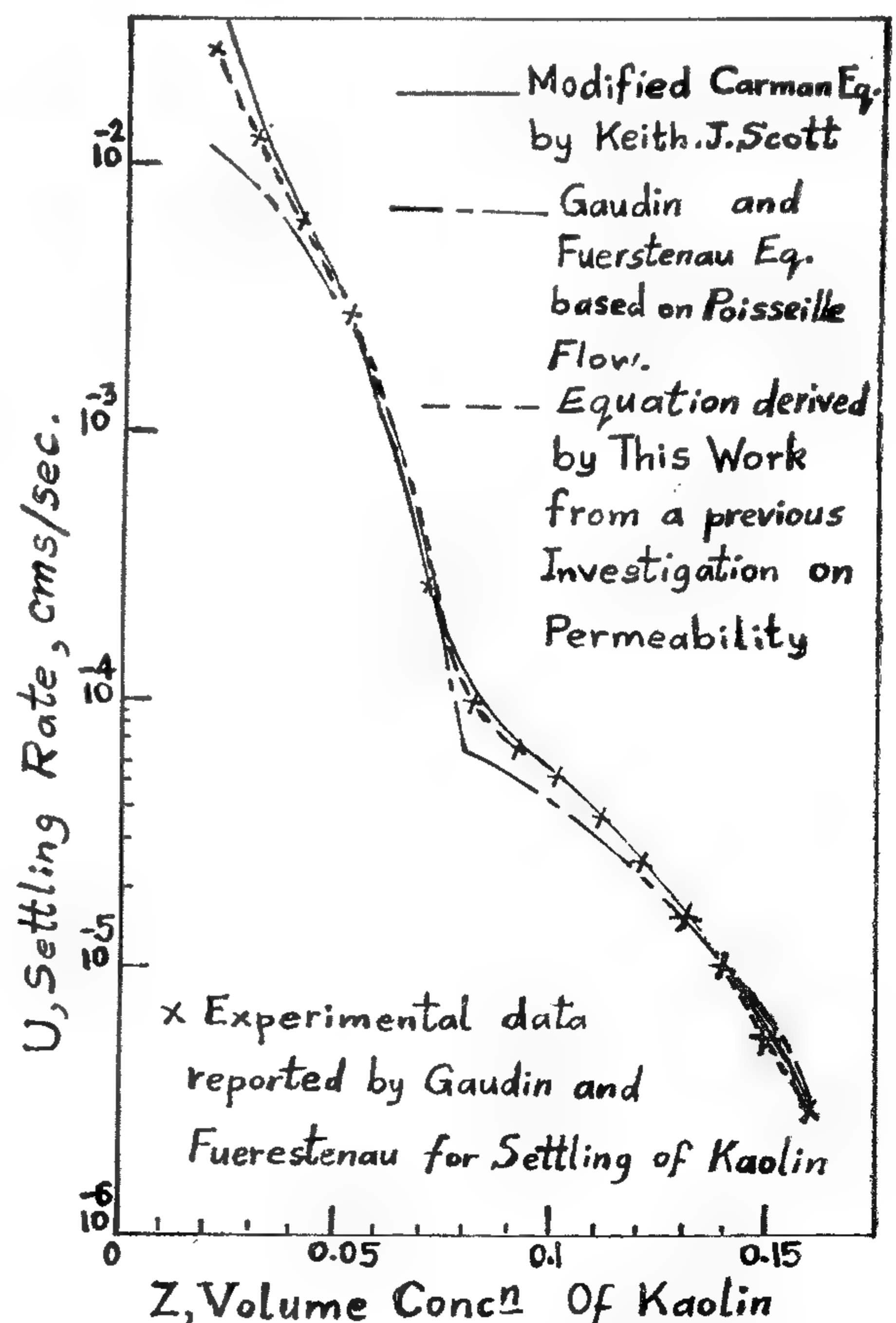


FIG.4. Comparison Of Three Models Of Thickening

dry solids, then, $\epsilon = 1 - cz$, and $(cz - z)$ proportional to Sz . Therefore, from equation (13) we get :

$$U = 0.1 \frac{(1 - cz)^2 (\rho_{floc} - \rho_{fluid}) g_c}{s^2 \times \mu \times cz} \quad (14)$$

ρ_{floc} represents the density of the descending units, consisting either of solid particles plus water shell or of individual flocs if the material is flocculated.

From the material balance we get :

$$\rho_{floc} - \rho_{fluid} = \frac{\rho_{solid} - \rho_{fluid}}{c} \quad (15)$$

Substituting in equation (14) gives :

$$U = 0.1 \frac{(\rho_{solid} - \rho_{fluid}) g_c}{s^2 \times \mu \times c^2} \times \frac{(1 - cz)^2}{z} \\ = K \frac{(1 - cz)^2}{z} \quad (16)$$

Applying the model developed by Gaudin (1), which describes two stage process of descent for flocculated kaolin, we get :

$$U = K \frac{(1 - cz)^2}{z} + k \frac{(1 - cz)^2}{z} \quad (17)$$

For $z > 0.08$, equation (17) reduces to:

$$(Uz)^{\frac{1}{2}} = K^{\frac{1}{2}} (1 - cz) \quad (18)$$

Figure (1) shows plots of $(Uz)^{\frac{1}{2}}$ against z as well as plots of $(Uz)^{\frac{1}{3}}$ against z . It is seen that both functions are represented by straight lines for values of "z" above which sending the straight line of the function $(Uz)^{\frac{1}{2}}$ for an alkalinity level equal to 0.1 gm CaO/Liter

$$U = 2.42 \times 10^{-5} (1 - 5.4 z)^2 / z \quad (19)$$

Figure (2) shows a comparison of the terms $(Uz)^{\frac{1}{2}}$ and $U^{\frac{1}{2}}$ versus the volume concentration "z". It is apparent that the $(Uz)^{\frac{1}{2}}$ function gives satisfactory straight lines, but the $U^{\frac{1}{2}}$ function cannot be defined by such lines.

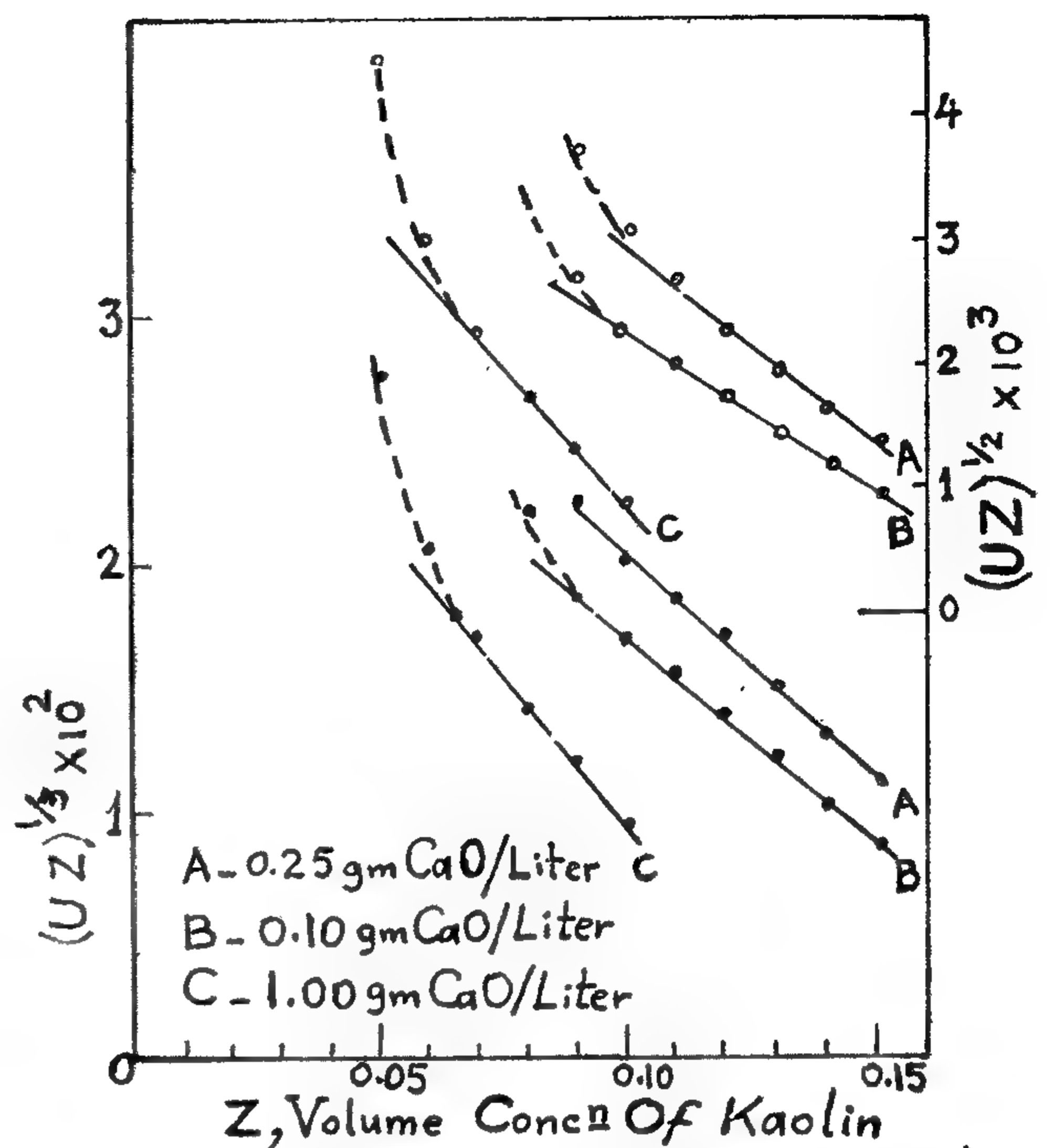


FIG.1. Comparison Of Functions $(Uz)^{\frac{1}{3}}$ and $(Uz)^{\frac{1}{2}}$ For Various Alkalinity Levels

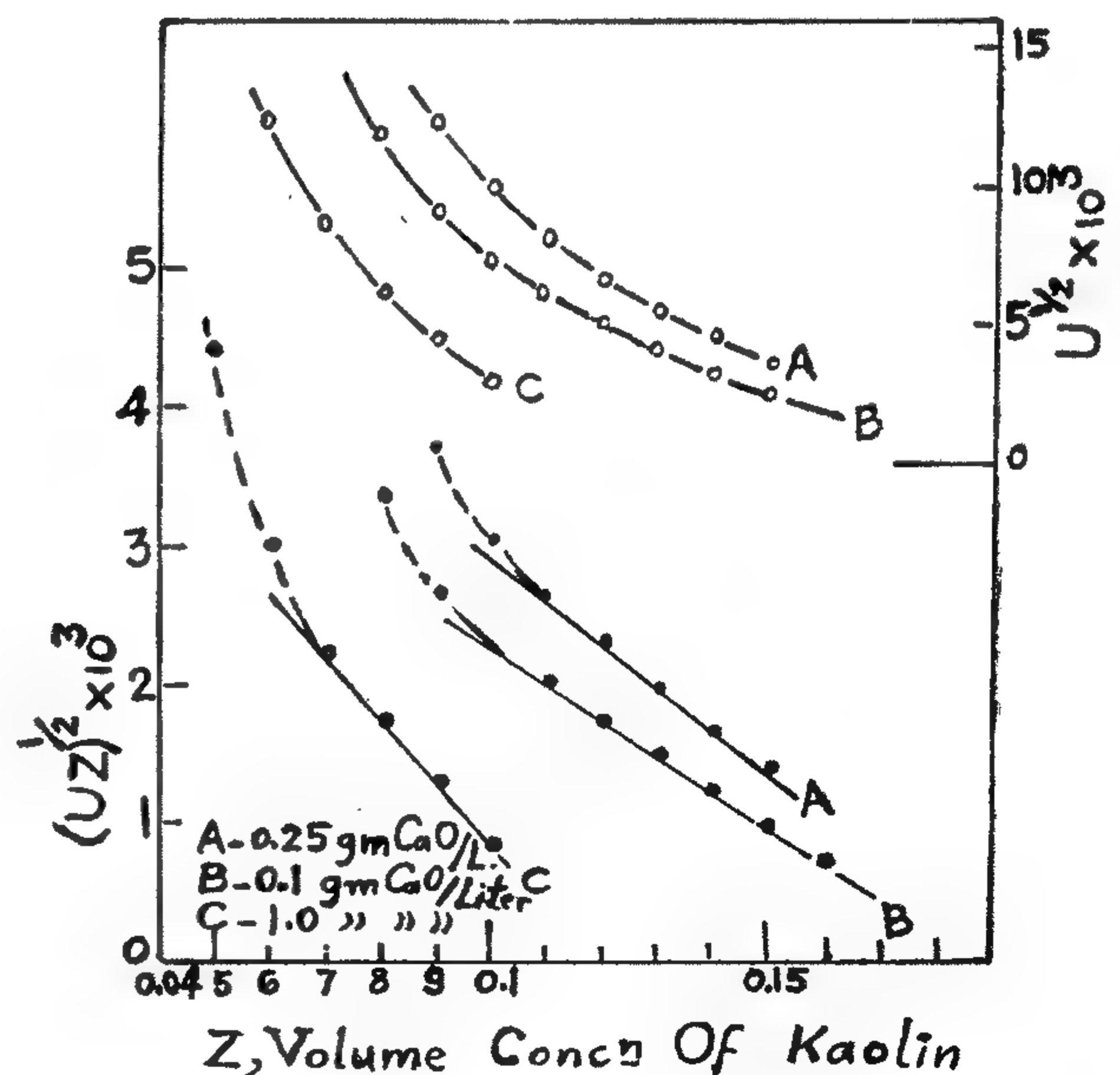


FIG.2. Comparison Of Functions $(Uz)^{\frac{1}{2}}$ and $U^{\frac{1}{2}}$ For Various Alkalinity Levels.

Substituting the numerical values for the constants M , m , K , k and the ratios c , and C as determined graphically from the settling rates of kaolin reported by Gaudin at an alkalinity level of 0.1 grm. CaO / liter, yielded the equations (5) proposed by Gaudin and (6) proposed by Keith :

$$U = 2.0 \times 10^{-2} (1 - 12.5 Z)^2 + 2.0 \times 10^{-4} (1 - 5.5 Z)^2 \quad (5)$$

$$U = 1.40 \times 10^{-3} (1 - 11.3 Z)^3 / Z + 3.75 \times 10^{-5} (1 - 4.8 Z)^3 / Z \dots (6)$$

Colin (6) used dimensionless groups for friction factor, ψ , against a modified Reyn-correlating sedimentation rates by plotting a olds number, B , called Blake Reynolds number. The correlation is of the type :

$$\psi = \frac{K}{B^N} \dots \dots \dots (7)$$

in which N and K are parameters. Colin assumed a plug flow to account for the constant settling rate; by forming force balance equations and using dimensionless groups, he derived a theoretical model represented by the following equations for ψ and B .

$$\psi = \frac{\epsilon^2}{U^2 S} \left(\frac{\rho_{solid} - \rho_{fluid}}{\rho_{fluid}} \right) \cdot g_c \dots \dots \dots (8)$$

$$B = U \cdot \rho_{fluid} / (1 - \epsilon) \cdot S \cdot \mu \dots \dots \dots (9)$$

Colin applied equations (8,9) to correlate the experimental data reported by Whitmore (7) for the sedimentation rates of two sets of spherical particles, and showed that when $\epsilon = 0.75$ and 0.8 then $N = 1$ and $K = 5.5$. The value of N remained constant at all porosities, but K increased with porosity, ranging from 6 when $\epsilon = 0.85$ to 13.5 when $\epsilon = 0.95$. This trend was attributed by Colin to be due to departure from plug flow and tend to become more serious as porosity increases.

Proposed Model and Discussion :—

Equation (10) was developed to correlate permeability in a previous investigation (8) :

$$\text{Permeability} = \frac{U \cdot \mu \cdot L}{\Delta p \cdot g_c} = 0.1 \times \frac{\epsilon^2}{S^2 (1 - \epsilon)^2} \dots \dots (10)$$

$$\text{(or)} \quad U = 0.1 \epsilon^2 \cdot \Delta p \cdot g_c / S^2 \cdot L \cdot (1 - \epsilon)^2 \dots \dots (11)$$

The most important expression in this equation is $\epsilon^2 / (1 - \epsilon)^2$ which correlates well the experimental data for flow through porous beds (8). A theoretical background favours the application of such expression than that proposed by Carman in equation (1). In the derivation of equation (1) from Poiseuille's equation for streamline flow in a pipe, the distance transversed by the fluid was assumed to be proportional to the depth of the porous bed, L , whereas it should be proportional to $(L \cdot \epsilon)$. The reason for this is that the porosity affects the length of the channels transversed by the fluid from one end to the other. The greater the porosity the longer the distance transversed by the fluid through the channels around the contacting particles.

In applying equation (11) to the sedimentation of solids, the pressure drop per unit length is equated to the net weight of solids supported hydraulically by unit height of pulp,

$$\frac{\Delta p}{L} g_c = (1 - \epsilon) (\rho_{solid} - \rho_{fluid}) g_c \quad (12)$$

Substituting in equation (11), we get :

$$U = 0.1 \frac{\epsilon^2 (1 - \epsilon) (\rho_{solid} - \rho_{fluid}) g_c}{S^2 \times \mu \times (1 - \epsilon)^2}$$

$$= 0.1 \frac{\epsilon^2 (\rho_{solid} - \rho_{fluid}) g_c}{S^2 \times \mu \times (1 - \epsilon)} \quad (13)$$

Assuming that some of the water adheres to the descending solid particles and that volume of this water is proportional to the dry solids surface. If "c" denotes the ratio of volume of water plus solid to volume of

MATHEMATICAL MODEL FOR THICKENING MECHANISM

By

Dr. M.Z. HATHOUT and Dr. M.F. CHILABI

ABSTRACT

A model based on flow through porous beds is proposed to elucidate the mechanism of thickening in concentrated suspensions. An equation is derived mathematically which explains the observed behaviour at all concentration levels during batch sedimentation. The equation was tested by means of the published transviewer data of Gaudin and Fuerstenau (1), and is shown to correlate with experimental data. The permeability correlation applied as basis for the model was found to agree with a theoretical sedimentation model given by Colin (6).

Many explanations of the processes occurring the thickening of relatively thick suspensions has been proposed in the literature. Gaudin and Fuerstenau (1) suggest a model based on Poiseuille's flow through a series of straight, parallel, circular tubes and tubules. They investigated the size distribution of these tubes in a second paper (2). Keith (3) considered the mechanism of thickening as the upward flow of water through a bed of particles. He used the previous work of Carman (4) in the field of porous beds as basis for an alternative model of thickening.

It has been demonstrated by Carman (4) that if we assume a bed to be composed of spheres of uniform diameter, d , the apparent flow velocity, U , is given by

$$U = \frac{d^2}{k^0 \mu} \times \frac{\epsilon^3}{36(1-\epsilon)^2} \times \frac{\Delta p}{L} \quad \dots \dots \dots (1)$$

Keith (3) regarded k^0 as constant of unknown value in the system under study, and in applying equation (1) to the sedimentation of solids, the pressure drop per unit length was

equated to the net weight of solid supported hydraulically by unit height of pulp. Keith assumed that some of the water adheres to the descending solid particles and that the volume of this water is proportional to the dry solids volume as had been previously reported in literature (1,5). Keith developed the following equation (2) mathematically.

$$U = \frac{d^2 (\rho_{solid} - \rho_{fluid}) g_c}{36 k^0 \mu c^2} \times \frac{(1-CZ)^3}{Z} \\ = K \cdot (1-CZ)^3 / Z \quad \dots \dots \dots (2)$$

where K is a constant for a given pulp at constant temperature, and U refers to the descent rate of the particles relative to the walls.

Gaudin (1) showed that for flocculated kaolin, the descent rate is essentially a two-stage process depending on the solids concentration. He assumed that in the dilute region most of the upward flow occurred in the spaces between the flocs (tubes), while at high concentration, when the flocs moved closer together, the only possible flow was within the uocs (tubules). The intrafloc was assumed to occur also in the dilute region. The termination of stage (1) was found to occur between 7 and 10% volume concentration for the kaolin water system. Gaudin described this two stage process by the following model :

$$U = M(1-CZ)^2 m(1 - CZ)^2 \dots (3)$$

The corresponding model developed by Keith was reported as:

$$U = \frac{K(1-CZ)^3}{Z} + \frac{k(1-cZ)^3}{Z} \dots (4)$$

1 — Professor of Mineral Dressing, Azhar University

2 — Assistant Professor of Chemical Engineering, Cairo University.

RAWMATERIALS & GHEMICAL INDUSTRIES

**INST. OF TINING, PETROLEUM &
METALLURGICAL ENGINEERS —
INST. OF CHEMICAL ENGINEERING**

CONTENTS

GENERAL SECTION :

BUILDING & CONSTRUCTION	INDUSRTY & PRODUCTION	RAW MATERIALS & CHEMICAL ENGINEERING
(ARABIC)	(ARABIC)	(ARABIC)
— Cairo Conference on Low Cost Housing Dr. G. NASSAR 8	Or ganization and re- vision of organization structures. Eng. H. NAGY 74	
— The Influence of tec- hnology on archic tural-creativity town Planning & Society -2- Dr. T. ABDEL-GA- WAD 11		
— O —	— O —	— O —
(ENGLISH)	(ENGLISH)	(ENGLISH)
— Treatment of forces in 3-Dimensions by or- thogcnal projection on two perpendicular pla- nes. Dr. S.H. ABDEL- SHAHID 26	— Soil Breakdown & its effect on the earth resistance Dr. A.G. ZEITOUN & A.M.K. EL-MORSHE- DY 93	— Mathematical model for thickening mecha- nism. Dr. M.Z. HATOUT & Dr. M.F. GHILABI 147
— Effect of stress his- tory on cyclic shear strength of sand Dr. A.A. MOUSSA ... 33	— Torsional vibration an- alysis for the pro- pulsion systems of large motor tankers. - 2 - Dr. F. BAHGAT, Dr. N. MAHAREM & A. EL-IRAKI 102	
— Finite element anal- —ysis of prestressed concrete beams. Dr. M.M. EL-HAS- HIMY, A. ABU EL- ENEIN & A.A. HA- MID 41	— Characteristic Time of oxygen : Calcula- tions and theoritical study Dr. A.R.M. ZAGU- LOUL, R.M. RAD- WAN & M.S. ABOU- SEADA 109	

JOURNAL OF THE EGYPTIAN SOCIETY OF ENGINEERS

VOL. XIV.

ISSUE No. 2 —

EPR-MAY-JAN - 1975)

EDITING BOARD

Editor

Dr. S. MORTADA

Assist. Editor &

Treasurer

Dr. G. NASSAR

Dr. H. AMER

Eng. T. ABD EL - GAWAD

Dr. F. BAHGAT

Dr. S. EL-SOBKY

Dr. M. ABU-ZIED

Dr. M. E. SELIM

Eng. A. EL-ASFORY

- Issued Quarterly Contributors are invited to submit material for editorial consideration addressed to the Editor. The Journal cannot accept responsibility for loss or damage to any material.

INSTRUCTIONS FOR AUTHORS OF ARTICLES

- The Journal publishes articles contributing to the advancement of engineering science and applications.
- Articles may be written in Arabic or English and presented in triplicate with an abstract in both languages.
- Authors' names to be given in full, together with their academic titles and professional occupation.
- Articles may not exceed 8 pages. In this respect, mathematical derivations may be abbreviated and tables replaced by curves.
- Curves to be drawn in black china ink, and to occupy half a page at most. Exceptionally, full page curves or plates are admitted. Curves presented will be scaled down to these sizes. Figures & lettering on curves should not be less than 3 mm even after scaling down.
- References to be given at the end of each article and classified alphabetically according to author's name followed by the name of the journal or book and the date of issue.
- Authors will be presented with two proofs, the first one accompanied by a correction convention chart to ease the work of type correction.

Society Subscriptions

Member	200 P.T.
Associate member	150 P.T.
Associate	100 P.T.

Magazine Subscriptions

Society members Free	
Engineers subscriptions	100 P.T.
Non-engineers subscription	300 P.T.
Organisations subscriptions	500 P.T.

ADVERTISING AGENT

Moassasset Misr for Printing and Publication
10, Souk El Tawfikieh Str. Cairo. Tel. 72192

مجلة جمعية المهندسين المصرية

المجلد الرابع عشر

العدد الثالث (يوليو - أغسطس - سبتمبر ١٩٧٥)

هيئة التحرير

رئيس التحرير

دكتور سيد مرتضى

سكرتير التحرير

وأمين الصندوق

دكتور جمال الدين نصار

مهندس توفيق احمد عبد الجواد

دكتور حامد حسنين عامر

مهندس عبد الملك العصفورى

دكتور فؤاد بهجت

دكتور صلاح السبكى

دكتور محمود أبو زيد

دكتور محيى الدين سليم

- تصدر المجلة ربع سنوية
- ترسل النصوص المطلوب موافقة هيئة التحرير على نشرها باسم السيد / رئيس التحرير . وهو غير مسئول عن فقد أو تلف أى نص .
- تنشر المجلة المقالات التى تسهم فى رفع مستوى العلوم الهندسية وطرق ممارستها .
- تقبل للنشر المقالات باحدى اللغتين العربية أو الانجليزية ، على أن تقدم من ثلاث نسخ مكتوبة على الآلة الكاتبة ومعها ملخص بكل من اللغتين .
- تذكر أسماء أصحاب المقالة كاملة باللغتين ومعها القابهم العلمية ووظائفهم .
- يراعى ألا تتجاوز المقالة ٨ صفحات بالمجلة ، وفى سبيل ذلك يختصر الاشتقاق الرياضى ويستعاض عن الجداول بمنحنيات مرسومة بالحبر الشينى الأسود ، على أن يشغل المنحنى نصف صفحة على الأكثر ولا يشغل صفحة كاملة الا فى حالات استثنائية وسيصفى أى منحن الى تلك المقاسات .
- ويراعى ألا يقل ارتفاع الحروف أو الأرقام على المنحنيات المنشورة عن ٣ مم بعد التصغير .
- يعنى بذكر المراجع المستقى منها المقال وتصنف تبعاً لاسم المؤلف ثم العنوان ثم المجلة أو الكتاب وتاريخه .
- تقدم لصاحب المقال تجربتان للطباعة وترفق بالأولى نسخة من مصطلحات التصحيح التى يؤدى اتباعها الى رفع كفاية التصحيح وتقليل الوقت الضائع فيه .

اشتراكات الجمعية :

العضو

العضو المنتسب

اشتراكات المجلة :

يتلقى أعضاء الجمعية نسخهم مجاناً .

ولغير الأعضاء :

الاشتراك السنوى للمهندسين

الاشتراك السنوى لغير المهندسين

الاشتراك السنوى للهيئات

تعطى أولوية النشر بالمجلة للسادة الزملاء

أعضاء جمعية المهندسين المصرية

الاعلانات :

مؤسسة مصر للطباعة والنشر

القاهرة ١٩ شارع سوق التوفيقية ت ٧٢١٩٢

رقم الايداع بدار الكتب ١٩٧٥/٢٩٨

محتويات العدد

التشييد والبناء	التصنيع والانتاج	الخامات الأولية والصناعات الكيميائية
<p>القسم العربى :</p> <p>— من اخبار المباني المالية : دكتور جمال الدين نصار ٤</p> <p>— التكنولوجيا والعمارة : التقدم التكنولوجى وأثره على العمارة والمدينة والمجتمع — ٣ — المعماري توفيق عبد الجواد ١٧</p>	<p>القسم العربى :</p> <p>— استخدام مفهوم المنظومات فى الإدارة للدكتورة أمينة الحفنى ٩٠</p> <p>— شبكات السكك الحديدية لتعمير منطقة القناة . (انشاء جسور الخطوط الحديدية) فوق التربة الضعيفة . للمهندس محمود عبد الوهاب ١١١</p>	<p>القسم العربى :</p> <p>— تكنولوجيا صناعة الطوب الرملى للدكتور يحيى عبد الفتاح ابو حسن ١٢٨</p>
<p>القسم الأفرنجى :</p> <p>— الاستطلاع الهيدروجيولوجى المبدئى قبل تجارب الضخ الاختبارى وتطبيقه على بعض المناطق بمصر للدكتور محمود السلاوى ٣٨</p> <p>— اضافة الى الكمرات المقوسة ذات الركائز البينية للدكتور محمد محمد الهاشمى والدكتور عبد الله سرور مهدى ٥١</p>	<p>القسم الأفرنجى :</p> <p>— طريقة جديدة لدراسة ايزان نظم القوى الكهربائية ذات الآلات المتعددة للدكتور محمد مصطفى سلام والدكتور مفتز زكريا غنيم والهندس محمد مصطفى الهنداوى ١٠٤</p> <p>— التحديد التحليلى لاتجاهات الأشعة النكسرة فى البلورات أحادية المخور . للدكتور محمد سالم سعيد ١٠٩</p>	<p>القسم الأفرنجى :</p> <p>— دراسة على النسبى الحجمية والخلط الخلفى للسريان المتوازى والمتعاكس فى أبراج الرش للدكتور شريف حسين عيسى ١٤١</p>

التشييد والبناء

جمعية المهندسين المدنيين
جمعية المهندسين المعماريين
جمعية مهندسي الري

3. Tall buildings must be justified for each particular case. Building them is reasonable as a rule only in crowded areas of big cities. Tall buildings should not be adopted as a solution for an entire city, but as a solution for part of a city. Their implementation should be consistent with regard to the general requirements of urban development.
4. Reinforced concrete will remain the basic building material for tall building construction in Romania for the foreseeable future. It will be used almost exclusively, and emphasis should be placed on the use of its efficient variants: lightweight concrete, prestressed concrete, etc.
5. Tall buildings built of reinforced concrete will have a secure life not of 20 or 30 years, but of 100 years or more. Therefore, attention should be given in design to sufficient functional flexibility, in order to provide possibilities of recycling.
6. The type of service system (heating, sanitary services) also enters into the definition of a tall building.
7. Tall buildings require higher construction quality than other buildings (permeability to air current could lead to serious air streams and to serious losses of heating energy).
8. Tall buildings raise specific economic problems. To optimize solutions, multi-criteria approaches are needed. Research in this direction is necessary to develop reasonable methodology of economic comparison.
9. We need more and more buildings. Technical solutions for structures, cladding etc. will be accepted only in cases where they are compatible with industrialized construction technology and with high productivity on the construction site.
10. A survey of existing buildings is necessary to avoid accidents due to damaged or worn out buildings. Buildings that do not fulfill safety standards should be repaired or demolished.
11. National programs for preventing serious earthquake effects and for rescue and rehabilitation after earthquakes should be set up.
12. Prefabricated buildings have their own characteristics and should not necessarily conform to monolithic buildings. Prefabricated structures should be designed so as to provide the required resistance and ductility.
13. Tall buildings must be the result of team work in design. Engineers, architects, planners, etc. should be educated to work together and to assume an interdisciplinary approach on planning and design.
14. Professional associations should recommend to authorities, engineers, etc., adoption of the most suitable policies in relation to tall building development.
15. Research and Development activities related to the specific problems of tall buildings should be stimulated and supported. R & D capacities should be increased with a view on common programs of specialists in various fields.

G. NASSAR

ROMANIA: 34th CONFERENCE ON TALL BUILDINGS

ROMANIAN CONCRETE BUILDINGS — AND EARTHQUAKES

Completing the series of 3 regional conferences held during October, was the 34th Regional Conference Oct. 14-16 in Iasi attended by 420 engineers and architects. Organized under Prof. Mazilu's leadership and with a fine team that made certain that all details were cared for, the 3-days encompassed a wide scope of subjects relating to Concrete Tall Buildings — especially earthquakes. 41 papers were presented. 3- participants attended from 15 countries outside Romania. The two volumes of Preprints (a total of 940 pages) will be followed by a third volume of Proceedings.

The earthquake conditions in Romania (ranging from 7 to 9 on the European scale of 1 to 9) create special conditions. Buildings that are fully prefabricated are limited to 5 stories. Beyond that height, some forms of cast-in-place frame and/or shear wall is essential.

Height categories are 5, 10, and 16 or 17, with 25 stories the maximum. The goal is to keep structures to 5 stories except in the biggest cities, where 10 story buildings are more common. Structural solutions are controlled by the need for using standardized components. Special problems are foundation settlement (due to loess and mining subsidence), maximum utilization of prefabrication in an earthquake-prone region, the need to improve the flexibility of design and use of prefabricated systems, and to make buildings more suitable to social needs.

The awareness of the need to control urban growth is reflected by criteria that limit the areas of towns and villages. (16% of the economy is agriculture based.)

One is impressed with the tree-lined streets and the many green spaces in both Iasi and Bucharest. Old historic buildings are preserved.

Condominiums account for about 50% of the apartments. A mix of building layouts, and play areas for children is characteristic in Bucharest. The newest housing area there, now being completed, will accommodate 1/4 — million people in 5, 10, and 18 story apartments. Densities are reported to be 3000/hectare.

The conference organizing committee recognized the need for implementation and took action to forward the recommendations to the appropriate ministries and agencies. A Tall Building Library has been established in Romania and their committee urges exchange of books between similar such libraries as quickly as they are established.

Some of the highlights follows :

1. The concept of tall buildings, as defined by the Joint Committee, should be extended. A proposal: buildings may be considered to be tall buildings when their height dictates special measures in design, in construction or in use when compared with buildings that are representative of ordinary construction.
2. The interaction of tall buildings with the environment should be considered in planning and designing. Tall buildings can exert a significant impact on the natural and urban environment.

TALL BUILDINGS NEWS

GREECE : 33rd CONFERENCE ON TALL BUILDINGS

THE GLORY OF GREECE

It was stritully "stauding room only" at the Conference Center in Athens. 480 specialists perticipated Oct. 7-9 in this 33rd Conference In the sessions on the philosophy of tall buildings the opinions swung perhaps more widely than in any conference to date.

And of course the view of the Acropolis and other ancient historic places remains a paramount concern in their urban planning.

The Greeks, in ancient times, had an alternative to "going up". Alternatives to tall buildings were part of the discussion, some of which claimed to provide a density comparable to that achieved by building skyward. An urban plan for Athens is currently being completed. Meanwhile, the construction of tall buildings in Atnens is slowed down although one has the impression of considerable construction ectivity.

As in other conferences there was discussion of the definition of a tall building and, in view of the exchanges, one might add a new one to the lists **A tall building-something that can start an argument.** It's interesting that the original developments that made the tall building possible are still dominant in the definition of tallness : the requirement of elevators and their econom and fire protaction.

Some specific points from the conference:

- Sooner or later tall buildings are inevitable. The should be studied from the standpoint of best incorporating then into culture.
- In order to protect the traditional character of the city, attention must be given to the histooric areas, to the smenities, to human reactions.
- Environment is a problem for all of soicity not just architects and engi-neers.
- Take care that regative reactions do not unduly slow down fundamental

examinations of tall buildings.

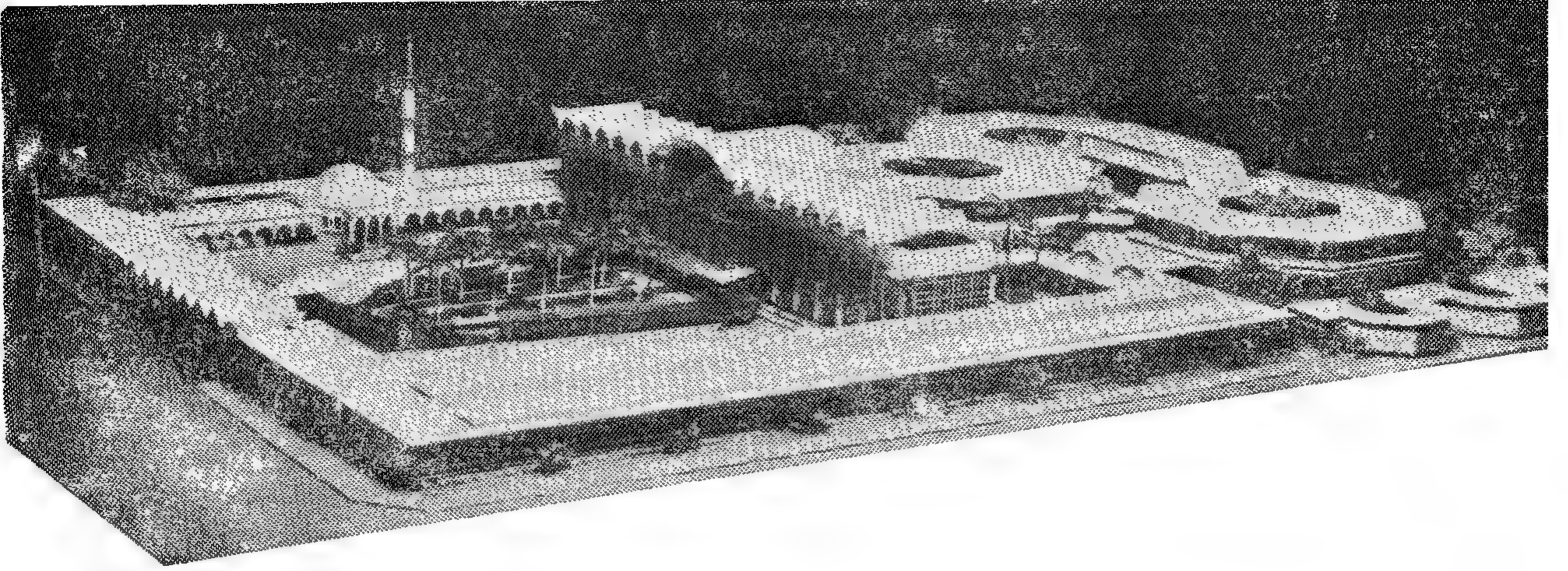
- Take another look at humidification. Is the corresponding energy demand justified?
- In earthquake regions avoid vertical discontinuities at the first floor.
- In reinforced concrete construction the desirability of ductile shear walls is heavily underscored.
- In severe earthquakes it is impossible to isolate "non-structural" panels. They must be included in the evaluation of the total response of the building.
- The preblems of noise and vibrations become particularly critical when the frequency coincides with the natural frequency of the individual. Human nature compels us to always want to take the next step. It is important to evaluate what the end of that "next step" might be.
- Tall buildings should be located in places where the buildings identify themselves with desired trends of the town.
- The future of tall buildings depends, in part, on how people will adapt themselves to new ideas and concepts.
- Comparisons of 6, 8 and 24 story buildings showed the high-rise building as having lower operating costs.
- Costs of air conditioning can be reduced 20 to 30% through reflecting window-panes, sunshading devices, reduced size of windows, attention to exterior wall insulation.
- The recommended teamwork having to do with air conditioning and conservation all too seldom is applied in practice.
- large panel construction of up to 24 stories can lead to economies in building construction.

G. NASSAR

اتجاه العمارة في المدن العربية

عيوبها .. فقدان الطابع المميز لها

المهندس المعماري : توفيق احمد عبد الجواد



١ : قصر الحكم في دولة الامارات العربية المتحدة أبو ظبي
وما يجب أن يكون نموذجا للعمارة العربية لدور الحكومة والمباني
الرسمية للدولة .

ولا يكذب . والعمارة توأم التاريخ ، فهي لا تخدع
ولا تكذب .

كانت العمارة دائما ، عبر العصور الماضية ،
هي الصورة الصادقة والتعبير الدقيق لحضارة
الإنسان وتطوره . وسارت حضارة الإنسان
وتقدمت ، وأسرعت تارة وتباطأت تارة أخرى ،
وسارت معها العمارة في تطور هادئ رزين لا يفارقها
طابعها المميز ، وكانت العمارة تتميز دائما بصفتين
متلازمتين لا يمكن فصلهما . فالي جانب الوجود
المادي المستمد من مواد البناء وطرق الانشاء ،
هناك المحتوى الحسي للمبنى وهو ما يتمتع به من
صفات فنية وهي ، الشخصية والوظيفة والفرض
بأسلوب خاص وتعبير معين .

● العمارة العربية احدى الحضارات أنست :

— من الغريب حقا أن نتجاهل ماضيينا
وحضارتنا وتراثنا المعماري الضخم ، في الوقت
الذي نرى فيه الكثير من علماء الغرب متعطشون
الى معرفة الكثير عنه لتزويد جامعاتهم به ،
والتخصص والتعميق في دراسته ، ولا نهتم نحن
العرب بدراسته وتعليمه في جامعاتنا العربية .

- نحو عمارة عربية معاصرة
- العمارة العربية احدى الحضارات الست
- المدن العربية تعيش في فوضى معمارية
- مسؤولية ضخمة أمام المجتمع والتاريخ
- التفكير الأيدلوجي وراء العمارة العربية

● أن كل ما يعمل به الإنسان مخالفات لقوانين
الطبيعة يكون مصيره الفشل . والبقاء للأصلح ،
وأصح النظريات ما كانت عملية ، وأصلح المبادئ
ما ضمنت مع ميلادها عوامل بقائها .

من الحقائق الثابتة ، والتي يعترف بها العالم ،
أن مهد الحضارة كان مقره الشرق العربي ، وأن
الشرق علم العالم أجمع في الماضي كيف تكون
الحضارة وكيف تكون العمارة ، وأن العرب أول من
علم الأمم كيف تتفق حرية الفكر مع استقامة الدين
وهذه هي حقيقة التاريخ الصحيح الذي لا يخدع

تسجل تاريخها وماضيها وحاضرها بعقلية متحررة على حوائط مبانيهم ، حيث آمنوا بأن العمارة هي التي تكتب التاريخ .

● مسؤولية ضخمة أمام التاريخ :

نرى في البلاد العربية ، مع الأسف الشديد ، ان النجاح في الكثير في المنشآت الكبرى الضخمة وفي ظل هذا التطور العالمى السريع هو الشيء الوحيد الشاذ الذى ما كان ينتظر حدوثه . وقد كان العكس في الماضي ، حيث كان الاخفاق هو الشيء البعيد الاحتمال . ان عمالقة الأساطير الشرقية ومشيدوا قصور صلاح الدين وقلاعه ومصمموا جامع السلطان حسن وابن طولون وسمراء وبابل والفيروان والفسطاط . . وغيرها من الروائع المعمارية ليسوا بسحرة ، ولكنهم كانوا عمالقة فعلا . وكم ينقصنا في أيامنا هذه من هؤلاء العمالقة الكثير .

لماذا ننكر هذا الاخفاق الذى بدأ يتكاثر حولنا في كل مكان حتى وكأننا نعاني من حمى الاخفاق لا اذا استثنينا بعض الأمثلة القليلة التى أنشأها قلة من المماريين يؤمنون برسالتهم وليسوا تجار مهنة ، يعرفون ما لهم وما عليهم من حقوق وواجبات نحو المهنة وكرامتها .

اننا نشعر بالمرارة حينما نرى تلك المباني العامة والهامة في المدن العربية على تلك الصورة الهزيلة التافهة ، التى ان دلت على شيء فانما تدل على ضعف المماري أو استهتاره وتهاونه بقدرسية المهنة وكرامتها ، ويساعده على ذلك قصور القوانين وضعف اللوائح والتشريعات الخاصة بالمباني والتخطيط وأعمال التنظيم والتى لا تحمى المدينة من هذا العبث والارتجال .

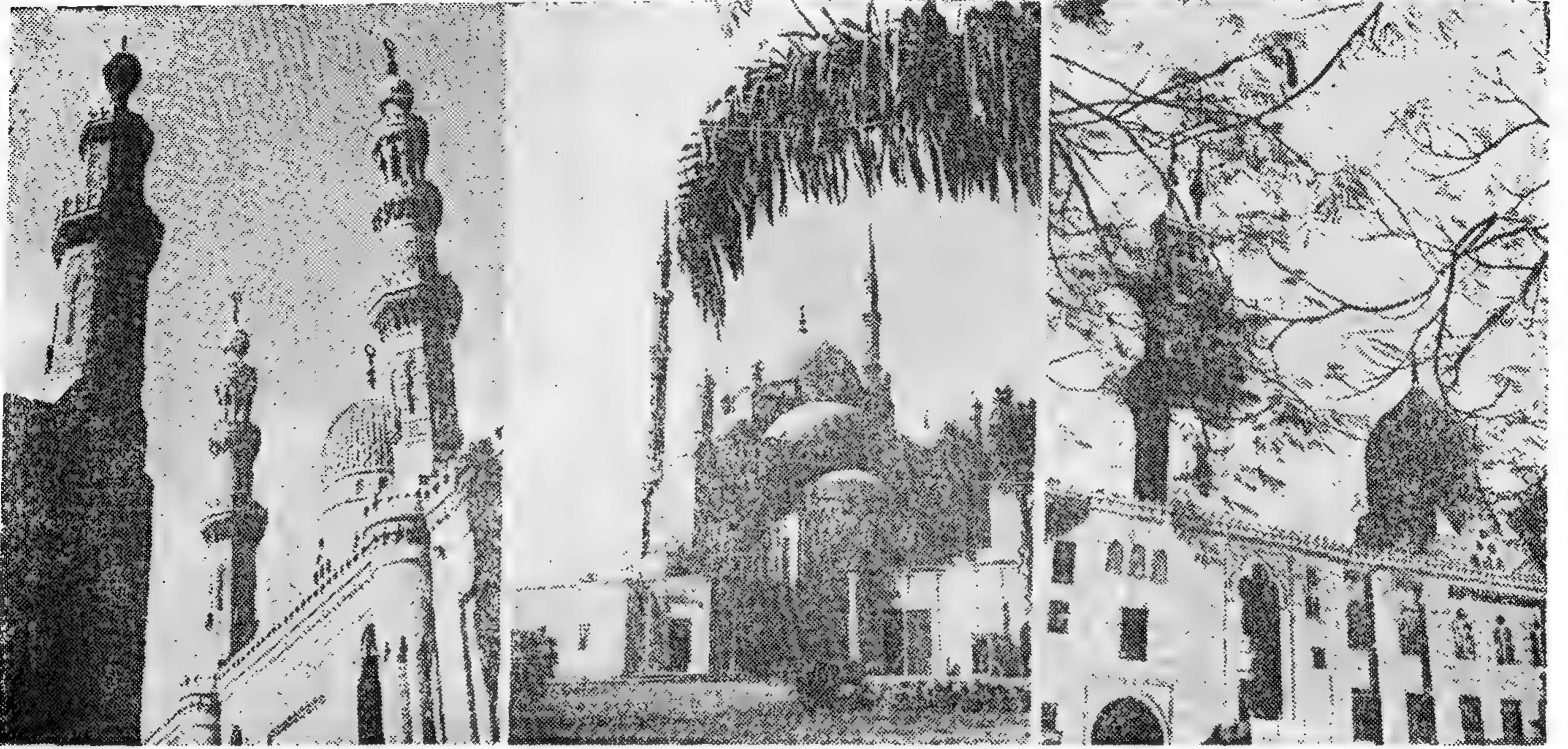
اننا نشعر بالضيق والضجر حينما نرى تلك الأبنية العامة والتى تحمل اسم هيئات حكومية جادة أصيلة أو تحمل اسم مؤسسات أو شركات عامة لها مكانها ومكانتها ، مصممة على شكل طائرة أو بارجة أو قاطرة . . وما أكثرها في المدن العربية وفي المناطق المنشأة حديثا ، في بيروت والكويت ، في القاهرة وفي الرياض ، في الاسكندرية وجدة . نرى تلك المباني على تلك الصور والمناظر الغير لائقة فهما وموضوعا ومعنى ونتساءل . . هل قصد المماري أن يصمم مبناه على تلك الصورة . . ؟ واذا كان التصميم جاء عن طريق الصدفة فالطاقة أكبر ، لأنه لو نقص المبنى بعض الذوق في التصميم أو الاخراج أو التكوين خير من أن يصمم المماري بالمصادفات .

وقد قال لى فرانك لويد رايت حين زيارته لمنطقة القلعة وجامع السلطان حسن عام ١٩٥٨ - كيف يجوز لقوم لديهم مثل هذه الروائع أن يتركوها ويستبدلوا بها سوءات العمارة الغربية التى يحاول الغربيون أنفسهم التخلص منها . . ؟

— من الغريب فعلا ان نتجاهل هذا التاريخ التليد ، وذلك الماضي المجتد ، وتلك الحضارة العربية الرائعة التى تعيش في واقعنا وفي عقولنا وأرواحنا ووجداننا ، ولا نحافظ عليها أو على الأقل لا نحاول الإبقاء عليها من الزوال . . بل ولا نكثر من تطبيقها في منشآتنا العامة ، ولا نضفى على المباني العامة التى تنشأ في بلادنا تلك الصبغة العربية الاسلامية التى تعبر عن شخصيتنا وبيئتنا وواقعنا .

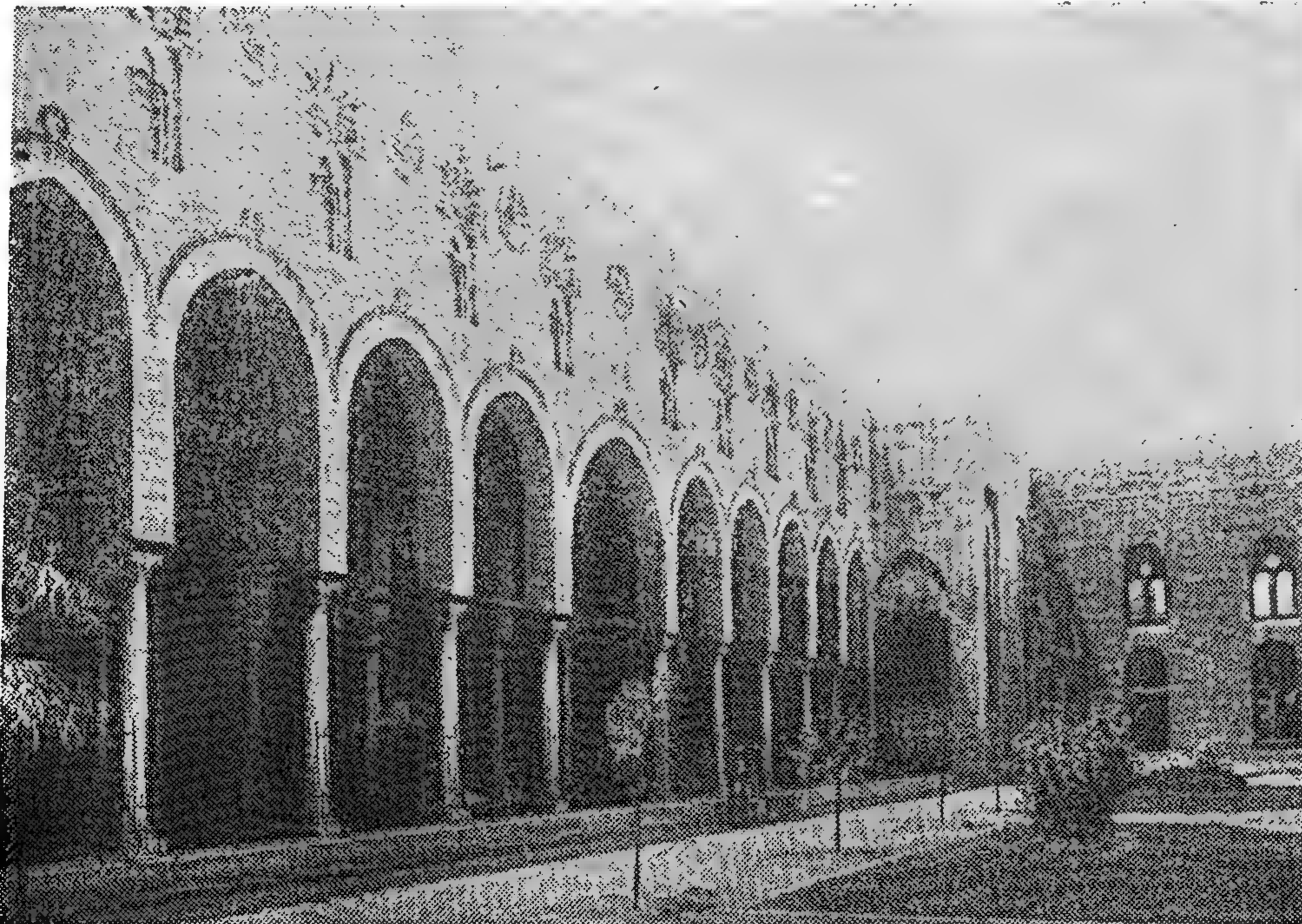
— من الغريب حقا أن نلمس في بعض الدول الأوروبية في الوقت الحاضر آثار التقاليد الاسلامية في معظم مظاهر الحياة العمرانية . فما زالت أسبانيا مثلا تحتفظ منذ ما يسمونه «بالاسترداد» ومعناه انتهاء دولة الاسلام بالأندلس بتراث هائل وثروة ضخمة من هذه التقاليد الاسلامية ، ومازالت مدنها تحمل ذلك الطابع الاسلامي العريق بفضل الروائع المعمارية الفنية التى خلفها مسلموا الأندلس في مدنها وقراهم . وتتمثل آثار العمارة الاسلامية في الأندلس في ثلاث مدن رئيسية ، كل منها تمثل مرحلة من مراحل التطور المعماري الاسلامي وهى : قرطبة ، وأشبيلية ، وغرناطة . — ومن الغريب أيضا أن نرى الكثير من المباني الهامة الحديثة تظهر في أوروبا وأمريكا تحمل ذلك الطابع الاسلامي العربي الأصيل مثل مبنى دار بلدية بوسطن بالولايات المتحدة الأمريكية ، ومبنى جامعة ساسكس بانجلترا ، ومبنى اتحاد الطلبة بجامعة ديرهام في انجلترا وغيرها من المباني الحديثة التى ظهرت مؤخرًا في هولندا يرجى أن تنظر أشكال أرقام ٦ ، ٧ ، ٨ ، ٩

— من الغريب أنه لا يزال حتى الآن الكثير من المماريين العرب ، الذين هم على مستوى المسؤولية في جميع البلاد العربية ، ينقلوا إلينا عمارة الغرب بأساليبها وتصميماتها وواجهاتها في بيئة مختلفة ومناخ مختلف ، وتقاليده وعادات واجتماعيات شرقية عربية مختلفة كل الاختلاف عن البيئة الغربية . . فكان أن ظهر هذا الخلط وذلك التناقض وانعدام الشخصية في المباني العامة والهامة في المدن العربية . في الوقت الذى بدأ فيه هذا العالم الغربى ، الذى ننقل عنه ، أن يستر رشده ويتحرر من سيطرة الآلة في مجال الانشاء والتعمير . بدأت كل دولة في أوروبا وأمريكا وآسيا تحاول ان



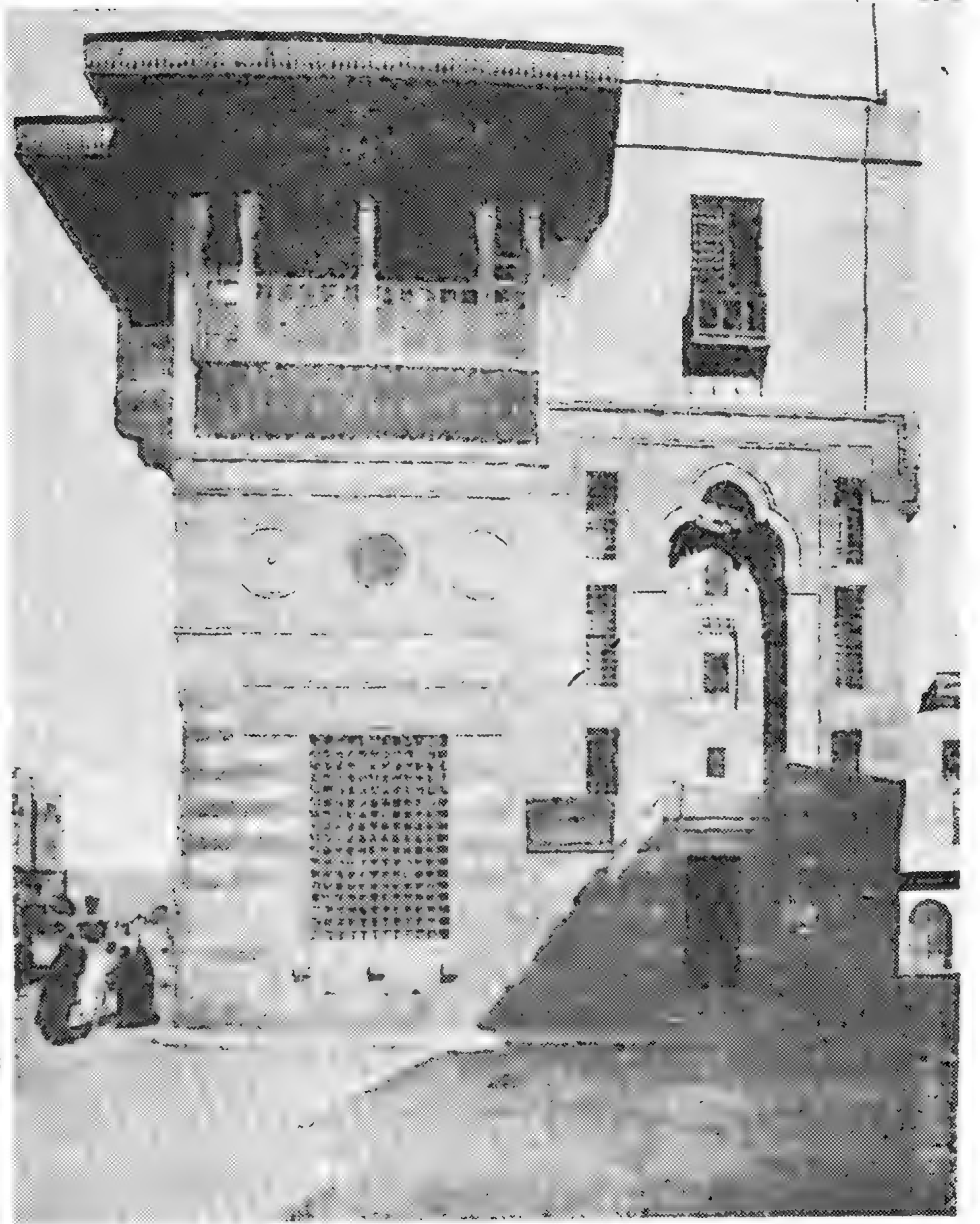
كلها على المعماري وحده ، ولكن يشترك معه في ذلك المجتمع في هذه المسئولية . في مصر ولبنان ، في دمشق وعمان ، في الكويت وتونس والسعودية خلط معماري غير مالوف لا يمت الى بيئة كل منها بصلة من حيث الموقع والمناخ ، من حيث مقتضيات المنطقة الحضرية والفنية والهندسية ، غير متناسق مع مقتضيات البيئة الأساسية ومع الظروف الاجتماعية هزيلة من الناحية الفلسفية والوظيفية والعملية حيث لابد وان تتناسب طبيعة المبنى الحسن مع بيئته لكي تدوم صفاته البارزة .

● لقد انفتحت الدول العربية في العشرين عاما الماضية آلاف الملايين من الجنيهات على التعمير واقامة المدن ، وكان هناك سباق جبار للانشاء والتعمير وبسرعة جنونية مذهلة . كان مبدأ التعمير هو الكمية وليست النوعية ، فكانت هذه الفوضى المعمارية وذلك التعمير المتدل ، كان من الممكن ان تكون نهضة معمارية أصيلة جادة تحمل بين طياتها وعلى صفحاتها طابعا عربيا معاصرا له أهميته ، مرتكزا على أسس طبيعية أصيلة لها فلسفتها وخصائصها ووظائفها . ولكنها جاءت هذه السرعة مخيبة للآمال لا يمكن بالطبع أن نضع المسئولية



٢ أعلا : من اليمين - جامع السلطان قايتباي بالقلعة - ١٤٧٥ م : مسجد محمد علي بالقلعة - ١٨٣٠ م ، جامع السلطان حسن القاهرة - ١٣٥٦ م
٣ - يسار مسجد المؤيد - القاهرة ١٤٢٠ م

● ان في تكرار الوحدات الزخرفية أو العناصر الكونية في المبنى تكرار النغم في الموسيقى العربية ، يدخل على النفس شعورا بالوحدة ، وإيماننا بالعقيدة وترباطا بالفكر الاسلامي .



٤ - مدرسة السلطان قايتباي - ١٤٧٢ من أهم ما يتميز به العمارة الإسلامية أو العمارة العربية دراسة الواجهات حتى تتبوا المكان المناسب لها . فتتألفت طبقات من مداميك أفقية من أحجار صفراء وأخرى حمراء داكنة ، أو عمل تجاوير أو حنايا عمودية تفتح فيها النوافذ أحيانا وتنتهي أعلاها بزخارف معمارية من المقرنصات وتظهر ذلك في أشرطة الزخارف والكتابات لآيات القرآنية أو الأحاديث ، وفي شرفات مسننة تتوج بها الواجهات .

واليابانية ، والروسية . وتلك مسئولية كبيرة ، وتحد كبير لا يمكن للهندسة المعمارية العربية الحالية في جميع أنحاء الشرق العربي أن تتحملها مع ما فيها من زيف وخط وتقليد .

إن العالم العربي يزخر بثروات طائلة من العلوم والفنون والثقافة والآداب والتراث الانشائي والمعماري ، ومن كنوز وثروات مادية ظاهرة وباطنة ، ومفاتيح الشرق لا تحصى ولا تعد . ولو أخذنا مثلا اللغة العربية بلهجاتها الحديثة المتعددة ، واللغة الكلاسيكية بقواعدها وشعرها ونثرها وأدبها ومرادفاتهما ، والخط العربي الجميل بصوره المتعددة واستعمالاته الخاصة التي عبر بها الفنان العربي عن ذوقه وأحاسيسه في ابتداء أنبل الأشكال الفنية التي يكتب بها كلمات الله . . سوف تدهشنا

ومن خلال دراستنا لتاريخ العمارة عبر العصور للطرز المختلفة . . ومن خلال تدريسنا لهذا التاريخ المعماري ، فإننا لم نصادف طيفا من الخيال يشبه في طرافته أو إيلامه أو الرتباك أو فتنه ما نشاهده يظهر إلى الوجود في المدن العربية الجديدة .

غير أن هناك بوادر تشير إلى أن هذا الاتجاه يسير إلى أحسن ، احتقا للحق ، في كل من لبنان وتونس والعراق ، وأن الطابع المعماري سينبثق من الأسس المناخية والعملية والحضارة للبلاد في كل منها .

ومع أن العرب في الدول العربية لا يزيد عددهم عن مائة مليون عربي ، إلا أنهم يمثلون إحدى الدعائم الأساسية الثقافية الست في العالم وهي الثقافة الأوروبية ، والهندسية والصينية ، والعربية ،

الحقيقة ثورة على الطرز المستوردة وعلى التقليد والمحاكاة لطرز لا تمت للبيئة أو الاقليم بصلة .

● ان التسلسل الطبيعي لشرح مفهوم العمارة الاقليمية في البيئة العربية سيقودنا حتما الى **الوظيفية في العمارة Function** ، حيث ان الوظيفة هي التي تميز العمارة عن الفنون الأخرى وعن العلوم المجردة في كونها فن وعلم يخدم احتياجات اجتماعية واقتصادية محدودة . ومن ثم ، تحدد لنا البيئة والمحيط Enviroment أو Ecology الأبعاد والطابع Character ، بينما يحدد لنا النظام والانتظام Order الايقاع والترديد والعضوية .

● أما الخطوة الثانية أو المرحلة الثانية من الدراسة فهي **دراسة الفراغ Space** ذلك العنصر الكوني الخالد بجميع مفاهيمه القديمة والحديثة ، الاقليمية والعالمية وتطوراته خلال مقاييس مختلفة تبدأ من العمل المعماري البسيط الى علاقة هذا العمل بالنسبة للمدينة أو حتى على مستوى الاقليم . حيث ان الفراغ جزء لا يتجزأ من هيكله المغلف للشكل الخارجى للمبنى .

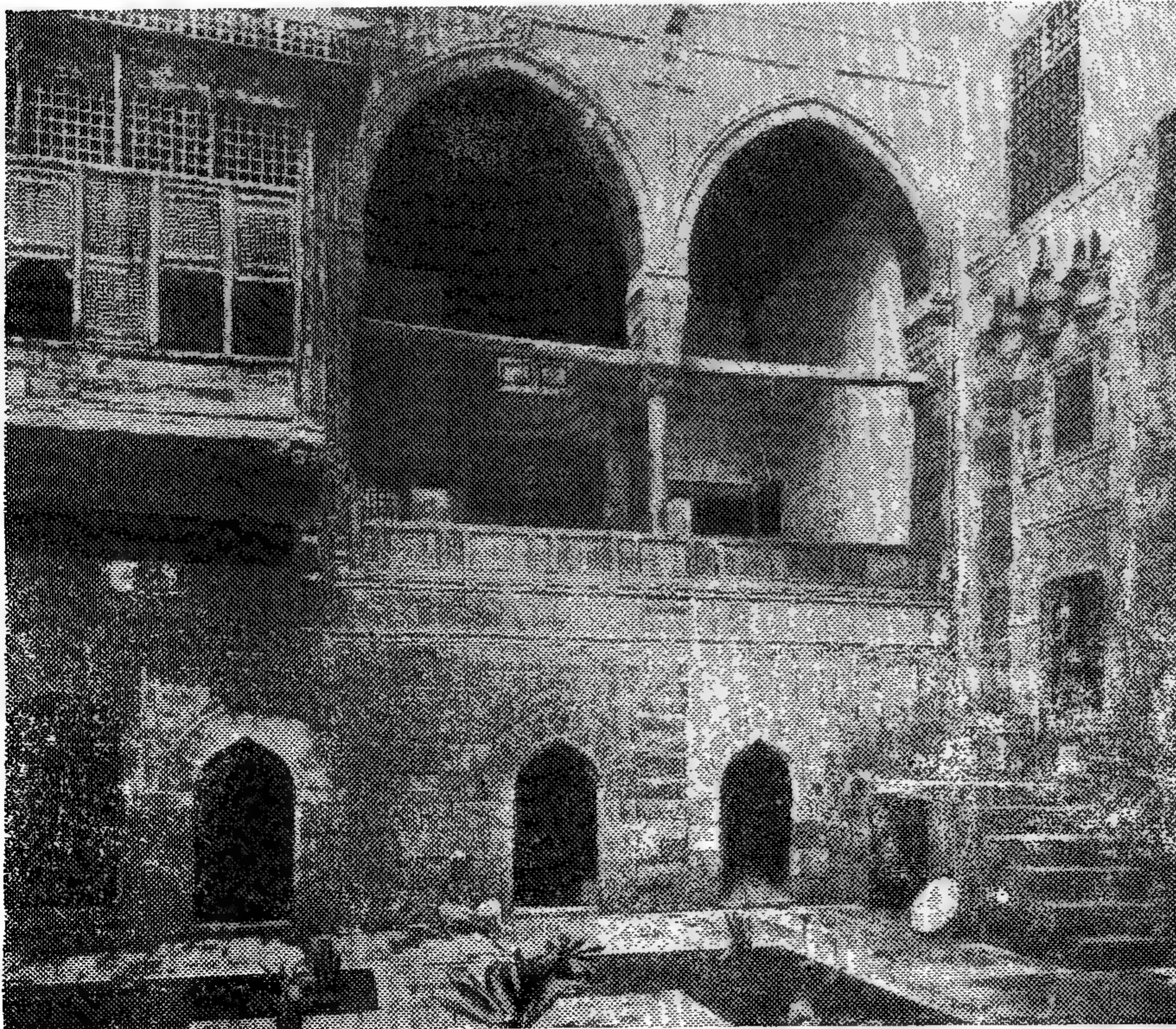
● والخطوة الثالثة في هذا التسلسل المنطقي هي معالجة **عنصر الإنشاء** ودوره في تحديد معالم المبنى ودراسة مواد البناء سواء أكان منها يستخدم انشائيا أو وظيفيا أو مطهريا من حيث الشكل والتكوين .

هذه الناحية وحدها لما يمتاز به العرب والعالم العربى . فما بالناس اذن بالتراث العربى الاسلامى وتاريخ العمارة العربية والمنشآت المعمارية العظيمة الخالدة . ولعل مشكلات العالم العربى تنبع من تعدد أنواع ثرواته وكنوزه وسحره ومفاته ، أقرب دليل على ذلك هى المشكلة التى نعيشها الآن .

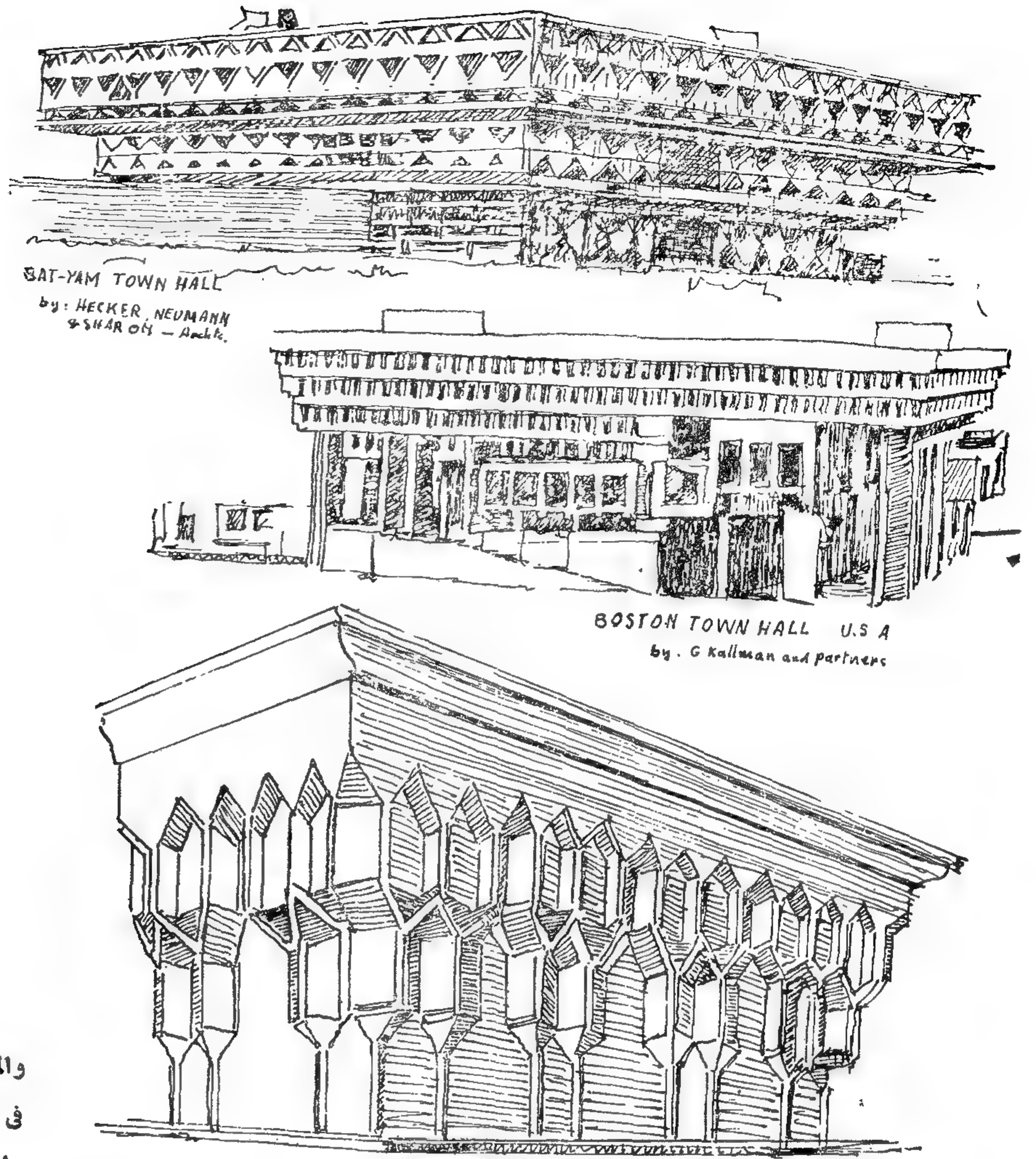
● التفكير الأيدولوجى وراء العمارة العربية :

باستقرار العرب فى مصر منذ القرن السابع ، قامت نهضة معمارية قوامها تفهم العرب لأسلوب العمارة القائمة وقتئذ وهى العمارة القبطية - وهى الامتداد الطبيعى للحضارة المصرية القديمة - وتطويرها دون محاولة ازلتها ومحوها ، وهنا تتمثل شخصية العرب فى الأمانة العلمية والثقافية والحضارية ، حيث كان يمكنهم التصميم على محوها أو على الأقل تغيير مكوناتها . فنجح العرب بذلك فى تحقيق استمرار مجرى الحضارة فى مصر - وهنا يؤكد العرب عملية الاستمرار الحضارى واقامة نهضة معمارية متمثلة فى نوعين من المباني هما : عمارة المساجد أى المباني الدينية ، وعمارة المساكن وبلغت هذه النهضة قممتها فى القرن السابع واستمرت الى القرن الثامن عشر ، ثم بدأت فى الانهيار فى منتصف هذا القرن .

سوف أتحدث عن العمارة العربية بالعمارة الاقليمية ، التى هى فى الواقع مرحلة متطورة للعمارة العالمية . لأن العمارة الاقليمية العربية هى فى

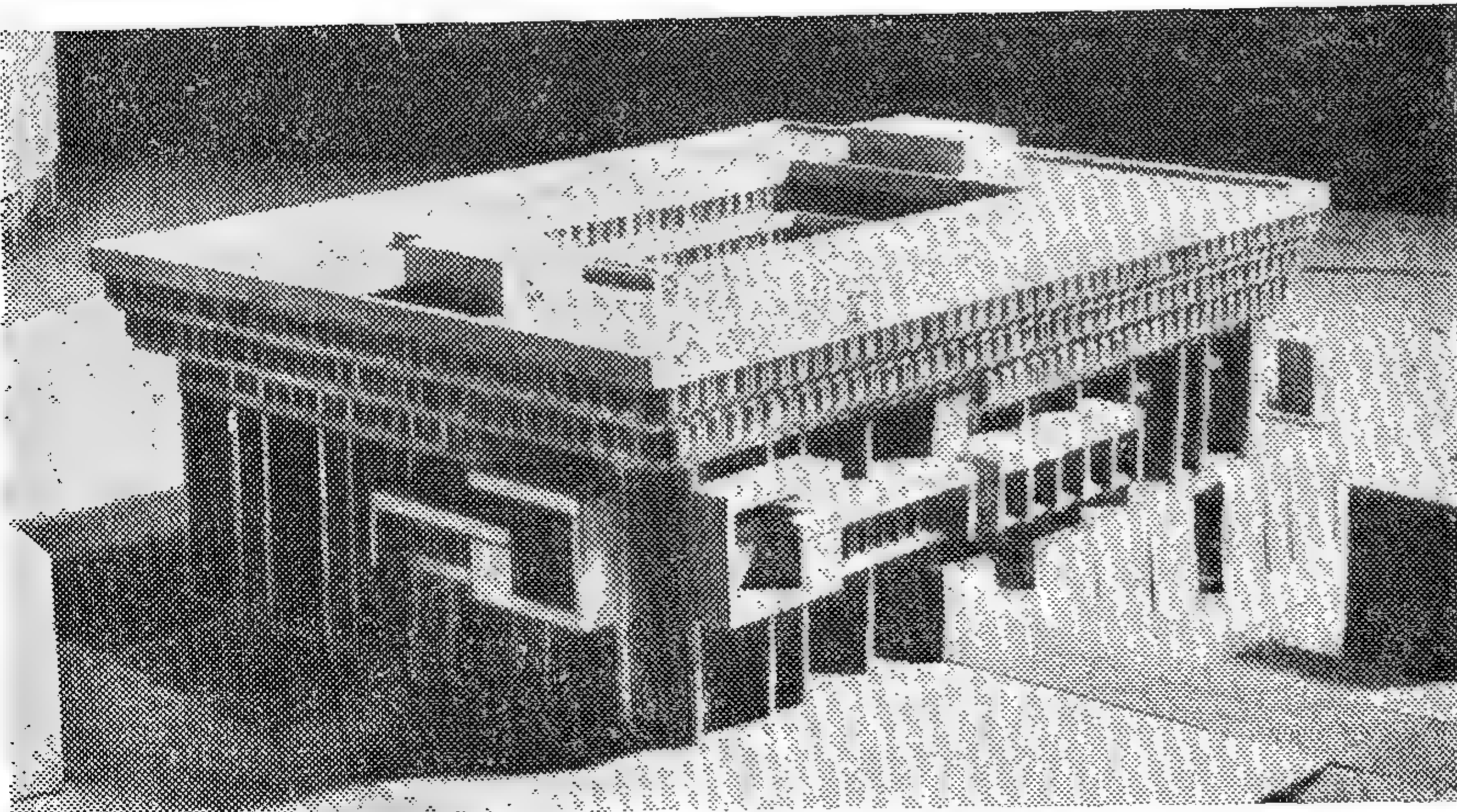


٥ - منزل جمال الدين الذهبى - القاهرة ١٦٤٨ م الفناء الداخلى فى المسكن العربى من أهم عناصر التكوين المعمارى . فالفناء الداخلى أو ما يسمى فى العصر الحديث - باثيو - معالجة معمارية تحجب عن الساكن التغيرات الجوية المختلفة ، وتترك له التمتع بالسماء وحدها . وتنبع هذه الفكرة من بذور الفكر الشرقى واستجابة صريحة لمقتضيات المناخ .



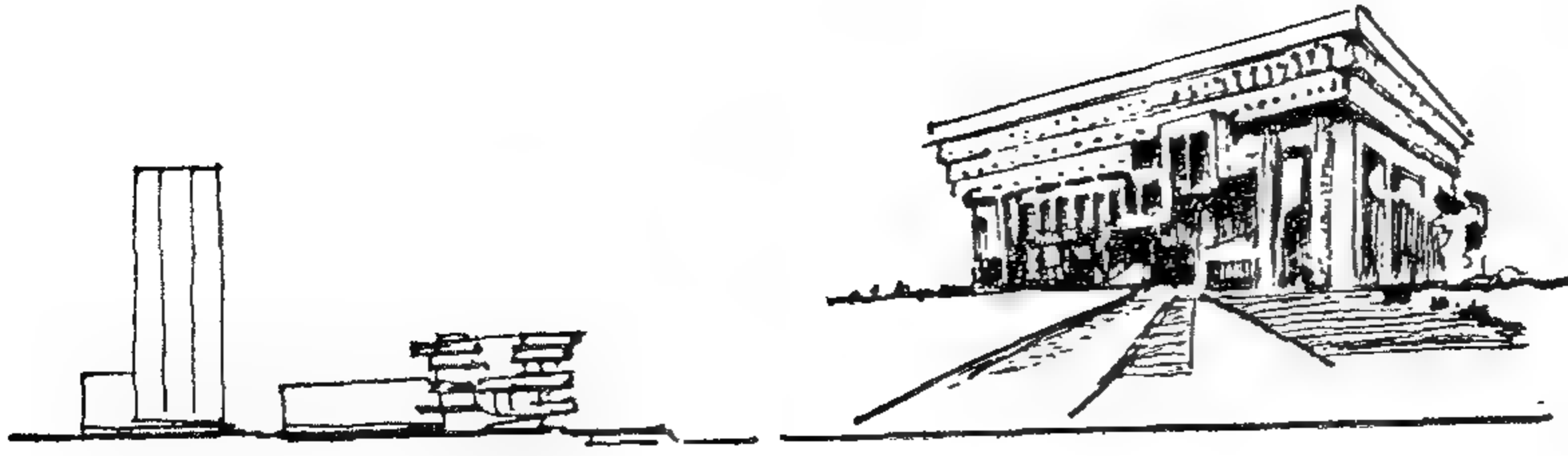
• استخدم علماء الغرب من الممارين والمخططين كثيرا من العناصر المعمارية الاسلامية في العمارة العربية وطبقوها في مبانيهم الهامة والعامة . ثم حوروها واستخدموا في انشائها مواد رخيصة ونسبوها الى انفسهم ، وسموها بالعمارة العالمية المعاصرة .

يرجى ان تنظر الاشكال ارقام ١٠،٩،٨،٧،٦

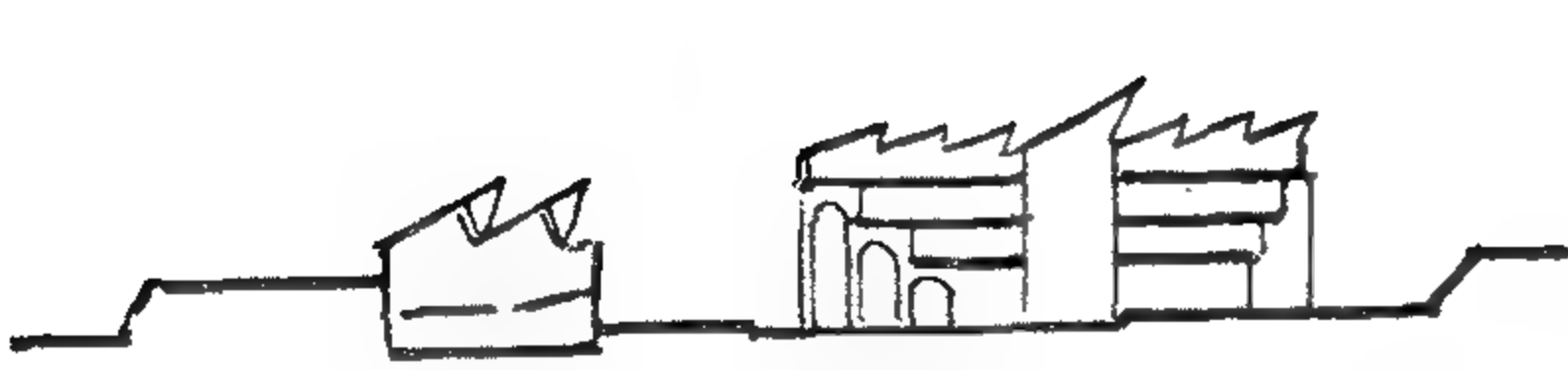


٦ أعلا : مبنى بلدية بوستن بالولايات المتحدة الامريكية . اسفل . الحراب الاسلامي الأصيل .

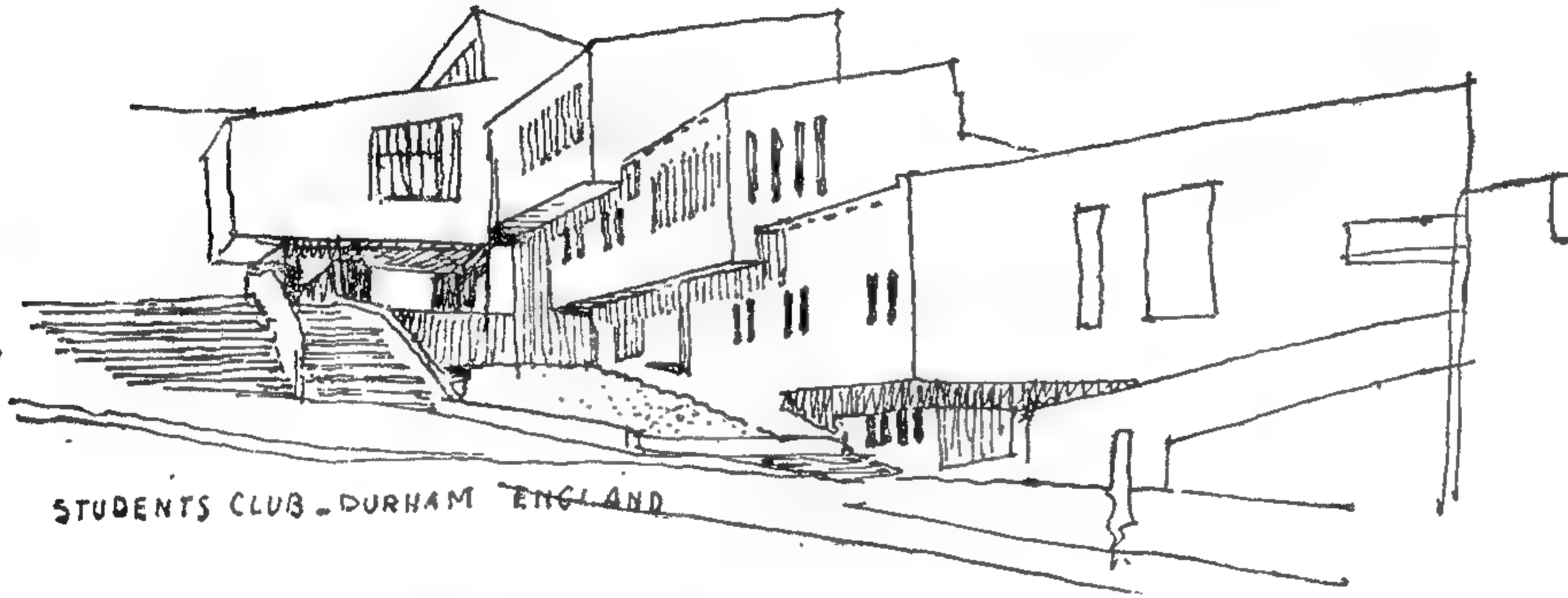
٧ - يسار : نموذج لمبنى بلدية بوستون



BOSTON TOWN HALL . USA



KHARTOUM TOWN HALL

SASSEX UNIVERSITY by BASIL SPENCE
ENGLAND

STUDENTS CLUB - DURHAM ENGLAND

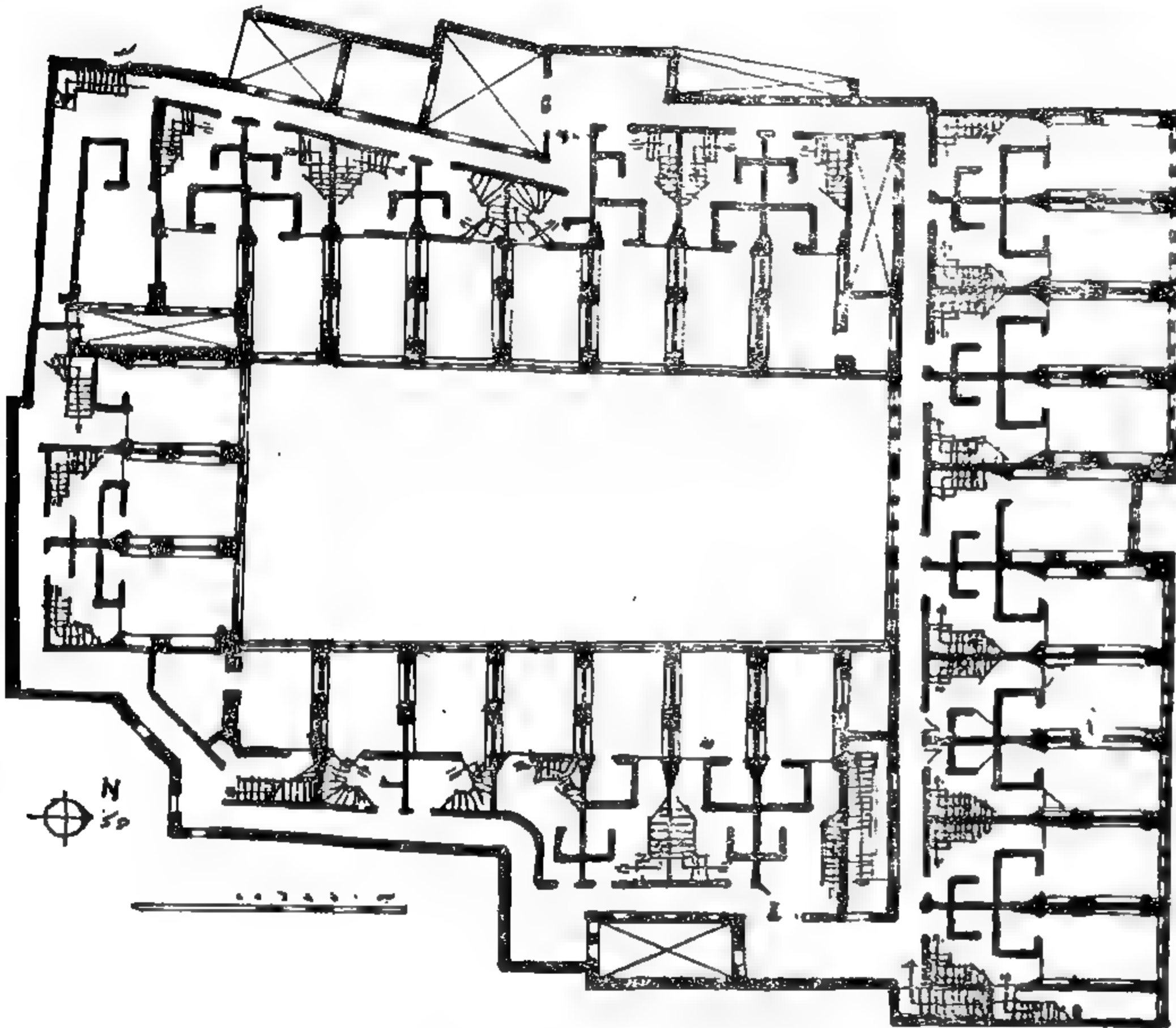
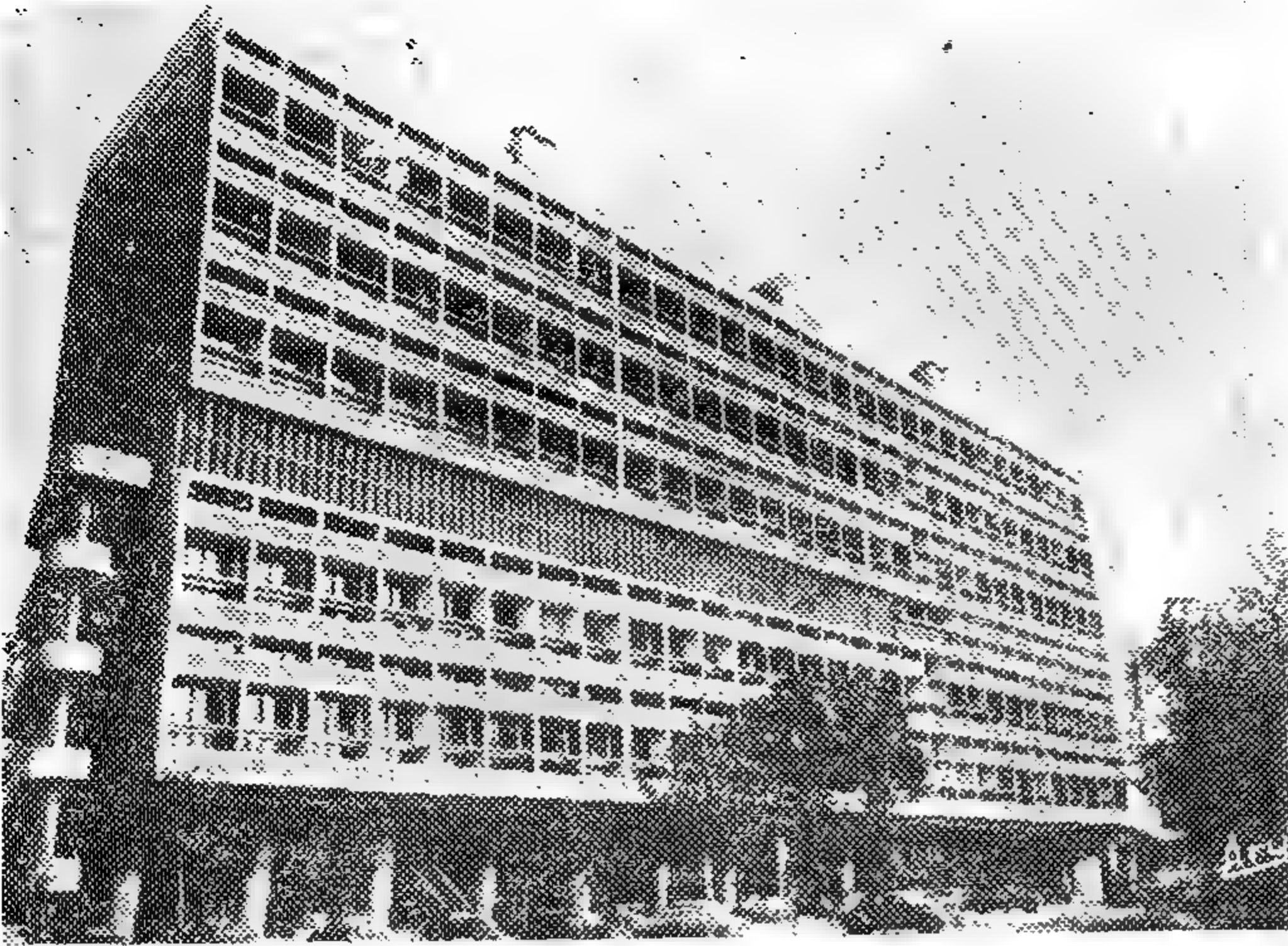
٨ • : بعض الأمثلة للمحاولات الغربية التي يحاول المهندسون
الإجانب استخدام العناصر المعمارية الإسلامية العربية الأصيلة في
مبانى العصر الحديث . وسموها بالعمارة العالية الحديثة أو العمارة
المعاصرة .

ويرى من أعلا الى اسفل : بلدية بوستن بالولايات المتحدة
الأمريكية ، بلدية مدينة الخرطوم بالسودان : جامعة ساكسى -
انجلترا ، نادى الطلبة جامعة ديرهام انجلترا .

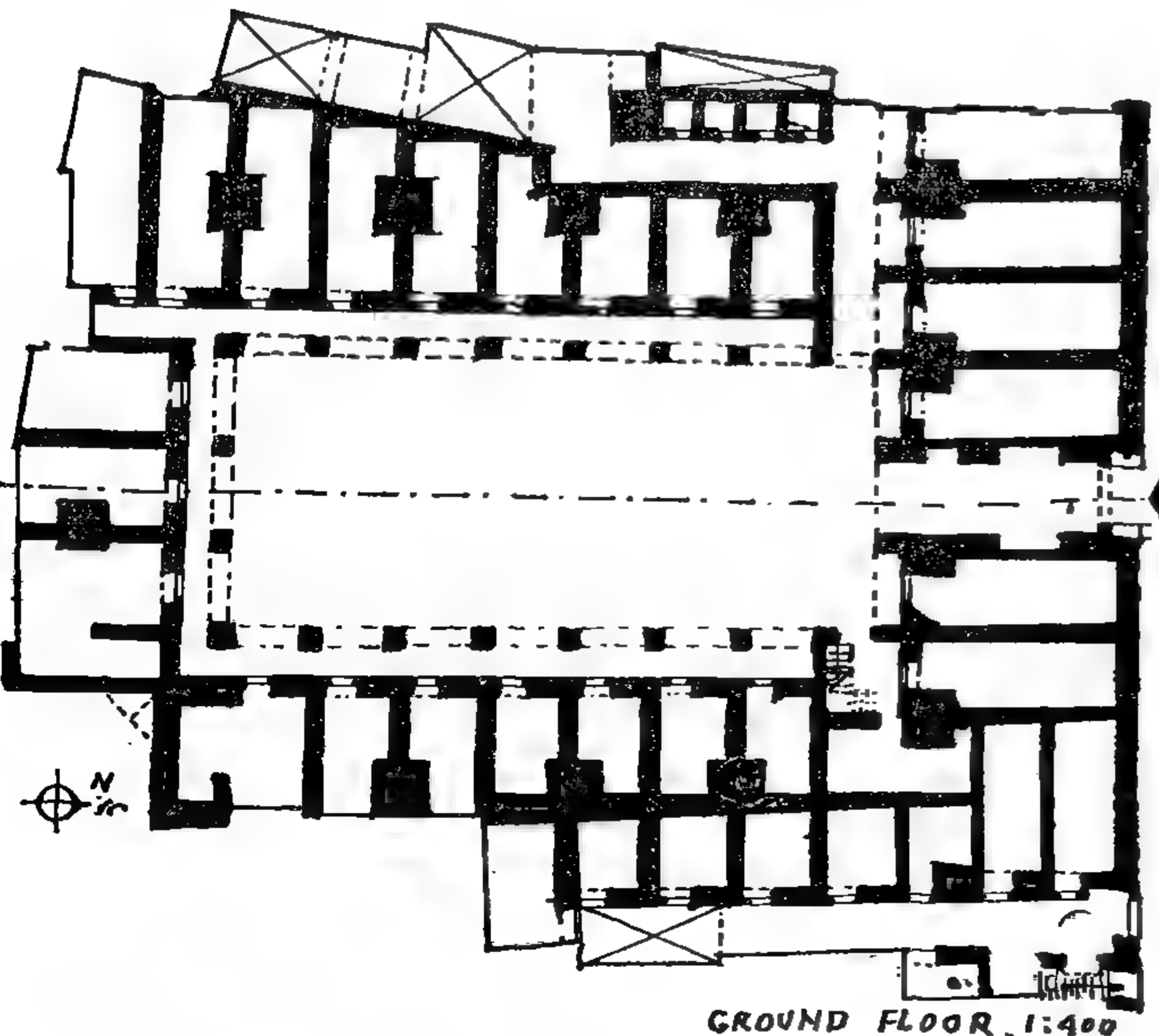
الطبيعة وتقبلها العرب وتحدها بالمجابهة بشكل
منطقى وخلاق . لأن الاستسلام لمثل هذه البيئة
قتل للشعور وتثبيط للهمم . فبالصبر والذكاء
والعلم والخبرة المكتسبة ، مضافا الى كل ذلك
التطور التدريجى للقدرات الفنية ، أمكن للعرب
مجاابه هذه البيئة القاسية والتحدى والبقاء .

هذه الخطوات الأساسية هي الركائز الثلاث
التي على أساسها تكونت العمارة العربية أو العمارة
الإقليمية وكيف كان ذلك . . ؟

— ان البيئة في حقيقة الأمر هي التي خلقت
العمارة العربية بشكل خاص والعمارة الإسلامية
بشكل عام . كانت بيئة قاسية مسيطرة فرضتها



THE DUBLEX SYSTEM - FIRST FLOOR 1:400



GROUND FLOOR 1:400

وهنا خلق العرب نظرية ال Contrast التضاد العضوي والبيئي بين الطبيعة القاسية وبين الأجواء الداخلية الرطبة المخضرة الفردوسية ، بين المناخ الحار الجاف وبين المناخ الرطب في الفناء الداخلى والنافورات السلسبيلية والعمارة الجميلة الفنية بالزخارف والألوان .

— ان الفراغ Space كان عند العرب عضوا وتلقائيا . وقد شكل الفراغ عدة رغبات ، اما لحماية المبانى من العوامل المناخية ، أو رغبة في التموه لأسباب دفاعية أو أسباب اجتماعية — وكذلك الفراغات الداخلية فقد عولجت معالجات معمارية تعكس الحركة وتعبر عن الوظيفة .

نلاحظ مثلا ان تعدد الأعمدة في المسجد يعطى شعورا فراغيا بالامتداد والانطلاق والانتهائية ، وتوحى تعدد وتكرار عقود هذه الأعمدة المتتابعة التي يتسلل الضوء من شبكات نوافذها فيصّل ضعيفا باهتا يؤثر في النفس ، فيستشعر المرء نفسه بعيدا عن نطاق الحقيقة ، ويظل مستغرقا مهيا للتطعم الى ما وراء الحس في صلاة خاشعة .

— ان في تكرار الوحدات سواء أكانت زخرفية أو عناصر تكوينية في المبنى كتكرار الموسيقى العربية ونغماتها ، يدخل على النفس شعورا بالوحدة ، وإيمانا بالعقيدة ، وترابطا بالفكر الإسلامى . تزداد الأمانة بهجة وانشراحا وتسبيحا برؤية للمساحات الجميلة والنغمات الحميمة التي تشع من خلال عقودها المتكررة ، ومن الظلال وأشباه الظلال التي تنعكس على هذه المسطحات الضخمة للحوائط لتعبر بأمانة وصدق عن العمارة الشرقية التي يتميز بها عالمنا العربى ، ويتلاءم مع طبيعة الجو والمناخ والمجتمع ، ويشع من خلالها الفن بكل ما يحمل من لهب في توافق تام مع التأليف المعمارى . يرجى أن تنظر الأشكال أرقام ١٢٤، ١٢٥، ١٢٦، ١٢٧ .

٩ : عمارة مارسيليا السكنية ، تصميم المعمارى ل . كوردبوزيه - ١٩٥٤ حيث اتبع في تصميمها النظرية التي ابتكرها العرب في بناء الوكالات في القرن الثامن عشر .

١٠ : مساقط أفقية لنموذج من نماذج الوكالات التي انتشرت في القرن الثامن عشر - وكالة الفورى .

● العناصر المعمارية في العمارة العربية :

سأحاول شرح بعض العناصر المعمارية الأصيلة في التكوين المعماري العربي الشرقي وكيف حاول الغرب محاكاته وتقليده ، ولكنه مع الأسف الشديد جانبه التوفيق . لأن العرب حينما ابتدعوا هذه التكوينات كانت نابعة من بيئتهم وواقعهم ووجدانهم بجانب الفلسفة الدينية والروحية التي على أساسها اشتقت هذه العناصر المعمارية : وأهم هذه العناصر المعمارية العربية ما يأتي :

- المشربية :

هي معالجة معمارية مصنوعة من الخشب الخروط لتغطية الفتحات ، الشبائيك أو البلكونات ، الشكمة ، تسمح بدخول الهواء اللطيف ولا تسمح بدخول أشعة الشمس ، وتستعمل أيضا لكسر حدة الضوء Glare الناتج من شدة الاستضاءة ، ذات مقاسات مطلقة لا يمكن أبدا تكبيرها أو تصغيرها . وتستعمل المشربيات ذات الفتحات الضيقة في الأجزاء السفلية من الحجرات لكسر حدة الضوء وتوفير الخصوصية ، أما الأجزاء المرتفعة فتستعمل الشبائيك ذات الفتحات الأوسع تساعد على التهوية ، يرجى أن ينظر شكل رقم ٤ .

أخذها الغرب وصنعوها بمواد من الجبس أو الخرسانة المسلحة أو الحجر الصناعي وغيرها مقاساتها وصدورها لنا باسم الكولاسترا أو كاسترات الشمس Sun Breakers . وينسب غير مدروسة فانت استعمالهم لهذه المشربيات تؤدي عكس الهدف منها فتزيد من حدة الضوء .

- الحوش :

أو الفناء الداخلي ، هو أيضا معالجة معمارية عربية أصيلة تحجب عن المساكن كل عناصر الطبيعة الخارجية وتترك له التمتع المطلق بالسماء . معالجة معمارية نابغة من بذور الفكر العربي واستجابة صريحة لظروف ومقتضيات مناخنا ، أخذها الغرب عنا وصدروه لنا باسم الباثيو - النافورة : فهي محاولة عربية أصيلة ، فهي

ترديد للعبة السماوية تعكس صورة السماء على صفحة مائها ، وتدخل السماء بما لها من قدسية وشفافية إلى المسكن . وهي دائما مربعة ترمز أركانها إلى عمود السماء الأربعة ، ثم تتحول إلى مثنى فتزد شكل القبة وينساب الماء داخل هذا المثنى . وفي ذلك ربط صريح بين الإنسان وأسلوبه الفكري الأساسي . وبالإضافة إلى عنصرها الجمالي فإنها عنصر فعال في تلطيف جو المسكن .

- ملاقف الهواء :

أحد المعالجات المعمارية التي توجه من الخارج في اتجاه الرياح النسمة البحرية ، وبذلك يمكن تهوية الحجرات والصنالات التي لا تفتح مباشرة على الاتجاه البحري - صدروه لنا باسم التكييف الطبيعي .

- الوكالة والربع :

في الوقت الذي كان فيه قوام النهضة المعمارية في أوروبا في القرن الثامن عشر استجابتها لاحتياجات الطبقة البورجوازية للمساكن الخاصة والفيلات الفاخرة والقصور ، بدأت تظهر في مصر عمارة من نوع جديد وهي عمارة المساكن المجمع - الاشتراكية العربية الأصيلة - لخدمة طبقات الصناع وصغار التجار لتحقيق رغباتهم ، فوجدت الوكالة ووجد الربع .

والوكالة عبارة عن فندق من نوع جديد ، حيث كانت الطوابق العلوية تحتوي على شقق صغيرة بدلا من الحجرات ، وكل شقة أو وحدة سكنية مستقلة تتكون من طابقين أو ثلاثة وتتصل هذه الطوابق بسلم داخلي لكل وحدة ، شكل رقم ١٠ .

والغريب في الأمر أن علماء الغرب أخذوا هذه الفكرة العربية الأصيلة ونسبوها إلى أنفسهم باسم الوحدات السكنية المجمع ، الدوبلكس والتريبلكس كما حدث في تصميم عمارة مارسيليا ١٩٥١/٤٩ للمعماري ل . كوربوزييه والتي اتخذت فيما بعد كنظرية جديدة من نظريات العمارة الحديثة . شكل رقم ٩ .

وتتكون الوكالة من دور أرضي يطل على فناء داخلي يحتوي على مخازن منفصلة وطوابق علوية مخصصة للسكن تطل على هذا الفناء الداخلي المفتوح . وكانت هذه الوكالات تخصص لأقامة التجار الذين يفدون من مختلف البلاد مع عائلاتهم لقضاء موسم التجارة حيث تخزن بضائعهم في المخازن حتى ينتهي كل تاجر من بيعها ثم يرحل . شكل رقم ١١ .

أما الربع : فكان صورة مبسطة للوكالة ، خصص أصلا للصناع وأصحاب الحرف ويتكون الدور الأرضي من ورش ومحلات ، والطابقان العلويان من شقق منفصلة مكونة من حجرة أو حجرتين وصالة معيشة ومطبخ ودورة مياه لعائلات الصناع أصحاب هذه المحلات .

وهناك الكثير من العناصر المعمارية العربية التي أخذها الغرب ونسبوها إلى أنفسهم مثل المباني المرفوعة على عمد وغيرها من العناصر المعمارية في العمارة العربية ، وكذلك العناصر المكلمة فيما يتعلق بالآثاث الثابت والدواليب داخل الحوائط والإضاءة والألوان . الخ .

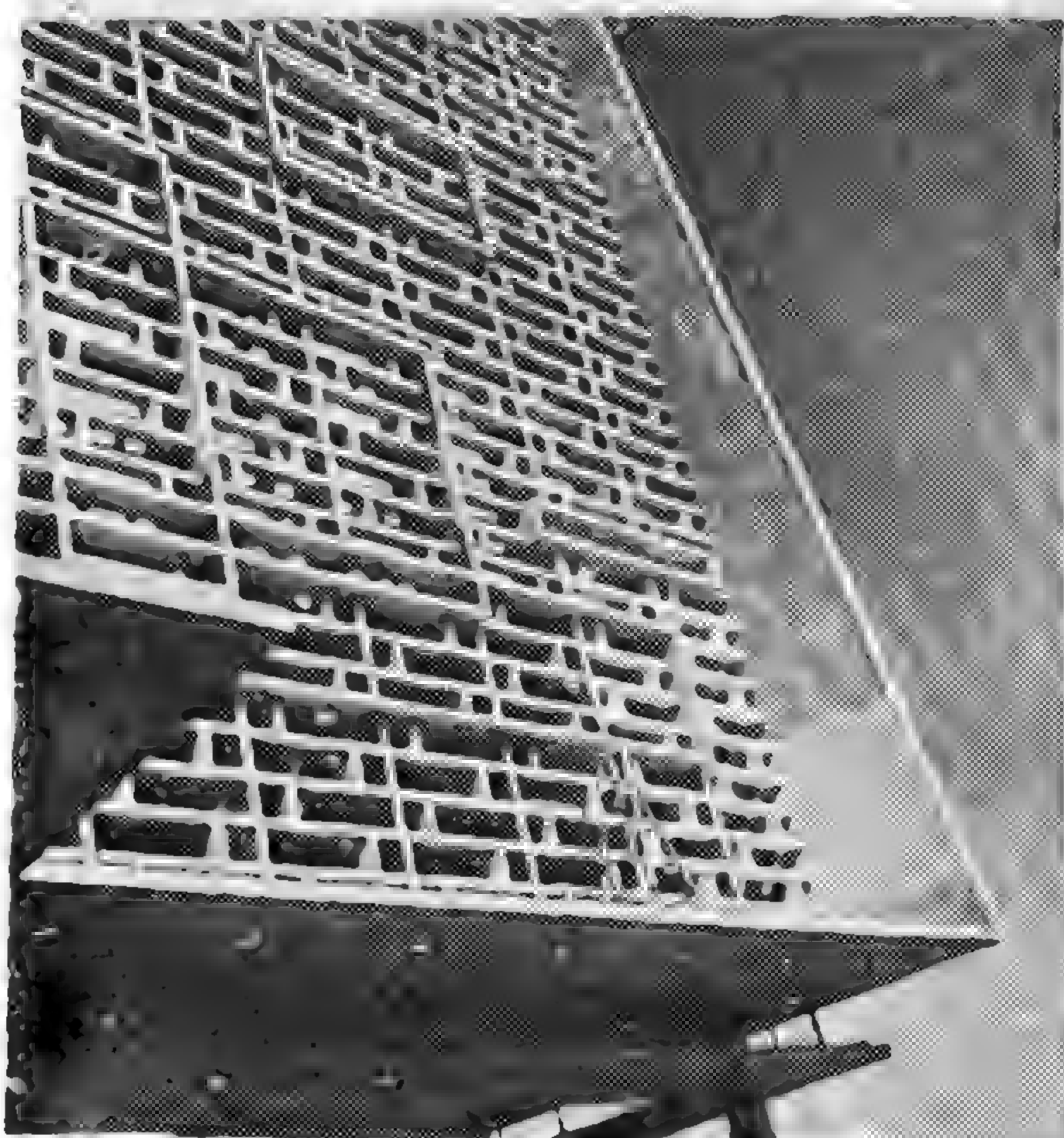
إن المباني التي شيدتها الأجيال السابقة وخاصة المباني ذات الطابع البيئي المحلي في البلدان العربية تتفوق كثيرا على معظم مباني الجيل الحالي ، خاصة إذا ما أخذ في الاعتبار عدم توفر معدات وأدوات البناء الحديثة في تلك العصور . وتكمن بعض أسباب تفوق البناء القديم على الحديث أن كان العمل في الماضي يتصف بالتروى والصدق

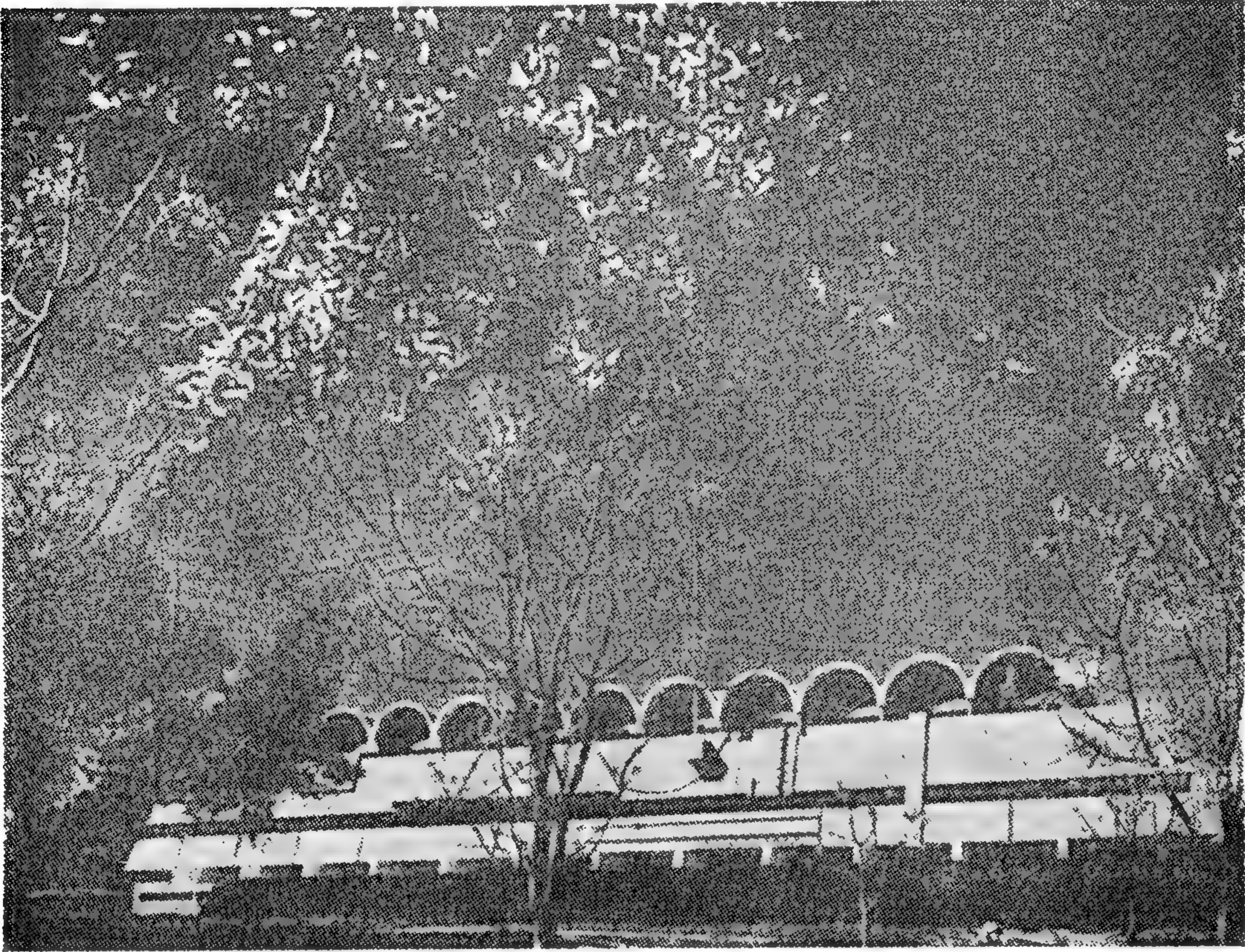


١١ أعلا : مجموعة
سكنية في بوستون/
أمريكا استخدمت فيها
العناصر المعمارية
العربية



١٢ أسفل : أمثلة
معمارية جادة تسم
بالوقار والاحترام
والتعق وتندمج مع
البيئة والمناخ والمجتمع
ويؤي من أعلا مدرسة
الباركية بالكويت
فيلا ، قاعة كبرى
للأحتفالات والاجتماعات
والسينما بالكويت
١٩٦٢





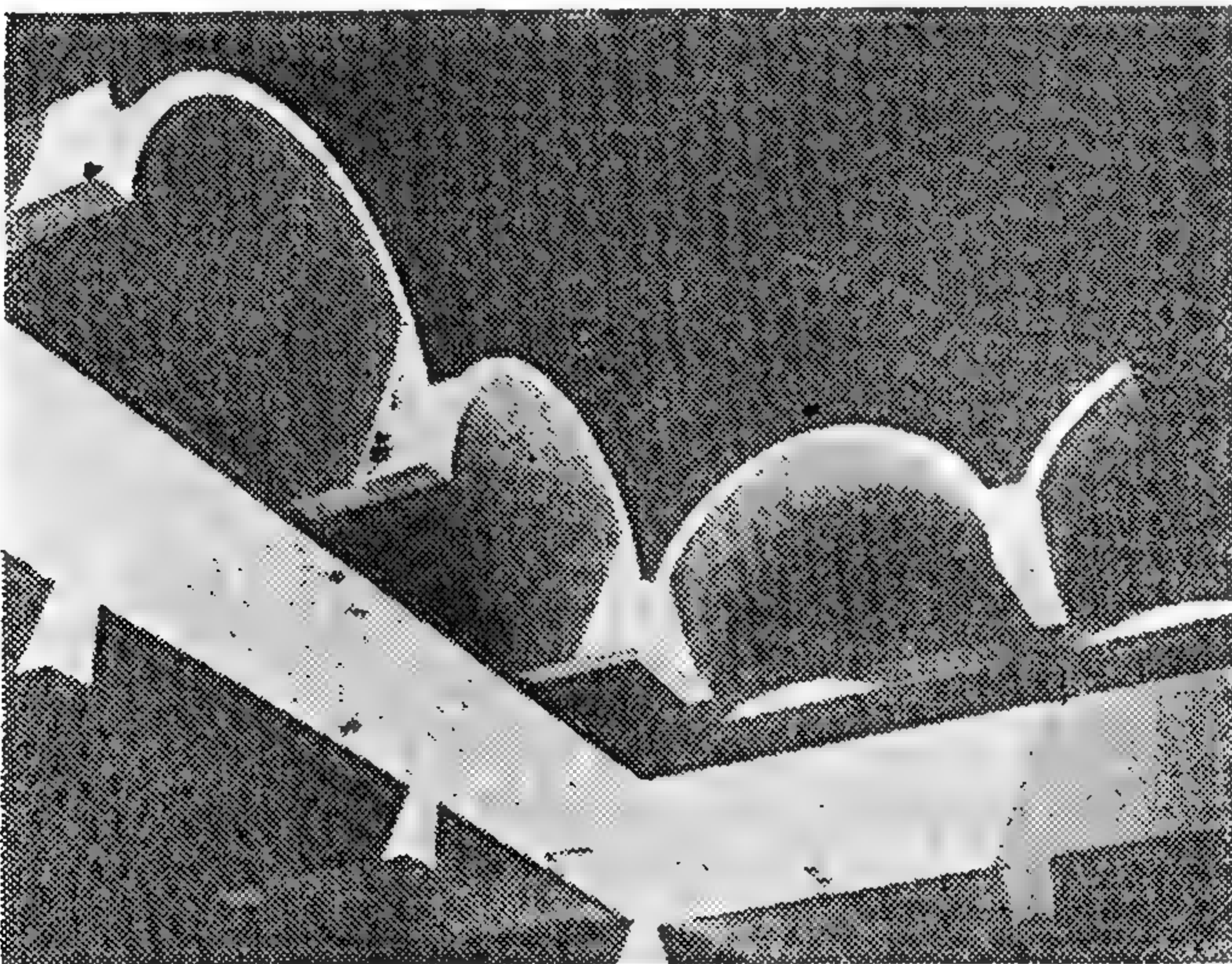
١٣ يسار : محكمة
جزئية - بنى ملال
مراكش ١٩٦٤
١٤ اسفل : تفاصيل
السقف بالمحكمة
الجزئية - بنى ملال .

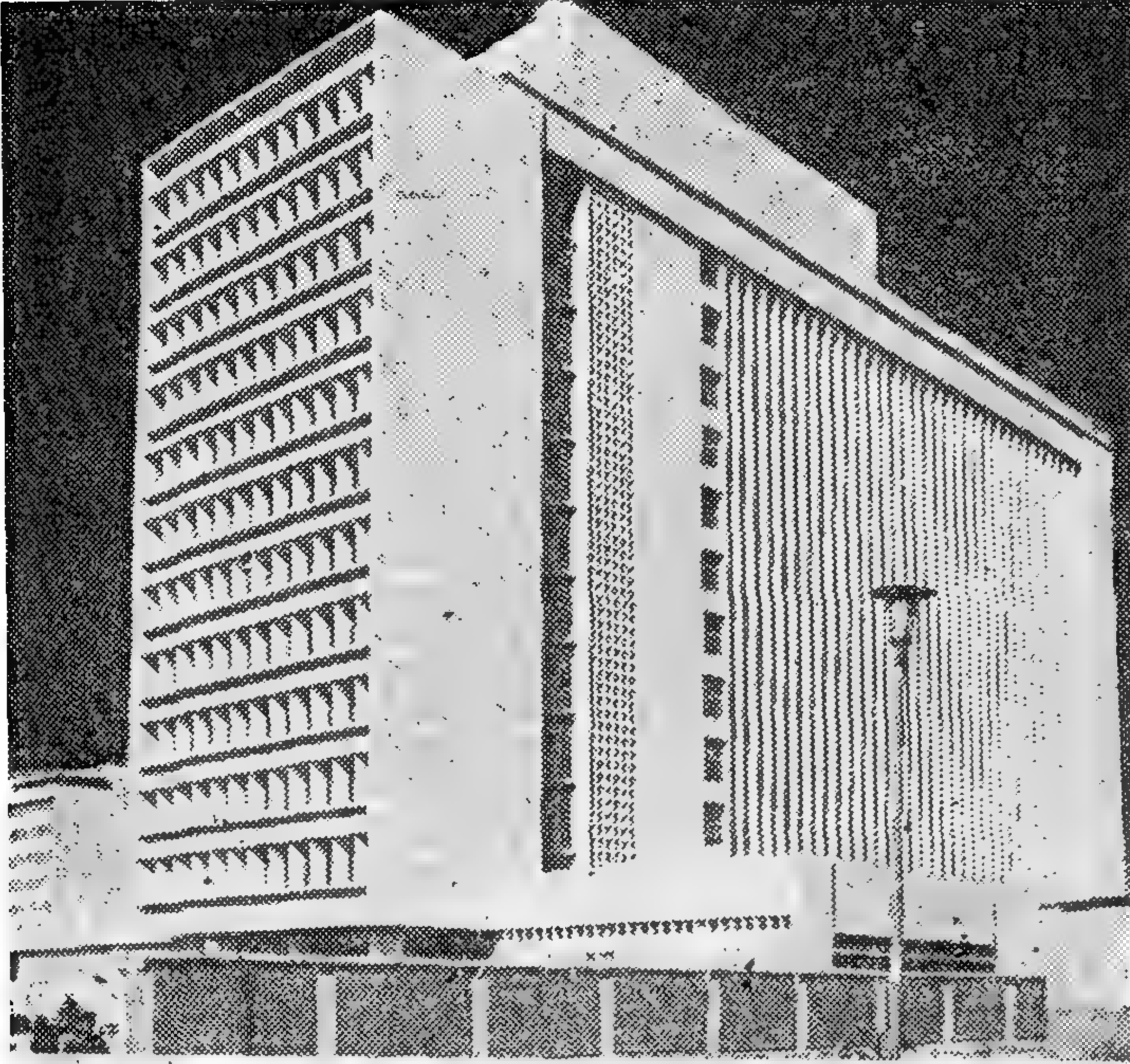
عمليات تكييف الهواء بالوسائل الميكانيكية للتحكم في ظروف المعيشة الداخلية ، ولكنها وسائل باهظة التكاليف لا يتحمل عبء تكاليفها وصيانتها الا الأثرياء ورؤساء مجالس ادارة مؤسسات وشركات القطاع العام . لماذا اذن لا نعود الى استخدام الوسائل الطبيعية في التصميم كما فعل العرب من قبل مع تطوير هذه الوسائل بالامكانيات المتاحة ..؟ لماذا اذن هذه الفتحات الزجاجية المتسعة في واجهات المباني القبلية والشرقية والغربية التي نراها في الرياض وجدة والكويت وبغداد والقاهرة

والامانة العلمية والفنية والمهنية ، وباعتزاز المرء بما تصنعه يده ، وان البناء كان يشيد في الماضي لكي يبقى طويلا ، وبسبب نظام التدريب وجدت أعظم براعة مهنية في التكوينات والعناصر المعمارية في العمارة العربية .

● وهنا تظهر أهمية ذلك السؤال الذي كثيرا ما رددناه وهو .. هل نعيش على ماضينا ، ام نبني حاضرا ونمهد لمستقبلنا ..؟ الجواب سهل وبسيط وهو ان العمارة تعكس آمال واماني الشعوب وقدرتها العلمية وذوقها وفلسفتها . فالعمارة تخص الانسان والمباني ، اما التخطيط فمرتبط بالانسان والمباني والمجتمع . والانسان هنا هو الانسان العربي ، والمجتمع هنا هو المجتمع العربي . لذلك يتحتم على المعمارى والمخطط العربى ان يأخذ كل منهما في الاعتبار في تصميماته وتخطيطاته جميع العلوم المتعلقة بالانسان العربى والبيئة والمجتمع .

● ان الشمس لا زالت ساطعة في مصر وفى العالم العربى بأسره كما كانت ساطعة بالأمس وستظل كذلك . ان ظروف المناخ المحلى في جميع البلاد العربية لم تتغير منذ آلاف السنين ، حار جاف صيفا ومعتدل قليل المطر شتاء ، هي نفس الظروف التى قامت فيها العمارة الفرعونية والعمارة الاسلامية ، وهى حضارات متصلة مترابطة . قد يقال ان تكنولوجيا العصر الحديث ادخلت لنا





١٥ : أعلا - مبنى وزارة العمل بمدينة نصر
القاهرة ١٩٦٩ أسفل - مبنى الجهاز المركزي
للتعبئة والاحصاء مدينة نصر - القاهرة ١٩٦٩

أو حلولا منقولة مستوردة ، أو مستوحاة من المشاريع الأجنبية .. ولكنه هو ذلك المعماري الأصل الحر الفنان ، الذي لا يتاجر بالمهنة ، الذي يتعاطف مع احتياجات عمله ويترجمها الى الاسلوب المعماري الذي يتلاءم مع البيئة والمناخ والمجتمع فالعمارة هي تفاعل وجدان الانسان مع البيئة ، وتفاعل وجدان المعماري العربي مع بيئة عربية يؤتى عمارة عربية .. والله ولي التوفيق .

فراغات وواجهات لا تتفق مع المناخ ولا مع الطابع العام ..؟ هذه المساكن أو هذه العمارات السكنية ابتعدت تماما عن مجرى حضارتنا وتطورها الطبيعي ، واتسمت بالجمود وعدم ملاءمتها للنمو الطبيعي للعائلة ، وعدم احترام عامل الاستقلال والخصوصية Privacy مما أدى الى خلق مشاكل اجتماعية خطيرة لا تخفى على أحد .

- كانت للمساجد ودور العبادة قدسية ومكانة ، كان لها وضع مميز في تخطيط الأحياء في المدن والقرى الغربية . اننا الان نختار مواقع هذه الأبنية المقدسة بطرق عشوائية ارتجالية . فيظهر المبنى بعد ذلك اما هزيلا بالنسبة لما يحيط به من مباني مرتفعة أو يفقد وقاره وجلاله نظرا لمباني الترفيه والتسلية التي تلتف حوله ، ويرجى ان ننظر اشكال أرقام ..

- كانت للحمامات الشعبية ، والأسواق التجارية والمكشوفة والمفطاة ، وأماكن الاجتماعات والمسارح في الهواء الطلق ، والمقاهي في الحدائق الداخلية المظلة ، وغير ذلك من المباني العربية الأصلية سواء في المدن أو في الريف أهمية خاصة في حياة المجتمع العربي .. أين هي الان ؟ لماذا لا نكثر منها ونطورها وهي استمرار وتطور طبيعي لطابع معماري عربي قائم ..؟

- واذا ما انتقلنا أخيرا الى امكانيات الفنون التطبيقية العليا نجد أمامنا طاقات محلية ضخمة للتعبير بها عن الفنون العربية الأصلية في مجال التطور المعماري الحديث في الشرق العربي أو بمعنى أصح في مجال التراث العربي . وهي الأشغال المعدنية بالنحاس والصدف ، وأعمال الخمرط الخشبي المطعم بالنسج والصدف والعاج ، وأعمال السيراميك الملون ، والفخار المزجج والقيشاني ، والزجاج الملون ، وأعمال السجاد والأكلمة والنسيج .. الى غير ذلك من المهارات والقدرات العربية التي تتعاون مع العمارة في تكوين مسطحات داخلية وخارجية وتشكيلها بدرجات عالية من الظل والنور واللون والتعبير .

● ان علينا تنقية مفهوم العمارة المعاصرة من الشوائب والخطط المعيب والزيف لكي نرفع العمارة الغربية الى مكانها الصحيح ووضعها السليم ، يجب علينا ان نفرق بين لفظ « معاصر وزائل » حيث يقول دانتي « قد يكون ما يسمى حديثا هو ما يستحق ان يبقى ليهدم » ومن المؤلم حقا ان نرى الكثير من كبار المعماريين العرب يختارون الزائل بدلا من المعاصر ، مثلهم في ذلك كمثل بعض طلبة أقسام العمارة في كلياتنا الذين يتبارون في خلق الاشكال المستحدثة التي لا معنى لها ، لمجرد انها تلفت النظر وتحوز على رضاء وتصفيق الجهلاء .

ان المعماري المطلوب ليس هو ذلك الانسان الذي يفرض حلولا جاهزة للمباني موحدة للجميع ،

$$Q = \frac{4 \pi K D S_w}{2.30 \log (2.25 K D t / S r_w^2)} \quad (4)$$

It should be noted that S is a constant for a free-flowing well and is equal to the difference between the static head and the out-flow openings of the well. For determination of the aquifer characteristics, the well is shut down for a period long enough for the pressure to become static, this can be measured with a pressure gauge fitted at the top of the well. Then the well is opened up again and the discharge rate is measured at intervals of from 30 to 60 second during the first minutes and afterwards with gradually increasing intervals. This method was used to calculate the hydrogeological parameters of some free-flowing wells in El-Kharga Oasis. Fig. (2) is the graphical illustration of the application of this method for El-Kharaga well No. 10. Approximate values of the transmissivity KD and storage coefficients obtained by using this method are 133 m²/day and 4×10^{-4} consequently. The values of these parameters obtained by Borelli, 1968 using long-term pumping test data are 144 m²/day and 1.5×10^{-3} . The graphical analysis of El-Kharga well No. 10 follows the following pattern :

1. Plot the values S_w / Q versus t on a semi-log paper (t on log scale).
2. Fit a straight line through the plotted points.
3. Extend this straight line till it intercepts the time-axis where $S_w / Q = 0$ at the point to
4. Introduce the value of the slope of the line S_w / Q i.e. the difference of S / Q per log cycle, of t into Eq (5) and calculate KD

$$KD = \frac{2.30}{4 \pi \Delta (S_w / Q)} \quad (5)$$

$$S' = \frac{2.25 K D t_0}{r_w^2} \quad (6)$$

Where $S' =$ Storage coefficient.

REFERENCES

- Jacob, C.E. and S.W. Lohman, 1952. Non-steady flow to a well of constant drawdown in an extensive aquifer. Am. Geophys. Union Trans, Vol. 33 : 559 — 569.
- Logan, J. 1964. Estimating transmissivity from routine production test of water wells. Groundwater, Vol. 2, nr. 1 : 35 — 37.

Well name	aquifer type	Screen diameter (in)	Well diameter (in)	$S_m W$ (m)	Well discharge range m/day	$KD(m^2/day)$	
						Borelli	Logan
Mahariq-7	Confined	9 $\frac{5}{8}$	13 $\frac{3}{8}$	2.68	3290	1172	1483
Mahariq-2	"	8	12	2.92	3000	1080	1250
El Sherka 34 A	"	5 $\frac{1}{2}$	9 $\frac{5}{8}$	0.70	800	1100	1400
E Kharga 1 A	"	6 $\frac{5}{8}$	8 $\frac{5}{8}$	1.95	2000	1431	1250
Bulaq-4	"	6 $\frac{5}{8}$	8 $\frac{5}{8}$	4.14	3240	749	950
Garmashin - 4	"	6 $\frac{5}{8}$	8 $\frac{5}{8}$	3.40	3070	1163	1100
Garmashin -10	"	6 $\frac{5}{8}$	8 $\frac{5}{8}$	1.58	2150	1228	1561
Baris - 6	"	7	8 $\frac{5}{8}$	2.78	2080	756	910
Ginah - 7	"	6 $\frac{5}{8}$	8 $\frac{5}{8}$	1.85	2310	1570	1510
Ginah - 6	"	8	12	5.36	4500	780	1020

2. Free-flowing wells :

Unsteady-state flow in confined aquifers

Although a free-flowing well is strictly speaking not pumped, the method of calculating the aquifer characteristics of an aquifer from observations made at such a well is so closely related to the analysis of pumping tests. As it is known, the free-flowing wells or artesian wells in a very famous and

frequent phenomena in the biggest underground-water basin in Egypt, the So-called the New-Valley in Western Desert, for this reason it is seemed useful to include that method here :

Jacob-Lohman's method :

Jacob and Lohman (1952) showed that the discharge rate of a free-flowing wells varies according to the following equations :

$$KD = \frac{2.30 Q \log r_{\max}/r_w}{2 \pi S_{mw}} \quad (1)$$

where : r_w radius of the pumped well
 r_{\max} = radius of influence = radius of depression
 s_{mw} = Maximum drawdown in the pumped well.

The accuracy of the calculation depends on the accuracy of the measurement of S_{mw} on which well losses may have a substantial influence and on the accuracy of the ratio r_{\max}/r_w .

The ratio of r_{\max}/r_w cannot be accurately determined without the use of piezometers.

Assuming average conditions of radii, a value of 3.33 for the log-ratio may be accepted as a rough approximation, substitution of this value into equation (1) gives :

$$KD = \frac{1.22 Q}{S_{mw}} \quad (2)$$

The above described method was used to calculate the hydrogeological parameters of some wells in El-Kharga Oasis in the New-Valley and then these results were correlated with the parameters calculated by (EGDDO) Borelli, 1968. The results obtained by using this simple method differ from these results obtained by Borelli by about 20.25% as it shown in tabe No. 1. It should be noted that the transmissivity value thus obtained are therefore only the first-time round approximation. However, in the absence of adequate data or in preliminary survey, this estimation method may be very useful.

The same line of reasoning may be followed for unconfined aquifer resulting in :

$$KD = \frac{1.22 Q}{(S_{mw})^0} \quad (3)$$

Where $(S_{mw})^0 = S_{mw} - S_{mw}^2 / 2D$

S_w/Q

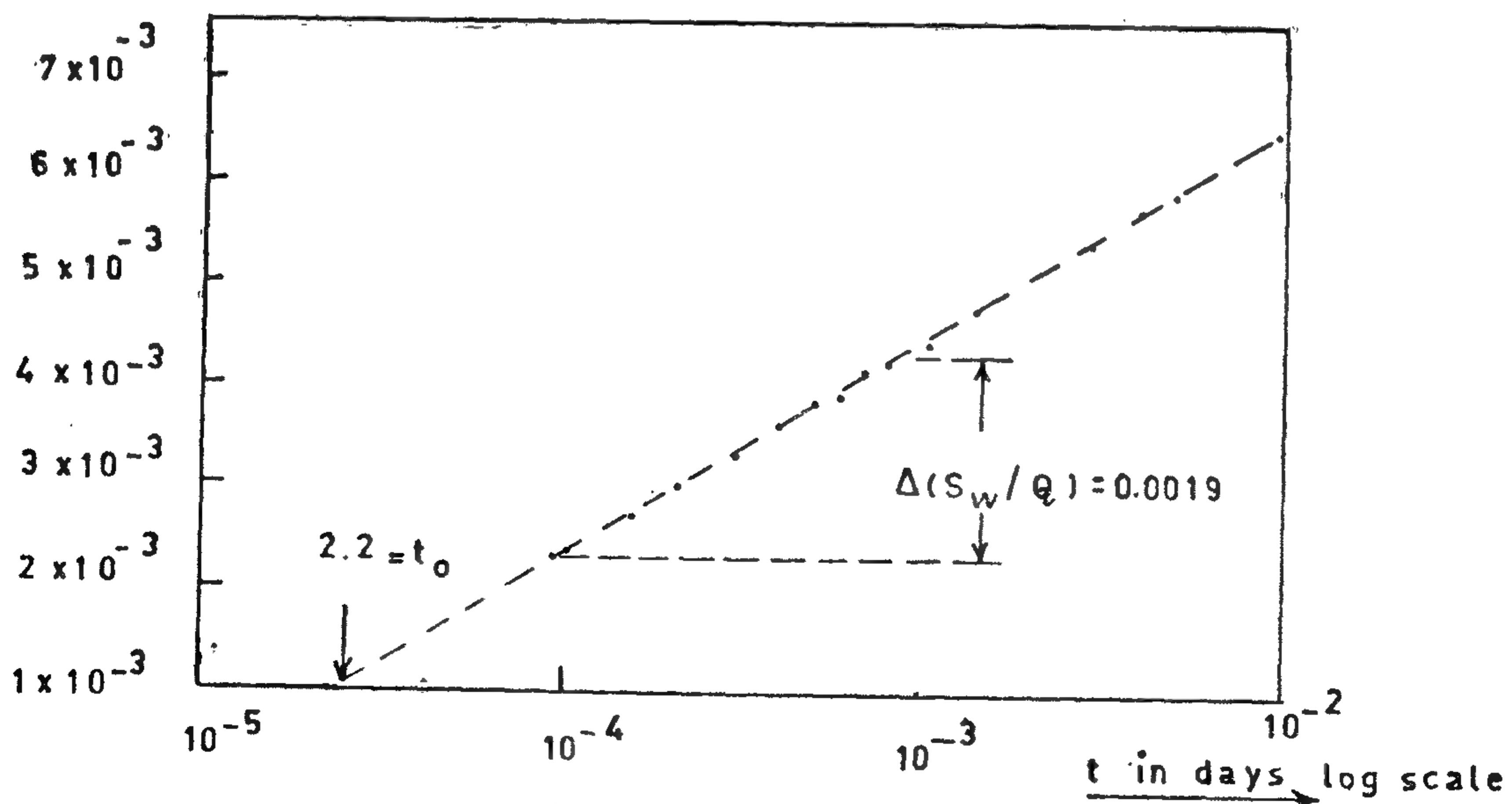


Fig.(2) Graphical illustration of the application of Jacob's method to El-kharga well No. 10.
 (Free-flowing well)

a piezometer outside the radius of influence of the pumped well so that the water table not affected by pumping can be measured. This piezometer should be placed several hundred meters from the well, or in certain cases, as far away as one kilometer or more.

3. The depth of piezometers :

In a uniform and homogeneous aquifer the piezometers should be installed at about the same depth as the middle of the well screen in the pumped well. For example if the pumped well is fully penetrating with a screen between 10 and 20 m below the ground surface, the screens in the piezometers should be installed at a depth of about 15 m below the ground surface,

For non-uniform aquifers with intercalated clay beds it is recommended that screens be installed above and below these clay beds to see if there is any hydraulic interconnection between the water-bearing layers.

When the aquifer to be tested is covered by a layer of low permeability, piezometers should be installed not only in the aquifer itself but also in the covering layer where the water table is found. These shallow piezometers are necessary to check the effect of pumping on the water table. This information is important for the analysis of pumping test data from semi-confined aquifers.

4 — Construction of piezometers :

Rapid and accurate measurements of the water levels are best obtained by small diameter piezometers. If the diameter is large, the volume of water contained in the piezometers may cause a time lag in changes of drawdown.

When hand methods of measuring the depth to water are employed the diameter of the piezometer need not be larger than

5 cm. If automatic water-level recorders are used the pipe must be wider.

Generally, the screen length of the piezometers not exceed 0.5 to 1 meter.

The annular space around the screen is filled with a uniform coarse sand in order to facilitate the entrance of water into the piezometer. The rest of the annular space may be filled with any material available except for those places where clay layers are present.

VII. Approximation methods for determination of the aquifer characteristics :

In reconnaissance surveys it is often impossible to perform proper pumping tests; and to get an impression of the order of magnitude of the hydraulic conductivity; less accurate methods have to be used. This is the case when, for example, a well already in existence is pumped and the drawdown data collected in this well are used to calculate the transmissivity of the aquifer or for the free-flowing wells in Artesian basin.

Approximate value of the aquifer characteristics can be obtained by using these methods.

Some of these approximation methods of analysis were used to determine the hydrogeological parameters in some localities in the new-valley in the Western Desert Of Egypt are now described:

Steady-State flow in confined and unconfined aquifers :

Logan's method

If a well in a confined homogeneous, isotropic and of an apparently infinite areal extent aquifer has been pumped for such a long period that the flow is in steady-state, the Logan method can be applied to calculate the order of magnitude of the transmissivity. Logan (1964) modified the Thiem formula for a confined aquifer as follows :

Simi confined aquifers have an intermediate positions

b — The magnitude of permeability :

The permeability of water-bearing material is also of great importance i.e. when the permeability of the aquifer material is high the cone of depression induced by pumping will be wide and flat, and on the other hand if the permeability is low the cone of depression will be steep and narrow. Therefore, in the first case piezometers can be placed further away from the pumped well than they can in the second.

c — The discharge rate :

If the discharge rate of the pumped well is high the cone of depression induced by pumping will be larger than with a low rate. Therefore, in the first case greater distances between the piezometers are allowed than in the second.

d — The well-screen length :

The choice of distances from the pumped well at which piezometers should be installed may be strongly influenced by the length of the well screen in the pumped well. If the pumped well is a fully penetrating one, the flow of the water to the pumped well will be horizontal. Therefore, drawdowns measured in piezometers placed even at short distances from the pumped well can be used for the analysis. It will be obvious that, if the aquifer to be tested is not very thick, it is always best to employ a fully penetrating well.

However, in many cases the aquifer to be tested is thick and conditions may not allow a well screen to be installed over the entire thickness of the aquifer. In such a partially penetrating well, the relatively short length of the well screen will cause a non-uniform distribution of head or drawdown which is most noticeable near the well. So, if the length of the well screen is considerably less than the saturated thickness of the aquifer, a distorted drawdown pattern is induced near the well, due to vertical flow components. Drawdown readings from wells

close to such a partially penetrating well may lead to incorrect results; and rather complicated correction methods have to be applied before those readings can be used for the analysis of the test data. These difficulties can be avoided if the piezometers are placed further away from the pumped well, where these abnormal effects do not appear. As a general rule it may be recommended that the nearest piezometers be placed at a distance which is at least equal to the thickness of the aquifer. At such a distance it may be assumed that the flow is horizontal.

e — Stratification :

Homogeneous aquifers seldom occur and most aquifers are stratified to some degree. As a result of this stratification the drawdown observed at a certain distance from the pumped well may be different at various depths within the aquifer, because of differences in permeability in vertical and horizontal directions. These differences in drawdown diminish as the time of pumping extends.

Furthermore, the greater the distance from the pumped well, the less is the effect of stratification upon distribution of drawdown.

From the above mentioned, it is obvious that several factors are involved in deciding how far from the pumped well the piezometers should be installed. A proper knowledge of the test site, especially of the type of aquifer, its thickness, average permeability and stratification, will make it easier to choose the proper distance at which the piezometers should be installed. Although no fixed rule can be given and the ultimate choice depends entirely on local conditions and the length of the well screen, placing piezometers about 10 to 100 m. from the pumped well will give good results in most cases. The distances must be greater for thick or stratified confined aquifer and the piezometers should be placed 100 to 250 m. or more from the pumped well in order to obtain reliable data. It is also useful to have

V. Selection of the pump :

The pump for an aquifer test should be capable of operating continuously at a constant discharge rate for a period of at least two days. In testing unconfined aquifers this period may even be too short, and the same is the true if drawdown from observation wells at great distances from the pumped well are to be used.

The capacity of the pump and the rate of discharge should be high enough to produce good measurable drawdowns in piezometers as far away say 100 or 200 m, depending on the aquifer conditions. After the pump is installed, the well should be developed by pumping at a low discharge rate. When the pumped water becomes clear, the discharge rate is enlarged and pumping is continued until the desired discharge rate for the actual test is reached or exceeded.

When all observation wells have been completed, the development of the discharging well provides a good opportunity of checking whether all observation wells are reacting satisfactorily.

VI. Piezometers or observation wells :

The principle of an aquifer test is that a well is pumped and the effect of this pumping on the water table in the vicinity is measured. For this purpose a number of piezometers or observation well should be available near the pumped well. Therefore, after the pumped well is completed one has to decide on the number and depth of these piezometers and howfar they should be located from the pumped well finally the construction of these piezometers. These important points are discussed in the following order :

1. Number of Piezometers :

The number of piezometer depends not only on the amount of information desired and the required degree of accuracy, but also on the funds available for the test.

Practice showed that the data obtained by measuring the drawdown in a single piezometer often permit calculation of the average permeability, transmissivity and storage coefficient of the aquifer.

The advantage of two or more piezometers placed at different distances and depths from the pumped well is that the drawdowns measured in these piezo meters can be analyzed in two ways : by studying both the time-drawdown and distancedrawdown relation-ships.

Obviously, the results of calculations thus obtained are more accurate and representative of a larger area. It is always best to many piezometers as conditions permit, while on the other hand it is recommended that at least three be employed.

2. Distance of piezometers from the pumped well :

Many factors govern the distance of the piezometers from the pumped well, the most important of them are the type of aquifer, the magnitude of permeability, the discharge rate, the well-screen length and finally the stratification of aquifers.

a — The type of aquifer :

In confined aquifers a loss of hydraulic head caused by pumping can propagate fast because the release of water from storage is entirely due to the compressibility of the aquifer material and that of water. Therefore, the loss of head may still be measurable at great distances, say few hundreds meters from the pumped well.

In unconfined or water-table aquifers the propogation of hydraulic head losses is rather slow because the release of water from storage is mostly due to dewatering of the zone through which the water is moving. Unless the period of pumping is extended for several days, the loss of hydraulic head caused by pumping is only measurable within rather short distances from the pumped well, for instance not much farther away than 100 m.

well may be assumed to be horizontal, and assumption which underlies nearly all pumping test formulas. Vertical flow components in the vicinity of the well, causing an extra drawdown, can thus be avoided and no correction need be made for partial penetration Fig. (1).

There are of course some expectations to this rule. In water table or unconfined aquifers it may be sufficient to screen the lower half or third of the aquifer because if appreciable drawdown occurs the upper part of the well screen may fall dry. It will also be apparent that if very thick aquifers are to be tested the length of the well screen will be reduced, simply for economical reasons. If the screen covers less than, say 70% of the aquifer thickness, the well is said to be partially penetrating well. Such a well induces vertical flow components within the aquifer over distances extending from the pumped well and roughly equalling the thickness of the aquifer D , see fig. (1).

Within this radius (r) measured drawdowns have to be corrected before they can be used to calculate the hydrogeological parameters see fig. (1).

With non-homogeneous aquifers, having continuous intercalated clay beds, it seems useful to make separate tests in the different aquifer parts. This may give a double check on the question whether the clay beds are impervious or leaky. Finally it should be noted that a proper screen should be utilized, having a sufficient total open area so that the entrance velocity is low, say less than about 3 cm per sec. At this velocity the friction losses in the screen openings will be negligible. The size of the screen openings is also of great importance. The size should be selected according to the grain size of the aquifer material.

IV. Gravel-pack : The entrance of water into the well screen is facilitated if the formation material immediately surrounding the screen is removed and replaced by artificially graded coarser material, a so-called gravel pack. When the well is pumped this graded gravel should retain all the formation material that would otherwise enter the well.

Gravel pack material should be clean, with rounded grains that are smooth and uniform. The thickness of the gravel pack should be at least 7 or 8 cm, in order to ensure that the envelope of gravel-pack-thickness should be about 20 cm.

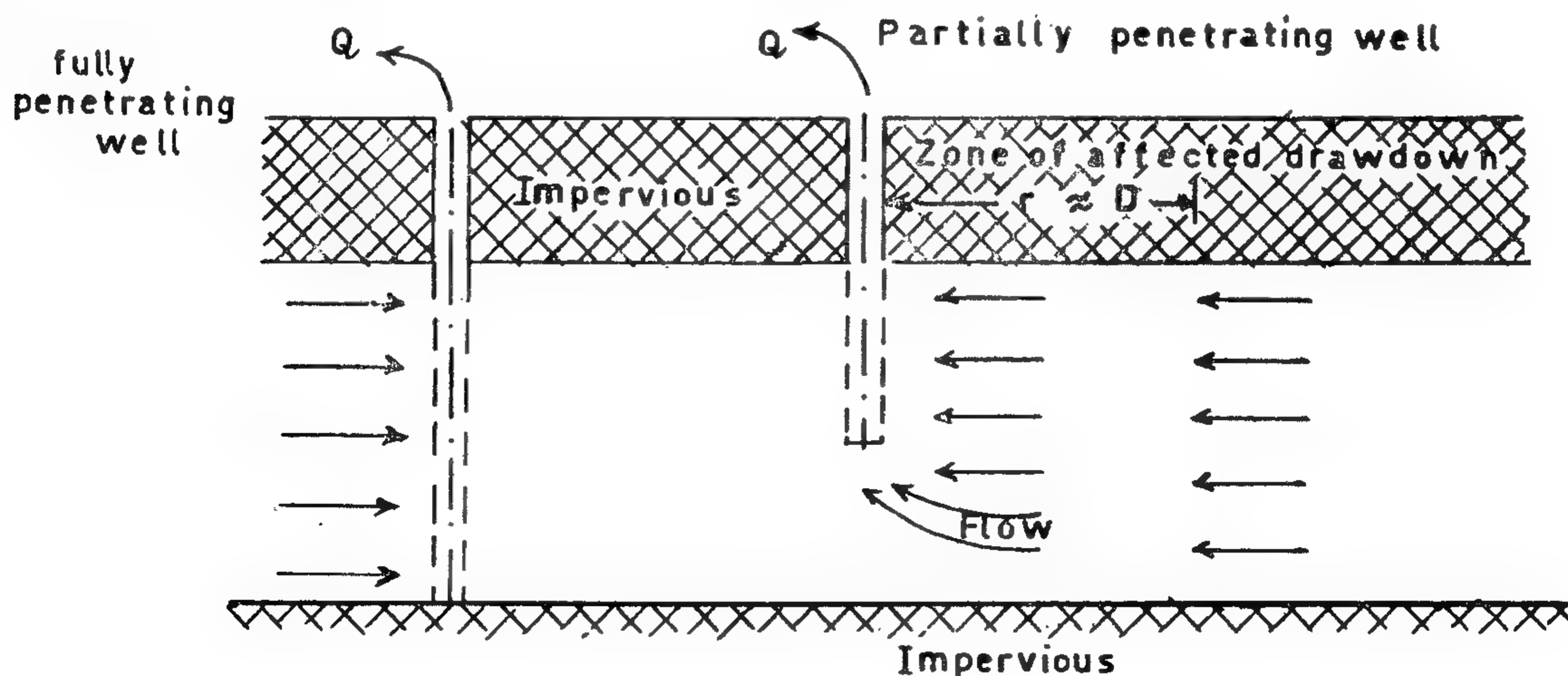


Fig.(1) Schematic section of a fully and partially penetrating well

for each test site a correction can be made on transmissivity values estimated from the logs of the wells located between these test sites.

Experience has shown that if accurate well logs are available the transmissivity can be estimated with reasonable accuracy. However, appreciable errors may be made when either very fine materials as clay and silt or very coarse as gravel are mixed with the sand. (Ernst, Deridder and De Vries, 1970). Nevertheless, in studying large ground water basin-like New Vally, Western Desert, Egypt this approach can be extremely useful. Obviously, this method cannot be recommended for the solution of local groundwater problems but generally for some studies on a regional scale.

III. Selection of test site :

One of the most important things during the Preliminary hydrogeological reconnaissance is the selection of the test site.

In certain cases the site of the test is predetermined and there is no possibility of moving to another more suitable site. This applies, for example, when existing wells to be used or when formation factors at a specific location are required. In regional ground-water studies one may be more or less free to select a suitable site.

In selecting the place of an aquifer test, the following remarks should be taken into consideration :

— The hydrogeological conditions of the site should not change over short distances and should be representative of the area or a large part of the area under studies.

— The pumped water must be discharged in a such away that it does not return to the aquifer.

— The gradient of the water table or piezometric surface should be low.

— Manpower and equipment must be able to reach the site easily. Obviously, a careful selection of the test site will prevent many difficulties during the evaluation of the test data.

IV. Pumped well :

After the test site has been selected, drilling operations on the pumped well can start. A pumped well is a well in which a tube is placed and this tube has a screen in the aquifer. The well is equipped with a pump to lift the water to the surface where it is discharged. Regarding the well design and construction, attention must paid to the following major and important points :

1. **Well diameter** : The well diameter must be chosen so as to satisfy two requirements; firstly, to accommodate the pump with proper clearance for installation and efficient operation; secondly, to assure hydraulic efficiency of the well.
2. **Well depth** : The expected depth of the well is usually determined from the log of a test hole, from the logs of other nearby wells, or during drilling. It is desirable that the well be completed to the bottom of the aquifer because then more of the aquifer thickness can be utilized as the intake portion of the well, resulting in a higher yield. A large drawdown can thus be realized which also permits a greater well yield.
3. **Well screen length** : It is known that increasing the diameter of the well screen results only in a slight increase of the well yield. The length of the screen, however, is more significant. The general rule is to screen 70—80% of the thickness of the aquifer because this makes it possible to obtain about 90% or more of the maximum yield that could be obtained if the entire aquifer were screened. Another great advantage of this screen length is that the groundwater flow towards the pumped

ried out. On the other hand, it should be noted that many successful aquifer tests have been made at places where little was known about the geology of the site. Sometimes impervious boundaries are hidden (buried fault) and their existence only shows up after a careful analysis of the drawdown plots.

Obviously, knowledge of the geology and hydrology of the area of study will be helpful in deciding on the type of drilling and pumping equipment needed and on the number and location of the tests.

Such knowledge may be also of great importance when the test data are being analysed and boundaries have to be taken into account.

When the available geological and hydrogeological data are studied, it will sometimes become apparent that some additional knowledge, especially concerning the deeper layers, is required before tentative evaluation of the hydrogeological conditions of the area can be made. The necessary information can often be obtained by drilling some additional exploration wells or bore holes.

In some areas, already existing wells which can be used to conduct aquifer tests, thus greatly reducing the cost; sometimes, however, they provide uncertain results because details of construction and condition of the wells may not be available.

II. Primary estimation of Transmissivity from well logs :

In the same time of drilling the poreholes of the pumping and observation wells, samples of the different geological formations that are penetrated should be collected and described lithologically. Special attention should be given to the grain-size of the various materials. On this basis the length of the pump screen and the depth at which this screen should be installed can be decided. In general, this will be the depth where the coarsest materials have been found. Fur-

ther Laboratory analysis for some samples sometime recommended. Firstly, geological analysis may provide information on the stratigraphic position of the various layers encountered in the borings. Secondly and of equal importance a more detailed lithologic description of the samples can be made, using binocular lens with a size scale. In this way the average grain size, the degree of sorting and the clay content of the sandy samples — all parameters which affect the hydraulic conductivity or permeability in a different way can be estimated more precisely than in the field. If funds are available grain size analyses of all samples could be made in order to determine these parameter.

These data can be used to obtain an initial impression of the permeability of the aquifer material and hence transmissivity of the aquifer.

A relationship can be established between the hydraulic conductivity or permeability and the grain size. In this relationship the effects of sorting and the clay and gravel content should be accounted.

If tables of this relationship are not readily at hand, one can divide the aquifer materials described in the Logs into a certain number of major groups, ranging from very fine sand to gravel, and assign by estimation a certain reasonable permeability coefficient to each group. For each layer described in the well Log this coefficient multiplied by the thickness of the layer to find the transmissivity of each layer. By summing these results the transmissivity of the aquifer at the well site may be found.

This geologic approach for determination transmissivity is repeated for each well used in the actual aquifer test and the results are averaged.

The estimated transmissivity value thus obtained can be compared with the result obtained from the actual test. If no agreement is found the error percentage should be determined. When this percentage is known

PRELIMINARY HYDROGEOLOGICAL RECONNAISSANCE PRIOR TO THE PERFORMANCE OF PUMPING TESTS AND ITS APPLICATION IN SOME LOCALITIES OF EGYPT

By **Dr. M.S. SALAWI***

INTRODUCTION :

There are numerous groundwater flow problems whose solution requires a proper knowledge of the hydrogeological characteristics of the aquifer. The number of pumping tests to be performed, the site of these tests, and the general set-up depend upon the kind of problem to be solved; the amount of information that is desired and of course upon the funds available for the test program.

The problem involved may be a local one of predicting future drawdowns where a new well field is to be established for domestic water supply. It may also be a more regional one for determining the exploitable reserves of a large groundwater basin, for example New Valley, Western Desert, Egypt. Owing to the high costs of aquifer testing and the usually limited funds available for such tests, their number in most regional groundwater studies must be restricted. For this reason a carefully and well-planned programme for preliminary hydrogeological and hydrological reconnaissance and survey must be prepared and performed before a pumping test has been conducted. In this work the author tries to make an approach to illuminate some important factors concerning this preliminary reconnaissance.

I. General geologo-hydrogeological features of the area :

Prior to the performance of pumping test the necessary information on the subsurface geological and hydrogeological con-

ditions has to be collected. By this we mean the geological features of the water-bearing layer, for example the lithologic character and thickness of the aquifer, its boundary conditions. With regard to these boundaries it is important to know the character and thickness of the beds overlying and underlying the aquifer.

Most of the pumping test formulas are based on the assumption that the tested aquifer is of infinite lateral extent. Although such aquifers do not exist, many aquifers are of such wide extent that for all practical purpose they can be considered infinite. Others however, are of limited extent because they terminate against impervious material. Such barrier boundaries are, for example, the impervious bedrock sides of a buried valley, a fault, or simply lateral changes in lithology of the aquifer material.

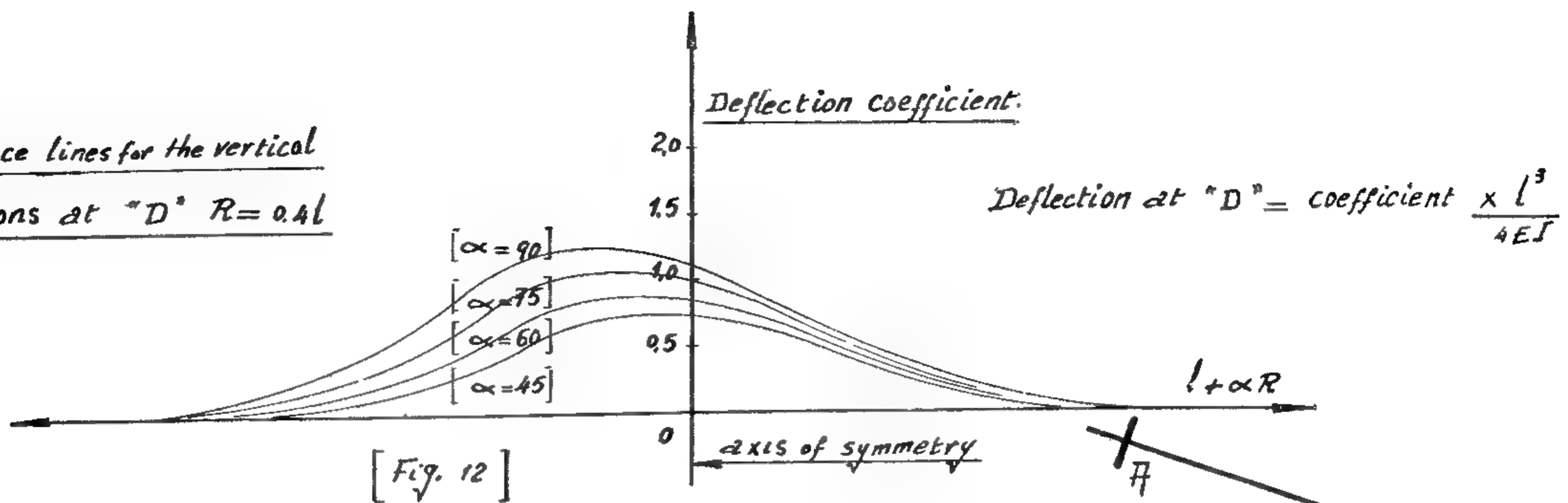
The recharge boundaries are also long which there is no drawdown also of equal importance, such boundary exists where an aquifer is freely connected hydraulically with a river, canal, lake, sea or ocean. If an aquifer is being tested near recharge or barrier boundaries, this fact must be considered in the analysis of the pumping test data.

Besides the position and nature of the hydrogeological boundaries it is also necessary to know the direction of groundwater flow, the water table gradients, and the regional water level trend.

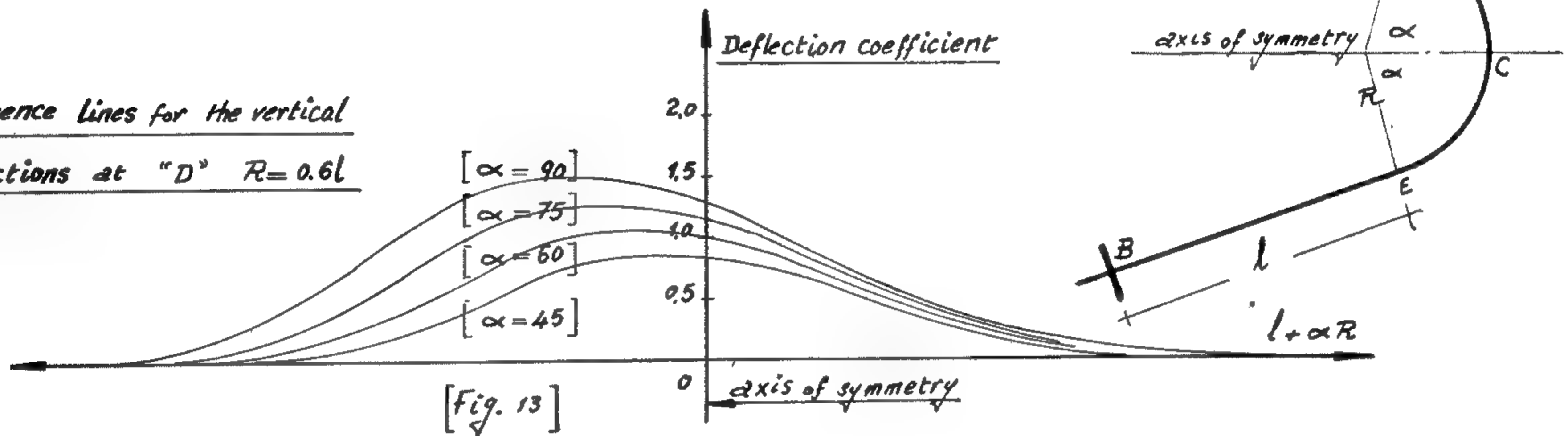
In most groundwater studies a great deal of the information is often already available before a pumping test program is car-

* Associate Professor, Water Resources Dept., Desert Institute, Matruh, Cairo.

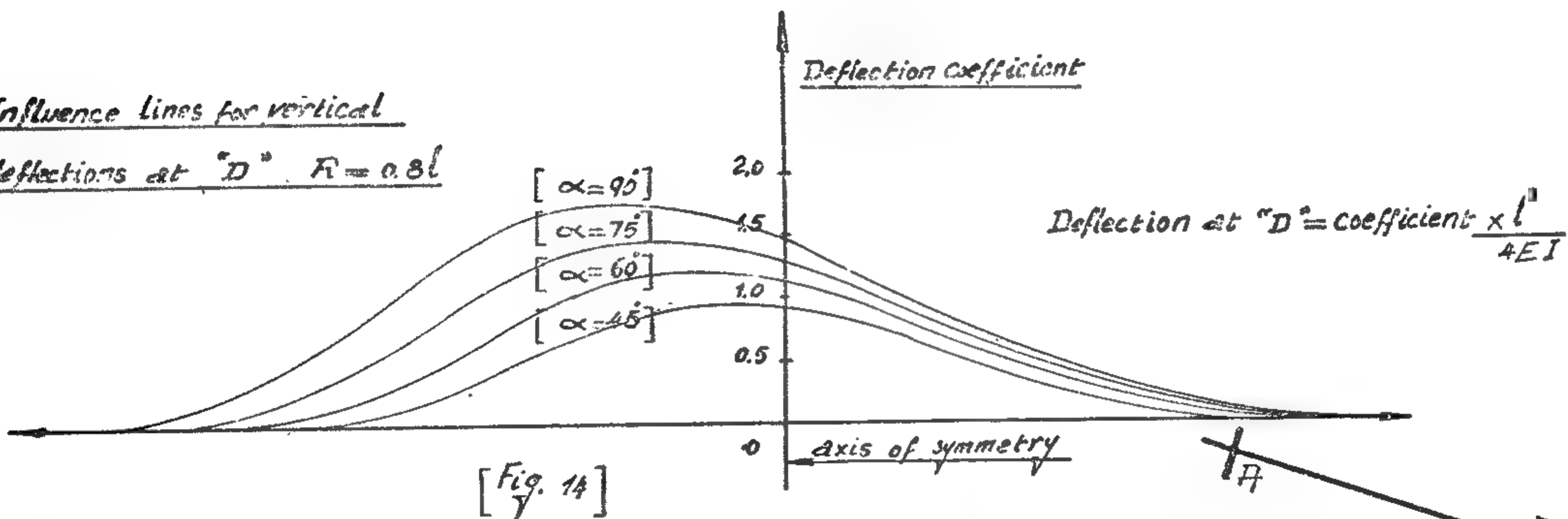
Influence lines for the vertical deflections at "D" $R=0.4l$



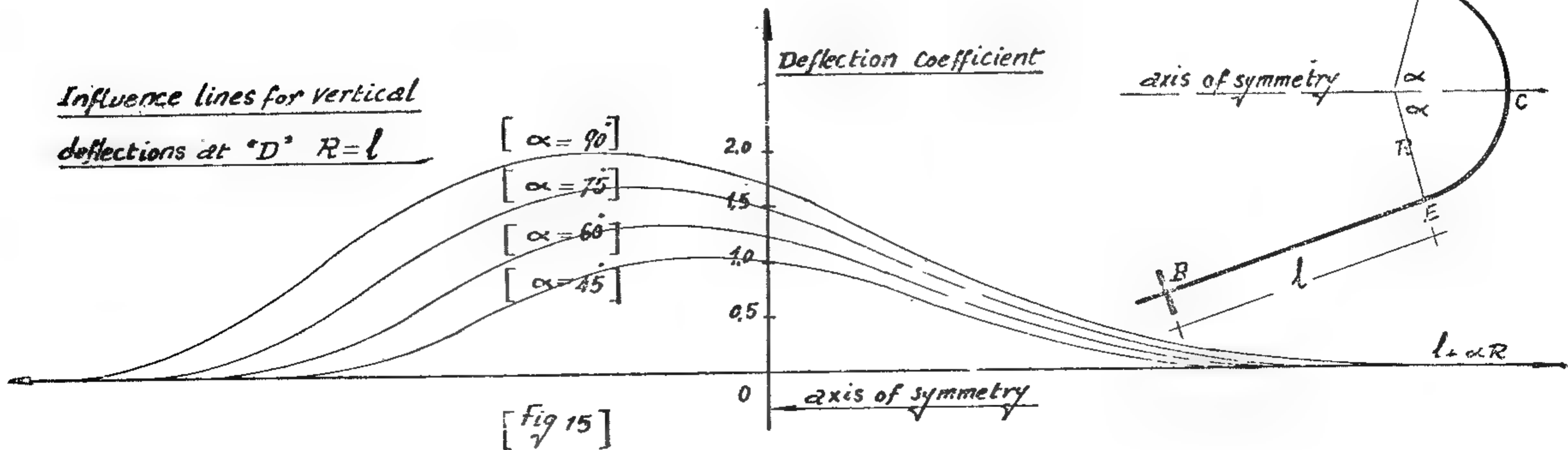
Influence lines for the vertical deflections at "D" $R=0.6l$

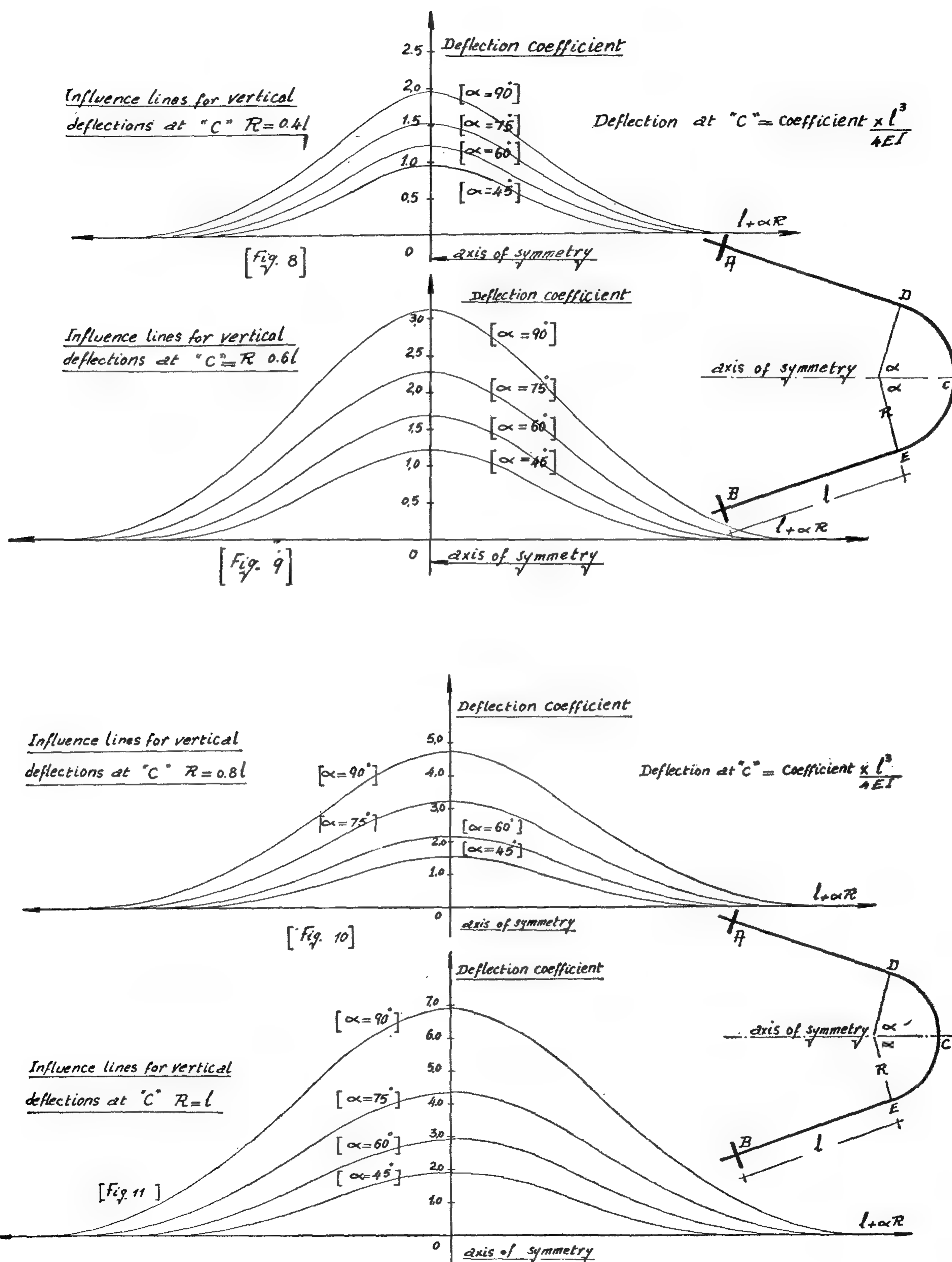


Influence lines for vertical deflections at "D" $R=0.8l$



Influence lines for vertical deflections at "D" $R=l$





where T_c & Q_c are given in (14 — a — b) respectively. The deflection at any point "n" on the curved part CD is attained as :

$EI \delta = \text{equation (13)} + \text{equation (15)}$ while the deflection at any point on the curved part CE is given by the difference of these equations respectively.

Influence lines for deflection :

Equations adopted in the previous two cases, enable the evaluation of the influence lines coefficients of vertical deflections at different sections of the bow girder curved part. In order to simplify the design for some special cases, the evaluation of these influence lines can be adopted in tables or curves form. This has the advantage of saving effort and time required for application of the corresponding equations directly.

The deflections, being dependant on the shape of the bow girder section, the deflection at a point can have a group of influence lines for the same girder, depending on the ratio corresponding to the section shape.

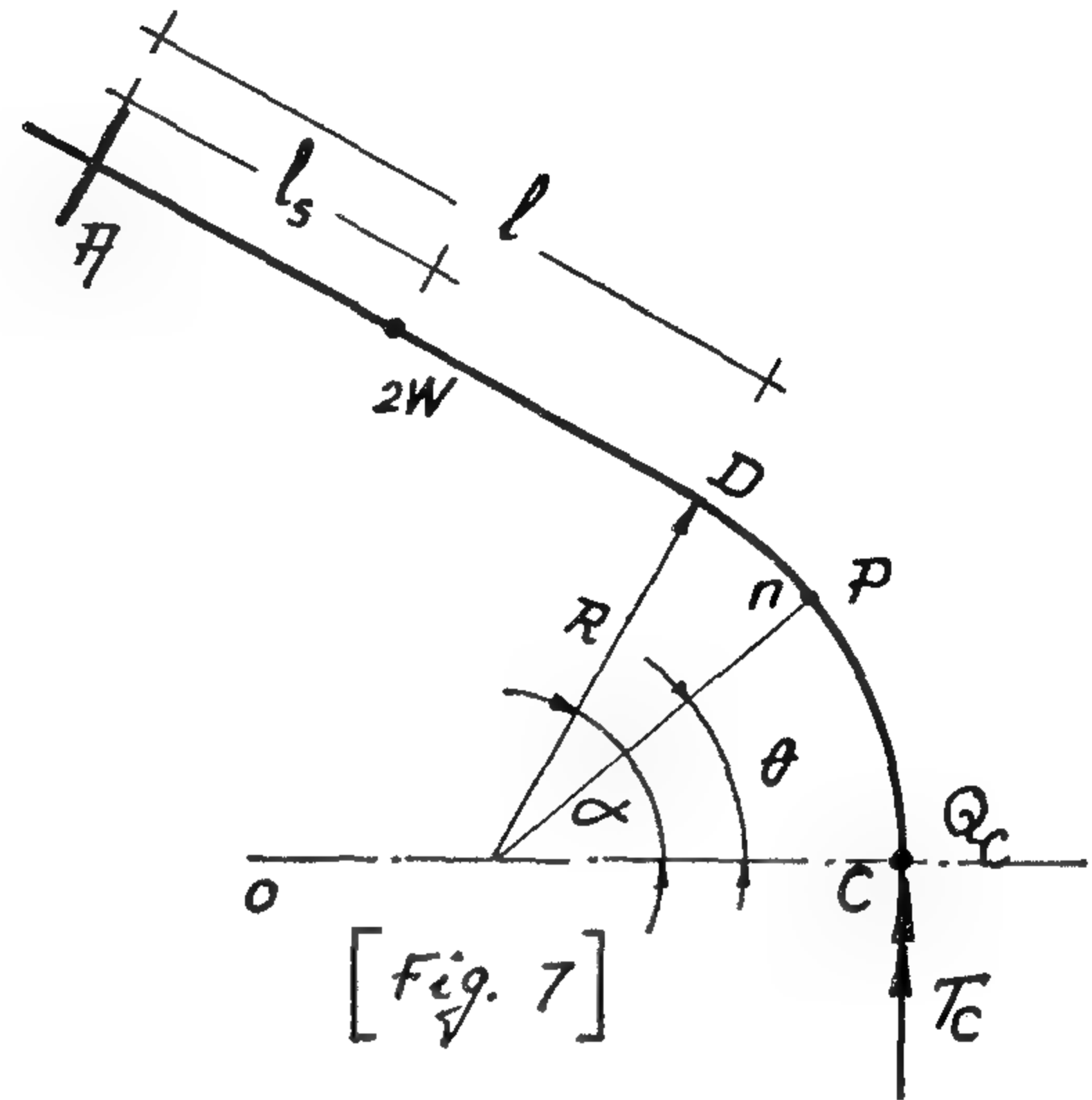
In figures (8, 9, 10 and 11) the influence lines for the vertical deflections at mid point "C" are given for girders of rectangular sections of sides ratio $\frac{b}{d}$

In figures (1, 13, 14 and 15) the influence lines for the vertical deflection at point of connection of the straight part 1 to that of the circular part (of radius R) "D" are given. The influence lines are given for different ratios of $\frac{R}{L}$ and different subtended angles 2α .

Regarding (fig. 7), where T_c and Q_c are introduced at section C, and applying moreover, an imaginary load P acting downwards at an angular distance (θ) from OC, then the bending moment and twisting moment at any section on the circular part and at any section on the straight part of the cantilever can be estimated. The deflection of this point

vertically will be given by : $\frac{\partial U}{\partial p}$, where U is the strain energy of the beam.

Forming equation (3) by integrating and equating $P = 0$ the deflection δ is given by :



$$\delta = \frac{1}{EI} \int M \frac{\partial M}{\partial P} ds + \frac{1}{GJ} \int T \frac{\partial T}{\partial P} ds.$$

The deflection δ is given in the form:

$$\begin{aligned} EI = & (T_c - Q_c R) \left[R^2 \left(\frac{\gamma - 1}{4} \right) \left\{ \sin (2\alpha - \theta) \right. \right. \\ & \left. \left. - \sin \theta \right\} + R^2 \left\{ \frac{(1 + \gamma)}{2} (\alpha - \theta) \cdot \cos \theta + \right. \right. \\ & \left. \left. (\sin \theta - \sin \alpha) \right\} + l_s \sin \alpha \left\{ R \sin (\alpha - \theta) \right. \right. \\ & \left. \left. + \frac{1}{2} l \right\} - \gamma R l \cos \alpha \left\{ 1 - \cos (\alpha - \theta) \right\} \right] \\ & + W l_s^2 \left\{ R \sin (\alpha - \theta) + \left(l - \frac{l_s}{3} \right) \right\} - Q_c l \\ & \left[\left\{ \frac{R}{2} l \sin (\alpha - \theta) + \frac{1}{3} l^2 \right\} + \gamma R^2 \left\{ 1 - \cos (\alpha - \theta) \right\} \right] \\ & - \gamma R^3 Q_c \left\{ (\alpha - \theta) - \sin (\alpha - \theta) \right\} \quad \dots (15) \end{aligned}$$

Applying this moment as shown in (fig. 6), to find the deflection at any point on the curved part at an angular distance θ from OC, a load P is imagined act down ward at the same point. The deflection of this point vertically will be given by : $\frac{\delta U}{\delta P}$, where U is the strain energy of the beam.

Forming equ. (3) by integrating, and equating P=0 the deflection δ is given by :

$$\begin{aligned} EI.\delta = & M_c \left[(\gamma - 1) \frac{R^2}{4} \left\{ \cos(2\alpha - \theta) - \cos \theta \right\} - R^2 \left\{ (1 + \gamma)(\alpha - \theta) \right. \right. \\ & \left. \left. + \frac{\sin \theta}{2} - \gamma (\cos \theta - \cos \alpha) \right\} + \right. \\ & \left. + l_s \sin \alpha \left\{ 1 - \cos(\alpha - \theta) \right\} + \right. \\ & \left. + l \cos \alpha \left\{ R \sin(\alpha - \theta) + \frac{1}{2} l \right\} \right. \\ & \left. + 2W l_s \left\{ \frac{R}{2} l_s \sin(\alpha - \theta) + \right. \right. \\ & \left. \left. \frac{l_s}{2} \left(l - \frac{l_s}{3} \right) \right\} \right] \dots\dots\dots (13) \end{aligned}$$

For the anti-symmetrical of loading, (fig. 5c) the two unknown statically indeterminate redandants, namely T_c and Q_c are given as:

$$T_c = W \left[\frac{D_1 B_2 + D_2 B_1}{A_1 B_2 - B_1 A_2} \right] \dots\dots\dots (14.a)$$

$$Q_c = W \left[\frac{D_1 A_2 + D_2 A_1}{B_1 A_2 - B_2 A_1} \right] \dots\dots\dots (14.b)$$

$$\text{Where. } A_1 = \frac{R}{2} \left\{ \alpha(1 + \gamma) + (\gamma - 1) \cdot \frac{\sin 2\alpha}{2} + l \left\{ 1 + (\gamma - 1) \cdot \cos^2 \alpha \right\} \right\}$$

$$\begin{aligned} B_1 = & \frac{R^2}{2} \left[\sin \alpha \left\{ \cos \alpha - \gamma \cdot (\cos \alpha - 2) - (1 + \gamma) \alpha \right\} \right. \\ & \left. - R l \left[1 - \cos \alpha \left\{ \cos \alpha + \gamma (1 - \cos \alpha) \right\} \right] - \frac{1}{2} l^2 \cdot \sin \alpha \right] \end{aligned}$$

$$D_1 = l_s^2 \cdot \sin \alpha$$

and

$$A_2 = \gamma R (R \sin \alpha + l \cos \alpha) - \frac{1}{2} l^2 \sin \alpha$$

$$\begin{aligned} B_2 = & l^2 \left(\frac{R}{2} \sin \alpha + \frac{1}{3} l \right) + \gamma R^2 \left\{ R(\alpha - \sin \alpha) \right. \\ & \left. + l (1 - \cos \alpha) \right\} \end{aligned}$$

$$D_2 = l_s^2 \left(l - \frac{l_s}{3} \right).$$

$$\begin{aligned}
& + 2W \left[R^3 \left\{ (1 - \gamma) \frac{\cos(\theta + \phi)}{4} (\sin 2\theta - \sin 2\alpha) \right. \right. \\
& + (1 - \gamma) \frac{\sin(\theta + \phi)}{4} (\cos 2\alpha - \cos 2\theta) \\
& + (1 + \gamma) \frac{(\alpha - \theta)^2}{2} \cos(\theta - \phi) \left. \right\} + \gamma R^3 \\
& (\alpha - \theta) - \sin(\alpha - \theta) - \sin(\alpha - \phi) + \sin(\theta - \phi) \left\{ \right. \\
& + R \ell \sin(\alpha - \phi) \left\{ \frac{1}{2} \ell + R \sin(\alpha - \theta) \right\} + \ell^2 \\
& \left. \left\{ \frac{R}{2} \sin(\alpha - \theta) + \frac{1}{3} \ell \right\} + \gamma R^2 \ell \left\{ 1 - \cos(\alpha - \phi) \right\} \right. \\
& \left. \left\{ 1 - \cos(\alpha - \phi) \right\} \right] - \gamma Q_c R^3 \cdot \left\{ (\alpha - \theta) - \sin(\alpha - \theta) \right\} \dots \dots \dots (8)
\end{aligned}$$

By superposition of the results obtained of these two cases, the deflection in point "n" of the totally fixed bow girder (Fig. 2a) under a concentrated load 4W, acting at an angular distance ϕ from centre line OC is found.

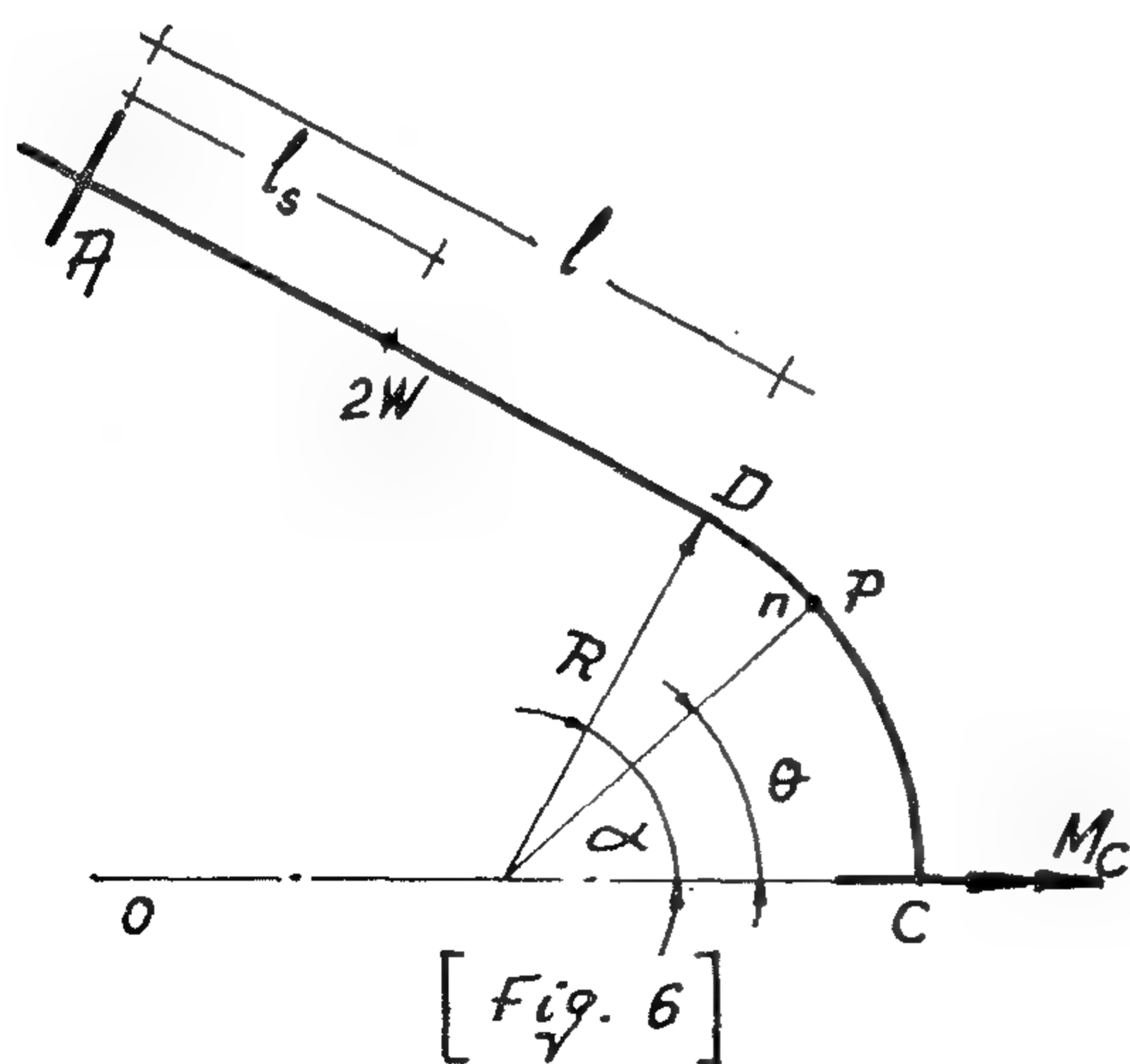
The deflection δ at any point "n" on the loaded part CD of the arc can be attained as follows.

for $\theta < \phi$
 $EI = \text{equation (4)} + \text{equation (7)} \dots (9)$

for $\theta \geq \phi$
 $\delta EI = \text{equation (5)} + \text{equation (8)} \dots \dots \dots (10)$

Similarly the deflection at any point "n" on the unloaded part CE of the arc is obtained for all values of θ as :

$\delta EI = \text{equation (4)} + \text{equation (7)} \dots \dots \dots (11)$



2. Deflection of a totally fixed circular bow girder ending with straight parts under loads acting on the straight part of the girder.

In this case, the girder, shown in (fig. 5a) is considered subjected to a concentrated load 4W at any point of the straight part AD, at a distance l_s from the fixed end A. Dividing this case in a symmetrical and anti-symmetrical case of loadings as shown in (Fig. 5b & 5c) respectively, the deflection at any point n will be the sum of the deflections at the same point in these latter two cases.

In the symmetrical case, (fig. 5b), two concentrated loads each of 2W act distances l_s from the fixed ends. As before, the only unknown statically indeterminate redant, if being considered as M_c at centre section C is given by:

$$M_c = - \frac{4W \int_s^2 \cdot \cos}{2R \left\{ \alpha(1 + \gamma) + (1 - \gamma) \cdot \frac{\sin 2\alpha}{2} + 4 \ell \left\{ 1 + (\gamma - 1) \cdot \sin^2 \alpha \right\} \right\}} \quad (12)$$

any section on the circular part or on the straight part can be estimated.

Applying equation (3), integrating and equating $P - \theta$, the deflection at any point at an angular distance θ from OC can be derived in the forms:

For $\theta < \phi$

$$\begin{aligned} \delta EI &= EI \frac{\partial U}{\partial P} \\ &= (T_c - Q_c R) \left[R^2 \left\{ (1 - \gamma) \cdot \frac{\sin \theta}{4} \cdot (\cos 2\alpha - \cos 2\theta) \right. \right. \\ &\quad \left. \left. + (1 + \gamma) \cdot (\alpha - \theta) \cdot \frac{\cos \theta}{2} + (\gamma - 1) \cdot \frac{\cos \theta}{4} \right. \right. \\ &\quad \left. \left. (\sin 2\alpha - \sin 2\theta) - \gamma (\sin \alpha - \sin \theta) \right\} + l \cdot \sin \alpha \cdot \right. \\ &\quad \left. \left\{ R \cdot \sin (\alpha - \theta) + \frac{1}{2} l \right\} - \gamma l R \cos \alpha \left\{ 1 - \cos (\alpha - \theta) \right\} \right] \\ &\quad - Q_c l \left[R \cdot \frac{1}{2} l \cdot \sin (\alpha - \theta) + \frac{1}{3} l^2 + \gamma R^2 \left\{ 1 - \cos \right. \right. \\ &\quad \left. \left. (\alpha - \theta) \right\} \right] + 2W \left[R^3 \left\{ (1 - \gamma) \cdot \frac{\cos (\phi + \theta)}{4} \cdot \right. \right. \\ &\quad \left. \left. (\sin 2\phi - \sin 2\alpha) + (1 - \gamma) \cdot \frac{\sin (\phi + \theta)}{4} \cdot \right. \right. \\ &\quad \left. \left. (\cos 2\alpha - \cos 2\phi) + (1 + \gamma) \cdot \frac{(\alpha - \phi)}{2} \cdot \cos (\phi - \theta) \right\} \right. \\ &\quad \left. + \gamma R^3 \left\{ (\alpha - \phi) - \sin (\alpha - \phi) + \sin (\phi - \alpha) \right. \right. \\ &\quad \left. \left. - \sin (\alpha - \phi) \right\} + R l \cdot \sin (\alpha - \phi) \left\{ \frac{1}{2} l + \right. \right. \\ &\quad \left. \left. + R \sin (\alpha - \theta) \right\} + l^2 \left\{ \frac{R}{2} \sin (\alpha - \theta) + \frac{1}{3} l \right\} \right. \\ &\quad \left. + \gamma R^2 \cdot l \left\{ 1 - \cos (\alpha - \phi) \right\} \times \left\{ 1 - \cos (\alpha - \theta) \right\} \right] \\ &\quad - \gamma Q_c R^3 \left\{ (\alpha - \theta) - \sin (\alpha - \theta) \right\} \dots \dots (7) \end{aligned}$$

Where T_c and Q_c are given in equation (6), and for $\theta > \phi$:

$$\begin{aligned} \delta EI &= EI \frac{\partial U}{\partial P} \\ &= (T_c - Q_c R) \left[R^2 \left\{ (1 - \gamma) \frac{\sin \theta}{4} (\cos 2\alpha - \cos 2\theta) \right. \right. \\ &\quad \left. \left. + (1 + \gamma) \cdot (\alpha - \theta) \frac{\cos \theta}{2} + (\gamma - 1) \cdot \frac{\cos \theta}{4} \right. \right. \\ &\quad \left. \left. (\sin 2\alpha - \sin 2\theta) - \gamma (\sin \alpha - \sin \theta) \right\} + \right. \\ &\quad \left. + l \cdot \sin \alpha \left\{ R \sin (\alpha - \theta) + \frac{1}{2} l \right\} - \gamma R l \cdot \right. \\ &\quad \left. \cos \alpha \left\{ 1 - \cos (\alpha - \theta) \right\} \right] - Q_c l \left[l R \frac{1}{2} \sin \cdot \right. \\ &\quad \left. (\alpha - \theta) + \frac{1}{3} l^2 + \gamma R^2 \left\{ 1 - \cos (\alpha - \theta) \right\} \right] + \end{aligned}$$

T_c and Q_c are:

$$\left. \begin{aligned} T_c &= 2W \cdot \frac{D_2 B_1 - 2D_1 B_2}{A_1 B_2 - B_1 A_2} \\ Q_c &= 2W \cdot \frac{D_2 A_1 - 2D_1 A_2}{B_1 A_2 - B_2 A_1} \end{aligned} \right\} \dots\dots\dots (6)$$

Where

$$\begin{aligned} A_1 &= R \left\{ 2\alpha \cdot (\gamma + 1) + (\gamma - 1) \cdot \sin 2\alpha \right\} + 4l \left\{ 1 + (\gamma - 1) \cos^2 \alpha \right\} \\ B_1 &= R^2 \left\{ (\gamma - 1)(2\alpha - \sin 2\alpha) - 4\gamma (\alpha - \sin \alpha) - 2l \left\{ l \sin \alpha + 2R \sin^2 \alpha - 2\gamma R \cdot \cos \alpha \cdot (1 - \cos \alpha) \right\} \right\} \\ D_1 &= R^2 \left[(\alpha - \theta) \cdot \cos \theta - \cos \alpha \cdot \sin (\alpha - \theta) - \gamma \left\{ 2 \sin \alpha - 2 \sin \theta - (\alpha - \theta) \cdot \cos \theta - \cos \alpha \cdot \sin (\alpha - \theta) \right\} \right] + l \left[2R \cdot \sin \alpha \sin (\alpha - \theta) + l \cdot \sin \alpha - 2R \gamma \cos \alpha \left\{ 1 - \cos (\alpha - \theta) \right\} \right] \end{aligned}$$

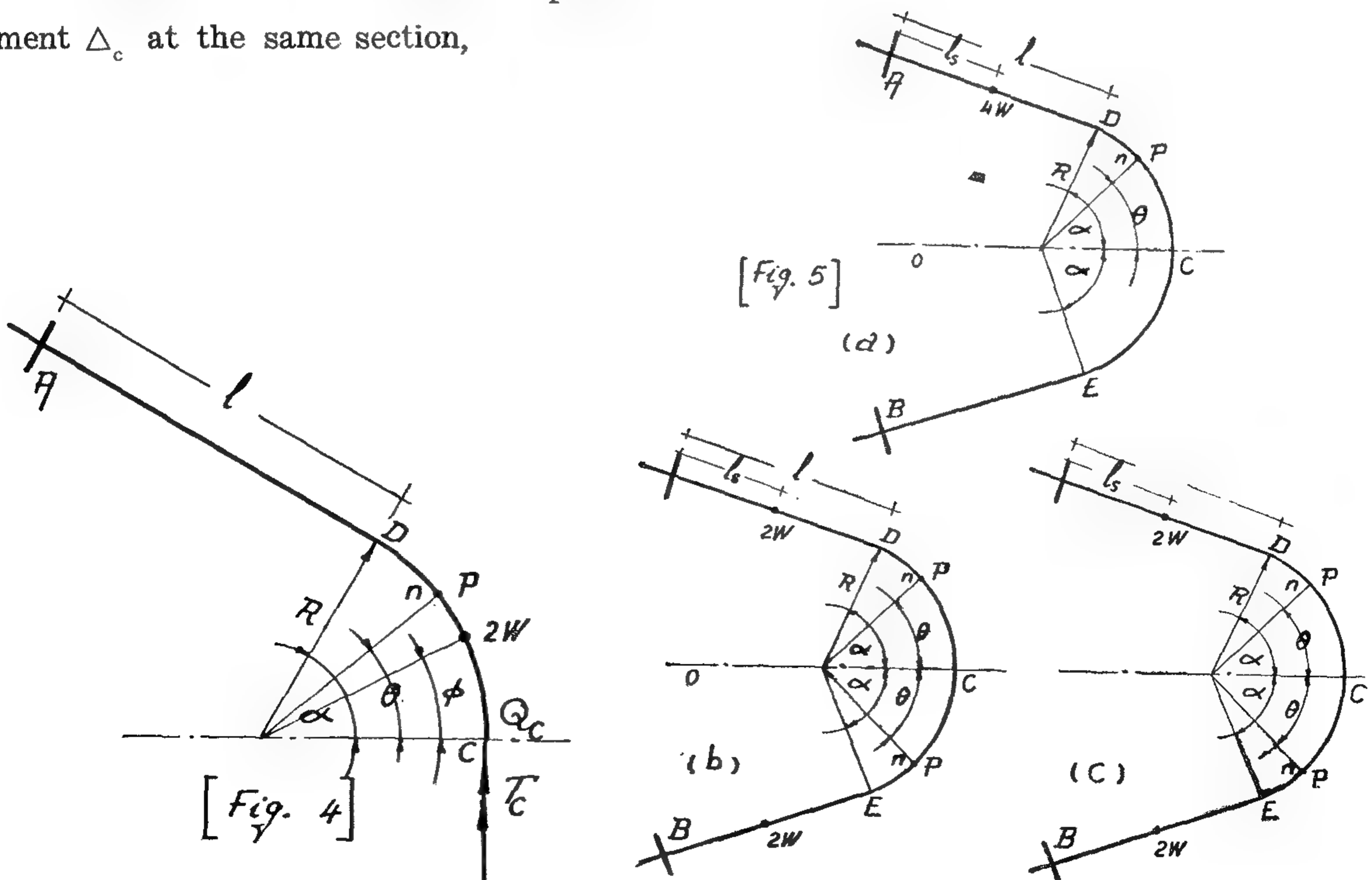
and

$$\begin{aligned} A_2 &= R \gamma \cdot \left\{ R \sin \alpha + l \cdot \cos \alpha \right\} - \frac{l^2}{2} \cdot \sin \alpha \\ B_2 &= l^2 \cdot \left(\frac{R}{2} \sin \alpha + \frac{l}{3} \right) + \gamma R^2 \cdot \left\{ R \cdot (\alpha - \sin \alpha) + l (1 - \cos \alpha) \right\} \\ D_2 &= -l^2 \left\{ \frac{1}{3} l + \frac{R}{2} \sin (\alpha - \theta) \right\} - \gamma R^2 \left[R (\alpha - \theta) - R \cdot \sin (\alpha - \theta) + l \left\{ 1 - \cos (\alpha - \theta) \right\} \right] . \end{aligned}$$

To find the deflection at any point at an angular distance θ , fig. (4), a load P is applied down wards at this point. The bending moment and twisting moment at

$$\begin{aligned}
& + \frac{1}{2} l^2 \} + \gamma l R \cdot \sin \alpha \left\{ 1 - \cos (\alpha - \theta) \right\} + \\
& + 2W \left[R^3 \cdot \left\{ (1 - \gamma) \cdot \frac{\cos (\theta + \alpha)}{4} \cdot (\sin 2\theta - \sin 2\alpha) \right. \right. \\
& + (1 - \gamma) \cdot \frac{\sin (\theta + \alpha)}{4} \cdot (\cos 2\alpha - \cos 2\theta) + \\
& + (1 + \gamma) \cdot \frac{(\alpha - \theta)}{2} \cdot \cos (\theta - \alpha) \left. \right\} + \gamma R^3 \\
& \left\{ (\alpha - \theta) - \sin (\alpha - \theta) - \sin (\alpha - \theta) + \sin \right. \\
& \left. (\theta - \alpha) \right\} + R l \cdot \sin (\alpha - \theta) \cdot \left\{ R \sin (\alpha - \theta) \right. \\
& + \frac{1}{2} l \left. \right\} + l^2 \cdot \left\{ \frac{R}{2} \cdot \sin (\alpha - \theta) + \frac{1}{3} l \right\} + \gamma R^2 l \cdot \\
& \left. \left\{ 1 - \cos (\alpha - \theta) \right\} \left\{ (1 - \cos (\alpha - \theta)) \right\} \right] \dots \dots (5)
\end{aligned}$$

In the anti-symmetrical case of loading. (as in fig. 2c) In this case, "C" will be totally free from bending moment and is only subjected to a torsional moment T_c and a shearing force Q_c . Due to condition that neither rotation γ_c at the centre section C nor vertical displacement Δ_c at the same section,



Neglecting the effect of the shearing force for its small effect, then the deflection can be represented as :

$$\begin{aligned} EI \delta &= EI \frac{\partial U}{\partial P} = \int M \frac{\partial M}{\partial P} ds \\ &+ \gamma \int T \frac{\partial T}{\partial P} ds \dots (3) \\ \text{where } \gamma &= \frac{EI}{GJ} \end{aligned}$$

The bending moment and twisting moment at any section on the circular part as well as the bending moment and the twisting moment at any section on the straight part can be estimated.

Integrating and equating $P = 0$ in equation (3), the deflection at any point at an angular distance θ from OC, due to this case of loading as in (fig. 2b) is obtained.

For points where $\theta \geq \phi$ the deflection equation will have the form :

$$\begin{aligned} \delta EI &= EI \frac{\partial U}{\partial P} \\ &= M_c \left[\frac{R^2}{4} (\gamma - 1) \{ \cos (2\alpha - \theta) \cos \theta \} - \right. \\ &\quad \left. - R^2 \cdot \left\{ (1 + \gamma) (\alpha - \theta) \cdot \frac{\sin \theta}{2} + \right. \right. \\ &\quad \left. \gamma (\cos \theta - \cos \alpha) \right\} + \cos \alpha \{ Rl \sin (\alpha - \theta) \\ &\quad \left. + \frac{1}{2} l^2 \right\} + l \gamma R \sin \alpha \{ 1 - \cos (\alpha - \theta) \} \Big] + \\ &\quad + 2W \left[R^3 \left\{ (1 + \gamma) \cdot \frac{\cos (\phi + \theta)}{4} \cdot \right. \right. \\ &\quad \left. (\sin 2\phi - \sin 2\alpha) + (1 - \gamma) \cdot \frac{\sin (\phi + \theta)}{4} \right. \\ &\quad \left. (\cos 2\alpha - \cos 2\phi) + (1 + \gamma) \frac{(\alpha - \phi)}{2} \cdot \right. \\ &\quad \left. \cos (\phi - \theta) \right\} + \gamma R^3 \left\{ (\alpha - \phi) - \sin \right. \\ &\quad \left. (\alpha - \phi) + \sin (\phi - \alpha) - \sin (\alpha - \phi) \right\} \\ &\quad \left. + Rl \sin (\alpha - \phi) \cdot \left\{ R \sin (\alpha - \theta) + \frac{1}{2} l \right\} \right. \\ &\quad \left. + l^2 \cdot \left\{ \frac{R}{2} \sin (\alpha - \theta) + \frac{1}{3} l \right\} + \gamma R^2 l \cdot \right. \\ &\quad \left. \left\{ 1 - \cos (\alpha - \phi) \right\} \left\{ 1 - \cos (\alpha - \theta) \right\} \right] \dots (4) \end{aligned}$$

While for sections at $\theta > \phi$ the deflection equation can be attained in the form:

$$\begin{aligned} \delta EI &= EI \frac{\partial U}{\partial P} \\ &= M_c \left[\frac{R^2}{4} (\gamma - 1) \cdot \left\{ \cos (2\alpha - \theta) - \cos \theta \right\} \right. \\ &\quad \left. - R^2 \left\{ (1 + \gamma) (\alpha - \theta) \cdot \frac{\sin \theta}{2} + \gamma (\cos \theta \right. \right. \\ &\quad \left. \left. - \cos \alpha) + \cos \alpha \left\{ l R \sin (\alpha - \theta) + \right. \right. \right. \end{aligned}$$

satisfying the condition that no rotation θ_c can happen at the centre section "C" in plan of action of M_c , this can be given as:

$$M_c = -4W \left[R^2 \left\{ (1 - \gamma) \cdot \sin \alpha \cdot \sin (\alpha - \phi) - (1 + \gamma) (\alpha - \phi) \cdot \sin \phi + \gamma (2 \cos \phi - 2 \cos \alpha) \right\} + 2l R \cos \alpha \cdot \sin (\alpha - \phi) + l^2 \cos \alpha + 2 \gamma R l \sin \alpha \left\{ (1 - \cos (\alpha - \phi)) \right\} \right] \\ + R \left\{ (1 - \gamma) \cdot \sin 2\alpha + 2\alpha(1 + \gamma) \right\} + 4l \left\{ 1 - (1 - \gamma) \cdot \sin^2 \alpha \right\} \dots \dots \dots (2)$$

in which $\gamma = \frac{E I}{G J}$ where E = modulus of elasticity

$$G = \text{shear modulus} = \frac{E}{2(1 + \nu)}$$

$$= \frac{E}{2.333} \text{ for reinforced concrete with poissons ratio}$$

$$\nu = \frac{1}{6}$$

I = moment of Inertia of the bow girder section about

its C.G. axis.

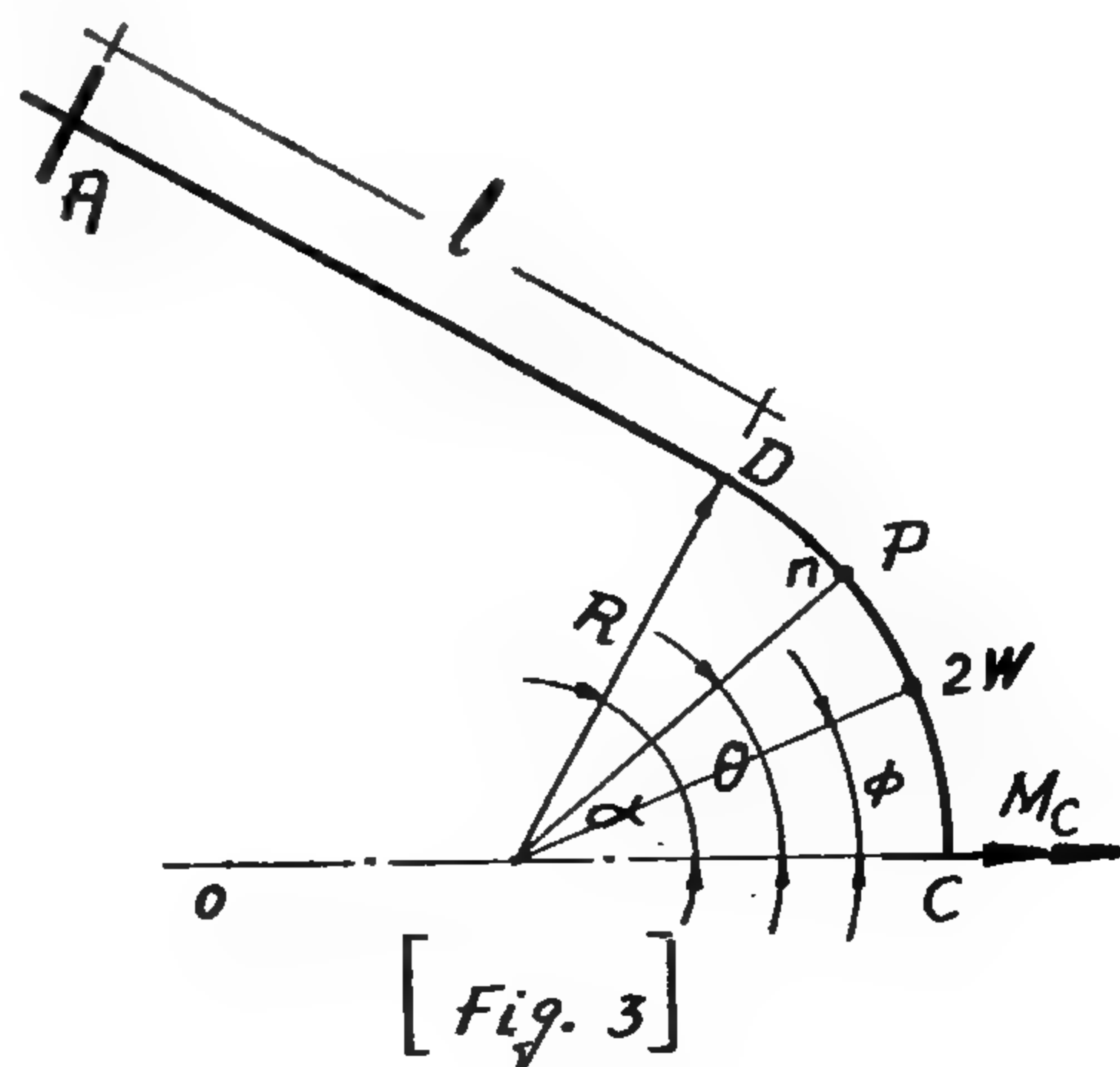
and \bar{J} = modified torsional second moment of Inertia for a rectangular section of area $A = b.d$ according to St. Venant's known formula = $\frac{A^4}{40 J}$

in which J = polar second moment of inertia =

$$\frac{bd^3 + db^3}{12}$$

Regarding (Fig. 3) to find the deflection δ due to this case at any point at a distance ϕ from axis OC an imaginary load P is assumed acting downwards at this point. The deflection is given by :

$\delta = \frac{du}{dp}$ where U is the strain energy of the beam.



the sum is equated to zero. Thus if, δ_{c_0} = deflection at support "C" due to the loading of the main system and

$\delta_{c1}, \delta_{c2}, \delta_{c3}, \dots, \delta_{c(n-1)}$ and δ_{cn} are the

deflections at the support "C" due to a unit vertical load at supports 1, 2, 3, 4 (n - 1) and n respectively then,

$$\delta_{c0} + x_1 \cdot \delta_{c1} + x_2 \cdot \delta_{c2} + x_3 \cdot \delta_{c3} + \dots + x_{(n-1)} \cdot \delta_{c(n-1)} + x_n \cdot \delta_{cn} = 0 \dots \dots \dots (1)$$

where $x_1, x_2, x_3, \dots, x_{n-1}$ and x_n are the values of the reactions at supports 1, 2, 3, (n - 1) and "n" respectively.

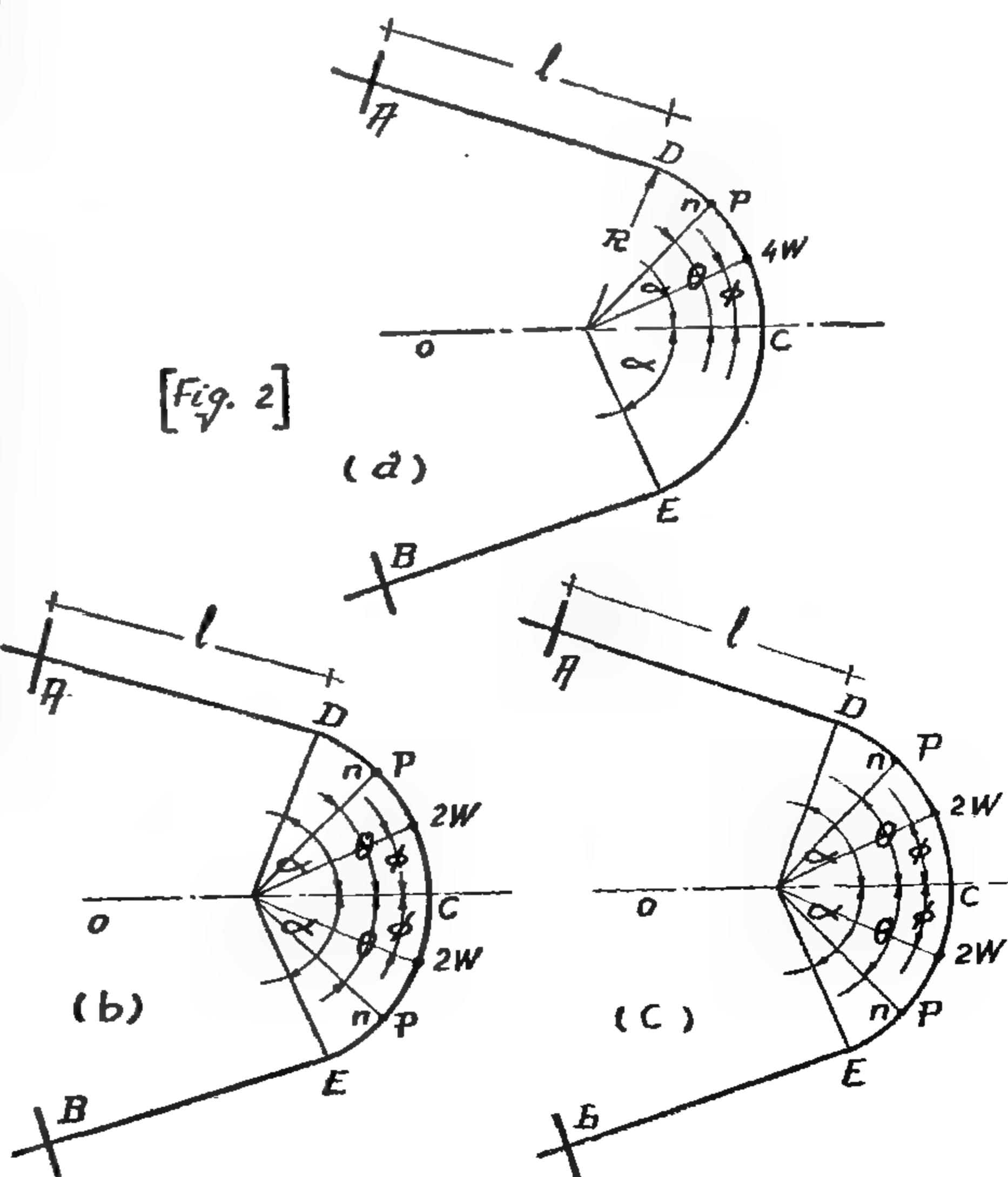
Hence "n" equations containing "n" unknowns, namely $x_1, x_2, x_3, \dots, x_{n-1}$ and x_n are obtained, the unknowns are determined by the simultaneous solution of these equations.

It is thus essential to find the equations for the deflection of the main system under different cases of loadings. In the following this is covered by the discussion of the next two cases, out of which, also influence lines for the deflection can be evaluated.

1. Deflection of a totally fixed circular bow girder ending with straight parts under loads acting on the circular part of the girder:

Fig. 2a. shows such a girder in which the circular part subtending an angle 2α at the centre and carrying a single load $4W$ on any point of the circular part, at an angular distance ϕ from the mid point "C". It is convenient for the solution to replace this case of loading by the superposition of a symmetrical and anti-symmetrical equivalent system of loadings as shown in fig. (2b and 2c).

In the symmetrical case, fig. (2b), due to symmetry, the statically indeterminate unknowns reduce simply to a bending moment M_c at mid section C. Considering the bending moment of positive sign if it tends to convex the beam upward, and



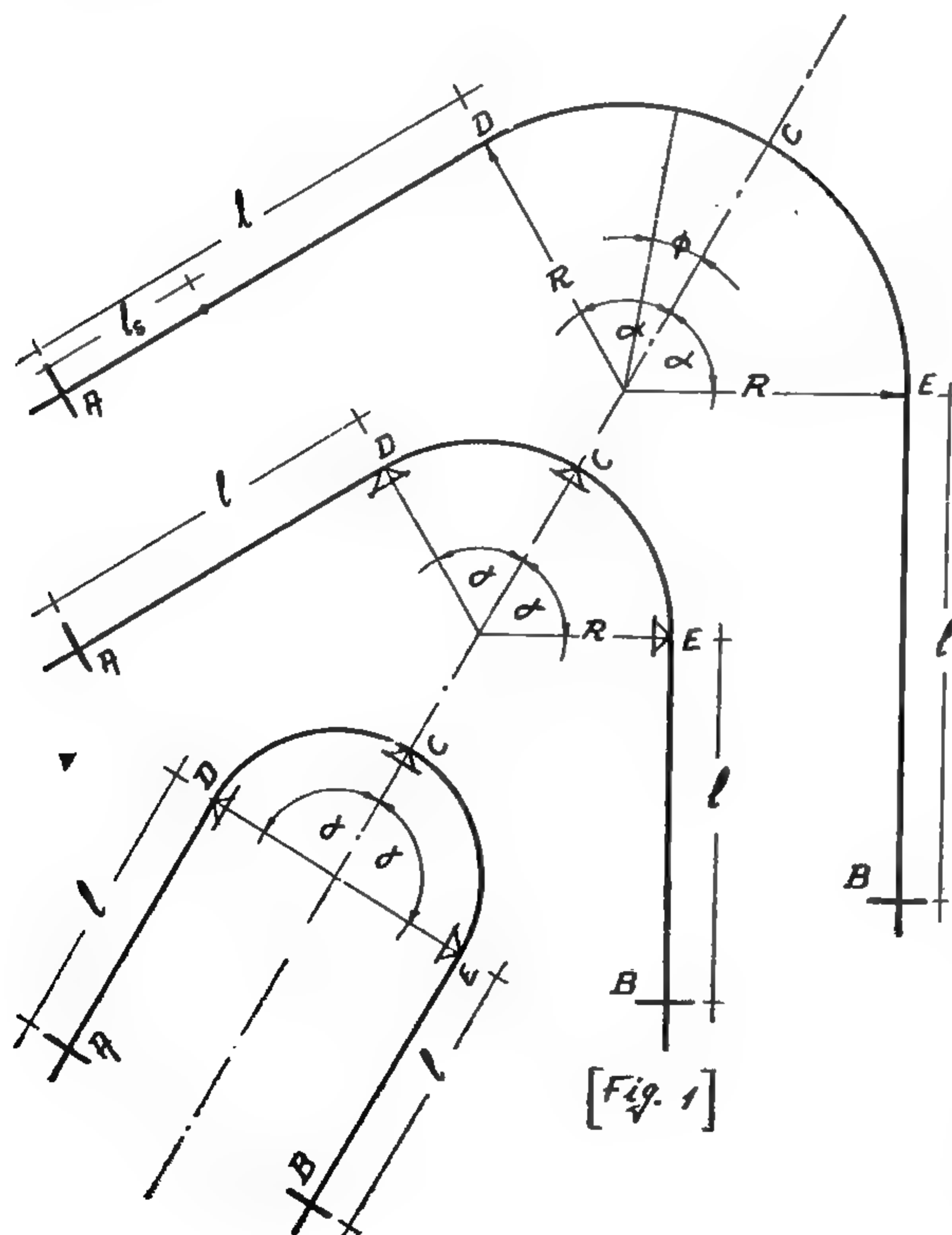
CONTRIBUTION TO BOW GIRDERS WITH INTERMEDIATE SUPPORTS

By

Professor Dr. Sc. Techn. **M.M. EL-HASHIMY ***

and Dr.-Ing. **ABDALLA S. MAHDY ****

The aim of this paper is to give the method of solution of bow girder, curved in plane and having two tangential straight parts fixed at their far ends, when intermediate supports are introduced. These intermediate supports, are assumed only capable of restraining deflections normal to the plane of the girder, but unable to prevent any rotation of the beam either in its radial or tangential directions.



A bow girder fixed at both ends with "n" intermediate supports fig. (1) is $(n + 3)$ times statically indeterminate. If the intermediate supports are relieved, the girder will be just a totally fixed bow beam, three times statically indeterminate which was dealt with previously by the writers of this paper***. The straining actions in this system, namely bending moments M , torsional moment T and shearing forces Q . An analysis was made by superposition, by applying the loading in both a symmetrical and anti-symmetrical equivalent systems. The straining actions in this system can thus be determined according to their corresponding equations, and frequently also with the aid of the relative evaluated curves and tables.

The procedure for solving the problem, fig. (1) is to consider the reactions of the supports as redundants. To find out the values of these redundants, the deflections at each intermediate support due to the loading as well as due to the loading as well as due to the redundants, are calculated and

* Prof. of Reinforced Concrete Ain Shams University.

** Lecturer of Reinforced Concrete EL AZHAR UNIVERSITY.

*** El-Hashimy, M. & Mahdy, A.-Circular Bow girders tangential to two straight parts & fixed at their far ends, The proceeding of the Engineering societies, October 1964.

BUILDING & CONSTRUCTION

**INSTITUTION OF IRRIGATION ENGINEERS
INSTITUTION OF ARCHITECTS
INSTITUTION OF CIVIL ENGINEERS**

التصنيع والانتاج

جمعية المهندسين الكهربائيين
والإلكترونيين
جمعية الهندسة الإدارية
جمعية المهندسين الميكانيكيين

ان التطور الحديث في التكنولوجيا يستلزم الاستعانة بطريقة المنظومات لعلاج المشاكل وللتخطيط والتنظيم والرقابة للمجالات الواسعة والمتشعبة . وهذا التطور نفسه ساهم في تسهيل الاستفادة من هذا الاسلوب المتكامل وذلك من خلال تطوير الامكانيات المستخدمة لها سواء اكانت آلية أو نظريات علمية .

كما ان نجاح استخدام هذا الاسلوب يتوقف على مدى كفاءة تصميم وتشغيل المنظومات وما تحتويه من خصائص ومزايا مثل البساطة والوضوح والرونة والدقة والاقتصاد . وكذلك مدى ادراك أهمية استخدام هذا الأسلوب وقبول تطبيقه .

مهندس عبد الملك محمد العصفوري
جمعية الهندسة الادارية

من حيث الصلاحية والضبط ، ووجود طلب على العمل الذي يؤديه ووضوح التعليمات الصادرة اليه . . الخ . كل ذلك يتوقف على عوامل خارجية ترتبط بالسوق واللوائح والسياسات السائدة في الدولة ، وعلى أنشطة أخرى داخلية مثل التخطيط والتخزين والصيانة . . وغيرها ، كما يتوقف أيضا على كفاءة الإدارة والتنظيم وعلى العلاقات الانسانية المحيطة بالعمل .

وما يقال عن عمل الفرد في جهة ما ، يسرى على عمل الجهات والقطاعات نفسها ، حيث يؤثر نشاطها ويتأثر بأنشطة الجهات والقطاعات الأخرى ، وبالظروف واللوائح المحيطة بها . ويتوقف عملها على عوامل تتحكم فيها وأخرى خارجة عن نطاق نفوذها وذلك نتيجة لارتباطها بأهداف تلك الجهة بالأهداف العامة للمجتمع المحيط بها . ومن ثم تأثرها بظروفه المالية والسياسية والاجتماعية، وباللوائح والقوانين السائدة فيه وبالسياسات العامة المرتبطة بالاستيراد والتصدير والتمويل والضرائب والقوى العاملة . . الخ .

ولذلك فان معالجة أى ضعف في انتاجية عمل ما ، لا يمكن أن يقتصر على مجرد دراسته وتبسيطه واعادة تنظيمه ، وعلى محاولة وضع نظام لربط الأجر بالانتاج بل لا بد من اعتباره جزءا من شبكة متكاملة من الأعمال التي تتباين في مضمونها وفي تخصصها وفاعليتها ، وان كانت وظائفها ترتبط بعضها ببعض وتتفاعل مع بعضها البعض من أجل تحقيق الهدف العام في الجهة التي بها هذا العمل .

ثانيا - مفهوم المنظومات كمدخل لأساليب العمل :
تعرف المنظومة System بأنها مجموعة متكاملة من عناصر مختلفة ترتبط بشكل معين من أجل تحقيق هدف محدد . وتتحدد خصائص المنظومة من طريقة تركيبها واسلوب

استخدام مفهوم المنظومات في الإدارة

للدكتورة أمينة الحفنى

أولا - مقدمة :

يؤدي التطور السريع في التكنولوجيا وما يتبعه من توسع في استخدام الآلات ، ومن تعدد في التخصصات الى التزايد المستمر في أحجام المشروعات والخدمات والى تشعب الأعمال وتعقد وتباين مجالات الأنشطة الداخلة فيها ، ثم تشابكها وتداخل وظائفها أثناء تحقيق أهدافها العامة ، مما يزيد في صعوبة وتعقيد تخطيطها وتنظيمها ورقابتها كما انه لم يعد من السهل حل المشاكل ومعالجة العيوب التي تظهر خلال العمل .

فعمل الشخص في أى مكان يرتبط بعمل غيره سواء اكان ذلك بطريق مباشر أو غير مباشر . فحصول الشخص على مستلزمات العمل من المواد بالكميات والجودة المطلوبتين لها ، وفي الوقت المحدد، ووجود المعدات التي يستخدمها في حالة جيدة

للانتهاء منه ، ومن حيث الاعتمادية المطلوبة لها .

٢ - حصر العناصر المكونة للمنظومة الرئيسية ، وتجميع المنظومات المتفرعة عنها ، ودراسة تكوين ووظيفة كل منها واهدافها الجزئية وترتيبها في المنظومة الرئيسية .

٣ - دراسة العلاقات بين العناصر المكونة للمنظومة الرئيسية ، وبين المنظومات المتفرعة عنها بعضها ببعض وتجديد أية تداخلات أو تفاعلات تنم بينها أثناء تشغيل المنظومة . كذلك تحليل أهداف كل من هذه المنظومات الفرعية ، والوسائل المثلى لتحقيقها وأثر ذلك في بلوغ التقسيمات الأخرى الأهداف ، وأثره كذلك في تحقيق أهداف المنظومة الرئيسية .

٤ - محاولة ترتيب المنظومة وتجميع التقسيمات المكونة لها ، بما ينسق بينها بعضها وبعض وينظم العلاقات الزمنية والمكانية بينها ، ويوفق بين تحقيق الأداء الأمثل لكل جزء منها وبين تحقيق أهداف المنظومة الرئيسية على أحسن وجه ممكن .

٥ - التحقق من صلاحية التجميع المتوصل اليه ومن أنه الأنسب لتحقيق الأهداف المطلوبة وذلك من خلال مقارنة نتائج أداء المنظومة الرئيسية بالأهداف المرسومة لها ، ومطابقة المنظومة المتوصل اليها للمنظومة المطلوب تصميمها كلاً وتفصيلاً وذلك لتحديد أية فروق بينها وأجراء أية تعديلات لازمة .

رابعاً - التخطيط والتنظيم والرقابة من خلال مفهوم المنظومات :

ان تصوير الأنشطة بأسلوب المنظومات يتطلب ادخال تغييرات معينة عند التخطيط والتنظيم لأداء هذه الأنشطة ، وكذلك لضبط ومتابعة وتقييم نتائج هذا الأداء حتى يتمشى مع مفهوم المنظومات .

فبدلاً من أن يتم أى من عمليات التخطيط أو التنظيم أو الرقابة على أجزاء بمعزل عن الأجزاء

ترتيب وتنظيم العناصر المكونة لها بعضها الى بعض . كما تتحدد وظيفتها العامة من نوعية ووظيفة كل عنصر من العناصر المكونة لها ، ودورها في تنفيذ العمل ، والتفاعلات التي تحدث بين هذه العناصر أثناء العمل نحو تحقيق الأهداف العامة للمنظومة .

ويطبق مفهوم المنظومات في الطبيعة على مجموعات الشمس والنجوم وعلى جسم الانسان و... غيرها . كما يطبق في النواحي الاقتصادية والاجتماعية لرسم السياسات العامة المتصلة بالاستثمار والانفاق وتكوين الدخل القومي والأسعار للقطاعات التخصصية المتصلة بالصناعة والزراعة والتجارة والخدمات وغيرها ، وذلك لتحقيق أكبر استفادة من الموارد المستخدمة فيها . اما في المجال الحربى فيطبق في تصميم وتشغيل الأسلحة وبخاصة الالكترونية منها كالرادار والصواريخ ... الخ . وقد طبق هذا المفهوم فعلاً في استطلاع القمر والصعود اليه .

ويساعد استخدام مفهوم المنظومات في الوصول الى تحقيق أحسن استفادة ممكنة من مجموعة عناصر عند تشغيلها لبلوغ معين .. وهذه العناصر وان كانت متباينة في تكوينها ، مختلفة في طبيعة وظيفتها ، فانها مرتبطة بعضها ببعض لأداء وظيفة معينة أو لتحقيق هدف محدد . كل ذلك في اطار محيط خارجي ويشتمل على عوامل وعناصر تؤثر في هذه المنظومة وتتأثر بها .

ثالثاً - خطوات تصميم المنظومة :

لعلاج مشكلة ما من خلال مفهوم المنظومات أو التخطيط والتنظيم لتنفيذ هدف ما أو لمتابعة مدى تحقيقه وتقييم نتائج هذا التنفيذ تتبع الخطوات الآتية : -

١ - توضيح وتحديد وتعريف الأهداف الرئيسية للمنظومة المتكاملة وذلك من حيث المطلوب تحقيقه أو الوصول اليه كما ونوعاً ، ومن حيث التكاليف المفروض ان يتم العمل في حدودها ، والزمن اللازم له والموعد المحدد

التشغيل . وهذا يتطلب التأكد من دخول هذه المعلومات ضمن اطار المنظومة ومعلومات متكاملة تربط الأنشطة المختلفة بعضها ببعض والمستويات المختلفة التي تتم من خلال معالجة المنظومة الرئيسية كذلك يجب أن يكون هذا التكامل في المعلومات وثيقا بحيث يغطي جميع مجالات الأعمال والأجزاء المكونة للمنظومة الرئيسية ، وتكون في خدمتها جميعا لتحقيق أهدافها ؛ وأن تسهل تطبيق العمليات الادارية وعلاج المشاكل الجزئية وذلك من خلال ومعالجة وحفظ وتوزيع اعداد كبيرة من البيانات تطبيق مفهوم المنظومات ويساعد التطور السريع في استخدام الحاسبات الالكترونية على تجميع ومعالجة وحفظ وتوزيع اعداد كبيرة من البيانات والمعلومات بسرعات هائلة .

ولكى ينجح استخدام المنظومات المتكاملة للبيانات والمعلومات لا بد من توافر المطلوب منها على أى مستوى وفى أى مكان ، وذلك فى الموعد المحدد لها . ومن ثم تظهر أهمية نوع ثالث من المنظومات هو منظومات الاتصالات التى تنظم تسلسل وتداول المعلومات بالسرعة التى توصل الى الاستفادة المثلى لها .

أى ان استخدام مفهوم المنظومات فى أى مجال يتطلب الآتى : -

١ - ترشيد عملية تداول المعلومات وزيادة الاستفادة منها وتنسيقها فى شكل متكامل يمكن من الافادة منها لتحقيق الأهداف العامة للمنظومة الرئيسية .

٢ - تصميم وسائل الاتصالات وخطوط سير البيانات والمعلومات بين المستويات والأنشطة المختلفة بما يساعد على سرعة الافادة من هذه البيانات والمعلومات .

الأخرى المرتبطة بها والتي تتكامل أنشطتها معها كجزء من نشاط أعم لمنظومة أشمل ، فان هذه العمليات الادارية تتم على أساس المستويات الآتية:

١ - المستوى الأعلى ويركز الاهتمام على ارتباط المنظومة ككل بالمحيط الخارجى الذى تعمل فى اطاره . وفيها تعالج العلاقات والتفاعلات التى تتم بين الأهداف العامة للمنظومة وبين السياسات العامة والعوامل الخارجية وبذلك ترسم الخطوط العريضة للمطلوب تحقيقه والظروف التى يتم فيها .

٢ - المستوى الذى يعنى بالعمليات الادارية فى مجال الحصول على الموارد المادية والبشرية والامكانيات اللازمة للعمل نحو تحقيق الأهداف العامة وفيه تقسم المنظومة الرئيسية الى عدة منظومات فرعية تعالج أمثل الوسائل لحصول أحسن على الموارد والامكانيات المطلوبة لكل نشاط أو جهة أو جزء من الأجزاء المتفرعة عن الهيكل العام للمنظومة الرئيسية

٣ - المستوى الذى يعنى بتنفيذ العمل ويتكون من منظومات أصغر متفرعة عن المنظومات الفرعية السابق تكوينها ، وتعنى بتفاصيل استغلال الموارد والامكانيات وتحقيق أمثل طرق لتوزيعها ولإستخدامها فى المواقع التى يتم فيها التنفيذ .

خامسا - تكامل المعلومات والاتصالات كمتطلبات تطبيق اسلوب المنظومات :

يتوقف تصميم وتشغيل أى منظومة سواء أكانت ميكانيكية أو اقتصادية اجتماعية على نوع وكمية البيانات الممكن الحصول عليها . كما يتوقف فاعلية تشغيل المنظومة على سرعة تداول المعلومات المرتبطة بالتنفيذ وامكانية الاستفادة من هذه المعلومات فى مواجهة أى تغير أو انحراف يصادف

b) For subsequent major intervals :

$$1 - \delta_i^{(1)}(t) = \delta_i^{(1)}(t - \Delta t) + \delta_i^{(2)}(t - \Delta t) \times \Delta t + \delta_i^{(3)}(t - \Delta t) \times \frac{\Delta t^2}{2!} + \dots + \delta_i^{(n)}(t - \Delta t) \frac{(\Delta t)^{n-1}}{(n-1)!} \dots$$

$$2 - \delta_i^{(2)}(t) = \frac{P_{Mi}}{M_i} + \sum_{\substack{j=1 \\ j \neq i}}^n \frac{P_{ij}}{M_i} \sin(\delta_{ij}^{(1)} + \alpha_{ij})$$

$$3 - \delta_i^{(3)}(t) = -\frac{1}{M_i} \frac{\pi}{180} \sum_{\substack{j=1 \\ j \neq i}}^n P_{ij} \delta_{ij}^{(1)}(t) \cos(\delta_{ij}^{(1)} + \alpha_{ij})$$

$$4 - \delta_i^{(4)}(t) = -\frac{1}{M_i} \frac{\pi}{180} \sum_{\substack{j=1 \\ j \neq i}}^n \left\{ P_{ij} \delta_{ij}^{(2)}(t) \cos(\delta_{ij}(t) + \alpha_{ij}) - \right.$$

$$\left. - \frac{\pi}{180} \left[\delta_{ij}^{(1)}(t) \right]^2 P_{ij} \sin(\delta_{ij}(t) + \alpha_{ij}) \right\}$$

$$5 - \delta_i^{(5)}(t) = -\frac{1}{M_i} \frac{\pi}{180} \sum_{\substack{j=1 \\ j \neq i}}^n \left\{ P_{ij} \delta_{ij}^{(3)}(t) \cos(\delta_{ij}(t) + \alpha_{ij}) - \right.$$

$$- 3 \left(\frac{\pi}{180} \right) \delta_{ij}^{(1)}(t) \delta_{ij}^{(2)}(t) P_{ij} \sin(\delta_{ij}(t) + \alpha_{ij}) -$$

$$\left. - \left(\frac{\pi}{180} \right)^2 \left[\delta_{ij}^{(1)}(t) \right]^2 P_{ij} \cos(\delta_{ij}^{(1)} + \alpha_{ij}) \right\}$$

$$6 - \delta_i^{(6)}(t) = -\frac{1}{M_i} \frac{\pi}{180} \sum_{\substack{j=1 \\ j \neq i}}^n \left\{ -4 \frac{\pi}{180} \delta_{ij}^{(3)}(t) P_{ij} \sin(\delta_{ij}(t) + \alpha_{ij}) \delta_{ij}^{(1)}(t) \right.$$

$$+ \delta_{ij}^{(4)}(t) P_{ij} \cos(\delta_{ij}(t) + \alpha_{ij}) - 6 \left(\frac{\pi}{180} \right)^2 \left[\delta_{ij}^{(1)}(t) \right]^2 \delta_{ij}^{(2)}(t) \times$$

$$P_{ij} \cos(\delta_{ij}(t) + \alpha_{ij}) - 3 \left(\frac{\pi}{180} \right) \left[\delta_{ij}^{(2)}(t) \right]^2 P_{ij} \sin$$

$$(\delta_{ij}(t) + \alpha_{ij}) + \left(\frac{\pi}{180} \right)^3 \left[\delta_{ij}^{(1)}(t) \right]^4 P_{ij} \sin(\delta_{ij}(t) + \alpha_{ij}) \left. \right\}$$

Appendix (II)

General Expression of the Rotor Angles Derivatives

a) For the first major interval: (t=0)

$$1 - \delta_i^{(1)}(0) = 0$$

$$2 - \delta_i^{(2)}(0) = \frac{P_{Mi}}{M_i} - \sum_{\substack{j=1 \\ j \neq i}}^n \frac{P_{ij}}{M_i} \sin(\delta_{ij}(0) + \alpha_{ij})$$

$$3 - \delta_i^{(3)}(0) = 0$$

$$4 - \delta_i^{(4)}(0) = \frac{-1}{M_i} \times \frac{\pi}{180} \sum_{\substack{j=1 \\ j \neq i}}^n \left[\left\{ P_{ij} \cos(\delta_{ij}(0) + \alpha_{ij}) \right\} \delta_{ij}^{(2)}(0) \right]$$

$$5 - \delta_i^{(5)}(0) = 0$$

$$6 - \delta_i^{(6)}(0) = \frac{-\pi}{180 M_i} \left[\sum_{\substack{j=1 \\ j \neq i}}^n \left[\delta_{ij}^{(4)}(0) P_{ij} \cos(\delta_{ij}(0) + \alpha_{ij}) - \right. \right. \\ \left. \left. - 3 \frac{\pi}{180} \left| \delta_{ij}^{(2)}(0) \right|^2 \times P_{ij} \sin(\delta_{ij}(0) + \alpha_{ij}) \right] \right]$$

$$7 - \delta_i^{(7)}(0) = 0$$

$$8 - \delta_i^{(8)}(0) = \frac{-1}{M_i} \frac{\pi}{180} \sum_{\substack{j=1 \\ j \neq i}}^n \left[-15 \delta_{ij}^{(2)}(0) \delta_{ij}^{(4)}(0) \frac{\pi}{180} P_{ij} \times \right. \\ \left. \sin(\delta_{ij}(0) + \alpha_{ij}) + \delta_{ij}^{(6)}(0) P_{ij} \cos(\delta_{ij}(0) + \alpha_{ij}) \right. \\ \left. - 15 (\delta_{ij}^{(2)}(0))^3 \left(\frac{\pi}{180} \right)^2 P_{ij} \cos(\delta_{ij}(0) + \alpha_{ij}) \right]$$

b)- Flow chart of the main program used for the solution of the swing equation by Taylor's series for time intervals equal to the major time intervals

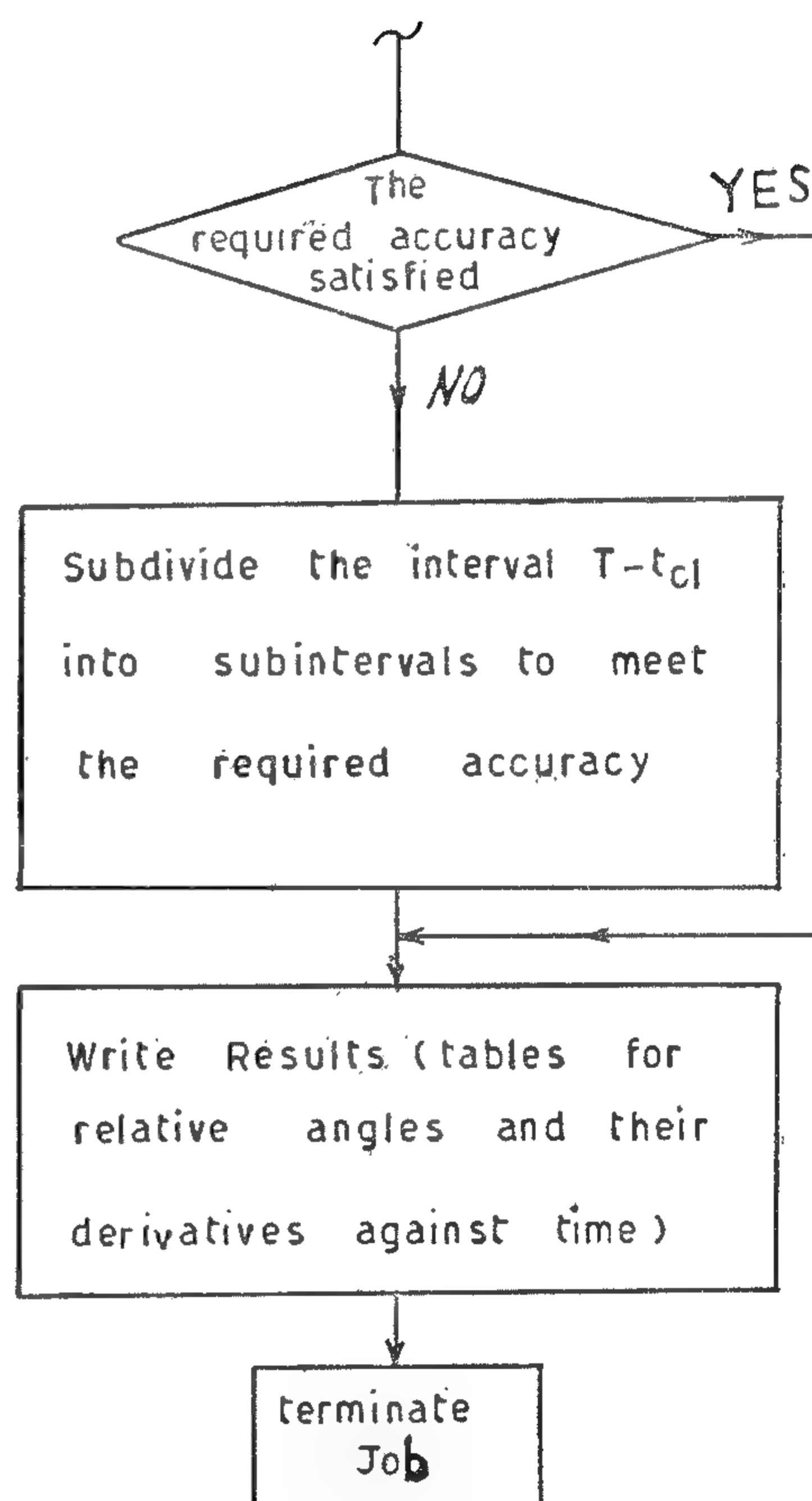
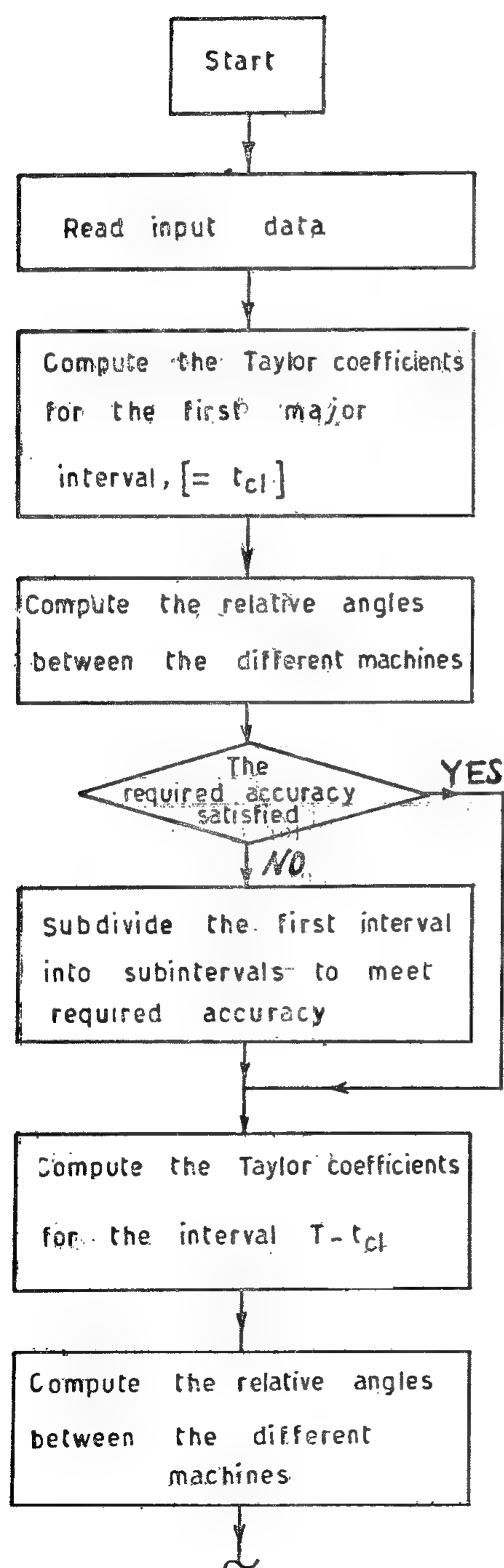


Table (II)

δ -t curve calculated by Taylor with $\epsilon = 0.001$
for major time intervals.
Computing time = 17 sec.

Tsec.	δ_{12}	δ_{23}	δ_{13}	δ_{12}	δ_{23}	δ_{13}
0.143	28.355	25.929	54.284	240.825	81.176	322.001
0.250	65.740	32.168	97.909	461.844	20.860	482.703
0.327	90.654	30.089	120.743	181.025	-64.111	116.914
0.417	91.387	22.896	114.283	-170.962	-81.346	-252.308
0.499	63.068	17.569	80.637	-518.713	-43.867	-562.580
0.564	22.250	15.923	38.173	-700.842	-7.737	-708.579
0.611	-10.402	16.045	5.642	-674.058	12.055	-662.002
0.675	-46.183	17.437	-28.686	-403.186	31.734	-371.432
0.748	-58.916	20.178	-38.738	66.063	37.245	103.307
0.819	-37.737	21.976	-15.761	507.290	6.604	513.894
0.874	-3.849	21.257	17.408	703.548	-32.513	671.036
0.938	41.419	18.351	59.770	667.519	-49.472	618.047
1.008	79.569	16.183	95.752	394.221	-2.687	391.534
1.091	96.734	19.466	116.200	25.716	79.258	104.973
1.179	82.724	27.992	110.715	-336.432	92.884	-243.547
1.250	49.866	31.988	81.853	-579.377	5.084	-574.293

CONCLUSIONS :

- 1) The results obtained by using the proposed method fits well with those given by the well known conventional methods such as the Rung-Kutta fourth order and the Euler modified.
- 2) The proposed method is advantageous in the following aspects :
 - a) The computational time required for the proposed method is less than any of the other known methods.

Table (III)

		Computing time - sec.	No. of steps	No. of major intervals
Taylor	$\epsilon = 0.01$	16	125	12
	$\epsilon = 0.005$	17		13
	$\epsilon = 0.001$	17		17
Rung - Kutta - 4		47		
Modified Euler		37		

- b) While the proposed method needs one power flow study at the beginning of each major interval, in order to calculate different derivative for that interval. The Rung-Kutta-4 and the modified Euler require more than a power flow study for each step. Taking into consideration that each major interval generally contains more than one step, it follows that the total computational time of the proposed

method will be less affected if load flow studies were carried out by iterative methods. Referring to the above example, the number of the major intervals were 12, 13 and 17 for the cases where ϵ was chosen to be 0.01, 0.005 and 0.001 respectively, while the number of steps were 125.

- c) While, there is no direct way by which the accuracy of the results obtained by using the Rung-Kutta or the modified Euler methods can be estimated [2], the accuracy of the obtained results by the suggested method can be clearly estimated, as it depends upon the chosen value of ϵ
- 3) For the case of persistent major disturbances in the power system such as a change in the loading condition or a disconnection of one or more line, the computational procedure will be highly simplified as the whole period of study may be considered as one major interval. This is due to the fact that, in spite of the higher order of the derivatives needed for a large major interval, the number of terms used in eqns. (6) is reduced, as in that case even derivatives are only present. Besides, the use of one major interval will result in a more accurate results (no accumulation of errors).

REFERENCES :

1. El-Sayed M.M. Azzouz, "New Methods for Stability Calculations of Simple Systems". Bulletin of Science and Technology — Assiut University, Vol. 6, 1963.
2. W.B. Humpage and B. Stott, "Predictor Corrector Method of Numerical Integration in Digital Computer Analysis of Power System Transient Stability". Proc. I.E.E., 1965, 112 (8) P. 1557.

TABLE (11)
The SWING CURVES FOR STEP OF 0.01 sec.

TIME	δ_{12}						δ_{23}						δ_{13}					
	TAYLOR			RUNG KUTTA-4	MODIFIED EULER		TAYLOR			RUNG KUTTA-4	MODIFIED EULER		TAYLOR			RUNG KUTTA-4	MODIFIED EULER	
	$\epsilon = 0.01$	$\epsilon = 0.005$	$\epsilon = 0.001$				$\epsilon = 0.01$	$\epsilon = 0.005$	$\epsilon = 0.001$				$\epsilon = 0.01$	$\epsilon = 0.005$	$\epsilon = 0.001$			
0	11.780	11.780	11.780	11.780	11.780		18.250	18.250	18.250	18.250	18.250		30.030	30.030	30.030	30.030	30.030	
0.05	13.737	13.737	13.736	13.736	13.735		19.412	19.417	19.413	19.413	19.417		33.149	33.149	33.149	33.149	33.152	
0.10	19.736	19.736	19.736	19.736	19.731		22.510	22.510	22.509	22.509	22.526		42.246	42.246	42.245	42.245	42.256	
0.15	30.124	30.124	30.124	30.124	30.114		26.506	26.506	26.506	26.507	26.535		56.630	56.630	56.630	56.630	56.649	
0.2	45.338	45.336	45.334	45.335	45.322		30.088	30.093	30.098	30.105	30.134		75.426	75.429	75.433	75.437	75.457	
0.25	65.767	65.753	65.741	65.741	65.735		32.087	32.130	32.164	32.167	32.183		97.855	97.883	97.906	97.907	97.918	
0.30	84.358	84.448	84.415	84.416	84.428		31.396	31.490	31.523	31.520	31.501		115.754	115.937	115.938	115.936	115.929	
0.35	93.826	93.811	93.829	93.876	93.904		28.349	28.403	28.441	28.427	28.376		122.175	122.215	122.270	122.303	122.280	
0.40	93.359	93.499	93.722	93.814	93.859		24.298	24.308	24.318	24.291	24.225		117.656	117.806	118.040	118.105	118.085	
0.45	82.682	82.957	83.459	83.643	83.702		20.455	20.397	20.382	20.358	20.305		103.138	103.354	103.841	104.001	104.008	
0.50	61.416	61.934	62.553	62.796	62.852		17.578	17.552	17.526	17.509	17.499		78.993	79.486	80.079	80.305	80.351	
0.55	30.650	31.368	32.098	32.362	32.383		16.090	16.097	16.086	16.095	16.142		46.740	47.464	48.184	48.457	48.526	
0.60	-4.282	-3.374	-2.984	-2.769	-2.807		15.875	15.916	15.940	15.974	16.066		11.593	12.536	12.956	13.205	13.259	
0.65	-35.127	-34.260	-34.386	-34.273	-34.349		16.677	16.725	16.784	16.888	16.925		-18.450	-17.536	-17.603	-17.445	-17.423	
0.70	-54.991	-53.820	-54.441	-54.387	-54.442		18.268	18.285	18.353	18.389	18.453		-36.724	-35.535	-36.087	-35.998	-35.989	
0.75	-59.467	-57.901	-58.891	-58.887	-58.872		20.238	20.186	20.253	20.269	20.278		-39.229	-37.715	-38.638	-38.619	-38.594	
0.80	-46.879	-45.416	-46.732	-46.855	-46.735		21.802	21.667	21.732	21.723	21.677		-25.077	-23.749	-25.000	-25.132	-25.058	
0.85	-19.472	-18.389	-20.173	-20.390	-20.150		21.957	21.770	21.849	21.825	21.739		2.486	3.381	1.676	1.435	1.588	
0.90	16.041	16.550	14.753	14.524	14.855		20.350	20.165	20.231	20.198	20.098		36.391	36.716	34.984	34.724	34.953	
0.95	50.908	50.802	49.326	49.105	49.438		17.870	17.778	17.778	17.746	17.675		68.778	68.579	67.104	66.851	67.113	
1.00	78.229	77.269	76.217	76.022	76.274		16.275	16.344	16.240	16.227	16.228		94.504	93.613	92.457	92.249	92.502	
1.05	94.898	92.585	92.220	92.058	92.197		16.922	17.179	16.969	16.991	17.086		111.820	109.764	109.188	109.049	109.283	
1.10	99.487	96.581	97.018	96.615	96.966		20.357	20.646	20.227	20.259	20.437		119.844	117.227	117.244	117.187	117.403	
1.15	93.773	90.253	91.239	91.224	91.191		25.341	25.279	25.084	25.112	25.329		119.114	115.532	116.323	116.337	116.521	
1.20	78.348	73.742	75.413	75.473	75.401		30.256	29.875	29.770	29.784	29.978		108.604	103.617	105.184	105.257	105.380	
1.25	53.653	48.194	50.437	50.546	50.457		32.769	31.925	32.039	32.041	32.146		86.422	80.119	82.470	82.587	82.603	

der are computed for the first major interval, while for other subsequent intervals derivatives till the 6th order were only obtained. General expressions for these derivatives are given in Appendix (2).

The transient stability study by Taylor's were done in two different ways :—

- 1) The swing curves of the different relative angles are obtained by solving the corresponding swing equations with steps of 0.01 sec. for different values of the accuracy parameter ϵ (for $\epsilon = 0.01, 0.005$ and 0.001). The obtained results are given in Table (1) where the relative angles, although computed for each 0.01 sec., are represented each 0.05 sec.
- 2) The relative angles are calculated at each major time interval only for $\epsilon = 0.001$. In this solution the reduction of the time intervals (item 3 pt V) was achieved by the formula

$$\Delta t_{\text{new}} = \frac{\Delta t}{1 + \Delta t}$$

The obtained results are given in Table (II).

It is expected that the obtained results from both ways will be similar. This can be judged out from Fig. (2), where the swing curves obtained with a step of 0.01 sec. as well as those obtained with major time intervals are represented.

For comparison purposes, the swing curves were also obtained by the two well known conventional methods of the Rung-Kutta fourth order and the modified Euler with steps of 0.01 sec., where they are given also in Table (I).

Comparison between the proposed method, the Rung-Kutta fourth order and the modified Euler, as regarding the computing time, the number of steps and the number of major time interval is given in Table (III).

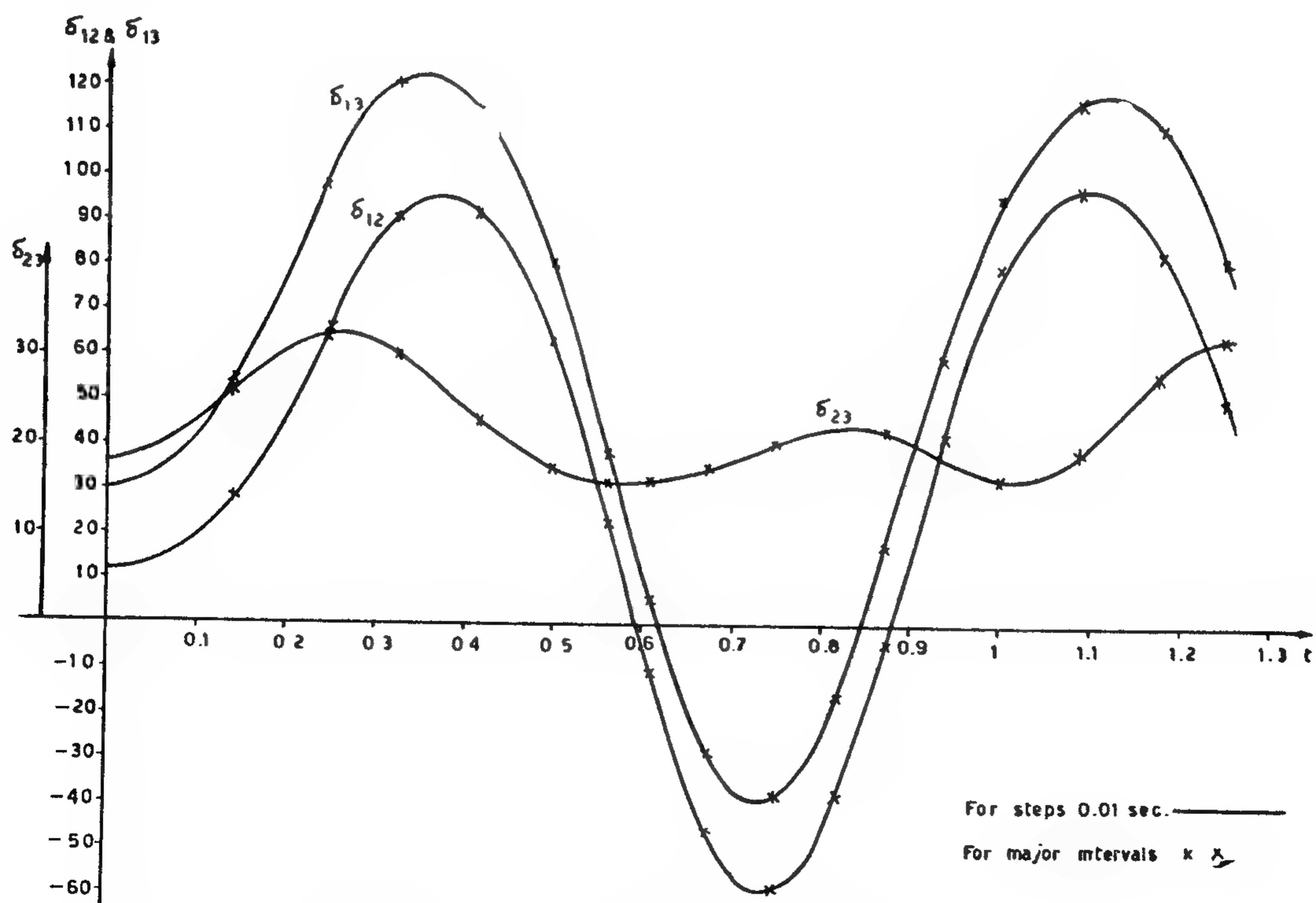


Fig. 2 - Swing curves obtained by Taylor's ($\epsilon = 0.001$)

following modifications of computational procedure given above are to be considered:

- I) The first step is the same as that given above.
- I) A time step Δt is introduced and the values of the relative angles are calculated after checking the accuracy requirements.
- III) The above procedure is repeated for time intervals of $2\Delta t$, $3\Delta t$, and so on, until the introduced time interval with the available number of derivatives does not satisfy the accuracy requirements. Suppose that, this interval is equal to $(m + 1)\Delta t$.
- IV) At the end of the m th step, new values of the derivatives are calculated and introduced for further study.
- V) Considering the end of the m th step as a new start, the processes

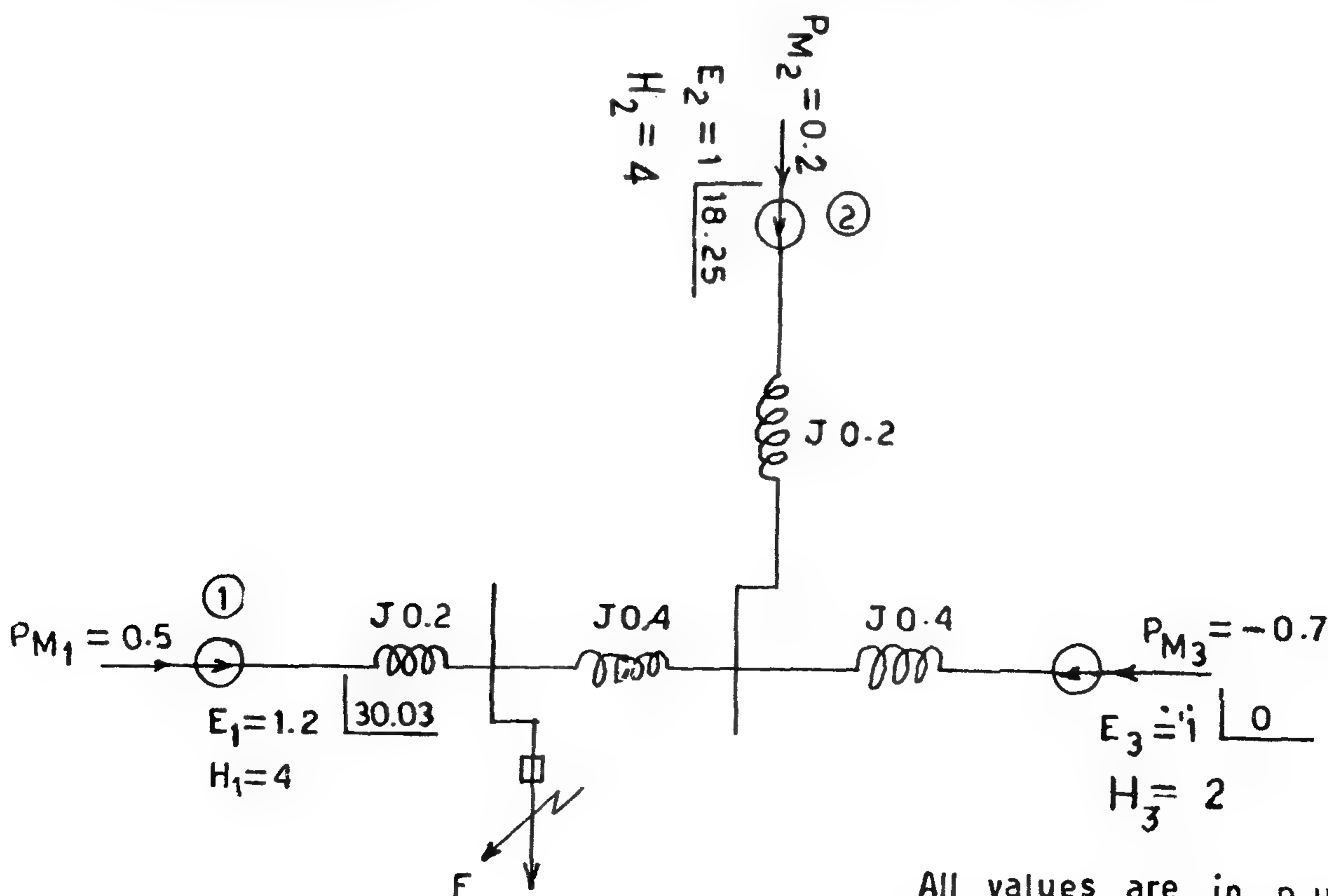
mentioned in items II, III and IV are repeated, either till the end of the period of study for persistent disturbance, or till t_{c1} for faults to be cleared.

- VI) Beginning with $t = t_{c1}$ the process is continued similarly till the end of the period of study T .

Flow chart representing the above mentioned computational procedures are given in Appendix (1). However, the corresponding computer programs (used for the solution of the illustrative example given below) are available upon request from the authors.

Illustrative Example :

In the power system shown in Fig. (1), a three phase fault taking place at point F is cleared after 0.25 sec. In order to check the stability of the above system by the proposed method (Taylor) derivatives of the relative angles till the 8th or-



All values are in p.u.

Fig. (1)

- the fault is to be cleared t_{c1} . For persistent disturbances, such as disconnection of lines, Δt is chosen to be the whole period of study T .
- III) The value of Δt is repetitively substituted in eqns. (6) where the relative angles are calculated every time with increasing number of terms. The parameter ϵ is checked every time a term is increased.
- IV) If with the available number of derivative, the given value of ϵ is reached the process is terminated and the values of the corresponding relative angles are accepted as those taking place at Δt .
- V) If with the available number of derivatives, the accuracy parameter ϵ cannot be realized, the interval Δt is to be reduced to Δt_{new} . Reduction of Δt may be achieved by any suitable formula.
- VI) The above procedure described in items III, IV, and V are repeated with Δt_{new} until an interval Δt_1 , at which the accuracy requirement could be realized, is reached. At that interval Δt_1 , the process is terminated and the corresponding relative angles are calculated. This interval is known as the first major interval.
- VII) Expressions for the derivatives of the relative angles till the n th order at time Δt_1 are to be deduced.
- VIII) A new time interval is introduced as a second step for further calculations. The second time interval is chosen equal to the difference between the preliminary introduced interval (t_{c1} or T) and the first major time interval Δt_1 , i.e. it is equal to $t_{c1} - \Delta t_1$ or $T - \Delta t_1$.
- IX) The whole previous computational procedure are repeated for the new time interval, until an interval Δt_2 , satisfying the accuracy requirements, is reached where the corresponding relative angles are calculated. Δt_2 is called the second major interval.
- X) The process is repeated by calculating the derivatives at the end of each major interval and introducing a new time interval for further calculations which is equal to the difference between the preliminary introduced time interval t_{c1} or T and the sum of all the previously obtained major time intervals. For persistent disturbances this will continue until the end of the period of study is reached. For faults to be cleared, the process is to be continued till t_{c1} where the new derivatives are computed and introduced for further calculations.
- XI) After fault clearing, the computation proceeds by the same way described above with the first time interval introduced (preliminary) $= T - t_{c1}$.
- XII) At the end of each major interval in addition to the determination of the relative angles between the machines, their first derivatives are also to be obtained.

The obtained results by the above mentioned procedure, although make it possible to judge about the system stability, it may not help in obtaining continuous $\delta - t$ curves. That is because, the different major intervals may be extremely large. In order to obtain continuous $\delta - t$ curves, each major interval is subdivided into steps, where the relative angles are calculated at the end of each step as previously described. However to avoid unnecessary accumulation of errors, the

3 — Higher Derivatives :

Any other derivative of order higher than the second may be obtained directly by successively differentiating the swing equations of the individual machines and subtracting. As an example the following higher derivatives of the individual rotor angle of the i th machine are given :

$$\delta_i^{(3)}(t) = \frac{-1}{M_i} \left[\sum_{\substack{j=1 \\ j \neq i}}^n \left\{ P_{ij} \cos(\delta_{ij}(t) + \alpha_{ij}) \right\} \delta_{ij}^{(1)}(t) \right] \frac{\pi}{180}$$

$$\delta_i^{(4)}(t) = \frac{-1}{180M_i} \sum_{\substack{j=1 \\ j \neq i}}^n \left[\left\{ P_{ij} \cos(\delta_{ij}(t) + \alpha_{ij}) \right\} \delta_{ij}^{(2)}(t) - \frac{\pi}{180} \left[\delta_{ij}^{(1)}(t) \right]^2 P_{ij} \sin(\delta_{ij}(t) + \alpha_{ij}) \right]$$

and the derivatives of the relative angles is then calculated from :

$$\delta_{ij}^{(n)}(t) = \delta_i^{(n)}(t) - \delta_j^{(n)}(t)$$

b — Determination of the Relative Angle Variation with Time

(δ_{ij} — t curve) :

After calculating the different derivatives of the relative angles, a substitution in eqns. (6), gives directly the magnitude of the relative angles at any desired time i.e. the δ — t curve. The accuracy of the obtained values of δ depends upon the number of terms used in its determination from the infinite series appearing in eqns. (6). The larger the number of terms used, the more accurate will be the obtained results. Theoretically, exact determination of δ is possible by using an infinite number of terms comprising derivatives till the infinite order. However, for practical purposes, the number of terms used is to be finite, and it may be determined as follows : —

As the series appearing in the right hand side of eqns. (6) is convergent, each angle δ is to be repetitively calcula-

ted by using successively increasing number of terms in sequence, until an addition of further term will not result in large change of the angle δ (i.e. successive approximation). For example if $\delta(n)$ and $\delta(n+1)$ are the magnitudes of the relative angle obtained by using n and $(n+1)$ terms of eqns. (6) respectively, the percentage increase due to the addition of the $(n+1)$ th term is given by :

$$\epsilon = \frac{\delta(n+1) - \delta(n)}{\delta(n+1)} \times 100$$

The use of $(n+1)$ term of eqns. (6) and hence $\delta(n+1)$ is considered acceptable, if ϵ as calculated above is lower than a given prescribed value. The choice of parameter ϵ depends upon the degree of accuracy required.

The computational procedure required for derivative calculations and determination of the number of terms to be used from eqns. (6) for a given value of ϵ together with obtaining the angles at any time t , were carried out using a computing machine. In the following item the computational procedures (Algorithm) as carried out by the computer is given.

3 — Computational Procedures :

- I) Taking the instant of disturbance occurrence to be the beginning of the time score, an expression for the derivatives of the relative angles are deduced and computed up till the n th order for $t = 0$.
- II) An interval (Δt), after which the relative angles are to be calculated, is introduced. The choice of Δt depends upon the nature of the disturbance. In case of a disturbance which is going to be cleared, such as short circuits, Δt is taken equal to the interval after which

Assuming that the synchronous machine is represented during transient performance by an e.m.f., that is maintained constant behind its transient reactance, the electrical power output P_e is given by the steady state network performance equations.

For n machine system P_e can be expressed as :

$$P_{ei} = \frac{E_i^2}{Y_{ii}} \sin \alpha_{ii} + \sum_{\substack{j=1 \\ j \neq i}}^n \frac{E_i}{E_j} \frac{1}{Y_{ij}} \sin (\delta_{ij} + \alpha_{ij}) \quad \dots (3)$$

where,

- P_{ei} — The electrical air gap power of the i th machine.
- E_i — e.m.f. of the i th machine behind its transient reactance.
- Y_{ii} — self admittance of the i th node.
- α_{ii} — The complement of the angle of the admittance Y_{ii} .
- Y_{ij} — Minus the mutual admittance between nodes i and j .
- α_{ij} — The complement of the angle of Y_{ij} .
- δ_{ij} — The relative angular displacement between machines i and j .
- and n — The number of the machines dealt with in the system.

Denoting $E_i/E_j/Y_{ij}$ by P_{ij} .

The swing equation for the i th machine may be written as :

$$\delta_i = \frac{1}{M_i} \left[P_{Mi} - \left\{ P_{ii} \sin \alpha_{ii} + \sum_{\substack{j=1 \\ j \neq i}}^n P_{ij} \sin (\delta_{ij} + \alpha_{ij}) \right\} \right] \quad \dots (4)$$

2 — The Proposed method for the Solution of the Swing Equation :

This method gives a direct relation between the angle δ and time in terms of its initial value and its derivatives (1). By means of Taylor's expansion series, the angle δ for any machine, say the i th, may be expressed as :

$$\delta_i(t+\Delta t) = \delta_i(t) + \delta_i^{(1)}(t) \Delta t + \delta_i^{(2)}(t) \frac{\Delta t^2}{2!} + \dots + \delta_i^{(n)}(t) \frac{\Delta t^n}{n!} \dots \dots \dots \quad \dots (5)$$

where $\delta_i^{(n)}$ is the n th derivative of the angle δ_i at time t and the relative angle between the i th and the j th machines is expressed as :

$$\delta_{ij}(t+\Delta t) = \delta_{ij}(t) + \delta_{ij}^{(1)}(t) \Delta t + \delta_{ij}^{(2)}(t) \frac{\Delta t^2}{2!} + \dots + \delta_{ij}^{(n)}(t) \frac{\Delta t^n}{n!} + \dots \dots \dots$$

Where $\delta_{ij}^{(n)}(t) = \delta_j^{(n)}(t) - \delta_i^{(n)}(t)$. . . (6)

The relative angles between the different machines at any time t and hence their variation with time depends upon the possibility of obtaining the derivatives encountered in eqns. (6). However, the accuracy by which the relative angles are obtained depends upon the number of terms taken into consideration from the infinite series represented by eqns. (6). Each of these two factors are studied in the following item :

a — Calculation of the Derivatives :

1 — First Derivative :

The first derivative of the angle δ_{ij} at any time t may be obtained in terms of its derivatives at any preceding instant,

$$\delta_{ij}^{(1)}(t) = \delta_{ij}^{(1)}(t-\Delta t) + \delta_{ij}^{(2)}(t-\Delta t) \Delta t + \delta_{ij}^{(3)}(t-\Delta t) \frac{\Delta t^2}{2!} + \dots + \delta_{ij}^{(n)}(t-\Delta t) \frac{\Delta t^{n-1}}{(n-1)!} + \dots$$

A special case of interest arises at the instant of the disturbance occurrence where $\delta_{ij}^{(1)}(0) = 0$.

2 — Second Derivative :

The second derivative is obtained directly from the swing eqns., i.e.

$$\delta_{ij}^{(2)}(t) = \frac{P_{Mi}}{M_i} - \frac{P_{Mj}}{M_j} - \left[\frac{P_{ii} \sin \alpha_{ii}}{M_i} - \frac{P_{ij} \sin \alpha_{ij}}{M_j} \right] - \left[\sum_{\substack{j=1 \\ j \neq i}}^n \frac{P_{ij}}{M_i} \sin (\delta_{ij}(t) + \alpha_{ij}) - \sum_{\substack{i=1 \\ i \neq j}}^n \frac{P_{ji}}{M_j} \sin (\delta_{ji}(t) + \alpha_{ji}) \right]$$

A NEW PROPOSED TECHNIQUE FOR TRANSIENT STABILITY STUDY OF MULTIMACHINE SYSTEMS

By

M.M. SALLAM* (Ph.D.), M.Z. GHONEIM**

(M.Sc., Ph.D)

M.M. EL-HINDAWI*** (B.Sc).

ABSTRACT :

The paper presents a new method for transient stability studies in multi-machine systems. In this method the relative angles between the machines are expressed by means of Taylor's expansion series. The methods used for the determination of the coefficients in the Taylor series as well as the number of terms to be used — for a given degree of accuracy — are given. The whole computational procedure is provided by using a digital computing machine. An example illustrating the transient stability of a three machine system using the proposed method, is given. The method compared with the known conventional methods for stability calculations (Rung Kutta-fourth order and Modified Euler), although giving almost the same results, is characterised by less computational time and clear error estimation.

1 — INTRODUCTION :

The capability of a power system to remain in synchronism during major disturbances, is usually checked by the character of variation of the relative angular displacements between the machines of the system with time. In order to determine the angular displacement between the machines of a power system, it is necessary to solve the differential equation describing the motion of the machine rotors. Generally the equation of

motion of the synchronous machine (swing equation) is given as : —

$$M \frac{d^2\delta}{dt^2} + K_d \frac{d\delta}{dt} = (P_M - \Delta P) - P_e \quad \dots (1)$$

where,

$M = GH/180$ f Mega—joules sec./electrical degree.

G — Machine rating in MVA.

H — Inertia constant of the machine in megawatt sec/MVA.

K_d — Damping coefficient.

P_m — Mechanical power input to the machine in MW.

ΔP_m — Change in P_m due to the governor action.

P_e — Electrical air gap power modified by the voltage regulator in MW.

δ — Electrical angular position in electrical degree of the rotor with respect to a synchronously rotating reference axis.

Neglecting the effects of the voltage regulator, the governor action and the machine damping, the swing equation is reduced to the simple form :

$$M \frac{d^2\delta}{dt^2} = P_M - P_e \quad \dots (2)$$

* Assistant Prof., Faculty of Engineering, Assiut University.

** Lecturer, Faculty of Engineering, Al-Azhar University.

*** Engineer, Electrical Eng. Lab., Al-Azhar University.

$$a_y \frac{\sin \theta_i}{n_e(\theta)} + a_z \sqrt{1 - \frac{\sin^2 \theta_i}{n_e^2(\theta)}} = \cos \theta \quad (\text{A-3})$$

Defining, $y = \tan^2 \theta$, (A-4)

$$q_1 \triangleq \frac{1}{n_o^2} \quad (\text{A-5})$$

$$q_2 \triangleq \frac{1}{n_e^2} \quad (\text{A-6})$$

$$q_3 \triangleq 1 - \frac{\sin^2 \theta_i}{n_o^2} \quad (\text{A-7})$$

$$q_4 \triangleq 1 - \frac{\sin^2 \theta_i}{n_e^2} \quad (\text{A-8})$$

Using (34) and (A-4) to (A-8), equation (A-3) reduces to

$$(a_y \sin \theta_i) \sqrt{q_1 + q_2 y} + a_z \sqrt{q_3 + q_4 y} = 1 \quad (\text{A-9})$$

Condensing this expression once more we define

$$q_3 + q_4 y \triangleq Q^2 \quad (\text{A-10})$$

Substituting in (A-9), we get

$$a_y \sin \theta_i \sqrt{(q_1 - \frac{q_2 q_3}{q_4}) + \frac{q_2}{q_4} Q^2} = 1 - a_z Q \quad (\text{A-11})$$

Defining

$$P_1 \triangleq \frac{q_2}{q_4} a_y^2 \sin^2 \theta_i - a_z^2 \quad (\text{A-12})$$

$$P_2 \triangleq \left\{ a_y^2 \sin^2 \theta_i (q_1 - \frac{q_2 q_3}{q_4}) - 1 \right\} \quad (\text{A-13})$$

We rewrite (-11) in the form

$$P_1 Q^2 + 2 a_z Q + P_2 = 0 \quad (\text{A-14})$$

which is a second-order algebraic equation whose solution is

$$Q = \frac{-a_z \pm \sqrt{a_z^2 - P_1 P_2}}{P_1} \quad (\text{A-15})$$

From (A-16) and (A-4) we get

$$\theta = \arctan \left\{ \sqrt{\frac{1}{q_4} (Q^2 - q_3)} \right\} \quad (\text{A-16})$$

Thus, by knowing θ_i and the parameters of the system, n and n , we can find q_1 , q_2 , q_3 , and q_4 from (A-5) —

(A-8), P_1 and P_2 from (A-12) and (A-13), Q from (A-15), and θ from (A-16). Then we calculate $n_e(\theta)$ from (34), and θ_{te} from (A1).

CONCLUSION

Given a plane wave that strikes the surface of a uniaxial crystal a part of its energy is reflected and the remainder is transmitted in the form of two rays, whose directions of propagation in the crystal have been analytically determined. For the ordinary ray, the direction of the ray is also that of the energy flow associated with that ray. For the extraordinary ray, however, the direction of energy flow is inclined to the direction of propagation as determined by Snell's law. The deviation angle α given by (35) is a function of θ , the angle between the direction of propagation in the crystal and the optic axis. The direction of energy flow of the extraordinary ray lies in a plane that contains the direction of e-ray propagation and the optic axis; this plane need not be the plane of incidence of the plane wave.

ACKNOWLEDGEMENT

The author wishes to extend his gratitude to Professors : Ahmed A. Kamal, Salah El-Sobky, and M. Fahim Sakr for their constant encouragement.

REFERENCES

- 1 — Longhurst. R.A., "Geometrical and physical optics", 2nd edition, Wiley, 1967.
- 2 — Jenkins, F.A. and White H.E., "Fundamentals of optics", 2nd edition McGraw Hill 1950.
- 3 — Born M., "Principles of Optics" 3rd edition, Pergamon Press 1965.
- 4 — Stone J.M. "Radiation and optics", McGraw Hill 1963.
- 5 — Klein M.V., "optics" Wiley 1970.
- 6 — Rossi B. "Optics" Oddison — Wesley 1957.
- 7 — Summerfeld A. "Optics". Academic Press 1954.

which are also perpendicular to \bar{a} , we have

$$\bar{u} \triangleq \frac{\bar{s}_{te} \times \bar{a}}{\sin \theta} \quad (18)$$

$$\bar{v} \triangleq \bar{a} \times \bar{u} \quad (19)$$

where θ is the angle between \bar{s}_{te} and \bar{a} . With these definitions we can represent our field vectors in the $\bar{a}, \bar{u}, \bar{v}$ system as

$$\bar{E}_{to} = E_{to} \frac{\bar{s}_{to} \times \bar{a}}{\sin \eta} \quad (20)$$

$$\bar{H}_{te} = -H_{te} \bar{u} \quad (21)$$

$$\bar{D}_{te} = D_{te} (\cos \theta \bar{v} - \sin \theta \bar{a}) \quad (22)$$

$$\bar{E}_{te} = E_{te} (\cos \psi \bar{v} + \sin \psi \bar{a}) \quad (23)$$

where η is the angle between \bar{a} and \bar{s}_{to} and ψ is the angle between \bar{E}_{te} and \bar{v} . Fig. 2 shows the vector relations for the e-wave with respect to the index ellipsoid.

We now express all our vectors in terms of physical unit vectors: the optic axis \bar{a} , and the directions of propagation \bar{s}_{to} and \bar{s}_{te} . Noting from Fig. 2 that

$$\bar{v} = \operatorname{cosec} \theta \bar{s}_{te} - \cot \theta \bar{a} \quad (24)$$

we get from (11)-(17) and (20)-(23) that

$$\bar{D}_{to} = \frac{n_o}{c} H_{to} \frac{\bar{s}_{to} \times \bar{a}}{\sin \eta} \quad (25)$$

$$\bar{E}_{to} = \frac{\mu c}{n_o} H_{to} \frac{\bar{s}_{to} \times \bar{a}}{\sin \eta} \quad (26)$$

$$\bar{H}_{te} = -\frac{n_e(\theta) \cos \alpha}{\mu c} E_{te} \frac{\bar{s}_{te} \times \bar{a}}{\sin \theta} \quad (27)$$

$$\bar{E}_{to} = E_{to} \left[(\sin \psi - \cos \psi \cot \theta) \bar{a} + \frac{\cos \psi}{\sin \theta} \bar{s}_{te} \right] \quad (28)$$

$$\bar{H}_{to} = \frac{H_{to}}{\sin \eta} [\cos \eta \bar{s}_{to} - \bar{a}] \quad (29)$$

$$\bar{D}_{te} = \frac{n_e^2(\theta)}{\mu c^2} \cos \alpha E_{te} [-\operatorname{cosec} \theta \bar{a} + \cot \theta \bar{s}_{te}] \quad (30)$$

$$\bar{s}_{to} = \frac{\mu c}{n_o} H_{to}^2 \bar{s}_{to} \quad (31)$$

$$\bar{s}_{te} = \frac{n_e(\theta) E_{te}^2}{\mu c} \cos \alpha \left[(\cos \psi + \sin \psi \cot \theta) \bar{a} - \frac{\sin \psi}{\sin \theta} \bar{s}_{te} \right], \quad (32)$$

where $\alpha = \theta + \psi$

is the angle between \bar{s}_{te} and \bar{S}_{te} the Poynting vector of the e-ray. The geometric relation among these vectors is illustrated in Fig. 3. In this figure we note

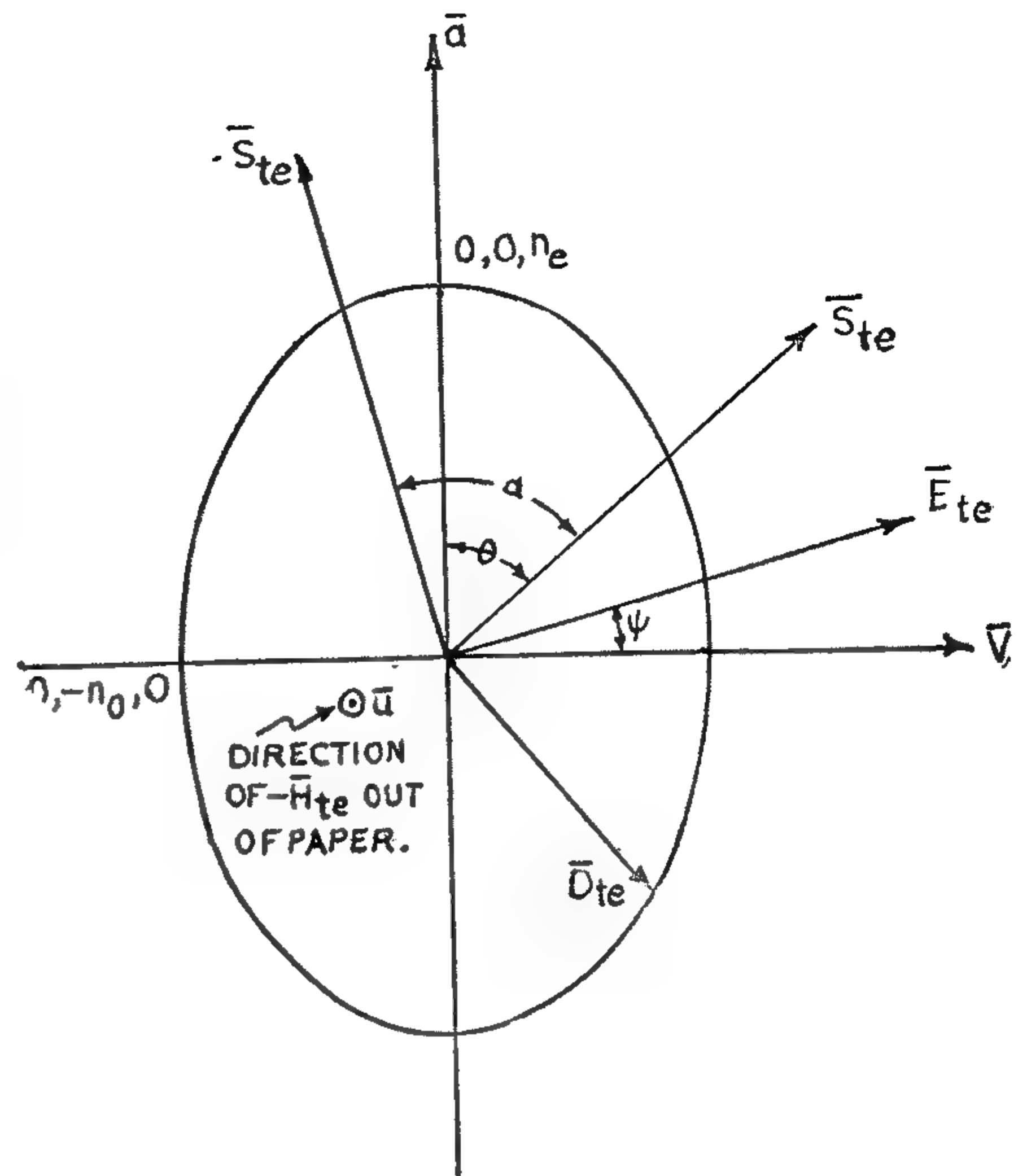


Fig. 2

vector relationships for the extraordinary wave

that \bar{s}_{te} and \bar{s}_{to} lie in the plane of incidence; however, this does not imply that the optic axis should also be contained in such a plane. This fact is illustrated in Fig. 4.

From the theory of the index ellipsoid, it can be shown (1, 3) that

$$\frac{\cos^2 \theta}{n_o^2} + \frac{\sin^2 \theta}{n_e^2} = \frac{1}{n_e^2(\theta)} \quad (34)$$

$$\text{and } \tan \psi = \cot \theta \frac{n_e^2(\theta) - n_o^2}{n_e^2(\theta) - n_e^2} \quad (35)$$

where n_e is called the extraordinary index of refraction. For negative uniaxial crystals $n_e < n_o$. From (34) and (35)

$$\tan \psi = -\left(\frac{n_o}{n_e}\right)^2 \tan \theta \quad (36)$$

$$\alpha = \theta + \arctan \left\{ -\left(\frac{n_o}{n_e}\right)^2 \tan \theta \right\} \quad (37)$$

We note that \bar{S}_{te} is specified completely by the fact that it makes an angle α with \bar{s}_{te} — which is determined by Snell's law — and lies in a plane that contains \bar{s}_{te} and the direction of the optic axis and is given by (32).

und different point sources on the wavefront is the extraordinary ray.

The purpose of this paper is to analytically formulate the tracing of these two rays and to determine their directions without resorting to Huygen's construction even for the most general cases of incidence.

ANGLE BETWEEN DOUBLY REFRACTED ORDINARY AND EXTRAORDINARY RAYS

For a plane wave incident from air on a plane surface of an anisotropic medium two possible directions of energy flow exist for the transmitted wave. We represent the direction of propagation of the ordinary wave by s_{to} and that of the extraordinary wave by s_{te} . Both vectors lie in the plane of incidence, which also contains the normal at the surface and s_i , the direction of propagation in air of the incident wave. The actual extraordinary ray (henceforth referred to as the e-ray), however, is not along the direction of s_{te} because of the anisotropy of the medium, but is in the direction of the Poynting vector. The Poynting vector is directed along the direction of flow of energy whereas the direction of propagation is the direction of phase advance.

The directions of propagation s_{to} , s_{te} , and s_i satisfy Snell's law. If θ_{to} , θ_{te} , and θ_i are the angles which the directions of propagation in the medium and the direction of propagation in air make with the normal to the surface, we have

$$\sin \theta_i = n_o \sin \theta_{to}, \quad (3)$$

$$\sin \theta_i = n_e(\theta) \sin \theta_{te} \quad (4)$$

Fig. 1 shows the relationship among the several vectors under consideration. Representing the incident plane wave by the phase factor

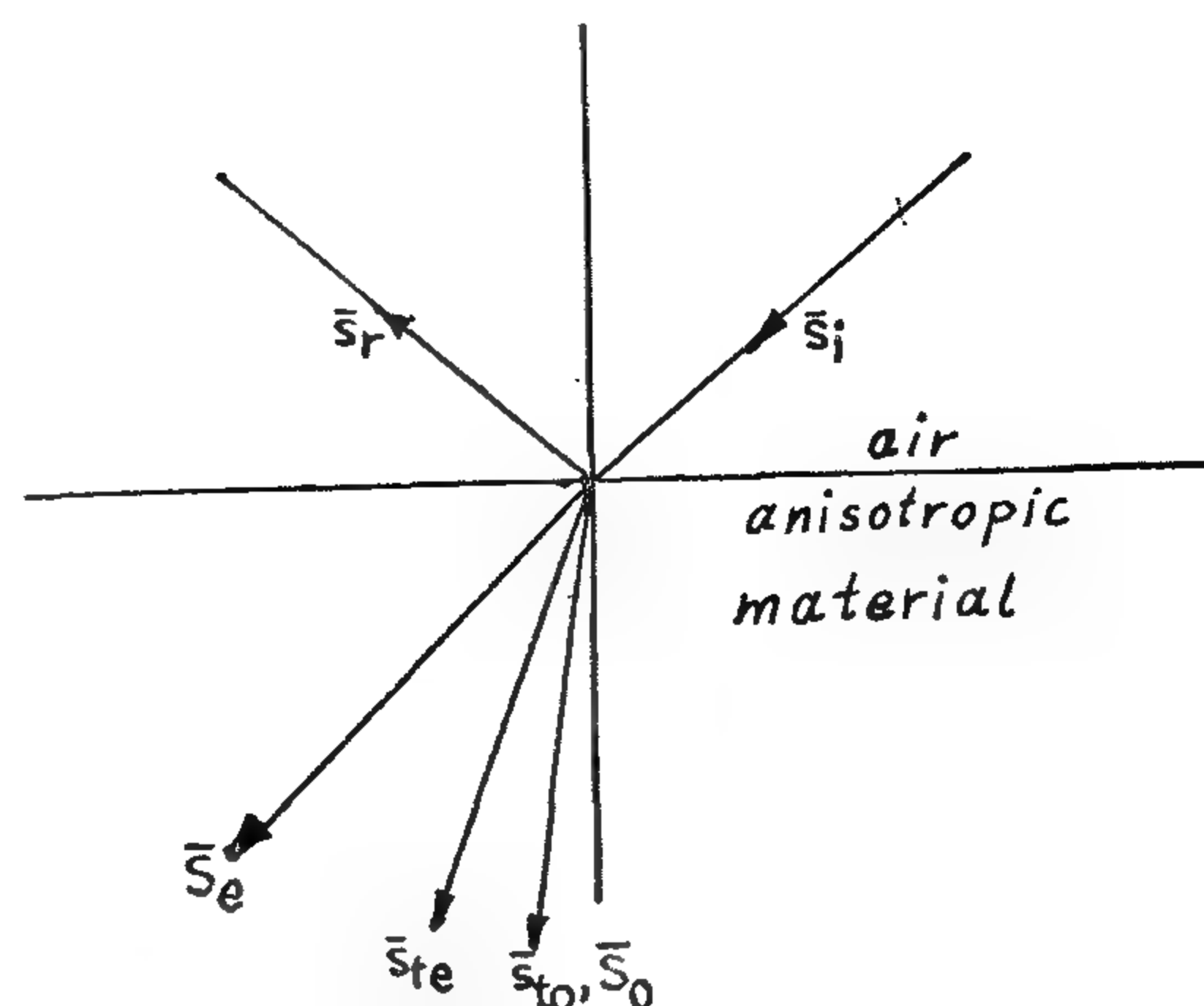


Fig. 1.
ray geometry at plane interface
between air and anisotropic
material

Maxwell's equations,

$$j_e w(t - n/c \text{ r.s.}), \quad (5)$$

$$\nabla \times \bar{E} = -\mu \frac{\partial \bar{H}}{\partial t} \quad (6)$$

$$\nabla \times \bar{H} = \frac{\partial \bar{D}}{\partial t} \quad (7)$$

$$\nabla \cdot \bar{D} = 0 \quad (8)$$

$$\nabla \cdot \bar{H} = 0 \quad (9)$$

$$\bar{s}_i \times \bar{H}_i = -\frac{\bar{E}_i}{\mu c} \quad (10)$$

$$\bar{s}_i \times \bar{E}_i = \mu c \bar{H}_i \quad (11)$$

$$\bar{s}_r \times \bar{E}_r = \mu c \bar{H}_r \quad (12)$$

$$\bar{s}_r \times \bar{H}_r = -\frac{\bar{E}_r}{\mu c} \quad (13)$$

$$\bar{s}_{to} \times \bar{E}_{to} = \frac{\mu c}{n_o} \bar{H}_{to} \quad (14)$$

$$\bar{s}_{to} \times \bar{H}_{to} = -\frac{n_o \bar{E}_{to}}{\mu c} \quad (15)$$

$$\frac{n_e(\theta)}{\mu c} (\bar{s}_{te} \times \bar{E}_{te}) = \bar{H}_{te} \quad (16)$$

$$\frac{e(\theta)}{c} (\bar{s}_{te} \times \bar{H}_{te}) = -\bar{D}_{te}, \quad (17)$$

where H is the magnetic field vector, E is the electric field vector, and D is the electric displacement vector. The suffixes to , te , r , and i denote ordinary transmitted, reflected, and incident, respectively.

Defining a as a unit vector in the direction of the optic axis and u and v as mutually perpendicular unit vectors

ANALYTICAL DETERMINATION OF THE DIRECTIONS OF DOUBLY REFRACTED RAYS IN A UNIAXIAL CRYSTAL

Dr. M. SAMEH SAID

ABSTRACT

The problem of propagation of plane waves through uniaxial crystals is solved for a general case of oblique incidence. The directions of propagation and energy flow of the ordinary and extraordinary rays are determined analytically without resort to Huygen's graphical construction.

INTRODUCTION

Transparent media may be classified as singly refracting or doubly refracting¹⁻⁵. The former includes homogeneous isotropic materials while the latter applies to transparent crystalline substances which, while homogeneous, are anisotropic. Thus, the velocity of a light wave propagating through them depends on the direction of propagation. In particular, a ray incident on a doubly refracting crystal is split into two rays in traversing the crystal — an **ordinary** ray whose directions of wave propagation and energy flow coincide, and an **extraordinary** ray for which these directions do not coincide. The extraordinary ray is distinguished by the fact that its index of refraction is a function of direction.

The general treatment of the propagation of light through doubly refracting crystals is usually presented graphically in terms of wave surfaces². The wave surface is defined as a wavefront entirely surrounding a point source of monochromatic light and is conceived with a know-

wledge of the index ellipsoid, e.g. 2,4,6 & 7. The relation between the wave surface and index ellipsoid can be illustrated by considering the defining equation of a wave surface and index ellipsoid can be illustrated by considering the defining equation of a wave surface.

$$\omega \frac{r.s}{V} = \text{constant}, \quad (1)$$

where r.s expresses the distance traversed by a wave of monochromatic radiation of frequency $\frac{\omega}{2\pi}$ with velocity v in direction s. In terms of the index of refraction n, this equation may be rewritten as

$$r.s = \frac{\text{constant}}{n} \quad (2)$$

For the ordinary ray the index of refraction n_o is a constant in all directions, while for the extraordinary ray, the index of refraction $n_e(\theta)$ is dependent on θ , the angle between the direction of propagation s and the direction of the optic axis.

Based on n_o and $n_e(\theta)$, two sets of Huygen's wavelets propagate, one set being spherical and the other ellipsoidal. The ray which corresponds to wave surfaces tangent to the spherical wavelets constitutes the ordinary ray; the ray corresponding to the planes tangent to the ellipsoidal wave surface formed aro-

INDUSTRY & PRODUCTION

INST. OF MECHASICAL ENGINEERS
INST. OF MECHANICAL ENGINEERS

الخدمات الأولية والصناعات الكيماوية

جمعية مهندسي المناجم والبترو
والفلزات
جمعية المهندسين الكيميائيين

تكنولوجيا صناعة الطوب الرملى

د. يحيى عبد الفتاح أبو حسين

ملخص :

تختلف صناعة الطوب الرملى عن صناعة الطوب الأحمر بأنه لا يتم حرق الخامات عند درجة حرارة عالية بل يتم لها تفاعل كيماوى عند ضغط ودرجة حرارة حوالى ٢٠٠م فقط وطرق هذه الصناعة مختلفة بحيث أن كل طريقة تكنولوجية تناسب خامات وظروف معينة . وبصفة عامة فإن الخامات اللازمة هي رمال سيلكا وجير حى يخلطان ويشكل الطوب تحت ضغط عالى في مكبس ثم ينقل الطوب الى أتوكلاف وتتم دورة الانتاج في زمن قياسي ٢٤ ساعة . هذا ويضم البحث مقارنة بين مختلف طرق الانتاج التكنولوجى لهذا الطوب .

كيمياء الصناعة :

الطوب الرملى عبارة عن سليكات الكالسيوم أو بعبارة أدق هو المادة اللاصقة المسمنتية سليكات الكالسيوم التى تسبب تماسك الطوب . وتتكون هذه المادة السمنتية من الجير والسليكا أثناء عمليات كيميائية تحت ضغط عال وبخار ماء يعطى الطوب صلابته وقوته .

ويصنع الطوب الرملى من رمل وجير بنسب تتوقف على تركيز أكسيد الكالسيوم الحرقى الجير وكذلك على نسبة السليكا فى الرمل وتكنولوجيا التصنيع والمعدات المستخدمة ومدى كفاءتها ويتم التفاعل بين الجير والرمل تحت تأثير الظروف أو العوامل المساعدة للتفاعل من الضغط ودرجة الحرارة والرطوبة فى الأتوكلاف كالتالى :

المرحلة الأولى : تبدأ باطفاء الجير الحى بالماء ليتحول الى أيدروكسيد الكالسيوم + حرارة (١٥ كيلو كالورى) .

المرحلة الثانية : يبدأ التفاعل بين الجير والرمل عقب التشكيل فورا وكذلك فى الفترة الأولى فى الأتوكلاف .

أيدروكسيد الكالسيوم + سليكا = هيدروسليلكات الكالسيوم الذائبة .

المرحلة الثالثة : تتم فى الأتوكلاف حتى نهاية الوقت تحت تأثير الضغط والحرارة هيدروسليلكات الكالسيوم هيدروسليلكات الكالسيوم المائية الغير ذائبة (أسمنت) .

وجدير بالذكر أن هذا التفاعل يتم على سطح حبيبات الرمال مكونا المادة السمنتية اللاصقة والتى تشبه فى تكوينها الكيميائى بعض مكونات الأسمنت البورتلاندى وهذه المادة السمنتية تملأ الفجوات بين حبيبات الرمل وتجعله يتماسك مع بعضه مكونا كتلة فى حجم تشكيل الطوبة مانحا إياها قوة الصلابة ومقاومة التآكل وجميع خواصه الطبيعية والكيميائية .

الجير المستعمل فى هذه الصناعة هو جير محروق فى أفران عند درجة حرارة ١١٥٠ ، وان هذا الجير هو أساس المادة السمنتية اللاصقة . وجدير بالذكر أن صناعة الطوب الرملى لا تحتاج الى حريق فى أفران كالطوب الأحمر الطفلى بل أن المعدات اللازمة تحتاج استثمار أقل من مصانع الطوب الطفلى الحديث . وهذه هى نقطة الخلاف بين مؤيدى صناعة الطوب الرملى وصناعة الطوب الطفلى فى حالة تواجد كلا الخامتين أى الرمال والطفله الصالحتين فى نفس المنطقة أو الموقع المقرر إقامة مصنع بها لانتاج الطوب . وفى حالة اضافة استثمارات مصنع الجير الى مصنع الطوب الرملى فإن الصورة تتغير بالنسبة الى رأس المال اللازمة لكل من صناعتي الطوب الرملى والطوب الطفلى . دولة الى أخرى وتصل الى مرحلة التنافس الشديد .

واذا قدر ثمن الجير الحى المستخدم فى صناعة الطوب الرملى بثمن بيع السوق السائدة فإن الصورة تتغير بالنسبة الى تكلفة ألف طوبة المنتجة وفى بعض الدول يرتفع سعر الطن وفى الأخرى ينخفض جدا لدرجة تجعل صناعة الطوب الرملى أكثر اقتصادا .

وتكنولوجيا الصناعة لها الأهمية الكبرى فى تحديد مواصفات الطوب المنتج واقتصاديات التشغيل والعمالة ويتوقف عليها نجاح المشروع الا أن مواصفات الخامات لها تأثيرها الفعال . لهذا تبدأ بها ثم بوصف طريقة الصناعة .

مواصفات الخامات

(١) الرمل :

توجد مواصفات مثالية للرمل أو أحسن أنواع الرمال التى تصلح ولكن لا يعنى ذلك أن الرمال الأقل جودة لا تصلح بل يمكن صناعة الطوب الرملى من أى رمال سيلكا بها نسبة معقولة من ثان أكسيد السيلكون لدرجة أن احصى الشركات الموردة

(ج) الماء أو الرطوبة :

يعتبر الماء احدى انخامات اللازمة لانتاج الطوب وان كانت نسبته قليلة فهي تماثل نسبة الجير تقريبا .

نسبة الماء في الخليط قبل التشكيل = ٦-٨٪

واذا فرضنا جودة الجير الحى (٨٠ ٪) فان النسبة المضافة منه = ٧٪ .

فلهذا يلزم كمية الماء اللازمة :

- ١ - استهلاك المياه لطفي الجير $٧ \times ٣٢ = ٢٢٤$ ٪
- ٢ - للتبخير أثناء الاطفاء (٣٢ ٪ بالوزن نظريا) $٧ = ٣٧$ ٪
- ٣ - للتبخير بحد الخلط أثناء الانتظار والنقل وخلافه ١٣٪
- ٤ - الماء اللازم للخليط قبل التشكيل في المكبس = ٧٪

مجموع المياه اللازمة ١٣٪
ولهذا فان نسبة الماء المطلوب صناعيا = ١٣٪

طريقة الانتاج

تستغرق جميع عمليات التصنيع حتى تخزين المنتج حوالى ٢١ - ٢٦ ساعة .

مرحلة الاعداد : يكسر الجير ويطحن بواسطة كسارة شواكيش تليها طاحونة كور ثم تتم معايرته بالوزن أو الحجم بنسبة ٧ - ١٠٪ من مجموع الخلطة ويتوقف ذلك على نسبة أكسيد الكالسيوم الحر وعلى طريقة الصناعة .

- بعد فصل الزلط من الرمل بواسطة مهزة خاصة ينقل الى المصنع بالسيارات أو بواسطة سير ناقل ثم تتم معايرته بالوزن أو الحجم أيضا بنسبة ٩٠ - ٩٣٪ من مجموع الخليط .

مرحلة الاطفاء والخلط :

يخلط الرمل والجير وتتم عملية الاطفاء للجير وبدء التفاعل باحدى الطرق الآتية :

(أ) الخلاط الكبير :

ويكون حجم الخليط كبير نسبيا (١٥٠ - ٢٠٠ م^٣) وتستمر عملية الاطفاء والخلط مدة طويلة نسبيا تتراوح بين ١٢ - ٢٠ ساعة وتتوقف على عوامل كثيرة مؤثرة . وتفضل هذه الطريقة عندما يحتوى الرمل على نسبة عالية من الرطوبة .

للمعدات تحدد المواصفات بأن لا تقل عن نسبة ٧٠٪ س أ فقط بينما موردين آخرين يشترط أن تكون أعلى من ٩٠٪ وخالى من الميسكا والطفلة والأثرية والأكاسيد وأن تكون الحبيبات ذات زوايا حادة غير شديدة الاستدارة ومتدرجة من أحجام مختلفة طبقا لمنحنى بيانى خاص .

ولكن في اعتقادى أن خواص الرمل الصالح هى :

- ١ - نسبة أكسيد السيليكون أعلى من ٧٠٪ س أ .
- ٢ - تفضل أن تكون الرمال من محاجر الرمال الصحراوية وليست من الرمال النهرية مثل رمال النيل أو البحرية أو الكثبان .
- ٣ - أن لا يزيد حجم حبيبات الرمل عن ملليمتر ويفضل أن تكون ٣ ملليمتر متدرجة بحيث يكون بها نسبة من الناعم تتراوح بين ١٠ - ١٥٪ يمر في منخل ١٠٠ مش .

والنسبة الناعمة تساعد على تقليل المسافات البينية بين حبيبات الرمل .

- ٤ - نسبة الشوائب المتواجدة بالرمل لا ضرر منها ما دامت موزعة توزيعا منتظما مع خام الرمال ولا تحتوى على مواد عضوية تأثر على اللون أو تغيره مثل بقايا الأعشاب وجذور الأشجار . وفى اعتقادى أن المواد الطفيلية وأكاسيد الحديد لا ضرر منها ما دامت منتظمة التوزيع .

(ب) الجير الحى :

كل جير محروق يمكن أن يصلح لصناعة الطوب الرملى ولكن تختلف النسب اللازمة وتكنولوجيا التصنيع وأهم الاشتراطات هى :

- ١ - يجب أن يكون محروقا جيدا لمدة معينة ودرجة حرارة تتراوح بين ١٠٠٠ - ١٢٠٠ م^٣ وأن لا يكون به أحجار جيرية غير كاملة الحريق أو محروقا أكثر من اللازم مما يبطئ اطفائه .
- ٢ - يفضل أن تكون نسبة أكسيد الكالسيوم الحر أعلى من ٨٠٪ كا أ

- ٣ - يستحسن أن لا تزيد نسبة أكسيد الماغنسيوم عن ٢٪ ما أ فى الجير لأنه يبطئ في اطفائه . وفى حالة تواجده يتم اطفائه بطريقة خاصة لمدة أطول وربما يظل في الخلاط أو الصهرج بعد اطفائه لمدة تتراوح بين ٨/٢٠ ساعة ويعتبر هذا وقت كاف لاطفائه وتحوله الى هيدروكسيد ماغنسيوم .

(ب) الخلاط المستمر :

يكون حجم الخليط متوسطا وحجمه = ٣م٤٠ ويتكون من خرسانة مسالحة قطره ٢ر٤م وعمليات الخلط تتم بطاقة ٧٥٠ كيلوات وتستمر عملية الأطفاء في مدة ٣ - ٤ ساعات بصفة مستمرة .

(ج) البرميل :

وهي أسرع طريقة للأطفاء والخلط .

حجم الخليط صغير نسبيا ويتوقف على سعة البرميل أو الشكل الأسطوانى وهو حوالى ٣م٢ر٥ أو أكثر حيث بلغت ٣م١٠ر٠ فى إنجلترا وطولها حوالى ٤ متر . ويتم اطفاء الجير داخل هذه الخلاطات التى تدور على محور أفقى وذلك بامرار كمية الماء اللازمة الى الخليط وبعد احكام القفل وبدء الدوران يمر بخار ماء تحت ضغط ٣ - ٥ جوى على أن تستكمل درجة الرطوبة الى ٧٪ . تتم فى مدة تتراوح بين ٤٠ - ٦٠ دقيقة .

(د) طريقة استخدام الجير المطفى :

هذه الطريقة تعتبر أبسط طرق الانتاج حيث يتم شراء الجير المطفى الجاهز وتتم معايرة كمية الجير المطفى من المخزن الخاص به وكذلك كمية الرمل ثم ينقل الخليط كله الى المرحلة التالية من الانتاج سواء كانت بريمة الخلط وتغذية المكبس أو طاحونة الخلط التى تسبق المكبس . وتوفر هذه مثال : (أ) أو (ب) أو (ج) .

وتتميز باستخدام نسبة ثابتة من الجير وهى النسبة الصحيحة .

— قلة امتصاص الماء .

الطوب الملون :

لانتاج طوب ملون يضاف اللون المناسب فى هذه المرحلة مع الجير والرمل سواء فى (أ) أو (ب) أو (ج) أو (د) بنسب ثابتة وبواسطة جهاز خاص لتحديد الوزن .

مرحلة التجهيز : بعد اعداد الخلطة بواسطة احدى الطرق سابقة الذكر يلزم لخلطها جيدا بطريقة مناسبة ويتم ذلك (فى إنجلترا) بواسطة طاحونة أسياخ .

أو فى طاحونة كور أو بواسطة بريمة مزدوجة .

— ويتوقف على هذه المرحلة من الخلط النهائى جودة اعداد الخليط لمرحلة التشكيل . ويمكن اضافة نسبة الماء اذا لزم لضبط النوعية .

— وفى أحد المصانع المتقدمة جدا فى الخبرة والتكنولوجيا يتم حساب نسبة الجير المطفى على أساس نوعية الطوب المطلوب حيث يوجد نوعان (أ) + (ب) .

فالنوع (ب) يستعمل ٧٪ أكسيد كالمسيوم فقط ويختزل الوقت اللازم فى الأتوكلاف الى ٣ ساعات عن انتاج طوب عادى النوعية قوة مقاومته للتهشم = ١٩٠٠ رطل بوصة (١٧٥ كجم / سم^٢) .

والنوع (أ) يستعمل ١٠٪ أكسيد كالمسيوم فى الوقت العادى فى الأتوكلاف وهو ٤ ساعات تحت ضغط ١٦ جوى (٢٣٥٤ رطل / بوصة مربعة يساوى ١٧٥ كجم / سم^٢) وهذا الطوب (أ) من النوع الممتاز المعروف بالطوب الهندسى وقوة مقاومته للتهشم أكثر من = ٢٩٠٠ رطل / بوصة بلمربعة (٢٠٣ كجم / سم^٢) . وجدير بالذكر أن النوعان (أ) ، (ب) لهما مواصفات كاملة فى المواصفات القياسية البريطانية رقم ١٨٧ لسنة ١٩٥٥ .

وتعتبر مراحل الأعداد والأطفاء والخلط والتجهيز ذات أثر فعال على مكبس التشكيل فعندما تتم كلها بدقة وكفاءة يصبح الخليط مناسباً للمكبس فان ذلك يوفر كثيرا فى صيانة فورم التشكيل ويرفع عمر استعمالها لمدد أطول .

مرحلة التشكيل : تعتبر هذه العملية أهم عملية فى الانتاج حيث يتوقف عليها نوعية المنتج وشكله ومظهره وكذلك قوة مقاومته للتهشم وتحمله .

وتوجد أنواع مختلفة من ماكينات التشكيل أو المكابس أهمها الأنواع التالية :

— مكبس صينية دواره .

— مكبس انحرافى .

— مكبس ازدواجى .

وتعمل المكابس بقوة ضغوط مختلفة تتراوح بين ١٥٠ - ٢٥٠ كيلو جرام على السنتمتر المربع ويصل بعضها الى حوالى ٨٠٠ كجم / سم^٢ وقوة ضغط المكبس لها تأثير فعال على قوة مقاومة التهشم للطوب المنتج فكلما زادت قوة المكبس تحسنت نوعية الطوب .

تزال قوالب الطوب من فورمة المكبس بالطريقة اليدوية أو أتماتيكية بواسطة جهاز خاص .

حيث ترص على عربات ديكوفيل بطريقة معينة . وينتج المكبس الواحد حوالى ٣٠٠٠ طوبة / ساعة

مرحلة التصليد والتقسية :

تعتبر هذه المرحلة هي النهائية لانتاج الطوب حيث يكتسب صفاته النهائية وخواصه ويتم فيها أهم التفاعلات الكيميائية واتخاذ أكسيد الكالسيوم بالسليكا مكونا مادة صلبة غير ذائبة تسبب تماسك حبيبات الرمال وتكسب الطوب قوة تحمله وخواصه. وهذه المادة لها نفس خواص الأسمنت وتعتبر إحدى مكوناته اللاصقة الهامة .

وتتم هذه المرحلة في أتوكلاف عبارة عن وعاء ضغط أسطواني له أحجام مختلفة طبقا لطاقة الانتاج والنوع الكبير قطره ٢ متر وطوله ٣٦ متر وله باب من كل جهة لادخال واخراج عربات الطوب وحجم عربة الطوب هو ١٨ × ١٨ متر . تسحب العربات الى داخل الأتوكلاف بواسطة سلك الونش الكهربائي ثم يحكم غلق الأبواب ثم يبدأ في فتح البخار الذي يمر خلال ماسورة خاصة ممتدة داخل الأتوكلاف حتى يصل إلى الضغط المطلوب . وتوجد حالتان للانتاج :

(١) في حالة الوصول الى ضغط ٨ جوى تتم الدورة الانتاجية في مدة ١٥ ساعة .

(ب) في حالة وصول الضغط الى ١٦ جوى تتم الدورة الانتاجية في مدة ٨ ساعات تشمل ٣-٤ ساعات فقط تحت الضغط المرتفع (١٦ جوى) .

بعد انتهاء هذا الوقت تفتح صمامات الأتوكلاف ثم الباب ثم تسحب العربات المحملة بالطوب .

وجدير بالذكر أنه يمكن استعمال بخار الأتوكلاف بعد انتهاء دورته وذلك بإمراره الى أتوكلاف آخر مجاور وهذه الطريقة توفر الوقود ويلزم تشغيل عدد من الأتوكلافات بصفة مستمرة معا وفي نظام تكنولوجي دقيق بالتناوب بحيث يلي بداية كل واحد نهاية دورة أتوكلاف آخر وذلك خلال ٢٤ ساعة عمل .

الطوب المنتج يتم سحب عرباته بواسطة الونش الى المخزن حيث يتم تحميله أو بوضعه بطريقة معينة في المخزن وذلك بواسطة ونش رفع يحمل كل حمولة العربة الى سطح اللورى أو الى مكان التخزين .

معدلات الاستهلاك : الانتاج ألف طوبة . (حجم عادى ٢٥ × ١٢ × ٦ سم) تحتاج الى :

جير حى = ٢٣٥ كجم - ٢٩٠ كم .

رمل = ١٩٩ متر مكعب .

وقود = ٥٥ - ٦٠ كيلو جرام مازوت (أو ما

يقابله بالسعر الحرارى من وقود آخر) .

كهرباء : ٢٦ ك . و . ساعة .

عمال : ٦٥ - ١ ساعة/عمالة .

أجسام طاحنة = ٤ ر . كجم/طن كرات طاحنة وشبكات .

الخواص والاستعمالات :

يوجد نوعان :

١ - طوب الواجهات ومنه عدة ألوان وغالبا حجمه ٢٥ × ١٢ × ٦ .

٢ - طوب المباني العادية وهو اما :

(أ) مصمت (ب) ذو فراغات أو ثقب وتتراوح درجة امتصاص الطوب الرملى للماء بين ٨ - ١٦ ٪ بالوزن .

ويتميز الطوب الرملى بما يلي :

— قوة تحمله للضغط عالية .

— انتظام الشكل .

— الوزن النوعى يتراوح بين ١٤ - ١٨ كجم/م^٣

— كمية المونة أو الأسمنت اللازمة اقل استهلاكاً من الأنواع الأخرى .

أهم المواصفات العالمية هي المواصفات البريطانية (١٨٧ لسنة ١٩٥٥) وظهرت المواصفات المصرية رقم ٤٢ - الطوب الرملى الجيرى - لسنة ١٩٦٥ .

TECHNOLOGY OF SAND LIME BRICKS MANUFACTURE

Synopsis :

Manufacture of sand bricks differs from that of red clay bricks since it is based on a chemical reaction under pressure and at a temperature of a 200°C only.

Technological processes for this type of production vary according to the type of raw materials and certain circumstances. In general, the raw materials are mixed, pressed, then transferred to autoclaves. Duration of the whole process is short comparatively, which is about 24 hours.

This paper also gives a comparison between the different methods of productions.

MOTION

O	Relative tracer concentration = $(C - C_r) / C_c - C_r$
C	Measured conductivity.
C_r	Conductivity of water.
C_c	Measured conductivity an column exit.
D	Column diameter, cm.
E_r	Mean effective axial dispersion coefficient, cm^2 / sec .
P_e	Modified Pellet number = $(V_r D) / E$, Dimensionless.
V_g	superficial gas velocity, cm/sec .
V_l	Superficial liquid velocity, cm/sec .
V	Actual liquid velocity = $V_l / (1 - \epsilon_g)$ cm/sec .
V_r	Actual relative velocity = $(V_l / V_g) - V$ cm/sec .
Z	Axial Position, cm.

LITERATURE CITED

1. Afschar, A.S., Diboun, M., and Schügerl, K., *Chem. Eng. Sci.* 23,253, 1968.
2. Anderson, J.L., and Quinn, J.A., *Chem. Eng. Sci.*, 25, 338, 1970.
3. Aoyoma, J., Ogushi, K., Koide, K., and Kubota, H., *Journal of Chemical Engineering of Japan*, 1,2, 1968.
4. Argo, W.B., and Cova, D.R., *Ind. Engf. Chem. Process Design and Develop.* 4,352, 1965.
5. Bischoff, K., and philips, J.B., *Ind. eng. Chem. Process Design and Develop.* 5,416, 1965.
6. Carbtree, J.R., and Bridgwater, J., *Chem., Eng. Sci.*, 26, 1971.
7. Diboun, M., and Schügerl, K., *Chem. Eng. Sci.*, 22, 147, 1967.
8. Diboun, M., and Schügerl, K., *Chem. Eng. Sci.* 22,, 161, 1967.
9. Duckler, A.E. Moyce Wicks, III, and Cleveland, R.G., *AIChE. J.* 10, 38, 1964.
10. E ssa, S.H., And El-Halwagi, M.M., *Conie Shimique*, -04, -1, 1971.
11. E ssa, SèH., El-Halwagi, M.M., and Saleh, M.A., 1 & EC Process Design and Develop. 1971.
12. Eissa, S.H., Ph.D.fl Thesis, Cairo Universityy, Egypt, -969.
13. El-Halwagi, M.M., andm Eissa, S.H., *Chem. Eng.*, 158 (Dec. 15), 1969.
14. Fair, J.R., Lambright, A.J. and Anderson, J.W., 1 & EC process Design and Develop. 1,33,1962.
15. Harry D. Mendeson, *AIChE, J.*, 132, 1697.
16. Hughmark,G.A., *Chem. Eng. Prog.* 58,62,1962.
17. Hughmark, G.A., 1 & EC Process Design Develop. 6,2,1967.
18. Lackme, C., *International Symp. on research in Courrent gas liquid flow*, University of waterloo, 1968, 44.1.
19. Reith, T., Renken, S., and Isral, S.A., *Chem. Eng. Sci.*, 23, 619, 1968.
20. Schügerl, K., *Chemiker Zeitung (German)*, 96,4, 1972.
21. Shinichiro, G., Shinbu, T., Kazuyochi, K., and Koichiro, K., *Chem. Eng. Sci.* 28,7,1973.
22. Siemes W., and W., *Chem. Tech.* 29, 727,1957.
23. Towell, G.D., Ackkerman, C.H., 5th European, second International symp. on Chemical reaction engineering, Amsterdam, May, 1972, B3—1.

Acknowledgment.

The authors gratefully acknowledge the Alexandre Von Humboldt Fcundation and «Boundsminister für Forschung and Technologie» for financial support and invaluable care.

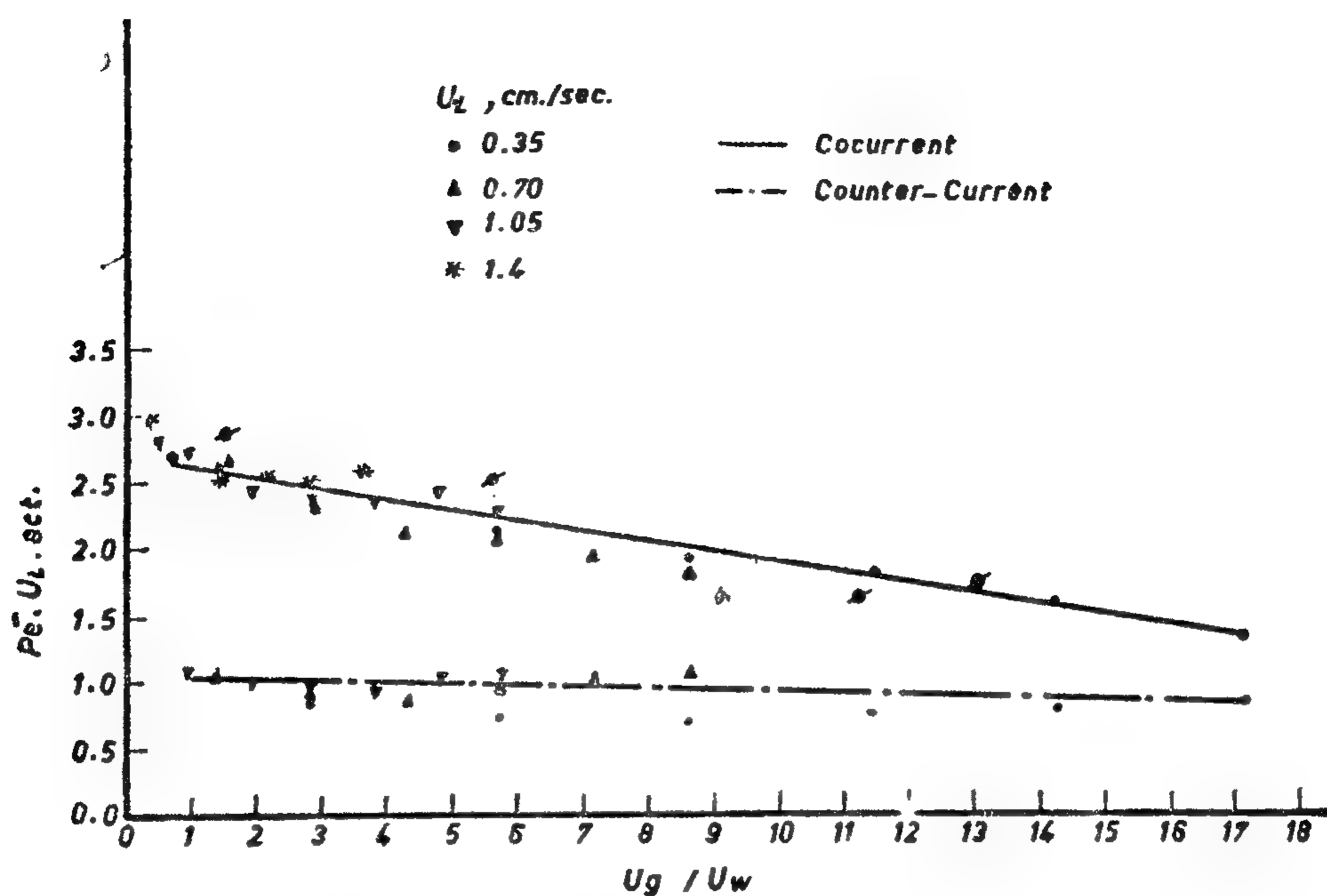


Figure 12 . A Proposed Correlation For This Wark's Data .

Table

Towel and Ackerman data. Column				This work data 15 — 9			
Diam., cm	height, cm	V_g	V_i	P_e^i	V_g	V_i	PC_i
40.64	149.86	2.196	0.68	2.18	0.7	2	2.89
		8.84	0.68	2.09	0.7	6	2.00
		2.196	1.36	2.90	1.4	2	1.61
		8.84	1.36	1.72	1.4	6	1.50
	284.58	1.92	0.68	1.58	0.7	3	2.59
		7.63	0.68	1.93	0.7	6	2.00
		1.92	1.36	1.94	1.4	3	1.56
		7.63	1.36	1.46	1.4	6	1.51
106.68	510.54	1.74	0.37	1.07	0.35	2	5.23
		3.475	0.37	1.32	0.35	4	4.28
		0.854	0.72	1.57	0.7	1	3.53
		1.738	0.72	0.94	0.7	2	2.89

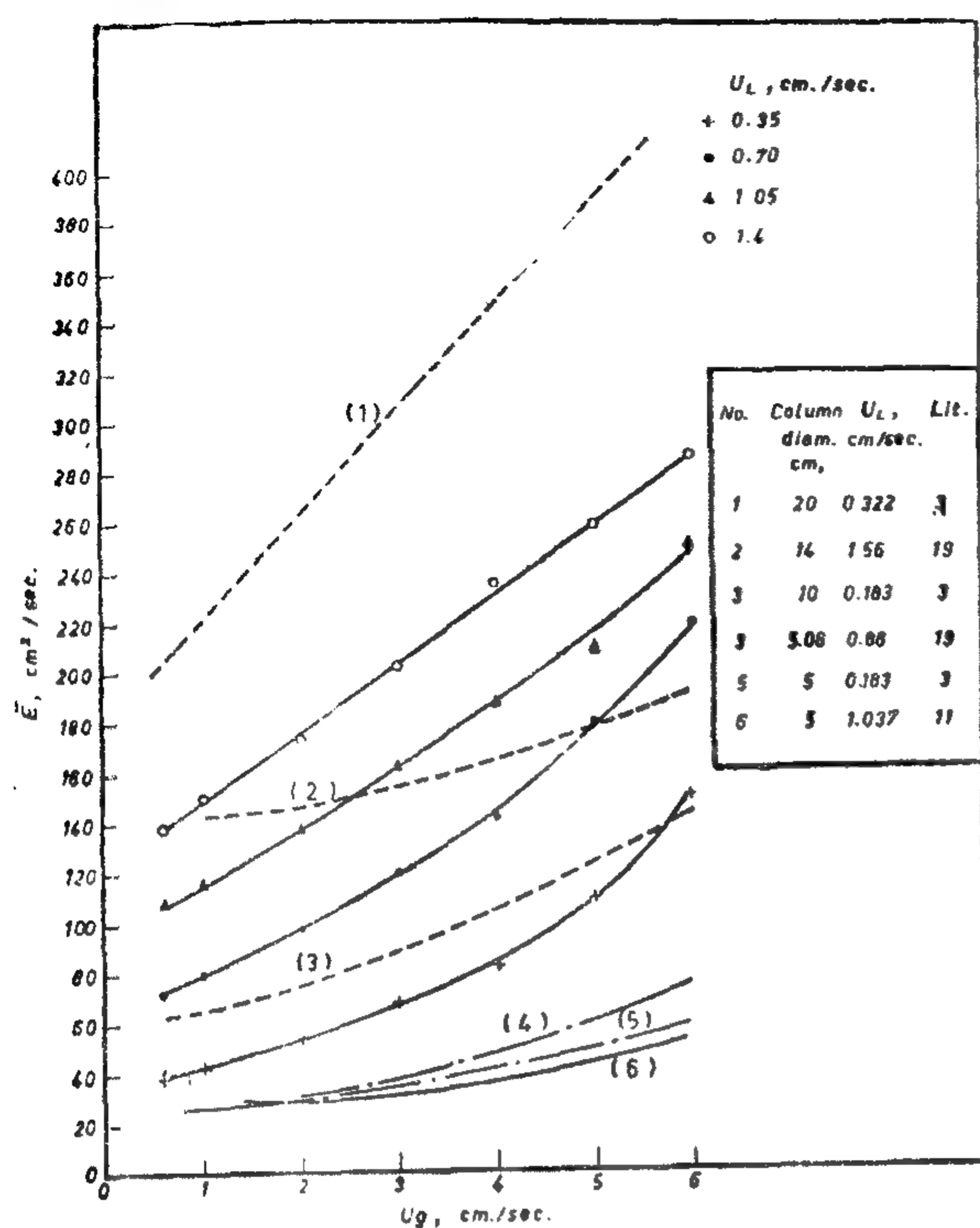


Figure 9 . Effect of Gas and Liquid Velocities on Mean Effective Axial Dispersion Coefficient For Cocurrent Flow .

data can be expressed in terms of a modified Peclet number based on the actual relative velocity and column diameter. Figure 11 shows the variation of such number with gas velocity for different liquid velocities and for both cocurrent and countercurrent cases. From this plot it can be seen that this number decreases with increasing gas velocity and increases with decreasing liquid velocity. It also seems to acquire an asymptotic value in the neighbourhood of 1.5 at gas velocities higher than 6 cm/sec for cocurrent case. A value of $\frac{v_r D}{E}$ was mentioned by Reith et al. A lower asymptotic value is to be expected for the countercurrent case because the relative velocity is smaller in this case and the mixing coefficient is of higher magnitude.

Table 3 shows a comparison with Towel and Ackermann data for large columns of different heights. As can be seen a fairly good agreement is maintained in spite of the experimental setup differences.

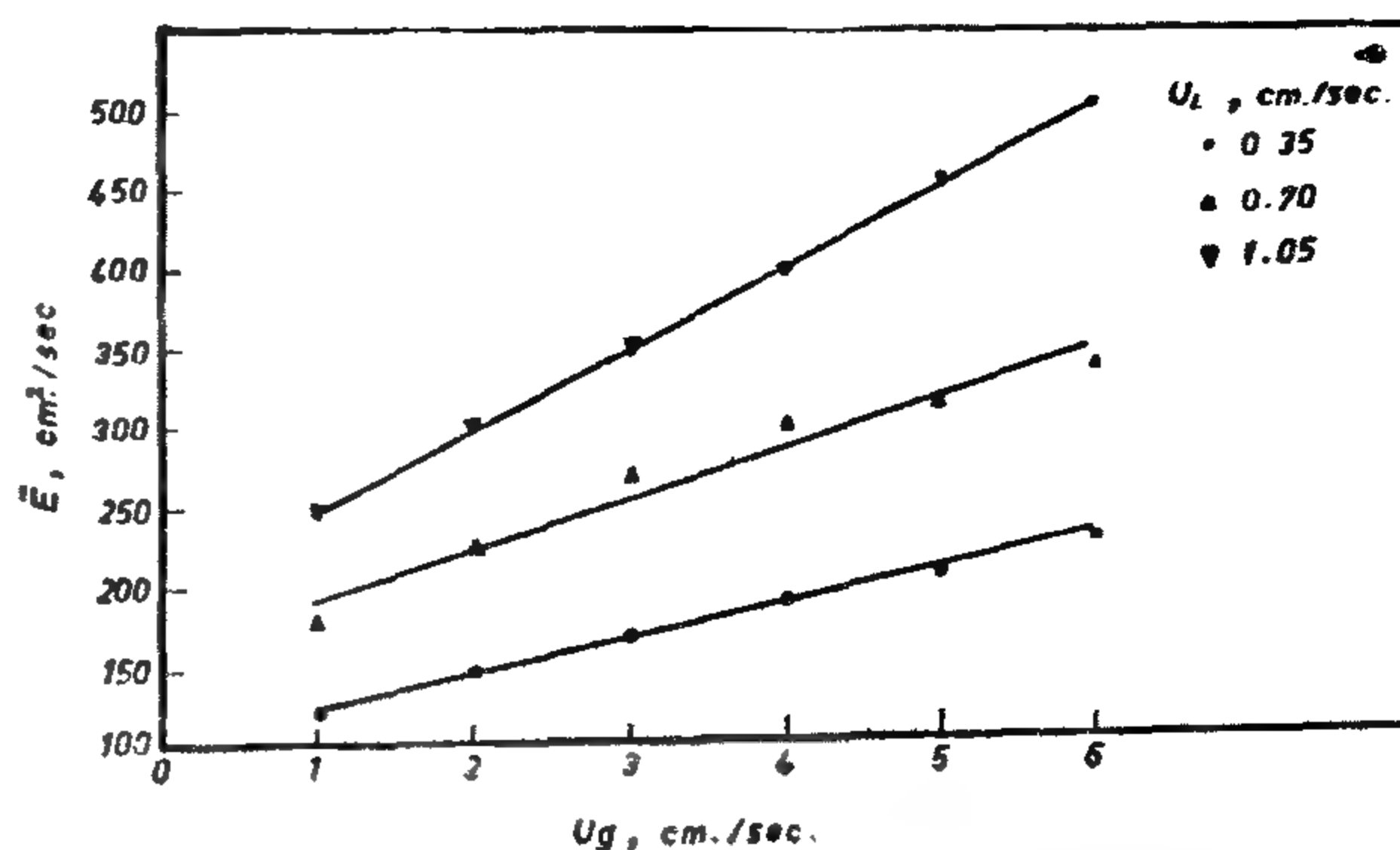


Figure 10 . Effect of Gas and Liquid Velocities on The Mean Effective Axial Dispersion Coefficient For Counter-Current Flow .

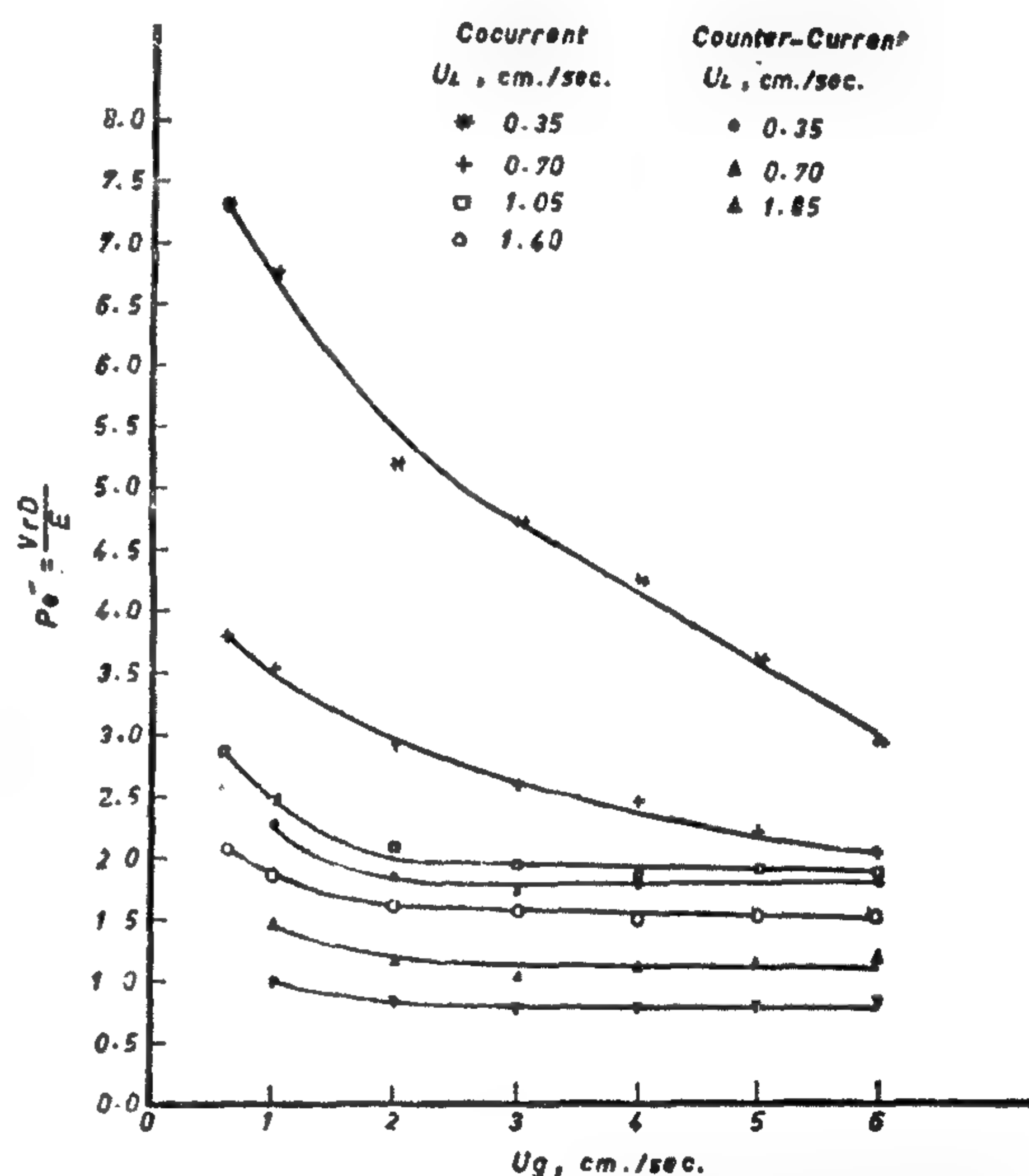


Figure 11 . Variation of The Modified Peclet Number With Gas Velocity For Both Cocurrent And Counter-Current Flow .

From Figure 11 it was conceived that if this number is multiplied by the actual velocity of the liquid phase and plotted for different gas to liquid velocities, straight lines may be obtained. Such a plot is shown in Figure 12 and indicates a reasonable correlation within the domain of the investigated conditions particularly for countercurrent case.

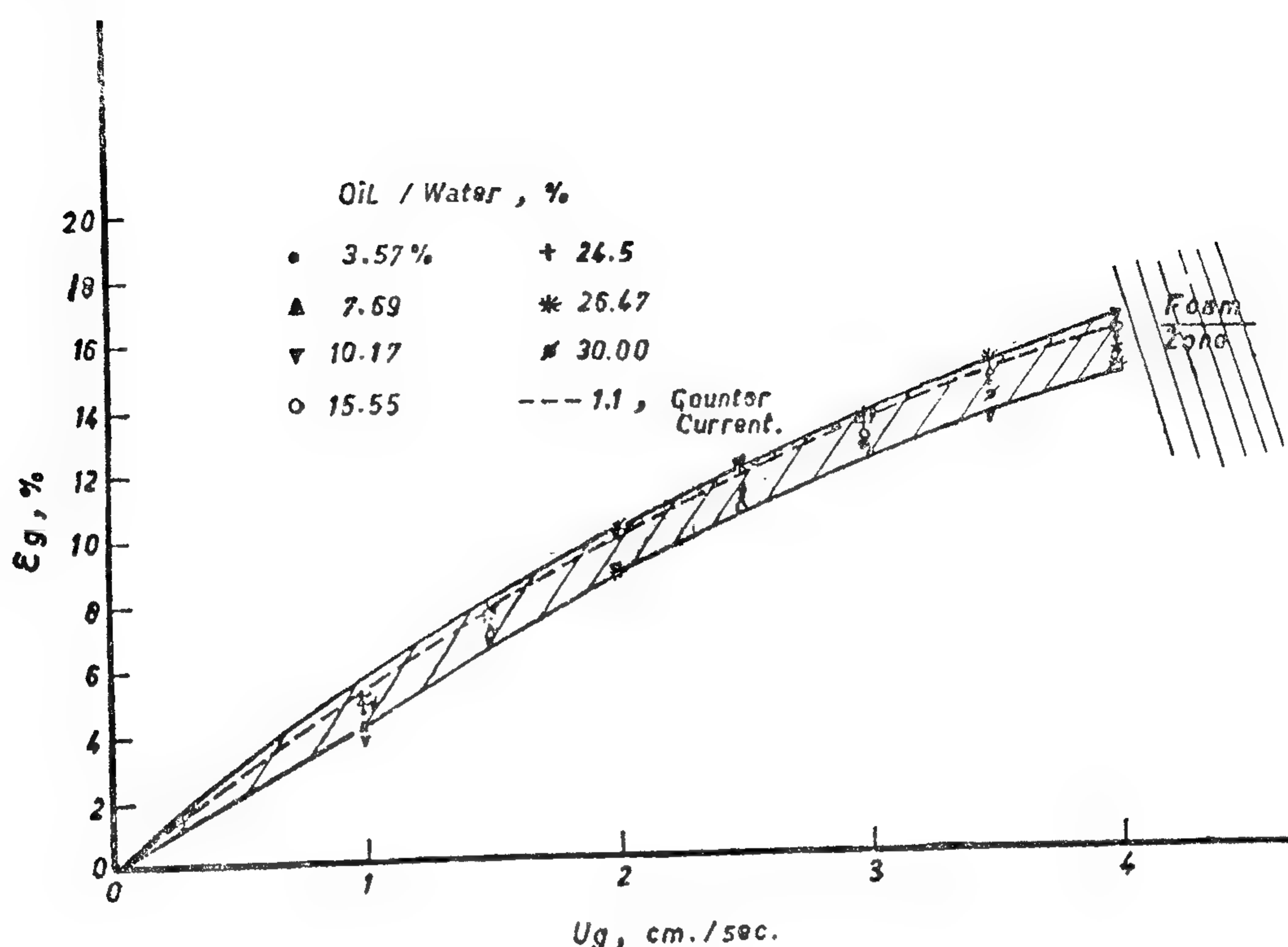


Figure 8 . Effect of Oil / Water Ratio on Gas Holdup .

Comparison of holdup data of this work and of previous investigators for air-water system indicates close resemblance both in trend and in the order-of-magnitude. However, it seems that gas-holdup decreases with increasing column diameter, presumably due to greater circulation patterns in large columns (2,14, 17, 18).

Variation of gas holdup for the system oil (diesel) — water-air for different oil to water concentrations with gas velocity can be seen in Figure 8. for a stagnant liquid and for the counter-current flow case. It can be observed that in both cases, oil to water ratio seems to have no clear effect on gas holdup.

B. Backmixing.

In this work axial-dispersed-plug-flow model gives good fit for the axial measured concentration profiles. According to which :

$$\bar{V} \frac{dC}{dZ} = E \frac{d^2C}{dZ^2}$$

Variation of the mean effective axial dispersion coefficient with gas and liquid velocities for cocurrent and countercurrent cases are given in figures 9 and 10. From these plots it can be seen that this coefficient increases with both gas and liquid velocities and has much higher values in the countercurrent flow case.

Comparison with pertinent literature data can be seen in Figure 9. A good agreement for both the general trend and the order-of-magnitude can be concluded. It is also to be observed that columns of larger diameters exhibit higher degree of axial mixing. This can be explained by the presence of much eddies in such columns in addition to the wakes behind bubbles which mainly causes mixing in smaller columns.

According to the turbulence theory and as suggested by Reith et al., Mixing

This behaviour can be explained in terms of the hindered gas bubble motion in viscous fluids. In which at relatively low viscosities, drag forces are not large enough to cause bubble coalescence. Moreover, these moderate forces could contribute to more uniform distribution of bubbles giving rise to higher gas holdups. Higher drag forces, however, promote coalescence resulting in lower gas holdups. This latter explanation was observed visually in this work in an experiment in which 99% glycerol was used. In this case very large deformed bubbles were observed even at the lowest gas velocities. This was also mentioned recently by Carbtree and Bridgwater (6).

From Figure 5 it can be seen that increasing the surface tension of the continuous phase is accompanied by a decrease of gas holdup. This can be explained in terms of bubble terminal velocity behaviour. According to Mendelson (15) and the wave theory, the terminal velocity of bubbles is proportional to the square root of the surface tension. Hence increasing the surface tension results in higher terminal velocities with consequent lower gas holdup.

Variation of gas holdup for Water-air

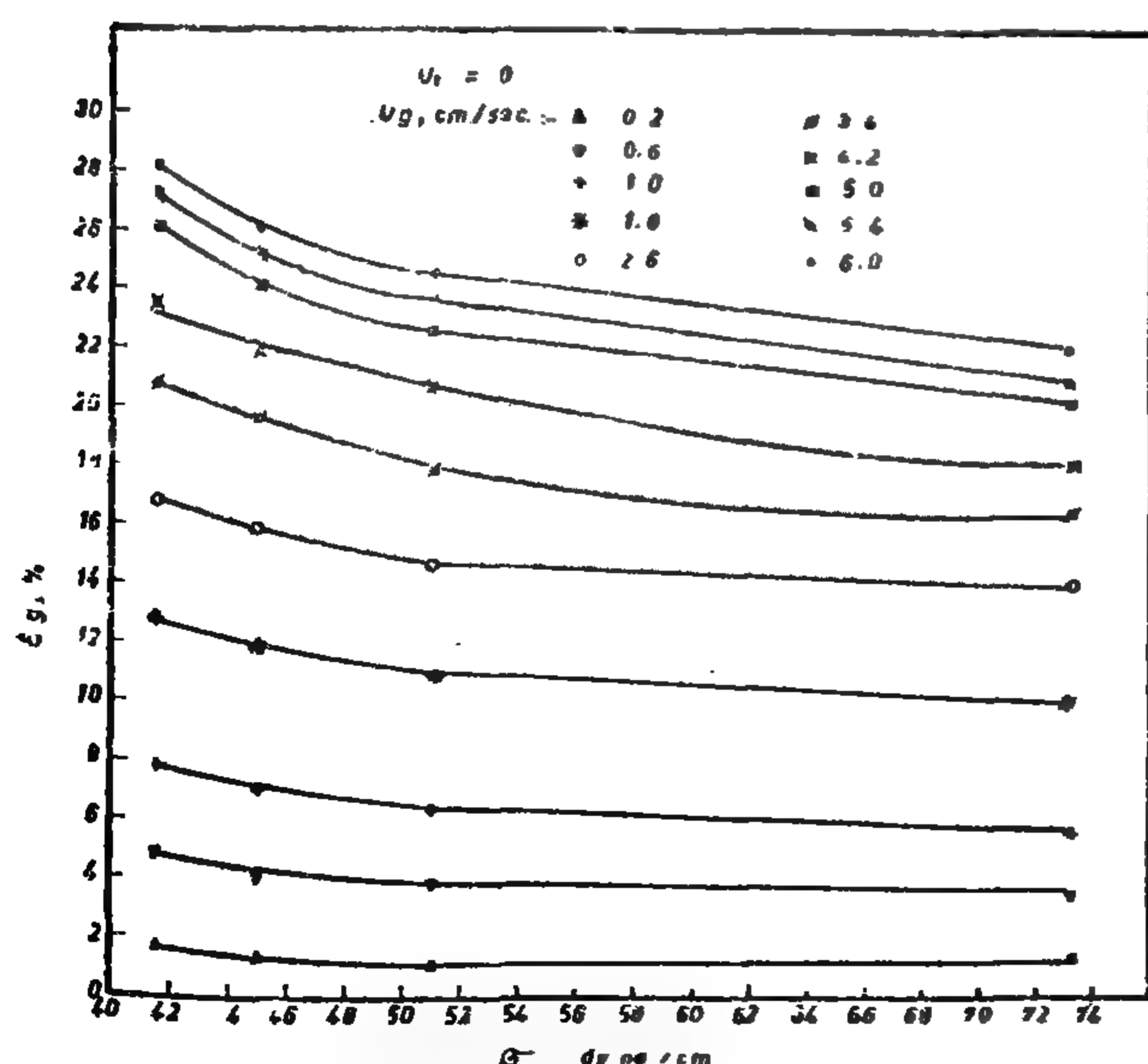


Figure 5. Variation of Gas-Holdup With Surface Tension.

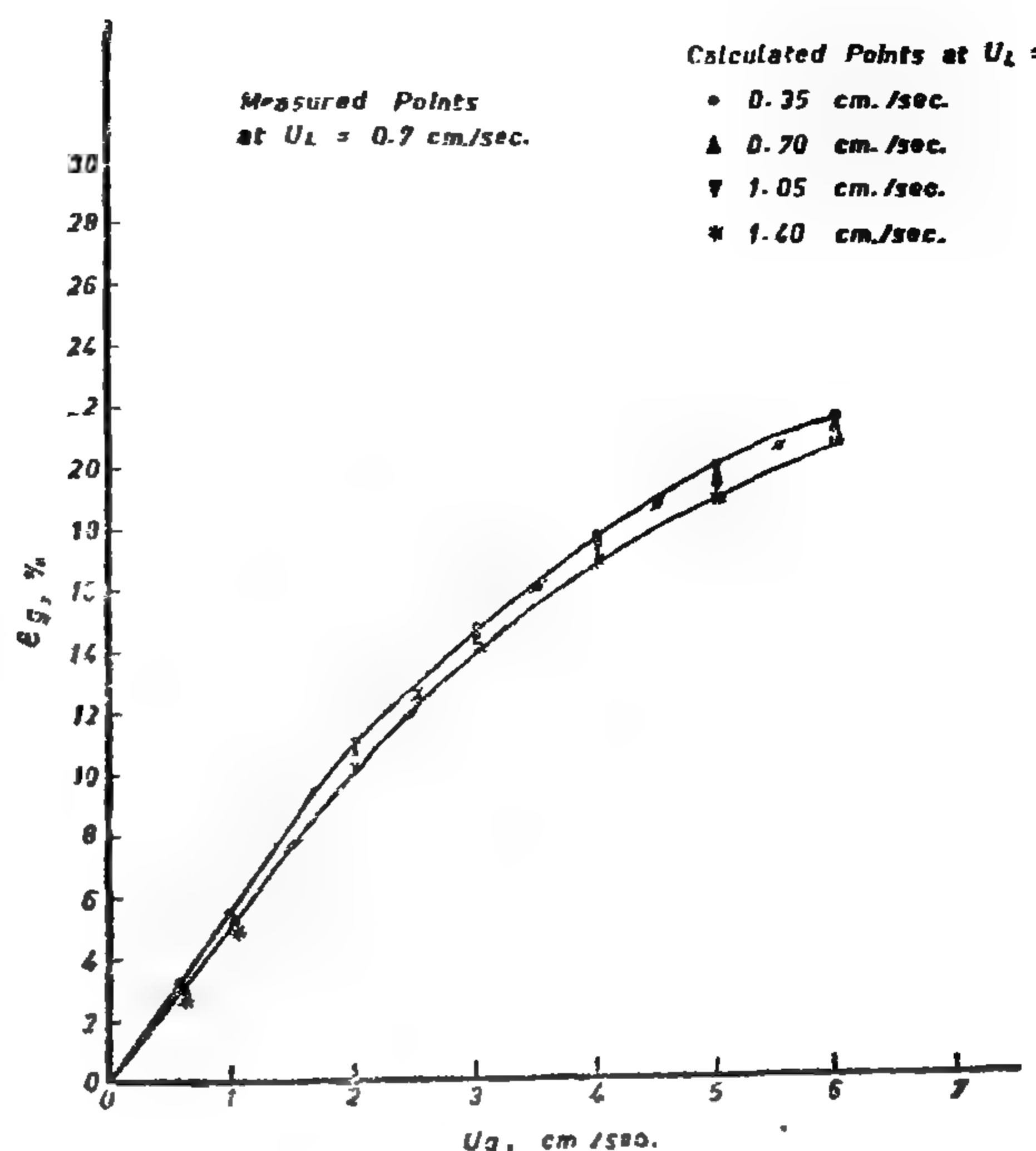


Figure 6. Calculated and Measured Gas-Holdup In Cocurrent Flow.

system for cocurrent and countercurrent cases can be seen in figures 6 and 7. In these figures holdups were calculated using the buoyant velocity component determined from the stagnant liquid measurements. A good agreement between measured and calculated values can be observed.

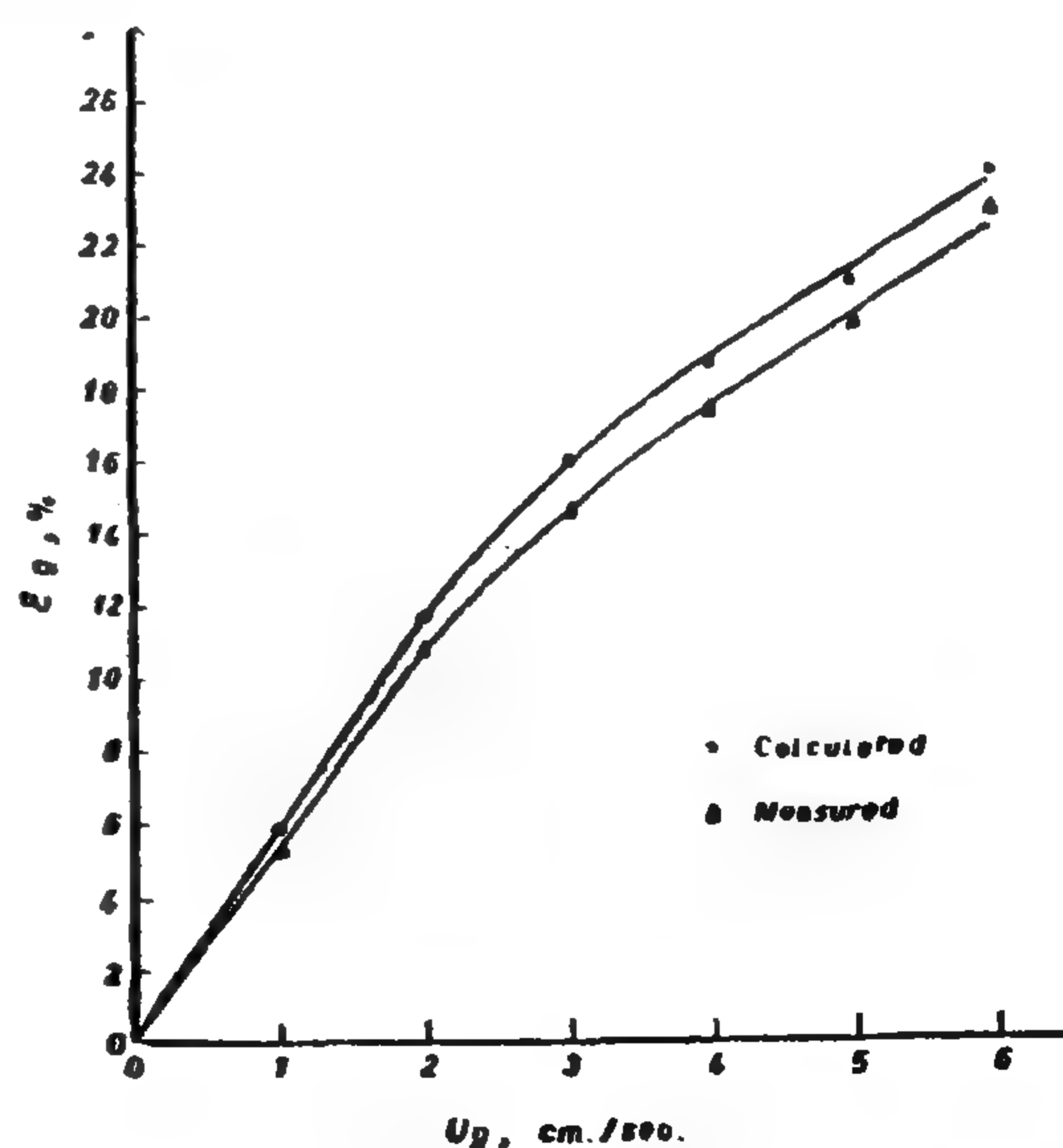


Figure 7. Measured & Calculated Gas Holdup For Counter-Current Flow at Liquid Velocity = 0.7 Cm./Sec.

Table 1

(water-glycerol)

Liquid No.	Viscosity cp	density, gm/cc	Surface tension dyne/cm
1	39.41	1.201	62.53
2	32.35	1.194	63.50
3	19.84	1.187	46.82
4	11.37	1.180	65.74
5	8.30	1.154	66.36
6	6.35	1.132	67.29
7	3.07	1.084	68.81
8	2.31	1.064	71.44
9	1	1	72.58

Table 2

(water-isopropanol)

10	1.7	0.982	41.5
11	1.61	0.985	45
12	1.42	0.990	51

From Figure 4, it can be seen that increasing the viscosity from 1 to about 11 cp is accompanied by increased gas holdup, reaching a maximum at about 3 cp and then decreasing more sharply at higher gas velocities. From about 11 cp till 39 an almost constant slow rate of gas holdup decrease with gas velocity is observed.

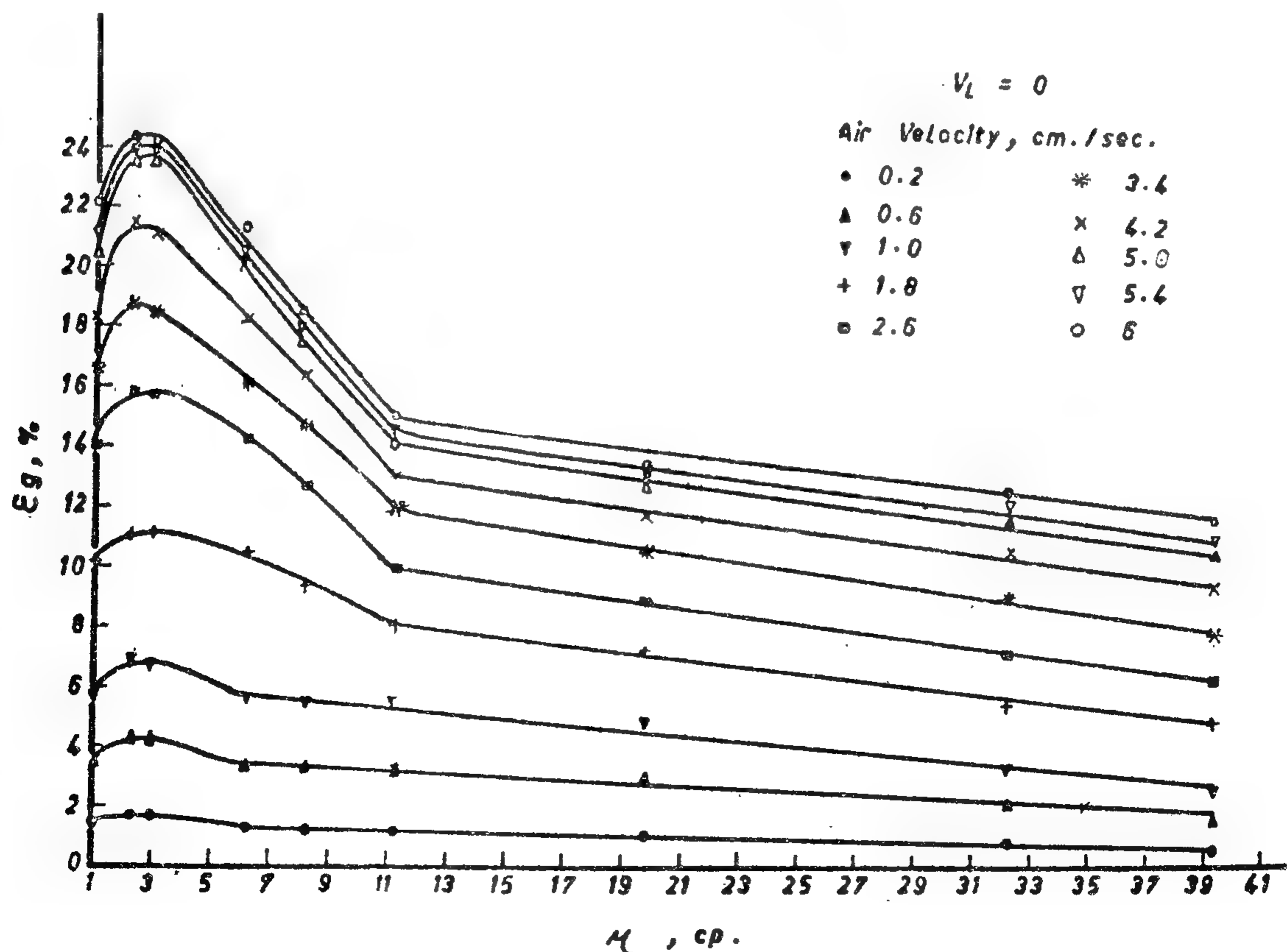


Figure 4 . Variation of Gas - Holdup With Liquid Viscosity .

For backmixing, the injection tube was inserted at the top or at the bottom of the test section pending whether the flow is cocurrent or countercurrent respectively, so as to provide a long axial measuring distance. The direction of the injection slot was always pointing up in the direction of the bulk flow. Attainment of already-state conditions was established by the constancy of the measured liquid conductivity at the column exit. Sampling of about 20 c.c/min.

was used. To have good representative samples a large amount of about 250 c.c. was collected at each investigated axial position.

RESULTS AND DISCUSSION.

A. Gas-holdup.

For a stagnant liquid, the variation of gas-holdup with gas velocity for some different liquid physical properties can be seen from figures 2 and 3. Table s 1 and 2 contain the properties of the used liquids.

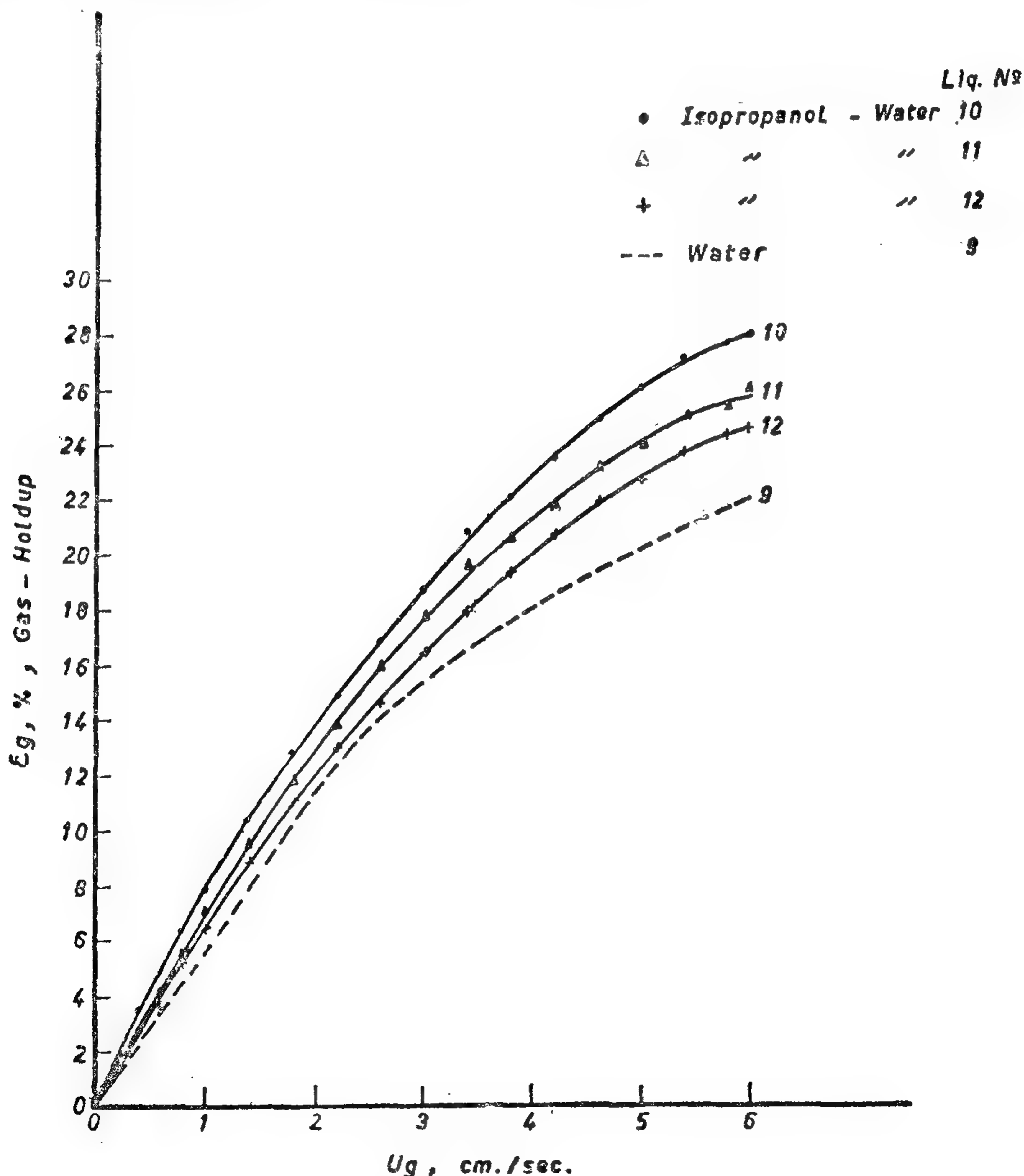


Figure 3 . Variation of Gas-Holdup With Gas Velocity For Water-Isopropanol Solutions .

an oil catcher, throttling valve, regulating valves, a set of rotameters, sudden stoppage magnetic valve, and then to the bottom of the column through a perforated stainless steel plate having 200 holes each of 2 mm. in diameter.

Water from mains passes through 1.5 m³ tank, a constant head feeding column, a pump, sudden stoppage magnetic valve, regulating valve rotameter, and then to the column either at the top or at the bottom through strainers pending whether the operation is countercurrent or cocurrent respectively.

The concentrated sodium chloride solution used as a tracer flows from a constant head feeder aided by a centrifugal pump to the column through an orifice meter, a U-tube manometer, and an injection tube. It has a slot of 2 mm. Width and 6 cm long so that the tracer can be injected over the central core of the column.

The test section of the column contains 19 radial openings for sampling, injection, and pressure drop measurements, each is at an axial distance of 5 cm from the other. Stainless steel tubes of 5 mm. outer diameter are used for sampling and injection, each can be radially moved from column wall to its center.

Concentrations of sodium chloride in the liquid phase were measured by conductivity transmitter (Philips type PR 9507) connected to a millivolt meter and an electrode (Philips type PW 9513).

PROCEDURES

In the case of stagnant liquid, average gas holdup, ϵ_g , was determined by measuring the height of the aerated liquid, H , and that of the clear liquid without aeration, H_0 , and applying :

$$\epsilon_g = (H - H_0) / H$$

It is to be noted that particularly at higher gas rates foam formation is considerable at the top of the column for most water-glycerol, water-isopropanol, and water-diesel oil systems. In these cases, H , was taken as the height of the aerated liquid level having a continuous surface as seen through the column wall.

Estimation of gas holdup was also done from pressure drop measurements across the test section of the column assuming that frictional head loss contribution is negligible compared to static head. This was justified in a previous work (12)

In countercurrent and cocurrent cases, holdups were also determined both by pressure drop measurements and heights of interfaces using sudden stoppage valves. Estimation was also done by the use of the buoyant velocity component concept (13).

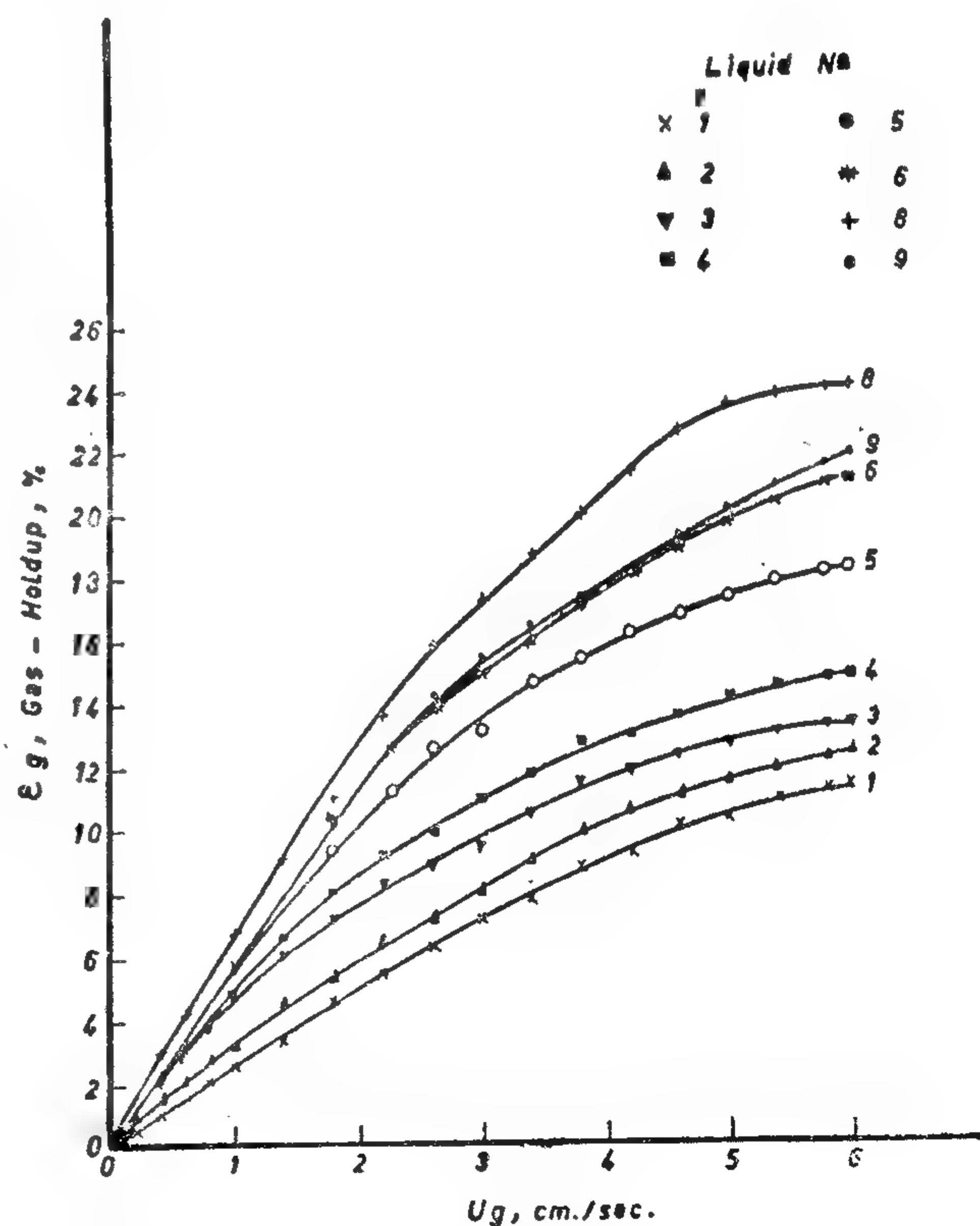


Figure 2 . Variation of Gas-Holdup With Gas Velocity For Water - Glycerol Solutions .

Diboun and Schügerl, and Afsher et al. published a three part series on axial mixing in cocurrent bubble columns. The steady-state tracer injection technique was used for the evaluation of axial mixing in both gas and liquid phases. Also Schügerl recently (20) published a review for multi-phase systems.

Reith et al. used 5.08, 14, and 29 cm column diameters for their investigations of axial dispersion at high gas velocities up to 45 cm/sec. They found that Pecelt number based on the relative velocity is constant for the 14 and 29 cm in diameter columns.

Eissa et al. investigated in a 5 cm in diameter column axial and adial mixing in cocurrent and countercurrent flow using the different dispersion models at gas velocities up to 8 cm/sec. It was concluded that the single-parameter axial dispersion model is adequate for characterizing the extent of mixing in terms of the axial dispersion coefficient.

Towel and Ackerman used large columns of 40.64 and 106.68 cm in diameter and studied the effect of column height and sparger type at different gas and liquid rates. A correlation for scaling up was proposed.

Shinichiro et al. studied axial mixing by large gas bubbles for cocurrent and countercurrent cases in 5 and 10 cm in diameter columns using the pulse injection technique. The mixing coefficients range from 5 — 20 cm²/sec for gas velocities 0.07 — 8 cm/sec. in the 5 cm column and 9 — 45 cm²/sec. for the 10 cm column in approximately the same gas range. It is however beleived that their columns are too short to measure axial mixing without much interference of end effects.

EXPERIMENTAL SETUP

A Schematic diagram for the experimental setup used is shown in Figure 1. Air from laboratory lines passes through

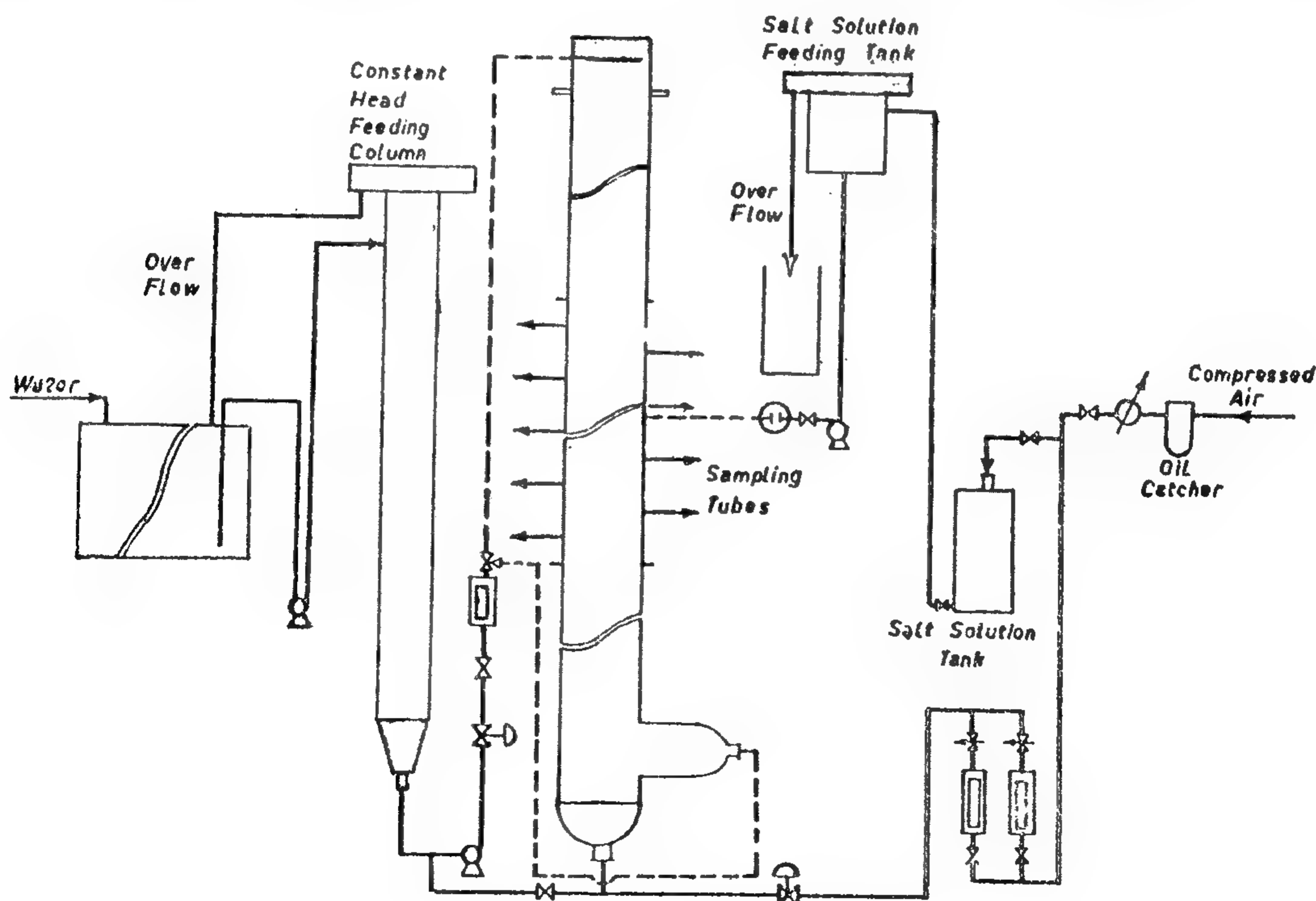


Figure 1. Experimental Setup .

HOLDUPS AND BACKMIXING INVESTIGATIONS IN COCURRENT AND COUNTERCURRENT BUBBLE COLUMNS

By

Dr. SHERIF H. EISSA* and K. SCHUGERL

SUMMARY

In a 15.9 cm in diameter and 390 cm in height glass column the effect of some liquid physical properties on gas-holdup was investigated. Oil emulsions were also employed. Data were obtained for the variation of the effective axial dispersion coefficient with gas and liquid velocities. The steady-state tracer injection technique and the axial-dispersed-plug-flow model were used. Results were compared with literature data for both smaller and larger columns.

INTRODUCTION AND PREVIOUS WORK

In spite of the industrially growing importance of bubble columns, relatively few recent studies have been reported on such equipment. Moreover, the published information and data seem to be to a practically large extent not consistent.

Concerning holdups, Duckler et al. (9) compiled nearly all the existing data on two-phase flow and checked the validity of the various proposed empirical correlations. They found that Hughmark's correlation (16) represents the existing data better than any other correlation. In a latter work (10) it was found to have considerable deviations. Hughmark (17) presented another correlation that considers the effects of both liquid surface tension and specific gravity. No terms liquid viscosity were included. Mendelson (15)

presented equations using the wave theory for holdup prediction which also did not include viscosity terms.

Axial mixing was studied in terms of dispersion models by Siemes and Weis (22), Argo and Cova (4), Bischoff and Philips (5), Diboun and Schugerl (7,8), Afsher et al. (1), Reith et al. (19), Eissa et al. (10,11), Towel and Ackermann (23), and recently by Shinichiro et al. (21).

Siemes and Weis used transient-state measurements to evaluate longitudinal mixing in 4.2 cm in diameter column with no liquid flow at gas velocities ranging from 1.6 to 6.4 cm/sec., axial dispersion coefficients of values from 2.5 to 65 were obtained using a simplified diffusion-type model.

Argo and Cova employed the steady-state injection technique and the axial coefficients were calculated using the axial dispersion model. Column diameters investigated were 4, 6, 10 and 45 cm. at gas velocities from 7 to 20 cm/sec. for the countercurrent case and 1.3 to 6.5 cm/sec. for the cocurrent case.

Bischoff and Philips obtained residence time distribution data in orifice-plate gas-liquid reactors for different plate designs. They calculated axial dispersion coefficient and proposed a correlation for their, as well as others, results.

* Institut of Technical Chemistry — Technical Univ. of Hanover.

** Present address : National research center, Cairo, Arab republic of EGYPT.

RAWMATERIALS & GHEMICAL INDUSTRIES

**INST. OF TINING, PETROLEUM &
METALLURGICAL ENGINEERS —
INST. OF CHEMICAL ENGINEERING**

CONTENIS

GENERAL SECTION :

BULDING & CONSTRUCTION	INDUSETY & PRODUCTION	RAW MATERIALS & CHEMICAL ENGINEERING
(ARABIC)	(ARABIC)	(ARABIC)
— Tall buildings news Dr. G. NASSR 4	— Application of mana- gement systems. Dr. A. EL-HEFNY ... 90	— Technology and sand- lime bricks Y.A. ABOHASSEIN 128
— The Influence of tec- hnology on archie tural-creativity, town planning & society -3- Dr. T. ABDEL-GA- WAD 17		
—O—	—O—	—O—
(ENGLISH)	(ENGLISH)	(ENGLISH)
— Preliminary hydrogeo- logical reconnaissance Prion. to the Perfor- mance of Pumping tests & its application in some localities of Egypt By. Dr. M.S. SALAWI 38	— A NEW Proposed te- chnique for transient stability study of Mul- timchine systems By. Dr. M.M. SALLAM, Dr. M.Z. GHONEIM Eng. M.M. EL-HIN- DAWI 92	— Holdup & Backmixinc investigations in co- current & counter- current bubble columns By Dr. S.H. EISSA & K. SCHUGERI 141
— Contribution to bow g.rders with interme- diate supports By. Dr. M.M. EL- HAHIMY & Dr. A.S. MAHDY 51	— Analytical determina- tion of the divections of doubly refracted rays in a uniaxial cr- ystal. B. Dr. M. SAMEH. SAID 109	

JOURNAL OF THE EGYPTIAN SOCIETY OF ENGINEERS

VOL. XIV.

ISSUE No. 3 — JUL — AUG — SEPTEMBER 1975)

EDITING BOARD

Editor

Dr. S. MORTADA

Assist. Editor &
Treasurer

Dr. G. NASSAR

Dr. H. AMER

Eng. T. ABD EL-GAWAD

Dr. F. BAHGAT

Dr. S. EL-SOBKY

Dr. M. ABU-ZIED

Dr. M. E. SELIM

Eng. A. EL-ASFORY

- Issued Quarterly Contributors are invited to submit material for editorial consideration addressed to the Editor. The Journal cannot accept responsibility for loss or damage to any material.

INSTRUCTIONS FOR AUTHORS OF ARTICLES

- The Journal publishes articles contributing to the advancement of engineering science and applications.
- Articles may be written in Arabic or English and presented in triplicate with an abstract in both languages.
- Authors' names to be given in full, together with their academic titles and professional occupation.
- Articles may not exceed 8 pages. In this respect, mathematical derivations may be abbreviated and tables replaced by curves.
- Curves to be drawn in black china ink, and to occupy half a page at most. Exceptionally, full page curves or plates are admitted. Curves presented will be scaled down to these sizes. Figures & lettering on curves should not be less than 3 mm even after scaling down.
- References to be given at the end of each article and classified alphabetically according to author's name followed by the name of the journal or book and the date of issue.
- Authors will be presented with two proofs, the first one accompanied by a correction convention chart to ease the work of type correction.

Society Subscriptions

Member	200 P.T.
Associate member	150 P.T.
Associate	100 P.T.

Magazine Subscriptions

Society members Free	
Engineers subscriptions	100 P.T.
Non-engineers subscription	300 P.T.
Organisations subscriptions	500 P.T.

ADVERTISING AGENT

Moassasset Misr for Printing and Publication
10, Souk El Tawfikieh Str. Cairo. Tel. 72192

مجلة جمعية المهندسين المصرية

العدد الرابع (أكتوبر - نوفمبر - ديسمبر ١٩٧٥)

المجلد الرابع عشر

هيئة التحرير

رئيس التحرير

دكتور سيد مرتضى

سكرتير التحرير

وأمين الصندوق

دكتور جمال الدين نصار

مهندس توفيق أحمد عبد الجواد

دكتور حامد حسنين عامر

مهندس عبد الملك العصفورى

دكتور فؤاد بهجت

دكتور صلاح السبكى

دكتور محمود أبو زيد

دكتور محيى الدين سليم

- تصدر المجلة ربع سنوية
- ترسل النصوص المطلوب موافقة هيئة التحرير على نشرها باسم السيد / رئيس التحرير . وهو غير مسئول عن فقد أو تلف أى نص .
- تنشر المجلة المقالات التى تسهم فى رفع مستوى العلوم الهندسية وطرق ممارستها .
- تقبل للنشر المقالات باحدى اللغتين العربية أو الانجليزية ، على أن تقدم من ثلاث نسخ مكتوبة على الآلة الكاتبة ومعها ملخص بكل من اللغتين .
- تذكر أسماء أصحاب المقالة كاملة باللغتين ومعها ألقابهم العلمية ووظائفهم .
- يراعى ألا تتجاوز المقالة ٨ صفحات بالمجلة ، وفى سبيل ذلك يختصر الاشتقاق الرياضى ويستعاض عن الجداول بمنحنيات مرسومة بالحبر الشينى الأسود ، على أن يشغل المنحنى نصف صفحة على الأكثر ولا يشغل صفحة كاملة إلا فى حالات استثنائية وسيصفى أى منح إلى تلك المقاسات .
- ويراعى ألا يقل ارتفاع الحروف أو الأرقام على المنحنيات المنشورة عن ٣ مم بعد التصغير .
- يعنى بذكر المراجع المستقى منها المقال وتصنف تبعاً لاسم المؤلف ثم العنوان ثم المجلة أو الكتاب وتاريخه .
- تقدم لصاحب المقال تجربتان للطباعة وتفرق بالأولى نسخة من مصطلحات التصحيح التى يؤدى اتباعها إلى رفع كفاية التصحيح وتقليل الوقت الضائع فيه .

اشتراكات الجمعية :

العضو

العضو المنتسب

اشتراكات المجلة :

يتلقى أعضاء الجمعية نسخهم مجاناً .

ولغير الأعضاء :

الاشتراك السنوى للمهندسين

الاشتراك السنوى لغير المهندسين

الاشتراك السنوى للهيئات

تعطى أولوية النشر بالمجلة للسادة الزملاء

أعضاء جمعية المهندسين المصرية

الاعلانات :

مؤسسة مصر للطباعة والنشر

القاهرة ١٩ شارع سوق التوفيقية ت ٧٢١٩٢

رقم الايداع بدار الكتب ١٩٧٥/٢٩٨

محتويات العدد

التشييد والبناء	التصنيع والانتاج	الخامات الأولية والصناعات الكيميائية
القسم العربى :	القسم العربى :	القسم العربى :
<ul style="list-style-type: none"> الاقصاد والمشاريع الهندسية . دكتور جمال نصار ٩ العمارة المصرية القديمة : دكتور سيد كريم ١٠ تقييم مشروع الصرف المغطى بدلتا نهر النيل دكتور محمود أبو زيد ١٥ 	<ul style="list-style-type: none"> المدخل لاستخدام مفهوم المكعب فى منظومات المعلومات الادارية . دكتور حامد كمال الدين ٨٤ تحسين كفاءة الطاقة الشمسية . دكتور عبد الحليم محمود شوشة مهندس محمد عبد الجواد ٩٠ حسابات الطاقة الكهربائية المتبادلة بين الانظمة المترابطة دكتور فاروق صمويل ثالث ٩٨ حساب انتقال الحرارة فى الافران المستمرة الاشتعال . دكتور محمود الزاهر محمد ١٠٥ 	<ul style="list-style-type: none"> تحلل اكسالات تيتانيل الباريوم وتقييم تيتانات الباريوم المحضر عند درجات حرارة مختلفة . دكتور محمد نبهان سويلم ودكتور احمد مراد جاد الله ١٤٣
القسم الأفرنجى :	القسم الأفرنجى :	القسم الأفرنجى :
<ul style="list-style-type: none"> أفضل منحني لتمثيل تصرف نهر النيل الطبيعى . دكتور مصطفى الجيزاوى ودكتور محمود أبو زيد ٣٤ دراسة عملية وحقلية لبعض أنواع التربة المنتفخة فى مصر . دكتور عبد الرحمن الرملى ودكتور مصطفى الدميرى ٤٢ المياه المكتسبة فى نهر النيل من الخزان الجوفى دكتور محمد حمدي الكاتب ومهندسة فاطمة عبد الرحمن ٥١ دراسات اقتصادية للأسقف المعلقة . دكتور احمد محرم ودكتور سفيان عبد الجواد والمهندس حسن حجاب ٥٩ 	<ul style="list-style-type: none"> المدخل لاستخدام مفهوم المكعب فى منظومات المعلومات الادارية . دكتور حامد كمال الدين ٨٤ تحسين كفاءة الطاقة الشمسية . دكتور عبد الحليم محمود شوشة مهندس محمد عبد الجواد ٩٠ حسابات الطاقة الكهربائية المتبادلة بين الانظمة المترابطة دكتور فاروق صمويل ثالث ٩٨ حساب انتقال الحرارة فى الافران المستمرة الاشتعال . دكتور محمود الزاهر محمد ١٠٥ 	<ul style="list-style-type: none"> تحلل اكسالات تيتانيل الباريوم وتقييم تيتانات الباريوم المحضر عند درجات حرارة مختلفة . دكتور محمد نبهان سويلم ودكتور احمد مراد جاد الله ١٤٣

التشييد والبناء

جمعية المهندسين المدنيين
جمعية المهندسين المعماريين
جمعية مهندسي الري

runs its completion date will cost more in that the contractors may be able to claim extra cost for delays, because working capital is in use over a long period, and because of the social cost of the loss of use of the completed project.

For all these strategies effective planning and management of the design and construction of the whole project is vital. The large construction project is complex, involving many different parties including many types of designers and specialist contractors and many material inputs. It is because of this complexity that management is so important, yet the amount of management used is often much less than for the equivalent value of turnover in manufacturing industry.

The choice of the method of letting the contract is important and so too is its effect on the local Egyptian industry. It is preferable to use local contractors where possible so that the Egyptian in-

dustry may be allowed to develop. Where this is not possible efficient expatriate contractors must be chosen. For this purpose it is essential to invite only a few contractors to tender. The costs of estimating and tendering are high and good contractors will not compete if their chances of success are low. Four contractors are enough for most purposes and eight should be the maximum. Expatriate contractors should be required as part of their contract to train Egyptian counterparts and if for this reason the project costs a little more, it will be money well spent for its long-term benefits.

Overall engineers should consider not only apparent money costs but also the real resources of men, materials and management which will be required, their likely availability and the long-term community costs of their use.

G. NASSAR

ECONOMICS AND THE CONSTRUCTION PROJECT

By

Dr. G. NASSAR*

after a lecture given by

Dr. PATRICIA HILLEBRANDT**

ECONOMICS AND THE CONSTRUCTION PROJECT

Economics is concerned with the allocation of scarce resources between alternative uses. Most people think economics is about money but money often obscures the real problem to be faced that is, to make the best use of the resources we have.

The scarce resources in Egypt seem to be skilled men, managements, some materials, foreign currency and capital. On the other hand unskilled labour and some materials are in plentiful supply while Egypt also appears to have a sufficient supply of university graduates in engineering and other subjects.

The objective of engineers in relation to the project is to construct it at as low a cost as possible and in as short a time as possible. They are concerned mostly with money cost but should take into account wherever possible the real costs to the community as whole including for example their effect in creating a healthy Egyptian industry. Moreover it is of little point to have a low estimated cost if the shortage of available resources will mean that the project is delayed. Time is important because it is only the finished product in use which benefits the client and the community. A large number of uncompleted projects which have used

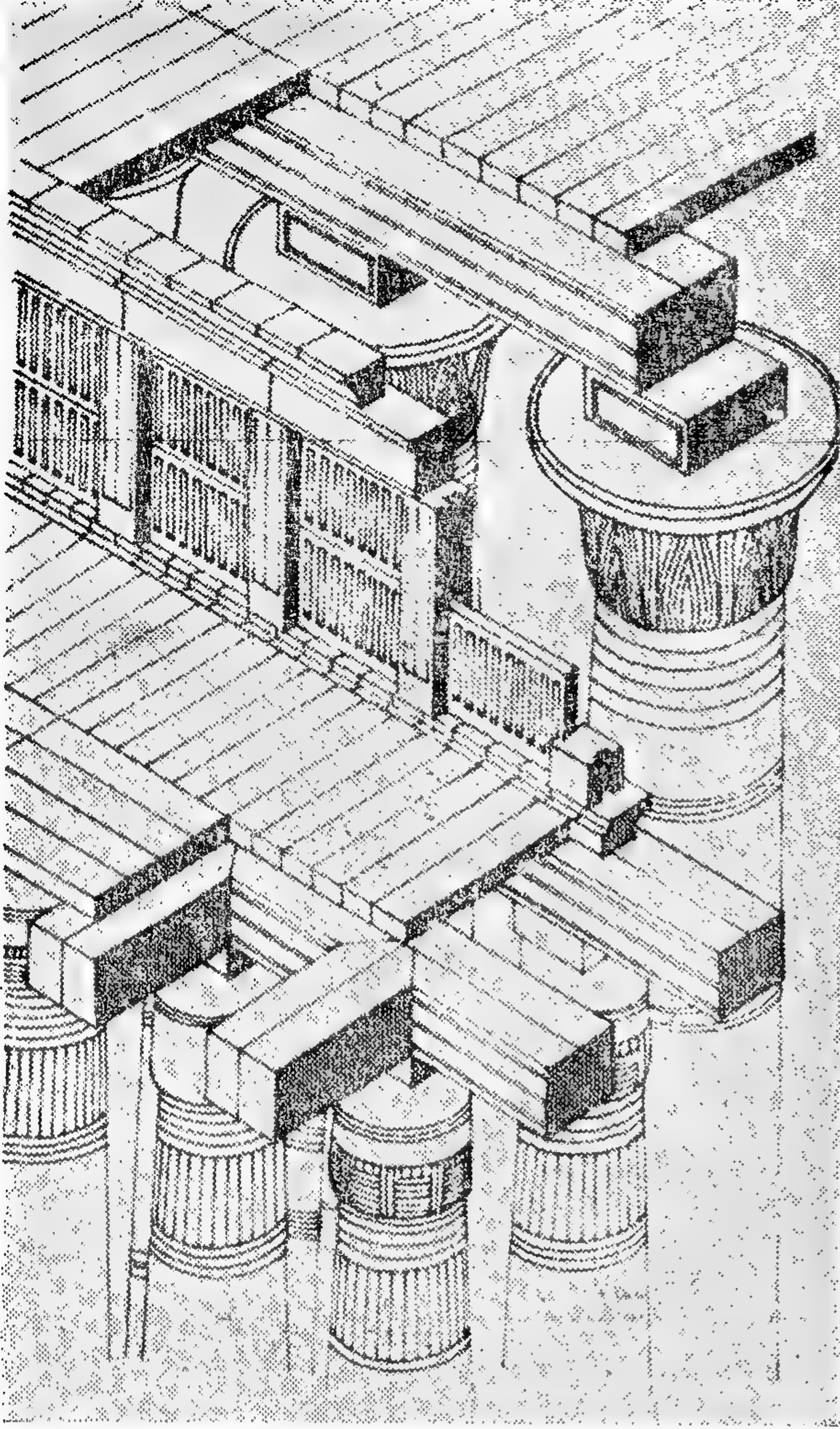
design and management skills as well as scarce materials and skills represent a waste of these resources which could more effectively have been concentrated on fewer projects to completion stage.

To achieve this objective various strategies have to be considered. At the design stage the availability of resources and the methods of production must be decided. Choice has to be made, for example, between labour intensive and capital intensive production; between buildings with a high initial cost and low maintenance or low initial cost and high maintenance; between the use of advanced imported components or more simple locally produced ones. Such choices cannot be based on money costs only. For example the low initial cost/high maintenance choice may be cheaper in money costs but this is irrelevant if the client will not in practice undertake the necessary maintenance work. Similarly imported components may apparently be cheaper in money terms but if the foreign exchange for them is not available the real cost in terms of delay may be much higher and the cost to the community of using imported components is also high because it takes away scarce foreign exchange from other sectors where its benefit might be higher.

The time period of construction is very important because a project which over-

* Faculty of Engineering, Ain Shams Univ.

** Univ. College, London.



□ العمارة المصرية القديمة

دكتور سيد كريم

THE EGYPTIAN ARCHITECTURE
& THE SKYLINE OF CIVILISATIONS

Dr. SAYED KARIM

• تتجمع جميع نظريات الهيكل الانشائي في بهو الأعمدة
بالكرنك بالأقصر - الأعمدة والكرات الرئيسية والفرعية
والبلطات والأضواء العلوية .

● العمارة هي مرآة الحضارة .

مصر مهد الحضارات رسمت بمهاراتها خط
السماء أو الخط البياني الذي أطلق عليه شريط
تسجيل ضربات نبض المدن .

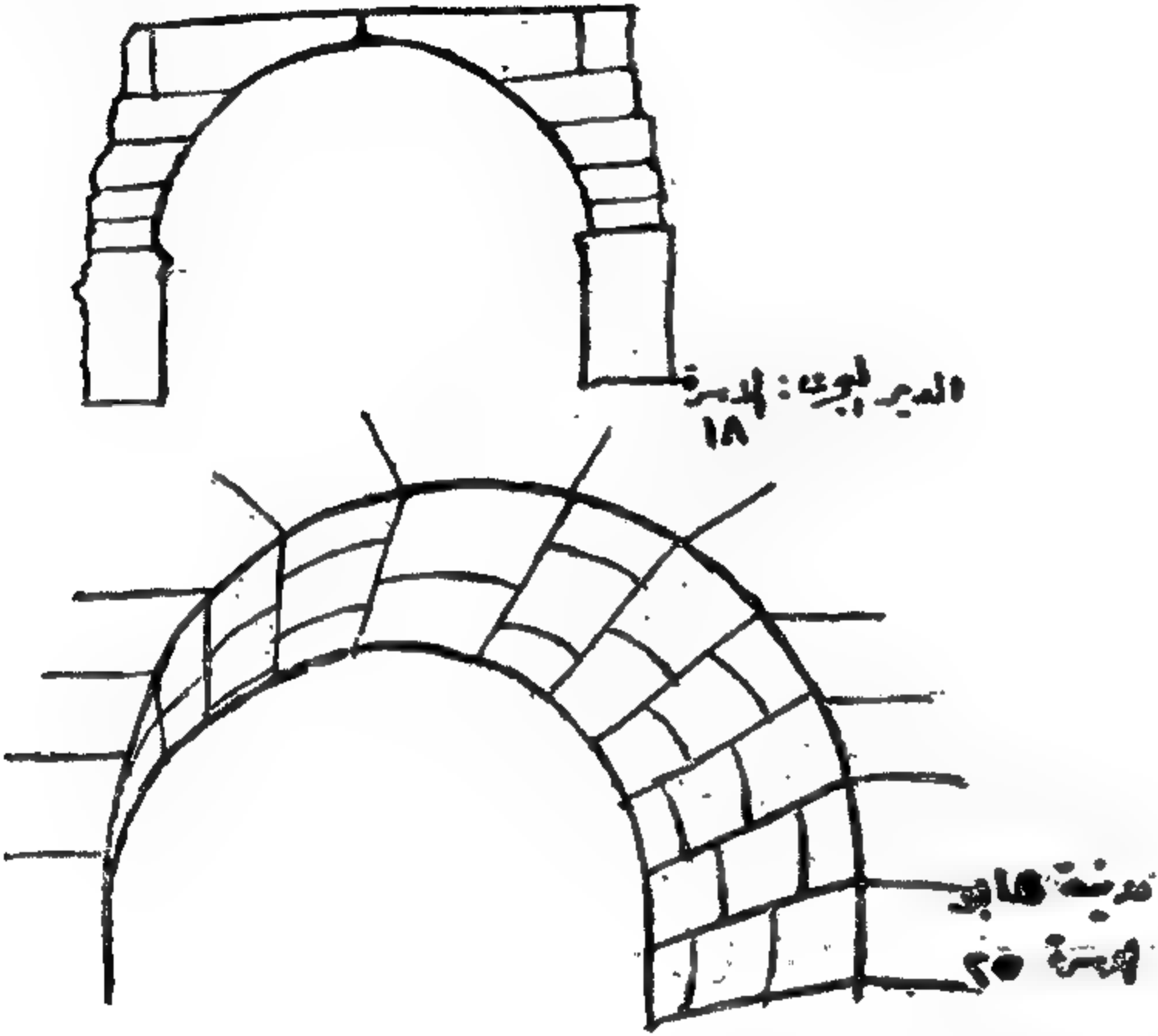
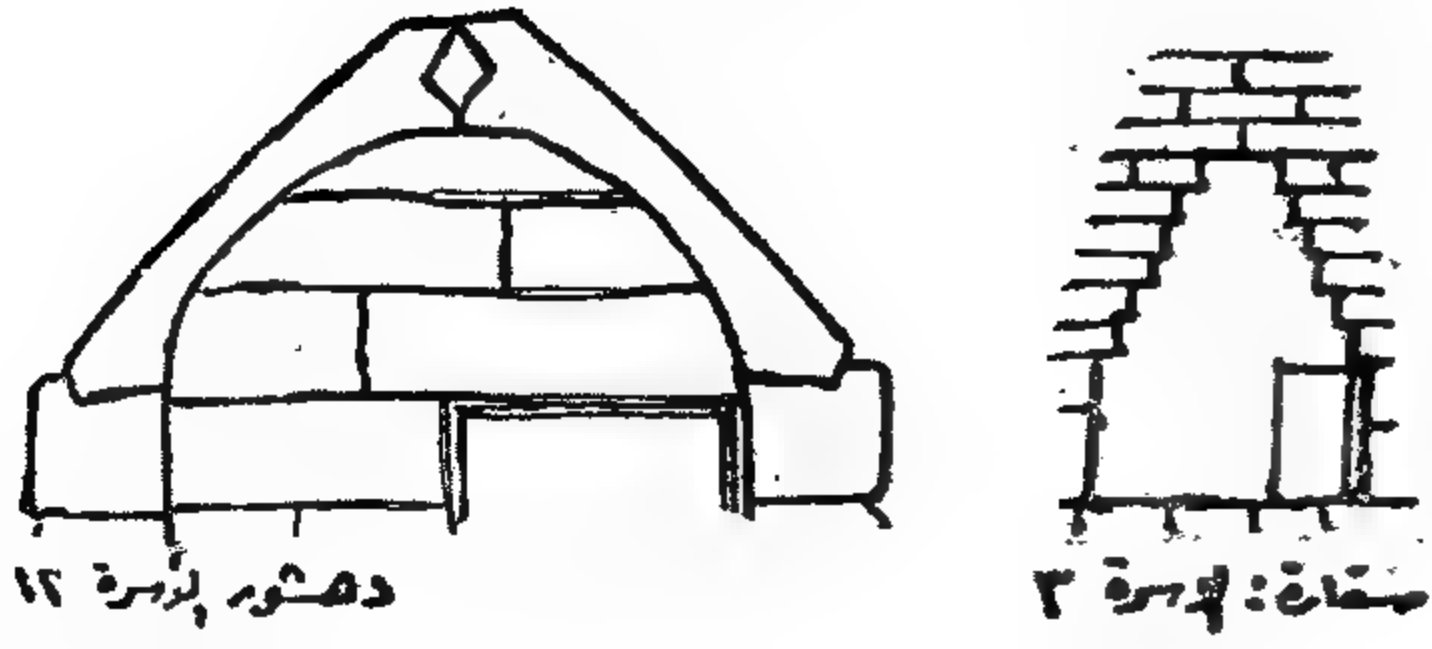
ان خط السماء هو الخط الذي تشكله قمم
المرتفعات فيفصل بين الأرض والسماء رسمته
الطبيعة بصخورها وجبالها وأشجارها . . ورسمته
يد الانسان بفنون عمارته . وكان المهندس المصري
القديم أول من شكل خطوطه الهندسية مع شروق
حضارته . ذلك الخط الذي بدأ بالسطوح الأفقية
التي غلت عن سطح الأرض ليعبر عنها بالمصاطب ،
وارتفعت متراصة فوق بعضها لتصنع الأهرامات
المدرجة التي تمثل سلم الصعود إلى السماء ومنها
إلى الأهرامات الهندسية والرياضية التكوينية
بأضلاعها المنحنية والمستقيمة وأسطحها الزخرفية
الملساء وارتفع الهرم بقاعدته عن سطح الأرض لتظهر

بوابات الشمس ثم يعلو فوق قائم يشق طريقه
نحو السماء لتظهر المسلات الرشيقة لتتناطح السحاب
وتكون أكثر قربا من السماء وتقربا إلى الإله .

ثم انتقلت العمارة من الحوائط العالية الضماء
إلى الدعامات والأعمدة التي تحمّل الأعتاب والكمرات
والأسقف وتصنيع أسس الهياكل الانشائية التي
تغيرت أبعادها ونسبها وتكويناتها تبعا لتغير مواد
البناء ونظريات انشائها فحددت طراز العمارة
الفرعونية ومراحل تطورها معالمها عبر التاريخ .

• ان تلك العمارة التي ارتفعت على شاطئ نهر
النيل وتجمعت في معرض طوله ألف كيلومتر يمتد
من شلالات أسوان الجرانيتية إلى شاطئ البحر
الأبيض المتوسط الرملية ليسجل تاريخ العمارة
المصرية خلال سبعة آلاف عام من عصر الانسانية .

• نشأة العقود وتطورها



• نشأة العقود وتطورها من الأسرة الثالثة الى الأسرة الخامسة والعشرين في العصر الفرعوني •

• ان خط السماء الذي رسمته العمارة الفرعونية من الصخور التي ترسب على شاطئ النيل ارتفع خلال أزمان بعيدة ليلقى ظلاله على ما ظهر حولها من حضارات فترك بصماته على طراز عمارة الاغريق والرومان منذ نشأتها وخلال تطورها .

ثم تابعت الشمس في غروبها لتعبر المحيط وتترك بصماتها على عمارة أمريكا في حضارتى المايا والأوزتيك فكانت الأهرامات بأنواعها وبوابات الشمس والمسلات أو ما رسم خط السماء في حضاراتها .

• كما تميزت الحضارة المصرية القديمة في جميع مقوماتها وعناصر تكوينها بارتكازها على البحث العلمى فكانت تلك المنجزات في علوم الطب والصيدلة والفلك والتنجيم والهندسة والرياضيات ومتحف علوم الحياة وفنونها ، وكذلك فن العمارة المصرية لم يكن وليد الاجتهاد والابتكار الفنى بل خلاصة تكنولوجيا علم البناء التي تعتبر نظرياتها جذور تكنولوجيا فن البناء وعلم الانشاء في مختلف الحضارات القديمة وامتدادها الى مدينة العصر الحديث .

لقد كان لمصر الفضل في وضع مثلث تكنولوجيا علم البناء للعالم أجمع ذلك المثلث الذي تتكون أضلاعه من :

١ - وحدة البناء : وهو قالب الطوب الذي شكله المهندس المصرى من ثمانية آلاف سنة من طمي النيل ثم من مختلف الأحجار بأبعاده الحالية وقدمه ليحتل مكانه في جميع الطرز المعمارية التي ظهرت في العالم ولا زال يحتل مكانه في العمارة العالمية الحديثة .

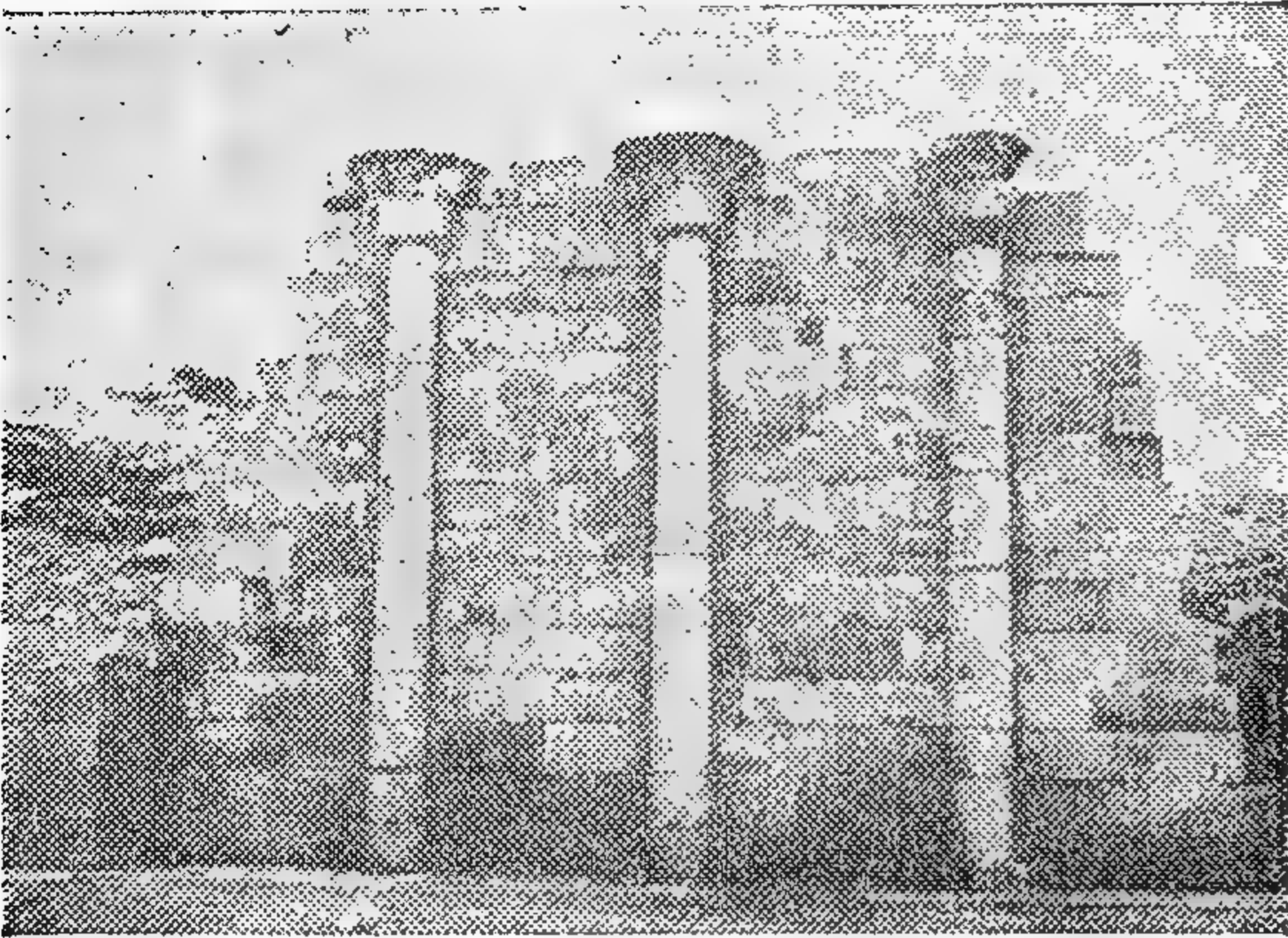
٢ - وحدة القياس : ابتداء من البوصة الهرمية الى الذراع المعماري وغيره من وحدات القياس وتقسيماتها العشرية والمئوية واستعمالها في تحديد حساب المسطحات والفراغ ووحدات كل منها مع ما ارتبط بها من نظريات رياضية .

٣ - وحدة التشكيل : ابتداء من الخط المستقيم الى مختلف الزوايا والدوائر والمنحنيات وتشكيلها وما ارتبط بها من نظريات هندسية .

بفضل تلك التكنولوجيا وعناصر تكوينها التي بدأت بقالب الطوب فخطط مبناه وفقا لتصميماته الهندسية والارتفاع بالحوائط في تكويناتها الهندسية الدقيقة العقود والقباب والقنوات التي توصل الى صناعتها في بادىء الامر بالطوب النيء .

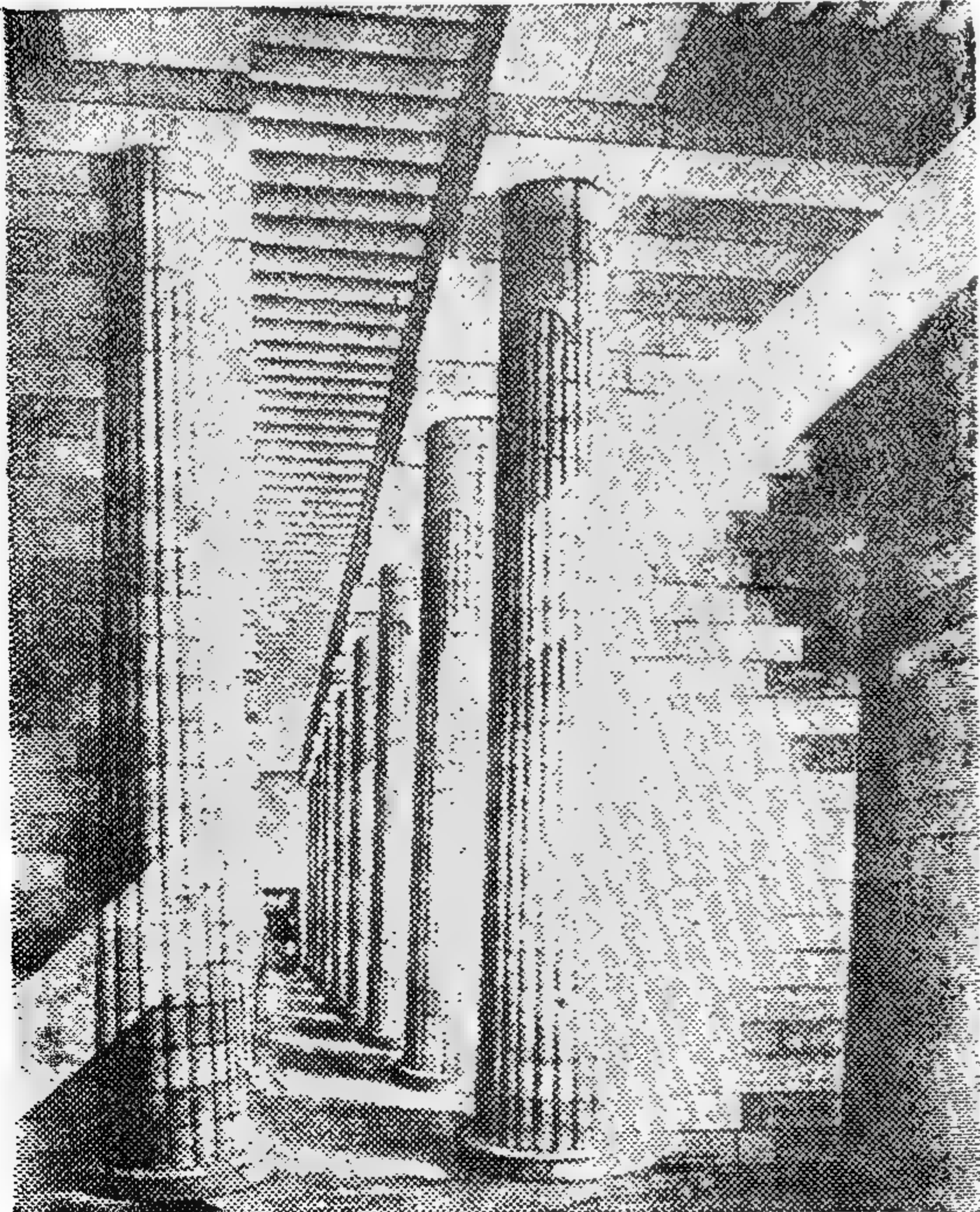


• معبد الرماسيوم في مدينة طيبة ، احد المخازن الملحقة بالمعبد . ويرى عقود الطوب في الوضع الطولى .



— أقدم أعمدة متوجة في التاريخ . أعمدة تيجان البردى
الرمز المميز لأسوار مدينة منف — الأسرة الثالثة .

• بهو الأعمدة في معبد زوسر الجانزي ومدينة الهرم
الدرج . أقدم مثل للأعمدة في العمارة المصرية الفرعونية
أخذت منه العمارة العالمية العمود الدورى الذى نقله
الاغريق عن مصر بعد ألفى سنة من ظهوره في مدينة منف



• كما كان المصرى القديم أول من اكتشف
الأعمدة التى تحمل الكمرات بدلا من الحوائط . لقد
أوحت اليه جذوع النخيل فكرة رفع الأسقف على
القوائم المتباعدة التى تحمل الأسقف ثم كسى جذوع
النخيل بالجبس والبياض لتصبح جزءا من المبنى
ثم تحول الى صناعتها من الطوب ثم الاحجار . .
ولم ينسى فضل النخلة التى أوحت له باكتشاف
فتوح أعمدته الحجرية بتاج يمثل زعف النخلة .

ويرجع اكتشاف المصرى القديم للأعمدة كوحدة
انشائية من وحدات العمارة الى عصر ما قبل
الأسرات ، اما نماذجها المعمارية المتطورة فقد بدأت في
كل من العصر العتيق والدولة القديمة . وكانت
الأعمدة من الطابع المميز لعمارة مدينة الجدار
الابيض واتخذت البوابة التى تحملها الأعمدة الدورية
شعارا لمدينة منف فظهر في مدينة منف ومعابد
سقارة العمود الدورى المفرز بالقنوات الراسية
والذى ظهر بعد ذلك في بنى حسن في الأسرة ١٣ ،
وانتقل منها الى اليونان ليصبح نواة العمارة
الاغريقية . ثم يظهر بعده العمود الايونى الذى نقله
الاغريق ايضا حيث يمثل تاجه لفاقتى البردى ،
وبعض أمثله اتخذ منحنياته الايونية من زخرفة
الابريق المرسومة على المساند التى ترجع الى عهد
تحتمس الثالث بالكرنك .

كما ان بقية التيجان النباتية كتيجان البردى
واللوتس والأعمدة المركبة من النباتات والزهور
الفرعونية انتقلت بدورها الى الأعمدة انكورثية في
أثينا وروما لتصبح من العناصر الأساسية في
العمارة الاغريقية والرومانية بعد استعمال زهور
الكانتس بدل اللوتس والنباتات الفرعونية وتنتقل
منها الى العمارة الأوروبية في عصورها المختلفة حتى
عصر النهضة .

ان الأعمدة التى تحمل رأس الاله حتحور وأعمدة
التماثيل في معابد دندرة وابو ستبل وجدت كلها
في العمارة الاغريقية والرومانية باسم الرياتيد .

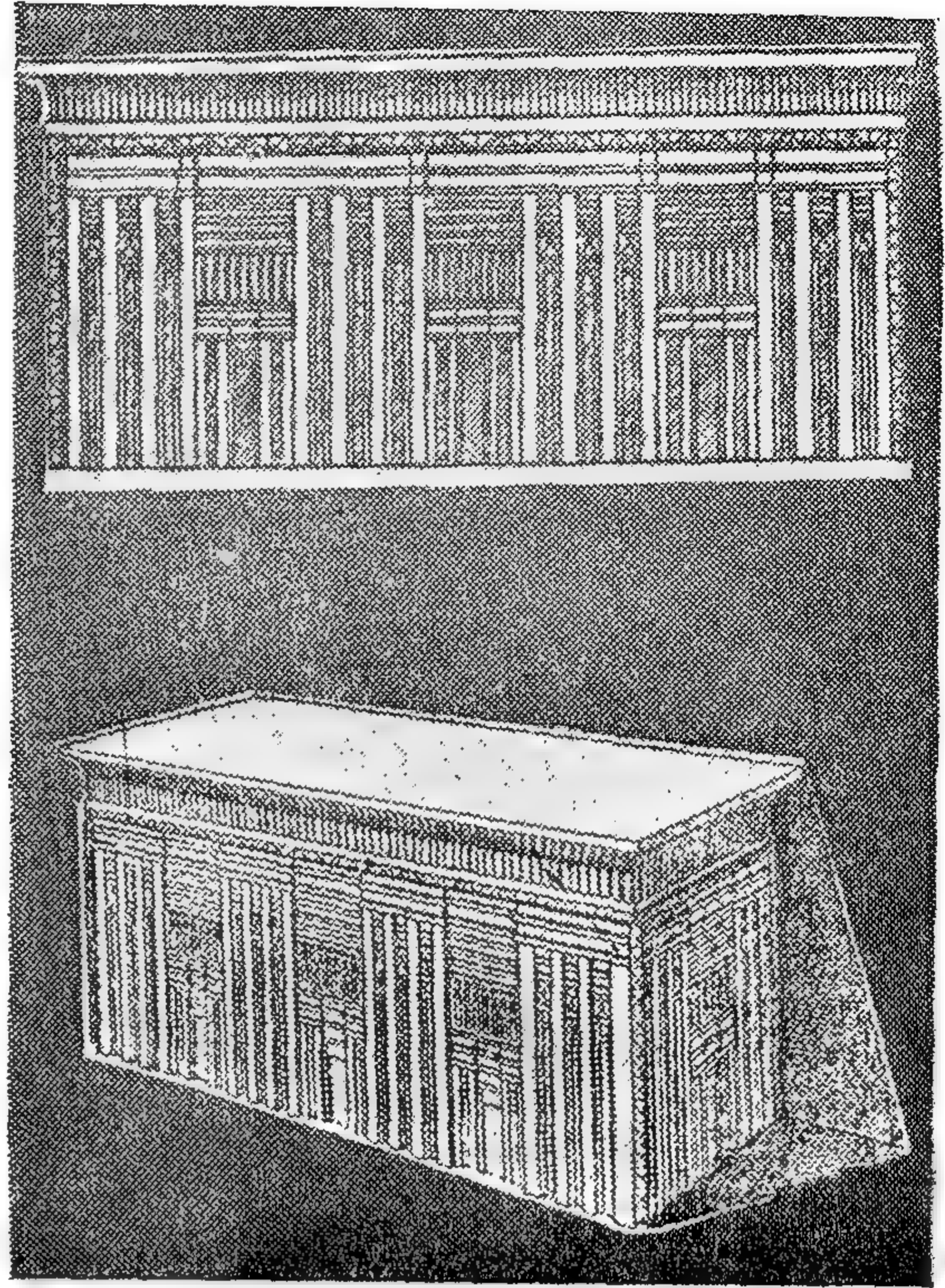
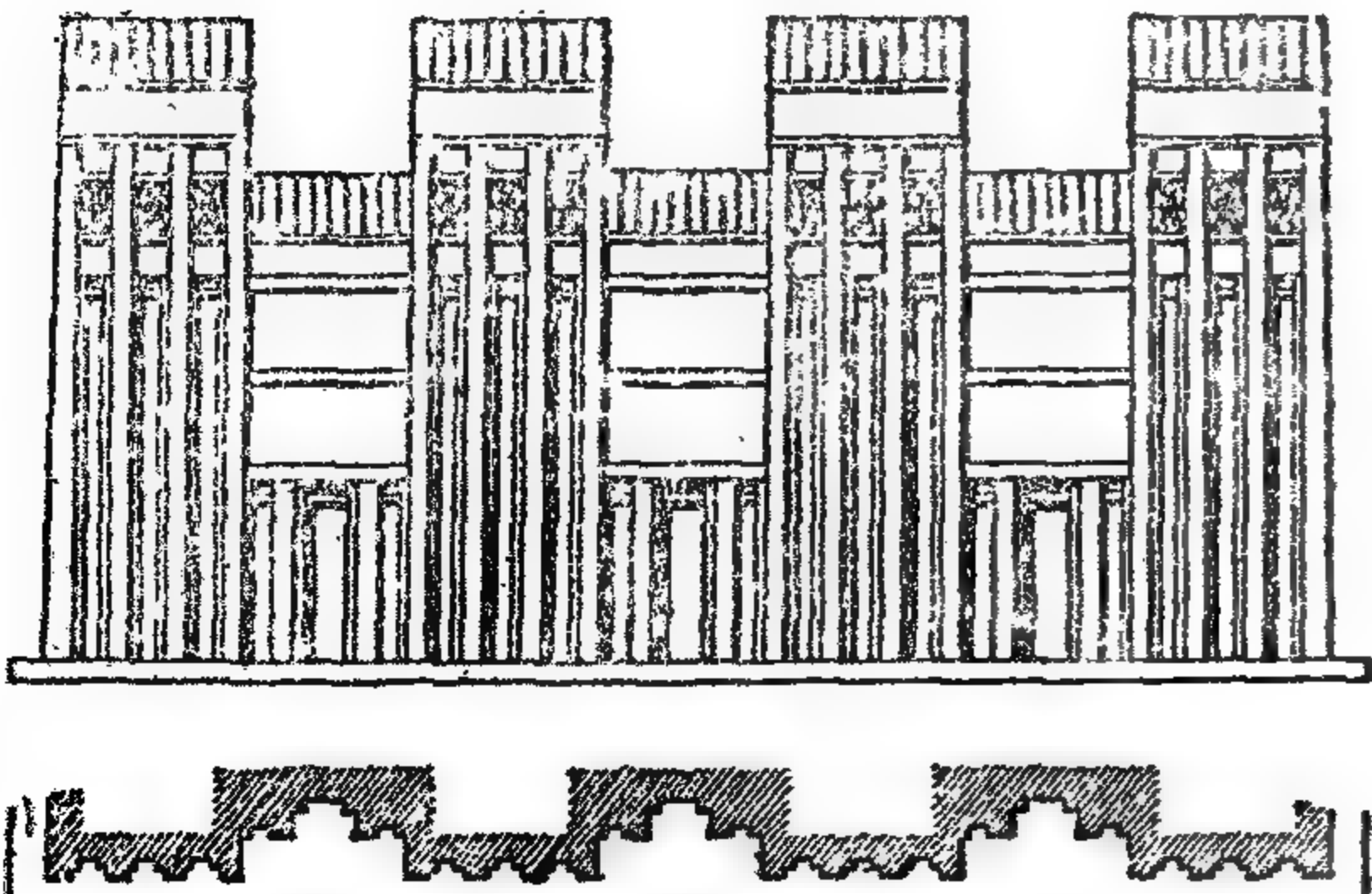
ان طرق قاعدة العمود الخارجية التى تميزت بها
العمارة الاغريقية وجدت لها مرجعا في معابد الدير
البحرى الذى سبق مثيلاتها في العمارة الاغريقية
بخمسة قرون .

ان طرق استعمال الكتل الضخمة لعمل الأعتاب
والكمرات التى تحمل الأسقف بأنواعها انتقلت الى
طراز تلك الحضارات من مصر مع الأعمدة ، وفي جميع
الأمثلة نجد أنها ظهرت في مصر قبل بدء ظهورها في
تلك الطراز بمئات السنين وفي بعضها كالطوب
والأعمدة والعقود بعدة آلاف من السنين .

● وان كانت تكنولوجيا العمارة الفرعونية قد وضعت أساس نظرية الانشاء المجهز بابتكار قالب الطوب .. أول وحدة جاهزة في فن العمارة . فقد تطورت نظرية الانشاء السابق التجهيز بتطبيق نظرية الوحدات الثابتة لمختلف أجزاء المبنى التي ظهرت متطورة في اقدم نماذجها بمدينة « خنت كاو » التي أنشئت عام ٣٥٦٥ ق . م في أواخر عصر الأهرامات بانتاج وحدات ثابتة الاشكال والأبعاد لمختلف أجزاء المبنى فأعدت نماذج موحدة للأبواب والشبابيك والوحدات الجاهزة لأعتاب الفتحات وكمرات الأسقف وبلاطات الأرضيات ومجاري المياه بجانب نماذج المساكن ومساقطها وأبعادها وحجراتها .

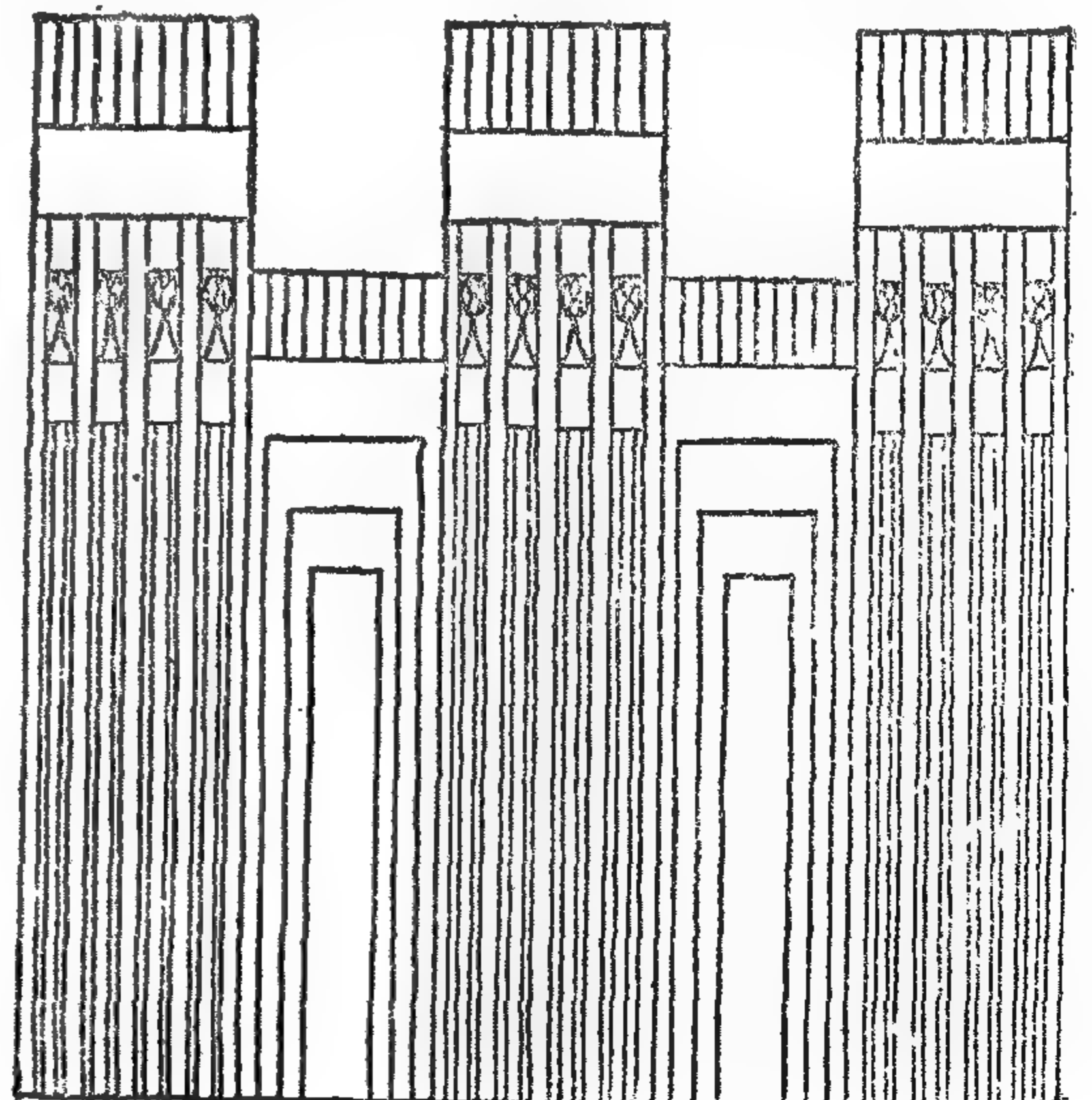
هناك مثل آخر تقديما وتطورا في علم المساكن الجاهزة والمباني السابقة التجهيز وهو مدينة اخت اتون بتل العمارة التي يرجع تاريخ انشائها الى عام ١٣٦٠ ق.م في الأسرة الثامنة عشرة . وقد شمل التجهيز الموحد كل حي من أحياء المدينة على حدة فظهرت بجانب النماذج الموحدة السابقة التجهيز للأبواب والشبابيك والاعتاب وبلاطات الأسقف وبلاط الأرضيات نماذج موحدة لدرجات السلالم والأفران والمخازن بجانب الزخرفة ونفسها فتوحدت نماذج الأعمدة والكرانيش الزخرفية بل انتقلت الى وضع نماذج موحدة للحمامات وأحواض السباحة ونافورات الحدائق وغيرها من وحدات البناء والانشاء .

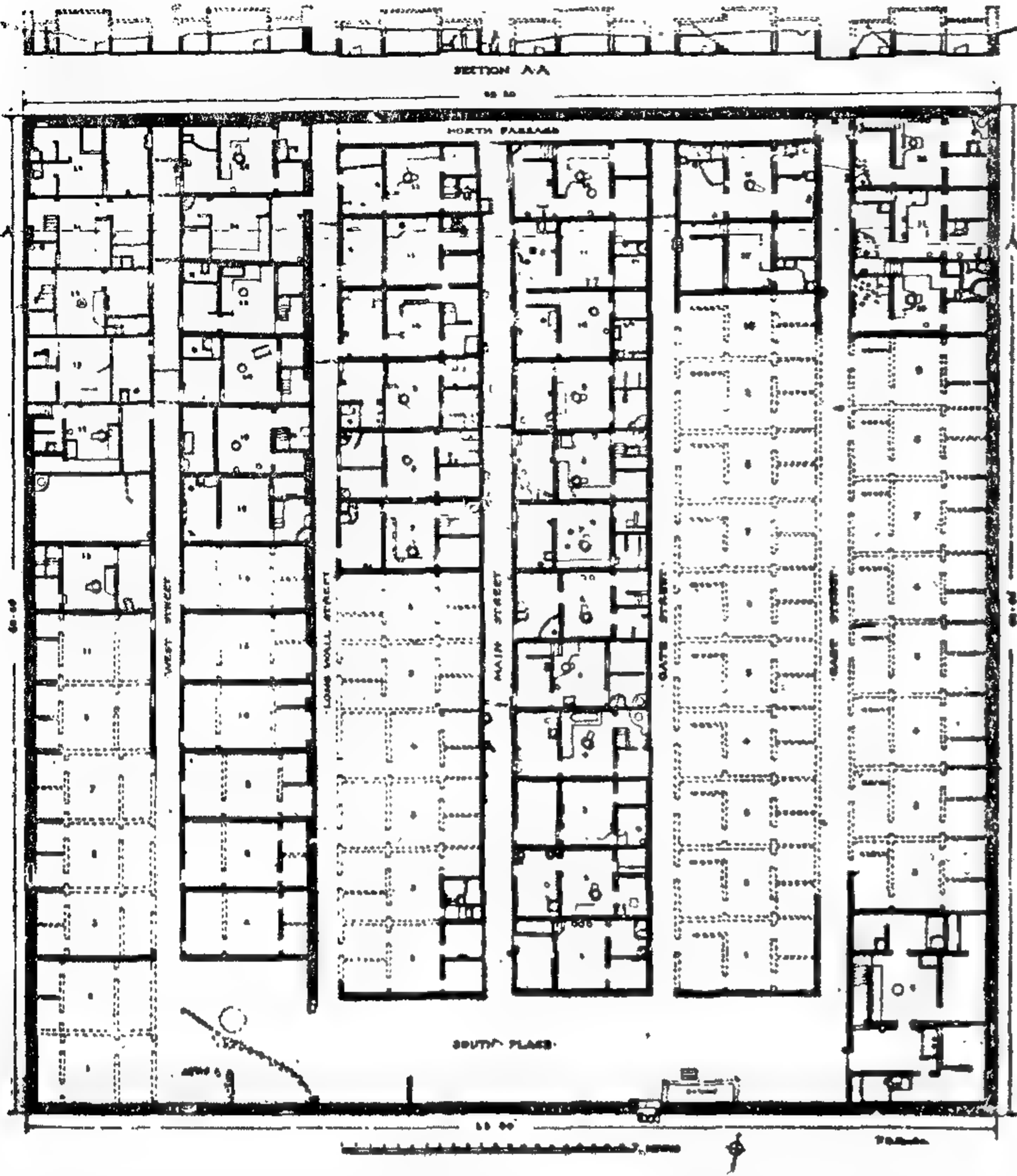
فالعمارة الفرعونية كان لها قصب السبق في ميدان المساكن الجاهزة والانشاء المجهز والوحدات السابقة التجهيز وانتاج الجملة والتي أصبحت الطابع المميز للعمارة العالمية الحديثة أو عمارة عصر التكنولوجيا .



● قصر الملك يواجي - الأسرة الاولى وجد محفورا على ستيل التتويج وعلى التابوت الملكي .

● واجهة قصر الملك ابراش من ملوك الأسرة الثالثة وجد محفورا على أحد أحجار مقبرته في أبيدوس .





● مدينة أخت آتون بتل العمارة ١٢٥٠ ق . م . مثل
من أمثلة التوحيد القياسى للحجرات ومساقطها وأبعادها ،
والنماذج الموحدة السابقة التجهيز للأبواب والشبابيك
والأرضيات والخمائم وغيرها من وحدات البناء والإنشاء

لقد بنى الفراعنة المساكن والقصور وخططوا المدن قبل بناء الأهرامات والمعابد وفن العمارة الفرعونية الذى ظهر قبل الأسرات سبق عمارة المصاطب والأهرامات ففي عهد الدولة القديمة وبداية الأسرات عندما بدأ الفراعنة بناء المصاطب التى بدأ بها مؤرخو العمارة المصرية كتابة تاريخ العمارة وتطورها نجد أن عمارة الحياة المصرية قد سجلت أروع الأمثلة فى عمارة القصور والقلاع والمدن قبل بداية الدولة القديمة نفسها . لم يفت المهندس الفرعونى القديم أن يخلد تصميماته وفنه المعماري فسجلها على جدران التوابيت الصخرية وفى بعض الأمثلة التى كشفت عنها الحفريات الأخيرة منطقة سقارة لجأ المعماري الى تصميم التابوت نفسه على شكل القصر الذى كان يعيش فيه فملك أو الأمير .

وهكذا تحايل المعماري القديم لتخليد نفسه الواقعى الذى يعبر عن عمارة الحياة وتسجل تاريخ العمارة وتطورها بحفظه ضمن عمارة الخلود .

فالمدينة المصرية القديمة . . والمساكن المصرى . . أو عناصر عمارة الحياة هى المرآة التى تعكس مدينة مصر على حقيقتها وتعبر عن مدى تقربها .

دكتور سيد كريم

● كلما ذكر اسم العمارة الفرعونية قفز الى الأذهان صورة تلك الأهرامات الخالدة والمعابد وبوابات الشمس والهيكل الجنائزية . . وما هى الا جانب واحد من جوانب العمارة الجانب الذى لا يعبر عن حقيقة المدينة وطابعها . فللعمارة وجهان كوجهى العملة الواحدة يكمل كل منهما الآخر أحدهما عمارة الحياة . . العمارة التى تخدم حياة المجتمع ، والمعابد والأهرامات . كانت الأولى تبنى لتعيش مع الانسان وتتطور مع مطالب حياته ، ولذا فكانت تبنى من الطوب والأخشاب والأحجار الجيرية وغيرها وتعبر عن كيانه وتطوره وتسجل واقع مدنيته ، وتتمثل فى المساكن ومختلف مباني خدمات المجتمع ونشاطاته والتى تمتد لتصل الى المدن وتخطيطها . والوجه الآخر وهو ما يطلق عليه عمارة الخلود التى تخدم العقائد والمعتقدات والتى تتمثل فى المقابر والمعابد والأهرامات . كانت الأولى تبنى من الطوب والأخشاب والأحجار الجيرية وغيرها من المواد التى لا يشترط فيها الدوام والبقاء وتستهلك مع استهلاك أغراضها وقابليتها لمسيرة التطور - بينما كانت الثانية التى روعى فيها أن تبقى أبد الدهر لتخدم العقيدة والعالم الآخر أو عالم الخلود تبنى من الأحجار الصلبة والجرانيت .

مشروع الصرف المغطى

بدلتا نهر النيل

* للدكتور محمود أبو زيد

مقدمة :

تعتبر مرحلة تقييم المشروعات من أهم المراحل الواجب القيام بها بعد التنفيذ خاصة وأن كانت هذه المشروعات لها أثر كبير على الاقتصاد القومى وتمثل جزءا كبيرا من استثمارات الدولة السنوية فإذا كانت هذه المشروعات تسير فى الاتجاه المرسوم لها أمكن المضى قدما فى التوسع فيها وإذا ما تعرضت لعوامل معوقة فيمكن اكتشافها وتصحيح مسارها .

وإذا ما تناولنا مشروعات الصرف المغطى فى مصر وأهمية الحاجة لها فى معظم الأراضى المنزرعة لنجد أن تنفيذها بمعدلات معقولة يتطلب رصد اعتمادات سنوية كبيرة ، ومن الضرورى إذن التأكد من أن هذه المشروعات تعود على البلاد بالفائدة المرجوة منها .

ويعتبر تقييم مشروعات الصرف من الأمور المعقدة التى يجب دراستها بحرص لا مكان الحصول على نتائج سليمة وذلك مرجعه بالطبع الى تعدد العوامل المؤثرة فى الانتاج الزراعى .

ويتضمن مشروع الصرف فى دلتا نهر النيل تنفيذ مشروعات الصرف فى مساحة ٩٥٠ ألف فدان بتكاليف قدرت بنحو ١٤٠ مليون دولار وفى فترة انشائية تبدأ من عام ١٩٧١ وحتى عام ١٩٥٨ ويشمل المشروع انشاء مصارف رئيسية جديدة وكذلك تعديل وتوسيع المصارف القائمة وانشاء محطة طلمبات صرف جديدة .

ويبلغ المكون الأجنبى للمشروع ٢٦ مليون دولار يتم الحصول عليها أثناء التنفيذ كقرض من هيئة التنمية الدولية احدى مؤسسات البنك الدولى للانشاء والتعمير .

هذا وتقع الأراضى التى يشملها المشروع الحالى بصفة رئيسية بالمنطقتين الجنوبية والوسطى من الدلتا . وهى تبلغ نحو ربع مساحة الأراضى المنزرعة حاليا بها . وتبلغ جملة المساحات التى سبق تزويدها بالصرف المغطى بالدلتا حوالى ٦٠ ألف فدان .

وقد قسمت منطقة المشروع الى ١٨ وحدة صرف catchment area (شكل ١) منها أربعة وحدات تصرف بالراحة دون حاجة الى ضخ وتقع بمنطقة شرق الدلتا ، أما باقى الوحدات فيتطلب صرفها انشاء محطات صرف جديدة .

وتقرر أن يشمل التقييم الحاصلات الرئيسية فقط بالمنطقة وهى : القن والقمح والأرز والشعير .

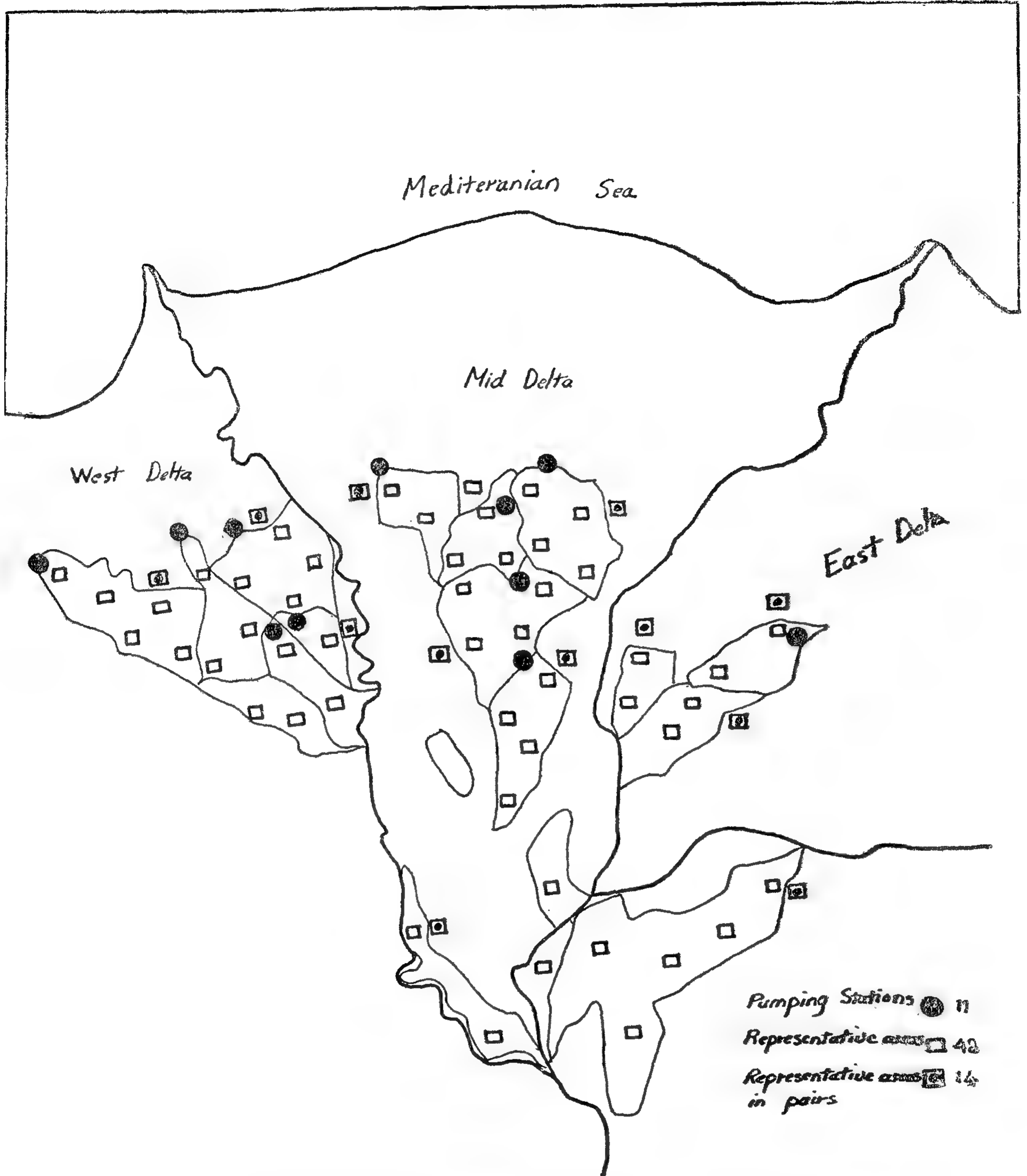
العوامل المؤثرة على الانتاج الزراعى :

يتأثر الانتاج الزراعى بعدة عوامل نذكر منها على سبيل المثال نوع البذور ، طريقة الري ، الخدمة الزراعية ، الأسمدة واستخداماتها ، الصرف ، العوامل الجوية ، المبيدات ... الخ ، وبدراسة هذه العوامل نجد أن بعضها يتوقف على الآخر فمثلا لا يمكن الحصول على زيادة معقولة فى المحصول باضافة الأسمدة عندما تكون حالة الصرف سيئة .

ويزيد من صعوبة فصل اثر هذه العوامل أن الارصاد السابقة لتنفيذ مشروعات الصرف غير دقيقة وان كانت هامة فى عملية التقييم ومن أمثلة هذه الارصاد كميات الأسمدة المضافة ونوعياتها وتركيزها وعدد الاضافات والفترات الزمنية بينها .

هذا ومن الأفضل اجراء المراقبة بالمناطق التى ينتظر أن يكون فيها استخدام الأسمدة كاملا ومتكافئا ان أمكن طوال فترة المراقبة ، والمناخ فى مصر بصفة عامة لا يحدث تغيرات جوهرية فى غلات المحاصيل من سنة لأخرى ، غير أنه قد تمر فترات من السنة تؤثر فيها درجة الحرارة على بعض المحاصيل . ومن ثم ينبغى تسجيل هذه التغيرات حينما تظهر فى الحقل .

وبالنسبة للرى فينبغى تسجيل كافة الاستخدامات الشاذة لمياه الرى التى تخالف القواعد المختارة للمنطقة والتى قد تؤثر فى خواص التربة وغللات المحاصيل .



شكل (١١) مشروع الصرف المغطى بدلتا نهر النيل

وكثير ما تصاب الحاصلات الزراعية بأفات وأوبئة مختلفة الأنواع ، ولذلك يجب عند تسجيل المعلومات عن غلات المحاصيل ذكر أية آثار قد تظهر .

وقد تتأثر غلة المحاصيل أيضا بالطرق المتبعة في الزراعة بسبب تغير الملاك أو المستأجرين أو توالى السلطات والاعتمادات ، كما يجب أيضا ملاحظة نوع البذور وتوافرها .

المحاصيل وعن الزيادة في الدخل الناتج عن ذلك .
كما تبين من الحسابات التي أجريت وجود عائد
على رأس المال المستثمر بنسبة اقتصادية قدرها
١٨ ٪ .

وهذا وقد تختلف غلة المحصول من منطقة
الى أخرى ، كما أن الزيادة في تلك الغلة تتغير تبعاً
لوقت الذي أنشئت فيه المصارف ونسبة الملوحة
في ذلك الوقت .

أثر موعد تنفيذ المشروع :

تختلف حاجة الأراضي الزراعية الى مشروعات
الصرف الحقل من منطقة لأخرى ويصعب لذلك
تحديد أولويات التنفيذ وتأخير هذه المشروعات
يضر بالانتاج فترتفع المياه الجوفية وتزيد ملوحة
التربة الى الدرجة التي قد تجعلها قلوية فيتطلب
الأمر بعض عمليات الاستصلاح الإضافية التي
كان من الممكن تلافيها اذا ما أمكن التبكير بهذه
المشروعات .

وفي الوقت نفسه فان الأراضي التي تبدأ
مشكلة الصرف فيها في الظهور ، في حاجة الى
تنفيذ الصرف الحقل في بداري الوقت محافظة
على مستوى الانتاج الزراعي ، ويبين شكل ٢
دياجراماً للعلاقات بين النقص في الانتاج والزيادة
في ملوحة التربة لعدم استكمال مشروعات
الصرف . ويلاحظ مقدار الزيادة في الانتاج وأثره
في نقص ملوحة التربة اذا ما نفذ المشروع في زمن
١، أو ٢ .

ويجب بالطبع دراسة دوال الزيادة في الانتاج
والتدهور حتى يمكن تحديد الموعد المثالي للبدء
في تنفيذ المشروع ، وقد تكون هناك بعض العوامل
التي لا تساعد على تنفيذ ذلك مثل الارتباط بنهـو
محطة طلبات أساسية للمشروع . وينظر
لمشروعات الصرف في هذه الحالة كعامل لتلافي
تدهور الانتاج بدلا من زيادة الانتاج وهو افتراض
ضروري لاستكمال الدراسات الاقتصادية
للمشروع . ويستلزم الأمر استنباط دوال خط
التدهور وخط التحسين .

برنامج التقييم :

نظراً لكبر المشروع فقد أجريت دراسات
شاملة لوضع برنامج عام للتقييم اشترك في اعداده
مجموعة من الخبراء العالمين والمحليين واعتمد
البرنامج الموضح فيما يلي :

وحيث أن الغرض الأساسي هو تحديد أثر
الصرف وحده على انتاجية الأراضي فلا بد أن
تشمل عمليات التقييم حساب الفوائد التي تستعود
على المنطقة من جراء تنفيذ مشروعات الصرف
المغطى وأهمها :

١ - تحسين التربة وتشمل :

(أ) تغيرات طبيعية مثل خفض منسوب
المياه الأرضية وما ينتج عنه من تحسين تهوية
التربة .

(ب) تحسن خواص التربة الكيميائية بانخفاض
نسبة ما تحتويه من أملاح .

(جـ) تحسين التربة من الناحية البيولوجية
وذلك بزيادة تنمية مكوناتها الدقيقة .

٢ - غلة المحصول :

(أ) ويمكن التوصل الى الزيادة في غلات
المحصول كما ونوعاً بطريقة مباشرة وذلك باجراء
عمليات الاحصاء الدقيق كل عام طوال فترات
معينة من السنين قبل وبعد انشاء الصرف
المغطى ، ويمكن بالتالي تقدير القيمة الاقتصادية
للك زيادة .

(ب) قد يؤدي تنفيذ مشروعات الصرف المغطى
الى امكانية ادخال زراعة محاصيل أخرى أكثر
تأثيراً بالملوحة وأكثر ربحاً .

٣ - المزايا الاقتصادية الأخرى :

من فوائد تنفيذ اختيار مشروعات الصرف
المغطى كأحد وسائل الصرف الحقل بدلا من
مشروعات الصرف المكشوف امكانية الاستفادة
بمساحات الأراضي الزراعية التي تشغلها المصارف
المكشوفة ، وهذه يمكن تقديرها اقتصادياً .

الدراسات السابقة عن الصرف المغطى :

لقد بدأ التنفيذ الميكانيكي لمشروعات الصرف
المغطى بدلتا النيل في عام ١٩٦٢ وأدى ذلك الى
زيادة المحاصيل عقب الانشاء بكل من مناطق
التجارب والمناطق الأخرى التي تم بها التنفيذ ،
وبلغت هذه الزيادة ٢٠ ٪ على الأقل دون
استخدام طاقات اضافية مثل الأسمدة أو البذور
المحسنة .

تقديرات هيئة التنمية الدولية لفوائد المشروع :

تضمن التقرير الذي أعدته هيئة التنمية
الدولية تقديرات عن الزيادة المنظورة في غلات

(ج) الادارة العامة للاحصاء والاقتصاد
بوزارة الزراعة .

(د) الادارة العامة للاراضى بوزارة الزراعة .
(هـ) كليات الزراعة بالجامعات .

وتكون الادارة العامة للاحصاء والاقتصادى
مسئولية عن جميع المعلومات الخاصة بفلات
المحاصيل والمعلومات الأخرى المتعلقة بذلك بعد
انشاء المصارف واثناء التنفيذ فى جميع أراضى
المشروع وداخل المناطق المختارة لتمثيلة .

هذا وتقوم الادارة العامة للاراضى بجمع
المعلومات الخاصة بتأثير الصرف على خواص
التربة . أما الادارة العامة للبحوث والتقييم
باليئة فهى تقوم بجمع وتحليل كافة المعلومات
التي تسجل بقصد حساب تكاليف المشروع
وفوائده الاقتصادية .

٣ - اختيار المناطق التى تمثل المشروع داخل وحدات الصرف :

يتوقف عدد هذه المناطق على حجم وحدة
الصرف ويختلف عددها لكل وحدة من واحدة الى
خمس ، غير أن المناطق المثلة يعتمد عددها اعتمادا
كبيرا على حالة المياه الجوفية وخواص التربة
داخل وحدة الصرف ، وتساعد الخرائط الكنتورية
لمناسيب المياه الجوفية وخواص التربة داخل
المنطقة على اختيار هذه المناطق .

وبالنسبة لمشروع الدلتا فقد اختير معظم
المناطق التى تمثل المشروع داخل وحدات الصرف
فى حدود 1000 ± 200 فدان لكل منها . ولما كان
كل مجمع صرف يخدم نحو 100 فدان فان كل
منطقة لتمثيل المشروع داخل وحدات الصرف
تشمل نحو عشرة مجمعات بما هو مرتب عليها
من حقليات .

١ - اختيار المناطق التى تمثل المشروع :

Representative Areas

تم اختيار مناطق صغيرة نسبيا ومنتشرة فى
كل منطقة المشروع . وتجرى عليها دراسات
تفصيلية عن تأثير الصرف على حالة التربة وغللات
المحاصيل . واختيرت هذه المناطق بحيث تصبح
كل منها تمثل جزءا معينا من المشروع ، وبذلك
يكون التقييم بها حينئذ منطبقا على منطقة
المشروع كلها .

هذا وقد قسمت منطقة المشروع الى عدد
من المناطق الجزئية Part areas مساحة كل
منها نحو 2000 فدان ، اختير بكل منطقة من
هذه المناطق الجزئية مساحة قدرها 1000 فدان
لتمثيلها ، وبهذه الطريقة يمكن القيام بدراسات
مفصلة لفوائد المشروع فى مساحة تبلغ نحو 50%
من مساحة المشروع الاجمالية .

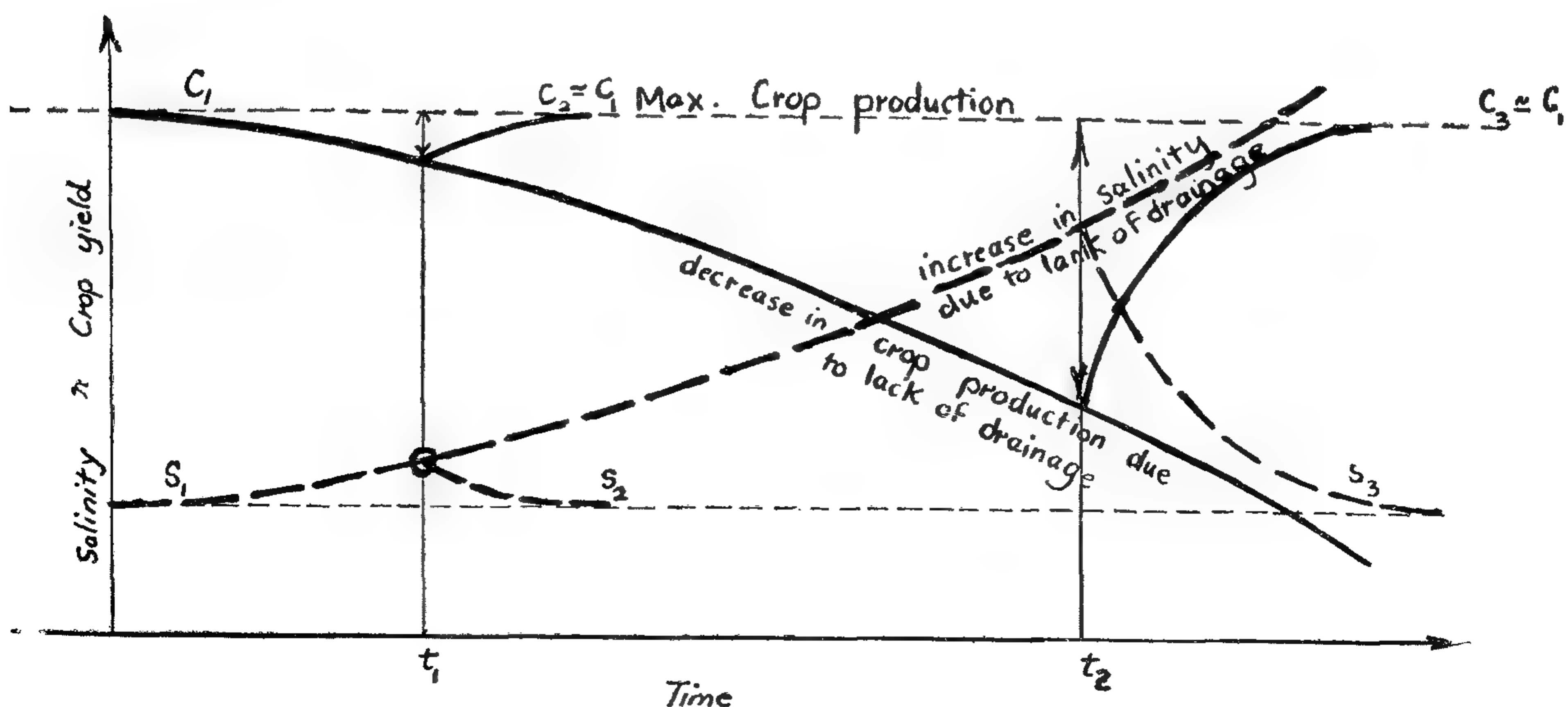
وتتضمن هذه الدراسات التفصيلية مناسيب
المياه الجوفية وملوحتها وملوحة التربة وقلويتها
وتكوينها والخواص الأخرى وكذلك غللات
المحاصيل ... الخ .

ومن أغراض اختبار هذه المناطق امكان دراسة
العائد الاقتصادى من المشروع فى حدود كل منطقة
أو وحدة صرف وذلك عن طريق استيفاء جميع
البيانات اللازمة لتقييم كل وحدة على حدة عن
طريق المناطق المثلة لها .

٢ - الجهات المشتركة فى أعمال التقييم ودور كل منها :

ثم تشكيل لجنة مشتركة للإشراف على أعمال
التقييم أعضاؤها من ممثلى الجهات الآتية :

- (أ) وزارة الري .
- (ب) الهيئة المصرية العامة لمشروعات الصرف .



شكل (٢) التغير فى ملوحة التربة ونتاجية الفدان مع وقت تنفيذ مشروعات الصرف المغطى

٤ - تسجيل غلات المحصول داخل المساحات التي تمثل المشروع :

تسجل غلات المحصول بوزن عينات تؤخذ من أحواض مختارة ، وتختار هذه العينات من مواقع مختلفة بحيث يصبح مقدار انحراف الخطأ المحتمل في الحدود الآتية :

بالنسبة لمركز إداري $\pm 7\%$

بالنسبة لمحافظة $\pm 3\%$

بالنسبة لمصر كلها $\pm 1\%$

وبالنسبة لمشروع الدلتا فان المساحة التي توزع سنوياً قطناً وأرزاً وأذرة داخل منطقة المشروع تتراوح بين ٣٠٠ ألف ، ٣٥٠ ألف فدان لكل محصول ، كما تبلغ بالنسبة للقمح نحو ٢٠٠ ألف فدان . وقد تقرر أن يؤخذ عدد العينات داخل المشروع بنسبة ١/٦ لكل فدان (بمعنى أنه اذا كانت مساحة وحدة الصرف ١٠ آلاف فدان فتؤخذ ٦٠ عينة) ، أما اذا كانت المساحة التي يشغلها المحصول تقل عن ١٠٠٠ فدان فان الحد الأدنى لعدد العينات يصبح خمس .

وتختار أحواض أخذ العينات بطريقة عشوائية . ومن ثم فانه بالنسبة لوحدة صرف مساحتها ١٠ آلاف فدان يجرى تقسيمها الى وحدات كل منها ٢٥٠ فدان أى الى ٥٠ وحدة مساحية . ثم يختار حوضين لأخذ العينات من كل وحدة مساحية . ونظراً لأنه سيتم أخذ ٦٠ عينة بواقع عینتين من كل وحدة مساحية فان عدد ما يختاره من الخمسين وحدة يصبح ٣٠ وحدة مساحية .

ويبلغ حجم كل حوض من الأحواض المخصصة لجميع العينات ٠.١ ر. فدان (٤٢ م^٢) بالنسبة للأذرة والأرز ، ٠.٢ ر. فدان (٨٤ م^٢) بالنسبة للقطن .

٥ - عدد السنوات اللازمة لتسجيل غلات المحاصيل :

هناك شبه اتفاق عام على أن تكون فترة المراقبة قبل انشاء مشروعات الصرف المغطى ينبغي أن تكون ثلاث سنوات على الأقل كما أن الأمر يستدعى فترة أخرى تمتد الى حوالى ثلاث سنوات أخرى قبل التعرف على التأثير الكامل للصرف المغطى على غلات المحاصيل ، ويجوز أن يكون هناك فترة ثالثة للمراقبة تبدأ بعد ثلاث سنوات من انشاء الصرف المغطى ، وقد تمتد الى ثلاث سنوات لتصل المدة الاجمالية للمراقبة الكاملة الى ٩ سنوات . وبعد الحصول على مزيد

من الخبرة قد يرى أنه من الممكن تقليل فترة المراقبة لتصل الى ٧ سنوات ، غير أنه ينبغي ألا تقل -بحال من الأحوال - عن ٥ سنوات .

٦ - ازدواج المساحة المثلة للمنطقة : Representative Areas in Pairs

لقد اقترح ان تكون كل مساحة ممثلة للمشروع مكونة من جزئين متجاوبين بقدر الامكان ومتماثلين تماماً من حيث حالة المياه الجوفية والتربة ، وتنفذ شبكة الصرف المغطى بأحد الجزئين ويؤجل تنفيذ الصرف المغطى في الجزء الثانى حتى نهاية مدة تنفيذ المشروع ، وبهذه الطريقة يمكن فصل جميع العوامل التي تؤثر في غلات المحاصيل والتي ليست لها علاقة بالصرف المغطى .

٧ - مناطق تمثيل المشروع المزدوجة خارج حدود المشروع :

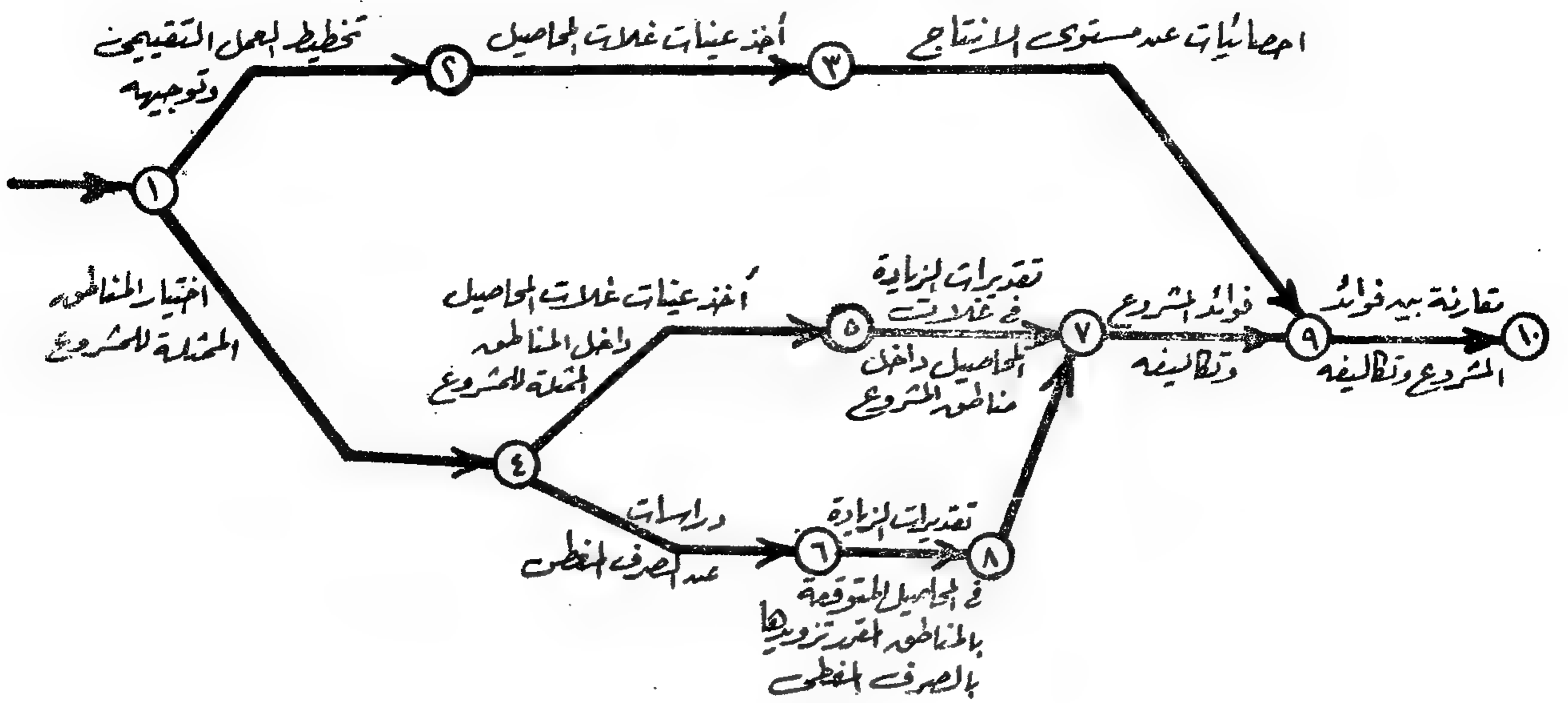
نظراً لطول المدة التي ستنقضى قبل تنفيذ الصرف المغطى بالأجزاء التي تقرر تركها بمناطق تمثيل المشروع المزدوجة داخل حدود المشروع بغرض المقارنة ، وبالإضافة الى احتمال تأثر مناسيب المياه الجوفية بهذه المناطق من جراء تنفيذ مشروعات الصرف المغطى بالمناطق المجاورة لها من أراضى المشروع - لذلك - فقد رُئى اختيار بعض المناطق المزدوجة بحيث تقع أجزاء منها خارج حدود وحدة الصرف ، وأجزائها الأخرى داخل وحدة الصرف .

ولما كان من المعتاد ان تفصل المصارف والترع بين حدود وحدات الصرف فان احتمال تأثر الجزء المتروك بدون تنفيذ الصرف - والخارج عن حدود المشروع - بمشروعات الصرف داخل المشروع احتمال ضئيل .

هذا وقد تقرر اختيار ٤٨ مساحة ممثلة للمشروع داخل منطقة المشروع ، ١٤ مساحة من المساحات المزدوجة أجزاء منها خارج منطقة المشروع .

٨ - التقييم الاقتصادي :

من المعتقد أن الحسابات الأساسية للتقييم الاقتصادي سوف لا تبدأ حتى عام ١٩٧٧ وللمناطق التي تم تنفيذها . أما التقييم الاقتصادي الشامل للمشروع فمن المحتمل أن يبدأ خلال عام ١٩٧٩ . وعلى أى حال فمن الضروري أن يحصل في بداية أعمال التقييم على الاتجاهات الرئيسية للتقييم حتى تكون منهجاً للأعمال المطلوبة في المراحل الأولى للدراسة .



شكل (٢) تخطيط وتنظيم أعمال التقييم .

(هـ) جمع عينات غلات المحاصيل من المساحات الممثلة للمشروع الادارية العامة للاحصاء والاقتصاد .

(و) دراسات عن الصرف المغطى وحالة التربة وغللات المحصول (الادارة العامة للاراضى) .

(ز) تقديرات الزيادة في غلات المحاصيل داخل : (الادارة العامة للتقييم) .

١ - كل منطقة جزئية داخل وحدات الصرف .

٢ - كل وحدة من وحدات الصرف .

٣ - كل منطقة المشروع .

(ح) تقديرات مسبقة لغللات المحاصيل المتوقعة بالمناطق المزمع ادخال الصرف المغطى بها (الادارة العامة للتقييم) .

(ط) فوائد المشروع وتكاليفه (الادارة العامة للتقييم) .

(ي) مقارنة بين فوائد المشروع وتكاليفه (المشتركة) .

ولقد بدأت أعمال الرصد منذ اعتماد برنامج التقييم ووضح من التحليل المبدئى لما أمكن الحصول عليه من بيانات فاعلية مشروعات الصرف المغطى وأثرها في زيادة الانتاج .

ونظرا لان بعض مناطق المشروع يتم تنفيذ مشروعاتها قبل الأخرى فيمكن تطبيق نفس الأسس على وحدة منفصلة يتم تنفيذ مشروعات الصرف المغطى لها ، وعلى ضوء هذا التقييم فقد يكون من الميسور اجراء تقرير لجميع النواحي الاقتصادية للمشروع .

هذا وينبغى تقدير تكاليف راس المال والتشغيل وأعمال الصيانة الدورية لكل وحدة صرف على حدة وأن يرجع في حسابات التقييم الاقتصادي الى مستوى أسعار معين يسبق تحديده بناء على دراسات عن تذبذب الأسعار العالمية والأسواق الممكنة لمنتجات المشروع بالإضافة الى التغيير في تكاليف المعدات والمواد الأولية اللازمة للتنفيذ .

٩ - تنظيم أعمال التقييم :

يتم تنظيم أعمال التقييم وتوالى الدراسات من بداية تخطيط العمل وحتى مقارنة فوائد المشروع بتكاليفه على النحو الموضح بالشكل ٣ وفيما يلى المكونات الرئيسية لأعمال التقييم :

(أ) تخطيط العمل التقييمى وتوجيهه (اللجنة المشتركة) .

(ب) أخذ عينات لغللات المحاصيل من منطقة المشروع (الادارة العامة للاحصاء والاقتصاد) .

(ج) احصائيات عن الزيادة في غلات المحاصيل بكل مناطق المشروع (والاقتصاد) .

(د) انشاء المساحات الممثلة للمشروع (الادارة العامة للتقييم) .

Serial number m	Year	Natural River Discharge Millard m ³ /year	Return period $\frac{n+1}{m}$ Gumbel	$\frac{n}{n-1/2}$ Hazen	Probability of occurrence $p=100\%$ $\frac{1}{n}$ Gumbel	Hazen	Probability of occurrence $(100-p)\%$ or $(100X \frac{1}{n-1})\%$ $\frac{1}{n-1}$ Gumbel	Hazen	Value of y accept- ding to Gumbel
1	2	3	4	5	6	7	8	9	10
73	1939-40	73	1.19	1.19	84.0	84.0	16.0	16.0	-0.60
74	1944-45	73	1.17	1.17	85.5	85.5	14.5	14.5	-0.65
75	1902-03	72	1.15	1.15	86.2	87.0	13.8	13.0	-0.68
76	1905-06	72	1.14	1.14	87.7	12.3	12.3	12.3	-0.74
77	1912-13	70	1.12	1.12	88.5	89.3	11.5	10.7	-0.78
78	1915-16	70	1.11	1.11	90.1	90.1	9.81	9.81	-0.81
79	1918-1919	69	1.10	1.10	90.9	90.9	9.09	9.09	-0.88
80	1925-26	69	1.08	1.08	91.8	91.8	8.26	8.26	-0.90
81	1930-31	68	1.07	1.07	93.5	93.5	6.55	6.55	-1.00
82	1941-42	68	1.06	1.06	94.3	94.3	5.66	5.66	-1.05
83	1907-08	66	1.04	1.04	96.1	96.1	3.84	3.84	-1.19
84	1940-41	66	1.03	1.03	97.1	97.1	2.92	2.92	-1.25
85	1899-1900	63	1.02	1.02	98.0	98.0	1.96	1.96	-1.37
86	1913-14	42	1.01	1.01	99.0	99.0	0.99	0.99	-1.53

Serial number m	Year	Natural River Discharge Milliard m^3/year	Return period T_p $\frac{n+1}{m}$ Gumbel	$\frac{n}{m-1/2}$ Hazen	Probability of occurrence $p=100\%$ $\frac{n}{m}$ Gumbel Hazen		Probability of non-occurrence $(100-p)\%$ or $(100 \times T_p - 1)\%$ $\frac{n}{m}$ Gumbel Hazen		Value of y according to Gumbel
1	2	3	4	5	6	7	8	9	10
55	1928-29	84	1.58	1.58	63.2	63.3	36.8	36.7	+ 0.02
56	1933-34	84	1.55	1.55	64.4	64.5	35.6	35.5	- 0.02
57	1943-44	84	1.53	1.52	65.5	65.8	34.5	34.2	- 0.06
58	1947-48	84	1.50	1.50	66.7	66.7	33.3	33.3	- 0.10
59	1942-43	82	1.47	1.47	67.8	68.0	32.2	32.0	- 0.13
60	1911-12	81	1.45	1.44	69.0	69.5	31.0	30.5	- 0.16
61	1937-38	81	1.43	1.42	70.0	70.5	30.0	29.5	- 0.18
62	1960-61	81	1.40	1.40	71.2	71.4	28.8	28.6	- 0.21
63	1920-21	80	1.38	1.38	72.4	72.5	27.6	27.5	- 0.25
64	1931-32	80	1.36	1.35	73.5	74.1	26.5	25.9	- 0.28
65	1904-05	77	1.34	1.33	74.7	75.2	25.3	24.8	- 0.31
66	1919-20	77	1.32	1.31	75.9	76.4	24.1	23.6	- 0.34
67	1952-53	76	1.30	1.29	77.0	77.5	23.0	22.5	- 0.38
68	1921-22	75	1.28	1.27	78.1	78.7	21.9	21.3	- 0.42
69	1951-52	75	1.26	1.26	79.4	79.4	20.6	20.6	- 0.45
70	1888-89	74	1.24	1.24	80.6	80.6	19.4	19.4	- 0.49
71	1957-58	74	1.22	1.22	81.3	82.0	18.7	18.0	- 0.52
72	1927-28	73	1.20	1.20	82.7	83.4	17.3	16.6	- 0.55

Serial Number m	Year	Natural River Discharge Milliard m ³ /year	Return period T_p $\frac{n+1}{m}$ Gumbel	$\frac{n}{m-1/2}$ Hazen	Probability of occurrence $p=100\%$ $\frac{T_p}{T_p}$ Gumbel	Hazen	Probability of non- occurrence $(100-p)\%$ or $(100X \frac{T_p}{T_p} - 1)\%$ Gumbel	Hazen	Value of y accor- ding to Gumbel
1	2	3	4	5	6	7	8	9	10
37	1963-64	94	2.35	2.36	42.5	42.4	57.5	57.6	0.61
38	1897-98	92	2.29	2.30	43.7	43.5	56.3	56.5	0.56
39	1906-07	92	2.23	2.24	44.8	44.6	55.2	55.4	0.54
40	1900-01	90	2.18	2.18	46.0	45.9	54.0	54.1	0.50
41	1914-15	90	2.12	2.12	47.1	47.1	52.9	52.9	0.47
42	1962-63	90	2.07	2.07	48.2	48.3	51.8	51.7	0.43
43	1932-33	89	2.02	2.02	49.4	49.5	50.6	50.5	0.40
44	1922-23	88	1.98	1.98	50.5	50.5	49.5	49.5	0.36
45	1923-24	88	1.93	1.93	51.7	51.8	48.3	48.2	0.33
46	1948-49	88	1.89	1.89	52.9	52.9	47.1	47.1	0.30
47	1950-51	88	1.85	1.85	54.0	54.0	46.0	46.0	0.27
48	1945-46	86	1.81	1.81	55.1	55.2	44.9	44.8	0.23
49	1949-50	86	1.78	1.77	56.3	56.5	43.7	43.5	0.21
50	1953-54	86	1.74	1.74	57.5	57.5	42.5	42.5	0.18
51	1936-37	85	1.71	1.70	58.5	58.8	41.5	41.2	0.14
52	1901-02	84	1.67	1.67	59.8	59.9	40.2	40.1	0.11
53	1924-25	84	1.64	1.64	60.9	61.0	39.1	39.0	0.08
54	1926-27	84	1.61	1.61	62.0	62.1	38.0	37.9	0.05

Serial number m	Year	Natural River Discharge Milliard m ³ /year	Return period T_p $\frac{n+1}{m}$ Gumbel	$\frac{n}{m-1/2}$ Hazen	Probability of occurrence $p = \frac{100\%}{T_p}$ Gumbel	Hazen	Probability of nonoccurrence (100-p)% or (100x $T_p - 1$)% $\frac{100}{T_p}$ Gumbel	Hazen	Value of y accor- ding to Gumbel
1	2	3	4	5	6	7	8	9	10
19	1938-39	104	4.58	4.65	21.8	21.5	78.2	78.5	1.42
20	1886-87	102	4.35	4.41	23.0	22.6	77.0	77.4	1.35
21	1909-10	102	4.15	4.20	24.2	23.8	75.8	76.2	1.29
22	1880-81	99	3.96	4.00	25.3	25.0	74.7	75.0	1.24
23	1882-83	99	3.78	3.82	26.4	26.2	73.6	73.8	1.19
24	1889-90	99	3.62	3.66	27.6	27.3	72.4	72.7	1.14
25	1956-57	99	3.48	3.51	28.8	28.5	71.2	71.5	1.10
26	1884-85	98	3.35	3.37	29.9	29.7	70.1	70.3	1.05
27	1903-04	98	3.22	3.24	31.0	30.9	69.0	69.1	1.00
28	1929-30	98	3.11	3.13	32.2	32.0	67.8	68.2	0.95
29	1959-60	98	3.00	3.02	33.3	33.1	66.7	66.9	0.92
30	1881-82	97	2.90	2.92	34.5	34.2	65.5	65.8	0.87
31	1885-86	97	2.81	2.82	35.6	35.5	64.4	64.5	0.83
32	1958-59	96	2.72	2.73	36.8	36.6	63.2	63.4	0.79
33	1934-35	95	2.64	2.64	37.9	37.9	62.1	62.1	0.75
34	1910-11	94	2.56	2.57	39.0	38.9	61.0	61.1	0.72
35	1935-36	94	2.49	2.50	40.2	40.0	59.8	60.0	0.68
36	1955-56	94	2.42	2.42	41.4	41.3	58.6	58.7	0.65

TABLE. 1. Aswan Total Natural River. Discharges (1879-1880) (1964-1965) Millions m³

Serial number	Year	Natural River Discharge Milliard m ³ /year	Return period $\frac{n+1}{m}$ Gumbel	Hazen $\frac{n}{m-1/2}$	Probability of occurrence $p = \frac{100\%}{T_p}$ Gumbel	Hazen T_p	Probability of non-occurrence (100-p)% or (100X $\frac{T_p}{T_p-1}$)% Gumbel	Hazen $\frac{T_p}{T_p-1}$	Value of γ according to Gumbel
1	2	3	4	5	6	7	8	9	10
1	1894-95	133	87.0	17.2	1.15	0.58	98.85	99.42	4.45
2	1892-93	131	43.5	57.3	2.30	1.75	97.70	98.25	3.75
3	1879-80	129	29.0	34.4	3.45	2.91	96.55	97.09	3.37
4	1964-65	123	21.8	24.6	4.60	4.07	95.40	95.93	3.05
5	1895-96	122	17.4	19.1	5.75	5.24	94.25	94.76	2.82
6	1896-97	122	14.5	15.6	9.90	6.41	93.10	93.59	2.64
7	1916-17	119	12.4	13.2	8.05	7.58	91.95	92.42	2.47
8	1890-91	118	10.9	11.5	9.20	8.70	90.80	91.30	2.32
9	1889-90	118	9.67	10.1	10.35	9.90	89.65	90.10	2.20
10	1917-18	117	8.70	9.06	11.5	11.0	88.5	89.0	2.10
11	1887-88	115	7.91	8.20	12.6	12.2	87.4	87.8	2.00
12	1883-84	111	7.25	7.48	13.8	13.4	86.2	86.6	1.91
13	1908-09	110	6.69	6.88	14.9	14.5	85.1	85.5	1.84
14	1893-94	109	6.21	6.37	16.1	15.7	83.9	84.3	1.75
15	1891-92	108	5.80	5.94	17.2	16.8	82.8	83.2	1.67
16	1946-47	107	5.44	5.55	18.4	18.0	81.6	82.0	1.60
17	1954-55	107	5.12	5.21	19.5	19.2	80.5	80.8	1.53
18	1961-62	107	4.83	4.91	20.7	20.4	79.3	79.6	1.47

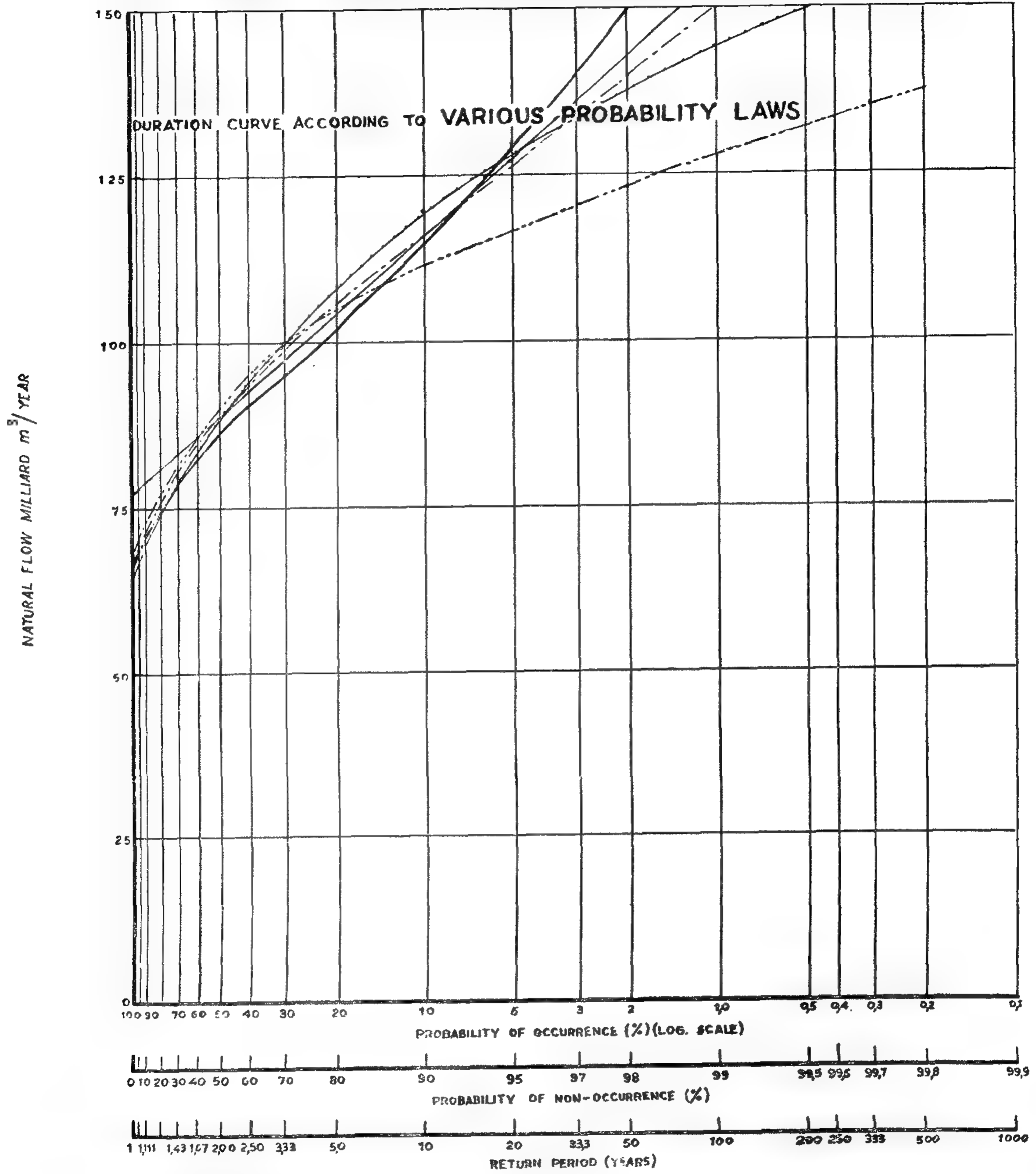
LIST OF REFERENCES :

- 1 — W. Fuller, The Asymptotice Distribution of the Range of Sume of Independent Random Variables. Ann. of Math. Stat., 22, 1951.
- 2 — Allen Hazen, Storage to be provided in Impounding Reservoirs for Muncipal Water Supply. Trans. Amer. Soc. Civ. Tngs. 77, 1914.
- 3 — Sir Gilbert Walker, Indian Mansoon and Nile floow-correlations with Warld Weather. Indian Meleorlogical Memoirs, 1910.
- 4 — E.E. Hurst long-term Storage Capacity of Reservoirs, Trans. Amer. Soc. Civ. Engs. 116, 1951.
- 5 — Hurst, Black and Simaika, The Nile Basin Vol. X-1966.

→



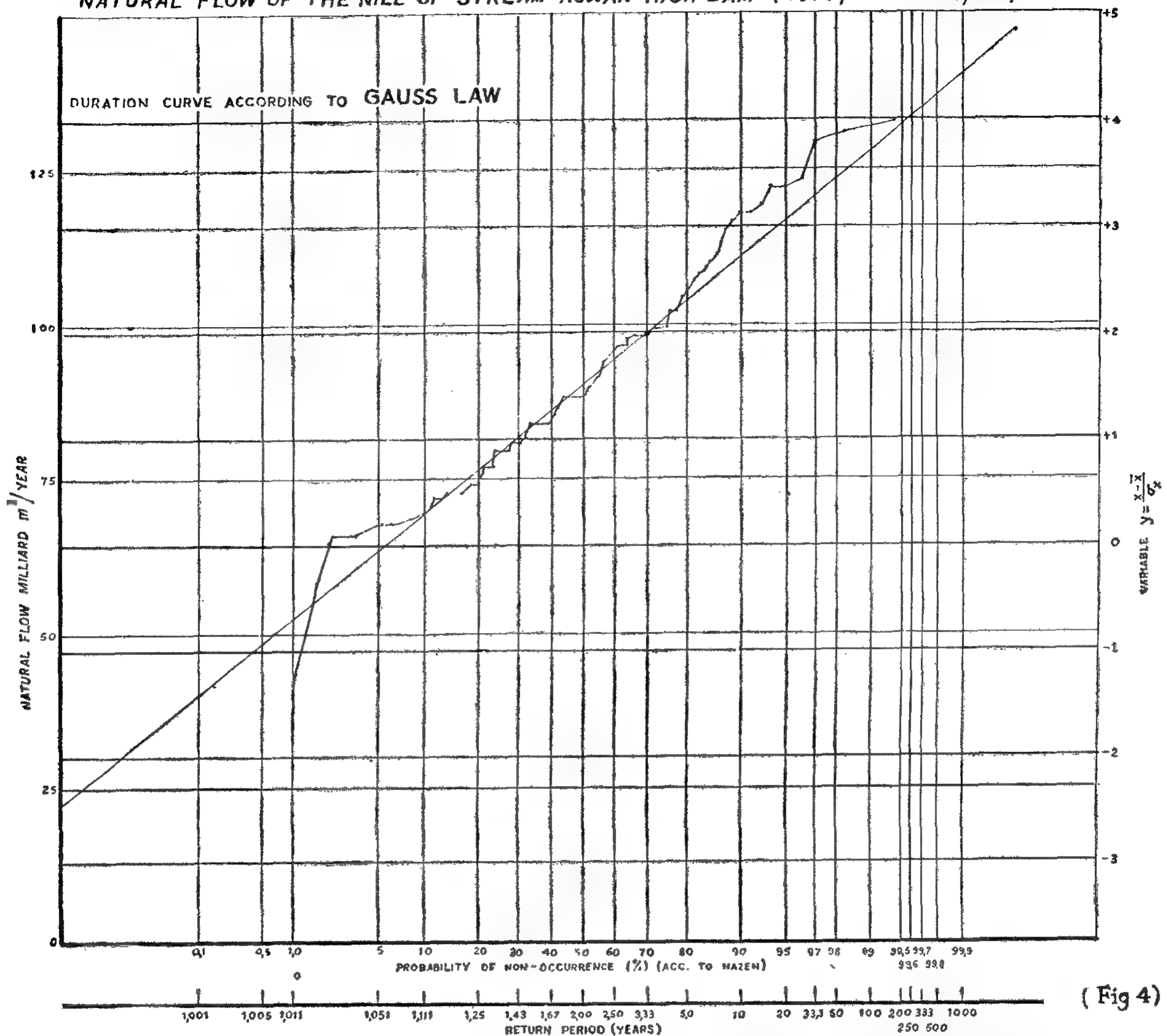
NATURAL FLOW OF THE NILE UP-STREAM ASWAN HIGH DAM (1879/80 - 1964/65)



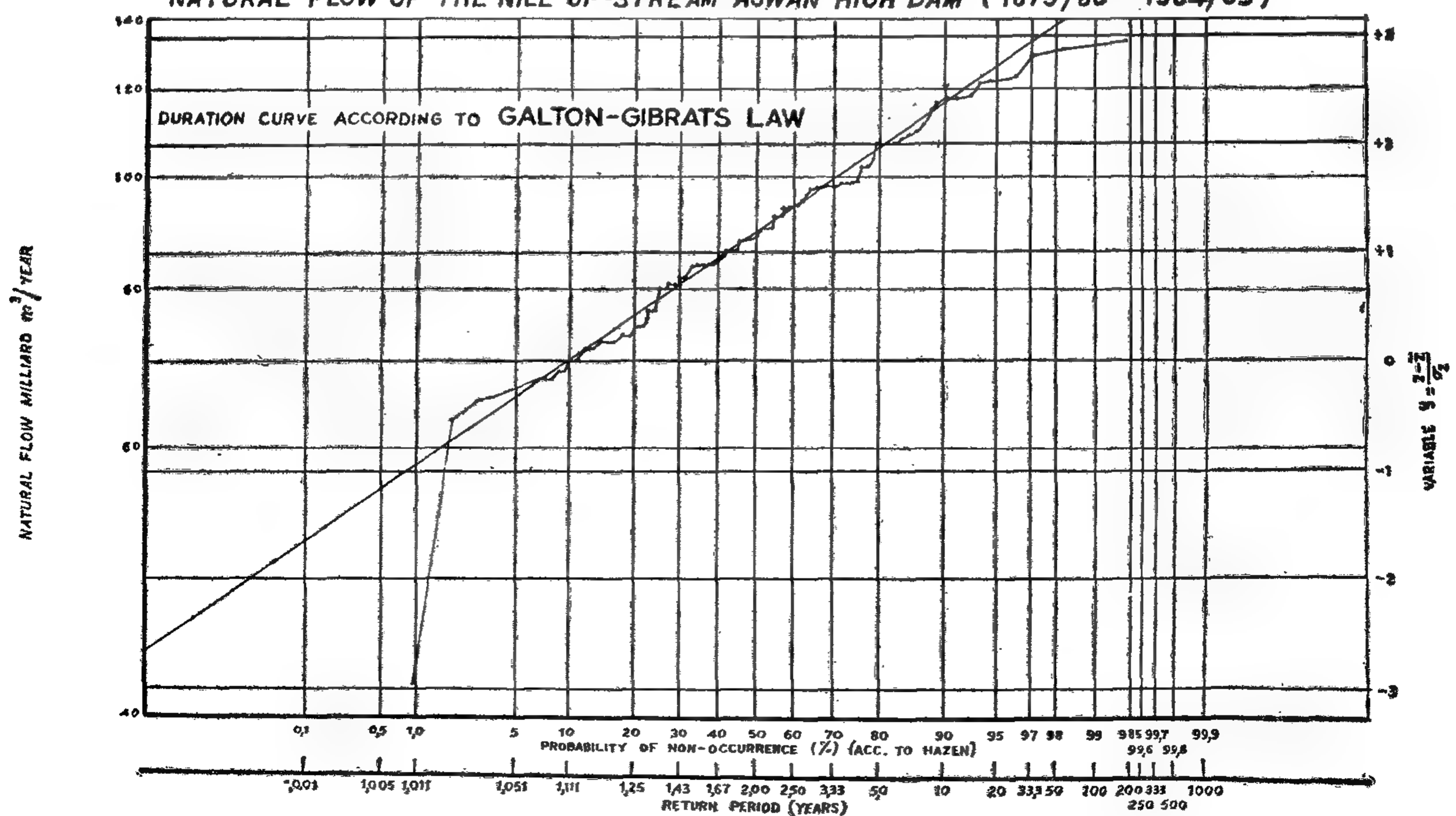
EXPLANATION

- GUMBEL'S LAW
- FRECHET'S LAW
- FULLER'S LAW CALCULATED
- " " GRAPHICAL SOLUTION
- ... GAUSS'S " "
- . - GALTON-GIBRAT'S LAW

NATURAL FLOW OF THE NILE UP-STREAM ASWAN HIGH DAM (1879/80 - 1964/65)



NATURAL FLOW OF THE NILE UP-STREAM ASWAN HIGH DAM (1879/80 - 1964/65)



NATURAL FLOW OF THE NILE UP-STREAM ASWAN HIGH DAM (1879/80 - 1964/65)

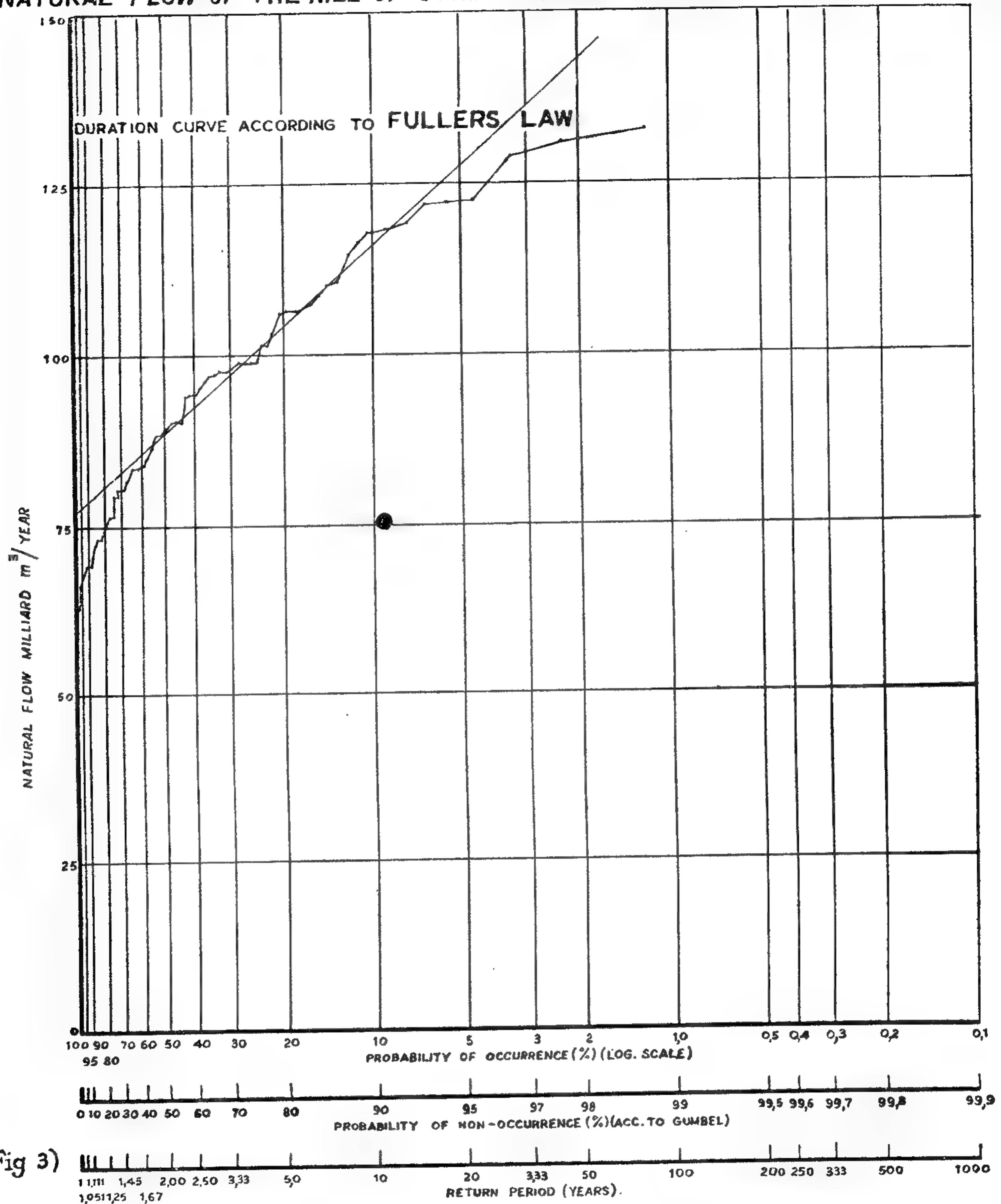


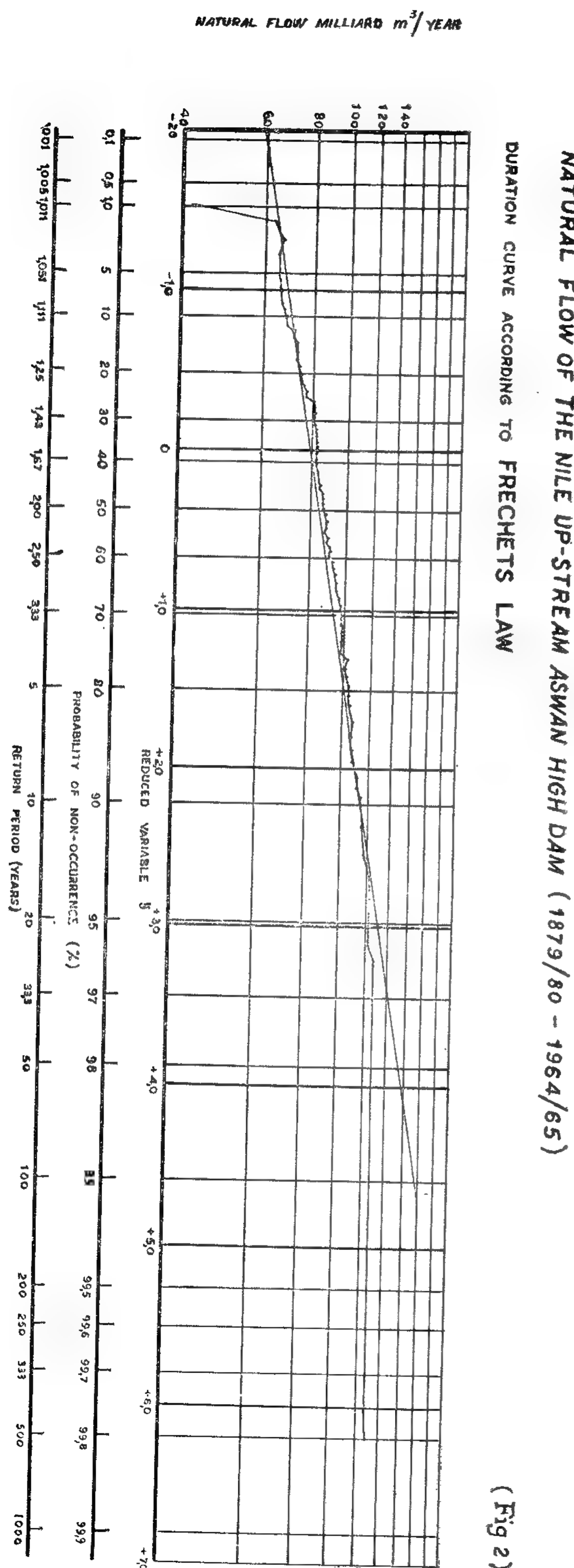
(Fig 3)

DATA BASIS

Dischargedata at Aswan :

From 1870 up to now gauge readings on Aswan downstream gauge are available, and from 1902 up to

now sluice measurents of discharges through the dam are availabe. Dic-charges for the last century have been computed from the general gauge discharge curve of all observations up till the construction of the dam and are therefore of lesser degree of accuracy than the subsequent ones, but it has been suggested that they should be rejected owing to the changes caused by the construc-



In such solution x has been assumed to be zero.

The ordinate represents flow (column 3) on a logarithmic scale.

As in Guass diagram, these ordinates have been plotted as a function of the probability of non-occurrence in% (column 9), based on the return period in years, according to Hazen (column 5), as indicated on the joint scale.

$$\bar{z} = 1.938 \quad (\text{as before})$$

$$\sigma_z = 0.109 \quad (\text{as before})$$

$$y = \frac{z - \bar{z}}{\sigma_z} = \frac{z - 1.938}{0.109}$$

$$z = 0.109 y + 1.938$$

CONCLUSION

Any Natural phenomena behaving as independent random events, their distribution follows the normal probability curve and hence it could be derived theoretically. There is no doubt that the curve on probability paper is a more useful device than the normal curve, since it shows the nature of the curve at its extremities.

In order to summarize the results, the various duration curves have been compiled in one diagram as used for Fuller's method. (Linear discharge scale and logarithmic probability scale). One curve could be concluded from the obtained diagram. This curve is shown on sheet No — (6), which is considered as the most fitting duration curve. The obtained duration curve can be used for the study of the log-term storage, and regulation of the High- Aswan Dam.

The arithmetic mean of the Natural flow $X = 91 \text{ m.m}^3/\text{year}$.

Standard deviation.

$$\begin{aligned} \text{tion } \sigma_x &= 17.5 \\ a &= \frac{1}{0.780 \sigma_x} = \frac{1}{0.780 \times 17.5} = 13.65 \\ \text{mode: } x_0 &= \bar{x} - 0.450 \sigma_x = 91 - 0.450 \times 17.5 \\ &= 91 - 7.875 = 83.125 \\ Y &= \frac{x - 83.125}{13.65} \\ x &= 13.65 Y + 83.125 \end{aligned}$$

6.2. Frèchet

On the basis of Frèchet's law the Natural flow (column 3) have been plotted on logarithmic scale as a function of the reduced variable y (column 10). Similar to Gumbel's method, scales for the probability of non-occurrence in % (column 8) and the return period in years (column 4) have been joined.

Duration curve calculations;

let $z = \log x$

arithmaic mean of $z = \bar{z} = 1.938$

$$\begin{aligned} \text{Standard deviation } \sigma_z &= 0.109 \\ a &= \frac{1}{0.780 \sigma_z} = \frac{1}{0.780 \times 0.109} = \frac{1}{0.085} \\ \text{mode: } z_0 &= \bar{z} - 0.450 \sigma_z = 1.938 - 0.450 \times 0.109 \\ &= 1.938 - 0.049 \\ &= 1.889 \end{aligned}$$

$$Y = \frac{z - 1.889}{0.085}$$

$$z = 0.085 Y + 1.889$$

6.3. Fuller

Natural flow frequency distributions of type of fuller's frequency formula (imperial) plotted lineary, using a linear

scale for Natural flow (column 3) and logarithmic scale for the probability of occurrence in % (column 6). These scales have been applied in the relevant diagram and joint scales for the probabability of non-occurrence in % (column 8) and the return period in years according to Gunding to Gumble (column 4) have been added.

duration curve calculations :

$$x = x_0 + \frac{1}{e} \ln T_P (X)$$

$$x_0 = 83.125$$

$$\frac{1}{e} = 13.65 \quad (\text{as before})$$

$$x = 83.125 + 13.65 \ln T_P (X)$$

$$x = 83.125 + 31.395 \log T_P (X)$$

6.4 Guass

Properly speaking Guass law does not apply here as the Natural flow series, they are not normally distributed. The relevent diagram is only prepared as an illustration. The Natural flow (column 3) have been plotted linearly as a function of the propability of non-occurrence in% (column 9), based on the return period in years, according to Hazen (column 5), which is indicated on a joint scale.

$$\bar{x} = 91 \text{ m.m}^3/\text{Year (as before)}$$

$$\sigma_x = 17.5 \quad (\text{as before})$$

$$y = \frac{x - \bar{x}}{\sigma_x} = \frac{x - 91}{17.5}$$

$$x = 17.5 y + 91$$

6.5. Galton — Gibrat

Galton transforms a non-normally distributes variable y , such that y is normally distributed.

Gibrat proposed for a Natural flow series (x)

$$y = a \log (x - x_0) + b$$

where : a , b and x_0 should be determined graphically by trial and error.

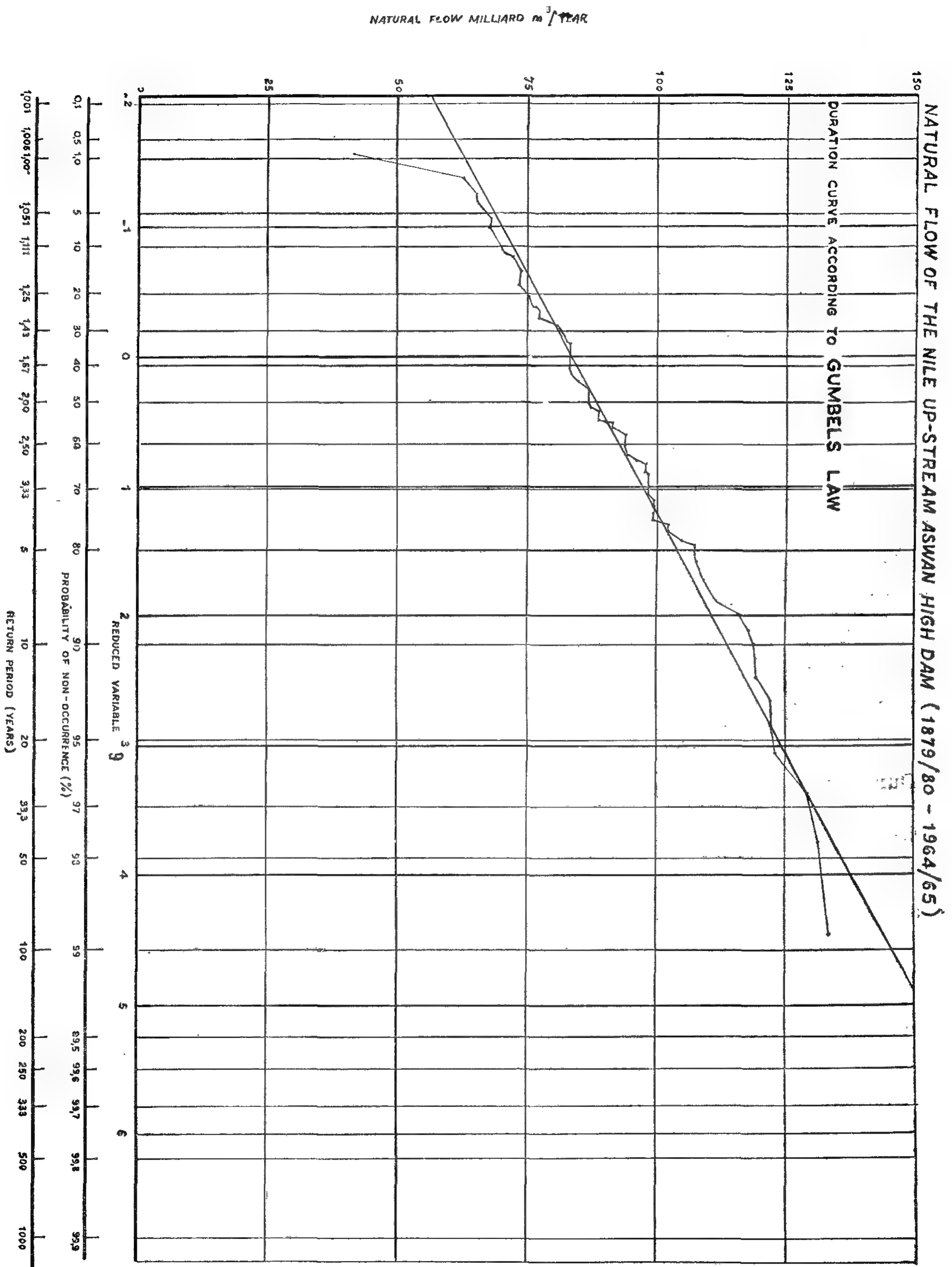


(Fig 1)

3. PURPOSE OF STUDY

The regulation of the Aswan High Dam was first derived in "Long term storage" by Hurst, Black and Simaika/5/, by making trial regulations on 20 samples each of which implies 100 years. These samples were produced from 88 years of discharges at Aswan by new Monte Carlo method.

In this paper, it is proposed to extend the work for the purpose giving a better fit to the river natural flow.

4. PROCEDURE OF STUDY

1. Analyse the natural flow of the Nile distributions.
2. Calculate all the requirements for plotting the data on the various probability papers mentioned in the Abstract.
3. Get the most suitable normal distribution curve to fit the Data of the Nile flow records.
4. Analyse the most fit normal distribution curve obtained.

5. OBTAINING NATURAL FLOW DURATION CURVES

Method of Calculation Required for Curves Plotting.

The annual Natural flow of the Nile, ranges from 42 to 133 milliards m³/year. The Natural flow magnitudes have been listed in a decreasing order in column 3 of table⁽¹⁾. Column 1 represents the serial numbers "m" from

1 to 86 Column 2 represents the years of occurrence. The return periods T have been calculated as follows :

- a) According to Gumbel (Column 4)

$$T_P = \frac{m+1}{m} = \frac{87}{m}$$

- b) According to Hazen (Column 5)

$$T_P = \frac{n}{m - \frac{1}{2}} = \frac{86}{m - \frac{1}{2}}$$

The probability of occurrence : P = 100/T % has been calculated in column 6 and 7 for the return periods listed in column 4 and 5. The supplements of 100% of these probabilities of occurrence give the probabilities of non-occurrence (100-P) %, listed in columns 8 and 9.

Column 10 shows the values of the reduced variables "y" of Gumbel, correspond to the probabilities of non-occurrence, as listed in column 8. These values have been read from a sheet of Gumbel's probability paper.

6. CURVE FITTING AND APPLIED SCALES.

6.1. Gumbel.

The natural flow (column 3) has been plotted linearly as a function of the reduced variable y (column 10). Scales for the probability of non-occurrence in% (column 8) and the return period (column 4) have been added as derived from a sheet of Gumbel's probability paper.

BEST FITTED DURATION CURVE FOR THE RIVER NILE NATURAL-FLOW

by

Dr. MOSTAFA EL-GIZAWI*,

& Dr. MAHMOUD ABU-ZEID⁽²⁾

I. ABSTRACT

Cumulative frequency distribution curves or duration curves based on various probability laws, have been calculated and drawn for annual natural flow of the Nile for the year 1879/80 to 1964/65 (86 years).

The frequency distribution curves are based on :

Gumble, Frechet, Fuller (i.e. The type of fuller empirical flood frequency formula), Gauss and Galton-Gibrat probability laws.

The results obtained by each of them have been compiled in one diagram which shows the duration curve of the River Nile. This diagram is very important for studying the over year storage of the High Aswan Dam.

2. INTRODUCTION

The annual flow of the Nile is capricious. In some years, it may be so low as to the extent of being insufficient to meet the required demands while in others the flow may be so high as to threaten the country for disastrous results. In order to guarantee demands, over-year storage is necessary so as store all water in excess to the requirements. Hence the construction of High Aswan Dam was

a necessity for Egypt. The over-year storage studies require statistical studies for a sound forecast of the flow series of the River Nile.

In many rivers, forecast of flow is possible for a future short interval. In the case of the Nile the discharge for several months in advance can be forecasted by analysis of rainfall data of the catchment area. However for long-term forecast, the probability theories have to be used. The use of probability in the runoff studies have been suggested to Fuller in 1986 by G.W. Rafter.

In 1914, Fuller gave the first real comprehensive study of statistical methods applied to floods in the U.S.A.

There are now many probability distributions which have been suggested as appropriate for hydrological analysis of a stream flow.

In this paper Duration curves based on various probability laws were plotted and the best fit curve was determined to give the probability of occurrence for the Natural flow, using the annual natural discharges of the Nile at Aswan for the period 1879 / 80 to 1965 / 65.

1) The Egyptian Public Authority for Drainage Projects.

2) Director, Water Distribution & Irrigation Methods Institute.

Boring No. 2

1.5									
4.5	2.5	4.5	55.0	15.0	13.4	2.8	11.8	2.00	0.61
7.0			49.0	23.0	11.3			2.04	
12.0									

Boring No 3

1.7								2.05	
4.0			89.0	20.0				1.90	
5.0	3.5	6.2	51.0	21.0	12.1	2.9	15.4	2.18	0.61
6.5	3.0	5.9	49.0	21.0	13.0	3.1	14.5	2.16	0.51
7.5			43.5	14.6				2.21	
9.00			38.0	16.2				2.24	
12.0	3.5	6.0	10.0	28.0	14.0	4.8	16.2	1.90	0.54

L.L. = Liquid limit.

P.L. = Plastic limit.

S.L. = Shrinkage limit.

CONCLUSION :

- 1) Field and laboratory tests bear good correlation qualitatively.
- 2) The swelling pressure measured in laboratory is still in a controversial state. The current methods require further studies to represent actual field behaviour.
- 3) The swelling characteristics of clayey soils depend not only on the clay mineral present but also, to the same degree on the initial compactness of the soil.
- 4) The use of values of P obtained from laboratory tests should be sus-

tained by long term field tests where the bulk of the soil under foundation level (and probably around foundation) is to be saturated and swelling is measured till the soil comes to equilibrium.

DEFERENCES :

- 1) Skempton (1953); "the colloidal activity of clays" Proceedure of the 3rd Int. Conf. on soil mechanics and Foundation Engineerigg- Zurich.
- 2) El Ramli "Swelling Characteristics of some Egyptian Clays"
Proc. of the Society of Engineering Cairo 1965.

The free swelling of the soils in the laboratory as well as in the field is relatively high as compared with the swelling under load. Experience shows that this characteristic is usually pertinent to either illites or calcium montmorillonites of poor crystalline order (Elramli 1965).

In our case where low activities are noticed one concludes that the predominant mineral could be illite.

The field tests show almost identical characteristics as laboratory tests. High free swelling is quite noticeable while a severe drop in the swelling takes place even under small loads, (see Figs 7, 8 and 9). The value of P_s in field tests as determined by interpolation from measured swelling under load (Figs. 7, 8 and 9) seems to bear some correlation with the values obtained experimentally by method (a) where the samples are saturated under constant volume and then stressed till 0.2% strain where the corresponding load is then considered to P_s . The authors believe that this correlation can be a fortuitous one.

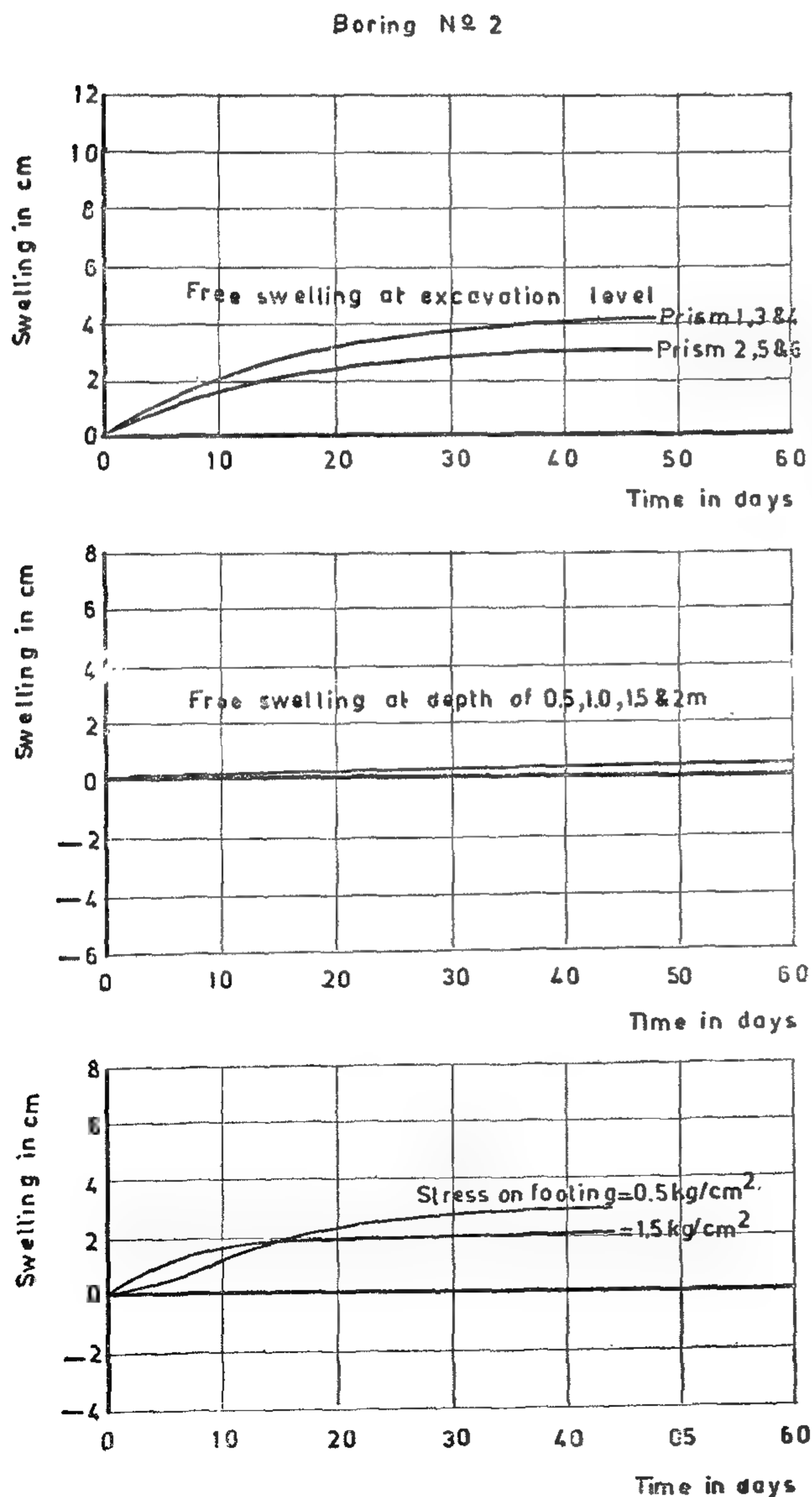


Fig. 8 TIME IN DAYS VERSUS SWELLING IN CENTEMETERS

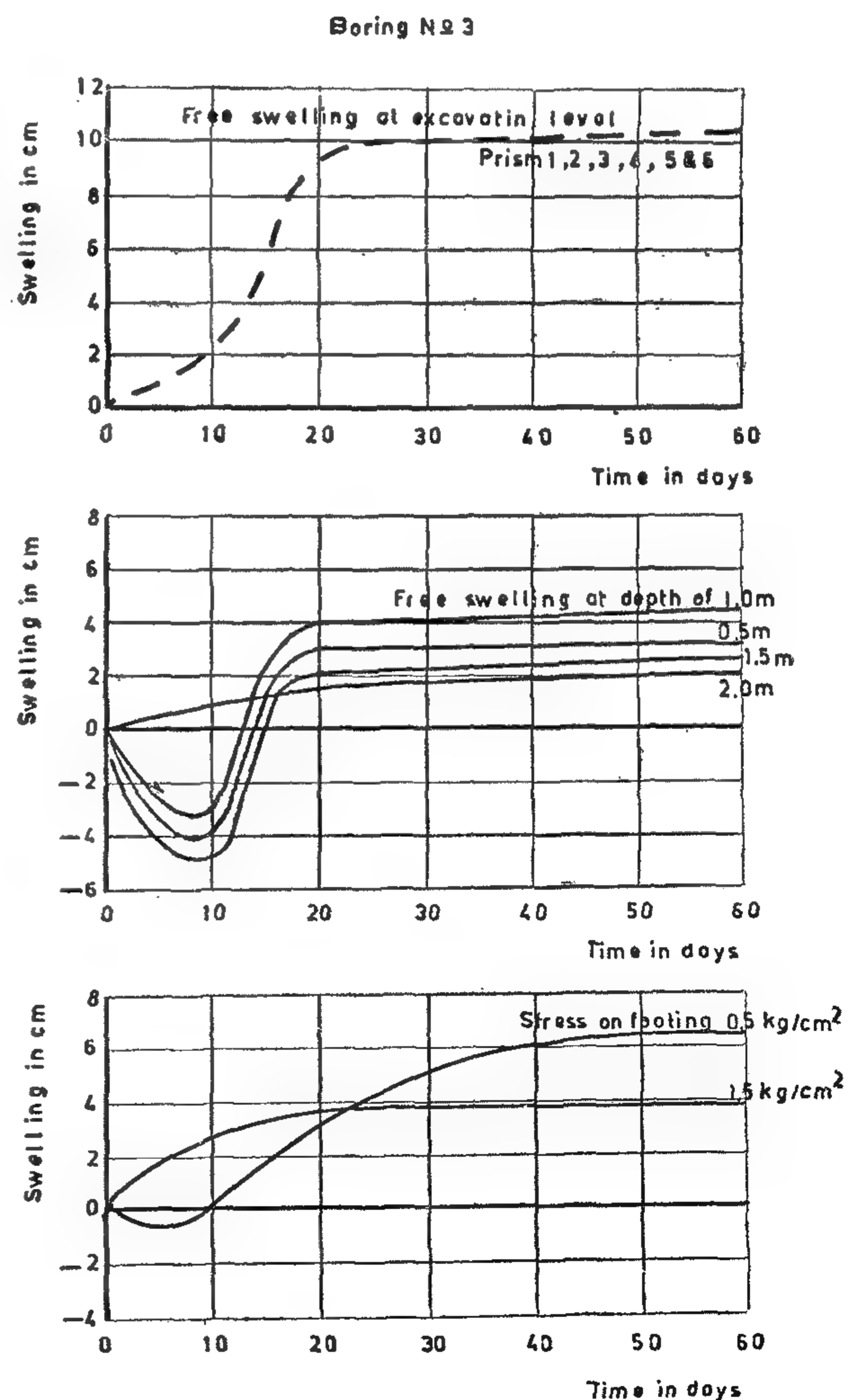


Fig. 9 TIME IN DAYS VERSUS SWELLING IN CENTEMETERS

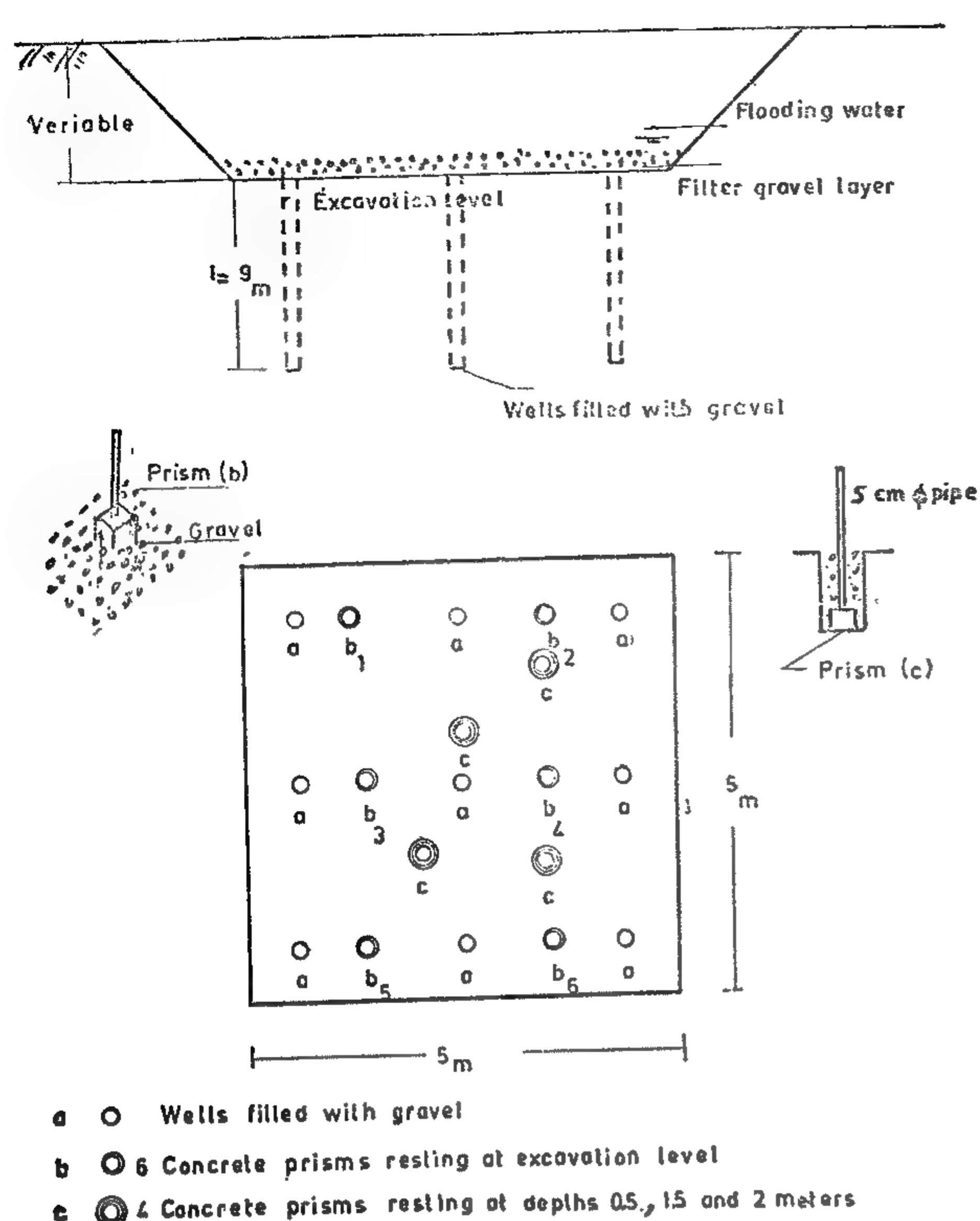


Fig. 6 ARRANGEMENT OF CONCRETE PRISMS

DISCUSSION

The different methods of laboratory determination for the value of the swelling pressure P are in fact not conclusive. While method "a" preserves the natural structure of the soil, method "b" does not. In fact the three or four samples tested by method "b" do not preserve their structure when they swell. The swelling under different loads gives eventually a different structures for each one of the samples which were initially identical with the result that the interpolated value P_s is not truly representing.

The values of P_{sa} and P_{sb} in (table 1) are at complete variance due partly to variations in the structure and partly to the fact that the chosen compression of

0.2% in method "a" may be smaller or greater than required to correspond to P_5

The correlation between activity and swelling pressure does not seem to be a conclusive one, contrary to that between shrinkage limit (as determined in the conventional way) and the swelling pressures. However, it is clear from laboratory tests that the initial dry density of the soil (the compactness) has also a great role in deciding the values of P

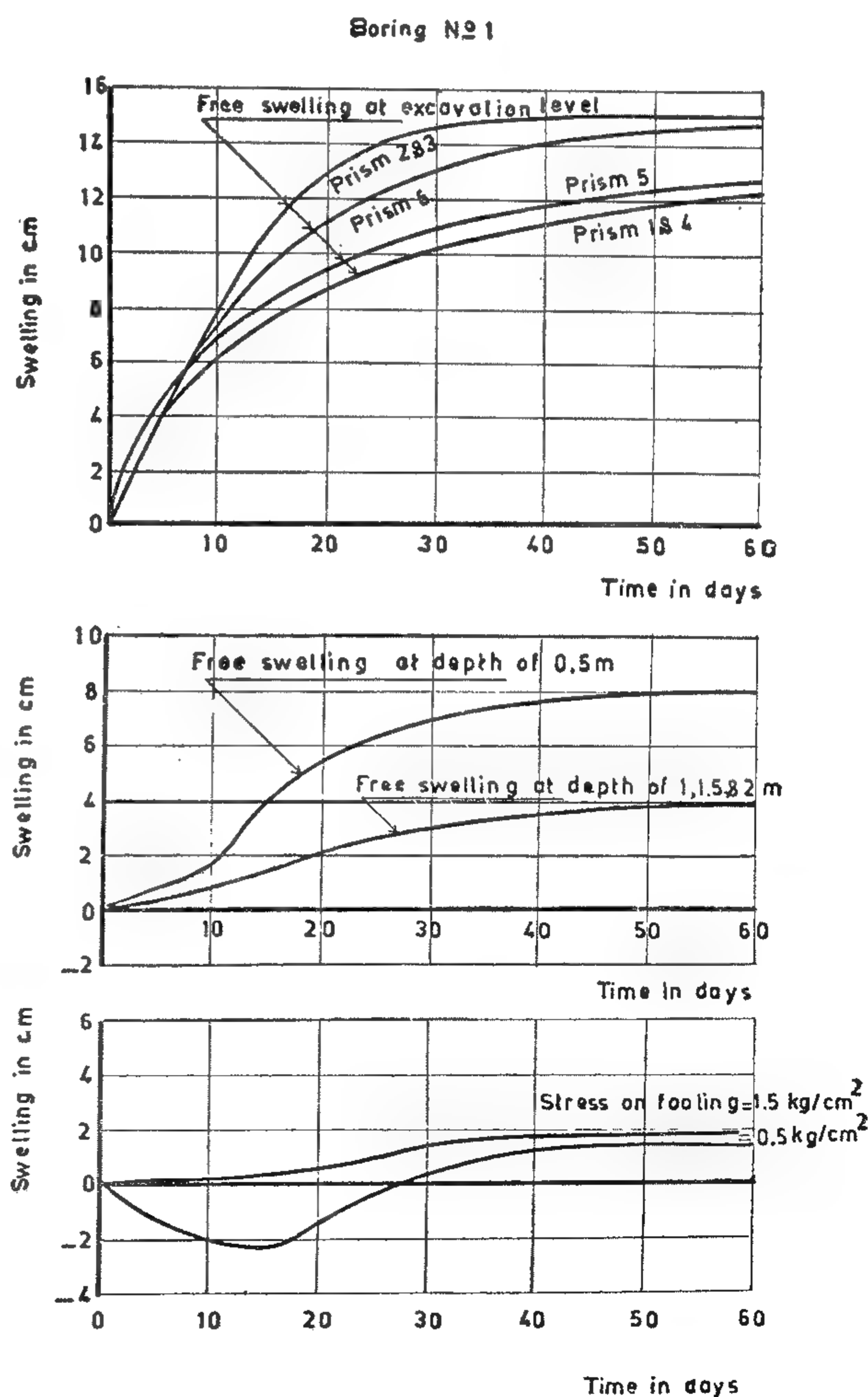


Fig. 7 TIME IN DAYS VERSUS SWELLING IN CENTIMETERS

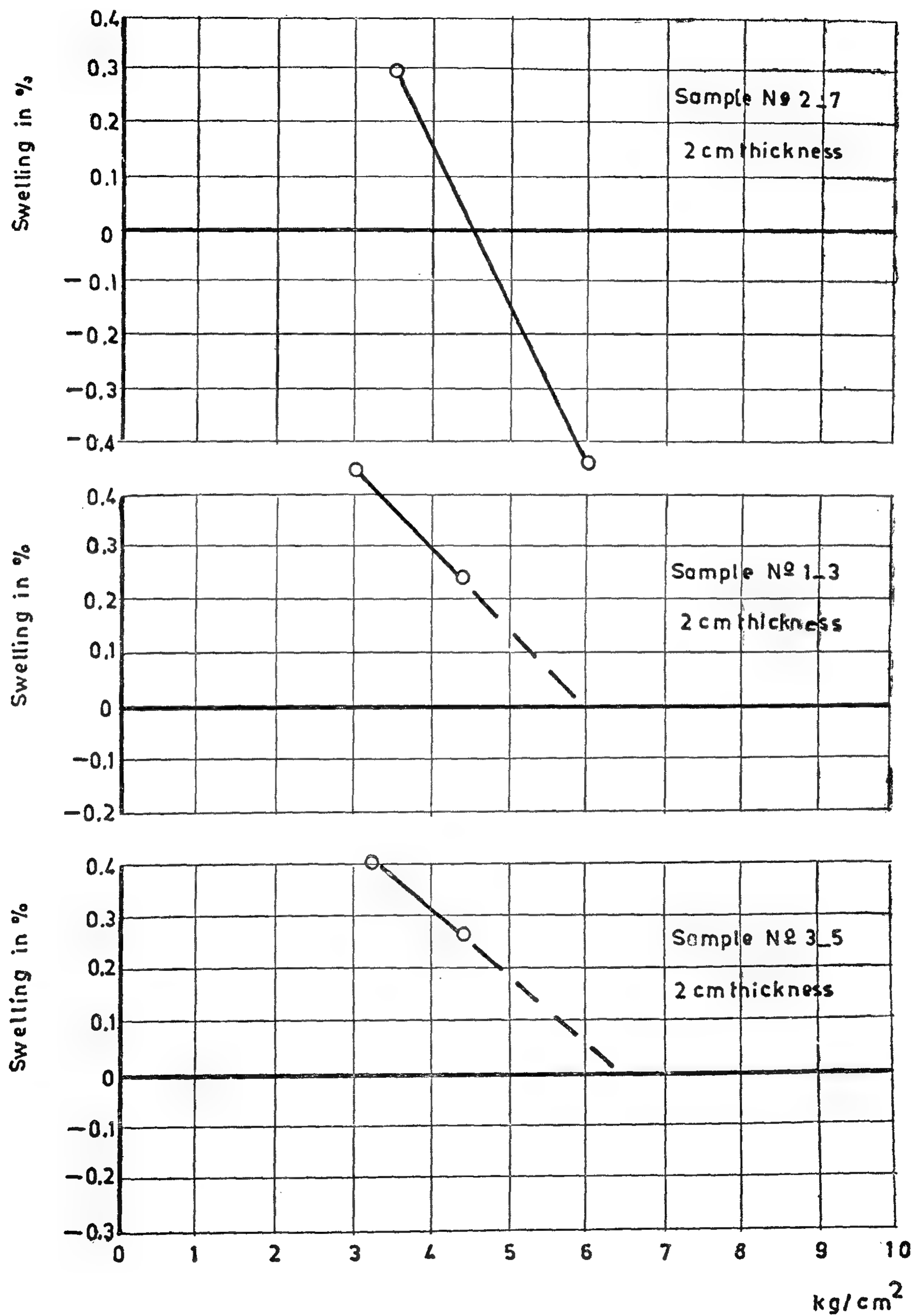


Fig. 5 Swelling in % For Three Undisturbed Soil Samples Under Various Vertical Stresses.

water is invading the soil sample. The results obtained by this method were to be sustained by a comparative study on the same samples by the more currently used method which follows :

- (b) This method of determining P_s is used in Egypt for many years and consists in testing three or more indential soil samples each under a different load. When water is allowed to seep into the sample, the final value of swelling is measured and plotting the results as shown in (Fig. 5) the swelling pressure is measured either by interpolation or by extrapolation. The results are shown in table 1. The swelling pressure is that causing zero volume change in the sample.

II — FIELD TESTS

- (a) Free swelling of soil :

This was done by digging a pit of about 5x5m and a depth varying according to the existance of swelling strata. In the bottom of the pit four (or more) 15 cm diameter wells were drilled in to a depth of about 9.0 m & filled with gravel (distance of wells is 2.0 m on centres). On the bottom of the pit there was placed six concrete prisms 15x15x30 cm at various

places and were provided with a staff (a gas pipe fitted with a scale). In addition four four prisms of the same size were placed in dug holes below bottom level of the pit at depths 0.5, 1.0, 1.5 and 2 m and provided with a scale similar to the above mentioned prisms (Fig. 6.). After the prisms were put in, a gravel layer was placed on the bottom of pit to a thickness of about 15 cm. The pit was then flooded gradually and carefully with water and the upward movements of the blocks were measured. Readings and flooding continued until the rate of rise is 2mm per week. This rate is considered as the eventual end of soil swelling (see Figs. 7, 8 and 9).

- (b) Swelling of loaded soil :

Loads of 5.0 & 1.5 Kg/cm² were applied to two test footings 70x70 cm in area. Each footing was fitted in an excavated pit similar to above mentioned ones. After adding the load on the dry soil through the test footing, flooding was started as before and measurement of the rise of the loaded footings continued till the rate was 2.0 mm per week (see Figs. 7.8 and 9).

Boring No. 1

Depth in m	Swelling Pressure P_s Kg/cm ²		Plasticity limits			nat- ural W/C	final W/C	δ gm/ cm ³	Acti- vity
	P_s (a)	P_s (b)	L.L	P.L.	S.L.				
1.0			51.0	17.5		2.50		2.09	
2.0			30.0	15.8		1.80		2.12	
3.0	3.0	5.9	45.0	20.0	12.1	2.62	14.4	1.96	0.45
5.0	3.5	6.1	54.0	25.0	11.0	2.74	15.0	2.00	0.52
7.0	3.5	5.5	48.0	22.0	14.4	1.74	11.5	2.06	0.61
10.0			49.5	19.0		1.85		2.08	
13.0			35.5	13.0		2.10		2.16	

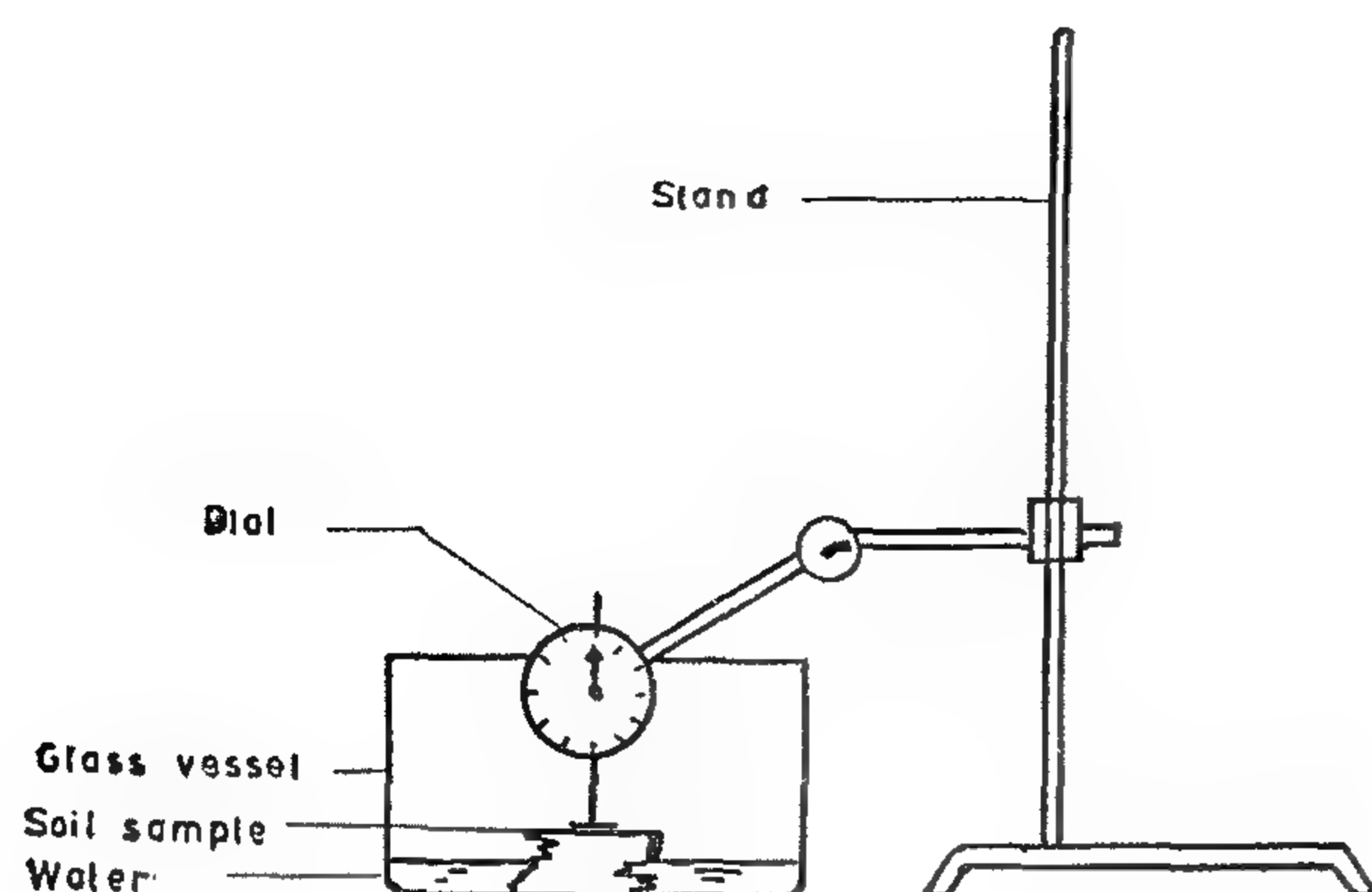


Fig. 2 SOIL SORTING DEVICE

reinforced concrete skeleton structure. Some engineers however, consider the "swelling pressure" as that pressure producing, in the test specimen, a certain value of swelling. Although this is a more realistic approach from the design point of view, it still bears to some extent the same misgivings as mentioned above.

Field testing also comprises the measurement of the "free swelling" together with loading tests on 70x70 cms test footing loaded (on the dry) by stresses of 0.5 & 1.5 Kg/cm² before the supporting soil is flooded. Laboratory swelling tests require a pre-determination of the time necessary for any sample to come to equilibrium with respect to water absorption. A special testing device was arranged (Fig. 3) where the soil sample is fitted in a ring and water is allowed to seep into it. The sample top touches a rod connected to a proving ring. The proving rings used have several flexibilities. The time for the proving ring to stop deformation is taken as the equilibrium time. Ranges of time were so small and bear almost no relation to the proving ring characteristics.

I — LABORATORY TESTS

Determination of swelling pressure

Ps:

- (a) The method of saturating the soil under constant volume :—

In this type of test the soil sample is brought to equilibrium under the effect of a percolating water (due to small hydraulic gradient) while its volume is kept constant by an arrester (Fig. 4), till the sample is fully saturated. At this stage the sample is loaded in the same as a compression sample. The load causing a deformation of 0.2% is considered conventionally as equal to P_s . Whether this is true or not for all types of clayey soils is still questionable. The technique is adopted in the U.S.S.R. and was applied on Egyptian clays as given in this paper. One of the merits of this method is the fact that the structure of the soil is kept almost intact while

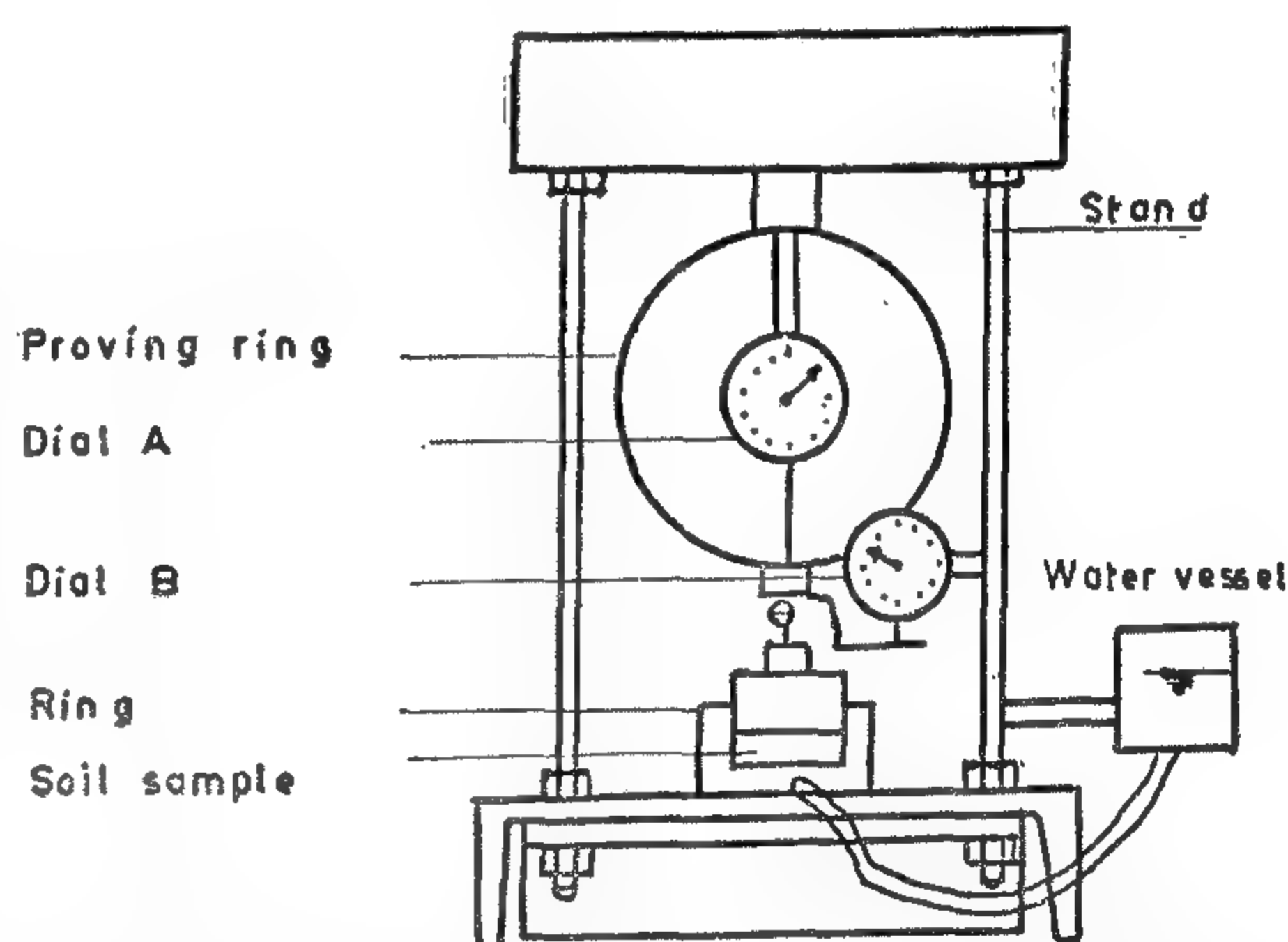


Fig. 3 SWELLIN STABILIZATION TIME APPARATUS

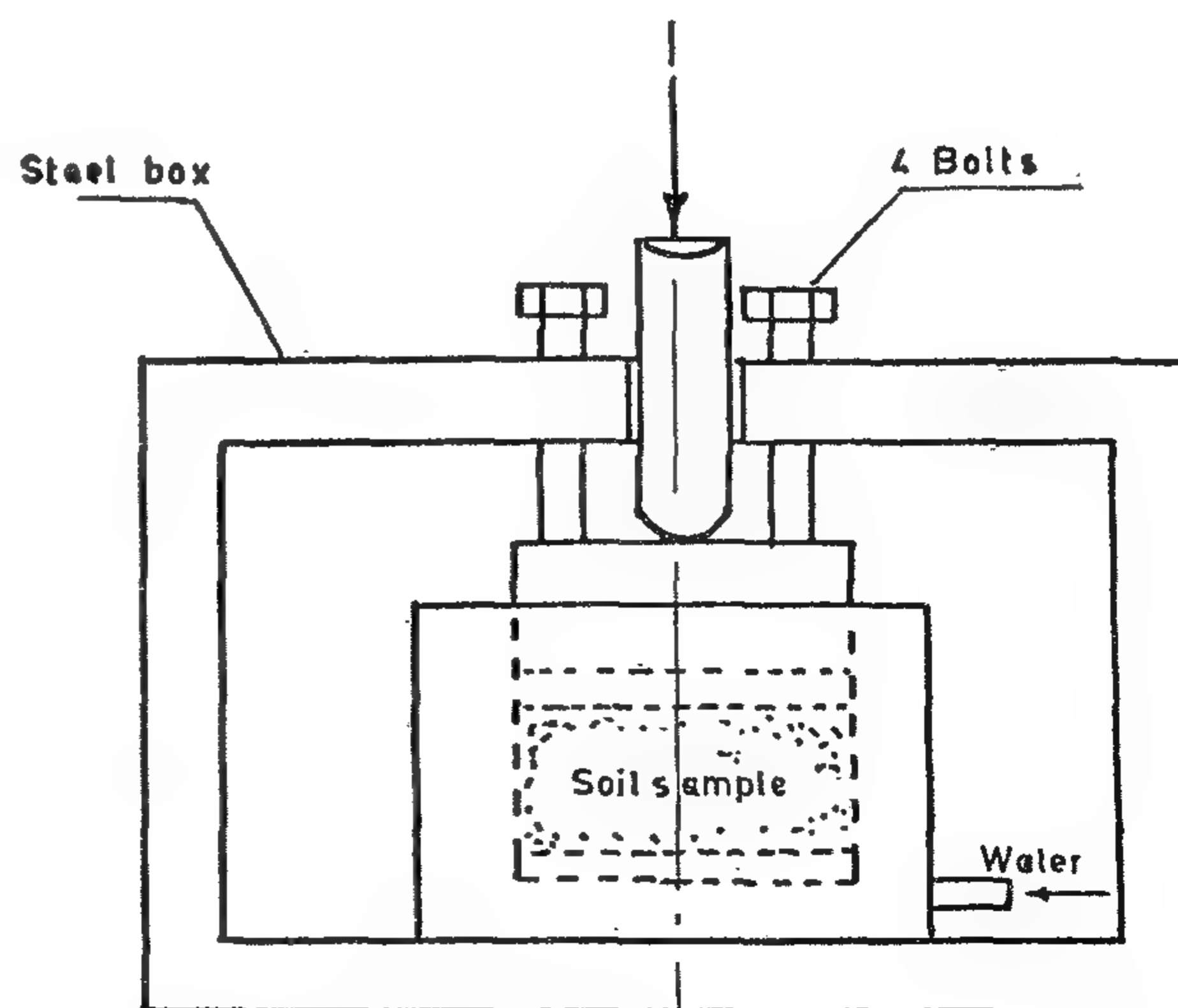


Fig. 4 CONSTANT VOLUME ARRESTER

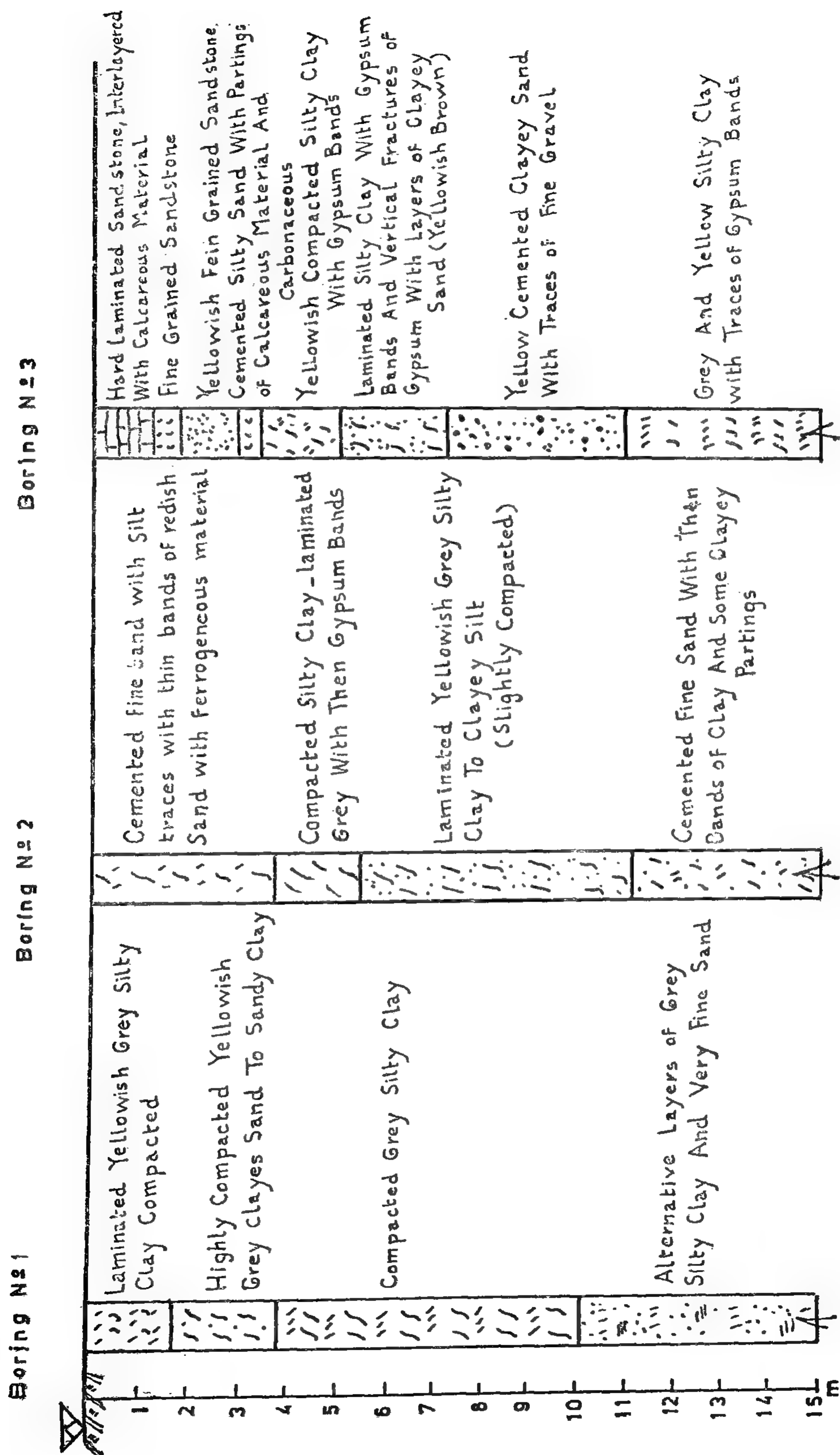


Fig.1 BORING SECTIONS

FIELD AND LABORATORY STUDIES ON CERTAIN SWELLING CLAYEY SOILS IN EGYPT

By

A. HELMI EL-RAMLI* D.I.C., M. Sc, Ph. D. &

MOUSTAFA EL-DEMERY** M. Sc, Ph. D.

INTRODUCTION

The swelling of dry soils in A.R.E. constitutes one of the challenging construction problems. In this paper a certain site was chosen for the construction of a large industrial plant where geological conditions lead to the formation of large depths of variegated shales containing some portions of swelling soils. A great part of such soils is relatively weathered. However the lower horizons are relatively intact and are formed of several layers of silty clay or interlayers of clays and fine sands in addition to occasional gypsiferous bands.

The general practice in Egypt when dealing with expansive soils, so far, was to found the structure on a cushion of sand with varying depth to "absorb" the swelling energy while the foundation is being reinforced with semelles in both directions. While this practice holds good for light construction, it may not prove satisfactory for structures of complex statical systems. This was also evidenced in some public buildings in many parts of the country that lie in the arid zones. The subject matter of this paper deals with one site where heavy construction is proposed & where extensive laboratory and field testing programs were made.

SOIL CONDITIONS

Three borings were made in the site and several samples were secured. Boring

sections and relevant soil description are given in Fig. 1.

SOIL TESTING

Experience with various soil types in Egypt can help in determining the swelling nature of soils visually. However in the present work the swelling nature was determined by a simple test on cut specimens subjected to water infiltration and then measuring its deformation (Fig. 2). The swelling specimens were thus reserved for future testing program. The testing program comprises the measuring of the free swelling as well as the swelling pressure.

While the term "free swelling" is self explanatory, the term "swelling pressure" is in some ways controversial. By "Swelling pressure" some engineers refer to that pressure that causes no swelling in the test specimen and hence in the soil underneath a foundation.

The swelling pressures measured in this way can be practically useful in cases of large rafts (as compared to the clay thickness) supporting a structure of relatively heavy weight i.e. exerting a pressure on the soil comparable to this said "swelling pressure". In case of footing foundations, the term may be completely misleading and a certain school in upper Egypt suffered upward movements of several centimeters and severe consequences were also sustained by the

* Professor of Soil Mechanics and Foundations Faculty of Engineering Cairo University.

** Building Research Institute Cairo.

specially after the conversion of Upper Egypt basins into perennial irrigation system.

6. Application of the proposed method has provided values of the seepage discharge gained into the Nile per meter run of its length. The annual discharge gained into the Nile as base flow is calculated approximately as 4.72 milliards of cubic meters in 1970, for the reach between km 80 and 910 km from Aswan.

APPENDIX — REFERENCES

1. Abd-elrahman, Fatma, «Parameters and Characteristics of the Ground water Reservoir in Upper Egypt», thesis submitted for the degree of master of Science, Cairo Univ., A.R.E 1974.
2. El-Kateb, M.H. and Fatma Abdel-Rahman, «Characteristics of the Ground Water Reservoir in Upper Egypt», Journal of the Egyptian Society of Engineers, Vol. XIV, No. 1 (Jan., Feb., March), 1975.
3. El-Korany, M. «Computer Simulation in Irrigation Problems», thesis submitted for the degree of Master of Science, Institute of Statistical Studies and Researches, Cairo Univ., A.R.E., 1974.
4. Hammad, H.Y., «Natural Drainage of River Valleys», Journal of The Irrigation and Drainage Division, ASCE, Vol. 91, No. IR2, Proc. Paper 4360, June 1965, pp. 39 — 49.
5. Hashem, A.S., «Effect of the High Aswan Dam on the Nile Hydrology and its Relation to Expansion Projects in Arab Republic of Egypt, Vol. II, Government Press, Ministry of Irrigation, October 1972.

TABLE 2.- VALUES OF ANNUAL DISCHARGES GAINED BY THE
NILE IN UPPER EGYPT

Sec. No.	Distance from Aswan	Permeability of Aquifer	Drainable Length		Average Q_{year}	Total Q_{year}
			λ_e	λ_w		
	(km)	(m/day)	(km)	(km)	(m ³ /year/m')	(mill.m ³ /year)
1	115.2	36.0	2.0	4.5	8000	520.0
2	170.4	21.5	0.0	3.5	4020	84.5
3	182.0	21.5	0.0	5.0	4880	88.0
4	202.5	21.5	3.0	5.0	7590	151.5
5	224	30.0	2.5	2.5	7000	210.0
6	256	72.0	5.0	3.0	13200	238.0
7	266	50.0	4.0	4.0	10200	153.0
8	285.8	50.0	4.0	2.0	7000	175.0
9	315.2	31.5	4.0	0.0	4220	105.0
10	383.5	85.0	2.0	3.0	8000	320.0
11	410.5	70.0	0.0	5.0	5000	150.0
12	454.3	65.0	3.0	5.0	12200	366.0
13	464.3	40.0	3.0	0.0	1780	18.0
14	513	40.0	5.0	5.0	4200	42.0
15	557	45.0	4.0	5.0	12200	488.0
16	594	51.0	0.0	4.0	7750	155.0
17	605.5	51.0	0.0	2.5	3400	95.0
18	661.2	35.0	0.0	6.0	7300	270.0
19	668.2	40.0	0.0	6.5	5900	71.0
20	687.3	40.0	0.0	3.0	2800	50.0
21	702.3	40.0	0.0	4.0	3200	35.0
22	709.3	40.0	0.0	6.0	4800	62.5
23	728.5	35.0	0.0	4.0	4850	72.5
24	740.6	31.5	0.0	5.5	5900	47.5
25	743.6	31.5	0.0	5.5	6050	49.0
26	755.3	31.5	0.0	5.0	4865	58.0
27	770.5	31.5	0.0	5.0	4300	56.0
28	781	31.5	0.0	5.0	4780	72.0
29	798.8	24.0	0.0	5.0	5700	74.0
30	809.3	24.0	0.0	4.5	3800	65.0
31	838.5	24.0	3.0	3.0	5000	120.0
32	849.7	20.0	4.0	3.0	5450	82.0
33	868	21.0	3.5	4.0	5450	87.5
34	883.2	20.0	2.0	4.0	5750	200.0
Total						4721

wan Dam, the field observations have indicated that the piezometric level of the ground water is lower than the water table in the silty-clay layer and higher than the Nile water stages except in the upstream of the barrages.

2. In the new regime, the ground water reservoir is a dynamic resource receiving the drainable excess water from irrigation process and discharging it into the Nile as base flow.

3. The discharge of the ground water in the longitudinal direction is found to be negligible in comparison with the discharge of the Nile.

4. The ground water reservoir downstream Aswan is not affected by the high stages of water stored in Nasser's Lake.

5. Replenishment of the ground water reservoir depends on excess water from irrigation and seepage losses from the system of canals and drains;

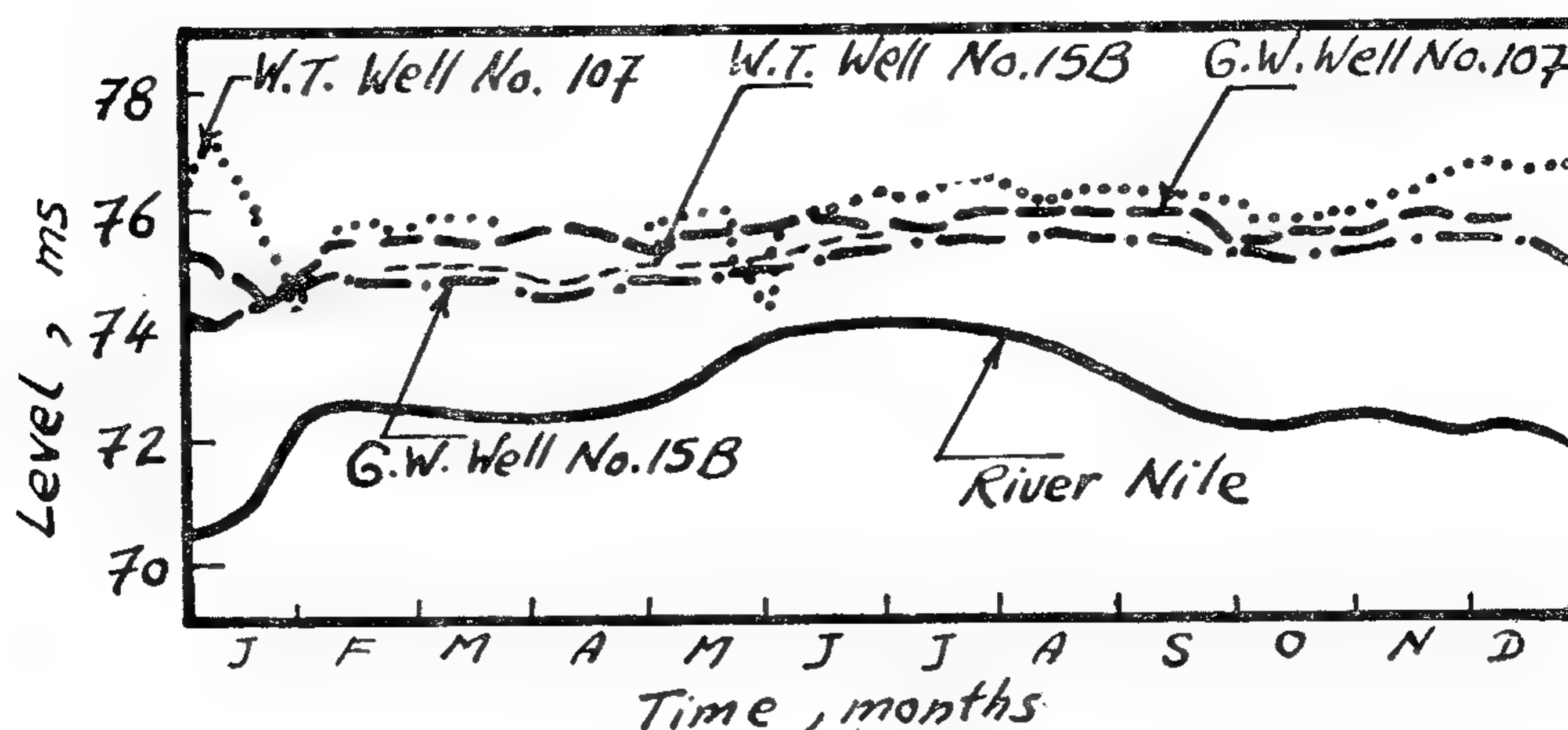


FIG. 8. HYDROGRAPHS OF WATER LEVELS AT SECTION, km. 202.5 FROM ASWAN

TABLE 1.- DETERMINATION OF THE MONTHLY SEEPAGE FLOW GAINED BY THE NILE AT ARMANT

Month	C_e	C_w	h_e	h_w	Q_e	Q_w	Q_n
	(m/day)	(m/day)	(m)	(m)	($m^3/d/m'$)	($m^3/d/m'$)	($m^3/d/m'$)
Jan.	4.45	3.9	3.61	4.02	16.1	15.7	31.8
Feb.	"	"	2.11	2.02	9.4	9.5	18.9
Mar.	"	"	2.13	2.80	9.5	10.9	20.4
Apr.	"	"	2.03	2.96	9.0	11.6	20.6
May	"	"	1.86	2.52	8.3	9.8	18.1
Jun.	"	"	1.28	1.91	5.7	7.5	13.2
Jul.	"	"	1.33	1.64	5.9	6.4	12.3
Aug.	"	"	1.66	2.17	7.4	8.5	15.9
Sep.	"	"	2.39	2.95	10.6	11.5	22.1
Oct.	"	"	2.88	3.21	12.8	12.5	25.3
Nov.	"	"	2.99	3.32	13.3	13.0	26.3
Dec.	"	"	3.12	3.65	13.9	14.3	28.2

Total = 253.1

$$Q_n = 251.1 \times 30 = 7593 \text{ m}^3/\text{year}/\text{m}'.$$

because sufficient data are not available.

Results are illustrated in Table 2 which indicates that the total seepage discharge gained into the Nile in 1970 between km 80 and km 910 is approximately 4.72 milliards of cubic meters per year.

CONCLUSIONS

From the study represented in this paper, the principal conclusions are summarized as follows :

1. Since the completion of the High As-

where Q = rate of seepage flow per unit length of river,

Q_e = rate of seepage flow from the eastern side of valley per unit length of river,

Q_w = rate of seepage flow from the western side of valley per unit length of river,

C_e = coefficient of the eastern side of valley,

C_w = coefficient of the western side of valley,

h_e = difference between piezometric level and Nile stage in the eastern side of valley,

h_w = difference between piezometric level and Nile stage in the western side of valley,

k_s = permeability coefficient of sand and gravel aquifer,

l_e = breadth of the eastern side of valley,

l_w = breadth of the western side of valley, and

r = half breadth of sandy bed of river.

If Q_n represents the monthly seepage flow per unit length of the Nile at any cross-section of the valley, the application of Eqs. 4,5,6,7 and 8 yields.

$$Q_n = \frac{1}{2} C_e (h_e)_n + \frac{1}{2} C_w (h_w)_n \quad (9)$$

$$\text{or } Q_n = \left[\frac{0.342 k_s (h_e)_n}{\log_{10} \frac{2 l_e}{\pi r}} + \frac{0.342 k_s (h_w)_n}{\log_{10} \frac{2 l_w}{\pi r}} \right] \quad (10)$$

in which $(h_e)_n$ and $(h_w)_n$ are the monthly average of difference in head between the Nile stage and the piezometric levels in the eastern and western sides of valley during any month n , respectively. Summation of Eq. 10 for the whole year gives the relation expressed on annual basis as,

$$Q_y = 0.342 \left[\frac{\sum_{n=1}^{12} (h_e)_n}{\log_{10} \frac{2 l_e}{\pi r}} + \frac{\sum_{n=1}^{12} (h_w)_n}{\log_{10} \frac{2 l_w}{\pi r}} \right] \quad (11)$$

in which Q_y is the annual seepage flow per unit length of the Nile at any cross-section.

APPLICATIONS

To illustrate the application of the proposed method, an example is given for a section perpendicular to the Nile near Armant. The calculations are based on actual records obtained from the field by the Ground Water Research Office of the Ministry of Irrigation in 1970. Fig. 8 shows the hydrographs of the water stage in the Nile, the piezometric levels and the water-table levels in two observation wells lying in the cross-section. The first well exists at 3 kilometers to the west of the Nile and the second well at 2.2 kilometers to the east of the Nile. Since the condition of geometrical symmetry is difficult to exist at any cross-section, analysis is made by the image method, as given by Fig. 11.

The corresponding parameters of the section in concern are determined as follows: l_e = 3 kilometers; l_w = 5 kilometers; πr = length of seepage face = 130 meters; d = 8 meters; b = 75 meters; k_e = 0.1 meter/day; k_s = 21.5 meters/day. The monthly difference between the Nile water stages and piezometric levels are illustrated in Fig. 8 and listed in Table 1, in order to calculate the seepage flow gained into the Nile according to Eqs. 7,8,9,10 & 11. It shows that the Nile gain at Armant in 1970 is 7593 cubic meters per year per meter length of the river.

For the rest of the sections across the Nile, calculations are made on annual basis. Few section have been dropped

where,

q = rate of seepage flow per unit length of river,

h = difference in piezometric level of ground water and water stage in the Nile,

k_c = permeability coefficient of silty-clay cap,

k_s = permeability coefficient of sand and gravel aquifer,

l = half breadth of the valley.

b = depth of aquifer,

d = depth of seepage face in clay cap, and

r = half breadth of sandy bed of river.

In the derivation of Fig. 1 Hammad assumed that the piezometric head is identical with the water table in the clay cap. In fact, the piezometric surface is almost lower than the water table as observed from field investigations. It is obvious that the seepage flow from the aquifer into the Nile is dependant on the difference in head between the piezometric level and the Nile stage.

During irrigation process, part of the water is used to supply moisture to the plants and the remainder for leaching as known for ideal use of irrigation water. The excess water drains under the action of gravity to join the subsoil water. When there is a difference between the surface water level and the ground water piezometric level, the excess water percolates vertically downwards. It represents the major source of water added to the ground water reservoirs in addition to seepage losses from waterways.

The formula given by Eq. 1 needs to be adapted for use in another convenient form. In general, the centerline of the river does not represent the axis of sym-

metry for the cross-section of the valley.

Also, the numerical value of the quantity $(\pi^2 bd/2k_c l^2)$ is very small in comparison with the second term in parentheses of Eq. 1. It can be neglected with no appreciable error. As a result, Eq. 1 reduces to

$$Q = \frac{\pi k_s h}{2.3 \log_{10} \left(\frac{2l}{\pi r} \right)^2} \quad (2)$$

or

$$Q = \frac{0.683 k_s h}{\log_{10} \left(\frac{2l}{\pi r} \right)} \quad (3)$$

It is obvious that the quantity (πr) represents the perimeter of the Nile section in the form of a semi-circle lying in touch with the aquifer.

Since, symmetry of the cross-section of the valley does not exist with respect to the centerline of the river, the analysis can be adjusted by the method of images. Each side of the valley with respect to the centerline of the Nile should be considered separately, namely : the eastern side and the western side. The rate of seepage flow into the Nile can be obtained by the method of images as follows :

$$Q = Q_e + Q_w \quad (4)$$

From Eq 3 it follows that

$$Q_e = \frac{1}{2} C_e h_e \quad (5)$$

and

$$Q_w = \frac{1}{2} C_w h_w \quad (6)$$

in which

$$C_e = \left(\frac{0.683 k_s}{\log_{10} \frac{2l_e}{\pi r}} \right) \quad (7)$$

and

$$C_w = \left(\frac{0.683 k_s}{\log_{10} \frac{2l_w}{\pi r}} \right) \quad (8)$$

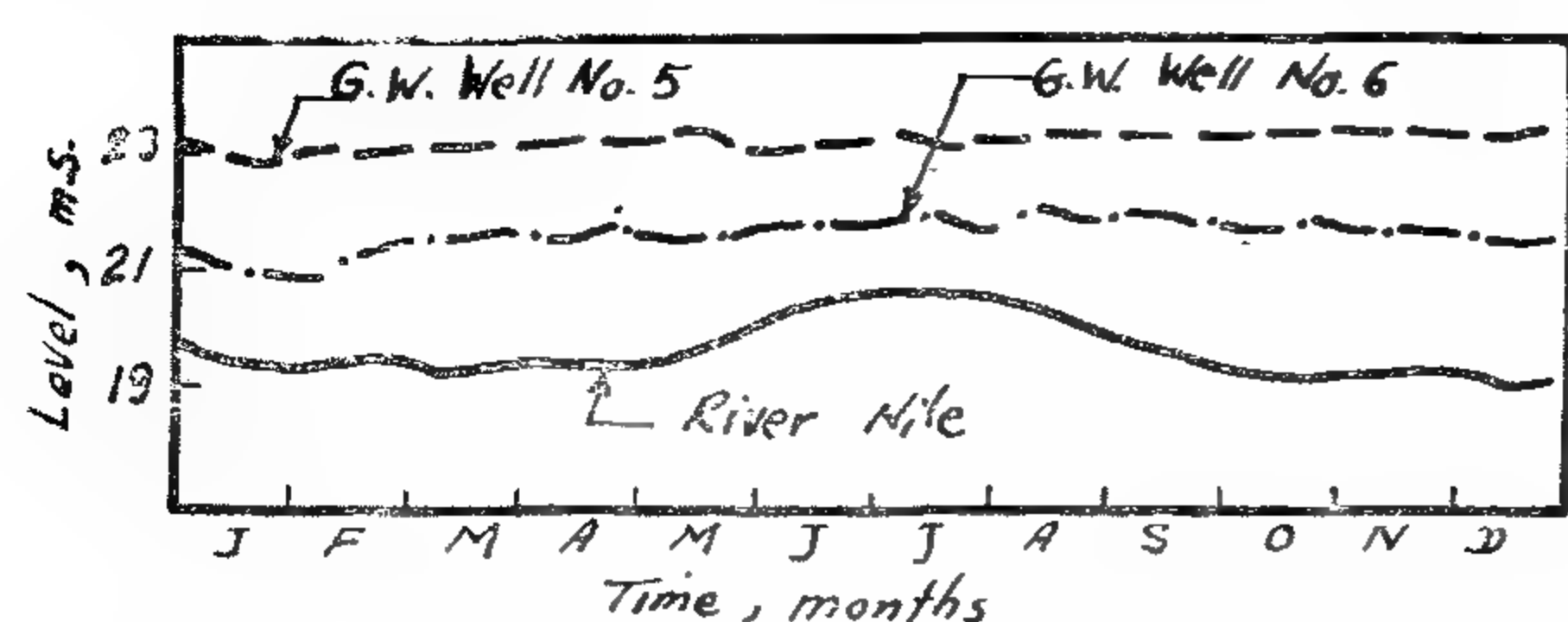


FIG. 6. - SECTION, km. 849.6 FROM ASWAN

water stages of the lake upstream the High Dam. To verify this opinion, the hydrographs of the piezometric levels inside a deep observation well, existing at 11.5 kilometers downstream Aswan; are studied for the years 1964 and 1970. Fig. 7 illustrates that there is no rise in the piezometric levels of the ground water to be correlated with the high water stage of the High reservoir. Another evidence is based on the construction of the old Aswan Dam in 1902. It is well-known that any gravity concrete dam cannot be built except on solid rock foundation to support its huge weight. This was the reason in choosing the location of the old Aswan Dam where the solid rock exists with a big depth. These facts assure that the rock formation existing in the reach of Aswan causes the discontinuity of the aquifer with the High Dam reservoir.

METHOD OF ANALYSIS

A typical cross-section of the Nile Valley in Upper Egypt is illustrated in Fig. 1. It shows a silty-clay cap overlying the sand and gravel aquifer. The measured permeability of the silty layer is observed by Fatma (1) to be very small in comparison with the high permeability of the aquifer. The Nile is in direct contact with the aquifer creating a response between the Nile water and the ground water. After the construction of the high Dam, water stages in the Nile are almost lower than the piezometric levels of the ground water which are in turn, lower than the water table in top silty-clay cap, as shown in Fig. 2. However, the Nile stages are higher than the piezometric levels in some reaches upstream the barrages, as shown in Fig. 3, upstream Naga-Hammadi Barrage. In general, there is seepage flow from the ground water reservoir into the Nile. In the new regime, the Nile is functioning as a big drain or an effluent stream. The effluent seepage flow gained into the Nile channel is defined as base flow component.

For this case, Yousef Hammad (4) obtained an analytical solution for the seepage flow in the form :

$$Q = \frac{\pi h}{\left(\frac{\pi^2 b d}{2k_c l^2} + \frac{2.3}{k_s} \log_{10} \frac{4 l^2}{\pi^2 r^2} \right)} \quad (1)$$

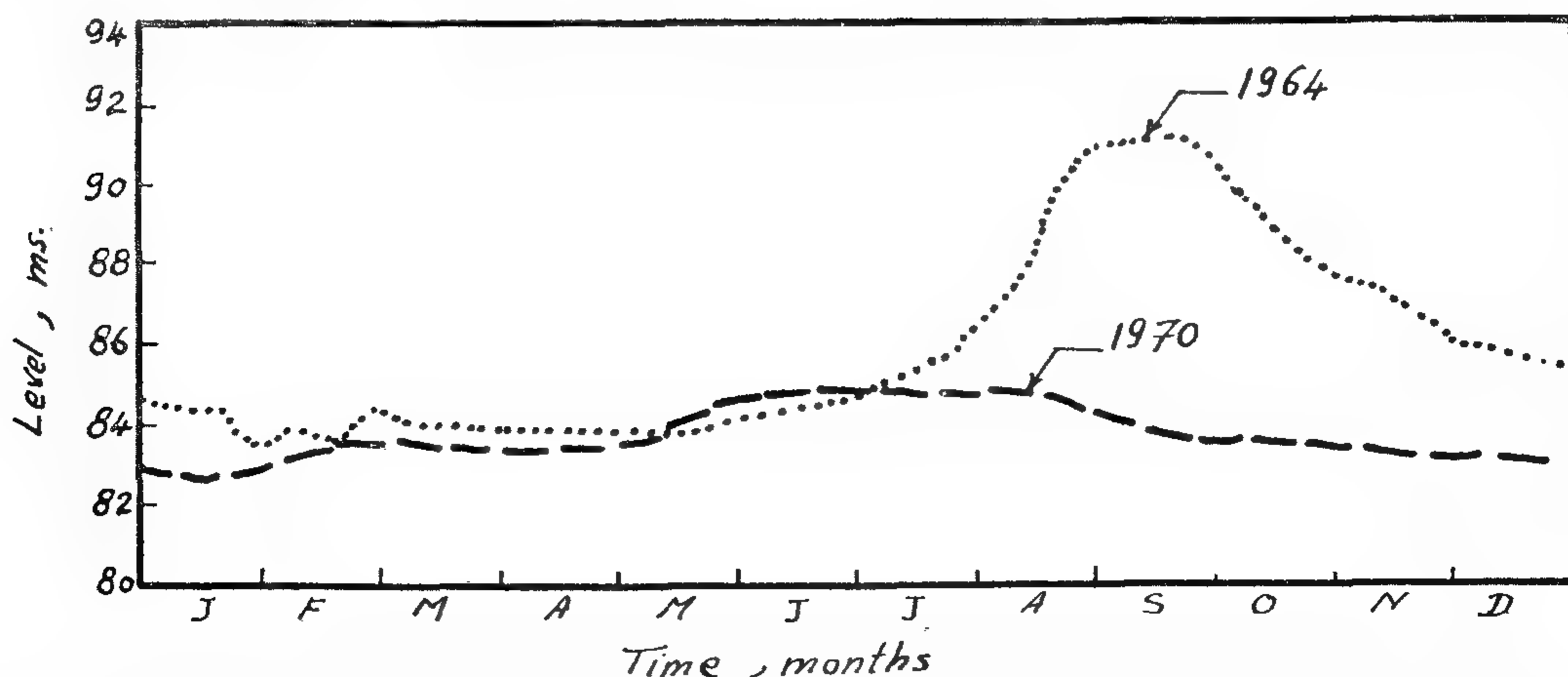


Fig. 7. - Hydrographs of water levels in a deep observation well at 11.5 km downstream Aswan

a previous paper (2). Since, the top layer is of lower permeability than the aquifer, the water table of the surface water and the piezometric heads in the aquifer are not the same. In fact, when the piezometric level is lower than the water-table level, water flows vertically downwards in to the ground-water reservoir, and vice versa. In the new regime, the comprehensive study of hydrographs obtained from deep and shallow observation wells, indicates that the water-table level is higher than the piezometric head, as illustrated in Fig. 2. This condition occurs at the majority of the cross-sections after the construction of the High Dam. Conversion from basin to perennial irrigation has resulted in increasing the drainable water due to continuous irrigation. This condition represents the main source of replenishment of the ground water reservoir in spite of low water stages in the Nile in its new regime. As a result, there is a continuous vertical motion downwards.

2 — Transversal Motion

Before the High Dam, observations indicated that the flood wave in the Nile was followed by a similar wave of the ground water in the valley with lag in time. In the new regime, the Nile has low water levels, taking the role of being a big drain for the valley as illustrated in the hydrographs of Fig. 2, 4 & 6. As a result, a natural drainage process occurs from the ground water into the Nile in a transversal direction. The observed piezometric levels of the ground water are almost higher than the water stages in the Nile except in some reaches upstream the barrages of Esna, Naga Hamadi, Assuit and the Delta, as shown in Fig. 3.

3 — Longitudinal Motion

The ground-water piezometric level declines from Aswan to Cairo with a slope varying from 5 to 8 centimeters per kilometer. It takes more or less the same slope as that of the land surface along the valley.

A fact must be mentioned here, is that the ground water reservoir in Upper Egypt is not affected by the high

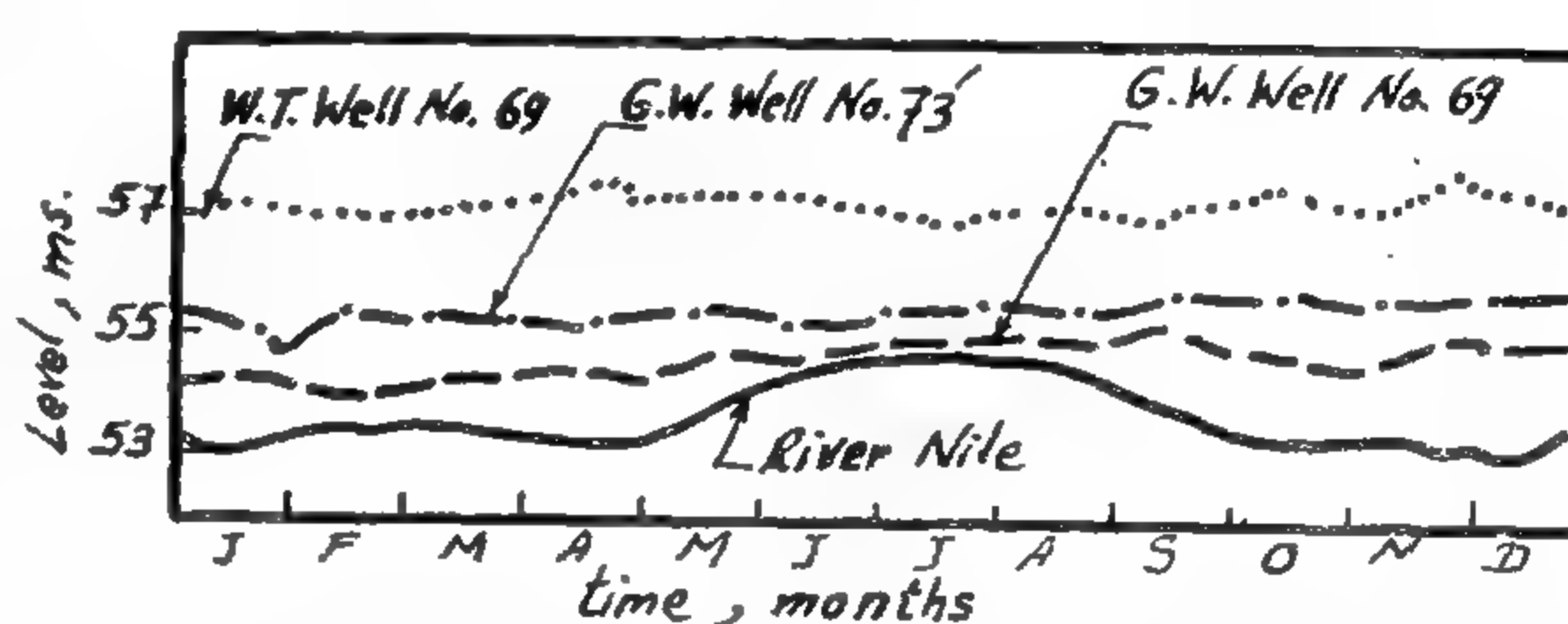


FIG. 2.- SECTION NO. 13, km 464.3 FROM ASWAN

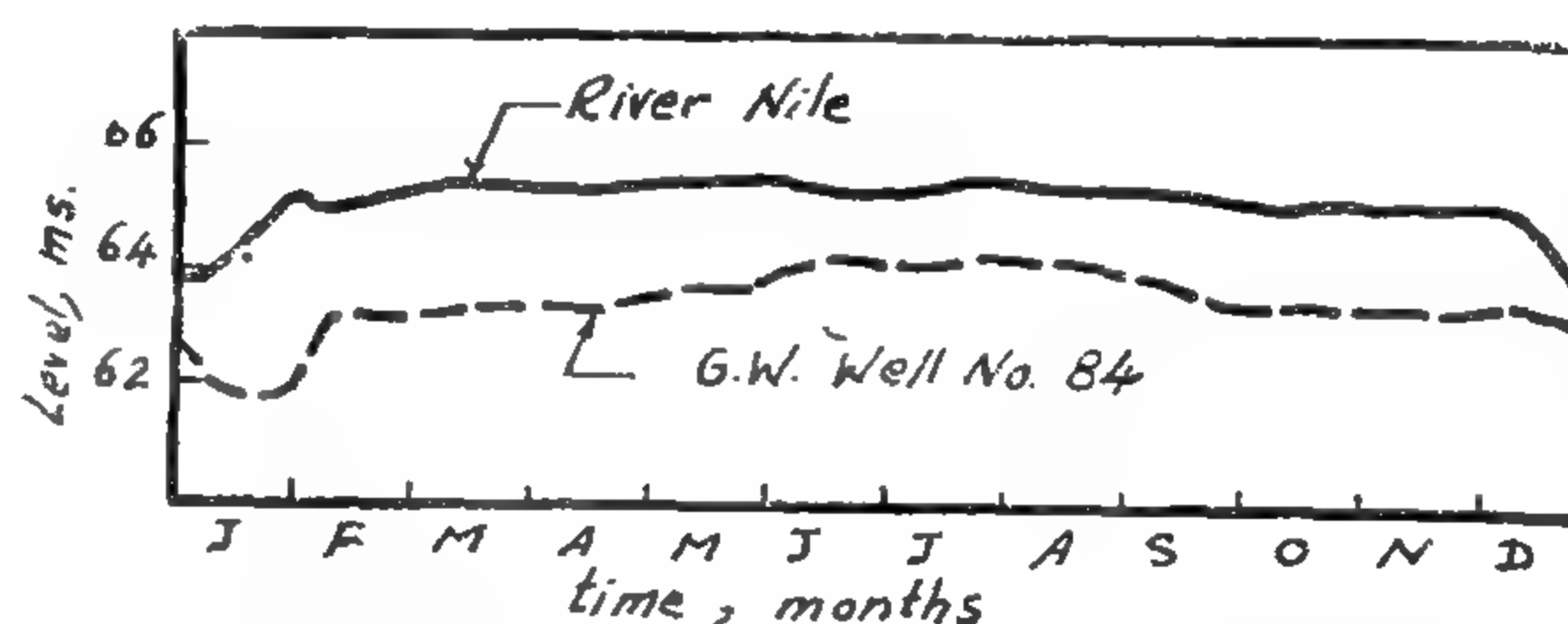


FIG. 3.- SECTION, km. 358.3 FROM ASWAN

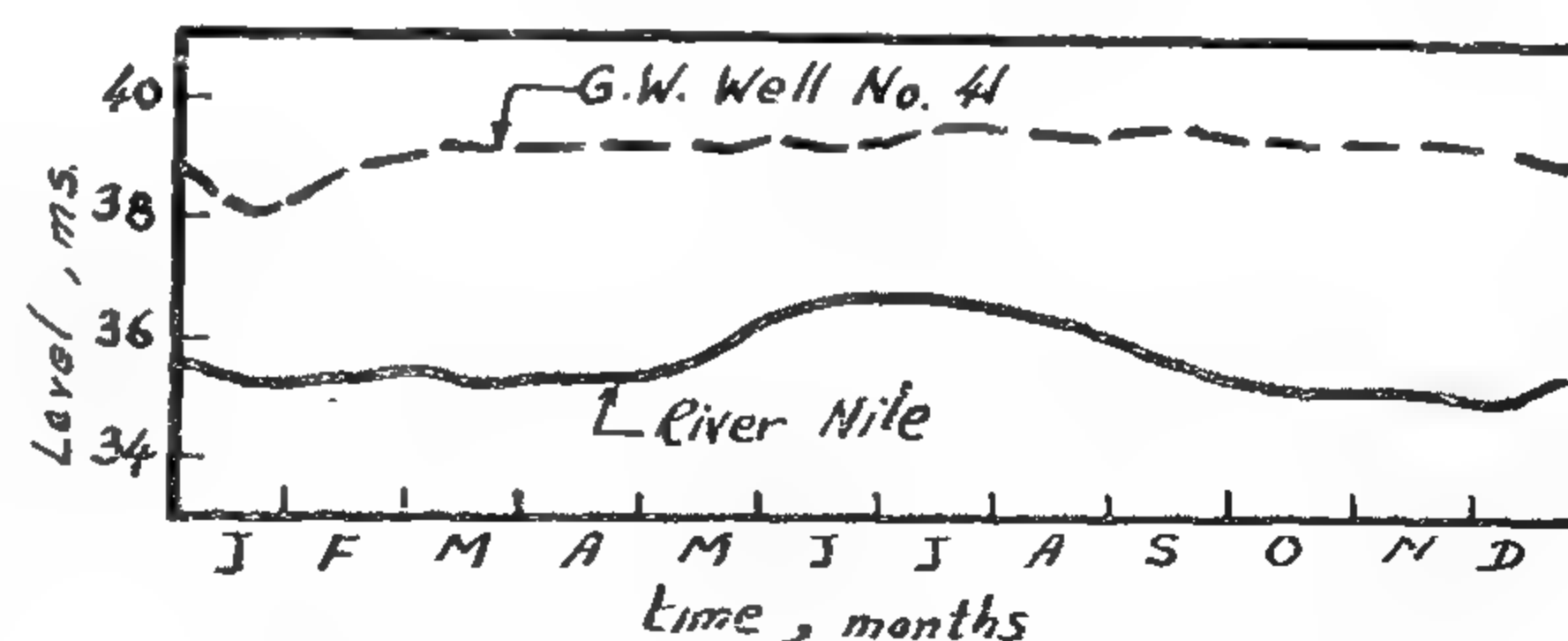


FIG. 4.- SECTION, km. 661.2 FROM ASWAN

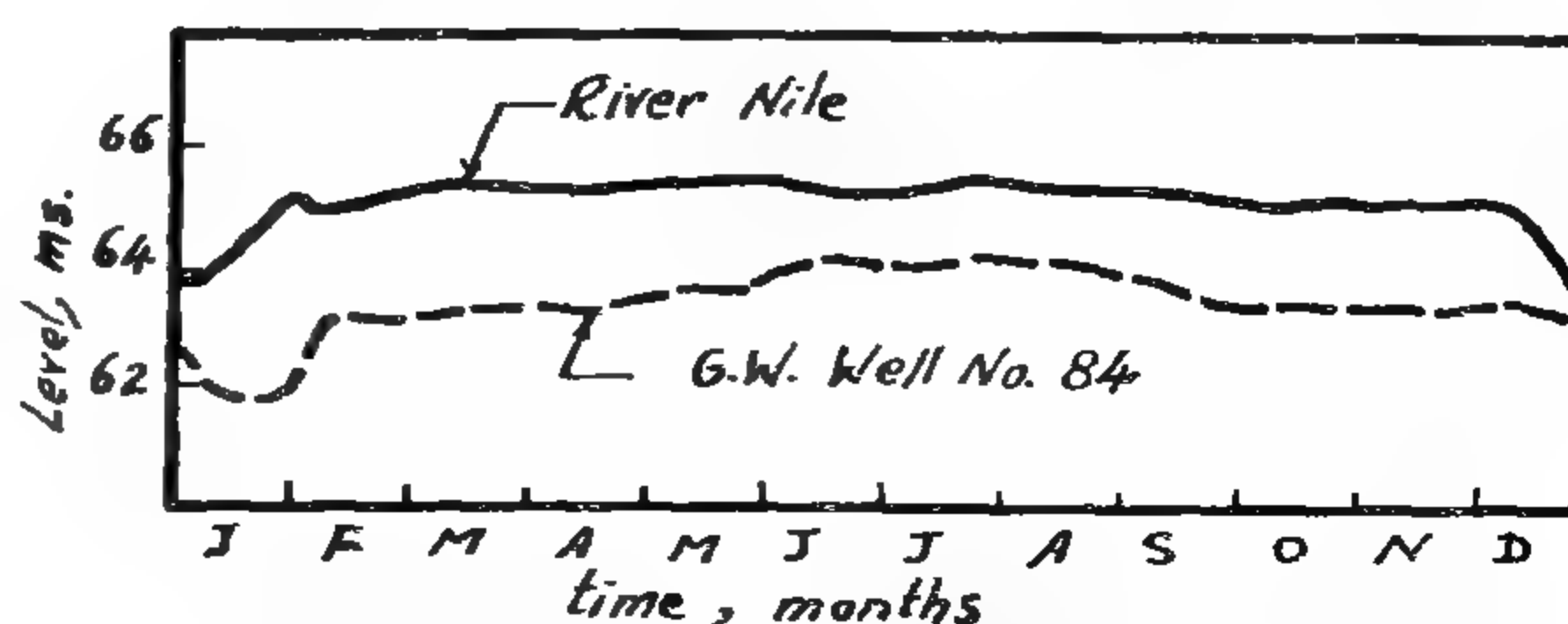


FIG. 3.- SECTION, km. 358.3 FROM ASWAN

The application of the foregoing relation depends on the knowledge of time of propagation of a certain discharge from Aswan to the different locations on the Nile. They have shown that the average Nile gain from the ground water within the period 1961 — 1971 is 2.747 milliards of cubic meters per year. In fact this approach is considered as a crude estimate of the actual ground water contribution as base flow.

The purpose of this study is to estimate the Nile gain from the ground water by knowledge of the seepage flow from the aquifer into the Nile channel. The study is based on the records of the piezometric heads measured in deep observations wells constructed at different cross-sections of the Nile as compared with the corresponding water levels in the Nile.

MOTION OF GROUND WATER IN NILE VALLEY

The flow through aquifers which are natural porous media, can be described by what is known as Darcy's law. Flow of water happens from a point of high pressure to one of small pressure. When this motion is analyzed in the space, three directions of flow are considered, namely : the longitudinal, transversal and vertical directions. The motion of the ground-water flow in the three main directions is summarized as follows :

1 — Vertical Motion

Water flows upwards or downwards due to the difference in pressures in both the aquifer and the top silty-clay cap, as shown in Fig. 1. In Upper Egypt, the aquifer of sand and gravel is considered as semi-confined. The silty-clay top layer is found to be semi-permeable, with a very low permeability, as already mentioned in

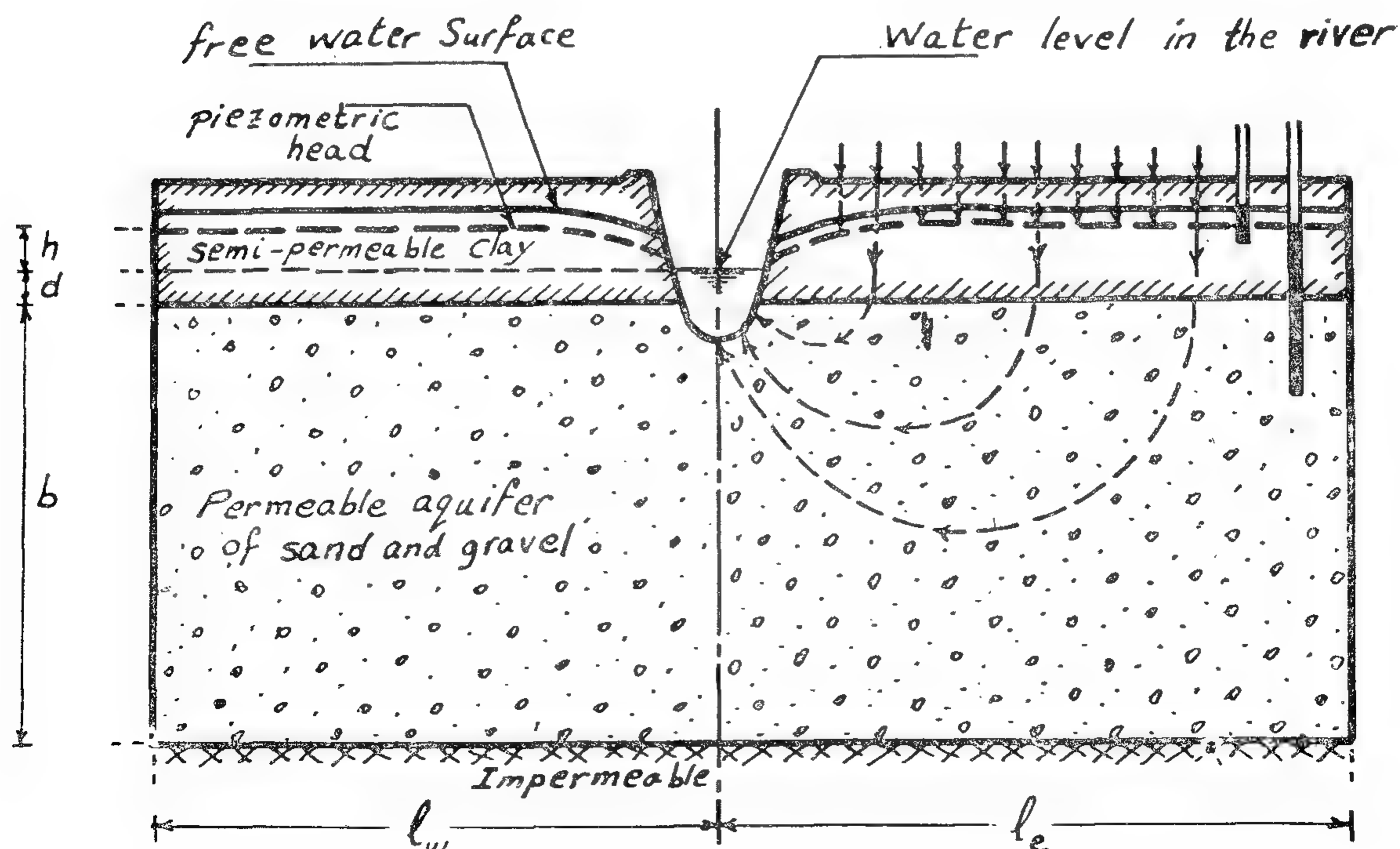


FIG. 1.- DEFINITION SKETCH OF AN IDEAL CROSS-SECTION OF THE NILE VALLEY

NILE GAIN FROM THE GROUND WATER RESERVOIR

By

MOHAMED HAMDY EL-KATEB¹, Ph. D., and

FATMA ABDEL-RAHMAN², M. Sc.

INTRODUCTION

In the distance between Aswan and Cairo, the river Nile passes through a valley of alluvial deposits of silty-clay cap over-lying an aquifer of sand and gravel. In a previous paper, written by the authors (2)³, it has been found that the average thickness of the silty-clay layer varies between 6 and 14 meters, while the average depth of the aquifer varies between 18 and 250 meters. The width of the valley ranges between 7 and 21 kilometers. In addition, the Nile bed is observed to be in direct contact with the aquifer causing a response between the Nile water and the ground water. Before the construction of the High Dam, there had been rises in water stages in the Nile downstream Aswan during the flood periods. This used to help the water to percolate into the ground water reservoir and then upwards into the silty cap. Later, when the Nile stage drops the water-table sinks again.

Since the completion of the High Dam, the Nile has lower stages because the maximum discharge of water requirements allowed down-stream Aswan is 230 millions of cubic meters per day in

July. In the new regime, the Nile performs its duty to act as a big drain, i.e., an effluent stream receiving ground water discharge. This fact depends on the relative water levels in the Nile and the piezometric heads of the ground water. That portion of the Nile discharge, coming from the ground water as a gain, is defined in hydrology as base flow. It is obvious that the ground water reservoir has become a dynamic resource receiving the drainable water during irrigation process and discharging it into the Nile.

An approximate method was adopted by El-Korany (3) and Hashem (5) to estimate the base flow gained by the Nile from the ground water reservoir in Upper Egypt. Their treatment was based on the application of the continuity equation of the Nile water according to the following relation :

Gain (or loss) of Nile water = Allowed discharge from the High Dam — Discharges of pump stations — Discharges diverted through Rayahs — Discharges through Delta Barrage + Changes in storage in the upstream reaches of the Barrages.

1. Assist. Prof. of Irrig. Eng., Cairo Univ., Giza, Arab Republic of Egypt.

2. Civil Engineer, Ground - Water Research Office, Ministry of Irrig., Arab Republic of Egypt.

3. Numerals in parentheses refer to corresponding items in the Appendix of references.

13. Thornton, C., and Birnstiel, C., "Three-Dimensional Suspension Structures", Journal of the Structural Division, ASCE, Vol. 93, No. ST2, Apr. 1967, Proc. Paper 5196, pp. 247-270.

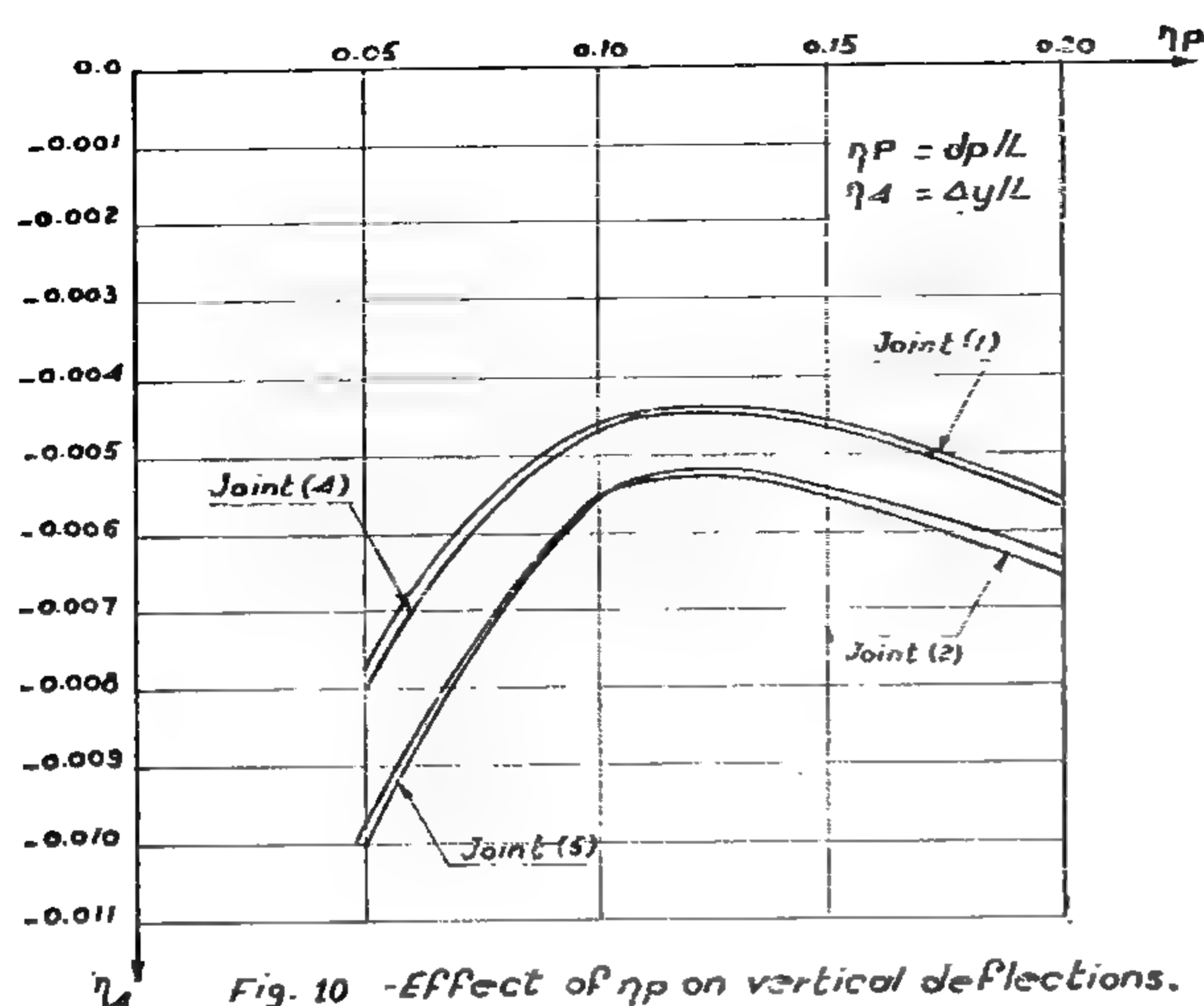
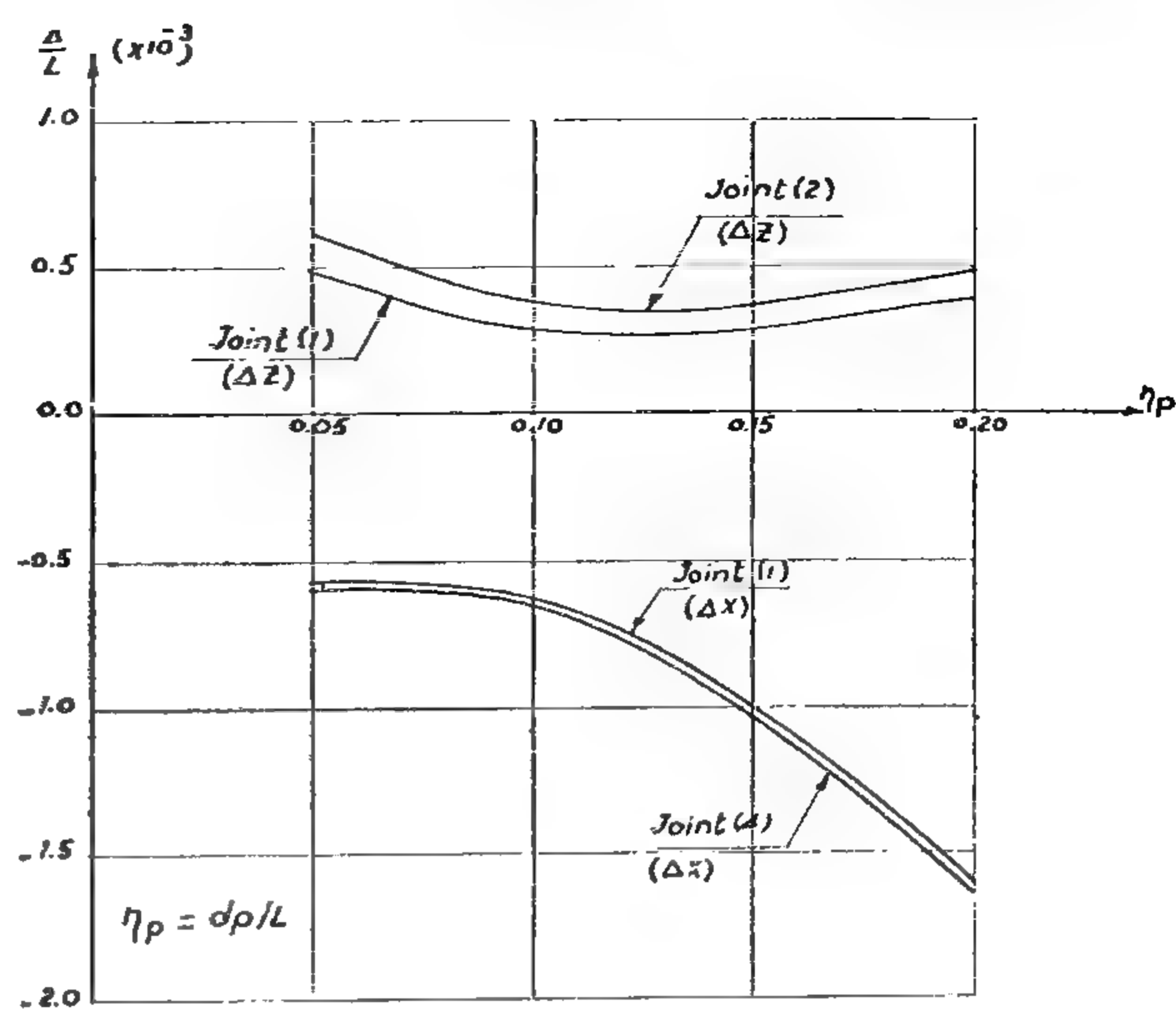
APPENDIX II. — NOTATION

The following symbols are used in this paper :

- A = cross-sectional area;
 d = central dip;
 d_p = central dip for cables having positive curvatures;
 d_n = central dip for cables having negative curvatures;
 E = Young's modulus of elasticity;
 G = tangent stiffness matrix;
 H = horizontal component of cable tension;
 h = difference in elevation of supports for unsymmetrical cables;

- \bar{K} = stiffness matrix corresponding to stress resultants Q;
 K = stiffness matrix corresponding to stress resultants P;
 L = span;
 P = acting load, stress resultants;
 \bar{P} = displacements;
 Q = stress resultants;
 q = displacements;
 w = applied pattern of loads;
 x,y,z = co-ordinate axes;

- $\Delta x, \Delta y, \Delta z$ = deflections in the x,y,z directions respectively;
 η_1 = dip-span ratio = d/L;
 η_2 = inclination of chord for unsymmetrical cables = h/L;
 η_p = $\Delta y / L$;
 η_{dp} = dp / L ;
 η_n = d_n / L ;
 β_1 = $H / \sum P$;
 β_2 = H / P ;
 δq = incremental displacements;
 Ψ = non-dimensional parameter for the weight of a suspension structure.

Fig. 10 - Effect of η_p on vertical deflections.Fig. 11 - Effect of η_p on horizontal deflections.

4. Moharram, A., Saafan, S.A., Hegab, H.I., "Suspension Roofs", Proceedings, 7th Conference for Statistical Studies and Scientific Computations, S.C.C., Cairo Univ., Giza, Egypt. April 1971, Vol. 3, pp. 371-383.
5. Mollmann, and Mortensen, P., "The Analysis of Prestressed Suspended Roofs (Cable Nets)", Space Structures, edited by R.M. Davies, Blackwell Scientific Publications, Oxford, 1967, pp. 873-889.
6. O'Brien, W.T., "General Solution of Suspended Cable Problems", Journal of the Structural Division, ASCE, Vol. 93, No. ST1, Feb. 1967, Proc. Paper 5085, pp. 1-26.
7. O'Brien, W.T., "Behaviour of Loaded Cable Systems", Journal of the Structural Division, ASCE, Vol. 94, No. ST10, Oct. 1968, Proc. Paper 6162, pp. 2281-2302.
8. Saafan, S.A. "Finite Deflection Analysis of Suspension Bridges," IIIth Proceedings, Scientific Conference's, Krynica, Poland, Sept., 1970.
9. Saafan, S.A., "Theoretical Analysis of Suspension Roofs", Journal of the Structural Division, ASCE, Vol. 96, No. ST2, Proc. Paper 7107, Feb. 1970, pp. 393-405.
10. Saafan, S.A., "Non-Linear Behaviour of Suspension Structures", Proceedings, International Symposium on Shell Structures, Beirut, Lebanon, April 1971.
11. Shore, S., and Bathish, G., "Membrane Analysis of Cable Roofs", Space Structures, edited by R.M. Davies, Blackwell Scientific Publications, Oxford, 1967, pp. 890-906.
12. Subcommittee on Cable Suspended Structures of the Task Committee on Special Structures, of the Committee on Metals of the Structural Division, John B. Scalzi, Chmn., "Cable-Suspended Roof Construction State-of-the-Art", Journal of the Structural Division, ASCE, Vol. 97, No. ST6, Proc. Paper 8190, June 1971, pp. 1715-1761.

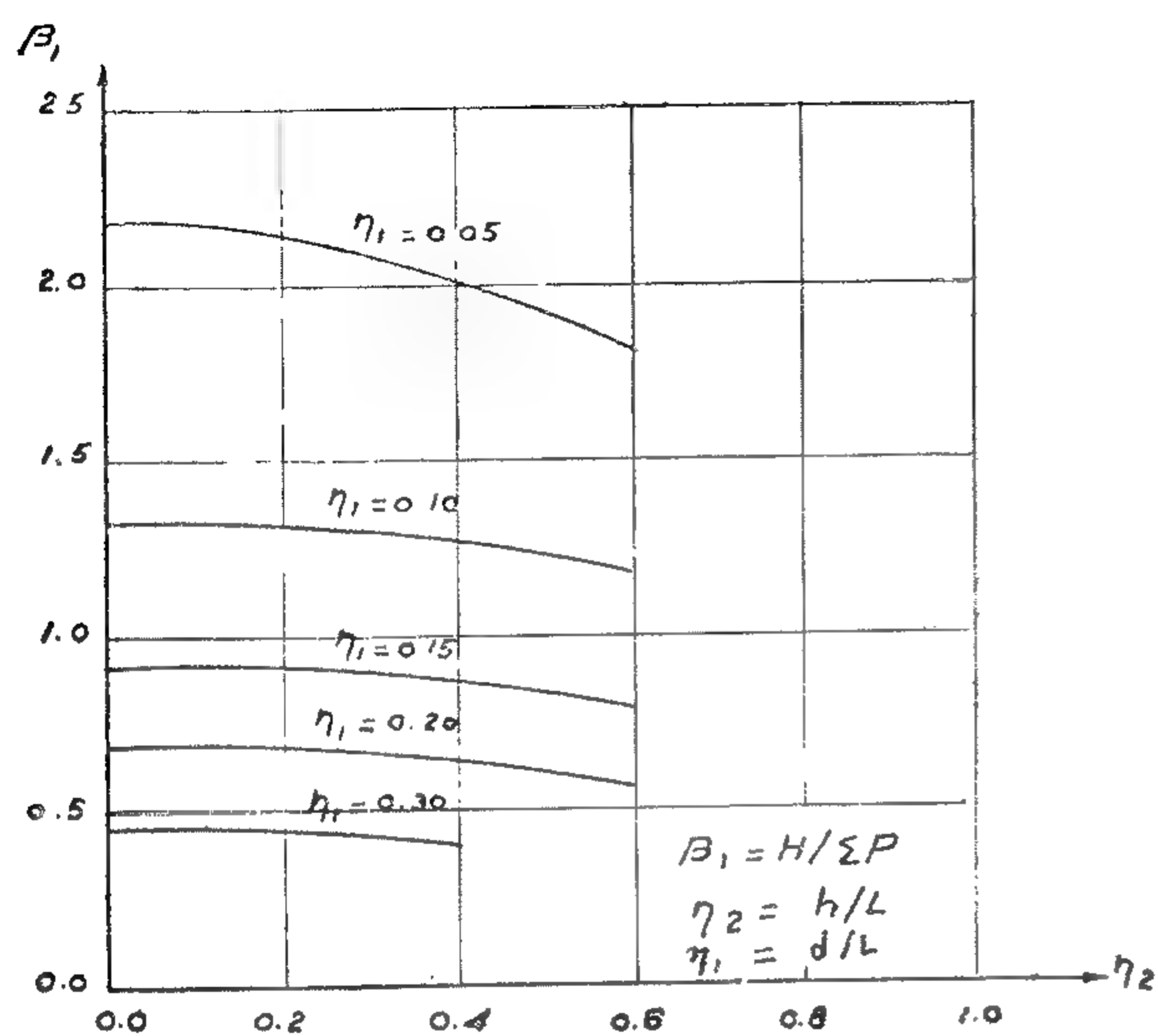


Fig. 7. - Relation Between η_1, η_2 and H For Unsymmetrical Cables Uniformly Loaded

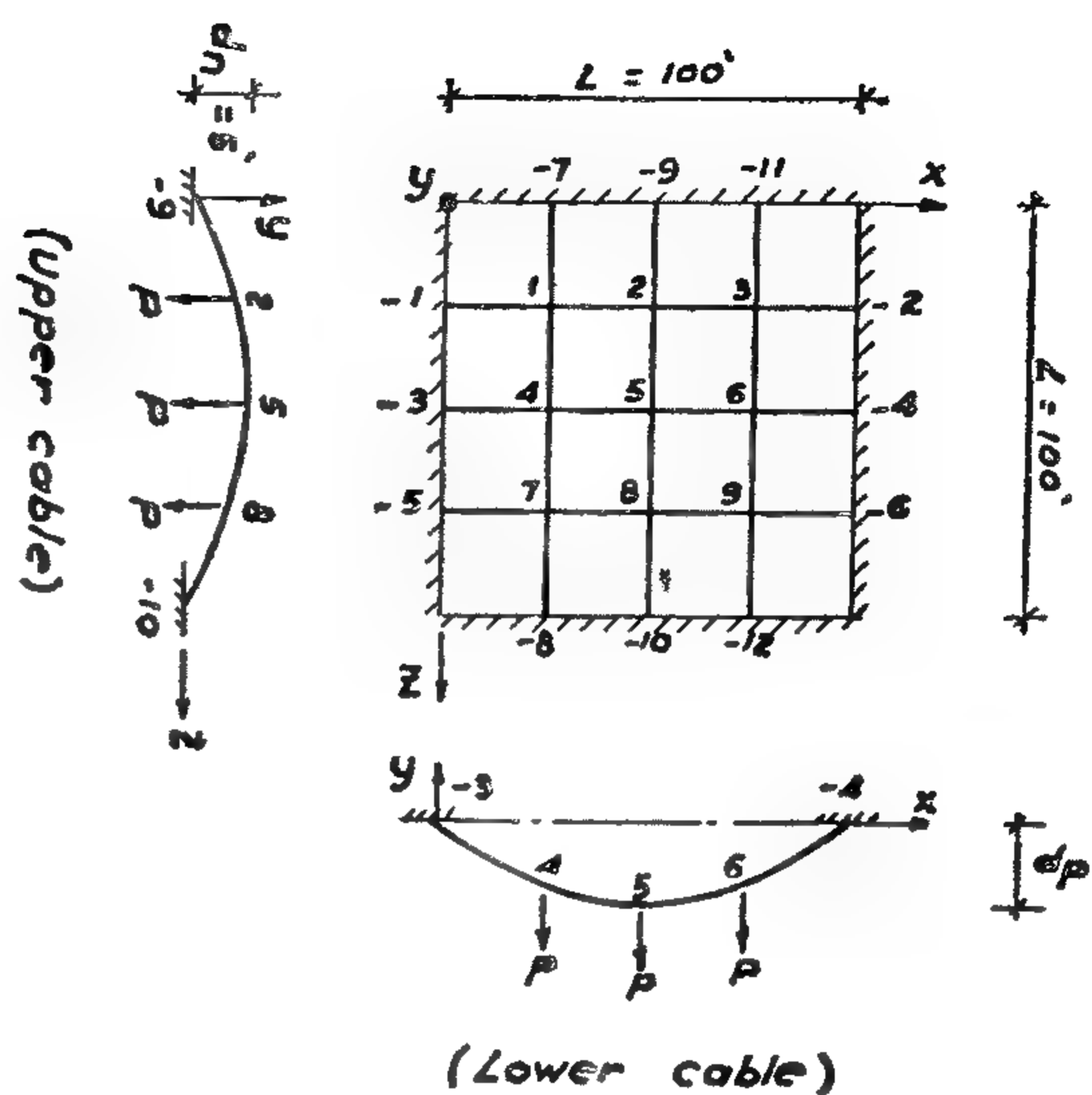


Fig. 8. - Hyperbolic paraboloid surface.

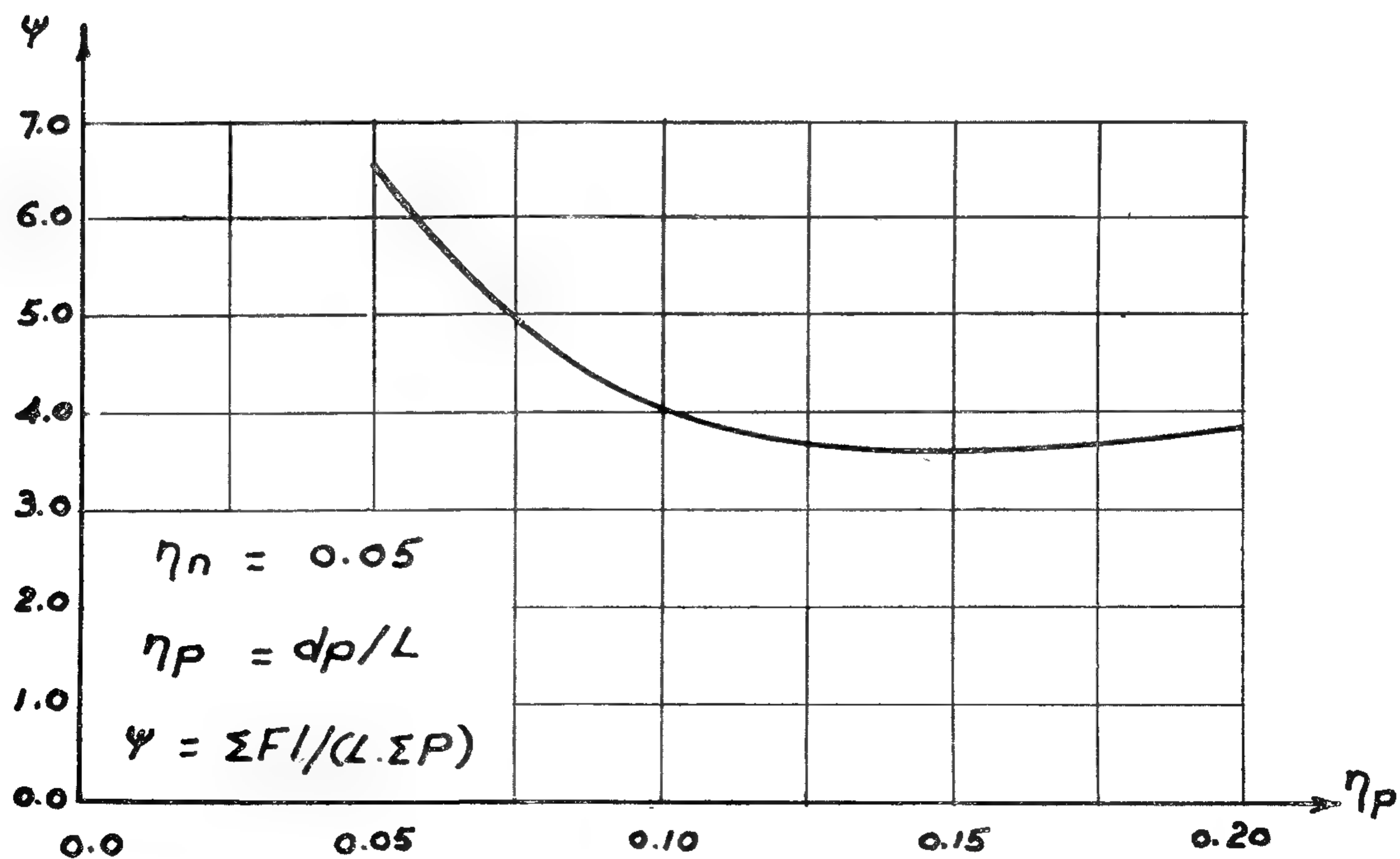


Fig. 9. - Relation between Sag of lower cables and weight of hyperbolic-paraboloid surface.

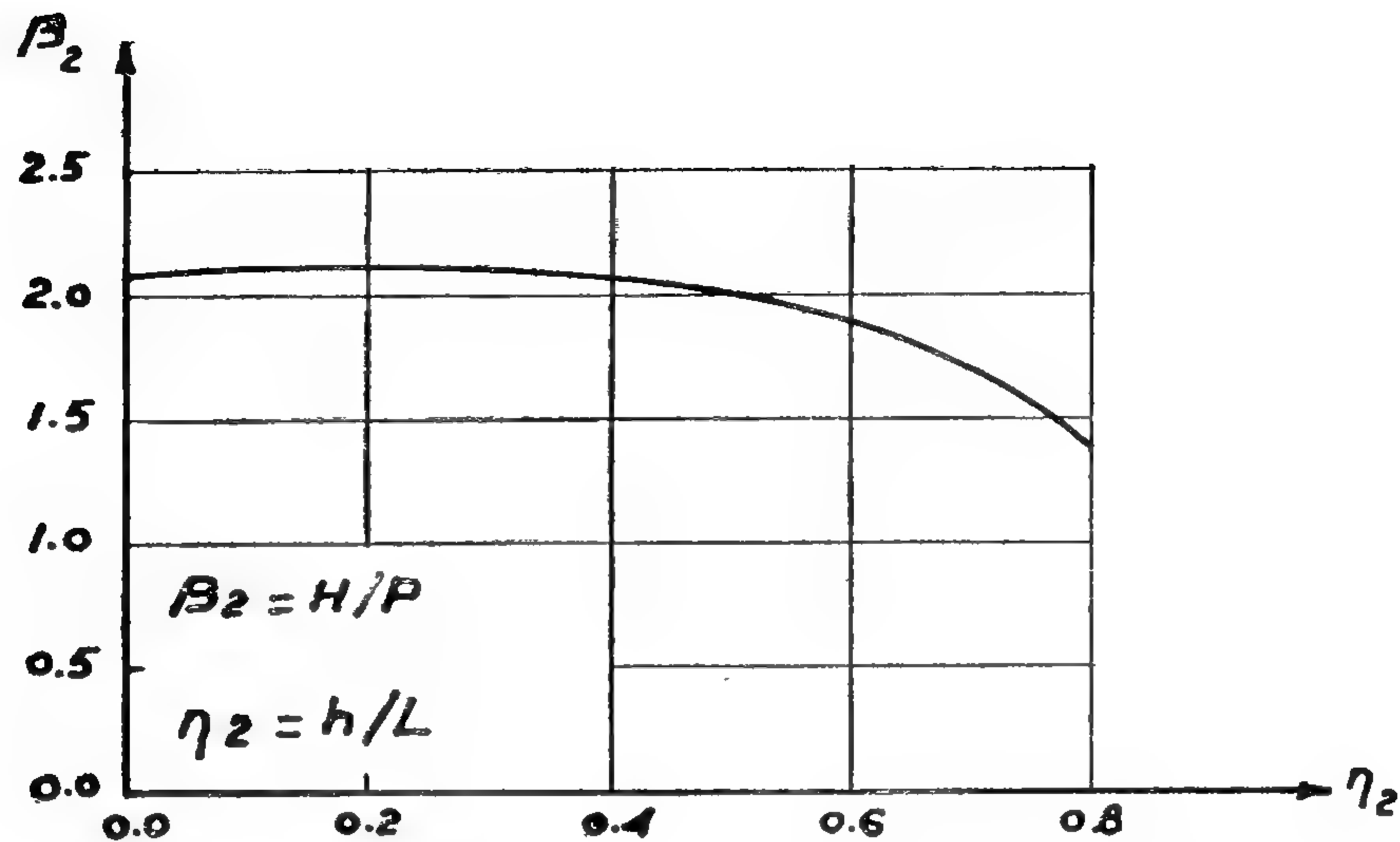


Fig. 6. - Effect of η_2 on H due to a Central load.

(i) Unsymmetrical Cables :—

1. The vertical deflections increase with the increase of the chord slope, η_2 . Deflections of all joints are minimum at a value of η_1 depending on the value of η_2 , Fig. 5.
2. The change of η_2 from 0.0 to 0.4 has insignificant effect on horizontal pull in the cable.

(ii) Hyperbolic Paraboloid Surface :—

1. The weight of the roof is minimum at a dip-span ratio, η_p , of the lower cables = 0.15.
2. The vertical deflections of all joints is minimum when $\eta_p = 0.13$.

ACKNOWLEDGEMENTS

This paper forms part of a research project on the optimum design of suspended structures being conducted in the De-

partment of Structural Engineering Ain Shams University, Cairo, Egypt.

APPENDIX I. — REFERENCES

1. Hegab, H.I., "Theoretical and Experimental Analysis of Suspension Roofs", M. Sc. Thesis, Struct. Tngrg. Dept., Faculty of Engrg. Ain Shams Univ., Cairo, Egypt, June 1972.
2. Krishna, P., and Sparkes, S., "Analysis of Pretensional Cable Systems" Proceedings, The Institution of Civil Engineers (London), Jan. 1968, Vol. 39.
3. Krishna, P., and Agarwal, T., "Study of Suspended Roof Model", Journal of the Structural Division, ASCE, Vol. 97, No. ST6, Proc. Paper 8168, June 1971, pp. 1671-1684.

Figs. 3 & 4 indicates the relation between the vertical deflections, the chord slope, η_2 and the dip-span ratio, η_1 , in which $\eta_2 = \frac{d}{L}$ and h = the difference in elevations of supports. It is seen that the vertical deflections increase with the increase of the chord slope, η_2 . For each value of η_2 , minimum deflections occur corresponding to a value of η_1 which increases with the decrease of η_2 as shown in Fig. 5.

Figs. 6 & 7 show that concentrated and uniform loads, the chord slope, η_2 , up to 0.40 has insignificant effect on the tension in the cable. Also, as in the case of symmetrical cables, the increase in the dip-span ratio, η_1 , reduces the tension in the cable when subjected to uniform loads.

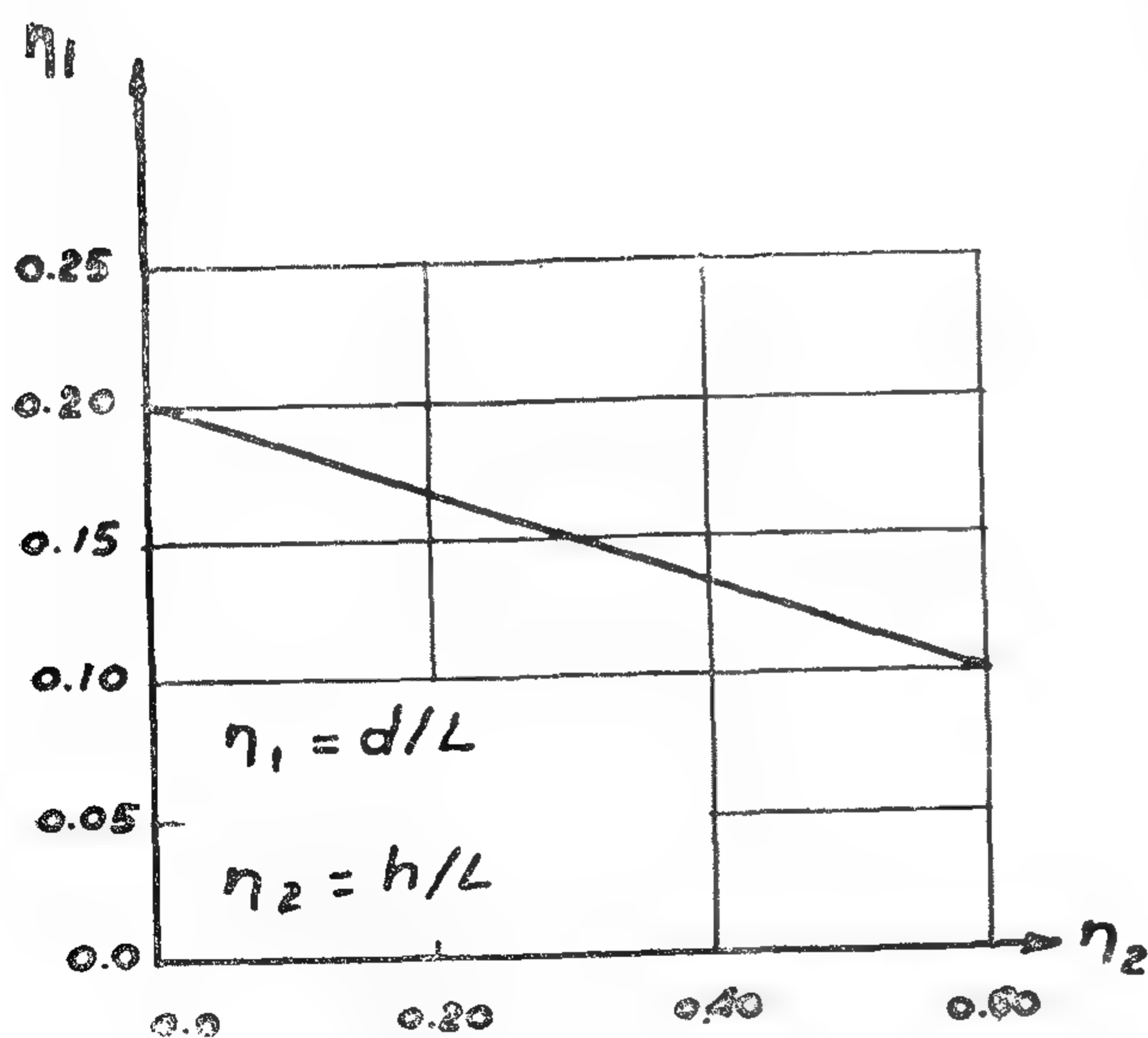


Fig. 5. Optimum dip-span ratio with respect to minimum deflection of unsymmetrical cables uniformly loaded.

HYPERBOLIC PARABOLOID SURFACE

The surface, Fig. 8, has opposite curvatures in the two main orthogonal directions x & z . Numerical studies have been carried out for the same case of loading (6.25 kips at each joint). The dip-span ratio, η_n of the upper cables is constant and equals 0.05, while that of the lower cables, η_p , ranges between 0.05 & 0.20. The span $L = 100$ ft., the cross-sectional area, A , of all cables = 0.8 sq. in., and the modulus of elasticity $E = 29151$ ksi.

It is intended to investigate the influence of the dip-span ratio, η_p , of the lower cables on the weight of the roof and the deflections of its joints. It can be seen from Fig. 9 that the optimum dip-span ratio of the lower cables is $\eta_p = 0.15$.

From Fig. 10, it can also be seen that the minimum vertical deflections for all joints are obtained at $\eta_p = 0.12$, and that the vertical deflections of all joints of any upper cable are almost the same. The outer upper cables move approximately parallel to themselves towards the boboundary, i.e. the horizontal out-of-plane deflections of all joints of an upper cable are nearly the same at each η_p and increase with the increase of η_p , Fig. 11.

For lower cables, horizontal out-of-plane deflections are directed towards the center of the roof, being minimum for $\eta_p = 0.12$.

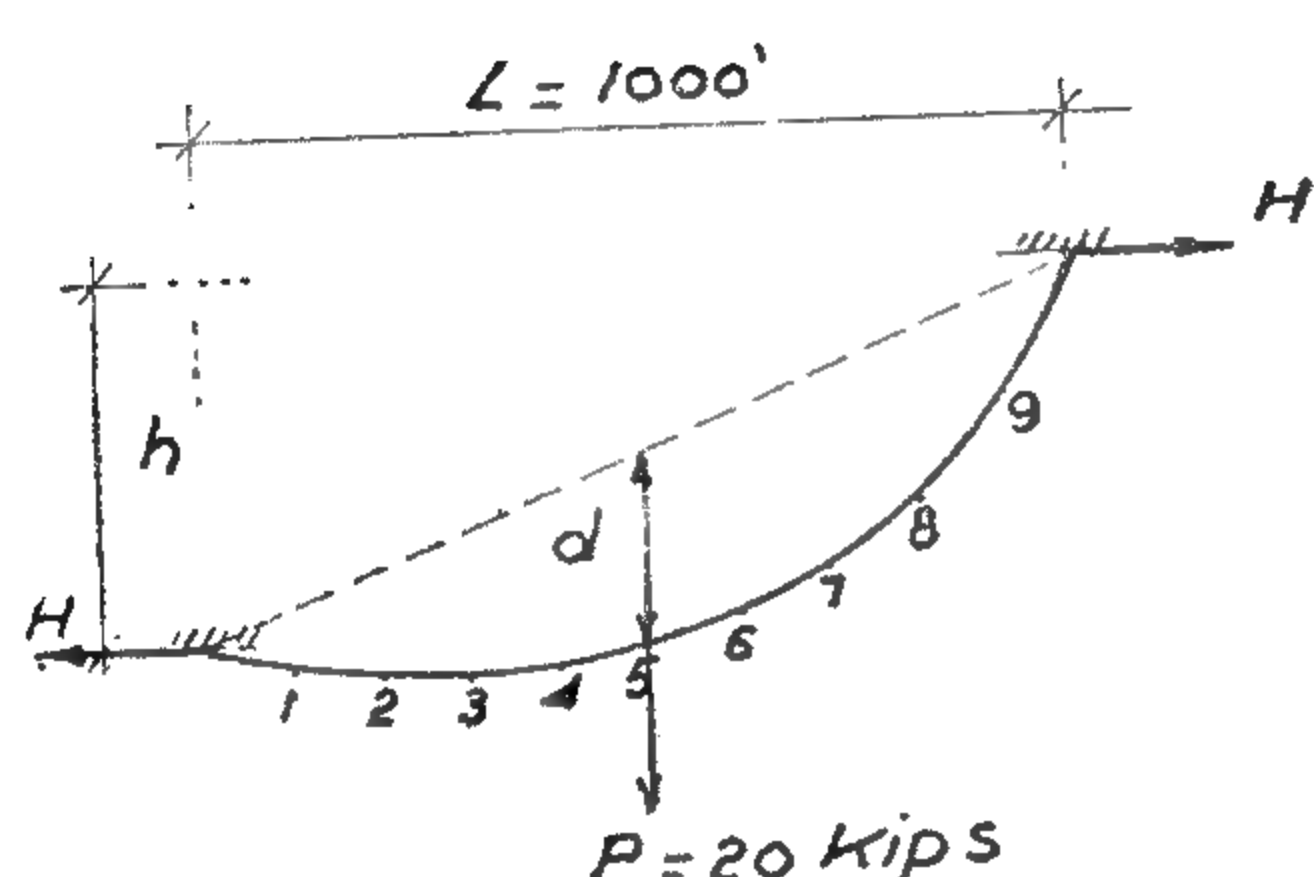
CONCLUSIONS

The most important conclusions of this investigation may be summarized as follows.

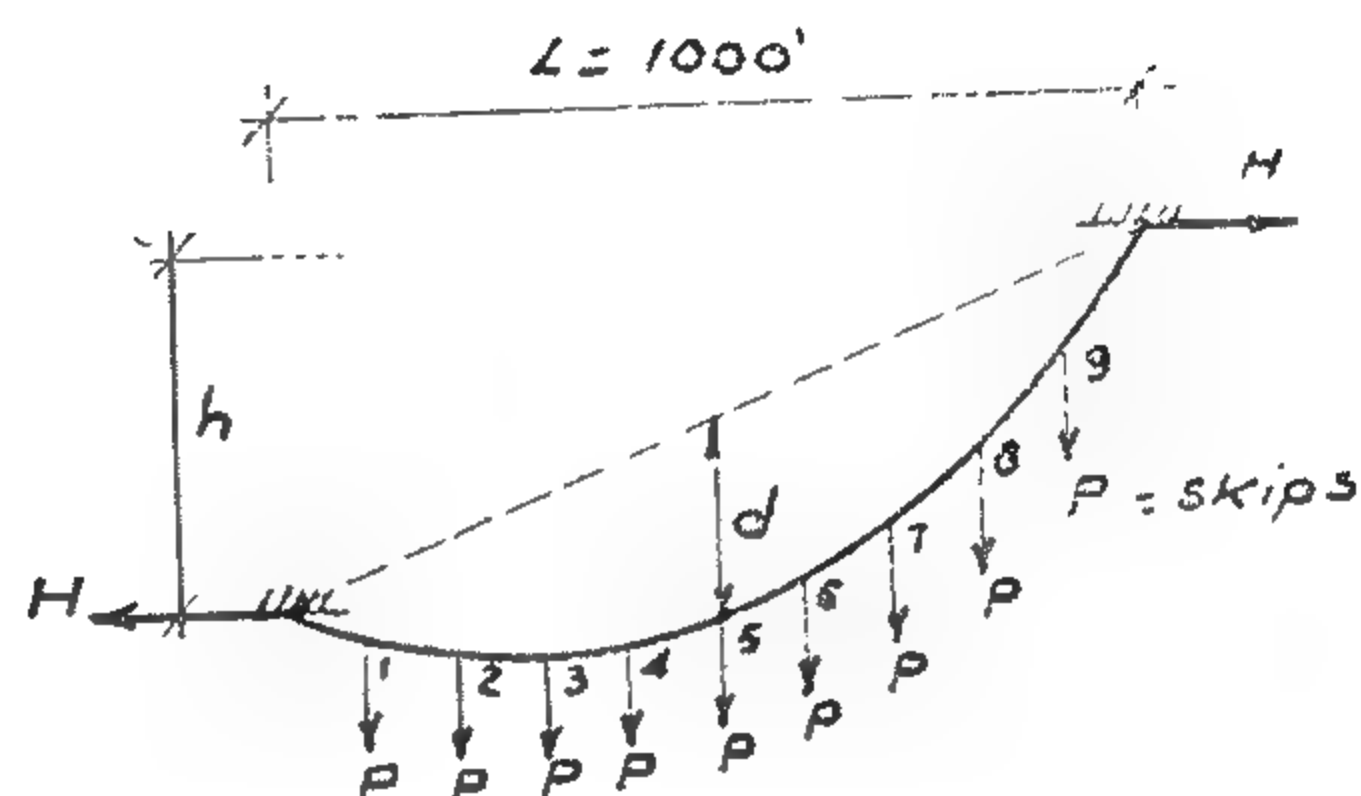
UNSYMMETRICAL CABLES

Similar numerical studies have been carried out for the two cases of loadings; a central vertical load $P = 20$ kips, and

uniform loads equivalent to 5 kips at each joint, Fig. 2. The span, $L = 1000$ ft, the modulus of elasticity, $E = 29151$ ksi, and the crosssectional area, $A = 0.85$ sq. in.



(a) Central Vertical Load



(b) Uniform Loads

Fig. 2: - Unsymmetrical cable.

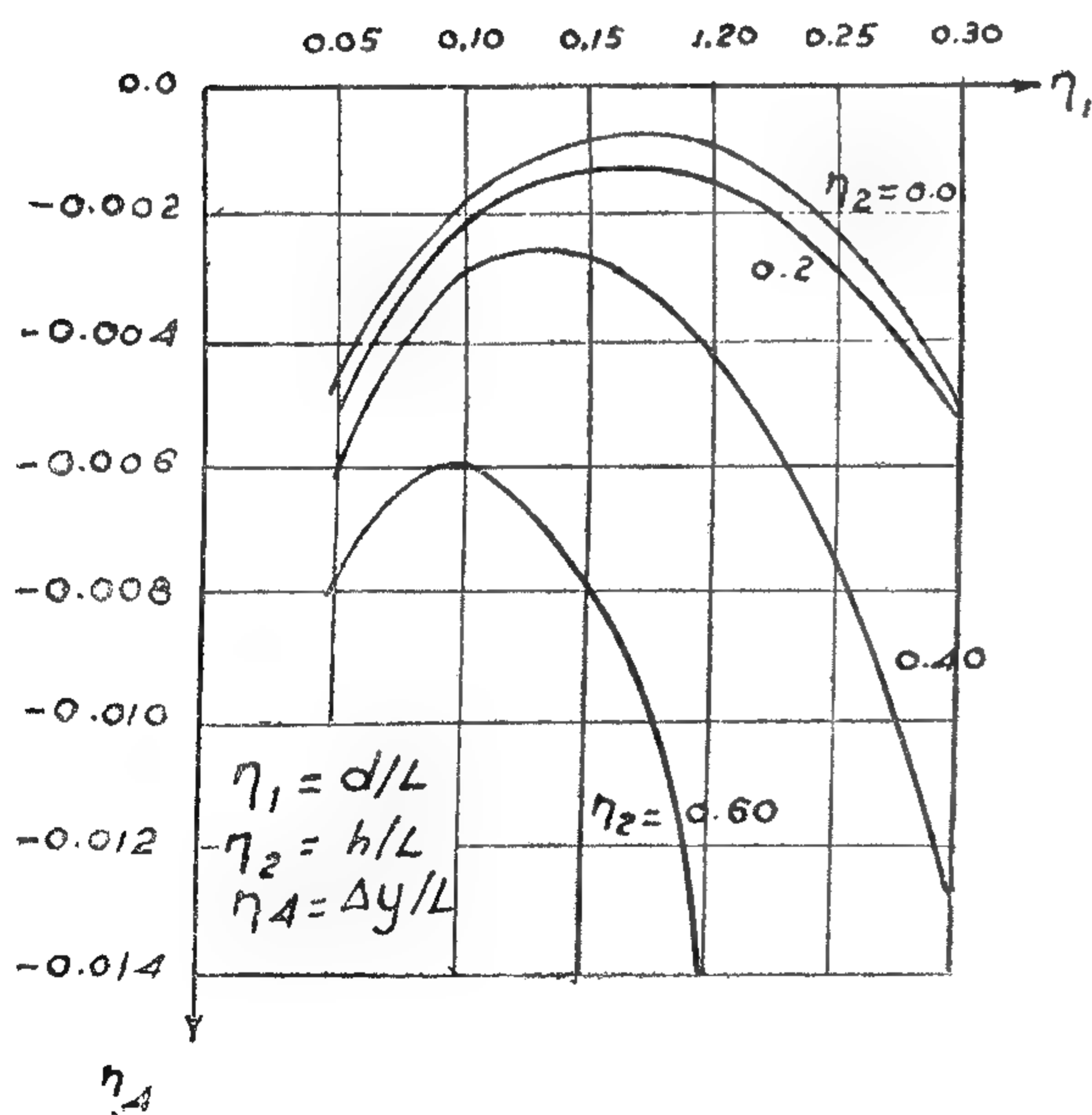


Fig. 3. - Deflection of joint (1).

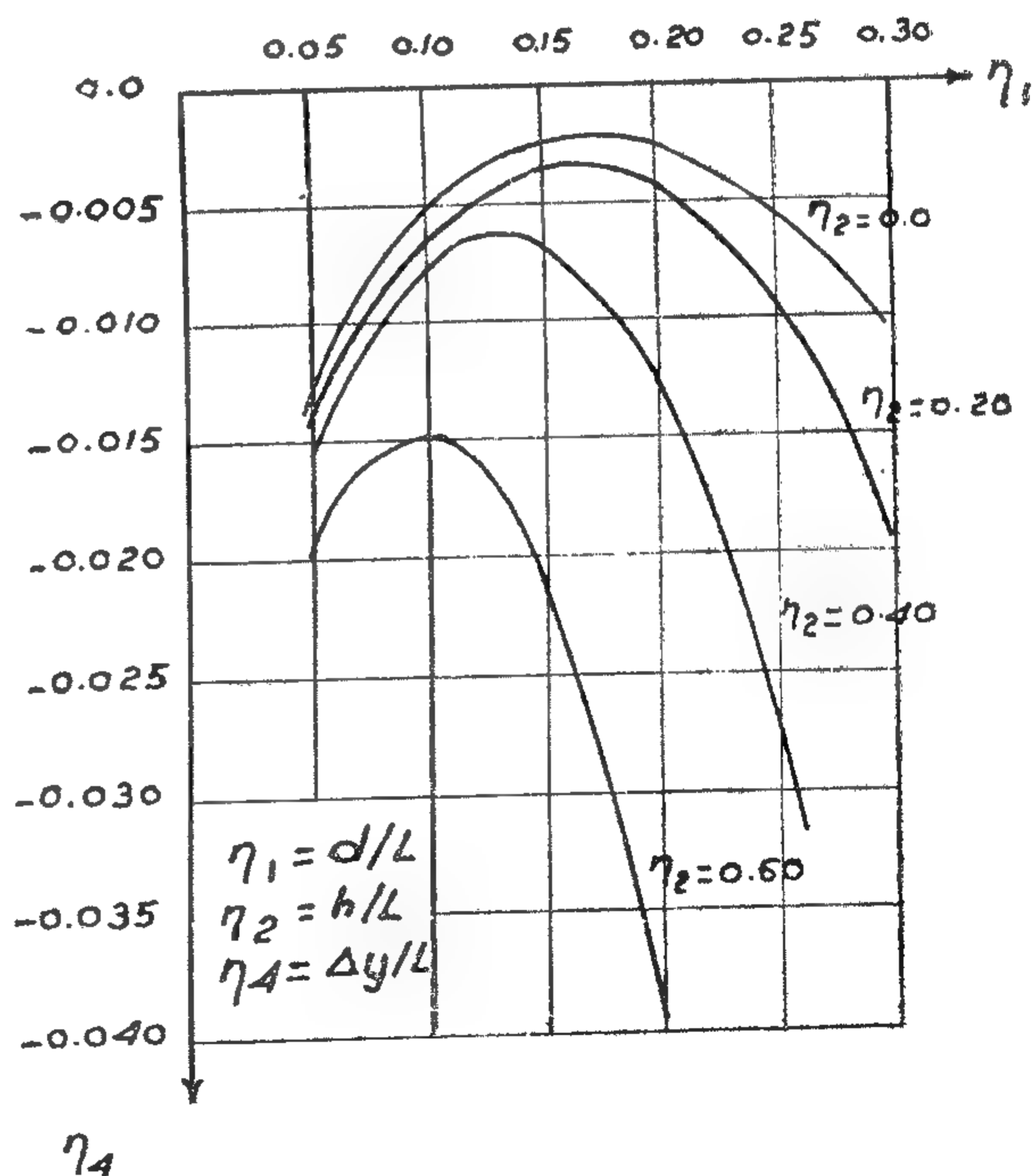


Fig. 4. - Deflections of joint (5).

$$[P] = [P_1, P_2, \dots, P_6] \dots (4a)$$

$$= [k][p] \dots (4b)$$

in which $[k]$ is the stiffness matrix corresponding to the stress resultants $[p]$.

The external loads corresponding to the joint displacements $[q]$ are designated as

$$[Q] = [Q_1, Q_2, \dots, Q_6] \dots (5)$$

The external loads $[Q]$ are related to the member loads $[P]$ as

$$[P] = [T][Q] \dots (6)$$

$$\text{or } [Q] = [T'] [P] = [T'] [k] [T] [q] = [K] [q] (7)$$

in which $[T^{-1}]$ is the orthogonal matrix inverse and $[K]$ indicates the stiffness matrix corresponding to the stress resultants $[Q]$.

In order to obtain a solution tangent to the actual nonlinear force-deflection curve at any intermediate stage, the elements of the tangent stiffness matrix $[G]$ are obtained as a partial derivation of vector $[Q]$ with respect to each one of the displacements $[q]$. Thus

$$(G) \partial Q / \partial q (8)$$

suppose there is a set of n simultaneous nonlinear equations in n unknowns,

$$\text{or } (G) (q) = (W) (9)$$

in which $[W]$ = the load column vector and $[Q]$ = the displacements column vector.

An approximate solution $[q_0]$ to Eq. 9 is obtained by solving the set of linear equations

$$[G_0][q_0] = [W] \dots (10)$$

in which $[G_0]$ = the tangent stiffness matrix for the initial state of deformation.

A better approximation is found by solving the set of linear equations

$$[G][\delta q] = [W] - [F] \dots (11a)$$

$$= [\delta W] \dots (11b)$$

in which $[G]$ = the tangent stiffness matrix, $[F]$ = the stress resultants' columns vector corresponding to the previous state of deformation (see Eq. 12); $[\delta W]$ = the restraints' column vector which together with stress resultants $[F]$ maintain the equilibrium at this state of deformation; and $[\delta q]$ = the incremental displacements' column vector caused by $[\delta W]$. Thus, the new displacements' column vector is $[q_1] = [q_0] + [\delta q_1]$. In general, at the n th state of deformation.

$$[q_n] = [q_0] + [\delta q_1] + [\delta q_2] + \dots + [\delta q_n] \dots (12)$$

is obtained.

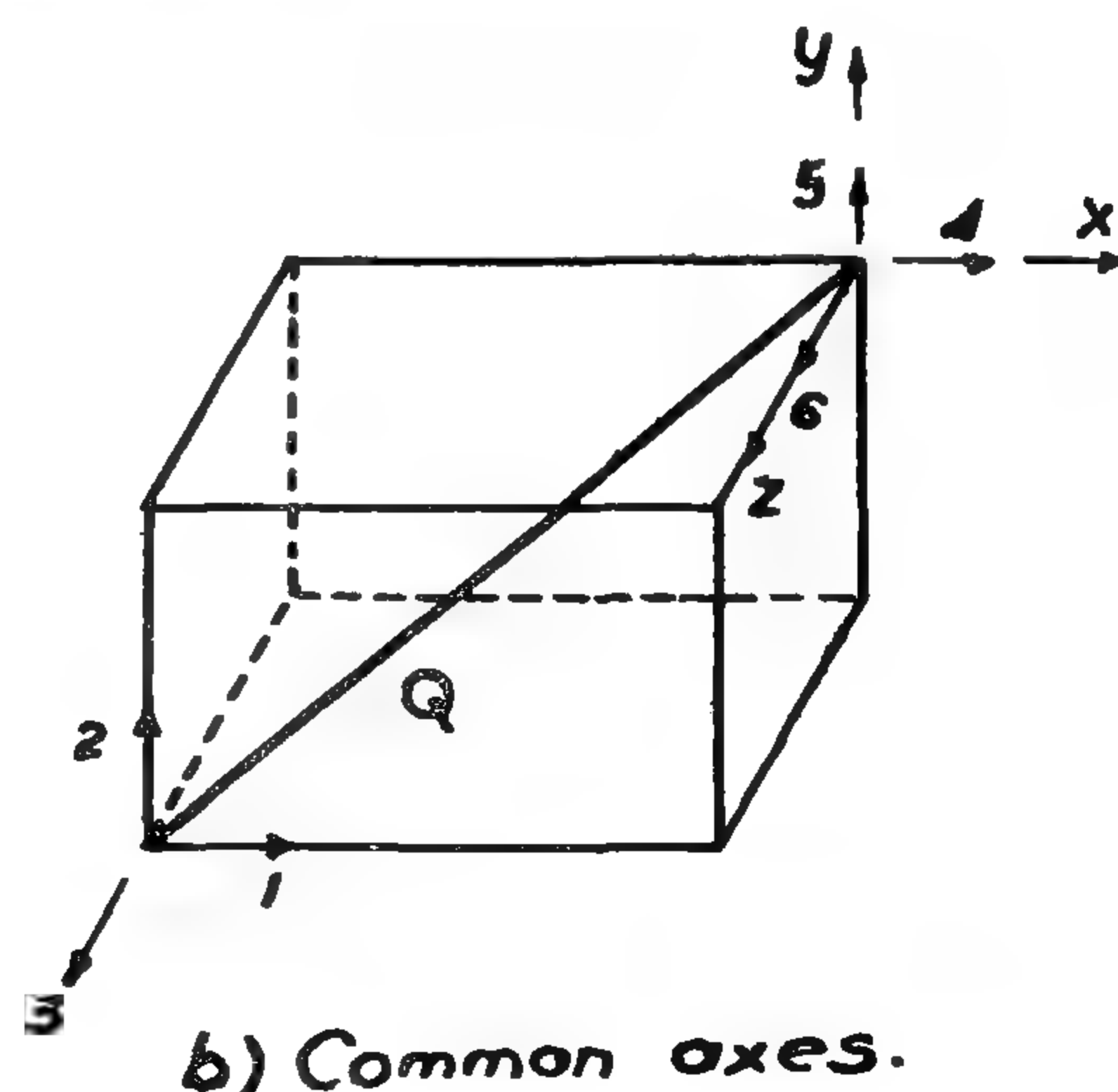
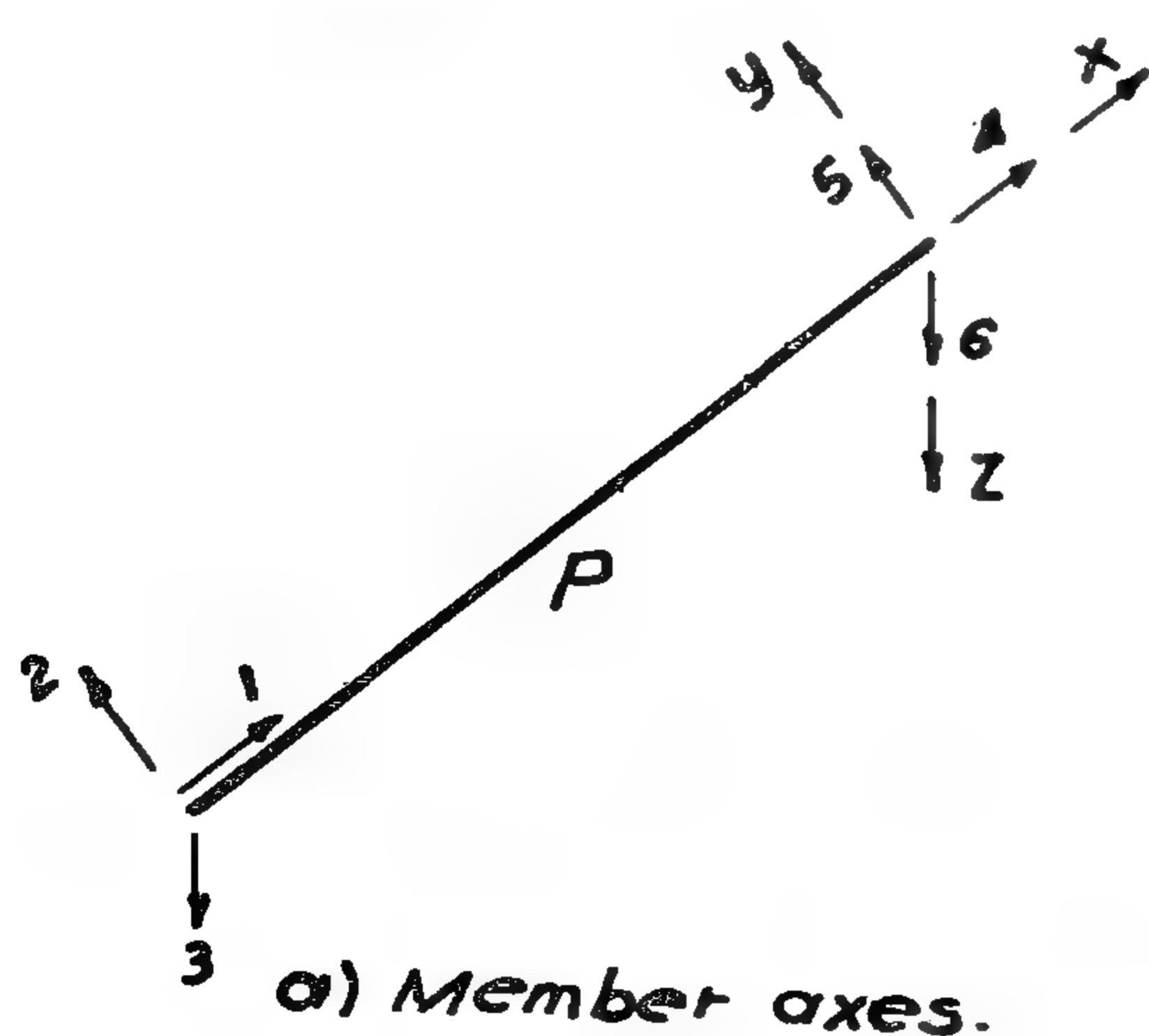


Fig. 1. - Definition of axes.

ECONOMICAL STUDY OF SUSPENSION STRUCTURES

By A. MOHARRAM¹, S.A. SAAFAN²,
& HASSAN I. HEGAB³

INTRODUCTION

Nowadays, there is abundance of literature on the theoretical analysis of suspension structures (5,6,9,10,11,14)⁴. How to decide the most economical solution for suspension roofs is usually considered as a matter of experience.

Theoretical and experimental treatises of suspension structures have been developed by many authors (2,3,6,7,13). A solution of suspended cable problems has been presented by O'Brien (6,7) based on the "Flexibility Method". Krishna and Sparkes (2) presented the "Influence coefficient Method" for the analysis of dual cables. An "Incremental load Method" has been presented by Thornton and Birnstiel (13) for the solution of three-dimensional suspension structures. A study of a suspended roof model for a hyperbolic cable network has been presented by Krishna and Agarwal (3).

The object of this paper is to introduce a study relating to the optimum design of suspension structures.

Numerical studies, using the Finite Deflection Theory (8,9), have been carried out on 4 types of suspension structures which are generally used (1,4). These are plane cables, paraboloid, hyperbolic paraboloid, and double surface suspension roofs.

ASSUMPTIONS

The following assumptions are made

1. The cables are divided by n points (joints) into $(n+1)$ segments (members);
2. The members of the suspension structures are of uniform cross-sections;
3. The initial shape of cables is parabolic;
4. The joints are frictionless;
5. The loads are concentrated at the joints; and
6. The edge elements of the suspension structure are cables, trusses, or fixed cable ends.

METHOD OF ANALYSIS

Let the displacements of member ij , Fig. 1 (a), with respect to the member axes, be designated by the column vector.

$$[p] = [p_1, p_2, \dots, p_6] \dots (1)^1$$

For a frame analysis, the displacements with respect to the common axes, Fig. 1 (b), are expressed by the column vector

$$[q] = [q_1, q_2, \dots, q_6] \dots (2)$$

The displacements $[p]$ can be defined as a function of the displacements $[q]$ as

$$[p] = [T] [q] \dots (3)$$

in which $[T]$ = the orthogonal transformation matrix.

Designating the forces in the members corresponding to the deformations $[P]$ as .

(1) Professor, Faculty of Engrg., Ain Shams Univ., Cairo, Egypt.

(2) Professor, Faculty of Engrg., Ain Shams Univ. Cairo, Egypt.

(3) Assoc. Lecturer, Faculty of Engrg., Ain Shams Univ., Cairo, Egypt.

(4) Numerals in parentheses refer to corresponding items in the Appendix I. — References.

(1) Notation is listed alphabetically in Appendix I.

BUILDING & CONSTRUCTION

**INSTITUTION OF CIVIL ENGINEERS
INSTITUTION OF ARCHITECTS
INSTITUTION OF IRRIGATION ENGINEERS**

التصنيع والانتاج

جمعية المهندسين الكهربائيين
والإلكترونيين
جمعية الهندسة الإدارية
جمعية المهندسين الميكانيكيين

These complex activities were assembled to produce a 3-dimensional cube shown in Figure 1.

Every cell (ijk) represents the subsystem for decision making within the three levels. For example, the shaded cell represents the allocation planning for warehouses in an affiliate.

It may be explained here that this cell was the first subsystem completed. This is because it is the product demand at the warehouse that sets in motion the whole chain of demands all the way up to the demand for reduced crude, and

thus triggers the corresponding inventories to meet these demands.

Needless to say that, as of today, many cells have been completed and the ultimate objective is to cover all the cells of the cube. The more cells covered, the closer we are to a total system for lube oils. The case study, briefly explained here, illustrates a system that can be described as "total" as one can get for the lube-oils segment of the petroleum industry.

The same cube concept can be applied as well to other segments of the petroleum industry. To that extent, it can be also used for other industries.

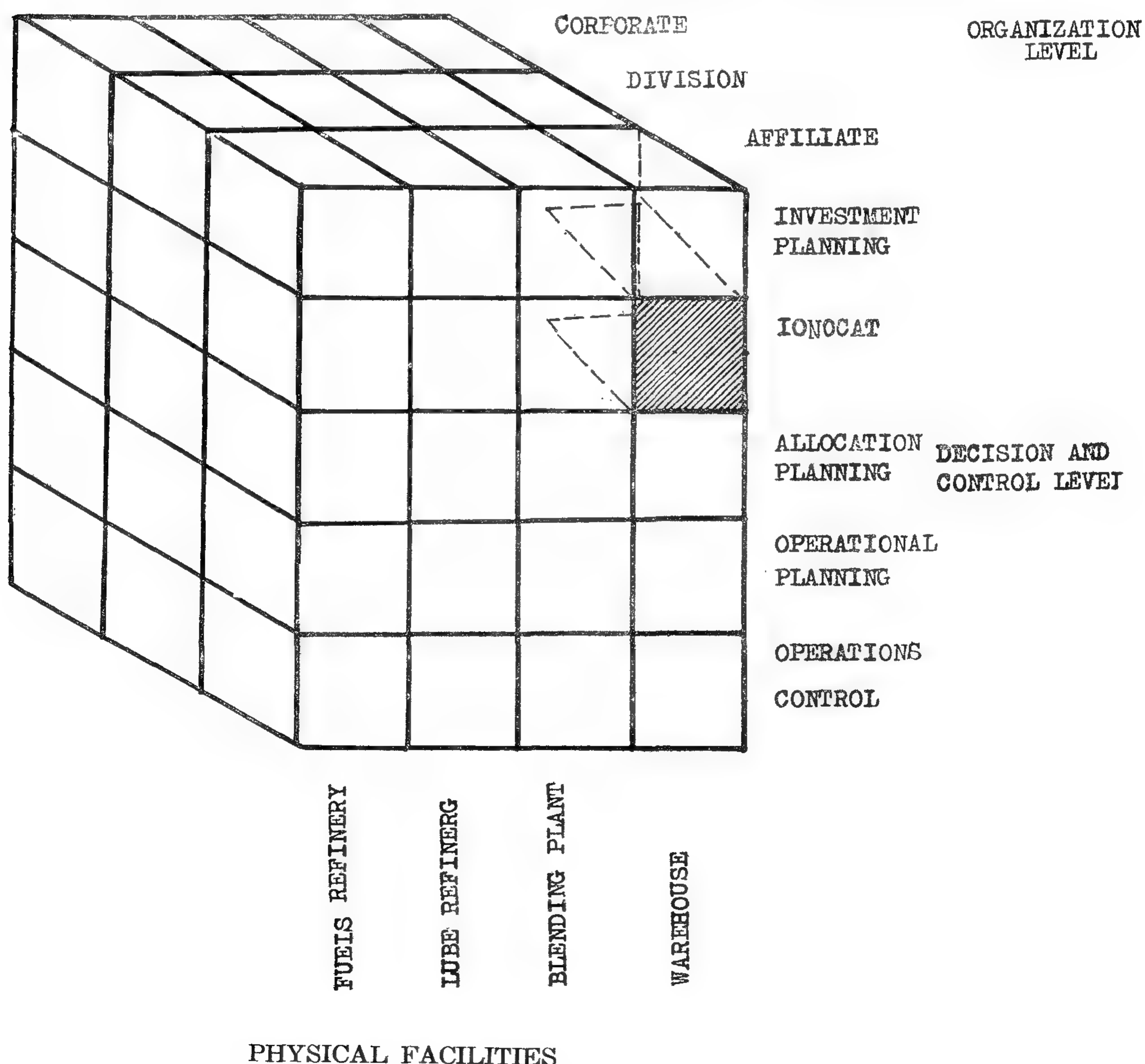


Figure 1. The "Cube Concept" approach to Management Information Systems

TOTAL SYSTEMS CONCEPT

The "total systems" approach implies that all subsystems in an organization should be integrated in a single information system. This total-systems approach is considered a "Dream" and can be translated to a computer-minded manager as follows : To have ALL the information, stored on RANDOM ACCESS equipment, in ONE location, continuously UP-DATED, and immediately available ON REQUEST. This is the concept of Total Management Information Systems.

This dream is not practical today for the following two main reasons:

1. Manpower limitations — we do not have qualified people to develop M.I.S.'s, even with our present, less-demanding equipment and techniques.

2. Economic considerations — the cost of compiling information, processing and retrieval is still high, in view of the present equipment capabilities and limitations.

There is no doubt that, at some time in the future, the concept of Total Management Information Systems will be possible and practicable. The fourth generation of computers, due in the early 1970's, promises hardware that is likely to be more advanced technically and separate from software. There will be improved cost/performance, larger high-speed memories, lower-cost random-access devices, greater multiprogramming and multiprocessing capability, more sophisticated on-line terminals, graphics-etc., increased use of operating systems, and improvements in the file management systems.

These improvements in computer technology will help overcome the economic and manpower limitations mentioned before. However, it may take a long time for the dream to materialize. Until such time, we should organize in a realistic manner to achieve real gains. The system's effectiveness depends on management ability in planning ahead of time

for the needs not only of today, but of the future as well. It is of vital importance at the outset to organize all the pertinent data within the planned parameters.

THE "CUBE CONCEPT" OF M.I.S.

The "cube concept" of M.I.S.'s is presented here as an approach to pre-planning the parameters of the total system and recognizing the sub-systems under two categories; those that should wait for future developments of computer technology, and those that can be handled immediately with the presently available capabilities of the computer applications.

The "cube concept" approach to M.I.S.'s will be illustrated by a brief description of a case study from the petroleum industry.

Case Study — In an international petroleum company, interest was expressed in developing and implementing tools to plan and control all elements falling within a major segment of the company. This segment was defined as that of manufacturing and distributing of lubricating oils (lube oils). A system was designed to provide information for decision-making at all organizational, physical, and functional levels of the company concerned with this segment of the business.

The parameters needed for a total lube-oils system were defined as follows:

1. Physical facilities level (i): These include the facilities required for the manufacture and distribution in the lube operations; refineries, blending plants, and warehouses.

2. Decision and control level (j): Functional decisionmaking is performed at levels involving investment and facilities planning, allocation of resources, operational planning, and scheduling control of daily operations.

3. Organizational level (k): Decisions are made at affiliate, division, and component levels.

It will take a long time to materialize the dream of total Management Information System. Let us not wait — let us organize our data and plan our parameters. We can achieve real gains from the present computer applications. We will continue to accomplish more cells of the cube as the improvement of computer technology permits, then the dream will materialize.

A.M. ELASFOURI

Management Engineering Association

THE CUBE CONCEPT APPROACH TO MANAGEMENT INFORMATION SYSTEMS

BY

Dr. Eng. HAMED KAMAL EL-DIN

INTRODUCTION

An effective management information system is a tool (among other management tools) to improve the manager's decision-making ability.

A meaningful definition of management is the function of establishing the objectives of the enterprise, allocating resources according to a predetermined plan and schedule, and reacting to deviations between predicted and actual results, to forestall the development of an unfavorable situation''.

Of course the effectiveness of management is measured by the results achieved. The objectives of an enterprise will vary according to its type. In business, the primary objective is to maximize return on investment i.e. to make profit. To accomplish this objective, management must be able to react instantly to varying sets of conditions and have a set of alternatives to consider in order to select the best course of action.

This is effective management, and system that helps management to do this is an effective Management Information System (M.I.S.).

OBJECTIVES OF THE M.I.S.

The objectives of the M.I.S. are two-fold: (1) To provide management with all the information necessary to create an operating plan; (2) To produce operating statistics for immediate correlation to the plan of the deviations between the initial plan and actual performance.

The information produced should be complete, useful, timely, accurate, and always economical. The cost of compiling information, in relation to its ultimate value to management, must be measured and understood. Also the feasibility of gathering and processing information, in view of equipment capabilities and limitations, must be determined.

Finally, it should satisfy all levels of management. Information needs of the various levels of management will differ, with greater reliance on detailed operating reports, for lower levels, and a lesser dependence on quantitative evaluation of operating reports at higher levels. Decision making at the lower levels tends to become somewhat repetitive and routine. Decision making at higher levels, however, is influenced by many factors that unfortunately do not easily lend themselves to quantification.

and CeO_2 ($n = 2.35$) can reduce the reflection loss below 1% over the major part of the spectral response of silicon solar cells. The optimum thicknesses of MgF_2 and CeO_2 films are seen to be $0.09 \mu\text{m}$ and $0.05 \mu\text{m}$ respectively.

4. OPTIMUM SERIES RESISTANCE

The series resistance of a solar cell has a pronounced effect on its conversion efficiency and the maximum available output power. A series resistance of only 5 ohms can reduce the available output power to less than 30 percent of the output power with zero resistance(6). Thus it is essential to minimize the cell series resistance.

The major component of the series resistance is usually the resistance of the diffused layer. As pointed out in Sec. 2.3, a high collection efficiency would require an extremely thin diffused layer. This requirement would lead to a high series resistance. Thus for a given cell configuration, there is an optimum thickness for the diffused layer which can be obtained by compromising between the diffused layer collection efficiency and its series resistance. This thickness would give the highest conversion efficiency and output power.

The resistance of the base layer is not critical since it is very easy to keep it below 0.25 ohm with thickness between 0.1 and 0.5 cm. The ohmic contact resistances can also be reduced to a negligible value through the use of contact grids.

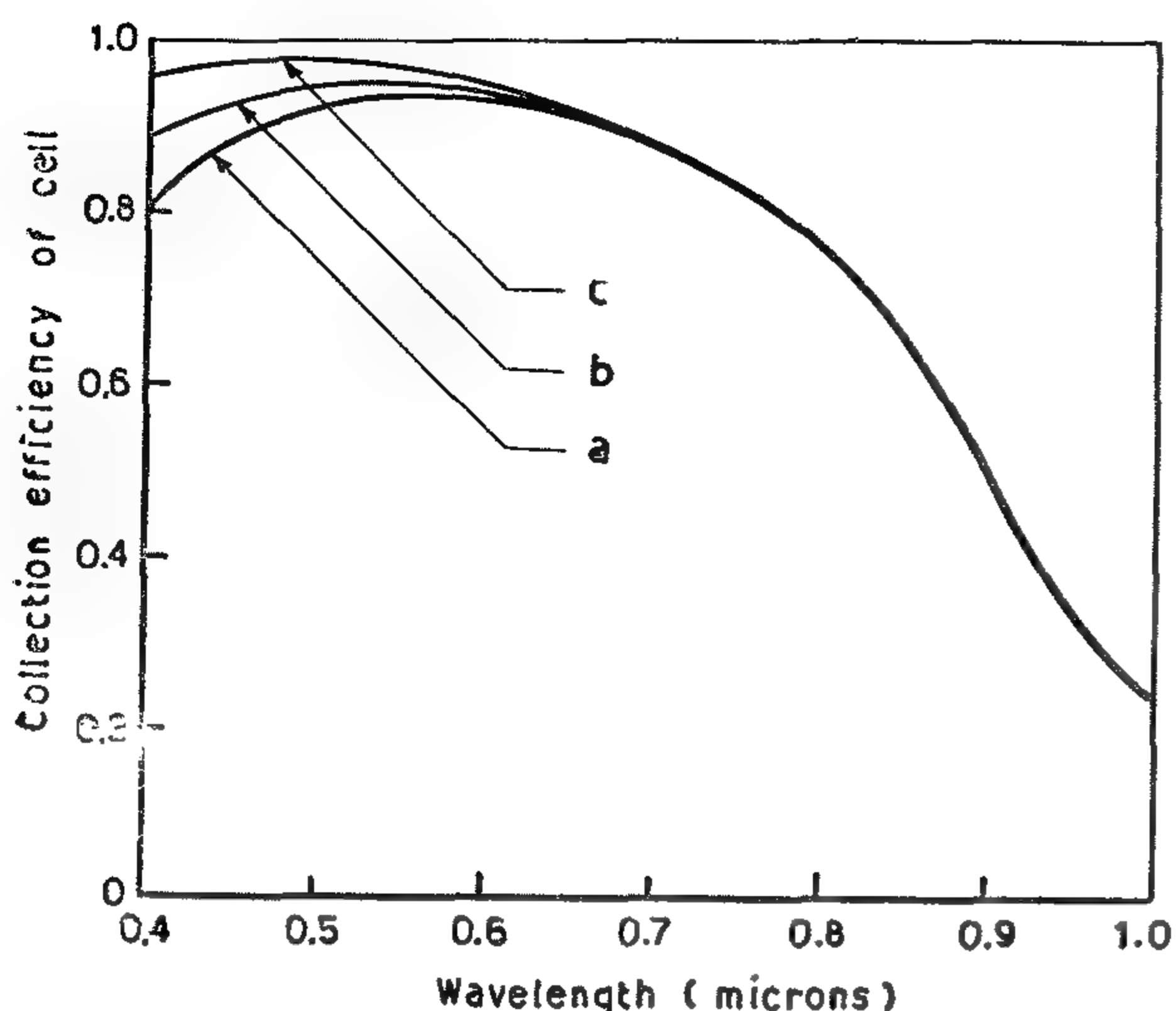
It is concluded that by proper design, it is possible to keep the cell series resistance below 0.5 ohm. For this value, the available output power will be more than 90 percent of the output power with zero resistance.

5. CONCLUSION

Collection efficiencies of about 97 percent over the major part of the spectral response are obtained for cells having exponential impurity profiles. While the typical collection efficiency for the field free cells is about 80 percent. Consequently, the conversion efficiency would increase from about 12 percent for the field free cells to about 15 percent for cells having exponential impurity profiles. Further increase in the conversion efficiency can be achieved through the use of double layer coatings and by minimizing the cell series resistance. The maximum possible conversion efficiency is 21.6 percent for silicon cells.

REFERENCES

- 1) M.M. Chapin, C.S. Fuller, and G.L. Pearson, A new silicon p-n junction cell for converting solar radiation into electrical power, J. Appl. Phys. 25, 676 (1954).
- 2) M.B Prince, "Silicon solar energy converters, J. Appl. Phys. 26, 534 (1955).
- 3) G.C. Jain and R.M.S. , Al-Rifai Effects of drift fields and field gradients on the quantum efficiency of photo cells, J. Appl. Phys. 38, 768
- 4) M. Abd El-Gawad, On the improvement of the conversion efficiency of solar cells, M. Sc. thesis, Cairo Univ. (1974).
- 5) W.C. Dash and R. Newman, Intrinsic Optical absorption in single crystal germanium and silicon, Phys. Rev. 99, 1151 (1955).
- 6) S.M. Sze, Physics of Semiconductor devices, J. Wiley (1969).



- (a) $N_0 / N_b = 10^4$
 (b) $N_0 / N_b = 10^2$
 (c) $N_0 / N_b = 10^4$ ($x_j = 0.5 \mu$, $x_t = -50 \mu$, $S_n = 10 \text{ cm scc}$, $S_p = 10^4 \text{ cm scc}^{-1}$, $D_n = 2 \text{ cm}^2 \text{ sec}^{-1}$, $\tau_n = 0.1 \mu \text{ sec}$, $\tau_p = 5 \mu \text{ sec}$)

FIG. (4) COLLECTION EFFICIENCY OF SOLAR CELL FOR EXPONENTIAL PROFILE WITH DIFFERENT VALUES FOR SURFACE-TO-JUNCTION ACCEPTOR CONCENTRATION RATIO.

th x_j , the better the collection efficiency. However if x_j gets too small, the efficiency falls off due to negligible absorption.

(2) The deeper the base layer edge x_t , the better the collection efficiency. However, if x_t exceeds a certain limit, the efficiency will not increase any more due to negligible increase in the absorption.

(3) Surface recombination velocity has a pronounced effect on the collection efficiency for high energy photons. However the collection efficiency for low energy photons does not depend greatly on the surface recombination velocity has a pronounced effect on the collection efficiency for high energy photons. However the collection efficiency for low energy photons does not depend greatly on the surface recombination velocity since they generate their electron — hole pair deep in the material.

3. COMPUTATION OF REFLECTION LOSS

Since the refractive index of most of

most of the semiconductors is high, the reflection loss from the cell surface is prohibitive unless some kind of antireflection coating is used. In practice, single layer or double layer antireflection coating is usually used to minimize the reflection loss. For the case of double layer coating the reflection coefficient is given by

$$r(\lambda) = \frac{r_1 + r_2 \exp(2\theta_1) + r_3 \exp(2\theta_1 + 2\theta_2) + r_1 r_2 r_3 \exp(2\theta_3)}{1 + r_1 r_2 \exp(2\theta_1) + r_1 r_3 \exp(2\theta_1 + 2\theta_2) + r_2 r_3 \exp(2\theta_3)} \quad (15)$$

where r_1 , r_2 , and r_3 are the Fresnel reflection coefficients and for normal incidence are given by

$$\theta_1 = -i(2\pi/\lambda)N_1 d_1 \text{ and } \theta_2 = -i(2\pi/\lambda)N_2 d_2$$

The reflectance $R(\lambda)$, which is the fraction of the incident light power reflected from the surface is

$$R(\lambda) = r(\lambda) r^*(\lambda) \quad (16)$$

The spectral response of a double layer coating on a silicon solar cell is given in (Fig. 5). The results show that a double layer coating of MgF_2 ($N_1 = 1.38$, $\tau =$

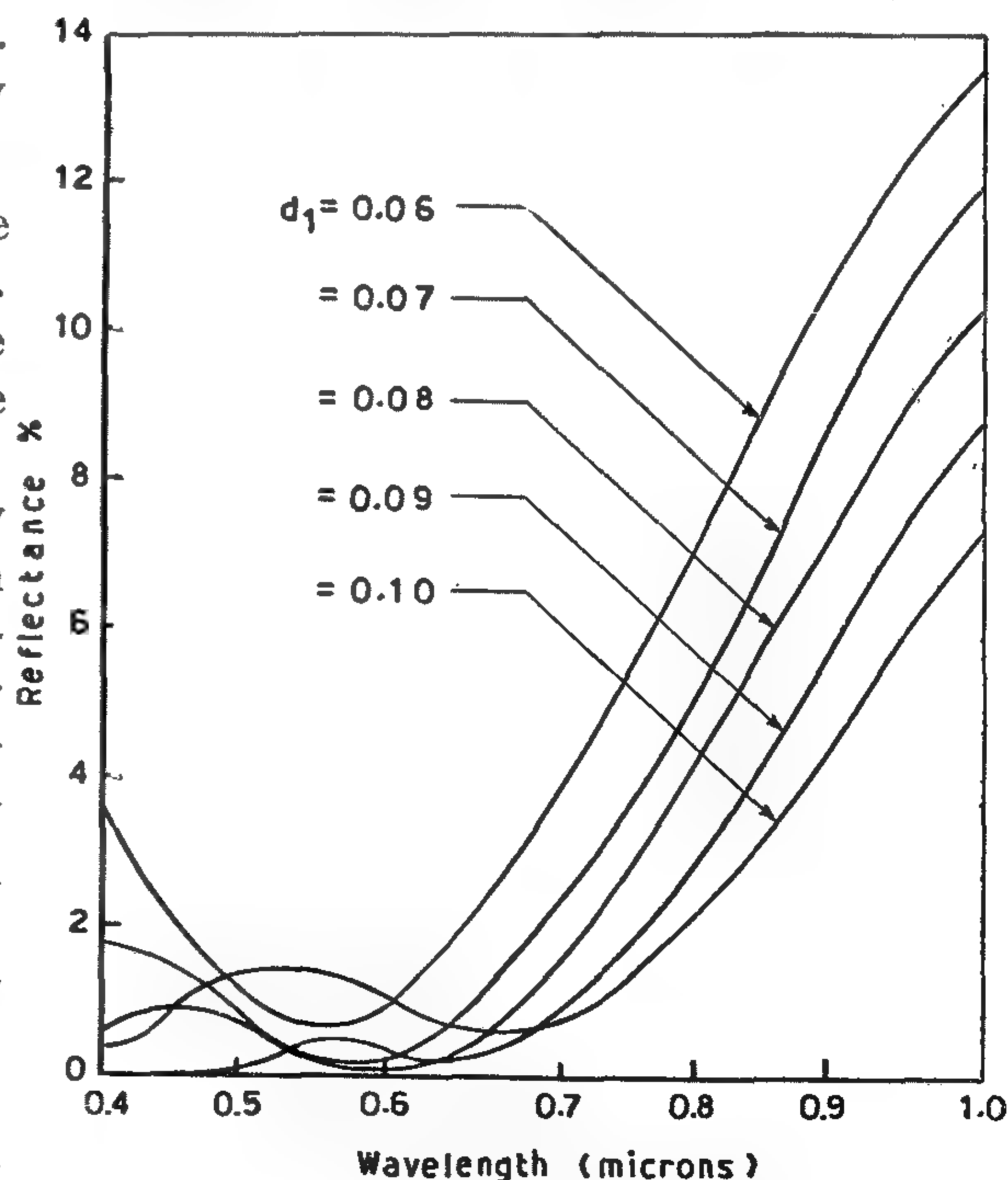


FIG. (5) REFLECTANCE VS WAVELENGTH FOR A MgF_2 - CeO_2 -Si STRUCTURE WITH $d_2 = 0.05 \mu$ AND FOR DIFFERENT VALUES OF FIRST FILM THICKNESS

2.2.1 Uniformly Doping Profiles : Field Free Case

In this case, Z_n and Z_p assume constant value except in the narrow depletion layer. The solutions of Eqs. (2) and (3) with the boundary conditions (4-6) yield

$$\eta_D = \frac{-\alpha}{\alpha^2 - w_n^2} \left[\alpha \exp(-\alpha y_1) + w_n \frac{(s_n \cosh(w_n y_1) + w_n \sinh(w_n y_1) \exp(-\alpha y_1) - (s_n + \alpha))}{s_n \sinh(w_n y_1) + w_n \cosh(w_n y_1)} \right] \quad (10)$$

$$\eta_B = \frac{\alpha}{\alpha^2 - w_p^2} \left[\alpha \exp(-\alpha y_2) + w_p \frac{(s_p \cosh(w_p y_2) - (s_p - \alpha) \exp(-\alpha y_2) - (s_p + \alpha) \sinh(w_p y_2) \exp(-\alpha y_2))}{s_p \sinh(w_p y_2) + w_p \cosh(w_p y_2)} \right] \quad (11)$$

where $\tilde{v}_p = w_p (y_t - y_2)$

2.2.2 Non Uniformly Doping Profiles a) Diffused Layer

For an exponential distribution of the form $N_a = N_0 \exp(-bx)$, the drift field is constant and equals $-(kT/q)b$. we can get for this case

$$\eta_D = \frac{\alpha}{\alpha^2 - 2N\alpha - w_n^2} \left[(2N - \alpha) \exp(-\alpha y_1) + (M - N) \left\{ (s_n - M - N) \exp(-\alpha y_1) - (s_n + \alpha - 2N) \exp((M - N)y) \right\} \exp(-My_1) - (M + N) \left\{ (s_n + \alpha - 2N) \exp((M - N)y_1) - (s_n + M - N) \exp(-\alpha y_1) \right\} \exp(My_1) \right] / ((s_n - M - N) \exp(-My_1) - (s_n + M - N) \exp(My_1)) \quad (12)$$

For variable field cases, it can be shown that

$$\eta_D = \frac{1}{1 + s_n} \left[\frac{\int_0^{y_1} z_n \exp(-\alpha y) dy}{\int_0^{y_1} z_n dy} \right] \exp(-\alpha y_1) \quad (13)$$

The integrals in eq. (13) can be obtained either analytically or numerically depending on the form of z_n .

b) Base Layer

A general expression for the base collection efficiency can be found to be

$$\eta_B = \exp(-\alpha y_2) - \left[\frac{(1 + LM)}{\alpha + w_p} + I_1 \right] / (R + I_2) \exp(-\alpha y_3) \quad (14)$$

$$\text{where } L = 2(s_p - w_p) / (1 + \exp(2w_p(y_t - y_3)))(s_p + w_p)$$

$$M = \frac{w_p}{\alpha - w_p} \left(1 - \frac{(s_p - \alpha) \alpha \exp(-\alpha w_p)(y_t - y_3)}{(s_p - w_p) w_p} \right)$$

$$R = (1 - L) / w_p$$

$$I_1 = \int_{y_1}^{y_3} (z_p / z_p(y_3)) \exp(-\alpha(y - y_3)) dy$$

$$I_2 = \int_{y_1}^{y_3} (z_p / z_p(y_3)) dy$$

2.3 Numerical Results

Fortran programs (Fig. 2) were written to compute the collection efficiency of cells having different doping profiles.

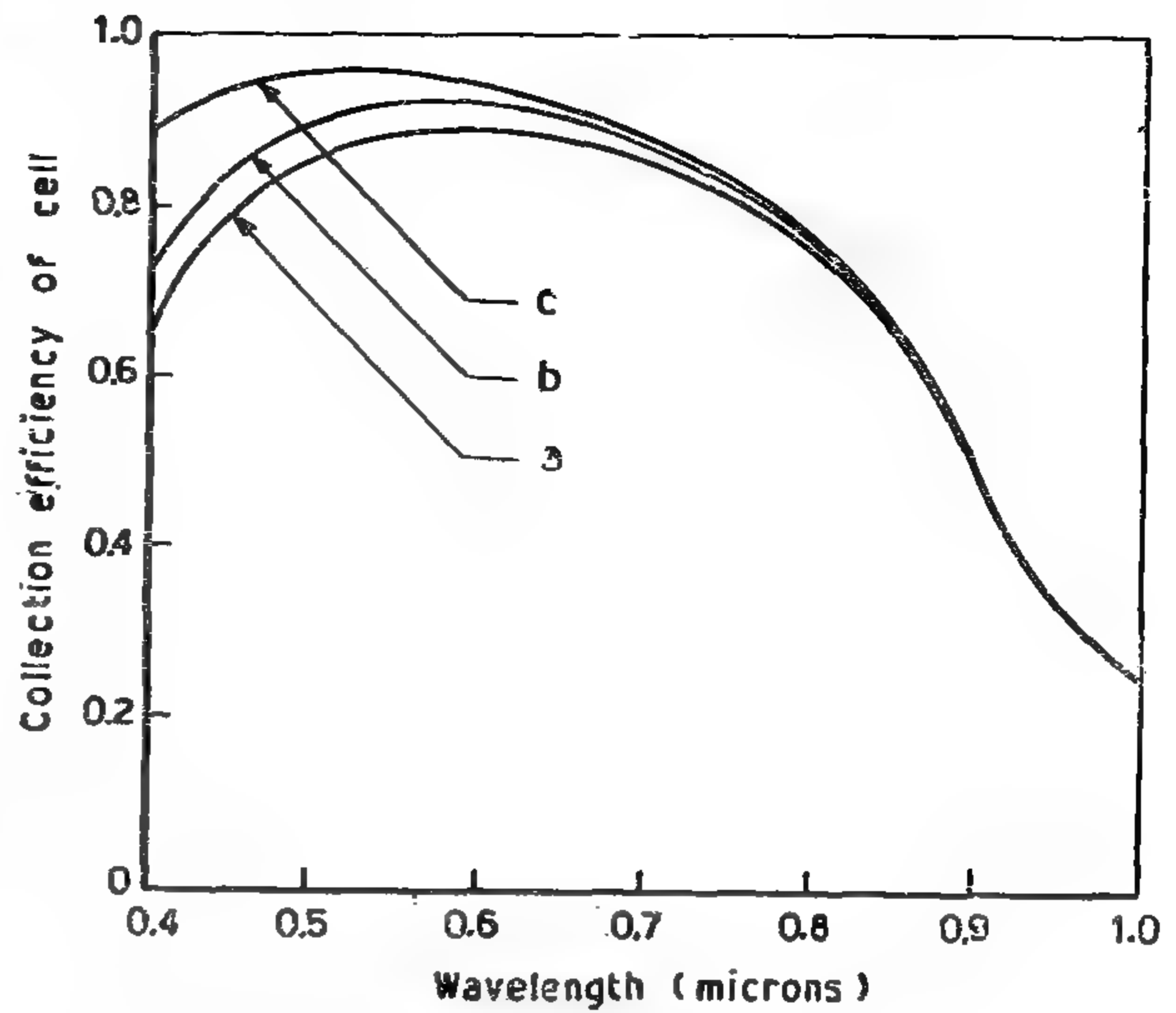


FIG.(3) COLLECTION EFFICIENCY OF SOLAR CELL
Inputs to the programs are the surface and background concentrations, the cell parameters and the optical absorption coefficient for silicon(5).
(a) Field free.
(b) Gaussian profile with $N_0/N_b = 10^2$
(c) Exponential profile with $N_0/N_b = 10^2$ ($x_j = 0.5 \mu$, $x_t = 0.45 \text{ mm}$, $D_n = D_p = 2 \text{ cm sec}^{-1}$, $\tau_n = 0.1 \mu \text{ sec}$, $\tau_p = 5 \mu \text{ sec}$, $S_n, S_p = 10^5, 10^4 \text{ cm sec}^{-1}$)

FIG.(3) COLLECTION EFFICIENCY OF SOLAR CELL

Inputs to the programs are the surface and background concentrations, the cell parameters and the optical absorption coefficient for silicon(5).

The results presented in (Fig. 3) show clearly that there is improvement in the collection efficiency when a drift field is established in the diffuse layer by using nonuniformly doped semiconductors. The best results are obtained for cells having exponential impurity profiles. Generally, the optimum profile is that which produces a high electrostatic field of small gradient. This is because the field aids the minority carriers to drift towards the junction and the field gradient impedes the motion of the minority carriers.

Fig. 4 shows that the collection efficiency can be increased by increasing the surface to back ground concentration ratio. Such an increase can be attributed to the increase in the established electrostatic field.

The computed results(4) show that

(1) The shallower the junction dep-

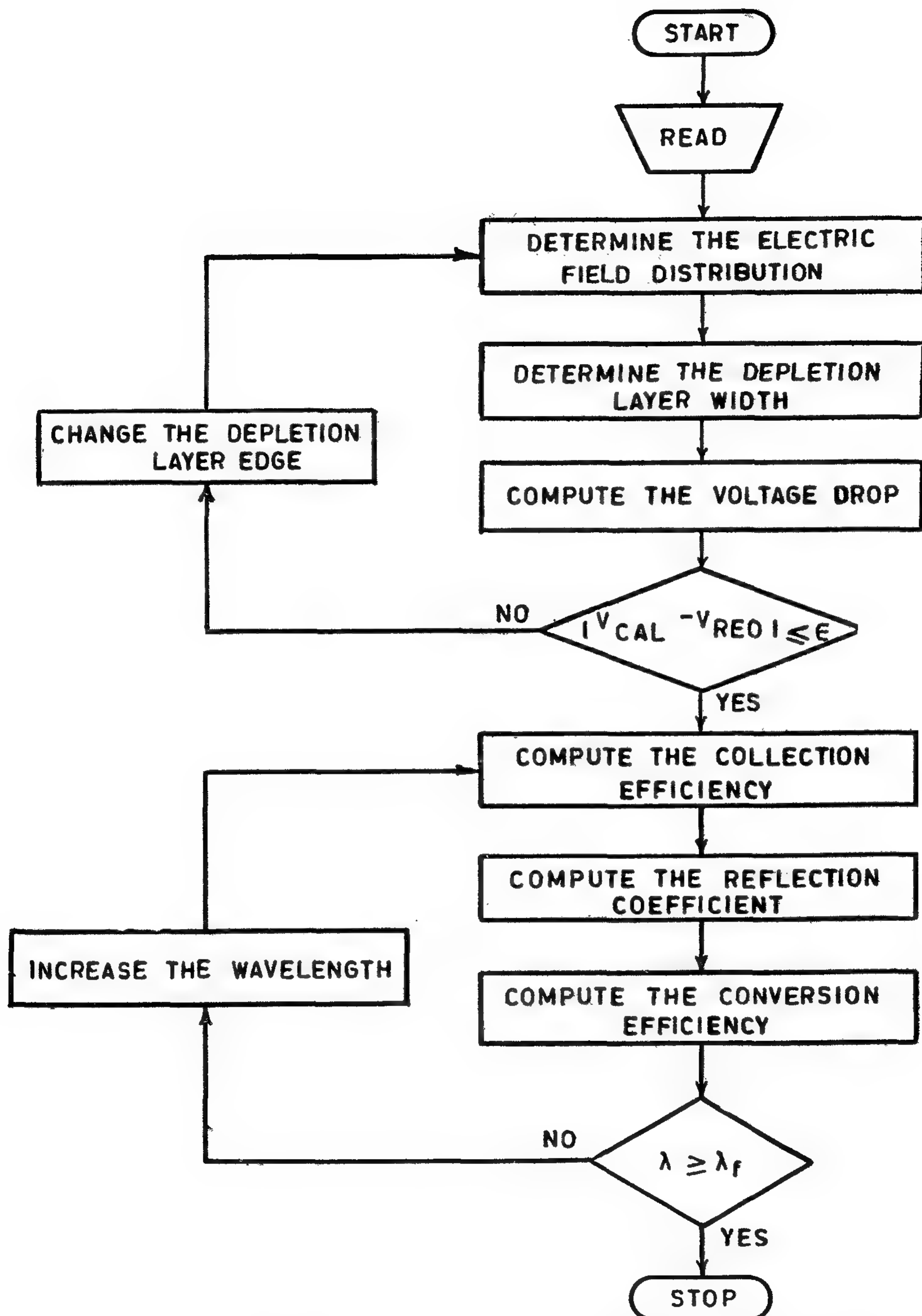


FIG. (2) FLOWCHART OF THE COMPUTER PROGRAM

2. COMPUTATION OF COLLECTION EFFICIENCY AND SPECTRAL RESPONSE

2.1 Continuity Equations for Minority Carriers

The excess minority carrier concentration n in the diffused p-layer (Fig. 1) is governed by the continuity equation

$$\frac{\partial n}{\partial t} - a(\lambda)F(\lambda)\exp(-a(\lambda)x) + \frac{1}{q} \frac{\partial J_n}{\partial x} - \frac{n}{\tau_n} \quad (1)$$

where $a(\lambda)$ is the optical absorption coefficient at wavelength λ , $F(\lambda)$ is the photon flux entering the p-layer per unit area per unit time, J_n is the electron current density ($= q(\mu_n n E + D_n \partial n / \partial x)$) and τ_n is the electron life time. It is convenient to rewrite eq. (1) in a normalized forms. Assuming nondegeneracy and thus using the Einstein relation ship ($\mu_n = q / kT) D_n$), we can get for the steady state operation

$$\frac{d^2 n}{dy^2} + \frac{d(\ln Z_n)}{dy} \cdot \frac{dn}{dy} + (\frac{d^2}{dy^2} (\ln Z_n) - w_n^2) n = -\alpha \beta \exp(-\alpha y) \quad (2)$$

$$\text{where } Z_n = \exp(-qV/kT), Y = x/x_j, \alpha = a(\lambda) X_j, \beta = X_j F(\lambda) / D_n \text{ and } w_n = X_j / \sqrt{D_n \tau_n}$$

Similarly for holes in the n-type base layer we get

$$\frac{d^2 p}{dy^2} + \frac{d(\ln Z_p)}{dy} \cdot \frac{dp}{dy} + (\frac{d^2}{dy^2} (\ln Z_p) - w_p^2) p = -\alpha \gamma \exp(-\alpha y) \quad (3)$$

$$\text{where } Z_p = \exp(qV/kT), \delta = X_j F(\lambda) / \nu_p, \text{ and } w_p = X_j / \sqrt{D_p \tau_p}$$

Solutions for Eqs. (2) and (3) must satisfy the boundary conditions

$$dn(0)/dy = [S_n - (d/dy)(\ln Z_n(0))]n(0) \quad (4)$$

$$n(y_1) = p(y_2) = 0 \quad (5)$$

$$dP(y_t)/dy = -S_p P(y_t) \quad (6)$$

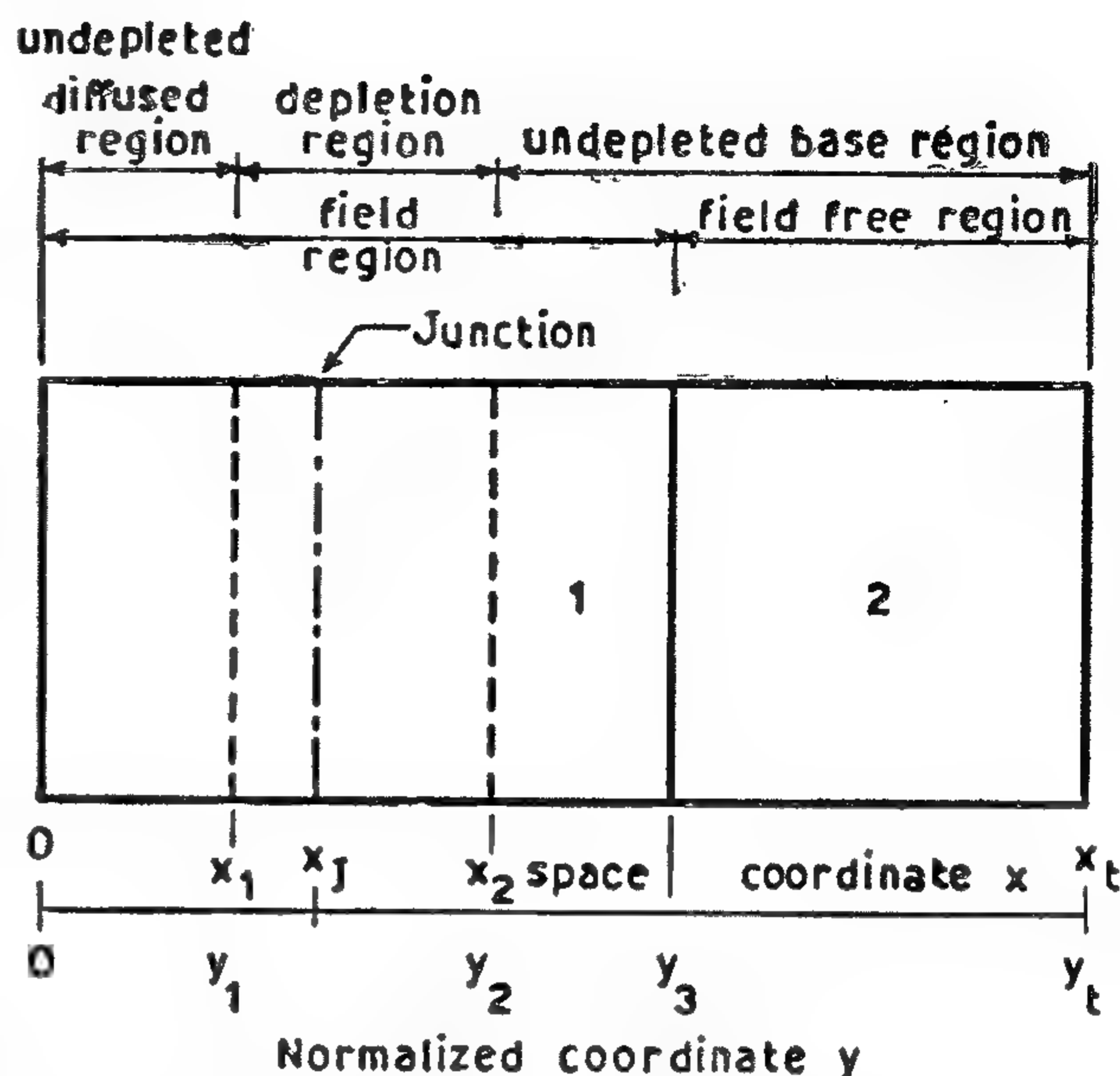


FIG. (1) GEOMETRICAL ORIENTATION OF THE CELL

where $S_n = s_n v_j / D_n$ and $S_p = s_p v_j / D_p$ are the normalized surface recombination velocities.

2.2 Expressions for the Collection Efficiency (4)

The collection efficiency is defined as

$$\eta_c = J_t / qF(\lambda)$$

where J_t is the total photo current density and has three components: J_d and J_b are the photocurrent density collected from the undepleted diffused layer and base layer, and J_{dl} is the photocurrent density due to absorption in the depletion layer. Assuming that each photon absorbed in the depletion layer contributes one current carrier, we get

$$J_{dl} = qF(\lambda)(\exp(-\alpha y_1) - \exp(-\alpha y_2)) \quad (8)$$

Thus Eq. (7) can be written as

$$\eta_c = \eta_D + \eta_{Dl} + \eta_B = -\beta^{-1} (dn/dy)_{y_1} + \exp(-\alpha y_1) - \exp(-\alpha y_2) + \delta^{-1} (dp/dy)_{y_2} \quad (9)$$

COMPUTER OPTIMIZED DESIGN OF SOLAR CELLS

By

Dr. M. ABDEL-GAWAD & A.H.M. SHOUSHA

ABSTRACT

The possibilities for improving the conversion efficiency of solar cells have been investigated with the aid of a computer model. The model is based on the macroscopic continuity equations for minority carriers. Solutions of these equations have been carried out to determine the effect of electrostatic drift fields and their gradients on the collection efficiency of p-n junction solar cells. Numerical computations for silicon solar cells have been performed using impurity profiles of the exponential, Gaussian and complementary error function types. It is found that there is improvement in the collection efficiency for any of the above distributions as compared to the field free case. The optimum impurity profile is that which produces a high electrostatic field of small gradient.

The present model also enables us to study the effects of antireflection coatings on the reflectance and transmittance of the incident light at the cell surface. The optimum thicknesses of antireflection coatings have been determined for several cases.

It is concluded that a conversion efficiency of about 15 percent can be achieved on silicon solar cells with exponential impurity profiles and proper design. This compares with about 12 percent for field free case.

1. INTRODUCTION

Since the first solar energy converter utilizing a silicon p-n junction was made by Chapin, Fuller and Pearson (1) in 1954, there have been many studies to improve the performance of the solar cell. The factors limiting the performance of such cells can be classified into two groups: basic limitations, such as the incomplete absorption of solar energy and partial utilization of photon energy, and technology determined limitations. The limit conversion efficiency, which is not affected by technique factors, has been found to be 21.6% for silicon solar cells (2) and it is not open to improvement for a given semiconductor. However, by proper design of the solar cell, its conversion efficiency can be improved.

The object of the present work is to investigate the dependence of the collection efficiency on impurity profiles of p-n solar cells, to develop a suitable antireflecting coatings and a study on the optimum series resistance in an attempt to improve the conversion efficiency.

$$\begin{aligned}
 f_{ex_k}(z) &= f_{ex_k}(|z|) P(z) \quad \text{if } |z| \neq M_i \\
 f_{ex_k}(M_i) &= P(M_i) \int_{M_i}^{f_2 \max(k)} f_{ex_k}(x) dx \\
 f_{ex_k}(-M_i) &= P(M_i) \int_{M_i}^{-f_1 \max(k)} f_{ex_k}(x) dx
 \end{aligned} \quad (12)$$

Where

$f_{ex_k}(Z)$ is the power interchange histogram taking the actual transmission line system into account.

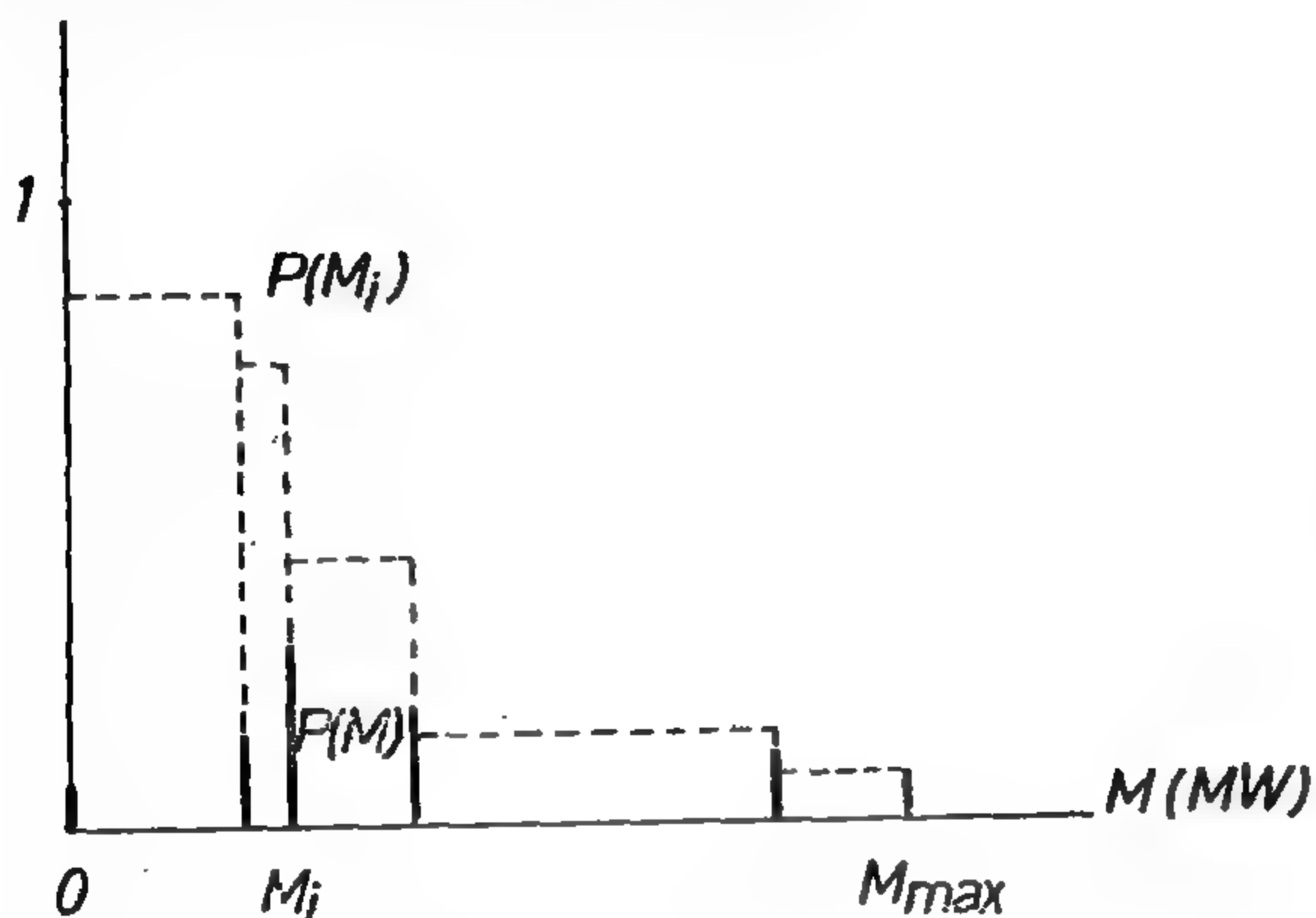


Fig.7 Capacity of a transmission line system.

The second and the third rows of Eq (12) express the fact that the total capacity M of the transmission system is utilized when this is the limiting factor for the transmission.

On the basis of the foregoing discussion, the amount of energy the transmission of which is prevented by the finite capacity of the transmission line system or an unexpected break-down, can be written as

$$D = \sum P(M_i) \left\{ \int_{M_i}^{f_2 \max(k)} (x - M_i) f_{ex_k}(x) dx + \int_{-f_1 \max(k)}^{-M_i} (x + M_i) f_{ex_k}(x) dx \right\}$$

SUMMARY :

The energetic systems are reduced to a point, their energy consumption and the available power station capacities are considered as probability variables and considering several operating policies. The histogram of the energy flow bet-

ween the two cooperating systems is determined. For real transmission line systems the histogram of the energy exchange not realized owing to limited line capacity or failure, is calculated, which, opposed to the capital costs of the transmission lines, leads to the determination of the economic optimum. The losses due to the limitation of the consumers are evaluated with the aid of a progressive circular function.

In this paper the first step has only be taken towards a complete dimensioning of an economic tie line. I intend to prepare a computer program for computing the algorithm, and to extend this work to the case of 3 or n systems and to develop cost accounting procedures outlined in the foregoing discussion.

REFERENCES

1. Szendy, Ch. : Economical Tie-line Capacity for an Interconnected system. P.A.S. July 1964 PP. 721 — 726
2. Central Electricity Generating Board (Great Britain) : Description of a Monte carlo Program for system Risk Assesment. (Manuscript for the CIGRE committee No. 13, 1966).
3. Fisher, M.J. : Power system Economic Load Allocation using a New Equation for transmission lines P.A. and S. (1960), 507.
4. De Salvo. C.A., Hoffman, C.H. and Ku, W.S. : A model for Transmission Planning by Logic. Ibid, Vol. 78 1959 (Febr. 1960 Section) PP. 1638 — 45.
5. Limmer, H.D. : Determination of Reserve and Interconnection Requirements. Ibid, Vol. 77, Aug. 1958, PP. 554-56.
6. Knight, U.G.W. : The logical Design of Electrical Networks using linear Programming Methods. The institution of Electrical Engineers, paper No. 31383, Dec. 1959.

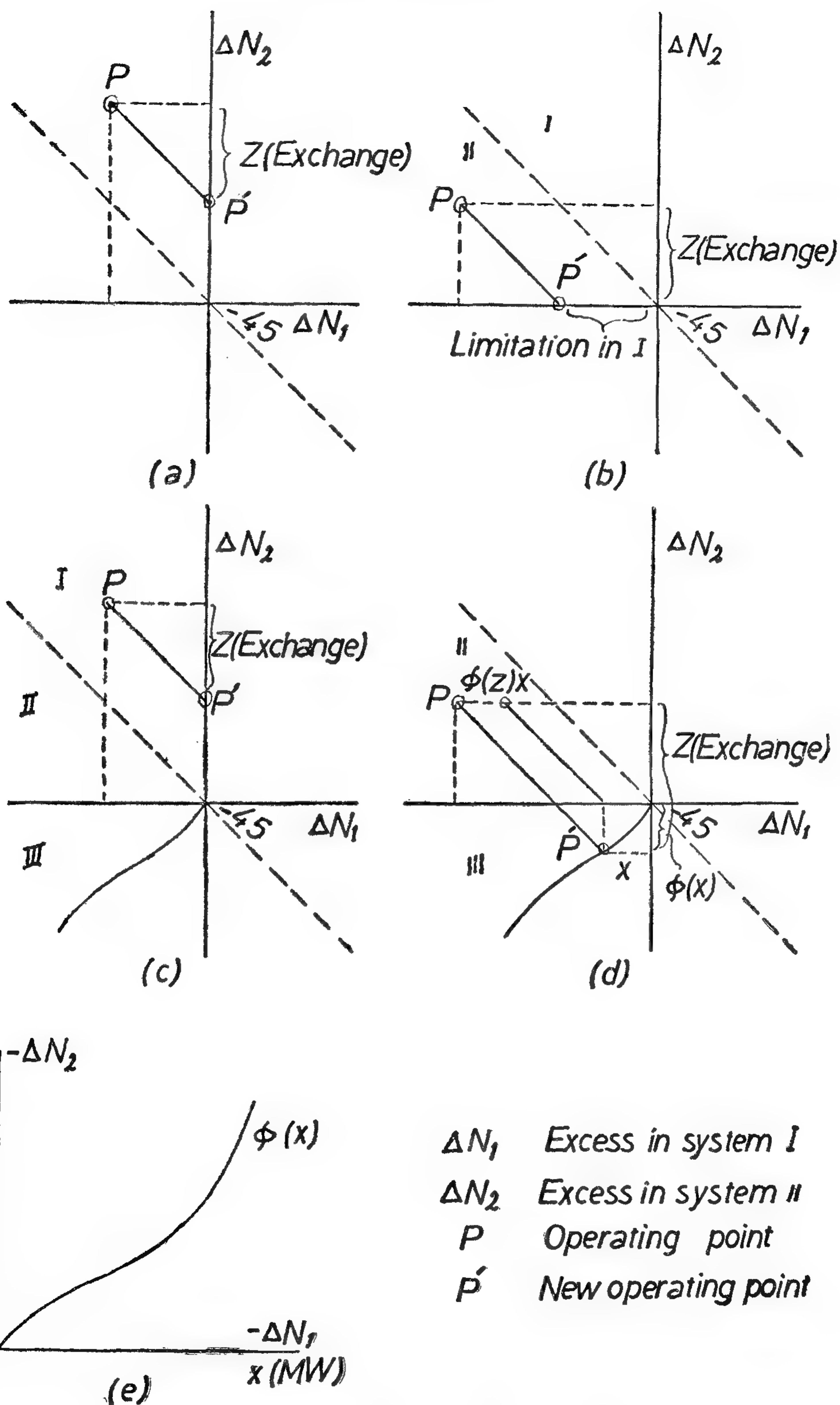


Fig.5 Operational policies of a tie-line system

of the deficiency is made possible — are shown in Fig. 5. The new operating point is placed along the vertical axis when the original operating point is in the first area, and if it is in the second area, it will be shifted to the curve. The exchange power density function is analogous to (9). The first terms correspond to area I and its image, while the second terms correspond to the combined area II—III and their respective areas. Thus the density function of the exchange power, in this case, can be written as:

$$f_{ex_k}(z) = \begin{cases} f_{1,k}(-z)[F_{2,k}(f_{2,max}(k)) - F_{2,k}(z)] + \\ \quad -G_{1,max}(k) - z \\ \quad + \int_0^{f_{2,max}(k)-z} f_{1,k}(-z-x) f_{2,k}(z-\phi(x)) dx & \text{if } z > 0 \\ \quad \text{From 2 to 1} \\ f_{2,k}(z)[F_{1,k}(f_{1,max}(k)) - F_{1,k}(-z)] + \\ \quad +G_{2,max}(k) + z \\ \quad + \int_0^{f_{1,max}(k)+z} f_{2,k}(z-x) f_{1,k}(-z-\phi^{-1}(x)) dx & \text{if } z < 0 \\ \quad \text{From 1 to 2} \\ 1 - \int_{f_{1,max}(k)}^{f_{2,max}(k)} f_{ex_k}(x) dx & \text{if } z=0 \text{ (no exchange)} \end{cases} \quad (10)$$

Note: The assistance policy discussed in (a) can be followed only in the case of an immediate intervention by the dispatcher. Conditions (b) are more closer to reality. Assuming that

$$\begin{aligned} \alpha_1 &= \alpha_2 \\ K_1 &= K_2 \end{aligned} \quad (11)$$

It is obvious that in this case the curve $\phi(x)$ (Fig. 5e) becomes a straight line and the deficiency must be divided between the two parties in proportion to the consumptions. Conditions (11) are fulfilled when nearly the same consumer structure is encountered in

the two systems, which involves a similarity of the power frequency factors.

2. Tie line with limited capacity and 100 percent reliability. Fig. 6. Shows a typical exchange-power hystogram. In long-range planning, the problem generally arises in such a form that an economic capacity M for the tie line must be determined. A useful approximate method to be used in performing economic calculations is as follows :

Both ends of the hystogram representing higher absolute values of the energy exchange are cut at M . The removed areas weighted with abscissa minus M are in proportion to the exchange in MWh which is unrealizable, because of the limited capacity of the tie line. This gives rise to a loss which gives a measure of the higher costs of a transmission line with greater capacity.

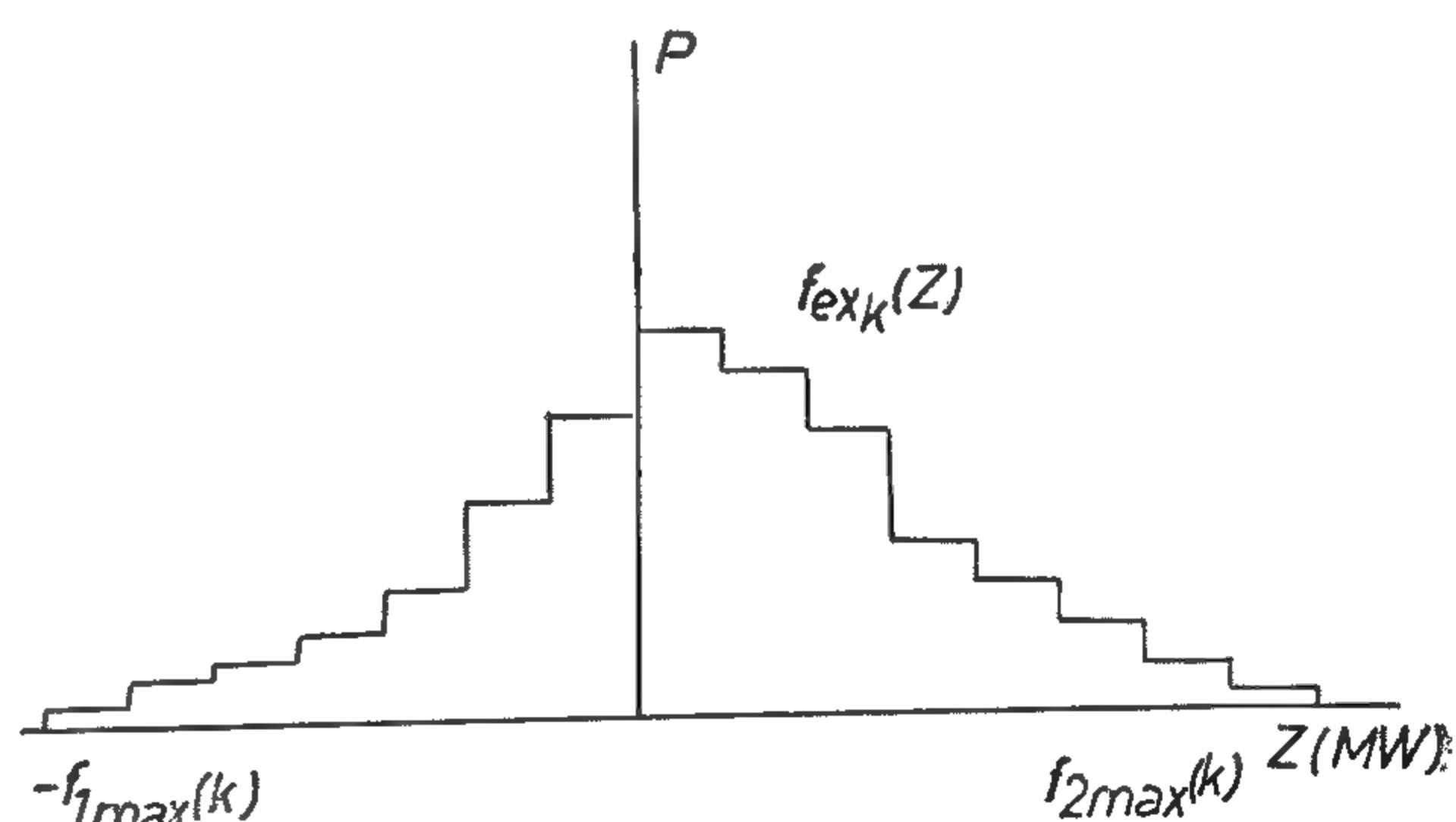


Fig. 6 A typical power exchange hystogram.

3. The probability distribution of the capacity of tie-line system is given by a hystogram.

Fig. 7 shows the capacity probability weights $p(M)$ and their cumulative $P(M)$ of a typical transmission line. In the calculations Eqs. (9) and (10) are modified according to the following relationships;

Where (ε) is the energy exchange deviation in the k th interval.

In practice, the distribution density function of the capacity excess and deficiency is replaced by a histogram. With $g_{l,k}(\chi)$ denoting the density function of the probability variable having the parameters defined by Eq. (6), the deficiency and excess density function $f_{l,k}$ is computed by using the following convolution integral:

$$f_{l,k} = \int_0^{G_{l,\max}} g_{l,k}(y-x) dH_l(y) \quad (7)$$

Where $H_l(x)$ is the cumulative of $h_l(x)$.

When $E(k)$ is considered to be a deterministic quantity rather than the expected value of a random variable, $\varepsilon(k)$ will be very small and can be neglected. Thus, the deficiency-excess distribution function and histogram can be written as:

$$\begin{aligned} F_{l,k}(x) &= H_l(x + G_l(k)) \\ f_{l,k}(x) &= h_l(x + G_l(k)) \end{aligned} \quad (8)$$

according to Eq. (7). Fig. 4 shows the histograms calculated in this way.

2.4. Calculation of exchange power

1. Tie line or tie-line system with unlimited capacity and 100 percent reliability in service.

(a) The case of the assistance policy (A) discussed in section 2.1. Fig. 5 represents the operational policies of a tie-line system. The second quarter is divided into two equal parts (I, II) by a straight line having a slope of 45 degrees. This is the so-called operating line, because, it allows the determination of the new operating point in the integrated system (Pand P' are the original and new opera-

ting points respectively). I, II denote the two areas where the deficiency of system 1 is fully or partially covered. The new operating point is shifted to the vertical axis in the former case and to the horizontal axis in the latter (Figs. 5 a and 5 b). The original operating point is shifted in direction parallel to the straight line to a position determined by the assistance policy. The displacement projected to one of the axes will give the furnished energy.

Thus, the density function of the exchange power $f_{ex}(z)$ can be written as;

$$f_{ex,k}(z) = \begin{cases} f_{1,k}(-z)[F_{2,k}(f_{2,\max}(k)) - F_{2,k}(z)] + f_{2,k}(z) \cdot [F_{2,k}(-z) - F_{2,k}(G_{1,\max}(k))] & \text{if } z > 0 \\ \text{To system 1 from system 2} \\ f_{2,k}(z)[F_{1,k}(f_{1,\max}(k)) - F_{1,k}(-z)] + f_{1,k}(-z) \cdot [F_{2,k}(z) - F_{2,k}(G_{2,\max}(k))] & \text{if } z < 0 \\ \text{To system 2 from system 1} \\ 1 - \int_{f_{1,\max}(k)}^{f_{2,\max}(k)} f_{ex,k}(x) dx & \text{if } z=0 \text{ (no exchange)} \end{cases} \quad (9)$$

The first and the second tow in this relationship express the reciprocity between each other. The first terms correspond to the values given by the operating point in area II.

(b) The case of the assistance policy (B) discussed in section 2.1.

The position of the operating points and the curve corresponding to equal losses in the two systems-by the aid of which, an optimal and the curve corresponding to equal losses in the two systems-by the aid of which, an optimal condition

The histogram is calculated by making use of a growing method. The initial and a general step of the algorithm are given by: Let the required capacity availability histogram be denoted by $h_1(x)$, where x is in MW.

a : Starting step

$$h_1(x) = \begin{cases} 1 & \text{if } x=0 \\ 0 & \text{if } x>0 \end{cases} \quad (4)$$

expressing that in a system without any generating unit, there will be a probability equal 1 that a capacity of (0 MW) is available.

Machines are then considered one by one and added to the system, with modifying the histogram in each time (Fig. 3).

b : General step.

Let the system already includes (includes $(i-1)$ machines. Then the i th machine now be added. We start from h_1 max. to the left in the direction of decreasing capacities and by making steps of K MW we proceed as follows :

$h_1(X + N_i)$ is increased by $h_1(x)$ $(1-p_i)$, and $h_1(x)$ is replaced by $h_1(x)$ (p_i) ; then another step is taken to advance from $x - K$.

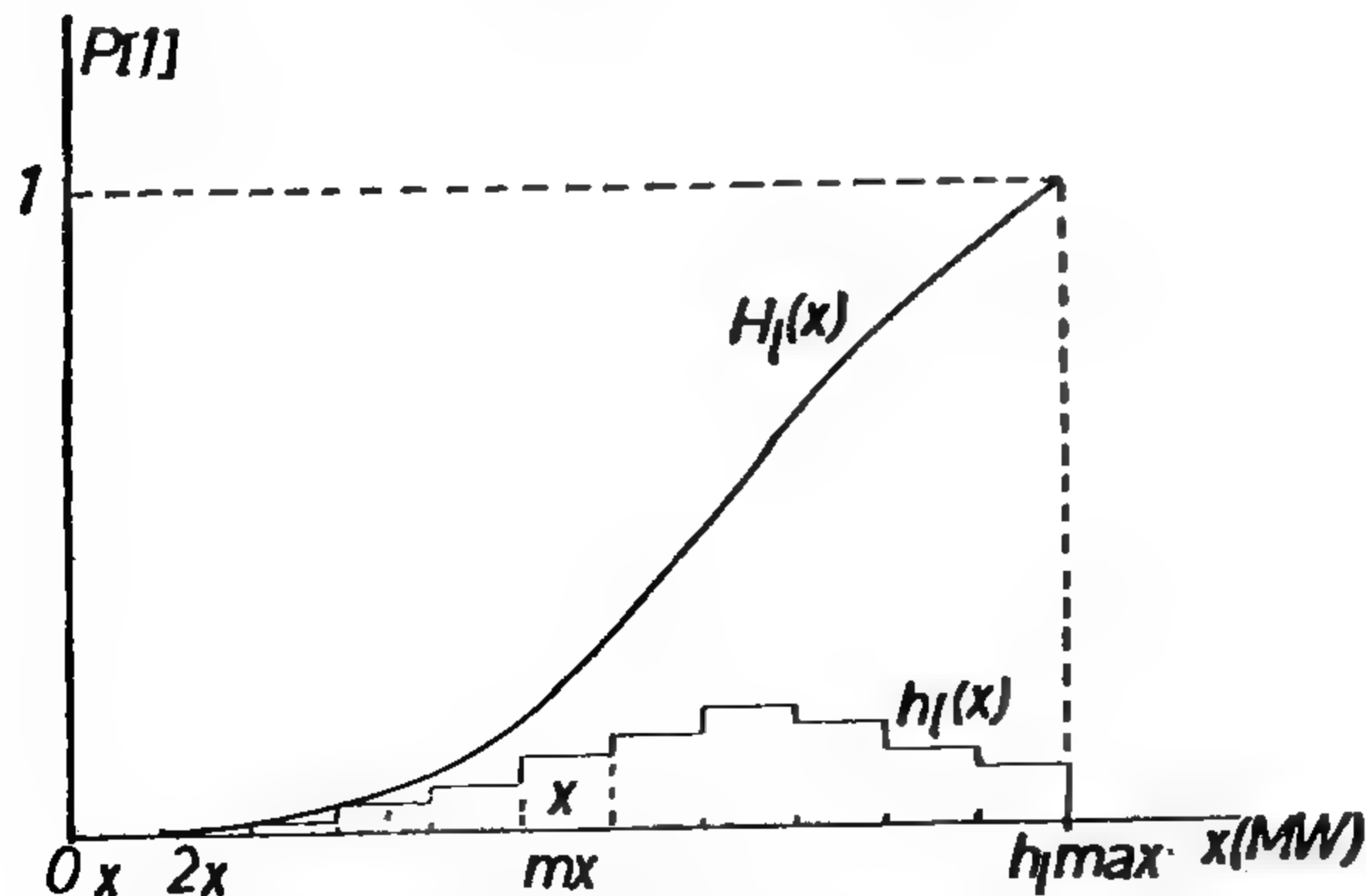


Fig. 3 Capacity availability histogram and distribution function

where

X (MW) width of a class
 m class of index

These two operations are performed for each x from h_1 max to 0, from right to left, and then the next machine is taken into consideration by repeating the procedure.

The histogram so obtained is obviously independent of the order in which the machines are added. The histogram is used to obtain the distribution function.

2.3. Calculation of deficiency — excess histogram.

As was discussed above, the machines installed in system "1" must furnish the algebraic sum of the energy demand by their own consumers and the net exchange of energy of the system. Since the sum of two normal distributions remains as a normal distribution, then, the consumption in the k th time interval $G_1(k)$ is a probability variable having a normal distribution with an expected value of :

$$G_1(k) = F_1(k) \pm E(k) \quad (5)$$

Where $F_1(K)$ is the expected value of consumer demand in the k th time interval and $E(k)$ is the expected value of net energy exchange (scheduled value) in the k th interval.

and a deviation of

$$\sigma_1^2(k) = \sigma_1^2(k) + E^2(k) \quad (6)$$

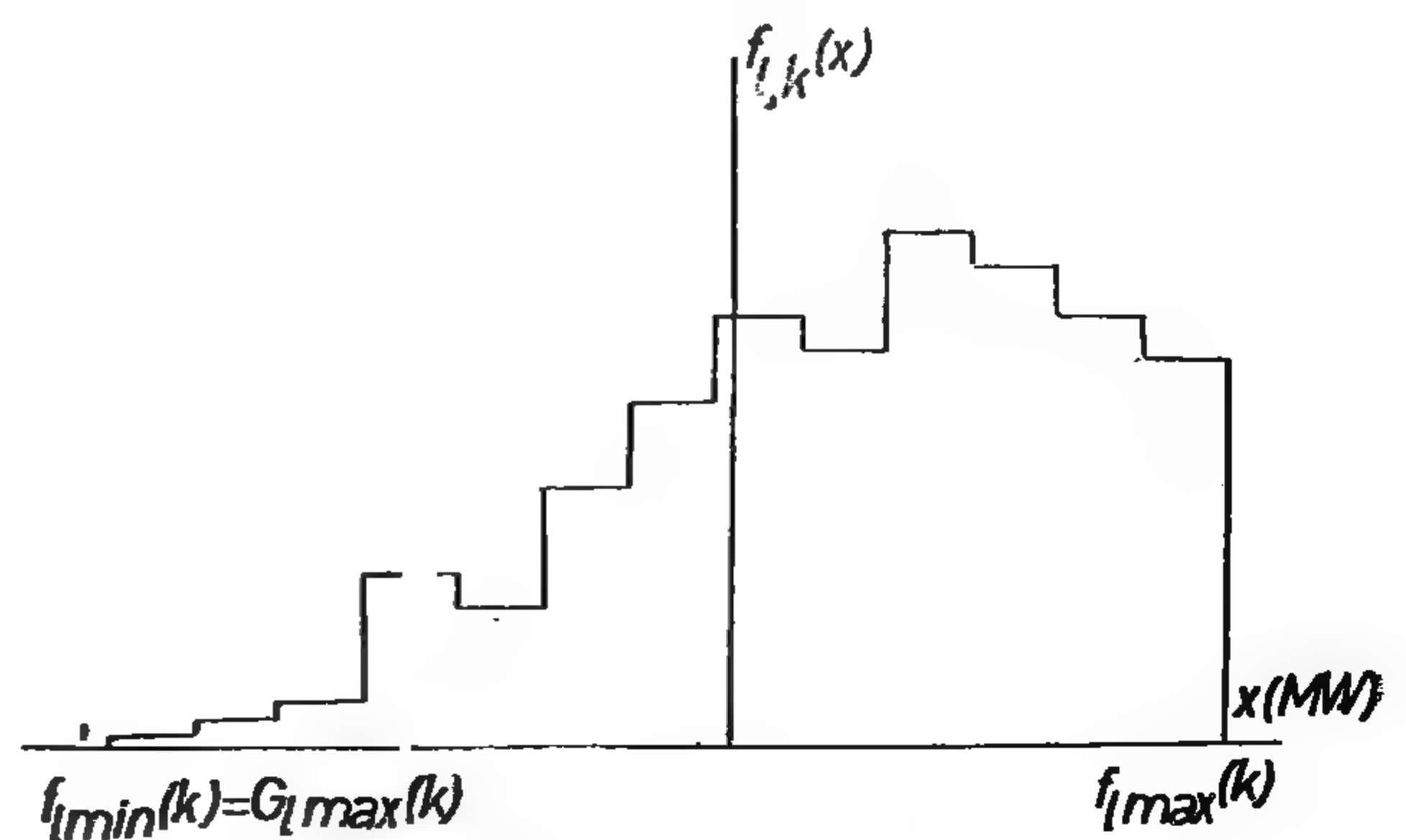


Fig. 4 Deficiency-excess histogram

Fig. 2 seems to be an appropriate practical approach.

In the case when Fig. 2 is used to determine the loss function the composition of the consumers must be assumed to be unchanged at each time interval (as the loss due to consumer restrictions is concerned) because " ∞_1 " is constant. This assumption together with the condition of linearity seems to be a permissible approximation from the viewpoint of long-range planning.

II. CALCULATION OF LOAD IN THE LINES

In view of the theoretical character of this paper, the modifications and approximations required by particular applications are not taking into consideration, unless they are absolutely necessary.

The equations for two systems and a period of one day will be presented in a form as general as possible and should be used in practice accordingly.

2.1. Operating interconnected systems.

Mutual help given in the case of an outage.

When the available capacity of one of the systems is reduced by an unforeseen event, it would be necessary to impose restrictions on its consumers. The co-operating partner can, in most cases, offer assistance to cover the total energy deficiency or a part of it. Thus, a more economic operation is ensured and the losses will be reduced.

Different assistance policies should be selected depending on the intention of minimising the loss due to restrictions on each system level separately, or the sum of losses in the two systems as a whole; the following two cases will be handled:

- (a) The assistance given in a particular case does not exceed the unutilized reserve, so that a ca-

capacity deficiency in one system cannot result in a consumer restriction in the other system giving assistance.

- (b) The two systems share the capacity deficiency in such a way as to obtain a minimum cost of the deficiency in the two systems, when the system which needs energy fails to obtain full assistance from the other system.

The deficiency is economically shared among the co-operating systems when the maximum specific loss is the same in each system, that is, the systems are operated at a point of equal losses. Megawatt-hour outage is constant in the grid, i.e, it is independent of the assistance policy.

Proof : Let us assume X (MW) deficiency in the integrated system. It will be divided into Z (say) for system 1 and $X - Z$ for system 2. Then the loss will be expressed as

$$K = K_1(Z) + K_2(X-Z) \quad [10^3 \text{ LE/hr}] \quad (2)$$

An extreme value as a function of Z is found in the following way:

$$\frac{dK}{dZ} = K'_1(Z) - K'_2(X-Z) = 0$$

$$\text{or } K'_1(Z) = K'_2(X-Z) \quad (3)$$

this is exactly that which was stated. From the curves K_1 and K_2 it is possible to determine a curve at the points of which the losses in the two systems are equal. In Fig. 5 e this curve $\phi(x)$ is presented in a completely general form with $x = -\Delta N_i$ as the independent variable.

2.2. Calculation of machine-power by an available histogram.

The probability distribution of the available machine power calculated from the maximum capacity of the individual generating units (N_i) and their failure probability (pi), is a discrete distribution. Therefore, it is given in the form of a histogram by the algorithm, anyway.

I. MATHEMATICAL MODELS OF ENERGY SYSTEM FACTORS

1.1. General blocks.

Generating blocks will be characterized by the following parameters :

N_i (MW) maximum power delivered to a bus (or the available power according to the interpretation).

$P_i(l)$ failure probability, depending on the age of the machine. (i and l being the machine unit index and system index respectively).

1.2. Representation of transmission lines.

A transmission line is represented by two data :

M_j (MW) transmission line capacity.

$r_j(l)$ transmission line failure probability (j being the line index).

1.3. The resultant consumer demand.

For each co-operating system the resultant consumer demand is assumed to be a random variable with normal distribution for all times. The expected values and deviations of the variable are considered constant along a given section. The curve of the expected values is shown in Fig. 1. It is assumed in this paper that the expected daily consumer schedule is a step-like function of time. The deviation is always given with res-

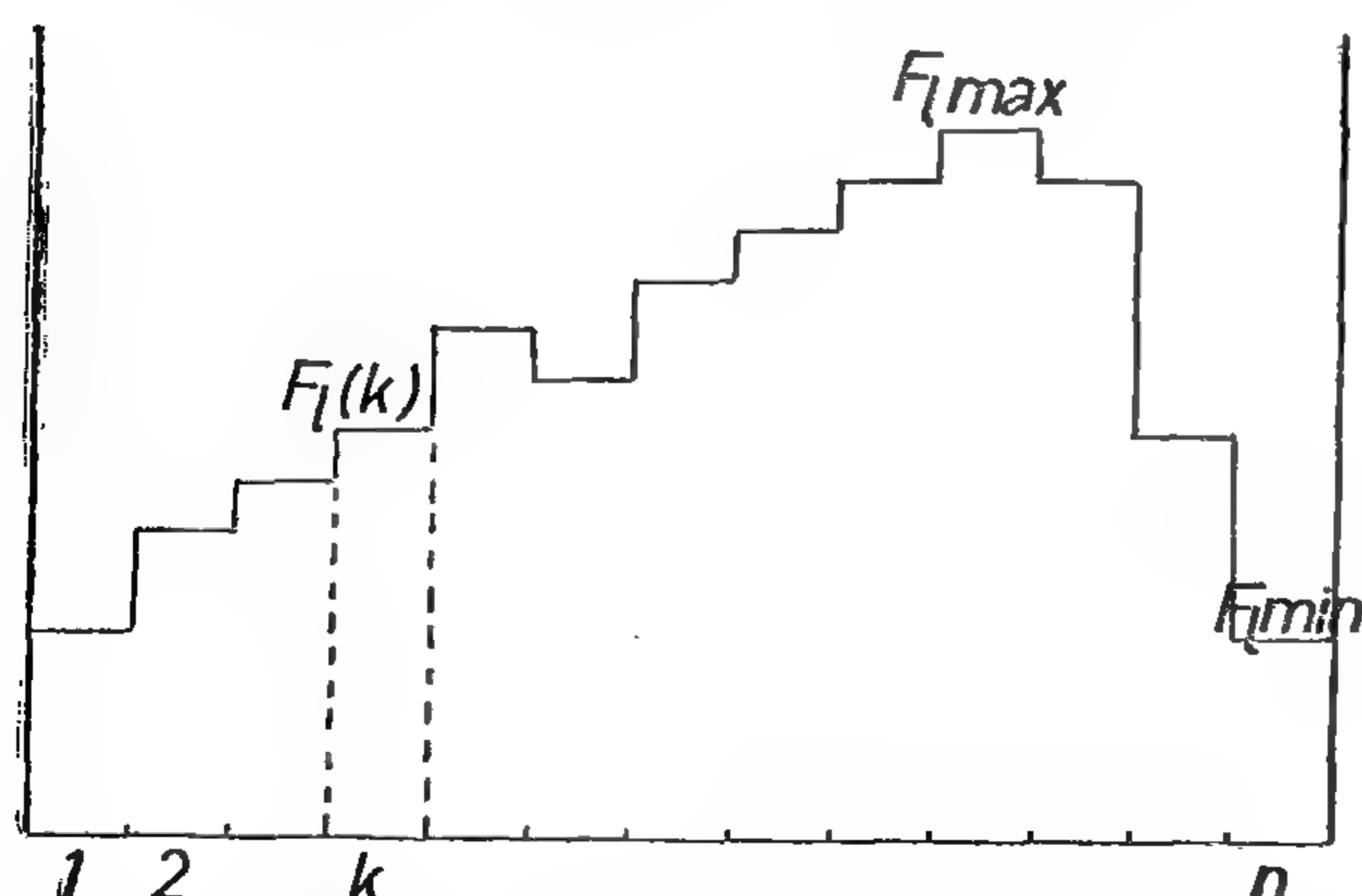


Fig. 1 A model of the daily variation in consumer demand.

Where : $F_l(k)$ is the expected value of consumer demand in the k th time interval. F_{lmax} and F_{lmin} are the maximum and minimum consumer demands expected on the investigated day respectively.

pect to the peak (F_{lmax}) in percent of the maximum deviation from the estimated value, so that, the probability of this maximum being surpassed is negligible.

For example, the consumer demand deviation in the k th time interval $\sigma_l(k)$ are approximated by using σ_{lmax} (deviation at F_{lmax}) according to the equation;

$$\sigma_l(k) = \sigma_{lmax} \sqrt{F_l(k)/F_{lmax}} \quad (1)$$

Which expresses the tendency that a lower load is associated with a lower absolute deviation and a higher relative deviation.

1.4. Loss due to consumer restrictions.

Experience shows that the loss due to consumer restrictions depends to a great extent on the momentary deficiency of capacity and the amount of energy which has not been delivered but has little influence on its value. As an adequate means to calculate actual loss, the so-called progressive loss function $K_l, K(Z)$ gives the loss due to a deficiency of capacity Z (MW) in a given period of time (e.g. an hour, a day). The use of the loss function defined in

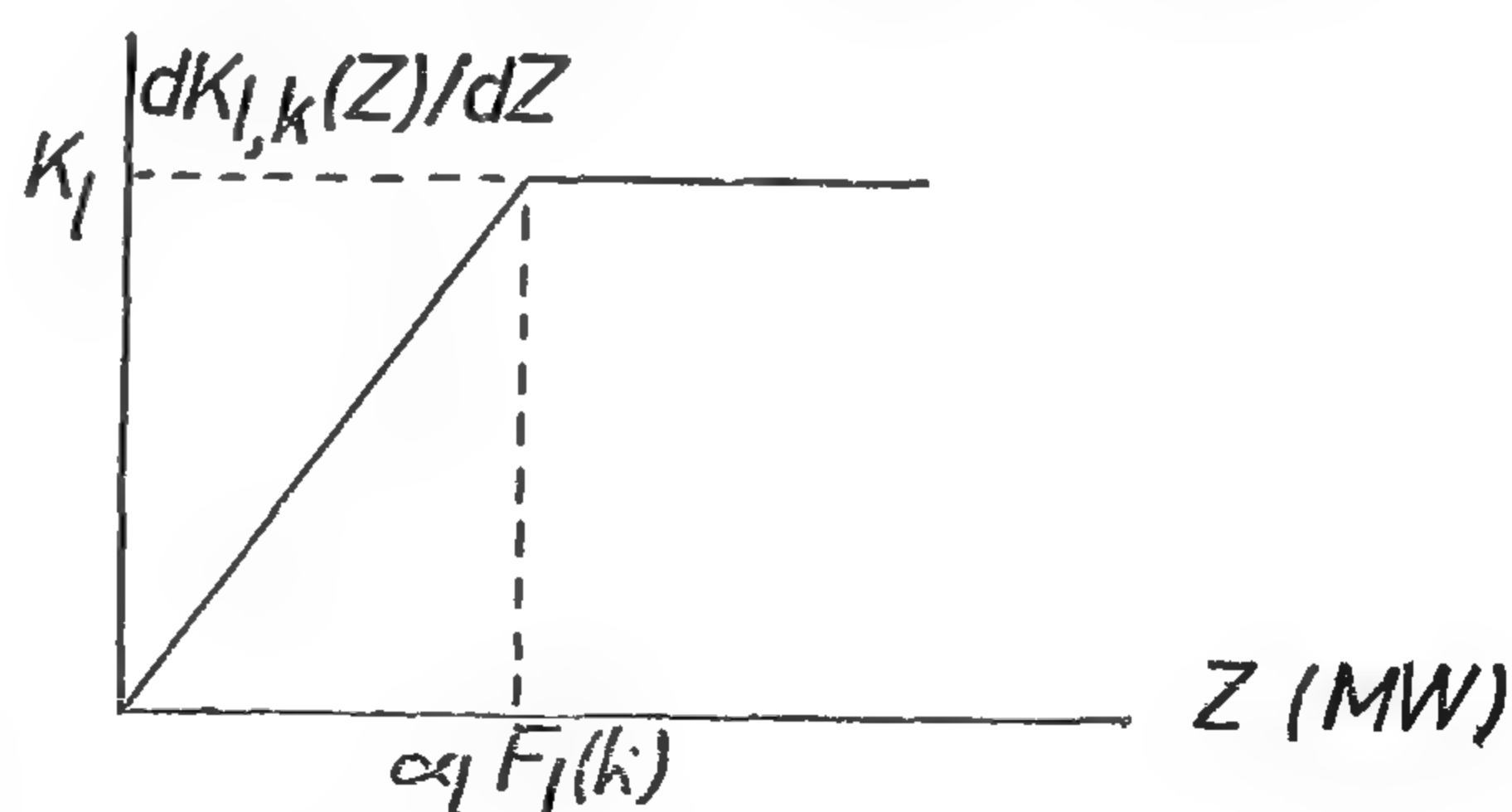


Fig.2 Derivative of loss function.

$$K'_{l,k}(Z) = dK_{l,k}(Z)/dZ = \begin{cases} \frac{K_l}{\alpha_l F_l(k)} Z & \text{if } Z < \alpha_l F_l(k) \\ K_l & \text{otherwise} \end{cases}$$

$$K'_{l,k}(0) = 0$$

$$\alpha_l = \text{Constant (about 0.2)}$$

$$K_l = LE / Kwh \text{ (about 0.12 LE/Kwh)}$$

These are estimated values

ELECTRICAL ENERGY EXCHANGE BETWEEN COOPERATING SYSTEMS

By

Dr. FAROUK SAMUEL THALOUTH

ABSTRACT

The paper presents a mathematical model and an algorithm for the calculation of the economic capacity of the cooperation Link between two energetic systems, taking the possibilities and requirements of computer work into consideration.

INTRODUCTION :

A solution based on economic calculations is offered by two basic principles :

1. The use of a simulation method allows the construction of an exact model describing actual conditions faithfully.
2. In the case when some reason impedes the use of a simulation method, the elaboration of a mathematical model will be a difficult task, because of the large number of variables and some special restrictions (e.g. maintenance problems, safety of operation and etc.).

Another factor which makes the algorithm more complex is the fact that a combined analysis of generating units and transmission lines, as a whole, leads to functions of the form $f(x) = \min(x_1, x_2)$, which are difficult to be evaluated. Some authors have no other choice but to simplify the actual conditions, for instance, by making use of the advantages of an assumed gaussian distribution, accomplishing calculations on a peak load

basis (1). The so-called fence method seems to be an interesting experiment to allow a number of interconnected systems to be analysed together (4). Because of the above mentioned difficulties designers still use experimental data instead of performing a logical economic and relying on its results.

An essential condition for calculating the economic operating conditions is a knowledge of the specifications for the interconnecting transmission lines or transmission line systems, that is, the expected demand which is necessary to determine the capacity of a tie line.

The first step in solving this complex problem is to calculate the load, that is, to determine some histograms or duration curves that will give informations about the time dependence of the interchange power flowing along the tie line system.

In analysing interconnected systems, the proposed algorithm makes use of the so called two-point model. That is, each of the two energy systems is reduced to a point representing the bus to which generators and consumers are connected. The tie lines are taken to interconnect these two points.

Instead of replacing the probability distribution of capacity availability by a familiar distribution law, a histogram based on the values of machine failure probability is used.

Table : 8

1	9	10	11	12	13	14	15	16
section number	heat to charge + losses in section	temperature of gases in section	initial temp. of gases in section	average flame temp. and average charge temp. in section	rate of heat transfer to charge	time required in section	length of section % of kiln length	distance from cold end % of kiln length
	K cal/ kg	°C	°C	°C	Kcal/ h	h/ kg	%	%
1	29.2	121	710	600 74	1,250,000	0.0000227	14.6	14.6
2	77.6	323	862	700 110	2,830,000	0.0000270	17.6	32.2
3	78.7	327	964	800 120	4,000,000	0.0000190	12.4	44.6
4	79.1	304	1052	900 120	5,620,000	0.0000135	8.7	53.3
5	104.3	400	1200	1000 335	6,080,000	0.0000160	10.5	63.8
6	200	740	1570	1200 700	6,550,000	0.0000294	19.2	83.0
7	163.4	583	1692	1400 1180	5,650,000	0.0000259	17.0	100.0

0.0001525

$$\text{Charge rate} = 1 / 0.0001525 = 6560 \text{ kg/h}$$

Although irregular and intermittent operation is, beyond doubt, the most important influence producing the variations of heat consumption, there are also other factors, such as :

- i. poor utilization of hearth area.
- ii. narrow furnace (increased wall losses in %).
- iii. excessive leaking of cold air.
- v. excessive area of water-cooled surfaces exposed to flame.
- iv. loss of heat through trouble doors by radiation and by escape of unburned gases.

For careful and safe operation, one can shift the calculated curve for each running conditions (heating rate) to higher values. The shift ranges normally bet 5-10 % of fuel consumption. In exceptional cases it rises up to 25% when all factors mentioned above are going together.

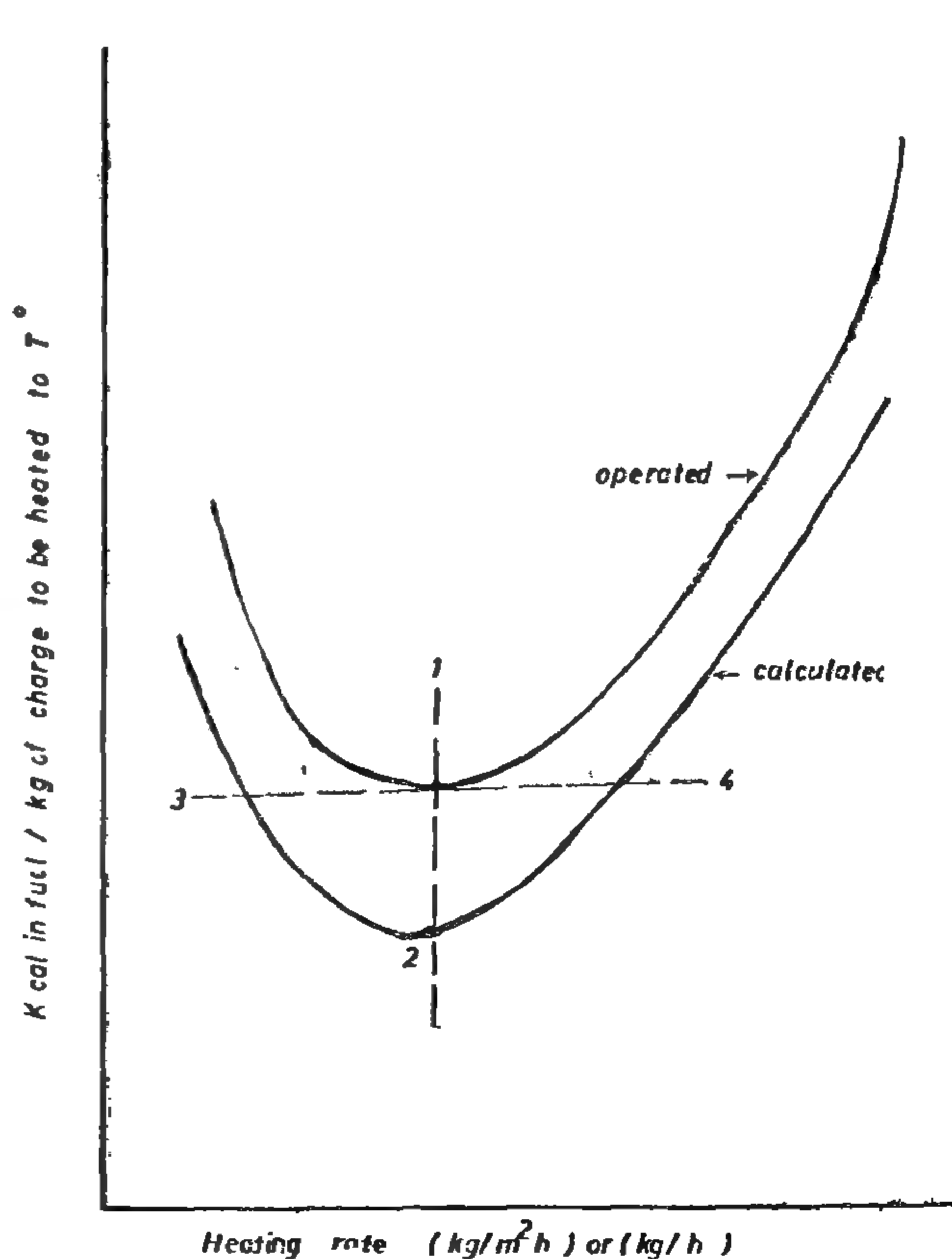


Fig. 9.

Table 7

1	2	3	4	5	6	7	8
section number	initial and final temperature of steel in section (tentative curve)	heat input per kg of steel in section	average temp. of flame and of steel in section (tentative curve)	average wall temperature in section	wall losses in section per m ² of steel surface	quantity of heat put into steel in section	ratio of wall losses to heat put to steel
	°C	Kcal/kg	°C	°C	Kcal/m ² h	Kcal/m ² h	%
1	48 — 100	28.3	600 — 74	350	750	36,000	2.08
2	100 — 120	76.5	700 — 110	500	1400	95,700	1.45
3	120 — 120	76.5	800 — 120	700	2700	95,700	2.82
4	120 — 120	76.5	900 — 120	800	33 000	95,7000	3.44
5	120 — 700	98.0	1000 — 420	900	39 000	60,3000	6.64
6	700 — 850	192.2	1200 — 775	1050	52 500	118,000	4.10
7	850 — 1250	146.6	1400 — 1180	1300	85 00	74,200	11.50

- Column 6 : $Q = K (T_i - T_a)$
- Column 7 = column 3 x heating rate desired.
- Column 8 = column 6 / column 7.
- Column 9 : 100 % + ratio of column 8.
- Column 10 : column 9 / sp. ht. of gases.
- Column 13 : $Q = 4.92$

$$\xi_1 \left[\left(\frac{T_{f1} + 273}{100} \right)^4 - \left(\frac{T_{oh} + 273}{100} \right)^4 \right] + k (T_{f1} - T_{oh}) + 4.92 \xi_2 \left[\left(\frac{T_w + 273}{100} \right)^4 - \left(\frac{T_{ch} + 273}{100} \right)^4 \right]$$

- Column 14 : column 3 / column 13.
- Column 15 : column 14 / Sum of column 15.

Check of calculations by practical running

It is desirable to check up the results of theoretical calculations by tests and operating data. But opportunities for tests that extend over a sufficiently long

period of time to establish equilibrium conditions are very scarce, because the demand for heated material is, generally, not regular.

If the heating rate (kg/m²h) or (kg/h) is plotted against head given from fuel per kg of charge heated to a given temp. T, we get a curve which has a min. This min. is the best running of the furnace. (S. Fig. 9.)

Let point (1) represents the point as obtained from operating record, while point (2) indicates the fuel consumption that might be expected from theoretical calculations.

But it is quite possible that furnace is driven very lightly, say at point (3) have the time (on account of troubles in mill or shear, lack of steel or troubles in fuel supply and burning) and driven very hard, say at point (4) the rest of the time, so as to maintain the tonnage of the mill. Then the resultant average must lie at (1) instead of at (2).

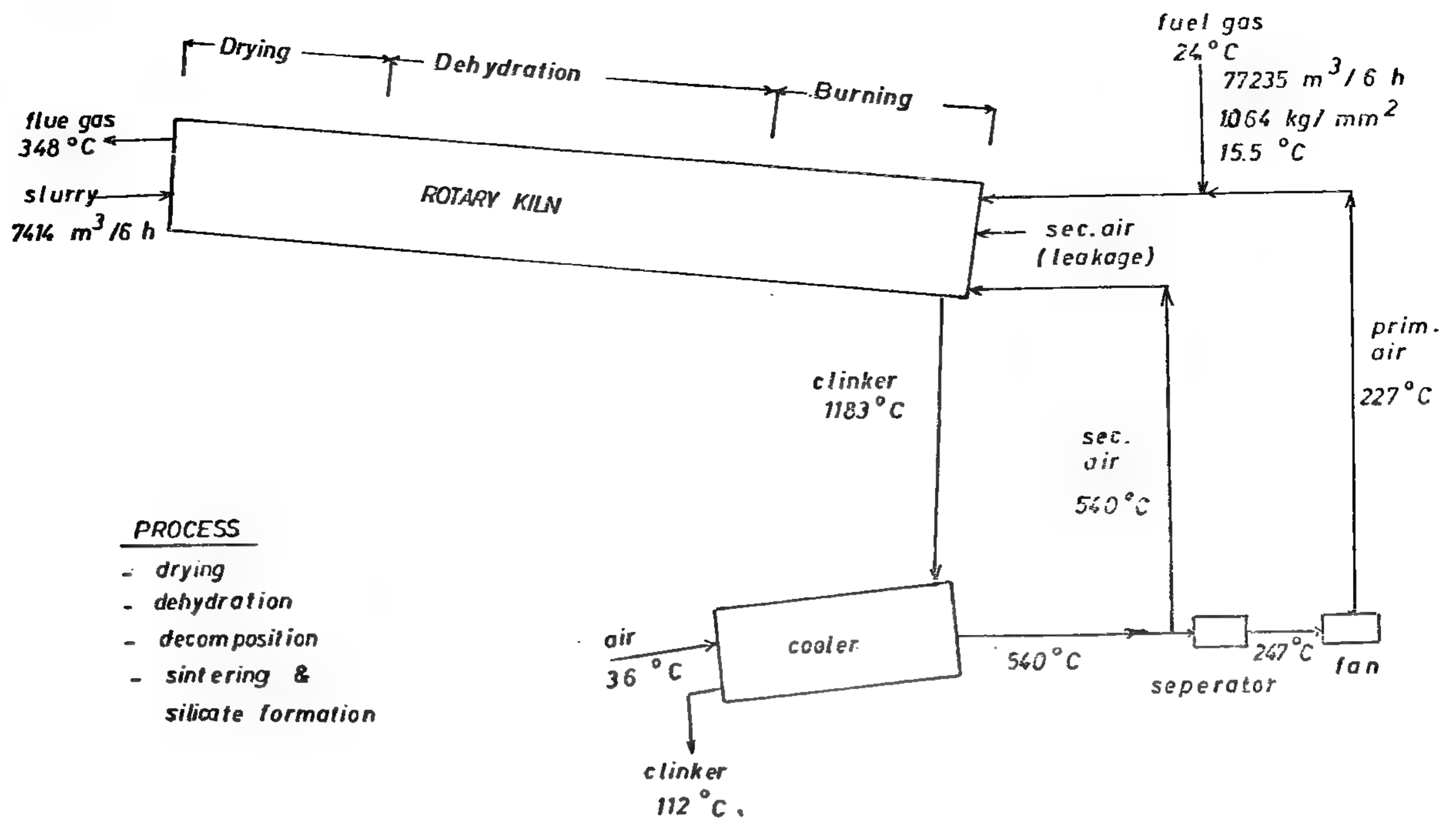


FIGURE : 5

Fig. 5. represents a sketch of the process of rotary kiln, with the data of mass and heat balance. Fig. 6. is the tentative curve, where the length is divided in seven sections. The dotted curve is the good coincidence of calculated in tentative curve.

Tables 7 and 8 shows the sequence of calculations.

N.B. The check of tentative curve is made by replotting the new calculated curve, where both are nearly coincident.

Moreover the check is made by calculating the rate of heating from the summation of values of column 14. The reciprocals of this summation is in fact the rate of heating.

— Column 2 of tables is deduced from tentative curve.

— Column 3 : $Q = W \times C \times \Delta T$

— Column 4 : from tentative curve

— Column 5 : $(T \text{ flame} + \text{stock}) / 2$.

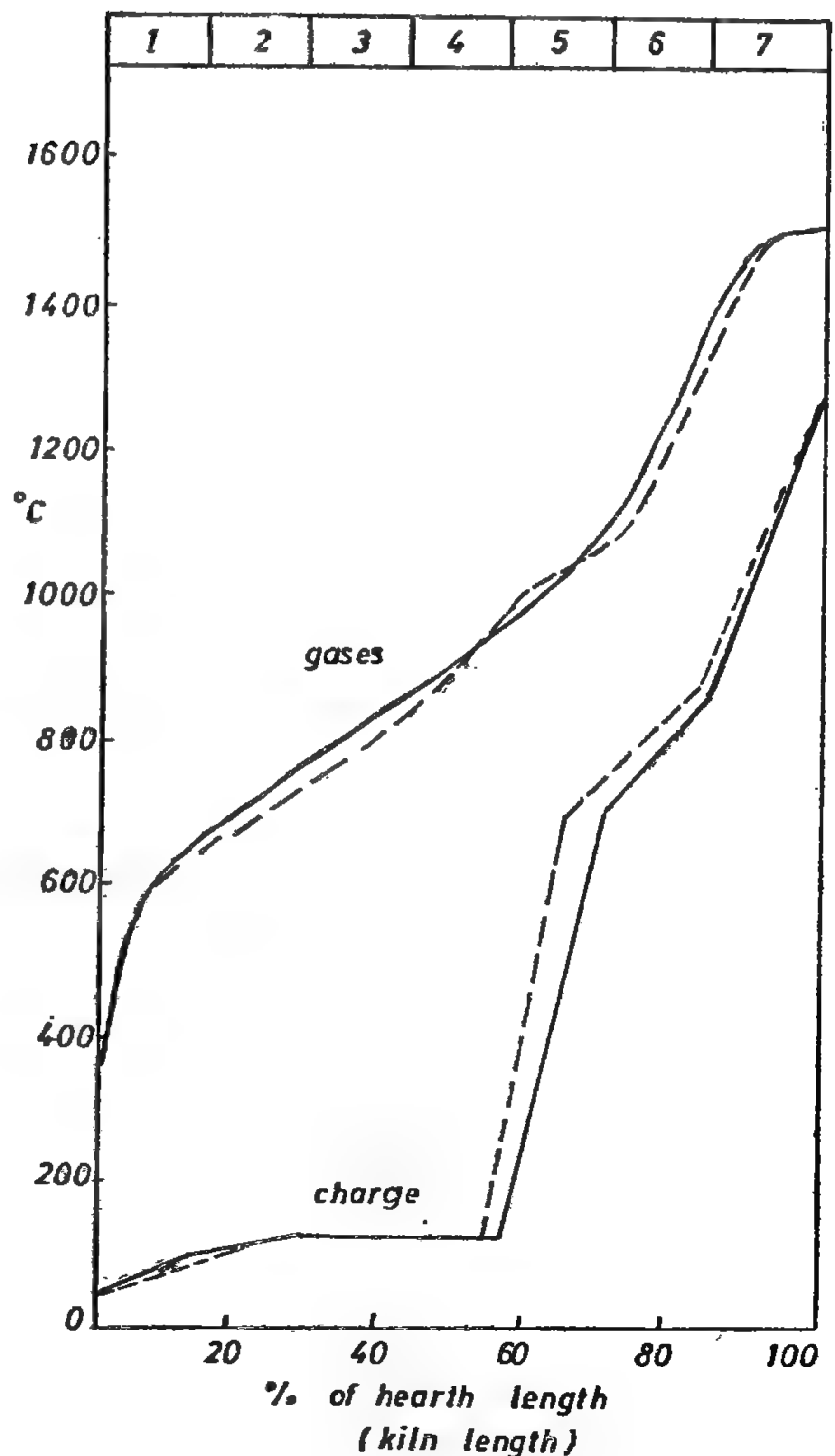


Fig. 6.

repeated. If the coincidence of assumed and calculated distribution is good, the rate of heating and the fuel consumption per kg of stock obtained from the first calculation were, of course, correct.

If the design of the furnace is similar to that of an existing or a previously calculated furnace, the shape of the gas-temperature versus gas-travel curve is known with sufficient accuracy. In any event, the exit temperature of the gases is known, because they give up as much heat as is required to heat the stock and to cover the losses.

* Let us see such calculation on two different furnaces :

i. Steel heating furnace (no chemical reaction).

Fig. 2. represents the problems and the tentative curve and the corrected curve (dotted lines). Tables 3 & 4 gives the sequence of calculations

ii. Rotary cement kiln (with chemical reaction) .

Table : 3

1	2	3	4	5	6	7	8
section number	initial and final temperature of steel in section (tentative curve)	heat input per kg of steel in section	average temp. of flame and of steel in section (tentative curve)	average wall temperature in section	wall losses in section per m ² of steel surface	quantity of heat put into steel in section	ratio of wall losses to heat input to steel
	°C	Kcal/kg	°C	°C	Kcal/m ² h	Kcal/m ² h	%
1	15 — 195	176	1010 — 105	555	251	780	32.3
2	195 — 365	230	1070 — 285	705	359	1020	35.1
3	365 — 555	285	1150 — 460	865	500	1265	39.5
4	555 — 715	352	1250 — 640	1020	655	1560	42.0
5	715 — 955	505	1350 — 830	1115	918	2240	41.1
6	955 — 1200	445	1370 — 1075	1300	1116	1970	58.8

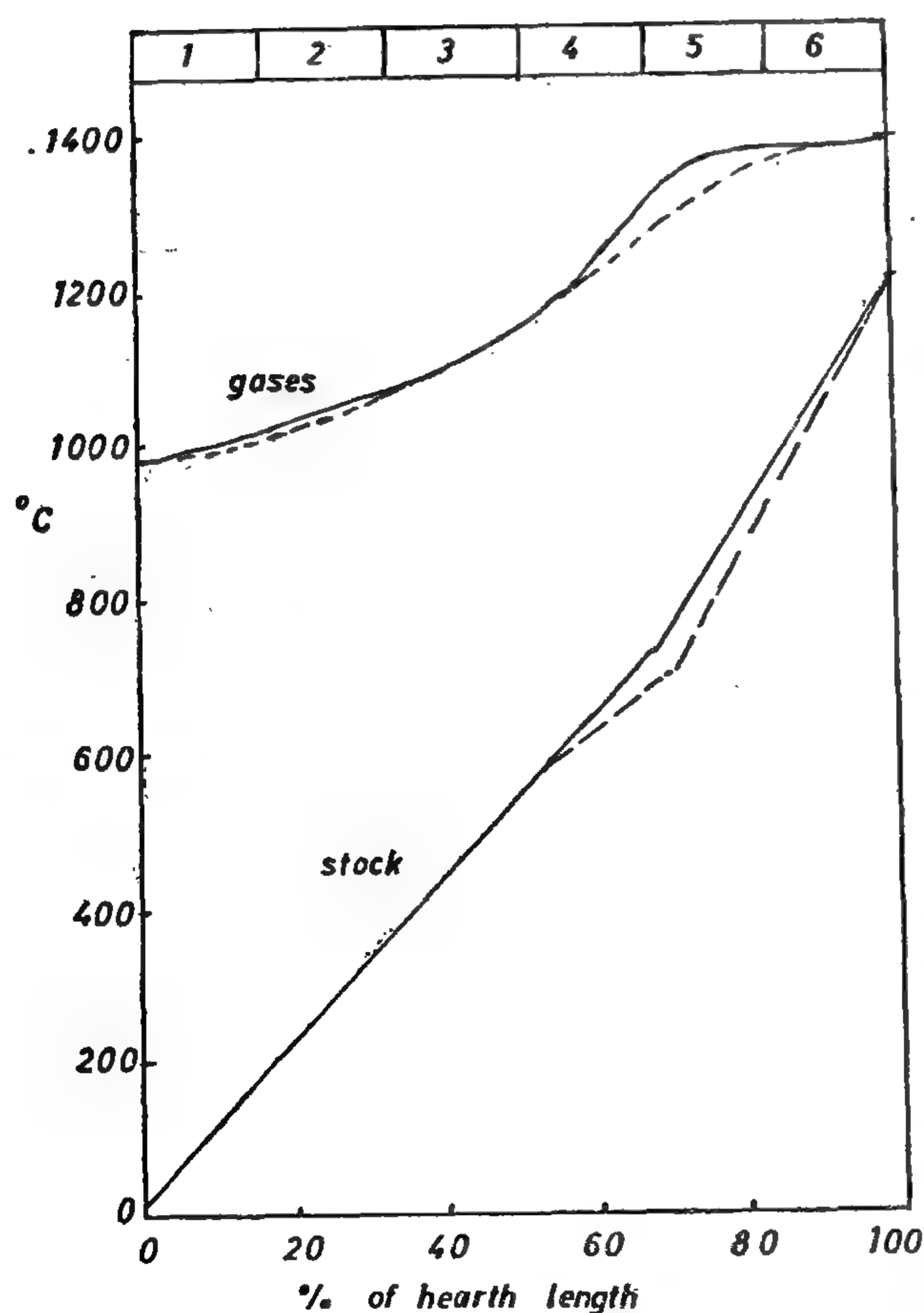
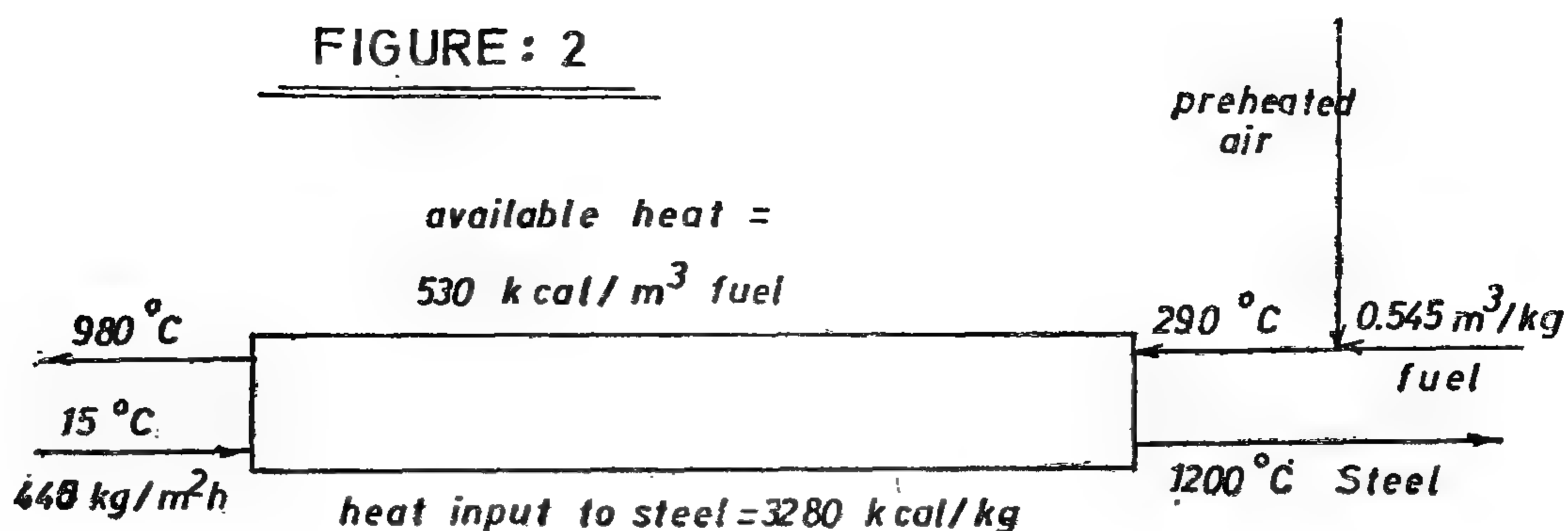
Table : 4

1	9	10	11	12	13	14	15	16
section number	heat to steel wall losses in section	temp. drop of gases in	initial temp. of gases in section	average flame temp. and average charge temp. in section	rate of heat transfer to charge	time required in section	length of section % of kiln length	distance from cold end % of kiln length
	Kcal/kg	°C	°C	°C	Kcal/h	h/kg	%	%
1	234	33	1026	1010 105	48,300	0.000364	16.2	16.2
2	312	51	1095	1070 285	59,900	0.000383	17.1	33.2
3	398	75	1188	1150 460	78,100	0.000365	16.0	49.3
4	500	92	1291	1250 640	106,000	0.000333	14.8	64.1
5	710	138	1360	1350 830	130,000	0.000388	17.3	81.4
6	707	138	1370	1370 1075	106,500	0.000417	18.6	100.0

0.002250

Heating rate = $1/0.00225 = 440$ kg/m²h

FIGURE : 2



this case represents no problem to calculate.

It has been already mentioned that in furnaces heating steel, copper, combustion is usually accompanied by luminous flame, extends through a considerable distance in the furnace. Since combustion requires time, the temperature of furnace gases at first remain constant, then drops

rapidly. The coefficient of heat transfer varies from place to place to such an extent that any calculation based on an overall heat-transf coefficient of experience would be correct only for exactly identical furnace conditions.

For a reasonably close approximation which is to be applicable to any continuous furnace, the furnace length must be divided into a number of sections, in each of which the heat transfer coefficient can be considered to be constant. The method of calculation is as follows :

A practical furnace length is called unity, and a number of temperatures of the products of combustion, at the points of leaving the furnace (or the stock), are sketched. For each of these "leaving" temperatures, a temperature distribution throughout the length of the furnace is tentatively sketched for the stock, on the bases of experience gained from previous calculations.

The necessity for assuming "tentative" temperature distribution is due to the fact that the ratio of wall losses to useful heat varies with temperature distribution and with the design of the wall.

With these temperature distributions, the transfer of heat is calculated by using the laws of heat transmission, and a new temperature distribution of stock and products of combustion is determined. If that distribution deviated much from the original assumption, the calculation is

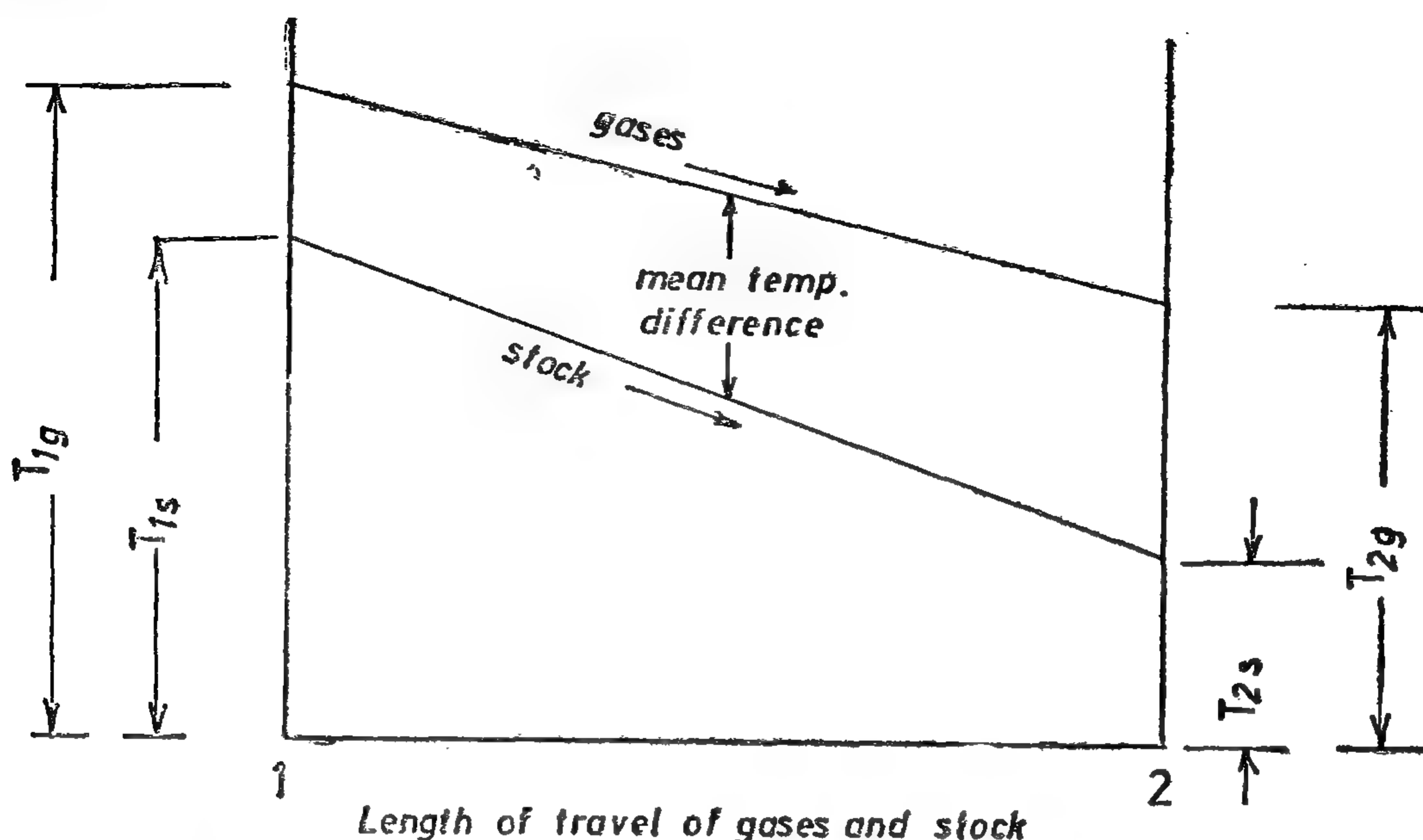


Fig. 1.

area is equal to the area of steel + $\frac{1}{2}$ the uncovered area of hearth at the sides + $\frac{1}{4}$ the height of the hearth).

In spite of that most of practical furnace engineer can base their heating-capacity figures on the actual area covered by the stock, rather than on the equivalent hearth area. This base will give rise to higher heating-capacity figures, but absolutely acceptable, particularly when the stock has no regular geometric shape.

With this brief introduction, it is possible now to understand the methods of calculating the relation between the rate of heating and fuel economy to put the results of calculation under consideration.

In continuous furnaces which heat light metals like Al 1 Mg and their alloys, the furnace temperature is low, and furnace gases are recirculated. Combustion is complete, when the furnace gases touch the stock, whereas combustion extends over a considerable portion of the length of the hearth in furnaces that heat steel or copper. In heating aluminium the sensible heat of the gases is the source of the major portion of the heat. The speci-

$$\begin{array}{c}
 \text{mean temp. difference} \quad \text{heat transfer coeff.} \\
 \downarrow \quad \downarrow \\
 \frac{1}{2} (T_{1g} - T_{1s} + T_{2g} - T_{2s}) \quad K A_{\text{exposed area}} = \\
 \text{specific heat} \\
 \downarrow \\
 (T_{1s} - T_{2s}) \quad W C = \\
 \text{temp. rise of stock} \quad \downarrow \quad \text{hourly wt. of stock} \\
 \text{efficiency factor} \quad \uparrow \quad \text{hourly wt. of furnace gases} \quad \uparrow \quad \text{sp. heat} \\
 f (T_{1g} - T_{2g}) W_g C_p
 \end{array}$$

fic heat of Al varies but little with temperature, on account of recirculation, furnace gases undergo but little change in temperature, while passing over the stock.

In view of the none too certain coefficients and constants of heat transfer, sufficiently close results are obtained if straight lines are substituted for the slightly curved lines of temperature distribution. If this be done, the following relations are derived from the figure (1) "which holds for heating of light metals".

This double equation gives perunits solving for two unknown quantities and

HEAT TRANSFER CALCULATIONS IN CONTINUOUS FIRED FURNACES

By

Dr. MAHMOUD EL-ZAHER MOHAMED

The growing importance of continuous furnaces makes it necessary to check the fuel economy, either in designing the furnace or after repair or maintenance and re-running.

Any attempt at a calculation of fuel consumption, per unit of material heated in a continuous furnace must reckon with the usual difficulties, such as non-uniform demand and improper regulation of combustion, as well as draft.

Since the fact has been established that fuel economy of combustion-type furnaces depend on the rate of heating, it is necessary to establish a unit for that rate. In the heating of steel the number of kgs. per unit area of hearth and hour commonly serve as such a measure, but for general purposes, the heat transferred to the stock per m^2 of hearth and hour is more usual unit. For a given final temperature of the stock, and for a given material, these units are convertible, and use is made of both of them in such calculations. In speaking of "rate of heating" input per m^2 and hour"; it should be clearly understood that in front-fired continuous furnaces, this rate is an average value only. At the cold end the rate is lower and at the hot end it is higher than the average rate.

For the sake of calculation the terms "hearth area" and "rate of heating per m^2 and hour" must be cleared because they can lead to greater rate of heat transfer if not properly considered.

In heating furnaces with long billets or smelting furnaces with low roofs, the

vacant spaces on the sides, between charge and sidewalls, are, in such a case, quite negligible. Practically all the heat that is transmitted to any part of the roof by the hot products of combustion is radiated back to the charge underneath. Compared to the heat-absorbing surfaces of the charge and of the roof, the surfaces of vacant spaces on the sides and the sidewalls are quite insignificant.

The situation is quite different, however, with short billets or slabs in heating furnace or with a high roofed furnace, or with special types like cement rotary kiln, (where it is quite improper to speak of side walls). In such cases, the rate of heating is increased by radiation of heat from the flame to the high side-walls and to the parts of the hearth not covered by the stock or charge and by radiation from those surface to the stock.

For more accurate calculation the "equivalent hearth area" must be deduced, which is different from case to case. It means that area that would be needed in a furnace with neglected sidewalls in order to absorb as much heat as is absorbed by the stock in a high furnace or a furnace with considerable side-walls radiation. It is certainly greater than the area of the exposed surface of the stock. How much it exceeds the latter area depends on the nature of the flame and on the relative amount of heat loss through the walls. (For steel heating furnace, one rule states that the equivalent hearth

INDUSTRY & PRODUCTION

**INST. OF MECHANICAL ENGINEERS
INST. OF ELECTRICAL ENGINEERS**

الخامات الأولية والصناعات الكيائية

جمعية مهندسى المناجم والبترول
والفلزات
جمعية المهندسين الكيمياءيين

4.4. SINTERABILITY OF BaTiO_3 PREPARED AT VARIOUS TEMPERATURES:

To determine the optimum conditions for preparing active BaTiO_3 , pellets were prepared by pressing at 3700 Kg/cm^2 before sintering at 1300°C for various soaking periods.

The results are shown in Figure 7.

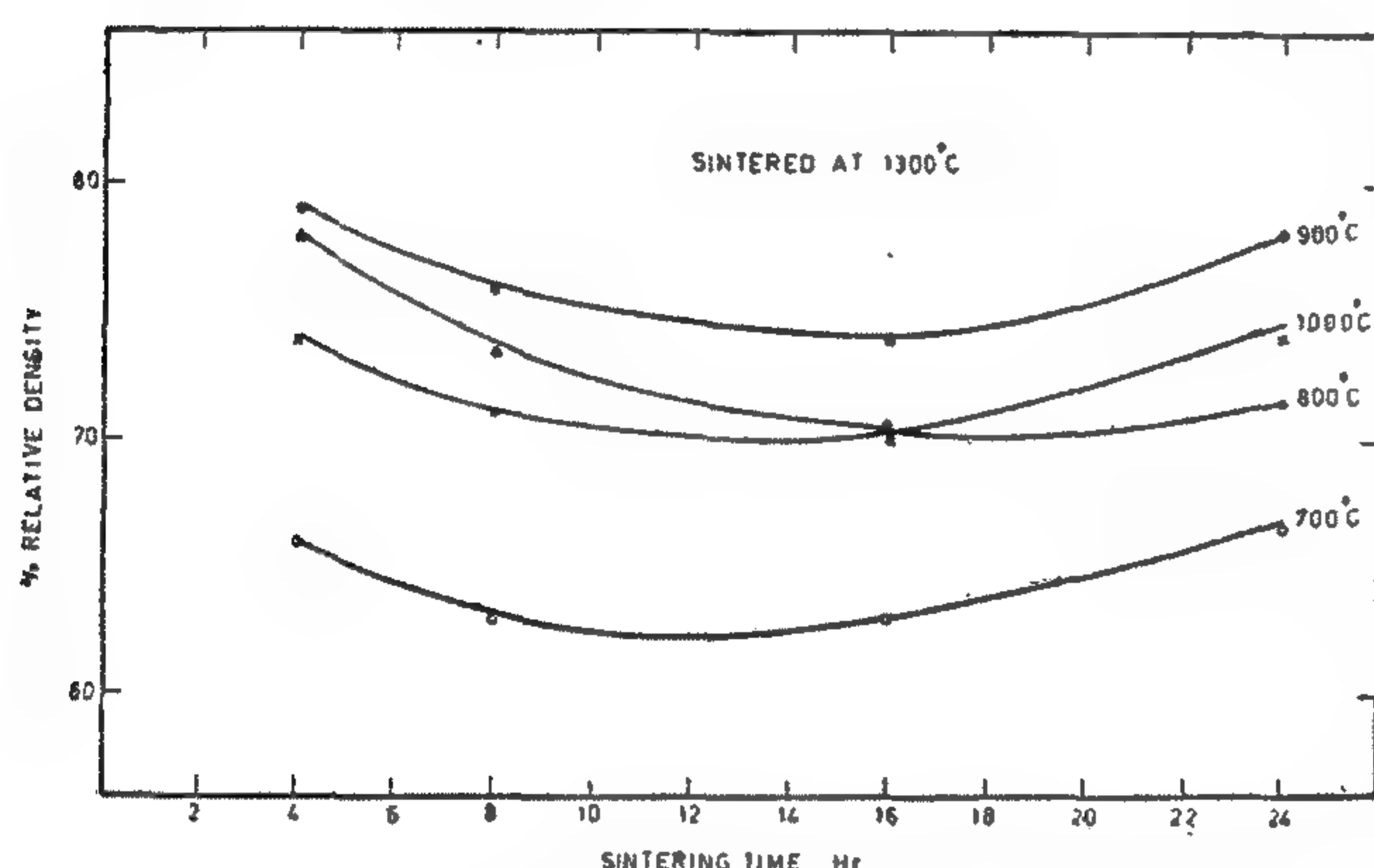


Figure 7: Sinterability of BaTiO_3 produced at various temperatures

As shown earlier, low temperature product will be of uniform low density particles with very high surface energy and higher tendency for agglomeration thus causing fissuring on sintering and low-

ering the density. Higher temperatures produce less active dense particles with various particle sizes encouraging exaggerated grain growth (with lower density) as shown by the curve obtained at 1000°C . The optimum temperature for preparation is 900°C .

The decrease in density at each temperature may be due to bloating effect in which gases diffuse from small pores with high pressure to large pores with low pressure.

REFERENCES

- 1) K. Kiss, J. Magder, M.S. Vukasovich, R.J. Lockhart, J. Amer. Ceram. Soc., **49**, 291, 1966.
- 2) B.V. Strizhkov, Zhur. Priklad Khim., **33**, 2009, 1960.
- 3) M. Yanase & K. Ono, Chem. Abst., **46**, 8973 f, 1966.
- 4) P.K. Gallagher, F. Schrey & F.V. Di Marcello, J. Amer. Ceram. Soc., **46**, 197 & 359, 1963.
- 5) P.K. Gallagher & J. Thomson, J. Amer. Ceram. Soc., **48**, 644, 1965.
- 6) H.P. Klug & L.E. Alexander, "X-ray Diffraction Procedures" J. Wiley & sons Ltd., New York, 1959.

red temperature was controlled before hanging the crucible. The results are shown in Fig. 4 indicating that at 600°C, 6 hours are needed, at 700°C an hour is enough and at 800 & 900°C less than 1/2 hr is required. These conditions are of extreme importance in preparing active material.

The mean crystal size "D" was determined from X-ray diffraction broadening using Scherrer's equation⁶). Since the crystal growth is inversely proportional to crystal size; $dD/dt = K/D$, by integrating, $D^2 = 2Kt$.

Since the rate constant K

$$= K_0 e^{-Q/RT}$$

it could be seen that,

$$\log (D^2/t) = \log 2K_0 - Q/2.303 RT.$$

Accordingly, on plotting $\log (D^2/t)$ against $1/T$, a straight line of slope $-Q/2.303 R$ was produced (Figure 5) giving activation energy for crystal growth of 21 K. cal.

4.3. EFFECT OF CALCINATION TEMPERATURE ON GREEN DENSITY OF BaTiO₃ COMPACTS :

The powder obtained by heating at various temperatures for the minimum time was compacted using a pressure of 4300 Kg/cm² and the green densities were measured using the mercury balance. The results are shown in Figure 6 relative to the true density (6.02 gm/cm³).

The higher the calcination temperature, the higher is the density. This effect can be attributed to the following reasons:

- a) At low temperature, the titanate formed agglomerates within the framework of the original crystal, with extremely fine pores between the crystallites and which may not be detected by surface area measurements (See Fig. 1). Higher temperatures cause the agglomerates to shrink to

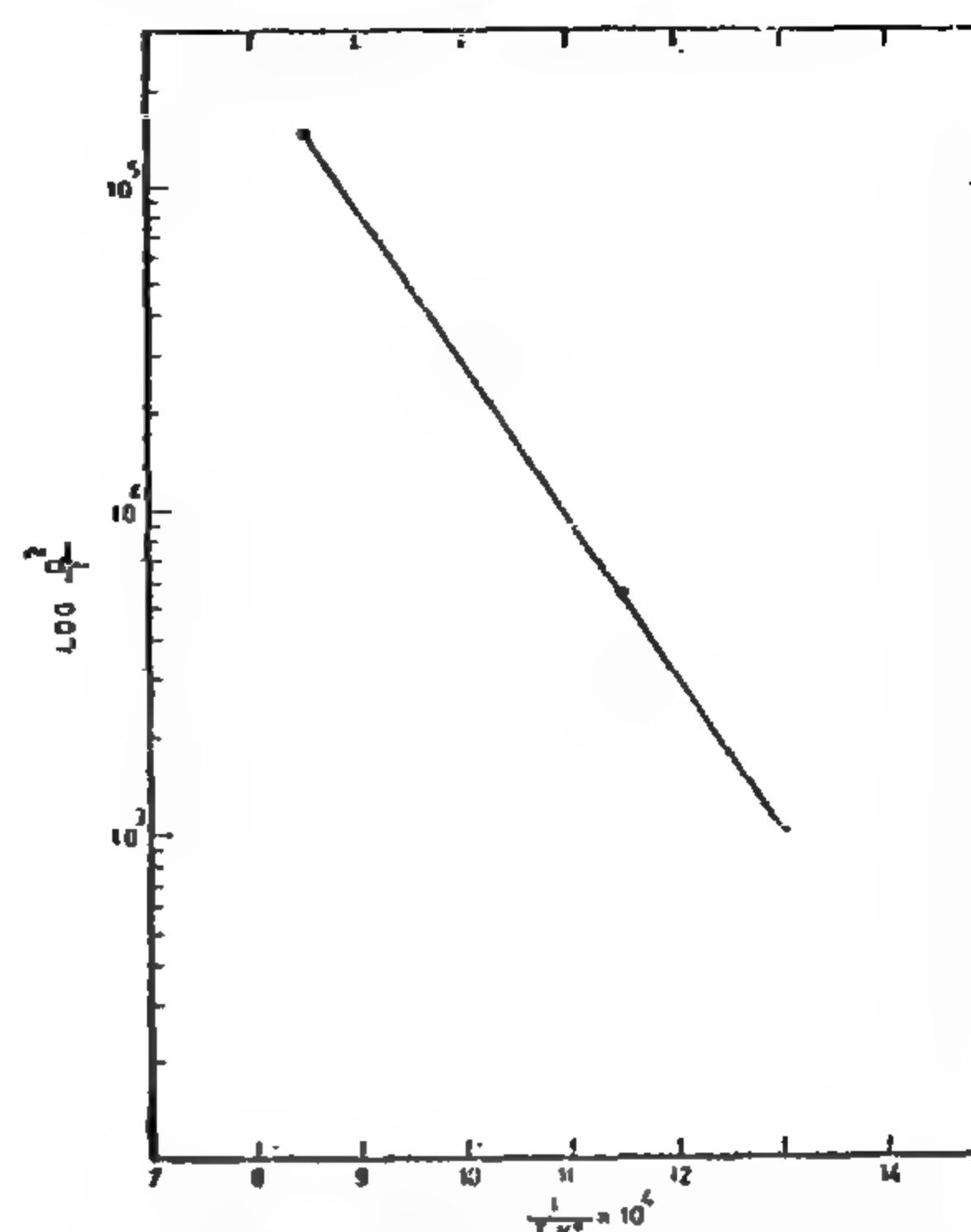


Figure 5 : Calculation of activation energy for crystal growth

much smaller particles eliminating these pores. This explains producing light material at low temperature and heavy material at high temperature.

- b) Calcination at low temperatures produce particles with narrow particle size distribution, while high temperatures caused sintering and production of wide ranges of particle sizes with lower surface energy. In the latter case, fine particles fit into interstices of coarse particles thus minimizing the porosity and increasing the density.

The curve shown in Fig. 6 can be used as a rough measure for the average particle size produced at various temperatures.

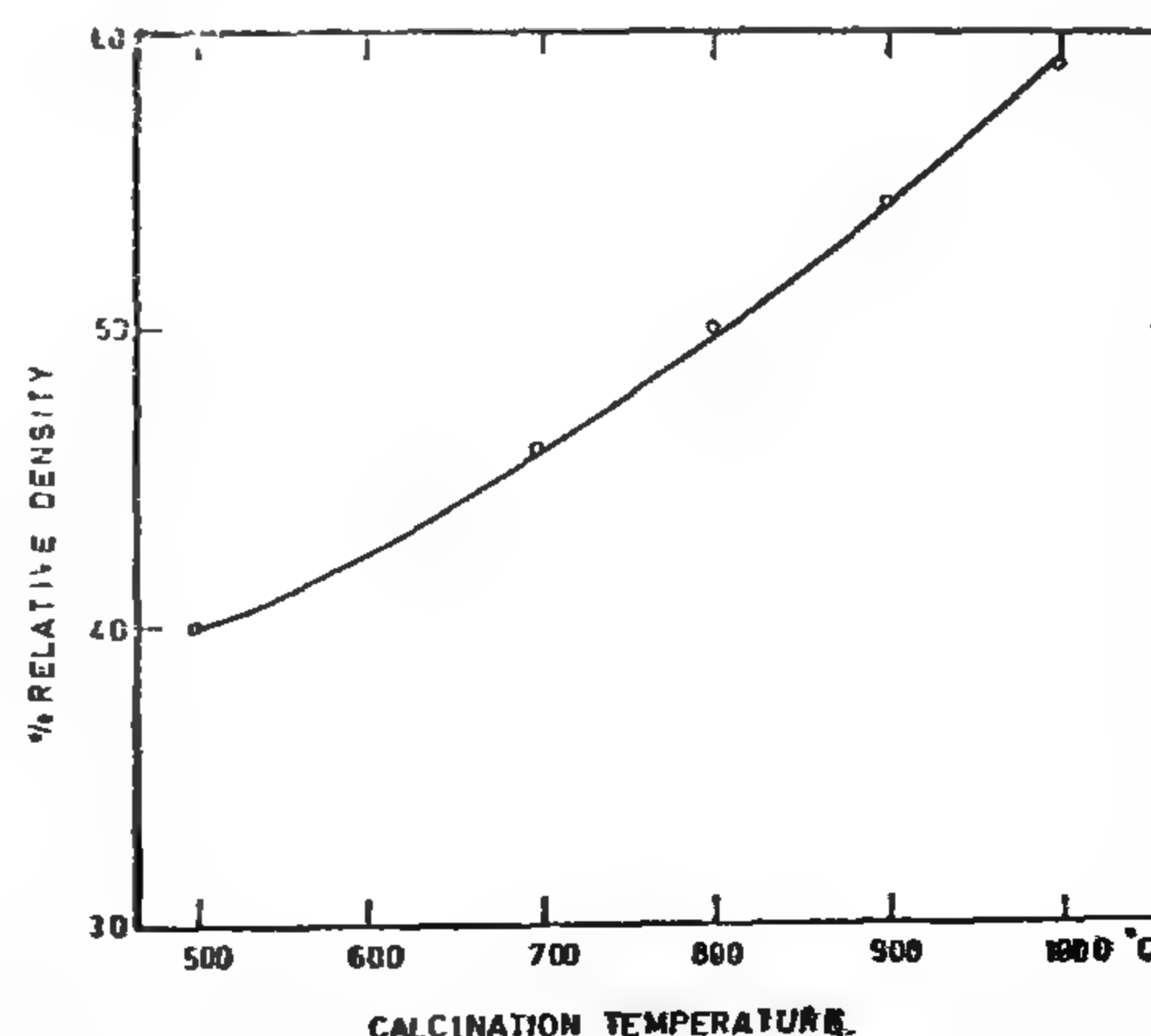


Figure 6: Variation of green density with calcination temperature

due to the dehydration which could be seen easily at higher magnifications (See Figure 2).

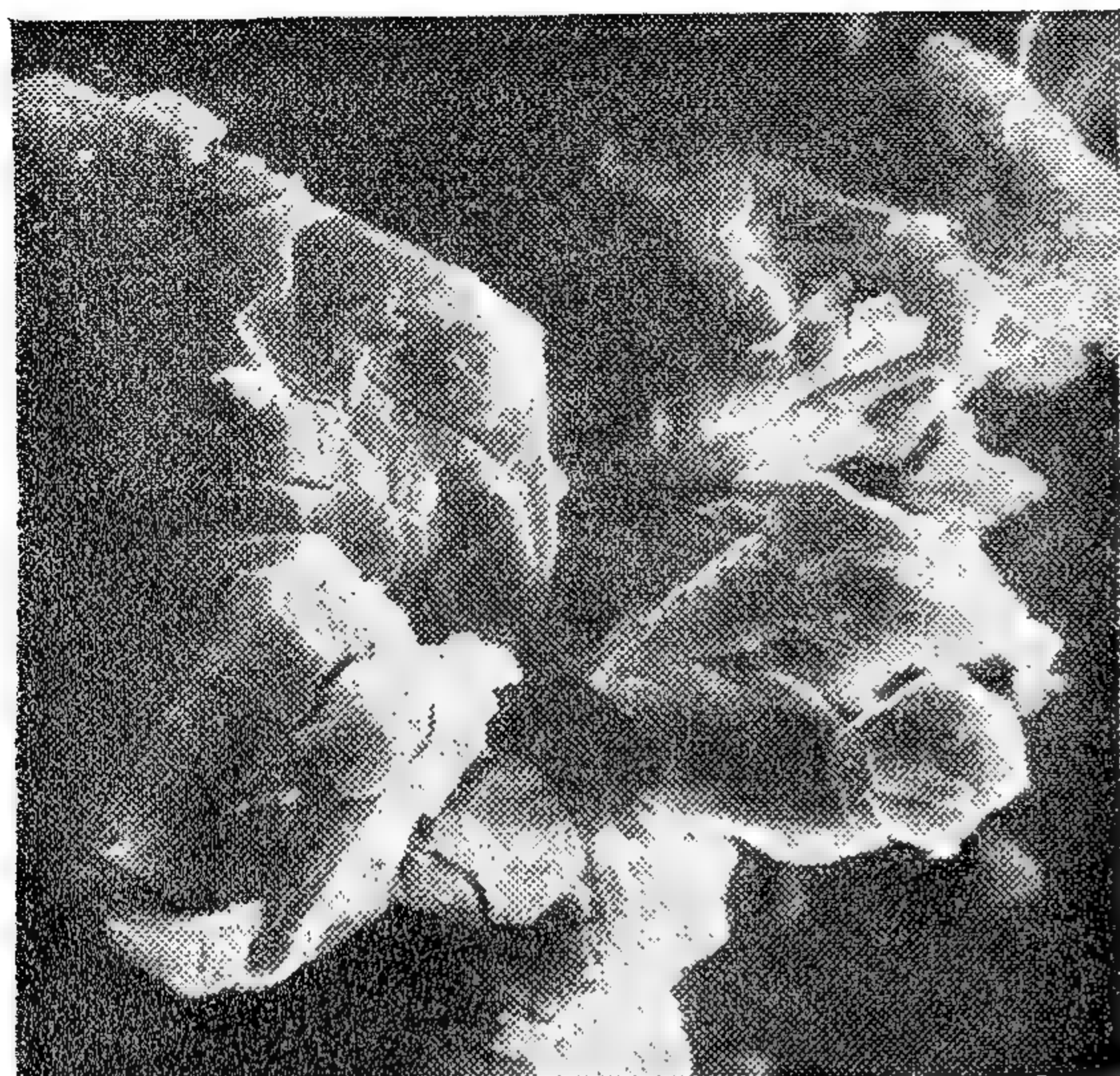


Figure 2 : Cracks developed due to dehydration of barium titanyl oxalate (at 170°C).

Just after the isothermal CO_2 loss at 300°C, the crystal structure was preserved with excessive cracks due to sudden evolution of gas, but larger magnification shows the formation of fine crystals inside the mother crystal. As the temperature increases, CO evolves and the crystals grow as indicated in Figure 1. Also X-rays proved that while at 300°C the material appeared amorphous, at 500°C starting of crystallization appeared giving the same pattern of BaTiO_3 with a regular shift towards lower values of θ and excessive broadening due to the ultrafine crystals formed. This supports the conclusion of the existence of the series of solid solutions.

To study the first part representing the sluggish dehydration process, thermal analysis was carried out and curves of DTG & TG are shown in Figure 3. Up to 185°C, water of crystallization evolved giving a break at 105°C on the DTA curve, on the DTG curve a small peak is followed by a large one implying that the water of crystallization is driven

off on two stages, one mole up to about 100°C and the other remaining there below 185°C. DTA curve showed also that with a rate of 10°/min. CO_2 was lost exothermally with a maximum rate at 350°C, and CO was lost endothermally over a range of temperatures.

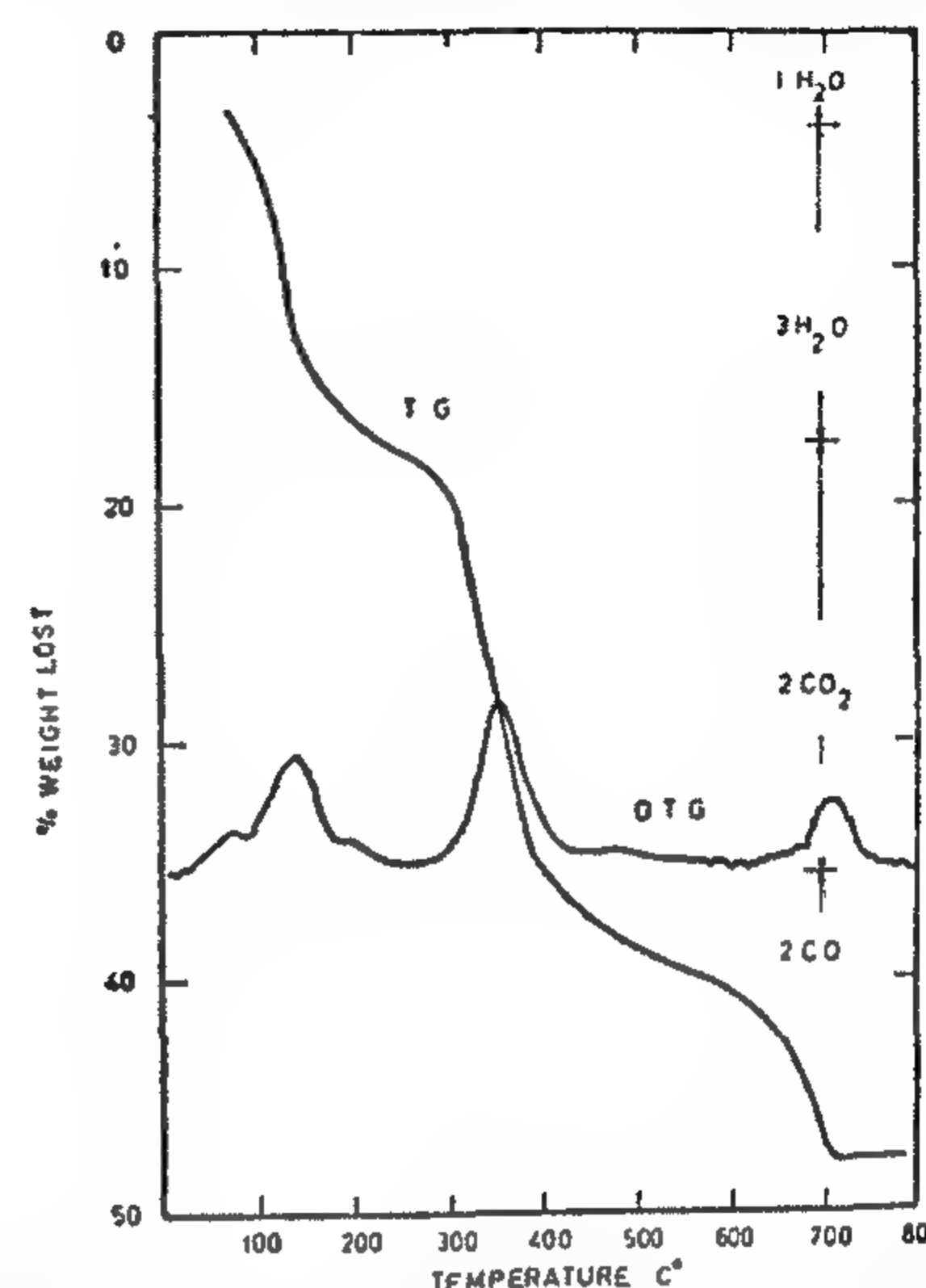


Figure 3 : Thermogravimetric analysis for barium titanyl oxalate. (10 / min.)

4.2. RATE OF FORMATION OF BaTiO_3 :

From the above results, it is evident that BaTiO_3 can be formed at temperatures above 600°C. To determine the minimum time required for each temperature, a thermobalance was used and the requi-

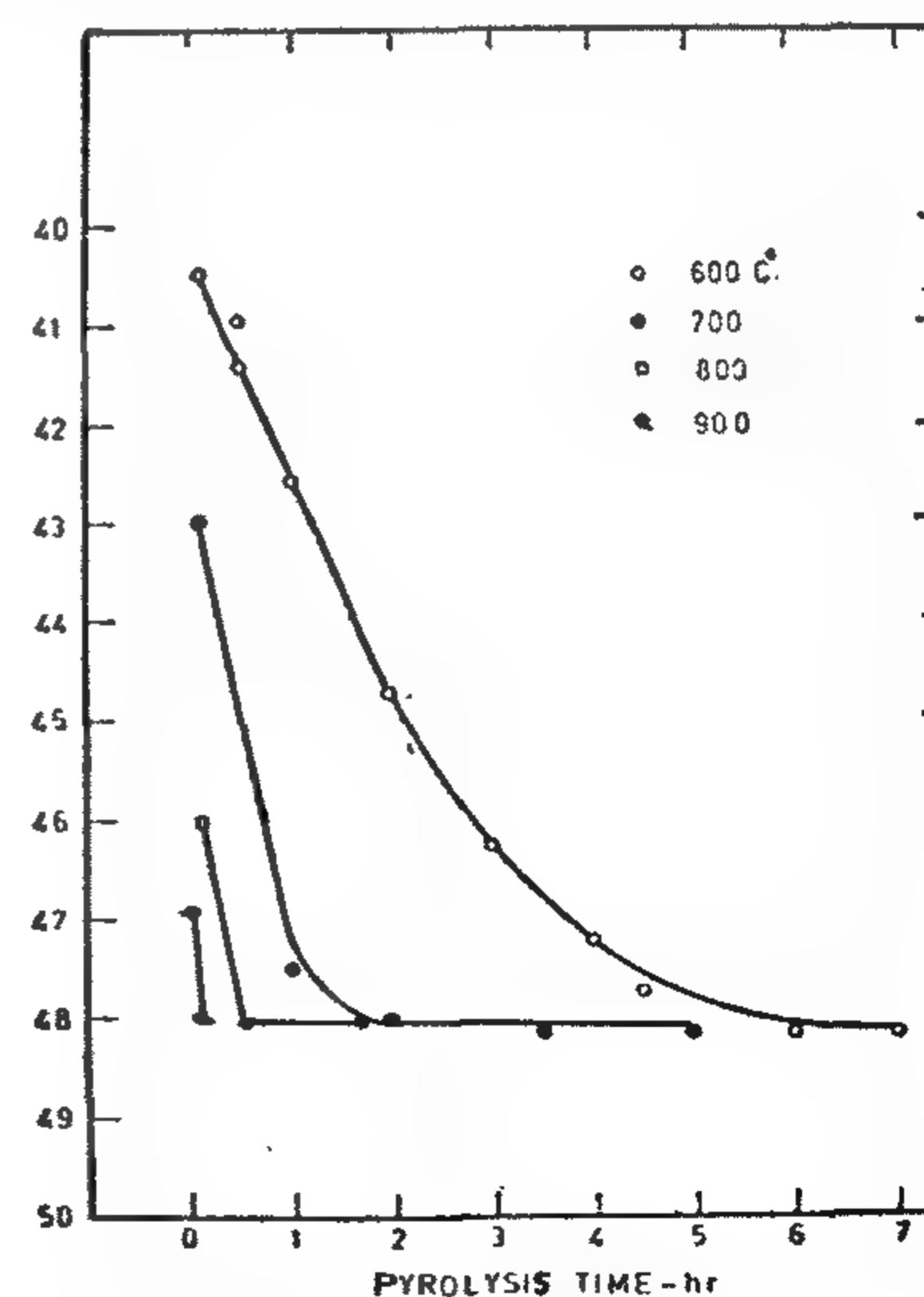
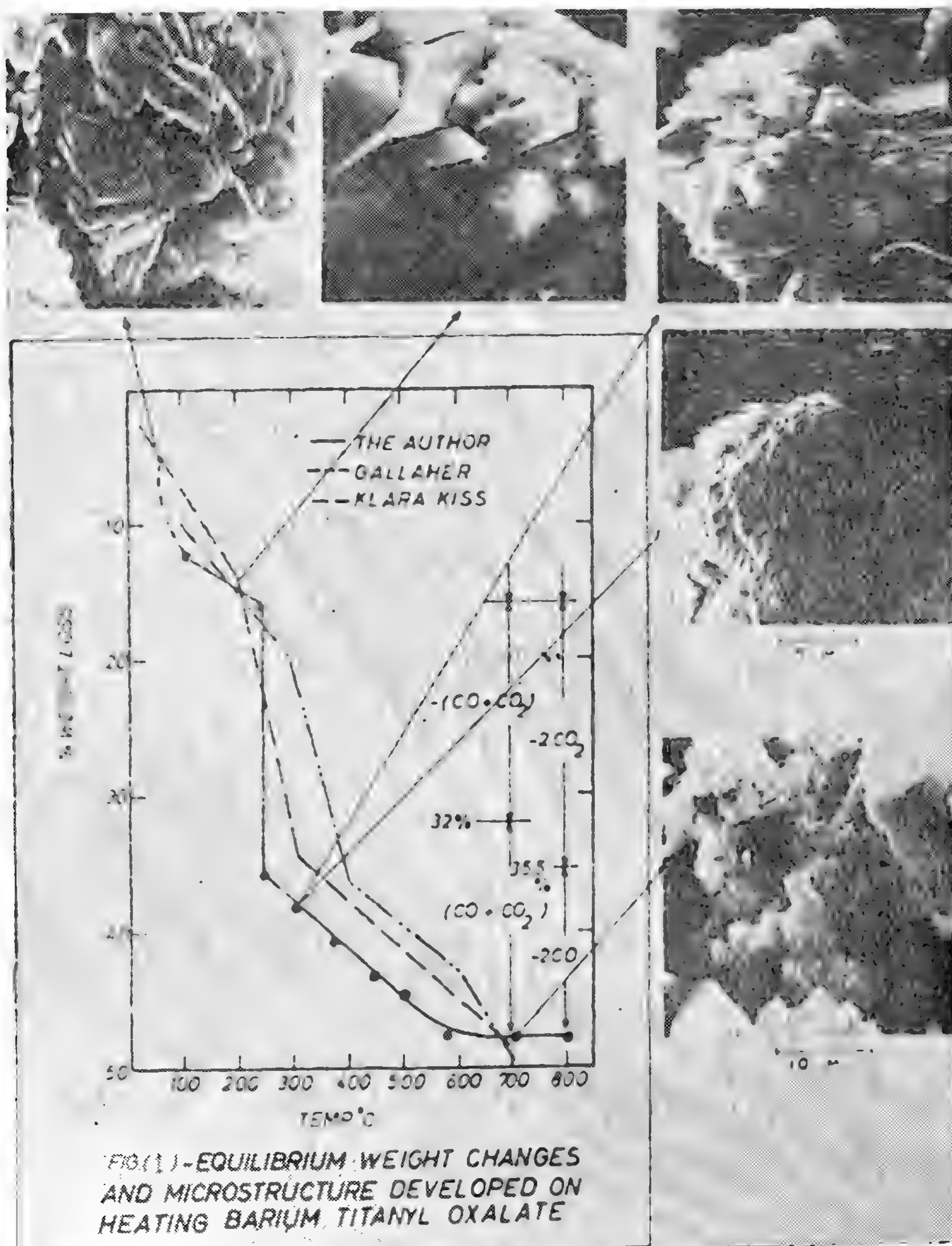


Figure 4: Kinetics of formation of barium titanate

To prove the above conclusion, barium titanyl oxalate was heated at selected temperatures of equilibrium and quenched then examined by ordinary and electron microscopes as well as by X-rays. The photomicrographs are shown in Figure 1. Barium titanyl oxalate consists

of fine crystals with high agglomeration tendency. Increasing the temperature in the first solid solution range caused the crystals to grow rapidly to well defined shapes (See the micrograph at 170°C) in spite of the cracks developed



Gallagher & Thomson⁵⁾ suggested that, after losing water of crystallization, oxygen is absorbed to form active BaCO_3 and TiO_2 which react to form BaTiO_3 .

3. PREPARATION OF BARIUM TITANYL OXALATE

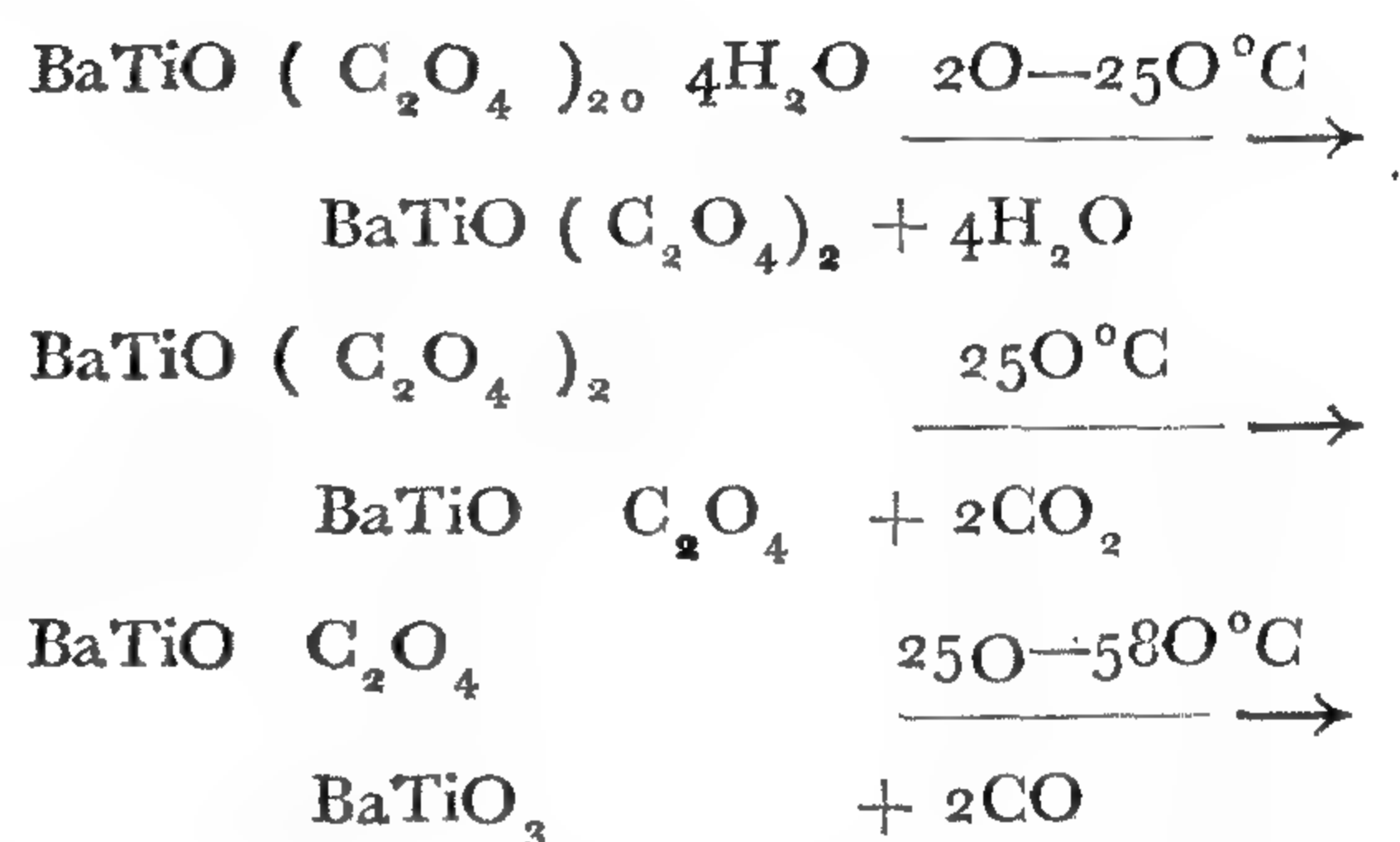
The technique used by Kiss et. al.¹⁾ and Gallagher⁴⁾ was adopted in preparing barium titanyl oxalate from TiCl_3 , BaCl_2 & oxalic acid. The stoichiometric ratio was checked by chemical analysis and batches which gave BaO/TiO_2 deviating from unity were not used²⁾ in this study.

4. RESULTS AND DISCUSSIONS

4.1. DECOMPOSITION OF BARIUM TITANYL OXALATE :

The results obtained from the weight loss reached at equilibrium at relative humidity of 54% in air are shown in Figure 1. To attain equilibrium at lower temperatures, long periods were required and the moisture content could not be fixed. Accordingly the fixed weight reached at 700° was considered to be 100% pure BaTiO_3 and the excess loss in weight than the calculated was considered the moisture content. To compare the present and the previous results, both were plotted on the same figure as well as the suggested mechanisms, which are shown to the right of the diagram. Since there is no doubt that 4 moles of water were lost first and since it was difficult to fix the corresponding weight changes at low temperatures, this portion was shown dashed. It is clear that the present curve lies below and to the left of the previous results implying that even soaking for 3 hours was not enough to reach equilibrium which needs days at low temperatures. A distinct three regions can be observed on the curve; a continuous cur-

change) then we followed by a vertical step (isothermal change) then gradual loss in weight till 580°C, at which a constant weight of BaTiO_3 was reached. These are corresponding to loss of 4 moles of water, 2 moles of CO_2 & 2 moles of CO respectively. The following reactions could be thus written :



Such mechanism is in agreement with the main steps suggested by Kiss et. al.¹⁾

Since this curve was obtained in air at fixed partial pressures of H_2O , CO_2 & CO, the condensed phase rule; $F=3-P$ could be applied to each reaction. An isothermal loss in Figure 1 (at 250°C) implies that the system is invariant and $P=3$ which are $\text{BaTiO} (\text{C}_2\text{O}_4)_2$, $\text{BaTiO} \cdot \text{C}_2\text{O}_4$ & the gas phase. Higher CO_2 partial pressures will increase the dissociation temperature. On the other hand, curves in Figure 1 implies the variation of composition over a range of temperatures and the system is monovariant, i.e. maximum number of phases in equilibrium is 2. Accordingly the compounds $\text{BaTiO} (\text{C}_2\text{O}_4)_2 \cdot 4\text{H}_2\text{O}$ & $\text{BaTiO} (\text{C}_2\text{O}_4)_2$ are one phase, i.e. they are isomorphous and form complete series of solid solutions. Similarly, $\text{BaTiO} \cdot \text{C}_2\text{O}_4$ & BaTiO_3 form another series of solid solutions.

DECOMPOSITION OF BARIUM TITANYL OXALATE

ASSESSMENT OF BARIUM TITANATE PRODUCED AT VARIOUS TEMPERATURES

M.N. SWILAM AND A.M. GADALLA

ABSTRACT :

The mechanism of decomposition of barium titanyl oxalate was studied using thermogravimetric analysis, D.T.A, X-rays and optical and electron microscopes. In air, water of crystallization was lost over a range of temperatures up to 250°C giving a series of solid solutions and at 250°C isothermal loss of 2 moles of CO₂ occurred. From 250 to 580°C the remaining 2 moles of CO were lost giving a second series of solid solutions. Rate of decomposition to form pure BaTiO₃ was determined at various temperatures and X-rays were used to determine the crystal size obtained at each temperature. The activation energy for crystal growth was also calculated. Green densities obtained using fixed pressure could be used as a measure for the average grain size. Sintering was used to assess the BaTiO₃ produced. Low temperature product was of uniform low density particles with very high surface energy and high tendency for agglomeration causing fissuring and lowering the density. Relatively high temperature produced less active dense particles thus lowering the final density reached. It was found that thus lowering the final density reached. It was found that the optimum temperature for preparing BaTiO₃ from barium titanyl oxalate was 900°C.

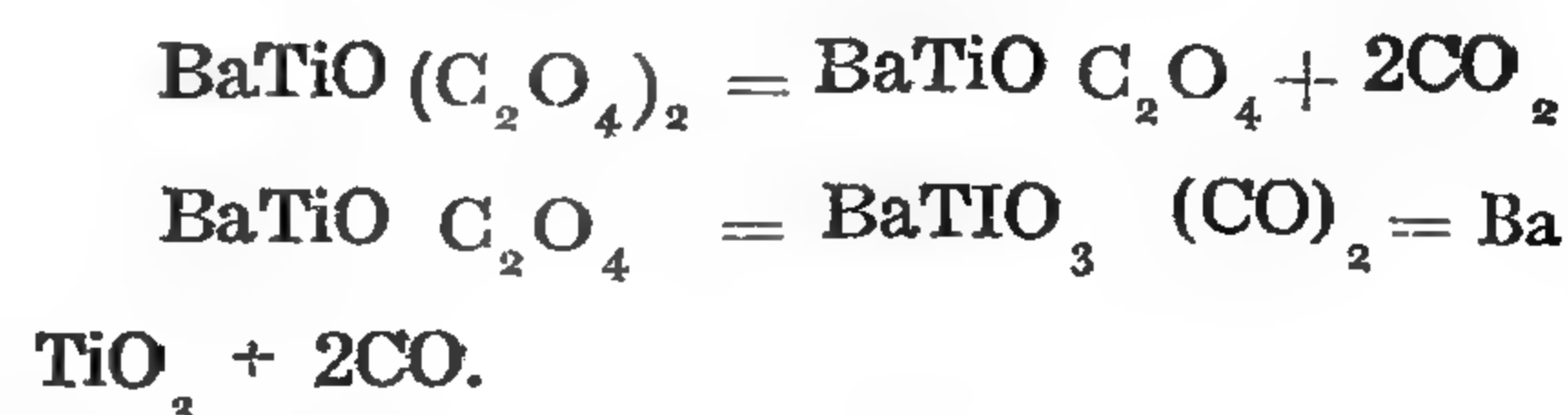
1. INTRODUCTION

The aim of this study is to prepare active BaTiO₃ suitable for electrical applications by controlling its rate of formation and growth using pure chemicals. Accordingly barium titanyl oxalate was prepared and its decomposition mechanism was studied to determine the minimum temperature for BaTiO₃ preparation. The product was assessed by measuring crystal size, green density and sinterability.

2. PREVIOUS WORK

Although several dissociation mechanisms, based on heating barium titanyl oxalate at a constant rate, were suggested, all results showed that BaTiO₃ was formed completely in the range of 600-800°C¹⁾²⁾³⁾.

There is a general agreement that the first step in dissociation is that 4 moles of water are lost at 20-300°C. While some authors¹⁾³⁾⁴⁾⁵⁾ suggested that at 250-360°C, 2 moles of CO₂ evolved and at 575-630°C, 2 moles of CO evolved;



others⁵⁾ believed that 300-360°C, 4 moles of CO evolved; $\text{BaTiO}(\text{C}_2\text{O}_4)_2 = \text{BaTiO}_5 + 4\text{CO}$.

The latter compound (with Titanium with a valence of 8) was considered to give BaTiO₃ and oxygen at 800-800°C.

RAWMATERIALS & CHEMICAL INDUSTRIES

**INST. OF MINING, PETROLEUM &
METALLURGICAL ENGINEERS
INST. OF CHEMICAL ENGINEERS**

CONTENIS

GENERAL SECTION :

BULDING & CONSTRUCTION	INDUSETY & PRODUCTION	RAW MATERIALS & CHEMICAL ENGINEERING
(ARABIC)	(ARABIC)	(ARABIC)
— Economics and the construction Project. Dr. G. NASSAR ... 9		
— The EGYPTIAN Ar- chitecture & the sky- line of civilisations Dr. S. KARIM ... 10		
— Eualuation of the Nile Dlta drainage praject Dr. M. ABU ZEID ... 15		
—	—	—
(ENGLISH)	(ENGLISH)	(ENGLISH)
— Best fitted duration curve for the river nile natural-flow Dr. M. EL-GIZAWI, Dr. M. ABU-ZEID 34	— The Cube concept approach to manage- ment information sys- tems. Dr. H.K. EL-DIN - 84	— Decomposition of bar- ium titanyl oxalate & assessment of Barium titanate produced at various temperatures Dr. M.N. SWELLAM & A.M. GADALLA 143
— Field & Laboratory studies on certain swelling clayey soils in EGYPT Dr. A.H. EL-RAMLI & M. EL-DEMERY 42	— Computer optimized design of solar cells Dr. M. ABDELGA- WAD & A.H.M. SHO- USHA ... 90	
— Nile gain from the ground water resevoir Dr. M.H. EL-KATEB & F. ABDEL-RAH- MAN ... 51	— Electrical energy ex- change between coo- perating systems Dr. F.S. THALOUTH 98	
— Economical study of suspension structures Dr. A. MOHARRAM, Dr. S.A. SAAFAN & H.I. HECAS ... 59	— Heat transfer calcu- lations in continuous fired furnaces Dr. M. EL-ZAHER MOHAMED ... 105	

JOURNAL OF THE EGYPTIAN SOCIETY OF ENGINEERS

VOL. XIV.

ISSUE No. 4 — OCT — NOV — DECEMBER 1975

EDITING BOARD

Editor

Dr. S. MORTADA

Assist. Editor &

Treasurer

Dr. G. NASSAR

Dr. H. AMER

Eng. T. ABD EL - GAWAD

Dr. F. BAHGAT

Dr. S. EL-SOBKY

Dr. M. ABU-ZIED

Dr. M. E. SELIM

Eng. A. EL-ASFORY

- Issued Quarterly Contributors are invited to submit material for editorial consideration addressed to the Editor. The Journal cannot accept responsibility for loss or damage to any material.

INSTRUCTIONS FOR AUTHORS OF ARTICLES

- The Journal publishes articles contributing to the advancement of engineering science and applications.
- Articles may be written in Arabic or English and presented in triplicate with an abstract in both languages.
- Authors' names to be given in full, together with their academic titles and professional occupation.
- Articles may not exceed 8 pages. In this respect, mathematical derivations may be abbreviated and tables replaced by curves.
- Curves to be drawn in black china ink, and to occupy half a page at most. Exceptionally, full page curves or plates are admitted. Curves presented will be scaled down to these sizes. Figures & lettering on curves should not be less than 3 mm even after scaling down.
- References to be given at the end of each article and classified alphabetically according to author's name followed by the name of the journal or book and the date of issue.
- Authors will be presented with two proofs, the first one accompanied by a correction convention chart to ease the work of type correction.

Society Subscriptions

Member	200 P.T.
Associate member	150 P.T.
Associate	100 P.T.

Magazine Subscriptions

Society members Free	
Engineers subscriptions	100 P.T.
Non-engineers subscription	300 P.T.
Organisations subscriptions	500 P.T.

ADVERTISING AGENT

Moassasset Misr for Printing and Publication
10, Souk El Tawfikieh Str. Cairo. Tel. 72192

